Glycoproteomic analysis of changes to the liver membrane

Albert Lee

B.Sc (Molecular Biotechnology) (University of Sydney)

M.Sc (Biotechnology) (Macquarie University)

Doctor of Philosophy

Department of Chemistry and Biomolecular Sciences

Macquarie University

Submission date: 13th May 2010

Table of Contents

Abstract 5

Declaration 8

Acknowledgements 9

Publications 10

Presentations 12

Awards 13

Abbreviations 14

Chapter 1: Introduction 16

1.1. Membrane glycoproteomics 17

1.2. What is the cell membrane? 19
1.2.1. The lipid bilayer 20
1.2.2. Lipid rafts 20
1.2.3. Types of membrane proteins 21
1.2.3.1. Peripheral membrane proteins 22
1.2.3.2. Integral membrane proteins 22
1.2.3.3. Lipid-Anchored Proteins 24

1.3. Protein glycosylation 26
1.3.1. Role(s) of protein glycosylation 29
1.3.2. Glycosylated membrane proteins in cancer 32
1.3.3. Glycosylated proteins in inflammation 36

1.4. Chacterisation of membrane glycoproteins 38
1.4.1. Proteomics 38
1.4.1.1. Characterising the membrane proteome 39
1.4.2. Glycomics 47
1.4.2.1. Characterising the membrane protein glycome 48
1.4.3. Glycoproteomics 53

1.5. Mouse liver membrane glycoproteomics 59
1.5.1. Liver structure and function 59
1.5.2. Mouse liver proteomics 61
1.5.3. Engelbreth-Holm Swarm (EHS) sarcoma 62
1.5.4. Colon 26 (C26) adenocarcinoma 64

1.6. Thesis Aims and Scope 67

Chapter 2: General Methods 68

2.1. Materials 69

2.2. Liver membrane preparation 70

2.3. Amino Acid Analysis (AAA) for protein quantitation 70

2.4. Gel electrophoresis and protein visualisation 71
2.4.1. SDS PAGE and protein visualization 71
2.4.2. Pro-Q Emerald staining for glycoprotein confirmation 71
2.4.3. Lectin blotting with WGA-HRP 72

2.4.4. Two-dimensional gel electrophoresis 72

2.5. Protein Identification by RP LC-MS/MS 73
2.5.1. In-solution digestion with trypsin 73
2.5.2. In-gel digestion with trypsin 73
2.5.3. RP LC-ESI-MS/MS 74
2.5.4. Protein Identification and Data Analysis 75
2.5.5. Calculation of protein Normalized Spectral Abundance Factors (NSAF) 75

2.6. N- and O-glycan identification by carbon LC-MS/MS 76
2.6.1. Preparation of *N*- and *O*-linked oligosaccharides 76
2.6.2. Purification of reduced *N*- and *O*-linked oligosaccharides. 77
2.6.3. Carbon LC-ESI-MS/MS 78

Chapter 3: Approaches for membrane glycoprotein analysis 80

3.1. Sample preparation 81
3.1.1. Comparison of detergents for membrane protein solubilisation 81
3.1.2. Detergent compatibility with ConA lectin affinity chromatography 84
3.1.3. AAA to quantitate detergent-solubilised proteins 86
3.1.4. Enrichment of rat liver membrane glycoproteins by lectin affinity chromatography 88
3.1.5. Triton X-114 phase partitioning for improved membrane protein enrichment 92
3.1.6. 2DGE of Triton X-114 phase partitioned rat liver membrane proteins 95

3.2. Proteomics 97
3.2.1. Rat liver membrane glycoproteome: enrichment by phase partitioning and glycoprotein capture (**Publication I**) 98
3.2.2. Glycopeptide capture as an alternative approach to identify membrane glycoproteins 110

3.3. Glycomics 112
3.3.1. The lectin riddle: glycoproteins fractionated from complex mixtures have similar glycomic profiles (**Publication II**) 114

Chapter 4: Liver membrane proteome glycosylation changes in mice bearing an extra-hepatic tumour (Publication III) 166

Chapter 5: Effects of a distal colon 26 adenocarcinoma on the liver membrane proteome of non-cachectic and cachectic mice 225

5.1. Introduction 226

5.2. Methods 229
5.2.1. Tumour transplantation 229

5.3. Results 230
5.3.1. Comparison of liver membrane proteins in cachectic, non-cachectic and normal mice. 230
5.3.2. Effects of a distal C26 tumour on the glycosylation machinery of the liver membrane glycoproteome 233
5.3.2.1. Cell surface receptors 233
5.3.2.2. Glycosylation pathway enzymes 234
5.3.2.3. Analysis of N-linked oligosaccharides on the liver membrane glycoproteins 236
5.3.2.4. Analysis of O-linked oligosaccharides 241
5.3.3. Effects of a C26 distal tumour on the metabolism of the liver 242
5.3.3.1. Xenobiotic metabolism (UGTs and cytochrome p450s) 242
5.3.3.2. Proteins involved in receptor-mediated endocytosis 244
5.3.3.3. Sugar Metabolism and Transport 245

5.4. Discussion 248
5.4.1. Differential expression of enzymes involved in protein glycosylation in the liver of C26 adenocarcinoma-bearing mice 248

5.4.2. *N*-glycans presented on liver membrane proteins differ between non-cachectic and cachectic mice... 252
5.4.3. Non-glycosylation related changes to liver metabolism in response to a distal C26 adenocarcinoma . 254
5.4.3.1. Immune-specific cell surface receptors ... 255
5.4.3.2. Xenobiotic metabolism ... 257
5.4.3.3. Endocytosis ... 259
5.4.3.4. Glycolysis and gluconeogenesis ... 261

Chapter 6: General Discussion ... 264

Appendices ... 274

References ... 293

Abstract

The study of membrane proteins has become increasingly important, as they play a number of cellular roles such as signal transduction, cell adhesion and cell communication. However, membrane proteomics has often been hampered by the low abundance, extreme hydrophobicity and large size of membrane proteins and therefore alternative enrichment strategies are required to efficiently analyse these types of proteins. In this thesis, we developed an alternative strategy for enriching membrane proteins by targeting both the hydrophobicity and glycosylation of these proteins, which involved (1) Triton X-114 detergent phase partitioning (2) isolation of glycosylphosphatidylinositol (GPI)-anchored proteins and (3) glycoprotein capture using either lectin affinity or hydrazine chemistry. Using this strategy we identified four predicted GPI-anchored proteins and two glycoproteins (Limbic system-associated membrane protein precursor (LSAMP) and Neuronal growth regulator 1 precursor) that have not previously been seen in the liver.

The capture of membrane glycoproteins by lectin affinity and hydrazine chemistry resulted in mostly different populations of enriched glycoproteins demonstrating the complementarity of the two glycocapture approaches. Lectins are often preferred as tools for studying glycoproteins because the sugars on the enriched proteins remain intact compared to the hydrazine capture approach. The selectivity and specificity of lectins for specific glycan structures however, was not reflected in the glycoforms retained from a complex mixture of proteins such as those present in the liver membrane. The use of ConA and WGA for enrichment of membrane glycoproteins showed little difference between the *N*-glycans on the bound proteins compared to those unbound. Only Jacalin appeared to enrich for *O*-glycan containing glycoproteins from the liver membrane preparation. Lectins are valuable tools for enrichment and fractionation of glycoproteins; however detailed structural analysis must be undertaken to define specific differences in the glycosylation of the proteins of interest in a complex mixture.

Applying label-free shotgun proteomics we determined that the presence of a distal Engelbreth-Holm Swarm (EHS) sarcoma and a distal colon 26 (C26) adenocarcinoma could induce differential expression of many metabolic classes of hepatic enzymes of cancer-bearing mice, demonstrating the extensive systemic effect of a distal cancer on the functions of the liver. In particular, we determined that many enzymes involved in the protein glycosylation machinery in the liver were differentially expressed in cancer-bearing mice. Glycomics analysis determined that differential expression of these enzymes was reflected in changes to specific glycan structures expressed on the liver membrane glycoproteins. Both distal cancer models (EHS sarcoma and C26 adenocarcinoma) resulted in an overall increased sialylation of *N*-glycans presented on the liver cell membrane proteins compared to the control. The liver membrane glycoproteins of EHS-bearing mice showed increased sialylation of core 1 and core 2 *O*-glycans containing NeuGc residues, whilst there were no observable *O*-glycan differences observed on the liver membrane proteins of non-cachectic and cachectic C26-bearing mice. Specifically, both EHS bearing mice and non-cachectic mice bearing the C26 adenocarcinoma were shown to preferentially display more *N*-acetyl neuraminic acids (NeuAc) than *N*-glycolylneuraminic acid (NeuGc) on their *N*-glycans. The preferred expression of NeuAc-containing glycans over the more common NeuGc-containing glycans suggests that the CMP-hydroxylase enzyme, which converts NeuAc to NeuGc, had impaired function and/or expression in these mice. There was also increased expression of *N*-glycan structures containing NeuAcα(2-3/6)Galβ(1-4)GlcNAcβ(1-2) (sialyl LacNAc) on the liver proteins in both cancer-bearing murine models compared to control livers. The expression of this specific glycan motif on the liver cell membrane of mice bearing two different distal cancers suggests that this glycan motif may serve as a marker for tumour-induced liver inflammation in the mouse.

The differential expression of the enzymes in the glycosylation pathway and the corresponding glycan products observed on the liver membrane glycoproteins of EHS-bearing

and C26-bearing mice strongly suggests that glycosylation of liver membrane proteins plays a role in the systemic inflammatory responses in the liver to the presence of distal cancers.

Declaration

I certify that the work presented in this thesis titled "Glycoproteomic analysis of changes to the liver membrane" has not previously been submitted, in either whole or part, for the purposes of obtaining any other degree to any other university or institution other than Macquarie University. Unless otherwise acknowledged, this work was carried out by the author.

Albert Lee
40682013

13th May 2010

Acknowledgements

There are many people I would like to thank for their support during my time at Macquarie University throughout my Master's and PhD degrees. Without the immense support none of this would be possible. Firstly, I would like to thank Mark Baker for his supervision and the opportunity to pursue this research project, and for also allowing me to develop my own thoughts under his guidance. I would also like to sincerely thank Nicki Packer, who introduced me to the 'sweet world' of sugars and glycomics and in hindsight, I am grateful that both worlds of proteins and sugars were explored during this project. Much appreciation goes out to you for your insight, optimism and creativitity, and giving me the motivation, guidance and encouragement to persevere during the tough times throughout the PhD years. Additionally, I would also like thank Susanna Lindman and Lars Andersson from GE Healthcare for their support during the project.

Many thanks to the current and former Macquarie University students and staff including Naveid, Karlie, Joel, Siba, Nandan, Katherine, Chi-Li, Pauliina, Rohit, Amit, Mehdi and Arun who have given me the support, conversations, advice and lunch hours (and shenanigans), which have made the whole PhD experience all that more enjoyable. I would also like to thank Lien for her conversations, amusement, support and hospitality during my time in Boston. Huge thanks go out to my 'in-lab' mentors Paul Haynes, Daniel Kolarich, Pia Jensen, Miyako Nakano and Mark Molloy for giving me advice, guidance and confidence to lead the student lab.

Finally, I am grateful to my extended family and friends who have always been there for me during the good and hard times, and for their ongoing support especially throughout the final months. To my parents and brothers, I will always be grateful for the love and support during these years, which have made this PhD even more worthwhile. Lastly, to Judy, your love, patience and support carried me through these years; with you by my side you make everything seem possible. This PhD would not be possible without you.

Publications

Publication I

Lee, A.; Kolarich, D.; Haynes, P. A.; Jensen, P. H.; Baker, M. S.; Packer, N. H., Rat liver membrane glycoproteome: enrichment by phase partitioning and glycoprotein capture. *J Proteome Res* **2009,** 8, (2), 770-81.

All work presented in this publication including membrane preparation, glycoprotein capture (lectin affinity and hydrazine chemistry) and RPLC-MS/MS for protein identification was carried out by the author of this thesis.

Publication II

Lee, A*.; Nakano, M*.; Hincapie, M.; Kolarich, D.; Baker, M. S.; Hancock, W.S.; Packer, N. H., The lectin riddle: glycoproteins fractionated from complex mixtures have similar glycomic profiles. *OMICS: A Journal of Integrative Biology* **2010.** OMI-2010-0075**.** Accepted Jun 15, 2010.

*Joint equal contribution

Lectin affinity fractionation of rat liver membrane glycoproteins and mass spectrometric analyses of *N*- and *O*-glycans were carried out by the author of this thesis. Lectin affinity fractionation of human plasma glycoproteins was performed by Dr. Marina Hincapie and, MS analyses of glycans corresponding to human plasma samples were carried out by Dr. Miyako Nakano. The author was responsible for drafting the manuscript.

Publication III

Lee, A*.; Chick, J. M*.; Kolarich, D.; Haynes, P. A.; Robertson, G. R.; Tsoli, M.; Jankova, L.; Clarke, S. J.; Packer, N. H.; Baker, M. S., Liver membrane proteome glycosylation changes in mice bearing an extra-hepatic tumour. *Mol Cell Proteomics* **2009:** M900538-MCP200v1. Accepted Feb 18, 2010.

*Joint equal contribution

Membrane enrichment and glycomic experiments including sample preparation, carbon LC-MS/MS and manual interpretation and validation of *N*- and *O*-glycans were carried out by the author of this thesis. Quantitation and statistical analyses to determine the relative abundance of glycosyltransferases, glycosidases and cell surface lectins were carried out by both the author and Dr. Joel M. Chick.

Publication IV (in preparation)

Lee, A.; Taylor, R.; Robertson, G. R.; Clarke, S.J.; Baker, M.S.; Packer, N.H., Liver membrane glycoproteomics reveals increased sialylation in non-cachectic and cachectic mice bearing a colon 26 adenocarcinoma. *Manuscript in preparation.*

Tumour implantation, liver harvesting and microarray data was contributed by Ryland Taylor and A/Prof. Graham Robertson. Membrane protein enrichment, *N*- and *O*-glycan preparation, 1D SDS PAGE separation, RP-LC-MS/MS, carbon LC-MS/MS, quantitation and statistical analyses and, manual intepretation and validation of *N*- and *O*-glycans were carried out by the author of this thesis.

Presentations

Lee, A.; Chick, J. M**;** Haynes, P.A.; Molloy, M.P.; Baker, M.S.; Uhlen, K.; Hornsten, L.; Bjellqvist, B.; Len, A.C.L., (2007) A comparative study of the shotgun proteomic techniques peptide immobilized pH gradient - isoelectric focusing coupled with LC-MS/MS and 2DLC-MS/MS using rat liver membrane proteins.

Poster presentation. *Lorne Proteomics*. Victoria, Australia

Lee, A.; Kolarich, D.; Haynes, P. A.; Jensen, P. H.; Baker, M. S.; Packer, N. H.,(2008) Enrichment of membrane proteins by phase partitioning combined with lectin affinity chromatography.

Poster presentation. *HUPO2008*. Amsterdam, Netherlands

Lee, A.; Kolarich, D.; Haynes, P. A.; Jensen, P. H.; Baker, M. S.; Packer, N. H., (2009) Proteomics and Glycomics: complementary approaches to study the membrane glycoproteome. Oral presentation. *Lorne Proteomics*. Victoria, Australia

Lee, A.; Chick, J. M.; Kolarich, D.; Haynes, P. A.; Robertson, G. R.; Tsoli, M.; Jankova, L.; Clarke, S. J.; Packer, N. H.; Baker, M. S. (2009) Membrane glycoproteomics of liver inflammation in the presence of a distal benign tumour.

Poster presentation. *HUPO2009*. Toronto, Canada

Lee, A.; Chick, J. M.; Kolarich, D.; Haynes, P. A.; Robertson, G. R.; Tsoli, M.; Jankova, L.; Clarke, S. J.; Packer, N. H.; Baker, M. S. (2010) Membrane glycoproteomics of liver inflammation in the presence of a distal benign tumour.

Poster presentation. *Lorne Proteomics*. Victoria, Australia

Awards

Australian Postgraduate Award (Industry) (APAI) GE Healthcare: Sept 2006 – March 2010

Macquarie University Postgraduate Research Fund (PGRF): June 2009

Macquarie University International Research Travel Grant: June 2009

HUPO 2009 Young Investigator Award: Sept 2009, Toronto, Canada

Lorne Proteomics Conference 2010 Poster Award: Feb 2010, Victoria, Australia

Abbreviations

1D SDS PAGE	One-dimensional sodium dodecyl sulphate polyacrylamide gel electrophoresis
2DGE	Two-dimensional gel electrophoresis
AAA	Amino Acid Analysis
B3GalT-VII	Beta-1,3-galactosyltransferase 7
B4GalT-III	Beta-1,4-galactosyltransferase 3
C1GalT-I	Beta-1,3-galactosyltransferase 1
C1GalT-II	Beta-1,3-galactosyltransferase 2
C26	Colon 26 Adenocarcinoma
CHAPS	3-[(3-Cholamidopropyl)-dimethylammonia]-1-propane sulfate
ConA	Concanavalin A
CYP	Cytochrome p450
DDM	n-dodecyl-β-D maltoside
dHex	Deoxyhexose
ECM	Extracellular Matrix
EHS	Engelbreth-Holm Swarm
ER	Endoplasmic Reticulum
ESI-MS	ElectroSpray Ionisation Mass Spectrometry
GA	Golgi Apparatus
Gal	Galactose
GalNAc	*N*-acetyl galactosamine
GalNT-I	Polypeptide *N*-acetyl galactosaminyltransferase 1
Glc	Glucose
GlcNAc	*N*-acetyl glucosamine
GO	Gene ontology
GPI	Glycosylphosphatidylinositol
GPM	Global Proteome Machine
GRAVY	GRand AVerage of HydropathY
Hex	Hexose
HexNAc	*N*-acetyl hexosamine
IPG-IEF	Immobilised pH Gradient-IsoElectric Focusing
MALDI-MS	Matrix-Assisted Laser Desorption/Ionization Mass Spectometry
Man	Mannose
Man1a-I	Mannosidase 1, alpha 1
Man1b-I	Mannosidase, alpha, class 1B, member 1

Man2a-I	Mannosidase 2, alpha 1
Mgat-I	Mannoside *N*-acetylglucosaminyltransferase 1
Mgat-II	Mannoside *N*-acetylglucosaminyltransferase 2
Mgat-V	Mannoside *N*-acetylglucosaminyltransferase 5
MMP	Matrix Metalloproteinase
MS/MS	Tandem mass spectometry
MudPit	Multi-Dimensional Protein Identification Technology
NeuAcα(2,3)	α(2,3)-linked *N*-acetyl neuraminic acid
NeuAcα(2,6)	α(2,6)-linked *N*-acetyl neuraminic acid
NeuGcα(2,3)	α(2,3)-linked *N*-glycolyl neuraminic acid
NeuGcα(2,6)	α(2,6)-linked *N*-glycolyl neuraminic acid
NSAF	Normalised Spectral Abundance Factors
OG	n-Octyl-β-D-glucopyranoside
OGT	Dolichol-oligosaccharide transferase
PNGase F	*N*-Glycosidase F
RPLC	Reverse Phase Liquid Chromatography
SB3-10	3-(Decyldimethylammonia) propanesulfonate inner salt
Siglec	Sialic acid immunoglobulin-like lectin
SLe*	Sialyl Lewis antigen (*specified as either x or a)
ST3Gal-I	Beta-galactoside alpha-2,3-sialyltransferase 1
ST6Gal-I	Beta galactoside alpha-2,6-sialyltransferase 1
ST6GalNAc-VI	Alpha-*N*-acetylgalactosaminide alpha-2,6-sialyltransferase 6
TMHMM	TransMembrane Helices in proteins
UGT	UDP-glucuronosyltransferase
WGA	Wheat Germ Agglutinin

Chapter 1: Introduction

1.1. Membrane glycoproteomics

Membrane proteins are involved in key biological functions such as signal transduction, cell adhesion and cell-cell communication. Because of their diverse functions, membrane proteins are the most elusive and sought after proteins in drug discovery as many of these proteins have been identified to be responsible for a range of diseases such as human cancers [1, 2], Alzheimer's disease [3] and autoimmunity [4]. Currently, approximately 70-80% of all drugs target membrane proteins [5] which include: G-protein coupled receptors (GPCR) (30%), ion channels (7%), transporters (4%) and nuclear hormone receptors (4%) [6]. Although membrane proteins are key targets for drug discovery, membrane proteomics has often been hampered by their low abundance and relatively high hydrophobicity and, therefore efficient methods to enrich for these types of proteins are essential for a better understanding of membrane organization and function.

Traditional proteomics approaches such as one-dimensional (1D SDS PAGE) and two-dimensional gel electrophoresis (2DGE) separation in combination with mass spectrometry are commonly used for separating and identifying soluble and mildly hydrophobic proteins. A major challenge with isolating and analyzing membrane proteins by these gel-based approaches is their low abundance and extreme hydrophobicity, which can make separating and identifying these proteins by gel electrophoresis difficult. Proteomic approaches currently used to overcome these issues are commonly based on "shotgun proteomics" methods using high resolution separation of proteolytic peptides in combination with tandem mass spectrometry [7-9].

The liver is involved in numerous biological functions such as xenobiotic metabolism, fatty acid metabolism, protein and ion transport, glycogen storage, plasma protein synthesis and bile acid biosynthesis, to name a few. In addition, the liver plays a functioning role in the immune system and is also responsible for conditioning and producing most plasma proteins [10]. Liver-derived plasma proteins and significant increases in serum acute phase

glycoproteins and their sialylation have generally been observed with most rodent experimental inflammation models [11-13]. Recently, it has been shown that mice bearing a distal Engelbreth Holm Swarm (EHS) sarcoma can induce differential expression of liver membrane proteins particularly those involved in xenobiotic metabolism and solute carrier transport [14-16], and these functions are thought to be correlated with the inability of many advanced cancer patients to metabolise and clear chemotherapeutic drugs leading to chemotoxicity. Patient deaths resulting from advanced stage cancers, particularly pancreatic and colon cancers, are mostly due to the condition of cachexia instead of the cancer itself [17]. In cachectic cancer patients, reduced levels of xenobiotic enzymes (e.g. cytochrome p450s), extreme body weight loss and loss of appetite is often associated with the condition. To emulate the condition of cachexia, murine studies employing the colon 26 (C26) adenocarcinoma are often used to induce inflammation of the liver and disorders of homeostasis [18].

The purpose of this chapter is to provide some background on what is currently known of membrane structure and function, the types of proteins that associate with the membrane and the approaches that are currently employed for studying the membrane proteome. In addition, since glycosylation of membrane proteins plays a significant role in processes such as cell adhesion, cell communication and cell signaling [19], and because of the importance of these processes in cancer we address how proteomics and glycomics can be used as complementary approaches to study the effect on liver membrane glycosylation of mice bearing a distal EHS non-metastasizing sarcoma and mice bearing a C26 adenocarcinoma with and without cachexia.

1.2. What is the cell membrane?

The major function of a plasma membrane is to act as a barrier between the cytosol of a cell and the extracellular environment. It also facilitates the removal of toxic molecules and ions, importation of nutrients to the cell, energy transduction, cell locomotion and reproduction, to name a few. Molecules such as oxygen, water, sugars, amino acids and proteins are able to pass across the membrane.

Eukaryotic plasma membranes are essentially composed of a lipid bilayer. The lipid bilayer consists of components such as lipids, proteins and carbohydrates. The structure of the plasma membrane was first described by Singer and Nicolson and named the 'Fluid Mosaic Model' [20]. This model presents the overall organization of the plasma membrane and its components where the phospholipid bilayer is a fluid matrix that is a two-dimensional solvent for proteins. Within plasma membranes, both lipids and proteins are capable of rotational and lateral movement [21]. The 'fluidity' of the lipid bilayer is the flexibility of lipids, which allows many of the proteins and carbohydrates associated with the plasma membrane to move to different locations on the surface of the cell. Lipids are composed of a terminal carboxyl group and a long hydrocarbon tail. The hydrocarbon tails of fatty acids pack together to form the lipid bilayer. The lipid molecules are arranged as a continuous double layer which provides the basic fluid structure of the membrane serving as a impermeable barrier to the passage of water-soluble molecules [22]. The transport of molecules and ions are assisted by the proteins that are associated with the membrane. Membrane proteins can be classified as peripheral, integral and lipid-anchored. Peripheral membrane proteins can associate with the lipid bilayer or with other membrane proteins by electrostatic interactions. Integral membrane proteins can either insert into one or both layers of the lipid bilayer [20]. Lipid-anchored proteins are mostly soluble proteins that are anchored by a lipid moiety either co-translationally, or post-translationally in the endoplasmic reticulum (ER) and/or Golgi Apparatus (GA) and are subsequently tethered to the membrane. The plasma membrane is

heavily glycosylated typically with carbohydrates covalently linked to membrane lipids (glycolipids) or to membrane proteins (glycoproteins). The fluid mosaic model which describes the cell membrane and its associated components has become a paradigm for studying eukaryotic membrane structures.

1.2.1. The lipid bilayer

Membrane lipids spontaneously form bilayers due to their amphipathic nature. All lipid molecules that make up cell membranes have a hydrophilic polar head and a hydrophobic tail. These lipid molecules can spontaneously form structures such as micelles, vesicles and bilayers through hydrophobic interactions between their fatty acid tails. Bilayers are the most common lipid structure found in eukaryotic membranes as their conformation is more energetically favourable [23]. Lipid bilayers are made up of three main classes of lipid molecules they are cholesterol, glycolipids and phospholipids. Lipid bilayers also form the basis for membrane boundaries of other eukaryotic organelles such as the nuclear envelope, ER, GA, mitochondria and peroxisomes.

1.2.2. Lipid rafts

The lipid bilayer of cell membranes are not planar but contain structures that are known as lipid assemblies or rafts, which provide fluid platforms that dynamically compartmentalize areas of the membrane [20, 23, 24]. Lipid rafts were first observed by Thompson and Tillack and described to be resistant to solubilisation with the non-ionic detergent Triton X-100 [25, 26] due to the tight packing of fatty acyl chain tails [27]. Lipid rafts are highly enriched in sphingolipids, cholesterol and some membrane proteins. Sphingolipids have long and saturated fatty hydrocarbon chains, which have interactions strong enough to hold adjacent molecules, being other sphingolipids or cholesterol [28]. They are thought to help organize proteins either by concentrating them for transport in small vesicles or to function as

platforms for the attachment of proteins and their internalization into the cell during signal transduction, endocytosis and cholesterol trafficking (Figure 1-1) [23, 28, 29]. A variety of proteins including caveolin [30], glycosylphosphatidylinositol (GPI)-anchored proteins [26] and other cell-signaling proteins [31, 32] are commonly found to be associated with lipid rafts.

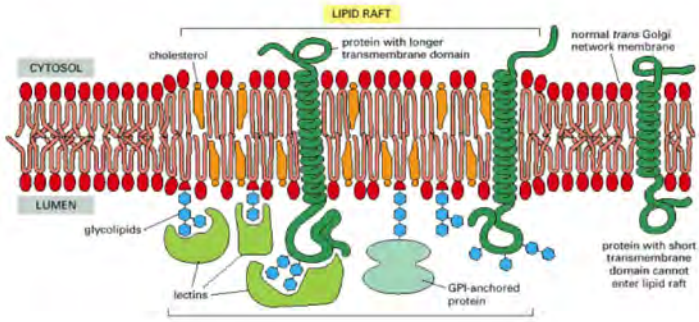

Figure 1-1. Lipid rafts consist of high concentrations of lipids and proteins that are clustered and concentrated in particular regions of the membrane. Many membrane proteins involved in cell-signaling and GPI-anchored proteins are often clustered in lipids rafts [33].

1.2.3. Types of membrane proteins

Based on the sequences from several genomes, membrane proteins have been predicted to comprise approximately 30% of eukaryotic proteomes [34]. Membrane proteins mediate and regulate the transport of metabolites, macromolecules and ions for the cell and their organelles and commonly act as intermediaries between the cell and the extracellular environment. Hormones and many other biological signal molecules and regulatory agents exert their effects via interactions with membrane proteins. Proteins are relatively large compared to lipid molecules – on average approximately 50 lipid molecules occupy the same hydrodynamic volumes as each membrane protein. Membrane proteins can be classified as 1) peripheral, 2) integral and 3) lipid-anchored.

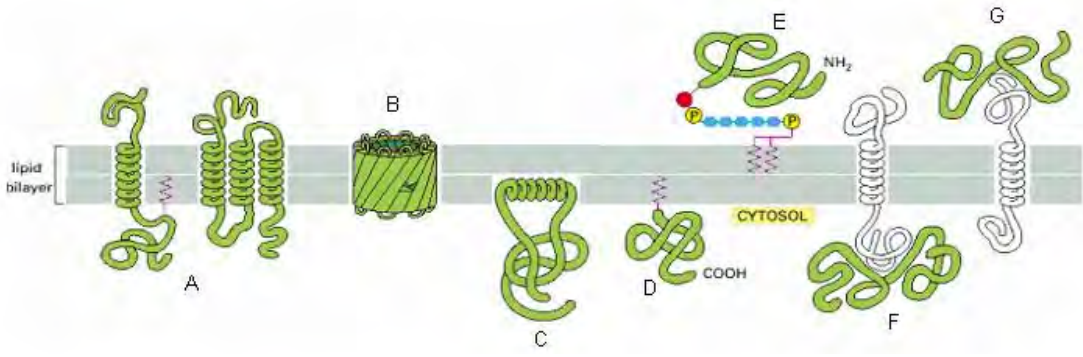

Figure 1-2. Various ways in which membrane proteins associate with the lipid bilayer as (A) single and multiple helices crossing the bilayer, (B) a β barrel, (C) anchored to the cytosolic surface by an amphipathic α helix that partitions into the cytosolic monolayer of the lipid bilayer through the hydrophobic face of the helix, (D) attached to the bilayer by a covalently attached by a fatty acid chain (E) attached via an oligosaccharide linker, to phosphatidylinositol in the non cytosolic monolayer and (F,G) proteins attached to the membrane only by non covalent interactions with other membrane proteins [22].

1.2.3.1. Peripheral membrane proteins

Peripheral proteins do not penetrate the lipid bilayer, however, they do associate with integral membrane proteins and the cytosolic and extracellular surface of the lipid bilayer by virtue of hydrophobic and electrostatic interactions, respectively [20] (Figure 1-2F and Figure 1-2G). They interact with the plasma membrane and integral transmembrane proteins by weak electrostatic forces, which can activate or inhibit signal pathways such as Protein Kinase C (PKC) family, which can induce processes such as cell proliferation, differentiation and apoptosis [35]. Other peripheral membrane proteins include Ras [36] and guanine nucleotide-binding proteins (G-proteins) [37] are also involved in many signal transduction pathways.

1.2.3.2. Integral membrane proteins

Integral membrane proteins are amphipathic in nature, where their hydrophobic regions pass through the membrane and interact with the hydrophobic tails of lipid molecules in the interior of the bilayer. The hydrophilic regions of transmembrane proteins are exposed to the extracellular and intracellular environment on either side of the membrane. In general, the structure of integral membrane proteins within the core of the lipid bilayer is dominated by complex tertiary protein structures. How integral membrane proteins cross the lipid bilayer is

determined by the conformation of the α-helices and peptide bonds [38]. Alpha helices either form as single-pass transmembrane proteins, crossing the bilayer only once or as multi-pass transmembrane proteins. Environmental cues prompt helices to undergo conformational changes that allow for ion channels to open and shut allowing transport of ions into the cell and the transfer of extracellular signals (Figure 1-2).

Integral membrane proteins can be either single-pass or have multiple-pass transmembrane regions. Single-pass transmembrane proteins are essentially anchored by a small hydrophobic polypeptide segment (usually in the form of a single α helix) and hydrophilic segments extending into either the cytoplasmic or extracellular space (Figure 1-2A). These membrane proteins often function as receptors for extracellular molecules and can act as recognition sites for the immune system [39, 40].

Multi-pass membrane proteins cross the membrane more than once and are often involved with transport and functions that require peptide binding [41]. They can cross the membrane in a globular shape with numerous hydrophobic α helical segments joined by hinge or loop regions (Figure 1-2A). Regions of single and multi-pass transmembrane proteins that are exposed to the extracellular surface of the plasma membrane often have hydrophilic oligosaccharides attached, which are exposed to the extracellular environment and act as recognition sites for other proteins and ligands [42].

Multi-pass transmembrane proteins can also be arranged as anti-parallel β sheets linked by β turns. They usually have a barrel-like structure and some are known as porins (Figure 1-2B). Porin proteins are made up of a cylindrical structure with polar amino acids lining the inside of the pore forming an aqueous channel, while the non-polar amino acids are projected on the outside of the barrel which interact with the lipid bilayer. The barrel motif forms a cavity that serves as a ligand binding region [43]. Porins control the diffusion of small metabolites like sugars, ions, and amino acids [43, 44]. Proteins mainly consisting of β pleated sheets are commonly found in gram-negative bacteria, mitochondrial and chloroplast

outer membranes including OmpC and OmpF from *E. coli* K-12 [45]; and the family of Translocator Outer Membrane (TOM) proteins found in mitochondria.

1.2.3.3. Lipid-Anchored Proteins

Lipid-anchored proteins are initially made as soluble proteins in the cytosol, where the ER identifies and attaches a lipid moiety and subsequently directs it to the plasma membrane via the Golgi apparatus (GA) (Figure 1-2D). The lipid that is anchored to the protein can modulate the activity of the attached protein [23, 26, 46, 47]. Lipid anchors can be reversibly attached to and detached from proteins and this provides a mechanism by which signal transduction pathways are controlled in eukaryotic cells [46-48]. There are currently four known types of lipid-anchoring motifs. These are amide-linked myristoyl [49], thioester-linked fatty acyl [50], thioether-linked prenyl [51] and amide-linked glycosyl phosphatidylinositol anchors [52].

Amide-linked myristoyl anchored proteins are formed by the linkage of the carboxyl end of myristic acid via a amide bond with the N-terminal glycine residues of a variety of eukaryotic and viral proteins [53]. Myristic acid is a saturated 14 carbon fatty acid chain, which is embedded into the lipid bilayer [49]. Thioester-linked fatty acyl anchored proteins are formed in the GA by ester linkages of fatty acids (Myristate [14 carbon], palmate [16 carbon], stearate [18 carbon] and oleate [unsaturated 18 carbon]) with cysteine, serine or threonine side chains of proteins [50]. Thioether farnesyl and geranyl are part of the long-chain polyisoprenoid lipid groups that can be attached to proteins at a cysteine residue in the polypeptide with the carboxy-terminal recognition sequence Cys-Ala-Ala-X (X: other amino acid).

Glycosylphosphatidylinositol (GPI) groups are structurally more complex membrane anchors than fatty acyl and prenyl groups (Figure 1-2E). Soluble glycoproteins are anchored in the outer leaflet of the plasma membrane by a moiety of phosphatidylinositol (PI), linked

via a glucosamine residue to a central glycan core composed of mannose residues (and often other sugars), which is coupled in the ER to the carboxyl group of the C-terminal amino acid of the protein via phosphoethanolamine (Figure 1-3). The GPI anchor is initially covalently linked to glucosamine, followed by deacetylation and addition of mannose residues and phosphoethanolamine [54, 55]. This GPI-anchor precursor is transferred to a specific site upstream of the C-terminal end of the target protein in the ER by the action of a transamidase complex, which simultaneously cleaves off the signal C-terminal peptide [56]. The C-terminal sequence of the protein thus acts as a signal for GPI attachment. The association of GPI-anchored proteins with lipid rafts occurs in the GA during outward trafficking of GPI-anchored proteins and helps to target them to the extracellular surface of the plasma membrane [57].

Unconjugated GPI lipids synthesized in the ER that are not attached to proteins are also directed to the cell surface [58]. The glycan core of unconjugated GPI lipids is different to GPI anchors linked to proteins instead consisting of galactose, *N*-acetylgalactosamine (GalNAc) and glucosamine. Mannose and ethanolamine are not present in unconjugated GPI lipids [54, 59]. A number of polypeptide growth factors, hormones and cytokines including insulin, insulin-like growth factor I, transforming growth factor-β, epidermal growth factor, interleukins 1 and 2, thyrotropin releasing hormone and thyroid stimulating hormone have been shown to stimulate hydrolysis of "free" GPI lipids as part of their mechanism for signal transduction [54, 59, 60].

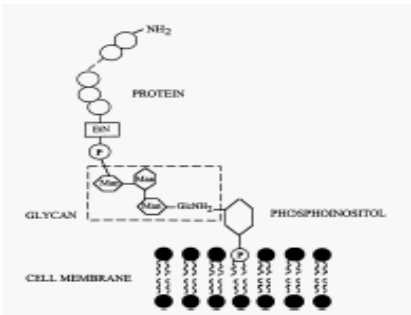

Figure 1-3. GPI-anchored proteins consist of an inositol region embedded in the lipid bilayer covalently attached to a glucosamine molecule. The glucosamine molecule is attached to mannose sugar molecules and ethanolamine. The ethanolamine is bound to the protein via an amide linkage [61].

1.3. Protein glycosylation

Glycosylation is an enzymatic process that covalently links glycans to proteins and/or lipids. There are two main types of protein glycosylation; *N*-linked and *O*-linked. *N*-linked glycosylated proteins are composed of *N*-acetylglucosamine (GlcNAc) linked to the amide nitrogen of asparagine side chains at the consensus sequence Asn-X-Ser/Thr (Cys), where X can be any amino acid except proline. *N*-glycans contain a common tri-mannose chitobiose core where additional monosaccharides are commonly elongated to the two outer mannose residues [Manα(1,3) and Manα(1,6)] producing three main classes of *N*-glycans: high-mannose, hybrid and complex (Figure 1-4 and Figure 1-5). *O*-linked glycosylation as described in this thesis refers to a GalNAc (*O*-GalNAc) monosaccharide α-linked to the hydroxyl groups of serine or threonine residues on proteins. However, other types of *O*-glycosylation also involve modification of serine and threonine residues in proteins, which include the attachment of fucose (*O*-fucose), glucose (*O*-glucose), *N*-acetylglucosamine (*O*-GlcNAc) or mannose (*O*-mannose). *O*-linked glycosylation does not have a consensus sequence for glycan attachment, and currently consists of eight characterised *O*-GalNAc linked core structures (Figure 1-6). Other types of glycosylation include the previously described GPI-anchors and *C*-glycosylation, which is often attached to tryptophan residues in some membrane-associated and secreted proteins [62].

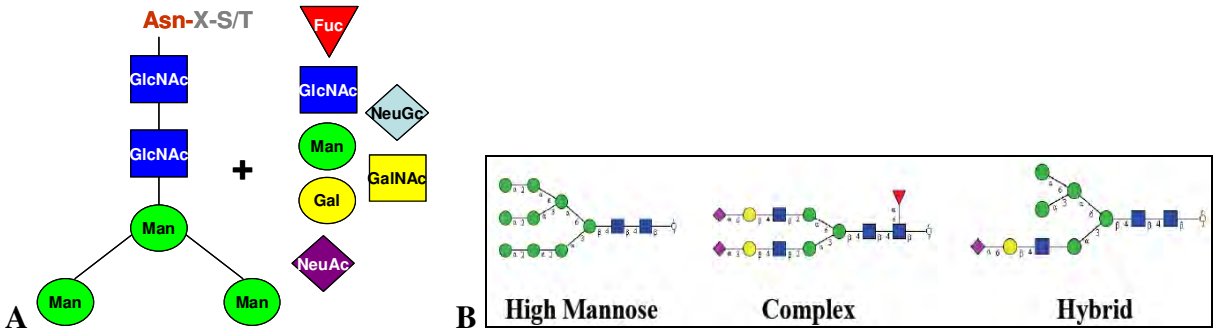

Figure 1-4. The tri-mannose chitobiose core which is commonly found in *N*-linked glycans consists of two *N*-acetylglucosamine residues linked to the asparigine residue in the consensus sequence (N-X-S/T) followed by three mannose residues (A). Other monosaccharide units can be attached to each of the two outer mannose residues producing high-mannose, hybrid and complex *N*-glycan structures (B). GlcNAc: *N*-acetylglucosamine, Man: mannose, Gal: galactose, Fuc: fucose, NeuAc: *N*-acetyl neuraminic acid

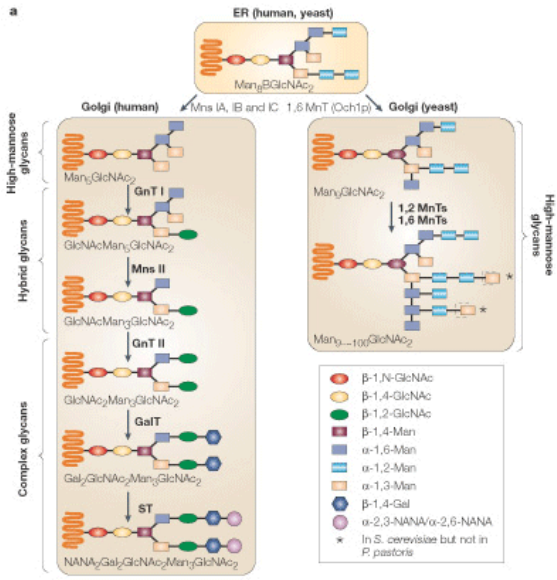

Figure 1-5. *N*-glycosylation pathway in humans (left) provides a template for humanizing N-glycosylation pathways in yeast (right). The glycosylation pathway begins in the ER and is synthesized by mannosyltransferases and mannosidases. The *N*-glycans are then further processed in the GA where a number of glycosyltransferases including *N*-acetylglucosaminyl transferases, galactosyltransferases and sialyltransferases catalyse the addition of other monosaccharide units to the maturing *N*-glycan. Different isoforms of glycosyltransferases are expressed in different cells, tissues and species. GalT, galactosyltransferase; GlcNAc, N-acetylglucosamine; GnT I, N-acetylglucosaminyl transferase I; GnT II, N-acetylglucosaminyl transferase II, Man, mannose; Mns II, mannosidase II; MnTs, mannosyltransferase; NANA, N-acetylneuraminic acid; ST, sialyltransferase.

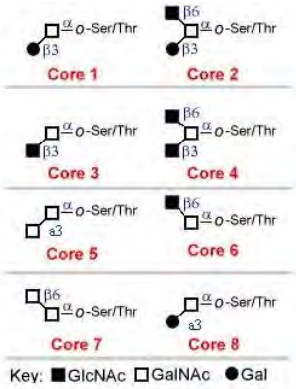

Figure 1-6. Main mammalian *O*-glycan core structures which are linked to the hydroxyl groups of Ser/Thr. Additional monosaccharide units can be attached to either of the eight core structures.

N-glycosylation can occur as co-translational and post-translational processes where attachment to proteins is catalyzed by a number of glycosyltransferases and glycosidases in the ER and GA compartments. The co-translational *N*-glycosylation process assists in the folding of glycoproteins. Many mammalian glycosyltransferases themselves are glycosylated as they possess the motif for *N*-glycosylation.

O-GalNAc linked glycosylation is catalysed by the enzyme UDP-*N*-acetyl-D-galactosamine:polypeptide *N*-acetylgalactosaminyltransferase in the GA at the latter stages of

protein processing (Figure 1-7) and is known to be involved in processes such as adhesion [63], immune regulation [64-66] and intracellular processing [67] in mammals. Intracellular glycosylation processes are also present in the cytoplasm and nucleus as single *O*-GlcNAc additions [68]. *O*-GlcNAc is added to serine or threonine by *O*-GlcNAc transferase on sites that would otherwise be phosphorylated by serine/threonine kinases [68]. Some of the other common monosaccharides found in oligosaccharides attached to proteins in mammals include: hexoses (mannose, galactose and glucose), hexosamines (*N*-acetyl glucosamine and *N*-acetyl galactosamine), deoxyhexoses (fucose) and sialic acids (*N*-acetyl neuraminic acid and *N*-glycolyl neuraminic acid).

Glycans are often heterogeneous since the monosaccharide units can be arranged in a number of combinatorial positions depending on the glycosyltransferases and glycosidases involved in the enzymatic processes (Figure 1-7). The different combinations of glycans that are attached to a protein can produce a number of glycoforms of the same protein, which often exhibit different physicochemical properties (e.g. hydrophilicity). However unlike the amino acids of proteins, which are linked in a linear structure, oligosaccharides are often branched-like structures formed by the different linkage(s) of one or more monosaccharides which can produce a number of different glycan structures (microheterogeneity). The numerous possible glycan structures and the lack of a template make it difficult to predict the type of structures that are produced and their different site(s) of attachment to glycoproteins (macrohetereogeneity).

Glycans can be recycled and re-used to glycosylate other proteins; this process is initiated by endoglycosidases that remove whole glycans from glycoproteins. The released oligosaccharides are further broken down into their individual monosaccharides components by exoglycosidases releasing them into the cytoplasm to be re-used as substrates for further protein glycosylation processing. In addition, sialic acids that are found “capped” at the end of glycans can also be removed and replaced with new monosaccharide units during endosomal

recycling without affecting the underlying sugar chain. Capping sugars such as sialic acids are usually α-linked, unlike the backbone residues, which are normally β-linked. α and β conformations, also known as stereoisomers, are determined by the position of the hydroxyl group that is attached to the anomeric carbon (carbon-1) which can be below the plane (α-linked) or above the plane (β-linked)

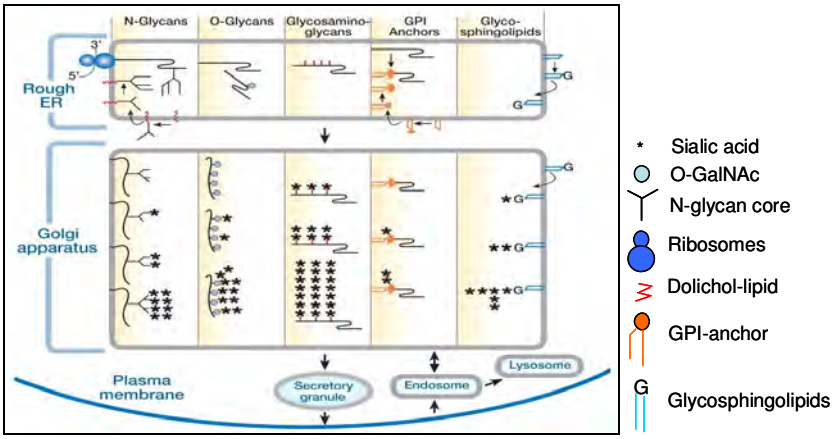

Figure 1-7. Summary of glycosylation processes (*N*-glycans, *O*-glycans, glycosaminoglycans, GPI anchored proteins and glycosphingolipids) that occur in the ER and GA [19]. Image reproduced from Varki *et al.* Essentials in Glycobiology [19]. Protein synthesis and initial stages of lipid and glycan attachment are carried out in the ER. Sialic acid capping of glycans and glycolipids is carried out in the GA.

1.3.1. Role(s) of protein glycosylation

As more knowledge of glycoproteins and their attached glycans emerges, there is growing evidence that the abundance and heterogeneity of glycans on the cell surface can reflect the differences in cell types and states [69]. Glycosylation of proteins has been shown to be associated with cell development, differentiation, implantation and morphogenesis [69] in diseases such as diabetes [70], cystic fibrosis (CF) [71], arthritis [72], Alzheimer's [73], autoimmunity [74] and cancer [75]. For example, increased glycoprotein expression of MUC2, MUC5AC and MUC5B and increased sulfation of *N*- and *O*-linked oligosaccharides on MUC5B in the lung cavity are often present in CF patients [71]. In addition, lung epithelial cells of CF patients often present increased expression of *N*-glycans containing Fucα(1,3) attached to the antennary GlcNAc, increased core fucosylation [Fucα(1-6)GlcNAc] and decreased expression of NeuAc residues [76]. The increased sulfation of MUC5B and

alterations to *N*- and *O*-glycans on the lung epithelial cell surface are thought to facilitate bacterial colonisation and leukyocyte recruitment in CF [76].

Another example of the role of glycosylation in diseases is the altered *N*-glycosylation of IgG (agalactosylated IgG/IgG_0) in the pathogenesis of rheumatoid arthritis, which exposes GlcNAc residues on *N*-glycans as the terminal sugars [77]. Additionally, monosaccharide compositions of total *N*-glycans from plasma proteins of arthritis patients have shown higher concentrations of mannose residues and reduced amounts of glucose residues compared to the normal [77]. The high mannose/glucose ratio in arthritis patients suggests the presence of unprocessed oligomannosidic glycan structures still attached to plasma proteins, which could be attributed to congenital disorders of glycosylation (CDGs). These two examples (CF and arthritis) demonstrate that aberrant protein glycosylation are features of these diseases and the study of protein glycosylation is important for the development of new diagnostics and identification of targets for therapeutic intervention.

All cells from all animal, plant and bacterial kingdoms are coated with abundant and heterogeneous glycans. Glycans have diverse functions, many of which are involved in modulating structure and functions of proteins to which they are attached. These glycans are presented as recognition sites for glycan-binding proteins known as lectins. Lectins are proteins found in plants, animals and microorganisms that have affinity for particular oligosaccharide structures presented on proteins and lipids. There are several major classes of animal lectins including galactose-type lectins (galectins), calcium-dependent type (C-type) lectins, cation-dependent type (P-type) lectins and immunoglobulin-like (I-type) lectins. Lectins serve many different biological functions in animals, including cell-adhesion (e.g. galactose-binding lectins [galectins]), immune system regulation (e.g. sialic acid immunoglobulin-like lectin [siglecs]), glycoprotein synthesis (e.g. calreticulin/calnexin) and degradation (e.g. mannose-6-phosphate receptor). The role of lectins in many of these biological phenomena relies mostly on the type of glycans and specific linkages that are

attached to proteins and/or lipids. For example, siglec-1, and siglec-2 are cell surface receptors expressed on leukocytes that play major roles in the immune system by specifically recognizing α(2,3)-linked and α(2,6)-linked sialic acids on *N*- and *O*-glycan structures [78, 79]. Therefore, correct protein glycosylation including the attachment of monosaccharide components and their specific linkages are important for their particular recognition by different lectin proteins.

Glycosylation of proteins is also commonly used for maintaining structural and thermal stability of glycoproteins, as well as signaling proteins for degradation by proteases. How a protein is glycosylated can determine the localization, activity and function of the glycoprotein [80], therefore glycosidases and glycosyltransferases play a crucial role in catalyzing and maintaining the correct glycosylation of proteins. Many glycan-specific diseases such as congenital disorders of glycosylation (CDGs), are caused by defects in the protein glycosylation machinery [81]. For example, diseases such as cancer and autoimmunity have been reported to possess altered glycosylation as a consequence of defective or altered glycosyltransferases [82-84]

Glycosyltransferases are a group of enzymes that synthesize the oligosaccharides on glycoproteins. There are approximately 30,000 glycosyltransferase sequences across all kingdoms (~500 genomes), of which there are around 90 different glycosyltransferase families based on primary DNA sequences [19]. Glycosyltransferases can catalyse the addition of the same monosaccharides but may differ in their starting substrates. For example ST3Gal-I and ST3Gal-II are two isoforms of sialyltransferases that are responsible for adding NeuAcα(2,3) to Galβ(1-3)GalNAc on proteins and lipids respectively [85]. Moreover, different isoforms of glycosyltransferases are also expressed in different cells and tissues.

Most glycoproteins are either secreted into the extracellular environment or attached to the plasma membrane; therefore changes to glycosyltransferases can ultimately influence the overall adhesive properties of the cell [84]. For example, changes in carbohydrate moieties of

membrane glycoproteins are extensively modified during cancer carcinogenesis and metastasis [86] due to reduced levels of sialyltransferases and increased expression of fucosyltransferases [87]. Sialyltransferases are responsible for catalyzing the addition of sialic acids to *N*- and *O*-glycans, which play an important role in cell-cell communication through protein-glycan and glycan-glycan interactions [88]. Fucosyltransferases catalyse the addition of fucose to *N*- and *O*- glycans and are responsible for synthesising Lewis x, y, a and b antigens, which are often found on the surface of red blood cells and are also determinants for secretory status [89]. Increased expression of SLe^x antigens is often associated with cancer and poor prognosis and it has been speculated that the degree of sialylation of the Lewis x antigen is a more confident marker of the aggressiveness of the tumour than the overall quantity of the antigen expressed [87, 90, 91].

1.3.2. Glycosylated membrane proteins in cancer

Membrane glycoproteins are currently used as markers for diagnosis and monitoring progression of cancer. Some of these glycoproteins which are used as general protein and/or glycan cancer markers include: Selectins, CD44 (protein and glycosylation), E-cadherin, Carcinoembyronic antigens (CEA), extracellular matrix (ECM) and basement membrane proteins and, matrix metalloproteinases (MMPs). The most common types of aberrant glycosylation observed on human cancer cell membrane proteins are 1) increased expression of Sialyl Lewis x and a antigens (SLe^x and SLe^a) on tumour cells [83, 86, 92], 2) increased β(1-6)GlcNAc antenna in *N*-linked structures resulting from enhanced or induced expression of GlcNAc transferase-V, 3) increased expression of Tn and Sialyl Tn antigens and 4) increased expression of poly-LacNAc (Galβ(1-4)GlcNAc) sequences. These glycoproteins and glycan epitopes are all associated with cancer, particularly in metastatic processes.

During cancer metastasis, tumour cells separate from the primary mass, enter the bloodstream, disperse through the body, migrate across vessel walls and generate distant

colonies. The ability of a cancer cell to adhere to the basement membrane and its interaction in the appropriate geometry with neighbouring cells is governed by the expression of the plasma membrane proteins (e.g. integrins) and associated glycans [93]. These factors are commonly mediated by adhesion molecules such as integrins and selectins. Integrins are heterodimeric (α, β subunits) transmembrane cell surface glycoproteins that act as receptors for ECM proteins and can also function as fibronectin receptors for metastasis [87, 94]. Integrins, together with selectins, play key roles in adhesion of tumour cells to microvascular endothelium and the migration of tumour cell colonies.

Selectins are a family of cell surface adhesion receptors expressed on endothelial cells, which have a high affinity for SLe^x and SLe^a antigens expressed on monocytes, granulocytes, T-lymphocytes [87] and metastatic colon cancer cells [95]. There are three classes of selectins: L, E and P selectins which are all expressed on the surface of leukocytes during inflammation and immune system regulation. The expression of SLe^x antigens by metastatic cancer cells promotes E-selectins to mediate adhesion of metastatic cancer cells to vascular endothelium. P-selectins promote initial attachment of metastatic cancer cells to blood vessel endothelium through protein interactions with α5β1 integrin promoting adhesion between cancer cells and platelets to form emboli [96]. This interaction has also been shown to activate p38 MAPK and PI3-K signaling pathways and as a result activate α5β1 integrin [96]. α5β1 integrin, which can also be activated by CD24 and CD44 stimulates the cell attachment and spreading of metastatic cancer cells [96].

Sialyl Lewis (SLe) x and a antigens are sialylated lacto-N-fucopentaose carbohydrate moieties that are normally expressed on leukocytes and interact with E-selectins to adhere to the endothelium and their extravasation to sites of inflammation. However, SLe antigens are also found on cell surface glycoproteins of metastatic tumour cells similarly to leukocytes, which are often use these antigens to aid metastasis, mimicking the still unknown mechanism of leukocyte extravasation [87, 97, 98]. The degree of sialylation of these antigens can affect

the polar orientation and adhesion of tumour cells to basement membranes during cancer metastasis [87]. SLe^x and SLe^a antigens which help to promote adhesion by selectins are also expressed on carcinoembryonic antigens (CEA) and on the surface of tumour cells.

CD44 is a single pass transmembrane glycoprotein that acts as a receptor for hyaluronan, fibronectin, collagen IV and laminin [99]. The interaction of these proteins with CD44 activates cell motility and proliferation [87, 99]. CD44 may also act as an anchor for epithelial cells in basement membranes to maintain their polar orientation and adhesive properties. The diverse functional roles of CD44 are governed by the sialylation and fucosylation of glycans attached to the molecule, which can influence the binding of CD44 to the different protein partners such as fibronectin, collagen and CEA [87, 92, 100-102]. The different CD44 variants arising from alternative splicing of mRNA and the degree of glycosylation can increase the size of CD44 to range from 37 kDa to 100 kDa [103-106], which can have profound effects in binding hyaluronidate, thus influencing the overall adhesive properties of the cancerous cells [103-106]. Decreased expression of CD44 in tumour cells can often lead to lymph node metastasis and poor prognosis [107]. Alternatively, elevated expression of CD44 can lead to increased binding of MMPs and cause venous invasion and hepatocellular carcinoma [108]. CD44 has been reported to be a protein involved with common cancers; however it is the glycosylation of CD44 which governs the adhesive properties of the cancerous cell which can influence the degree of metastasis [108].

Adhesion molecules maintain epithelial cell integrity and cellular architecture of normal cells. The architecture of tumour cells loses its capacity to adhere through degradation of the collagen meshwork of the ECM and basement membranes by MMPs, thus facilitating their dettachment from the primary tumour mass. Cell adhesion events following detachment can be regulated by cadherin and catenin complexes. There are three types of cadherins: N-cadherin found in neurons, P-cadherin found in the placenta and, E-cadherin found on epithelial cells. E-cadherin requires α and β catenins to bind to complete a cadherin-catenin

complex. This complex interacts with CD44 to facilitate and sustain the adhesive functions of normal cells, and it has been shown to suppress invasion and metastasis of cancer [109]. The decreased or loss of expression of either the cadherin-catenin complex or CD44 is often correlated with poor prognosis and survival [109].

Carcinoembyronic antigens (CEA) are soluble glycoproteins secreted to the cell surface of metastatic and Duke's C (non-metastatic) colon and liver cancer cells. CEA contains high concentrations of SLe^x and SLe^a antigens. Levels of CEA and fibronectin concentration are being examined as potential prognostic markers for cancer. However, CEA has been described as a poor diagnostic marker since secretion of this antigen is normally considered to be a secondary phenomenon following cell adhesion and metastasis [110]. In addition, the binding of CEA to its specific receptor on Kupffer cells triggers the degradation of CEA itself whilst also releasing cytokines (for example interleukin-6 (IL-6) and tumour necrosis factor-α (TNF-α)) into the sinusoid environment causing increased growth of tumour cells [111, 112].

Cancer metastasis involves the interaction of tumour cells with ECM and basement membranes at distant locations. In the liver, the principal ECM components are collagen type I and IV as the structural skeleton and laminin as the glycoprotein attachment to the basement membrane. The basement membrane and ECM can be broken down by MMPs releasing tumour cells to distant locations. There are over 20 types of MMPs, which are found as secreted and membrane bound proteinases. Many of the MMPs which have been studied focus on the degradation of ECM and basement membranes, most commonly collagen IV and fibronectin (MMP 2, 9 and 11) [113-115]. In addition to degradation of ECM components, MMPs with plasminogen activators participate in the processing of angiogenesis and proliferation of endothelial cells. The breakdown of ECM components releases mitogens and growth factors such as vascular endothelial growth factor (VEGF) and platelet derived endothelial growth factor (PDGF) [116] which can further promote tumour growth.

Although there are many factors that influence the adhesion and metastasis of cancer cells and multitude of biological processes, it is both the proteins and glycans in concert that ultimately govern the interaction of the cancerous cells with the basement membranes and neighbouring cells [87, 99, 109]. In a study by Casey *et al.* [99] to determine the effect of glycosylation on the metastatic potential of tumour cells, ovarian carcinoma cells were treated with glycosidases (chondroitinase, hyaluronidase and neuraminidase) to remove chondroitin sulfate, hyaluronan and sialic acid respectively from the surface of cells. Carcinoma cells with removed glycans were subjected to cell adhesion assays and were demonstrated to have altered adhesion, migration and invasion towards ECM components. This treatment also reduced the adhesion of CD44 to hyaluronan influencing cell adhesion and migration via signal transduction through c-src kinase, Ras and Rac 1 [99]. This study demonstrated that a detailed understanding of cancer-associated glycoproteins and their attached glycans can provide further understanding of the roles of glycosylation mechanisms in cancer. An example of such an application is a recently approved diagnostic test for hepatocarcinoma, which measures the percentage of *N*-glycans that carry a fucose near the reducing end in a α(1,6) linkage attached to alpha-fetoprotein in the blood [117].

1.3.3. Glycosylated proteins in inflammation

The concentration of acute phase proteins and their glycosylation status have been reported to be altered in the presence of cancer and/or inflammation [118-120]. Inflammatory cytokines such as interleukin-6 (IL-6), IL-1b, tumour necrosis factor α (TNF-α), Interferon γ and transforming growth factor β (TGF-β) are produced by a variety of cell types including macrophages and monocytes during inflammatory processes [121]. These secreted cytokines circulate from the initial site of disturbances to distant organs such as the liver, resulting in the increased synthesis and modulation of acute phase proteins and inflammation. Some major acute phase glycoproteins include: C-reactive protein (CRP), serum amyloid A (SAA), α-1-

acid glycoprotein (AGP), haptoglobin (HPT), protease inhibitors such as α-1-antitrypsin and α-1-antichymotrypsin (ACT) and complement proteins. The release of acute phase proteins from the liver is part of the acute phase innate response that mediates non-specific phagocytosis by Kupffer cells, initiating non-specific cell killing by liver natural killer cells (pit cells) and assists in the endocytosis of circulating macromolecules by liver sinusoidal endothelial cells. The purpose of the acute phase response is to restore homeostasis by removing injury, infection or diseases (e.g. cancer) that can cause disturbances to systemic and metabolic functions. These perturbations to homeostasis which can result in chronic inflammation can induce persistent acute phase responses and contribute to the development of the disease and lead to other metabolic disturbances such as cachexia [122].

Tumours and their microenvironments are rich sources of cytokines, which are released into the plasma and can trigger chronic inflammation in the liver. These factors promote acute phase protein synthesis and enhance the expression of specific glycosyltransferases, such as sialyltransferases and fucosyltransferases [123], which result in specific *N*- and *O*-glycosylation modifications of some acute phase proteins in the plasma of cancer patients. Changes in the serum glycome of cancer patients have been well characterised with many *N*-glycosylation modifications including increased levels of tri- and tetra-antennary *N*-glycan structures, SLe^x epitopes and agalactosylated bi-antennary *N*-glycans [118]. These *N*- and *O*-glycosylation modifications are also found on the plasma membrane of tumour cells [119]. In addition, increased levels of acute phase glycoproteins containing SLe^x antigens have been also correlated with the increased concentration of C-reactive protein in the serum, and is considered a strong inflammatory protein marker [124].

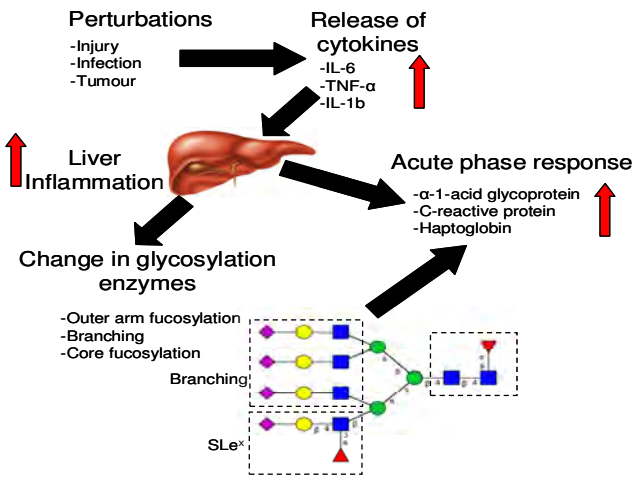

Figure 1-8. Perturbations to homeostasis can cause alterations to a multitude of different biological processes. For example, a tumour is able to release pro-inflammatory cytokines into the bloodstream and cause inflammation of the liver. This inflammation can result in the increase secretion of acute phase proteins and change the expression of glycosyltransferases resulting in aberrant glycosylation of these acute phase proteins.

Cancer is well known to cause inflammation to the liver due to the release of increased levels of pro-inflammatory cytokines by the tumour into the bloodstream, which can cause alterations to the glycosyltransferases in the liver and ultimately lead to aberrant glycosylation of acute phase glycoproteins [125]. Several glycosylation markers have been linked to both cancer and chronic inflammatory diseases which promote questions about their biological correlation. However, the effect of cancer and liver inflammation on the glycosylation of liver membrane proteins is not known.

1.4. Chacterisation of membrane glycoproteins

1.4.1. Proteomics

Proteomics is the large-scale study of proteins with particular relevance to their identification, quantitation, structure and function. The study of the proteome now attempts to address not only the identification of the representative proteins in any given cell, but the set of all isoforms and modifications, interactions between them, structural descriptions of the proteins and their higher order complexes and everything 'post genome' [126]. Most importantly, while the genome is a relatively constant entity, the proteome differs from cell to cell, cell

location, and differentiation status and is constantly changing due to environmental cues and through biochemical interactions. One organism, cell and/or tissue type may have different protein expression patterns in different parts of its body, in different stages of its life cycle and under different environmental conditions [127]. Proteomics promises to provide a better understanding of the structure and function(s) of expressed proteins and has the potential to identify diagnostic and prognostic markers of disease and disease states which may offer therapeutic value.

1.4.1.1. Characterising the membrane proteome

A major challenge with isolating and analyzing integral membrane proteins by traditional proteomic methods is that membrane proteins are often present in low abundance and are poorly soluble in many aqueous buffers. In addition, many integral membrane proteins tend to be very large. For example; human Ca^{2+} channel proteins (e.g. voltage-dependent anion channels) can have up to 24 transmembrane helices and are typically over 200 kDa in size. It is likely that a combination of hydrophobicity, low abundance and size of membrane proteins account for the problematic isolation of integral membrane proteins by gel-based approaches such as one-dimensional gel electrophoresis (1D SDS PAGE) and two-dimensional gel electrophoresis (2DGE).

One-dimensional gel electrophoresis (1D SDS PAGE)

The separation of proteins by 1D SDS PAGE involves the denaturation of proteins by sodium dodecyl-sulfate (SDS). SDS is an anionic detergent that coats proteins with a net negative charge by disrupting the intermolecular forces, such as hydrogen bonding and van der Waals forces that contribute to protein folding. 1D SDS PAGE is commonly used to separate complex mixtures of proteins, investigate subunit compositions and verify homogeneity of protein samples. However, 1D SDS PAGE often poorly separates complex mixtures of proteins and often gives inaccurate mass determinations of proteins that are globular in shape

and those that are posttranslationally modified [128]. The shape or 'linearity' of a protein can influence the level of migration in the gel as the separation of proteins is influenced by their Stokes' radius [129]. In addition, protein modifications such as glycosylation and phosphorylation can induce a net negative charge on a protein, restricting the binding of SDS to the protein backbone due to steric hindrance, and causing proteins to migrate slower through a gel and show a higher apparent molecular weight [130]. Nevertheless, 1D SDS PAGE is still commonly used for separating crude protein mixtures and membrane proteins for subsequent applications such as western blotting and shotgun proteomics.

Two-dimensional gel electrophoresis (2DGE)

Two-dimensional gel electrophoresis (2DGE) has been widely used for more comprehensive analysis of proteins by first separating proteins based on their isoelectric point using immobilized pH gradient (IPG) strips (first dimension) followed by separation according to their apparent molecular weight (second dimension) [131]. While IPG-IEF focusing has been a superior technique in separating soluble and mildly hydrophobic proteins in the first dimension; separation of membrane and other extremely hydrophobic proteins have often resulted in poor focusing [132]. This is due to the hydrophobic interactions within and/or between membrane proteins and also the interactions of these proteins with the basic acryl-amido derivatives of the IPG matrix, which can produce protein aggregates and impede IPG-IEF [133]. Although there are many considerations and alternative solubilisation strategies, such as the use of chaotropes, surfactants and reducing agents, it has been reported that separation of proteins with GRAVY (Grand Average Hydropathy) scores > 0.3 are poorly underrepresented by 2DGE [134]. The GRAVY score of a protein is the relative value for hydrophobic residues of a protein, where decreasing GRAVY values below 0 represent increasing protein hydrophilicity [135, 136].

2DGE utilising narrow pH ranges have been applied to increase the resolution of proteins from complex protein mixtures. Modified isoforms of proteins such as glycosylated proteins have different pIs and apparent molecular weight, which can be separated into individual protein spots on a 2D gel. Because 2DGE can isolate proteins into their different isoforms it is still considered the preferred method for separating protein isoforms. Additionally, the staining intensity of protein isoforms can reflect the relative amounts of protein present within a protein mixture, providing quantitative information of the different protein isoforms. The expression of these different protein isoforms may be useful for diagnostic purposes [137]. However, alternative approaches to study membrane proteins are now based on 'shotgun proteomics' methods using high resolution separation of proteolytic peptides to overcome the solubility issues associated with membrane proteins.

Shotgun proteomics for protein identification

The combination of 1D SDS PAGE or 2DGE with mass spectrometry (Matrix Assisted Laser Desorption Ionisation Mass Spectrometry (MALDI-MS) and/or Electrospray Ionisation Mass Spectrometry (ESI-MS)) and the sequencing of many genomes has allowed for accurate and efficient identification and characterisation of proteins [138]. This approach is termed as "top-down" proteomics since proteins are initially separated and subsequently digested with a protease to obtain proteolytic peptides. These peptides are then separated by an analytical technique (e.g. liquid chromatography) and separated peptides are identified by mass spectrometry. 2DGE separation in combination with mass spectrometry has been successfully used for separating and identifying soluble hydrophilic and mildly hydrophobic proteins in many systems.

With improvements in mass spectrometry and software now enabling the rapid and sensitive identification of thousands of proteins and peptides by mass, approaches to study membrane proteins are usually now based on 'shotgun proteomics' methods which uses

protease total digests of complex protein mixtures to overcome the solubility issues associated with membrane proteins. This approach is termed “bottom-up” proteomics. The digestion of proteins into peptides alleviates the solubility contraints associated with membrane proteins since peptides are generally more soluble in aqueous solutions [139]. The high resolution separation of proteolytic peptides is commonly achieved by 1) strong cation exchange and reverse phase chromatography (MudPit) and/or 2) peptide immobilized pH gradient isoelectric focusing (peptide IPG-IEF) in combination with tandem mass spectrometry [7, 8]. Other shotgun proteomics approaches such as capillary peptide electrophoresis [140] and ampholyte-free liquid-phase isoelectric peptide focusing [141] separation techniques are also commonly used to separate peptides for identifying membrane proteins.

Multi-dimensional protein identification technology (MudPit)

Multi Dimensional Protein Identification Technology (MudPit) is a shotgun proteomics technique that incorporates strong cation exchange (SCX) and reverse phase (RP) chromatography to separate proteolytic peptides followed by tandem mass spectrometry. MudPit can be performed either ‘offline’ or ‘online’ [142]. Offline systems fractionate proteins or peptides using SCX, which can be further desalted, concentrated and digested with a protease (commonly trypsin and/or proteinase K). Proteolytic peptides are then subjected to RP chromatographic separation and analysed by tandem mass spectrometry.

SCX fractions that are directly eluted onto an RP trap or coupled onto the RP portion of a biphasic microcapillary column are described as ‘online’ systems. The biphasic microcapillary column is first packed with RP phase media followed by SCX resin and is interfaced with a HPLC pump. The biphasic microcapillary column elutes ionized peptides and acts as the ion source for tandem mass spectrometry. The spectra obtained from MS/MS analysis of eluted peptides are searched using a database such as Sequest, Mascot or the Global Proteome Machine (GPM) for protein identification. [143].

MudPit has been demonstrated to identify largely different subsets of proteins compared to gel-based approaches but is considered to be a better technique for protein identification, by identifying greater numbers of peptides corresponding to more protein identifications [144, 145]. MudPit approaches have also been used to study differential expression of proteins in advanced prostate cancer patients using quantitative labeling methods such as Isotope Coded Affinity Tag (ICAT), Stable Istope Labelling of Amino acids in Cell Culture (SILAC) and Isotope Tags for Relative Abundance Quantitation (iTRAQ) [146], and found that the androgen receptor and its binding partners in prostate cancer were determined to be elevated using these quantitation methods. MudPit has also recently been used to detect some minor protein post-translational modifications [147]. The main advantage of using standard RP LC-MS/MS and MudPit shotgun approaches for protein identification is the ability to perform experiments on limited quantities of sample since the entire proteolytic digest can be directly subjected to LC separation and tandem MS. However, a major disadvantage of MudPIT is the inability to readily provide comprehensive information on protein isoforms and their post-translational modifications.

1D SDS PAGE and RPLC-MS/MS

An alternative two-dimensional fractionation approach for characterizing membrane proteins involves initially separating proteins by 1D SDS PAGE, and each gel lane is subsequently cut into smaller fractions and in-gel digested with trypsin. Tryptic peptides are extracted and analysed by RPLC-MS/MS [145]. This shotgun proteomics approach has been effectively used to characterize the yeast [145], HeLa cells [148, 149], human peripheral blood mononuclear cells [150] and rat liver [151] proteomes. 1D SDS PAGE separation and RPLC-MS/MS has many advantages in fractionating and analyzing membrane proteins most notably because of the ability of SDS to solubilise membrane proteins, whilst maintaining the solubility of membrane proteins during gel electrophoresis. In addition, the procedure is relatively quick and easy compared with other shotgun techniques. A limitation of this

approach for analyzing membrane proteins is the poor separation of higher molecular weight (>250 kDa) membrane proteins, which are not often resolved by 1D SDS PAGE, and therefore these proteins are not identified.

Peptide IPG-IEF

The use of IPG-IEF to separate proteins on the basis of their isoelectric point is widely used as a first dimension technique in 2DGE. One of the first studies using IEF for protein separation by O'Farrell demonstrated the separation of 1100 proteins from a protein mixture [152] and this technique has been widely used as a first dimension separation technique in many other 2DGE proteomic studies. Peptide IPG-IEF, however, is a recent development in which the peptides from digestion of complex mixtures of proteins, usually with trypsin, are rehydrated into an IPG strip and separated by IEF. Peptides are focused according to the p*I* of the individual peptides and the focused strip can be cut into equal fractions, and peptides extracted for RPLC-MS/MS analyses [153]. IPG-IEF has several advantages as a high resolution shotgun proteomics technique most notably because of its high sample loading capacity (up to 1 mg) [8, 139] and increased solubility of peptides from hydrophobic proteins. This method has previously been demonstrated to provide more confident and reproducible protein identifications compared to 1D SDS PAGE [154] and MudPit [155] by using the theoretical p*I* of peptides as an additional filtering criteria to reduce false discovery rates [8].

Peptide IPG-IEF, 1D SDS PAGE and MudPit analyses can be used for comparative label-free quantitative proteomics by using a protein's calculated normalised spectral abundance factor (NSAF) of a protein and it has recently been applied to study the yeast [156, 157], rat and mouse liver membrane proteome [8, 139] (See Chapter 4). Normalized spectral abundance factors (NSAF) for quantitation of proteins as described by Zybailov et al.,[156] is calculated by the total number of tandem mass spectra that match peptides to a particular protein, and normalized against the entire protein and spectra datasets to measure the relative

abundance of proteins in a complex mixture. This label-free method takes into account the sample-to-sample variation that is obtained when carrying out replicate analyses of a sample and also that longer proteins tend to have more peptide identifications than shorter proteins. NSAF for quantitative proteomic analysis has been applied to study expressional changes of membrane proteins in *S. cerevisiae* [156] and human transcriptional regulatory complexes [158]. This NSAF statistical approach for quantitating proteomic data has also been shown to have a high degree of statistical similarity to Affymetrix GeneChip™ analysis demonstrating its reproducibility and accuracy for quantitation [159].

While shotgun proteomics has demonstrated its utility in identifying membrane proteins, one of the disadvantages of shotgun proteomics is that specific information such as post-translational modifications (e.g. phosphorylation and glycosylation) of protein isoforms is not obtained [160]. In addition, the large data sets obtained from these experiments can be complex and difficult to interpret, therefore alternative pre-fractionation methods such as chromtography approaches (ion exchange, size-exclusion and/or lectin affinity) are needed to reduce sample complexity prior to chromatographic separation and MS analyses [150].

Protein identification and data analysis

The integration of the different algorithms such as Sequest, Mascot and X!Tandem to interpret tandem mass spectra for identifying proteins is now easily and routinely performed. The output from software platforms (e.g. Bioworks™ [Thermo], Mascot [Matrix science] and Global Proteome Machine (GPM) [Beavis Informatics]) that use these algorithms provide large collections of protein identifications; however they do not provide information of the biological significance of these proteins in relation to the entire subset of identified proteins.

Gene ontology (GO) analysis is commonly used to address the need for consistent descriptions of gene products and functions from different databases [161]. GO analysis has three categories that describe gene products in terms of their associated 1) biological

processes, 2) cellular components and 3) molecular functions in a species-independent manner. The analysis involves the development and maintenance of the ontologies themselves within a analysed sample set; the annotation of gene products and assembling of their associations between the ontologies and the genes and gene products in the collaborating databases (also termed GO mapping); and the use of ontologies to find all the gene products that are involved in specific functions (e.g. signal transduction) [161].

The cellular component GO category determines the subcellular location(s) of the gene products. The molecular function GO category describes activities (e.g. catalytic or binding activities) that occur at the molecular level of individual gene products which describe functional activities rather than their entities (molecules or complexes) that perform the specific function. The biological process GO component describes a series of events accomplished by one or more ordered assemblies of molecular functions.

Another tool that is also used to functionally categorise collections of proteins is Kyoto Encylopedia of Genes and Genomes (KEGG) Pathway Mapping [162-165]. KEGG pathway mapping is a collection of manually drawn pathway maps representing current knowledge and reported literature on the molecular interaction and reaction networks of proteins involved in various biological pathways such as 1) metabolism (e.g. glycolysis/gluconeogenesis, fatty acid oxidation and glycan biosynthesis) 2) genetic information processing (e.g. transcription, translation and protein folding) 3) environmental information processing (e.g. membrane transport, signal transduction and cell interactions) 4) cellular processes (e.g. cell transport, motility and communication) 5) organismal systems (e.g. immune, endocrine and circulatory systems) and, 6) human diseases (e.g. cancers, metabolic and infectious diseases). These maps can be used to match identified proteins against the biological pathways that have been previously reported.

Several software platforms such as Ingenuity™ [166, 167] and Blast2GO [168] have been recently developed to provide easier analysis and interpretation of protein compilations

by using GO analysis, KEGG pathway mapping, Interpro and Enzyme code mapping. These 'all-in-one' software platforms are now becoming increasingly used for interpretation of proteomics data to provide better insights into the biological significance of large datasets of identified proteins from shotgun proteomics experiments.

1.4.2. Glycomics

Analogous to genomics and proteomics, which is the study of a whole set of genes and proteins respectively, glycomics is the study of a whole set of glycans produced in a single cell, organism or tissue [169]. Glycomics is an emerging field in biology, which can provide complementary information to the genome and proteome. Many of the well-established techniques used in proteomics (such as 1D SDS PAGE, 2DGE and mass spectrometry) are applicable to studying the glycome. Glycomics can involve the fundamentals of the monosaccharide composition and how they diverge (structural), comparative observations of how glycans change through biochemistry and evolution (comparative), and how glycans and glycosylation can affect the function of biological processes (functional). It is important to study glycans and their associated proteins because not only are they markers to characterize cell types and states, but they are also involved in numerous biological phenomena. In addition, the hydrophilicity of glycans can affect the physicochemical properties of glycoproteins and analysis of the mature glycoprotein.

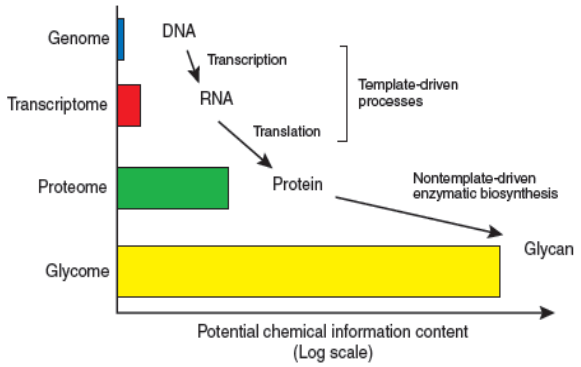

Figure 1-9. The genome and transcriptome of most organisms have been sequenced and protein information is mostly derived from these completed genomes. Unlike proteins which are linked in a linear amino acid structure, the difficulty with studying glycans is that the monosaccharide units can be linked in a number of combinatorial positions and there is no template from which produced glycans can be predicted [170].

Protein sequence information from most organisms is derived from completed genomes and transcriptomes, and is more easily determined because of the ordered linear structure and composition of amino acids that produce proteins. However, unlike proteins, the difficulty with studying glycans is that the monosaccharide units can be linked in a number of combinatorial positions producing a number of different isoforms of glycans (microheterogenity) (Figure 1-9) [170]. In addition, the heterogeneity of glycans and the lack of a template make it difficult to determine the micro- and macroheterogeneity of glycans that may be present on glycoproteins. Several approaches used for proteomics are currently modified for studying the glycome but strategies for studying glycomics are still in their infancy [169, 171]. The field of glycomics is expected to expand due to the complexity and importance of glycans and their roles in biology and disease.

1.4.2.1. Characterising the membrane protein glycome

Release of glycans from glycoproteins

N- and *O*-linked glycans can be globally released from complex mixtures of proteins or from individual glycoproteins for further analysis. Global *N*- and *O*-linked glycan profiling of membrane proteins enables the characterization of all possible glycans that are produced by a particular cell. This provides an overview of the entire subset of different types of glycans that are produced and attached to the cell membrane at a particular time and/or state. However, this global glycan analysis approach cannot provide detailed glycan information with regards to the specific glycans and their site(s) of attachment to individual glycoproteins. Glycomic analysis of individual *N*-linked glycoproteins is commonly carried out by separating complex mixtures of proteins by 1D SDS PAGE or 2DGE [128], excising the glycoprotein isoforms and treating with *N*-glycosidase F (PNGase F) to release *N*-linked oligosaccharides [172-178]. PNGase F hydrolyzes the amide bond between the *N*-glycan and the side chain of asparagine, which releases the glycan and converts the asparagine to aspartic acid. The glycosidase

releases nearly all bound *N*-linked glycans, except for glycans containing fucose attached in a α(1,3) linkage to the reducing GlcNAc residue [179]. These PNGase F-resistant glycans, which are commonly found in plants and nematodes, can be hydrolyzed by PNGase A [180]. The *N*-linked oligosaccharides released from these enzymatic methods can be reduced with sodium borohydride, derivatized via reductive amination with chromophores or fluorophores, or further analysed without derivatisation [179].

O-linked glycans are attached to the hydroxyl groups of serine and threonine residues of glycoproteins. There is no common enzyme available, such as the PNGase F used to release *N*-glycans that can be used to cleave this linkage. *O*-linked glycans are usually released by reductive alkaline β-elimination in the presence of high concentrations of sodium borohydride which reduces terminal reducing end residues and prevents the released glycan from undergoing subsequent peeling and destruction in the alkali. Both released *N*- and *O*-linked oligosaccharides can be analysed by MS to determine the composition and/or structures of these glycans.

Oligosaccharide analysis

The two most common ionization methods for MS characterization in glycomics are Matrix Assisted Laser Desorption Ionisation (MALDI) and Electrospray Ionisation (ESI). MALDI-MS and ESI-MS are commonly used to analyse complex mixtures of proteins and peptides, but they can also be applied to study *N*- and *O*-linked oligosaccharides. The characterization of glycans using MALDI involves the mixture of the sample with a matrix compound such as 3,5-dimethoxy-4-hydroxycinnamic acid (sinapinic acid), α-cyano-4-hydroxycinnamic acid or 2,5-dihydroxybenzoic acid (DHB), which protects the samples from being destroyed directly by the laser and allows crystallization of the sample: matrix mixture. The ionization of the mixture is triggered by a laser (normally a nitrogen laser), which vapourises the mixture into a gas-state and it is thought that the matrix provides charge to the analyte [181]. The mass of

the oligosaccharide is then examined using either time-of-flight (TOF), quadrupole TOF (Q-TOF), quadrupole ion-trap (Q-IT) or TOF-TOF mass spectrometers and ions are usually observed by MALDI as singly charged species (e.g. $[M+H]^+$ and/or $[M+Na]^+$) [182-184]. On the other hand, ESI involves the flow of analytes in organic solutions through a capillary that is under high voltage. This allows the oligosaccharides to be dispersed in a gas-state, and under high-vacuum they can be analysed by the same mass detectors as previously described. The oligosaccharide ions produced by ESI are often seen as multiply charged species.

Both MALDI-MS and ESI-MS have advantages and disadvantages for MS characterization of glycans. MALDI-MS is sometimes considered a more sensitive technique than ESI-MS since the multiple charged ions formed by ESI-MS can reduce the sensitivity of detection as a result of the resultant signal splitting [185]. In addition, detection of larger molecules by MALDI is relatively constant, in contrast to that observed for ESI, where the ionization efficiency decreases with increasing molecular weight [186]. For the analysis of oligosaccharides, MALDI is usually applied in positive ion mode where it is effective for characterizing neutral and mono- or de-sialylated oligosaccharides both for molecular mass determination and for fragmentation analysis [187]. Most neutral oligosaccharides present as intense signals corresponding to their $[M+Na]^+$ ions. However, complex glycans containing sialic acids are more difficult to analyse by MALDI-MS due to loss of sialic acid by the laser ionization and loss of sialic acids in the mass analyzer. It has been reported that detailed profiling of sialylated oligosaccharides by MALDI-MS can be achieved in linear ion mode in TOF analysis [184].

To prevent the loss of sialic acid during MALDI-MS and ESI-MS analysis, sialylated oligosaccharides are often permethylated to remove the negative charge on the carboxyl groups and thus increase the sensitivity of detecting ions in positive ion mode. Permethylation of oligosaccharides stabilizes the sialic acid residues in acidic oligosaccharides by converting the negatively charged sialic acids into methyl esters or lactones, yielding more predictable

ion products when subjected to MS/MS experiments. Permethylation also allows for oligosaccharides to be subsequently analysed by gas chromatography mass spectrometry (GC-MS) for quantitative monosaccharide analysis after hydrolysis [188].

ESI-MS has been widely used to analyse mixtures of *N*- and *O*-linked oligosaccharides in both positive and negative ion modes [187], and ESI-MS has been shown to provide good analysis of neutral and acidic oligosaccharides [189, 190]. The generation of multiply charged and stable parent ions in ESI can provide more informative fragmentation spectra compared with MALDI, which requires a constant accumulation of spectra from concentrated regions of analytes on the MALDI target to produce adequate parent ion intensities. Both positive and negative ionization methods for ESI-MS are commonly used for analyzing *N*- and *O*-linked oligosaccharides, and both have their advantages and disadvantages (Table 1-1). A recently study to compare ESI-MS ionization in both positive and negative ion modes demonstrated that positive ion mode was more effective in ionising oligomannosidic structures than negative ion mode [191]. Conversely, negative ion mode was shown to have better sensitivity and ionization efficiency of acidic glycans [191, 192].

Recent studies to compare MALDI-MS and ESI-MS for oligosaccharide analysis have demonstrated that both MS techniques can be effectively and reproducibly used for characterizing neutral and sialylated oligosaccharides by using either (i) MALDI mass fingerprinting complemented by sequencing of mixtures of permethylated glycans or (ii) on-line LC-ESI-MS in the negative ion mode of native glycans [193, 194]. Both approaches are routinely semi-quantitative making them applicable for comparative glycomics.

Table 1-1. Summary of different MS ion modes for MALDI and ESI-MS used for oligosaccharide analysis. *Refers to ESI-MS.

Mode	Glycan derivative	MS
Positive	Free or alditols	Metal adducts (e.g. Na). Difficult to detect acidic sialylated and sulfated oligosaccharides. Metastable ions detected in MALDI reflectron mode for sialylated oligosaccharides.
Positive	Permethylated	Metal adducts (e.g. Na). Permethylation of sulfated oligosaccharides are difficult. Sialic acids are converted into methyl esters. Mixtures of neutral and sialylated oligosaccharides can be analysed together. Excellent MSn
Positive	Reducing end derivatives	Derivatives of quaternary amines and amines with high pKa give H and metal adducts. Good MSn.
Negative*	Free or alditols	[M-xH] ions of neutral and acidic oligosaccharides. Both neutral and acidic oligosaccharides can be analysed together by ESI
Negative*	Permethylated	Not often reported

Chromatographic separation of glycans

HPLC systems can be coupled online with ESI-MS, which can separate oligosaccharides either by reverse-phase, anion-exchange or graphitized carbon chromatography prior to MS analyses. Of these three chromatographic methods, graphitized carbon chromatography is most widely used for separating native oligosaccharides. The glycan separation is based on polar interactions of the hydroxyl groups on oligosaccharides with the stationary phase, which separates these glycans depending on the increasing elongation of the glycan chains. The separation also allows for the analysis of both neutral and sialylated oligosaccharides in the one separation. The retention time of eluted glycans using graphitized carbon allows for the separation and identification of isobaric glycan isomers and MS fragmentation of the separated oligosaccharides from LC-ESI-MS experiments, together with their chromatographic retention time, can produce both composition and linkage information of analysed glycans [189].

Other means of chromatographic separation of glycans can be carried out by reducing end derivatization (reductive amination) which introduces functional groups such as 2-aminobenzamide (AB) (monoisotopic mass increment 138.08) and 2-aminopyridin (PA) (monoisotopic mass increment 96.07) into oligosaccharides. The most frequently used reducing end derivatives are low molecular weight amines that do not significantly change the mass range in which the oligosaccharides can be detected by mass spectrometry. The

functional group can include features such as a chromophore or fluorophore which can make the oligosaccharide detectable by UV or fluorescence [195]. Additionally, the attachment of a hydrophobic chromophore or fluorophore to the oligosaccharide allows for RP chromatographic separation prior to MS analysis.

Structural determination of glycans

A suite of glyco-informatic tools can used to interpret data obtained from MALDI-MS and ESI-MS experiments to interpret peak lists obtained from MS analyses and to compare observed fragmentation masses with the predicted masses and compositions in glycan databases such as GlycoMod [196] (http://www.expasy.org/tools/glycomod/), Cartoonist (MALDI only) [197], GlycoSidIQ [198], GlycoSearch (http://www.glycosciences.de) (MALDI only) [199] and OSCAR (http://glycome.unh.edu/tools/GlySpy/) [200]. Unlike the genome and proteome, the difficulty with studying the glycome is that there is no template for which glycans can be predicted and thus predictive databases cannot be created but rely on experimentally determined structural information (e.g. GlycoSuiteDB, GlycomeDB and Consortium of Functional Glycomics (CFG)). Glycomics currently lacks the informatics necessary for high-throughput and facile molecular sequencing of glycans and structural determination relies heavily on the manual interpretation of mass spectra. It is hoped that improvements and advances in glyco-informatics in the near future will help improve the analysis and interpretation of mass spectrometric data for analysing glycans.

1.4.3. Glycoproteomics

Glycoproteomics brings proteomics and glycomics together in order to 1) identify the glycoprotein or glycopeptides of interest, 2) locate potential glycosylation site(s) and, 3) structurally analyse the glycans that are attached to the protein or peptide. With the creation of many genome and proteome databases, identification of proteins is relatively easy, fast and

automated, and usually involves i) 1D or 2DGE for protein separation, followed by tryptic digestion and MALDI-MS or ii) LC separation of tryptic peptides, followed by ESI-MS [7, 201]. Identifying glycoproteins and glycopeptides by mass spectrometry can be challenging due to their low level of abundance in complex mixtures often caused by the attachment of structurally different glycans (microhetereogeneity) that can occupy (to varying degrees) different glycosylation sites (macroheterogeneity). The heterogeneity of glycans and their numerous sites of attachment can result in a number of glycoforms of the same glycoprotein. Therefore, full characterization of glycoproteins from biological systems is a challenge which can be facilitated by enriching the glycoproteins/glycopeptides from the complex mixtures. At present, the two most used methods for capturing glycoproteins and glycopeptides include hydrazine coupling of *N*-linked glycoproteins and glycopeptides to a solid support [202] and immobilized lectin chromatography that employs the affinity of these proteins for particular glycan sub-structures [203].

Enrichment by hydrazine coupling

The hydrazine chemistry method immobilizes the *N*-linked glycoprotein or glycopeptide onto a solid-phase support by first oxidizing with periodate those attached carbohydrates that contain vicinal hydroxyl groups into aldehydes [204]. The resulting aldehydes then react with hydrazide groups on an agarose media support to form stable hydrazone bonds. The immobilized glycoproteins can be subsequently treated with trypsin, releasing peptides for mass spectrometry analysis and identification of the bound proteins. The immobilized *N*-linked glycosylated peptides can also be treated with PNGase F to release and identify the attached peptide. This hydrazine chemistry approach has been used to identify glycosylated proteins in human cerebrospinal fluid (CSF) [205], saliva [206], plasma [207] human platelet proteins [208] and cell surface proteins from the LNCaP prostate cancer epithelial cell line [202]. The disadvantage of using the hydrazine chemistry approach is that the carbohydrates

are destroyed by the oxidative chemical coupling leaving the glycans no longer able to be identified and characterized.

Enrichment by lectin affinity

The use of lectins as a glycocapture method is considered to be a more favourable approach for glycosylation analysis since the integrity of the attached glycans or their sites of attachment is maintained during the fractionation. Lectins are carbohydrate binding proteins of non-immune origin that are capable of recognition and reversible binding to carbohydrates of glycoconjugates [209]. Different lectins have affinities for particular oligosaccharide epitopes (Table 1-2) and have been used in glycomics to examine the microheterogeneity of carbohydrates [69]. Lectins are frequently used in cytology and histology to stain glycoproteins [210] due to their ability to recognize specific carbohydrate sub-structures. In many clinical applications, detection of glyco biomarkers is based on lectin recognition which is a rapid and sensitive detection of differences in samples. Several lectins with different specificities have been used sequentially [211] and in parallel [203] on complex mixtures; to enrich glycoproteins for identification of low abundance plasma proteins [203], examine the microheterogeneity of carbohydrates associated with disease and disease progression [69, 70], targeting specific glycosylation sites on proteins [171] and for isolating glycopeptides [171, 212, 213].

Table 1-2. Specificity of some common plant lectins used for recognising glycoproteins. ConA: Concanavalin A, LCA: Lens culinaris agglutinin, PSA: Pisum Sativum agglutinin, GNL: Galanthus nivalis lectin, ECL: Erthrina cristagalli lectin, GSL: Griffonia simplicifolia lectin, PNA: Peanut agglutinin, RCA: Ricinus communis agglutin, AAL: Aleuria aurantia lectin, LTL: Lotus tetragonolobus lectin, VVL: Vicia Villosa lectin, WFA: Wisteria Floribunda agglutinin, WGA: Wheat germ agglutinin, SNA: Sambus Nigra agglutinin, MAL: Maackia amurensis lectin. Table reproduced from Vector Laboratories.

Specificity Guide for Lectins

Sugar	Lectin
Glucose	Con A, LCA, PSA
Mannose	Con A, GNL, HHL, LCA, NPL, PSA
Galactose	ACL, ECL, EEL, GSL I, GSL I-B_4, Jacalin, MAL I, PNA, RCA_{60}, RCA_{120}, SBA
Fucose	AAL, LTL, UEA I
N-Acetyl Galactosamine	BPL, DBA, GSL I, MPL, PTL, RCA_{60}, RCA_{120}, SJA, SBA, VVA, WFA
N-Acetyl Glucosamine	DSL, GSL II, LEL, STL, WGA
Sialic Acid	MAL II, SNA
Complex Structures	PHA-E, PHA-L

Enrichment by hydrophilic interaction (HILIC) and electrostatic repulsion (ERLIC) liquid chromatography

Hydrophilic interaction chromatography (HILIC) has been used for enrichment and targeted analysis of post-translational modifications (PTMs) such as N-acetylation [214], phosphorylation [215] and glycosylation [216] in many proteomics applications. HILIC is characterized by the use of a hydrophilic stationary phase and a hydrophobic organic mobile phase that separates polar compounds such as oligosaccharides [217]. The order of elution is based on the increasing hydrophilicity of compounds with those that are more hydrophilic being retained longer, which is reversed relative to reversed-phase chromatography (RP) [218]. Unlike lectin affinity, which targets particular glycan epitope sub-structures, the capture potential of the HILIC medium is dependent on the size of the glycans and not their specific sub-structures [219, 220]. Several HILIC applications have been used on complex mixtures; to enrich glycopeptides from human serum [221], platelets [222], and plasma and cellular fibronectins [223] for glycosylation site analysis.

A special type of HILIC called electrostatic repulsion–hydrophilic interaction chromatography (ERLIC) specifically utilizes the electrostatic interactions in HILIC by selecting a stationary phase that has a similar charge to the analytes to be separated [224]. These compounds are repelled by the stationary phase but are retained by the aqueous layer

surrounding the stationary phase. These opposing interactions allow for isocratic resolution of the analysed compounds [224].

Glycosylation site analysis

Glycopeptides are difficult to detect in MALDI-MS and ESI-MS analysis of tryptic mixtures due to the limited control of the size of glycopeptides as masses can be > 2000 Da, which includes the tryptic peptide and attached oligosaccharides. In addition, the separation and enrichment of tryptic glycopeptides by RP chromatography is also complicated by the physicochemical properties (e.g. size and charge) of the tryptic peptide and attached glycan. Finding glycopeptides in a complex mixture can be facilitated by software such as GlycoSpectrumScan [225] and GlycoMiner [226] which can locate m/z ions corresponding to potential glycopeptides in a MS spectrum. Alternatively, detection of intact tryptic glycopeptides in a MS spectrum can be facilitated by the loss of specific diagnostic ions from a series of peptide masses corresponding to saccharide unit mass differences (Hex: m/z 162, HexNAc: m/z 203 and NeuAc m/z 291), which give an indication of the ions that may correspond to a family of glycopeptides within the sample. These mass ions in MS2 fragmentation of the glycopeptides will also give identification of which parent peptide ions are glycosylated in a MS spectrum. The CID-MS/MS spectrum of a glycopeptide (Figure 1-10A) will give information on the overall composition and with the help of some specific diagnostic ions can give some structural linkage information (e.g. core fucose [Fucα(1-3)GlcNAc] m/z 350.1 and sialyl LacNAc [NeuAcα(2-3/6)Galβ(1-4)GlcNAc] m/z 655.2). Further fragmentation (MS3) can either give information on the underlying peptide sequence (Figure 1-10B) or provide further specific diagnostic structural ions. In addition, differential display of peptides before and after PNGase F digestion can provide information on the possible sites of *N*-glycosylation attachment. The site of attachment on the previously glycosylated peptide will be converted from asparagine to aspartic acid after PNGase F

digestion resulting in a peptide mass increase of +1 Da compared to the predicted peptide mass [178]. To effectively study glycoproteomics, two separate experiments need to be carried out in parallel to 1) identify the peptide and glycopeptides to determine the underlying glycoprotein and glycosylation site(s) (proteomics) and 2) structural characterization of released oligosaccharides (glycomics).

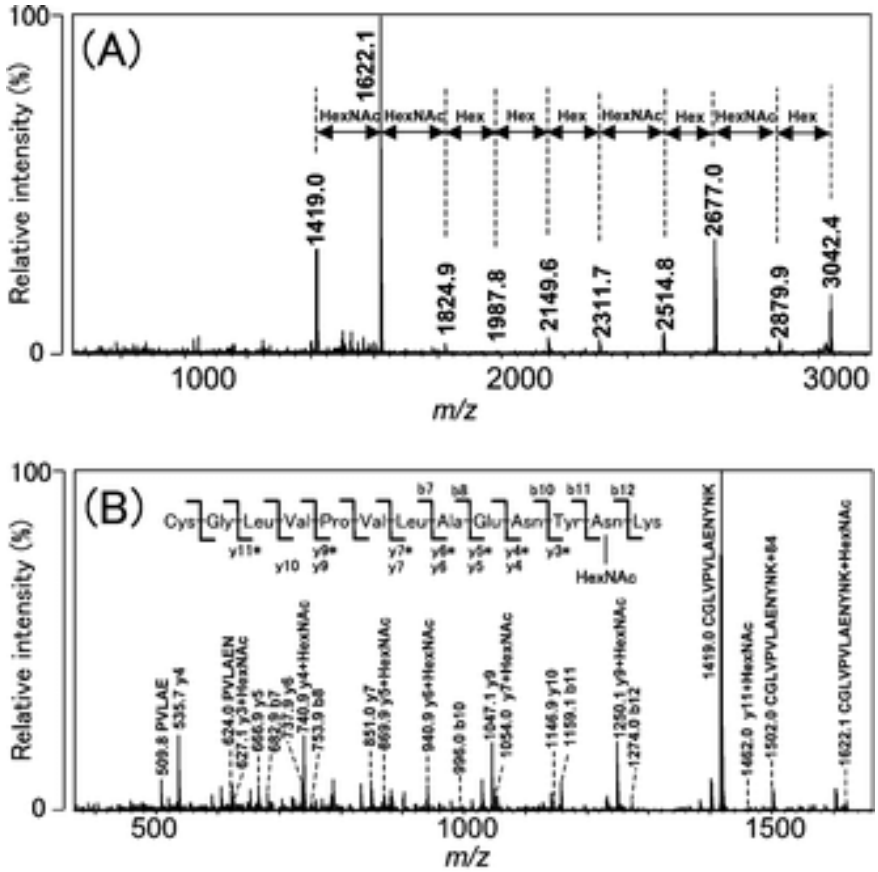

Figure 1-10. MALDI-QIT-TOF MS/MS of glycopeptides derived from ribonuclease B followed by SNA-lectin affinity chromatography. MS/MS spectrum indicates B ions corresponding to Hex (m/z 162) and HexNAc (m/z 203) (A) and MS/MS/MS fragmentation indicates amino acid sequence and Y ions with attached HexNAc to the Asn residue (B). Image adapted from Kubota *et al.*, [227].

1.5. Mouse liver membrane glycoproteomics

The liver has been well studied at both the genomic and proteomic levels with particular emphasis on diseases such as hepatitis [228, 229], hepatocellular carcinoma (HCC) [229], and alcoholism [230]. Infection of the liver by hepatitis B and C viruses are the major contributing factors in predisposition to HCC [231]. The main symptoms associated with most liver diseases involve inflammation of the liver due to extensive damage and apoptosis of hepatic cells. This is followed by the replacement of the destroyed liver cells with connective tissue (fibrosis), which can eventually result in the loss of normal liver function and interference with blood flow throughout the liver. Liver and liver-associated diseases are very often poorly diagnosed, with most diagnoses associated with low survival rates due to relatively poor detection at early stages of disease. Therefore, studying the liver proteome in health and disease is of great importance as it may provide further information which could assist in the early diagnosis and prognosis of diseases that affect the liver.

1.5.1. Liver structure and function

The liver is a crucial organ in the body which is responsible for a range of functions such as detoxification, protein synthesis, and xenobiotic metabolism [232]. Other functions also include glycogen storage, production of cholesterol, breakdown of red blood cells, plasma protein synthesis and the production of bile, which assists in the digestion of lipids. The bile that is produced by the liver is stored and released by the gall bladder for absorption of fatty acids from the intestines and metabolism of xenobiotics. The liver also maintains blood glucose levels by storing excess glucose as glycogen or breaking it down and secreting the resulting glucose into the blood stream; these factors are governed by external cues such as insulin and glucagon. Furthermore, the liver is also involved in the breakdown and storage of fatty acids in adipose tissue and catabolism processes which convert excess amino acids into ammonia through the urea cycle.

The liver is the only internal human organ capable of natural regeneration of lost tissue [232]; these are promoted by hepatocytes and a number of different growth and regulatory factors such as hepatocyte growth factor (HGF), epidermal growth factor (EGF) and interleukin-6 (IL-6). The liver acts as a detoxifier with numerous enzymes from different liver cells breaking down toxins and chemicals found in food and medicines. There are a number of different cells in the liver which are involved in these processes; some of these include hepatocytes, stellate cells, endothelial cells, kupffer cells and epithelial cells.

Hepatocytes make up 70-80% (w/w) of the cytoplasmic mass of the liver. Hepatocytes are organised into plates separated by vascular channels (sinusoids) [233]. These cells are involved in protein synthesis, protein storage, transformation of carbohydrates, detoxification, modification and excretion of exogenous and endogenous substances and, synthesis of cholesterol, bile salts and phospholipids [233, 234]. Hepatocytes also initiate the formation and secretion of bile into the bile canaliculi. Stellate cells are responsible for fat and vitamin A storage and the accumulation of ECM proteins [234]. Endothelial cells are a thin layer of cells that are found in the sinusoid and line the interior surface of blood vessels forming an interface between circulating blood in the lumen and the rest of the vessel wall. Endothelial cells are responsible for blood clotting, formation of new blood vessels, inflammation and also provide a barrier between blood vessels and the surrounding tissue controlling the transport of white blood cells. Kupffer cells are liver-specific macrophages located in the sinusoid of the liver and are responsible for phagocytosis of red blood cells [234]. Epithelial cells are usually tightly packed together in one or more layers and are specialized in covering and lining all internal and external body surfaces. Epithelial cells line the connective, muscle and nervous tissue of the liver.

1.5.2. Mouse liver proteomics

A comprehensive proteomics study of the mouse liver and corresponding plasma proteomes has provided a strong foundation for employing mouse models to better understand the effect of liver-associated diseases [235]. Large-scale proteomic studies using mouse models are relevant to further improve our understanding of hepatic processes that occur during progression of diseases such as cancer.

Previous proteomic approaches using sucrose density gradient centrifugation to enrich for mouse liver plasma membrane proteins followed by 2DGE separation identified 175 nonredundant proteins, of which 88 were determined to be integral membrane proteins with one to seven transmembrane domains [236]. Approximately 40% of the integral membrane proteins were annotated to contain some enzymatic function such as proteins belonging to the UDP-glucuronosyltransferase family [236]. A more recent study using a combination of 1D SDS PAGE and MudPit separation followed by Fourier Transform Ion Cyclotron Resonance (FT-ICR) mass spectrometry characterized the mouse liver and plasma proteomes. This study identified 7099 proteins in the liver and 4727 in the plasma respectively which had a dynamic concentration range of 4 orders of magnitude [235]. Comparison of the liver and plasma protein datasets demonstrated that a significant number of proteins identified in the liver were also detected in the plasma with most proteins identified to be involved in complement and coagulation, fatty acid metabolism, gluconeogenesis, glycolysis, protein ubiquitination and insulin, interleukin-4, epidermal growth factor, and platelet-derived growth factor signaling (Figure 1-11).

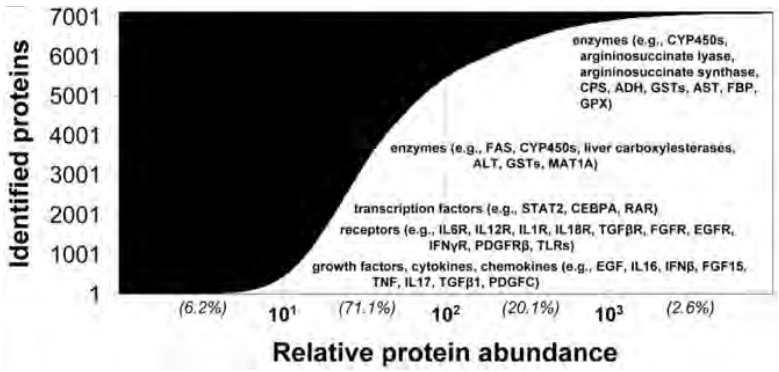

Figure 1-11. Dynamic range of the abundance of identified liver proteins [235]. Hepatic enzymes make up the majority of the liver proteome, most of which are membrane-associated proteins such as cytochrome p450s and fatty acid binding proteins.

The most abundant proteins that were identified included cytochrome p450s, glutathione S-transferases, phosphorylation enzymes, ribosomes and histones [235]. Cytochrome p450s and glutathione S-transferases are peripheral enzymatic membrane proteins that are involved in 70% of phase I and II xenobiotic metabolism and transport [237]. The identification of these peripheral enzymatic membrane proteins is important since it has been described that reduced levels of cytochrome p450s is correlated with inflammation of the liver [14, 238]. Not surprisingly, integral membrane proteins such as cell surface receptors were vastly underrepresented in this study which further substantiates the fact that membrane enrichment strategies are required to reduce the sample complexity and improve the identification of membrane proteins by mass spectrometry.

1.5.3. Engelbreth-Holm Swarm (EHS) sarcoma

Mouse models have been widely used as model systems to study parallel aspects of human disease (e.g. cancer) to further improve our understanding of the mechanisms involved with these diseases. Two different distal xenograft cancers have been used in this thesis to investigate the effects of tumour-induced liver inflammation on membrane protein glycosylation. The first distal xenograft cancer mouse model is an encapsulated non-metastatic EHS sarcoma and the second model is a metastatic colon 26 adenocarcinoma. Most membrane proteomic studies that investigate tumour-induced inflammatory effects on the

liver are predominately focused on enzymes involved in xenobiotic metabolism (e.g. cytochrome p450s, UDP-glucuronosyltransferases and glutathione-S-transferases), which are often found to be repressed in expression and enzymatic function [14-16, 18].

Liver inflammation and reduced expression of these enzymes have been linked to the lack of safety of many chemotherapeutic drugs, due to the inability of many advanced cancer patients to metabolize and clear these drugs [14-16]. Previous mRNA expression studies of mice bearing the Engelbreath-Holm Swarm (EHS) sarcoma have demonstrated that increased levels of pro-inflammatory cytokines can initiate an hepatic acute phase response and cause reduced hepatic gene expression of cytochrome p450 enzymes (Figure 1-12) [14-16]. Advanced cancer patients often have reduced levels of CYP3A4, usually mediated by pro-inflammatory cytokines such as tumour necrosis factor (TNF-α), IL-6, IL-8 and IL-17 [239, 240] and, it is now known that once a cancer is established these cytokines are continuously released into the tumour microenvironment which promote tumour cell proliferation, metastasis and liver inflammation (Figure 1-13).

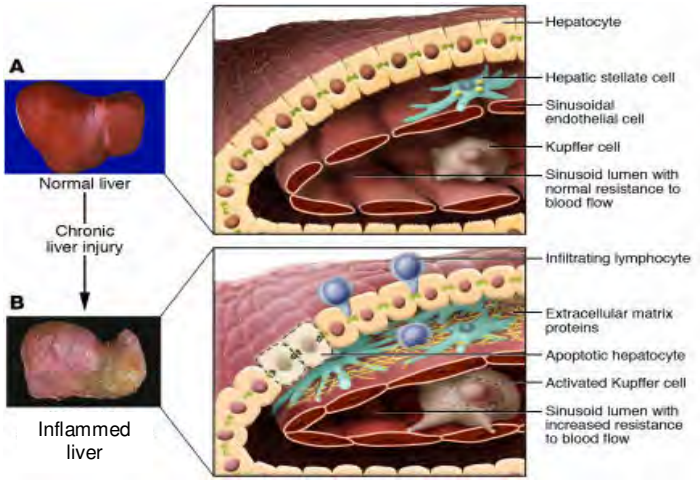

Figure 1-12. Comparison of normal liver and inflamed liver shows that the colouration of the surface of the liver has changed. This is partly due to the 'smoothing' of liver endothelial cells which line the cellular membrane of the liver. This can give rise to increased resistance to blood flow in and out of the liver and restricts infilterating lymphocytes from getting into the sinusoid and attending to activated Kupffer cells [234].

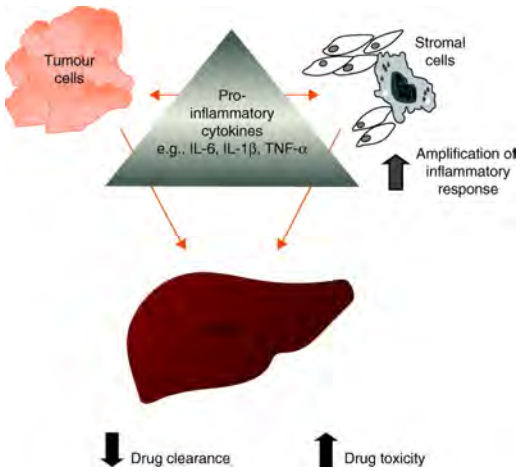

Figure 1-13. Tumour and stromal cells secrete pro-inflammatory cytokines into the blood stream which interact with the liver. This can result in cytokine signaling in the liver which can lead to reduced hepatic expression of cytochromes and ultimately to reduced drug clearance and increased chemotoxicity [241].

In a parallel, as yet unpublished study in our lab (Chick J.M., *Liver Membrane Proteome Dynamics in Cancer Bearing Mice.* In preparation) using peptide IPG-IEF separation and label-free quantitation employing NSAF to investigate the effect of a distal EHS sarcoma and its associated inflammation on the mouse liver membrane proteome, 1625 proteins were identified from sodium carbonate-treated membrane preparations. Of the total proteins, 813 were classified as integral membrane proteins. A large proportion of these integral membrane proteins (236) were determined to be differentially expressed and were mostly responsible for solute carrier transport, electron transport chain metabolism (TCA cycle) and fatty acid oxidation. Although many studies [14-16] have investigated the EHS sarcoma mouse model with strong emphasis on its inflammatory effects on the liver membrane proteome and liver metabolism, it is not known whether liver membrane glycosylation is also affected by the presence of this distal EHS sarcoma.

1.5.4. Colon 26 (C26) adenocarcinoma

The murine colon 26 xenograft adenocarcinoma is an undifferentiated colon carcinoma induced by the carcinogen *N*-nitro-*N*-methylurethane [242]. The C26 adenocarcinoma Balb/c mouse model is useful for studying liver inflammation and cancer cachexia as very few

animal transplantable tumours and tumour xenografts are able to induce inflammation, cachexia and disorders of homeostasis [18, 242]. The presence of a distal C26 adenocarcinoma has been shown to reduce the abundance and activity of cytochrome p450 drug metabolizing enzymes in the liver [18]. It is also capable of inducing inflammation and increasing levels of acute phase response proteins in the plasma such as fibrinogen, serum amyloid, α-1-antitrypsin and α-2-macroglobulin in response to tissue damage and inflammation [243, 244]. In addition to the inflammatory effects, the C26 adenocarcinoma has also been shown to induce cancer cachexia in some hosts [242].

Cachexia is the loss of lean body mass that cannot be controlled and/or reversed nutritionally. Cachexia is often seen in patients with advanced stages of diseases such as cancer, autoimmunity and pulmonary diseases [245, 246]. The risk of death is dramatically increased in cachectic patients as therapeutic intervention is further complicated by this condition. Cachectic cancer patients often exhibit increased energy expenditure, possibly due to increased thermogenesis and increased operation of the Cori cycle in the skeletal muscles [247]. The loss of skeletal muscle as a result of cachexia is mostly caused by the reduced protein synthesis and increased protein degradation by the ubiquitin-proteome and lysosomal pathways [248, 249]. Depending on the tumour type and stage, weight loss occurs in 30-80% of cancer patients with pancreatic and gastric cancers having the highest frequency of weight loss [250]. The exact mechanism in which these diseases cause cachexia is poorly understood, but it is thought that pro-inflammatory cytokines such as TNF-α, interferon gamma (IFNγ) and IL-6, as well as the tumor-secreted proteolysis inducing factor (PIF) are increased in the blood and transported across the blood-brain barrier where they interact with the luminal surface of brain endothelial cells and affect appetite [17].

Figure 1-14. Phenotypic difference between normal (control) and cachectic mice. Mice were considered cachectic if there was loss of least 25% of its original weight. The C26 cells are injected subcutaneously into the intracellular muscle and allowed to grow for 18-21 days.

A recent study combining proteomics and glycomics approaches to investigate the plasma glycoproteome of mice bearing a distal metastasizing C26 adenocarcinoma demonstrated that levels of leukocytes and acute phase proteins in the blood of tumour-bearing mice were significantly increased compared to controls [11]. In addition, overall increased sialylation of acute phase glycoproteins in tumour-bearing mice was observed with increased high mannose and complex bi- and tetra-antennary *N*-glycan structures with terminating NeuAcα(2-3/6)Galβ(1-4)GlcNAc (sialyl LacNAc) sequences. Complex *N*-glycans with *N*-glycolylneuraminic acid (NeuGc) attached to the termini were found to be downregulated in the plasma of tumour-bearing mice, which suggested either a downregulation or impaired function of the CMP-hydroxylase enzyme in tumour-bearing mice [11]. This enzyme is responsible for hydroxylating *N*-acetylneuraminic acid (NeuAc) to NeuGc [251]. The findings in this study suggested that glycosylation of liver-derived acute phase proteins found in the plasma were altered during cancer metastasis. However, it is not known whether similar glycosylation changes are also reflected on the liver cell membrane proteins of C26 cancer-bearing mice.

1.6. Thesis Aims and Scope

Most membrane proteins are glycosylated. Therefore, studying both proteins and glycans will improve the chracterisation of a membrane glycoproteome. The aim of this thesis was to use proteomics, glycomics and glycoproteomics approaches to gain insight into the changes that occur to liver membrane glycoprotein status in response to a host bearing distal extra-hepatic tumours. The specific aims were:

1. To develop enrichment strategies to better isolate and characterise the membrane glycoproteome using rat liver tissue as a model system. A range of detergents that are commonly used for solubilising membrane proteins was trialled to determine their applicability for studying membrane proteins by 1D SDS PAGE, lectin affinity chromatography and mass spectrometry. Two common glycoprotein capture methods (lectin affinity and hydrazine chemistry) were compared as alternative strategies for membrane glycoprotein enrichment and identification.

2. To apply the optimized membrane glycoprotein enrichment strategies to proteomic and glycomic analyses to investigate whether the presence of a distal non-metastasizing EHS tumour influences the liver membrane glycoproteome. Expression of the enzymes involved in the glycosylation machinery of the liver was correlated with the glycan products of the pathway.

3. To apply similar strategies to examine expressional changes of liver membrane proteins as well as their associated glycans, of mice bearing a distal metastasising C26 adenocarcinoma. Mice bearing early stages of the distal C26 adenocarcinoma, which did not phenotypically display cachexia (non-cachectic), were also compared.

Overall, the thesis studies the effects on the liver membrane glycoproteome of the presence of distal extra-hepatic non-metastatic and metastatic tumours.

Chapter 2: General Methods

2.1. Materials

Tris, sodium chloride, sodium hydroxide, sodium carbonate, EDTA, Bradford reagent, PBS tablets, ammonium bicarbonate (NH_4HCO_3), formic acid, 3-[(3-Cholamidopropyl)dimethylammonio]-1-propanesulfonate (CHAPS), 3-(Decyldimethylammonia) propanesulfonate inner salt (SB3-10), n-Octyl-β-D glucopyranoside (OG), n-dodecyl-β-D maltoside (DDM), Triton X-100, Triton X-114, dithiothreitol (DTT), iodoacetamide (IAA), methyl-α-glucopyranoside, galactose, sodium dihydrogen orthophosphate (NaH_2PO_4), α-1-antitrypsin from human serum, ovalbumin from *Gallus gallus,* sodium *meta*-periodate, *N*-acetyl-glucosamine (GlcNAc), WGA conjugated to Horse Radish Peroxidase (HRP), agarose bound Jacalin with protein concentration of 5 mg/mL and binding capacity of 1-2 mg human IgA/mL and, agarose bound WGA with protein concentration of 5 mg/mL and binding capacity 1-2 mg ovomucoid/mL were obtained from Sigma (St. Louis, MO, USA). NuPAGE 10% Bis-Tris pre-cast gradient gels, 3-(*N*-morpholino) propane sulfonic acid (MOPS) running buffer and phospholipase C from *Bacillus cereus* were obtained from Invitrogen (San Diego, CA, USA). Agarose bound Concanavalin A (ConA) with protein concentration of 10-16 mg/mL and binding capacity of 20-45 mg porcine thyroglobulin/mL was obtained from GE Healthcare (Uppsala, Sweden). Sequencing-grade trypsin was obtained from Promega (Madison, WI, USA). Immobolin-P Polyvinylidene Fluoride (PVDF) and Immobilon Western Chemiluminescence Substrate was obtained from Millipore (MA, USA). Hydrazide Gel was obtained from Pierce (Rockford, IL, USA). Recombinant N-Glycosidase F (PNGase F, cloned from *Flavobacterium meningosepticum* and expressed in *Escherichia. coli*) lyophilized in 10 mM sodium phosphate buffer, pH 7.2 was acquired from Roche Diagnostics (Basel, Switzerland). AG50W-X8 cation-exchange resin and Criterion pre-cast gels were obtained from Bio-Rad (Hercules CA, USA) and C_{18} tips were obtained from Eppendorf (Hamburg, Germany).

2.2. Liver membrane preparation

Rat livers obtained from 8 week old Dark Agouti rats (Save Sight Institute, Sydney Eye Hospital, Australia) and mouse livers from 8-10 week old Balb/c mice (Concord Repatriation Hospital, Australia) were perfused with 0.9% (w/v) phosphate buffered saline (PBS). Liver tissue (rat ~3 g and mice ~1.5 g) was homogenized in 5 mL of lysis buffer (pH 7.4) containing 50 mM Tris-HCl, 0.1 M NaCl, 1 mM EDTA & protease inhibitor cocktail (3 mg of antipain-dihydrochloride, 0.5 mg of aprotinin, 0.5 mg of bestatin, 1 mg of chymostatin, 3 mg of E-64, 10 mg of EDTA-Na2, 0.5 mg of leupeptide, 20 mg of Pefabloc SC, 0.5 mg of pepstatin, 3 mg of phosphoramidon) (Roche Diagnostics, Switzerland) using an Omni TH homogenizer (Omni International Inc., VA, USA).

The homogenized liver tissue was centrifuged at 2,000g for 20 min at room temperature. The supernatant containing cellular proteins was removed and diluted with binding buffer (20 mM Tris-HCl, 0.1 M NaCl, 1 mM $MnCl_2$, 1 mM $MgCl_2$ and 1 mM $CaCl_2$, pH 7.4) to a final volume of 40 mL and chilled on ice for 1 hr. This was to ensure that the sample was compatible for lectin affinity chromatography. The diluted proteins were sedimented by ultracentrifugation at 120 000 g_{avg} for 1 hr and 20 mins. The supernatant was removed, and the membrane pellet was washed twice with 0.1 M sodium carbonate (pH 11) and was stored at -80 °C if not used immediately. Membrane pellets were homogenised in binding buffer containing 1% (w/v) detergent and protein quantification was performed by Bradford Assay (Sigma-Aldrich, MO, USA).

2.3. Amino Acid Analysis (AAA) for protein quantitation

Membrane pellets were homogenized separately in 5 mL binding buffer containing 1% (w/v) detergent and incubated at 4°C for 1 hr with gentle rocking. Homogenised membrane proteins were subsequently centrifuged at 10,000 g for 20 mins to remove any remaining insoluble compounds and the supernatant was obtained for AAA. AAA was performed by Dr. Leon

McQuade from the Australian Proteome Analysis Facility (APAF). Detergent-solubilised membrane protein samples underwent 24 hr gas phase hydrolysis with 6 M HCl at 110ºC. Amino acids were analysed using the Waters AccQTag chemistry and cysteine and tryptophan were not analysed by this method as these amino acids are destroyed by acid hydrolysis. Samples were analysed in duplicate and results were expressed as an average. A constituent of both the undiluted and diluted buffers used in the preparation of the samples eluted from the UPLC column at the same position as serine and therefore serine could not be quantitated.

2.4. Gel electrophoresis and protein visualisation

2.4.1. SDS PAGE and protein visualization

Approximately 10 µg of protein was applied per lane onto NuPAGE 10% Bis-Tris pre-cast gradient gels with MOPS running buffer. Electrophoresis conditions were set to 200 V, 125 mA for 60 mins. The gels were fixed in 7% (v/v) acetic acid and 10% (v/v) methanol and stained overnight with Sypro Ruby (Invitrogen, San Diego, CA). Gel images were obtained using Typhoon Trio Variable Mode Imager (GE Healthcare, Uppsala, Sweden).

2.4.2. Pro-Q Emerald staining for glycoprotein confirmation

For glycoprotein confirmation, 1D SDS PAGE separated membrane proteins were stained with Pro-Q® Emerald 300 glycoprotein stain (Invitrogen, San Diego, CA) according to the manufacturer's instructions to determine if N-linked glycoproteins were present in lectin-fractionated samples. Briefly, gels were fixed in 5% (v/v) acetic acid/50% (v/v) methanol for 30 mins and subsequently washed with 3% (v/v) acetic acid to ensure SDS was completely washed out of the gel. Glycoproteins were oxidized with 10 mM periodic acid for 30 mins, and washed again with 3% (v/v) acetic acid. Gels were stained with Pro-Q® Emerald 300 stock solution in the dark for 90 mins and washed with 3% (v/v) acetic acid for 15 mins at

room temperature. Gel images were obtained using Fujifilm LAS-3000 CCD camera with the excitation filter set at 280 nm and the emission filter set at 530 nm.

2.4.3. Lectin blotting with WGA-HRP

Lectin fractionated rat liver membrane proteins were separated by 1D SDS PAGE and separated proteins were electroblotted onto PVDF according to manufacturer's instructions (Invitrogen, San Diego, CA). PVDF membranes were initially wet with 100% (v/v) methanol and subsequently buffered with NuPAGE Transfer Buffer containing 20% (v/v) methanol. Electroblotting of proteins onto PVDF membranes was carried out at 30 V for 2 hrs. PVDF membranes were washed three times in PBS containing 2% (v/v) Tween-20 for 15 mins each wash, and further rinsed in PBS. PVDF membranes were incubated with 1 µg/ml WGA-HRP in PBS containing 0.05% (v/v) Tween-20, 1 mM $CaCl_2$, 1 mM $MnCl_2$ and 1mM $MgCl_2$ overnight at room temperature. After incubation, blots were washed with PBS and incubated with Millipore Immobilon Western Chemiluminescence Substrate for 5 mins. Images were obtained from the Fujifilm LAS-3000 CCD camera with a 510 nm emission filter and an excitation at 460 nm.

2.4.4. Two-dimensional gel electrophoresis

Triton X-114 phase partitioned membrane proteins were precipitated in ice-cold acetone at -20ºC overnight. Precipitated aqueous and detergent phase containing proteins were resolubilised and buffer exchanged in 7 M urea, 2 M thiourea and 4% CHAPS until the conductivity < 300 $\mu S.cm^{-1}$. Samples were then diluted with 7 M urea, 2 M thiourea, 4 % CHAPS, 40 mM Tris, 5 mM TBP and 10 mM acrylamide to reduce and alkylate the proteins and subsequently incubated at room temperature for 90 mins. Approximately 250 µg of protein was passively rehydrated onto an 11 cm Immobilised pH gradient (IPG) 3-10, 3-6 and 4-7 strips overnight. Isoelectric focusing (IEF) was conducted on a Protean IEF Cell (Bio-

Rad, MA, USA) with a current limit of 50 μA per strip with the following focusing program: 300 V for 5 hrs, a linear gradient to 8000 V for 8 hrs and 8000 V until 100 kVh was reached.

Focused IPG-strips were equilibrated with 6 M urea, 2 % (w/v) SDS and 2 % (v/v) glycerol for 30 mins. The second dimension was run on 10-20% Criterion Tris-HCl Pre-cast gels (Bio-Rad, MA, USA) with the following running program: 10 mA for 30 mins, 35 mA for 2 hrs and 50 mA for 10 mins. Gels were fixed in 7 % (v/v) acetic acid/10% (v/v) methanol and stained with Sypro Ruby (Invitrogen, MO, USA). Gel images were obtained using Typhoon Trio Variable Mode Imager (GE Healthcare, Uppsala, Sweden).

2.5. Protein Identification by RP LC-MS/MS

2.5.1. In-solution digestion with trypsin

Phase partitioned proteins were buffer exchanged with 100mM NH_4HCO_3, pH 7.8 using a Microcon YM-10 Centrifugal Filter unit (Millipore, MA, USA). The samples were reduced with 25mM DTT for 30 mins and alkylated with 55mM IAA in the dark for 45 mins. The samples were buffer exchanged again with 100mM NH_4HCO_3, pH 7.8 and concentrated. After concentration the proteins were digested with trypsin (trypsin:protein 1:50 (w/w)) and prepared for lectin affinity chromatography for isolating glycopeptides and RPLC-MS/MS analysis as below.

2.5.2. In-gel digestion with trypsin

Following 1D SDS PAGE, gel lanes were cut into 12 equal fractions and equilibrated with 100 mM NH_4HCO_3 pH 7.8 for 10 mins. Gel pieces were dehydrated in 50 mM NH_4HCO_3/50% (v/v) ACN for 20 mins with intermittent vortexing followed by 100% (v/v) ACN for 20 mins. Dehydrated gel pieces were reduced with 25 mM DTT at 37ºC for 30 mins and alkylated with 55 mM IAA in the dark at room temperature for 45 mins. The samples were buffer exchanged again with 100 mM NH_4HCO_3, pH 7.8 for 20 min, followed by 50

mM NH_4HCO_3/50% (v/v) ACN pH 7.8 for 20 mins and dehydrated again with 100% (v/v) ACN. The gel pieces were digested with 1:50 trypsin:protein (w/w) with sequencing-grade trypsin (Promega, Madison, WI) for 18 hours at 37 °C. The tryptic peptides were extracted with twice with 50% (v/v) ACN/2% (v/v) formic acid and dried under vaccum centrifuge until all ACN was removed. Each fraction was desalted using C_{18} tips (PerfectPure C_{18} Tips) (Eppendorf®, Germany) and the eluate was dried using a vacuum centrifuge followed by resuspension in 0.1% (v/v) formic acid in preparation for RPLC-MS/MS [252].

2.5.3. RP LC-ESI-MS/MS

The extracted tryptic peptides were analyzed by nanoLC-MS/MS using a LTQ-XL ion-trap mass spectrometer (Thermo, CA). Reversed phase columns were packed in-house to approximately 7 cm (100 µm i.d.) using 100 Å, 5 mM Zorbax C_{18} resin (Agilent Technologies, CA) in a fused silica capillary with an integrated electrospray tip. A 1.8 kV electrospray voltage was applied via a liquid junction upstream of the C_{18} column. Samples were injected onto the C_{18} column using a Surveyor autosampler (Thermo, CA). Each sample was loaded onto the C_{18} column followed by initial wash step with Buffer A (5% (v/v) ACN, 0.1% (v/v) formic acid) for 10 mins at 1 µL/min. Peptides were subsequently eluted from the C_{18} column with 0–50% Buffer B (95% (v/v) ACN, 0.1% (v/v) formic acid) over 58 mins at 500 nL/min followed by 50–95% Buffer B over 5 min at 500 nL/min. The column eluate was directed into a nanospray ionization source of the mass spectrometer and spectra were scanned over the range 400–1500 amu. Automated peak recognition, dynamic exclusion, and tandem MS of the top 6 most intense precursor ions at 35% normalized collision energy were performed using the Xcalibur software (Thermo, CA).

2.5.4. Protein Identification and Data Analysis

Spectra files were converted to mzXML format and processed through the global proteome machine (GPM) software (version 2.2.1), an open source protein identification system that uses the X!Tandem algorithm [253]. The spectra obtained from each experiment were processed sequentially and a nonredundant output file generated for protein identifications with Log(e) values less than −1. Peptide identification was determined using a peptide ion tolerance of +3 Da and -0.5 Da a fragment ion tolerance of 0.4 Da. Carbamidomethyl was considered as a complete modification and partial modifications were also considered, including oxidation of methionine and threonine, and deamidation of asparagine and glutamine. MS/MS spectra were searched against the *Rattus norvegicus* and *Mus musculus* databases (Database derived from Swiss-prot, Ensembl and NCBI) and reverse database searching was used for estimating false discovery rates [254]. The assignment of an identified protein as being located in the membrane was made using a combination of predictions using Transmembrane Hidden Markov Model (TMHMM) (available at http://www.cbs.dtu.dk/services/TMHMM) [255] and information on membrane location derived from UniProt, GO annotation and the Swiss-Prot database. In this context, membrane proteins were considered to be both integral and peripheral to total cellular membranes. Protein identifications that have contributed to this thesis are attached as a CD.

2.5.5. Calculation of protein Normalized Spectral Abundance Factors (NSAF)

Normalized spectral abundance factors (NSAF) were calculated according to Zybailov et al., [156] using the following formula: NSAF = (Spc/L)/∑(Spc/L), where Spc refers to spectral count (number of nonredundant peptide identifications for a given protein), L is the length of the protein. Protein identifications were only included in NSAF data analysis if a given protein was identified in each of the triplicates. In addition, only identified proteins containing at least five nonredundant peptides were used for label-free quantitation analysis. The reduced

protein list was then adjusted with a fraction of a spectral count (in these datasets a factor of 0.25 was used) to allow the incorporation of proteins with zero spectral counts for statistical analysis [156]. The protein and peptide identifications used to generate this protein dataset are available on a CD and are attached with this thesis. An optimal adjustment factor was determined through fitting the natural log of the NSAF values to a Gaussian curve, assessed by computing both R^2 values and applying a Shapiro–Wilk test. To satisfy the Shapiro–Wilk test, a W value > 0.05 was required. Statistical analysis was conducted with Microsoft Excel using the Student t-test with equal sample sizes and $P \leq 0.05$ for assignment of statistical confidence. Origin8 software package was used for assessing Gaussian distribution of data for label-free quantitation by computing both R^2 values and a Shapiro–Wilk test. The rigorous statistical approach used in the experiments (through the use of a reduced protein list, Shapir*O*-Wilk analysis and Student t-test) was designed to address concerns of analytical reproducibility.

2.6. N- and O-glycan identification by carbon LC-MS/MS

2.6.1. Preparation of *N*- and *O*-linked oligosaccharides

N- and *O*-linked oligosaccharides were sequentially released according to Wilson *et al.*[178]. Immobilon-P PVDF membranes were pre-wet with 100% (v/v) ethanol. Triton X-114 phase partitioned membrane proteins and lectin eluates were dot-blotted (2 x 2.5 µL) and left to dry overnight. PVDF membranes were then washed with water followed by methanol to remove residual salts and detergents. The membrane was stained with Direct Blue 71 so that proteins could be visually recognized. Protein spots were cut from the PVDF membrane and placed in separate wells of a 96-well microtiter plate. The spots were blocked with 100 µL of 1% (w/v) polyvinylpyrrolidone (PVP) 40 000 in 50% (v/v) methanol, agitated for 20 mins, and washed thoroughly with water. *N*-linked oligosaccharides were released from the protein by incubation with 5 µL of PNGase F (0.5 units/µL) for 15 mins at 37°C, and subsequently

topped up with 10 µL water and incubated overnight at 37°C. The sample wells were surrounded by wells containing water to prevent evaporation, and the plate was sealed tightly with parafilm.

To recover *N*-linked oligosaccharides, the samples were sonicated in a water bath (in the 96-well plate) for 20 mins, and the supernatant containing released *N*-linked oligosaccharides was collected. Spots were washed two times with 50 µL water and combined with the supernatant and were reduced to alditols prior to LC separation. Before reduction the released *N*-linked oligosaccharides were incubated with 100 mM CH_3COONH_4 pH 5 (final concentration 15 mM) for 1 hr at room temperature to ensure complete regeneration of the reducing terminus and were reduced with 1 M $NaBH_4$/50 mM KOH (20 µL) at 50ºC for 2 hrs. The reduction was quenched with 5 µL glacial acetic acid.

β-elimination of *O*-linked oligosaccharides was carried out after the PNGase F release of the *N*-linked oligosaccharides by re-wetting the protein spots with 2 µL methanol and incubation overnight with 0.5 M $NaBH_4$/50 mM KOH (20 µL) at 50ºC. The reaction was quenched with 2 µL acetic acid and both reduced *N*- and *O*-linked oligosaccharides were purified as described below.

2.6.2. Purification of reduced *N*- and *O*-linked oligosaccharides.

Homemade cation exchange columns comprising 20 µL of AG50W-X8 cation-exchange resin (H^+–form) (BioRad, Hercules, CA) were packed on top of µC_{18} ZipTips[256]. Columns were prepared by washing 3 x 50 µL 1 M HCl, followed by 3 x 50 µL methanol and 3 x 50 µL water. *N*- and *O*-linked oligosaccharide alditols were eluted with 2 x 60 µL of water and dried. The borate was removed by the addition of 100 µL methanol and drying under vacuum five times. The oligosaccharides were re-suspended in 10 µL of water for Carbon LC–ESI–MS/MS analysis.

2.6.3. Carbon LC-ESI-MS/MS

N- and *O*-linked oligosaccharide alditols were analyzed by porous graphitized carbon LC-MS/MS using a HCT Ultra ETD II ion-trap mass spectrometer (Bruker BioSciences Corporation, MA USA). The samples were applied to a Hypercarb porous graphitized carbon column (5 µm Hypercarb, 0.32 × 100 mm, Thermo Hypersil, Runcorn UK). *N*-linked oligosaccharides were separated using a linear gradient with 0-45% (v/v) ACN/10 mM NH_4HCO_3 for 83 mins, followed by a 10 mins wash with 90% (v/v) ACN/10 mM NH_4HCO_3 at a flow rate of 5 µL/min. *O*-linked oligosaccharides were separated using a linear gradient with 0-90% (v/v) ACN/10 mM NH_4HCO_3 for 45 min, followed by a 10 min wash with 90% (v/v) ACN/10 mM NH_4HCO_3 at a flow rate of 5 µL/min. ESI–MS was performed in negative ion mode with three scan events: full scan with mass range *m*/*z* 100–2500 amu, dependent zoom scan, and dependent MS/MS scan after collision induced fragmentation. Automated peak recognition and tandem MS of the top three most intense precursor ions at 40% normalised collision energy was performed with an activation time of 30 ms. The composition of glycans was determined using the monoisotopic masses of detected ions and was verified by their associated MS/MS. Monoisotopic masses were searched using the GlycoMod software (available at http://www.expasy.ch/tools/glycomod) with parameters of ±0.7 Da to predict the possible glycan compositions corresponding to these masses.

The general workflow for studying the liver membrane proteome and glycome are outlined in Figure 2-1.

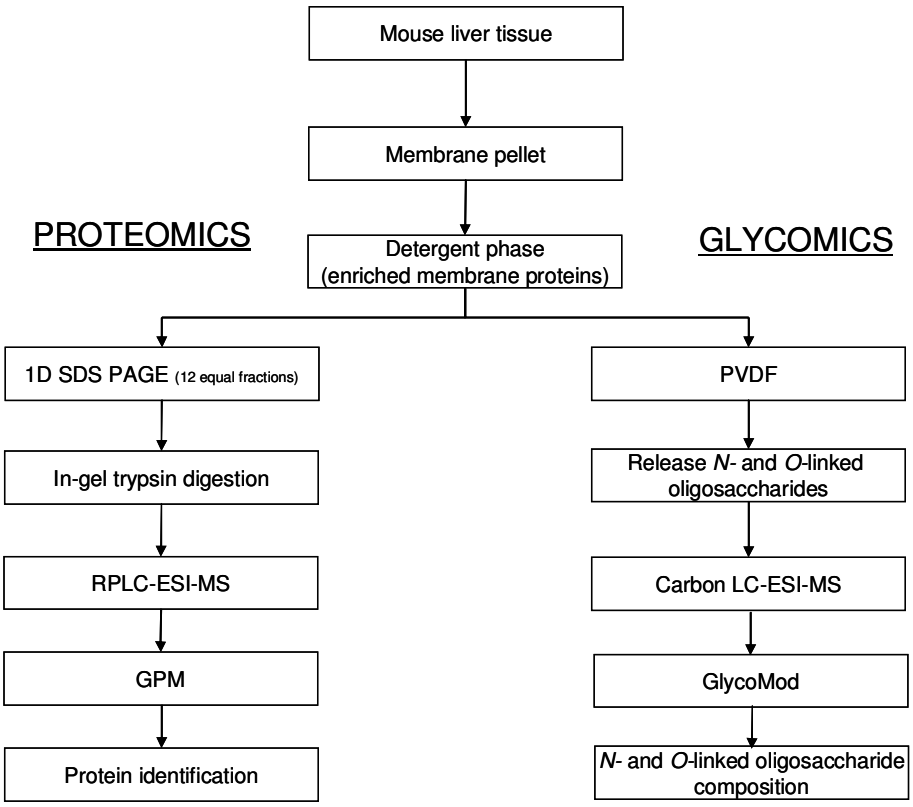

Figure 2-1. General workflow used to study the liver membrane proteome and glycome

Chapter 3: Approaches for membrane glycoprotein analysis

3.1. Sample preparation

It is currently not known how many membrane proteins are expressed in a cell at any given time. It has been speculated that human membrane proteins contribute 26% (5539) of all protein-encoded genes [257], and because of their diverse biological roles and functions in the cell membrane they are the most sought after proteins in drug discovery. Despite membrane proteins constituting approximately 70% of all human protein based drug targets, studying membrane proteins is often hindered by their low abundance, large size and relatively high hydrophobicity. Therefore, optimization and development of enrichment methods was carried out using rat liver as a model system to improve the isolation of membrane proteins.

Sodium carbonate stripping [258] has been used to isolate plasma and intracellular membranes from a range of cell types and tissues including prokaryotic cells [45], eukaryotic cells [259], archaebacteria [260] and rat liver microsomes [261]. The procedure consists of diluting prepared organelles in cold sodium carbonate followed by high-speed centrifugation to isolate total cell membranes. The treatment of these membranes with sodium carbonate converts closed vesicles into open membrane sheets releasing the cytoplasmic protein contents within organelle membranes and the high pH ionizes and releases many loosely bound proteins [258]. Therefore, sodium carbonate ultracentrifugation was used as the first step in all membrane preparation protocols.

3.1.1. Comparison of detergents for membrane protein solubilisation

Membrane proteins are often difficult to resolubilise in aqueous buffers and therefore it is necessary to solubilise these proteins in the presence of organic solvents or detergents. Solubilisation of membrane proteins is required for further functional and structural studies using techniques such as mass spectrometry, nuclear magnetic resonance spectroscopy (NMR) [262] and x-ray crystallography [263]. In this study, we investigated some

commercially available detergents for their ability to solubilise membrane proteins and their suitability for protein gel electrophoresis and lectin affinity chromatography.

We evaluated six different detergents for membrane protein solubilisation that suited our general criteria for further analytical studies such as protein gel electrophoresis, lectin affinity chromatography and mass spectrometry. Ideally membrane solubilisation can be achieved using SDS, which was shown to be solubilise more membrane proteins that the other non-ionic detergents as shown in Figure 3-1. However, SDS cannot be used for subsequent studies of membrane proteins as it causes denaturation of the proteins and is incompatible with lectin affinity and mass spectrometry. Although, non-ionic detergents did not solubilise the equivocal amounts of protein as compared to SDS, they were selected for membrane solubilisation as they do not cause protein denaturation and many non-ionic detergents are compatible for subsequent studies.

Membrane protein solubilisation with non-ionic detergents involves the penetration of the lipid bilayer with the hydrophobic tails of the detergent and interaction with the hydrophobic regions of lipids and proteins that are embedded within the lipid bilayer. The polar head groups of the detergent allow the detergent-protein complex to be soluble and exist in both hydrophobic and hydrophilic phases. A number of common and commercially available non-ionic detergents were compared for efficient membrane solubilisation, which included: 3-[(3-Cholamidopropyl)-dimethylammonia]-1-propane sulfate (CHAPS), 3-(Decyldimethylammonia) propanesulfonate inner salt (SB3-10), n-Octyl-β-D glucopyranoside (OG), n-dodecyl-β-D maltoside (DDM), Triton X-100 and Triton X-114. The rat liver membrane pellet was homogenised in binding buffer (Chapter 2.2) containing 1% (w/v) detergent and the protein extraction was monitored by 1D SDS PAGE (Figure 3-1).

Rat liver membrane proteins from a carbonate stripped total membrane preparation (Chapter 2.2) solubilised in Triton X-100, Triton X-114 or with no detergent showed very poor protein solubilisation and poor separation as judged by 1D SDS PAGE (Figure 3-1: lanes

5, 6 and 7). Prior to 1D SDS PAGE separation, Triton-X detergents were shown to effectively solubilise rat liver membrane proteins. However, the poor separation of Triton X-solubilised membrane proteins by 1D SDS PAGE could be due to the ability of Triton X detergents to inhibit SDS from binding to proteins thus providing lack of negative charge to proteins for 1D SDS PAGE separation which were subsequently not visualized on the gel [264]. On the other hand, membrane proteins solubilised with CHAPS, OG, DDM and SB3-10 showed a very similar distribution of proteins on the 1D gel (Figure 3-1). The same amount of solubilised protein was loaded in each lane as judged by the Bradford assay but OG and DDM appear to have much more intense protein bands compared to the other detergents. This could be due to the inaccuracies and interferences with the Bradford assay in determining protein concentrations in the presence of glycosidic detergents, which can often underestimate the amount of protein assayed (Product information from Sigma-Aldrich). An equivalent volume of proteins solubilised by Triton-X detergents were loaded in lanes 5 and 6.

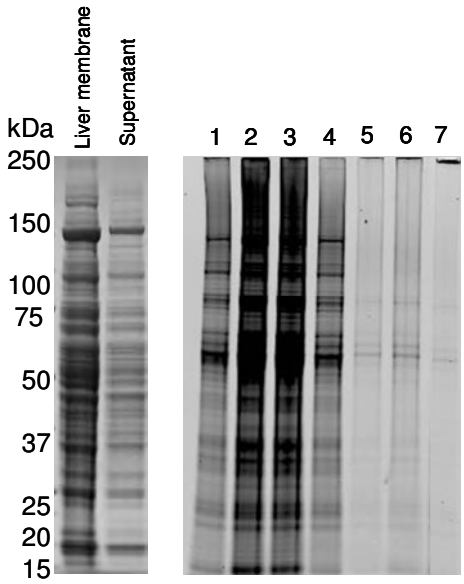

Figure 3-1. 1D SDS PAGE of rat liver membrane proteins prepared by ultracentrifugation and subsequently solubilised in 1% (w/v) CHAPS (lane 1), OG (lane 2), DDM (lane 3), SB3-10 (lane 4), Triton X-100 (lane 5), Triton X-114 (lane 6) and with no detergent (lane 7). Rat liver membrane proteins prepared by ultracentrifugation and solubilised in only SDS (liver membrane).

To determine the success of the detergents in enriching for membrane proteins from the crude membrane pellet, the enriched membrane pellets were homogenised in the presence

of CHAPS, digested in-solution with trypsin and analysed by RPLC-MS/MS. In total, 195 common proteins were identified, of which membrane proteins (transmembrane and membrane associated proteins) as determined by GO analysis, comprised 48% (95) of the total protein identifications (protein identifications have been included as supplementary information on a CD). Identified membrane proteins localized to the mitochondria and endoplasmic reticulum/Golgi apparatus represented 15% and 17% of the membrane protein identifications respectively. Membrane proteins localized to lysosomes/peroxisomes and plasma membrane proteins represented 10% and 6% of the data set respectively, but cytoplasmic proteins still comprised 48% of the total protein identifications in the membrane pellet. Two percent of the protein identifications were not able to be assigned (Figure 3-2). The percentage of identified membrane proteins in this study reflects similarly to most shotgun proteomic studies that employ ultracentrifugation as their primary membrane enrichment strategy [8, 139, 265]. For example, enrichment of membrane proteins from *D. radiodurans* strain R1 cells by sodium carbonate treatment identified 503 proteins in total, of which 268 (53%) were classified as membrane proteins [265].

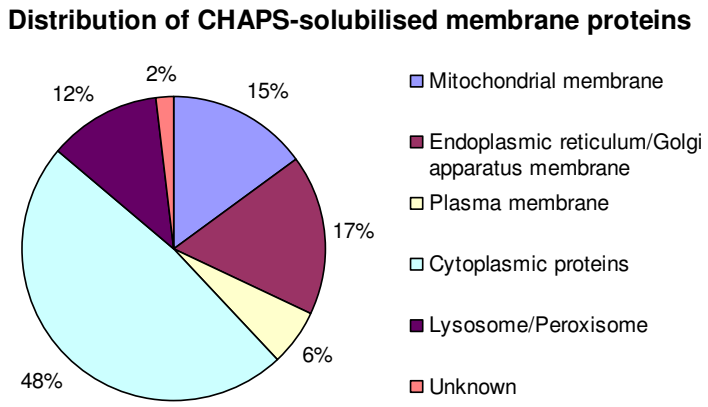

Figure 3-2. Distribution of cellular components of identified proteins from CHAPS-solubilised rat liver membrane proteins.

3.1.2. Detergent compatibility with ConA lectin affinity chromatography

With the aim of further enrichment of membrane proteins by targeting their glycosylation using lectins, the compatibility of these six non-ionic detergents with lectin affinity

chromatography was investigated. Agarose-bound ConA lectin (0.5 mL) were packed in disposable gravity-flow Poly-Prep chromatography columns (Bio-Rad, Hercules MA) and initially washed with 10 mL of elution buffer A (20 mM Tris-HCl, 0.1 M NaCl, 0.2 M methyl-α-D glucopyranoside) followed by equilibration with 20 mL binding buffer. The membrane pellet was homogenised in binding buffer containing either 1 % (w/v) CHAPS, OG, DDM, SB3-10, Triton X-100 or Triton X-114 and approximately 80 µg of each detergent-solubilised membranes were subjected to ConA affinity fractionation. The ConA column was washed with binding buffer (20 mM Tris-HCl, 0.1 M NaCl, 1 mM $MnCl_2$, 1 mM $MgCl_2$ and 1 mM $CaCl_2$, pH 7.4) to remove proteins that were not retained by the lectin and bound proteins were competitively eluted with 0.2 M methyl-α-glucopyranoside. ConA unbound and bound fractions were desalted and concentrated using an Amicon Ultra-10 centrifugal device with 10 kDa nominal molecular weight limit (NMWL) (Millipore, MA) and concentrated proteins were separated by 1D SDS PAGE (Figure 3-3).

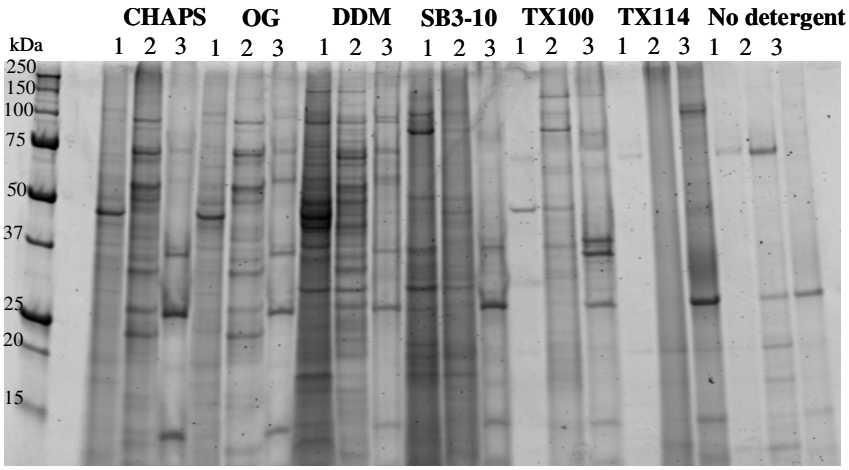

Figure 3-3. Solubilised rat liver membrane proteins in 1%(w/v) detergent (CHAPS, OG, DDM, SB3-10, Triton X-100, Triton X-114) or with no detergent followed by ConA affinity fractionation with different detergents. Homogenised rat liver membrane proteins in 1% (w/v) detergent (1), ConA flow through (2), and ConA bound fractions (3).

Membranes solubilised with Triton X-100 and Triton X-114 were again not visible by 1D SDS PAGE however, a few proteins were seen to be fractionated by ConA. This is possibly due to reduced concentration and dilution of Triton-X detergents during the elution process. This indicated that Triton X detergents were not suitable for enriching membrane

proteins for further analytical studies such as lectin affinity enrichment. Membrane proteins solubilised with SB3-10, particularly proteins with an apparent molecular weight > 75 kDa, were not observed on the 1D gel which suggested poor solubilisation and lectin fractionation of larger proteins. SB3-10 has been previously reported to only solubilise membrane proteins with an apparent molecular weight ranging between 10-80 kDa [266] and is known to cause precipitation of proteins with high concentrations of chaotropes (>5 M urea) [267, 268]. For these reasons, membrane proteins that are solubilised with SB3-10 were not suitable for anion-exchange and size exclusion chromatography [269] and as shown by this study, not suitable for lectin affinity. CHAPS, OG and DDM were visually assessed to be the best detergents for membrane protein solubilisation and lectin affinity.

Rat liver membrane proteins were then solubilised in different concentrations (0.01% (w/v), 0.1% (w/v), 1% (w/v) and 5% (w/v)) of CHAPS, OG and DDM to determine the most appropriate concentration of these detergents for solubilising membrane proteins. We observed that the detergent concentrations 0.1% (w/v), 1% (w/v) and 5% (w/v) solubilised similar protein amounts as determined by the Bradford assay and visual assessment of 1D SDS PAGE gel (Appendix C-1). Therefore, we standardized the detergent concentration for subsequent experiments to 1% (w/v) to ensure that the detergent:protein ratio of molecules was approximately 3:1, which would allow for efficient solubilisation of membrane proteins and easy removal of excess detergent monomers [270]. Other common non-ionic detergents such as Brij and Tween detergents were not compared in our study as they have been reported to offer poor solubilisation of membrane proteins and often cause precipitation of proteins in chaotrope mixtures during protein gel electrophoresis [271].

3.1.3.AAA to quantitate detergent-solubilised proteins

Monitoring the protein solubilisation by 1D SDS PAGE is seen to be difficult to interpret accurately and quantitately. Amino acid analysis (AAA) is one of the most robust methods for

protein quantitation. AAA was used to compare the amount of protein solubilised in 1% (w/v) CHAPS, OG and DDM and to quantitate the amount of solubilised protein bound to the ConA column.

Table 3-1. Amino Acid Analysis (AAA) of rat liver membrane proteins solubilised in CHAPS, OG and DDM. AAA was performed in duplicates and protein concentrations were expressed as an average.

Detergent	AAA of diluted rat liver membrane proteins (µg/ml)	Concentration of solubilised rat liver membrane proteins in original pellet (mg/ml)	Concentration of rat liver membrane proteins bound to ConA column (µg/ml)	% bound
CHAPS	668.60	6.43	196.10	12.2 %
OG	275.71	2.64	96.10	23.4%
DDM	694.80	6.67	226.90	13.5%

CHAPS (0.669 mg/ml) and DDM (0.695 mg/ml) solubilised similar concentrations of crude membrane proteins. This was approximately 2.5 times more protein, compared to that solubilised by OG (0.275 mg/ml), although solubilisation with OG resulted in a larger percentage of these proteins bound to the ConA column (by approximately 10%) when compared to CHAPS and DDM ([quantity of protein bound]/[quantity of protein loaded] x 100) % (Table 3-1). Previous studies using serial and array biosensor technologies for determining ligand-membrane protein interactions have shown that both CHAPS and DDM are the best detergents for solubilising membrane proteins for functional and interaction studies. This is mostly due to their ability to solubilise membrane proteins efficiently whilst also maintaining protein native structure and function in solution [272, 273]. From these results, OG, DDM and CHAPS appear to be equally able to solubilise proteins whilst being compatible with lectin affinity.

Glycosidic detergents such as OG and DDM have been reported to solubilise membrane glycoproteins for anion exchange and lectin affinity chromatography and are generally very efficient in solubilising membrane proteins for functional and protein interaction studies [274, 275]. These glycosidic detergents are acid labile and have high critical micelle concentrations making them easily removable by dialysis. Similarly, CHAPS also has a high critical micelle concentration and it is readily available in the laboratory and

cheaper than both glycosidic detergents. CHAPS has been used to solubilise MHC membrane glycoproteins from tumour cells prior to lectin affinity chromatography [276], and was shown to be more effective in disrupting protein-protein interactions compared to other non-ionic detergents such as Triton X-100 and NP-40. CHAPS was also shown to improve the binding of membrane glycoproteins to the lectin *Lens culinaris* [276]. In addition, the CMC of CHAPS allows the detergent to be easily removed by dialysis and it is also compatible with trypsin digestion [277] and mass spectrometric analysis [278]. Overall, all three detergents (CHAPS, OG and DDM) were evaluated as suitable detergent(s) for membrane protein solubilisation with applicability to further analytical studies such as lectin affinity chromatography, protein gel electrophoresis and mass spectrometry, but CHAPS was chosen as the best overall for further experimentation.

3.1.4. Enrichment of rat liver membrane glycoproteins by lectin affinity chromatography

Membrane proteins are often glycosylated on the extracellular surface of the plasma membrane and this characteristic was targeted as an enrichment strategy for isolating membrane glycoproteins. Agarose-bound lectins (ConA, Jacalin and WGA) (0.5 mL of each lectin) were packed in separate disposable gravity-flow columns and initially washed with 10 ml of their corresponding elution buffer (20 mM Tris-HCl, 0.1 M NaCl with 0.2 M methyl-α-D glucopyranoside [ConA] or 0.5 M α-D galactose [Jacalin] or 0.5 M *N*-acetyl glucosamine [WGA], pH 7.4) and then equilibrated with 20 ml binding buffer. The membrane pellet was homogenised in binding buffer containing 1% (w/v) CHAPS and loaded on each lectin column. The lectin columns were washed with 20 ml binding buffer to remove proteins that were not retained by the lectins. Competing monosaccharides were used to elute bound proteins from ConA (0.2 M methyl-α-glucopyranoside), Jacalin (0.5 M α-D galactose) and WGA (0.5 M GlcNAc) columns. Each fraction was desalted and concentrated using an Amicon Ultra-10 centrifugal device with 10 kDa nominal molecular weight limit (NMWL)

(Millipore, MA). Concentrated proteins were digested in-solution with trypsin and prepared for RPLC-MS/MS analysis for protein identification.

The three lectins used in parallel isolated 383 proteins in total, which included 148 (39%) membrane proteins as defined by GO analysis (protein identifications are included attached on CD). A common subset of only 20 membrane proteins was isolated by the three lectins used in parallel. ConA, which recognizes α-mannose (and α-glucose), isolated 33 unique membrane proteins. Jacalin isolated 16 unique membrane proteins and WGA, which recognizes GlcNAc and sialic acid, isolated 38 unique membrane proteins (Figure 3-4). ConA and WGA are two of the most common lectins used for isolating *N*-linked glycoproteins and glycopeptides. Both lectins captured 132 (89%) of the total 148 membrane proteins isolated with a 36% overlap of common proteins isolated by both ConA and WGA.

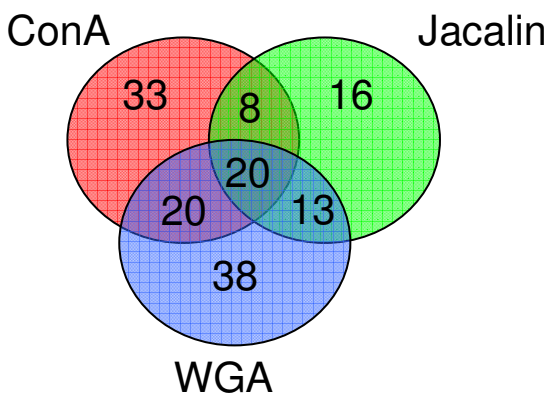

Figure 3-4. Number of proteins identified from rat liver membranes solubilised with 1% CHAPS using immobilized lectins: ConA, Jacalin and WGA, in parallel.

The proteins that bound to the individual lectins were separated by 1D SDS PAGE and stained with Pro-Q Emerald 300 glycoprotein stain (Invitrogen, MO, USA) to determine if the lectin-bound proteins were glycosylated. This stain is commonly used to detect carbohydrates that consist of vicinal hydroxyl groups for example, mannose and galactose, which are found in *N*- and *O*-glycans. Many proteins in the CHAPS-solubilised membrane pellet and those that bound to the ConA and WGA column were seen to be glycoproteins (Figure 3-5). Jacalin is a

general lectin commonly used to isolate *O*-linked glycoproteins due to its specificity for Galβ(1,3)GalNAc and less glycoproteins were seen in this separation.

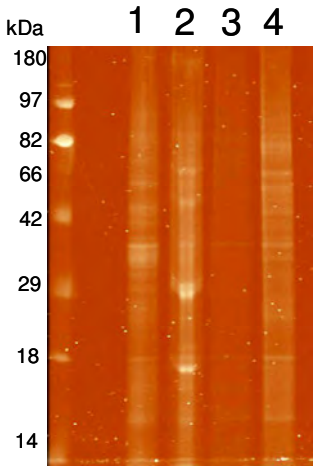

Figure 3-5. ProQ-Emerald 300 glycoprotein staining to confirm glycosylated proteins in lectin eluates. Membrane pellet solubilised in 1% (w/v) CHAPS (lane 1), bound glycoproteins eluted from ConA (lane 2), Jacalin (lane 3) and WGA (lane 4).

To further examine the cross-reactivities of the three lectins for the different subsets of glycoproteins, lectin eluates were separated by 1D SDS PAGE, followed by electroblotting of separated proteins onto PVDF which was probed for *N*-linked glycoproteins containing GlcNAc and sialic acid with WGA-HRP. Surprisingly, WGA-HRP was shown to recognize glycoproteins in both lectin unbound and bound fractions from all three lectins. Moreover, WGA-HRP reacted with proteins in the unbound fraction of the WGA lectin column which may suggest that the WGA column may be overloaded and become saturated with glycoproteins (Figure 3-6). However, in these experiments only ~80 µg of solubilised membrane proteins (as determined by Bradford assay) were applied to 0.5 mL of each lectin column to ensure that the amount of protein loaded was well below the maximum binding capacity (binding capacity specified by manufacturer as 20-45 mg/ml thyroglobulin [ConA], 1-2 mg human IgA/ml [Jacalin] and 1-2 mg/ml ovomucoid [WGA]) of the columns.

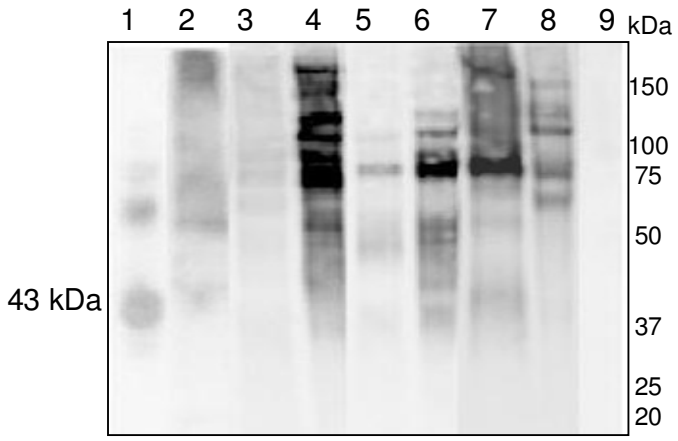

Figure 3-6. WGA-HRP blot to determine whether there was cross reactivity between the other WGA and lectin eluates. Ovalbumin was used as a positive control (lane 1), membrane pellet (lane 2), ConA flow through (lane 3), ConA bound (lane 4), Jacalin flow through (lane 5), Jacalin bound (lane 6), WGA flow through (lane 7), WGA bound (lane 8) and, BSA was used as a negative control (lane 9).

The results presented here illustrate that lectin affinity chromatography has potential for fractionating membrane glycoproteins although there is no absolute correlation between the presence of specific glycoprotein epitopes and their retention by the lectin. The low percentage of membrane proteins, relative to the number of cytoplasmic proteins, that were identified using lectin affinity and annotated by GO to be membrane-associated could be due to the high percentage of contaminating cytoplasmic proteins in the initial membrane preparation, which may reduce the spatial environment and propensity for the lectins to specifically target glycoproteins. It is also possible that these cytoplasmic proteins may be bound non-specifically to the support media and/or to other bound glycoproteins.

To improve the fractionation of membrane glycoproteins using lectin affinity, additional methods are required to increase the enrichment of membrane proteins prior to fractionation. As seen from the decreased solubilisation of membrane proteins by non-ionic detergents compared with SDS (Figure 3-1 [lane: liver membrane] and Figure 3-3), initial membrane protein solubilisation is being compromised by the need to make the solution compatible with lectin affinity chromatography and mass spectrometry. Another approach which has been shown to solubilise membrane proteins well, whilst also separating soluble cytoplasmic proteins from enriched hydrophobic proteins is solubilisation with the detergent Triton X-114 followed by aqueous phase partitioning [279].

3.1.5. Triton X-114 phase partitioning for improved membrane protein enrichment

Triton X-114 was previously shown to be incompatible with protein gel electrophoresis (Chapter 3.1.1) and lectin affinity (Chapter 3.1.2). However, Triton X-114 has been used effectively to solubilise hydrophobic proteins to improve the enrichment of membrane proteins from complex mixtures [148, 149, 279].

Crude membrane preparations obtained from differential centrifugation of carbonate-stripped liver homogenate were subjected to Triton X-114 phase partitioning [279] to further enrich membrane proteins. Triton X-114 effectively solubilises membrane proteins by forming mixed micelles with proteins at 4ºC and when heated to its cloud point temperature (20°C) exhibits phase partitioning with water [279, 280], which permits the isolation of integral membrane proteins and membrane-associated proteins from soluble proteins [148, 279].

Approximately 100 µl (equivalent to approximately 0.5-1 mg) of the rat liver membrane pellet was homogenised with 4 volumes of binding buffer (20 mM Tris-HCl, 0.1 M NaCl, 1 mM $MnCl_2$, 1 mM $MgCl_2$ and 1 mM $CaCl_2$, pH 7.4) containing 1% (v/v) Triton X-114 and chilled on ice with intermittent vortexing for 20 mins. The samples were heated at 37°C for 20 mins and phase partitioned by centrifugation at 300 g for 5 mins. The upper aqueous phase was removed and stored. The detergent phase was further diluted with 4 volumes of binding buffer containing 1% (v/v) Triton X-114 and phase partitioning was repeated. Because of the temperature-sensitive and detergent properties of Triton X-114 which can influence chromatographic separation and mass spectrometric analyses, the proteins in the combined aqueous, and Triton X-114 phases were precipitated with 9 volumes of ice-cold acetone and centrifuged at 300 g for 5 mins. Precipitated membrane proteins were resolubilised in binding buffer containing 1% (w/v) CHAPS. Proteins partitioned between the aqueous and detergent phases were digested in-solution with trypsin and analysed by RPLC-MS/MS.

Enrichment of proteins in the detergent phase of Triton X-114 phase partitioning identified 245 proteins in total, of which 188 (76.7%) were classified as membrane proteins by GO analysis (protein identifications are provided on CD). Of these membrane proteins, 46% and 29% were localized to the mitochondria and endoplasmic reticulum/Golgi apparatus respectively with 12% of the proteins (Appendix A-1), many of which contained predicted *N*-linked glycosylation sites, classified as plasma membrane proteins (**Publication I**). Some of these plasma membrane proteins included cell adhesion proteins (e.g. cadherins), cell surface receptors (e.g. basigin) and many solute carrier transporters (e.g. solute carrier family 25). Based on the number of membrane protein identifications, Triton X-114 phase partitioning improved the initial enrichment of membrane proteins by 29% relative to stand-alone differential centrifugation.

Interestingly, 13 membrane proteins identified in the detergent phase were also found to be present in the aqueous phase (Table 3-2). Based on the information obtained from the Swiss Prot database, 11 of these membrane proteins also found in the aqueous phase contained multiple glycosylation sites (*N*- and/or *O*-linked). PNGase F treatment of the crude membrane proteins to remove *N*-linked glycans prior to Triton X-114 phase partitioning resulted in seven of these proteins no longer partitioning to the aqueous phase suggesting that *N*-glycosylation was responsible for their apparent partitioning into the hydrophilic fraction. The four membrane-associated proteins (Kupffer cell receptor, cadherin-2, cadherin-17 and E-cadherin) which remained soluble in the aqueous phase after PNGase F treatment were classified as proteins involved in cell adhesion and had relatively low GRAVY (Grand Average Hydropathy) scores. A GRAVY score is the relative value for the hydrophobic residues of a protein, where decreasing GRAVY values represent increasing protein hydrophilicity [135, 136]. These membrane proteins that remained in the aqueous phase thus had a large distribution of hydrophilic amino acids, which could contribute to their solubility and partitioning behaviour. In addition to glycosylation, protein isoforms such as those

modified by phosphorylation [281] and acetylation [282] may also influence the solubility of these membrane proteins.

Table 3-2. Triton X-114 phase partitioning of membrane proteins showed that 13 of the 188 membrane proteins partitioned to the detergent phase were also present in the aqueous phase. Of these, 11 were either *N*- and/or *O*- glycosylated.*Membrane-associated proteins remaining in aqueous phase after treatment with PNGase F followed by Triton X-114 phase partitioning.

Identifier	Protein description	Location	Glycosylation (N-X-S/T)	GRAVY score
ENSRNOP00000017101	Membrane-associated progesterone receptor component 1	Membrane	0	-0.598
ENSRNOP00000010579	Microsomal glutathione S-transferase 1	Membrane	0	0.193
ENSRNOP00000025254	Asialoglycoprotein receptor 1 (ASGPR 1)	Membrane	3 N	-0.625
ENSRNOP00000017472	Prohibitin-2	Membrane	2 N	-0.266
ENSRNOP00000005853	Polymeric-immunoglobulin receptor precursor	Membrane	4 N	-0.501
ENSRNOP00000000177	Lysosome-associated membrane glycoprotein 2	Membrane	16 N	0.048
ENSRNOP00000050252	Basigin precursor (OX-47 antigen)	Membrane	3 N	-0.305
ENSRNOP00000014235	Long-chain-fatty-acid--CoA ligase 1	Membrane	3 N	-0.08
ENSRNOP00000056976	Translocon-associated protein subunit	Membrane	2 N	-0.176
ENSRNOP00000017643*	C-type lectin domain family 4 (Kupffer cell receptor)	Membrane associated	6 N	-0.576
ENSRNOP00000021170*	Cadherin-2 precursor (Neural-cadherin)	Membrane associated	8 N	-0.347
ENSRNOP00000021612*	Cadherin-17 precursor	Membrane associated	7 N	-0.256
ENSRNOP00000027346*	Epithelial-cadherin precursor (E-cadherin)	Membrane associated	2 N	-0.431

The anomalous phase partitioning of some of these membrane proteins strongly suggests that posttranslational modifications such as glycosylation influences their solubility. This phenomenon has also been observed with Triton X-114 phase partitioning of acetylcholinesterase from *Torpedo californica* (4 *N*-linked glycosylation sites), Na',K^+-ATPase from kidney microsomes (3 *N*-linked glycosylation sites) and Ca^{2+} ATPase from sarcoplasmic reticulum membranes (3 *N*-linked glycosylation sites) [283]. The anomalous partitioning of these membrane glycoproteins is also contributed to the presence of high numbers of hydrophilic amino acids, which may explain the reason that 4 of the membrane glycoproteins remained in the aqueous phase after deglycosylation [283].

3.1.6. 2DGE of Triton X-114 phase partitioned rat liver membrane proteins

To determine whether 2DGE could be used for further characterizing membrane proteins Triton X-114 phase partitioned rat liver membrane proteins were separated by 2DGE using broad range (pH 3-10) (Figure 3-7) and mid-range (pH 3-6, 4-7) IPG strips (Figure 3-7 and Appendix C-3). In-gel rehydration of Triton X-114 phase partitioned rat liver membrane proteins was used to reduce the problems associated with precipitation of membrane proteins during isoelectric focusing. In-gel rehydration has been shown to resolve murine mammary epithelial cell membranes on 2D gels far better than cup-loading [131].

Most Triton X-114 detergent phase proteins separated by 2DGE were visible in the pH 4 to pH 8 region with many higher molecular weight proteins, particularly those with apparent molecular weight >150 kDa observed. These higher molecular weight proteins were not clearly resolved on the gel suggesting poor entry into the second dimension gel. This could be due to the poor solubility of membrane proteins in isoelectric focusing buffers which often leads to protein precipitation [136], or very high molecular weight and/or heterogeneity. 'Trains' of protein spots were observed in the pH 3-10 gel (Figure 3-7). These spots are usually posttranslationally modified proteins, for example glycoproteins and phosphoproteins, which can often reduce the overall pI of these protein isoforms making them more hydrophilic and amenable for 2DGE separation [284].

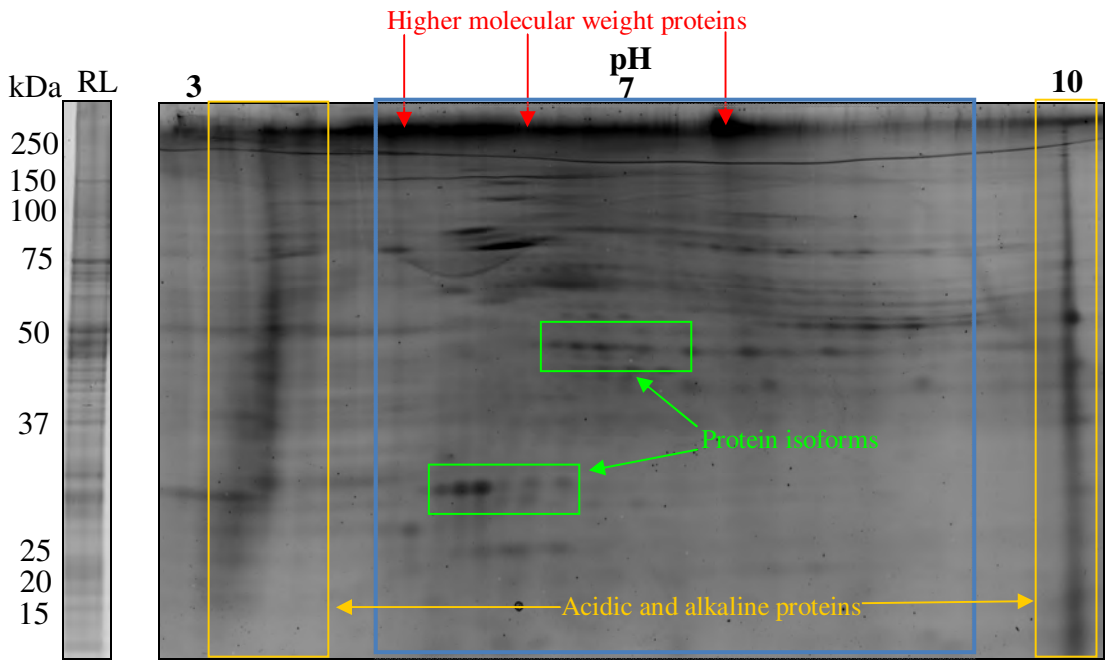

Figure 3-7. Triton X-114 phase partitioned rat liver membrane proteins were focused on pH 3-10 IPG strips and stained with Sypro Ruby. RL: Triton X-114 phase partitioned rat liver membrane proteins separated by 1D SDS PAGE. Membrane proteins were more clearly resolved in the pH range 5 to 8 (blue). Higher molecular weight were poorly solubilised and not separated by 2DGE (red). Trains of protein spots (protein isoforms) were resolved on the 2DGE (green). Acidic and alkaline membrane proteins were poorly resolved in regions with pH < 4 and pH > 9 (yellow).

While 2DGE has been shown to be a technique for separating soluble and mildly hydrophobic proteins; membrane and other extremely hydrophobic proteins have often resulted in poor separations [132]. In particular, integral membrane proteins which are 'designed' to be soluble in lipid bilayers and not in aqueous solvents are often difficult to solubilise with the urea-detergent mixtures in water-based environments that are used in 2DGE. In addition, the poor separation of membrane and hydrophobic proteins by 2DGE can be also attributed to hydrophobic interactions between these types of proteins and the basic acryl-amido derivatives of the IPG matrix, forming protein aggregates that impede isoelectric focusing [133].

Other components found in membrane preparations, such as lipids and contaminating soluble proteins, can also interfere with membrane solubilisation in IEF sample buffers and can often be presented as protein spots on the 2D gel [285]. Vertical streaking was observed in the basic region of the pH 3-10 2D gel due to the alkaline pIs that membrane proteins often exhibit and are not clearly resolved on 2D gels [134]. Precipitation and loss of membrane

proteins may have also occurred during IEF since horizontal streaking was observed on all 2D gels. This study showed that 2DGE fractionation of Triton X-114 enriched rat liver membrane proteins provided limited separation and resolution of proteins, and as a result 2DGE was not used in further comparative studies.

The investigation of methods to improve membrane protein analysis described here have demonstrated that Triton X-114 phase partitioning following carbonate stripping and centrifugation improves the enrichment of membrane proteins from rat liver tissue whilst lectin affinity chromatography using ConA, Jacalin and WGA was shown to have some potential in isolating membrane proteins by targeting their glycosylation. In our further studies both the hydrophobic and glycosylation properties of membrane proteins were exploited by combining these two analytical methods as a strategy for isolating membrane glycoproteins for characterisation.

3.2. Proteomics

The optimised sample preparation methods developed in Chapter 3.1 were applied to investigate the glycoproteomic complement of the liver membrane using two common glycoprotein capture approaches (lectin affinity and hydrazine chemistry). Here we report the strategy and results of the analysis of the tissue membrane glycoproteome which involves (1) Triton X-114 phase partitioning (2) isolation of glycosylphosphatidylinositol (GPI)-anchored proteins and (3) glycoprotein capture using lectin affinity or hydrazine chemistry. Triton X-114 phase partitioning was used to enrich rat liver membrane glycoproteins following differential ultracentrifugation as it was shown (Chapter 3.1.5) to improve the number of membrane protein identifications. Phase partitioned membrane proteins were resolubilised with CHAPS, as this was shown (Chapter 3.1.1, 3.1.2 and 3.1.3) to be a good detergent for membrane solubilisation, and solubilised membrane proteins were then subjected to lectin

affinity chromatography and hydrazine chemistry to compare these as a method of glycoprotein enrichment.

3.2.1. Rat liver membrane glycoproteome: enrichment by phase partitioning and glycoprotein capture (Publication I) Reprinted with permission from Albert Lee, Daniel Kolarich, Paul A. Haynes, Pia H. Jensen, Mark S. Baker, and Nicolle H. Packer, Journal of Proteome Research 2009 8 (2), 770-781 DOI: 10.1021/pr800910w. Copyright 2009 American Chemical Society

research articles Journal of proteome research

Rat Liver Membrane Glycoproteome: Enrichment by Phase Partitioning and Glycoprotein Capture

Albert Lee,[†] Daniel Kolarich,[†] Paul A. Haynes,[†] Pia H. Jensen,[†] Mark S. Baker,[†,‡] and Nicolle H. Packer*,[†]

Department of Chemistry and Biomolecular Sciences, Macquarie University, Sydney Australia 2109, and Australian Proteome Analysis Facility (APAF), Macquarie University, Sydney Australia 2109

Received October 28, 2008

Past proteomic studies of membrane proteins have often been hampered by the low abundance and relatively high hydrophobicity of these proteins. Proteins are often glycosylated, particularly on the extracellular surface of the plasma membrane, and this characteristic was targeted as an enrichment strategy for identifying membrane proteins. Here, we report a strategy for identifying the tissue membrane glycoproteome, which involves (1) Triton X-114 phase partitioning, (2) isolation of glycosylphosphatidylinositol (GPI)-anchored proteins, and (3) glycoprotein capture using lectin affinity or hydrazine chemistry. Surprisingly, the capture of membrane proteins by lectin affinity and hydrazine chemistry resulted in mostly different populations of enriched glycoproteins. Lectins enriched high molecular weight functional membrane proteins with more potential glycosylation such as those involved in signal transduction and cell adhesion. Conversely, hydrazine chemistry isolated a higher proportion of smaller, enzymatic and peripheral membrane proteins such as solute carrier transporters and cytochrome p450s. We have applied our strategy to characterize the rat liver membrane glycoproteome and identified four new predicted GPI-anchored proteins and two that have not previously been seen in the liver. We also identified 424 nonredundant membrane proteins, of which 335 had potential N-linked glycosylation sites.

Keywords: Membrane proteins • phase partitioning • glycosylphosphatidylinositol (GPI)-anchored proteins • lectin affinity • hydrazine chemistry • glycosylation • glycoproteins

Downloaded by MACQUARIE UNIV on September 2, 2009 | http://pubs.acs.org
Publication Date (Web): January 6, 2009 | doi: 10.1021/pr800910w

Introduction

The study of membrane proteins is an important field in proteomics because they represent 30% of the genome and constitute approximately 70% of all human protein based drug targets.[1] Membrane proteins play an important role in homeostasis of cells and are responsible for the transportation of molecules in and out of cells, the recognition of molecules, and cell−cell adhesion events. Because of their properties, they are the most elusive and sought after proteins in drug discovery, and therefore, efficient methods to enrich for these types of proteins are essential for a better understanding of membrane organization and function.

Membrane proteins can be classified as peripheral, integral and lipid-anchored.[2] Their amino acid composition is typically hydrophobic and they are often glycosylated and located on the extracellular surface of the plasma membrane. The attached carbohydrates can be covalently linked to the hydroxyl groups of serine or threonine (and hydroxylysine) residues (O-linked) or to the amide nitrogen of asparagine residues (N-linked) via the consensus sequence Asn-X-Ser/Thr (Cys), where X can be any amino acid except proline.[3] Glycosylation of membrane proteins plays a significant role in processes such as signal transduction, cell adhesion and cell recognition.[4] As more knowledge of glycoproteins and their attached glycans emerges, there is growing evidence that the abundance and heterogeneity of glycans on the cell surface can reflect the differences in cell types and states.[5] This has been shown to influence cell development, differentiation, implantation and morphogenesis[5] in diseases such as diabetes,[6] cystic fibrosis,[7] arthritis,[8] Alzheimer's,[9] autoimmunity[10] and cancer.[11]

A subset of membrane proteins are modified by a covalently attached glycosylphosphatidylinositol (GPI) moiety at the C terminus of the protein[12] and a number of glycoproteins have been found to be tethered by a GPI anchor to the extracellular face of eukaryotic plasma membranes.[13] GPI-anchored proteins are assumed to be located in sphingolipid and cholesterol rich microdomains, known as lipid rafts[13] and have been proposed to act as platforms for signal transduction across the plasma membrane through a large number of cellular receptors that are spatially segregated into these discrete microdomains.[14−17] Although the exact function of the GPI anchor has been the subject of much discussion, some of their roles include facilitating the transportation of folate,[18] transfer of surface

* To whom correspondence should be addressed. Prof. Nicolle H. Packer, Bldg E8C Room 307, Department of Chemistry and Biomolecular Sciences, Macquarie University, NSW 2109, Australia. Phone: +61 2 9850 8176. E-mail: npacker@cbms.mq.edu.au.

[†] Department of Chemistry and Biomolecular Sciences, Macquarie University.

[‡] Australian Proteome Analysis Facility (APAF), Macquarie University.

Published on Web 01/06/2009
10.1021/pr800910w CCC: $40.75
© 2009 American Chemical Society

proteins to neighboring cells[19] and cell–cell adhesion.[20] Their structural diversity and relatively low abundance has made the isolation of GPI-anchored proteins difficult, so that their enrichment will allow a better understanding of their function in the plasma membrane.

Two-dimensional gel electrophoresis (2DGE) and mass spectrometry are commonly used for separation and identification of soluble proteins. A major challenge with isolating and analyzing membrane proteins by 2DGE is their low abundance and poor solubility in the first-dimension isoelectric focusing buffers. In addition, many integral membrane proteins tend to be very large; for example, human calcium channels have up to 24 transmembrane helices and are typically over 200 kDa in size.[21] It is likely that a combination of hydrophobicity, low abundance and size of membrane proteins account for the historically problematic isolation of integral membrane proteins by 2DGE. Proteomic approaches currently used to overcome these issues are commonly based on "shotgun proteomics" methods using high resolution separation of tryptic peptides by liquid chromatography (MudPit) or peptide immobilized pH gradient isoelectric focusing (peptide IPG-IEF) in combination with tandem mass spectrometry.[22,23] While shotgun proteomics has demonstrated its utility in analyzing membrane proteins,[22−24] one of the disadvantages of this approach is that specific information such as post-translational modifications of protein isoforms is not obtained.[25] In addition, the large data sets obtained from these experiments can be complex and difficult to interpret, and alternative prefractionation methods are therefore needed to reduce sample complexity prior to MS analyses.[26] The primary objective of our research was to develop an efficient method for isolating membrane proteins by targeting both the hydrophobicity and glycosylation of these proteins.

Isolation of membrane proteins usually involves the solubilization of the membrane with a suitable detergent. The choice of this surfactant is important as it must be able to disrupt and solubilize cell membranes as well as being suitable for further studies of cell membrane components by such techniques as mass spectrometry. Triton X-114 has been previously used to solubilize integral membrane proteins at 4 °C and, when heated to its cloud point temperature (20 °C), exhibits phase partitioning.[27,28] Phase partitioning was shown to separate integral membrane proteins and soluble proteins that formed mixed micelles with the detergent.[27] When Triton X-114 phase partitioning was applied to crude membrane proteins, soluble proteins were segregated and removed from the enriched membrane protein fraction.[27,29] Some GPI-anchored proteins were enriched in this membrane fraction and were subsequently treated with phospholipase C to specifically cleave the phosphatidylinositol from GPI-anchored proteins to release the attached soluble glycoprotein. Previous studies using this strategy on *Arabidopsis thaliana* membrane preparations identified 44 GPI-anchored proteins, which is the largest number of GPI-anchored protein identifications from a single study to date.[29]

Lectins are proteins found in plants, animals and microorganisms that have selective affinities for particular oligosaccharide epitope structures displayed on proteins and lipids.[30,31] They have been used together to enrich cell surface glycoproteins for identification of low-abundance plasma proteins[32] and to examine the microheterogeneity of carbohydrates associated with disease and disease progression.[5,6] Three lectins, Concanavalin A (ConA), Jacalin and Wheat Germ Agglutinin (WGA), immobilized on agarose beads, were used sequentially to fractionate rat liver membrane glycoproteins based on their attached glycans. ConA recognizes α-mannose (and α-glucose), which are commonly found in N-linked glycans.[33] Jacalin has been acknowledged as a general lectin for O-glycans for its recognition of galactosyl (β-1, 3) *N*-acetyl-galactosamine, lactose and galactose.[34,35] In addition, Jacalin has been shown to also recognize mannose, oligomannosides, glucose, *N*-acetylneuraminic acid and *N*-acetylmuramic acid.[35] WGA recognizes *N*-acetyl glucosamine (GlcNAc) and has also been observed to have affinity for sialic acid.[36]

Recently, one of the more common methods used for identifying glycoproteins is a solid-phase extraction procedure for N-linked glycoproteins and glycopeptides using hydrazine coupling chemistry.[37] This method immobilizes the glycoprotein or glycopeptide onto a solid-phase support by first oxidizing the attached carbohydrates containing vicinal hydroxyl groups into aldehydes with periodate. The resulting aldehydes then react with hydrazide groups on an agarose media support to form stable hydrazone bonds. Immobilized glycoproteins can be subsequently treated with trypsin, releasing peptides for mass spectrometry analysis and identification of the bound glycoprotein. The immobilized N-linked glycosylated peptides can also be treated with PNGase F to release and identify the attached peptide. This hydrazine chemistry approach has been used to identify the proteins that are glycosylated in human cerebrospinal fluid (CSF),[38] saliva[39] and plasma.[40] The disadvantage of this approach is that the carbohydrates are destroyed, and therefore, the glycans are no longer able to be identified and characterized.

In this study, a number of analytical approaches were combined including Triton X-114 extraction and phase partitioning to enrich the membrane proteins from rat liver tissue. The identification of membrane glycoproteins in parallel using either immobilized lectin affinity chromatography or solid-phase hydrazine coupling chemistry was compared. The results presented here demonstrate the utility of targeting protein glycosylation as an enrichment strategy for identifying membrane proteins in tissue samples.

Materials and Methods

Materials. Tris, sodium chloride, sodium hydroxide, sodium carbonate, EDTA, Bradford reagent, HEPES, PBS tablets, ammonium bicarbonate (NH_4HCO_3), formic acid, Triton X-114, 3-[(3-Cholamidopropyl)dimethylammonio]-1-propanesulfonate (CHAPS), dithiothreitol (DTT), iodoacetamide (IAA), methyl-α-glucopyranoside, galactose, sodium dihydrogen orthophosphate (NaH_2PO_4), sodium *meta*-periodate, *N*-acetylglucosamine, agarose bound Jacalin with protein concentration of 5 mg/mL and binding capacity of 1−2 mg human IgA/mL and, agarose bound WGA with protein concentration of 5 mg/mL and binding capacity 1−2 mg ovomucoid/mL were obtained from Sigma (St. Louis, MO). NuPAGE 10% Bis-Tris precast gradient gels, 3-(*N*-morpholino) propane sulfonic acid (MOPS) running buffer and phospholipase C from *Bacillus cereus* were obtained from Invitrogen (San Diego, CA). Agarose bound Concanavalin A (ConA) with protein concentration of 10−16 mg/mL and binding capacity of 20−45 mg porcine thyroglobulin/mL was obtained from GE Healthcare (Uppsala, Sweden). Ultralink Hydrazide Gel was obtained from Pierce (Rockford, IL). Sequencing-grade trypsin was obtained from Promega (Madison, WI).

Downloaded by MACQUARIE UNIV on September 2, 2009 | http://pubs.acs.org
Publication Date (Web): January 6, 2009 | doi: 10.1021/pr800910w

Rat Liver Membrane Preparation. Rat livers obtained from 8 week old Dark Agouti rats (Save Sight Institute, Sydney Eye Hospital, Australia) were perfused with 0.9% (w/v) phosphate buffered saline (PBS). Rat liver tissue (3 g) was homogenized in 5 mL of lysis buffer (pH 7.4) containing 50 mM Tris-HCl, 0.1 M NaCl, 1 mM EDTA and protease inhibitor cocktail (3 mg of antipain-dihydrochloride, 0.5 mg of aprotinin, 0.5 mg of bestatin, 1 mg of chymostatin, 3 mg of E-64, 10 mg of EDTA-Na_2, 0.5 mg of leupeptide, 20 mg of Pefabloc SC, 0.5 mg of pepstatin, 3 mg of phosphoramidon) (Roche Diagnostics, Switzerland) using an Omni TH homogenizer (Omni International, Inc., VA).

The homogenized rat liver tissue was centrifuged at 2000*g* for 20 min at room temperature. The supernatant containing cellular proteins was removed and diluted with binding buffer (20 mM Tris-HCl, 0.1 M NaCl, 1 mM $MnCl_2$, 1 mM $MgCl_2$ and 1 mM $CaCl_2$, pH 7.4) to a final volume of 40 mL and chilled on ice for 1 h. This was to ensure that the sample was compatible for lectin affinity chromatography. The diluted proteins were sedimented by ultracentrifugation at 120 000g_{avg} for 1 h and 20 min. The supernatant was removed, and the membrane pellet was washed twice with 0.1 M sodium carbonate (pH 11) and was stored at −80 °C if not used immediately. Membrane pellets were homogenized in binding buffer and protein quantification was performed by Bradford Assay (Sigma-Aldrich, MO).

Triton X-114 Phase Partitioning. Approximately 100 μL (0.5−1 mg) of the rat liver membrane pellet was homogenized with 4 vol of binding buffer containing 1% (v/v) Triton X-114 and chilled on ice with intermittent vortexing for 20 min. The samples were heated at 37 °C for 20 min and phase partitioned by centrifugation at 300*g* for 5 min. The upper aqueous phase was removed and stored. The detergent phase was further diluted with 4 vol of binding buffer containing 1% (v/v) Triton X-114 and phase partitioning was repeated. The combined aqueous phases were mixed with 9 vol of ice-cold acetone to precipitate proteins and remove any detergent. Membrane proteins contained in the Triton X-114 detergent phase were either subjected to phospholipase C (PI-PLC) treatment (see below) or were precipitated with 9 vol of ice-cold acetone. Precipitated membrane proteins were resolubilized in binding buffer containing 1% (w/v) CHAPS and stored at −80 °C if not used immediately.

PNGase F Treatment. Homogenized crude membrane proteins in binding buffer were treated with 5 μL of PNGase F (0.5 units/μL) and incubated at 37 °C overnight. The sample was then diluted with 4 vol of binding buffer containing 1% (v/v) Triton X-114 and phase partitioned as above to obtain the de-N-glycosylated enriched membrane fraction.

Isolation of GPI-Anchored Proteins. Following Triton X-114 phase partitioning, the detergent phase was diluted with 4 vol of binding buffer containing 1% (v/v) Triton X-114 and 10 μL of phospholipase C from *B. cereus* (specific activity 100 U/mL) was added. The sample was chilled on ice for 20 min with gentle mixing and then incubated at 37 °C for 1 h with shaking before being phase partitioned by centrifugation as above. The proteins in the aqueous and detergent phases were precipitated with 9 vol of ice-cold acetone for protein analysis. The aqueous phase precipitant was resolubilized in water, and the detergent phase precipitant was resolubilized in binding buffer containing 1% (w/v) CHAPS, then these were heated at 96 °C for 6 min to inactivate any protease activity.

***Escherichia coli* Cell Lysate and Crude Membrane Preparation.** *E. coli* K-12 strain was grown aerobically at 37 °C with shaking as described.[41] *E. coli* cells were collected by centrifugation at 2500*g* for 8 min. The cells were resuspended in 50 mM Tris-HCl, pH 7.4 for washing, and then pelleted by centrifugation at 2500*g* for 10 min. *E. coli* cells were ruptured in an Aminco French press with three presses at 9.6×10^7 Pa and the unbroken cells were removed by centrifugation at 2500*g* for 10 min. The supernatant containing cellular proteins was frozen at −80 °C.

E. coli membrane proteins were enriched for by diluting approximately 4 mg of *E. coli* total cellular proteins with 0.1 M sodium carbonate (pH 11) to a final volume of 40 mL and chilled on ice for 1 h. The treated proteins were sedimented by ultracentrifugation at 120 000g_{avg} for 1 h and 20 min. The supernatant was removed, and the crude membrane pellet was washed twice with 0.1 M sodium carbonate (pH 11). Membrane pellets were stored at −80 °C if not used immediately.

Lectin Affinity Chromatography. Agarose-bound lectins (ConA, Jacalin and WGA) (0.5 mL) were initially washed with 10 mL of their corresponding elution buffer A (20 mM Tris-HCl, 0.1 M NaCl, 0.2 M methyl-α-D glucopyranoside [ConA], 0.5 M α-D galactose [Jacalin] and 0.5 M *N*-acetyl glucosamine [WGA], pH 7.4) and then equilibrated with 20 mL of binding buffer. Eighty micrograms of detergent-partitioned proteins in 0.5 mL of binding buffer was mixed with each of the immobilized lectins and incubated at 4 °C overnight. Each mixture was packed in disposable gravity-flow Poly-Prep chromatography columns (Bio-Rad, Hercules, MA) and the three lectin columns were washed with 10 bed volumes of binding buffer. Bound proteins were then eluted with 10 column volumes of elution buffer A, followed by 10 bed volumes of corresponding higher concentration elution buffer B (20 mM Tris-HCl, 0.1 M NaCl, 1 M methyl-α-D glucopyranoside [ConA], 1 M α-D galactose [Jacalin] or 1 M *N*-acetyl glucosamine [WGA], pH 7.4). Further elution of tightly bound proteins was performed using 10 bed volumes of the relevant elution buffer C (20 mM Tris-HCl, 0.1 M NaCl, 1.5 M methyl-α-D glucopyranoside [ConA], 1.5 M α-D galactose [Jacalin] and 1.5 M *N*-acetyl glucosamine [WGA], pH 7.4). All eluted samples were desalted and concentrated using an Amicon Ultra-10 centrifugal device with 10 kDa Nominal Molecular Weight Limit (NMWL) (Millipore, MA). Lectin eluates with high concentrations of monosaccharides were diluted with water to assist in the diafiltration and concentration of proteins.

SDS PAGE and Protein Visualization. Approximately 10 μg of protein was applied per lane onto NuPAGE 10% Bis-Tris precast gradient gels with MOPS running buffer. Electrophoresis conditions were set to 200 V, 125 mA for 60 min. The gels were fixed in 7% (v/v) acetic acid and 10% (v/v) methanol and stained overnight with Sypro Ruby (Invitrogen, San Diego, CA). Gel images were obtained using Typhoon Trio Variable Mode Imager (GE Healthcare, Uppsala, Sweden).

Immobilization of Glycoproteins by Hydrazine Chemistry. Immobilization by hydrazine coupling of proteins partitioned into the Triton X-114 detergent phase was performed as per manufacturer's instructions (Pierce). The oligosaccharides in approximately 80 μg of protein in 0.1 M NaH_2PO_4, pH 7.0 (1 mL) were oxidized in sodium *meta*-periodate at 25 mM final concentration and incubated at room temperature in the dark for 30 min. Samples were desalted with 0.1 M NaH_2PO_4, pH

Downloaded by MACQUARIE UNIV on September 2, 2009 | http://pubs.acs.org
Publication Date (Web): January 6, 2009 | doi: 10.1021/pr8009910w

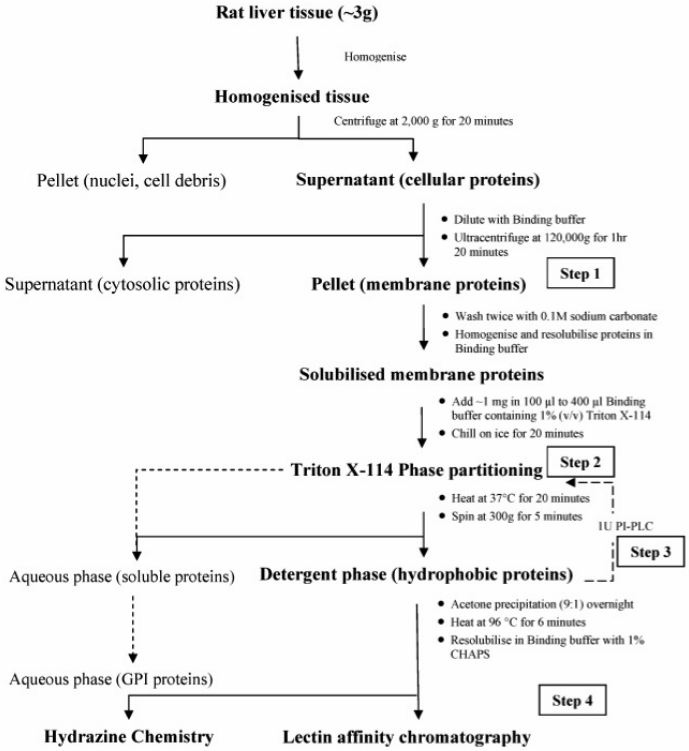

Figure 1. Enrichment of membrane proteins workflow. Step (1), homogenized rat liver tissue was sedimented by centrifugation at 120 000*g* for 80 min. Step (2), the membrane pellet was resolubilized in Binding buffer and membrane proteins were enriched by Triton X114 phase partitioning. Step (3), the detergent phase was treated with phospholipase C and the mixture was phase partitioned again releasing GPI-anchored proteins into the aqueous phase. Step (4), lectin affinity chromatography: the acetone-precipitated detergent phase was heated at 96 °C for 6 min and solubilized with 1% (w/v) CHAPS. Samples were loaded onto ConA, Jacalin and WGA affinity columns for glycoprotein enrichment. Hydrazine chemistry: proteins precipitated from the detergent phase were conjugated to Ultralink hydrazine gel (Pierce).

Downloaded by MACQUARIE UNIV on September 2, 2009 | http://pubs.acs.org
Publication Date (Web): January 6, 2009 | doi: 10.1021/pr800910w

7.0, using a Microcon YM-10 Centrifugal Filter unit (Millipore, MA). Ultralink hydrazide gel was packed in disposable gravity-flow Poly-Prep chromatography columns (Bio-Rad, Hercules, MA) and equilibrated with 5 bed volumes of 0.1 M NaH_2PO_4, pH 7.0. The oxidized sample was applied to the equilibrated hydrazine gel-bed and incubated overnight at room temperature with gentle mixing. The gel-bed was washed with 5 bed volumes of 1 M NaCl followed by 5 bed volumes of PBS. The gel-bed was equilibrated with 100 mM NH_4HCO_3, pH 7.8, and the immobilized proteins were reduced with 10 mM DTT for 30 min and alkylated with 55 mM IAA in the dark for 45 min. The gel-bound proteins were then digested with 1:50 Trypsin/Protein (w/w) with sequencing-grade trypsin (Promega, Madison, WI) for 18 h at 37 °C. The tryptic peptides were eluted by washing the gel-bed with 5 bed volumes of 100 mM NH_4HCO_3, pH 7.8, followed by 5 bed volumes methanol. Each fraction was desalted using C_{18} tips (PerfectPure C18 Tips) (Eppendorf, Germany) and the eluate was dried using a vacuum centrifuge followed by resuspension in 0.1% (v/v) formic acid in preparation for nanoLC-MS/MS.[42] All experiments were done in triplicate using the same original rat liver crude membrane preparation so that both methods can be directly compared.

In-Solution Digestion with Trypsin. Phase partitioned proteins and lectin eluates were buffer exchanged with 100 mM NH_4HCO_3, pH 7.8, using a Microcon YM-10 Centrifugal Filter unit (Millipore, MA). The samples were reduced with 25 mM DTT for 30 min and alkylated with 55 mM IAA in the dark for 45 min. The samples were buffer exchanged again with 100 mM NH_4HCO_3, pH 7.8, and concentrated. After concentration, the proteins were digested with trypsin and prepared for nanoLC-MS/MS analysis as below.

RP-HPLC and Mass Spectrometry. The tryptic peptide mixtures were analyzed by nanoLC-MS/MS using a LTQ linear ion-trap mass spectrometer (ThermoFinnigan, CA). Reversed-phase columns were packed in-house to approximately 7 cm (100 μm i.d.) using 100 Å, 5 mM Zorbax C_{18} resin (Agilent Technologies, CA), in a fused silica capillary with an integrated electrospray tip. A 1.8 kV electrospray voltage was applied via a liquid junction upstream of the C_{18} column. Samples were injected onto the C_{18} column using a Surveyor autosampler. Each sample was loaded onto the C_{18} column followed by an initial wash step with Buffer A (5% (v/v) acetonitrile, 0.1% (v/v) formic acid) for 10 min at 1 μL/min. Peptides were subsequently eluted from the C_{18} column with 0−50% Buffer B (95% (v/v) acetonitrile, 0.1% (v/v) formic acid) for 58 min at 500 nL/min followed by 50−95% buffer B for 5 min at 500 nL/min. The column eluate was directed into a nanospray ionization source of the mass spectrometer. Spectra were scanned over the range 400−1500 amu. Automated peak recognition, dynamic exclusion, and tandem MS of the top six most intense

precursor ions at 40% normalization collision energy were performed using the Xcalibur software (ThermoFinnigan, CA).

Protein Identification and Data Analysis. Spectra files were converted to mzXML format and processed through the global proteome machine (GPM) software, an open source protein identification system that uses the Tandem algorithm.[43] Peptide identification was determined using a 0.4 Da fragment ion tolerance. Carbamidomethyl was considered as a complete modification, and partial modifications were also considered, which included oxidation of methionine and threonine and deamidation of asparagine and glutamine. MS/MS spectra were searched against the *Rattus norvegicus* and *E. coli* databases (Database derived from Swiss-Prot, Ensemble and NCBI), and reverse database searching was used for estimating false discovery rates.[44] Protein identifications were validated using a 1% false discovery rate assessed by reverse database searching, which was applied to nonredundant protein lists. A minimum of two unique peptide matches identified in at least two replicates was used to validate protein identifications.

The assignment of an identified protein as being located in the membrane was made using a combination of predictions using Transmembrane Hidden Markov Model (TMHMM) (available at http://www.cbs.dtu.dk/services/TMHMM)[45] and information on membrane location derived from UniProt, GO annotation and the Swiss-Prot database. In this context, membrane proteins were considered to be both integral and peripheral to total cellular membranes. Identification of GPI anchor signals were determined by Kohonen Self Organizing Mapping (GPI-SOM)[46] (available at http://gpi.unibe.ch).[46] N-linked glycosylation sites (N-X-S/T) were predicted using NetNGlyc (available at http://www.cbs.dtu.dk/services/NetNGlyc).

Downloaded by MACQUARIE UNIV on September 2, 2009 | http://pubs.acs.org
Publication Date (Web): January 6, 2009 | doi: 10.1021/pr800910w

Results

We have developed a procedure for identifying membrane proteins based on their properties of hydrophobicity (Triton X-114 phase partitioning[27]), and glycosylation (lectin affinity chromatography[30] and hydrazine chemistry[37]) as outlined in Figure 1. We have defined membrane proteins as comprising integral membrane proteins, lipid-anchored proteins and membrane-associated proteins as determined by TMHMM together with information derived from UniProt, GO annotation and the Swiss-Prot database.

Isolation of Crude Membrane Proteins. Rat liver membranes were prepared by differential centrifugation, after the crude pellet was washed briefly with sodium carbonate to minimize contamination from soluble proteins.[47] The membrane pellet was homogenized in binding buffer and the proteins in the supernatant and pellet fractions were separated by 1D SDS-PAGE (Figure 2) which showed differential protein enrichment.

The enriched membrane fraction was digested in-solution with trypsin and analyzed by nanoLC-MS/MS. In total, 195 proteins were identified. Membrane proteins (transmembrane and membrane associated proteins) contributed to 48% (95) of total protein identifications. Of these, membrane proteins localized to the mitochondria and endoplasmic reticulum/Golgi apparatus represented 15% and 17% of the data set, respectively. Plasma membrane proteins represented 6% of the data set. Cytoplasmic proteins comprised 49% of protein identifications in this fraction Two percent of the proteins had no known function (Supporting Information Table 1).

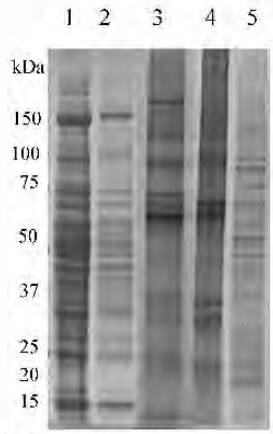

Figure 2. SDS-PAGE separation of proteins from homogenated rat liver tissue (lane 1), supernatant following ultracentrifugation (lane 2), and the enriched membrane pellet following ultracentrifugation (lane 3) Triton X-114 phase partitioning, detergent phase (lane 4), and aqueous phase of rat liver proteins (lane 5).

Enrichment of Membrane Proteins by Triton X-114 Phase Partitioning. To further enrich for membrane proteins, the crude membrane preparations were subjected to Triton X-114 phase partitioning. Proteins in the aqueous and detergent phases were digested in-solution with trypsin and analyzed by nanoLC-MS/MS. Enrichment of membrane proteins in the detergent phase of the Triton X-114 phase partitioning identified 245 proteins in total, of which 188 (76.7%) were classified as membrane proteins (Figure 3A). Of these membrane proteins, 46% and 29% were localized to the mitochondria and endoplasmic reticulum/Golgi apparatus, respectively (Figure 3B). Twelve percent of the proteins, many of which contained predicted N-linked glycosylation sites, were classified as plasma membrane proteins. Some of these plasma membrane proteins included cell adhesion proteins, cell surface receptors and many solute carrier transporters (Supporting Information Table 2).

Interestingly, 13 membrane proteins identified in the detergent phase were also found to be present in the aqueous phase. On the basis of the information obtained from the Swiss-Prot database, 11 of these membrane proteins found in the aqueous phase contained multiple glycosylation sites (N- and/or O-linked). PNGase F treatment of the crude membrane proteins to remove N-linked glycans prior to Triton X-114 phase partitioning resulted in seven of these proteins no longer partitioning to the aqueous phase suggesting that N-glycosylation was responsible for their hydrophilicity. The four proteins which remained soluble in the aqueous phase after PNGase F treatment were classified as membrane-associated proteins involved in cell adhesion and had relatively low GRAVY (Grand Average Hydropathy) scores. A GRAVY score is the relative value for the hydrophobic residues of a protein, where decreasing GRAVY values represent increasing protein hydrophilicity.[48,49] The membrane proteins found in the aqueous phase had a large distribution of hydrophilic amino acids, which could contribute to their solubility and partitioning behavior. In addition, protein isoforms such as those modified by phos-

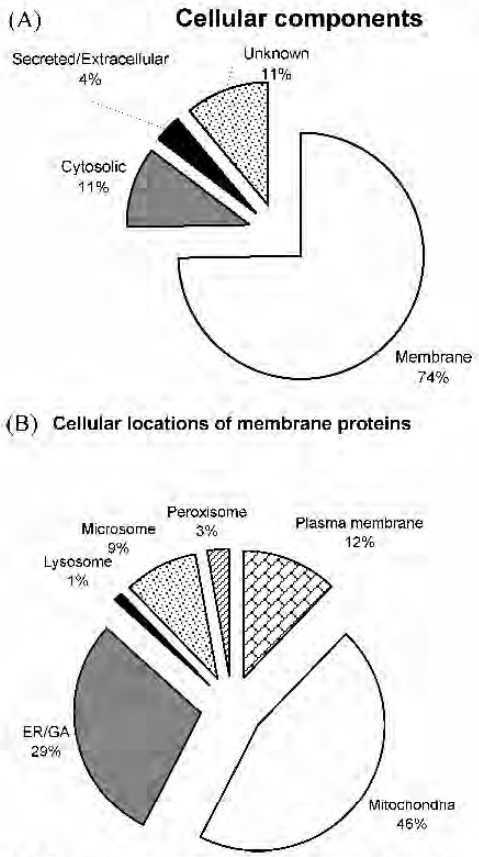

Figure 3. Proteins partitioned to the detergent phase following Triton X-114 phase partitioning. (A) Distribution of identified proteins cellular components. (B) Distribution of membrane proteins cellular location. All identified proteins were annotated using UniProt and GO annotation.

Downloaded by MACQUARIE UNIV on September 2, 2009 | http://pubs.acs.org
Publication Date (Web): January 6, 2009 | doi: 10.1021/pr800910w

phorylation[50] and acetylation[51] may also influence the solubility of these membrane proteins.

Glycosylphosphatidylinositol (GPI)-Anchored Proteins. GPI-anchored proteins are soluble glycoproteins that are tethered to the extracellular surface of the plasma membrane by a phosphatidylinositol anchor. This GPI lipid anchor would be expected to isolate these proteins in the detergent phase but no GPI-anchored proteins were identified in this fraction. The isolated detergent phase was subjected to PI-PLC to hydrolyze the phosphatidylinositol moiety, which released 13 soluble GPI-proteins from the enriched membrane fraction into the aqueous phase (Table 1). Nine of these are described in the Swiss-Prot database as GPI-anchored proteins. Four other proteins were identified to contain GPI-anchor signals by Kohonen Self Organizing Mapping (GPI-SOM). To our knowledge, the nervous system (CNS) proteins, LSAM and Neuronal growth regulator 1 were identified in the rat liver for the first time.

Parallel Lectin Affinity Chromatography of Enriched Membrane Proteins. Proteins precipitated with ice-cold acetone from the Triton X-114 detergent phase were resolubilized in binding buffer containing 1% (w/v) CHAPS and heated at 96 °C for 6 min to destroy any possible protease activity. These proteins were then incubated at 4 °C with rotating overnight with ConA, Jacalin and WGA lectins immobilized on agarose beads. High concentrations of competing sugar were required to elute the membrane glycoproteins from the ConA (1.5 M methyl-α-D glucopyranoside), Jacalin (1.5 M α-D galactose) and WGA (1.5 M *N*-acetyl glucosamine) columns.

The eluted fractions from each of the lectin affinity columns were digested in-solution with trypsin and subjected to nanoLC-MS/MS. With the use of the three lectins in parallel as an enrichment strategy, 423 proteins were identified in total, including 277 membrane proteins, of which 202 (71%) of these proteins contained predicted N-linked glycosylation sites (N-X-T/S) (Figure 4). The three lectins isolated 44 membrane proteins in common, of which 27 had predicted N-linked glycosylation sites. ConA, a common N-linked glycoprotein affinity lectin, also isolated 67 unique membrane proteins, of which 48 had predicted N-linked glycosylation sites. Jacalin isolated 42 unique membrane proteins; of these, 30 had predicted N-linked glycosylation sites, and WGA, which recognizes GlcNAc as well as sialic acid, isolated 61 unique membrane proteins, of which 50 had predicted N-linked glycosylation sites. The possibility of O-glycosylation accounting for the affinities of the other proteins was not able to be reliably predicted. The proteins identified comprised a large proportion of cell adhesion proteins, receptors, solute carrier transporters and cytochrome p450s (Supporting Informaiton Tables 3−5).

Identifying Glycosylated Proteins Using Hydrazine Chemistry. An aliquot of enriched membrane proteins of the same detergent fraction as that used for enrichment by lectin affinity was used to compare the effectiveness of the lectin approach with the more general hydrazine chemistry approach. In principle, hydrazine chemistry should react with all glycoproteins because of the specificity of the initial oxidation by periodic acid of the vicinal hydroxyl groups found on sugars. The hydrazine on the beads reacts with these oxidized sugars and immobilizes the glycoproteins from a mixture for subsequent trypsin digest and identification. In total, 367 proteins were identified using hydrazine chemistry, of which 269 were classified as membrane proteins (Figure 5A,B). Approximately 78% (210) of these membrane proteins were predicted by NetNGlyc to possess potential N-linked glycosylation sites. It should be noted however that, contrary to expectation, there were also 53 cytoplasmic proteins with predicted N-linked glycosylation sites also retained by the hydrazide beads.

The two glycoprotein enrichment methods surprisingly yielded very different results. The two methods pulled out 148 of the same proteins, with only 77 of these with predicted N-linked glycosylation sites (Figure 5C). Most (122) of these 148 proteins were membrane proteins. There were, however, a large number of glycoproteins which were enriched by lectin affinity (275) but not by hydrazine binding. Conversely, there were many glycoproteins which were selected by hydrazine (219) but were not captured by any of the lectins. Not all of these proteins had N-linked glycoprotein motifs with 52% and 43%, respectively, of the lectin-enriched and hydrazine-coupled proteins not having an N-linked glycosylation site. There is no reliable way to predict which of these may have O-linked glycosylation sites. It is clear though that most of the membrane proteins that are enriched are glycosylated (73% and 78%, respectively). In summary, lectin affinity chromatography and hydrazine chemistry were able to fractionate common and

Table 1. Thirteen GPI-Anchored Proteins Were Identified after PI-PLC Treatment of the Precipitated Proteins from the TX-114 Detergent Phase[a]

identifier	protein description (GPI-anchored proteins)	location	accession no.
ENSRNOP00000015057	5′-nucleotidase precursor (CD73 antigen)	Lymphoid tissue	P21588
ENSRNOP00000040165	Limbic system-associated membrane protein precursor (LSAMP)	CNS	Q62813
ENSRNOP00000006306	CD48 antigen precursor (MRC OX-45 surface antigen)	Lymphocytes	P10252
ENSRNOP00000023977	Monocyte differentiation antigen CD14 precursor	Lymphoid tissue	Q63691
ENSRNOP00000019004	Alkaline phosphatase, tissue-nonspecific	Liver	P08289
ENSRNOP00000021397	Dipeptidase 1 precursor (Microsomal dipeptidase)	Lung/Kidney	P31430
ENSRNOP00000042811	Neuronal growth regulator 1 precursor	Brain	Q9Z0J8
ENSRNOP00000008685	Thy-1 membrane glycoprotein	Lymphoid tissue	P01830
ENSRNOP00000026925	Folate receptor 1 alpha	All tissues	
ENSRNOP00000010209[a]	Dolichyl-diphosphooligosaccharide-protein glycosyltransferase (Ribophorin II)	All tissues	P25235
ENSRNOP00000004864[a]	Dimethylaniline monooxygenase 3 (Hepatic flavin-containing monooxygenase 3)	Liver	Q9EQ76
ENSRNOP00000015956[a]	Aspartate aminotransferase (Transaminase A)	Brain/CNS	P00507
ENSRNOP00000035497[a]	Uncharacterized protein KIAA0152 homologue precursor	Unknown	Q5FVQ4

[a] Four of these proteins were predicted by GPI-SOM to contain conserved GPI-anchored protein N- or C-terminal domains.

Downloaded by MACQUARIE UNIV on September 2, 2009 | http://pubs.acs.org
Publication Date (Web): January 6, 2009 | doi: 10.1021/pr8009910w

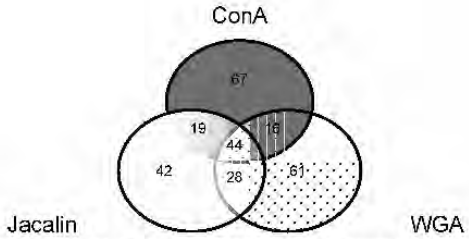

Figure 4. Number of proteins identified using immobilized lectins: ConA, Jacalin and WGA.

unique subsets of membrane proteins, and provided a good representation of the rat liver membrane glycoproteome (Figure 6).

Nonspecific Binding to Lectin Affinity and Hydrazine Chemistry Affinity Media. Nonspecific protein binding could explain the high percentage of differentially retained proteins by the two approaches. The extent of nonselective affinity of the two capture matrices used was determined by subjecting an *E. coli* cell lysate to the two enrichment methods. *E. coli* proteins are not glycosylated and should not be retained by either lectins or hydrazine chemistry. *E. coli* cell lysate and *E. coli* crude membranes were prepared and fractionated by ConA affinity and hydrazine chemistry, in exactly the same way as the fractionation of rat liver membrane proteins. Many proteins from *E. coli* cell lysates and membranes bound nonspecifically to both the Con A and the hydrazine resin and different proteins were enriched from *E. coli* cell lysates and crude membranes (Figure 7). NanoLC-MS/MS of ConA eluates identified many nonglycosylated high-abundance *E. coli* proteins such as protein chain elongation factors, outer membrane porin proteins and ribosomal proteins (Supporting Information Tables 7 and 8).

Similarly, hydrazine coupling chemistry was used to immobilize proteins from *E. coli* cell lysates and crude membranes onto hydrazide gel. In addition to the major proteins identified by ConA affinity, hydrazine chemistry captured a large number of nonglycosylated proteins including chaperones, ATP synthases and lipoproteins (Supporting Information Tables 9 and 10). The binding of *E. coli* proteins to both ConA and the hydrazine resin suggests that both glycoprotein enrichment strategies are capable of binding nonglycosylated proteins; this

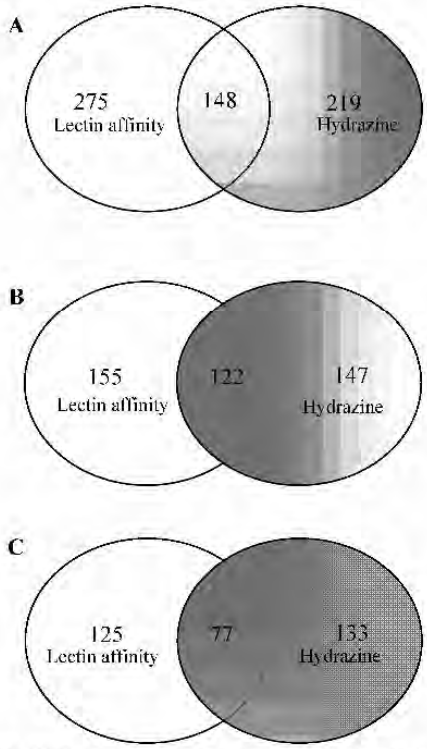

Figure 5. (A) Total proteins identified from lectin affinity chromatography and hydrazine chemistry. (B) Membrane proteins identified from lectin affinity chromatography and hydrazine chemistry. (C) Membrane glycoproteins (N-linked) identified from ConA, Jacalin, WGA and hydrazine chemistry.

provides an explanation for the capture of the many nonglycosylated rat liver proteins using both these methods.

Discussion

Enrichment of Membrane Proteins from Rat Liver Tissue. Different membrane enrichments methods such as sodium carbonate stripping,[41,47] aqueous phase partitioning,[52]

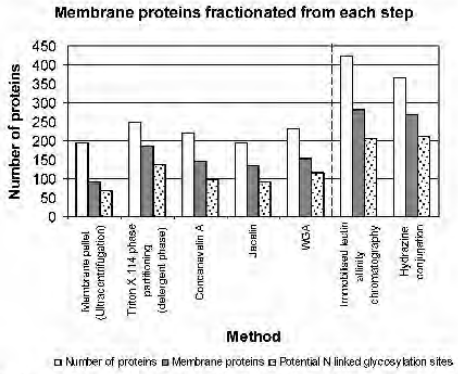

Figure 6. Number of membrane proteins identified from each step of our enrichment strategy.

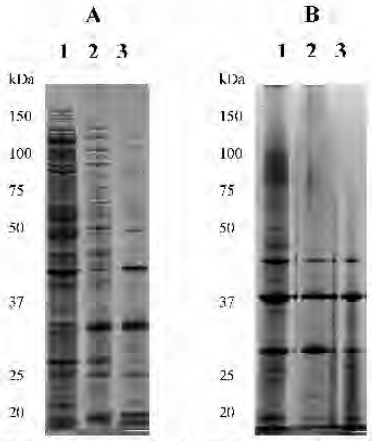

Figure 7. 1D SDS-PAGE of ConA affinity controls (A) *E. coli* K-12 cell lysates subjected to ConA affinity fractionation. *E. coli* cell lysates (lane 1), ConA flow through (lane 2) and ConA bound proteins (lane 3). (B) *E. coli* K-12 cell membranes subjected to ConA affinity fraction. *E. coli* cell membrane (lane 1), ConA flow through (lane 2) and ConA bound proteins (lane 3).

Downloaded by MACQUARIE UNIV on September 2, 2009 | http://pubs.acs.org
Publication Date (Web): January 6, 2009 | doi: 10.1021/pr800910w

sucrose density gradient centrifugation[53] and sequential protein extraction[54] have been used in pilot studies to compare membrane solubilization and removal of soluble proteins such as cytoplasmic and ribosomal proteins from enriched membrane fractions. In our enrichment strategy, Triton X-114 phase partitioning was chosen as the ideal method for removing soluble proteins from membrane preparations.[27] Membrane protein annotations and N-linked glycosylation sites were determined using a suite of prediction programs available online. Although many prediction programs are never completely reliable and currently available methods use their own algorithms, there is no universal method for determining transmembrane segments.[45] In our study, we have employed Transmembrane Hidden Markov Model (TMHMM 2.0), which is frequently used for evaluating large amounts of proteomic data for predicting transmembrane segments.[55] Membrane proteins were also determined using information derived from UniProt, GO annotation and the Swiss-Prot database.[56] NetNGlyc was used to predict N-linked glycosylation sites (N-X-S/T), and has been previously used to construct the human liver glycoproteome.[56] NetOGlyc is an available tool for predicting O-glycosylation sites, but as there is no amino acid motif for this modification, it is difficult to evaluate for its predictive correctness and was not used.

Triton X-114 effectively solubilizes membrane proteins by forming mixed-micelles with proteins, which permits the isolation of integral membrane proteins and membrane-associated proteins by phase partitioning with water. MS analyses of the proteins in the detergent phase identified 188 nonredundant membrane proteins partitioning to the detergent phase. The anomalous phase partitioning of some of these membrane proteins suggests that glycosylation may influence their solubility. This phenomenon has been observed with acetylcholinesterase from *Torpedo californica* (4 N-linked glycosylation sites), Na^{+},K^{+}-ATPase from kidney microsomes (3 N-linked glycosylation sites) and Ca^{2+} ATPase from sarcoplasmic reticulum membranes (3 N-linked glycosylation sites).[57] It has also been suggested that the anomalous partitioning of these membrane glycoproteins could be due to large strings of hydrophilic amino acids present in these proteins, which could explain why 4 of the membrane glycoproteins remained in the aqueous phase after deglycosylation.[57] The basis of the anomalous detergent partitioning of membrane glycoproteins is not fully understood.

Triton X-114 has been previously shown to influence chromatographic separation, so we precipitated the proteins from the detergent phase with ice-cold acetone for further separation by gel electrophoresis and lectin affinity chromatography after solubilization in CHAPS containing buffer. CHAPS has been used to solubilize MHC membrane glycoproteins from tumor cells prior to lectin affinity chromatography.[4] These authors concluded that CHAPS was effective in disrupting protein–protein interactions and significantly improved binding of membrane proteins to the lectin *Lens culinaris*.[4] In addition, the critical micelle concentration (CMC) of CHAPS allows the detergent to be easily removed by dialysis and is also compatible with trypsin digestion[58] and mass spectrometric analysis.[59]

GPI-Anchored Protein Enrichment. Lipid raft preparations are commonly used to isolate GPI-anchored proteins by solubilizing the membrane in Triton X-100 and separating the detergent-resistant membrane (DRM) containing lipid rafts.[13,15] The largest number of GPI-anchored proteins that have been identified in an individual proteomic study from lipid raft preparations found 36 integral membrane proteins localized in lipid rafts; of these, 13 were annotated as GPI-anchored proteins.[60]

We used an alternative approach for enriching GPI-anchored proteins from the detergent phase of the Triton X-114 partitioning step by treating with PI-PLC to release the GPI-protein into the aqueous phase.[29] This approach has been previously applied for isolating GPI-anchored proteins from *A. thaliana*[29] and was included in the workflow to isolate GPI-anchored proteins, as the subsequent glycoprotein fractionation of enriched membrane proteins by lectin affinity and hydrazine chemistry were unable to retrieve this class of membrane glycoproteins.

We isolated a total of 13 GPI-anchored proteins from rat liver membranes using this strategy, of which four previously unidentified GPI-anchored proteins were predicted. Limbic system-associated membrane protein precursor (LSAMP) and Neuronal growth regulator 1 were identified in the rat liver for the first time as previous studies have only suggested their involvement in the CNS.[61,62] LSAMP has been described as being expressed by neurons responsible for mediating selective

neuron growth and axon targeting. Overexpression of LSAMP has been shown to cause neuritic and synaptic dysfunction in schizophrenia and bipolar disorder.[61] Neuronal growth factor regulator 1 has only been identified to be expressed in the brain as a cell adhesion molecule and may also function as a neural growth promoting factor for axon development.[62] The function of these neuronal proteins in the liver remains to be elucidated. A total of 61 GPI-anchored proteins from the total rat proteome have been identified to date with the majority identified in the brain (13), kidney (12) CNS (10) and lung/gut (9) based on Swiss-Prot annotations. PI-PLC is specific for hydrolyzing the GPI-anchor, but palmitoylation of the GPI-anchor at the myo-inositol 2-position and/or 3-position of the inositol ring can prohibit cleavage by PI-PLC.[63]

Lectin Affinity Enrichment of Membrane Proteins. The combination of immobilized lectins ConA, Jacalin and WGA has been used as a multilectin affinity support for identifying biomarkers in serum and plasma.[32,64] The multilectin affinity technique has been demonstrated to fractionate glycoproteins with great reproducibility and high yield. We used these three lectins in parallel to attempt to distinguish different subsets of glycoproteins fractionated by these lectins. There was differential enrichment of some rat liver proteins using ConA, Jacalin and WGA with each lectin capturing some glycoproteins uniquely and with many N-linked glycoproteins captured by all three lectins. Another study[65] has used ConA to enrich for membrane glycoproteins from *Caenorhabditis elegans*. The tryptic glycopeptides were enriched using ConA and treated with PNGase F to determine N-glycosylation sites.

Jacalin is widely used in affinity chromatography as a general lectin for O-linked glycoproteins due to its specificity for Gal(β1-3)GalNAc.[34] However, surface-plasmon-resonance measurements and X-ray crystallographic studies have demonstrated that Jacalin binds mannose and oligomannosides, as well as glucose, *N*-acetylneuraminic acid and *N*-acetylmuramic acid.[35] Our results show that Jacalin fractionated a large number of membrane proteins containing potential N-linked glycosylation sites; and these were shown to overlap with some proteins fractionated by ConA and WGA. Potential O-glycosylated proteins isolated by Jacalin were not assessed in this study, as their glycan attachments do not have a consensus sequence as with *N*-glycosylation. The results presented in this study support the notion that, in addition to specificity for O-glycans, Jacalin may also have affinity for N-glycans.

ConA and WGA are the most common lectins used to isolate N-linked glycoproteins and glycopeptides and have been used to isolate membrane surface glycoproteins.[30] ConA and WGA have relative affinities for different sugar epitopes and common as well as unique proteins have been captured by the two lectins.[30,66] The application of both lectins allows greater coverage in capturing N-linked glycoproteins. Previous studies to enrich for membrane proteins from K562 cells using ConA and WGA isolated a total of 158 proteins containing 36 and 18 membrane proteins, respectively.[30] In our study, lectin affinity chromatography fractionated 423 proteins in total; 277 of these proteins were characterized as membrane proteins. Out of the 277 membrane proteins, 202 (73%) were predicted to contain N-linked glycosylation sites, which included receptors, membrane-associated ligands, proteases, phosphatases, and structural and adhesion proteins. A large subset of nonglycosylated cytoplasmic proteins (146) was identified to bind to the lectins. High-abundance nonglycosylated *E. coli* proteins were also shown to bind ConA, demonstrating that nonspecific binding of proteins to lectins occurs and may account for this nonselectivity.

Enrichment of Membrane Proteins by Hydrazine Immobilization. An alternative approach for enriching glycoproteins uses oxidation of the sugars and coupling of the glycoprotein onto a hydrazide resin. The captured glycoprotein is then hydrolyzed by trypsin and the eluted peptides are used to identify the protein. This approach has been used to identify glycoproteins from human cerebrospinal fluid (CSF),[38] human platelet proteins[67] and cell surface proteins from the LNCaP prostate cancer epithelial cell line.[68] Using hydrazine chemistry to enrich for rat liver membrane glycoproteins showed that 78% (210) of the membrane proteins identified had predicted N-linked glycosylation sites. Surprisingly, 14% (53) of these proteins were classified as cytoplasmic and nuclear proteins with putative N-glycosylation motifs. Many cytoplasmic and nuclear proteins are known to be modified by the single monosaccharide *O*-*N*-acetylglucosamine (*O*-GlcNAc). However, studies to identify *O*-GlcNAc modification sites on microtubule-associated proteins showed that *O*-GlcNAc was not affected by periodate oxidation,[69] and therefore could not account for our finding. To check for the possibilities of either nonspecific binding or oxidation of amino acids and hydrazine binding of the protein, we carried out the hydrazine coupling chemistry using *E. coli* cell lysates and membranes. NanoLC-MS/MS identified a significant number of *E. coli* proteins immobilized on the hydrazide gel, which supports the notion that nonglycosylation dependent conjugation of proteins to the hydrazine resin can occur.

Comparison of Lectin Affinity and Hydrazine Coupling Chemistry for Enrichment of Membrane Proteins. Fractionating membrane proteins using lectin affinity has the advantage of eluting bound proteins while maintaining the glycans intact. This enables further analyses of their attached glycans, which have been shown to be important for vaccine targeting[70] and assessing disease progression.[11,70,71] Although the hydrazine chemistry approach for enriching membrane proteins destroys the attached glycans in the process of attaching the proteins, the recovery from fractionating complex mixtures is easier and quicker,[70] as the eluted peptides can be directly subjected to MS analysis. In the case of lectin affinity fractionation, lectin eluates require the removal of the competing monosaccharides prior to trypsin digestion and MS analysis.

It was expected that the more general approach of hydrazine chemistry would enrich a significantly higher number of membrane glycoproteins compared with lectin affinity chromatography. However, approximately the same number of, but largely different, membrane proteins were identified by both approaches. Analysis of their distribution and characteristics demonstrated that the two approaches selected for different properties. A large proportion of the membrane proteins fractionated by lectin affinity chromatography were localized to the extracellular surface of the plasma membrane. Some of these proteins are known to have functional roles in protein and ion binding (54%), protein and ion transport (11%) and signal transduction (7%) (Supporting Information). Interestingly, lectin affinity (40) also fractionated a larger proportion of membrane proteins with predicted molecular weight >100 kDa compared to hydrazine chemistry (17) (Figure 8A). In addition, lectin affinity was able to fractionate a larger proportion of membrane proteins with multiple N-linked glycosylation sites (>3 predicted N-linked glycosylation sites) (Figure 8B). We suspect that size, physicochemical properties and glycoside

Downloaded by MACQUARIE UNIV on September 2, 2009 | http://pubs.acs.org
Publication Date (Web): January 6, 2009 | doi: 10.1021/pr800910w

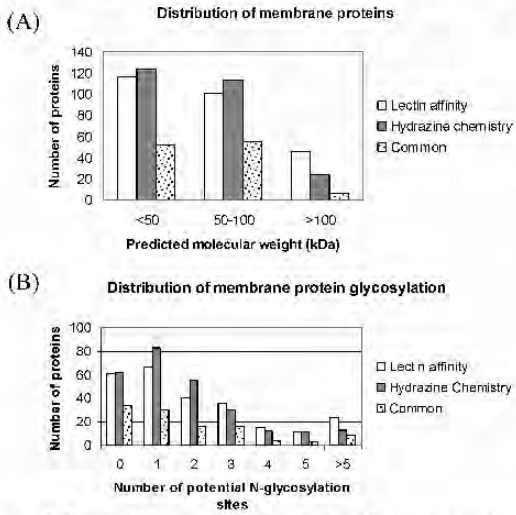

Figure 8. Size and glycosylation distribution of unique membrane proteins isolated by lectin affinity and hydrazine chemistry. (A) Size distribution of the membrane proteins enriched by lectin affinity chromatography and hydrazine chemistry (B) Distribution of potential N-linked glycosylation sites on membrane proteins fractionated by lectin affinity chromatography and hydrazine chemistry

clustering of these membrane proteins with their attached glycans could contribute to the differential enrichment by lectin affinity chromatography. The multimeric complex of lectins means that they are able to vary their structure to change specificity and select for multivalent carbohydrate ligands.[72]

Hydrazine chemistry fractionated a larger proportion of intracellular membrane proteins including UDP-transferases, cytochrome p450s and solute carrier transporters. Many of these are predominately responsible for protein and ion binding (54%), catalytic activity (37%), and protein and ion transport (5%) (Supporting information).

On the basis of our results, the differences observed in the enrichment of membrane proteins with predicted N-linked glycosylation sites by lectin affinity compared to hydrazine coupling may be explained by (1) the structural flexibility and conformation of lectin binding sites, (2) saturation of the affinity columns due to a large number of membrane proteins with glycosylation sites, and/or (3) nonspecific protein binding to the support media.

With the goal of developing a strategy for identifying membrane proteins from tissue samples and based on the localization of glycosylated proteins on the cell surface, we have used Triton X-114 phase partitioning followed by glycoprotein capture by lectin affinity chromatography or hydrazine chemistry to enrich and identify rat liver membrane proteins. A similar approach has very recently been applied by another laboratory to analyze a cancer cell line glycoproteome.[73] From the detergent fraction, lectin affinity chromatography fractionated 277 membrane proteins, while hydrazine chemistry pulled down 269 membrane proteins. Both techniques isolated a common subset of 122 membrane proteins. In total, 424 nonredundant membrane proteins were identified using both fractionation methods. Of these, 335 had potential N-glycosylation sites. To our knowledge, this represents the first study to characterize the rat liver membrane glycoproteome and has utility for further studies to characterize GPI-anchored proteins and the membrane glycoproteome of other systems.

Abbreviations: LC, liquid chromatography; MS, mass spectrometry; MS/MS, tandem mass spectrometry; ConA, concanavalin A; WGA, wheat germ agglutinin.

Acknowledgment. The research was supported by the Australian Research Council and GE Healthcare, Sweden. The authors would like to thank Lars Andersson, Susanna Lindman, and Brian Hood. This research project was facilitated by access to the Australian Proteomics Analysis Facility (APAF) established under the Australian Government's NCRIS program.

Supporting Information Available: Supporting Information contains nonredundant membrane protein identifications at each step of our workflow. In addition, the list of membrane proteins identified in the aqueous phase following phase partitioning, and summarized results of the subcellular location of membrane proteins identified from lectin affinity and hydrazine chemistry. This material is available free of charge via the Internet at http://pubs.acs.org.

References

(1) Qoronfleh, M. W.; Benton, B.; Ignacio, R.; Kaboord, B. Selective enrichment of membrane proteins by partition phase separation for proteomic studies. *J. Biomed. Biotechnol.* **2003**, *2003* (4), 249–255.
(2) Singer, S. J.; Nicolson, G. L. The fluid mosaic model of the structure of cell membranes. *Science* **1972**, *175* (23), 720–31.
(3) Jentoft, N. Why are proteins O-glycosylated. *Trends Biochem. Sci.* **1990**, *15* (8), 291–294.
(4) Holland, N. B.; Qiu, Y.; Ruegsegger, M.; Marchant, R. E. Biomimetic engineering of non-adhesive glycocalyx-like surfaces using oligosaccharide surfactant polymers. *Nature* **1998**, *392* (6678), 799–801.
(5) Hirabayashi, J.; Kasai, K. Separation technologies for glycomics. *J. Chromatogr., B: Anal. Technol. Biomed. Life Sci.* **2002**, *771* (1–2), 67–87.
(6) Vlassara, H.; Palace, M. R. Diabetes and advanced glycation endproducts. *J. Intern. Med.* **2002**, *251* (2), 87–101.
(7) Kirkham, S.; Sheehan, J. K.; Knight, D.; Richardson, P. S.; Thornton, D. J. Heterogeneity of airways mucus: variations in the amounts and glycoforms of the major oligomeric mucins MUC5AC and MUC5B. *Biochem. J.* **2002**, *361* (Pt 3), 537–546.
(8) Reddy, G. K.; Dhar, S. C. Studies on carbohydrate moieties of glycoproteins in established adjuvant induced arthritis. *Agents Actions* **1988**, *25* (1–2), 63–70.
(9) Ahmed, N.; Thornalley, P. J. Chromatographic assay of glycation adducts in human serum albumin glycated in vitro by derivatization with 6-aminoquinolyl-N-hydroxysuccinimidyl-carbamate and intrinsic fluorescence. *Biochem. J.* **2002**, *364* (Pt 1), 15–24.
(10) Sato, T.; Kawada, T.; Sugimachi, M.; Sunagawa, K. Bionic technology revitalizes native baroreflex function in rats with baroreflex failure. *Circulation* **2002**, *106* (6), 730–734.
(11) Xiong, L.; Andrews, D.; Regnier, F. Comparative proteomics of glycoproteins based on lectin selection and isotope coding. *J. Proteome Res.* **2003**, *2* (6), 618–625.
(12) Ferguson, M. A.; Homans, S. W.; Dwek, R. A.; Rademacher, T. W. Glycosyl-phosphatidylinositol moiety that anchors Trypanosoma brucei variant surface glycoprotein to the membrane. *Science* **1988**, *239* (4841 Pt 1), 753–759.
(13) Sharom, F. J.; Lehto, M. T. Glycosylphosphatidylinositol-anchored proteins: structure, function, and cleavage by phosphatidylinositol-specific phospholipase C. *Biochem. Cell Biol.* **2002**, *80* (5), 535–549.
(14) Brown, D. A. Interactions between GPI-anchored proteins and membrane lipids. *Trends Cell Biol* **1992**, *2* (11), 338–43.
(15) Sharom, F. J.; Radeva, G. GPI-anchored protein cleavage in the regulation of transmembrane signals. *Subcell. Biochem.* **2004**, *37*, 285–315.
(16) Simons, K.; Ikonen, E. Functional rafts in cell membranes. *Nature* **1997**, *387* (6633), 569–572.

Downloaded by MACQUARIE UNIV on September 2, 2009 | http://pubs.acs.org
Publication Date (Web): January 6, 2009 | doi: 10.1021/pr800910w

(17) Simons, K.; Vaz, W. L. Model systems, lipid rafts, and cell membranes. *Annu. Rev. Biophys. Biomol. Struct.* **2004**, *33*, 269–295.
(18) Rothberg, K. G.; Ying, Y. S.; Kolhouse, J. F.; Kamen, B. A.; Anderson, R. G. The glycophospholipid-linked folate receptor internalizes folate without entering the clathrin-coated pit endocytic pathway. *J. Cell Biol.* **1990**, *110* (3), 637–649.
(19) Kooyman, D. L.; Byrne, G. W.; McClellan, S.; Nielsen, D.; Tone, M.; Waldmann, H.; Coffman, T. M.; McCurry, K. R.; Platt, J. L.; Logan, J. S. In vivo transfer of GPI-linked complement restriction factors from erythrocytes to the endothelium. *Science* **1995**, *269* (5220), 89–92.
(20) Nosjean, O.; Briolay, A.; Roux, B. Mammalian GPI proteins: sorting, membrane residence and functions. *Biochim. Biophys. Acta* **1997**, *1331* (2), 153–186.
(21) Williams, M. E.; Brust, P. F.; Feldman, D. H.; Patthi, S.; Simerson, S.; Maroufi, A.; McCue, A. F.; Velicelebi, G.; Ellis, S. B.; Harpold, M. M. Structure and functional expression of an omega-conotoxin-sensitive human N-type calcium channel. *Science* **1992**, *257* (5068), 389–395.
(22) Washburn, M. P.; Wolters, D.; Yates, J. R., III. Large-scale analysis of the yeast proteome by multidimensional protein identification technology. *Nat. Biotechnol.* **2001**, *19* (3), 242–247.
(23) Chick, J. M.; Haynes, P. A.; Molloy, M. P.; Bjellqvist, B.; Baker, M. S.; Len, A. C. Characterization of the rat liver membrane proteome using peptide immobilized pH gradient isoelectric focusing. *J. Proteome Res.* **2008**, *7* (3), 1036–1045.
(24) Rabilloud, T. Membrane proteins ride shotgun. *Nat. Biotechnol.* **2003**, *21* (5), 508–510.
(25) Nesvizhskii, A. I.; Aebersold, R. Interpretation of shotgun proteomic data: the protein inference problem. *Mol. Cell. Proteomics* **2005**, *4* (10), 1419–1440.
(26) Everberg, H.; Peterson, R.; Rak, S.; Tjerneld, F.; Emanuelsson, C. Aqueous two-phase partitioning for proteomic monitoring of cell surface biomarkers in human peripheral blood mononuclear cells. *J. Proteome Res.* **2006**, *5* (5), 1168–1175.
(27) Bordier, C. Phase separation of integral membrane proteins in Triton X-114 solution. *J. Biol. Chem.* **1981**, *256* (4), 1604–1607.
(28) Haynes, P. A.; Gooley, A. A.; Ferguson, M. A.; Redmond, J. W.; Williams, K. L. Post-translational modifications of the Dictyostelium discoideum glycoprotein PsAGlycosylphosphatidylinositol membrane anchor and composition of O-linked oligosaccharides. *Eur. J. Biochem.* **1993**, *216* (3), 729–737.
(29) Elortza, F.; Nuhse, T. S.; Foster, L. J.; Stensballe, A.; Peck, S. C.; Jensen, O. N. Proteomic analysis of glycosylphosphatidylinositol-anchored membrane proteins. *Mol. Cell. Proteomics* **2003**, *2* (12), 1261–1270.
(30) Ghosh, D.; Krokhin, O.; Antonovici, M.; Ens, W.; Standing, K. G.; Beavis, R. C.; Wilkins, J. A. Lectin affinity as an approach to the proteomic analysis of membrane glycoproteins. *J. Proteome Res.* **2004**, *3* (4), 841–850.
(31) Jones, M. N. Surfactants in membrane solubilisation. *Int. J. Pharm.* **1999**, *177* (2), 137–159.
(32) Yang, Z.; Hancock, W. S. Approach to the comprehensive analysis of glycoproteins isolated from human serum using a multi-lectin affinity column. *J. Chromatogr., A* **2004**, *1053* (1−2), 79–88.
(33) Reeke, G. N., Jr.; Becker, J. W.; Cunningham, B. A.; Wang, J. L.; Yahara, I.; Edelman, G. M. Structure and function of concanavalin A. *Adv. Exp. Med. Biol.* **1975**, *55*, 13–33.
(34) Roque-Barreira, M. C.; Campos-Neto, A. Jacalin: an IgA-binding lectin. *J. Immunol.* **1985**, *134* (3), 1740–1743.
(35) Bourne, Y.; Astoul, C. H.; Zamboni, V.; Peumans, W. J.; Menu-Bouaouiche, L.; Van Damme, E. J.; Barre, A.; Rouge, P. Structural basis for the unusual carbohydrate-binding specificity of jacalin towards galactose and mannose. *Biochem. J.* **2002**, *364* (Pt 1), 173–180.
(36) Nagata, Y.; Burger, M. M. Wheat germ agglutinin. Molecular characteristics and specificity for sugar binding. *J. Biol. Chem.* **1974**, *249* (10), 3116–3122.
(37) Tian, Y.; Zhou, Y.; Elliott, S.; Aebersold, R.; Zhang, H. Solid-phase extraction of N-linked glycopeptides. *Nat. Protoc.* **2007**, *2* (2), 334–339.
(38) Pan, S.; Wang, Y.; Quinn, J. F.; Peskind, E. R.; Waichunas, D.; Wimberger, J. T.; Jin, J.; Li, J. G.; Zhu, D.; Pan, C.; Zhang, J. Identification of glycoproteins in human cerebrospinal fluid with a complementary proteomic approach. *J. Proteome Res.* **2006**, *5* (10), 2769–2779.
(39) Ramachandran, P.; Boontheung, P.; Xie, Y.; Sondej, M.; Wong, D. T.; Loo, J. A. Identification of N-linked glycoproteins in human saliva by glycoprotein capture and mass spectrometry. *J. Proteome Res.* **2006**, *5* (6), 1493–1503.
(40) Zhang, H.; Liu, A. Y.; Loriaux, P.; Wollscheid, B.; Zhou, Y.; Watts, J. D.; Aebersold, R. Mass spectrometric detection of tissue proteins in plasma. *Mol. Cell. Proteomics* **2007**, *6* (1), 64–71.
(41) Molloy, M. P.; Herbert, B. R.; Slade, M. B.; Rabilloud, T.; Nouwens, A. S.; Williams, K. L.; Gooley, A. A. Proteomic analysis of the Escherichia coli outer membrane. *Eur. J. Biochem.* **2000**, *267* (10), 2871–2881.
(42) Miller, I.; Haynes, P.; Eberini, I.; Gemeiner, M.; Aebersold, R.; Gianazza, E., III. Gender-related differences in protein concentration under baseline conditions and upon experimental inflammation as evaluated by two-dimensional electrophoresis. *Electrophoresis* **1999**, *20* (4−5), 836–845.
(43) Craig, R.; Beavis, R. C. TANDEM: matching proteins with tandem mass spectra. *Bioinformatics* **2004**, *20* (9), 1466–1467.
(44) Peng, J.; Elias, J. E.; Thoreen, C. C.; Licklider, L. J.; Gygi, S. P. Evaluation of multidimensional chromatography coupled with tandem mass spectrometry (LC/LC-MS/MS) for large-scale protein analysis: the yeast proteome. *J. Proteome Res.* **2003**, *2* (1), 43–50.
(45) Krogh, A.; Larsson, B.; von Heijne, G.; Sonnhammer, E. L. Predicting transmembrane protein topology with a hidden Markov model: application to complete genomes. *J. Mol. Biol.* **2001**, *305* (3), 567–580.
(46) Fankhauser, N.; Maser, P. Identification of GPI anchor attachment signals by a Kohonen self-organizing map. *Bioinformatics* **2005**, *21* (9), 1846–1852.
(47) Fujiki, Y.; Hubbard, A. L.; Fowler, S.; Lazarow, P. B. Isolation of intracellular membranes by means of sodium carbonate treatment: application to endoplasmic reticulum. *J. Cell Biol.* **1982**, *93* (1), 97–102.
(48) Molloy, M. P.; Herbert, B. R.; Walsh, B. J.; Tyler, M. I.; Traini, M.; Sanchez, J. C.; Hochstrasser, D. F.; Williams, K. L.; Gooley, A. A. Extraction of membrane proteins by differential solubilization for separation using two-dimensional gel electrophoresis. *Electrophoresis* **1998**, *19* (5), 837–844.
(49) Kyte, J.; Doolittle, R. F. A simple method for displaying the hydropathic character of a protein. *J. Mol. Biol.* **1982**, *157* (1), 105–132.
(50) Mengesdorf, T.; Althausen, S.; Mies, G.; Olah, L.; Paschen, W. Phosphorylation state, solubility, and activity of calcium/calmodulin-dependent protein kinase II alpha in transient focal ischemia in mouse brain. *Neurochem. Res.* **2002**, *27* (6), 477–484.
(51) Lin, P. P.; Barry, R. C.; Smith, D. L.; Smith, J. B. In vivo acetylation identified at lysine 70 of human lens alphaA-Crystallin. *Protein Sci.* **1998**, *7* (6), 1451–1457.
(52) Widell, S.; Lundborg, T.; Larsson, C. Plasma membranes from oats prepared by partition in an aqueous polymer two-phase system: on the use of light-induced cytochrome b reduction as a marker for the plasma membrane. *Plant Physiol* **1982**, *70* (5), 1429–1435.
(53) Zhang, L. J.; Wang, X. E.; Peng, X.; Wei, Y. J.; Cao, R.; Liu, Z.; Xiong, J. X.; Yin, X. F.; Ping, C.; Liang, S. Proteomic analysis of low-abundant integral plasma membrane proteins based on gels. *Cell. Mol. Life Sci.* **2006**, *63* (15), 1790–1804.
(54) Molloy, M. P. Two-dimensional electrophoresis of membrane proteins using immobilized pH gradients. *Anal. Biochem.* **2000**, *280* (1), 1–10.
(55) Speers, A. E.; Wu, C. C. Proteomics of integral membrane proteins--theory and application. *Chem. Rev.* **2007**, *107* (8), 3687–3714.
(56) Ghosh, D.; Beavis, R. C.; Wilkins, J. A. The identification and characterization of membranome components. *J. Proteome Res.* **2008**, *7* (4), 1572–1583.
(57) Maher, P. A.; Singer, S. J. Anomalous interaction of the acetylcholine receptor protein with the nonionic detergent Triton X-114. *Proc. Natl. Acad. Sci. U.S.A.* **1985**, *82* (4), 958–962.
(58) Zhang, N.; Li, L. Effects of common surfactants on protein digestion and matrix-assisted laser desorption/ionization mass spectrometric analysis of the digested peptides using two-layer sample preparation. *Rapid Commun. Mass Spectrom.* **2004**, *18* (8), 889–896.
(59) Loo, R. R.; Dales, N.; Andrews, P. C. Surfactant effects on protein structure examined by electrospray ionization mass spectrometry. *Protein Sci.* **1994**, *3* (11), 1975–1983.
(60) Martosella, J.; Zolotarjova, N.; Liu, H.; Moyer, S. C.; Perkins, P. D.; Boyes, B. E. High recovery HPLC separation of lipid rafts for membrane proteome analysis. *J. Proteome Res.* **2006**, *5* (6), 1301–1312.
(61) Behan, A.; Byrne, C.; Dunn, M. J.; Cagney, G.; Cotter, D. R. Proteomic analysis of membrane microdomain-associated proteins in the dorsolateral prefrontal cortex in schizophrenia and bipolar disorder reveals alterations in LAMP, STXBP1 and BASP1 protein expression. *Mol. Psychiatry* **2008**, in press.

Downloaded by MACQUARIE UNIV on September 2, 2009 | http://pubs.acs.org
Publication Date (Web): January 6, 2009 | doi: 10.1021/pr800910w

(62) Funatsu, N.; Miyata, S.; Kumanogoh, H.; Shigeta, M.; Hamada, K.; Endo, Y.; Sokawa, Y.; Maekawa, S. Characterization of a novel rat brain glycosylphosphatidylinositol-anchored protein (Kilon), a member of the IgLON cell adhesion molecule family. *J. Biol. Chem.* **1999**, *274* (12), 8224–8230.
(63) Ferguson, M. A. Site of palmitoylation of a phospholipase C-resistant glycosylphosphatidylinositol membrane anchor. *Biochem. J.* **1992**, *284* (Pt 2), 297–300.
(64) Yang, Z.; Harris, L. E.; Palmer-Toy, D. E.; Hancock, W. S. Multilectin affinity chromatography for characterization of multiple glycoprotein biomarker candidates in serum from breast cancer patients. *Clin Chem* **2006**, *52* (10), 1897–1905.
(65) Kaji, H.; Saito, H.; Yamauchi, Y.; Shinkawa, T.; Taoka, M.; Hirabayashi, J.; Kasai, K.; Takahashi, N.; Isobe, T. Lectin affinity capture, isotope-coded tagging and mass spectrometry to identify N-linked glycoproteins. *Nat. Biotechnol.* **2003**, *21* (6), 667–672.
(66) Xu, Z.; Zhou, X.; Lu, H.; Wu, N.; Zhao, H.; Zhang, L.; Zhang, W.; Liang, Y. L.; Wang, L.; Liu, Y.; Yang, P.; Zha, X. Comparative glycoproteomics based on lectins affinity capture of N-linked glycoproteins from human Chang liver cells and MHCC97-H cells. *Proteomics* **2007**, *7* (14), 2358–2370.
(67) Lewandrowski, U.; Moebius, J.; Walter, U.; Sickmann, A. Elucidation of N-glycosylation sites on human platelet proteins: a glycoproteomic approach. *Mol. Cell. Proteomics* **2006**, *5* (2), 226–233.
(68) Zhang, H.; Li, X. J.; Martin, D. B.; Aebersold, R. Identification and quantification of N-linked glycoproteins using hydrazide chemistry, stable isotope labeling and mass spectrometry. *Nat. Biotechnol.* **2003**, *21* (6), 660–666.
(69) Ding, M.; Vandre, D. D. High molecular weight microtubule-associated proteins contain O-linked-N-acetylglucosamine. *J. Biol. Chem.* **1996**, *271* (21), 12555–12561.
(70) Atwood, J. A., 3rd; Minning, T.; Ludolf, F.; Nuccio, A.; Weatherly, D. B.; Alvarez-Manilla, G.; Tarleton, R.; Orlando, R. Glycoproteomics of Trypanosoma cruzi trypomastigotes using subcellular fractionation, lectin affinity, and stable isotope labeling. *J. Proteome Res.* **2006**, *5* (12), 3376–3384.
(71) Springer, D. L.; Auberry, D. L.; Ahram, M.; Adkins, J. N.; Feldhaus, J. M.; Wahl, J. H.; Wunschel, D. S.; Rodland, K. D. Characterization of plasma membrane proteins from ovarian cancer cells using mass spectrometry. *Dis. Markers* **2003**, *19* (4–5), 219–228.
(72) Loris, R. Principles of structures of animal and plant lectins. *Biochim. Biophys. Acta* **2002**, *1572* (2–3), 198–208.
(73) McDonald, C. A.; Yang, J. Y.; Marathe, V.; Yen, T. Y.; Macher, B. A. Combining results from lectin affinity chromatography and glycocapture approaches substantially improves the coverage of the glycoproteome. *Mol. Cell. Proteomics* **2008**, in press.

PR800910W

Downloaded by MACQUARIE UNIV on September 2, 2009 | http://pubs.acs.org
Publication Date (Web): January 6, 2009 | doi: 10.1021/pr800910w

3.2.2. Glycopeptide capture as an alternative approach to identify membrane glycoproteins

In our previous study (Chapter 3.2.1) rat liver membrane glycoproteins were enriched using Triton X-114 phase partitioning and glycoprotein capture using lectin affinity and hydrazine chemistry. This approach identified 424 membrane proteins annotated by gene ontology to be membrane-associated, of which 335 (79%) of these proteins contained a predicted *N*-linked glycosylation site (N-X-S/T). In this section, we examine whether enriching for rat liver membrane tryptic glycopeptides, rather than glycoproteins, using three common glycopeptide capture methods could increase the number of membrane protein identifications. The glycopeptide capture methods used were: tri-lectin affinity (ConA, Jacalin and WGA) [203], hydrazine chemistry and hydrophilic interaction chromatography (HILIC). The glycopeptides strategy for identifying rat liver membrane glycoproteins was employed to tackle the challenges associated with selective enrichment of membrane glycoproteins due to their poor solubility in the aqueous buffers used for lectin and hydrazine-binding. The previous criteria for validating protein identifications using a minimum of two peptides was not applied here because glycopeptides generally represent only 2-5% of an entire tryptic digest [220] and many glycoproteins often contain less than two unique glycopeptides. Therefore, identified *N*-linked glycopeptides were manually validated by the presence of an *N*-glycosylation site (N-X-S/T). *N*-linked glycopeptides enriched by all three approaches were treated with PNGase F to remove *N*-glycans prior to RPLC-MS/MS analysis and protein identification.

Approximately 250 µg of rat liver membrane proteins were digested in-solution with trypsin as specified in Chapter 2. Lectin affinity and hydrazine chemistry to capture glycopeptides were carried out as previously described in **Publication I**. To isolate *N*-linked glycopeptides by HILIC, tryptic peptides were dried using a vacuum centrifuge, resuspended in 80% (v/v) ACN/5% (v/v) formic acid. HILIC resin (Waters, MA, USA) was packed on top of μC_{18} pipette tips and the HILIC resin was activated with 0.1% (v/v) formic acid followed by equilibration with 80% (v/v) ACN/5% (v/v) formic acid. Resuspended tryptic peptides

were loaded on top of the HILIC resin and washed with 80% (v/v) ACN/5% (v/v) formic acid to remove unbound peptides. Bound glycopeptides from all three capture methods were eluted with 0.1% (v/v) formic acid and subsequently digested with 5 µl PNGase F (0.5 U/µl) overnight at 37ºC. De-glycosylated peptides were analysed by RPLC-MS/MS as described in Chapter 2.

Hydrazine chemistry isolated more (44) unique *N*-linked glycopeptides compared to HILIC (32) and lectin affinity (24). All three methods isolated a common subset of 13 *N*-linked glycopeptides which matched to 12 glycoproteins. The largely different populations of *N*-linked glycopeptides isolated by lectin affinity, hydrazine chemistry and HILIC is most likely due to the different chemistries that the three methods use for capturing glycopeptides [220, 221]. For example, lectin affinity is based on the recognition of particular glycan epitopes and, hydrazine chemistry is based on the coupling of oxidized carbohydrates containing vicinal hydroxyl groups to the hydrazide groups on agarose support media. On the other hand, HILIC enrichment of glycopeptides is based on the interaction between polar species such as oligosaccharides and hydrophilic amino acids to either cellulose or Sepharose gel matrices [218] and/or to zwitterionic beads (Zic-HILIC) [286].

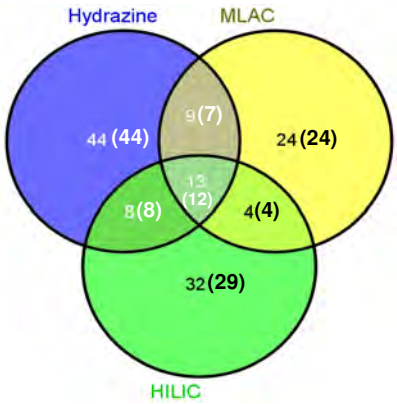

Figure 3-8. Number of N-linked glycopeptides containing the N-X-S/T sequence enriched using lectin affinity, hydrazine chemistry and HILIC. Numbers in brackets indicate matched proteins

Membrane proteins identified by all three glycopeptides capture approaches were localized to the plasma membrane (20%), mitochondria (16%), endoplasmic reticulum/Golgi apparatus (16%) and lysosomes and peroxisomes (6%). Cytoplasmic and peripheral

membrane proteins represented 35% of the total identified membrane glycoproteins (Appendix C-5).

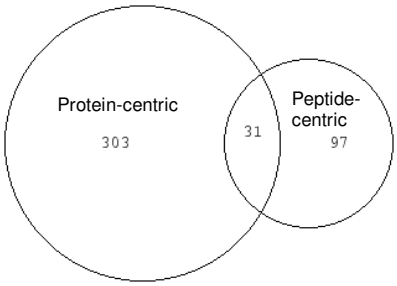

Figure 3-9. Number of membrane proteins containing a *N*-glycosylation site identified using glycopeptide- (lectin affinity, hydrazine chemistry and HILIC) and protein-centric approaches (lectin affinity and hydrazine chemistry).

Lectin affinity, hydrazine chemistry and HILIC enriched mostly different populations of *N*-linked glycopeptides demonstrating the complementarity of these strategies for glycopeptide identification (Figure 3-8). In total, 134 *N*-linked glycopeptides were identified from the three glycopeptide capture methods which corresponded to 128 unique glycoproteins (Figure 3-8 and Appendix C-5). This compares with the 334 *N*-linked membrane glycoproteins identified using the two glycoprotein (lectin affinity and hydrazine chemistry) capture methods (Chapter 3.2.1) (Figure 3-9). In addition, the identities of the proteins corresponding to the matched glycopeptides were largely different to the glycoproteins identified by protein-centric approaches (Figure 3-9). Generally, we observed less membrane protein identifications using the combined three approaches of glycopeptide enrichment and therefore targeting glycopeptides for membrane protein characterisation was not adopted for subsequent studies.

3.3.Glycomics

The approach of using hydrazine chemistry to identify membrane glycoproteins has been shown (Chapter 3.2) to result in a higher level of glycoprotein identifications (78%) compared to lectin enrichment (71%). However, lectin affinity approaches to glycoprotein enrichment have the advantage of maintaining the attached protein carbohydrates intact and able to be

characterised. Mass spectrometry (MS) has proven to be a useful technique for detailed glycomic analysis of glycans and glycoconjugates in complex biological samples. However, identification of low abundance glycoconjugates is often difficult in complex samples and therefore strategies for targeting and isolating these molecules are required to reduce the complexity and improve their characterization by MS. One of the most common methods used for isolating glycoconjugates and free oligosaccharides is lectin affinity chromatography. Lectins are proteins found in plants, animals and microorganisms that display affinity towards different oligosaccharide epitope structures. However, the mechanism(s) of how carbohydrate residues and sequences are recognized by lectins in complex mixtures of proteins are largely unknown. In the present study, three lectins (ConA, Jacalin and WGA) were used to enrich *N*- and *O*-linked glycoproteins from Triton X-114 phase partitioned rat liver membrane proteins. Enrichment of glycoproteins has been shown to result from the use of these lectins (Chapter 3.2.1) and analysis of the glycosylation of proteins that were bound and flowed through the lectin columns was carried out to determine the efficacy of using this approach to study the membrane glycoproteome.

3.3.1. The lectin riddle: glycoproteins fractionated from complex mixtures have similar glycomic profiles (Publication II)

OMICS: A Journal of Integrative Biology

OMICS: A Journal of Integrative Biology: http://mc.manuscriptcentral.com/omics

The lectin riddle: glycoproteins fractionated from complex mixtures have similar glycomic profiles

Journal:	*OMICS: A Journal of Integrative Biology*
Manuscript ID:	OMI-2010-0075
Manuscript Type:	Original Article
Date Submitted by the Author:	15-Jun-2010
Complete List of Authors:	Lee, Albert; Macquarie University, Chemistry and Biomolecular Sciences Nakano, Miyako; Macquarie University, Chemistry and Biomolecular Sciences Hincapie, Marina; Northeastern University, Chemistry and Chemical Biology Kolarich, Daniel; Macquarie University, Chemistry and Biomolecular Sciences Baker, Mark; Macquarie University, Chemistry and Biomolecular Sciences Hancock, William; Northeastern University, Chemistry and Chemical Biology Packer, Nicolle; Macquarie University, Chemistry and Biomolecular Sciences
Keyword:	Proteomics, Proteome, Other

Mary Ann Liebert, Inc., 140 Huguenot Street, New Rochelle, NY 10801

The lectin riddle: glycoproteins fractionated from complex mixtures have similar glycomic profiles

Albert Lee[1*], Miyako Nakano[1*], Marina Hincapie[2], Daniel Kolarich[1], Mark S. Baker[1], William S. Hancock[2], Nicolle H. Packer[1†]

1. Department of Chemistry and Biomolecular Sciences, Macquarie University, NSW 2109 Australia

2. Department of Chemistry and Chemical Biology, Northeastern University, Boston MA 02115 USA

*These authors contributed equally

†Corresponding author

Prof Nicolle H. Packer

Bldg E8C Room 307

Department of Chemistry and Biomolecular Sciences

Macquarie University

NSW 2109

Australia

Contact: +61 2 9850 8176

Email: nicki.packer@mq.edu.au

For Peer Review

Abstract

One common method used for analysing the glycoproteome is chromatography using multiple lectins that display different affinities towards oligosaccharide structures. Much has been done to determine lectin affinity using standard glycoproteins with known glycosylation, however a knowledge of the selectivity and specificity of lectins exposed to complex mixtures of proteins is required if they are to be used as a means of studying the glycoproteome. In the present study, three lectins (Concanavalin A, Jacalin and Wheat Germ Agglutinin) were used to fractionate glycoproteins from two different complex environments 1) cell membranes and 2) plasma. Reproducible enrichment of glycoproteins from these samples has been shown to result from the combined use of these lectins. However, the global glycan profiles of the released *N*- and *O*-linked oligosaccharides from the glycoproteins retained by the lectins, and from those glycoproteins that did not bind, using both these complex samples, were found to be very similar. That is, although the lectins selectively and reproducibly retained some glycoproteins, other proteins with the same attached oligosaccharide structures did not bind. Some small *N*- and *O*-glycan differences were observed in the bound fractions but there was little absolute specificity towards individual oligosaccharide structures known to have high affinity to these lectins. These data indicate that lectins are useful for fractionating glycoproteins from complex mixtures, but that the overall glycoproteome is not isolated by this approach.

Introduction

Proteins secreted into the plasma or those destined to be localized to the cellular membrane are often glycosylated, and can serve a variety of structural and functional roles such as signal transduction, cell adhesion and protein localization (Holland et al.,1998). The attached carbohydrates can be covalently linked to the hydroxyl groups of serine or threonine (and hydroxylysine) residues (*O*-linked) or to the amide nitrogen of asparagine residues (*N*-linked) via the consensus sequence Asn-X-Ser/Thr (Cys), where X can be any amino acid except proline (Jentoft.1990). As more knowledge of glycoproteins and their attached glycans emerges, there is growing evidence that the abundance and heterogeneity of glycans can reflect the differences in cell types and states (Hirabayashi et al.,2002, Kanie et al.,2009) in diseases such as diabetes (Dayarathna et al.,2008, Vlassara et al.,2002), cystic fibrosis (Kirkham et al.,2002, Schulz et al.,2007), autoimmunity (Sato et al.,2002, Van Beneden et al.,2009) and cancer (Arnold et al.,2008, Xiong et al.,2003). Glycans are composed of monosaccharides that are covalently linked by glycosidic bonds, either in α or β configurations. However unlike proteins, which are linked in a linear structure, oligosaccharides are heterogeneous with branched structures formed by the different linkage(s) of one or more monosaccharides. The heterogeneity of glycans and lack of a template make it difficult to predict the type of glycans that are produced and their specific site(s) of attachment to proteins.

Recently, mass spectrometry has become increasingly used in glycoproteomics to 1) identify the glycosylated protein and peptides, 2) determine *N*- and *O*-glycosylation site(s) and, 3) analyse the structures of the attached glycan moieties (Tissot et al.,2009). With the completion of many genome and proteome databases, identification of proteins

is relatively easy, fast and automated, and usually involves i) 2DGE for protein separation, followed by MALDI-MS or ii) LC separation of proteins or peptides, followed by ESI-MS (Lim et al.,2003, Washburn et al.,2001). Identifying glycoproteins and glycopeptides by mass spectrometry in this context can be challenging due to the low level of different glycoforms of the same protein in complex mixtures, due to the attachment of structurally different glycans (microhetereogeneity) that can occupy (to varying degrees) different glycosylation sites (macroheterogeneity). Therefore, full characterization of glycoproteins from biological systems is a challenge which can be facilitated by enriching the glycoproteins from the complex mixtures of proteins. At present, the two most used methods for capturing glycoproteins are hydrazine coupling of *N*-linked glycoproteins and glycopeptides to a solid support (Zhang et al.,2003) and immobilized lectin chromatography that employs the affinity of these proteins for particular glycan sub-structures (Yang et al.,2004). The disadvantage of using the hydrazine chemistry approach is that the carbohydrates are destroyed by the oxidative chemical coupling to the hydrazine leaving the glycans no longer able to be identified and characterized. The use of lectins as a glycocapture method is considered to be a more favourable approach for glycosylation analysis since the integrity of the attached glycans is maintained during the fractionation.

Lectins are proteins found in plants, animals and micro-organisms and have different affinities for particular oligosaccharide structures displayed on proteins and lipids and are frequently used in cytology and histology to stain glycoproteins (Collins et al.,1982). Several lectins with different specificities have been used sequentially (Lee et al.,2009) and in parallel (Yang et al.,2004) to enrich glycoproteins from complex

mixtures; to identify low abundance plasma proteins (Yang et al.,2004), to examine the microheterogeneity of carbohydrates associated with disease and disease progression (Hirabayashi et al.,2002, Vlassara et al.,2002), to identify liver membrane glycoproteins (Lee et al.,2009) and to target specific glycosylation sites on proteins (Kaji et al.,2003). Although lectins have been used to isolate glycopeptides (Hirabayashi.,2004, Hirabayashi et al.,2002, Kaji et al.,2003) the focus of this paper is on investigating the role of lectins as a means of enriching glycoproteins from complex samples.

Three lectins, Concanavalin A (ConA), Jacalin and Wheat Germ Agglutinin (WGA) are commonly used in these types of experiments and have been used as a multi-lectin affinity chromatography (M-LAC) system for reproducibly enriching serum or plasma glycoproteins from breast cancer patients (Yang et al.,2006), autoimmune (Plavina et al.,2007) and metabolic syndrome diseases (Dayarathna et al.,2008). Using a mixture of lectins such as the M-LAC system has been demonstrated to increase the binding of glycoproteins compared to the use of a single lectin (Ralin et al.,2008). This is presumably due to the heterogeneity of glycosylation on individual proteins which could lead to multi-site attachment between the glycoprotein and the different lectins in the M-LAC system. ConA is a lectin found in the jack bean *Canavalia ensiformis* that is composed of identical protomers that combine to form a tetrameric complex. Each monomer is approximately 25 kDa in size and contains one saccharide binding site, which allows for four saccharides to be bound to the lectin at any given time (Becker et al.,1975, Cunningham et al.,1975, Edelman et al.,1972, Reeke et al.,1975). ConA primarily recognises α-mannose residues that are arranged in a trimannosyl (Manα(1,3)[Manα(1,6)]Man) configuration which is always part of the *N*-glycan core

structure (Goldstein.1975, Goldstein et al.,1965, Goldstein et al.,1965, Reeke et al.,1975). Con A has increased affinity for tri-mannosyl oligosaccharide structures that are elongated by α(1-2) linked mannose (or α-glucose) residues on high mannose and hybrid *N*-glycan structures (Brewer et al.,1986). However, tri- and tetra-antennary *N*-glycans and *N*-glycan structures that consist of a bisecting *N*-acetyl-D-glucosamine (GlcNAc) or a fucosylated core show reduced or no binding to ConA (Brewer et al.,1986, Cummings et al.,1982).

Jacalin is a lectin found in seeds of jack fruit (*Artocarpus integrifolia*) and is a homotetrameric glycoprotein of four identical protomers consisting of a light (β) and a heavy (α) polypeptide chain of 20 and 133 amino acid residues, respectively (Young et al.,1991). Jacalin undergoes a series of co- and post-translational processing events including signal peptide cleavage and *N*-linked glycosylation to produce the mature and functional tetrameric lectin. Jacalin has been acknowledged as a general lectin for *O*-glycans by its recognition of the ubiquitous *O*-linked structure galactosyl β(1-3) *N*-acetyl-galactosamine (Galβ(1-3)GalNAc), although it also has affinity for lactose and galactose (Bourne et al.,2002, Roque-Barreira et al.,1985). In addition, X-ray crystallography and surface plasmon resonance measurements have indicated that a relatively large carbohydrate-binding site enables Jacalin to also bind a number of different monosaccharides including mannose, oligomannosides, glucose, *N*-acetylneuraminic acid (NeuAc) and *N*-acetylmuramic acid (Bourne et al.,2002, Do et al.,1998). The affinity for these different sugars is thought to occur at the same binding site as galactose in the *O*-linked disaccharide and not at two distinct binding sites with different specificities (Bourne et al.,2002).

WGA is a lectin isolated from *Triticum vulgaris* that functions as a dimeric protein for carbohydrate binding, with each monomer having two oligosaccharide binding sites (Kronis et al.,1985, Nagata et al.,1972, Nagata et al.,1974). The two identical WGA monomers have a combined molecular weight of approximately 35 kDa with amino acid sequence made up of mostly glycine and half-cystine amino acids, with none of the half-cystines present as cysteines (Nagata et al.,1972). WGA exhibits a primary affinity for GlcNAcβ(1-4)GlcNAc and is commonly used to bind sialylated complex *N*-glycan structures due to its secondary affinity for NeuAcα(2,3) (Nagata et al.,1974). Despite its recognition of some sialylated glycans, WGA has very little or no affinity for NeuAcα(2,6) and NeuAcα(2,8) sialylated glycans (Iskratsch et al.,2009) and shows no recognition of core fucosylated *N*-glycan structures (Cummings et al.,1982, Iskratsch et al.,2009).

In this study, three immobilized lectins (ConA, Jacalin and WGA) commonly used to enrich *N*- and *O*-linked glycoproteins were applied to two different biological systems (Triton X-114 phase partitioned rat liver membranes, and albumin and IgG-depleted human plasma) to examine the differential enrichment of glycoproteins and their attached glycans. The global *N*- and *O*-glycan profiles of the lectin unbound and bound glycoproteins from rat liver membrane and human plasma were compared to try to understand the basis of the glycoprotein separation by lectin affinity chromatography in two different complex biological systems. We have previously described that these three lectins can be effectively and reproducibly used for proteomic studies to isolate subsets of glycoproteins from complex mixtures (Kullolli et al.,2010). The results presented here

demonstrate that lectin affinity for fractionating glycoproteins from complex samples can have limitations for glycomic analysis, which was not resolved by this approach.

For Peer Review

Materials and Methods

Materials

Tris, sodium chloride, ammonium bicarbonate (NH_4HCO_3), formic acid, Triton X-114, 3-[(3-Cholamidopropyl)dimethylammonio]-1-propanesulfonate (CHAPS), ammonium acetate (CH_3COONH_4), dithiothreitol (DTT), iodoacetamide (IAA), methyl-α-glucopyranoside, galactose, *N*-acetyl-glucosamine, urea, thiourea, tributyl phosphine (TBP), ovalbumin from *Gallus gallus*, glycerol, SDS, agarose bound Jacalin with protein concentration of 5 mg/mL and binding capacity of 1-2 mg human IgA/mL and, agarose bound WGA with protein concentration of 5 mg/mL and binding capacity 1-2 mg ovomucoid/mL were obtained from Sigma (St. Louis, MO, USA). α_1-protease inhibitor (A1PI) from human serum was a donation from Baxter Bioscience, Austria. Agarose bound Concanavalin A (ConA) with protein concentration of 10-16 mg/mL and binding capacity of 20-45 mg porcine thyroglobulin/mL was obtained from GE Healthcare (Uppsala, Sweden). Sequencing-grade trypsin was obtained from Promega (Madison, WI, USA). *N*-Glycosidase F (PNGase F, recombinant cloned from *Flavobacterium meningosepticum* and expressed in *Escherichia coli*) lyophilized in 10 mM sodium phosphate buffer, pH 7.2 was acquired from Roche Diagnostics (Basel, Switzerland). Immobilon-P polyvinylidene fluoride (PVDF) was purchased from Millipore (MA, USA). AG50W-X8 cation-exchange resin was obtained from Bio-Rad (Hercules CA, USA).

Rat liver membrane preparation

Rat liver membrane proteins were prepared according to our previous method (Lee et al.,2009). Briefly, rat liver tissue (~1.5 g) was homogenized in 5 mL lysis buffer (pH 7.4) containing 50 mM Tris-HCl, 0.1 M NaCl, 1 mM EDTA & protease inhibitor cocktail (Roche Diagnostics, Switzerland) using an Omni TH homogenizer (Omni International Inc, VA, USA) and centrifuged at 2,000g for 20 mins at room temperature. The supernatant containing cellular proteins was removed and diluted with binding buffer (20 mM Tris-HCl, 0.1 M NaCl, 1 mM $MnCl_2$, 1 mM $MgCl_2$ and 1 mM $CaCl_2$, pH 7.4) to a final volume of 40 mL and chilled on ice for 1 hr. This was to ensure that the applied sample was compatible with lectin affinity chromatography. The diluted proteins were sedimented by ultracentrifugation at 120 000 g_{avg} for 1 hr and 20 mins. The membrane pellet was washed twice with 0.1 M sodium carbonate (pH 11).

Approximately 100 µl (equivalent to approximately 0.5 mg) of the rat liver membrane pellet was homogenised with 4 volumes of binding buffer containing 1% (v/v) Triton X-114 and chilled on ice with intermittent vortexing for 20 mins. The samples were heated at 37 °C for 20 mins and phase partitioned by centrifugation at 300g for 5 mins. The upper aqueous phase was removed and stored and phase partitioning was repeated. The combined aqueous phases were mixed with 9 volumes of ice-cold acetone to precipitate proteins and remove any detergent. Membrane proteins contained in the Triton X-114 detergent phase were precipitated with 9 volumes of ice-cold acetone. Precipitated membrane proteins were resolubilised in binding buffer containing 1% (w/v) CHAPS, heated at 96°C for 6 mins, and stored at -80 °C if not used immediately. Protein quantification was performed using a Bradford Assay (Sigma-Aldrich, MO, USA)

Lectin affinity chromatography of rat liver membranes

Lectin affinity chromatography was carried out as previously described (Lee et al.,2009) Approximately 80 μg of detergent-partitioned proteins in 0.5 mL of binding buffer containing CHAPS was mixed with 0.25 ml of agarose-bound ConA (protein concentration 10-16 mg/ml and binding capacity of 20-45 mg porcine thyroglobulin/ml), 0.5 ml agarose-bound Jacalin (protein concentration 5 mg/ml and binding capacity of 1-2 mg human IgA/ml) and 0.5 ml of agarose-bound WGA (protein concentration 5 mg/ml and binding capacity of 1-2 mg ovomucoid/ml) and incubated at 4°C overnight. Each mixture was packed in disposable gravity-flow Poly-Prep chromatography columns (Bio-Rad, Hercules MA) and the three lectin columns were washed with 10 bed volumes of binding buffer. Bound proteins were then eluted with 10 column volumes of elution buffer A (20 mM Tris-HCl, 0.1 M NaCl, 0.2 M methyl-α-D glucopyranoside [ConA], 0.5 M α-D galactose [Jacalin] or 0.5 M *N*-acetyl glucosamine [WGA], pH 7.4), followed by 10 bed volumes of corresponding higher concentration elution buffer B (20 mM Tris-HCl, 0.1 M NaCl, 1 M methyl-α-D glucopyranoside [ConA], 1 M α-D galactose [Jacalin] or 1 M *N*-acetyl glucosamine [WGA], pH 7.4). Further elution of tightly bound proteins was performed using 10 bed volumes of the relevant elution buffer C (20 mM Tris-HCl, 0.1 M NaCl, 1.5 M methyl-α-D glucopyranoside [ConA], 1.5 M α-D galactose [Jacalin] and 1.5 M *N*-acetyl glucosamine [WGA], pH 7.4). All eluted samples were desalted and concentrated using an Amicon Ultra-10 centrifugal device with 10 kDa Nominal Molecular Weight Limit (NMWL) (Millipore, MA). Lectin eluates with high

concentrations of monosaccharides were diluted with water to assist in the diafiltration and concentration of proteins.

Lectin affinity chromatography of human plasma proteins

Human plasma glycoproteins were prepared as described (Kullolli et al.,2010). Briefly, 2 mL of human plasma (from a normal female volunteer) was depleted using a protein A and polystyrene-divinylbenzene support matrix (POROS) anti-HSA column to remove IgG and albumin from plasma respectively. Depleted plasma proteins (50 µl) were diluted 1:4 with binding buffer and subjected to a single chromatographic mixed bed support containing equal volumes of ConA (protein concentration 15 mg/ml and binding capacity of ~10 mg/ml fetuin and thyroglobulin), Jacalin (protein concentration 15 mg/ml and binding capacity of ~10 mg/ml fetuin and thyroglobulin) and WGA lectins (protein concentration 15 mg/ml and binding capacity of ~10 mg/ml fetuin and thyroglobulin) immobilized to POROS matrix beads (total bed volume ~0.5 ml) (Kullolli et al.,2008). The lectin column was initially washed with 5 column volumes of 50 mM Tris-HCl, 0.5 M NaCl, pH 7.4 (unbound fraction) to elute unbound proteins followed by 5 column volumes of 100 mM acetic acid, pH 4 to elute bound proteins. Both lectin bound and flow through (FT) fractions were transferred to a C4-reverse phase cartridge to concentrate and desalt the samples. Concentrated proteins were then lyophilized using a vacuum centrifuge and prepared for *N*- and *O*-linked oligosaccharide analysis.

SDS PAGE

Approximately 10 μg of phase partitioned membrane proteins was applied per lane onto NuPAGE 10% Bis-Tris pre-cast gradient gels with MOPS running buffer. Electrophoresis conditions were set to 200 V, 125 mA for 60 mins. The gels were fixed in 7% (v/v) acetic acid and 10% (v/v) methanol and stained overnight with Sypro Ruby (Invitrogen, San Diego, CA). Gel images were obtained using Typhoon Trio Variable Mode Imager (GE Healthcare, Uppsala, Sweden).

Release of *N*- and *O*-linked oligosaccharides

N- and *O*-linked oligosaccharides were sequentially released from lectin-fractionated rat liver membrane and human plasma proteins as described (Wilson et al.,2002) Briefly, Immobilon-P PVDF membranes were pre-wet with 100% (v/v) ethanol. Rat liver membrane proteins and lyophilized human plasma proteins were re-solubilised in 20 μl 8 M urea and dot-blotted (2 x 2.5 μL) on the PVDF membrane and left to dry overnight. PVDF membranes were then washed with methanol followed by water to remove residual salts and detergents. Protein spots were cut from the PVDF membrane and placed in separate wells of a 96-well microtiter plate. The spots were blocked with 100 μL of 1% (w/v) polyvinylpyrrolidone (PVP) 40 000 in 50% (v/v) methanol, agitated for 20 min, and washed thoroughly with water. *N*-linked oligosaccharides were released from the protein by incubation with 5 μL of PNGase F (0.5 units/μL) for 15 min at 37°C, and subsequently topped up with 10 μL water and incubated overnight at 37°C. The sample wells were surrounded by wells containing water to prevent evaporation, and the plate was sealed tightly with parafilm.

To recover *N*-linked oligosaccharides, the samples were sonicated in a water bath (in the 96-well plate) for 20 min, and the supernatant containing released *N*-linked oligosaccharides were collected. Spots were washed twice with 50 µL water, and combined with the supernatant and then reduced to alditols prior to LC separation. Before reduction the released *N*-linked oligosaccharides were incubated with 100 mM CH_3COONH_4 pH 5 (final concentration 15 mM) for 1 hr at room temperature to ensure complete regeneration of the reducing terminus. *N*-linked oligosaccharides were dried under vacuum centrifuge and reduced with 1 M $NaBH_4$/50 mM KOH (20 µL) at 50°C for 3 hrs. The reduction was quenched with 2 µL glacial acetic acid.

β-elimination of *O*-linked oligosaccharides was carried out after the PNGase F release of the *N*-linked oligosaccharides by re-wetting the protein spots with 2 µL methanol, and incubating 16 hrs with 0.5 M $NaBH_4$/50 mM KOH (20 µL) at 50°C. The reaction was quenched with 2 µL acetic acid and both reduced *N*- and *O*-linked oligosaccharides were purified as described below.

Purification of reduced *N*- and *O*-linked oligosaccharides.

Homemade cation exchange columns comprising 20 µL of AG50W-X8 cation-exchange resin (H^+–form) (BioRad, Hercules, CA) were packed on top of µC_{18} ZipTips (Schulz et al.,2002). Columns were prepared by washing 3 x 50 µL 1 M HCl, followed by 3 x 50 µL methanol and 3 x 50 µL water. *N*- and *O*-linked oligosaccharide alditols were eluted with 2 x 60 µL of water and dried. The borate was removed by the addition of 100 µL methanol and drying under vacuum five times. The oligosaccharides were re-suspended in 10 µL of 10 mM NH_4HCO_3 pH 7.8 for Carbon LC–ESI–MS/MS analysis.

Carbon LC-ESI-MS/MS

N- and *O*-linked oligosaccharide alditols were analyzed by porous graphitized carbon LC-MS/MS on a capillary LC-MS/MS using an Agilent MSD ion-trap XCT Plus mass spectrometer coupled to a Agilent 1100 capillary LC (Agilent Technologies, CA USA). The samples were applied to a Hypercarb porous graphitized carbon column (5 µm Hypercarb, 0.32 × 100 mm, Thermo Hypersil, Runcorn UK). *N*-linked oligosaccharides were separated using a linear gradient with 2-16% (v/v) ACN/10 mM NH_4HCO_3 for 45 min, followed by a gradient from 16-45% over 20 min before washing the column with 45% (v/v) ACN/10 mM NH_4HCO_3 at a flow rate of 5 µL/min for 6 minutes and re-equilibrating in 10 mM NH_4HCO_3. *O*-linked oligosaccharides were separated using a linear gradient with 0-25% (v/v) ACN/10 mM NH_4HCO_3 for 25 min, followed by a 10 min wash with 72% (v/v) ACN/10 mM NH_4HCO_3 at a flow rate of 5 µL/min. ESI–MS was performed in negative ion mode with two scan events: full scan with mass range *m/z* 100–2000 amu and dependent MS/MS scan after collision induced fragmentation. Automated peak recognition and tandem MS of the top three most intense precursor ions at 40% normalised collision energy was performed with an activation time of 30 ms. The composition of glycans was determined using the monoisotopic masses of detected ions and was verified by their associated MS/MS. Monoisotopic masses were searched using the GlycoMod software (available at http://www.expasy.ch/tools/glycomod) with parameters of ±0.3 Da to predict the possible glycan compositions corresponding to these masses.

Results and Discussion

Rat liver membranes and plasma were chosen to compare the capacity of the same three lectins (ConA, Jacalin and WGA) to enrich glycoproteins from highly heterogeneous mixtures of hydrophobic and hydrophilic proteins respectively. In addition, different elution conditions of the bound glycoproteins, via high concentrations of competing monosaccharides (membrane glycoproteins) or by a change in pH (plasma glycoproteins) were used to test for their efficacy in enriching for glycoproteins. The different binding and eluting buffers were necessary because of the particular conditions required to maintain the solubility of the hydrophobic membrane. and hydrophilic plasma. glycoproteins.

Lectin affinity chromatography of standard glycoproteins.

We first evaluated the characteristics of the binding of two standard *N*-linked glycoproteins (mixture of α_1-antitrypsin and ovalbumin) to the columns of immobilized ConA, Jacalin and WGA. α_1-antitrypsin and ovalbumin both contain three possible *N*-linked glycosylation sites and have not been reported to contain any attached *O*-glycans. α_1-antitrypsin predominately has attached biantennary complex *N*-glycans and some triantennary and tetraantennary *N*-glycan structures (Kolarich et al.,2006). Ovalbumin has mostly high mannose *N*-glycan structures attached, but also contains hybrid and complex *N*-glycan structures (Harvey et al.,2000). A mixture of both standard *N*-glycoproteins (approximately 10 μg of each standard protein) together with an excess of the unglycosylated human serum albumin (HSA) (50 μg) were fractionated on separate lectin

chromatography columns containing 0.25 ml of ConA (lectin concentration 10-16 mg/ml and binding capacity 20-45 mg/ml porcine thyroglobulin), 0.5 ml of Jacalin (lectin concentration 5 mg/ml and binding capacity of 1-2 mg/ml human IgA) and 0.5 ml of WGA (lectin concentration 5 mg/ml and binding capacity of 1-2 mg/ml ovomucoid) to test for their retention when present in relatively low abundance. Bound glycoproteins were eluted with 1.5 M methyl-α-glucopyranoside, 1.5 M galactose and 1.5 M GlcNAc respectively to competitively elute the glycoproteins from the lectins. Proteins that flowed through, or were bound and subsequently eluted from the lectin column, were diafiltered, concentrated and separated by 1D SDS PAGE (Figure 1).

ConA bound α_1-antitrypsin and ovalbumin with mostly HSA in the flow through (FT; Figure 1B and 1C) and confirms ConA as binding to glycoproteins containing α-mannose in their *N*-glycans. Both of these *N*-linked glycoproteins, α_1-antitrypsin and ovalbumin, were not retained well by the Jacalin column although α_1-antitrypsin was partially bound (Figure 1D and 1E). This suggests that Jacalin, in addition to its primary selectivity for *O*-glycans (Galβ(1-3)GalNAc), may have some recognition for *N*-linked glycoproteins through its reported recognition of monosaccharides, including mannose and *N*-acetylneuraminic acid (NeuAc) (Bourne et al.,2002, Do et al.,1998) and its large oligosaccharide binding site (Arockia Jeyaprakash et al.,2005). We have previously observed that Jacalin binds *N*-linked glycoproteins from a rat liver membrane preparation (Lee et al.,2009). WGA, which recognises GlcNAc and NeuAcα(2,3), bound α_1-antitrypsin and ovalbumin strongly (Figure 1F and 1G). The excess unglycosylated human serum albumin (HSA) (50 μg) was shown predominately in the FT fraction of all lectin columns as expected. The presence of the small amount of HSA in the bound

fraction could be due to non-specific interactions to the support media, the lectins and/or to the two bound glycoproteins.

Lectin affinity chromatography of rat liver membrane and human plasma glycoproteins

Triton X-114 phase partitioned rat liver membrane proteins solubilized in binding buffer containing CHAPS were incubated separately overnight with immobilized ConA, Jacalin and WGA lectins before mixing and packing into a single tri-lectin column. As seen in Figure 2 some proteins were not bound (FT) but many of the rat liver membrane proteins were retained by the lectin column and were eluted (B) by using competing monosaccharides at a concentration of 1.5 M.

Proteomic analysis by mass spectrometry of the tryptic digests of these fractions have previously identified (Lee et al.,2009) that a total of 277 membrane proteins could be enriched by ConA, Jacalin and WGA lectins, of which 44 (16%) common proteins were isolated by the three lectins when used separately. The identified membrane proteins comprised a large proportion of cell adhesion proteins, receptors, solute carrier transporters and cytochrome p450 enzymes.

In an alternate approach, albumin and IgG depleted-plasma glycoproteins were fractionated using a single column containing an equal volume of immobilized ConA, Jacalin and WGA lectins (M-LAC) with each lectin having the same concentration (15 mg/ml). As plasma proteins are water soluble, bound plasma glycoproteins were able to be successfully eluted from the M-LAC column with a low pH buffer. 1D SDS PAGE of

the fractionated proteins demonstrated that the bound plasma proteins were largely different to the unbound proteins in the FT from the column (Kullolli et al.,2010).

Although the glycoprotein retention capacity of the amount of lectin used in the column (~10 mg retention capacity of each as determined by the manufacturer using standard proteins) was far in excess of the total protein sample load (~100 μg) the possibility of protein saturation of the lectin columns was checked by re-injecting the bound and FT fractions separately back onto the M-LAC column (Kullolli et al.,2010). The same chromatographic behaviour of the fractions occurred i.e. the bound fraction was shown to completely re-bind to the lectin column and the original FT fraction again did not bind at all to the lectins on the second pass through the column. Thus the three lectins reproducibly bound to the same glycoproteins and protein saturation of the column was not a contributory factor to the differential protein fractionation by the lectins.

Analysis of *N*-linked oligosaccharides from lectin-fractionated rat liver membrane and human plasma glycoproteins.

ConA and WGA are two of the most commonly used lectins for isolating *N*-linked glycoproteins. The combination of both these plant-derived lectins has been widely used for improving the analysis of PNGase F released *N*-linked oligosaccharides from human serum and plasma proteins (Sparbier et al.,2007, Sparbier et al.,2005) and human colon carcinoma cell membrane proteins (Vercoutter-Edouart et al.,2008). Many plant lectins are themselves *N*-glycosylated (Kabir.1995), and extended use of agarose-bound lectins, particularly those conjugated by cyanogen bromide linkages leads to leaching of the immobilized lectins. Thus plant lectins can sometimes be seen to co-elute

with the analysed glycoproteins, and their glycans may contaminate the subsequent analysis. However, the glycans that were derived from any leached lectin proteins can be differentiated from those that were attached to mammalian glycoproteins, since most plant oligosaccharides contain pentose sugars (such as xylose) (Carrington et al.,1985, Kisiel et al.,1996, Kolarich et al.,2000, Wilson et al.,2001), which are not normally found in mammalian *N*- and *O*-linked oligosaccharides. In addition, plant oligosaccharides often contain non-mammalian α(1,3) linked core fucose and these will not be released by PNGase F.

To determine how the specificity of the three lectins is reflected in the overall *N*-glycosylation of the fractionated proteins, *N*-linked oligosaccharides were released from both the retained and flow through fractions of the lectin-partitioned rat liver membrane and human plasma glycoproteins by PNGase F digestion. The compositions of these *N*-glycans were determined using graphitized carbon LC-ESI-MS in negative ion mode. The average MS of *N*-linked oligosaccharides released from lectin-fractionated rat liver membrane proteins is shown in Figure 3 and assigned *N*-glycan compositions are indicated in Table 1. Surprisingly, the *N*-glycan global profile of lectin-fractionated rat liver membrane proteins in both the tri-lectin bound and unbound (FT) fractions were remarkably similar. Both show the same relative content of high mannose *N*-glycan structures (for example m/z of $(860.3)^{2-}$ and $(941.3)^{2-}$) and sialylated complex *N*-glycan structures (for example m/z of $(965.8)^{2-}$ and $(1111.4)^{2-}$).

Every effort was made to ensure that the protein load (~80 μg) was well below the maximum binding capacity of the column (binding capacity 5-10 mg [ConA] and 0.5-1 mg [Jacalin and WGA]) and membrane proteins were solubilised with binding buffer

containing CHAPS and filtered prior to incubation with immobilized lectins to minimize the amount of particulates in the sample. It is of course possible that membrane proteins may have precipitated during overnight incubation with the lectins and lost their binding specificity.

To try and understand the result of an almost identical *N*-glycosylation profile of the different proteins that were bound to the lectins compared to those that did not bind, *N*-glycan profiling of human plasma proteins fractionated by M-LAC (ConA, WGA and Jacalin) lectin affinity chromatography was also compared. Again, the average MS (over retention time 35-65 min) of the separated *N*-glycans related from plasma glycoproteins bound to the lectin column (and eluted by a change in pH) and those glycoproteins that did not bind were almost identical (Figure 4E and 4K). Both the bound and unbound fractions consisted of high mannose *N*-glycan structures (for example m/z $(860.3)^{2-}$ and $(941.3)^{2-}$), complex asialo *N*-glycan structures (for example m/z $(731.3)^{2-}$ and $(820.3)^{2-}$), complex mono-sialo *N*-glycan structures (for example m/z $(965.8)^{2-}$ and $(1038.9)^{2-}$), complex di-sialo *N*-glycan structures (for example m/z $(1111.4)^{2-}$ and $(1184.4)^{2-}$) and even traces of a complex tri- and tetra-sialo *N*-glycan structures (Table 1).

The base peak chromatograms (Figure 4A and 4F) of the *N*-linked glycomic profile were further interrogated in detail to determine if there were any significant glycosylation structural differences on the protein subset that was retained by the three lectins on the column, compared to the glycans on those proteins that were not bound. Graphitized carbon chromatography is able to distinguish and separate isomeric glycans, which may have the same mass and/or composition but differ in specific monosaccharide linkages and thus may exhibit different structural affinities for the lectins.

Using extracted ion chromatograms (EIC) of masses that correspond to specific m/z ions, we selected for the EIC of MS/MS m/z 290.1 (diagnostic ion for NeuAc) (Figure 4B and 4G) and, m/z 350.2 (diagnostic ion for core fucose (Fucα(1-6)GlcNAc-ol)(Figure 4C and 4H). The EIC of MS/MS m/z 290.1 suggests that the three lectins bound more proteins containing complex sialylated *N*-glycan isoforms than were in the flow through. Conversely, the EIC of MS/MS m/z 350.1 showed that proteins containing core fucosylated *N*-glycan structures were present in higher abundance in the FT fraction compared to the bound fraction indicating that these three lectins had somewhat reduced affinity to the fucosylated core motif.

To further evaluate the binding of these lectins for specific *N*-glycan structures, we selected EIC of m/z $(1038.9)^{2-}$ (Figure 4D and 4I) which has the *N*-glycan composition $(Hex)_2(HexNAc)_2(Fuc)_1(NeuAc)_1 + (Man)_3(GlcNAc)_2$ and was identified to be a core fucosylated mono-sialylated complex biantennary *N*-glycan based on the MS/MS fragmentation data. The elution profile of EIC of m/z $(1038.9)^{2-}$ in the bound and FT fractions showed that two isomeric peaks were eluted at 54 and 61 min respectively. The peak shown at 54 min corresponds to NeuAc attached in an α(2,6) linkage to the terminus of the complex biantennary *N*-glycan and the peak shown at 61 min corresponds to NeuAc attached in an α(2,3) linkage to the terminus of the complex biantennary *N*-glycan structure. The biantennary *N*-glycan structure consisting of NeuAcα(2,6) was shown to be present in both bound and FT fractions, whereas the *N*-glycan structure consisting of NeuAcα(2,3) was observed in much greater abundance on the bound proteins than in the FT fraction. The identity of these isomers and their specific NeuAc linkages was confirmed by their having the same MS/MS fragmentation pattern and the

same elution position as that of corresponding standard *N*-glycans (data not shown). Based on the EIC data the combination of ConA, WGA and Jacalin lectins apparently recognizes specifically *N*-glycan structures containing terminal NeuAcα(2,3) but not NeuAcα(2,6). In agreement with this observation, the WGA lectin has been reported previously to recognize mostly NeuAcα(2,3) with no recognition for NeuAcα(2,6) and NeuAcα(2,8) (Iskratsch et al.,2009). All three lectins used have been reported not to bind to core fucosylated *N*-glycan structures (Cummings et al.,1982, Iskratsch et al.,2009) which correlates with the predominance of core fucosylated *N*-glycans in the flow through fraction in this study, however, core fucosylated *N*-glycans with terminal Neuα(2,3) did bind to the M-LAC column (Supplementary Figure 1). This example demonstrates the complexity of the competing interactions between the heterogeneously glycosylated proteins and the lectin binding affinities.

Analysis of *O*-linked oligosaccharides from lectin-fractionated rat liver membrane and depleted human plasma glycoproteins.

As in the *N*-linked global glycomic profile, the *O*-linked oligosaccharide profile on the glycoproteins bound and unbound to the lectins was similar overall. The combined EIC of $[M-H]^{1-}$ $(675.2)^{1}$, $(878.2)^{1}$, $(966.3)^{1}$ and $(1331.5)^{1}$ m/z (Figure 5) monitors the masses corresponding to *O*-glycans previously identified in the rat (Funakoshi et al.,1982, Hull et al.,1984, Nato et al.,1986) and corresponds to *O*-glycan compositions consisting of $(Hex)_1(HexNAc)_1(NeuAc)_1$, $(Hex)_1(HexNAc)_2(NeuAc)_1$, $(Hex)_1(HexNAc)_1(NeuAc)_2$ and $(Hex)_2(HexNAc)_2(NeuAc)_2$ as seen in the total liver membrane glycoproteins (Figure 5A and Table 2). MS/MS fragmentation of the major ions m/z $(675.2)^{1-}$ and $(966.3)^{1-}$

(Figure 5B and 5C) found in both the lectin bound and flow through fractions of rat liver membrane glycoproteins identified a mono- and di-sialylated core 1 *O*-glycan structure (Supplementary Figure 2, Table 2).

More detailed analysis of the *O*-linked oligosaccharides from the lectin-fractionated rat liver membrane glycoproteins was able to show some low abundance differences between the bound and FT fractions. The average MS of masses eluting in the narrow window of retention time 23 to 24 min identified the ions of m/z $(878.2)^{1-}$ m/z and $(1331.5)^{1-}$ m/z in the lectin bound fraction (Figure 5B) but not in the flow through (Figure 5C). These masses were identified to be mono- and di-sialylated core 2 *O*-glycan structures by MS/MS fragmentation (Supplementary Figure 2, Table 2). The enrichment of these low abundance *O*-linked oligosaccharides in the lectin bound fraction presumably was due to the preference of the Jacalin lectin for these structures.

O-linked oligosaccharides released from lectin-fractionated human plasma glycoproteins also showed the two major ions of m/z $(675.2)^{1-}$ and $(966.3)^{1-}$ corresponding to the mono- and di-sialylated core 1 *O*-glycan structures as confirmed by MS/MS (Table 2). These were present in higher abundance in the M-LAC bound fraction compared to the flow through (Figure 6) suggesting that most glycoproteins containing these two *O*-glycan structures had bound to the M-LAC column.

These results provide evidence that Jacalin, which is the lectin with preference for binding *O*-glycans, is suitable for enriching *O*-linked glycoproteins when used in the multi-lectin format. Moreover, the inclusion of WGA, that recognises NeuAcα(2,3), in the tri-lectin mixture, may also assist in the binding and isolation of *O*-linked glycoproteins containing these sialylated core 1 and core 2 *O*-glycan structures. The

enrichment of *O*-linked glycoproteins using the combination of the three lectins was consistently observed in both biological systems.

Although, using detailed structural analysis, there is some preferential binding of specific low abundance oligosaccharide structures to the lectin columns, it is clear, in the case of both the rat liver membrane and the plasma samples, that not all glycoproteins were captured by the tri-lectin column and that overall, the oligosaccharides on the proteins that were bound to the lectins were mostly the same as those on the proteins that were not retained.

The explanation for this surprising finding is difficult at this stage but we speculate that it may be due to the complexity of interactions that occur in a mixture of the many hundreds of proteins and their glycoforms that comprise these two samples. It has been shown that the tri-lectin M-LAC system has an enhanced affinity for glycoproteins compared to single lectins (Ralin et al.,2008) due to multi-site attachment between the glycoproteins and the different lectins. This is supported by the fact that lectins found *in vivo* exhibit high affinity and specificity for particular glycoproteins presented on cell membranes (Drickamer.1995). However, protein-protein interactions are considered to be much stronger than the binding of lectins to carbohydrates (Hoebeke et al.,1978, Schreiber.,2002). The dissociation equilibrium constant (K_d) is the propensity for protein complexes to separate reversibly into their components, where lower K_d values indicate stronger binding of a ligand to a particular protein. For example, the affinity of ConA for *N*-glycans attached to chicken ovalbumin has been reported to have a $K_d \sim 0.34$ μM (Ohyama et al.,1985), whereas interactions between proteins such as synapsin I and rat brain synaptic vesicles have been reported to have a lower $K_d \sim 10$ nM

(Stefani et al.,1997). Therefore, the weaker affinity of lectins for oligosaccharide structures (K_d ~ μM) compared to the interaction between different proteins in complex mixtures (K_d ~ nM) may offer one explanation of why similar glycomic profiles are observed on glycoproteins in the lectin bound and unbound fractions.

Conclusions

The data from our previously published proteomic studies (Kullolli et al.,2010, Lee et al.,2009) on the same complex mixtures of rat liver membrane proteins and human plasma proteins as described in this paper, showed that the three lectins (ConA, WGA and Jacalin) reproducibly enriched different subsets of proteins. However, this glycomic study shows, with some exceptions, that similar global oligosaccharide profiles are found on both lectin-bound and -unbound glycoproteins. This suggests that the selectivity of these lectins for specific oligosaccharide structures attached to proteins in complex mixtures appears to be compromised. Such properties as lectin multivalency, the presence of heterogeneous populations of glycans attached to the same protein, the abundance of some structures, the concentration-dependent competing affinities of lectins for the same structures, and/or the competing protein-protein or protein complex interactions may be involved, such that lectin binding cannot simply be explained by their preferred sugar epitopes.

In glycoproteomic studies, lectins are often used and perceived as a method for enriching all intact glycoproteins from complex mixtures. The riddle of lectins presented here, is that the combination of immobilized ConA, Jacalin and WGA lectins, which are commonly used to enrich *N*- and *O*-linked glycoproteins, did not completely capture the

entire glycoproteome in rat liver membranes and depleted human plasma, but rather partitioned the proteins into distinct subsets of glycoproteins.

The study emphasizes that the use of lectins in proteomics studies is a valuable tool for the fractionation of different glycoprotein subsets from complex mixtures. The glycomics analysis of these lectin affinity fractionated glycoproteins however indicates that both the flow through as well as the bound glycoprotein fractions need to be considered for biomarker discovery studies, and that the mechanisms responsible for lectins partitioning complex glycoprotein mixtures might not be the same as those that have been established for purified and well characterized standard protein mixtures. The almost identical glycomic profiles of unbound and bound glycoproteins cannot be fully explained, but we deduce from our experiments that there appear to be more parameters than simple oligosaccharide recognition that influence the binding (or no binding) of glycoproteins to lectins when complex mixtures are subjected to this kind of enrichment approach.

Acknowledgements

The authors would like to thank their ARC Linkage industry partner GE Healthcare. This research project was supported by access to the Australian Proteome Analysis Facility (APAF) established under the Australian Government's NCRIS program and to the mass spectrometry infrastructure funded by a NSW Cancer Institute Infrastructure grant.

Author Disclosure Statement

The authors declare no conflict of interest.

References

ARNOLD, J. N., SALDOVA, R., HAMID, U. M., and RUDD, P. M. (2008) Evaluation of the serum N-linked glycome for the diagnosis of cancer and chronic inflammation. Proteomics **8**, 3284-3293

AROCKIA JEYAPRAKASH, A., JAYASHREE, G., MAHANTA, S. K., SWAMINATHAN, C. P., SEKAR, K., SUROLIA, A., et al. (2005) Structural basis for the energetics of jacalin-sugar interactions: promiscuity versus specificity. J Mol Biol **347**, 181-188

BECKER, J. W., REEKE, G. N., JR., WANG, J. L., CUNNINGHAM, B. A., and EDELMAN, G. M. (1975) The covalent and three-dimensional structure of concanavalin A. III. Structure of the monomer and its interactions with metals and saccharides. J Biol Chem **250**, 1513-1524

BOURNE, Y., ASTOUL, C. H., ZAMBONI, V., PEUMANS, W. J., MENU-BOUAOUICHE, L., VAN DAMME, E. J., et al. (2002) Structural basis for the unusual carbohydrate-binding specificity of jacalin towards galactose and mannose. Biochem J **364**, 173-180

BREWER, C. F., and BHATTACHARYYA, L. (1986) Specificity of concanavalin A binding to asparagine-linked glycopeptides. A nuclear magnetic relaxation dispersion study. J Biol Chem **261**, 7306-7310

CARRINGTON, D. M., AUFFRET, A., and HANKE, D. E. (1985) Polypeptide ligation occurs during post-translational modification of concanavalin A. Nature **313**, 64-67

COLLINS, R. D., JACOBSON, W., and STODDART, R. W. (1982) Lectin staining of carbohydrates of haemic cells. III. The cells of Hodgkin's disease and other lymphomas. Histopathology **6**, 601-616

CUMMINGS, R. D., and KORNFELD, S. (1982) Fractionation of asparagine-linked oligosaccharides by serial lectin-Agarose affinity chromatography. A rapid, sensitive, and specific technique. J Biol Chem **257**, 11235-11240

CUNNINGHAM, B. A., WANG, J. L., WAXDAL, M. J., and EDELMAN, G. M. (1975) The covalent and three-dimensional structure of concanavalin A. II. Amino acid sequence of cyanogen bromide fragment F3. J Biol Chem **250**, 1503-1512

DAYARATHNA. M. K., HANCOCK, W. S., and HINCAPIE. M. (2008) A two step fractionation approach for plasma proteomics using immunodepletion of abundant proteins and multi-lectin affinity chromatography: Application to the analysis of obesity, diabetes, and hypertension diseases. J Sep Sci **31**, 1156-1166

DO, S. I., and LEE, K. Y. (1998) Jacalin interacts with Asn-linked glycopeptides containing multi-antennary oligosaccharide structure with terminal alpha-linked galactose. FEBS Lett **421**, 169-173

DRICKAMER, K. (1995) Multiplicity of lectin-carbohydrate interactions. Nat Struct Biol **2**, 437-439

EDELMAN, G. M., CUNNINGHAM, B. A., REEKE, G. N., JR., BECKER, J. W., WAXDAL, M. J., and WANG, J. L. (1972) The covalent and three-dimensional structure of concanavalin A. Proc Natl Acad Sci U S A **69**, 2580-2584

FUNAKOSHI, I., and YAMASHINA, I. (1982) Structure of O-glycosidically linked sugar units from plasma membranes of an ascites hepatoma, AH 66. J Biol Chem **257**, 3782-3787

GOLDSTEIN, I. J. (1975) Studies on the combining sites of concanavalin A. Adv Exp Med Biol **55**, 35-53

GOLDSTEIN, I. J., HOLLERMAN, C. E., and MERRICK, J. M. (1965) Protein-Carbohydrate Interaction. I. The Interaction of Polysaccharides with Concanavalin A. Biochim Biophys Acta **97**, 68-76

GOLDSTEIN, I. J., HOLLERMAN, C. E., and SMITH, E. E. (1965) Protein-Carbohydrate Interaction. Ii. Inhibition Studies on the Interaction of Concanavalin a with Polysaccharides. Biochemistry **4**, 876-883

HARVEY, D. J., WING, D. R., KUSTER, B., and WILSON, I. B. (2000) Composition of N-linked carbohydrates from ovalbumin and co-purified glycoproteins. J Am Soc Mass Spectrom **11**, 564-571

HIRABAYASHI, J. (2004) Lectin-based structural glycomics: glycoproteomics and glycan profiling. Glycoconj J **21**, 35-40

HIRABAYASHI, J., HASHIDATE, T., and KASAI, K. (2002) Glyco-catch method: A lectin affinity technique for glycoproteomics. J Biomol Tech **13**, 205-218

HIRABAYASHI, J., and KASAI, K. (2002) Separation technologies for glycomics. J Chromatogr B Analyt Technol Biomed Life Sci **771**, 67-87

HOEBEKE, J., FORIERS, A., SCHREIBER, A. B., and STROSBERG, A. D. (1978) Equilibrium and kinetic studies of the binding of Lens culinaris lectin to rabbit erythrocytes by a quantitative fluorometric method. Biochemistry **17**, 5000-5005

HOLLAND, N. B., QIU, Y., RUEGSEGGER, M., and MARCHANT, R. E. (1998) Biomimetic engineering of non-adhesive glycocalyx-like surfaces using oligosaccharide surfactant polymers. Nature **392**, 799-801

HULL, S. R., LAINE, R. A., KAIZU, T., RODRIGUEZ, I., and CARRAWAY, K. L. (1984) Structures of the O-linked oligosaccharides of the major cell surface sialoglycoprotein of MAT-B1 and MAT-C1 ascites sublines of the 13762 rat mammary adenocarcinoma. J Biol Chem **259**, 4866-4877

ISKRATSCH, T., BRAUN, A., PASCHINGER, K., and WILSON, I. B. (2009) Specificity analysis of lectins and antibodies using remodeled glycoproteins. Anal Biochem **386**, 133-146

JENTOFT, N. (1990) Why are proteins O-glycosylated? Trends Biochem Sci **15**, 291-294

KABIR, S. (1995) The isolation and characterisation of jacalin [Artocarpus heterophyllus (jackfruit) lectin] based on its charge properties. Int J Biochem Cell Biol **27**, 147-156

KAJI, H., SAITO, H., YAMAUCHI, Y., SHINKAWA, T., TAOKA, M., HIRABAYASHI, J., et al. (2003) Lectin affinity capture, isotope-coded tagging and mass spectrometry to identify N-linked glycoproteins. Nat Biotechnol **21**, 667-672

KANIE, Y., YAMAMOTO-HINO, M., KARINO, Y., YOKOZAWA, H., NISHIHARA, S., UEDA, R., et al. (2009) Insight into the regulation of glycan synthesis in Drosophila chaoptin based on mass spectrometry. PLoS One **4**, e5434

KIRKHAM, S., SHEEHAN, J. K., KNIGHT, D., RICHARDSON, P. S., and THORNTON, D. J. (2002) Heterogeneity of airways mucus: variations in the amounts and glycoforms of the major oligomeric mucins MUC5AC and MUC5B. Biochem J **361**, 537-546

KISIEL, D. G., GINDZIENSKI, A., and ZWIERZ, K. (1996) Is wheat germ agglutinin (WGA) a glycosylated protein? Rocz Akad Med Bialymst **41**, 284-292

KOLARICH, D., and ALTMANN, F. (2000) N-Glycan analysis by matrix-assisted laser desorption/ionization mass spectrometry of electrophoretically separated nonmammalian proteins: application to peanut allergen Ara h 1 and olive pollen allergen Ole e 1. Anal Biochem **285**, 64-75

KOLARICH, D., WEBER, A., TURECEK, P. L., SCHWARZ, H. P., and ALTMANN, F. (2006) Comprehensive glyco-proteomic analysis of human alpha1-antitrypsin and its charge isoforms. Proteomics **6**, 3369-3380

KRONIS, K. A., and CARVER, J. P. (1985) Wheat germ agglutinin dimers bind sialyloligosaccharides at four sites in solution: proton nuclear magnetic resonance temperature studies at 360 MHz. Biochemistry **24**, 826-833

KULLOLLI, M., HANCOCK, W. S., and HINCAPIE, M. (2008) Preparation of a high-performance multi-lectin affinity chromatography (HP-M-LAC) adsorbent for the analysis of human plasma glycoproteins. J Sep Sci **31**, 2733-2739

KULLOLLI, M., HANCOCK, W. S., and HINCAPIE, M. (2010) Automated platform for fractionation of human plasma glycoproteome in clinical proteomics. Anal Chem **82**, 115-120

LEE, A., KOLARICH, D., HAYNES, P. A., JENSEN, P. H., BAKER, M. S., and PACKER, N. H. (2009) Rat liver membrane glycoproteome: enrichment by phase partitioning and glycoprotein capture. J Proteome Res **8**, 770-781

LIM, H., ENG, J., YATES, J. R., 3RD, TOLLAKSEN, S. L., GIOMETTI, C. S., HOLDEN, J. F., et al. (2003) Identification of 2D-gel proteins: a comparison of MALDI/TOF peptide mass mapping to mu LC-ESI tandem mass spectrometry. J Am Soc Mass Spectrom **14**, 957-970

NAGATA, Y., and BURGER, M. M. (1972) Wheat germ agglutinin. Isolation and crystallization. J Biol Chem **247**, 2248-2250

NAGATA, Y., and BURGER, M. M. (1974) Wheat germ agglutinin. Molecular characteristics and specificity for sugar binding. J Biol Chem **249**, 3116-3122

NATO, F., GOULUT, C., BOURRILLON, R., VAN HALBEEK, H., and VLIEGENTHART, J. F. (1986) The structure of the O-glycosidic oligosaccharide chains of the major Zajdela hepatoma ascites-cell-membrane glycoprotein. Eur J Biochem **159**, 303-308

OHYAMA, Y., KASAI, K., NOMOTO, H., and INOUE, Y. (1985) Frontal affinity chromatography of ovalbumin glycoasparagines on a concanavalin A-sepharose column. A quantitative study of the binding specificity of the lectin. J Biol Chem **260**, 6882-6887

PLAVINA, T., WAKSHULL, E., HANCOCK, W. S., and HINCAPIE, M. (2007) Combination of abundant protein depletion and multi-lectin affinity chromatography (M-LAC) for plasma protein biomarker discovery. J Proteome Res **6**, 662-671

RALIN, D. W., DULTZ, S. C., SILVER, J. E., TRAVIS, J. C., KULLOLLI, M., HANCOCK, W. S., et al. (2008) Kinetic Analysis of Glycoprotein-Lectin Interactions by Label Free Internal-Reflection Ellipsometry. Clinical Proteomics **4**, 37-46

REEKE, G. N., JR., BECKER, J. W., CUNNINGHAM, B. A., WANG, J. L., YAHARA, I., and EDELMAN, G. M. (1975) Structure and function of concanavalin A. Adv Exp Med Biol **55**, 13-33

REEKE, G. N., JR., BECKER, J. W., and EDELMAN, G. M. (1975) The covalent and three-dimensional structure of concanavalin A. IV. Atomic coordinates, hydrogen bonding, and quaternary structure. J Biol Chem **250**, 1525-1547

ROQUE-BARREIRA, M. C., and CAMPOS-NETO, A. (1985) Jacalin: an IgA-binding lectin. J Immunol **134**, 1740-1743

SATO, T., KAWADA, T., SUGIMACHI, M., and SUNAGAWA, K. (2002) Bionic technology revitalizes native baroreflex function in rats with baroreflex failure. Circulation **106**, 730-734

SCHREIBER, G. (2002) Kinetic studies of protein-protein interactions. Curr Opin Struct Biol **12**, 41-47

SCHULZ, B. L., OXLEY, D., PACKER, N. H., and KARLSSON, N. G. (2002) Identification of two highly sialylated human tear-fluid DMBT1 isoforms: the major high-molecular-mass glycoproteins in human tears. Biochem J **366**, 511-520

SCHULZ, B. L., SLOANE, A. J., ROBINSON, L. J., PRASAD, S. S., LINDNER, R. A., ROBINSON, M., et al. (2007) Glycosylation of sputum mucins is altered in cystic fibrosis patients. Glycobiology **17**, 698-712

SPARBIER, K., ASPERGER, A., RESEMANN, A., KESSLER, I., KOCH, S., WENZEL, T., et al. (2007) Analysis of glycoproteins in human serum by means of glycospecific magnetic bead separation and LC-MALDI-TOF/TOF analysis with automated glycopeptide detection. J Biomol Tech **18**, 252-258

SPARBIER, K., KOCH, S., KESSLER, I., WENZEL, T., and KOSTRZEWA, M. (2005) Selective isolation of glycoproteins and glycopeptides for MALDI-TOF MS detection supported by magnetic particles. J Biomol Tech **16**, 407-413

STEFANI, G., ONOFRI, F., VALTORTA, F., VACCARO, P., GREENGARD, P., and BENFENATI, F. (1997) Kinetic analysis of the phosphorylation-dependent interactions of synapsin I with rat brain synaptic vesicles. J Physiol **504** (**Pt 3**), 501-515

TISSOT, B., NORTH, S. J., CERONI, A., PANG, P. C., PANICO, M., ROSATI, F., et al. (2009) Glycoproteomics: past, present and future. FEBS Lett **583**, 1728-1735

VAN BENEDEN, K., COPPIETERS, K., LAROY, W., DE KEYSER, F., HOFFMAN, I. E., VAN DEN BOSCH, F., et al. (2009) Reversible changes in serum immunoglobulin galactosylation during the immune response and treatment of inflammatory autoimmune arthritis. Ann Rheum Dis **68**, 1360-1365

VERCOUTTER-EDOUART, A. S., SLOMIANNY, M. C., DEKEYZER-BESEME, O., HAEUW, J. F., and MICHALSKI, J. C. (2008) Glycoproteomics and glycomics

investigation of membrane N-glycosylproteins from human colon carcinoma cells. Proteomics **8**, 3236-3256

VLASSARA, H., and PALACE, M. R. (2002) Diabetes and advanced glycation endproducts. J Intern Med **251**, 87-101

WASHBURN, M. P., WOLTERS, D., and YATES, J. R., 3RD. (2001) Large-scale analysis of the yeast proteome by multidimensional protein identification technology. Nat Biotechnol **19**, 242-247

WILSON, I. B., ZELENY, R., KOLARICH, D., STAUDACHER, E., STROOP, C. J., KAMERLING, J. P., et al. (2001) Analysis of Asn-linked glycans from vegetable foodstuffs: widespread occurrence of Lewis a, core alpha1,3-linked fucose and xylose substitutions. Glycobiology **11**, 261-274

WILSON, N. L., SCHULZ, B. L., KARLSSON, N. G., and PACKER, N. H. (2002) Sequential analysis of N- and O-linked glycosylation of 2D-PAGE separated glycoproteins. J Proteome Res **1**, 521-529

XIONG, L., ANDREWS, D., and REGNIER, F. (2003) Comparative proteomics of glycoproteins based on lectin selection and isotope coding. J Proteome Res **2**, 618-625

YANG, Z., and HANCOCK, W. S. (2004) Approach to the comprehensive analysis of glycoproteins isolated from human serum using a multi-lectin affinity column. J Chromatogr A **1053**, 79-88

YANG, Z., HARRIS, L. E., PALMER-TOY, D. E., and HANCOCK, W. S. (2006) Multilectin affinity chromatography for characterization of multiple glycoprotein

biomarker candidates in serum from breast cancer patients. Clin Chem **52**, 1897-1905

YOUNG, N. M., JOHNSTON, R. A., and WATSON, D. C. (1991) The amino acid sequences of jacalin and the Maclura pomifera agglutinin. FEBS Lett **282**, 382-384

ZHANG, H., LI, X. J., MARTIN, D. B., and AEBERSOLD, R. (2003) Identification and quantification of N-linked glycoproteins using hydrazide chemistry, stable isotope labeling and mass spectrometry. Nat Biotechnol **21**, 660-666

For peer review

Table 1. Total assigned *N*-glycan compositions observed in lectin-fractionated human plasma glycoproteins. *indicates those *N*-glycan structures also identified in lectin-fractionated rat liver membrane glycoproteins.

	Structure No	Composition + N-linked core[a]	$[M-2H]^{2-}$
High Mannose	1*	$(Hex)_2$	617.2
	2*	$(Hex)_3$	698.2
	3*	$(Hex)_4$	779.3
	4*	$(Hex)_5$	860.3
	5*	$(Hex)_6$	941.3
	6*	$(Hex)_7$	1022.3
Asialo N-glycan	7	$(HexNAc)_2$	658.2
	8	$(Hex)_2 (HexNAc)_1$	718.8
	9	$(HexNAc)_2 (Fuc)_1$	731.3
	10	$(Hex)_1 (HexNAc)_2$	739.3
	11	$(Hex)_3 (HexNAc)_1$	799.8
	12	$(Hex)_1 (HexNAc)_2 (Fuc)_1$	812.3
	13*	$(Hex)_2 (HexNAc)_2$	820.3
	14	$(HexNAc)_3 (Fuc)_1$	832.8
	15	$(Hex)_1 (HexNAc)_3$	840.8
	16	$(Hex)_2 (HexNAc)_2 (Fuc)_1$	893.3
	17	$(Hex)_1 (HexNAc)_3 (Fuc)_1$	913.8
	18	$(Hex)_2 (HexNAc)_3$	921.8
	19	$(Hex)_2 (HexNAc)_3 (Fuc)_1$	994.9
	20	$(Hex)_2 (HexNAc)_3 (Fuc)_2$	1067.9
Monosialo N-glycan	21	$(Hex)_1 (HexNAc)_1 (NeuAc)_1$	783.3
	22	$(Hex)_2 (HexNAc)_1 (NeuAc)_1$	864.3
	23	$(Hex)_1 (HexNAc)_2 (NeuAc)_1$	884.8
	24	$(Hex)_2 (HexNAc)_1 (Fuc)_1 (NeuAc)_1$	937.3
	25	$(Hex)_3 (HexNAc)_1 (NeuAc)_1$	945.3
	26	$(Hex)_1 (HexNAc)_2 (Fuc)_1 (NeuAc)_1$	957.8
	27*	$(Hex)_2 (HexNAc)_3 (NeuAc)_1$	965.8
	28*	$(Hex)_1 (HexNAc)_3 (NeuAc)_1$	986.4
	29*	$(Hex)_2 (HexNAc)_2 (Fuc)_1 (NeuAc)_1$	1038.9
	30	$(Hex)_1 (HexNAc)_3 (Fuc)_1 (NeuAc)_1$	1059.4
	31	$(Hex)_2 (HexNAc)_3 (NeuAc)_1$	1067.4
	32	$(Hex)_1 (HexNAc)_3 (Fuc)_2 (NeuAc)_1$	1132.4
	33	$(Hex)_2 (HexNAc)_3 (Fuc)_1 (NeuAc)_1$	1140.4
	34	$(Hex)_3 (HexNAc)_3 (NeuAc)_1$	1148.4
	35	$(Hex)_2 (HexNAc)_3 (Fuc)_1 (NeuAc)_1$	1221.4
	36	$(Hex)_4 (HexNAc)_4 (NeuAc)_1$	1331
Disialo N-glycan	37*	$(Hex)_2 (HexNAc)_2 (NeuAc)_2$	1111.4
	38*	$(Hex)_2 (HexNAc)_2 (Fuc)_1 (NeuAc)_2$	1184.4
	39	$(Hex)_2 (HexNAc)_3 (NeuAc)_2$	1212.9
	40*	$(Hex)_2 (HexNAc)_3 (Fuc)_1 (NeuAc)_2$	1286
	41	$(Hex)_3 (HexNAc)_3 (NeuAc)_2$	1294
	42	$(Hex)_2 (HexNAc)_3 (Fuc)_1 (NeuAc)_2$	1367
	43	$(Hex)_4 (HexNAc)_4 (NeuAc)_2$	1476.5
Trisialo N-glycan	44	$(Hex)_2 (HexNAc)_3 (NeuAc)_3$	1439.5
	45	$(Hex)_2 (HexNAc)_3 (Fuc)_1 (NeuAc)_3$	1512.5
	46	$(Hex)_2 (HexNAc)_3 (Fuc)_2 (NeuAc)_3$	1585.6
	47	$(Hex)_4 (HexNAc)_4 (NeuAc)_3$	1622.1
Tetrasialo N-glycan	48	$(Hex)_4 (HexNAc)_4 (NeuAc)_4$	1767.6

[a] N-linked core = $(Man)_3 (GlcNAc)_2$

Table 2. Assigned *O*-glycan structures present in rat liver membrane glycoproteins (structures 49-52) and human plasma glycoproteins (structures 49 and 50) fractionated by lectin affinity chromatography.

O-glycans

Structure No.	Composition	$[M-H]^-$
49		675.2
50	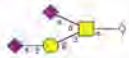	966.3
51	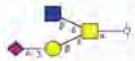	878.2
52		1331.5

N-acetylgalactosamine N-acetylglucosamine
Galactose N-acetylneuraminic acid

Figure Legends

Figure 1

Lectin affinity fractionation of standard *N*-linked glycoproteins (mixture of human α_1-antitrypsin [10 µg], chicken ovalbumin [10 µg] and human serum albumin [50 µg]). HSA: Human serum albumin (67 kDa), A1PI: α_1-antitrypsin (53kDa) and OVA: chicken ovalbumin (45 kDa). FT: flow through of a mixture of A1PI, OVA and HSA with ConA (B), Jacalin (D) and WGA columns (F). B: bound fractions of a mixture of A1PI, OVA and HSA with ConA (C), Jacalin (E) and WGA columns (G)

Figure 2

Tri-lectin affinity (ConA, Jacalin and WGA) bound (B) and flow through (FT) of Triton X-114 phase partitioned rat liver membrane proteins (RL) eluted from a column containing a mixture of 0.25 ml ConA (10-16 mg/ml), 0.5 ml Jacalin (5 mg/ml) and 0.5 ml WGA (5mg /ml) with 1.5 M methyl-α-glucopyranoside, 1.5 M galactose and 1.5 M *N*-acetyl glucosamine.

Figure 3

Average MS of released *N*-linked oligosaccharides (retention time 35-65 min) from rat liver membrane proteins and the tri-lectin (ConA, Jacalin and WGA) bound and FT fractions. Masses $[M-2H]^{2-}$ corresponding to known rat glycan compositions were observed in all three samples (See Table 1). †Same *N*-glycan structure but singly charged $[M-H]^{1-}$.

Figure 4

Depleted human plasma glycoproteins fractionated by a mixture of immobilized ConA, Jacalin and WGA lectins. Base peak chromatogram (BPC) of *N*-linked oligosaccharides released from the bound (A) and unbound fractions (F). Extracted ion chromatogram (EIC) of m/z 290.1 (NeuAc) of the bound (B) and unbound fractions (G) and, EIC of m/z 350.2 (Fucα(1,6)GlcNAc) of the bound (C) and unbound fractions (H). EIC of m/z $(1038.9)^{2}$ of the bound (D) and unbound fractions (I) and average MS of released *N*-linked oligosaccharides (retention time 35-65 min) from bound (E) and unbound fractions (K)

Figure 5

Combined extracted ion chromatogram of m/z $(675.2)^{1-}$, $(878.2)^{1-}$, $(966.3)^{1-}$ and $(1331.5)^{1-}$ from Triton X-114 phase partitioned rat liver membrane proteins (A), lectin bound fraction (B) and lectin FT fraction (C). Insert shows the average MS (over retention time 23-24 min)

Figure 6

Base peak chromatogram (BPC) and average MS (retention time 23-27min) of human plasma proteins fractionated by lectin affinity chromatography shows core 1 *O*-glycans present in the bound fraction (A and B) and FT fraction (C and D).

Supplementary Figure 1

Analysis of *N*-linked oligosaccharides from fetuin, and lectin bound and unbound human plasma glycoproteins shows the base peak chromatograph (BPC) (A) and extracted ion chromatograms (EIC) of m/z $(965.8)^{2-}$ (B), $(1038.9)^{2-}$ (C), $(1111.4)^{2-}$ (D)

and $(1184.4)^{2-}$ (E). The EIC of m/z $(965.8)^{2-}$ (B) which corresponds to *N*-glycan composition $(Hex)_2$ $(HexNAc)_2(NeuAc)_1$ + $(Man)_3(GlcNAc)_2$ eluted at 46 mins and was shown to be present in both bound and unbound fractions whereas; the EIC of m/z $(1038.9)^{2-}$ (C) which corresponds to *N*-glycan composition $(Hex)_2(HexNAc)_2(Fuc)_1(NeuAc)_1$ + $(Man)_3(GlcNAc)_2$ was shown to contain one isomer at 54 mins in both unbound and bound fractions. This *N*-glycan isomer corresponds to α(2,6)-linked NeuAc. Interestingly, a second isomer of m/z ion $(1038.9)^{2-}$ was shown to be present at 62 mins in only the unbound fraction but not in the bound fraction. This isomer corresponds to α(2,3)-linked NeuAc. The EIC of m/z $(1111.4)^{2-}$ (D) and $(1184.4)^{2-}$ (E) which corresponds to *N*-glycan compositions $(Hex)_2(HexNAc)_2$ $(NeuAc)_2$ + $(Man)_3(GlcNAc)_2$ and $(Hex)_2$ $(HexNAc)_2(Fuc)_1(NeuAc)_2$ + $(Man)_3(GlcNAc)_2$ respectively, were shown to be very similar in both unbound and bound fractions of lectin-fractionated human plasma glycoproteins.

Supplementary Figure 2

MS/MS fragmentation of m/z $(675.3)^{1-}$ (A), $(878.2)^{1-}$ (B), $(966.3)^{1-}$ (C) and $(1331.5)^{1-}$ (D), which corresponds to *O*-glycan compositions consisting of mono- and di-sialylated core 1 *O*-glycan structure as seen in the total liver membrane glycoproteins.

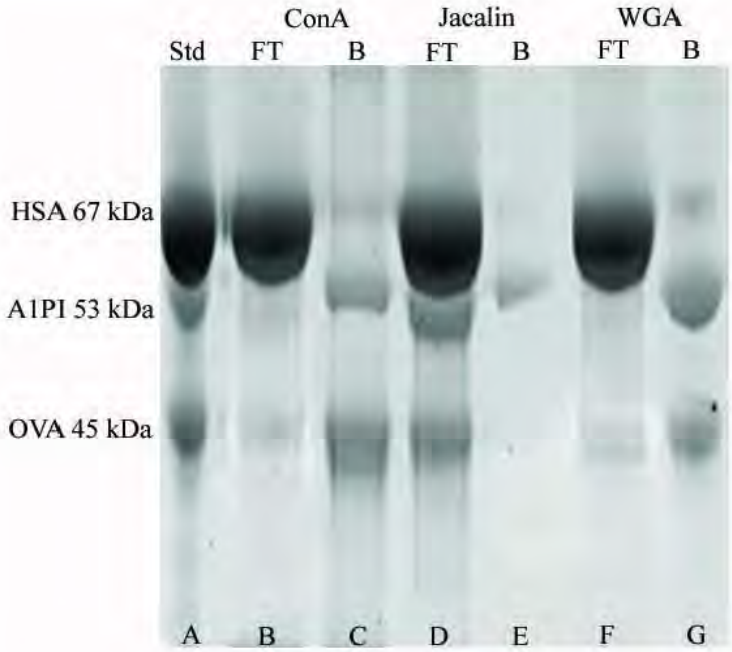
ConA
Jacalin
WGA
Std
FT
B
FT
B
FT
B
HSA 67 kDa
A1PI 53 kDa
OVA 45 kDa
A
B
C
D
E
F
G

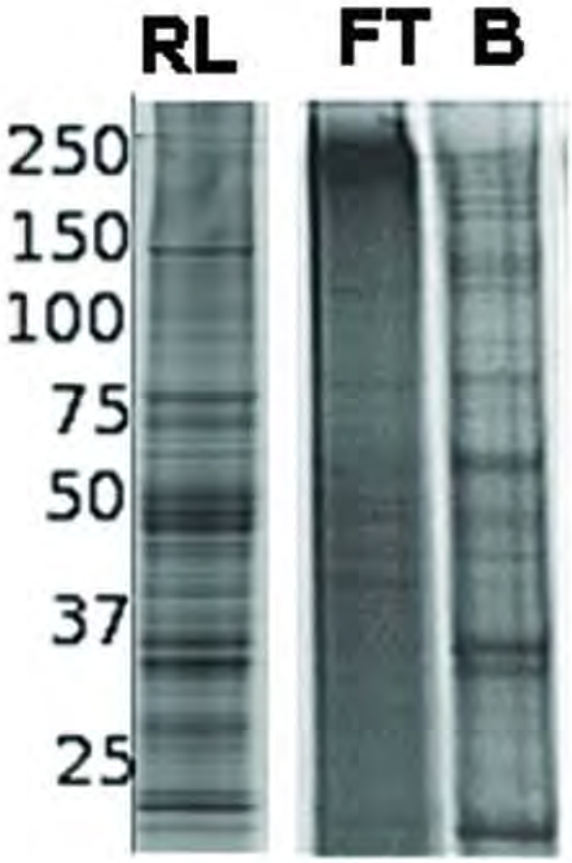

40x58mm (300 x 300 DPI)

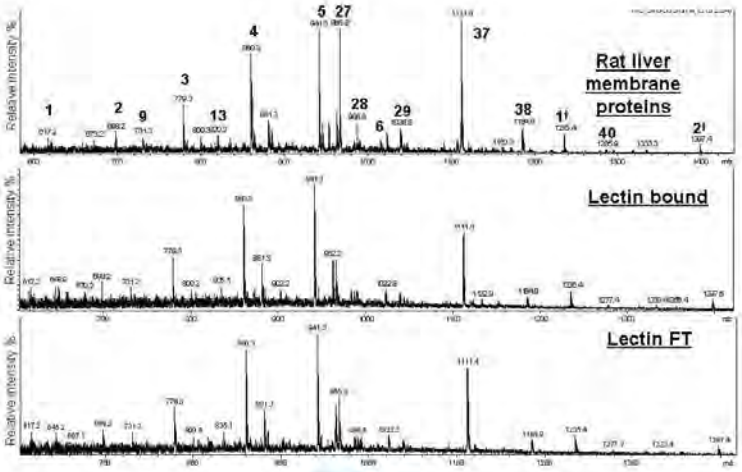
Rat liver membrane proteins
Lectin bound
Lectin FT
Relative intensity %
1
2
9
3
13
4
5
27
28
6
29
37
38
11
40
21

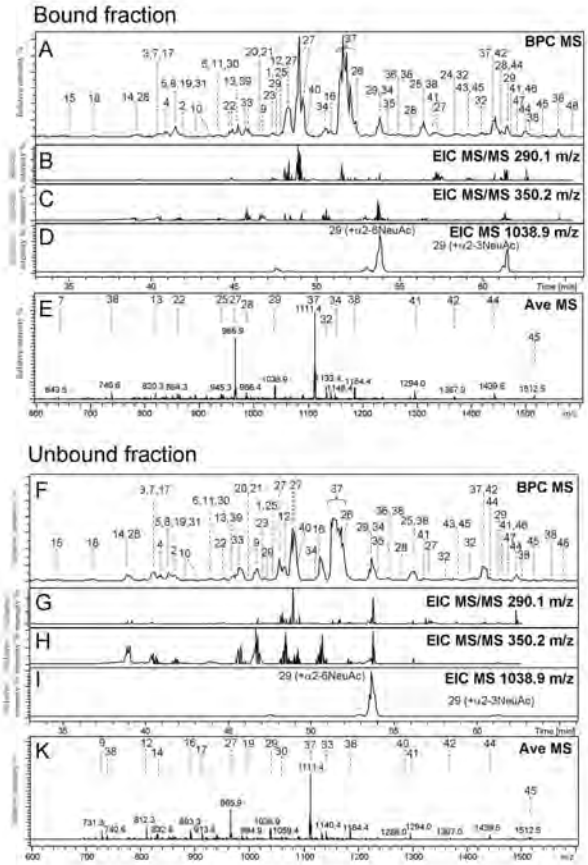

190x254mm (300 x 300 DPI)

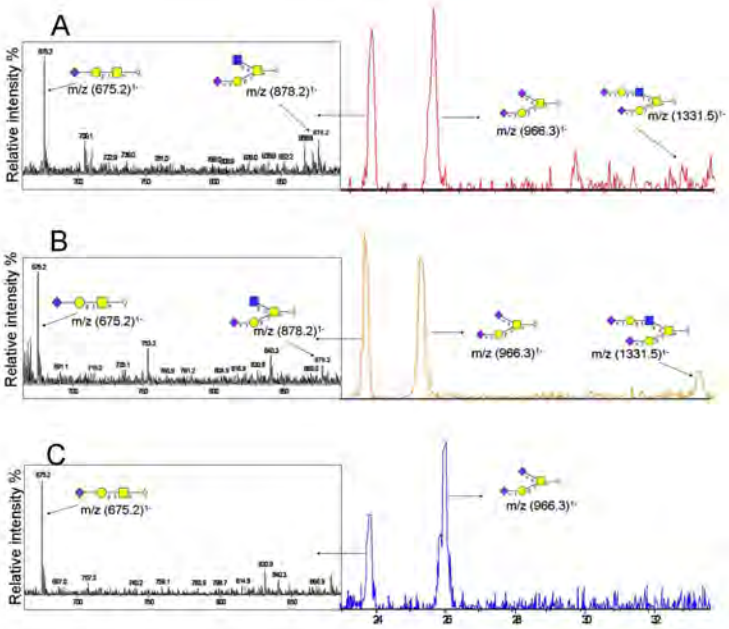

199x174mm (300 x 300 DPI)

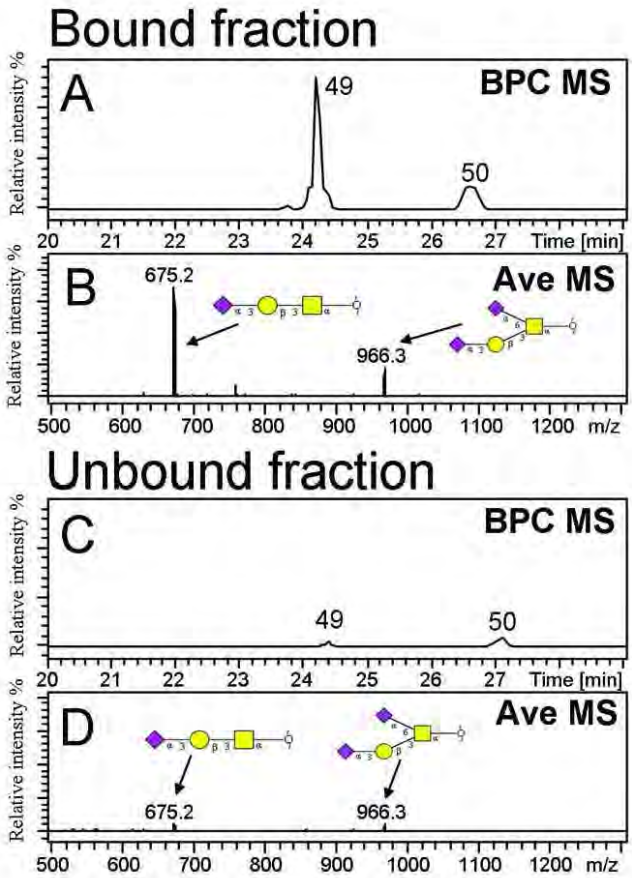

60x77mm (300 x 300 DPI)

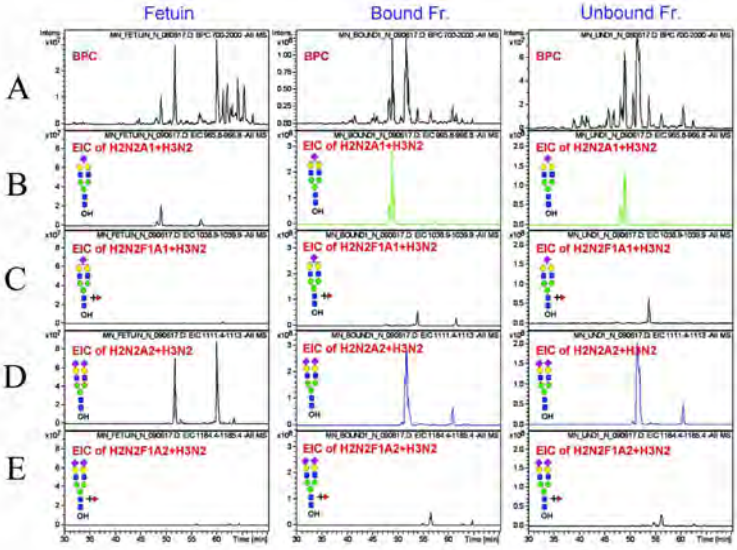

184x140mm (300 x 300 DPI)

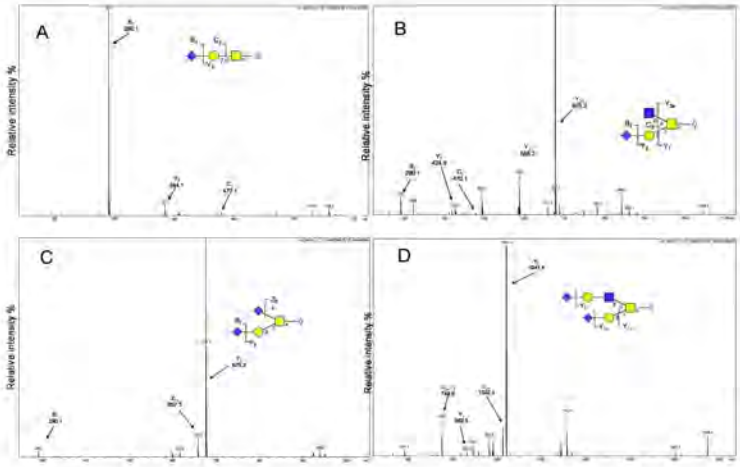

150x99mm (300 x 300 DPI)

The study presented in this paper emphasizes that whilst the use of lectins in glycoproteomics is a valuable tool for enrichment and fractionation of glycoproteins, detailed structural analysis must be undertaken to define specific differences in the glycosylation of the proteins of interest in a complex mixture. Global glycan profiling of released *N*- and *O*-linked oligosaccharides from the lectin-fractionated proteins showed that overall, both *N*- and *O*-glycan structures were very similarly attached to the lectin bound proteins and those glycoproteins not retained by the lectins. There is currently growing interest in using lectins to study protein glycosylation and these results indicate that care should be taken when interpreting results from using lectins to enrich glycoproteins from complex samples. Due to the largely different subsets of glycoproteins isolated by the different capture approaches investigated in this chapter, the unfractionated Triton X-114 phase partitioned membrane protein fraction was used as the preferred sample preparation method for enriching liver membrane proteins for subsequent studies into the effect of distal cancers on the liver glycoproteome.

Chapter 4: Liver membrane proteome glycosylation changes in mice bearing an extra-hepatic tumour (Publication III)

The optimized workflow for enrichment and analysis of liver membrane proteins that was developed in Chapter 3 was applied to study liver membrane glycoproteomic changes in mice bearing a distal tumour. In this study, proteomic and glycomic analyses were used together to determine whether liver membrane protein glycosylation was affected in mice bearing the Engelbreth-Holm Swarm (EHS) sarcoma.

MCP Papers in Press. Published on February 18, 2010 as Manuscript M900538-MCP200

Liver membrane proteome glycosylation changes in mice bearing an extra-hepatic tumour

Albert Lee[1*], Joel M. Chick[1*], Daniel Kolarich[1], Paul A. Haynes[1], Graham R. Robertson[2], Maria Tsoli[2], Lucy Jankova[2], Stephen J. Clarke[2], Nicolle H. Packer[1†], Mark S. Baker[1†].

1. Department of Chemistry and Biomolecular Sciences, Macquarie University, NSW 2109 Australia

2. ANZAC Research Institute, University of Sydney, Concord, RG Hospital NSW 2139 Australia

* These authors contributed equally

† Can be considered joint last authors

Corresponding author

Prof Nicolle H. Packer

Bldg E8C Room 307

Department of Chemistry and Biomolecular Sciences

Macquarie University

NSW 2109

Australia

Contact: +61 2 9850 8176

Email: npacker@cbms.mq.edu.au

Running title: Liver membrane glycoproteome changes in benign cancer

Copyright 2010 by The American Society for Biochemistry and Molecular Biology, Inc.

Abbreviations:

EHS, Engelbreth Holm Swarm

Peptide IPG-IEF, peptide immobilized pH gradient-isoelectric focusing

NSAF, normalised spectral abundance factor

Man1a-I, Mannosidase 1, alpha

Man1b-I, Mannosidase, alpha, class 1B, member 1

Man2a-I, Mannosidase 2, alpha 1

Mgat-I, Mannoside N-acetylglucosaminyltransferase 1

Mgat-II, Mannoside N-acetylglucosaminyltransferase 2

Mgat-V, Mannoside N-acetylglucosaminyltransferase 5

ST3Gal-I, Beta-galactoside alpha-2,3-sialyltransferase 1

ST6Gal-I, Beta galactoside alpha 2,6 sialyltransferase 1

ST6GalNAc-VI, Alpha-N-acetylgalactosaminide alpha-2,6-sialyltransferase 6

B3GalT-VII, Beta-1,3-galactosyltransferase 7

B4GalT-III, Beta-1,4-galactosyltransferase 3

C1GalT-I, Beta1,3-galactosyltransferase 1

C1GalT-II, Beta1,3-galactosyltransferase 2

GalNT-I, Polypeptide N-acetylgalactosaminyltransferase 1

NeuAc, N-acetyl neuraminic acid

NeuGc, N-glycolyl neuraminic acid

TMHMM, TransMembrane Hidden Markov Model

Summary

Cancer is well known to be associated with alterations in membrane protein glycosylation(1-3). Equally, it has been well established that tumour-associated inflammation through the release of pro-inflammatory cytokines is a common cause of reduced hepatic drug metabolism and increased toxicity in advanced cancer patients being treated with cytotoxic chemotherapies. However, little is known about the impact of bearing a tumour (and downstream effects like inflammation) on liver membrane protein glycosylation.

In this study, proteomic and glycomic analyses were used in combination to determine whether liver membrane protein glycosylation was affected in mice bearing the Engelbreth-Holm Swarm (EHS) sarcoma. Peptide IPG-IEF and label-free quantitation determined that many enzymes involved in the protein glycosylation pathway specifically; mannosidases (Man1a-I, Man1b-I and Man2a-I), mannoside N-acetylglucosaminyltransferases (Mgat-I and Mgat-II), galactosyltransferases (B3GalT-VII, B4GalT-I, B4GalT-III, C1GalT-I, C1GalT-II and GalNT-I) and sialyltransferases (ST3Gal-I, ST6Gal-I and ST6GalNAc-VI) were upregulated in all livers of tumour-bearing mice (n=3) compared to non-tumour bearing controls (n=3). In addition, many cell surface lectins: Sialoadhesin-1 (Siglec-1), C-type lectin family 4f (Kupffer cell receptor) and Galactose-binding lectin 9 (Galectin-9) were determined to be upregulated in the liver of tumour-bearing compared to control mice. Global glycan analysis identified seven N-glycans and two O-glycans that had changed on the liver membrane proteins derived from tumour-bearing mice.. Interestingly, α(2,3) sialic acid was found to be upregulated on the liver membrane of tumour-bearing mice which reflected the increased expression of its associated sialyltransferase and lectin receptor (siglec-1). The overall increased sialylation on the liver membrane of EHS

bearing mice correlates with the increased expression of their associated glycosyltransferases and suggests that glycosylation of proteins in the liver plays a role in tumour-induced liver inflammation

Introduction

Despite membrane proteins constituting approximately 70% of all human protein based drug targets, studying membrane proteins is often hindered by their low abundance, large size and relatively high hydrophobicity. Isolation and separation of membrane proteins by two-dimensional gel electrophoresis (2DGE) has been particularly problematic due to their poor solubility in various isoelectric focusing buffers. Alternative proteomic approaches such as shotgun proteomics have recently become the preferred method for identifying membrane proteins utilising high resolution separation of proteolytic peptides by liquid chromatography (MudPit)(4), capillary isoelectric focusing (cIEF)(5) or peptide immobilised pH gradient isoelectric focusing (peptide IPG-IEF)(6) in combination with reverse phase chromatography and tandem mass spectrometry.

We have recently demonstrated the use of broad and narrow range peptide IPG-IEF as an alternative method for shotgun proteomics of rat liver membrane proteins(6). Peptide IPG-IEF has several advantages as a high-resolution shotgun proteomics technique most notably because of its high sample loading capacity. It has previously been demonstrated to provide more confident and reproducible protein identifications compared to 1D SDS PAGE(7) and/or SCX(8) by using the theoretical p*I* of peptides as an additional filtering criteria to reduce false discovery rates(6). In addition, peptide IPG-IEF followed by RPLC-MS/MS can be used for comparative label-free quantitative proteomics by using a protein's calculated normalised spectral abundance factor (NSAF)(9-12).

Shotgun proteomics has demonstrated its utility in identifying membrane proteins; however information on posttranslational modifications is not obtained. Membrane proteins can be classified as peripheral, integral and/or lipid-anchored and are often glycosylated. The

extracellular surface of the plasma membrane is often decorated with glycans, glycolipids and glycoproteins which mediate many cellular events such as cell signalling, ion transport and cell recognition and adhesion. The carbohydrates attached to the proteins are covalently linked to the amide nitrogen of asparagine residues (i.e., *N*-linked) via the consensus sequence Asn-X-Ser/Thr, where X can be any amino acid except proline or to the hydroxyl groups of serine or threonine (i.e., *O*-linked).

Analogous to genomics and proteomics, which are the studies of a whole set of genes and proteins respectively, glycomics is the study of the whole set of glycans produced in a cell, tissue or organism at a particular time in health and disease. Glycans can act as markers to characterize cell types and states and they are also involved in numerous biological functions and processes such as modulating structure and function of proteins, fertilization, cell division, anti-coagulation, and inflammatory responses(13-15). Glycans are composed of monosaccharides that are covalently linked by glycosidic bonds, either in α or β conformations. However unlike proteins, which are linked in a linear structure, oligosaccharides often display diverse microheterogeneity as they are often branched-like structures formed by the different linkage/s of one or more monosaccharides.

The hydrophilicity of glycans can affect the physicochemical properties of glycoproteins thus influencing the folding, solubility, subcellular distribution and stability of the mature protein. The heterogeneity of glycans and lack of a template make it difficult to predict the type of glycans that are produced and their specific site(s) of attachment to proteins. How a protein is glycosylated can determine the localization, activity and function of the glycoprotein, therefore glycosidases and glycosyltransferases play crucial roles in catalyzing and maintaining the correct glycosylation of proteins. Many glycan-specific diseases such as congenital disorders of

glycosylation (CDGs), are caused by defects in the protein glycosylation machinery(16). For example, diseases such as cancer and autoimmunity have been reported to possess altered glycosylation as a consequence of defective or altered glycosyltransferases(2, 17, 18).

Glycosylation is known to play a role in cancer carcinogenesis and metastasis in many common cancers, and it has been shown to affect the function of many membrane proteins such as CD44(19), matrix metalloproteinases (MMPs)(20-22), selectins(23) and cadherins(24) on cancer cells. Glycosyltransferases are a group of enzymes that catalyse the addition of monosaccharides to core proteins. Most glycoproteins are either secreted into the extracellular environment or attached to the plasma membrane of the cancer cell; therefore changes to glycosyltransferases can ultimately influence the overall adhesive properties (2). Reduced levels of sialyltransferases and increased expression of fucosyltransferases, which are known to occur during cancer carcinogenesis and metastasis, extensively modify carbohydrate moieties on the cell surface(25). The degree of sialylation on the cell surface of a cancer cell acts as a confident marker of the aggressiveness of some tumours(26, 27). In addition, Sialyl Lewis X (SLe^x) antigens which are sialylated lacto-N-fucopentaose carbohydrate moieties are commonly found on cell surface glycoproteins of metastatic tumour cells (28). The degree of sialylation of these antigens can affect the polar orientation and adhesion of tumour cells during cancer metastasis(28).

The clinical relevance of inflammation both in contributing to the development of cancer and in determining prognosis is well established (29, 30). Our interest in tumour-associated inflammation has arisen as a result of our clinical findings that cancer patients with evidence of an acute phase inflammatory response in plasma (elevated C-reactive protein and alpha-1 acid glycoprotein) exhibit reduced clearance of hepatically metabolised cytotoxic drugs resulting in

increased toxicity. The murine studies described in this paper have been designed to explain these clinical findings by providing insights into the pathogenesis of the tumour-induced inflammatory effects.

Inflammation is a symptom of a disease or infection that regulates the expression of specific proteins that mediate innate and adaptive immune responses to promote healing of the affected site. Previous studies using lectin and immunoblot analyses have shown that turpentine oil-induced inflammation in mice leads to changes in the sialylation patterns of serum glycoproteins(31). Reverse transcription- polymerase chain reaction (RT-PCR) analysis of the expression profiles of mRNA for the known sialyltransferases involved in the synthesis of these sugars identified increased levels of β-galactoside α(2,3)-sialyltransferases (ST3Gal-I and ST3Gal-III), β-*N*-acetylgalactosaminide α(2,6)-sialyltransferase (ST6GalNAc-VI) and β-galactoside α(2,6)-sialyltransferase (ST6Gal-I)(31). These sialyltransferases are mostly involved in the addition of α(2,3) and α(2,6) sialic acids onto *N*- and *O*-glycans. Most plasma proteins are derived from the liver and significant increases in serum acute phase glycoproteins and their sialylation have generally been observed with most rodent experimental inflammation models (31-33).

Previous studies of mice bearing the Engelbreth-Holm Swarm (EHS) sarcoma have demonstrated that increased levels of pro-inflammatory cytokines can initiate a hepatic acute phase response and cause reduced hepatic gene expression of cytochrome enzymes(34, 35), particularly hepatic cytochrome *P*450 3A4 (CYP3A4). In cancer patients, reduced hepatic CYP3A4 function in response to tumour-associated liver inflammation has been associated with reduced drug metabolism and increased drug toxicity(36). The impact of the EHS tumour and its associated inflammatory response on the liver membrane proteome has recently been

reported(30, 36), however little is known about whether tumour-associated liver inflammation can influence membrane protein glycosylation.

In the present study, peptide IPG-IEF and label-free quantitation were used to identify and determine the relative abundance of glycosyltranferases and cell surface lectins on the liver membrane of mice bearing a distal benign tumour. Triton X-114 phase partitioning(37) was employed to further enrich membrane proteins for global glycan profiling to determine whether the changes in glycosyltransferases identified by peptide IPG-IEF reflected the structures of the glycans presented on the membrane. The combination of proteomics and glycomics approaches could help determine potentially important biological changes resulting from the EHS tumour on liver cellular membrane.

Experimental Procedures

Materials

Tris, sodium chloride, sodium hydroxide, sodium carbonate, EDTA, Bradford reagent, HEPES, PBS tablets, ammonium bicarbonate (NH_4HCO_3), ammonium acetate (NH_4COOH), formic acid, Triton X-114, dithiothreitol (DTT), iodoacetamide (IAA), LC grade acetonitrile (ACN) and sodium borohydride ($NaBH_4$) were obtained from Sigma (St. Louis, MO, USA). NuPAGE 10% Bis-Tris pre-cast gradient gels and 3-(*N*-morpholino) propane sulfonic acid (MOPS) running buffer were purchased from Invitrogen (San Diego, CA, USA). IPG strips were a generous gift from GE Healthcare (Uppsala, Sweden). Sequencing-grade trypsin was obtained from Promega (Madison, WI, USA). N-Glycosidase F (PNGase F, recombinant cloned from *Flavobacterium meningosepticum* and expressed in *Escherichia. coli*) lyophilized in 10 mM sodium phosphate buffer, pH 7.2 was acquired from Roche Diagnostics (Basel, Switzerland). Immobolin-P Polyvinylidene Fluoride (PVDF) was obtained from Millipore (MA, USA). AG50W-X8 cation-exchange resin was obtained from Bio-Rad (Hercules CA, USA) and C_{18} tips were obtained from Eppendorf (Hamburg, Germany).

Tumour transplantation

Eight to ten week old transgenic FvB male mice (n=3) were aseptically inoculated using a 14-gauge needle with 0.3 mL suspension of EHS sarcoma cells (containing 10^6 cells) in 0.9% (w/v) PBS into the quadriceps of the right hind leg. Control mice (n=3) were injected with 0.3 mL of 0.9% (w/v) PBS. Tumour mass reached approximately 3 g or 10% (w/w) total body weight over 18 to 21 days. Tumour and control mice were euthanized and livers were harvested. To address concerns of biological reproducibility, all proteomic and glycomic experiments were conducted on three biological replicates of individual control and tumor-bearing mice. All animal work was

approved by the Concord Repatriation General Hospital local area health service Animal Ethics Committee.

Membrane Protein Extraction

Mouse livers (n=3, ~1.5g) were perfused with 0.9% (w/v) phosphate buffered saline and homogenized in 10 mM HEPES buffer (pH 7.8) supplemented with 2 mM NaCl, 10 mM NaOH, 500 mM EDTA and protease inhibitors (3 mg of antipain-dihydrochloride, 0.5 mg of aprotinin, 0.5 mg of bestatin, 1 mg of chymostatin, 3 mg of E-64, 10 mg of EDTA-Na2, 0.5 mg of leupeptin, 20 mg of Pefabloc SC, 0.5 mg of pepstatin, 3 mg of phosphoramidon) one tablet per 100 ml of buffer (Roche Diagnostics, Switzerland) using an Omni TH homogenizer (Omni International, Inc., VA).

The homogenized tissue was then centrifuged at 13,000g for 15 min at room temperature (RT) to remove unbroken cells and cell debris. Total cell membrane proteins were isolated from the supernatant using a modified sodium carbonate stripping method(38). Briefly, the supernatant was diluted to a final volume of 20 mL in 0.1 M sodium carbonate (pH 11), then incubated for 1 h rotating at 4 °C. The carbonate-treated membranes were sedimented by ultracentrifugation at 120,000g for 1 h at 4 °C. The supernatant was then removed and the membrane pellet was washed twice with ammonium bicarbonate (10 mM NH_4HCO_3, pH 7.8), then 1 ml of 0.5 M TEAB, 0.05% SDS was added and pellet was transferred to a 20 mL glass scintillation vial and pulse-sonicated using a Branson 450 Sonifier (Branson, Danbury, CT) using 2 s bursts for 15 intervals on ice, and stored at -80 °C if not used immediately.

Membrane protein enrichment by Triton X-114 phase partitioning

Approximately 100 µl (equivalent to ~0.5-1 mg) of the mouse liver membrane pellet was homogenised in 4 volumes TBS buffer containing 1% (v/v) Triton X-114 and chilled on ice with

intermittent vortexing for 20 min(37). The samples were heated to 37 °C for 20 min and phase partitioned followed by centrifugation at 300g for 5 min. The upper aqueous phase was removed and stored. The detergent phase was further diluted with 4 volumes of TBS buffer containing 1% (v/v) Triton X-114 and phase partitioning repeated. The proteins in the combined aqueous phases and detergent phase were each precipitated with 9 volumes of ice-cold acetone and incubated overnight at -20°C. Acetone-precipitated proteins were resuspended in 20 µL 8 M urea.

Membrane protein digestion

The sonicated membrane sample was reduced with 10 mM DTT for 1 h at 37 °C and subsequently alkylated with 55 mM IAA in the dark at RT for 30 min. Protein quantification was conducted using a Bradford Assay (Sigma-Aldrich, MO, USA) using BSA as the standard. Trypsin digestion was carried out in the presence of 60% (v/v) methanol in 10 mM NH_4HCO_3 (pH 7.8) for approximately 8 h at 37 °C as previously described(6). All digested samples were evaporated to dryness in a vacuum centrifuge and resuspended in 250 µL of 8 M urea supplemented with a trace of Bromophenol Blue.

Preparation of *N*- and *O*-linked oligosaccharides

N- and *O*-linked oligosaccharides were sequentially released from approximately 10 µg of Triton X-114 partitioned membrane proteins according to Wilson *et al.*(39) Briefly, Immobilon-P PVDF membranes were pre-wet with 100% (v/v) ethanol and Triton X-114 phase partitioned membrane enriched proteins were dot-blotted (2.5 µL) onto the PVDF and left to dry. The PVDF was then washed with water followed by methanol to remove residual salts and detergents. The membrane was stained with Direct Blue 71 so that proteins could be visually recognized. Protein spots were excised from the PVDF membrane and placed into separate wells of a 96-well microtiter plate. The spots were blocked with 100 µL of 1% (w/v) polyvinylpyrrolidone (PVP)

40000 in 50% (v/v) methanol, agitated for 20 min, and washed thoroughly with water. *N*-linked oligosaccharides were released from the protein by incubation with 5 µL of PNGase F (0.5 units/µL) for 15 min at 37°C, and subsequently topped up with 10 µL water to reduce loss by evaporation and incubated overnight at 37°C. The sample wells were surrounded by wells containing water to further prevent evaporation, and the plate was sealed tightly with parafilm.

To recover *N*-linked oligosaccharides, the plate was sonicated in a water bath for 20 min and supernatants from each well containing released *N*-linked oligosaccharides were collected. Spots were washed twice with 50 µL water, and combined with the supernatant and were reduced to alditols prior to LC separation. Before reduction the released *N*-linked oligosaccharides were incubated with 100 mM NH_4COOH pH 5 (final concentration 15 mM) for 1 h at room temperature to ensure complete regeneration of the reducing terminus and were reduced with 1 M $NaBH_4$/50 mM KOH (20 µL) at 50ºC for 2 h. The reduction was quenched with 5 µL glacial acetic acid.

For release of N-linked oligosaccharides from SDS PAGE separated proteins, gel pieces were equilibrated and dehydrated. Each gel piece was treated with 5 µl PNGase F (0.5 U/µL) by passive diffusion, topped up with 20 µL water and incubated at 37ºC overnight. *N*-linked oligosaccharides were recovered by washing gel pieces with 3 x 20 µL water and sonicated. Released *N*-linked oligosaccharides were reduced as above and purified as described below.

Reductive β-elimination of *O*-linked oligosaccharides was carried out on the same samples after PNGase F release of the *N*-linked oligosaccharides by re-wetting the protein spots with 2 µL methanol, and incubating overnight with 0.5 M $NaBH_4$/50 mM KOH (20 µL) at 50ºC. The reaction was quenched with 2 µL acetic acid and both reduced *N*- and *O*-linked oligosaccharides were purified as described below.

Purification of reduced *N*- and *O*-linked oligosaccharides.

Homemade cation exchange columns comprising 20 µL of AG50W-X8 cation-exchange resin (H^+–form) (BioRad, Hercules, CA) were packed on top of µC_{18} ZipTips(40). Columns were prepared by washing 3 x 50 µL 1 M HCl, followed by 3 x 50 µL methanol and 3 x 50 µL water. The reduced *N*- and *O*-linked oligosaccharide alditols were applied to the column and eluted with 2 x 60 µL of water and dried. Borate was removed by the addition of 100 µL methanol and drying under vacuum five times. The oligosaccharides were re-suspended in 10 µL of water for porous graphitized carbon LC–ESI–MS/MS separation and analysis.

Neuraminidase digestion

To determine sialic acid linkages, purified *N*-linked oligosaccharides were digested in either 3 µL α(2,3) neuraminidase (Takara Bio, Japan) or 1 µL α(2,3,6) neuraminidase (Northstar Bioproducts, MA USA) in 100 mM NH_4COOH, pH 6 at 37°C for 10 min and overnight respectively. Neuraminidase activity was terminated by heating at 99°C for 3 min before carbon LC-ESI-MS/MS re-analyses of the desialylated oligosaccharides.

SDS PAGE

Approximately 10 µg of protein was applied per lane onto NuPAGE 10% Bis-Tris pre-cast gradient gels with MOPS running buffer. Electrophoresis conditions were set to 200 V, 125 mA for 60 min. The gels were fixed in 7% (v/v) acetic acid and 10% (v/v) methanol for 30 min and stained overnight with SYPRO Ruby (Invitrogen, San Diego, CA). Gel images were obtained using the Typhoon Trio Variable Mode Imager (GE Healthcare, Uppsala, Sweden). Lanes were cut into six equal fractions and equilibrated with 100 mM NH_4HCO_3 pH 7.8 for 10 min. Gel pieces were dehydrated in 50 mM NH_4HCO_3/50% (v/v) ACN for 20 min with intermittent vortexing followed by 100% (v/v) ACN for 20 min. Dehydrated gel pieces were reduced with 25

mM DTT at 37ºC for 30 min and alkylated with 55 mM IAA in the dark at room temperature for 45 min.

Peptide IPG-IEF separation

Trypsin-digested proteins (1 mg) in 8 M urea were used to passively rehydrate linear pH 3–10 (in which the actual pH range of the IPG strip is 3.85–9.36, information available at www.gehealthcare.com) 18 cm IPG strips (broad range) for 6 h at room temperature in triplicate. Isoelectric focusing was conducted on an IPGPhorII (GE Healthcare) with a current limit of 50 μA per strip for the BR IPG strip at 20°C with the following focusing program: 300 V for 1 h, a gradient to 1000 V for 1 h, a gradient to 4000 V for 3 h, a gradient to 8000 V for 3 h and 8000 V until 100 kVh was reached(6, 9). The strips were then cut (with plastic backing still in place) with a scalpel blade into 24 equal length pieces. Peptides were extracted from each fraction by incubation in 100 μL of 0.1% (v/v) formic acid for 1 h at RT. The extraction was repeated twice and subsequently combined with the initial fractions. Combined peptide extracts were desalted using C_{18} tips (Omix, Varian, Inc., CA) and the eluate was dried using a vacuum centrifuge followed by resuspension in 0.1% (v/v) formic acid.

RP LC-ESI-MS/MS

Each of the 24 IPG-IEF separated peptides fractions (from a 1 mg tryptic digest) from triplicate experiments were analyzed by nanoLC-MS/MS using a LTQ-XL ion-trap mass spectrometer (Thermo, CA). Reversed phase columns were packed in-house to approximately 7 cm (100 μm i.d.) using 100 Å, 5 mM Zorbax C_{18} resin (Agilent Technologies, CA) in a fused silica capillary with an integrated electrospray tip. A 1.8 kV electrospray voltage was applied via a liquid junction upstream of the C_{18} column. Samples were injected onto the C_{18} column using a Surveyor autosampler (Thermo, CA). Each sample was loaded onto the C_{18} column followed by

initial wash step with Buffer A (5% (v/v) ACN, 0.1% (v/v) formic acid) for 10 min at 1000 nL/min. Peptides were subsequently eluted from the C_{18} column with 0–50% Buffer B (95% (v/v) ACN, 0.1% (v/v) formic acid) over 58 min at 500 nL/min followed by 50–95% Buffer B over 5 min at 500 nL/min. The column eluate was directed into a nanospray ionization source of the mass spectrometer and spectra were scanned over the range 400–1500 amu. Automated peak recognition, dynamic exclusion, and tandem MS of the top 6 most intense precursor ions at 35% normalized collision energy were performed using the Xcalibur software (Thermo, CA).

Carbon LC-ESI-MS/MS

N- and *O*-linked oligosaccharide alditols released from approximately 10 µg of Triton X-114 phase partitioned membrane proteins were analyzed by capillary LC-MS/MS using a HCT Ultra ETD II ion-trap mass spectrometer (Bruker Biosciences Corporation, MA USA) and a capillary LC-MS/MS using a Agilent 6330 ion-trap mass spectrometer (Agilent Technologies, CA USA). The samples were applied to a Hypercarb porous graphitized carbon HPLC column (5 µm Hypercarb, 0.32 × 150 mm, Thermo Hypersil, Runcorn UK). *N*-linked oligosaccharides were separated using a linear gradient with 0-45% (v/v) ACN/10 mM NH_4HCO_3 for 83 min, followed by a 10 min wash with 90% (v/v) ACN/10 mM NH_4HCO_3 at a flow rate of 5 µL/min. *O*-linked oligosaccharides were separated using a linear gradient with 0-90% (v/v) ACN/10 mM NH_4HCO_3 for 45 min, followed by a 10 min wash with 90% (v/v) ACN/10 mM NH_4HCO_3 at a flow rate of 5 µL/min. ESI–MS was performed in negative ion mode with three scan events: full scan with mass range *m/z* 100–2500 amu, dependent zoom scan, and dependent MS/MS scan after collision induced fragmentation. Automated peak recognition, dynamic exclusion and tandem MS of the top 3 most intense precursor ions at 40% normalised collision energy was performed with an activation time of 30 s. The composition of glycans was determined using the

monoisotopic masses of detected ions and was verified manually by their associated MS/MS. Monoisotopic masses were searched using the GlycoMod software (available at http://www.expasy.ch/tools/glycomod) with parameters of ±0.7 Da to predict the possible glycan compositions corresponding to these masses. Ratios of glycans were determined by calculating the peak area of the extracted ion chromatogram (EIC) corresponding to the glycans of interest, and glycan differences were considered significant if observed in all three biological replicates.

Protein Identification and Data Analysis

Spectra files were converted to mzXML format and processed through the global proteome machine (GPM) software (version 2.1.1), an open source protein identification system that uses the X!Tandem algorithm(41). For each experiment, 24 fractions were processed sequentially with output files for each individual fraction and a merged, nonredundant output file generated for protein identifications with Log(e) values less than –1. Peptide identification was determined using a parent ion mass error of +3 Da and -0.5 Da and fragment ion tolerance of 0.4 Da(41). Mass spectra were searched based on peptide trypticity with up to three miss cleavages. Carbamidomethyl was considered as a complete modification and partial modifications were also considered, including oxidation of methionine and threonine, and deamidation of asparagine and glutamine. MS/MS spectra were searched against the *Mus musculus* database (Database derived from SwissProt, Ensemble and NCBI, released 01/06/2006) and reverse database searching was used for estimating false discovery rates.(42) The actual number of proteins in the database that were actually searched was 64,684. Mass spectra for single peptide identifications are provided as supplementary information.

Protein identifications were validated using peptide pI filtering as described previously(6). Briefly, pI was calculated through an open source pI calculator, Compute pI from

ExPASy (http://au.expasy.org/tools/pi_tool.html), which calculates peptide pI from amino acid values(43). Peptide pI filtering was conducted on the data obtained from each of the fractions by removal of statistical outliers that were defined as peptides with pI values that fall outside the pI boundaries, determined using ±0.5 of the standard deviation (calculated over the entire fraction) from the median pI value of the fraction. For analysis of total protein identifications, proteins were further validated using a 1% false discovery rate by searching the MS spectra against a reverse database and applying the following formula: FDR = reverse/(reverse + forward) × 100.

The assignment of an identified protein as being located in the membrane was made using a combination of prediction using Transmembrane Hidden Markov Model (TMHMM) (available at http://www.cbs.dtu.dk/services/TMHMM)(44) together with information on membrane location derived from UniProt, GO annotation and the Swiss-Prot database. In this study we have defined membrane proteins as comprising of integral membrane proteins, lipid-anchored proteins and membrane-associated proteins.

Calculation of peptide Normalized Spectral Abundance Factors (NSAF)

Normalized spectral abundance factors (NSAF) were calculated according to Zybailov et al.,(12) using the following formula: NSAF = (Spc/L)/$\sum$(Spc/L), where Spc refers to spectral count (number of nonredundant peptide identifications for a given protein), L is the length of the protein. Protein identifications were only included in NSAF data analysis if a given protein was identified in each of the triplicates. The reduced protein list was then adjusted with a fraction of a spectral count (in these datasets a factor of 0.18 was used) to allow the incorporation of proteins with zero spectral counts for statistical analysis (9, 12). The protein and peptide identifications used to generate this protein dataset are available in supplementary tables 1. An optimal adjustment factor was determined through fitting the natural log of the NSAF values to a

Gaussian curve, assessed by computing both R^2 values and applying a Shapiro–Wilk test. To satisfy the Shapiro–Wilk test, a W value > 0.05 was required. Statistical analysis was conducted with Microsoft Excel using the Student t-test with equal sample sizes and $P \leq 0.05$ for assignment of statistical confidence. Origin8 software package was used for assessing Gaussian distribution of data for label-free quantitation by computing both R^2 values and a Shapiro–Wilk test. The rigorous statistical approach used in the experiments (through the use of isoelectric point filtering, a reduced protein list, Shapiro-Wilk analysis and Student t-test) was designed to address concerns of analytical reproducibility.

Results

We have applied peptide IPG-IEF separation and RPLC-ESI-MS/MS to identify mouse liver membrane proteins from control (n=3) and tumour-bearing mice (n=3) and quantitated the relative abundance by calculating the NSAF(9-12) of all proteins whose gene ontology mapping suggests involvement with the glycosylation machinery. Mouse liver membrane proteins were further enriched by Triton X-114 phase partitioning and the detergent phase subjected to PNGase F digestion and reductive β-elimination to release both *N*- and *O*-linked oligosaccharides respectively for analysis by carbon LC-ESI-MS/MS. In this study we have defined membrane proteins as comprising of integral membrane proteins, lipid-anchored proteins and membrane-associated proteins as determined by TMHMM together with information derived from UniProt, GO annotation and the Swiss-Prot databases.

Label-free quantitation using peptide IPG-IEF separation

Mouse liver membranes were prepared by differential ultracentrifugation using a modified sodium carbonate stripping method(38). The membrane pellet was pulse sonicated and digested with trypsin in the presence of 60% (v/v) methanol as this solvent has been previously shown to improve membrane protein coverage.(6) In our previous study (Chick, J. M., Haynes, P. A., Robertson, G. R., and Baker, M. S. (2009) Liver Membrane Proteome Dynamics in Cancer Bearing Mice, manuscript in preparation) in which we characterized the mouse liver membrane proteome by this approach, we identified 1625 proteins of which 236 were determined to be differentially expressed proteins involved metabolic pathways such as liver metabolism, solute carrier transport and drug detoxification.

In this study, we identified 33 membrane proteins involved in glycosylation of which 15 were found to be significantly and differentially expressed (i.e., fold change greater than 1.3 and $p \leq 0.05$) in the livers of all tumour-bearing mice (Figure 1, Supplementary Table 1 and Supplementary Figure 1). These include mannosidases (Man1a-I, Man1b-I and Man2a-I), which were found to be upregulated (1.38, 5.98 and 1.86 fold respectively); and mannoside N-acetylglucosaminyltransferases (Mgat-I, Mgat-II and Mgat-V) which were also determined to be upregulated (4.22, 2.33 and 16.31 fold respectively) in the liver of tumour-bearing mice. Mannosidases are often found in the ER and cytoplasm and are mostly involved in the hydrolysis and removal of mannose monosaccharides from glycans that are attached to lipids and proteins. They are also involved in the synthesis of complex glycoconjugates by the degradation of immature glycoproteins that permit further modification by other glycosyltransferases. Mannoside N-acetylglucosaminyltransferases (Mgats) are involved in the catalysis of GlcNAc from uridine diphospho-GlcNAc (UDP-GlcNAc) to terminal branched α-mannosyl (Man) residues on glycolipids and glycoproteins in both the endoplasmic reticulum (ER) and Golgi apparatus (GA).

The 6 galactosyltransferases (B3GalT-VII, B4GalT-I, B4GalT-III, C1GalT-I, C1GalT-II and GalNT-I) were all found to be upregulated in the liver of tumour-bearing mice (Figure 1) with a range between 6 and 11 fold change. Galactosyltransferases and sialyltransferases are usually localized to the GA membrane and are involved in *N*- and *O*-glycan biosynthesis. Galactosyltransferases are responsible for catalyzing the transfer of galactose from UDP-galactose to *N*- and *O*-linked glycans via β(1-4), β(1-3), α(1-3) and α(1-4) linkages and are also involved in lactose biosynthesis. Sialyltransferases (ST3Gal-I, ST6Gal-I and ST6GalNAc-VI) were also found to be upregulated (5.45, 5.25 and 11.67 fold respectively) in the liver of tumour-

bearing mice. These enzymes are responsible for catalyzing the addition of α(2,3) and α(2,6) neuraminic acid to the non-reducing termini of glycolipids and of *N*- and *O*-linked glycans on glycoproteins. Other glycan-processing enzymes such as alpha(1-3)-mannosyltransferases (Alg2, Alg3), ST3Gal-III, ST3Gal-IV and GalNT-II were determined to have no significant change in abundance (Figure 1, Supplementary Table 1). Collectively, the upregulation of these enzymes suggests an overall increase in activity of the glycosylation machinery in the liver of tumour-bearing mice.

We identified siglec-1 upregulated (~43 fold) in liver membrane proteins from tumour-bearing mice in this study compared to the controls (Figure 2). Other lectins including calcium dependent-type (C-type), lectin 4f (Clec4f) and galactose-binding lectin 9 (Lgals9) were also upregulated in tumour-bearing mice (Figure 2). Clec4f has been reported to mediate pathogen recognition and cell-cell interactions using structurally related Ca^{2+}-dependent carbohydrate-recognition domains on macrophages and natural killer cells in the immune system(45). Lgals9 is known to promote anti-inflammatory responses in the innate and adaptive immune system when stimulated by pro-inflammatory cytokines(46).

Global analysis of oligosaccharides

To determine whether the increased expression of glycosyltransferases and mannosidases in the liver influenced the glycosylation of liver membrane proteins, global glycan analysis was performed on control and tumour-bearing mouse liver membrane proteins. The identification of any global *N*- and/or *O*-glycan differences would determine if the significant differential expression of glycosylation-related proteins was converted to observable enzymatic activity reflected in altered substrate glycosylation status. *N*-linked oligosaccharides were released from

the membrane glycoproteins by PNGase F and analysed using graphitized carbon LC-ESI-MS in negative ion mode.

The combined mass spectra of the global liver membrane N-linked oligosaccharides attached from control and tumour-bearing mice are shown in Figure 3 and the *N*-glycan differences observed in the liver membrane proteins of tumour-bearing mice are shown in Table 1. Ions corresponding to *N*-glycans were found as doubly charged $[M-2H]^{2-}$ ions in the combined mass spectra. Several masses assigned to *N*-glycan compositions were seen in the liver membranes of tumour-bearing mice and not in the control. Both control and tumour-bearing mouse liver membrane proteins expressed high mannose structures (for example $[M-2H]^{2-}$ of m/z 860.3 and 941.3) and sialylated complex type *N*-glycan structures (for example $[M-2H]^{2-}$ of m/z 1127.4). Specifically, six *N*-glycan structures were found to be present only on liver membrane proteins from EHS tumour-bearing mice ($[M-2H]^{2-}$ of m/z 965.9, 1022.4, 1038.9, 1111.4, 1184.4 and 1280.9). Of these, four are complex *N*-glycans terminating with *N*-acetyl neuraminic acid (NeuAc), with two containing a fucosylated core. Two low abundance ions corresponding to N-glycan masses of m/z $(1022.4)^{2-}$ and $(1038.9)^{2-}$ appeared to be present in higher amounts in the tumour–bearing mice in the average MS taken over the chromatography retention time of 20-65 min (Figure 3A and 3B). We have substantiated the tumour-specific difference in the abundance of these ions by using a combined EIC of m/z 941.3, 1022.4 and 1038.9 (+/- 0.5 Da) to detect the specific abundance of each relative to nearby peaks (Figure 3C and 3D). Average MS of the narrower retention time (21-28min) of where the m/z ion (1022.4) elutes confirms that this mass ion is present in the tumour-bearing mice but is not detectable in the normal mice. The masses corresponding to the assigned glycan structures have been previously identified in the mouse by

the references indicated in Table 1. Assigned glycan structures have been included as supplementary information (Supplementary Table 2).

The expression of di-*N*-glycolyl neuraminic acid (NeuGc) biantennary *N*-glycan structure ($[M-2H]^{2-}$ of m/z 1127.4) which was verified by MS/MS fragmentation (Figure 4C) was observed in both control and tumour-bearing. This mass was seen to exist as two isomers in the extracted ion chromatogram (EIC) at 30 min and at 41 min (Figure 4A and 4B). Based on the EIC and peak area, the control mice (Figure 4A) expressed a different ratio of these two isomers (approximately 9:1 (isomer 1:2, n=3)) whilst the tumour-bearing mouse had a ratio of 2.3:1(isomer 1:2, n=3).

The presence of two isobaric N-linked structures at ($[M-2H]^{2-}$ of m/z 1127.4) suggests that the isomers may have different linkages to the two terminal NeuGc. The N-linked oligosaccharides from membrane proteins of tumour-bearing mice were digested with α(2,3) neuraminidase to determine the specific linkages of the NeuGc attached specifically to the non-reducing termini of the biantennary N-glycan. This enzyme has been shown to remove NeuGc as well as NeuAc(47). The first isomer eluted at 54 min was not affected by digestion and thus must consist of two NeuGcα(2,6)Galβ1 moieties attached to the non-reducing termini (Figure 5B). The isomer observed at 62 min (Figure 5A) was no longer present after digestion, implying that this isomer consisted of two α(2,3) linked NeuGc moieties attached to the non-reducing termini. Interestingly, following α(2,3) neuraminidase digestion two additional peaks corresponding to the same mass ($[M-2H]^{2-}$ of m/z 1127.4) appeared, eluting at the retention times different to those above relative to the NeuGcα(2,6)Galβ1. That is, α(2,3) linked NeuGc had been removed from a precursor oligosaccharide producing two different biantennary di-sialylated glycans different from the double α(2,6) NeuGc terminated structure eluting at 54 min. Therefore, this

suggested that in the original sample, a tri-sialylated biantennary N-glycan consisting of three NeuGc may also be present. A peak of $[M-2H]^{2-}$ of m/z 1280.9 was present at 55 and 60 mins which would correspond to a composition of $(NeuGc)_3(Hex)_2(HexNAc)_2$ + $(Man)_3(HexNAc)_2$. The structural isomers after treatment with neuraminidase, corresponding to m/z $(1127.4)^{2-}$ observed in Figure 4 and in the EIC of m/z $(1127.4)^{2-}$ in Figures 5 and 6 appear to differ in elution times. These samples had been analysed by carbon chromatography on two different mass spectrometric systems; Agilent HCT and the Bruker Ultra ETD II ion-trap mass spectrometers, and resulted in different retention times. The consistent identity of these isomers was confirmed by their having the same MS/MS fragmentation pattern of the mass ion m/z $(1127.4)^{2-}$ and the same elution position as that of standard glycans chromatographed on the same instruments.

Identification of a biantennary *N*-glycan with three N-glycolyl neuraminic acids

To determine the structures of the tri-sialylated N-glycan, the N-linked oligosaccharides were digested with α(2,3,6) neuraminidase to remove both terminal NeuGcα(2-3)Galβ1 and NeuGcα(2-6)Galβ1 linkages. After 10 min digestion all di-sialylated and tri-sialylated masses (m/z of $(1127.4)^{2-}$ and $(1280.9)^{2-}$) had disappeared with only non-sialylated and mono-sialylated structures remaining (Figure 6B). After further overnight digestion with α(2,3,6) neuraminidase there remained evidence of a single resistant NeuGc residue with m/z of $(973.8)^{2-}$ corresponding to a mono-sialylated biantennary N-glycan. MS/MS fragmentation of the remaining mono-sialylated glycan mass (m/z of $(973.8)^{2-}$) showed a diagnostic ion (c_2 m/z ion $(509.1)^{-1}$) which corresponded to the mass of a NeuGc attached to GlcNAc suggesting possible existence of the two structures depicted in Figure 6D. It is of course possible that the α(2,3,6) sialidase digestion could have been incomplete and/or that some of the three NeuGc residues were resistant to

cleavage. In particular, it is possible that the unusual NeuGc-GlcNAc linkage may not be cleaved by this enzyme so that the exact linkages of this tri-sialylated biantennary structure cannot be unequivocally assigned. Interestingly, liver membrane proteins from EHS tumour-bearing mice expressed this tri-sialylated glycan structure ($[M-2H]^{2-}$ of m/z 1280.9), which the control mice did not express. This particular *N*-glycan has recently been identified in the mouse liver(48).

Analysis of O-linked oligosaccharides

EIC of the *O*-linked oligosaccharides released by β-elimination from liver membranes of control and tumour-bearing mice show distinct differences. The combined EIC of m/z $(675.3)^{1-}$, $(691.3)^{1-}$ $(966.2)^{1-}$, $(982.3)^{1-}$, $(998.4)^{1-}$ and $(681.3)^{2-}$ (Figure 7A and 7B) monitors the masses corresponding to O-glycans previously identified in the mouse (49-51). These ions were mostly singly charged ions $[M-H]^{-1}$. Liver membranes from both control and tumour-bearing mice mostly expressed similar compositions containing both NeuAc and NeuGc ($[M-H]^{1-}$ of m/z 675.3 $((Hex)_1(HexNAc)_1(NeuAc)_1)$, 691.3 $((Hex)_1(HexNAc)_1(NeuGc)_1)$, 966.2 $((Hex)_1(HexNAc)_1(NeuAc)_2)$ and 982.3 $((Hex)_1\ (HexNAc)_1\ (NeuAc)_1\ (NeuGc)_1)$ as shown in Figure 7A and 7B.

Interestingly, the average MS between retention time 17.2 to 17.9 min indicated an ion of m/z $(998.4)^{1-}$ in tumour–bearing but not in control mice. MS/MS fragmentation of this ion identified a core 1 structure consisting of $(HexNAc)_1(Hex)_1(NeuGc)_2$ (Figure 7C). In addition, a O-glycan of composition $(HexNAc)_2(Hex)_2(NeuGc)_2$ ($[M-H]^{2-}$ of m/z 681.3) was observed on the liver membrane of tumour-bearing mice and not in the controls (Figure 7B). This O-glycan of composition $(HexNAc)_2(Hex)_2(NeuGc)_2$ ($[M-H]^{2-}$ of m/z 681.3) was shown to be a core 2 structure by MS/MS fragmentation (Figure 7D).

Glycan profile changes on fractionated membrane proteins

To determine whether the differences in glycans observed in the liver of EHS tumour-bearing mice were occurring on all membrane proteins or on specific protein(s), Triton X-114 phase partitioned membrane proteins were separated by 1D SDS PAGE and gel lanes cut into 6 equal fractions of descending mass with each fraction digested with PNGase F to release *N*-linked oligosaccharides. The analysis of *N*-linked oligosaccharides released from each of the 6 fractions showed that the same *N*-glycans seen in the global N-glycn profile were overall reflected similarly on all membrane proteins (Figure 8).

Discussion

Previous characterization of the mouse liver membrane proteome reported that many of the identified proteins are involved in cellular processes such as coagulation, fatty acid metabolism, gluconeogenesis , glycolysis, and protein ubiquitination. The liver has been well studied at both the genomic and proteomic level with strong emphasis on liver diseases such as hepatitis(52, 53), hepatocellular carcinoma(53) and alcoholism(54). Mouse models have been widely used as model systems to study parallel aspects of human disease to further improve our understanding of the mechanisms involved with these diseases. The specific model used in the current study involves systemic inflammation produced by the EHS sarcoma, which has been previously shown to result in repression of multiple hepatic drug metabolizing enzymes and transporters (30, 36). The inflammatory reaction is associated with elevated plasma concentrations of pro-inflammatory cytokines produced by the tumour and the surrounding stromal cells (29, 35, 55). These changes can lead to reduced liver metabolism and clearance of drugs resulting in increased toxicity from chemotherapy. In this study we determined that the glycosylation of liver membrane proteins was also affected by the presence of this tumour.

Glycosylation pathway enzymes change in the liver of tumour-bearing mice

Peptide IPG-IEF and label-free quantitation analyses determined that mannosidases and many glycosyltransferases (mgat, galactosyltransferases and sialyltransferases) were upregulated in the liver membrane of tumour-bearing mice. Mannosidases are often found in the ER and cytoplasm and they are responsible for trimming mannose residues from *N*-linked glycans that are attached to proteins for correct folding and orientation. They are also involved in the degradation of mature glycoproteins forming glycoconjugate intermediates that permit further modification by other glycosyltransferases such as Mgats.

Mgat I (GlcNAcT-I) and Mgat-II (GlcNAcT-II) are responsible for the transfer of GlcNAc in a β(1,2) glycosidic linkage to the Manα(1,3) and Manα(1,6) arm of a N-linked glycan respectively in a [Manα(1,3)/Manα(1,6)]Manβ(1,4)GlcNAcβ(1,4)GlcNAc–Asn sequence, and are both essential in initiating the biosynthesis of complex *N*-glycans within the lumen of the Golgi apparatus. It has been reported that the loss of either enzyme can reduce the number of complex-type N-glycans whilst increasing the number of hybrid-type *N*-glycans on the cell surface causing alterations to cell adhesion and other cellular interactions(56). Mgat-II deficiencies in mice display phenotypic signs similar to those reported in human congenital disorders of glycosylation. Mgat-V (GlcNAcT-V) transfers GlcNAc to the hydroxyl on carbon 6 of α-linked mannose in the preliminary sequence GlcNAcβ(1,2)Manα(1,6)Manβ(1,4)GlcNAcβ(1,4)GlcNAc–Asn, which is present as the *N*-glycan intermediate at the medial Golgi apparatus stage of glycosylation. Knockout studies of mouse Mgat-V have found that Mgat-V-deficient mice were susceptible to autoimmune diseases, reduced cancer progression and T-cell hypersensitivity(57, 58).

Galactosyltransferases (B3GalT-VII, B4GalT-I, B4GalT-III, C1GalT-I, C1GalT-II and GalNT-I) were identified be up-regulated in the liver of tumour-bearing mice. These enzymes are responsible for catalyzing the transfer of galactose to *N*- and *O*-linked glycans via β(1-4) and β(1-3) linkages, and they are also involved in lactose biosynthesis. B3GalT-VII and C1GalT1 are responsible for the formation of the core 1 disaccharide O-glycan (Galβ(1–3)GalNAc), known as the T antigen. The core 1 O-glycan is the precursor for the synthesis of many of the extended mucin-type O-glycans, which are commonly found on mammalian glycoproteins. The loss of B3GalT-VII and C1GalT-I enzymatic activity has been reported to cause hemolytic anemia due to the lack of T antigens on blood cells(59). It has been proposed that C1GalT-II functions as a

molecular chaperone together with C1GalT-1 in the synthesis of core 1 O-glycans(60). B4GalT-I is ubiquitously expressed and has two enzymatic activities. As a monomer it transfers Gal to GlcNAc-acceptors and when associated with α-lactalbumin, B4GalT-I catalyses the transfer of Gal to Glc producing lactose(60). B4GalT-I is active towards GlcNAc in a range of glycoconjugates (*N*- and O-glycans and glycolipids) and deficiencies in this enzyme in mice present with skin lesions, decreased fertility and absence of lactose in milk(60). The function of B4GalT-III appears to be in the synthesis of the first N-acetyllactosamine unit of poly-N-acetyllactosamine chains on glycoconjugates(61). Furthermore, GalNT-I is one of the enzymes responsible for the transfer of GalNAc to serine and threonine residues on many O-linked glycoproteins(60).

Sialyltransferases (ST3Gal-I, ST6Gal-I and ST6GalNAc-VI) were also observed to be up-regulated on the liver membrane proteins of tumour-bearing mice. ST3Gal-I is highly abundant in the spleen, liver, bone marrow, thymus, and salivary glands of humans and mice. It is responsible for the transfer of sialic acid from CMP-NeuAc to the terminal galactose residues through α(2,3) linkages and has been reported to preferentially transfer sialic acid to core 1 O-glycan structures(62). NeuAc is modified to NeuGc in mice by the enzyme CMP-hydroxylase, which catalyzes the hydroxylation of CMP-NeuAc to CMP-NeuGc in the presence of hydrogen donor (NADH), cytochrome b5 and NADH-cytochrome b5 reductase(63, 64). Mice with ST3Gal-I deficiency exhibit decreased cytotoxic T-cell immune responses and increased apoptosis of $CD8^+$ T-cells(65). The sialylation of core 1 and core 2 O-glycans presented on $CD8^+$ T-cells is crucial in controlling the differential binding of these cells to MHC-I. Moreover, ST6Gal-I and ST6GalNAc-VI are responsible for catalyzing the transfer of sialic acid to terminal galactose and *N*-acetylgalactoseamine (GalNAc) residues through an α(2,6) linkage. ST6Gal-I is

ubiquitously expressed and plays important roles in the immune system, as it has been demonstrated that mice lacking ST6Gal-I display reduced serum IgM levels and impaired B-cell proliferation(66). The increased expression of many enzymes involved in glycosylation suggest that this could result in dramatic changes in the structure of metabolically significant N and O-glycans found collectively on membrane proteins as a result of bearing a benign tumour.

Presence of tumour increases sialylation on liver membrane glycoproteins

It has been reported that the release of inflammatory cytokines stimulates the expression of glycosyltransferases in tumour, as well as hepatocyte cells, which results in increased glycan branching and Sialyl Lewis X (SLe^x) (NeuAcα(2,3)Galβ(1,4)[Fucα(1,3)]GlcNAc) structures on secreted glycoproteins in humans (67). In addition to the expressional changes of acute phase proteins the prevalence of tri- and tetra-antennary glycans with SLe^x structures have also been shown to be altered during systemic autoimmune liver inflammation. During short-term acute liver inflammation, α1-acid glycoprotein displayed increased expression of biantennary *N*-glycans. However, during long-term acute liver inflammation α1-acid glycoprotein expressed primarily tri- and tetra-antennary *N*-glycan forms(67). The increased levels of tri- and tetra-antennary and SLe^x structures of acute phase serum proteins is considered a secondary outcome following the secretion of pro-inflammatory cytokines from human diseases such as stomach(67) and ovarian cancer(68), as well as rheumatoid arthritis(69). Although much attention has been paid to identifying alterations in phase serum glycoproteins during acute liver inflammation, our goal was to determine if changes in glycan composition were observed on the liver membrane proteome correlating with observed glycosylation enzyme expression changes.

Liver membrane glycoproteins from tumour-bearing mice showed increased sialylation on complex-type biantennary *N*-linked glycans with terminating *N*-acetyl- and *N*-glycolyl-

neuraminic acid, and increased *N*-glycolyl sialylation on core 1 and core 2 O-glycans. In addition, the ratios of different isomers of biantennary complex-type *N*-glycans with two NeuGc attached to Galβ(1-4)GlcNAcβ(1-2)Manα(1-3)[Galβ(1-4)GlcNAcβ(1-2)Manα(1-6)]Manβ(1-4)GlcNAcβ(1-4)GlcNAc differed between control and tumour-bearing mice. Interestingly, liver membrane proteins from tumour-bearing mice, and not control mice, expressed a tri-sialylated biantennary *N*-glycan with three NeuGc. Neuraminidases with different specificities were used to determine the linkages of the three attached NeuGc. Together with MS/MS fragmentation data, the presence of a NeuGcα(2-6)GlcNAcβ1 linkage was confirmed. This biantennary N-glycan structure with three NeuGc attached was shown to be present only in the liver of tumour-bearing mice and not in the control. This N-glycan has been reported previously to be present in the liver of control and insulin-resistant mice (48).

Similar glycosylation changes were observed on all SDS-PAGE fractionated membrane proteins from tumour-bearing mice, this was not surprising since hepatocytes make up approximately 80% (w/w) of the cytoplasmic mass of the liver and, both *N*- and *O*-glycosylation are processed through the same protein glycosylation machinery in the ER and Golgi apparatus. The N-glycan profiles of the different mass range proteins separated by gel electrophoresis were generally similar between all fractions and reflect the gross overall profile shown in the global glycan anlysis (Figure 8). This observation emphasizes the fact that alterations in the abundance of glycosylation enzymes in a cell affect all expressed glycoproteins. There are some differences observed in the relative intensities of some peaks corresponding to N-glycans in the average MS of the different gel fractions and these small variations are most likely attributed to subtle differences in glycosylation of individual membrane glycoproteins. The effect of these observed

glycosylation changes on the function of individual membrane glycoproteins remains to be determined experimentally.

Both NeuAc and NeuGc belong to a family of sialic acids that are typically found attached to the terminal positions of several classes of cell-surface and secreted *N*- and *O*-glycans. They are also presented on glycans to increase the hydrophilicity of glycoproteins for export to the extracellular environment and/or the cell surface for cell interaction events. Sialic acids often act as ligands for selectins and sialic acid-binding lectin (Siglecs) for glycan-mediated cellular interactions, such as B- and T-cell activation in adaptive immunity(65, 70), and the increased expression of NeuAc and NeuGc in the liver of tumour-bearing mice may play roles in response to inflammatory stimuli.

Siglecs are a family of sialic acid-binding immunoglobulin (Ig)-like lectins that are found either secreted into the extracellular environment or attached to the surface of cells where they interact specifically with sialic acid on glycan structures. For example, siglec-1 binds to the sialic acids on the surface of B-cells in activating the adaptive immune system(71). Siglec-1 is also expressed by resident and inflammatory macrophages in the liver, lung, and spleen in response to inflammation and is responsible for binding sialylated ligands. The lectin specifically recognises α(2,3) sialic acid on *N*- and *O*-glycans in a NeuAc/NeuGcα(2-3)Galβ(1-4)GlcNAc sequence(72) on other hemopoietic cells, neutrophils, monocytes, natural killer cells, B cells and a subset of $CD8^+$ T lymphocytes(73). The increased expression of sialylation observed in this study on the surface of the liver membrane in response to the distal tumour could therefore act as a ligand for macrophage receptors like siglec-1 whereby it could modify cell adhesion and interaction.

The data presented in this study indicates that many enzymes involved in the protein glycosylation pathway in inflamed livers of mice bearing a distal benign tumour were found to

be significantly up-regulated. Cell surface lectins and receptors were also determined to be up-regulated in these tumour-bearing mice. These enzymes and receptors correlated with the changes in *N*- and *O*-linked glycan structures which were expressed only on the liver membrane of tumour-bearing mice and were reflected on all membrane glycoproteins. Specifically, increased *N*-acetyl and *N*-glycolyl sialylation were only identified on the membrane proteins from livers of tumour-bearing mice. The presence of cancer is well-known to be associated with alterations in membrane protein glycosylation but differential expression of these glycan structural differences, together with their associated synthetic enzymes and receptors demonstrate that downstream effects of cancer are seen in the liver which is distant from the tumour itself.

Acknowledgements

The authors would like to thank their ARC Linkage industry partner GE Healthcare. This research project was supported by access to the Australian Proteome Analysis Facility (APAF) established under the Australian Government's NCRIS program and to the mass spectrometry infrastructure funded by the NSW Cancer Institute.

References

1. Bird, N. C., Mangnall, D., and Majeed, A. W. (2006) Biology of colorectal liver metastases: A review. *J Surg Oncol* 94, 68-80.

2. Dimitroff, C. J., Pera, P., Dall'Olio, F., Matta, K. L., Chandrasekaran, E. V., Lau, J. T., and Bernacki, R. J. (1999) Cell surface n-acetylneuraminic acid alpha2,3-galactoside-dependent intercellular adhesion of human colon cancer cells. *Biochem Biophys Res Commun* 256, 631-636.

3. Arcinas, A., Yen, T. Y., Kebebew, E., and Macher, B. A. (2009) Cell surface and secreted protein profiles of human thyroid cancer cell lines reveal distinct glycoprotein patterns. *J Proteome Res* 8, 3958-3968.

4. Washburn, M. P., Wolters, D., and Yates, J. R., 3rd (2001) Large-scale analysis of the yeast proteome by multidimensional protein identification technology. *Nat Biotechnol* 19, 242-247.

5. Wang, W., Guo, T., Rudnick, P. A., Song, T., Li, J., Zhuang, Z., Zheng, W., Devoe, D. L., Lee, C. S., and Balgley, B. M. (2007) Membrane proteome analysis of microdissected ovarian tumor tissues using capillary isoelectric focusing/reversed-phase liquid chromatography-tandem MS. *Anal Chem* 79, 1002-1009.

6. Chick, J. M., Haynes, P. A., Molloy, M. P., Bjellqvist, B., Baker, M. S., and Len, A. C. (2008) Characterization of the rat liver membrane proteome using peptide immobilized pH gradient isoelectric focusing. *J Proteome Res* 7, 1036-1045.

7. Krijgsveld, J., Gauci, S., Dormeyer, W., and Heck, A. J. (2006) In-gel isoelectric focusing of peptides as a tool for improved protein identification. *J Proteome Res* 5, 1721-1730.

8. Slebos, R. J., Brock, J. W., Winters, N. F., Stuart, S. R., Martinez, M. A., Li, M., Chambers, M. C., Zimmerman, L. J., Ham, A. J., Tabb, D. L., and Liebler, D. C. (2008) Evaluation of strong cation exchange versus isoelectric focusing of peptides for multidimensional liquid chromatography-tandem mass spectrometry. *J Proteome Res* 7, 5286-5294.

9. Chick, J. M., Haynes, P. A., Bjellqvist, B., and Baker, M. S. (2008) A combination of immobilised pH gradients improves membrane proteomics. *J Proteome Res* 7, 4974-4981.

10. Pavelka, N., Fournier, M. L., Swanson, S. K., Pelizzola, M., Ricciardi-Castagnoli, P., Florens, L., and Washburn, M. P. (2008) Statistical similarities between transcriptomics and quantitative shotgun proteomics data. *Mol Cell Proteomics* 7, 631-644.

11. Sardiu, M. E., Cai, Y., Jin, J., Swanson, S. K., Conaway, R. C., Conaway, J. W., Florens, L., and Washburn, M. P. (2008) Probabilistic assembly of human protein interaction networks from label-free quantitative proteomics. *Proc Natl Acad Sci U S A* 105, 1454-1459.

12. Zybailov, B., Mosley, A. L., Sardiu, M. E., Coleman, M. K., Florens, L., and Washburn, M. P. (2006) Statistical analysis of membrane proteome expression changes in Saccharomyces cerevisiae. *J Proteome Res* 5, 2339-2347.

13. Rudd, P. M., Elliott, T., Cresswell, P., Wilson, I. A., and Dwek, R. A. (2001) Glycosylation and the immune system. *Science* 291, 2370-2376.

14. Dwek, R. A. (1996) Glycobiology: Toward Understanding the Function of Sugars. *Chem Rev* 96, 683-720.

15. Varki, A., *et al*. (1999) *Essentials in Glycobiology*.

16. Freeze, H. H. (2006) Genetic defects in the human glycome. *Nat Rev Genet* 7, 537-551.

17. Green, R. S., Stone, E. L., Tenno, M., Lehtonen, E., Farquhar, M. G., and Marth, J. D. (2007) Mammalian N-glycan branching protects against innate immune self-recognition and inflammation in autoimmune disease pathogenesis. *Immunity* 27, 308-320.

18. Hakomori, S. (2002) Glycosylation defining cancer malignancy: new wine in an old bottle. *Proc Natl Acad Sci U S A* 99, 10231-10233.

19. Casey, R. C., Oegema, T. R., Jr., Skubitz, K. M., Pambuccian, S. E., Grindle, S. M., and Skubitz, A. P. (2003) Cell membrane glycosylation mediates the adhesion, migration, and invasion of ovarian carcinoma cells. *Clin Exp Metastasis* 20, 143-152.

20. Mori, M., Barnard, G. F., Mimori, K., Ueo, H., Akiyoshi, T., and Sugimachi, K. (1995) Overexpression of matrix metalloproteinase-7 mRNA in human colon carcinomas. *Cancer* 75, 1516-1519.

21. Yamamoto, H., Itoh, F., Senota, A., Adachi, Y., Yoshimoto, M., Endoh, T., Hinoda, Y., Yachi, A., and Imai, K. (1995) Expression of matrix metalloproteinase matrilysin (MMP-7) was induced by activated Ki-ras via AP-1 activation in SW1417 colon cancer cells. *J Clin Lab Anal* 9, 297-301.

22. Zeng, Z. S., and Guillem, J. G. (1998) Unique activation of matrix metalloproteinase-9 within human liver metastasis from colorectal cancer. *Br J Cancer* 78, 349-353.

23. Reyes-Reyes, M. E., George, M. D., Roberts, J. D., and Akiyama, S. K. (2006) P-selectin activates integrin-mediated colon carcinoma cell adhesion to fibronectin. *Exp Cell Res* 312, 4056-4069.

24. Ngan, C. Y., Yamamoto, H., Seshimo, I., Ezumi, K., Terayama, M., Hemmi, H., Takemasa, I., Ikeda, M., Sekimoto, M., and Monden, M. (2007) A multivariate analysis of adhesion molecules expression in assessment of colorectal cancer. *J Surg Oncol* 95, 652-662.

25. Petretti, T., Kemmner, W., Schulze, B., and Schlag, P. M. (2000) Altered mRNA expression of glycosyltransferases in human colorectal carcinomas and liver metastases. *Gut* 46, 359-366.

26. Hasegawa, H., Watanabe, M., Arisawa, Y., Teramoto, T., Kodaira, S., and Kitajima, M. (1993) Carbohydrate antigens and liver metastasis in colorectal cancer. *Jpn J Clin Oncol* 23, 336-341.

27. Matsushita, Y., Cleary, K. R., Ota, D. M., Hoff, S. D., and Irimura, T. (1990) Sialyl-dimeric Lewis-X antigen expressed on mucin-like glycoproteins in colorectal cancer metastases. *Lab Invest* 63, 780-791.

28. Berg, E. L., Robinson, M. K., Mansson, O., Butcher, E. C., and Magnani, J. L. (1991) A carbohydrate domain common to both sialyl Le(a) and sialyl Le(X) is recognized by the endothelial cell leukocyte adhesion molecule ELAM-1. *J Biol Chem* 266, 14869-14872.

29. Kacevska, M., Robertson, G. R., Clarke, S. J., and Liddle, C. (2008) Inflammation and CYP3A4-mediated drug metabolism in advanced cancer: impact and implications for chemotherapeutic drug dosing. *Expert Opin Drug Metab Toxicol* 4, 137-149.

30. Robertson, G. R., Liddle, C., and Clarke, S. J. (2008) Inflammation and altered drug clearance in cancer: transcriptional repression of a human CYP3A4 transgene in tumor-bearing mice. *Clin Pharmacol Ther* 83, 894-897.

31. Yasukawa, Z., Sato, C., and Kitajima, K. (2005) Inflammation-dependent changes in alpha2,3-, alpha2,6-, and alpha2,8-sialic acid glycotopes on serum glycoproteins in mice. *Glycobiology* 15, 827-837.

32. Lin, S. Y., Chen, Y. Y., Fan, Y. Y., Lin, C. W., Chen, S. T., Wang, A. H., and Khoo, K. H. (2008) Precise mapping of increased sialylation pattern and the expression of acute phase proteins accompanying murine tumor progression in BALB/c mouse by integrated sera proteomics and glycomics. *J Proteome Res* 7, 3293-3303.

33. Chavan, M. M., Kawle, P. D., and Mehta, N. G. (2005) Increased sialylation and defucosylation of plasma proteins are early events in the acute phase response. *Glycobiology* 15, 838-848.

34. Fang, C., Yoon, S., Tindberg, N., Jarvelainen, H. A., Lindros, K. O., and Ingelman-Sundberg, M. (2004) Hepatic expression of multiple acute phase proteins and down-regulation of nuclear receptors after acute endotoxin exposure. *Biochem Pharmacol* 67, 1389-1397.

35. Morgan, E. T., Goralski, K. B., Piquette-Miller, M., Renton, K. W., Robertson, G. R., Chaluvadi, M. R., Charles, K. A., Clarke, S. J., Kacevska, M., Liddle, C., Richardson, T. A., Sharma, R., and Sinal, C. J. (2008) Regulation of drug-metabolizing enzymes and transporters in infection, inflammation, and cancer. *Drug Metab Dispos* 36, 205-216.

36. Charles, K. A., Rivory, L. P., Brown, S. L., Liddle, C., Clarke, S. J., and Robertson, G. R. (2006) Transcriptional repression of hepatic cytochrome P450 3A4 gene in the presence of cancer. *Clin Cancer Res* 12, 7492-7497.

37. Lee, A., Kolarich, D., Haynes, P. A., Jensen, P. H., Baker, M. S., and Packer, N. H. (2009) Rat liver membrane glycoproteome: enrichment by phase partitioning and glycoprotein capture. *J Proteome Res* 8, 770-781.

38. Fujiki, Y., Hubbard, A. L., Fowler, S., and Lazarow, P. B. (1982) Isolation of intracellular membranes by means of sodium carbonate treatment: application to endoplasmic reticulum. *J Cell Biol* 93, 97-102.

39. Wilson, N. L., Schulz, B. L., Karlsson, N. G., and Packer, N. H. (2002) Sequential analysis of N- and O-linked glycosylation of 2D-PAGE separated glycoproteins. *J Proteome Res* 1, 521-529.

40. Schulz, B. L., Oxley, D., Packer, N. H., and Karlsson, N. G. (2002) Identification of two highly sialylated human tear-fluid DMBT1 isoforms: the major high-molecular-mass glycoproteins in human tears. *Biochem J* 366, 511-520.

41. Craig, R., and Beavis, R. C. (2004) TANDEM: matching proteins with tandem mass spectra. *Bioinformatics* 20, 1466-1467.

42. Peng, J., Elias, J. E., Thoreen, C. C., Licklider, L. J., and Gygi, S. P. (2003) Evaluation of multidimensional chromatography coupled with tandem mass spectrometry (LC/LC-MS/MS) for large-scale protein analysis: the yeast proteome. *J Proteome Res* 2, 43-50.

43. Bjellqvist, B., Hughes, G. J., Pasquali, C., Paquet, N., Ravier, F., Sanchez, J. C., Frutiger, S., and Hochstrasser, D. (1993) The focusing positions of polypeptides in immobilized pH gradients can be predicted from their amino acid sequences. *Electrophoresis* 14, 1023-1031.

44. Krogh, A., Larsson, B., von Heijne, G., and Sonnhammer, E. L. (2001) Predicting transmembrane protein topology with a hidden Markov model: application to complete genomes. *J Mol Biol* 305, 567-580.

45. Weis, W. I., Taylor, M. E., and Drickamer, K. (1998) The C-type lectin superfamily in the immune system. *Immunol Rev* 163, 19-34.

46. Tsuboi, Y., Abe, H., Nakagawa, R., Oomizu, S., Watanabe, K., Nishi, N., Nakamura, T., Yamauchi, A., and Hirashima, M. (2007) Galectin-9 protects mice from the Shwartzman reaction by attracting prostaglandin E2-producing polymorphonuclear leukocytes. *Clin Immunol* 124, 221-233.

47. Zhang, Y., Inoue, Y., Inoue, S., and Lee, Y. C. (1997) Separation of oligo/polymers of 5-N-acetylneuraminic acid, 5-N-glycolylneuraminic acid, and 2-keto-3-deoxy-D-glycero-D-galacto-nononic acid by high-performance anion-exchange chromatography with pulsed amperometric detector. *Anal Biochem* 250, 245-251.

48. Parry, S., Hadaschik, D., Blancher, C., Kumaran, M. K., Bochkina, N., Morris, H. R., Richardson, S., Aitman, T. J., Gauguier, D., Siddle, K., Scott, J., and Dell, A. (2006) Glycomics investigation into insulin action. *Biochim Biophys Acta* 1760, 652-668.

49. Dell, A., Chalabi, S., Easton, R. L., Haslam, S. M., Sutton-Smith, M., Patankar, M. S., Lattanzio, F., Panico, M., Morris, H. R., and Clark, G. F. (2003) Murine and human zona pellucida 3 derived from mouse eggs express identical O-glycans. *Proc Natl Acad Sci U S A* 100, 15631-15636.

50. Easton, R. L., Patankar, M. S., Lattanzio, F. A., Leaven, T. H., Morris, H. R., Clark, G. F., and Dell, A. (2000) Structural analysis of murine zona pellucida glycans. Evidence for the expression of core 2-type O-glycans and the Sd(a) antigen. *J Biol Chem* 275, 7731-7742.

51. Kotani, N., Asano, M., Iwakura, Y., and Takasaki, S. (1999) Impaired galactosylation of core 2 O-glycans in erythrocytes of beta1,4-galactosyltransferase knockout mice. *Biochem Biophys Res Commun* 260, 94-98.

52. Ichibangase, T., Moriya, K., Koike, K., and Imai, K. (2007) A proteomics method revealing disease-related proteins in livers of hepatitis-infected mouse model. *J Proteome Res* 6, 2841-2849.

53. El-Aneed, A., and Banoub, J. (2006) Proteomics in the diagnosis of hepatocellular carcinoma: focus on high risk hepatitis B and C patients. *Anticancer Res* 26, 3293-3300.

54. Baranova, A., Liotta, L., Petricoin, E., and Younossi, Z. M. (2007) The role of genomics and proteomics: technologies in studying non-alcoholic fatty liver disease. *Clin Liver Dis* 11, 209-220, xi.

55. Michael, M., Thompson, M., Hicks, R. J., Mitchell, P. L., Ellis, A., Milner, A. D., Di Iulio, J., Scott, A. M., Gurtler, V., Hoskins, J. M., Clarke, S. J., Tebbut, N. C., Foo, K., Jefford, M., and Zalcberg, J. R. (2006) Relationship of hepatic functional imaging to irinotecan pharmacokinetics and genetic parameters of drug elimination. *J Clin Oncol* 24, 4228-4235.

56. Wang, Y., Schachter, H., and Marth, J. D. (2002) Mice with a homozygous deletion of the Mgat2 gene encoding UDP-N-acetylglucosamine:alpha-6-D-mannoside beta1,2-N-acetylglucosaminyltransferase II: a model for congenital disorder of glycosylation type IIa. *Biochim Biophys Acta* 1573, 301-311.

57. Demetriou, M., Granovsky, M., Quaggin, S., and Dennis, J. W. (2001) Negative regulation of T-cell activation and autoimmunity by Mgat5 N-glycosylation. *Nature* 409, 733-739.

58. Morgan, R., Gao, G., Pawling, J., Dennis, J. W., Demetriou, M., and Li, B. (2004) N-acetylglucosaminyltransferase V (Mgat5)-mediated N-glycosylation negatively regulates Th1 cytokine production by T cells. *J Immunol* 173, 7200-7208.

59. Berger, E. G. (1999) Tn-syndrome. *Biochim Biophys Acta* 1455, 255-268.

60. Hennet, T. (2002) The galactosyltransferase family. *Cell Mol Life Sci* 59, 1081-1095.

61. Amado, M., Almeida, R., Schwientek, T., and Clausen, H. (1999) Identification and characterization of large galactosyltransferase gene families: galactosyltransferases for all functions. *Biochim Biophys Acta* 1473, 35-53.

62. Takashima, S. (2008) Characterization of mouse sialyltransferase genes: their evolution and diversity. *Biosci Biotechnol Biochem* 72, 1155-1167.

63. Kozutsumi, Y., Kawano, T., Yamakawa, T., and Suzuki, A. (1990) Participation of cytochrome b5 in CMP-N-acetylneuraminic acid hydroxylation in mouse liver cytosol. *J Biochem* 108, 704-706.

64. Takematsu, H., Kawano, T., Koyama, S., Kozutsumi, Y., Suzuki, A., and Kawasaki, T. (1994) Reaction mechanism underlying CMP-N-acetylneuraminic acid hydroxylation in mouse liver: formation of a ternary complex of cytochrome b5, CMP-N-acetylneuraminic acid, and a hydroxylation enzyme. *J Biochem* 115, 381-386.

65. Van Dyken, S. J., Green, R. S., and Marth, J. D. (2007) Structural and mechanistic features of protein O glycosylation linked to CD8+ T-cell apoptosis. *Mol Cell Biol* 27, 1096-1111.

66. Hennet, T., Chui, D., Paulson, J. C., and Marth, J. D. (1998) Immune regulation by the ST6Gal sialyltransferase. *Proc Natl Acad Sci U S A* 95, 4504-4509.

67. Arnold, J. N., Saldova, R., Hamid, U. M., and Rudd, P. M. (2008) Evaluation of the serum N-linked glycome for the diagnosis of cancer and chronic inflammation. *Proteomics* 8, 3284-3293.

68. Turner, G. A., Goodarzi, M. T., and Thompson, S. (1995) Glycosylation of alpha-1-proteinase inhibitor and haptoglobin in ovarian cancer: evidence for two different mechanisms. *Glycoconj J* 12, 211-218.

69. Thompson, S., Dargan, E., Griffiths, I. D., Kelly, C. A., and Turner, G. A. (1993) The glycosylation of haptoglobin in rheumatoid arthritis. *Clin Chim Acta* 220, 107-114.

70. Jin, L., McLean, P. A., Neel, B. G., and Wortis, H. H. (2002) Sialic acid binding domains of CD22 are required for negative regulation of B cell receptor signaling. *J Exp Med* 195, 1199-1205.

71. Collins, B. E., Smith, B. A., Bengtson, P., and Paulson, J. C. (2006) Ablation of CD22 in ligand-deficient mice restores B cell receptor signaling. *Nat Immunol* 7, 199-206.

72. Varki, A. (2007) Glycan-based interactions involving vertebrate sialic-acid-recognizing proteins. *Nature* 446, 1023-1029.

73. Hartnell, A., Steel, J., Turley, H., Jones, M., Jackson, D. G., and Crocker, P. R. (2001) Characterization of human sialoadhesin, a sialic acid binding receptor expressed by resident and inflammatory macrophage populations. *Blood* 97, 288-296.

74. Coombs, P. J., Taylor, M. E., and Drickamer, K. (2006) Two categories of mammalian galactose-binding receptors distinguished by glycan array profiling. *Glycobiology* 16, 1C-7C.

75. Takahashi, N., Yamada, W., Masuda, K., Araki, H., Tsukamoto, Y., Galinha, A., Sautes, C., Kato, K., and Shimada, I. (1998) N-glycan structures of a recombinant mouse soluble Fcgamma receptor II. *Glycoconj J* 15, 905-914.

76. Krogh, T. N., Bachmann, E., Teisner, B., Skjodt, K., and Hojrup, P. (1997) Glycosylation analysis and protein structure determination of murine fetal antigen 1 (mFA1)--the circulating

gene product of the delta-like protein (dlk), preadipocyte factor 1 (Pref-1) and stromal-cell-derived protein 1 (SCP-1) cDNAs. *Eur J Biochem* 244, 334-342.

77. Angel, A. S., Gronberg, G., Krotkiewski, H., Lisowska, E., and Nilsson, B. (1991) Structural analysis of the N-linked oligosaccharides from murine glycophorin. *Arch Biochem Biophys* 291, 76-88.

78. Debray, H., Dus, D., Wieruszeski, J. M., Strecker, G., and Montreuil, J. (1991) Structures of the alpha(1-3)-galactose-containing asparagine-linked glycans of a Lewis lung carcinoma cell subline resistant to Aleuria aurantia agglutinin: elucidation by 1H-NMR spectroscopy. *Glycoconj J* 8, 29-37.

79. Palamarczyk, G., and Elbein, A. D. (1985) The effect of castanospermine on the oligosaccharide structures of glycoproteins from lymphoma cell lines. *Biochem J* 227, 795-804.

80. Coddeville, B., Regoeczi, E., Strecker, G., Plancke, Y., and Spik, G. (2000) Structural analysis of trisialylated biantennary glycans isolated from mouse serum transferrin. Characterization of the sequence Neu5Gc(alpha 2-3)Gal(beta 1-3)[Neu5Gc(alpha 2-6)]GlcNAc(beta 1-2)Man. *Biochim Biophys Acta* 1475, 321-328.

81. Nagae, M., Nishi, N., Murata, T., Usui, T., Nakamura, T., Wakatsuki, S., and Kato, R. (2009) Structural analysis of the recognition mechanism of poly-N-acetyllactosamine by the human galectin-9 N-terminal carbohydrate recognition domain. *Glycobiology* 19, 112-117.

Figure Legends

Figure 1 Relative abundance of glycosyltransferases and mannosidases determined by peptide IPG-IEF followed by label-free quantitation. NSAF values describe the relative fold difference between samples with $p \leq 0.05$. *Selected glycosyltransferases that did not change in abundance (Supplementary Table 1)

Figure 2 Cell surface lectins play a role in the immune system and were found to be significantly upregulated in the liver of tumour-bearing mice $p \leq 0.05$. A detailed glycan array profiling of the Kupffer cell receptor has indicated it is primarily a galactose- and GalNAc-binding receptor(74).

Figure 3 Combined LC-ESI-MS (retention time 20-65 min) of globally released N-linked oligosaccharides from mouse liver membrane proteins from control(A) and tumour-bearing mice (B). Combined extracted ion chromatogram (EIC) of m/z $(941.3)^{2-}$, $(1022.4)^{2-}$ and $(1038.9)^{2-}$ and average MS (retention time 21-28 min) of control (C) and tumour-bearing mice (D). Ions corresponding to m/z $(1022.4)^{2-}$ and $(1038.9)^{2-}$ were observed in low abundance in the average MS spectra in both control (A) and tumour-bearing (B) mice but were clearly observable by their combined EIC (C and D). Averaging MS spectra of the narrower retention time (21-28 min) reveals the presence of m/z $(1022.4)^{2-}$. Some major ions corresponding to N-glycans have been assigned possible structures (Supplementary Table 2). *Representative $[M-2H]^{2-}$ ions correspond to identified structures found only in tumour-bearing mice (Table 1).

Figure 4 Extracted ion chromatogram (EIC) of m/z $(1127.4)^{2-}$ shows the different ratios of the biantennary *N*-glycan with two NeuGc attached shown in (A) control (n=3, $p \leq 0.05$) and (B) tumour-bearing mouse liver membranes (n=3, $p \leq 0.05$) (C) MS/MS fragmentation of glycan isomer observed at 41 min in tumour-bearing mice indicates the position of the two NeuGc. Isomer 1 and 2 are two isomeric forms of m/z $(1127.4)^{2-}$.

Figure 5 *N*-linked oligosaccharides were treated with α(2,3) neuraminidase to remove α(2,3) linked NeuGc on di-sialylated biantennary N-glycan corresponding to m/z of $(1127.4)^{2}$. EIC of m/z $(1127.4)^{2-}$ with no neuraminidase digestion and combined MS (A) over 40-65 min. EIC of m/z $(1127.4)^{2-}$ following a overnight α(2,3) neuraminidase digestion of N-linked oligosaccharides and combined MS (B) over 40-65 min.*Generated additional di-sialylated N-glycans.

Figure 6 Identification of N-glycan with three glycolyl neuraminic acids. Structures are depicted as biantennary N-glycans since this is the most likely configuration of the compositions in the mouse. EIC of $(1127.4)^{2-}$ and $(1280.9)^{2-}$ and combined MS spectrum (A) over 40-65 min. Digestion of purified N-linked oligosaccharides with α(2,3,6) neuraminidase for 10 min and combined MS spectrum (B) over 40-65 min. Overnight digestion of purified N-linked oligosaccharides with α(2,3,6) neuraminidase and combined MS spectrum (C) over 40-65 min (D). MS/MS fragmentation of the resultant monosialylated N-glycan (m/z of $(973.8)^{2-}$) confirms a NeuGc attached to a GlcNAc(m/z ion 509.1) thus predicting the structures shown.

Figure 7 Combined EIC of $(675.3)^{1-}$, $(691.3)^{1-}$, $(966.2)^{1-}$, $(982.3)^{1-}$, $(998.4)^{1-}$ and $(681.3)^{2-}$ and average MS of *O*-linked oligosaccharides (retention time 17.2-17.9 min) from liver membranes from control (A) and tumour-bearing mice (B) MS/MS fragmentation of m/z $(998.4)^{1-}$ (C) and MS/MS fragmentation of m/z $(681.3)^{2-}$(D) confirming the structures shown.

Figure 8 1D SDS PAGE followed by in-gel PNGase F digestion of proteins of decreasing mass to release N-linked oligosaccharides. Combined MS of 20-65min of the N-glycans released from the proteins with each band show a similar global profile to the total protein glycoprofile.

Table 1 Summarized results of glycan differences observed on liver membranes of control and tumour-bearing mice

N-glycan changes	m/z	N-glycan structure based on known structures found in the mouse	Reference
Only expressed in tumour-bearing	$(1038.9)^{2-}$		(75, 76)
	$(1111.4)^{2-}$		(77, 78)
	$(965.9)^{2-}$		(77, 78)
	$(1022.4)^{2-}$	6x 1x	(79)
	$(1184.4)^{2-}$		(77, 78)
	$(1280.9)^{2-}$		(80)
Different ratios of glycan isomers	$(1127.4)^{2-}$		(50, 80)
O-glycan changes		**O-glycan structure based on known structures found in the mouse**	
Only expressed in tumour-bearing	$(998.4)^{1-}$	(core 1)	(49, 50)
	$(681.3)^{2-}$	*(core 2)	(51)*

Galactose, Mannose, Glucose, N-acetyl glucosamine, N-glycolyl-neuraminic acid, N-acetyl galactosamine, Fucose, N-acetyl-neuraminic acid

*O-glycan structure has been previously identified by high pH anion-exchange chromatography in mouse erythrocytes and consists of two NeuAc rather than two NeuGc on the non-reducing terminal.

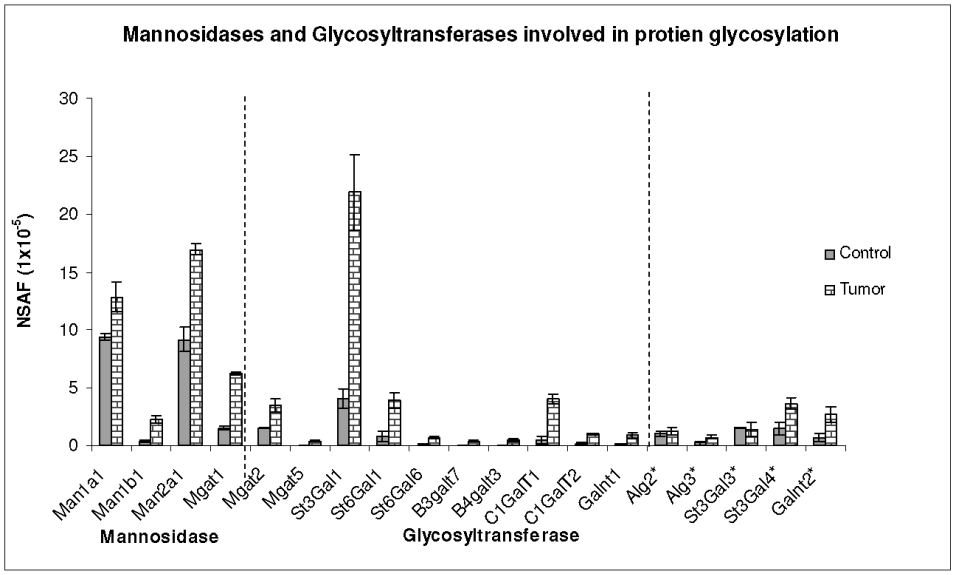
Mannosidases and Glycosyltransferases involved in protien glycosylation
NSAF (1x10-5)
30
25
20
15
10
5
0
Control
Tumor
Man1a1
Man1b1
Man2a1
Mgat1
Mgat2
Mgat5
St3Gal1
St6Gal1
St6Gal6
B3galt7
B4galt3
C1GalT1
C1GalT2
Galnt1
Alg2*
Alg3*
St3Gal3*
St3Gal4*
Galnt2*
Mannosidase
Glycosyltransferase

Figure 1

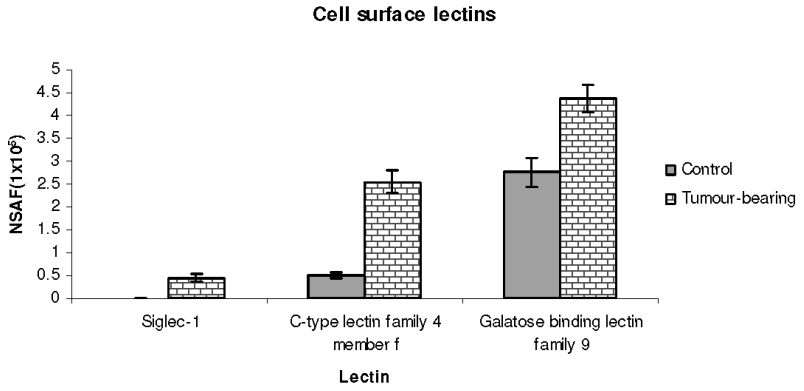

Lectin	Recognition	Reference
Sialoadhesin (Siglec-1)	NeuGc/NeuAcα(2-3)Galβ(1-4)GlcNAc	(72)
C-type lectin family 4 member f (Kupffer cell receptor)	Galactose, GalNAc	(45, 74)
Galactose binding lectin family 9 (Galectin-9)	Galβ(1-4)GlcNAc	(81)

Figure 2

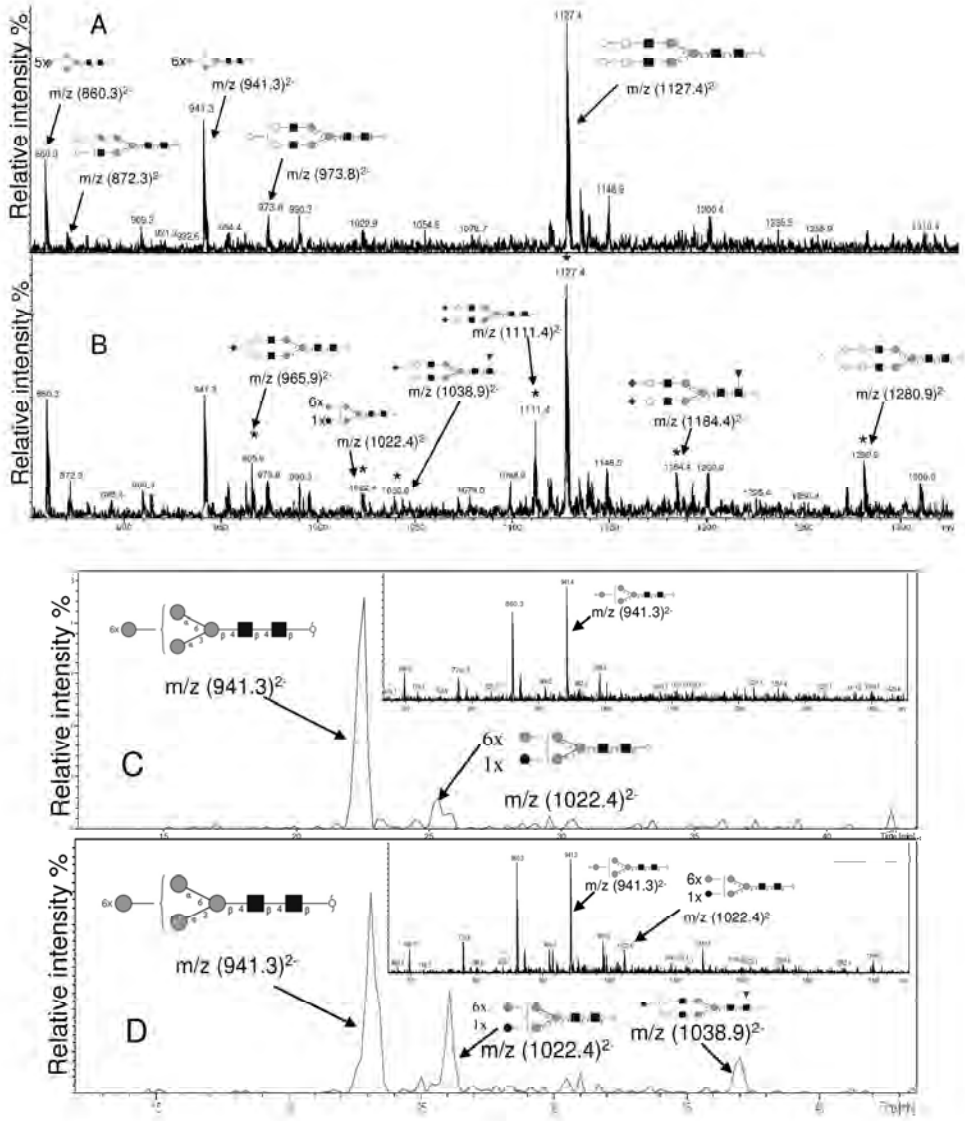
A
Relative intensity %
m/z (860.3)2-
m/z (872.3)2-
m/z (941.3)2-
m/z (973.8)2-
m/z (1127.4)2-
B
m/z (965.9)2-
m/z (1038.9)2-
m/z (1111.4)2-
m/z (1022.4)2-
m/z (1184.4)2-
m/z (1280.9)2-
C
m/z (941.3)2-
m/z (1022.4)2-
D
m/z (941.3)2-
m/z (1022.4)2-
m/z (1038.9)2-

Figure 3

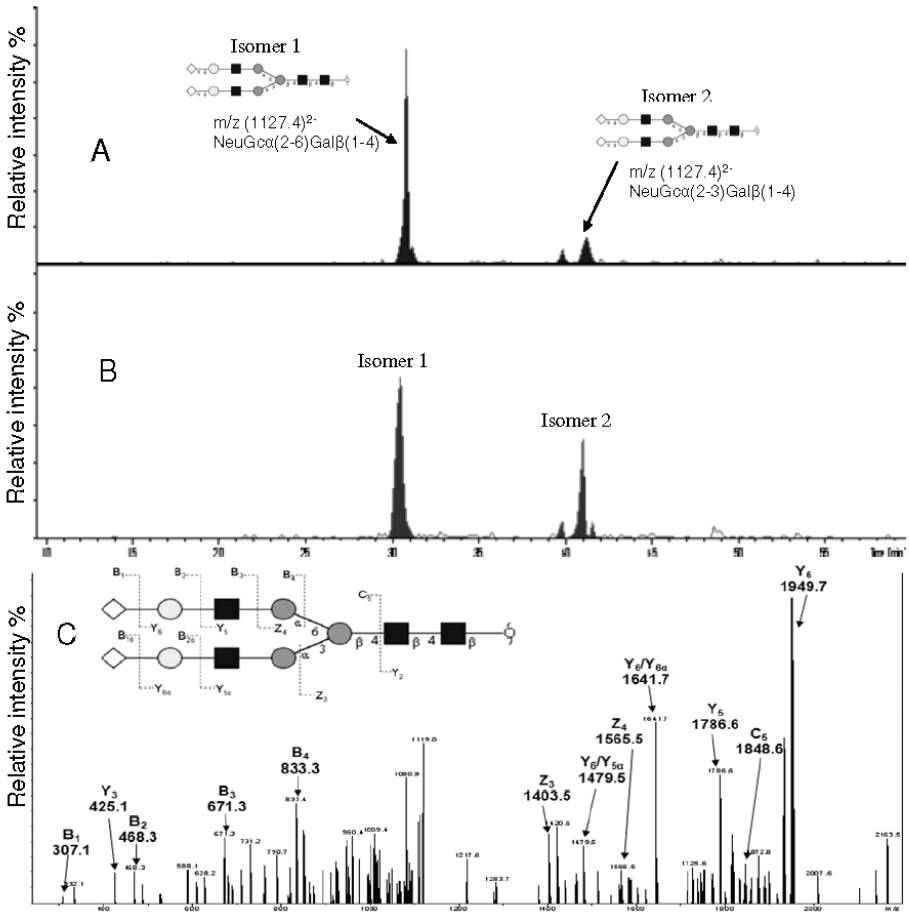
Relative intensity %
A
Isomer 1
m/z (1127.4)2-
NeuGcα(2-6)Galβ(1-4)
Isomer 2
m/z (1127.4)2-
NeuGcα(2-3)Galβ(1-4)
B
Isomer 1
Isomer 2
C
Y6
1949.7
Y6/Y6α
1641.7
Z4
1565.5
Y5
1786.6
C5
1848.6
Y6/Y5α
1479.5
Z3
1403.5
B4
833.3
B3
671.3
Y3
425.1
B2
468.3
B1
307.1

Figure 4

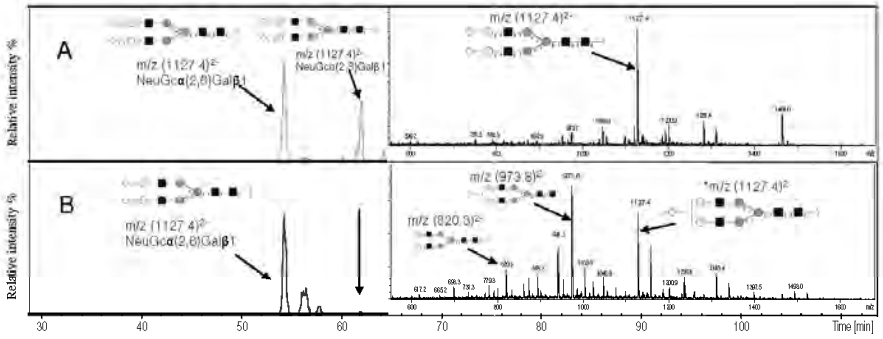
A
B
Relative intensity %
Relative intensity %
m/z (1127.4)2-
NeuGcα(2,6)Galβ1
m/z (1127.4)2-
NeuGcα(2,3)Galβ1
m/z (973.8)2-
m/z (820.3)2-
30
40
50
60
70
80
90
100
Time [min]

Figure 5

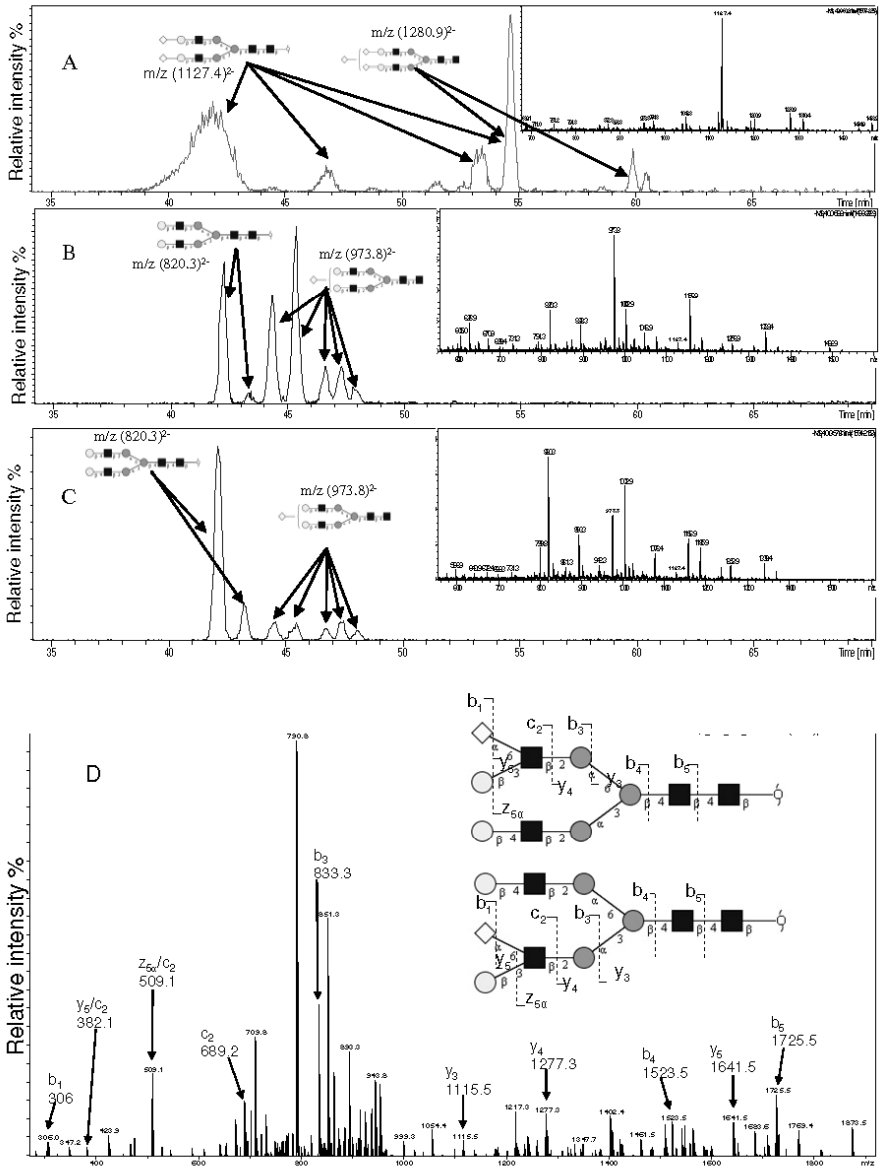
A
m/z (1127.4)2-
m/z (1280.9)2-
B
m/z (820.3)2-
m/z (973.8)2-
C
m/z (820.3)2-
m/z (973.8)2-
Relative intensity %
Time [min]
D
b1
306
y5/c2
382.1
z5α/c2
509.1
c2
689.2
b3
833.3
y3
1115.5
y4
1277.3
b4
1523.5
y5
1641.5
b5
1725.5
m/z

Figure 6

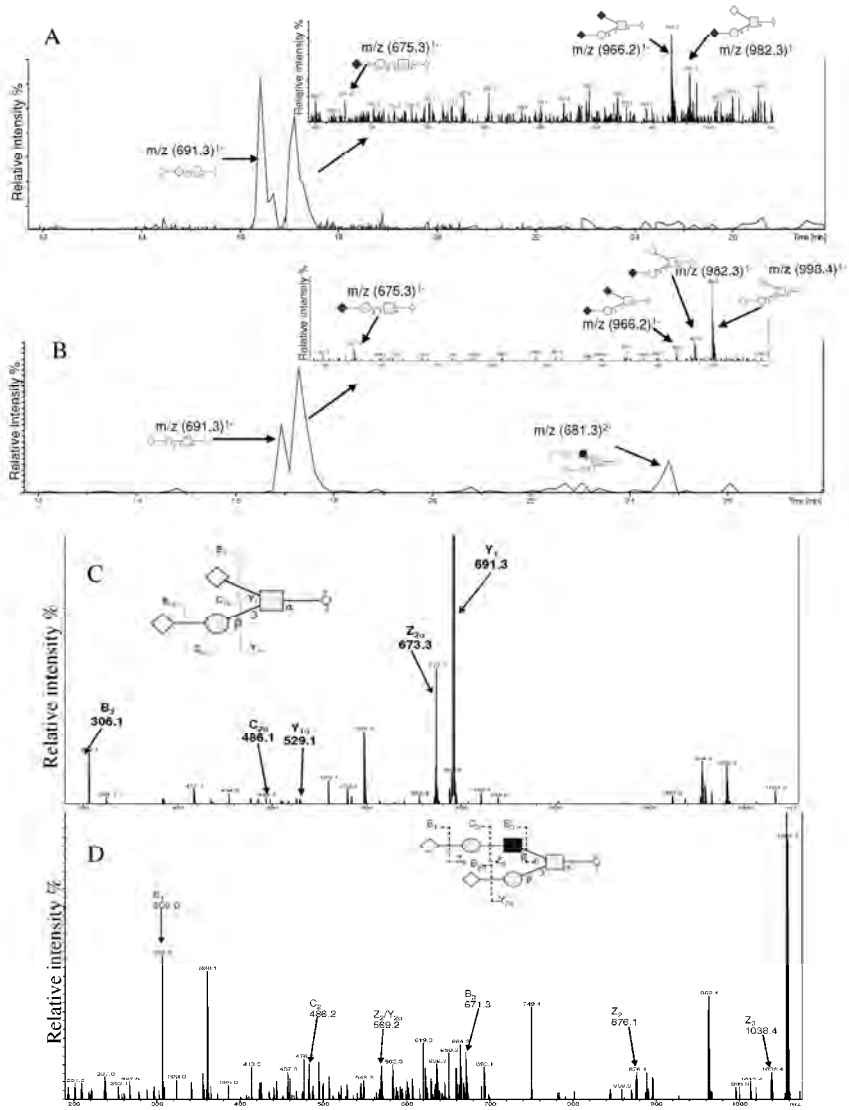
A
Relative intensity %
m/z (691.3)
m/z (675.3)
m/z (966.2)
m/z (982.3)
B
m/z (691.3)
m/z (675.3)
m/z (966.2)
m/z (982.3)
m/z (681.3)
C
Relative intensity %
Y1 691.3
Z2α 673.3
B2 306.1
C2α 486.1
Y1α 529.1
D
Relative intensity %
B2 306.0
C2 486.2
Z2/Y2α 589.2
B3 671.3
Z3 676.1
Z3 1038.4

Figure 7

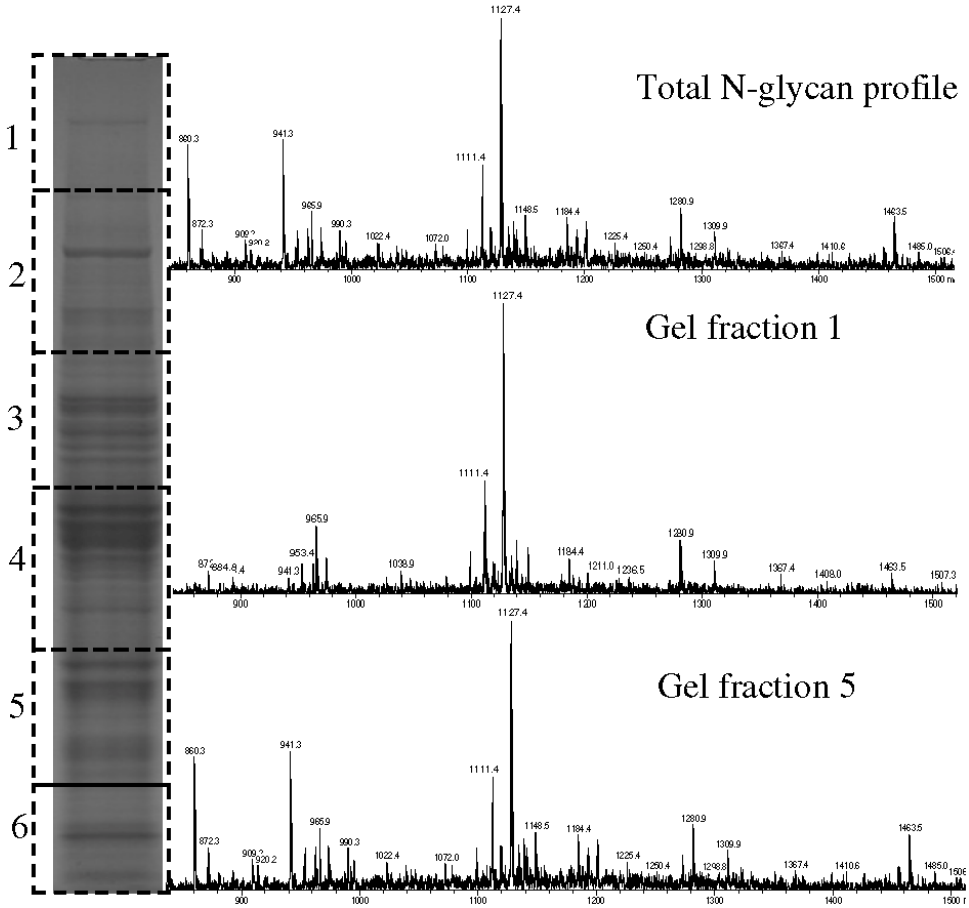

Figure 8

Chapter 5: Effects of a distal colon 26 adenocarcinoma on the liver membrane proteome of non-cachectic and cachectic mice

Both cancer and inflammation are known to cause changes to protein glycosylation. The murine model examined in Chapter 4 involves systemic liver inflammation produced by a distal non-metastasizing EHS sarcoma, which was shown to cause perturbations to liver metabolism as well as chronic liver inflammation. Specifically, the presence of a distal non-metastasizing EHS tumour was shown to cause differential expression of glycosyltransferases and cell surface lectins in the liver of cancer-bearing mice. These changes were shown to reflect an overall increased sialylation of glycans on liver membrane proteins. These enzymatic and glycan differences in the liver membrane of EHS-bearing mice provided the basis to study glycosylation changes in another mouse model bearing a metastasizing distal cancer of the C26 adenocarcinoma.

5.1. Introduction

The liver is the main organ that is responsible for conditioning and producing approximately 70% protein yield of plasma in the body [235]. In addition, the liver also contains large numbers of leukocytes which upon stimulation by pro-inflammatory cytokines play key roles in the immune system in removing antigens, pathogens and toxins. The release of pro-inflammatory cytokines from a tumour can often stimulate the immune system and induce liver inflammation, which is a common cause of reduced hepatic drug metabolism and increased toxicity in advanced cancer patients being treated with cytotoxic chemotherapies. Additionally, the increased levels of pro-inflammatory cytokines can also initiate hepatic acute phase responses and cause reduced hepatic gene expression of major classes of membrane proteins such as UDP-glucuronosyltransferases and cytochromes p450s, which are responsible for phase I xenobiotic metabolism [4, 5].

The C26 adenocarcinoma mouse model is a distal metastasizing tumour that is capable of reducing the abundance and activity of cytochrome p450 drug metabolizing enzymes in the liver [18]. It is also able to induce increased levels of acute phase response proteins in the plasma such as fibrinogen, serum amyloid, α-1-antitrypsin and α-2-macroglobulin in response to tissue damage and inflammation [18, 242-244]. In this study, the C26 adenocarcinoma mouse model was used to investigate the effects of bearing a distal metastasizing cancer on liver membrane protein glycosylation, and to compare the glycosylation changes with those observed in the non-metastasizing EHS-bearing mice (Chapter 4). In addition, the C26 mouse model also offers an opportunity to study the effects of cachexia on the liver as a consequence of bearing a distal metastasizing tumour [18, 242].

The C26 adenocarcinoma is a unique cancer model that sometimes manifests severe weight loss (cachexia) as well as liver inflammation. Cachexia is the loss of lean body mass that cannot be controlled and/or reversed nutritionally. Cachexia is often seen in patients with advanced stages of diseases such as cancer, autoimmunity and pulmonary diseases. The risk

of death is dramatically increased in cachectic patients as therapeutic intervention is further complicated by this condition. Cachectic cancer patients often exhibit increased energy expenditure, due to increased thermogenesis and increased operation of the Cori cycle in the skeletal muscles. In addition, the loss of skeletal muscle as a result of cachexia is also caused by the reduced protein synthesis and increased protein degradation by the ubiquitin-proteome and lysosomal pathways, which utilize these by-products for catabolic processes.

Depending on the tumour type and stage, weight loss occurs in 30-80% of cancer patients, with pancreatic and gastric cancers having the highest frequency of weight loss [250]. The exact mechanism by which these diseases cause cachexia is poorly understood, but it is thought that pro-inflammatory cytokines such as TNF-α, IFNγ and IL-6, as well as the tumor-secreted proteolysis inducing factor (PIF) are increased in the blood and transported across the blood-brain barrier where they interact with the luminal surface of brain endothelial cells and affect appetite [17]. The mechanism of how PIF affects appetite is not known.

The clinical relevance of liver inflammation and cachexia both in contributing to the development of cancer and in determining prognosis has been well established [11, 14, 17, 287]. The C26 adenocarcinoma murine model studies described in this chapter have been designed to provide insights into the pathogenesis of the tumour-induced inflammatory effects and cachexia on liver. A recent study combining proteomics and glycomics approaches to investigate the plasma glycoproteome of mice bearing a metastasizing C26 xenograft adenocarcinoma demonstrated that levels of leukocytes and acute phase proteins in the blood of tumour-bearing mice were significantly increased compared to the normal [11]. An overall increased sialylation of acute phase glycoproteins in plasma of tumour-bearing mice was observed with increased high mannose and complex bi- and tetra-antennary *N*-glycan structures with terminating NeuAcα(2-3/6)Galβ(1-4)GlcNAc (sialyl LacNAc) sequences. Complex *N*-glycans with *N*-glycolylneuraminic acid (NeuGc) attached to the termini were found to be downregulated in the plasma of tumour-bearing mice, which suggested either a

downregulation or impaired function of the CMP-hydroxylase enzyme in tumour-bearing mice. This enzyme is responsible for hydroxylating N-acetylneuraminic acid (NeuAc) to NeuGc [11]. The findings from this study suggested that glycosylation of most liver-derived acute phase proteins in the plasma can be altered in the presence of the C26 adenocarcinoma and during cancer metastasis. However, it is not known whether similar glycosylation changes are also observed on the liver cell membrane of mice bearing the C26 adenocarcinoma.

In the present study, shotgun proteomics employing 1D SDS PAGE separation of Triton X-114 phase partitioned mouse liver membrane proteins and label-free quantitation employing NSAF [139, 156, 159, 288] was used to identify and determine the relative abundance of liver membrane proteins in mice bearing a distal C26 adenocarcinoma. Mice bearing the distal C26 adenocarcinoma, which display either the phenotype for cachexia or non-cachexia, were also compared with normal mice. Specifically, membrane proteins involved in the cellular glycosylation machinery were focused on, with any protein changes in other metabolic pathways also documented, to determine protein expression differences between the livers of the two cancer models (non-cachectic and cachectic) and normal livers. Global glycan profiling of Triton X-114 phase partitioned liver membrane proteins from the livers of non-cachectic and cachectic mice was used to determine if glycosylation of the liver membrane proteins was also affected by the presence of a distal metastasizing C26 adenocarcinoma. The study of the liver membrane proteome using a combination of proteomic and glycomic approaches could help determine potentially important biological changes that occur during tumour-induced liver inflammation and cancer cachexia.

5.2. Methods

5.2.1. Tumour transplantation

Eight to ten week old transgenic BALB/c male mice (n=3) were aseptically inoculated using a 14-gauge needle with 0.3 mL suspension of mouse colon 26 adenocarcinoma cells (containing 10^6 cells) in 0.9% (w/v) PBS into the subcutaneous right flank muscle[1]. Control mice (n=3) were injected with 0.3 mL of 0.9% (w/v) PBS. Reduced food intake was observed after 9 to 10 days with no apparent loss of weight. Tumour mass reached approximately 3 g or 10% (w/w) total body weight over 14 to 16 days where approximately 20% (w/w) of weight was lost in cachectic mice. Tumour and control mice were euthanized and livers were harvested. To address concerns of biological reproducibility, all proteomic and glycomic experiments were conducted on three biological replicates of individual control and tumor-bearing mice. All animal work was approved by the Concord Repatriation General Hospital local area health service Animal Ethics Committee. Triton X-114 phase partitioning to enrich rat liver membrane proteins, 1D SDS PAGE protein separation and, RPLC-MS/MS for protein identification, and analysis of *N*-linked oligosaccharides was carried out as described in the Chapter 2.

[1] Tumour implantation and liver harvesting was carried by A/Prof. Graham Robertson from Concord Hospital Repatriation General Hospital.

5.3. Results

Liver membrane proteins from control (n=3), non-cachectic (n=3) and cachectic (n=3) mice were prepared by differential ultracentrifugation using a modified sodium carbonate stripping method [258]. Membrane proteins were further enriched by Triton X-114 phase partitioning and separated by 1D SDS PAGE. Each gel lane was cut into 12 equal fractions, in-gel digested with trypsin and tryptic peptides were analysed by RPLC-MS/MS for protein identification. The relative abundance of identified proteins was quantitated by calculating the NSAF [139, 156, 159, 288] of all membrane-associated proteins. Gene ontology mapping suggested the membrane proteins were involved in the glycosylation machinery, xenobiotic metabolism, endo- and exocytosis, glycolysis and gluconeogenesis and fatty acid metabolism. In this study we have defined membrane proteins as comprising of integral membrane proteins, lipid-anchored proteins and membrane-associated proteins as determined by TMHMM together with information derived from UniProt, GO annotation and the Swiss-Prot databases. GO mapping of comprehensive lists of sequences were arranged into the different GO categories (biological process, molecular function and cellular component) using Blast2GO [168]. Although GO annotations have not been fully characterised it is currently one of the more suitable informatic methods for determining cellular roles and biological pathways of proteins in a given cell and/or tissue [289].

5.3.1. Comparison of liver membrane proteins in cachectic, non-cachectic and normal mice.

A large number of common and unique proteins were identified from control, non-cachectic and cachectic mouse liver membrane preparations. GO mapping of the comprehensive list of nonredundant proteins obtained from control, non-cachectic and cachectic mouse liver membrane preparations illustrated that there was a similar distribution of proteins in all the mice across all subcellular locations. For example, proteins found in the cytosol and mitochondria from the control, non-cachectic and cachectic mouse liver made up

approximately 33% and 30% of their corresponding data sets respectively (Appendix D-1). Similarly, proteins found localized to the plasma membrane and the ER made up approximately 17% and 9 % of the identified proteins in each dataset.

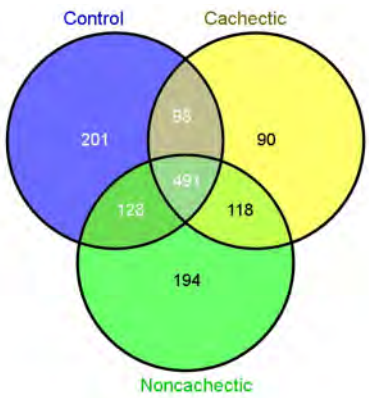

Figure 5-1. Common and unique subsets of proteins identified from control (A), non-cachectic (B) and cachectic (C) mouse liver membrane preparations.

Proteins belonging to the GO categories: 1) biological and 2) cellular processes made up 46 % (control), 48% (non-cachectic) and 47% (cachectic) of the total proteins with proteins responsible for molecular functions such as 1) protein and ion binding and 2) catalytic and enzymatic activity comprising approximately 43% and 33% respectively (Appendix D-1). The identified proteins from normal, non-cachectic and cachectic mouse liver membrane preparations were similarly distributed in all GO annotation categories and as a collection could not be used to interpret specific changes to particular biological functions of the liver as a result of a distal adenocarcinoma. Therefore, label-free quantitation of proteins was used to determine their relative abundance in specific biological pathways.

Using label-free quantitation employing NSAF [139, 156, 159, 288] we determined the relative abundance of identified proteins from control, non-cachectic and cachectic mouse liver membranes (Figure 5-2, Figure 5-3 and Figure 5-4). Applying the natural log to the NSAF values of all proteins normalizes the distribution to allow for significance testing and quantitation of proteins in low abundance (Figure 5-2). Proteins were determined to be confident identifications if found in all three biological replicates of each murine model, with at least five nonredundant peptides per protein identification. We identified 1143 common

proteins between non-cachectic and normal mice, of which 581 were annotated by GO to be membrane-associated. Approximately 45% (516, $p \leq 0.05$) of the total proteins were determined to be differentially expressed (up- and downregulated by at least 1.5-fold) (Figure 5-3A).

Additionally, 1050 common proteins were identified between cachectic and normal mice, of which 539 were annotated by GO to be membrane-associated. Approximately 29% (312, $p \leq 0.05$) of the total proteins were determined to be differently expressed (up- and downregulated by at least 1.5-fold) (Figure 5-3B). A heat map summarizing the differentially expressed proteins provided helpful information of the expressed proteins that may be related to particular biological pathways (Figure 5-4). The percentage of differentially expressed proteins in the liver membranes of both non-cachectic (45%) and cachectic (29%) relative to the control appear to be quite high with many protein identifications from a diverse range of metabolic pathways. Some of these identified protein classes included: ribosomal, cytoplasmic and, cytoskeletal proteins such as tubulin and actin, as well as biological pathways involved in xenobiotic metabolism, endo- and exocytosis, glycolysis and gluconeogenesis, fatty acid metabolism (Appendix D-2) and the glycosylation pathways. This chapter describes those changes evident in the glycosylation pathway in the first instance, in order to compare the effects of the C26 metastatic distal tumour on this pathway in the liver with that of the non-metastatic EHS tumour (described in Chapter 4).

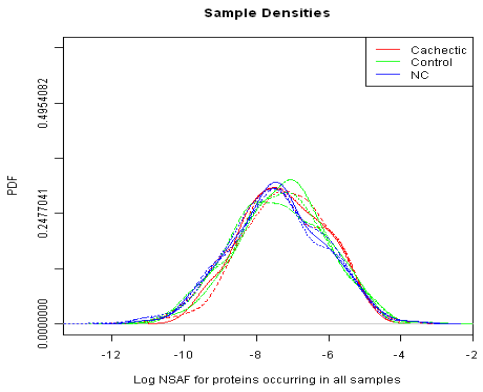

Figure 5-2. Log NSAF of all proteins in control, non-cachectic and cachectic mouse liver membrane preparations. The sample densities show that after applying log to the NSAF, the distribution has become normal allowing for quantitation and statistical analyses. Applying natural log to the the NSAF of proteins also allows for low abundance proteins (low spectral counts) to be quantitated.

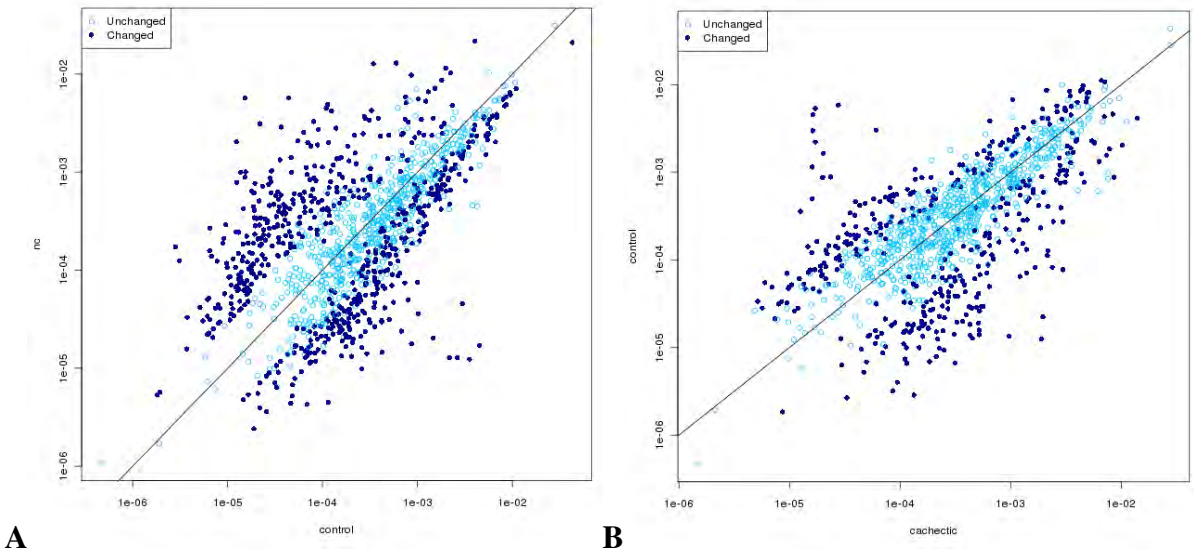

Figure 5-3. Comparison of identified proteins between the control and non-cachectic (A) and cachectic (B) mice. Dark blue spots are proteins determined to be differentially expressed. Light blue spots indicate proteins that did not change in expression ($p \leq 0.05$, fold change > 1.5).

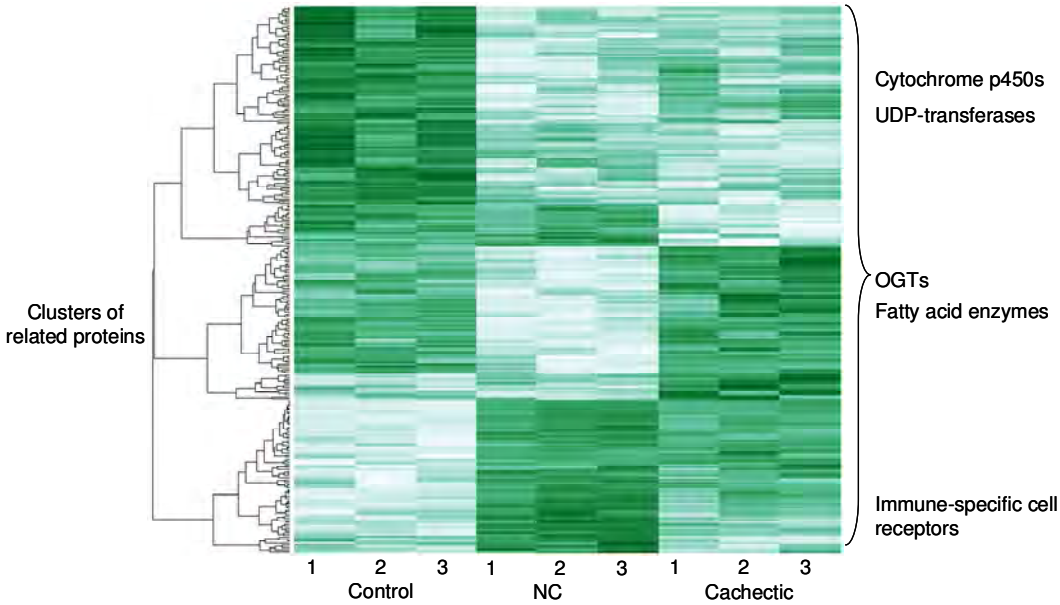

Figure 5-4. Heat map of the differentially expressed proteins in control, non-cachectic (NC) and cachectic mouse liver membrane preparations. Collections of proteins belonging to some biological pathways (xenobiotic metabolism, fatty acid metabolism and glycosylation) were shown to be differentially expressed.

5.3.2. Effects of a distal C26 tumour on the glycosylation machinery of the liver membrane glycoproteome

5.3.2.1. Cell surface receptors

The majority of cell surface receptors involved in antigen recognition by T-cells for immune regulation and in the orchestration of cell-adhesion and cell-signalling events are glycoproteins [290]. Glycosylation of these immune-specific cell surface receptors markedly

change the properties and modulate the function of these glycoproteins [291]. Three membrane receptors which were described by GO to be involved in immune-specific cell surface responses and cytokine signaling were identified to be upregulated by at least 1.5-fold in the livers of non-cachectic mice compared to the normal (Figure 5-5A). These included H2 histocompatibility antigen (6.11±4.30 fold upregulated), lymphatic endothelial hyaluronic acid receptor (8.05±3.37 fold upregulated) and tumour necrosis factor receptor associated protein (TRAP-1) (9.51±3.52 fold upregulated). H2 Class I Histocompatibility antigen is known to be expressed on the surface of hepatocytes, which can act as antigen-presenting cells (APCs) for CD1 or MHC class I-restricted T-cells during liver inflammation [232]. Lymphatic vessel endothelial hyaluronan receptor is a homolog of CD44 which is widely expressed on leukocytes, dendritic cells, and tumor cells [292] and, TRAP-1 associates with the intracellular domain of TNF receptor 1 and is essential for mediating programmed cell death by inducing apoptosis and activation of NF-kappa B [19].

5.3.2.2. Glycosylation pathway enzymes

Many glycosyltransferases and glycosidases were downregulated in the liver of non-cachectic mice but showed very little change in expression in the cachectic mice. Some of these enzymes included: alpha (1-3)-mannosyltransferase, dolichol-diphospholigosaccharide protein glycosyltransferases, mannosyl-oligosaccharide glucosidase, neutral alpha glucosidase AB and alpha mannosidase II (Figure 5-5B). These identified glycosyltransferases and glycosidases are mostly localised to the ER membrane and are responsible for the initial biosynthesis of *N*-glycans.

Interestingly, bifunctional UDP-GlcNAc 2 epimerase/*N*-acetylmannosamine kinase was determined to be upregulated by approximately 20 fold in the liver of both non-cachectic and cachectic mice (Figure 5-5A). The bifunctional enzyme UDP-GlcNAc 2 epimerase/*N*-acetylmannosamine kinase, encoded by the GNE gene, catalyzes the first two committed,

rate-limiting steps in the biosynthesis of NeuAc but is not involved in the attachment of NeuAc to complex glycans. Therefore, this enzyme plays a crucial role in biosynthesis and addition of sialic acids to *N*- and *O*-glycans, and is significantly upregulated in the liver in response to distal tumour whether cachexia is a symptom or not.

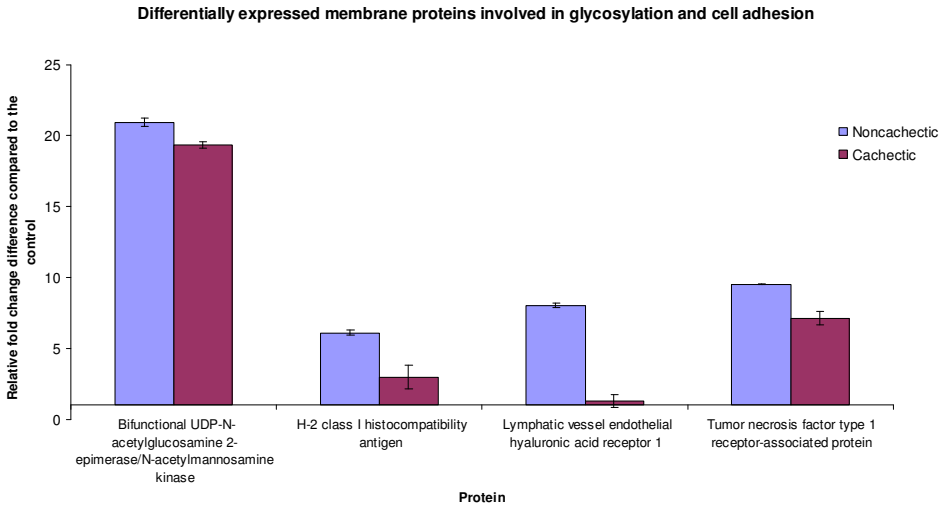

A

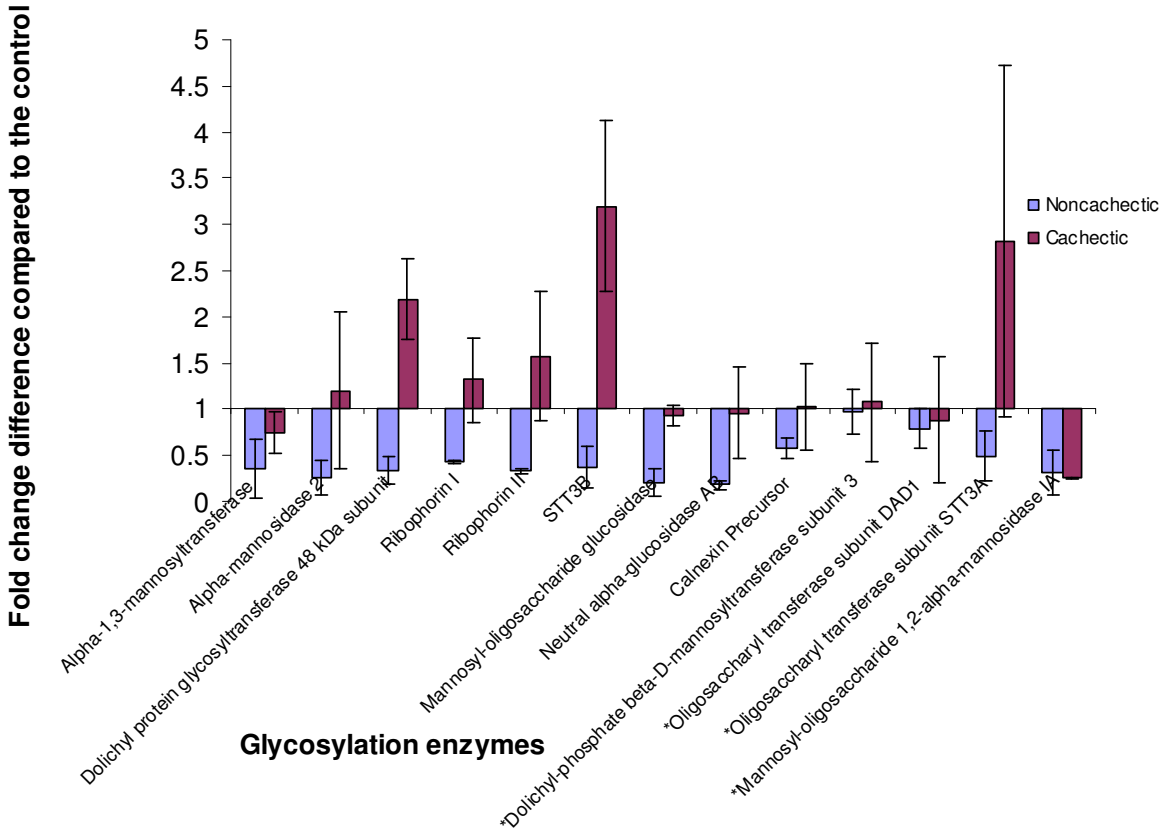

B

Figure 5-5. Relative fold change difference of UDP-GlcNAc epimerase and cell receptors involved in immune responses proteins (A) and proteins involved in the initial stages of *N*-linked glycosylation (B). *indicates proteins that did change in expression in both non-cachectic and cachectic mouse livers.

5.3.2.3. Analysis of N-linked oligosaccharides on the liver membrane glycoproteins

To determine whether the observed differential expression of glycosyltransferases and glycosidases in the liver of cancer-bearing mice influenced the glycosylation of liver membrane proteins, global *N*-glycan analysis was performed on Triton X-114 phase partitioned liver membrane proteins from control, non-cachectic and cachectic mice. The identification of any global *N*-glycan differences would determine if the significant differential expression of glycosylation-related enzymes was reflected in an altered product glycosylation status of the glycoproteins in the cell membrane. *N*-linked oligosaccharides were released from Triton X-114 phase partitioned mouse liver membrane proteins by PNGase F and analysed using graphitized carbon LC-ESI-MS in negative ion mode.

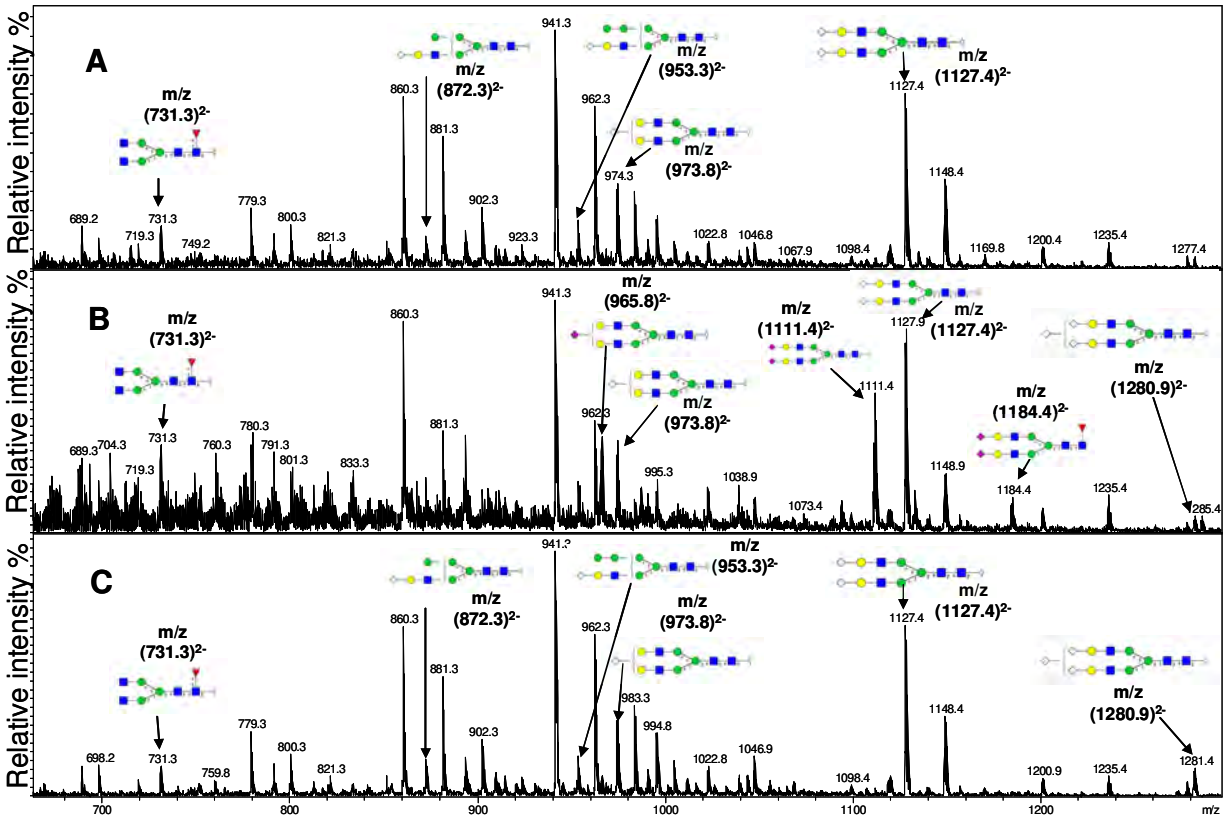

Figure 5-6. Average MS of *N*-glycans from control (A), non-cachectic (B) and cachectic (C) shows that the major *N*-glycans in normal and cachectic mice are similarly distributed. Non-cachectic mice were however shown to have biantennary *N*-glycans with two NeuAc, whilst both non-cachectic and cachectic expressed a biantennary *N*-glycan with three NeuGc (m/z (1280.9)$^{2-}$).

The combined mass spectra of the released *N*-linked oligosaccharides from liver membrane proteins from control, non-cachectic and cachectic are shown in Figure 5-6. Ions

corresponding to *N*-glycans were found as doubly charged $[M-2H]^{2-}$ ions in the combined mass spectra. Several masses assigned to *N*-glycan compositions were seen in the liver membranes of all three mouse models with all mice expressing high mannose structures (for example $[M-2H]^{2-}$ of m/z 860.3 and 941.3), hybrid (for example $[M-2H]^{2-}$ of m/z 872.3 and 953.3) and sialylated complex type *N*-glycan structures (for example $[M-2H]^{2-}$ of m/z 973.8 and 1127.4). *N*-glycans assigned to these masses are shown in Table 5-1.

Interestingly, a tri-sialylated complex *N*-glycan structure of m/z $(1280.9)^{2-}$ with composition $(NeuGc)_3(HexNAc)_2(Hex)_2$ + $(Man)_3(HexNAc)_2$ was identified on the liver membrane glycoproteins of non-cachectic and cachectic mice but not in the control. We have substantiated the relative tumour-specific difference in the abundance of these structures by using a combined EIC of m/z 973.8 and 1280.9 (+/- 0.5 Da) to detect the specific abundance of this ion normalised to the m/z 973.8 chromatographic peak (Figure 5-7). Although at low abundance, several isomers of this structure are apparent in the chromatogram of the *N*-linked oligosaccharides released from the liver membrane glycoproteins from the tumour-bearing mice. Average MS of the narrower retention time (50-65min) window of elution of the m/z ion $(1280.9)^{2-}$ confirms that this mass ion is present in both non-cachectic and cachectic mice but is not detectable in the normal mice. This same tri-sialylated complex biantennary *N*-glycan with three NeuGc attached has been previously identified on serotransferrin [29] and on the liver membrane of mice bearing a distal EHS sarcoma as described in Chapter 4.

Table 5-1. Total assigned *N*-glycan compositions identified on the liver membrane of normal, non-cachectic and cachectic mice.

$(M-H)^{2-}$	Assigned N-glycan compositions *
617.3	$(Hex)_2$
658.2	$(HexNAc)_2$
698.3	$(Hex)_3$
731.3	$(HexNAc)_2$ $(Deoxyhexose)_1$
779.3	$(Hex)_4$
791.3	$(Hex)_1$ $(HexNAc)_1$ $(NeuGc)_1$
799.8	$(Hex)_3(HexNAc)_1$
812.3	$(Hex)_1(HexNAc)_2(Deoxyhexose)_1$
820.3	$(Hex)_2$ $(HexNAc)_2$
832.8	$(HexNAc)_3$ $(Deoxyhexose)_1$
860.3	$(Hex)_5$
872.3	$(Hex)_2$ $(HexNAc)_1$ $(NeuGc)_1$
884.8	$(Hex)_1$ $(HexNAc)_2$ $(NeuAc)_1$
893.9	$(Hex)_1$ $(HexNAc)_2$ $(NeuGc)_1$
913.8	$(Hex)_1$ $(HexNAc)_3$ $(Deoxyhexose)_1$
941.3	$(Hex)_6$
952.9	$(Hex)_3$ $(HexNAc)_1$ $(NeuGc)_1$
961.8	$(Hex)_5$ $(HexNAc)_1$
965.9	$(Hex)_2$ $(HexNAc)_2$ $(NeuAc)_1$
973.8	$(Hex)_2$ $(HexNAc)_2$ $(NeuGc)_1$
994.5	$(Hex)_2$ $(HexNAc)_3$ $(Deoxyhexose)_1$
1022.4	$(Hex)_7$
1038.9	$(Hex)_2$ $(HexNAc)_2$ $(Deoxyhexose)_1$ $(NeuAc)_1$
1046.4	$(Hex)_1$ $(HexNAc)_2$ $(NeuGc)_2$
1067.5	$(Hex)_2(HexNAc)_3(Deoxyhexose)_2$
1103.4	$(Hex)_8$
1111.4	$(Hex)_2$ $(HexNAc)_2$ $(NeuAc)_2$
1119.9	$(Hex)_3$ $(HexNAc)_2$ $(Deoxyhexose)_1$ $(NeuAc)_1$
1127.5	$(Hex)_2$ $(HexNAc)_2$ $(NeuGc)_2$
1148.6	$(Hex)_2$ $(HexNAc)_3$ $(Deoxyhexose)_1$ $(NeuGc)_1$
1148.6	$(Hex)_3$ $(HexNAc)_3$ $(NeuAc)_1$
1169.4	$(Hex)_2$ $(HexNAc)_4$ $(NeuAc)_1$
1184.4	$(Hex)_2$ $(HexNAc)_2$ $(Deoxyhexose)_1$ $(NeuAc)_2$
1192.4	$(Hex)_2$ $(HexNAc)_2$ $(Deoxyhexose)_1$ $(NeuAc)_1$ $(NeuGc)_1$
1200.5	$(Hex)_2$ $(HexNAc)_2$ $(Deoxyhexose)_1$ $(NeuGc)_2$
1221.4	$(Hex)_3$ $(HexNAc)_3$ $(Deoxyhexose)_1$ $(NeuAc)_1$
1280.9	$(Hex)_2$ $(HexNAc)_2$ $(NeuGc)_3$
1293.9	$(Hex)_3$ $(HexNAc)_3$ $(NeuAc)_2$
1302.4	$(Hex)_4$ $(HexNAc)_3$ $(Deoxyhexose)_1$ $(NeuAc)_1$
1309.9	$(Hex)_3$ $(HexNAc)_3$ $(NeuGc)_2$
1331.4	$(Hex)_4$ $(HexNAc)_4$ $(NeuAc)_1$
1463.5	$(Hex)_3$ $(HexNAc)_3$ $(NeuGc)_3$

* $(Man)_3(GlcNAc)_2$ core N-glycan structure

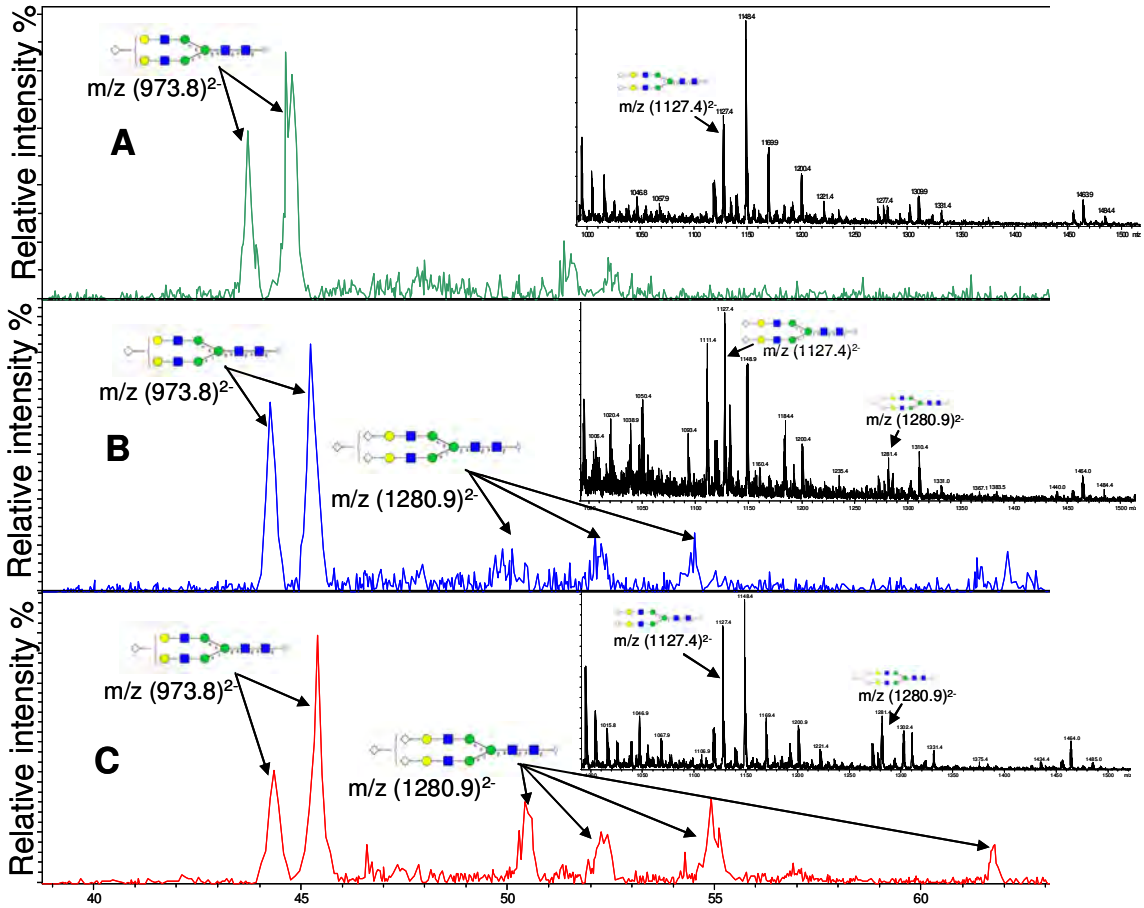

Figure 5-7. Combined extracted ion chromatogram (EIC) m/z $(973.8)^{2-}$ and m/z $(1280.9)^{2-}$ and average MS over LC retention time 50-65 min of N-glycans released from the liver membrane of control (A) non-cachectic (B) cachectic(C) mice.

In addition, three mass ions m/z of $(965.8)^{2-}$, $(1111.4)^{2-}$ and $(1184.4)^{2-}$ were observed in the *N*-glycans released from liver membrane glycoproteins of non-cachectic mice but were not detectable in the control and cachectic mice. These ions correspond to *N*-glycan compositions of $(NeuAc)_1(Hex)_2(HexNAc)_2$ + $(Man)_3(GlcNAc)_2$, $(NeuAc)_2(Hex)_2(HexNAc)_2$ + $(Man)_3(GlcNAc)_2$ and $(dHex)_1(NeuAc)_2(Hex)_2(HexNAc)_2$ + $(Man)_3(GlcNAc)_2$ respectively and these compositions have been previously assigned in mouse erythrocytes [293, 294]. MS/MS fragmentation of these ions deduced the detail of the *N*-glycan structures as depicted in Figure 5-8. Non-cachectic mice were shown to express *N*-glycans with the motif consisting of NeuAcα(2-3/6)Galβ(1-4)GlcNAc, which was also observerd on the liver membrane of EHS-bearing mice (Chapter 4). Therefore, the expression of *N*-glycans consisting of the NeuAcα(2-3/6)Galβ(1-4)GlcNAc motif may serve as an important inflammatory glycan marker on the liver membrane of tumour-bearing mice. Normal mice predominately express

NeuGc on their sialylated glycans so, the increased expression of NeuAc over NeuGc in the plasma of C26 cancer-bearing mice has been suggested to be caused by the loss or impaired function of the CMP-hydroxylase that converts CMP-NeuAc to CMP-NeuGc [8]. This was not the case in the cachectic mice.

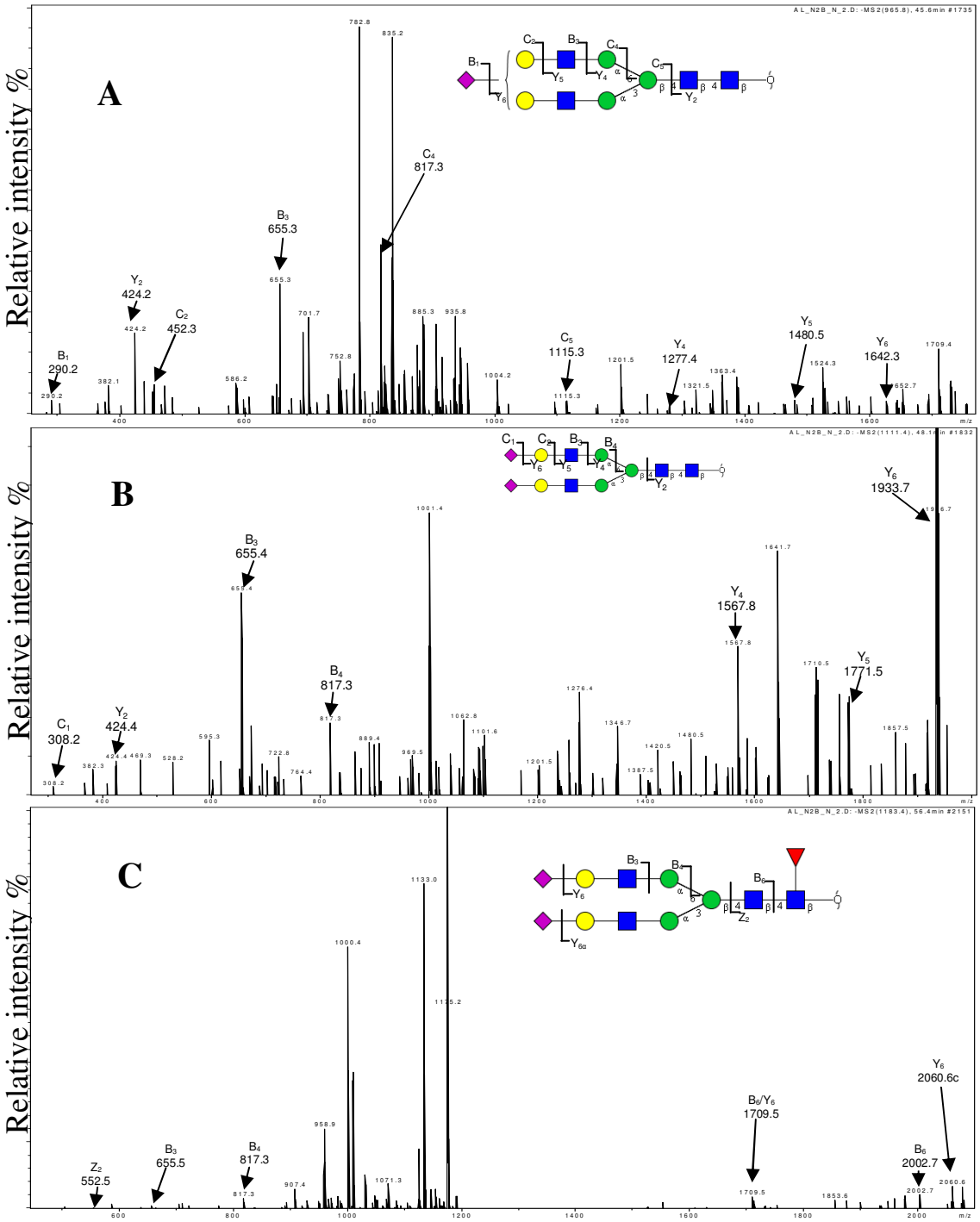

Figure 5-8. MS/MS fragmentation of m/z $(965.8)^{2-}$ (A), $(1111.4)^{2-}$(B) and $(1184.4)^{2-}$(C) which was only observed in non-cachectic mice and not in the normal and cachectic mice

5.3.2.4. Analysis of O-linked oligosaccharides

The average MS (LC retention time 20-25 min) of *O*-linked oligosaccharides released by β-elimination from liver membranes of control and tumour-bearing mice show no observable differences between m/z 600-1200. Ions corresponding to known *O*-glycan structures which have been previously identified in the mouse were seen as singly charged ions $[M-H]^{1-}$ [295, 296] (Figure 5-9), indicating that the liver membranes from control and tumour-bearing mice (non-cachectic and cachectic) expressed similar compositions containing both NeuAc and NeuGc terminal residues: ($[M-H]^{1-}$ of m/z 675.3 ($(Hex)_1(HexNAc)_1(NeuAc)_1$), m/z 691.3 ($(Hex)_1(HexNAc)_1(NeuGc)_1$), m/z 877.3 ($(Hex)_1(HexNAc)_2(NeuAc)_1$, m/z 895.3 ($(Hex)_2(HexNAc)_2(dHex)_1$, m/z 966.2 ($(Hex)_1(HexNAc)_1(NeuAc)_2$), m/z 982.3 ($(Hex)_1(HexNAc)_1$ $(NeuAc)_1$ $(NeuGc)_1$) and m/z 998.4 ($(Hex)_1(HexNAc)_1(NeuGc)_2$) (Table 5-2). MS/MS fragmentation of these mass ions identified mono- (m/z 675.3, 691.3 and 877.3) and di-sialylated (m/z 966.2, 982.3 and 998.4) core 1 structures and a mono-sialylated core 2 structure (m/z $(877.3)^{1-}$) in both control and tumour-bearing mice. The mass ions m/z $(877.3)^{1-}$ in the control mice and m/z $(895.3)^{1-}$ were more abundant in cachectic mice compared with the non-cachectic mice as shown by the average MS spectra, but interrogation using EIC of these masses confirmed that these ions were present in all mice (data not shown). Overall, there were no significant *O*-glycan differences observed in either control, non-cachectic or cachectic mouse liver membranes.

Table 5-2. Total assigned *O*-glycan compositions identified on the liver membrane of normal, non-cachectic and cachectic mice.

[M-H]	Assigned O-glycan compositions
675.5	$(Hex)_1$ $(HexNAc)_1$ $(NeuAc)_1$
691.3	$(Hex)_1$ $(HexNAc)_1$ $(NeuGc)_1$
877.3	$(Hex)_1$ $(HexNAc)_2$ $(NeuAc)_1$
895.3	$(Hex)_2$ $(HexNAc)_2$ $(Deoxyhexose)_1$
966.5	$(Hex)_1$ $(HexNAc)_1$ $(NeuAc)_2$
982.3	$(Hex)_1$ $(HexNAc)_1$ $(NeuAc)_1$ $(NeuGc)_1$
998.3	$(Hex)_1$ $(HexNAc)_1$ $(NeuGc)_2$

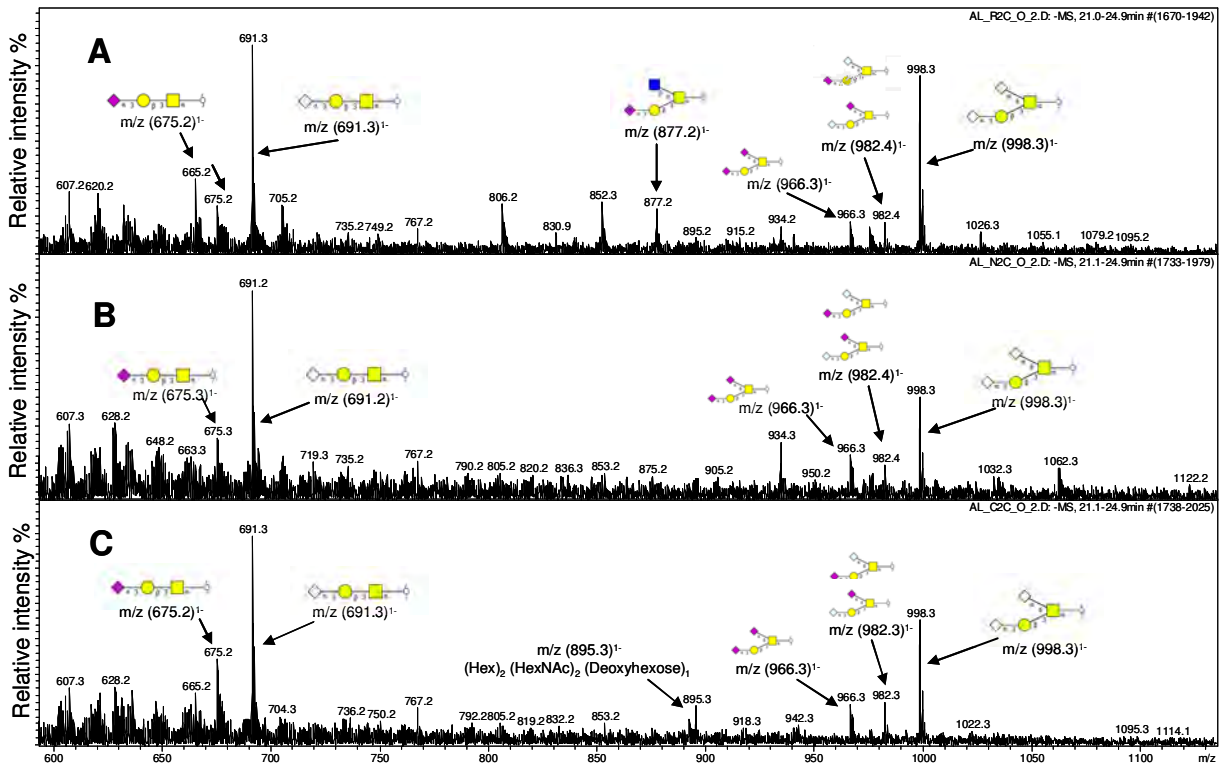

Figure 5-9. Average MS (over LC retention time 20-25 min) of released *O*-linked oligosaccharides from control (A), non-cachectic (B) and cachectic (C) mouse liver membrane proteins. Mono-(m/z (675.3)$^{1-}$ and (691.3)$^{1-}$) and di-sialylated (m/z (966.3)$^{1-}$, (982.4)$^{1-}$ and (998.3)$^{1-}$) core 1 *O*-glycans, and a mono-sialylated core 2 *O*-glycan (m/z (877.2)$^{1-}$) were identified on the liver membranes of all mice.

5.3.3. Effects of a C26 distal tumour on the metabolism of the liver

5.3.3.1. Xenobiotic metabolism (UGTs and cytochrome p450s)

The family of enzymes responsible for metabolism, glucuronidation and clearance of xenobiotic compounds are the UDP-glucuronosyltransferases (UGT) and cytochrome p450s. Metabolism and removal of xenobiotics such as bilirubin, fatty acid derivatives, drugs and antibiotic compounds require the glucuronidation of the molecule prior to transport out of the cell. In total, 18 UGT isoforms were identified, of which 12 were determined to be downregulated in both the non-cachectic and cachectic mouse livers compared to the normal (Figure 5-10).

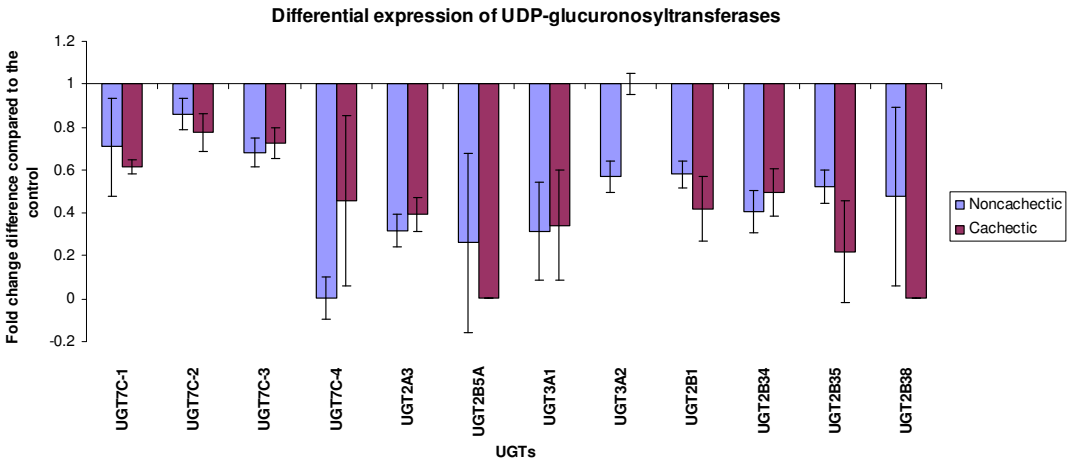

Figure 5-10. Differential expression of UDP-gluronosyltransferases in the liver of non-cachectic and cachectic mice.

Cytochromes p450s form part of the multi-component electron transfer chains and use both exogenous and endogenous compounds as substrates for enzymatic reactions. We identified 36 different cytochrome p450 isoforms, of which 27 were determined to be downregulated in the liver of non-cachectic mice. In addition, 21 of these same cytochrome p450 enzymes were determined to be downregulated in both non-cachectic and cachectic mice and two had not changed in abundance compared to the control (Figure 5-11A). Significantly, four cytochrome p450s, CYP2E1 (1.35±0.06 fold change), CYP3A13 (3.03±1.76 fold change), CYP2B19 (1.27±0.1 fold change) and CYP17A1 (72.1±27.26 fold change) were determined to be significantly upregulated in the liver of only cachectic mice ($p \leq 0.05$, Figure 5-11) compared to the normal. CYP2E1 is responsible for the hydroxylation of oleic acid in rat liver microsomes in fatty acid metabolism [297] whereas CYP3A13 is responsible for metabolizing and clearing the carcinogenic mycotoxin aflatoxin B [298], whose associated protein aflatoxin B aldehyde reductase was also determined to be significantly upregulated in cachectic mice. CYP2B19 is involved in the NADPH-dependent electron transport pathway and oxidizes a variety of compounds, including steroids, fatty acids, and xenobiotics. Very significantly, CYP17A1 was determined to be at least 40 fold upregulated in the liver of cachectic mice (Figure 5-11B). It is a key enzyme involved in

glucocorticoid production, which is known to play a major role in cancer cachexia by mediating the ubiquitin-proteosome pathway [17].

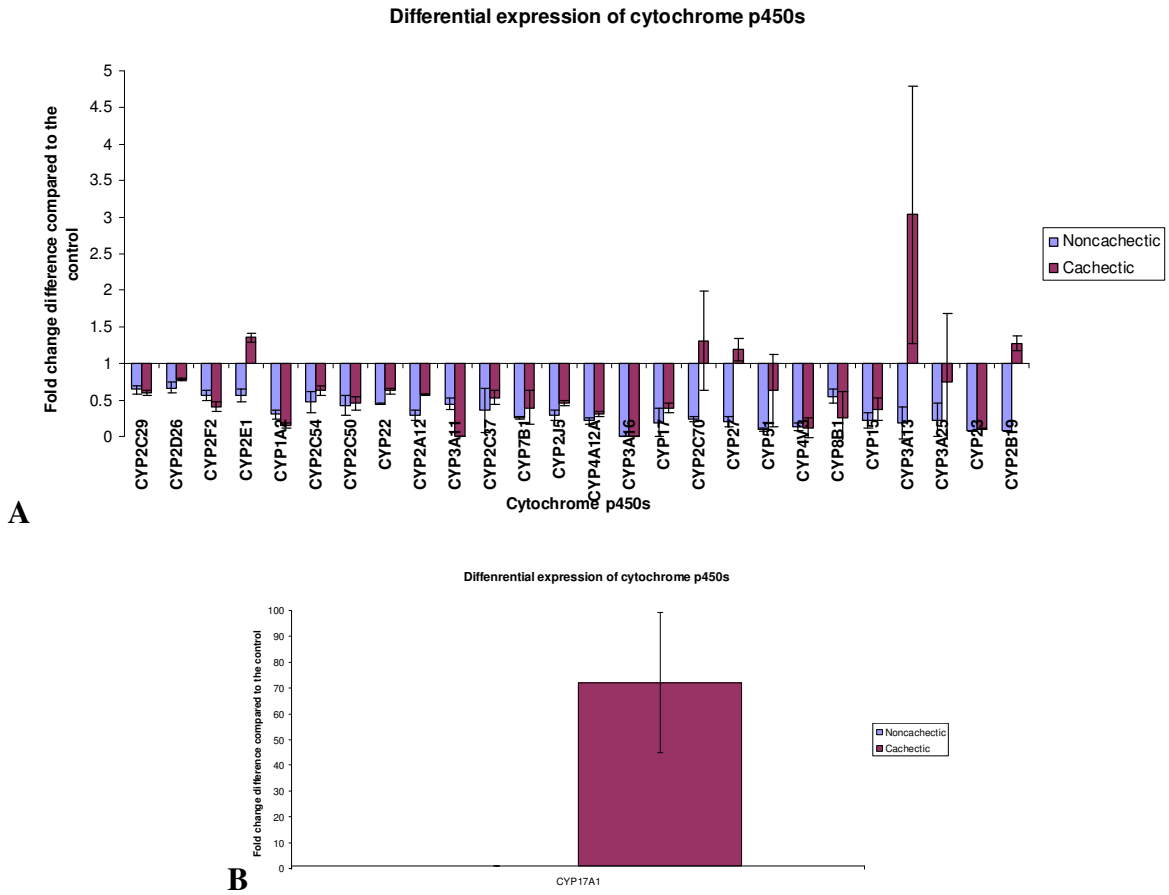

Figure 5-11. Differential expression of cytochrome p450s in the liver of non-cachectic and cachectic mice (A) and cytochrome p450 17A1 (B), which was not identified in either control or non-cachectic mouse livers.

5.3.3.2. Proteins involved in receptor-mediated endocytosis

Membrane proteins described by GO annotations to be involved in endo- and exocytosis were determined to be generally downregulated, particularly in the non-cachectic mice. Specifically, transferrin receptor (0.28±0.17 fold change), clathrin interactor (0.32±0.02 fold change), asialoglycoprotein receptor 1 (0.48±0.04 fold change), Adapter protein 2 (AP-2) alpha 1 (0.5±0.15 fold change) and 2 (0.56±0.05 fold change) and mannose-6-phosphate receptor (0.43±0.17 fold change) were identified to be downregulated in non-cachectic mice but not in the cachectic mice (Figure 5-12). These receptors and adapter proteins are all associated with clathrin-mediated endocytosis of apoptotic cells[299]. In addition, vesicular

integral membrane protein VIP36 (0.66±0.09 fold change), scavenger receptor (0.43±0.08 fold change) and sarcoplasmic reticulum calcium ATPase 2 (0.23±0.06 fold change) were determined to be downregulated in the liver of only non-cachectic mice, and are also involved in the endocytosis (not clathrin-mediated). Interestingly, AP-3 complex subunit beta-1 was determined to be significantly upregulated in the livers of cachectic mice (4.69±1.77 fold change) but showed no change in the non-cachectic mice.

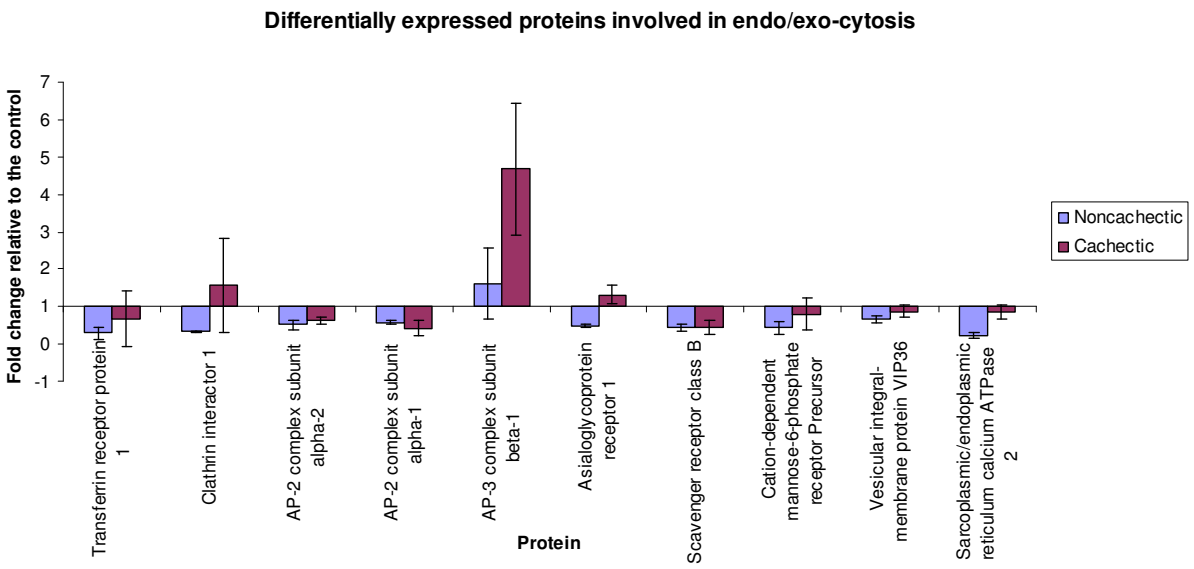

Figure 5-12. Differentially expressed proteins involved in endo and exocytosis.

5.3.3.3. Sugar Metabolism and Transport

Protein kinases that are responsible for phosphorylating key enzymes involved in sugar metabolism and transport were identified to be upregulated in the liver of both non-cachectic and cachectic mice. These include: 6-phosphofructokinase, glycerol kinase, probable glucokinase, glucokinase regulatory protein, galactokinase and glucokinase (Figure 5-13), all of which belong to the major hexokinase family. Glucokinase is a hexokinase isozyme which can mediate the phosphorylation of glucose to glucose-6-phosphate (G6P) in preparation for glycogen synthesis and glycolysis. On the other hand, galactokinases and fructokinases mediate the phosphorylation of galactose to galactose-1-phosphate and fructose to fructose-1-phosphate respectively, which can be further used as substrates for carbohydrate metabolism. In addition, aflatoxin B aldehyde reductase, glucose-6-phosphatase and UDP-glucose-6-

dehydrogenase were identified to be upregulated in both non-cachectic and cachectic mice. UDP-glucose-6-dehydrogenase is responsible for converting the nucleotide sugar UDP-glucose to glucose-6-phosphate through a number of reactions, which could be used as an intermediate substrate for either glycolysis or gluconeogenesis (Figure 5-15).

GDH-endoplasmic bifunctional protein and fructose bisphosphate adolase did not change in expression in either non-cachectic or cachectic mice. However, sugar transporters such as glucose-transporter 2 (GLUT 2) and solute carrier family 37 (glucose-6-phosphate) transporter were determined to be downregulated in the liver of both non-cachectic and cachectic mice.

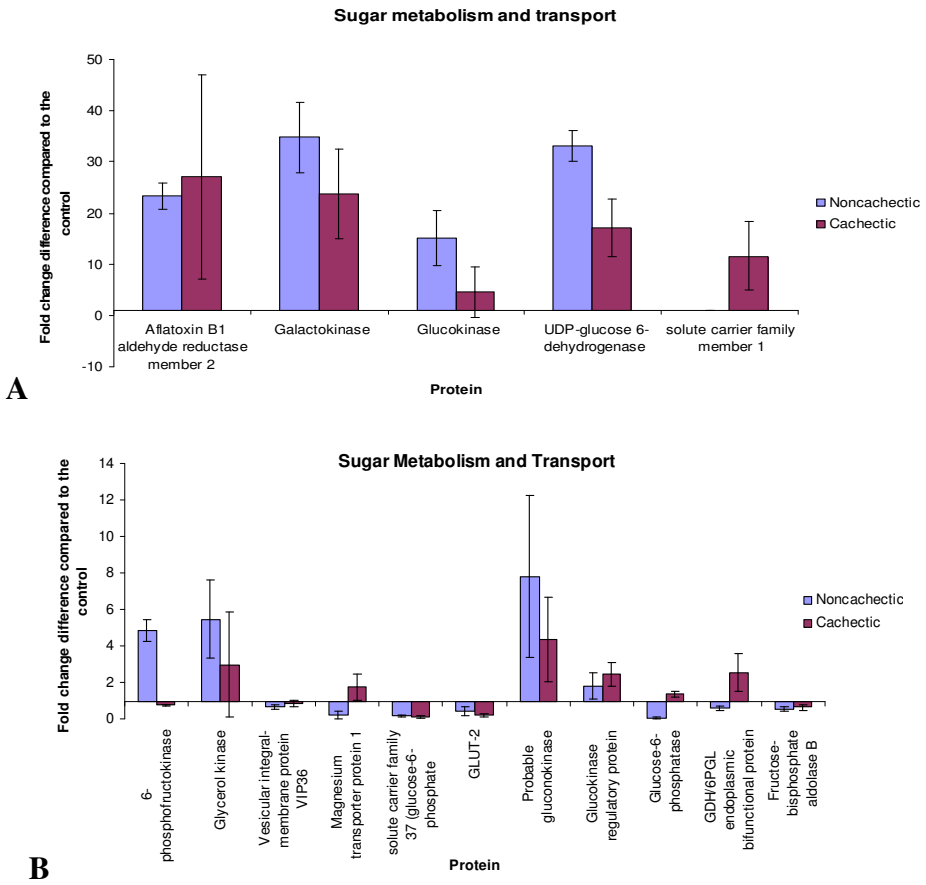

Figure 5-13 Differential expression of kinases involved in sugar metabolism (A) and enzymes involved in sugar metabolism and transport (B)

Many enzymes involved in the gluconeogenesis metabolic pathway were determined to be upregulated in abundance (Figure 5-13), particularly in the liver of cachectic mice including: glucose-6-phosphatase (3.66±0.14 fold change), glycerate kinase (37.46±10.48fold

change), alpha enolase (29.14±15.16 fold change), pyruvate carboxylase (4.33±2.21 fold change), dihydroxyacetone kinase (4.66±0.82 fold change) and glycerol-3-dehydrogenase (3.24±0.94 fold change). Some enzymes responsible for glycolysis including pyruvate kinase (0.133±0.004 fold change) and phosphoglycerate kinase (0.68±0.83) were determined to be either downregulated or unchanged in the liver of cancer-bearing cachectic mice.

5.4.Discussion

The colon 26 (C26) adenocarcinoma is one of the few animal transplantable tumours that are able to induce liver inflammation, cachexia and disorders of homeostasis in different hosts. The C26 mouse model was employed to study the effects of bearing a distal metastasizing tumour on liver membrane protein glycosylation, and to compare these glycosylation changes with those observed on the liver membrane proteins in EHS-bearing mice (Chapter 4). This cachexia model results in systemic inflammation of the liver produced by the C26 adenocarcinoma, and has been previously demonstrated to show a reduction in hepatic cytochrome p450 drug metabolizing enzyme activity and alterations to other metabolic processes (e.g. glycolysis/gluconeogenesis and fatty acid metabolism) [242]. The tumour and surrounding stromal macrophages, which are among the first to respond to the adenocarcinoma, release pro-inflammatory cytokines such as interleukin-1 (IL-1) and interleukin-6 (IL-6), TNF-α and interferons, into the bloodstream [18]. The increased levels of these cytokines are able to induce liver inflammation and liver regeneration [232] causing elevated secretion of acute phase proteins such as fibrinogen and sialic acid-rich glycoproteins into the plasma [11, 18]. In addition to the inflammatory effects, the C26 adenocarcinoma is a unique cancer model that is capable manifesting severe weight loss (cachexia) in some hosts, which provides an opportunity to study the effects of cachexia on the liver.

5.4.1. Differential expression of enzymes involved in protein glycosylation in the liver of C26 adenocarcinoma-bearing mice.

It is well known that alterations to protein glycosylation play a major role in ligand-selectin interaction in inflammatory and immune responses [118]. The enzymes responsible for protein glycosylation are the family of glycosyltransferases (such as fucosyltransferases, sialyltransferases and galactosyltransferases) and glycosidases, which are often found localized to the ER and Golgi Apparatus membrane, and are often implicated in the generation of glycan ligands that are responsible for responding to inflammatory stimuli

[120]. The expression and function of these protein glycosylation enzymes as well as their resultant glycans are often altered in parallel during tumour-induced inflammation (Chapter 4).

The family of dolichol-diphospholigosaccharide transferases and alpha (1,3)-mannosyltransferases were downregulated by at least 1.5-fold in the liver of non-cachectic mice but showed little or no significant change in cachectic mice. These transferases are involved in the first steps of the *N*-glycosylation pathway which is carried out on the cytosolic face of the ER membrane. The first step consists of the formation of an oligosaccharide-lipid complex containing a chitobiose *N*-glycan core with six mannose and three glucose residues linked to a dolichol moiety. Alpha (1,3)-mannosyltransferase is responsible for adding the first mannose residue on to the chitobiose *N*-glycan core. It is not known what the cause or overall effect of decreased expression of dolichol-diphospholigosaccharide protein transferases and mannosyltransferases has on the liver however, the decreased expression of these transferases has previously been reported to occur as a result of ethanol-induced liver injury and inflammation [300]. The reduced expression of these transferases has also been correlated with decreased concentrations of intracellular dolichol and reduced levels of transferrin [300].

Mannosyl oligosaccharide glucosidase, neutral alpha glucosidase AB and alpha mannosidase 2 were also downregulated by 4.8, 5.4 and 3.8-fold respectively in the liver of non-cachectic mice but showed no significant change in expression in cachectic mice. These enzymes trim the α(1,2) and α(1,3) linked glucose residues of the attached $Glc_3Man_9GlcNAc_2$-dolichol *N*-glycan precursor structure and cleave terminal mannose residues on both the Manα(1,3) and Manα(1,6) arms of precursor *N*-glycans in preparation for complex *N*-glycan biosynthesis. Chronic ethanol-induced injury to the liver has been shown to reduce glucosidase and mannosidase activity [301].

The final step of the *N*-glycosylation pathway is the addition of neuraminic acid to complex *N*-glycan structures. The first two steps in neuraminic acid biosynthesis are catalysed by the bifunctional UDP-GlcNAc 2 epimerase/*N*-acetylmannosamine kinase (Figure 5-14). UDP-GlcNAc 2 epimerase/*N*-acetylmannosamine kinase was significantly upregulated by 20.9 and 19.3 fold in the livers of non-cachectic and cachectic mice respectively. UDP-GlcNAc 2 epimerase/*N*-acetylmannosamine kinase is phosphorylated by several isoforms of protein kinase C and is a key enzyme in regulating neuraminic acid biosynthesis in the rat and mouse liver [302, 303]. It catalyzes the synthesis of neuraminic acid in the cytosol by the conversion of UDP-GlcNAc to ManAc and the subsequent phosphorylation to ManAc-6-phosphate [303]. The activity of UDP-GlcNAc 2 epimerase/*N*-acetylmannosamine kinase is feedback-regulated by the concentration of CMP-NeuAc [304]. Alterations to metabolic processes, for example reduced xenobiotic enzyme expression, can often lead to lack of CMP-NeuAc feedback-inhibition of UDP-GlcNAc 2 epimerase/*N*-acetylmannosamine kinase resulting in overexpression of NeuAc (Figure 5-14) [11, 302]. Therefore, UDP-GlcNAc 2 epimerase/*N*-acetylmannosamine kinase is the major determinant of cell surface sialylation and is critical for the function of most cell surface adhesion molecules [302].

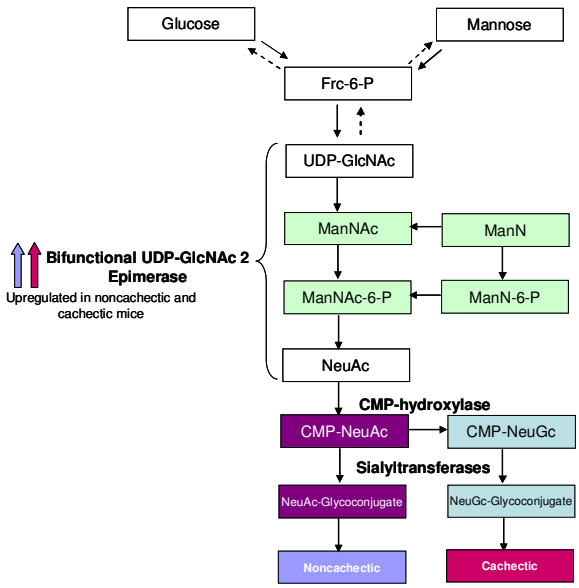

Figure 5-14. The function and activity of UDP-GlcNAc 2 epimerase/*N*-acetylmannosamine kinase is crucial in the biosynthesis of NeuAc and NeuGc [302]. This enzyme is responsible for converting UDP-GlcNAc to ManAc and the phosphorylation to ManAc-6-phosphate and is the rate limiting step in producing NeuAc.

The elevated expression of UDP-GlcNAc 2 epimerase/*N*-acetylmannosamine kinase gives some clues as to how the presence of the C26 adenocarcinoma may affect the overall sialylation status of glycans as seen in the cancer-bearing mice. Both non-cachectic and cachectic mice were observed to have increased expression of UDP-GlcNAc epimerase/*N*-acetylmannosamine kinase but differed in the nature of the sialylation of the liver cell membrane with less NeuGc attached to non-cachectic liver membrane glycoproteins. This suggests that the CMP-hydroxylase, which converts CMP-NeuAc to CMP-NeuGc, was downregulated in the non-cachectic mice (Figure 5-14).

The specific glycosyltransferases and sialyltransfases that carry out the final additions of neuraminic acid to glycans were not identified in this study as they are in very low abundance. To correlate these sialylation changes with the expression of specific transferases, other confirmatory methods such as RT-PCR would need to be used in future work to measure the level of mRNA transcripts corresponding to the sialyltransferases. It should be noted that mRNA levels may not correlate with the actual levels of protein present, such that Western blot analysis, ELISA and peptide IPG-IEF separation and label-free quantitation employing NSAF may have to be used to identify and quantitate the relative abundance of specific glycosyltransferases. Such determination of the differential expression of sialyltransferases has been shown to explain some, but not all, observed differential sialylation of membrane proteins [302, 305]. For example, human B lymphoma cells displayed differential sialylation of proteins on the cell membrane as a result of leukemia treatment, which correlated to reduced levels of α(2,6) and α(2,3)-linked sialic acids on their glycan structures. However, the activity and abundance of the enzymes responsible for these structures: β-galactoside α(2,6) sialyltransferase (ST6Gal-I) and β-galactoside α(2,3) sialyltransferase (ST3Gal-I) were unchanged [306, 307]. This suggests that the degree of sialylation of glycans, in addition to the abundance of their responsible sialyltransferases, may

also be dependent on the concentration of the CMP-NeuAc substrate, which is in turn controlled and maintained by UDP-GlcNAc 2 epimerase/N-acetylmannosamine kinase.

5.4.2. *N*-glycans presented on liver membrane proteins differ between non-cachectic and cachectic mice.

Glycosylation changes to the liver membrane proteins of mice reflected the differential expression of the glycosylation pathway enzymes seen in the livers of mice bearing a distal metastasizing C26 adenocarcinoma. The *N*-glycan profiles of both cachectic and non-cachectic mouse liver membranes were observed to be very similar to the normal but both expressed an additional unusual biantennary *N*-glycan containing three NeuGc that was not detectable in the normal. The expression of this tri-sialylated complex biantennary *N*-glycan on the mouse liver membrane and its relationship to cancer and cachexia has not been previously reported. This *N*-glycan was also identified in this thesis on the liver membrane of mice bearing a distal EHS tumour (Chapter 4) suggesting strongly that this *N*-glycan is expressed in response to pertubations to liver metabolism and homeostasis which may be caused by either a metastatic or non-metastatic distal tumour.

Interestingly, liver membranes from non-cachectic mice expressed complex biantennary *N*-glycans with terminal NeuAc, which were not expressed in either the cachectic or normal mice that express only terminal NeuGc. The expression of both NeuAc and NeuGc on the *N*-glycan structures presented on the liver membrane of non-cachectic mice suggests that the liver is affected by an inflammatory response, since the increased expression of NeuAc-containing glycans is directly correlated with perturbations to the immune system [79, 308-312]. This inflammatory effect was confirmed by the expression of these same specific *N*-glycans containing NeuAc determinants also identified on the liver membrane of mice bearing a distal EHS-tumour as described in Chapter 4. These NeuAc-containing *N*-glycans are the preferential ligands for selectins and sialic acid-binding lectins (Siglecs) for glycan-mediated cellular interactions such as B- and T-cell activation in the immune system in mice

[79, 308-312]. Siglecs are commonly expressed by resident and inflammatory macrophages in the liver, lung, and spleen, which are found either secreted into the extracellular environment or attached to the surface of cells where they interact specifically with the sialic acids on glycan structures. In the mice, siglecs have a higher affinity for NeuAc-containing glycans compared to those consisting of NeuGc [308, 312-316]. The presence of these NeuAc-containing *N*-glycans suggests that the activity of the CMP-hydroxylase that converts NeuAc to NeuGc in the liver of non-cachectic mice may be impaired.

CMP-hydroxylase catalyses the hydroxylation of CMP-NeuAc to CMP-NeuGc in the presence of hydrogen donor NADH, cytochrome b5 and NADH-cytochrome b5 reductase and is the rate limiting reaction in expressing NeuGc [310, 311]. Knockout studies of the CMP-hydroxylase gene in mice have demonstrated that the loss or reduced activity of this enzyme leads to hyperactivation of B-cells and, interestingly the change of expression from NeuGc to NeuAc-containing glycans leads to further activation of leukocytes in the mouse liver and spleen [313, 314, 317]. Humans are defective for the CMP-hydroxylase gene and therefore this enzyme is not normally expressed in human tissues [309]. Therefore the differences in sialic acid determinants observed in these mouse models may not truly reflect the glycosylation status observed in humans.

In this study, liver membrane protein glycosylation was shown to differ in the two mouse models bearing the same distal C26 adenocarcinoma with differences in their cachectic condition. Increased *N*-glycans containing NeuAcα(2,3/6)Galβ(1,4)GlcNAcβ(1,2) were observed on the liver membrane of only non-cachectic mice which also expressed a higher ratio of NeuAc compared to NeuGc. These *N*-glycan structures containing the NeuAcα(2,3/6)Galβ(1,4)GlcNAcβ(1,2) motif were also observed to be highly expressed on the liver membrane proteins of EHS-bearing mice, and it suggests that these *N*-glycan structures may be expressed in response to inflammatory stimuli [11, 309]. In addition, a biantennary *N*-glycan with three attached NeuGc was observed in both non-cachectic and

cachectic cancer-bearing mice but not in the normal. These differences in sialic acid determinants correlates with the observed upregulation of the sialic acid pathway enzyme, bifunctional UDP-GlcNAc 2 epimerase/*N*-acetylmannosamine kinase (Chapter 5.4.1), in both the non-cachectic and cachectic mice. The complementary results suggest that the feedback-inhibition mechanism of CMP-NeuAc may differ with the same cancer showing differed phenotypic effects (i.e. cachexia). That is, the liver of cachectic mice may have normal biosynthesis of NeuGc, whereas livers of non-cachectic mice may have reduced or impaired CMP-hydroxylase activity favouring the remaining presence of NeuAc (Figure 5-14). The differences in abundance of sialylation and of the corresponding synthesized glycan structures also suggest that there may also be functional and/or expressional differences in the sialyltransferases downstream in the protein glycosylation pathway.

Overall, the protein glycosylation changes observed on the liver membrane proteins of non-cachectic and cachectic C26-bearing mice described here and EHS-bearing mice (Chapter 4) strongly suggests that glycosylation is a general feature of liver responses to distal tumours. The specific differences in sialic acid determinants on *N*-glycan structures on the liver cell membrane of non-cachectic and cachectic mice and its relationship to tumour-induced liver inflammation and cancer cachexia is not fully understood. However, this data suggests that the CMP-hydroxylase enzyme and the sialic acid synthetic pathway may play a role in response to perturbations to the mouse liver by distal cancers.

5.4.3. Non-glycosylation related changes to liver metabolism in response to a distal C26 adenocarcinoma

Examination of the liver membrane proteins also revealed a multitude of effects of the distal C26 tumour in addition those observed in the protein glycosylation pathway and its glycan structural products. The liver plays a crucial role in maintaining metabolic functions such as processing of carbohydrates, lipids and amino acids. It is also responsible for detoxification, digestion of xenobiotics, phagocytosis of molecules from the portal circulation and in the

regulation of the immune system. The major cell type that carries out most of the functions of the liver are the hepatocytes. Hepatocytes make up approximately 80% (v/v) of the liver and are known to modify amino acid uptake and gluconeogenesis whilst also increasing synthesis of acute phase proteins after exposure to pro-inflammatory cytokines (e.g. IL-6) [232]. Hepatocytes can modify the host immune response by releasing immunomodulatory molecules which can signal to the immune system and act as scavengers for inflammatory mediators [232]. In addition, they can express various molecules on their surfaces (e.g. MHC class I and II molecules such as CD1 and CD40L) that can initiate mechanisms that serve to eliminate infection(s) whilst also restoring the structural and functional integrity of any associated liver damage resulting from the infection [232].

Loss of adipose tissue and skeletal muscle coupled with subsequent weight loss is often associated with cachectic cancer patients. This is due to increased resting energy expenditure as a result of increased thermogenesis and operation of the Cori cycle in skeletal muscles. The loss of adipose tissue and skeletal muscle is also due to decreased protein synthesis and increased protein degradation by the 1) lysosomal system including cathepsins to degrade extracellular proteins and cell receptors, 2) calcium-activated calpains which are involved in tissue necrosis and autolysis and, 3) ubiquitin-proteosome which is responsible for degrading myofibrillar proteins [17].

5.4.3.1. Immune-specific cell surface receptors

Immune-specific cell surface receptors such as H2 histocompatibility class I antigen receptor, lymphatic vessel endothelial hyaluronan receptor and tumour necrosis factor receptor associated protein (TRAP-1) were upregulated in the livers of non-cachectic C26-bearing mice but not in the cachectic mice. H2 histocompatibility class I antigen receptor is involved in antigen processing and presentation of peptide antigens on the surface of the plasma membrane for recognition by cytotoxic CD_8^+ T-cells. They are found on all cells except red

blood cells and are responsible for triggering cytotoxic T-cell responses to kill infected and abnormal cells [318]. It has been speculated that MHC class I antigen expression is related to natural killer (NK) cell development leading to effective recognition of infected cells by the host immune system [319]. The elevated expression of H2 histocompatibility class I antigen receptor in non-cachectic mice suggests that the liver may be regulating the immune system in response to inflammation caused by the presence of the tumour.

Lymphatic vessel endothelial hyaluronic acid receptor 1 (LYVE-1) is a homolog of the hyaluronan receptor CD44, which is widely expressed on the cell surface of leukocytes, dendritic cells and tumour cells as well as sinusoidal endothelial and Kupffer cells within the liver [292]. LYVE-1 together with hyaluronan is an important component of the extracellular matrix and a key mediator of cell migration in tissues during inflammation and wound healing [320]. It is thought that LYVE-1 may be involved in the lymphatic system providing fluid drainage of immune cells and foreign antigens from the liver to the peripheral lymph nodes, where they are sampled by antigen-presenting cells and phagocytes, stimulating the immune system [321]. In addition, it is thought that the expression of LYVE-1 may play a similar role to CD44 in promoting adhesion to the lymphatic endothelium during inflammation and cancer [292], and the elevated expression of this receptor in the livers of non-cachectic mice could be related to these stresses.

Tumour necrosis factor (TNF) is produced predominately by macrophages that are activated by infections and/or malignancies. It is involved in promoting immunity, inflammation and altering metabolic processes [322]. The TNF receptor is an integral membrane protein that is embedded on the extracellular monolayer of the plasma membrane, and does not contain an intrinsic cytoplasmic domain for protein tyrosine kinase activity and intracellular signalling. The tumour necrosis factor receptor associated protein (TRAP-1) interacts with the cytoplasmic monolayer of the plasma membrane and with the intracellular domain of the TNF receptor for intracellular signaling [322, 323]. The interaction of TNF

with its associated receptor (TNF receptor) and subsequently TRAP-1 mediates programmed cell death by inducing apoptosis and activation of NF-kappa B. TRAP-1 has also been described to mediate TNF-α and TNF receptor signaling to modulate N-cadherin expression and regulation of cell adhesion during cancer and inflammation [323, 324]. In addition, TRAP-1 is considered a novel marker of localized and metastatic prostate cancer, which has only recently been used as a therapeutic target for preventing cancer in human patients [323]. The upregulation of the three cell surface receptors: H2 histocompatibility class I antigen receptor, LYVE-1 and TRAP-1 have all been reported to be related to immune system regulation in response to perturbations such as inflammation and/or cancer, and in this study it strongly suggests that the livers of non-cachectic C26 cancer-bearing mice may be related to these stresses.

5.4.3.2. Xenobiotic metabolism

Hepatic xenobiotic metabolism is carried out by the family of cytochrome p450s, UDP-glucuronosyltransferases and glutathione-S-transferases (GSTs). Cytochrome p450s introduce reactive and polar groups such as carboxyl groups into xenobiotic compounds during phase I metabolism. These modified compounds are then glucuronidated by UGTs adding a glucuronosyl group from uridine 5'-disphospho-glucuronic acid to the hydroxylated compound during phase II metabolism. The glucuronidated compound is subsequently conjugated to a glutathione group by GSTs where the final conjugated xenobiotics are further processed and transported by solute carrier transporters (ABC transporters) out of the liver and into the bile or urine (phase III) [325]. Previous studies to monitor the levels and activity of hepatic UGTs in lipopolysaccharide (LPS) induced inflammation of mouse livers have shown that both the abundance and activity of UGTs are generally downregulated during inflammation [326]. In addition, the expression of UGTs is often closely correlated with the

expressional levels of cytochrome p450 enzymes as both are required for efficient glucuronidation and xenobiotic metabolism [326].

Decreased expression of UGTs were directly correlated in this study with the reduced expression of most cytochrome p450s in the liver of non-cachectic and cachectic mice, suggesting that reduced expression of hepatic xenobiotic enzymes are a common feature of liver inflammation. Four cytochrome p450 enzymes (CYP2E1, CYP2B19, CYP3A13 and CYP17A1) were determined to be upregulated in the liver of only cachectic mice. The CYP2E1 enzyme is responsible for the hydroxylation of oleic acid in rat liver microsomes in the fatty acid oxidation pathway [297] and may reflect the elevated energy expenditure and loss of muscle experienced by the cachectic mice, which would require the breakdown and oxidation of fatty acid stores for more energy [327]. CYP2B19 is involved in the NADPH-dependent electron transport pathway and has been described to oxidize a variety of structurally unrelated compounds, including steroids, fatty acids, and xenobiotics. CYP2B19 plays an important role in drug metabolism as well as in the bioactivation and disposition of fatty acids and lipids. It is also implicated in formation and regulation of squamous epithelial tissue [328]. However, it is not known what the role of elevated CYP2B19 has in the liver of cachectic C26-bearing mice. CYP3A13 is part of the CYP3A subclass of cytochrome p450 enzymes and is responsible for phase I metabolism of 45–60% of clinically administered drugs [329] and metabolizing and clearing the carcinogenic mycotoxin aflatoxin B [298]. The elevated expression of this enzyme in the liver of cachectic mice has never been observed but may be correlated with the elevated expression of aflatoxin reductase in cachectic mice (Figure 5-13A).

One of the most dominant changes was in CYP17A1, which was determined to be at least 40-fold upregulated in only the liver of cachectic mice. This cytochrome p450 enzyme is a key enzyme in the steroidogenic pathway that produces progestins, mineralocorticoids and glucocorticoids and is responsible for mediating the ubiquitin-proteosome pathway in cancer

cachexia [17, 330-332]. The increase in glucocorticoids can explain some of the metabolic alterations that occur during cancer cachexia, such as the induction of hepatic enzymes promoting gluconeogenesis [333, 334], the increased synthesis of acute phase proteins [335, 336] and, the regulation of the production of IL-1 [337] and TNF [338] mediators. In addition, increased levels of glucocorticoids may help to maintain the physiological homeostasis that is perturbed by the C26 adenocarcinoma [18]. CYP17A1 has been reported to be elevated in cancer patients and is considered a marker of cancer development and progression in humans [330-332], which correlates well with our findings in the mouse model and extends its use to the possible differentiation between the cancer-induced cachectic phenotype. The four cytochrome p450 enzymes that were determined to be upregulated in cachectic mouse livers have been described to be functionally related to fatty acid metabolism and steroid production, suggesting that these enzymes play a major role in reconditioning the liver and synthesizing hormones and metabolites during cachexia.

5.4.3.3. Endocytosis

Receptor-mediated endocytosis and vesicular trafficking is often impaired in hepatocarcinoma and as such, unbalanced recycling of cell surface receptors (such as integrins and cadherin-based adhesion complexes) are often associated with the disease [339]. Impaired receptor-mediated endocytosis in the liver can also be affected by other means of liver injury such as alcoholism, hepatitis and cirrhosis [340]. We observed many proteins involved in receptor-mediated endocytosis to be downregulated in the liver of non-cachectic mice that did not change in abundance in cachectic mice. These proteins included: asialoglycoprotein receptor 1, cation dependent mannose-6-phosphate receptor, adaptor proteins, transferrin receptor and clathrin-interacting protein.

Hepatic asialoglycoprotein receptor is responsible for the endocytosis of serum glycoproteins containing terminal galactose and/or *N*-acetyl galactosamine such as transferrin,

alkaline phosphatase and immunoglobulins. Increased levels of pro-inflammatory cytokines and liver inflammation have been attributed to reduced synthesis and function of the hepatic asialoglycoprotein receptor [341] in several diseases such as cancer, viral hepatitis and cirrhosis [342]. The decreased expression of the asialoglycoprotein receptor in non-cachectic C26-bearing mice suggests that the livers of these mice are affected by inflammation as a consequence of bearing a distal cancer and that cachexia does not involve this pathway.

The transferrin receptor is responsible for binding and internalizing iron and transferrin into the liver. The downregulation of the transferrin receptor in both non-cachectic and cachectic mouse liver membranes suggests either reduced expression of the transferrin receptor or increased shedding of the receptor on the cell surface [343]. The increased shedding of the membrane-bound transferrin receptors can occur as a result of increased concentrations of TNF-α in the blood and chronic liver inflammation, which can activate a cascade of proteases that initiate the digestion of the receptor [343].

The cation dependent mannose-6-phosphate receptor, clathrin-interacting protein, vesicular integral membrane protein 36 (VIP36) and adapter proteins (AP-1 and AP-2) were determined to be downregulated in the liver of non-cachectic mice but not in the cachectic mice. These proteins are all involved in clathrin-mediated endocytosis and vesicular trafficking of newly synthesized soluble acid hydrolases by binding specifically to high mannose and mannose 6-phosphate (Man-6-P) residues found on their *N*-glycans [299, 344]. The reduced expression of the identified membrane proteins responsible for clathrin-mediated endocytosis is a common feature in tumour-induced inflammation [339]. Overall, the downregulation of these proteins involved in endocytosis have been previously described to occur as a consequence of liver inflammation and cancer [339, 341, 345] further suggesting that an inflammatory response may be a characteristic of the non-cachectic mouse liver, but that other responses dominate the cachectic phenotype.

5.4.3.4. Glycolysis and gluconeogenesis

Although many studies have focused on the mechanisms of cachexia in tissue-wasting, little is known about how metabolic processes such as glycolysis, gluconeogenesis and fatty acid metabolism are altered in the liver. We examined the liver membrane proteins associated with glycolysis and gluconeogenesis. The abundance of most proteins involved in liver glycolysis was downregulated in the cachectic mice which showed approximately 20% weight loss compared to the non-cachectic mice. Proteins involved in gluconeogenesis were concomitantly upregulated in the cachectic mice including pyruvate carboxylase, 2-phosphoglycerate and glycerate kinase. The increased expression of these enzymes may also suggest that the liver of cachectic mice may be favouring glucose production for transport to other parts of the body such as the skeletal muscles and/or to the tumour itself.

Increased gluconeogenesis is well known to be associated with cancer cachexia [346]. The process of gluconeogenesis involves converting pyruvate to glucose-6-phosphate followed by its conversion to glucose by the enzyme glucose-6-phosphatase (Figure 5-15). We determined glucose-6-phosphatase to be upregulated by at least 3-fold in the liver of cachectic mice suggesting that gluconeogenesis is indeed increased in these mice [347]. The increased production of free glucose in the liver can be transported via the bloodstream to other parts of the body such as the skeletal muscles, or to the tumour itself, which can then utilize the glucose for energy production. This outcome is often observed to be reversed in the skeletal muscles of cachectic mice. That is, skeletal muscles of cachectic mice often experience increased glycolysis and decreased gluconeogenesis to allow increased ATP production and increased energy expenditure [17].

Conversely, hexokinases (such as galactokinase and glucokinase), which are involved in the first steps of glycoslysis, were upregulated in the liver of cachectic mice suggesting that the initial stages of glycolysis may be upregulated. This initial step in glycolysis involves the phosphorylation of glucose by hexokinases to produce glucose-6-phosphate for glycolysis or

glycogen storage. This class of hexokinases together with glucose transporters (e.g. GLUT2) are known to interact between the glucose transport system, hepatic glucose production and glycogen storage, which have been described to be altered during cancer cachexia [348].

The upregulation of the two antagonistic processes of glycolysis and gluconeogenesis in the liver show that these processes can be upregulated simultaneously under certain metabolic conditions which would result in increased cycling between glucose and glucose-6-phosphate [348]. Under normal conditions these two metabolic processes complement each other i.e. glycolysis is activated whilst the gluconeogenesis is disabled.

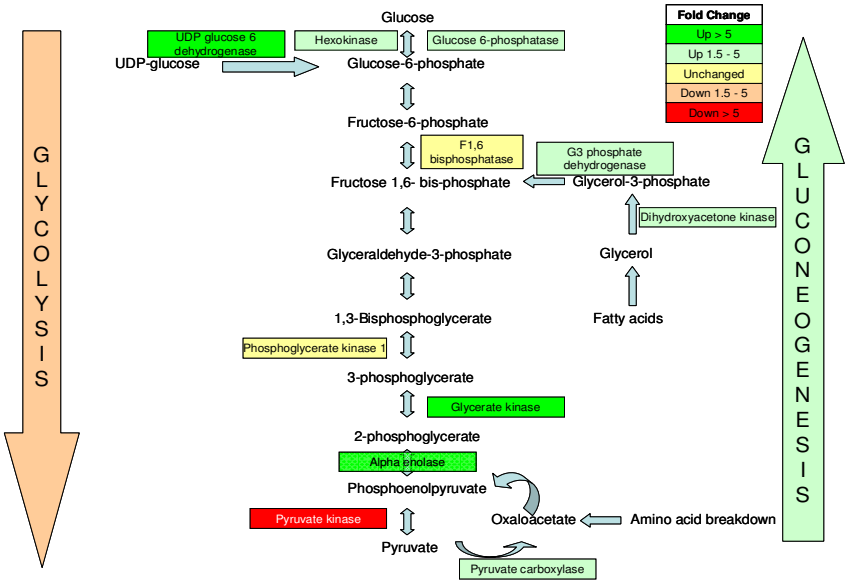

Figure 5-15. Summary of the glycolysis and gluconeogenesis pathways with identified proteins coloured to signify level of abundance in the liver of cachectic mice.

The process of breaking down glycogen stores involves the conversion of UDP-glucose to glucose-1-phosphate by the enzyme UDP-glucose-pyrophosphorylase, which is then subsequently converted to glucose-6-phosphate and thereafter into glucose. The transport of glucose between the liver and the bloodstream is carried by glucose transporter 2 (GLUT2), which is the major isoform expressed in hepatocytes, pancreatic β-cells, intestines and kidneys. Although the expression of this transporter would be expected to increase to deal with the increased rate of glucose production in the liver of cachectic mice, GLUT2 transporter was downregulated in these mice. This may indicate that the transport of glucose

from the liver of cachectic mice into the bloodstream is being carried out by other means (e.g. Na^+/glucose transport) besides GLUT2 transport [348].

Based on these results, we propose that livers of non-cachectic mice bearing a distal C26 adenocarcinoma may be reacting with an inflammatory response whereas, cachectic mice bearing the same distal C26 adenocarcinoma show less of an inflammatory response, as their metabolism switches to favour more essential cellular processes such as energy metabolism and liver cell homeostasis which do not affect the protein glycosylation pathway. This scenario is plausible since most of the glycans presented on the liver membrane of cachectic mice were very similar to the normal control. This speculation warrants further investigation in the future.

In this study, in addition to changes in glycosylation of liver membrane glycoproteins, we determined changes in the relative abundance of proteins involved in many important biological processes, specifically those related to xenobiotic metabolism, endo- and exocytosis, glycolysis and gluconeogenesis and fatty acid metabolism induced in the liver as a consequence of a C26 adenocarcinoma distal to the liver. The identification and quantitation of enzymes involved in the protein glycosylation pathway together with complementary information on the *N*- and *O*-glycans on the liver cell membrane also provided insights into the effects of tumour-induced liver inflammation and cancer cachexia on protein glycosylation.

Chapter 6: General Discussion

The work presented in this thesis describes the optimization of methods for isolating liver membrane glycoproteins and the application of these methods to study the liver membrane glycoproteome of two murine models as models of tumour-induced liver inflammation. The two murine cancer models examined have been established [14, 15, 241, 287] and described by our collaborators at the ANZAC Research Institute (Concord Hospital, NSW, Australia) to be involved in systemic liver inflammation produced by a distal non-metastasizing EHS sarcoma (Chapter 4) and a distal metastasizing C26 adenocarcinoma (Chapter 5) (Table 6-1). The EHS sarcoma is an encapsulated xenograft murine non-metastasizing tumour, which contains ECM basement membrane extracts that are rich in laminin, growth factors, entactin/nidogen, type IV collagen, and heparan sulfate proteoglycan [349]. In contrast, the colon 26 adenocarcinoma is an undifferentiated grade IV carcinoma induced by the carcinogen *N*-nitroso-*N*-methylurethane that is capable of metastasis and causing cachexia [242]. In this study, immune-specific cell surface receptors such as siglec-1 and TRAP-1, which are often used as markers for determining inflammatory status, were determined to be upregulated [323, 350] in liver membrane preparations and is concordant with the proposed inflammatory murine models.

Table 6-1. Summary of the changes determined by proteomics analysis of metabolic pathways relative to normal metabolism.

	Distal Tumour		
Metabolic process	**EHS Sarcoma**	**C26 carcinoma non-cachectic**	**C26 carcinoma cachectic**
Glycosylation - sialylated structures - CMP-hydroxylase activity - Glycosyltransferases (OGTs) - Galactosyl/Sialyltransferases - O-linked glycosylation	**Up** NeuAc & NeuGc structures Impaired/Reduced Increased expression Increased expression Increased sialylation	**Up** NeuAc & NeuGc structures Impaired/Reduced Decreased expression Increased expression No change	**Up** Only NeuGc structures No change No change Increased expression No change
Xenobiotic metabolism - UDP-glucuronosyltransferases - Cytochrome p450s	**Down*** Decreased expression Decreased expression	**Down** Decreased expression Decreased expression	**Down** Decreased expression Decreased expression (except CYP17A, CYP2E1, CYP3A13 & CYP2B19)
Immune-cell specific receptors	**Up***	**Up**	**No change**
Endocytosis	**Down***	**Down**	**No change**
Gluconeogenesis	**Down***	**Down**	**Up**
Glycolysis	**Up***	**Up**	**Up (first step only)**
Fatty acid oxidation and metabolism	**Down***	**No change**	**Up**

***Data obtained with permission from Dr. Joel Chick from the PhD thesis titled "Proteomic Analysis of Liver Membranes through an Alternative Shotgun Methodology", Macquarie University 2009.**

Liver inflammation, cancer and perturbations to liver metabolism are factors that are well-known to result in alterations to the protein glycosylation machinery and have been reported extensively to cause aberrations to the glycosylation of plasma glycoproteins [118, 351-353]. It was not known whether these external cues (inflammation, cancer and/or liver metabolism) can influence the glycosylation of proteins presented in an implicated organ such as the liver. The presence of a distal non-metastasizing EHS tumour was shown to influence the expression of glycosyltransferases and cell surface lectins expressed on the membrane of the liver of EHS-bearing mice. Global glycan analysis confirmed that the changes in expression of these enzymes were reflected in the status of their *N*- and *O*-glycan products that were attached to the liver membrane proteins of EHS-bearing mice and were not observed in the non-tumour bearing mice. Most differences were observed to occur in the *N*-linked glycans with four unique biantennary *N*-glycans containing NeuAc moieties present only on the liver membrane proteins of EHS-bearing mice.

Whether these glycosylation changes were attributable to the type of distal cancer was investigated by studying whether the same glycosylation changes occur in other cancer models such as the C26 adenocarcinoma bearing mice. These have the added variable of resulting in weight loss (cachexia) in a sub-population and thus provide a further model in which to study the downstream effects of a distal tumour on the liver. Differences in sialic acid determinants were also observed in the *N*-glycans of liver membrane proteins in both the non-cachectic and cachectic C26-bearing mice. Liver membrane proteins however showed different effects on the sialylation of their attached glycans, with biantennary complex *N*-glycans containing three NeuGc being expressed on glycoproteins of cachectic C26-bearing mice, whilst non-cachectic C26-bearing mice expressed complex *N*-glycans containing both NeuGc and NeuAc residues. The expression of NeuAc-containing glycans rather than the normally expressed NeuGc in mice has been previously reported to increase upon B-cell

activation in the mouse liver and spleen during inflammatory stimuli [317] and has also been reported to be present on acute phase plasma glycoproteins in C26-bearing mice [11].

Specifically, both non-cachectic mice bearing the C26 adenocarcinoma and EHS-bearing mice were shown to have increased expression of *N*-glycans with the glycan motif NeuAcα(2,3/6)Galβ(1-4)GlcNAcβ(1-2). *N*- and *O*-glycans containing this motif have been reported to be highly expressed in inflammation and cancer [118, 125]. The results presented from the two different murine non-cachectic cancer models in this thesis suggest that this motif could be a glycan epitope biomarker for tumour-induced liver inflammation in the mouse. This thesis reports for the first time that glycosylation of membrane proteins in non-cachectic mouse livers is altered in the presence of a distal non-metastatic EHS tumour and a metastatic C26 adenocarcinoma, and it substantiates that protein glycosylation of membrane proteins in the liver may play a role in systemic responses in the liver to distal cancers.

In contrast, cachectic mice bearing the C26 adenocarcinoma did not show these changes in sialylation of the protein *N*-glycans and their metabolism appears to favour more essential processes that involve energy metabolism and liver cell homeostasis. In addition, the changes observed in the livers of C26-bearing mice may not be a complete reflection of the liver inflammatory effects of bearing colon cancer since the adenocarcinoma was injected into the subcutaneous muscle in these experiments. Future studies employing other distal cancers such as pancreatic or prostate cancers should also be compared to monitor for glycosylation changes on liver membrane proteins. Further studies to determine the activity of some glycosylation enzymes found to be over-expressed in the liver of mice with a distal tumour (e.g. CMP-hydroxylase and sialyltransferases) as well as the concentration of substrates (e.g. CMP-NeuAc) would be interesting to carry out in order to confirm whether substrate dependency and specific enzymatic activity, rather than only protein expression, are contributing factors to the differential glycan expression observed in these murine cancer models. These studies will give further insights into liver responses to cancer as this thesis has

demonstrated that physical condition (cachexia), that is a cancer phenotype affected by factors such as nutrition and tissue wasting does not result in substantial glycosylation changes to liver proteins, whilst tumour-induced liver inflammation in non-cachectic mice is seen to significantly influence the protein glycosylation pathway.

One of the challenges with determining glycosylation changes and identifying glycan markers in animal models that are used to reflect human diseases is the distinction between expressed glycans containing NeuGc and NeuAc moieties. As demonstrated in this thesis, compared to normal mice that express mostly NeuGc (95%) in the liver, cancer-bearing mice exhibit the expression of NeuAc in response to tumour-induced inflammation. The differential expression of these residues on liver membrane proteins is unlikely be reflected in humans since humans express only NeuAc (not NeuGc) in their tissues, however, NeuGc has been reported to be expressed in some human cancers [354-356]. Extension to these murine studies could be made by using rats as model organisms, since rats preferentially express NeuAc (89%) over NeuGc (11%) [312]. Glycosylation changes of rat (or other mammals including humans) liver membrane proteins may be more relevant and reflective of the changes that may occur in humans.

In addition to the changes in the glycosylation pathway, cancer and liver inflammation was observed to affect a multitude of metabolic pathways in the liver including immune system regulation, endocytosis, xenobiotic metabolism and energy metabolism. The liver plays an important role in both innate and specific immune regulation. The innate response of the liver to inflammation is the secretion of acute phase plasma proteins as a part of the acute-phase response, mediation of non-specific phagocytosis by Kupffer cells, initiation of non-specific cell killing by liver natural killer cells and endocytosis of circulating macromolecules by liver sinusoidal endothelial cells. The results presented in this study, as well as results from the PhD thesis "Proteomic Analysis of Liver Membranes through an Alternative Shotgun Methodology" by Dr. Joel Chick show that proteins involved in endocytosis were

downregulated in expression in the livers of non-cachectic EHS- and C26-bearing mice, but were shown to have no significant change in cachectic C26-bearing mice. The decreased expression of these proteins have been shown to be directly correlated with cancer and chronic and recurring liver inflammation [339, 345] and it indicates that the livers of non-cachectic EHS- and C26-bearing mice may be under extreme inflammatory stress.

Injury, infection, inflammation and diseases (e.g. cancer) that disturb homeostasis involve several systemic and metabolic changes that make up the acute phase response which can also perturb other metabolic pathways such as xenobiotic metabolism. In advanced cancer, the persistence of the acute phase response and chronic liver inflammation can lead to numerous metabolic disturbances and cachexia. Tumour-induced inflammation has been attributed to decreased expression of hepatic UGTs and cytochrome p450s [15, 241], both of which were observed in the livers of all cancer-bearing mice examined in these studies. This further supports the notion that decreased expression of hepatic xenobiotic metabolic enzymes, such as these proteins, is a general feature and is directly correlated with the presence of cancer and systemic tumour-induced liver inflammation.

The body of work presented in this thesis describes changes in glycans and their associated glycosyltransferases in tumour-bearing mouse livers, the structures of which have been implicated in cancer and chronic inflammatory diseases. Proteomics and glycomics were used as complementary experimental approaches to study these glycosylation changes to the liver membrane proteins of mice bearing distal non-metastatic and metastatic tumours. Both proteomics and glycomics, as separate entities, have their advantages and disadvantages for glycoproteomic analysis. In this study, proteomics approaches identified and quantitated the relative abundance of membrane proteins and enzymes involved in different biological pathways including the glycosylation pathways, and gave a perspective of other pathways that were affected in response to tumour-induced liver inflammation. In most proteomic applications, differentially expressed proteins are often validated using Western blot analysis

with specific antibodies to these proteins, which can give supportive information on their relative abundance. However, Western blot analysis may be complicated by the specificity of the antibodies to different protein isoforms and to those proteins with similar sequence homology. More importantly, neither Western blot analysis nor proteomics can determine whether the differentially expressed proteins and enzymes have different functional activity.

Glycomics is a separate experimental approach which gave detailed information on the abundance and the types of structures and linkages of the glycans that were differentially expressed on liver cell membrane proteins of tumour-bearing mice. For example, increased sialylation of *N*-glycans was observed on the liver cell membrane proteins of all cancer-bearing mice, which indicated that one or more sialyltransferases may have been upregulated. An alternative explanation may be that the nucleotide-sugar substrates for this family of enzymes may be in excess.

In Chapters 4 and 5, both proteomics and glycomics approaches were used to study changes to total liver membrane glycoproteins in response to a distal tumour. Differentially expressed glycan structures were determined and were correlated directly to the specific enzyme(s) that were up or down regulated in the biosynthesis of these glycans. The application of these analytical approaches, which we term "reverse translational glycoproteomics", identified both the glycan products and their corresponding glycosylation enzymes and highlights that glycomics can be used as a confirmatory approach for verification of both the differential expression of glycosylation enzyme abundance and the resultant enzymatic activity (Figure 6-1).

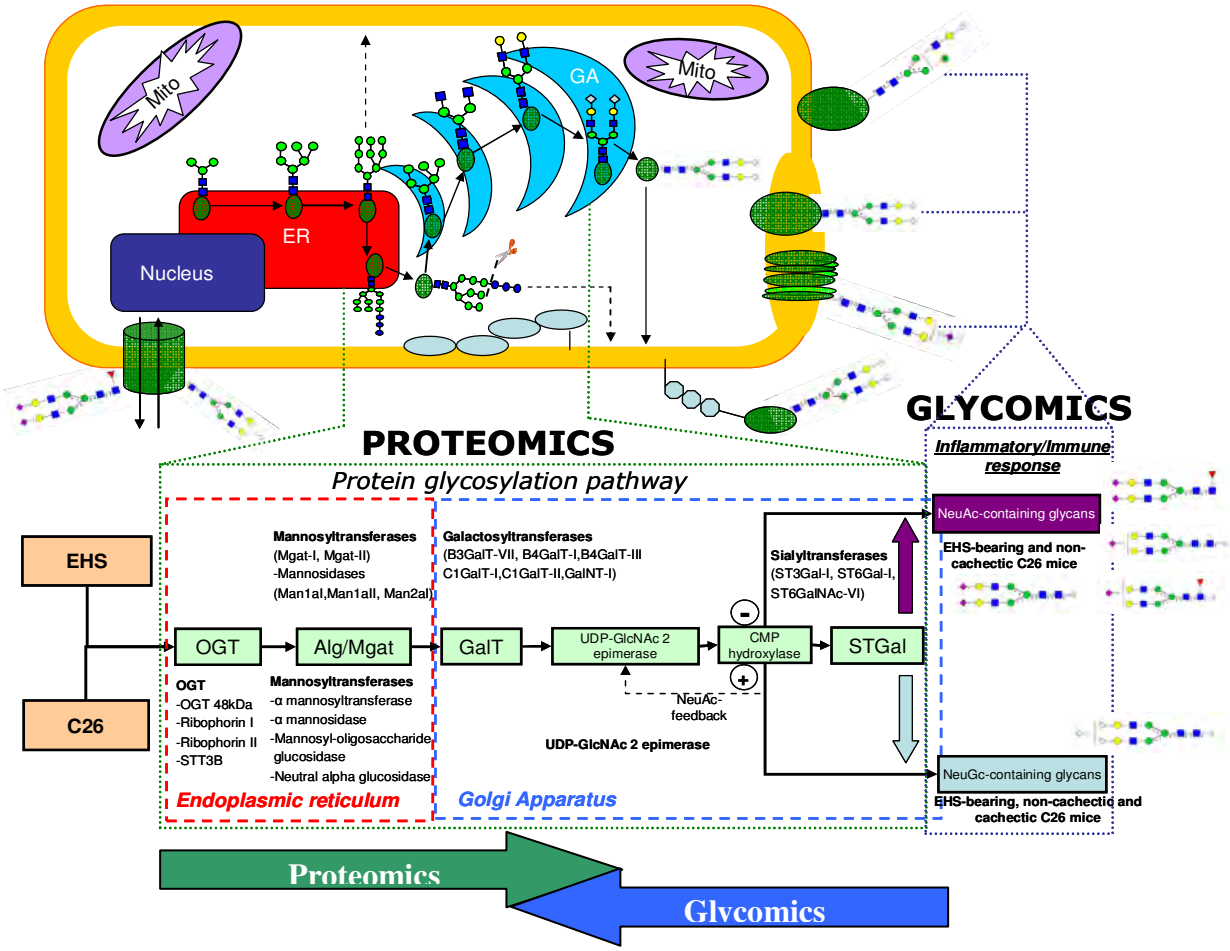

Figure 6-1. Summary of the protein glycosylation pathway in normal, EHS-bearing and non-cachectic and cachectic mouse livers. OGT – dolichol-oligosaccharide transferase, Alg/Mgat – mannosyltransferases and mannosyl N-acetylglucosaminyltransferase, GalT – galactosyltransferase, STGal – sialyltransferase and CMP - cytidine monophosphate. (+) - Normal activity/expression, (-) - Reduced activity/expression, ↑ - synthesis of NeuAc-containing glycans due to reduced CMP-hydroxylase activity/expression. ↓ - synthesis of NeuGc-containing glycans due to normal CMP-hydroxylase activity/expression. Enzymes of the protein glycosylation pathway that were observed in this study are indicated.

The information gathered from the combination of these analytical approaches also provided more detail on the effects of cancer on liver protein glycosylation between non-cachectic and cachectic C26-bearing mice. For example, non-cachectic and cachectic mice bearing the same distal C26 adenocarcinoma were shown to both have elevated expression of the bifunctional UDP-GlcNAc 2 epimerase/*N*-acetylmannosamine kinase that is a key enzyme in the addition of both NeuAc and NeuGc sialic acids at the termini of *N*- and *O*-glycans (Figure 6-1). The upregulation of this enzyme using an exclusive proteomics approach may lead us to simply conclude that this enzyme may cause increased downstream sialylation of the glycans on membrane glycoproteins. Further verification by glycomics identified the

specific glycan structures that were affected and the differences in the specific sialic acid determinants (NeuAc and NeuGc) as well as the glycan linkage information (α(2,3) and/or α(2,6)) of the sialic acids, that were altered.

In this way, glycomics analysis significantly increased the information on the fine detail of the induced changes; that the sialylation of the *N*-glycans on the liver cell membrane proteins of non-cachectic and cachectic mice were very different i.e. non-cachectic mice expressed *N*-glycans containing NeuAc whereas cachectic mice expressed only NeuGc. These sialylation differences imply that there are also functional and/or expressional alterations to the CMP-hydroxylase that converts NeuAc to NeuGc as a consequence of tumour-induced liver inflammation. This deduction could not have been made using proteomics alone as CMP-hydroxylase was not identified in the study, probably due to its low abundance. The results presented in this thesis demonstrate that both proteomics and glycomics experimental approaches add value to glycoproteomic analysis of the protein glycosylation pathway.

This thesis emphasizes that tumour-induced liver inflammation can affect the glycosylation pathway in the liver to produce different glycan structures presented on liver membrane glycoproteins, in two different cancer models. The differential expression of the enzymes in the glycosylation pathway and the resultant glycan products observed on the liver membrane glycoproteins of EHS-bearing and C26-bearing mice strongly suggests that glycosylation of liver membrane proteins plays a role in systemic responses to liver inflammation in the presence of distal cancers. The changes to the glycosylation status and the expression of unique glycan structures on liver membrane glycoproteins of tumour-bearing mice that are different to those displayed in normal mice may indicate that these glycans may play some role as immunomodulatory molecules in the liver as a consequence of infections and/or inflammation. The unique glycans expressed only in tumour-bearing mice could be used diagnostically for determining inflammatory status of the liver. In addition to the aberrant glycosylation of serum glycoproteins which have been extensively reported, the work

presented in this thesis establishes that changes to liver membrane protein glycosylation are also evident in cancer-induced liver inflammation.

Appendices

Appendix A: Publication I Supplementary Information

Appendix A-1: *Subcellular localization of membrane proteins isolated by lectin affinity and hydrazine chemistry*

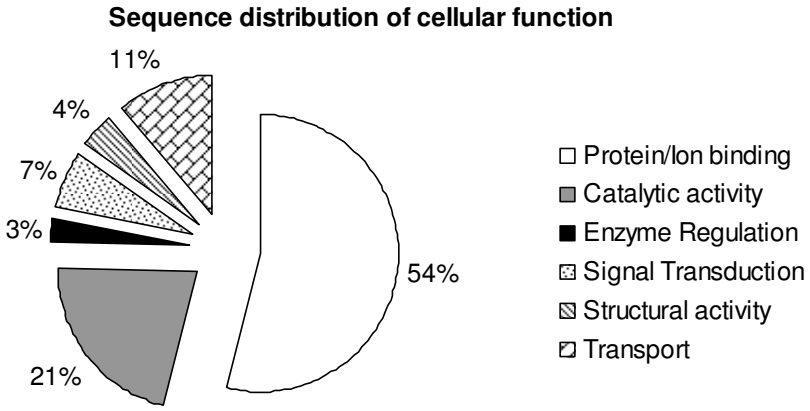

A: Distribution of cellular functions of membrane proteins isolated using lectin affinity chromatography

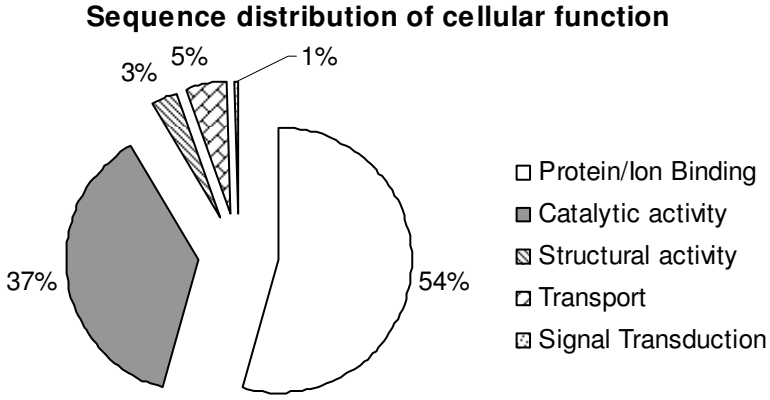

B: Distribution of cellular functions of membrane proteins isolated using hydrazine chemistry

Figure A-1-1. Distribution of cellular functions of membrane proteins isolated using lectin affinity chromatography B: Distribution of cellular functions of membrane proteins isolated using hydrazine chemistry

Appendix B: Publication III Supplementary Information

Appendix B-1: *Assigned N- and O-glycans in normal and EHS tumour-bearing mice*

N-glycans		
(M-H)2-	(M-H)1-	Glycan assignment
617.3	1235.6	$(Hex)_2 + (Man)_3(GlcNAc)_2$
658.2	1317.4	$(HexNAc)_2 + (Man)_3(GlcNAc)_2$
698.3	1397.6	$(Hex)_3 + (Man)_3(GlcNAc)_2$
779.3	1559.6	$(Hex)_4 + (Man)_3(GlcNAc)_2$
791.3	1583.6	$(Hex)_1\ (HexNAc)_1\ (NeuGc)_1 + (Man)_3(GlcNAc)_2$
799.8	1600.6	$(Hex)_3(HexNAc)_1 + (Man)_3(GlcNAc)_2$
812.3	1625.6	$(Hex)_1(HexNAc)_2(Deoxyhexose)_1 + (Man)_3(GlcNAc)_2$
820.3	1641.6	$(Hex)_2\ (HexNAc)_2 + (Man)_3(GlcNAc)_2$
832.8	1666.6	$(HexNAc)_3\ (Deoxyhexose)_1 + (Man)_3(GlcNAc)_2$
860.3	1721.6	$(Hex)_5 + (Man)_3(GlcNAc)_2$
872.3	1745.6	$(Hex)_2\ (HexNAc)_1\ (NeuGc)_1 + (Man)_3(GlcNAc)_2$
884.8	1770.6	$(Hex)_1\ (HexNAc)_2\ (NeuAc)_1 + (Man)_3(GlcNAc)_2$
893.9	1788.8	$(Hex)_1\ (HexNAc)_2\ (NeuGc)_1 + (Man)_3(GlcNAc)_2$
913.8	1828.6	$(Hex)_1\ (HexNAc)_3\ (Deoxyhexose)_1 + (Man)_3(GlcNAc)_2$
941.3	1883.6	$(Hex)_6 + (Man)_3(GlcNAc)_2$
952.9	1906.8	$(Hex)_3\ (HexNAc)_1\ (NeuGc)_1 + (Man)_3(GlcNAc)_2$
961.8	1924.6	$(Hex)_5\ (HexNAc)_1 + (Man)_3(GlcNAc)_2$
965.9	1932.8	$(Hex)_2\ (HexNAc)_2\ (NeuAc)_1 + (Man)_3(GlcNAc)_2$
973.8	1948.6	$(Hex)_2\ (HexNAc)_2\ (NeuGc)_1 + (Man)_3(GlcNAc)_2$
994.5	1990	$(Hex)_2\ (HexNAc)_3\ (Deoxyhexose)_1 + (Man)_3(GlcNAc)_2$
1022.4	2045.8	$(Hex)_7 + (Man)_3(GlcNAc)_2$
1038.9	2078.8	$(Hex)_2\ (HexNAc)_2\ (Deoxyhexose)_1\ (NeuAc)_1 + (Man)_3(GlcNAc)_2$
1046.4	2093.8	$(Hex)_1\ (HexNAc)_2\ (NeuGc)_2 + (Man)_3(GlcNAc)_2$
1067.5	2136	$(Hex)_2(HexNAc)_3(Deoxyhexose)_2 + (Man)_3(GlcNAc)_2$
1103.4	2207.8	$(Hex)_8 + (Man)_3(GlcNAc)_2$
1111.4	2223.8	$(Hex)_2\ (HexNAc)_2\ (NeuAc)_2 + (Man)_3(GlcNAc)_2$
1119.9	2240.8	$(Hex)_3\ (HexNAc)_2\ (Deoxyhexose)_1\ (NeuAc)_1 + (Man)_3(GlcNAc)_2$
1127.5	2256	$(Hex)_2\ (HexNAc)_2\ (NeuGc)_2 + (Man)_3(GlcNAc)_2$
1148.6	2298.2	$(Hex)_2\ (HexNAc)_3\ (Deoxyhexose)_1\ (NeuGc)_1 + (Man)_3(GlcNAc)_2$
1148.6	2298.2	$(Hex)_3\ (HexNAc)_3\ (NeuAc)_1 + (Man)_3(GlcNAc)_2$
1184.4	2369.8	$(Hex)_2\ (HexNAc)_2\ (Deoxyhexose)_1\ (NeuAc)_2 + (Man)_3(GlcNAc)_2$
1200.5	2402	$(Hex)_2\ (HexNAc)_2\ (Deoxyhexose)_1\ (NeuGc)_2 + (Man)_3(GlcNAc)_2$
1280.9	2562.8	$(Hex)_2\ (HexNAc)_2\ (NeuGc)_3 + (Man)_3(GlcNAc)_2$
1309.9	2620.8	$(Hex)_3\ (HexNAc)_3\ (NeuGc)_2 + (Man)_3(GlcNAc)_2$
1463.5	2928	$(Hex)_3\ (HexNAc)_3\ (NeuGc)_3 + (Man)_3(GlcNAc)_2$
O-glycans		
	675.5	$(Hex)_1\ (HexNAc)_1\ (NeuAc)_1$
	691.3	$(Hex)_1\ (HexNAc)_1\ (NeuGc)_1$
	966.5	$(Hex)_1\ (HexNAc)_1\ (NeuAc)_2$
	982.3	$(Hex)_1\ (HexNAc)_1\ (NeuAc)_1\ (NeuGc)_1$
	998.3	$(Hex)_1\ (HexNAc)_1\ (NeuGc)_2$
681.3	1363.6	$(Hex)_2\ (HexNAc)_2\ (NeuGc)_2$

Appendix B-2: *MS/MS fragmentation of N-glycans observed only in tumour-bearing mice*

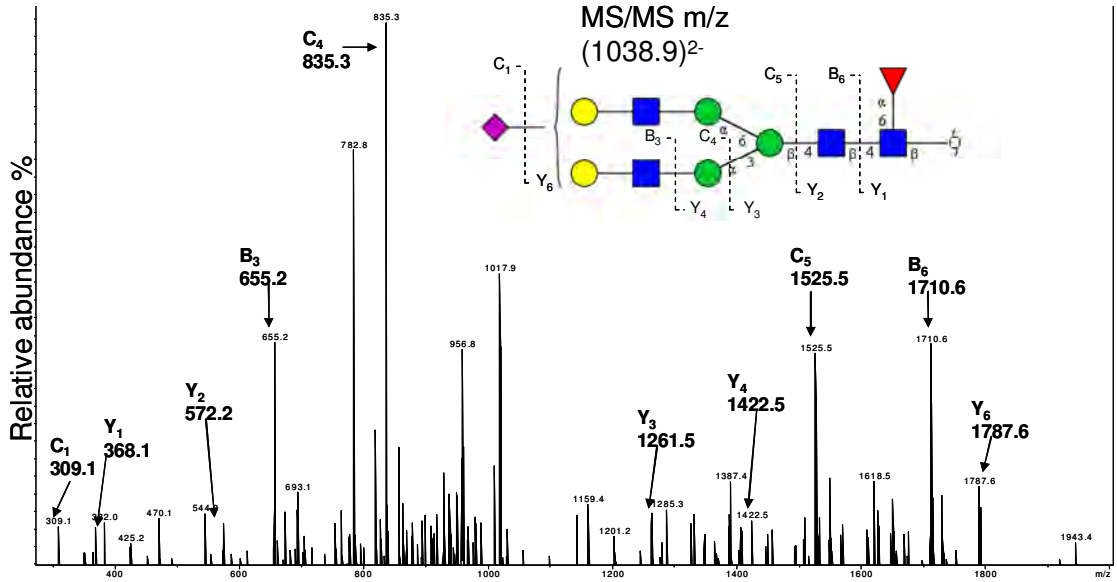

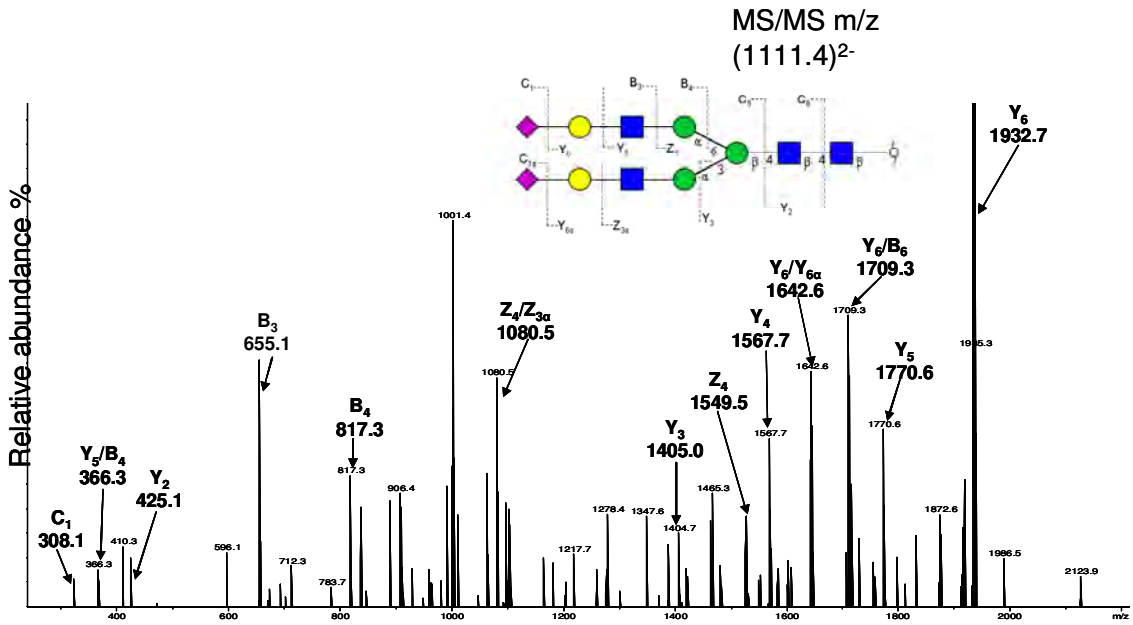

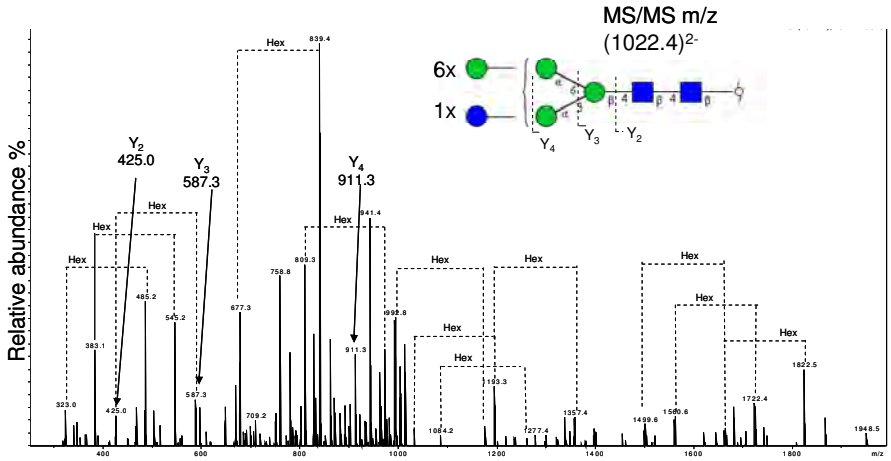
MS/MS m/z
(1022.4)2-
6x
1x
Y4
Y3
Y2
Y2
425.0
Y3
587.3
Y4
911.3
Hex
Relative abundance %
m/z

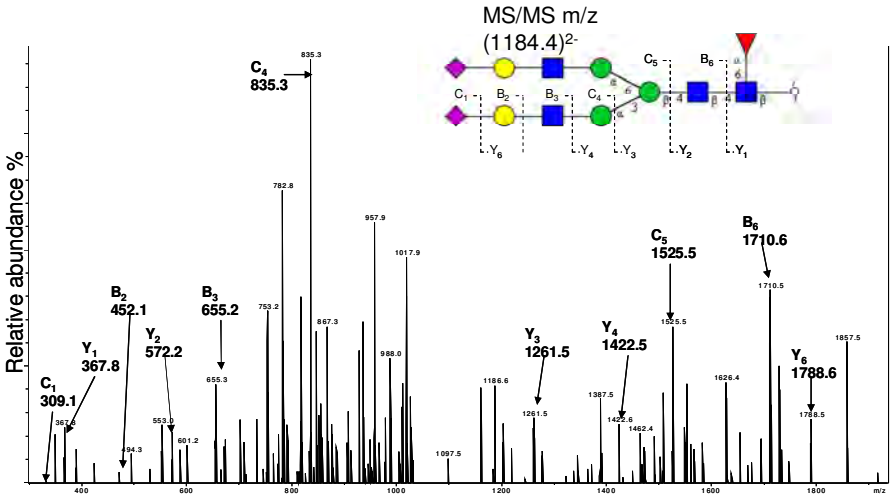
MS/MS m/z
(1184.4)2-
C4
835.3
B2
452.1
B3
655.2
Y1
367.8
Y2
572.2
C1
309.1
Y3
1261.5
Y4
1422.5
C5
1525.5
B6
1710.6
Y6
1788.6
Relative abundance %
m/z

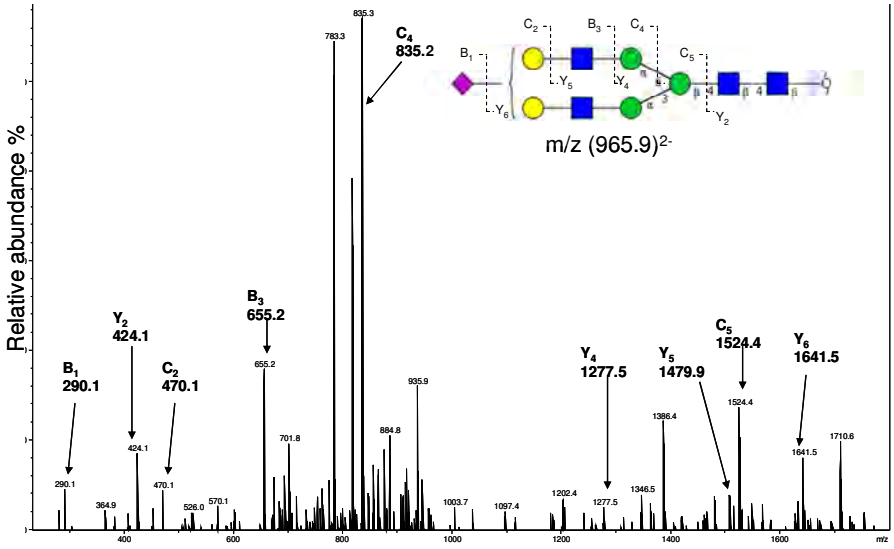
C4
835.2
m/z (965.9)2-
B3
655.2
Y2
424.1
B1
290.1
C2
470.1
Y4
1277.5
Y5
1479.9
C5
1524.4
Y6
1641.5
Relative abundance %
m/z

Appendix C: Approaches for membrane glycoprotein analysis

Appendix C-1: *Titration of detergent concentration for solubilising membrane proteins*

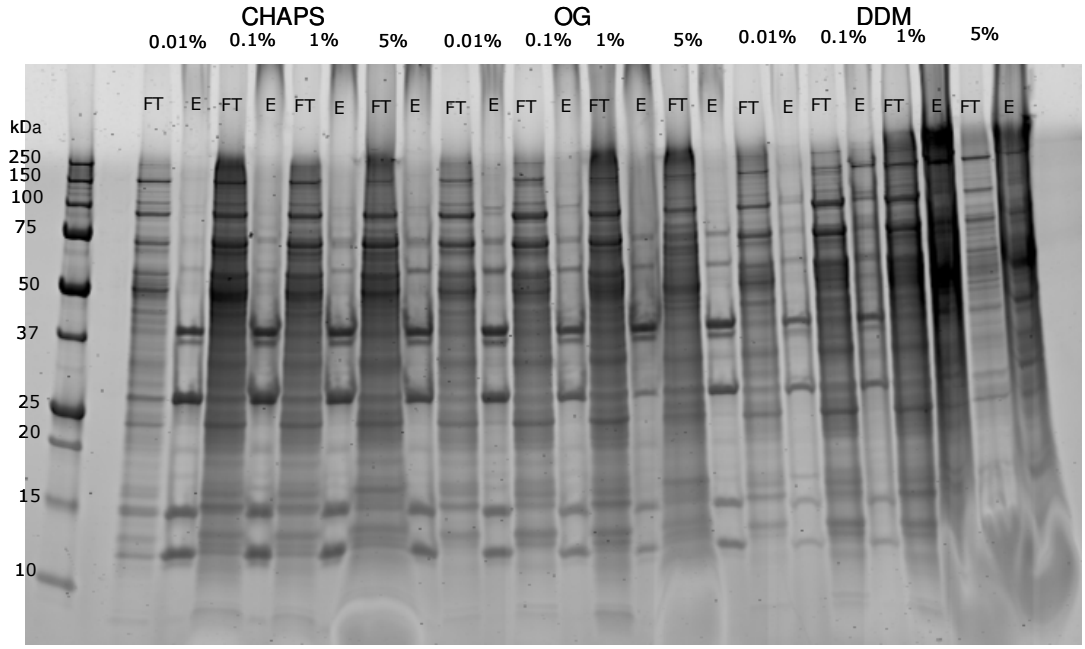

Figure C-1-1. Rat liver membrane proteins were solubilised in different concentrations (0.01% (w/v), 0.1% (w/v), 1% (w/v) and 5% (w/v)) of CHAPS, OG and DDM and subjected to ConA lectin affinity chromatography to determine the most appropriate concentration to be used for membrane solubilisation

Appendix C-2: *Amino acid analysis of solubilised rat liver membrane proteins*

AMINO ACID ANALYSIS REPORT

High Sensitivity Amino Acid Analysis – Result

Sample No: 1

Amino Acid	Amino Acid (–H_2O) (µg/ml)*	Mole %
Histidine	19.64	2.39
Arginine	52.89	5.66
Glycine	32.00	9.39
Aspartic acid	68.36	9.93
Glutamic acid	89.34	11.57
Threonine	33.96	5.61
Alanine	36.48	8.57
Proline	31.69	5.45
Lysine	59.47	7.75
Tyrosine	33.84	3.47
Methionine	19.08	2.43
Valine	42.09	7.09
Isoleucine	36.51	5.39
Leucine	71.42	10.54
Phenylalanine	41.89	4.75
Total	668.60	100.00

AMINO ACID ANALYSIS REPORT

High Sensitivity Amino Acid Analysis – Result

Sample No: 2

Amino Acid	Amino Acid (–H_2O) (µg/ml)*	Mole %
Histidine	7.63	2.25
Arginine	22.24	5.66
Glycine	15.23	10.82
Aspartic acid	27.85	9.58
Glutamic acid	35.94	10.88
Threonine	14.72	5.78
Alanine	15.35	8.75
Proline	14.95	6.15
Lysine	24.99	7.84
Tyrosine	13.93	3.41
Methionine	3.52	0.98
Valine	18.44	7.50
Isoleucine	15.09	5.40
Leucine	29.08	10.39
Phenylalanine	16.78	4.62
Total	275.71	100.00

AMINO ACID ANALYSIS REPORT

High Sensitivity Amino Acid Analysis – Result

Sample No: 3

Amino Acid	Amino Acid (–H_2O) (µg/ml)*	Mole %
Histidine	20.77	2.44
Arginine	54.69	5.64
Glycine	31.57	8.92
Aspartic acid	70.77	9.91
Glutamic acid	91.71	11.45
Threonine	35.52	5.66
Alanine	37.98	8.61
Proline	33.27	5.52
Lysine	61.42	7.72
Tyrosine	34.79	3.44
Methionine	20.15	2.47
Valine	44.25	7.19
Isoleucine	38.29	5.45
Leucine	75.14	10.70
Phenylalanine	44.52	4.87
Total	694.80	100.00

AMINO ACID ANALYSIS REPORT

High Sensitivity Amino Acid Analysis – Result

Sample No: 5

Amino Acid	Amino Acid (–H_2O) (µg/ml)*	Mole %
Histidine	5.31	2.13
Arginine	11.43	4.04
Glycine	11.41	11.05
Aspartic acid	26.16	12.55
Glutamic acid	22.41	9.58
Threonine	13.34	7.28
Alanine	12.34	9.58
Proline	9.50	5.39
Lysine	14.18	6.10
Tyrosine	8.16	2.76
Methionine	3.03	1.27
Valine	13.39	7.45
Isoleucine	11.45	5.58
Leucine	21.16	10.31
Phenylalanine	13.18	4.94
Total	196.40	100.00

AMINO ACID ANALYSIS REPORT

High Sensitivity Amino Acid Analysis – Result

Sample No: 7

Amino Acid	Amino Acid (–H_2O) (µg/ml)*	Mole %
Histidine	2.40	1.95
Arginine	5.85	4.06
Glycine	6.64	13.05
Aspartic acid	15.05	14.67
Glutamic acid	10.95	9.33
Threonine	6.96	7.64
Alanine	5.88	9.23
Proline	4.99	5.64
Lysine	5.39	4.70
Tyrosine	4.21	2.84
Methionine	0.78	0.67
Valine	6.46	7.22
Isoleucine	5.47	5.40
Leucine	9.39	9.21
Phenylalanine	5.82	4.41
Total	96.21	100.00

AMINO ACID ANALYSIS REPORT

High Sensitivity Amino Acid Analysis – Result

Sample No: 8

Amino Acid	Amino Acid (–H_2O) (µg/ml)*	Mole %
Histidine	68.69	2.56
Arginine	172.77	5.65
Glycine	101.30	9.07
Aspartic acid	213.56	9.50
Glutamic acid	271.92	10.78
Threonine	114.08	5.77
Alanine	119.11	8.57
Proline	106.35	5.60
Lysine	192.43	7.68
Tyrosine	112.11	3.51
Methionine	64.37	2.51
Valine	141.66	7.31
Isoleucine	124.23	5.61
Leucine	239.29	10.81
Phenylalanine	145.66	5.06
Total	2187.48	100.00

Figure C-2-1. Amino Acid Analysis (AAA) of rat liver membrane proteins solubilised in CHAPS, OG and DDM. AAA was performed in duplicates and protein concentrations were expressed as an average. Amino acid analysis of (1) Solubilised membrane proteins in 1 % (w/v) CHAPS (2) Solubilised membrane proteins in 1 % (w/v) OG (3) Solubilised membrane proteins in 1 % (w/v) DDM (5) Lectin bound membrane proteins in 1 % (w/v) CHAPS(7) Lectin bound membrane proteins in 1 % (w/v) OG (8) Lectin bound membrane proteins in 1 % (w/v) DDM

Appendix C-3: *2D gels of Triton X-114 phase partitioned rat liver membrane proteins*

The purpose of using 2DGE to fractionate Triton X-114 phase partitioned membrane proteins was to complement the number of protein identifications obtained from our previous study, which employed in-solution digestion with trypsin in combination with LC-ESI-MS analyses. Due to the very limited number of protein spots that were observed on these 2DGE gels using pH 3-10, pH 4-7 and pH 3-6 IPG strips, protein spots were not excised for further mass spectrometric analysis and identification. Whilst membrane proteins were poorly separated by 2DGE, it did reveal that a large proportion of membrane proteins (of those observable) are likely post-translationally modified.

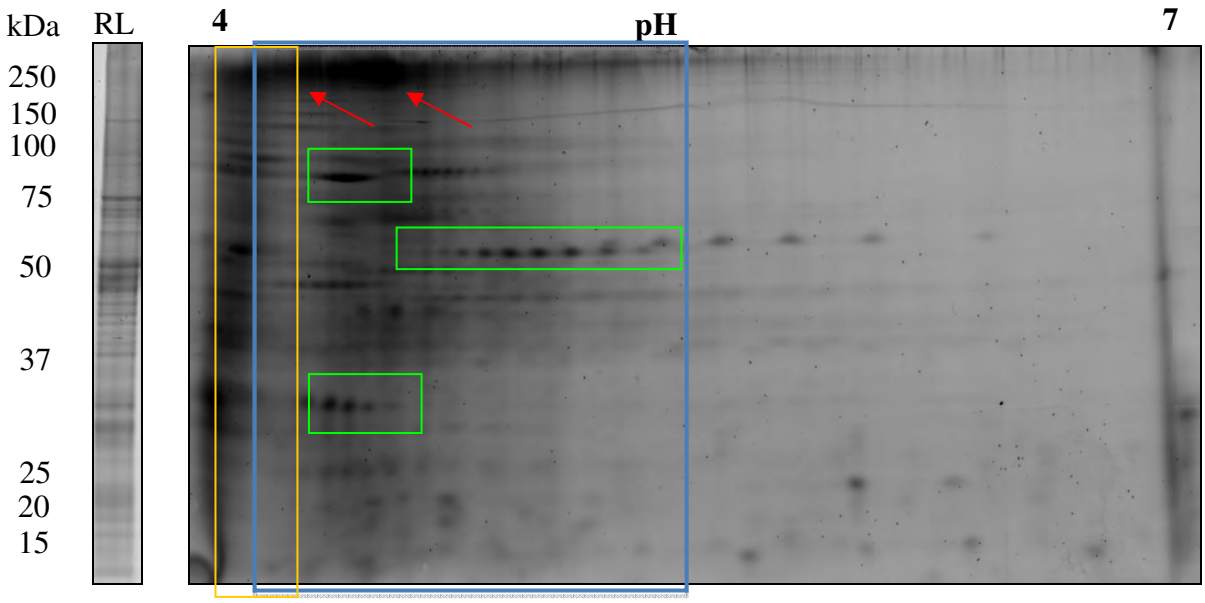

Figure C-3-1. Triton X-114 phase partitioned rat liver membrane proteins were focused on pH 4-7 IPG strips and stained with Sypro Ruby. RL: Triton X-114 phase partitioned rat liver membrane proteins. Membrane proteins that were clearly resolved in the pH range 4.5 to 5.5 (blue). Higher molecular weight were poorly solubilised and not separated by 2DGE (red). Trains of protein spots (protein isoforms) were clearly resolved on the 2DGE (green). Acidic membrane proteins were poorly resolved in regions with pH < 4.5 (yellow).

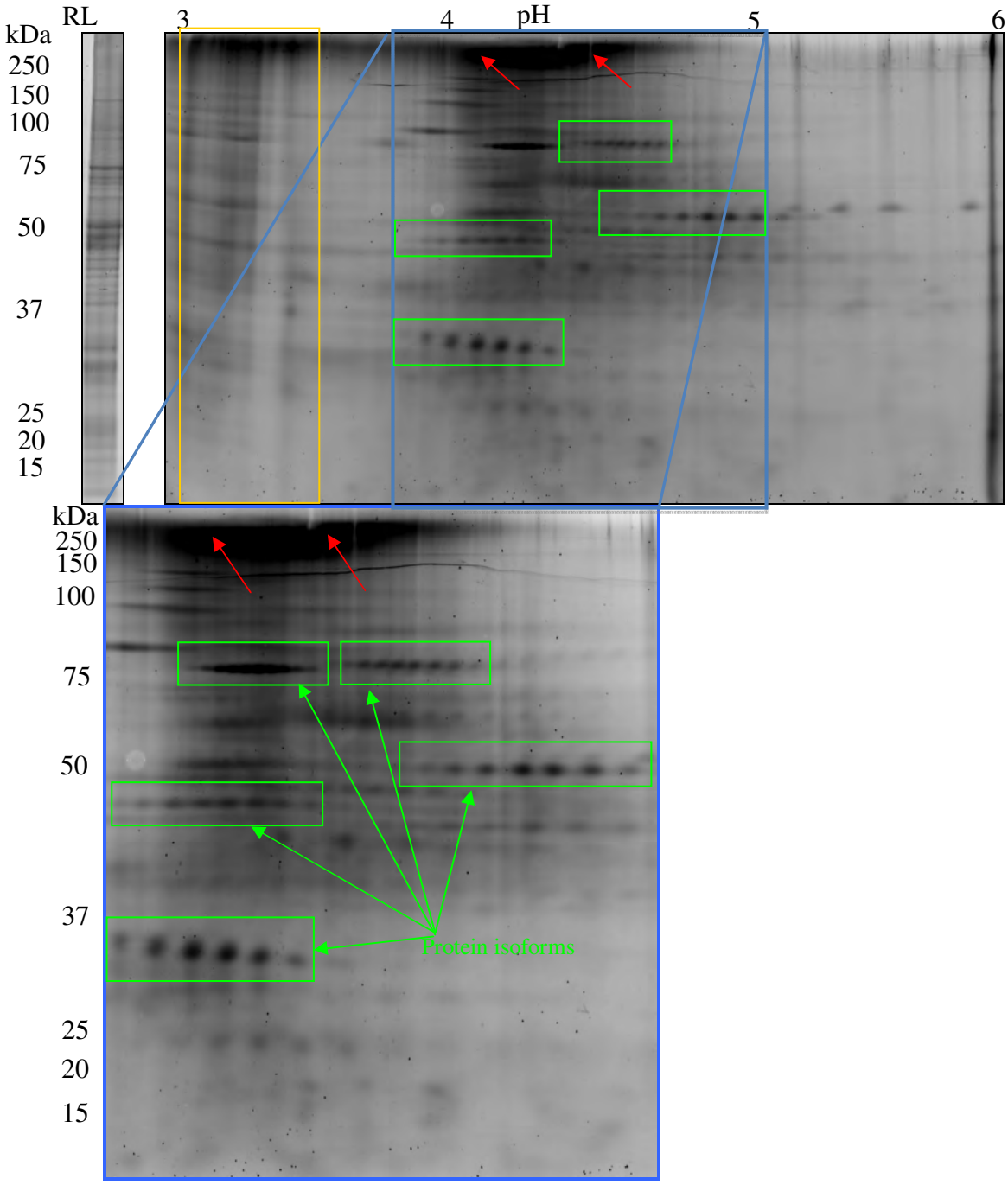

Figure C-3-2. Triton X-114 phase partitioned rat liver membrane proteins were focused on pH 3-6 IPG strips and stained with Sypro Ruby. RL: Triton X-114 phase partitioned rat liver membrane proteins. Most membrane glycoproteins that could be separated by 2DGE were localized between pH 4 and pH 5.25 (blue). Higher molecular weight were poorly solubilised and not separated by 2DGE (red). Trains of protein spots (protein isoforms) were clearly resolved on the pH 3-6 2D gel (green). Acidic membrane proteins were poorly resolved in regions with pH 3 (yellow).

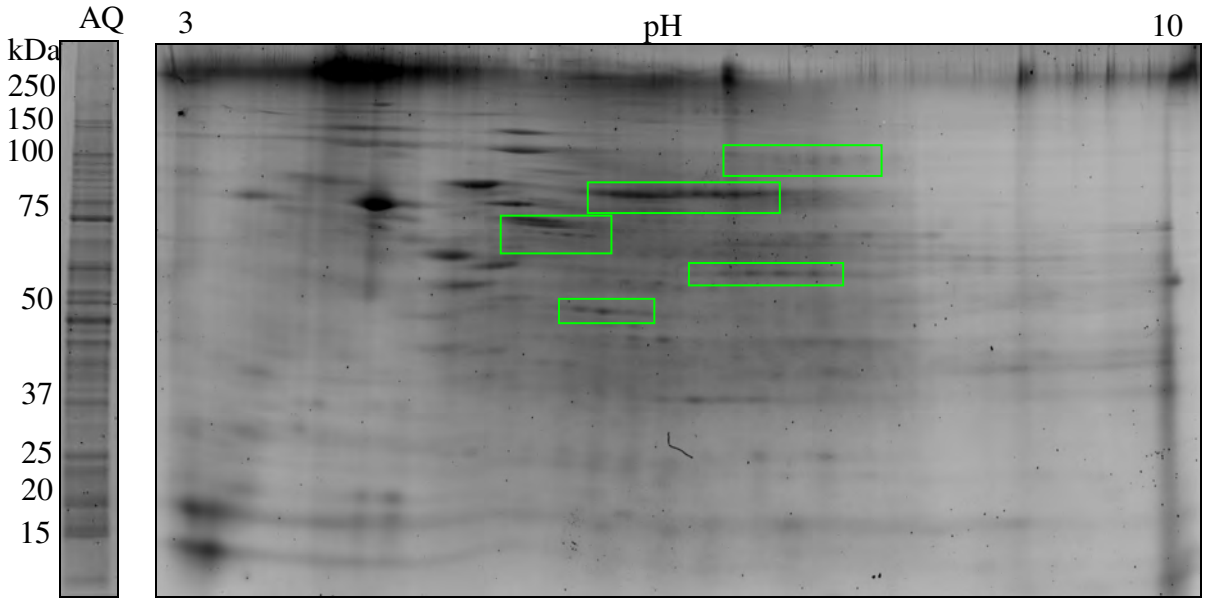

Figure C-3-3. 2DGE separation of the aqueous phase obtained from Triton X-114 phase partitioning using pH 3-10 strips and stained with Sypro Ruby. AQ: Aqueous phase proteins separated by 1D SDS PAGE. Trains of protein spots were observed in the 2DGE separated aqueous fraction (green).

Appendix C-4: *Differential isolation of rat liver membrane glycoproteins using ConA, Jacalin and WGA*

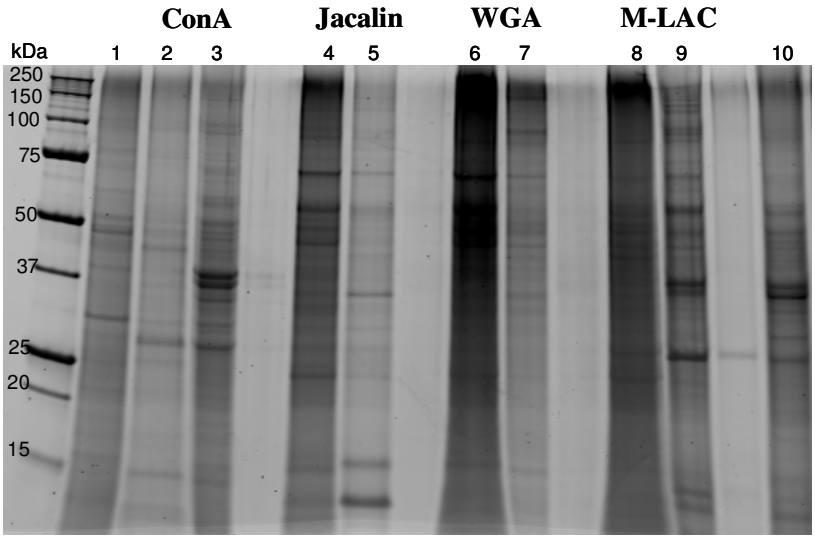

Figure C-4-1. Triton X-114 phase partitioned rat liver membrane proteins solubilised in binding buffer containing CHAPS were incubated with immobilized ConA, Jacalin and WGA lectins. Bound membrane glycoproteins were eluted using a combination of high concentrations of displacing monosaccharides (1.5 M methyl-α-glucopyranoside, 1.5 M galactose and 1.5 GlcNAc) and showed enrichment of common and unique subsets of glycoproteins. Liver membrane proteins [Lane 1], ConA FT [lane 2], ConA bound [lane 3], Jacalin FT [lane 4], Jacalin bound [lane 5], WGA FT [lane 6], WGA bound [lane 7], M-LAC FT [lane 8], M-LAC bound [lane 9] and combination of all individual bound fractions from ConA, Jacalin and WGA [lane 10]

Appendix C-5: *Enrichment of glycopeptides*

Table C-5-1. Triton X-114 phase partitioned rat liver membrane N-linked glycopeptides obtained from M-LAC enrichment.

Accession	Protein Description	Glycopeptide identified	UniProt/SwissProt No#
ENSRNOP00000000327	forkhead box O3a	fkdk197 **GDSNSSAGWK NSIR** 210hnls	RefSeq_peptide NP_001099865
ENSRNOP00000001960	Transmembrane protein 120A (Transmembrane protein induced by tumor necrosis factor alpha).	eltk43 **LQDNCTNSIT R** 53qkkr	Q5HZE2
ENSRNOP00000002366	D-beta-hydroxybutyrate dehydrogenase, mitochondrial precursor (EC 1.1.1.30) (BDH) (3-hydroxybutyrate	akgr191 **VVNISSMLGR** 200manp	P29147
ENSRNOP00000002738	CD166 antigen precursor (Activated leukocyte cell adhesion molecule) (Protein MEMD) (HB2) (SB-10 antigen) (KG-CAM).	yysk473 **IIISPEENVT LTCTAENQLE** R 493tvns	O35112
ENSRNOP00000003052	Lysosome membrane protein 2 (Lysosome membrane protein II) (LIMP II) (Scavenger receptor class B member 2) (85 kDa lysosomal membrane sialoglycoprotein) (LGP85) (CD36 antigen	lmk98 **ANVQFGENGT TISAVTNK** 115ayif	P27615
ENSRNOP00000003334	Guanine nucleotide-binding protein subunit beta-2-like 1 (Receptor of activated protein kinase C 1) (RACK1) (Receptor for activated C kinase).	scvr159 **FSPNSSNPII VSCGWDK** 175lvkv	P63245
ENSRNOP00000006359	60S ribosomal protein L19.	gkkk21 **VWLDPNETNE IANANSR** 37qqir	P84100
ENSRNOP00000007398	Myosin-9 (Myosin heavy chain 9) (Myosin heavy chain, non-muscle IIa) (Non-muscle myosin heavy chain IIa) (NMMHC II-a) (NMMHC-IIA) (Cellular myosin heavy chain, type A) (Non-muscle myosin heavy chain-A) (NMMHC- A).	leak1816 **IAQLEEQLDN ETK** 1828erqa	Q62812
ENSRNOP00000007870	Corticosteroid 11-beta-dehydrogenase isozyme 1 (EC 1.1.1.146) (11-DH) (11-beta-hydroxysteroid dehydrogenase 1)	pmlk158 **QSNGSIAIIS SMAGK** 172mtqp	P16232
ENSRNOP00000008094	No other features on this peptide	nslk144 **IVSNASCTTN CLAPLAK** 160vihd	
ENSRNOP00000008477	Voltage-dependent anion-selective channel protein 1 (VDAC-1) (rVDAC1) (Outer mitochondrial membrane protein porin 1).	fsak253 **VNNSSLIGLG YTQTLKPGIK** 272ltls	Q9Z2L0
ENSRNOP00000010383	40S ribosomal protein S6.	1 **LNISFPATGC QK** 12liev	P62755
ENSRNOP00000010932	elastin microfibril interfacer 1	lslr561 **LNLTAAQLSQ LEGLLQAR** 578gdeg	RefSeq_peptide NP_001100180
ENSRNOP00000011823	Serum paraoxonase/arylesterase 1 (EC 3.1.1.2) (EC 3.1.8.1) (PON 1) (Serum aryldialkylphosphatase 1) (A-esterase 1) (Aromatic esterase 1).	nafr33 **EVTPVDLPNC TLVK** 46giea	P55159
ENSRNOP00000011922	Teneurin-2 (Ten-2) (Tenascin-M2) (Ten-m2) (Protein Odd Oz/ten-m homolog 2) (Neurestin).	tigr2632 **KVLESGVNVT VSQPTLLVNG R** 2652trrf	Q9R1K2
ENSRNOP00000013230	Solute carrier organic anion transporter family member 1C1 (Solute carrier family 21 member 14) (Blood-brain barrier-specific anion transporter 1) (BBB-specific anion transporter	aapk535 **SGNWSGMMGR CQK** 547dngc	Q9EPZ7
ENSRNOP00000014235	Long-chain-fatty-acid--CoA ligase 1 (EC 6.2.1.3) (Long-chain acyl-CoA synthetase 1) (LACS 1) (Long-chain-fatty-acid--CoA ligase, liver isozyme).	digk545 **WLPNGTLK** 552iidr rv**nr261 TKPKPPEPED LAIIC** 275ftsg	P18163
ENSRNOP00000015947	similar to Protein C20orf129 (predicted) (RGD1311988_predicted), mRNA	peqk555 **EVNSCTTGSS NSTIIGSQGR** 574dtpk	RefSeq_dna NM_001108169
ENSRNOP00000016353	Integrin alpha-1 precursor (Laminin and collagen receptor) (VLA-1) (CD49a antigen).	pcvk77 **LDLPVNTSIP NVTEIK** 92enmt	P18614
ENSRNOP00000017339	No description available.Protein Family: MACROPHAGE SCAVENGER RECEPTOR TYPES I AND II MACROPHAGE ACETYLATED LDL RECEPTOR I AND II	qevk246 **VLNNITNDLR** 255lkdw	
ENSRNOP00000017950	TGF-beta receptor type-2 precursor (EC 2.7.11.30) (TGF-beta receptor type II) (TGFR-2) (TGF-beta type II receptor) (Transforming growth factor-beta receptor type II) (TbetaR-II).	sqek582 **IPEDGSLNTT K** 592	P38438
ENSRNOP00000018043	No description available.Protein Family: TRANSMEMBRANE 9 SUPERFAMILY MEMBER PRECURSOR	ngnr168 **IVDVNLTSEG K** 178vklv	
ENSRNOP00000018328	transglutaminase 2, C polypeptide	svlk415 **SINNSLVVGQ K** 425istk	RefSeq_peptide NP_062259
ENSRNOP00000018682	Cerebellin-2 (Cerebellin-like protein).	gsak93 **VAFSATRSTN HEPSEMSNR 111t**mti	P98087
ENSRNOP00000018850	3-ketoacyl-CoA thiolase, mitochondrial (EC 2.3.1.16) (Beta-ketothiolase) (Acetyl-CoA acyltransferase) (Mitochondrial 3-oxoacyl- CoA thiolase).	dpsk336 **TNVSGGAIAL GHPLGGSGSR** 355itah	P13437
ENSRNOP00000019021	Carbamoyl-phosphate synthase , mitochondrial precursor (EC 6.3.4.16) (Carbamoyl-phosphate synthetase I) (CPSase I).	manr317 **GQNQPVLNIT NR** 328qafi	P07756
ENSRNOP00000019162	60S ribosomal protein L35.	siar56 **VLTVINQTQK** 65enlr	P17078
ENSRNOP00000021221	similar to small nuclear ribonucleoprotein D2 (LOC680309),	qsvk38 **NNTQVLINCR** 47nnkk	Source: RefSeq_dna NM_0011093
ENSRNOP00000021514	Cytochrome b-c1 complex subunit 2, mitochondrial precursor (Ubiquinol- cytochrome-c reductase complex core protein 2) (Core protein II) (Complex III subunit 2).	nqvk359 **AVAQGNLSSA DVQAAK** 374nklk hikr301 **GNNTTSLLSQ SVAK** 314gsqq	P32551
ENSRNOP00000022150	T-cell surface glycoprotein CD1d precursor (CD1d antigen).	egtr175 **ETVQILLNDT CPQFVR** 190glle	Q63493
ENSRNOP00000023811	NADH dehydrogenase (ubiquinone) 1 alpha subcomplex, 2	gqek75 **NVSLNNLSAA EVTK** 88amen	RefSeq_peptide NP_001099623
ENSRNOP00000024707	Sideroflexin-1 (Tricarboxylate carrier protein) (TCC).	nslk144 **IVSNASCTTN CLAPLAK** 160vihd relk203 **VGIPVTDENG TR** 214lges	Q63965
ENSRNOP00000025025	LIM domain binding 1	rkrk301 **MSGGSTMSSG GGNTNNSNSK** 320kksp	RefSeq_peptide NP_001101071
ENSRNOP00000025254	Asialoglycoprotein receptor 1 (ASGPR 1) (ASGP-R 1) (Hepatic lectin 1) (RHL-1).	rvlr74 **QNFSNFTVST EDQVK** 88altt	P02706
ENSRNOP00000025446	Enoyl-CoA hydratase, mitochondrial precursor (EC 4.2.1.17) (Short chain enoyl-CoA hydratase) (SCEH) (Enoyl-CoA	kkgk44 **NSSVGLIQLN RPK** 56alna	P14604
ENSRNOP00000025655	40S ribosomal protein S14.	lrat101 **GGNRTKTPGP GAQSALR** 117alar	P13471

Table C-5-2. Triton X-114 phase partitioned rat liver membrane N-linked glycopeptides obtained from hydrazine chemistry enrichment.

Accession	Protein Description	Glycopeptide identified	UniProt/SwissProt No#
ENSRNOP00000000327	forkhead box O3a	fkdk197 **GDSNSSAGWK NSIR** 210hnls	RefSeq_peptide NP_001099865
ENSRNOP00000001960	Transmembrane protein 120A (Transmembrane protein induced by tumor necrosis factor alpha).	eltk43 **LQDNCTNSIT R** 53qkkr	Q5HZE2
ENSRNOP00000002366	D-beta-hydroxybutyrate dehydrogenase, mitochondrial precursor (EC 1.1.1.30) (BDH) (3-hydroxybutyrate	akgr191 **VVNISSMLGR** 200manp	P29147
ENSRNOP00000002738	CD166 antigen precursor (Activated leukocyte cell adhesion molecule) (Protein MEMD) (HB2) (SB-10 antigen) (KG-CAM).	yysk473 **IIISPEENVT LTCTAENQLE** R 493tvns	O35112
ENSRNOP00000003052	Lysosome membrane protein 2 (Lysosome membrane protein II) (LIMP II) (Scavenger receptor class B member 2) (85 kDa lysosomal membrane sialoglycoprotein) (LGP85) (CD36 antigen	lrnk98 **ANVQFGENGT TISAVTNK** 115ayif	P27615
ENSRNOP00000003334	Guanine nucleotide-binding protein subunit beta-2-like 1 (Receptor of activated protein kinase C 1) (RACK1) (Receptor for activated C kinase).	scvr159 **FSPNSSNPII VSCGWDK** 175lvkv	P63245
ENSRNOP00000006359	60S ribosomal protein L19.	gkkk21 **VWLDPNETNE IANANSR** 37qqir	P84100
ENSRNOP00000007398	Myosin-9 (Myosin heavy chain 9) (Myosin heavy chain, non-muscle IIa) (Non-muscle myosin heavy chain IIa) (NMMHC II-a) (NMMHC-IIA) (Cellular myosin heavy chain, type A) (Non-muscle myosin heavy chain-A) (NMMHC- A).	leak1816 **IAQLEEQLDN ETK** 1828erqa	Q62812
ENSRNOP00000007870	Corticosteroid 11-beta-dehydrogenase isozyme 1 (EC 1.1.1.146) (11-DH) (11-beta-hydroxysteroid dehydrogenase 1)	pmlk158 **QSNGSIAIIS SMAGK** 172mtqp	P16232
ENSRNOP00000008094	No other features on this peptide	nslk144 **IVSNASCTTN CLAPLAK** 160vihd	
ENSRNOP00000008477	Voltage-dependent anion-selective channel protein 1 (VDAC-1) (rVDAC1) (Outer mitochondrial membrane protein porin 1).	fsak253 **VNNSSLIGLG YTQTLKPGIK** 272ltls	Q9Z2L0
ENSRNOP00000010383	40S ribosomal protein S6.	1 **LNISFPATGC QK** 12liev	P62755
ENSRNOP00000010932	elastin microfibril interfacer 1	lslr561 **LNLTAAQLSQ LEGLLQAR** 578gdeg	RefSeq_peptide NP_001100180
ENSRNOP00000011823	Serum paraoxonase/arylesterase 1 (EC 3.1.1.2) (EC 3.1.8.1) (PON 1) (Serum aryldialkylphosphatase 1) (A-esterase 1) (Aromatic esterase 1).	nafr33 **EVTPVDLPNC TLVK** 46giea	P55159
ENSRNOP00000011922	Teneurin-2 (Ten-2) (Tenascin-M2) (Ten-m2) (Protein Odd Oz/ten-m homolog 2) (Neurestin).	tigr2632 **KVLESGVNVT VSQPTLLVNG R** 2652trrf	Q9R1K2
ENSRNOP00000013230	Solute carrier organic anion transporter family member 1C1 (Solute carrier family 21 member 14) (Blood-brain barrier-specific anion transporter 1) (BBB-specific anion transporter	aapk535 **SGNWSGMMGR CQK** 547dngc	Q9EPZ7
ENSRNOP00000014235	Long-chain-fatty-acid--CoA ligase 1 (EC 6.2.1.3) (Long-chain acyl-CoA synthetase 1) (LACS 1) (Long-chain-fatty-acid--CoA ligase, liver isozyme).	digk545 **WLPNGTLK** 552iidr rv**nr261 TKPKPPEPED LAIIC** 275ftsg	P18163
ENSRNOP00000015947	similar to Protein C20orf129 (predicted) (RGD1311988_predicted), mRNA	peqk555 **EVNSCTTGSS NSTIIGSQGR** 574dtpk	RefSeq_dna NM_001108169
ENSRNOP00000016353	Integrin alpha-1 precursor (Laminin and collagen receptor) (VLA-1) (CD49a antigen).	pcvk77 **LDLPVNTSIP NVTEIK** 92enmt	P18614
ENSRNOP00000017339	No description available.Protein Family: MACROPHAGE SCAVENGER RECEPTOR TYPES I AND II MACROPHAGE ACETYLATED LDL RECEPTOR I AND II	qevk246 **VLNNITNDLR** 255lkdw	
ENSRNOP00000017950	TGF-beta receptor type-2 precursor (EC 2.7.11.30) (TGF-beta receptor type II) (TGFR-2) (TGF-beta type II receptor) (Transforming growth factor-beta receptor type II) (TbetaR-II).	sqek582 **IPEDGSLNTT K** 592	P38438
ENSRNOP00000018043	No description available.Protein Family: TRANSMEMBRANE 9 SUPERFAMILY MEMBER PRECURSOR	ngnr168 **IVDVNLTSEG K** 178vklv	
ENSRNOP00000018328	transglutaminase 2, C polypeptide	svlk415 **SINNSLVVGQ K** 425istk	RefSeq_peptide NP_062259
ENSRNOP00000018682	Cerebellin-2 (Cerebellin-like protein).	gsak93 **VAFSATRSTN HEPSEMSNR 111t**mti	P98087
ENSRNOP00000018850	3-ketoacyl-CoA thiolase, mitochondrial (EC 2.3.1.16) (Beta-ketothiolase) (Acetyl-CoA acyltransferase) (Mitochondrial 3-oxoacyl- CoA thiolase).	dpsk336 **TNVSGGAIAL GHPLGGSGSR** 355itah	P13437
ENSRNOP00000019021	Carbamoyl-phosphate synthase , mitochondrial precursor (EC 6.3.4.16) (Carbamoyl-phosphate synthetase I) (CPSase I).	manr317 **GQNQPVLNIT NR** 328qafi	P07756
ENSRNOP00000019162	60S ribosomal protein L35.	siar56 **VLTVINQTQK** 65enlr	P17078
ENSRNOP00000021221	similar to small nuclear ribonucleoprotein D2 (LOC680309),	qsvk38 **NNTQVLINCR** 47nnkk	Source: RefSeq_dna NM_0011093
ENSRNOP00000021514	Cytochrome b-c1 complex subunit 2, mitochondrial precursor (Ubiquinol- cytochrome-c reductase complex core protein 2) (Core protein II) (Complex III subunit 2).	nqvk359 **AVAQGNLSSA DVQAAK** 374nklk hikr301 **GNNTTSLLSQ SVAK** 314gsqq	P32551
ENSRNOP00000022150	T-cell surface glycoprotein CD1d precursor (CD1d antigen).	egtr175 **ETVQILLNDT CPQFVR** 190glle	Q63493
ENSRNOP00000023811	NADH dehydrogenase (ubiquinone) 1 alpha subcomplex, 2	gqek75 **NVSLNNLSAA EVTK** 88amen	RefSeq_peptide NP_001099623
ENSRNOP00000024707	Sideroflexin-1 (Tricarboxylate carrier protein) (TCC).	nslk144 **IVSNASCTTN CLAPLAK** 160vihd relk203 **VGIPVTDENG TR** 214lges	Q63965
ENSRNOP00000025025	LIM domain binding 1	rkrk301 **MSGGSTMSSG GGNTNNSNSK** 320kksp	RefSeq_peptide NP_001101071
ENSRNOP00000025254	Asialoglycoprotein receptor 1 (ASGPR 1) (ASGP-R 1) (Hepatic lectin 1) (RHL-1).	rvlr74 **QNFSNFTVST EDQVK** 88altt	P02706
ENSRNOP00000025446	Enoyl-CoA hydratase, mitochondrial precursor (EC 4.2.1.17) (Short chain enoyl-CoA hydratase) (SCEH) (Enoyl-CoA	kkgk44 **NSSVGLIQLN RPK** 56alna	P14604
ENSRNOP00000025655	40S ribosomal protein S14.	lrat101 **GGNRTKTPGP GAQSALR** 117alar	P13471

Table C-5-3. Triton X-114 phase partitioned rat liver membrane N-linked glycopeptides obtained from HILIC enrichment.

Accession No	Protein description	Glycopeptides	UniProt/SwissProt No
ENSRNOP00000002067	No description available.Protein Family: MITOGEN ACTIVATED KINASE	kyyr683 GSVSL**NSS**PK 692gryg	
ENSRNOP00000042159	No description available.Protein Family: UNKNOWN	qhgk26 VEIIANDQG**N R** 36ttps	
ENSRNOP00000015365	Filamin-A-interacting protein 1 (FILIP).	kgmk1021 AGKPVVAASG AG**NLT**K 1036fqpr	Q8K4T4
ENSRNOP00000049709	No other features on this peptide	ktgr64 VC**NVT**QHAVG IIVNK 78qvkg	
ENSRNOP00000011275	Basigin precursor (OX-47 antigen) (Glycoprotein CE9) (CD147 antigen).	ltcf159 L**NSS**GIDIVG HR 170wmrg	P26453
ENSRNOP00000011275	Basigin precursor (OX-47 antigen) (Glycoprotein CE9) (CD147 antigen).	vwfk259 TSDTGDQTIS **NGT**EANSK 276yvii	P26453
ENSRNOP00000034321	Low affinity immunoglobulin gamma Fc region receptor II precursor (Fc- gamma RII) (FcRII) (IgG Fc receptor II beta) (CD32 antigen).	ytfk110 ATV**NDS**GEYR 119crme	Q63203
ENSRNOP00000018850	3-ketoacyl-CoA thiolase, mitochondrial (EC 2.3.1.16) (Beta-ketothiolase) (Acetyl-CoA acyltransferase) (Mitochondrial 3-oxoacyl- CoA thiolase).	dpsk336 T**NVS**GGAIAL GHPLGGSGSR 355itah	P13437
ENSRNOP00000019021	Carbamoyl-phosphate synthase , mitochondrial precursor (EC 6.3.4.16) (Carbamoyl-phosphate synthetase I) (CPSase I).	manr317 GQNQPVL**NIT** NR 328qafi	P07756
ENSRNOP00000041174	Cytochrome P450 2D1 (EC 1.14.14.1) (CYPIID1) (P450-DB1) (P450-CMF1A) (P450-UT-7) (Debrisoquine 4-hydroxylase).	fmal254 LDNLLAE**NR** 262ttwd	P10633
ENSRNOP00000041174	Cytochrome P450 2D1 (EC 1.14.14.1) (CYPIID1) (P450-DB1) (P450-CMF1A) (P450-UT-7) (Debrisoquine 4-hydroxylase).	qppr273 **NLT**DAFLAEV EK 284akgn	P10633
ENSRNOP00000013262	Electron transfer flavoprotein-ubiquinone oxidoreductase, mitochondrial precursor (EC 1.5.5.1) (ETF-QO) (ETF-ubiquinone oxidoreductase) (ETF dehydrogenase) (Electron-transferring- flavoprotein dehydrogenase).	pvnr548 **NLS**IYDGPEQ R 558fcpa	Q6UPE1
ENSRNOP00000021514	Cytochrome b-c1 complex subunit 2, mitochondrial precursor (Ubiquinol- cytochrome-c reductase complex core protein 2) (Core protein II) (Complex III subunit 2).	nqvk359 AVAQG**NLS**SA DVQAAK 374nklk	P32551
ENSRNOP00000042159	No description available.Protein Family: UNKNOWN	qhgk26 VEIIANDQG**N R** 36ttps	
ENSRNOP00000032635	60S ribosomal protein L9.	[mk3 TILS**NQT**VDI PENVDITLK 21grtv	P17077
ENSRNOP00000028237	Cytochrome P450 2A1 (EC 1.14.14.1) (CYPIIA1) (Steroid hormones 7- alpha-hydroxylase) (Testosterone 7-alpha-hydroxylase) (P450-UT-F).	ekvr253 Q**NHS**TLDPNS PR 264nfid	P11711
ENSRNOP00000045650	Sodium/potassium-transporting ATPase subunit alpha-1 precursor (EC 3.6.3.9) (Sodium pump subunit alpha-1) (Na(+)/K(+) ATPase alpha-1 subunit).	aiak361 GVGIISEG**NE T**VEDIAAR 378lnip	Q8VDN2
ENSRNOP00000006359	60S ribosomal protein L19.	gkkk21 VWLDP**NET**NE IANANSR 37qqir	P84100
ENSRNOP00000024707	Sideroflexin-1 (Tricarboxylate carrier protein) (TCC).	relk203 VGIPVTDE**NG T**R 214lges	Q63965
ENSRNOP00000025446	Enoyl-CoA hydratase, mitochondrial precursor (EC 4.2.1.17) (Short chain enoyl-CoA hydratase) (SCEH) (Enoyl-CoA hydratase 1).	kkgk44 **NSS**VGLIQLN RPK 56alna	P14604
ENSRNOP00000025351	glyceraldehyde-3-phosphate dehydrogenase (Gapdh),	mafr186 VPTP**NVS**VVD LTCR 199lekp	RefSeq_dna NM_017008
ENSRNOP00000011230	Catalase (EC 1.11.1.6).	kavk481 **NFT**DVHPDYG AR 492vqal	P04762
ENSRNOP00000026122	Hydroxymethylglutaryl-CoA synthase, mitochondrial precursor (EC 2.3.3.10) (HMG-CoA synthase) (3-hydroxy-3-methylglutaryl coenzyme A synthase).	fyhk442 V**NFS**PPGDTS NLFPGTWYLE R 462vde	P22791
ENSRNOP00000012255	No other features on this peptide	mvvr12 **NCS**SFLIK 19rnkq	
ENSRNOP00000004228	succinate dehydrogenase complex, subunit C	fwnk45 **NTS**SNRPVSP HLTIYR 60wslp	RefSeq_peptide NP_0010
ENSRNOP00000039607	coronin, actin binding protein 1C	dflk886 SACYTPTPSS ISS**NLT**R 902ssss	RefSeq_peptide NP_0011
ENSRNOP00000045344	ribosomal protein L27a (predicted) (Rpl27a_predicted)	hlkr68 **NQS**FCPTVNL DK 79lwtl	RefSeq_dna NM_0011062
ENSRNOP00000046281	No description available.Protein Family: 60S RIBOSOMAL L35	siar57 VLTVI**NQT**QK 66enlr	
ENSRNOP00000039099	60S ribosomal protein L35a.	ykak55 **NNT**VTPGGKP NK 66trvi	P04646
ENSRNOP00000046448	No description available.Protein Family: HEAT SHOCK	qimk396 AQVLRD**NST**M GYMMAK 411kqle	
ENSRNOP00000003020	Starch-binding domain-containing protein 1 (Genethonin-1).	sesk91 DLG**NLT**EAQR 100lqnv	Q5FVN1
ENSRNOP00000018460	No description available.Protein Family: GAMMA TUBULIN COMPLEX COMPONENT 4	vaek276 ILFVGESVQM FENQNV**NL**TR 295kgsi	
ENSRNOP00000013789	Glutamate dehydrogenase 1, mitochondrial precursor (EC 1.4.1.3) (GDH) (Memory-related protein 2) (MRG-2).	inpk192 **NYT**DNELEK 200itrr	P10860
ENSRNOP00000044696	Cytochrome b-c1 complex subunit 1, mitochondrial precursor (Ubiquinol- cytochrome-c reductase complex core protein 1) (Core protein I) (Complex III subunit 1).	dlpk143 VVELLADIVQ **NIS**LEDSQIE K 163erdv	Q68FY0
ENSRNOP00000025351	glyceraldehyde-3-phosphate dehydrogenase (Gapdh),	nslk97 IVS**NAS**CTTN CLAPLAK 113vihd	RefSeq_dna NM_017008
ENSRNOP00000055369	Cytochrome P450 1A2 (EC 1.14.14.1) (CYPIA2) (P450-P2/P450-P3).	sskd225 FVE**NVT**SGNA VDFFPVLR 242ylpn	P00186
ENSRNOP00000051846	solute carrier family 25 (mitochondrial carrier; dicarboxylate transporter), member 10	sqrr139 **NYS**HALDGLY R 149vare	RefSeq_peptide NP_5969
ENSRNOP00000000627	splicing factor, arginine/serine-rich 3 (SRp20)	ldck12 VYVGNLGNNG **NK** 23tele	RefSeq_peptide NP_0010

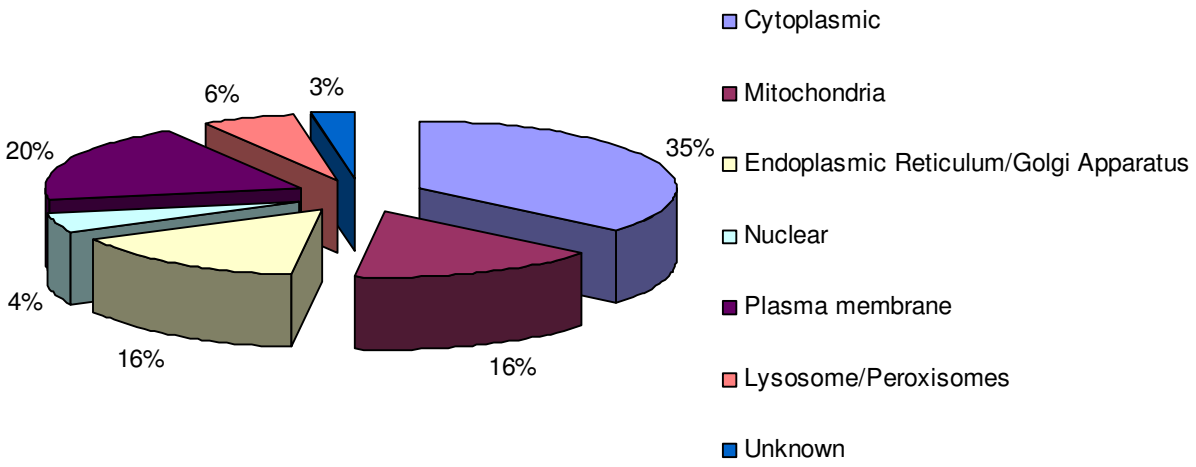

Figure C-5-1. Subcellular location annotated by gene ontology, of all identified membrane proteins enriched using a 'peptide-centric' approach employing M-LAC, hydrazine chemistry and HILIC. Approximately 35% of the membrane protein identifications were annotated by GO to be cytoplasmic/peripheral membrane proteins and 20% of identifications were determined to be localized to the plasma membrane.

Appendix D: Effects of a distal C26 adenocarcinoma on the liver membrane glycoproteome of non-cachectic and cachectic mice.

Appendix D-1: *Subcellular Localisation of proteins in control, non-cachectic and cachectic mouse liver membranes.*

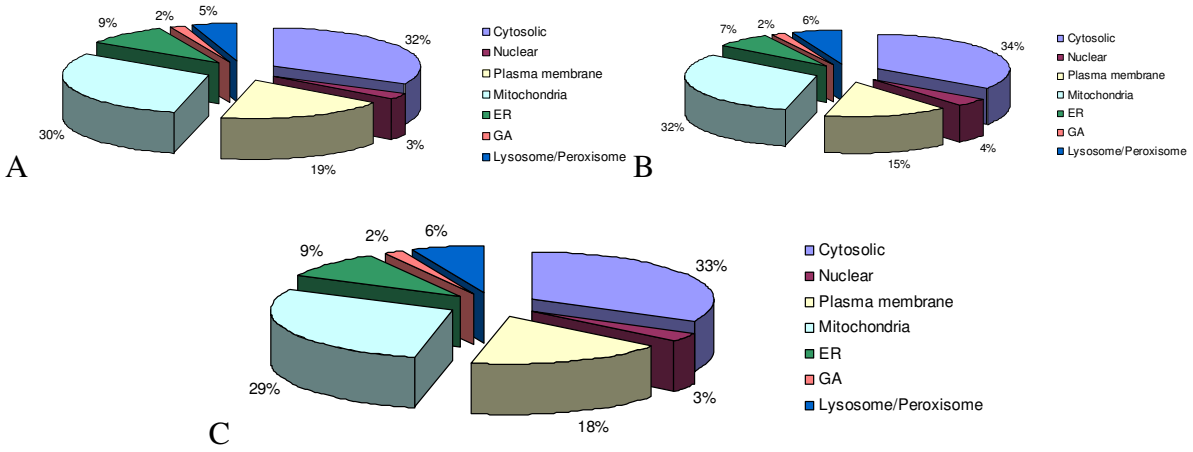

Figure D-1-1. Subcellular Location of identified proteins from control (A) non-cachectic (B) and cachectic (C) shows very little differences

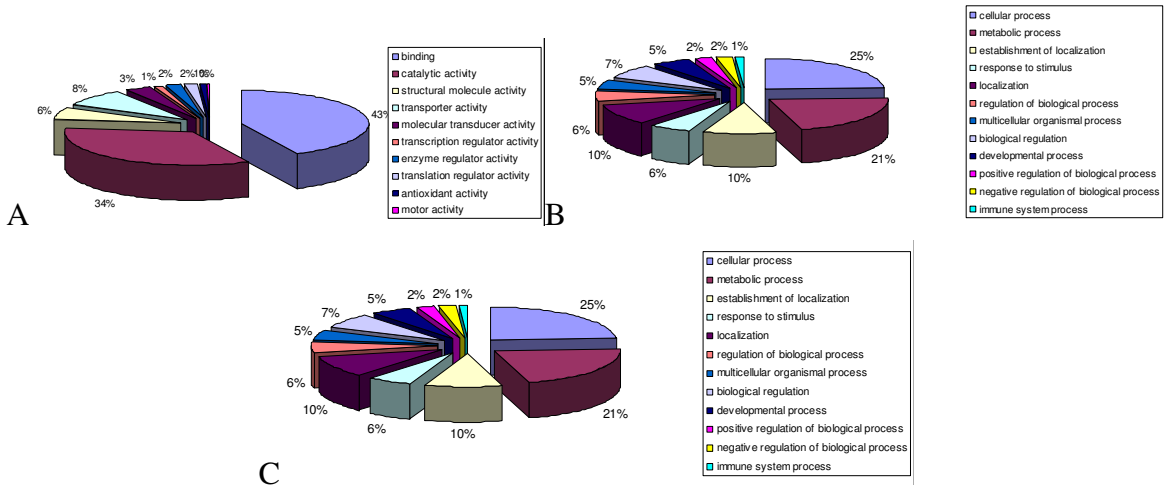

Figure D-1-2. Distribution of proteins involved in various molecular functions (A) and biological processes (B) also shows no distinct differences between control, non-cachectic and cachectic mice.

Appendix D-2: *Fatty acid oxidation and metabolism in cachectic mice*

The process of fatty acid metabolism requires the breakdown and oxidation of long chains of fatty acids into acetyl-coA. The process of fatty acid oxidation is initiated by the dehydrogenation of long chain fatty acids by acyl-coA dehydrogenase. This is followed by hydration by enoyl-coA hydratase and further dehydrogenation by hydroxyl-coA dehydrogenase. Each cycle removes two carbons off the fatty acid carbon chain and the oxidation cycle continues until the fatty acid chain has been completely oxidised yielding both acetyl-coA and propionyl-CoA (Figure D-2-1). Excess acetyl-coA is often converted to ketone bodies by ketogenesis, which can then be transported from the liver to other tissues such as the heart and brain for further energy consumption.

Label-free quantitation determined that many membrane-associated enzymes involved in fatty acid oxidation were upregulated in abundance in the liver of cachectic mice. These enzymes included: very long acyl-coA dehydrogenase (1.65±0.48 fold change), acyl-coA synthetase (18.89±2.32 fold change), enoyl-coA hydratase (11.62±2.25 fold change), hydroxyacyl-coA dehydrogenase (2.61±0.77 fold change), acetyl-coA acetyltransferase (1.86±0.86 fold change), 2,4 dienoyl-coA reductase (1.28±0.5 fold change) and short chain enoyl-coA hydratase (4.97±2.57 fold change) (Figure D-2-2). The elevated expression of fatty acid metabolic enzymes in the livers of cachectic mice serves as a good control that is indicative of cachexia [17].

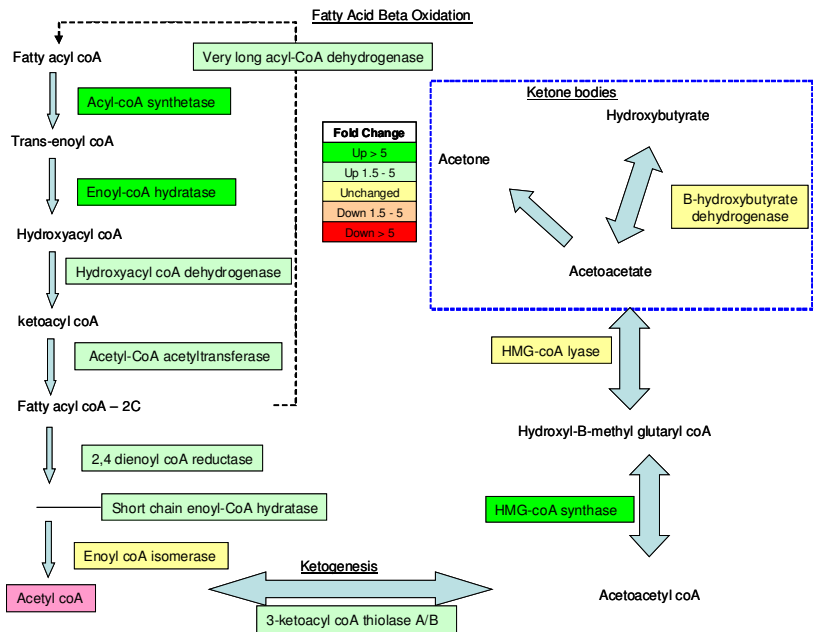

Figure D-2-1. Summary flow diagram of identified proteins involved in fatty acid oxidation and ketogenesis

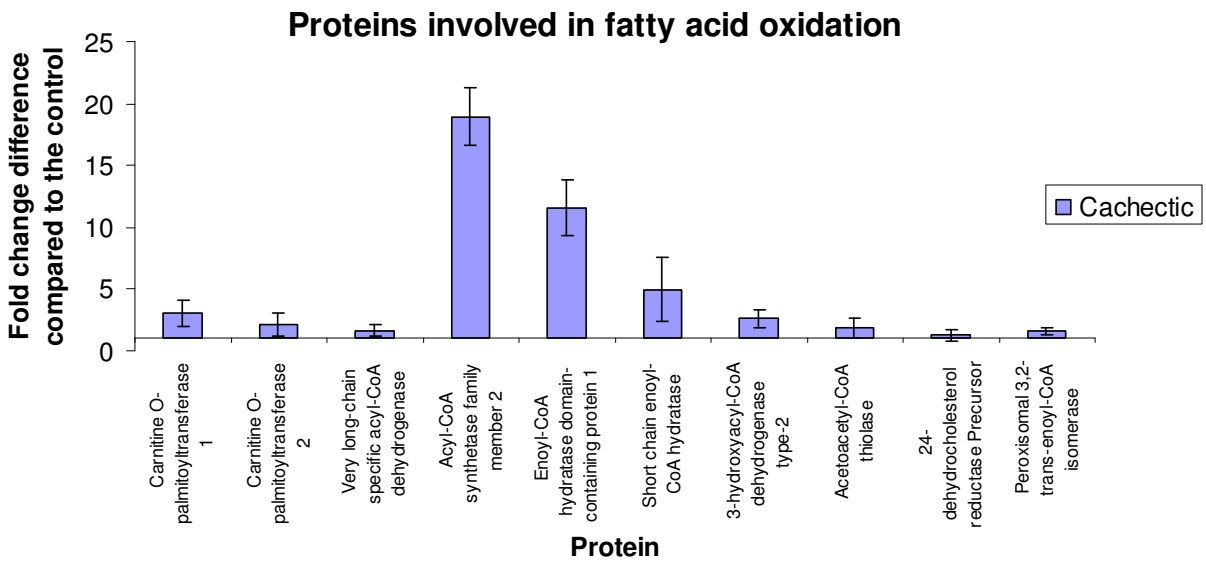

Figure D-2-2. Proteins identified to be involved in fatty acid oxidation and metabolism in the liver of cachectic mice.

Excess acetyl-coA can be converted to ketone bodies by ketogenesis, which can be transported and used for energy in the brain, heart and/or skeletal muscles. Enzymes responsible for producing ketone bodies including: 3-ketoacyl-coA thiolase A (3.09±0.53 fold change) and B (1.32±0.28 fold change) and HMG-coA synthase (9.86±3.85 fold change) were determined to be upregulated in the liver of cachectic mice (Figure D-2-3). Interestingly, HMG-coA synthase was determined to be upregulated by > 5 fold and it is the enzyme

responsible for converting acetyl-coA to acetoacetyl-coA to form 3-hydroxy-3-methylglutaryl-coA (HMG-coA), which is the starting substrate for producing ketone bodies.

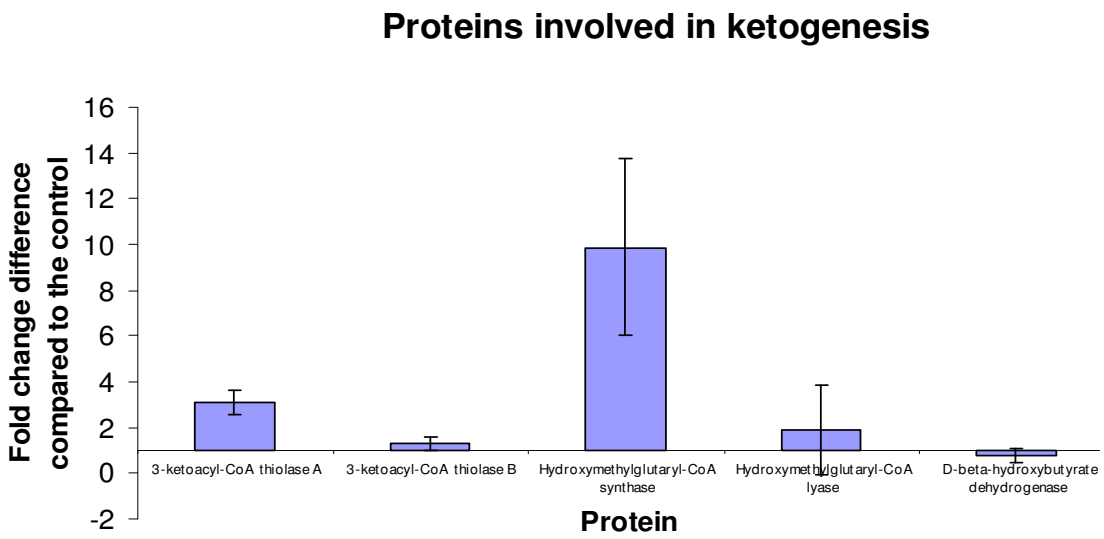

Figure D-2-3 Proteins identified to be involved in ketogenesis in the formation of ketone bodies.

The tumour itself deprives the host of available glucose that is either extracted from food or the glycogen storages in the liver. Other tissues including the liver have to rely mainly on the aerobic oxidation of fatty acids to acetyl-coA for energy. Lipid metabolism in the liver is a complex process involving the synthesis of very low density lipoproteins (VLDL), ketone bodies, as well as fatty acid oxidation. The enzymes responsible for fatty acid oxidation and metabolism were determined to be elevated in the liver of cachectic mice and this is a common feature among cachectic cancer patients [357]. These enzymes function by oxidizing the long hydrocarbon chains of fatty acids to produce acetyl-coA, which can be subsequently used for metabolism via the Krebs cycle or the fatty acids can be converted to ketone bodies and transported to other tissues such as the heart and/or the brain for further metabolism. It was not surprising that many of the enzymes involved in fatty acid oxidation processes had elevated expression in the liver of cachectic mice, and this outcome is often reflected in many patients with advanced stages of cancer cachexia.

References

1. Srivastava, S., M. Verma, and D.E. Henson, Biomarkers for early detection of colon cancer. *Clin Cancer Res*, 2001. **7**(5): p. 1118-26.
2. Srinivas, P.R., S. Srivastava, S. Hanash, and G.L. Wright, Jr., Proteomics in early detection of cancer. *Clin Chem*, 2001. **47**(10): p. 1901-11.
3. Mitchell, R.M., E.J. Neafsey, and M.A. Collins, Essential involvement of the NMDA receptor in ethanol preconditioning-dependent neuroprotection from amyloid-betain vitro. *J Neurochem*, 2009. **111**(2): p. 580-8.
4. Doranz, B.J., J.F. Berson, J. Rucker, and R.W. Doms, Chemokine receptors as fusion cofactors for human immunodeficiency virus type 1 (HIV-1). *Immunol Res*, 1997. **16**(1): p. 15-28.
5. Qoronfleh, M.W., B. Benton, R. Ignacio, and B. Kaboord, Selective Enrichment of Membrane Proteins by Partition Phase Separation for Proteomic Studies. *J Biomed Biotechnol*, 2003. **2003**(4): p. 249-255.
6. Hopkins, A.L. and C.R. Groom, The druggable genome. *Nat Rev Drug Discov*, 2002. **1**(9): p. 727-30.
7. Washburn, M.P., D. Wolters, and J.R. Yates, 3rd, Large-scale analysis of the yeast proteome by multidimensional protein identification technology. *Nat Biotechnol*, 2001. **19**(3): p. 242-7.
8. Chick, J.M., P.A. Haynes, M.P. Molloy, B. Bjellqvist, M.S. Baker, and A.C. Len, Characterization of the rat liver membrane proteome using peptide immobilized pH gradient isoelectric focusing. *J Proteome Res*, 2008. **7**(3): p. 1036-45.
9. Rabilloud, T., Membrane proteins ride shotgun. *Nat Biotechnol*, 2003. **21**(5): p. 508-10.
10. Mackiewicz, A. and K. Mackiewicz, Glycoforms of serum alpha 1-acid glycoprotein as markers of inflammation and cancer. *Glycoconj J*, 1995. **12**(3): p. 241-7.
11. Lin, S.Y., Y.Y. Chen, Y.Y. Fan, C.W. Lin, S.T. Chen, A.H. Wang, and K.H. Khoo, Precise mapping of increased sialylation pattern and the expression of acute phase proteins accompanying murine tumor progression in BALB/c mouse by integrated sera proteomics and glycomics. *J Proteome Res*, 2008. **7**(8): p. 3293-303.
12. Yasukawa, Z., C. Sato, and K. Kitajima, Inflammation-dependent changes in alpha2,3-, alpha2,6-, and alpha2,8-sialic acid glycotopes on serum glycoproteins in mice. *Glycobiology*, 2005. **15**(9): p. 827-37.
13. Chavan, M.M., P.D. Kawle, and N.G. Mehta, Increased sialylation and defucosylation of plasma proteins are early events in the acute phase response. *Glycobiology*, 2005. **15**(9): p. 838-48.
14. Kacevska, M., G.R. Robertson, S.J. Clarke, and C. Liddle, Inflammation and CYP3A4-mediated drug metabolism in advanced cancer: impact and implications for chemotherapeutic drug dosing. *Expert Opin Drug Metab Toxicol*, 2008. **4**(2): p. 137-49.
15. Morgan, E.T., K.B. Goralski, M. Piquette-Miller, K.W. Renton, G.R. Robertson, M.R. Chaluvadi, K.A. Charles, S.J. Clarke, M. Kacevska, C. Liddle, T.A. Richardson, R. Sharma, and C.J. Sinal, Regulation of drug-metabolizing enzymes and transporters in infection, inflammation, and cancer. *Drug Metab Dispos*, 2008. **36**(2): p. 205-16.
16. Michael, M., M. Thompson, R.J. Hicks, P.L. Mitchell, A. Ellis, A.D. Milner, J. Di Iulio, A.M. Scott, V. Gurtler, J.M. Hoskins, S.J. Clarke, N.C. Tebbut, K. Foo, M. Jefford, and J.R. Zalcberg, Relationship of hepatic functional imaging to irinotecan pharmacokinetics and genetic parameters of drug elimination. *J Clin Oncol*, 2006. **24**(26): p. 4228-35.
17. Tisdale, M.J., Mechanisms of cancer cachexia. *Physiol Rev*, 2009. **89**(2): p. 381-410.
18. Tanaka, Y., H. Eda, T. Tanaka, T. Udagawa, T. Ishikawa, I. Horii, H. Ishitsuka, T. Kataoka, and T. Taguchi, Experimental cancer cachexia induced by transplantable colon 26 adenocarcinoma in mice. *Cancer Res*, 1990. **50**(8): p. 2290-5.

19. Varki, A., *et al*., *Essentials in Glycobiology*, ed. C.S.H.L. Press. 1999.
20. Singer, S.J. and G.L. Nicolson, The fluid mosaic model of the structure of cell membranes. *Science*, 1972. **175**(23): p. 720-31.
21. Garret, R.H. and C.M. Grisham, *Biochemistry: 2nd Edition*. Vol. 9. 1999: Brooks/Cole-Thomson Learning Inc. 292-293.
22. Alberts, B., A. Johnson, J. Lewis, M. Raff, K. Roberts, and P. Walter, *Molecular biology of the cell*. Vol. 4th edition. 2002: Garland Science. 583-614.
23. Simons, K. and W.L. Vaz, Model systems, lipid rafts, and cell membranes. *Annu Rev Biophys Biomol Struct*, 2004. **33**: p. 269-95.
24. Singer, S.J. and G.L. Nicolson, The structure and chemistry of mammalian cell membranes. *Am J Pathol*, 1971. **65**(2): p. 427-37.
25. Thompson, T.E. and T.W. Tillack, Organization of glycosphingolipids in bilayers and plasma membranes of mammalian cells. *Annu Rev Biophys Biophys Chem*, 1985. **14**: p. 361-86.
26. Brown, D.A. and J.K. Rose, Sorting of GPI-anchored proteins to glycolipid-enriched membrane subdomains during transport to the apical cell surface. *Cell*, 1992. **68**(3): p. 533-44.
27. Lim, K.I. and J. Yin, Localization of receptors in lipid rafts can inhibit signal transduction. *Biotechnol Bioeng*, 2005. **90**(6): p. 694-702.
28. Simons, K. and E. Ikonen, Functional rafts in cell membranes. *Nature*, 1997. **387**(6633): p. 569-72.
29. Brown, D.A. and E. London, Structure and function of sphingolipid- and cholesterol-rich membrane rafts. *J Biol Chem*, 2000. **275**(23): p. 17221-4.
30. Rothberg, K.G., J.E. Heuser, W.C. Donzell, Y.S. Ying, J.R. Glenney, and R.G. Anderson, Caveolin, a protein component of caveolae membrane coats. *Cell*, 1992. **68**(4): p. 673-82.
31. Foster, L.J., C.L. De Hoog, and M. Mann, Unbiased quantitative proteomics of lipid rafts reveals high specificity for signaling factors. *Proc Natl Acad Sci U S A*, 2003. **100**(10): p. 5813-8.
32. von Haller, P.D., S. Donohoe, D.R. Goodlett, R. Aebersold, and J.D. Watts, Mass spectrometric characterization of proteins extracted from Jurkat T cell detergent-resistant membrane domains. *Proteomics*, 2001. **1**(8): p. 1010-21.
33. Julicher, F. and M. Zapotocky. *Signal transduction in olfactory cilium: stochastic dynamics of ion channels*. [Website] 2005 [cited 14th September 2006]; Available from: http://www.mri.ernet.in/~manoj/res.html.
34. Wallin, E. and G. von Heijne, Genome-wide analysis of integral membrane proteins from eubacterial, archaean, and eukaryotic organisms. *Protein Sci*, 1998. **7**(4): p. 1029-38.
35. Dennehy, K.M., A. Kerstan, A. Bischof, J.H. Park, S.Y. Na, and T. Hunig, Mitogenic signals through CD28 activate the protein kinase Ctheta-NF-kappaB pathway in primary peripheral T cells. *Int Immunol*, 2003. **15**(5): p. 655-63.
36. Philips, M.R., Compartmentalized signalling of Ras. *Biochem Soc Trans*, 2005. **33**(Pt 4): p. 657-61.
37. Fishburn, C.S., S.K. Pollitt, and H.R. Bourne, Localization of a peripheral membrane protein: Gbetagamma targets Galpha(Z). *Proc Natl Acad Sci U S A*, 2000. **97**(3): p. 1085-90.
38. Karle, I.L., M. Sukumar, and P. Balaram, Parallel packing of alpha-helices in crystals of the zervamicin IIA analog Boc-Trp-Ile-Ala-Aib-Ile-Val-Aib-Leu-Aib-Pro-OMe.2H2O. *Proc Natl Acad Sci U S A*, 1986. **83**(24): p. 9284-8.
39. van Beek, E.M., F. Cochrane, A.N. Barclay, and T.K. van den Berg, Signal regulatory proteins in the immune system. *J Immunol*, 2005. **175**(12): p. 7781-7.
40. Patel, T.B., Single transmembrane spanning heterotrimeric g protein-coupled receptors and their signaling cascades. *Pharmacol Rev*, 2004. **56**(3): p. 371-85.

41. Kessler, M., K.E. Gottschalk, H. Janovjak, D.J. Muller, and H.E. Gaub, Bacteriorhodopsin folds into the membrane against an external force. *J Mol Biol*, 2006. **357**(2): p. 644-54.
42. Marchesi, V.T., Structure and function of the erythrocyte membrane skeleton. *Prog Clin Biol Res*, 1984. **159**: p. 1-12.
43. LaLonde, J.M., D.A. Bernlohr, and L.J. Banaszak, The up-and-down beta-barrel proteins. *Faseb J*, 1994. **8**(15): p. 1240-7.
44. De Pinto, V., J.A. al Jamal, R. Benz, G. Genchi, and F. Palmieri, Characterization of SH groups in porin of bovine heart mitochondria. Porin cysteines are localized in the channel walls. *Eur J Biochem*, 1991. **202**(3): p. 903-11.
45. Molloy, M.P., B.R. Herbert, M.B. Slade, T. Rabilloud, A.S. Nouwens, K.L. Williams, and A.A. Gooley, Proteomic analysis of the Escherichia coli outer membrane. *Eur J Biochem*, 2000. **267**(10): p. 2871-81.
46. Brown, D.A., Interactions between GPI-anchored proteins and membrane lipids. *Trends Cell Biol*, 1992. **2**(11): p. 338-43.
47. Lee, A.G., How lipids affect the activities of integral membrane proteins. *Biochim Biophys Acta*, 2004. **1666**(1-2): p. 62-87.
48. Pucadyil, T.J. and A. Chattopadhyay, Role of cholesterol in the function and organization of G-protein coupled receptors. *Prog Lipid Res*, 2006. **45**(4): p. 295-333.
49. Gordon, J.I., R.J. Duronio, D.A. Rudnick, S.P. Adams, and G.W. Gokel, Protein N-myristoylation. *J Biol Chem*, 1991. **266**(14): p. 8647-50.
50. Sefton, B.M. and J.E. Buss, The covalent modification of eukaryotic proteins with lipid. *J Cell Biol*, 1987. **104**(6): p. 1449-53.
51. Glomset, J.A., M.H. Gelb, and C.C. Farnsworth, Prenyl proteins in eukaryotic cells: a new type of membrane anchor. *Trends Biochem Sci*, 1990. **15**(4): p. 139-42.
52. Doering, T.L., W.J. Masterson, G.W. Hart, and P.T. Englund, Biosynthesis of glycosyl phosphatidylinositol membrane anchors. *J Biol Chem*, 1990. **265**(2): p. 611-4.
53. Towler, D.A., S.P. Adams, S.R. Eubanks, D.S. Towery, E. Jackson-Machelski, L. Glaser, and J.I. Gordon, Myristoyl CoA:protein N-myristoyltransferase activities from rat liver and yeast possess overlapping yet distinct peptide substrate specificities. *J Biol Chem*, 1988. **263**(4): p. 1784-90.
54. Jones, D.R. and I. Varela-Nieto, The role of glycosyl-phosphatidylinositol in signal transduction. *Int J Biochem Cell Biol*, 1998. **30**(3): p. 313-26.
55. Brodbeck, U., Signalling properties of glycosylphosphatidylinositols and their regulated release from membranes in the turnover of glycosylphosphatidylinositol-anchored proteins. *Biol Chem*, 1998. **379**(8-9): p. 1041-4.
56. Ikezawa, H., Glycosylphosphatidylinositol (GPI)-anchored proteins. *Biol Pharm Bull*, 2002. **25**(4): p. 409-17.
57. Muniz, M. and H. Riezman, Intracellular transport of GPI-anchored proteins. *Embo J*, 2000. **19**(1): p. 10-5.
58. Singh, N., L.N. Liang, M.L. Tykocinski, and A.M. Tartakoff, A novel class of cell surface glycolipids of mammalian cells. Free glycosyl phosphatidylinositols. *J Biol Chem*, 1996. **271**(22): p. 12879-84.
59. Varela-Nieto, I., Y. Leon, and H.N. Caro, Cell signalling by inositol phosphoglycans from different species. *Comp Biochem Physiol B Biochem Mol Biol*, 1996. **115**(2): p. 223-41.
60. Petitfrere, E., H. Sartelet, D. Vivien, I. Varela-Nieto, H. Elbtaouri, L. Martiny, and B. Haye, Glycosyl phosphatidylinositol (GPI)/inositolphosphate glycan (IPG): an intracellular signalling system involved in the control of thyroid cell proliferation. *Biochimie*, 1998. **80**(12): p. 1063-7.

61. Hooper, N. and T. Turner. *GPI Membrane Anchors*. [Website] 2005 [cited 18th September 2006]; Available from: http://www.bmb.leeds.ac.uk/staff/nmh/project3.html.
62. Hofsteenge, J., D.R. Muller, T. de Beer, A. Loffler, W.J. Richter, and J.F. Vliegenthart, New type of linkage between a carbohydrate and a protein: C-glycosylation of a specific tryptophan residue in human RNase Us. *Biochemistry*, 1994. **33**(46): p. 13524-30.
63. Tsuiji, H., S. Takasaki, M. Sakamoto, T. Irimura, and S. Hirohashi, Aberrant O-glycosylation inhibits stable expression of dysadherin, a carcinoma-associated antigen, and facilitates cell-cell adhesion. *Glycobiology*, 2003. **13**(7): p. 521-7.
64. Moody, A.M., S.J. North, B. Reinhold, S.J. Van Dyken, M.E. Rogers, M. Panico, A. Dell, H.R. Morris, J.D. Marth, and E.L. Reinherz, Sialic acid capping of CD8beta core 1-O-glycans controls thymocyte-major histocompatibility complex class I interaction. *J Biol Chem*, 2003. **278**(9): p. 7240-6.
65. Van Dyken, S.J., R.S. Green, and J.D. Marth, Structural and mechanistic features of protein O glycosylation linked to CD8+ T-cell apoptosis. *Mol Cell Biol*, 2007. **27**(3): p. 1096-111.
66. Zapata, D.A., W.W. Schamel, P.S. Torres, B. Alarcon, N.E. Rossi, M.N. Navarro, M.L. Toribio, and J.R. Regueiro, Biochemical differences in the alphabeta T cell receptor.CD3 surface complex between CD8+ and CD4+ human mature T lymphocytes. *J Biol Chem*, 2004. **279**(23): p. 24485-92.
67. Atiya-Nasagi, Y., H. Cohen, O. Medalia, M. Fukudan, and R. Sagi-Eisenberg, O-glycosylation is essential for intracellular targeting of synaptotagmins I and II in non-neuronal specialized secretory cells. *J Cell Sci*, 2005. **118**(Pt 7): p. 1363-72.
68. Hart, G.W., M.P. Housley, and C. Slawson, Cycling of O-linked beta-N-acetylglucosamine on nucleocytoplasmic proteins. *Nature*, 2007. **446**(7139): p. 1017-22.
69. Hirabayashi, J. and K. Kasai, Separation technologies for glycomics. *J Chromatogr B Analyt Technol Biomed Life Sci*, 2002. **771**(1-2): p. 67-87.
70. Vlassara, H. and M.R. Palace, Diabetes and advanced glycation endproducts. *J Intern Med*, 2002. **251**(2): p. 87-101.
71. Kirkham, S., J.K. Sheehan, D. Knight, P.S. Richardson, and D.J. Thornton, Heterogeneity of airways mucus: variations in the amounts and glycoforms of the major oligomeric mucins MUC5AC and MUC5B. *Biochem J*, 2002. **361**(Pt 3): p. 537-46.
72. Reddy, G.K. and S.C. Dhar, Studies on carbohydrate moieties of glycoproteins in established adjuvant induced arthritis. *Agents Actions*, 1988. **25**(1-2): p. 63-70.
73. Ahmed, N. and P.J. Thornalley, Chromatographic assay of glycation adducts in human serum albumin glycated in vitro by derivatization with 6-aminoquinolyl-N-hydroxysuccinimidyl-carbamate and intrinsic fluorescence. *Biochem J*, 2002. **364**(Pt 1): p. 15-24.
74. Sato, T., T. Kawada, M. Sugimachi, and K. Sunagawa, Bionic technology revitalizes native baroreflex function in rats with baroreflex failure. *Circulation*, 2002. **106**(6): p. 730-4.
75. Xiong, L., D. Andrews, and F. Regnier, Comparative proteomics of glycoproteins based on lectin selection and isotope coding. *J Proteome Res*, 2003. **2**(6): p. 618-25.
76. Rhim, A.D., V.A. Kothari, P.J. Park, A.E. Mulberg, M.C. Glick, and T.F. Scanlin, Terminal glycosylation of cystic fibrosis airway epithelial cells. *Glycoconj J*, 2000. **17**(6): p. 385-91.
77. Raghav, S.K., B. Gupta, C. Agrawal, A. Saroha, R.H. Das, V.P. Chaturvedi, and H.R. Das, Altered expression and glycosylation of plasma proteins in rheumatoid arthritis. *Glycoconj J*, 2006. **23**(3-4): p. 167-73.

78. Crocker, P.R. and S. Gordon, Properties and distribution of a lectin-like hemagglutinin differentially expressed by murine stromal tissue macrophages. *J Exp Med*, 1986. **164**(6): p. 1862-75.
79. Varki, A., Glycan-based interactions involving vertebrate sialic-acid-recognizing proteins. *Nature*, 2007. **446**(7139): p. 1023-9.
80. Gut, A., F. Kappeler, N. Hyka, M.S. Balda, H.P. Hauri, and K. Matter, Carbohydrate-mediated Golgi to cell surface transport and apical targeting of membrane proteins. *Embo J*, 1998. **17**(7): p. 1919-29.
81. Freeze, H.H., Genetic defects in the human glycome. *Nat Rev Genet*, 2006. **7**(7): p. 537-51.
82. Green, R.S., E.L. Stone, M. Tenno, E. Lehtonen, M.G. Farquhar, and J.D. Marth, Mammalian N-glycan branching protects against innate immune self-recognition and inflammation in autoimmune disease pathogenesis. *Immunity*, 2007. **27**(2): p. 308-20.
83. Hakomori, S., Glycosylation defining cancer malignancy: new wine in an old bottle. *Proc Natl Acad Sci U S A*, 2002. **99**(16): p. 10231-3.
84. Dimitroff, C.J., P. Pera, F. Dall'Olio, K.L. Matta, E.V. Chandrasekaran, J.T. Lau, and R.J. Bernacki, Cell surface n-acetylneuraminic acid alpha2,3-galactoside-dependent intercellular adhesion of human colon cancer cells. *Biochem Biophys Res Commun*, 1999. **256**(3): p. 631-6.
85. Lee, Y.C., N. Kurosawa, T. Hamamoto, T. Nakaoka, and S. Tsuji, Molecular cloning and expression of Gal beta 1,3GalNAc alpha 2,3-sialyltransferase from mouse brain. *Eur J Biochem*, 1993. **216**(2): p. 377-85.
86. Hakomori, S., Aberrant glycosylation in tumors and tumor-associated carbohydrate antigens. *Adv Cancer Res*, 1989. **52**: p. 257-331.
87. Bird, N.C., D. Mangnall, and A.W. Majeed, Biology of colorectal liver metastases: A review. *J Surg Oncol*, 2006. **94**(1): p. 68-80.
88. Popescu, O., I. Checiu, P. Gherghel, Z. Simon, and G.N. Misevic, Quantitative and qualitative approach of glycan-glycan interactions in marine sponges. *Biochimie*, 2003. **85**(1-2): p. 181-8.
89. Grubb, R., Correlation between Lewis blood group and secretor character in man. *Nature*, 1948. **162**(4128): p. 933.
90. Hasegawa, H., M. Watanabe, Y. Arisawa, T. Teramoto, S. Kodaira, and M. Kitajima, Carbohydrate antigens and liver metastasis in colorectal cancer. *Jpn J Clin Oncol*, 1993. **23**(6): p. 336-41.
91. Matsushita, Y., K.R. Cleary, D.M. Ota, S.D. Hoff, and T. Irimura, Sialyl-dimeric Lewis-X antigen expressed on mucin-like glycoproteins in colorectal cancer metastases. *Lab Invest*, 1990. **63**(6): p. 780-91.
92. Hakomori, S., Tumor malignancy defined by aberrant glycosylation and sphingo(glyco)lipid metabolism. *Cancer Res*, 1996. **56**(23): p. 5309-18.
93. Paget, S., The distribution of secondary growths in cancer of the breast. 1889. *Cancer Metastasis Rev*, 1989. **8**(2): p. 98-101.
94. Ono, M. and S. Hakomori, Glycosylation defining cancer cell motility and invasiveness. *Glycoconj J*, 2004. **20**(1): p. 71-8.
95. Nakamori, S., M. Kameyama, S. Imaoka, H. Furukawa, O. Ishikawa, Y. Sasaki, Y. Izumi, and T. Irimura, Involvement of carbohydrate antigen sialyl Lewis(x) in colorectal cancer metastasis. *Dis Colon Rectum*, 1997. **40**(4): p. 420-31.
96. Reyes-Reyes, M.E., M.D. George, J.D. Roberts, and S.K. Akiyama, P-selectin activates integrin-mediated colon carcinoma cell adhesion to fibronectin. *Exp Cell Res*, 2006. **312**(20): p. 4056-69.
97. Dimitroff, C.J., M. Lechpammer, D. Long-Woodward, and J.L. Kutok, Rolling of human bone-metastatic prostate tumor cells on human bone marrow endothelium under shear flow is mediated by E-selectin. *Cancer Res*, 2004. **64**(15): p. 5261-9.

98. Witz, I.P., The involvement of selectins and their ligands in tumor-progression. *Immunol Lett*, 2006. **104**(1-2): p. 89-93.
99. Casey, R.C., T.R. Oegema, Jr., K.M. Skubitz, S.E. Pambuccian, S.M. Grindle, and A.P. Skubitz, Cell membrane glycosylation mediates the adhesion, migration, and invasion of ovarian carcinoma cells. *Clin Exp Metastasis*, 2003. **20**(2): p. 143-52.
100. Hanley, W.D., S.L. Napier, M.M. Burdick, R.L. Schnaar, R. Sackstein, and K. Konstantopoulos, Variant isoforms of CD44 are P- and L-selectin ligands on colon carcinoma cells. *FASEB J*, 2006. **20**(2): p. 337-9.
101. Napier, S.L., Z.R. Healy, R.L. Schnaar, and K. Konstantopoulos, Selectin ligand expression regulates the initial vascular interactions of colon carcinoma cells: the roles of CD44v and alternative sialofucosylated selectin ligands. *J Biol Chem*, 2007. **282**(6): p. 3433-41.
102. Thomas, S.N., F. Zhu, R.L. Schnaar, C.S. Alves, and K. Konstantopoulos, Carcinoembryonic antigen and CD44 variant isoforms cooperate to mediate colon carcinoma cell adhesion to E- and L-selectin in shear flow. *J Biol Chem*, 2008. **283**(23): p. 15647-55.
103. Takeuchi, K., A. Yamaguchi, T. Urano, T. Goi, G. Nakagawara, and H. Shiku, Expression of CD44 variant exons 8-10 in colorectal cancer and its relationship to metastasis. *Jpn J Cancer Res*, 1995. **86**(3): p. 292-7.
104. Gotley, D.C., J. Fawcett, M.D. Walsh, J.A. Reeder, D.L. Simmons, and T.M. Antalis, Alternatively spliced variants of the cell adhesion molecule CD44 and tumour progression in colorectal cancer. *Br J Cancer*, 1996. **74**(3): p. 342-51.
105. Sneath, R.J. and D.C. Mangham, The normal structure and function of CD44 and its role in neoplasia. *Mol Pathol*, 1998. **51**(4): p. 191-200.
106. Coppola, D., M. Hyacinthe, L. Fu, A.B. Cantor, R. Karl, J. Marcet, D.L. Cooper, S.V. Nicosia, and H.S. Cooper, CD44V6 expression in human colorectal carcinoma. *Hum Pathol*, 1998. **29**(6): p. 627-35.
107. Asao, T., J. Nakamura, Y. Shitara, S. Tsutsumi, E. Mochiki, T. Shimura, S. Takenoshita, and H. Kuwano, Loss of standard type of CD44 expression in invaded area as a good indicator of lymph-node metastasis in colorectal carcinoma. *Dis Colon Rectum*, 2000. **43**(9): p. 1250-4; discussion 1254-5.
108. Mathew, J., J.E. Hines, J.O. Obafunwa, A.W. Burr, K. Toole, and A.D. Burt, CD44 is expressed in hepatocellular carcinomas showing vascular invasion. *J Pathol*, 1996. **179**(1): p. 74-9.
109. Ngan, C.Y., H. Yamamoto, I. Seshimo, K. Ezumi, M. Terayama, H. Hemmi, I. Takemasa, M. Ikeda, M. Sekimoto, and M. Monden, A multivariate analysis of adhesion molecules expression in assessment of colorectal cancer. *J Surg Oncol*, 2007. **95**(8): p. 652-62.
110. Minami, S., J. Furui, and T. Kanematsu, Role of carcinoembryonic antigen in the progression of colon cancer cells that express carbohydrate antigen. *Cancer Res*, 2001. **61**(6): p. 2732-5.
111. Thomas, P., A. Gangopadhyay, G. Steele, Jr., C. Andrews, H. Nakazato, S. Oikawa, and J.M. Jessup, The effect of transfection of the CEA gene on the metastatic behavior of the human colorectal cancer cell line MIP-101. *Cancer Lett*, 1995. **92**(1): p. 59-66.
112. Jessup, J.M., S. Ishii, T. Mitzoi, K.H. Edmiston, and Y. Shoji, Carcinoembryonic antigen facilitates experimental metastasis through a mechanism that does not involve adhesion to liver cells. *Clin Exp Metastasis*, 1999. **17**(6): p. 481-8.
113. Mori, M., G.F. Barnard, K. Mimori, H. Ueo, T. Akiyoshi, and K. Sugimachi, Overexpression of matrix metalloproteinase-7 mRNA in human colon carcinomas. *Cancer*, 1995. **75**(6 Suppl): p. 1516-9.
114. Yamamoto, H., F. Itoh, A. Senota, Y. Adachi, M. Yoshimoto, T. Endoh, Y. Hinoda, A. Yachi, and K. Imai, Expression of matrix metalloproteinase matrilysin (MMP-7) was

induced by activated Ki-ras via AP-1 activation in SW1417 colon cancer cells. *J Clin Lab Anal*, 1995. **9**(5): p. 297-301.
115. Zeng, Z.S. and J.G. Guillem, Unique activation of matrix metalloproteinase-9 within human liver metastasis from colorectal cancer. *Br J Cancer*, 1998. **78**(3): p. 349-53.
116. Rmali, K.A., M.C. Puntis, and W.G. Jiang, Tumour-associated angiogenesis in human colorectal cancer. *Colorectal Dis*, 2007. **9**(1): p. 3-14.
117. Li, D., T. Mallory, and S. Satomura, AFP-L3: a new generation of tumor marker for hepatocellular carcinoma. *Clin Chim Acta*, 2001. **313**(1-2): p. 15-9.
118. Arnold, J.N., R. Saldova, U.M. Hamid, and P.M. Rudd, Evaluation of the serum N-linked glycome for the diagnosis of cancer and chronic inflammation. *Proteomics*, 2008. **8**(16): p. 3284-93.
119. Rudd, P.M., T. Elliott, P. Cresswell, I.A. Wilson, and R.A. Dwek, Glycosylation and the immune system. *Science*, 2001. **291**(5512): p. 2370-6.
120. Sperandio, M., C.A. Gleissner, and K. Ley, Glycosylation in immune cell trafficking. *Immunol Rev*, 2009. **230**(1): p. 97-113.
121. Gabay, C. and I. Kushner, Acute-phase proteins and other systemic responses to inflammation. *N Engl J Med*, 1999. **340**(6): p. 448-54.
122. Skipworth, R.J., G.D. Stewart, C.H. Dejong, T. Preston, and K.C. Fearon, Pathophysiology of cancer cachexia: much more than host-tumour interaction? *Clin Nutr*, 2007. **26**(6): p. 667-76.
123. Narisada, M., S. Kawamoto, K. Kuwamoto, K. Moriwaki, T. Nakagawa, H. Matsumoto, M. Asahi, N. Koyama, and E. Miyoshi, Identification of an inducible factor secreted by pancreatic cancer cell lines that stimulates the production of fucosylated haptoglobin in hepatoma cells. *Biochem Biophys Res Commun*, 2008. **377**(3): p. 792-6.
124. Marnell, L., C. Mold, and T.W. Du Clos, C-reactive protein: ligands, receptors and role in inflammation. *Clin Immunol*, 2005. **117**(2): p. 104-11.
125. Peracaula, R., A. Sarrats, and P.M. Rudd, Liver proteins as sensor of human malignancies and inflammation. *Proteomics Clinical Applications*, 2010. **4**(1-6): p. 426-431.
126. Twyman, R.M., *Principles of proteomics*. 2004, New York: BIOS Scientific Publishers.
127. Flower, D.R., The lipocalin protein family: structure and function. *J Biochem*, 1996. **318 (Pt 1)**: p. 1-14.
128. Kuster, B., T.N. Krogh, E. Mortz, and D.J. Harvey, Glycosylation analysis of gel-separated proteins. *Proteomics*, 2001. **1**(2): p. 350-61.
129. Page, M. and C. Godin, On the determination of the Stokes radius of glutamate dehydrogenase monomer by gel filtration of Sephadex G-200. *Biochim Biophys Acta*, 1969. **194**(1): p. 329-31.
130. Shapiro, A.L., E. Vinuela, and J.V. Maizel, Jr., Molecular weight estimation of polypeptide chains by electrophoresis in SDS-polyacrylamide gels. *Biochem Biophys Res Commun*, 1967. **28**(5): p. 815-20.
131. Pasquali, C., I. Fialka, and L.A. Huber, Preparative two-dimensional gel electrophoresis of membrane proteins. *Electrophoresis*, 1997. **18**(14): p. 2573-81.
132. Molloy, M.P., Two-dimensional electrophoresis of membrane proteins using immobilized pH gradients. *Anal Biochem*, 2000. **280**(1): p. 1-10.
133. Righetti, P.G., C. Gelfi, and M.L. Bossi, Hydrophobic interaction between alkaline immobilines and ferritin during isoelectric focusing in immobilized pH gradients. *J Chromatogr*, 1987. **392**: p. 123-32.
134. Wilkins, M.R., E. Gasteiger, J.C. Sanchez, A. Bairoch, and D.F. Hochstrasser, Two-dimensional gel electrophoresis for proteome projects: the effects of protein hydrophobicity and copy number. *Electrophoresis*, 1998. **19**(8-9): p. 1501-5.

135. Kyte, J. and R.F. Doolittle, A simple method for displaying the hydropathic character of a protein. *J Mol Biol*, 1982. **157**(1): p. 105-32.
136. Molloy, M.P., B.R. Herbert, B.J. Walsh, M.I. Tyler, M. Traini, J.C. Sanchez, D.F. Hochstrasser, K.L. Williams, and A.A. Gooley, Extraction of membrane proteins by differential solubilization for separation using two-dimensional gel electrophoresis. *Electrophoresis*, 1998. **19**(5): p. 837-44.
137. Hoffmann, A., M. Nimtz, and H.S. Conradt, Molecular characterization of beta-trace protein in human serum and urine: a potential diagnostic marker for renal diseases. *Glycobiology*, 1997. **7**(4): p. 499-506.
138. Monribot, C. and H. Boucherie, *Proteome Research: Two-Dimensional Gel Electrophoresis and Identification Methods*. 2000, New York: Springer.
139. Chick, J.M., P.A. Haynes, B. Bjellqvist, and M.S. Baker, A combination of immobilised pH gradients improves membrane proteomics. *J Proteome Res*, 2008. **7**(11): p. 4974-81.
140. Wang, W., T. Guo, P.A. Rudnick, T. Song, J. Li, Z. Zhuang, W. Zheng, D.L. Devoe, C.S. Lee, and B.M. Balgley, Membrane proteome analysis of microdissected ovarian tumor tissues using capillary isoelectric focusing/reversed-phase liquid chromatography-tandem MS. *Anal Chem*, 2007. **79**(3): p. 1002-9.
141. Xiao, Z., T.P. Conrads, D.A. Lucas, G.M. Janini, C.F. Schaefer, K.H. Buetow, H.J. Issaq, and T.D. Veenstra, Direct ampholyte-free liquid-phase isoelectric peptide focusing: application to the human serum proteome. *Electrophoresis*, 2004. **25**(1): p. 128-33.
142. Swanson, S.K. and M.P. Washburn, The continuing evolution of shotgun proteomics. *Drug Discov Today*, 2005. **10**(10): p. 719-25.
143. Yates, J.R., 3rd, J.K. Eng, A.L. McCormack, and D. Schieltz, Method to correlate tandem mass spectra of modified peptides to amino acid sequences in the protein database. *Anal Chem*, 1995. **67**(8): p. 1426-36.
144. Fujii, K., T. Nakano, T. Kawamura, F. Usui, Y. Bando, R. Wang, and T. Nishimura, Multidimensional protein profiling technology and its application to human plasma proteome. *J Proteome Res*, 2004. **3**(4): p. 712-8.
145. Breci, L., E. Hattrup, M. Keeler, J. Letarte, R. Johnson, and P.A. Haynes, Comprehensive proteomics in yeast using chromatographic fractionation, gas phase fractionation, protein gel electrophoresis, and isoelectric focusing. *Proteomics*, 2005. **5**(8): p. 2018-28.
146. Comuzzi, B. and M.D. Sadar, Proteomic analyses to identify novel therapeutic targets for the treatment of advanced prostate cancer. *Cellscience*, 2006. **3**(1): p. 61-81.
147. McDonald, W.H. and J.R. Yates, 3rd, Shotgun proteomics and biomarker discovery. *Dis Markers*, 2002. **18**(2): p. 99-105.
148. Elortza, F., T.S. Nuhse, L.J. Foster, A. Stensballe, S.C. Peck, and O.N. Jensen, Proteomic analysis of glycosylphosphatidylinositol-anchored membrane proteins. *Mol Cell Proteomics*, 2003. **2**(12): p. 1261-70.
149. Elortza, F., S. Mohammed, J. Bunkenborg, L.J. Foster, T.S. Nuhse, U. Brodbeck, S.C. Peck, and O.N. Jensen, Modification-specific proteomics of plasma membrane proteins: identification and characterization of glycosylphosphatidylinositol-anchored proteins released upon phospholipase D treatment. *J Proteome Res*, 2006. **5**(4): p. 935-43.
150. Everberg, H., R. Peterson, S. Rak, F. Tjerneld, and C. Emanuelsson, Aqueous two-phase partitioning for proteomic monitoring of cell surface biomarkers in human peripheral blood mononuclear cells. *J Proteome Res*, 2006. **5**(5): p. 1168-75.
151. Schindler, J., U. Lewandrowski, A. Sickmann, E. Friauf, and H.G. Nothwang, Proteomic analysis of brain plasma membranes isolated by affinity two-phase partitioning. *Mol Cell Proteomics*, 2006. **5**(2): p. 390-400.

152. O'Farrell, P.H., High resolution two-dimensional electrophoresis of proteins. *J Biol Chem*, 1975. **250**(10): p. 4007-21.
153. Cargile, B.J., J.R. Sevinsky, A.S. Essader, J.L. Stephenson, Jr., and J.L. Bundy, Immobilized pH gradient isoelectric focusing as a first-dimension separation in shotgun proteomics. *J Biomol Tech*, 2005. **16**(3): p. 181-9.
154. Krijgsveld, J., S. Gauci, W. Dormeyer, and A.J. Heck, In-gel isoelectric focusing of peptides as a tool for improved protein identification. *J Proteome Res*, 2006. **5**(7): p. 1721-30.
155. Slebos, R.J., J.W. Brock, N.F. Winters, S.R. Stuart, M.A. Martinez, M. Li, M.C. Chambers, L.J. Zimmerman, A.J. Ham, D.L. Tabb, and D.C. Liebler, Evaluation of strong cation exchange versus isoelectric focusing of peptides for multidimensional liquid chromatography-tandem mass spectrometry. *J Proteome Res*, 2008. **7**(12): p. 5286-94.
156. Zybailov, B., A.L. Mosley, M.E. Sardiu, M.K. Coleman, L. Florens, and M.P. Washburn, Statistical analysis of membrane proteome expression changes in Saccharomyces cerevisiae. *J Proteome Res*, 2006. **5**(9): p. 2339-47.
157. Mosley, A.L., L. Florens, Z. Wen, and M.P. Washburn, A label free quantitative proteomic analysis of the Saccharomyces cerevisiae nucleus. *J Proteomics*, 2009. **72**(1): p. 110-20.
158. Paoletti, A.C., T.J. Parmely, C. Tomomori-Sato, S. Sato, D. Zhu, R.C. Conaway, J.W. Conaway, L. Florens, and M.P. Washburn, Quantitative proteomic analysis of distinct mammalian Mediator complexes using normalized spectral abundance factors. *Proc Natl Acad Sci U S A*, 2006. **103**(50): p. 18928-33.
159. Pavelka, N., M.L. Fournier, S.K. Swanson, M. Pelizzola, P. Ricciardi-Castagnoli, L. Florens, and M.P. Washburn, Statistical similarities between transcriptomics and quantitative shotgun proteomics data. *Mol Cell Proteomics*, 2008. **7**(4): p. 631-44.
160. Nesvizhskii, A.I. and R. Aebersold, Interpretation of shotgun proteomic data: the protein inference problem. *Mol Cell Proteomics*, 2005. **4**(10): p. 1419-40.
161. Ashburner, M., C.A. Ball, J.A. Blake, D. Botstein, H. Butler, J.M. Cherry, A.P. Davis, K. Dolinski, S.S. Dwight, J.T. Eppig, M.A. Harris, D.P. Hill, L. Issel-Tarver, A. Kasarskis, S. Lewis, J.C. Matese, J.E. Richardson, M. Ringwald, G.M. Rubin, and G. Sherlock, Gene ontology: tool for the unification of biology. The Gene Ontology Consortium. *Nat Genet*, 2000. **25**(1): p. 25-9.
162. Kanehisa, M. and S. Goto, KEGG: kyoto encyclopedia of genes and genomes. *Nucleic Acids Res*, 2000. **28**(1): p. 27-30.
163. Ogata, H., S. Goto, W. Fujibuchi, and M. Kanehisa, Computation with the KEGG pathway database. *Biosystems*, 1998. **47**(1-2): p. 119-28.
164. Ogata, H., S. Goto, K. Sato, W. Fujibuchi, H. Bono, and M. Kanehisa, KEGG: Kyoto Encyclopedia of Genes and Genomes. *Nucleic Acids Res*, 1999. **27**(1): p. 29-34.
165. Wixon, J. and D. Kell, The Kyoto encyclopedia of genes and genomes--KEGG. *Yeast*, 2000. **17**(1): p. 48-55.
166. Jimenez-Marin, A., M. Collado-Romero, M. Ramirez-Boo, C. Arce, and J.J. Garrido, Biological pathway analysis by ArrayUnlock and Ingenuity Pathway Analysis. *BMC Proc*, 2009. **3 Suppl 4**: p. S6.
167. Mayburd, A.L., A. Martlinez, D. Sackett, H. Liu, J. Shih, J. Tauler, I. Avis, and J.L. Mulshine, Ingenuity network-assisted transcription profiling: Identification of a new pharmacologic mechanism for MK886. *Clin Cancer Res*, 2006. **12**(6): p. 1820-7.
168. Conesa, A. and S. Gotz, Blast2GO: A Comprehensive Suite for Functional Analysis in Plant Genomics. *Int J Plant Genomics*, 2008. **2008**: p. 619832.
169. Hirabayashi, J., Y. Arata, and K. Kasai, Glycome project: concept, strategy and preliminary application to Caenorhabditis elegans. *Proteomics*, 2001. **1**(2): p. 295-303.

170. Turnbull, J.E. and R.A. Field, Emerging glycomics technologies. *Nat Chem Biol*, 2007. **3**(2): p. 74-7.
171. Kaji, H., H. Saito, Y. Yamauchi, T. Shinkawa, M. Taoka, J. Hirabayashi, K. Kasai, N. Takahashi, and T. Isobe, Lectin affinity capture, isotope-coded tagging and mass spectrometry to identify N-linked glycoproteins. *Nat Biotechnol*, 2003. **21**(6): p. 667-72.
172. Charlwood, J., J.M. Skehel, and P. Camilleri, Analysis of N-linked oligosaccharides released from glycoproteins separated by two-dimensional gel electrophoresis. *Anal Biochem*, 2000. **284**(1): p. 49-59.
173. Kuster, B., S.F. Wheeler, A.P. Hunter, R.A. Dwek, and D.J. Harvey, Sequencing of N-linked oligosaccharides directly from protein gels: in-gel deglycosylation followed by matrix-assisted laser desorption/ionization mass spectrometry and normal-phase high-performance liquid chromatography. *Anal Biochem*, 1997. **250**(1): p. 82-101.
174. Mills, P.B., K. Mills, A.W. Johnson, P.T. Clayton, and B.G. Winchester, Analysis by matrix assisted laser desorption/ionisation-time of flight mass spectrometry of the post-translational modifications of alpha 1-antitrypsin isoforms separated by two-dimensional polyacrylamide gel electrophoresis. *Proteomics*, 2001. **1**(6): p. 778-86.
175. Packer, N.H., M.A. Lawson, D.R. Jardine, J.C. Sanchez, and A.A. Gooley, Analyzing glycoproteins separated by two-dimensional gel electrophoresis. *Electrophoresis*, 1998. **19**(6): p. 981-8.
176. Powell, A.K. and D.J. Harvey, Stabilization of sialic acids in N-linked oligosaccharides and gangliosides for analysis by positive ion matrix-assisted laser desorption/ionization mass spectrometry. *Rapid Commun Mass Spectrom*, 1996. **10**(9): p. 1027-32.
177. Wheeler, S.F. and D.J. Harvey, Extension of the in-gel release method for structural analysis of neutral and sialylated N-linked glycans to the analysis of sulfated glycans: application to the glycans from bovine thyroid-stimulating hormone. *Anal Biochem*, 2001. **296**(1): p. 92-100.
178. Wilson, N.L., B.L. Schulz, N.G. Karlsson, and N.H. Packer, Sequential analysis of N- and O-linked glycosylation of 2D-PAGE separated glycoproteins. *J Proteome Res*, 2002. **1**(6): p. 521-9.
179. Morelle, W., K. Canis, F. Chirat, V. Faid, and J.C. Michalski, The use of mass spectrometry for the proteomic analysis of glycosylation. *Proteomics*, 2006. **6**(14): p. 3993-4015.
180. Takahashi, N. and H. Nishibe, Some characteristics of a new glycopeptidase acting on aspartylglycosylamine linkages. *J Biochem*, 1978. **84**(6): p. 1467-73.
181. Knochenmuss, R., Ion formation mechanisms in UV-MALDI. *Analyst*, 2006. **131**(9): p. 966-86.
182. Harvey, D.J., R.H. Bateman, R.S. Bordoli, and R. Tyldesley, Ionisation and fragmentation of complex glycans with a quadrupole time-of-flight mass spectrometer fitted with a matrix-assisted laser desorption/ionisation ion source. *Rapid Commun Mass Spectrom*, 2000. **14**(22): p. 2135-42.
183. Lewandrowski, U., A. Resemann, and A. Sickmann, Laser-induced dissociation/high-energy collision-induced dissociation fragmentation using MALDI-TOF/TOF-MS instrumentation for the analysis of neutral and acidic oligosaccharides. *Anal Chem*, 2005. **77**(10): p. 3274-83.
184. Mechref, Y., M.V. Novotny, and C. Krishnan, Structural characterization of oligosaccharides using MALDI-TOF/TOF tandem mass spectrometry. *Anal Chem*, 2003. **75**(18): p. 4895-903.
185. Wuhrer, M., M.I. Catalina, A.M. Deelder, and C.H. Hokke, Glycoproteomics based on tandem mass spectrometry of glycopeptides. *J Chromatogr B Analyt Technol Biomed Life Sci*, 2007. **849**(1-2): p. 115-28.

186. Harvey, D.J., Quantitative aspects of the matrix-assisted laser desorption mass spectrometry of complex oligosaccharides. *Rapid Commun Mass Spectrom*, 1993. **7**(7): p. 614-9.
187. Zaia, J., Mass spectrometry of oligosaccharides. *Mass Spectrom Rev*, 2004. **23**(3): p. 161-227.
188. Ciucanu, I. and F. Kerek, Rapid and simultaneous methylation of fatty and hydroxy fatty acids for gas—liquid chromatographic analysis. *Journal of Chromatography A*, 1984. **284**: p. 179-185.
189. Karlsson, N.G., N.L. Wilson, H.J. Wirth, P. Dawes, H. Joshi, and N.H. Packer, Negative ion graphitised carbon nano-liquid chromatography/mass spectrometry increases sensitivity for glycoprotein oligosaccharide analysis. *Rapid Commun Mass Spectrom*, 2004. **18**(19): p. 2282-92.
190. Ninonuevo, M., H. An, H. Yin, K. Killeen, R. Grimm, R. Ward, B. German, and C. Lebrilla, Nanoliquid chromatography-mass spectrometry of oligosaccharides employing graphitized carbon chromatography on microchip with a high-accuracy mass analyzer. *Electrophoresis*, 2005. **26**(19): p. 3641-9.
191. Pabst, M. and F. Altmann, Influence of electrosorption, solvent, temperature, and ion polarity on the performance of LC-ESI-MS using graphitic carbon for acidic oligosaccharides. *Anal Chem*, 2008. **80**(19): p. 7534-42.
192. Harvey, D.J., Collision-induced fragmentation of underivatized N-linked carbohydrates ionized by electrospray. *J Mass Spectrom*, 2000. **35**(10): p. 1178-90.
193. Wada, Y., P. Azadi, C.E. Costello, A. Dell, R.A. Dwek, H. Geyer, R. Geyer, K. Kakehi, N.G. Karlsson, K. Kato, N. Kawasaki, K.H. Khoo, S. Kim, A. Kondo, E. Lattova, Y. Mechref, E. Miyoshi, K. Nakamura, H. Narimatsu, M.V. Novotny, N.H. Packer, H. Perreault, J. Peter-Katalinic, G. Pohlentz, V.N. Reinhold, P.M. Rudd, A. Suzuki, and N. Taniguchi, Comparison of the methods for profiling glycoprotein glycans--HUPO Human Disease Glycomics/Proteome Initiative multi-institutional study. *Glycobiology*, 2007. **17**(4): p. 411-22.
194. Wada, Y., A. Dell, S.M. Haslam, B. Tissot, K. Canis, P. Azadi, M. Backstrom, C.E. Costello, G.C. Hansson, Y. Hiki, M. Ishihara, H. Ito, K. Kakehi, N. Karlsson, K. Kato, N. Kawasaki, K.H. Khoo, K. Kobayashi, D. Kolarich, A. Kondo, C. Lebrilla, M. Nakano, H. Narimatsu, J. Novak, M.V. Novotny, E. Ohno, N.H. Packer, M.B. Renfrow, M. Tajiri, K.A. Thomsson, H. Yagi, S.Y. Yu, and N. Taniguchi, Comparison of Methods for Profiling O-glycosylation: HUPO Human Disease Glycomics/Proteome Initiative Multi-Institutional Study of IgA1. *Mol Cell Proteomics*.
195. Honda, S., S. Suzuki, and A. Taga, Analysis of carbohydrates as 1-phenyl-3-methyl-5-pyrazolone derivatives by capillary/microchip electrophoresis and capillary electrochromatography. *J Pharm Biomed Anal*, 2003. **30**(6): p. 1689-714.
196. Cooper, C.A., E. Gasteiger, and N.H. Packer, GlycoMod--a software tool for determining glycosylation compositions from mass spectrometric data. *Proteomics*, 2001. **1**(2): p. 340-9.
197. Goldberg, D., M. Sutton-Smith, J. Paulson, and A. Dell, Automatic annotation of matrix-assisted laser desorption/ionization N-glycan spectra. *Proteomics*, 2005. **5**(4): p. 865-75.
198. Joshi, H.J., M.J. Harrison, B.L. Schulz, C.A. Cooper, N.H. Packer, and N.G. Karlsson, Development of a mass fingerprinting tool for automated interpretation of oligosaccharide fragmentation data. *Proteomics*, 2004. **4**(6): p. 1650-64.
199. Lohmann, K.K. and C.W. von der Lieth, GlycoFragment and GlycoSearchMS: web tools to support the interpretation of mass spectra of complex carbohydrates. *Nucleic Acids Res*, 2004. **32**(Web Server issue): p. W261-6.

200. Lapadula, A.J., P.J. Hatcher, A.J. Hanneman, D.J. Ashline, H. Zhang, and V.N. Reinhold, Congruent strategies for carbohydrate sequencing. 3. OSCAR: an algorithm for assigning oligosaccharide topology from MSn data. *Anal Chem*, 2005. **77**(19): p. 6271-9.
201. Lim, H., J. Eng, J.R. Yates, 3rd, S.L. Tollaksen, C.S. Giometti, J.F. Holden, M.W. Adams, C.I. Reich, G.J. Olsen, and L.G. Hays, Identification of 2D-gel proteins: a comparison of MALDI/TOF peptide mass mapping to mu LC-ESI tandem mass spectrometry. *J Am Soc Mass Spectrom*, 2003. **14**(9): p. 957-70.
202. Zhang, H., X.J. Li, D.B. Martin, and R. Aebersold, Identification and quantification of N-linked glycoproteins using hydrazide chemistry, stable isotope labeling and mass spectrometry. *Nat Biotechnol*, 2003. **21**(6): p. 660-6.
203. Yang, Z. and W.S. Hancock, Approach to the comprehensive analysis of glycoproteins isolated from human serum using a multi-lectin affinity column. *J Chromatogr A*, 2004. **1053**(1-2): p. 79-88.
204. Tian, Y., Y. Zhou, S. Elliott, R. Aebersold, and H. Zhang, Solid-phase extraction of N-linked glycopeptides. *Nat Protoc*, 2007. **2**(2): p. 334-9.
205. Pan, S., Y. Wang, J.F. Quinn, E.R. Peskind, D. Waichunas, J.T. Wimberger, J. Jin, J.G. Li, D. Zhu, C. Pan, and J. Zhang, Identification of glycoproteins in human cerebrospinal fluid with a complementary proteomic approach. *J Proteome Res*, 2006. **5**(10): p. 2769-79.
206. Ramachandran, P., P. Boontheung, Y. Xie, M. Sondej, D.T. Wong, and J.A. Loo, Identification of N-linked glycoproteins in human saliva by glycoprotein capture and mass spectrometry. *J Proteome Res*, 2006. **5**(6): p. 1493-503.
207. Zhang, H., A.Y. Liu, P. Loriaux, B. Wollscheid, Y. Zhou, J.D. Watts, and R. Aebersold, Mass spectrometric detection of tissue proteins in plasma. *Mol Cell Proteomics*, 2007. **6**(1): p. 64-71.
208. Lewandrowski, U., J. Moebius, U. Walter, and A. Sickmann, Elucidation of N-glycosylation sites on human platelet proteins: a glycoproteomic approach. *Mol Cell Proteomics*, 2006. **5**(2): p. 226-33.
209. Wilson, N.L., N.G. Karlsson, and P. N.H., *Enrichment of Glycoproteins in the proteome*. Separation methods in proteomics, ed. G.S.a.G. Lazarev. 2006: CRC Press.
210. Collins, R.D., W. Jacobson, and R.W. Stoddart, Lectin staining of carbohydrates of haemic cells. III. The cells of Hodgkin's disease and other lymphomas. *Histopathology*, 1982. **6**(5): p. 601-16.
211. Ghosh, D., R.C. Beavis, and J.A. Wilkins, The identification and characterization of membranome components. *J Proteome Res*, 2008. **7**(4): p. 1572-83.
212. Hirabayashi, J., Lectin-based structural glycomics: glycoproteomics and glycan profiling. *Glycoconj J*, 2004. **21**(1-2): p. 35-40.
213. Hirabayashi, J., T. Hashidate, and K. Kasai, Glyco-catch method: A lectin affinity technique for glycoproteomics. *J Biomol Tech*, 2002. **13**(4): p. 205-18.
214. Boersema, P.J., N. Divecha, A.J. Heck, and S. Mohammed, Evaluation and optimization of ZIC-HILIC-RP as an alternative MudPIT strategy. *J Proteome Res*, 2007. **6**(3): p. 937-46.
215. McNulty, D.E. and R.S. Annan, Hydrophilic interaction chromatography reduces the complexity of the phosphoproteome and improves global phosphopeptide isolation and detection. *Mol Cell Proteomics*, 2008. **7**(5): p. 971-80.
216. Hagglund, P., J. Bunkenborg, F. Elortza, O.N. Jensen, and P. Roepstorff, A new strategy for identification of N-glycosylated proteins and unambiguous assignment of their glycosylation sites using HILIC enrichment and partial deglycosylation. *J Proteome Res*, 2004. **3**(3): p. 556-66.
217. Alpert, A.J. and P.C. Andrews, Cation-exchange chromatography of peptides on poly(2-sulfoethyl aspartamide)-silica. *J Chromatogr*, 1988. **443**: p. 85-96.

218. Hemstrom, P. and K. Irgum, Hydrophilic interaction chromatography. *J Sep Sci*, 2006. **29**(12): p. 1784-821.
219. Wada, Y., M. Tajiri, and S. Yoshida, Hydrophilic affinity isolation and MALDI multiple-stage tandem mass spectrometry of glycopeptides for glycoproteomics. *Anal Chem*, 2004. **76**(22): p. 6560-5.
220. Liu, X., L. Ma, and J. Li, Recent Developments in the Enrichment of Glycopeptides for Glycoproteomics. *Analytical Letters*, 2008. **41**(2): p. 268-277.
221. Calvano, C.D., C.G. Zambonin, and O.N. Jensen, Assessment of lectin and HILIC based enrichment protocols for characterization of serum glycoproteins by mass spectrometry. *J Proteomics*, 2008. **71**(3): p. 304-17.
222. Lewandrowski, U., K. Lohrig, R.P. Zahedi, D. Wolters, and A. Sickmann, Glycosylation Site Analysis of Human Platelets by Electrostatic Repulsion Hydrophilic Interaction Chromatography. *Clinical Proteomics*, 2008. **4**(1-2): p. 25-36.
223. Tajiri, M., S. Yoshida, and Y. Wada, Differential analysis of site-specific glycans on plasma and cellular fibronectins: application of a hydrophilic affinity method for glycopeptide enrichment. *Glycobiology*, 2005. **15**(12): p. 1332-40.
224. Alpert, A.J., Electrostatic repulsion hydrophilic interaction chromatography for isocratic separation of charged solutes and selective isolation of phosphopeptides. *Anal Chem*, 2008. **80**(1): p. 62-76.
225. Deshpande, N., P.H. Jensen, N.H. Packer, and D. Kolarich, GlycoSpectrumScan: fishing glycopeptides from MS spectra of protease digests of human colostrum sIgA. *J Proteome Res*, 2010. **9**(2): p. 1063-75.
226. Ozohanics, O., J. Krenyacz, K. Ludanyi, F. Pollreisz, K. Vekey, and L. Drahos, GlycoMiner: a new software tool to elucidate glycopeptide composition. *Rapid Commun Mass Spectrom*, 2008. **22**(20): p. 3245-54.
227. Kubota, K., Y. Sato, Y. Suzuki, N. Goto-Inoue, T. Toda, M. Suzuki, S. Hisanaga, A. Suzuki, and T. Endo, Analysis of glycopeptides using lectin affinity chromatography with MALDI-TOF mass spectrometry. *Anal Chem*, 2008. **80**(10): p. 3693-8.
228. Ichibangase, T., K. Moriya, K. Koike, and K. Imai, A proteomics method revealing disease-related proteins in livers of hepatitis-infected mouse model. *J Proteome Res*, 2007. **6**(7): p. 2841-9.
229. El-Aneed, A. and J. Banoub, Proteomics in the diagnosis of hepatocellular carcinoma: focus on high risk hepatitis B and C patients. *Anticancer Res*, 2006. **26**(5A): p. 3293-300.
230. Baranova, A., L. Liotta, E. Petricoin, and Z.M. Younossi, The role of genomics and proteomics: technologies in studying non-alcoholic fatty liver disease. *Clin Liver Dis*, 2007. **11**(1): p. 209-20, xi.
231. Brechot, C., [Hepatitis B and C viruses and primary liver cancer]. *Rev Prat*, 1995. **45**(2): p. 190-6.
232. Markiewski, M.M., R.A. DeAngelis, and J.D. Lambris, Liver inflammation and regeneration: two distinct biological phenomena or parallel pathophysiologic processes? *Mol Immunol*, 2006. **43**(1-2): p. 45-56.
233. Zhou, H.J., Y.K. Liu, J.F. Chui, Q.L. Sun, W.J. Lu, K. Guo, H. Jin, L.M. Wei, and P.Y. Yang, A glycoproteome database of normal human liver tissue. *J Cancer Res Clin Oncol*, 2007. **133**(6): p. 379-87.
234. Bataller, R. and D.A. Brenner, Liver fibrosis. *J Clin Invest*, 2005. **115**(2): p. 209-18.
235. Lai, K.K., D. Kolippakkam, and L. Beretta, Comprehensive and quantitative proteome profiling of the mouse liver and plasma. *Hepatology*, 2008. **47**(3): p. 1043-51.
236. Zhang, L., J. Xie, X. Wang, X. Liu, X. Tang, R. Cao, W. Hu, S. Nie, C. Fan, and S. Liang, Proteomic analysis of mouse liver plasma membrane: use of differential extraction to enrich hydrophobic membrane proteins. *Proteomics*, 2005. **5**(17): p. 4510-24.

237. Evans, W.E. and M.V. Relling, Pharmacogenomics: translating functional genomics into rational therapeutics. *Science*, 1999. **286**(5439): p. 487-91.
238. Siewert, E., R. Bort, R. Kluge, P.C. Heinrich, J. Castell, and R. Jover, Hepatic cytochrome P450 down-regulation during aseptic inflammation in the mouse is interleukin 6 dependent. *Hepatology*, 2000. **32**(1): p. 49-55.
239. Rivory, L.P., K.A. Slaviero, and S.J. Clarke, Hepatic cytochrome P450 3A drug metabolism is reduced in cancer patients who have an acute-phase response. *Br J Cancer*, 2002. **87**(3): p. 277-80.
240. Slaviero, K.A., S.J. Clarke, and L.P. Rivory, Inflammatory response: an unrecognised source of variability in the pharmacokinetics and pharmacodynamics of cancer chemotherapy. *Lancet Oncol*, 2003. **4**(4): p. 224-32.
241. Charles, K.A., L.P. Rivory, S.L. Brown, C. Liddle, S.J. Clarke, and G.R. Robertson, Transcriptional repression of hepatic cytochrome P450 3A4 gene in the presence of cancer. *Clin Cancer Res*, 2006. **12**(24): p. 7492-7.
242. Corbett, T.H., D.P. Griswold, Jr., B.J. Roberts, J.C. Peckham, and F.M. Schabel, Jr., Tumor induction relationships in development of transplantable cancers of the colon in mice for chemotherapy assays, with a note on carcinogen structure. *Cancer Res*, 1975. **35**(9): p. 2434-9.
243. Ghezzi, P., B. Saccardo, and M. Bianchi, Recombinant tumor necrosis factor depresses cytochrome P450-dependent microsomal drug metabolism in mice. *Biochem Biophys Res Commun*, 1986. **136**(1): p. 316-21.
244. Ghezzi, P., B. Saccardo, P. Villa, V. Rossi, M. Bianchi, and C.A. Dinarello, Role of interleukin-1 in the depression of liver drug metabolism by endotoxin. *Infect Immun*, 1986. **54**(3): p. 837-40.
245. Houten, L. and A.A. Reilley, An investigation of the cause of death from cancer. *J Surg Oncol*, 1980. **13**(2): p. 111-6.
246. Kotler, D.P., A.R. Tierney, J.A. Culpepper-Morgan, J. Wang, and R.N. Pierson, Jr., Effect of home total parenteral nutrition on body composition in patients with acquired immunodeficiency syndrome. *JPEN J Parenter Enteral Nutr*, 1990. **14**(5): p. 454-8.
247. Holroyde, C.P., C.L. Skutches, G. Boden, and G.A. Reichard, Glucose metabolism in cachectic patients with colorectal cancer. *Cancer Res*, 1984. **44**(12 Pt 1): p. 5910-3.
248. Khal, J., S.M. Wyke, S.T. Russell, A.V. Hine, and M.J. Tisdale, Expression of the ubiquitin-proteasome pathway and muscle loss in experimental cancer cachexia. *Br J Cancer*, 2005. **93**(7): p. 774-80.
249. Schersten, T. and K. Lundholm, Lysosomal enzyme activity in muscle tissue from patients with malignant tumor. *Cancer*, 1972. **30**(5): p. 1246-51.
250. Wigmore, S.J., C.E. Plester, R.A. Richardson, and K.C. Fearon, Changes in nutritional status associated with unresectable pancreatic cancer. *Br J Cancer*, 1997. **75**(1): p. 106-9.
251. Takematsu, H., T. Kawano, S. Koyama, Y. Kozutsumi, A. Suzuki, and T. Kawasaki, Reaction mechanism underlying CMP-N-acetylneuraminic acid hydroxylation in mouse liver: formation of a ternary complex of cytochrome b5, CMP-N-acetylneuraminic acid, and a hydroxylation enzyme. *J Biochem*, 1994. **115**(3): p. 381-6.
252. Miller, I., P. Haynes, I. Eberini, M. Gemeiner, R. Aebersold, and E. Gianazza, Proteins of rat serum: III. Gender-related differences in protein concentration under baseline conditions and upon experimental inflammation as evaluated by two-dimensional electrophoresis. *Electrophoresis*, 1999. **20**(4-5): p. 836-45.
253. Craig, R. and R.C. Beavis, TANDEM: matching proteins with tandem mass spectra. *Bioinformatics*, 2004. **20**(9): p. 1466-7.
254. Peng, J., J.E. Elias, C.C. Thoreen, L.J. Licklider, and S.P. Gygi, Evaluation of multidimensional chromatography coupled with tandem mass spectrometry (LC/LC-

MS/MS) for large-scale protein analysis: the yeast proteome. *J Proteome Res*, 2003. **2**(1): p. 43-50.
255. Krogh, A., B. Larsson, G. von Heijne, and E.L. Sonnhammer, Predicting transmembrane protein topology with a hidden Markov model: application to complete genomes. *J Mol Biol*, 2001. **305**(3): p. 567-80.
256. Schulz, B.L., D. Oxley, N.H. Packer, and N.G. Karlsson, Identification of two highly sialylated human tear-fluid DMBT1 isoforms: the major high-molecular-mass glycoproteins in human tears. *Biochem J*, 2002. **366**(Pt 2): p. 511-20.
257. Fagerberg, L., K. Jonasson, G. von Heijne, M. Uhlen, and L. Berglund, Prediction of the human membrane proteome. *Proteomics*, 2010. **10**(6): p. 1141-9.
258. Fujiki, Y., A.L. Hubbard, S. Fowler, and P.B. Lazarow, Isolation of intracellular membranes by means of sodium carbonate treatment: application to endoplasmic reticulum. *J Cell Biol*, 1982. **93**(1): p. 97-102.
259. Fujiki, Y., S. Fowler, H. Shio, A.L. Hubbard, and P.B. Lazarow, Polypeptide and phospholipid composition of the membrane of rat liver peroxisomes: comparison with endoplasmic reticulum and mitochondrial membranes. *J Cell Biol*, 1982. **93**(1): p. 103-10.
260. Pease, T.K., E.S. Van Vleet, and J.S. Barre, Diphytanyl glycerol ether distributions in sediments of the Orca Basin. *Geochim Cosmochim Acta*, 1992. **56**(9): p. 3469-79.
261. Kravchenko, L.V., S.V. Morozov, and V.A. Tutel'yan, Effect of lycopine on the resistance of rat liver microsomes to in vitro induced LPO. *Bull Exp Biol Med*, 2003. **136**(1): p. 66-9.
262. Spadaccini, R., G. D'Errico, V. D'Alessio, E. Notomista, A. Bianchi, M. Merola, and D. Picone, Structural characterization of the transmembrane proximal region of the hepatis C virus E1 glycoprotein. *Biochim Biophys Acta*, 2009.
263. Alisio, A. and M. Mueckler, Purification and Characterization of Mammalian Glucose Transporters Expressed in Pichia Pastoris. *Protein Expr Purif*, 2009.
264. Hummel, K.M., A.R. Penheiter, A.C. Gathman, and W.W. Lilly, Anomalous estimation of protease molecular weights using gelatin-containing Sds-Page. *Anal Biochem*, 1996. **233**(1): p. 140-2.
265. Blonder, J., M.B. Goshe, R.J. Moore, L. Pasa-Tolic, C.D. Masselon, M.S. Lipton, and R.D. Smith, Enrichment of integral membrane proteins for proteomic analysis using liquid chromatography-tandem mass spectrometry. *J Proteome Res*, 2002. **1**(4): p. 351-60.
266. Zintl, A., S.R. Pennington, and G. Mulcahy, Comparison of different methods for the solubilisation of Neospora caninum (Phylum Apicomplexa) antigen. *Vet Parasitol*, 2006. **135**(3-4): p. 205-13.
267. Rabilloud, T., C. Adessi, A. Giraudel, and J. Lunardi, Improvement of the solubilization of proteins in two-dimensional electrophoresis with immobilized pH gradients. *Electrophoresis*, 1997. **18**(3-4): p. 307-16.
268. Chevallet, M., V. Santoni, A. Poinas, D. Rouquie, A. Fuchs, S. Kieffer, M. Rossignol, J. Lunardi, J. Garin, and T. Rabilloud, New zwitterionic detergents improve the analysis of membrane proteins by two-dimensional electrophoresis. *Electrophoresis*, 1998. **19**(11): p. 1901-9.
269. Beis, K., C. Whitfield, I. Booth, and J.H. Naismith, Two-step purification of outer membrane proteins. *Int J Biol Macromol*, 2006. **39**(1-3): p. 10-4.
270. le Maire, M., B. Arnou, C. Olesen, D. Georgin, C. Ebel, and J.V. Moller, Gel chromatography and analytical ultracentrifugation to determine the extent of detergent binding and aggregation, and Stokes radius of membrane proteins using sarcoplasmic reticulum Ca2+-ATPase as an example. *Nat Protoc*, 2008. **3**(11): p. 1782-95.

271. Luche, S., V. Santoni, and T. Rabilloud, Evaluation of nonionic and zwitterionic detergents as membrane protein solubilizers in two-dimensional electrophoresis. *Proteomics*, 2003. **3**(3): p. 249-53.
272. Navratilova, I., M. Dioszegi, and D.G. Myszka, Analyzing ligand and small molecule binding activity of solubilized GPCRs using biosensor technology. *Anal Biochem*, 2006. **355**(1): p. 132-9.
273. Rich, R.L., A.R. Miles, B.K. Gale, and D.G. Myszka, Detergent screening of a G-protein-coupled receptor using serial and array biosensor technologies. *Anal Biochem*, 2009. **386**(1): p. 98-104.
274. Gan, L., J.M. Alexander, A. Wittelsberger, B. Thomas, and M. Rosenblatt, Large-scale purification and characterization of human parathyroid hormone-1 receptor stably expressed in HEK293S GnTI- cells. *Protein Expr Purif*, 2006. **47**(1): p. 296-302.
275. Taylor, R.M., J.B. Burritt, T.R. Foubert, M.A. Snodgrass, K.C. Stone, D. Baniulis, J.M. Gripentrog, C. Lord, and A.J. Jesaitis, Single-step immunoaffinity purification and characterization of dodecylmaltoside-solubilized human neutrophil flavocytochrome b. *Biochim Biophys Acta*, 2003. **1612**(1): p. 65-75.
276. Labeta, M.O., N. Fernandez, and H. Festenstein, Solubilisation effect of Nonidet P-40, triton X-100 and CHAPS in the detection of MHC-like glycoproteins. *J Immunol Methods*, 1988. **112**(1): p. 133-8.
277. Zhang, N. and L. Li, Effects of common surfactants on protein digestion and matrix-assisted laser desorption/ionization mass spectrometric analysis of the digested peptides using two-layer sample preparation. *Rapid Commun Mass Spectrom*, 2004. **18**(8): p. 889-96.
278. Loo, R.R., N. Dales, and P.C. Andrews, Surfactant effects on protein structure examined by electrospray ionization mass spectrometry. *Protein Sci*, 1994. **3**(11): p. 1975-83.
279. Bordier, C., Phase separation of integral membrane proteins in Triton X-114 solution. *J Biol Chem*, 1981. **256**(4): p. 1604-7.
280. Haynes, P.A., A.A. Gooley, M.A. Ferguson, J.W. Redmond, and K.L. Williams, Post-translational modifications of the Dictyostelium discoideum glycoprotein PsA. Glycosylphosphatidylinositol membrane anchor and composition of O-linked oligosaccharides. *Eur J Biochem*, 1993. **216**(3): p. 729-37.
281. Mengesdorf, T., S. Althausen, G. Mies, L. Olah, and W. Paschen, Phosphorylation state, solubility, and activity of calcium/calmodulin-dependent protein kinase II alpha in transient focal ischemia in mouse brain. *Neurochem Res*, 2002. **27**(6): p. 477-84.
282. Lin, P.P., R.C. Barry, D.L. Smith, and J.B. Smith, In vivo acetylation identified at lysine 70 of human lens alphaA-crystallin. *Protein Sci*, 1998. **7**(6): p. 1451-7.
283. Maher, P.A. and S.J. Singer, Anomalous interaction of the acetylcholine receptor protein with the nonionic detergent Triton X-114. *Proc Natl Acad Sci U S A*, 1985. **82**(4): p. 958-62.
284. Celis, J.E. and P. Gromov, 2D protein electrophoresis: can it be perfected? *Curr Opin Biotechnol*, 1999. **10**(1): p. 16-21.
285. Santoni, V., M. Molloy, and T. Rabilloud, Membrane proteins and proteomics: un amour impossible? *Electrophoresis*, 2000. **21**(6): p. 1054-70.
286. Thaysen-Andersen, M., I.B. Thogersen, H.J. Nielsen, U. Lademann, N. Brunner, J.J. Enghild, and P. Hojrup, Rapid and individual-specific glycoprofiling of the low abundance N-glycosylated protein tissue inhibitor of metalloproteinases-1. *Mol Cell Proteomics*, 2007. **6**(4): p. 638-47.
287. Robertson, G.R., C. Liddle, and S.J. Clarke, Inflammation and altered drug clearance in cancer: transcriptional repression of a human CYP3A4 transgene in tumor-bearing mice. *Clin Pharmacol Ther*, 2008. **83**(6): p. 894-7.
288. Sardiu, M.E., Y. Cai, J. Jin, S.K. Swanson, R.C. Conaway, J.W. Conaway, L. Florens, and M.P. Washburn, Probabilistic assembly of human protein interaction networks

from label-free quantitative proteomics. *Proc Natl Acad Sci U S A*, 2008. **105**(5): p. 1454-9.
289. Camon, E., M. Magrane, D. Barrell, D. Binns, W. Fleischmann, P. Kersey, N. Mulder, T. Oinn, J. Maslen, A. Cox, and R. Apweiler, The Gene Ontology Annotation (GOA) project: implementation of GO in SWISS-PROT, TrEMBL, and InterPro. *Genome Res*, 2003. **13**(4): p. 662-72.
290. Rudd, P.M., M.R. Wormald, R.L. Stanfield, M. Huang, N. Mattsson, J.A. Speir, J.A. DiGennaro, J.S. Fetrow, R.A. Dwek, and I.A. Wilson, Roles for glycosylation of cell surface receptors involved in cellular immune recognition. *J Mol Biol*, 1999. **293**(2): p. 351-66.
291. Grakoui, A., S.K. Bromley, C. Sumen, M.M. Davis, A.S. Shaw, P.M. Allen, and M.L. Dustin, The immunological synapse: a molecular machine controlling T cell activation. *Science*, 1999. **285**(5425): p. 221-7.
292. Banerji, S., J. Ni, S.X. Wang, S. Clasper, J. Su, R. Tammi, M. Jones, and D.G. Jackson, LYVE-1, a new homologue of the CD44 glycoprotein, is a lymph-specific receptor for hyaluronan. *J Cell Biol*, 1999. **144**(4): p. 789-801.
293. Angel, A.S., G. Gronberg, H. Krotkiewski, E. Lisowska, and B. Nilsson, Structural analysis of the N-linked oligosaccharides from murine glycophorin. *Arch Biochem Biophys*, 1991. **291**(1): p. 76-88.
294. Debray, H., D. Dus, J.M. Wieruszeski, G. Strecker, and J. Montreuil, Structures of the alpha(1-3)-galactose-containing asparagine-linked glycans of a Lewis lung carcinoma cell subline resistant to Aleuria aurantia agglutinin: elucidation by 1H-NMR spectroscopy. *Glycoconj J*, 1991. **8**(1): p. 29-37.
295. Easton, R.L., M.S. Patankar, F.A. Lattanzio, T.H. Leaven, H.R. Morris, G.F. Clark, and A. Dell, Structural analysis of murine zona pellucida glycans. Evidence for the expression of core 2-type O-glycans and the Sd(a) antigen. *J Biol Chem*, 2000. **275**(11): p. 7731-42.
296. Kotani, N., M. Asano, Y. Iwakura, and S. Takasaki, Impaired galactosylation of core 2 O-glycans in erythrocytes of beta1,4-galactosyltransferase knockout mice. *Biochem Biophys Res Commun*, 1999. **260**(1): p. 94-8.
297. Adas, F., F. Berthou, D. Picart, P. Lozac'h, F. Beauge, and Y. Amet, Involvement of cytochrome P450 2E1 in the (omega-1)-hydroxylation of oleic acid in human and rat liver microsomes. *J Lipid Res*, 1998. **39**(6): p. 1210-9.
298. Yanagimoto, T., S. Itoh, M. Sawada, H. Hashimoto, and T. Kamataki, Molecular cloning and functional expression of a mouse cytochrome P-450 (Cyp3a-13): examination of Cyp3a-13 enzyme to activate aflatoxin B1 (AFB1). *Biochim Biophys Acta*, 1994. **1201**(3): p. 405-10.
299. Ghosh, P. and S. Kornfeld, The GGA proteins: key players in protein sorting at the trans-Golgi network. *Eur J Cell Biol*, 2004. **83**(6): p. 257-62.
300. Cottalasso, D., C. Domenicotti, N. Traverso, M. Pronzato, and G. Nanni, Influence of chronic ethanol consumption on toxic effects of 1,2-dichloroethane: glycolipoprotein retention and impairment of dolichol concentration in rat liver microsomes and Golgi apparatus. *Toxicology*, 2002. **178**(3): p. 229-240.
301. Lauro, P., P.S. Lechner, A. Okolo, P.K. Eagon, and R.H. Glew, Effect of chronic ethanol ingestion on alpha-mannosidase isoenzymes in rat liver. *Clin Chim Acta*, 1988. **174**(3): p. 291-8.
302. Keppler, O.T., S. Hinderlich, J. Langner, R. Schwartz-Albiez, W. Reutter, and M. Pawlita, UDP-GlcNAc 2-epimerase: a regulator of cell surface sialylation. *Science*, 1999. **284**(5418): p. 1372-6.
303. Horstkorte, R., S. Nohring, K. Danker, K. Effertz, W. Reutter, and L. Lucka, Protein kinase C phosphorylates and regulates UDP-N-acetylglucosamine-2-epimerase/N-acetylmannosamine kinase. *FEBS Lett*, 2000. **470**(3): p. 315-8.

304. Kornfeld, S., R. Kornfeld, E.F. Neufeld, and P.J. O'Brien, The Feedback Control of Sugar Nucleotide Biosynthesis in Liver. *Proc Natl Acad Sci U S A*, 1964. **52**: p. 371-9.
305. Keppler, O.T., G. Moldenhauer, M. Oppenlander, R. Schwartz-Albiez, E.G. Berger, S. Funderud, and M. Pawlita, Human Golgi beta-galactoside alpha-2,6-sialyltransferase generates a group of sialylated B lymphocyte differentiation antigens. *Eur J Immunol*, 1992. **22**(11): p. 2777-81.
306. Keppler, O.T., M.E. Peter, S. Hinderlich, G. Moldenhauer, P. Stehling, I. Schmitz, R. Schwartz-Albiez, W. Reutter, and M. Pawlita, Differential sialylation of cell surface glycoconjugates in a human B lymphoma cell line regulates susceptibility for CD95 (APO-1/Fas)-mediated apoptosis and for infection by a lymphotropic virus. *Glycobiology*, 1999. **9**(6): p. 557-69.
307. Wagers, A.J., L.M. Stoolman, R. Craig, R.N. Knibbs, and G.S. Kansas, An sLex-deficient variant of HL60 cells exhibits high levels of adhesion to vascular selectins: further evidence that HECA-452 and CSLEX1 monoclonal antibody epitopes are not essential for high avidity binding to vascular selectins. *J Immunol*, 1998. **160**(10): p. 5122-9.
308. Brinkman-Van der Linden, E.C., E.R. Sjoberg, L.R. Juneja, P.R. Crocker, N. Varki, and A. Varki, Loss of N-glycolylneuraminic acid in human evolution. Implications for sialic acid recognition by siglecs. *J Biol Chem*, 2000. **275**(12): p. 8633-40.
309. Irie, A. and A. Suzuki, CMP-N-Acetylneuraminic acid hydroxylase is exclusively inactive in humans. *Biochem Biophys Res Commun*, 1998. **248**(2): p. 330-3.
310. Kawano, T., Y. Kozutsumi, T. Kawasaki, and A. Suzuki, Biosynthesis of N-glycolylneuraminic acid-containing glycoconjugates. Purification and characterization of the key enzyme of the cytidine monophospho-N-acetylneuraminic acid hydroxylation system. *J Biol Chem*, 1994. **269**(12): p. 9024-9.
311. Kozutsumi, Y., T. Kawano, T. Yamakawa, and A. Suzuki, Participation of cytochrome b5 in CMP-N-acetylneuraminic acid hydroxylation in mouse liver cytosol. *J Biochem*, 1990. **108**(5): p. 704-6.
312. Lepers, A., L. Shaw, P. Schneckenburger, R. Cacan, A. Verbert, and R. Schauer, A study on the regulation of N-glycoloylneuraminic acid biosynthesis and utilization in rat and mouse liver. *Eur J Biochem*, 1990. **193**(3): p. 715-23.
313. Kelm, S., R. Brossmer, R. Isecke, H.J. Gross, K. Strenge, and R. Schauer, Functional groups of sialic acids involved in binding to siglecs (sialoadhesins) deduced from interactions with synthetic analogues. *Eur J Biochem*, 1998. **255**(3): p. 663-72.
314. Kelm, S., R. Schauer, J.C. Manuguerra, H.J. Gross, and P.R. Crocker, Modifications of cell surface sialic acids modulate cell adhesion mediated by sialoadhesin and CD22. *Glycoconj J*, 1994. **11**(6): p. 576-85.
315. Blixt, O., B.E. Collins, I.M. van den Nieuwenhof, P.R. Crocker, and J.C. Paulson, Sialoside specificity of the siglec family assessed using novel multivalent probes: identification of potent inhibitors of myelin-associated glycoprotein. *J Biol Chem*, 2003. **278**(33): p. 31007-19.
316. Crocker, P.R., J.C. Paulson, and A. Varki, Siglecs and their roles in the immune system. *Nat Rev Immunol*, 2007. **7**(4): p. 255-66.
317. Naito, Y., H. Takematsu, S. Koyama, S. Miyake, H. Yamamoto, R. Fujinawa, M. Sugai, Y. Okuno, G. Tsujimoto, T. Yamaji, Y. Hashimoto, S. Itohara, T. Kawasaki, A. Suzuki, and Y. Kozutsumi, Germinal center marker GL7 probes activation-dependent repression of N-glycolylneuraminic acid, a sialic acid species involved in the negative modulation of B-cell activation. *Mol Cell Biol*, 2007. **27**(8): p. 3008-22.
318. Hennecke, J. and D.C. Wiley, T cell receptor-MHC interactions up close. *Cell*, 2001. **104**(1): p. 1-4.
319. Yamasaki, T., G. Klein, H.G. Ljunggren, K. Karre, K. Moritake, J.T. Paine, and H. Kikuchi, Role of histocompatibility antigen gene and protooncogene expressions in

intracerebral tumorigenicity of mouse neuroblastoma. *J Neurosurg*, 1993. **78**(4): p. 619-29.
320. Lee, J.Y. and A.P. Spicer, Hyaluronan: a multifunctional, megaDalton, stealth molecule. *Curr Opin Cell Biol*, 2000. **12**(5): p. 581-6.
321. Prevo, R., S. Banerji, D.J. Ferguson, S. Clasper, and D.G. Jackson, Mouse LYVE-1 is an endocytic receptor for hyaluronan in lymphatic endothelium. *J Biol Chem*, 2001. **276**(22): p. 19420-30.
322. Song, H.Y., J.D. Dunbar, Y.X. Zhang, D. Guo, and D.B. Donner, Identification of a protein with homology to hsp90 that binds the type 1 tumor necrosis factor receptor. *J Biol Chem*, 1995. **270**(8): p. 3574-81.
323. Leav, I., J. Plescia, H.L. Goel, J. Li, Z. Jiang, R.J. Cohen, L.R. Languino, and D.C. Altieri, Cytoprotective mitochondrial chaperone TRAP-1 as a novel molecular target in localized and metastatic prostate cancer. *Am J Pathol*. **176**(1): p. 393-401.
324. Aplin, A.E., A. Howe, S.K. Alahari, and R.L. Juliano, Signal transduction and signal modulation by cell adhesion receptors: the role of integrins, cadherins, immunoglobulin-cell adhesion molecules, and selectins. *Pharmacol Rev*, 1998. **50**(2): p. 197-263.
325. King, C.D., G.R. Rios, M.D. Green, and T.R. Tephly, UDP-glucuronosyltransferases. *Curr Drug Metab*, 2000. **1**(2): p. 143-61.
326. Roberson, P.L., Quantitative autoradiography for the study of radiopharmaceutical uptake and dose heterogeneity. *J Nucl Med*, 1992. **33**(10): p. 1833-5.
327. Takahashi, H., I. Johansson, S.W. French, and M. Ingelman-Sundberg, Effects of dietary fat composition on activities of the microsomal ethanol oxidizing system and ethanol-inducible cytochrome P450 (CYP2E1) in the liver of rats chronically fed ethanol. *Pharmacol Toxicol*, 1992. **70**(5 Pt 1): p. 347-51.
328. Du, L., V. Yermalitsky, P.A. Ladd, J.H. Capdevila, R. Mernaugh, and D.S. Keeney, Evidence that cytochrome P450 CYP2B19 is the major source of epoxyeicosatrienoic acids in mouse skin. *Arch Biochem Biophys*, 2005. **435**(1): p. 125-33.
329. Down, M.J., S. Arkle, and J.J. Mills, Regulation and induction of CYP3A11, CYP3A13 and CYP3A25 in C57BL/6J mouse liver. *Arch Biochem Biophys*, 2007. **457**(1): p. 105-10.
330. Llorente, A., B. van Deurs, and K. Sandvig, Cholesterol regulates prostasome release from secretory lysosomes in PC-3 human prostate cancer cells. *Eur J Cell Biol*, 2007. **86**(7): p. 405-15.
331. Locke, J.A., L. Fazli, H. Adomat, J. Smyl, K. Weins, A.A. Lubik, D.B. Hales, C.C. Nelson, M.E. Gleave, and E.S. Tomlinson Guns, A novel communication role for CYP17A1 in the progression of castration-resistant prostate cancer. *Prostate*, 2009. **69**(9): p. 928-37.
332. Locke, J.A., E.S. Guns, A.A. Lubik, H.H. Adomat, S.C. Hendy, C.A. Wood, S.L. Ettinger, M.E. Gleave, and C.C. Nelson, Androgen levels increase by intratumoral de novo steroidogenesis during progression of castration-resistant prostate cancer. *Cancer Res*, 2008. **68**(15): p. 6407-15.
333. Gunn, J.M., R.W. Hanson, O. Meyuhas, L. Reshef, and F.J. Ballard, Glucocorticoids and the regulation of phosphoenolpyruvate carboxykinase (guanosine triphosphate) in the rat. *Biochem J*, 1975. **150**(2): p. 195-203.
334. Seitz, H.J., M.J. Muller, P. Nordmeyer, W. Krone, and W. Tarnowski, Concentration of cyclic AMP in rat liver as a function of the insulin/glucagon ratio in blood under standardized physiological conditions. *Endocrinology*, 1976. **99**(5): p. 1313-8.
335. Okamoto, H., Y. Ohashi, and N. Itoh, Involvement of leukocyte and glucocorticoid in the acute-phase response of angiotensinogen. *Biochem Biophys Res Commun*, 1987. **145**(3): p. 1225-30.

336. Thompson, W.L., F.B. Abeles, F.A. Beall, R.E. Dinterman, and R.W. Wannemacher, Jr., Influence of the adrenal glucocorticoids on the stimulation of synthesis of hepatic ribonucleic acid and plasma acute-phase globulins by leucocytic endogenous mediator. *Biochem J*, 1976. **156**(1): p. 25-32.
337. Snyder, D.S. and E.R. Unanue, Corticosteroids inhibit murine macrophage Ia expression and interleukin 1 production. *J Immunol*, 1982. **129**(5): p. 1803-5.
338. Beutler, B., N. Krochin, I.W. Milsark, C. Luedke, and A. Cerami, Control of cachectin (tumor necrosis factor) synthesis: mechanisms of endotoxin resistance. *Science*, 1986. **232**(4753): p. 977-80.
339. Mosesson, Y., G.B. Mills, and Y. Yarden, Derailed endocytosis: an emerging feature of cancer. *Nat Rev Cancer*, 2008. **8**(11): p. 835-50.
340. Lee, S.M., C.A. Casey, and B.L. McVicker, Impact of asialoglycoprotein receptor deficiency on the development of liver injury. *World J Gastroenterol*, 2009. **15**(10): p. 1194-200.
341. Treichel, U., E. Paietta, T. Poralla, K.H. Meyer zum Buschenfelde, and R.J. Stockert, Effects of cytokines on synthesis and function of the hepatic asialoglycoprotein receptor. *J Cell Physiol*, 1994. **158**(3): p. 527-34.
342. Sawamura, T., H. Nakada, H. Hazama, Y. Shiozaki, Y. Sameshima, and Y. Tashiro, Hyperasialoglycoproteinemia in patients with chronic liver diseases and/or liver cell carcinoma. Asialoglycoprotein receptor in cirrhosis and liver cell carcinoma. *Gastroenterology*, 1984. **87**(6): p. 1217-21.
343. Kaup, M., K. Dassler, C. Weise, and H. Fuchs, Shedding of the transferrin receptor is mediated constitutively by an integral membrane metalloprotease sensitive to tumor necrosis factor alpha protease inhibitor-2. *J Biol Chem*, 2002. **277**(41): p. 38494-502.
344. Hara-Kuge, S., T. Ohkura, A. Seko, and K. Yamashita, Vesicular-integral membrane protein, VIP36, recognizes high-mannose type glycans containing alpha1-->2 mannosyl residues in MDCK cells. *Glycobiology*, 1999. **9**(8): p. 833-9.
345. Murata, K. and A. Sakamoto, Impairment of clathrin-mediated endocytosis via cytoskeletal change by epithelial to fibroblastoid conversion in HepG2 cells: a possible mechanism of des-gamma-carboxy prothrombin production in hepatocellular carcinoma. *Int J Oncol*, 2008. **33**(6): p. 1149-55.
346. Butler, P.C., E.J. Kryshak, W.F. Schwenk, M.W. Haymond, and R.A. Rizza, Hepatic and extrahepatic responses to insulin in NIDDM and nondiabetic humans. Assessment in absence of artifact introduced by tritiated nonglucose contaminants. *Diabetes*, 1990. **39**(2): p. 217-25.
347. Tayek, J.A., A review of cancer cachexia and abnormal glucose metabolism in humans with cancer. *J Am Coll Nutr*, 1992. **11**(4): p. 445-56.
348. Doi, C., Y. Noguchi, T. Ito, T. Yoshikawa, T. Makino, and A. Matsumoto, Alteration in immunoexpression of glucose transporter 2 in liver of tumour-bearing rats. *Int J Exp Pathol*, 1998. **79**(1): p. 25-31.
349. Kibbey, M.C., Maintenance of the EHS sarcoma and Matrigel preparation. *Journal of Tissue Culture Methods*, 1994. **16**(3-4): p. 227-230.
350. Xiong, Y.S., Y.H. Zhou, G.H. Rong, W.L. Wu, Y. Liang, Z.X. Yang, H.L. Geng, and R.Q. Zhong, Siglec-1 on monocytes is a potential risk marker for monitoring disease severity in coronary artery disease. *Clin Biochem*, 2009. **42**(10-11): p. 1057-63.
351. Arcinas, A., T.Y. Yen, E. Kebebew, and B.A. Macher, Cell surface and secreted protein profiles of human thyroid cancer cell lines reveal distinct glycoprotein patterns. *J Proteome Res*, 2009. **8**(8): p. 3958-68.
352. Comunale, M.A., M. Lowman, R.E. Long, J. Krakover, R. Philip, S. Seeholzer, A.A. Evans, H.W. Hann, T.M. Block, and A.S. Mehta, Proteomic analysis of serum associated fucosylated glycoproteins in the development of primary hepatocellular carcinoma. *J Proteome Res*, 2006. **5**(2): p. 308-15.

353. Dwek, M.V., H.A. Ross, and A.J. Leathem, Proteome and glycosylation mapping identifies post-translational modifications associated with aggressive breast cancer. *Proteomics*, 2001. **1**(6): p. 756-62.
354. Diaz, S.L., V. Padler-Karavani, D. Ghaderi, N. Hurtado-Ziola, H. Yu, X. Chen, E.C. Brinkman-Van der Linden, A. Varki, and N.M. Varki, Sensitive and specific detection of the non-human sialic Acid N-glycolylneuraminic acid in human tissues and biotherapeutic products. *PLoS One*, 2009. **4**(1): p. e4241.
355. Padler-Karavani, V., H. Yu, H. Cao, H. Chokhawala, F. Karp, N. Varki, X. Chen, and A. Varki, Diversity in specificity, abundance, and composition of anti-Neu5Gc antibodies in normal humans: potential implications for disease. *Glycobiology*, 2008. **18**(10): p. 818-30.
356. Kim, Y.J. and A. Varki, Perspectives on the significance of altered glycosylation of glycoproteins in cancer. *Glycoconj J*, 1997. **14**(5): p. 569-76.
357. Bongaerts, G.P., H.K. van Halteren, C.A. Verhagen, and D.J. Wagener, Cancer cachexia demonstrates the energetic impact of gluconeogenesis in human metabolism. *Med Hypotheses*, 2006. **67**(5): p. 1213-22.

Supplementary Tables Index (Attached CD)

Supplementary Table 1: Proteins identified in the membrane pellet following differential centrifugation.

Supplementary Table 2: Lectin affinity fractionation of the sodium carbonate-treatment membrane pellet.

Supplementary Table 3: Membrane proteins identified in the detergent phase following Triton X-114 phase partitioning.

Supplementary Table 4a: Triton X-114 phase partitioned membrane proteins followed by ConA lectin affinity chromatography.

Supplementary Table 4b: Triton X-114 phase partitioned membrane proteins followed by Jacalin lectin affinity chromatography.

Supplementary Table 4c: Triton X-114 phase partitioned membrane proteins followed by WGA lectin affinity chromatography.

Supplementary Table 5: Triton X-114 phase partitioned membrane proteins followed by hydrazine chemistry.

Supplementary Table 6: Enzymes involved in the glycosylation pathway and cell surface lectins identified in the livers of EHS-bearing mice (Chapter 4)

Supplementary Table 7: Assigned *N*- and *O*-glycans identified in EHS-bearing and control mice.

Supplementary Table 8, 8-1 and 8-2: Protein identifications from control, non-cachectic and cachectic C26-bearing mouse liver membrane preparations. Spectral counts of each identified protein and their normalised values to their molecular weight and total spectra in the entire protein dataset.

Supplementary Tables

Supplementary Table 1
Proteins identified in the membrane pellet following differential centrifugation (Chapter 3)

Identifier	# peptides	log(e) score	Description	Glycosylation (N-X-S/T)	Accession No.
ENSRNOP00000003965	149	-173.8	ATP synthase subunit beta, mitochondrial precursor (EC 3.6.3.14).	0	P10719
ENSRNOP00000022892	118	-135.5	ATP synthase subunit alpha, mitochondrial precursor (EC 3.6.3.14).	1	P15999
ENSRNOP00000002732	56	-85.3	ATP synthase O subunit, mitochondrial precursor (EC 3.6.3.14) (Oligomycin sensitivity conferral protein) (OSCP).	0	Q06647
ENSRNOP00000043239	47	-82.5	UDP-glucuronosyltransferase 2B3 precursor (EC 2.4.1.17) (UDPGT) (Testosterone, dihydrotestosterone, and beta-estradiol specific) (17-beta-hydroxysteroid specific) (UDPGTr-3) (RLUG38).	0	P08542
ENSRNOP00000044296	10	-61	Actin, cytoplasmic 1 (Beta-actin).	1	P60711
ENSRNOP00000013816	43	-51.8	No other features on this peptide	0	
ENSRNOP00000017472	45	-51.3	Prohibitin-2 (B-cell receptor-associated protein BAP37) (BAP-37).	2	Q5XIH7
ENSRNOP00000014235	38	-48.7	Long-chain-fatty-acid--CoA ligase 1 (EC 6.2.1.3) (Long-chain acyl-CoA synthetase 1) (LACS 1) (Long-chain-fatty-acid--CoA ligase, liver isozyme).	3	P18163
ENSRNOP00000014630	10	-48.1	No description available.Protein Family: MICROSOMAL TRIGLYCERIDE TRANSFER LARGE SUBUNIT PRECURSOR	1	
ENSRNOP00000051841	26	-46.4	Protein disulfide-isomerase precursor (EC 5.3.4.1) (PDI) (Prolyl 4-hydroxylase subunit beta) (Cellular thyroid hormone-binding protein)	0	P04785
ENSRNOP00000014464	10	-43.3	Annexin A6 (Annexin-6) (Annexin VI) (Lipocortin VI) (P68) (P70) (Protein III) (Chromobindin-20) (67 kDa calelectrin) (Calphobindin-II) (CPB-II) (Calcium-binding protein CATA 65/67).	1	P48037
ENSRNOP00000042597	20	-41.6	Liver carboxylesterase 4 precursor (EC 3.1.1.1) (Carboxyesterase ES-4) (Microsomal palmitoyl-CoA hydrolase) (Kidney microsomal carboxylesterase).	1	Q64573
ENSRNOP00000034723	55	-41.5	UDP-glucuronosyltransferase 2B2 precursor (EC 2.4.1.17) (UDPGT) (3- hydroxyandrogen specific) (UDPGTr-4) (RLUG23)	1	P08541
ENSRNOP00000010209	7	-41.3	Dolichyl-diphosphooligosaccharide--protein glycosyltransferase 63 kDa subunit precursor (EC 2.4.1.119) (Ribophorin II) (RPN-II).	2	P25235
ENSRNOP00000012413	9	-39.9	Cytochrome P450 2D26 (EC 1.14.14.1) (CYPIID26) (P450-DB2) (P450-CMF2) (Debrisoquine 4-hydroxylase).	3	P10634
ENSRNOP00000021920	12	-37.4	ATP synthase B chain, mitochondrial precursor (EC 3.6.3.14)	0	P19511
ENSRNOP00000020002	5	-34.2	Aminopeptidase N (EC 3.4.11.2) (rAPN) (Alanyl aminopeptidase) (Microsomal aminopeptidase) (Aminopeptidase M) (APM) (Kidney Zn peptidase) (KZP) (CD13 antigen)	6	P15684

ENSRNOP00000012425	13	-34.1	No description available.Protein Family: NADH DEHYDROGENASE IRON SULFUR 3 MITOCHONDRIAL PRECURSOR EC_1.6.5.3 EC_1.6.99.- 3 NADH UBIQUINONE OXIDOREDUCTASE 30 KDA SUBUNIT COMPLEX I 30KD CI 30KD	0	
ENSRNOP00000046414	16	-30.7	Cytochrome c oxidase subunit 2 (EC 1.9.3.1) (Cytochrome c oxidase polypeptide II).	0	P00406
ENSRNOP00000004941	5	-26.7	Leucine-rich repeat-containing protein 59 (Protein p34)	1	Q5RJR8
ENSRNOP00000015913	19	-25.5	ADP/ATP translocase 2 (Adenine nucleotide translocator 2) (ANT 2) (ADP,ATP carrier protein 2) (Solute carrier family 25 member 5).	1	Q09073
ENSRNOP00000050581	14	-25.4	Corticosteroid 11-beta-dehydrogenase isozyme 1 (EC 1.1.1.146) (11-DH) (11-beta-hydroxysteroid dehydrogenase 1) (11-beta-HSD1)	2	P16232
ENSRNOP00000045002	19	-24	UDP-glucuronosyltransferase 2B3 precursor (EC 2.4.1.17) (UDPGT) (Testosterone, dihydrotestosterone, and beta-estradiol specific) (17-beta-hydroxysteroid specific) (UDPGTr-3) (RLUG38).	0	P08542
ENSRNOP00000015802	6	-23.6	No description available.Protein Family: CYTOCHROME P450 2	1	
ENSRNOP00000053675	7	-22.1	No other features on this peptide	1	
ENSRNOP00000004686	6	-22	Ornithine carbamoyltransferase, mitochondrial precursor (EC 2.1.3.3) (OTCase) (Ornithine transcarbamylase).	3	P00481
ENSRNOP00000002712	12	-21.6	UDP-glucuronosyltransferase 2B4 precursor (EC 2.4.1.17) (UDPGT) (UDP- glucuronosyltransferase 2B12).	0	P36511
ENSRNOP00000034293	4	-21.5	Epoxide hydrolase 1 (EC 3.3.2.9) (Microsomal epoxide hydrolase) (Epoxide hydratase).	1	P07687
ENSRNOP00000041174	11	-21.3	Cytochrome P450 2D1 (EC 1.14.14.1) (CYPIID1) (P450-DB1) (P450-CMF1A) (P450-UT-7) (Debrisoquine 4-hydroxylase).	4	P10633
ENSRNOP00000008477	9	-20.1	Voltage-dependent anion-selective channel protein 1 (VDAC-1) (rVDAC1) (Outer mitochondrial membrane protein porin 1).	2	Q9Z2L0
ENSRNOP00000045886	10	-18.9	Fatty aldehyde dehydrogenase (EC 1.2.1.3) (Aldehyde dehydrogenase, microsomal) (Aldehyde dehydrogenase family 3 member A2) (Aldehyde dehydrogenase 10).	0	P30839
ENSRNOP00000001816	9	-18.8	Aldehyde dehydrogenase, mitochondrial precursor (EC 1.2.1.3) (ALDH class 2) (ALDH1) (ALDH-E2).	1	P11884
ENSRNOP00000051846	6	-17.8	solute carrier family 25 (mitochondrial carrier; dicarboxylate transporter), member 10 Source: RefSeq_peptide NP_596909	1	O89035_RAT
ENSRNOP00000020306	3	-17.7	dolichyl-di-phosphooligosaccharide-protein glycotransferase (predicted) Source: RefSeq_peptide NP_001012104	0	
ENSRNOP00000016883	8	-17.4	Cytochrome P450 2E1 (EC 1.14.14.1) (CYPIIE1) (P450-J) (P450RLM6).	2	P05182

ENSRNOP00000019624	3	-17.4	No description available.Protein Family: NADH DEHYDROGENASE 1 BETA SUBCOMPLEX SUBUNIT 10 EC_1.6.5.3 EC_1.6.99.- 3 NADH UBIQUINONE OXIDOREDUCTASE PDSW SUBUNIT COMPLEX I PDSW CI PDSW	1	
ENSRNOP00000046654	3	-17.2	Carcinoembryonic antigen-related cell adhesion molecule 1 precursor (Cell-CAM 105) (C-CAM 105) (Ecto-ATPase) (ATP-dependent taurocolate- carrier protein) (GP110) (pp120)	16	P16573
ENSRNOP00000055824	3	-16.8	Dipeptidyl peptidase 4 (EC 3.4.14.5) (Dipeptidyl peptidase IV) (DPP IV) (T-cell activation antigen CD26) (GP110 glycoprotein) (Bile canaliculus domain-specific membrane glycoprotein) [Contains: Dipeptidyl peptidase 4 membrane form (Dipeptidyl peptidase IV	9	P14740
ENSRNOP00000019571	4	-16.5	All-trans-retinol 13,14-reductase precursor (EC 1.3.99.23) (All-trans-13,14-dihydroretinol saturase) (RetSat) (RMT-7)	0	Q8VHE9
ENSRNOP00000021215	6	-14.7	similar to prohibitin (LOC364817), mRNA Source: RefSeq_dna XR_005946	1	0
ENSRNOP00000048711	2	-13.6	Cytochrome P450 2D3 (EC 1.14.14.1) (CYPIID3) (P450-DB3) (Debrisoquine 4-hydroxylase)	1	P12938
ENSRNOP00000026794	2	-13.2	No description available.Protein Family: ALPHA GLUCOSIDASE	7	
ENSRNOP00000054537	2	-12.4	lysosomal-associated membrane protein 1	18	
ENSRNOP00000028237	5	-12.2	Cytochrome P450 2A1 (EC 1.14.14.1) (CYPIIA1) (Steroid hormones 7- alpha-hydroxylase) (Testosterone 7-alpha-hydroxylase) (P450-UT-F).	1	P11711
ENSRNOP00000017101	2	-12.2	Membrane-associated progesterone receptor component 1 (Acidic 25 kDa protein) (25-DX) (Ventral midline antigen) (VEMA)	0	P70580
ENSRNOP00000020681	2	-12	Vesicle-associated membrane protein-associated protein A (VAMP-associated protein A) (VAMP-A) (VAP-A) (33 kDa Vamp-associated protein) (VAP-33).	5	Q9Z270
ENSRNOP00000017310	3	-11.2	Cytochrome P450 2C11 (EC 1.14.14.1) (CYPIIC11) (P-450(M-1)) (P450H) (P450-UT-A) (UT-2).	1	P08683
ENSRNOP00000041608	4	-11.1	Phosphate carrier protein, mitochondrial precursor (PTP) (Solute carrier family 25 member 3)	0	P16036
ENSRNOP00000018336	7	-10.7	Succinate dehydrogenase flavoprotein subunit, mitochondrial precursor (EC 1.3.5.1) (Fp) (Flavoprotein subunit of complex II)	0	Q920L2
ENSRNOP00000015598	3	-10.6	Ras-related protein Rab-11A (Rab-11) (24KG).	0	P62494
ENSRNOP00000025045	3	-10.3	UDP-glucuronosyltransferase 1-1 precursor (EC 2.4.1.17) (UDPGT) (UGT1*1) (UGT1-01) (UGT1.1) (UGT1A1) (B1).	2	Q64550
ENSRNOP00000010579	20	-9.7	Microsomal glutathione S-transferase 1 (EC 2.5.1.18) (Microsomal GST- 1) (Microsomal GST-I).	0	P08011

ENSRNOP00000026290	21	-9.5	3 beta-hydroxysteroid dehydrogenase type 5 (3 beta-hydroxysteroid dehydrogenase type V) (3-beta-HSD V) (NADPH-dependent 3-beta-hydroxy- Delta(5)-steroid dehydrogenase) (EC 1.1.1.-) (3-beta-hydroxy-5-ene steroid dehydrogenase) (Progesterone reductase).	2	P22071
ENSRNOP00000013279	3	-9.3	butyrylcholinesterase Source: RefSeq_peptide NP_075231	8	
ENSRNOP00000013262	2	-9.3	Electron transfer flavoprotein-ubiquinone oxidoreductase, mitochondrial precursor (EC 1.5.5.1) (ETF-QO) (ETF-ubiquinone oxidoreductase) (ETF dehydrogenase) (Electron-transferring-flavoprotein dehydrogenase).	1	Q6UPE1
ENSRNOP00000040859	7	-9.2	Calnexin precursor.	1	P35565
ENSRNOP00000054078	5	-9.1	Cytochrome P450 2A3 (EC 1.14.14.1) (CYPIIA3) (Coumarin 7-hydroxylase)	1	P20812
ENSRNOP00000002724	4	-8.9	UDP-glucuronosyltransferase 2B1 precursor (EC 2.4.1.17) (UDPGT) (UDPGTr-2).	2	P09875
ENSRNOP00000015851	2	-8.8	NADH-ubiquinone oxidoreductase 75 kDa subunit, mitochondrial precursor (EC 1.6.5.3) (EC 1.6.99.3).	1	Q66HF1
ENSRNOP00000029578	2	-8.7	nicotinamide nucleotide transhydrogenase Source: RefSeq_peptide NP_001013175	5	Q61941
ENSRNOP00000026290	21	-9.5	3 beta-hydroxysteroid dehydrogenase type 5 (3 beta-hydroxysteroid dehydrogenase type V) (3-beta-HSD V) (NADPH-dependent 3-beta-hydroxy- Delta(5)-steroid dehydrogenase) (EC 1.1.1.-) (3-beta-hydroxy-5-ene steroid dehydrogenase) (Progesterone reductase)	2	P22071
ENSRNOP00000057816	2	-8.3	Polymeric-immunoglobulin receptor precursor (Poly-Ig receptor) (PIGR)	3	P15083
ENSRNOP00000023526	2	-8.1	No description available.Protein Family: NADH DEHYDROGENASE IRON SULFUR 8 MITOCHONDRIAL PRECURSOR EC_1.6.5.3 EC_1.6.99.- 3 NADH UBIQUINONE OXIDOREDUCTASE 23 KDA SUBUNIT COMPLEX I 23KD CI 23KD	0	
ENSRNOP00000004836	15	-8.1	No description available.Protein Family: ATP SYNTHASE D CHAIN MITOCHONDRIAL EC_3.6.3.14	1	
ENSRNOP00000026574	3	-7.8	Bile acyl-CoA synthetase (EC 6.2.1.7) (BACS) (Bile acid CoA ligase) (BA-CoA ligase) (BAL) (Cholate--CoA ligase) (Very long chain acyl-CoA synthetase-related protein) (VLACS-related) (VLACSR) (Fatty acid transport protein 5) (FATP-5) (Solute carrier family	1	Q9ES38
ENSRNOP00000000177	2	-7.6	Lysosome-associated membrane glycoprotein 2 precursor (LAMP-2) (Lysosomal membrane glycoprotein-type B) (LGP-B) (LGP-96) (LGP-110) (CD107b antigen)	16	P17046

ENSRNOP00000044696	2	-7.5	Ubiquinol-cytochrome-c reductase complex core protein 1, mitochondrial precursor (EC 1.10.2.2) (Core I protein).	2	Q68FY0
ENSRNOP00000049879	2	-7.4	ATP synthase gamma chain, mitochondrial (EC 3.6.3.14).	4	P35435
ENSRNOP00000017180	4	-6.9	similar to eukaryotic translation elongation factor 1 alpha 2 (LOC364172), mRNA Source: RefSeq_dna XR_006078	1	
ENSRNOP00000030668	2	-6.8	transmembrane emp24 protein transport domain containing 9 Source: RefSeq_peptide NP_001009703	1	
ENSRNOP00000019552	2	-6.7	Annexin A5 (Annexin-5) (Annexin V) (Lipocortin V) (Endonexin II) (Calphobindin I) (CBP-I) (Placental anticoagulant protein I) (PAP-I) (PP4) (Thromboplastin inhibitor) (Vascular anticoagulant-alpha) (VAC-alpha) (Anchorin CII).	0	P14668
ENSRNOP00000043148	2	-6.6	Catechol O-methyltransferase (EC 2.1.1.6)	0	P22734
ENSRNOP00000017237	2	-6.3	Cytochrome P450 2C6 (EC 1.14.14.1) (CYPIIC6) (P450 PB1) (PTF2).	3	P05178
ENSRNOP00000006855	2	-6.3	Surfeit locus protein 1	1	Q9QXU2
ENSRNOP00000048723	3	-5.7	No other features on this peptide	1	
ENSRNOP00000024973	5	-5.7	Very-long-chain specific acyl-CoA dehydrogenase, mitochondrial precursor (EC 1.3.99.-) (VLCAD)	3	P45953
ENSRNOP00000024423	2	-5.7	Dimethylaniline monooxygenase 5 (EC 1.14.13.8) (Hepatic flavin-containing monooxygenase 5) (FMO 5) (Dimethylaniline oxidase 5)	2	Q8K4C0
ENSRNOP00000027760	2	-5.4	CD81 antigen (26 kDa cell surface protein TAPA-1) (Target of the antiproliferative antibody 1)	0	Q62745
ENSRNOP00000035416	2	-5.4	No description available.Protein Family: SYNAPTIC GLYCOPROTEIN SC2	3	0
ENSRNOP00000004864	2	-5.3	Dimethylaniline monooxygenase 3 (EC 1.14.13.8) (Hepatic flavin-containing monooxygenase 3) (FMO 3) (Dimethylaniline oxidase 3)	3	Q9EQ76
ENSRNOP00000010760	2	-4.9	Methyltransferase-like protein 7B precursor (EC 2.1.1.-) (Associated with lipid droplet protein 1) (ALDI).	0	Q562C4
ENSRNOP00000012448	14	-4.3	Cytochrome P450 4X1 (EC 1.14.14.1) (CYPIVX1)	3	Q8K4D6
ENSRNOP00000012233	2	-4.3	Dolichyl-diphosphooligosaccharide--protein glycosyltransferase subunit DAD1 (EC 2.4.1.119) (Oligosaccharyl transferase subunit DAD1) (Defender against cell death 1) (DAD-1)	0	P61805
ENSRNOP00000052656	2	-4.2	Clathrin heavy chain	6	P11442
ENSRNOP00000013607	3	-4.2	Solute carrier family 27 (Fatty acid transporter), member 2	2	Q66HN6
ENSRNOP00000027520	2	-3.7	Mitochondrial carnitine/acylcarnitine carrier protein (Carnitine/acylcarnitine translocase) (CAC) (Solute carrier family 25 member 20)	0	P97521
ENSRNOP00000039545	2	-3.5	Cytochrome P450 4F4 (EC 1.14.14.1) (CYPIVF4)	3	Q498D5
ENSRNOP00000009511	2	-3.3	Ras-related protein Rap-1b precursor (GTP-binding protein smg p21B).	0	Q62636

ENSRNOP00000051361	2	-3.1	Dimethylaniline monooxygenase 1 (EC 1.14.13.8) (Hepatic flavin-containing monooxygenase 1) (FMO 1) (Dimethylaniline oxidase 1)	2	P36365
ENSRNOP00000002806	2	-3	Annexin A3 (Annexin-3) (Annexin III) (Lipocortin III) (Placental anticoagulant protein III) (PAP-III) (35-alpha calcimedin)	1	P14669
ENSRNOP00000045029	2	-3	Cytochrome P450 2C7 (EC 1.14.14.1) (CYPIIC7) (P450F) (PTF1)	1	P05179
ENSRNOP00000011773	5	-26	Actin, alpha cardiac muscle 1 (Alpha-cardiac actin).	1	P68035
ENSRNOP00000005990	3	-4.1	Alpha-actinin-1 (Alpha-actinin cytoskeletal isoform) (Non-muscle alpha-actinin-1) (F-actin cross-linking protein)	1	Q9Z1P2
ENSRNOP00000011158	3	-19.6	Nipsnap1 protein (Fragment). Source: Uniprot/SPTREMBL Q5EBA4		
ENSRNOP00000053689	3	-15.9	No description available.Protein Family: UNKNOWN		
ENSRNOP00000010512	1	-5.7	No description available.Protein Family: PRECURSOR		
ENSRNOP00000034144	1	-3	nitrilase family, member 2 Source: RefSeq_peptide NP_001029298		
ENSRNOP00000034135	2	-2.9	Ndufa9 protein (Fragment). Source: Uniprot/SPTREMBL Q5BK63		
ENSRNOP00000056312	17	-34	tumor rejection antigen gp96 (predicted) Source: RefSeq_peptide NP_001012197		
ENSRNOP00000024452	4	-9.8	No description available.Protein Family: SERINE BETA LACTAMASE LACTB MITOCHONDRIAL PRECURSOR EC_3.4.-.-		
ENSRNOP00000024517	1	-4	NADH dehydrogenase (ubiquinone) flavoprotein 1, 51kDa Source: RefSeq_peptide NP_001006973		
ENSRNOP00000019021	110	-233.6	Carbamoyl-phosphate synthase , mitochondrial precursor (EC 6.3.4.16) (Carbamoyl-phosphate synthetase I) (CPSase I). Source: Uniprot/SWISSPROT P07756		
ENSRNOP00000002366	62	-115.1	D-beta-hydroxybutyrate dehydrogenase, mitochondrial precursor (EC 1.1.1.30) (BDH) (3-hydroxybutyrate dehydrogenase). Source: Uniprot/SWISSPROT P29147		
ENSRNOP00000025064	39	-91.1	78 kDa glucose-regulated protein precursor (GRP 78) (Heat shock 70 kDa protein 5) (Immunoglobulin heavy chain-binding protein) (BiP) (Steroidogenesis-activator polypeptide). Source: Uniprot/SWISSPROT P06761		
ENSRNOP00000020478	20	-55.9	Protein disulfide-isomerase A3 precursor (EC 5.3.4.1) (Disulfide isomerase ER-60) (ERp60) (58 kDa microsomal protein) (p58) (ERp57) (HIP-70) (Q-2). Source: Uniprot/SWISSPROT P11598		
ENSRNOP00000003921	68	-54.3	Serum albumin precursor. Source: Uniprot/SWISSPROT P02770		
ENSRNOP00000001958	23	-53.5	Malate dehydrogenase, mitochondrial precursor (EC 1.1.1.37). Source: Uniprot/SWISSPROT P04636		
ENSRNOP00000040121	20	-52.7	Transitional endoplasmic reticulum ATPase (TER ATPase) (15S Mg(2+)- ATPase p97 subunit) (Valosin-containing protein) (VCP). Source: Uniprot/SWISSPROT P46462		

ENSRNOP00000014177	40	-42.4	Carbonic anhydrase 3 (EC 4.2.1.1) (Carbonic anhydrase III) (Carbonate dehydratase III) (CA-III). Source: Uniprot/SWISSPROT P14141		
ENSRNOP00000001518	16	-39.6	60S acidic ribosomal protein P0 (L10E). Source: Uniprot/SWISSPROT P19945		
ENSRNOP00000011333	11	-39.4	40S ribosomal protein S7 (S8). Source: Uniprot/SWISSPROT P62083		
ENSRNOP00000021812	27	-39.4	Carboxylesterase 3 precursor (EC 3.1.1.1) (Liver carboxylesterase 10) (Carboxyesterase ES-10) (pI 6.1 esterase) (ES-HVEL). Source: Uniprot/SWISSPROT P16303		
ENSRNOP00000026122	10	-37.3	Hydroxymethylglutaryl-CoA synthase, mitochondrial precursor (EC 2.3.3.10) (HMG-CoA synthase) (3-hydroxy-3-methylglutaryl coenzyme A synthase). Source: Uniprot/SWISSPROT P22791		
ENSRNOP00000004091	12	-36.9	Calreticulin precursor (CRP55) (Calregulin) (HACBP) (ERp60) (CALBP) (Calcium-binding protein 3) (CABP3). Source: Uniprot/SWISSPROT P18418		
ENSRNOP00000025224	7	-35.7	40S ribosomal protein SA (p40) (34/67 kDa laminin receptor). Source: Uniprot/SWISSPROT P38983		
ENSRNOP00000017911	9	-34.6	Arginase-1 (EC 3.5.3.1) (Type I arginase) (Liver-type arginase). Source: Uniprot/SWISSPROT P07824		
ENSRNOP00000043608	16	-29.1	3-hydroxyacyl-CoA dehydrogenase type-2 (EC 1.1.1.35) (3-hydroxyacyl- CoA dehydrogenase type II) (Type II HADH) (3-hydroxy-2-methylbutyryl- CoA dehydrogenase) (EC 1.1.1.178) (Endoplasmic reticulum-associated amyloid beta-peptide-binding protein). Source: U		
ENSRNOP00000039050	20	-27.6	Glutathione S-transferase Mu 1 (EC 2.5.1.18) (GSTM1-1) (Glutathione S- transferase Yb-1) (GST Yb1) (GST 3-3). Source: Uniprot/SWISSPROT P04905		
ENSRNOP00000014637	18	-27.2	Trifunctional enzyme subunit beta, mitochondrial precursor (TP-beta) . Source: Uniprot/SWISSPROT Q60587		
ENSRNOP00000025939	15	-26.8	Glutathione S-transferase Mu 2 (EC 2.5.1.18) (GSTM2-2) (Glutathione S- transferase Yb-2) (GST Yb2) (GST 4-4). Source: Uniprot/SWISSPROT P08010		
ENSRNOP00000010573	10	-26.4	Acetyl-CoA acetyltransferase, mitochondrial precursor (EC 2.3.1.9) (Acetoacetyl-CoA thiolase). Source: Uniprot/SWISSPROT P17764		
ENSRNOP00000013789	4	-25.7	Glutamate dehydrogenase 1, mitochondrial precursor (EC 1.4.1.3) (GDH) (Memory-related protein 2) (MRG-2). Source: Uniprot/SWISSPROT P10860		
ENSRNOP00000021970	11	-25.6	Uricase (EC 1.7.3.3) (Urate oxidase). Source: Uniprot/SWISSPROT P09118		

ENSRNOP00000048250	26	-25.5	Hemoglobin subunit beta-1 (Hemoglobin beta-1 chain) (Beta-1-globin) (Hemoglobin beta chain, major-form). Source: Uniprot/SWISSPROT P02091		
ENSRNOP00000055923	7	-25.1	similar to ribosomal protein L10a (LOC435570), mRNA Source: RefSeq_dna XR_004012		
ENSRNOP00000011784	3	-23.8	3,2-trans-enoyl-CoA isomerase, mitochondrial precursor (EC 5.3.3.8) (Dodecenoyl-CoA isomerase) (Delta(3),Delta(2)-enoyl-CoA isomerase) (D3,D2-enoyl-CoA isomerase). Source: Uniprot/SWISSPROT P23965		
ENSRNOP00000014658	15	-23.8	Hydroxyacyl-coenzyme A dehydrogenase, mitochondrial precursor (EC 1.1.1.35) (Short chain 3-hydroxyacyl-CoA dehydrogenase) (HCDH) (Medium and short chain L-3-hydroxyacyl-coenzyme A dehydrogenase). Source: Uniprot/SWISSPROT Q9WVK7		
ENSRNOP00000037786	8	-23.6	Glutathione S-transferase alpha-2 (EC 2.5.1.18) (Glutathione S-transferase Ya-2) (GST Ya2) (GST 1b-1b) (GST A2-2). Source: Uniprot/SWISSPROT P04903		
ENSRNOP00000009111	11	-23.3	Fructose-bisphosphate aldolase B (EC 4.1.2.13) (Liver-type aldolase). Source: Uniprot/SWISSPROT P00884		
ENSRNOP00000017954	4	-23.1	Fumarylacetoacetase (EC 3.7.1.2) (Fumarylacetoacetate hydrolase) (Beta-diketonase) (FAA). Source: Uniprot/SWISSPROT P25093		
ENSRNOP00000019912	5	-23	60 kDa heat shock protein, mitochondrial precursor (Hsp60) (60 kDa chaperonin) (CPN60) (Heat shock protein 60) (HSP-60) (Mitochondrial matrix protein P1) (HSP-65). Source: Uniprot/SWISSPROT P63039		
ENSRNOP00000029068	35	-22.3	Keratin, type II cytoskeletal 8 (Cytokeratin-8) (CK-8) (Keratin-8) (K8) (Cytokeratin endo A). Source: Uniprot/SWISSPROT Q10758		
ENSRNOP00000023935	5	-21.2	40S ribosomal protein S3. Source: Uniprot/SWISSPROT P62909		
ENSRNOP00000024782	6	-20.9	Dehydrogenase/reductase SDR family member 4 (EC 1.1.1.184) (NADPH- dependent carbonyl reductase/NADP-retinol dehydrogenase) (CR) (PHCR) (Peroxisomal short-chain alcohol dehydrogenase) (NADPH-dependent retinol dehydrogenase/reductase) (NDRD). Source: Unipr		
ENSRNOP00000035423	25	-20.1	Retinol dehydrogenase 2 (EC 1.1.1.105) (Retinol dehydrogenase type II) (RODH II) (29 k-protein). Source: Uniprot/SWISSPROT P50170		
ENSRNOP00000021512	6	-19.8	Peroxisomal trans-2-enoyl-CoA reductase (EC 1.3.1.38) (RLF98) (Peroxisomal 2,4-dienoyl CoA reductase) (PX-2,4-DCR1). Source: Uniprot/SWISSPROT Q9WVK3		
ENSRNOP00000056469	6	-19.1	No description available.Protein Family: HISTONE H2A		

ENSRNOP00000043510	8	-17.3	Glutathione S-transferase alpha-1 (EC 2.5.1.18) (Glutathione S-transferase Ya-1) (GST Ya1) (Ligandin) (GST 1a-1a) (GST B) (GST 1-1) (GST A1-1). Source: Uniprot/SWISSPROT P00502		
ENSRNOP00000042159	3	-16.6	No description available.Protein Family: UNKNOWN		
ENSRNOP00000039702	2	-16	triosephosphate isomerase Source: RefSeq_peptide NP_001028244		
ENSRNOP00000028770	35	-15.6	No description available.Protein Family: HISTONE H2B		
ENSRNOP00000009467	6	-15.4	Alpha-1-macroglobulin precursor (Alpha-1-M) . Source: Uniprot/SWISSPROT Q63041		
ENSRNOP00000056595	3	-14.8	No description available.Protein Family: UNKNOWN		
ENSRNOP00000011823	6	-14.1	Serum paraoxonase/arylesterase 1 (EC 3.1.1.2) (EC 3.1.8.1) (PON 1) (Serum aryldialkylphosphatase 1) (A-esterase 1) (Aromatic esterase 1). Source: Uniprot/SWISSPROT P55159		
ENSRNOP00000042628	5	-14.1	similar to Tubulin alpha-2 chain (Alpha-tubulin 2) (predicted) (RGD1565476_predicted), mRNA Source: RefSeq_dna NM_001044270		
ENSRNOP00000044081	17	-13.3	hemoglobin alpha 2 chain Source: RefSeq_peptide NP_001007723		
ENSRNOP00000025844	6	-12.9	60S ribosomal protein L14. Source: Uniprot/SWISSPROT Q63507		
ENSRNOP00000041462	6	-12.7	60S ribosomal protein L12. Source: Uniprot/SWISSPROT P23358		
ENSRNOP00000057443	7	-12.6	Glutathione S-transferase alpha-5 (EC 2.5.1.18) (Glutathione S-transferase Yc-2) (GST Yc2) (GST A5-5). Source: Uniprot/SWISSPROT P46418		
ENSRNOP00000038073	15	-12.5	Trifunctional enzyme subunit alpha, mitochondrial precursor (TP-alpha) . Source: Uniprot/SWISSPROT Q64428		
ENSRNOP00000042411	5	-12.2	Histone H4 . Source: Uniprot/SWISSPROT P62804		
ENSRNOP00000050293	17	-10.9	No description available.Protein Family: 40S RIBOSOMAL S10		
ENSRNOP00000004491	11	-9.5	No description available.Protein Family: HETEROGENEOUS NUCLEAR RIBONUCLEOPROTEIN HNRNP		
ENSRNOP00000015336	8	-9.4	Betaine--homocysteine S-methyltransferase 1 (EC 2.1.1.5). Source: Uniprot/SWISSPROT O09171		
ENSRNOP00000056824	4	-9.3	Dihydrolipoyl dehydrogenase, mitochondrial precursor (EC 1.8.1.4) (Dihydrolipoamide dehydrogenase). Source: Uniprot/SWISSPROT Q6P6R2		
ENSRNOP00000009431	5	-9.2	60S ribosomal protein L7. Source: Uniprot/SWISSPROT P05426		
ENSRNOP00000049473	1	-8.8	Alpha-1-inhibitor 3 precursor (Alpha-1-inhibitor III) (Alpha-1- inhibitor 3 variant II). Source: Uniprot/SWISSPROT P14046		
ENSRNOP00000018820	12	-8.6	60S acidic ribosomal protein P1. Source: Uniprot/SWISSPROT P19944		
ENSRNOP00000026528	4	-8.5	40S ribosomal protein S5. Source: Uniprot/SWISSPROT P24050		

ENSRNOP00000022828	1	-8.3	Peptidyl-prolyl cis-trans isomerase B precursor (EC 5.2.1.8) (PPIase) (Rotamase) (Cyclophilin B) (S-cyclophilin) (SCYLP) (CYP-S1). Source: Uniprot/SWISSPROT P24368		
ENSRNOP00000005611	1	-8.3	4-trimethylaminobutyraldehyde dehydrogenase (EC 1.2.1.47) (TMABADH) (Aldehyde dehydrogenase 9A1) (EC 1.2.1.3). Source: Uniprot/SWISSPROT Q9JLJ3		
ENSRNOP00000020544	1	-8	Electron transfer flavoprotein subunit alpha, mitochondrial precursor (Alpha-ETF). Source: Uniprot/SWISSPROT P13803		
ENSRNOP00000004278	9	-7.4	ribosomal protein S4, X-linked		
ENSRNOP00000056413	3	-7.4	Hypoxia up-regulated protein 1 precursor (150 kDa oxygen-regulated protein) (Orp150). Source: Uniprot/SWISSPROT Q63617		
ENSRNOP00000039338	3	-7.3	Thiosulfate sulfurtransferase (EC 2.8.1.1) (Rhodanese). Source: Uniprot/SWISSPROT P24329		
ENSRNOP00000046175	3	-7.2	No description available.Protein Family: HISTONE H2A		
ENSRNOP00000016346	10	-7.2	Alcohol dehydrogenase 1 (EC 1.1.1.1) (Alcohol dehydrogenase A subunit). Source: Uniprot/SWISSPROT P06757		
ENSRNOP00000041707	1	-7.2	No description available.Protein Family: 60S RIBOSOMAL L9		
ENSRNOP00000036106	1	-7.1	No other features on this peptide		
ENSRNOP00000013588	5	-6.5	No description available.Protein Family: 40S RIBOSOMAL S24		
ENSRNOP00000025794	2	-6.2	Superoxide dismutase , mitochondrial precursor (EC 1.15.1.1). Source: Uniprot/SWISSPROT P07895		
ENSRNOP00000022089	1	-6.2	NADH dehydrogenase 1 alpha subcomplex subunit 10, mitochondrial precursor (EC 1.6.5.3) (EC 1.6.99.3) (NADH-ubiquinone oxidoreductase 42 kDa subunit) (Complex I-42kD) (CI-42kD). Source: Uniprot/SWISSPROT Q561S0		
ENSRNOP00000026696	2	-6.2	Stress-70 protein, mitochondrial precursor (75 kDa glucose-regulated protein) (GRP 75) (Heat shock 70 kDa protein 9) (Peptide-binding protein 74) (PBP74) (MTHSP70) (Mortalin). Source: Uniprot/SWISSPROT P48721		
ENSRNOP00000026316	2	-5.2	Pyruvate carboxylase, mitochondrial precursor (EC 6.4.1.1) (Pyruvic carboxylase) (PCB). Source: Uniprot/SWISSPROT P52873		
ENSRNOP00000054026	1	-5.2	2-oxoglutarate dehydrogenase E1 component, mitochondrial precursor (EC 1.2.4.2) (Alpha-ketoglutarate dehydrogenase). Source: Uniprot/SWISSPROT Q5XI78		
ENSRNOP00000034299	1	-5.2	Keratin, type I cytoskeletal 18 (Cytokeratin-18) (CK-18) (Keratin-18) (K18). Source: Uniprot/SWISSPROT Q5BJY9		
ENSRNOP00000021055	2	-5	Plasma retinol-binding protein precursor (PRBP) (RBP). Source: Uniprot/SWISSPROT P04916		
ENSRNOP00000045215	1	-5	No description available.Protein Family: 60S RIBOSOMAL L18		

ENSRNOP00000018850	1	-5	3-ketoacyl-CoA thiolase, mitochondrial (EC 2.3.1.16) (Beta-ketothiolase) (Acetyl-CoA acyltransferase) (Mitochondrial 3-oxoacyl-CoA thiolase). Source: Uniprot/SWISSPROT P13437		
ENSRNOP00000000134	4	-4.8	Adenylate kinase isoenzyme 2, mitochondrial (EC 2.7.4.3) (ATP-AMP transphosphorylase). Source: Uniprot/SWISSPROT P29410		
ENSRNOP00000026928	1	-4.6	Proteasome subunit alpha type 5 (EC 3.4.25.1) (Proteasome zeta chain) (Macropain zeta chain) (Multicatalytic endopeptidase complex zeta chain). Source: Uniprot/SWISSPROT P34064		
ENSRNOP00000012050	2	-4.6	Serum paraoxonase/lactonase 3 (EC 3.1.1.-). Source: Uniprot/SWISSPROT Q68FP2		
ENSRNOP00000025446	1	-4.5	Enoyl-CoA hydratase, mitochondrial precursor (EC 4.2.1.17) (Short chain enoyl-CoA hydratase) (SCEH) (Enoyl-CoA hydratase 1). Source: Uniprot/SWISSPROT P14604		
ENSRNOP00000013863	3	-4.5	Tubulin beta-2C chain. Source: Uniprot/SWISSPROT Q6P9T8		
ENSRNOP00000028875	1	-4.1	similar to heterogeneous nuclear ribonucleoprotein A2/B1 (predicted) (RGD1562992_predicted), mRNA Source: RefSeq_dna XR_008579		
ENSRNOP00000024083	1	-4	Electron transfer flavoprotein subunit beta (Beta-ETF). Source: Uniprot/SWISSPROT Q68FU3		
ENSRNOP00000008503	1	-3.8	Apoptosis-inducing factor 1, mitochondrial precursor (EC 1.-.-.-) (Programmed cell death protein 8). Source: Uniprot/SWISSPROT Q9JM53		
ENSRNOP00000017332	1	-3.7	glycogen synthase 2		
ENSRNOP00000022307	1	-3.6	Glycine N-methyltransferase (EC 2.1.1.20) (Folate-binding protein). Source: Uniprot/SWISSPROT P13255		
ENSRNOP00000015234	1	-3.6	40S ribosomal protein S9. Source: Uniprot/SWISSPROT P29314		
ENSRNOP00000011330	2	-3.4	2,4-dienoyl-CoA reductase, mitochondrial precursor (EC 1.3.1.34) (2,4- dienoyl-CoA reductase). Source: Uniprot/SWISSPROT Q64591		
ENSRNOP00000048563	1	-3	C-reactive protein precursor. Source: Uniprot/SWISSPROT P48199		
ENSRNOP00000008728	2	-3	Protein disulfide-isomerase A4 precursor (EC 5.3.4.1) (Protein ERp-72) (ERp72) (Calcium-binding protein 2) (CaBP2). Source: Uniprot/SWISSPROT P38659		
ENSRNOP00000027494	2	-3.8	similar to heterogeneous nuclear ribonucleoprotein L isoform a (LOC679914), mRNA Source: RefSeq_dna XR_005602		
ENSRNOP00000014819	1	-4.4	Uncharacterized protein C10orf58 homolog precursor. Source: Uniprot/SWISSPROT Q6AXX6		

Supplementary Table 2

Lectin affinity fractionation of the membrane pellet (Chapter 3)

Identifier	Protein	SwissProt/Uniprot	ConA	Jacalin	WGA
ENSRNOP00000026290	3 beta-hydroxysteroid dehydrogenase type 5	P27364	13	6	3
ENSRNOP00000013816	Adenine nucleotide translocator 1		4	23	21
ENSRNOP00000015913	ADP/ATP translocase 2	Q09073	11	21	15
ENSRNOP00000022892	ATP synthase subunit alpha, mitochondrial precursor (EC 3.6.3.14).	P15999	2	4	6
ENSRNOP00000003965	ATP synthase subunit beta, mitochondrial precursor (EC 3.6.3.14).	P10719	1	2	3
ENSRNOP00000046414	Cytochrome c oxidase subunit 2 (EC 1.9.3.1) (Cytochrome c oxidase polypeptide II).	P00406	9	6	1
ENSRNOP00000017310	Cytochrome P450 2C11 (EC 1.14.14.1) (CYPIIC11) (P-450(M-1)) (P450H) (P450-UT-A) (UT-2).	P08683	10	5	5
ENSRNOP00000012413	Cytochrome P450 2D26 (EC 1.14.14.1) (CYPIID26) (P450-DB2) (P450-CMF2) (Debrisoquine 4-hydroxylase).	P10634	6	3	16
ENSRNOP00000010209	Dolichyl-diphosphooligosaccharide--protein glycosyltransferase 63 kDa subunit precursor (EC 2.4.1.119) (Ribophorin II) (RPN-II).	P25235	6	4	3
ENSRNOP00000034293	Epoxide hydrolase 1 (EC 3.3.2.9) (Microsomal epoxide hydrolase) (Epoxide hydratase).	P07687	2	2	2
ENSRNOP00000045886	Fatty aldehyde dehydrogenase (EC 1.2.1.3) (Aldehyde dehydrogenase, microsomal) (Aldehyde dehydrogenase family 3 member A2) (Aldehyde dehydrogenase 10).	P30839	6	14	9
ENSRNOP00000019772	Fibronectin precursor (FN).	P04937	5	8	4
ENSRNOP00000003334	Guanine nucleotide-binding protein subunit beta 2-like 1 (Receptor of activated protein kinase C 1) (RACK1) (Receptor for activated C kinase).	P63245	4	5	13
ENSRNOP00000042597	Liver carboxylesterase 4 precursor (EC 3.1.1.1) (Carboxyesterase ES-4) (Microsomal palmitoyl-CoA hydrolase) (Kidney microsomal carboxylesterase).	Q64573	46	6	11
ENSRNOP00000014235	Long-chain-fatty-acid--CoA ligase 1 (EC 6.2.1.3) (Long-chain acyl-CoA synthetase 1) (LACS 1) (Long-chain-fatty-acid--CoA ligase, liver isozyme).	P18163	11	69	39
ENSRNOP00000017101	Membrane-associated progesterone receptor component 1 (Acidic 25 kDa protein) (25-DX) (Ventral midline antigen) (VEMA).	P70580	3	2	2

ENSRNOP00000010579	Microsomal glutathione S-transferase 1 (EC 2.5.1.18) (Microsomal GST- 1) (Microsomal GST-I).	P08011	11	23	12
ENSRNOP00000012878	NADH-cytochrome b5 reductase 3 (EC 1.6.2.2) (Cytochrome b5 reductase) (B5R) (Diaphorase-1) .	P20070	1	2	4
ENSRNOP00000034954	Perlecan (Fragment). Laminin	O08591	2	2	2
ENSRNOP00000008477	Voltage-dependent anion-selective channel protein 1 (VDAC-1) (rVDAC1) (Outer mitochondrial membrane protein porin 1).	Q9Z2L0	4	16	4
ENSRNOP00000019571	All-trans-retinol 13,14-reductase precursor (EC 1.3.99.23) (All-trans- 13,14-dihydroretinol saturase) (RetSat) (RMT-7).	Q8VHE9	6	5	0
ENSRNOP00000024106	Alpha-enolase (EC 4.2.1.11) (2-phospho-D-glycerate hydro-lyase) (Non- neural enolase) (NNE) (Enolase 1).	P04764	6	2	0
ENSRNOP00000015956	Aspartate aminotransferase, mitochondrial precursor (EC 2.6.1.1) (Transaminase A) (Glutamate oxaloacetate transaminase 2).	P00507	2	2	0
ENSRNOP00000005755	Calmodulin (CaM).	P62161	2	3	0
ENSRNOP00000040859	Calnexin precursor.	P35565	2	2	0
ENSRNOP00000050581	Corticosteroid 11-beta-dehydrogenase isozyme 1 (EC 1.1.1.146) (11-DH) (11-beta-hydroxysteroid dehydrogenase 1) (11-beta-HSD1).	P16232	5	5	0
ENSRNOP00000017237	Cytochrome P450 2C6 (EC 1.14.14.1) (CYPIIC6) (P450 PB1) (PTF2).	P05178	3	2	0
ENSRNOP00000016965	NADH dehydrogenase flavoprotein 2, mitochondrial precursor (EC 1.6.5.3) (EC 1.6.99.3) (NADH-ubiquinone oxidoreductase 24 kDa subunit).	P19234	2	2	0
ENSRNOP00000002732	ATP synthase O subunit, mitochondrial precursor (EC 3.6.3.14) (Oligomycin sensitivity conferral protein) (OSCP).	Q06647	4	0	13
ENSRNOP00000050252	Basigin precursor (OX-47 antigen) (Glycoprotein CE9) (CD147 antigen).	P26453	13	0	9
ENSRNOP00000026574	Bile acyl-CoA synthetase (EC 6.2.1.7) (BACS) (Bile acid CoA ligase) (BA-CoA ligase) (BAL) (Cholate--CoA ligase) (Very long chain acyl-CoA synthetase-related protein) (VLACS-related) (VLACSR) (Fatty acid transport protein 5) (FATP-5) (Solute carrier family		5	0	9
ENSRNOP00000021407	choline dehydrogenase precursor	RefSeq_peptide NP_942026	38	0	5
ENSRNOP00000020446	Cytochrome b5.	P00173	2	0	20
ENSRNOP00000041174	Cytochrome P450 2D1 (EC 1.14.14.1) (CYPIID1) (P450-DB1) (P450-CMF1A) (P450-UT-7) (Debrisoquine 4-hydroxylase).	P10633	7	0	31

ENSRNOP00000012233	Dolichyl-diphosphooligosaccharide--protein glycosyltransferase subunit DAD1 (EC 2.4.1.119) (Oligosaccharyl transferase subunit DAD1) (Defender against cell death 1) (DAD-1).	P61805	1	0	1
ENSRNOP00000020306	dolichyl-di-phosphooligosaccharide-protein glycotransferase (predicted)	RefSeq_peptide NP_001012104	1	0	4
ENSRNOP00000020775	Liver carboxylesterase 3 precursor (EC 3.1.1.1) (Carboxyesterase ES-3) (pI 5.5 esterase) (ES-HTEL).	Q63108	6	0	9
ENSRNOP00000000177	Lysosome-associated membrane glycoprotein 2 precursor (LAMP-2) (Lysosomal membrane glycoprotein-type B) (LGP-B) (LGP-96) (LGP-110) (CD107b antigen).	P17046	1	0	1
ENSRNOP00000001961	NADPH--cytochrome P450 reductase (EC 1.6.2.4) (CPR) (P450R).	P00388	20	0	31
ENSRNOP00000026794	No Description Available. Protein family: Alpha glucosidase		11	0	5
ENSRNOP00000053474	No description available.Protein Family: COLLAGEN ALPHA 1 CHAIN		2	0	1
ENSRNOP00000015802	No description available.Protein Family: CYTOCHROME P450 2		1	0	1
ENSRNOP00000014630	No description available.Protein Family: MICROSOMAL TRIGLYCERIDE TRANSFER LARGE SUBUNIT PRECURSOR		7	0	8
ENSRNOP00000058260	Prohibitin-2 (B-cell receptor-associated protein BAP37) (BAP-37).	Q5XIH7	13	0	8
ENSRNOP00000025045	UDP-glucuronosyltransferase 1-1 precursor (EC 2.4.1.17) (UDPGT) (UGT1*1) (UGT1-01) (UGT1.1) (UGT1A1) (B1).	Q64550	4	0	1
ENSRNOP00000002724	UDP-glucuronosyltransferase 2B1 precursor (EC 2.4.1.17) (UDPGT) (UDPGTr-2).	P09875	1	0	7
ENSRNOP00000034723	UDP-glucuronosyltransferase 2B2 precursor (EC 2.4.1.17) (UDPGT) (3- hydroxyandrogen specific) (UDPGTr-4) (RLUG23).	P08541	7	0	10
ENSRNOP00000043239	UDP-glucuronosyltransferase 2B3 precursor (EC 2.4.1.17) (UDPGT) (Testosterone, dihydrotestosterone, and beta-estradiol specific) (17- beta-hydroxysteroid specific) (UDPGTr-3) (RLUG38).	P08542	4	0	7
ENSRNOP00000020670	ATP synthase delta chain, mitochondrial precursor (EC 3.6.3.14).	P35434	2	0	0
ENSRNOP00000000072	ATP synthase e chain, mitochondrial (EC 3.6.3.14).	P29419	5	0	0
ENSRNOP00000040969	ATP synthase, H+ transporting, mitochondrial F0 complex, subunit G	RefSeq_peptide NP_997681	6	0	0
ENSRNOP00000015724	Carboxylesterase precursor (EC 3.1.1.1) (Fragment).	O35535	3	0	0

ENSRNOP00000024033	Cytochrome c oxidase subunit 4 isoform 1, mitochondrial precursor (EC 1.9.3.1) (Cytochrome c oxidase subunit IV isoform 1) (COX IV-1) (Cytochrome c oxidase polypeptide IV).	P10888	13	0	0
ENSRNOP00000025525	Cytochrome c oxidase subunit 5A, mitochondrial precursor (EC 1.9.3.1) (Cytochrome c oxidase polypeptide Va).	P11240	3	0	0
ENSRNOP00000028249	Cytochrome P450 2A2 (EC 1.14.14.1) (CYPIIA2) (Testosterone 15-alpha- hydroxylase) (P450-UT-4).	P15149	12	0	0
ENSRNOP00000045567	Cytochrome P450 4A14 precursor (EC 1.14.15.3) (CYPIVA14) (Lauric acid omega-hydroxylase) (P450-LA-omega 3).	P20817	13	0	0
ENSRNOP00000006533	Cytochrome P450 4F1 (EC 1.14.14.1) (CYPIVF1) (P450-A3).	P33274	16	0	0
ENSRNOP00000055824	Dipeptidyl peptidase 4 (EC 3.4.14.5) (Dipeptidyl peptidase IV) (DPP IV) (T-cell activation antigen CD26) (GP110 glycoprotein) (Bile canaliculus domain-specific membrane glycoprotein) [Contains: Dipeptidyl peptidase 4 membrane form (Dipeptidyl peptidase IV		2	0	0
ENSRNOP00000013262	Electron transfer flavoprotein-ubiquinone oxidoreductase, mitochondrial precursor (EC 1.5.5.1) (ETF-QO) (ETF-ubiquinone oxidoreductase) (ETF dehydrogenase) (Electron-transferring- flavoprotein dehydrogenase).	Q6UPE1	64	0	0
ENSRNOP00000034828	eukaryotic translation elongation factor 1 delta	RefSeq_peptide NP_001013122	2	0	0
ENSRNOP00000027880	Hormone-sensitive lipase (EC 3.1.1.79) (HSL).	P15304	2	0	0
ENSRNOP00000016353	Integrin alpha-1 precursor (Laminin and collagen receptor) (VLA-1) (CD49a antigen).	P18614	2	0	0
ENSRNOP00000004941	Leucine-rich repeat-containing protein 59 (Protein p34).	Q5RJR8	9	0	0
ENSRNOP00000011485	MAL2 proteolipid protein	RefSeq_peptide NP_942081	1	0	0
ENSRNOP00000015851	NADH-ubiquinone oxidoreductase 75 kDa subunit, mitochondrial precursor (EC 1.6.5.3) (EC 1.6.99.3).	Q66HF1	3	0	0
ENSRNOP00000004836	No description available.Protein Family: ATP SYNTHASE D CHAIN MITOCHONDRIAL EC_3.6.3.14		4	0	0
ENSRNOP00000029426	No description available.Protein Family: ATP SYNTHASE F CHAIN MITOCHONDRIAL EC_3.6.3.14		1	0	0
ENSRNOP00000057649	No description available.Protein Family: LIVER CARBOXYLESTERASE PRECURSOR EC_3.1.1.1		3	0	0

ENSRNOP00000012425	No description available.Protein Family: NADH DEHYDROGENASE IRON SULFUR 3 MITOCHONDRIAL PRECURSOR EC_1.6.5.3 EC_1.6.99.- 3 NADH UBIQUINONE OXIDOREDUCTASE 30 KDA SUBUNIT COMPLEX I 30KD CI 30KD		4	0	0
ENSRNOP00000003611	Nucleoside diphosphate kinase B (EC 2.7.4.6) (NDK B) (NDP kinase B) (P18).	P19804	1	0	0
ENSRNOP00000041608	Phosphate carrier protein, mitochondrial precursor (PTP) (Solute carrier family 25 member 3).	P16036	10	0	0
ENSRNOP00000001500	Phosphatidylethanolamine-binding protein 1 (PEBP-1) (HCNPpp) (23 kDa morphine-binding protein) (P23K) .	P31044	1	0	0
ENSRNOP00000039493	Receptor expression-enhancing protein 6 (Polyposis locus protein 1- like 1).	Q5XI60	1	0	0
ENSRNOP00000026047	Rho guanine nucleotide exchange factor (GEF) 17		2	0	0
ENSRNOP00000024707	Sideroflexin-1 (Tricarboxylate carrier protein) (TCC).	Q63965	3	0	0
ENSRNOP00000021215	similar to prohibitin (LOC364817),	RefSeq_dna XR_005946	2	0	0
ENSRNOP00000044696	Ubiquinol-cytochrome-c reductase complex core protein 1, mitochondrial precursor (EC 1.10.2.2) (Core I protein).	Q68FY0	2	0	0
ENSRNOP00000020558	UDP-glucose:glycoprotein glucosyltransferase 1 precursor (EC 2.4.1.-) (UDP-glucose ceramide glucosyltransferase-like 1) (UDP-- Glc:glycoprotein glucosyltransferase) (RUGT).	Q9JLA3	3	0	0
ENSRNOP00000035497	Uncharacterized protein KIAA0152 homolog precursor.	Q5FVQ4	14	0	0
ENSRNOP00000018462	Voltage-dependent anion-selective channel protein 2 (VDAC-2) (Outer mitochondrial membrane protein porin 2) (B36-VDAC).	P81155	2	0	0
ENSRNOP00000026197	Voltage-dependent anion-selective channel protein 3 (VDAC-3) (rVDAC3) (Outer mitochondrial membrane protein porin 3).	Q9R1Z0	6	0	0
ENSRNOP00000018711	Adenylyl cyclase-associated protein 1 (CAP 1).	Q08163	0	2	2
ENSRNOP00000014464	Annexin A6 (Annexin-6) (Annexin VI) (Lipocortin VI) (P68) (P70) (Protein III) (Chromobindin-20) (67 kDa calelectrin) (Calphobindin-II) (CPB-II) (Calcium-binding protein CATA 65/67).	P48037	0	5	3
	Asialoglycoprotein receptor 1 (ASGPR 1) (ASGP-R 1) (Hepatic lectin 1) (RHL-1).	P02706	0	2	5
ENSRNOP00000014058	Cytochrome c, somatic.	P62898	0	3	2
ENSRNOP00000006087	epidermal growth factor receptor	RefSeq_peptide NP_113695	0	2	3
ENSRNOP00000046750	Major urinary protein precursor (MUP) (Alpha-2u-globulin) (Alpha(2)- euglobulin) (Allergen Rat n 1) (Rat n I) .	P02761	0	3	2

ENSRNOP00000007398	Myosin-9 (Myosin heavy chain 9) (Myosin heavy chain, nonmuscle IIa) (Nonmuscle myosin heavy chain IIa) (NMMHC II-a) (NMMHC-IIA) (Cellular myosin heavy chain, type A) (Nonmuscle myosin heavy chain-A) (NMMHC- A).	Q62812	0	3	2
ENSRNOP00000052490	No description available.Protein Family: SOLUTE CARRIER ORGANIC ANION TRANSPORTER FAMILY MEMBER SOLUTE CARRIER FAMILY 21 MEMBER ORGANIC ANION TRANSPORTER ORGANIC ANION TRANSPORTING POLYPEPTIDE		0	1	1
ENSRNOP00000051841	Protein disulfide-isomerase precursor (EC 5.3.4.1) (PDI) (Prolyl 4- hydroxylase subunit beta) (Cellular thyroid hormone-binding protein).	P04785	0	12	4
ENSRNOP00000022233	Prothrombin precursor (EC 3.4.21.5) (Coagulation factor II) .	P18292	0	1	3
ENSRNOP00000012725	Serotransferrin precursor (Transferrin) (Siderophilin) (Beta-1-metal- binding globulin) (Liver regeneration-related protein LRRG03).	P12346	0	6	4
ENSRNOP00000018336	Succinate dehydrogenase flavoprotein subunit, mitochondrial precursor (EC 1.3.5.1) (Fp) (Flavoprotein subunit of complex II).	Q920L2	0	11	13
ENSRNOP00000021514	Ubiquinol-cytochrome-c reductase complex core protein 2, mitochondrial precursor (EC 1.10.2.2) (Core protein II) (Complex III subunit II).	P32551	0	6	7
ENSRNOP00000009266	Adrenergic receptor, alpha-2A SH2 motif Proline-rich region Vacuolar sorting protein 9, subgroup Vacuolar sorting protein 9 RA		0	2	0
ENSRNOP00000013629	AP-2 complex subunit beta-1 (Adapter-related protein complex 2 beta-1 subunit) (Beta-adaptin) (Plasma membrane adaptor HA2/AP2 adaptin beta subunit) (Clathrin assembly protein complex 2 beta large chain) (AP105B).	P62944	0	1	0
ENSRNOP00000016247	Cell adhesion molecule-related/down-regulated by oncogenes precursor.	O35158	0	4	0
ENSRNOP00000019338	K+ channel tetramerization protein	RefSeq_peptide NP_001014044	0	1	0
ENSRNOP00000042136	Latrophilin-2 precursor (Calcium-independent alpha-latrotoxin receptor 2) (CIRL-2).	O88923	0	1	0
ENSRNOP00000013496	Low-density lipoprotein receptor precursor (LDL receptor).	P35952	0	3	0
ENSRNOP00000034210	Lrp1 protein (Fragment).	Q5I0H1	0	23	0
ENSRNOP00000017360	MAP-kinase activating death domain	RefSeq_peptide NP_446037	0	1	0
ENSRNOP00000051616	No description available.Protein Family: CYTOCHROME		0	4	0

	P450 2				
ENSRNOP00000028680	No description available.Protein Family: NODAL MODULATOR PRECURSOR PM5		0	1	0
ENSRNOP00000030087	Nociceptin receptor (Orphanin FQ receptor) (Kappa-type 3 opioid receptor) (KOR-3) (ROR-C) (XOR1).	P35370	0	1	0
ENSRNOP00000020737	P11 protein (Cdtw1), Protein of unknown function UPF0136, Transmembrane	RefSeq_dna NM_134395	0	1	0
ENSRNOP00000040018	Plectin-1 (PLTN) (PCN).	P30427	0	2	0
ENSRNOP00000028189	Shab voltage-gated K+ channel Shaker voltage-gated K+ channel Kv9 voltage-gated K+ channel Sodium Shal voltage-gated K+ channel Ion transport K+ channel tetramerisation Kv channel Voltage-dependent potassium		0	1	0
ENSRNOP00000033224	Sodium channel protein type 11 subunit alpha (Sodium channel protein type XI subunit alpha) (Voltage-gated sodium channel subunit alpha Nav1.9) (Sensory neuron sodium channel 2) (NaN).	O88457	0	1	0
ENSRNOP00000017145	TLC domain-containing protein 1 precursor.	Q5U2T1	0	3	0
ENSRNOP00000043164	Acyl-coA-binding protein, ACBP		0	0	1
ENSRNOP00000018711	Adenylyl cyclase-associated protein 1 (CAP 1).	Q08163	0	0	2
ENSRNOP00000047811	ADP-ribosylation factor 3 (Liver regeneration-related protein LRRG202).	P61206	0	0	7
ENSRNOP00000001816	Aldehyde dehydrogenase, mitochondrial precursor (EC 1.2.1.3) (ALDH class 2) (ALDH1) (ALDH-E2).	P11884	0	0	4
ENSRNOP00000003910	Amine oxidase A (EC 1.4.3.4) (Monoamine oxidase type A) (MAO-A).	P21396	0	0	2
ENSRNOP00000043466	Amine oxidase B (EC 1.4.3.4) (Monoamine oxidase type B) (MAO-B).	P19643	0	0	8
ENSRNOP00000027337	Anion exchange protein 3 (Neuronal band 3-like protein) (Solute carrier family 4 member 3).	P23348	0	0	2
ENSRNOP00000018761	Arylacetamide deacetylase (EC 3.1.1.-) (AADAC).	Q9QZH8	0	0	1
ENSRNOP00000021920	ATP synthase B chain, mitochondrial precursor (EC 3.6.3.14).	P19511	0	0	6
ENSRNOP00000049879	ATP synthase gamma chain, mitochondrial (EC 3.6.3.14).	P35435	0	0	8
ENSRNOP00000045650	ATPase, Na+/K+ transporting, alpha 1 polypeptide		0	0	14
ENSRNOP00000043148	Catechol O-methyltransferase (EC 2.1.1.6).	P22734	0	0	2
ENSRNOP00000027760	CD81 antigen (26 kDa cell surface protein TAPA-1) (Target of the antiproliferative antibody 1).	Q62745	0	0	1

ENSRNOP00000016083	Ceruloplasmin precursor (EC 1.16.3.1) (Ferroxidase). Source: Uniprot/SWISSPROT P13635		0	0	7
ENSRNOP00000052656	Clathrin heavy chain.	P11442	0	0	5
ENSRNOP00000018545	Complement component C9 precursor.	Q62930	0	0	1
ENSRNOP00000051608	Cytochrome P450 2C70 (EC 1.14.14.1) (CYPIIC70) (P-450Md) (P450 P49).	P19225	0	0	1
ENSRNOP00000012681	Cytochrome P450, E-class, group II		0	0	1
ENSRNOP00000007074	D(1B) dopamine receptor (D(5) dopamine receptor).	P25115	0	0	1
ENSRNOP00000041026	ectonucleoside triphosphate diphosphohydrolase 5	RefSeq_peptide NP_955426	0	0	1
ENSRNOP00000006141	Junctional adhesion molecule A precursor (JAM-A) (Junctional adhesion molecule 1) (JAM-1) (CD321 antigen).	Q9JHY1	0	0	1
ENSRNOP00000021638	lectin, mannose-binding 2		0	0	1
ENSRNOP00000003052	Lysosome membrane protein 2 (Lysosome membrane protein II) (LIMP II) (Scavenger receptor class B member 2) (85 kDa lysosomal membrane sialoglycoprotein) (LGP85) (CD36 antigen-like 2).	P27615	0	0	2
ENSRNOP00000022985	NAD(P) dependent steroid dehydrogenase-like	RefSeq_peptide NP_001009399	0	0	3
ENSRNOP00000017067	No description available.Protein Family: CYTOCHROME C1 HEME PROTEIN MITOCHONDRIAL PRECURSOR		0	0	8
ENSRNOP00000035416	No description available.Protein Family: SYNAPTIC GLYCOPROTEIN SC2		0	0	3
ENSRNOP00000001905	No description available.Protein Family: TRANSFERRIN RECEPTOR		0	0	1
ENSRNOP00000021512	Peroxisomal trans-2-enoyl-CoA reductase (EC 1.3.1.38) (RLF98) (Peroxisomal 2,4-dienoyl CoA reductase) (PX-2,4-DCR1).	Q9WVK3	0	0	4
ENSRNOP00000005853	Polymeric-immunoglobulin receptor precursor (Poly-Ig receptor) (PIGR) .	P15083	0	0	5
ENSRNOP00000022532	Prenylcysteine oxidase precursor (EC 1.8.3.5) (Chloride ion pump- associated 55 kDa protein).	Q99ML5	0	0	2
ENSRNOP00000017878	Rim ABC transporter AAA+ ATPase, core ABC transporter related		0	0	2
ENSRNOP00000001299	Scavenger receptor class B member 1 (SRB1) (SR-BI).	P97943	0	0	2
ENSRNOP00000043207	similar to Alpha-enolase (2-phospho-D-glycerate hydro-lyase) (Non-neural enolase) (NNE) (Enolase 1) (LOC435375),	RefSeq_dna XR_001998	0	0	4

ENSRNOP00000007825	Sodium/bile acid cotransporter (Na(+)/bile acid cotransporter) (Na(+)/taurocholate transport protein) (Sodium/taurocholate cotransporting polypeptide) (Solute carrier family 10 member 1)	P26435	0	0	4
ENSRNOP00000006855	Surfeit locus protein 1.	Q9QXU2	0	0	2
ENSRNOP00000015043	translocase of inner mitochondrial membrane 8 homolog a (yeast) (Timm8a),	RefSeq_dna NM_053370	0	0	2
ENSRNOP00000010663	UDP-glucose pyrophosphorylase 2	RefSeq_peptide NP_001019914	0	0	2
ENSRNOP00000024973	Very-long-chain specific acyl-CoA dehydrogenase, mitochondrial precursor (EC 1.3.99.-) (VLCAD).	P45953	0	0	6

Supplementary Table 3
Membrane proteins identified in Triton X-114 detergent phase (Chapter 3)

Identifier	# peptides	log (e) score	Description	Glycosylation (N-X-S/T)	Accession No.
ENSRNOP00000014235	49	-351.4	Long-chain-fatty-acid--CoA ligase 1 (EC 6.2.1.3) (Long-chain acyl-CoA synthetase 1) (LACS 1) (Long-chain-fatty-acid--CoA ligase, liver isozyme).	3	P18163
ENSRNOP00000043239	58	-351.1	UDP-glucuronosyltransferase 2B3 precursor (EC 2.4.1.17) (UDPGT) (Testosterone, dihydrotestosterone, and beta-estradiol specific) (17- beta-hydroxysteroid specific) (UDPGTr-3) (RLUG38).	0	P08542
ENSRNOP00000013816	40	-261.6	No other features on this peptide	0	
ENSRNOP00000041174	39	-203.2	Cytochrome P450 2D1 (EC 1.14.14.1) (CYPIID1) (P450-DB1) (P450-CMF1A) (P450-UT-7) (Debrisoquine 4-hydroxylase)	4	P10633
ENSRNOP00000017310	27	-159.5	Cytochrome P450 2C11 (EC 1.14.14.1) (CYPIIC11) (P-450(M-1)) (P450H) (P450-UT-A) (UT-2)	2	P08683
ENSRNOP00000040266	35	-196.6	Cytochrome P450 2D10 (EC 1.14.14.1) (CYPIID10) (P450-DB5) (P450-CMF1B) (Debrisoquine 4-hydroxylase).	4	P12939
ENSRNOP00000003965	32	-209.8	ATP synthase subunit beta, mitochondrial precursor (EC 3.6.3.14).	0	P10719
ENSRNOP00000048711	27	-181.5	Cytochrome P450 2D3 (EC 1.14.14.1) (CYPIID3) (P450-DB3) (Debrisoquine 4-hydroxylase).	1	P12938
ENSRNOP00000012413	35	-227.4	Cytochrome P450 2D26 (EC 1.14.14.1) (CYPIID26) (P450-DB2) (P450-CMF2) (Debrisoquine 4-hydroxylase)	3	P10634
ENSRNOP00000026574	21	-181.5	Bile acyl-CoA synthetase (EC 6.2.1.7) (BACS) (Bile acid CoA ligase) (BA-CoA ligase) (BAL) (Cholate--CoA ligase) (Very long chain acyl-CoA synthetase-related protein) (VLACS-related) (VLACSR) (Fatty acid transport protein 5) (FATP-5) (Solute carrier family	1	Q9ES38
ENSRNOP00000010209	15	-164.8	Dolichyl-diphosphooligosaccharide--protein glycosyltransferase 63 kDa subunit precursor (EC 2.4.1.119) (Ribophorin II) (RPN-II).	2	P25235
ENSRNOP00000025045	34	-212.9	UDP-glucuronosyltransferase 1-1 precursor (EC 2.4.1.17) (UDPGT) (UGT1*1) (UGT1-01) (UGT1.1) (UGT1A1) (B1)	2	Q64550
ENSRNOP00000008477	13	-70.1	Voltage-dependent anion-selective channel protein 1 (VDAC-1) (rVDAC1) (Outer mitochondrial membrane protein porin 1).	2	Q9Z2L0
ENSRNOP00000034723	34	-170.6	UDP-glucuronosyltransferase 2B2 precursor (EC 2.4.1.17) (UDPGT) (3- hydroxyandrogen specific) (UDPGTr-4) (RLUG23)	1	P08541

ENSRNOP00000010579	34	-152.4	Microsomal glutathione S-transferase 1 (EC 2.5.1.18) (Microsomal GST- 1) (Microsomal GST-I).	0	P08011
ENSRNOP00000017237	19	-143.2	Cytochrome P450 2C6 (EC 1.14.14.1) (CYPIIC6) (P450 PB1) (PTF2).	2	P05178
ENSRNOP00000001961	16	-106.4	NADPH--cytochrome P450 reductase (EC 1.6.2.4) (CPR) (P450R).	1	P00388
ENSRNOP00000004864	15	-84.9	Dimethylaniline monooxygenase 3 (EC 1.14.13.8) (Hepatic flavin-containing monooxygenase 3) (FMO 3) (Dimethylaniline oxidase 3)	3	Q9EQ76
ENSRNOP00000015913	38	-179.1	ADP/ATP translocase 2 (Adenine nucleotide translocator 2) (ANT 2) (ADP,ATP carrier protein 2) (Solute carrier family 25 member 5).	1	Q09073
ENSRNOP00000005875	14	-97.6	Retinol dehydrogenase 7 (EC 1.1.1.105) (Retinol dehydrogenase type III) (RODH III).	1	P55006
ENSRNOP00000022892	25	-162.7	ATP synthase subunit alpha, mitochondrial precursor (EC 3.6.3.14).	1	P15999
ENSRNOP00000035423	11	-95.9	Retinol dehydrogenase 2 (EC 1.1.1.105) (Retinol dehydrogenase type II) (RODH II) (29 k-protein).	0	P50170
ENSRNOP00000043466	15	-76.8	Amine oxidase B (EC 1.4.3.4) (Monoamine oxidase type B) (MAO-B).	1	P19643
ENSRNOP00000024423	8	-44.7	Dimethylaniline monooxygenase 5 (EC 1.14.13.8) (Hepatic flavin-containing monooxygenase 5) (FMO 5) (Dimethylaniline oxidase 5).	2	Q8K4C0
ENSRNOP00000002712	18	-88.1	UDP-glucuronosyltransferase 2B4 precursor (EC 2.4.1.17) (UDPGT) (UDP- glucuronosyltransferase 2B12).	1	P36511
ENSRNOP00000049879	8	-51.1	ATP synthase gamma chain, mitochondrial (EC 3.6.3.14).	4	P35435
ENSRNOP00000026290	10	-59.9	3 beta-hydroxysteroid dehydrogenase type 5 (3 beta-hydroxysteroid dehydrogenase type V) (3-beta-HSD V) (NADPH-dependent 3-beta-hydroxy- Delta(5)-steroid dehydrogenase) (EC 1.1.1.-) (3-beta-hydroxy-5-ene steroid dehydrogenase) (Progesterone reductase)	3	P22071
ENSRNOP00000013789	19	-128.5	Glutamate dehydrogenase 1, mitochondrial precursor (EC 1.4.1.3) (GDH) (Memory-related protein 2) (MRG-2).	1	P10860
ENSRNOP00000021514	19	-108.9	Ubiquinol-cytochrome-c reductase complex core protein 2, mitochondrial precursor (EC 1.10.2.2) (Core protein II) (Complex III subunit II).	3	P32551
ENSRNOP00000045567	18	-138	Cytochrome P450 4A14 precursor (EC 1.14.15.3) (CYPIVA14) (Lauric acid omega-hydroxylase) (P450-LA-omega 3).	3	P20817
ENSRNOP00000003910	14	-79	Amine oxidase A (EC 1.4.3.4) (Monoamine oxidase type A) (MAO-A).	1	P21396

ENSRNOP00000020670	2	-16.8	ATP synthase delta chain, mitochondrial precursor (EC 3.6.3.14).	0	P35434
ENSRNOP00000013262	13	-80	Electron transfer flavoprotein-ubiquinone oxidoreductase, mitochondrial precursor (EC 1.5.5.1) (ETF-QO) (ETF-ubiquinone oxidoreductase) (ETF dehydrogenase) (Electron-transferring-flavoprotein dehydrogenase).	1	Q6UPE1
ENSRNOP00000017472	13	-85.6	Prohibitin-2 (B-cell receptor-associated protein BAP37) (BAP-37).	2	Q5XIH7
ENSRNOP00000012681	12	-75.4	No other features on this peptide	1	
ENSRNOP00000011494	17	-81.8	Phosphate carrier protein, mitochondrial precursor (PTP) (Solute carrier family 25 member 3).	0	P16036
ENSRNOP00000002724	16	-114.1	UDP-glucuronosyltransferase 2B1 precursor (EC 2.4.1.17) (UDPGT) (UDPGTr-2).	1	P09875
ENSRNOP00000012878	15	-89.3	NADH-cytochrome b5 reductase 3 (EC 1.6.2.2) (Cytochrome b5 reductase) (B5R) (Diaphorase-1)	0	P20070
ENSRNOP00000028237	11	-71.4	Cytochrome P450 2A1 (EC 1.14.14.1) (CYPIIA1) (Steroid hormones 7- alpha-hydroxylase) (Testosterone 7-alpha-hydroxylase) (P450-UT-F).	1	P11711
ENSRNOP00000011846	4	-17.2	mitochondrial carrier homolog 2 Source: RefSeq_peptide NP_001099958	1	
ENSRNOP00000025525	21	-63.4	Cytochrome c oxidase subunit 5A, mitochondrial precursor (EC 1.9.3.1) (Cytochrome c oxidase polypeptide Va).	0	P11240
ENSRNOP00000020446	8	-29.6	Cytochrome b5	1	P00173
ENSRNOP00000029578	17	-120.8	nicotinamide nucleotide transhydrogenase Source: RefSeq_peptide NP_001013175	5	Q61941
ENSRNOP00000028249	10	-71.2	Cytochrome P450 2A2 (EC 1.14.14.1) (CYPIIA2) (Testosterone 15-alpha- hydroxylase) (P450-UT-4).	2	P15149
ENSRNOP00000020306	7	-32.6	dolichyl-di-phosphooligosaccharide-protein glycotransferase (predicted) Source: RefSeq_peptide NP_001012104	2	
ENSRNOP00000024033	10	-44.7	Cytochrome c oxidase subunit 4 isoform 1, mitochondrial precursor (EC 1.9.3.1) (Cytochrome c oxidase subunit IV isoform 1) (COX IV-1) (Cytochrome c oxidase polypeptide IV).	0	P10888
ENSRNOP00000001291	6	-56	Cytochrome P450 3A2 (EC 1.14.14.1) (CYPIIIA2) (P450-PCN2) (P450/6- beta-A) (Testosterone 6-beta-hydroxylase).	2	P05183
ENSRNOP00000017840	3	-29.6	Cytochrome P450 2C23 (EC 1.14.14.1) (CYPIIC23) (Arachidonic acid epoxygenase).	1	P24470
ENSRNOP00000018455	11	-48.5	Protein transport protein Sec61 subunit alpha isoform 1 (Sec61 alpha- 1).	0	P61621
ENSRNOP00000015851	11	-86.3	NADH-ubiquinone oxidoreductase 75 kDa subunit, mitochondrial precursor (EC 1.6.5.3) (EC 1.6.99.3).	1	Q66HF1

ENSRNOP00000002732	8	-63.8	ATP synthase O subunit, mitochondrial precursor (EC 3.6.3.14) (Oligomycin sensitivity conferral protein) (OSCP).	0	Q06647
ENSRNOP00000017067	5	-27	No description available.Protein Family: CYTOCHROME C1 HEME PROTEIN MITOCHONDRIAL PRECURSOR	0	
ENSRNOP00000044696	10	-91.1	Ubiquinol-cytochrome-c reductase complex core protein 1, mitochondrial precursor (EC 1.10.2.2) (Core I protein).	2	Q68FY0
ENSRNOP00000055369	5	-17.9	cytochrome P450, family 1, subfamily a, polypeptide 2	3	
ENSRNOP00000016883	9	-58.2	Cytochrome P450 2E1 (EC 1.14.14.1) (CYPIIE1) (P450-J) (P450RLM6).	2	P05182
ENSRNOP00000051846	15	-89.3	solute carrier family 25 (mitochondrial carrier; dicarboxylate transporter), member 10 Source: RefSeq_peptide NP_596909	1	O89035_RAT
ENSRNOP00000024707	6	-44.4	Sideroflexin-1 (Tricarboxylate carrier protein) (TCC).	3	Q63965
ENSRNOP00000028194	12	-65.6	7-dehydrocholesterol reductase (EC 1.3.1.21) (7-DHC reductase) (Sterol Delta(7)-reductase).	3	Q9Z2Z8
ENSRNOP00000000306	10	-58.6	Tricarboxylate transport protein, mitochondrial precursor (Citrate transport protein) (CTP) (Tricarboxylate carrier protein) (Solute carrier family 25 member 1).	0	P32089
ENSRNOP00000045650	11	-68.2	ATPase, Na+/K+ transporting, alpha 1 polypeptide	3	
ENSRNOP00000004836	11	-39.5	No description available.Protein Family: ATP SYNTHASE D CHAIN MITOCHONDRIAL EC_3.6.3.14	1	
ENSRNOP00000040859	9	-48.9	Calnexin precursor.	1	P35565
ENSRNOP00000034293	10	-109.3	Epoxide hydrolase 1 (EC 3.3.2.9) (Microsomal epoxide hydrolase) (Epoxide hydratase).	0	P07687
ENSRNOP00000051445	7	-41.1	Long-chain-fatty-acid--CoA ligase 5 (EC 6.2.1.3) (Long-chain acyl-CoA synthetase 5) (LACS 5).	1	O88813
ENSRNOP00000035497	3	-15.7	Uncharacterized protein KIAA0152 homolog precursor.	1	Q5FVQ4
ENSRNOP00000045029	6	-28.6	Cytochrome P450 2C7 (EC 1.14.14.1) (CYPIIC7) (P450F) (PTF1).	1	P05179
ENSRNOP00000021920	8	-56	ATP synthase B chain, mitochondrial precursor (EC 3.6.3.14).	0	P19511
ENSRNOP00000019571	10	-65.4	All-trans-retinol 13,14-reductase precursor (EC 1.3.99.23) (All-trans- 13,14-dihydroretinol saturase) (RetSat) (RMT-7).	0	Q8VHE9
ENSRNOP00000013607	9	-45.9	Solute carrier family 27 (Fatty acid transporter), member 2.	2	Q66HN6
ENSRNOP00000003498	5	-31.5	No description available.Protein Family: BETA DEHYDROGENASE BETA HYDROXYSTEROID DEHYDROGENASE	3	
ENSRNOP00000036519	6	-37	dehydrogenase/reductase (SDR family) member 7 Source: RefSeq_peptide NP_001013116	0	
ENSRNOP00000024517	5	-12.8	NADH dehydrogenase (ubiquinone) flavoprotein 1, 51kDa Source: RefSeq_peptide NP_001006973	1	
ENSRNOP00000015802	4	-34.3	No description available.Protein Family: CYTOCHROME P450 2	1	

ENSRNOP00000005005	5	-42	Kynurenine 3-monooxygenase (EC 1.14.13.9) (Kynurenine 3-hydroxylase).	2	O88867
ENSRNOP00000001738	12	-94.4	Sarcoplasmic/endoplasmic reticulum calcium ATPase 2 (EC 3.6.3.8) (Calcium pump 2) (SERCA2) (SR Ca(2+)-ATPase 2) (Calcium-transporting ATPase sarcoplasmic reticulum type, slow twitch skeletal muscle isoform) (Endoplasmic reticulum class 1/2 Ca(2+) ATPase).	3	Q64578
ENSRNOP00000022487	6	-34.9	Cytochrome c oxidase subunit 5B, mitochondrial precursor (EC 1.9.3.1) (Cytochrome c oxidase polypeptide Vb) (Cytochrome c oxidase subunit VIA*).	1	P12075
ENSRNOP00000027520	8	-53.3	Mitochondrial carnitine/acylcarnitine carrier protein (Carnitine/acylcarnitine translocase) (CAC) (Solute carrier family 25 member 20)	0	P97521
ENSRNOP00000018462	5	-31.2	Voltage-dependent anion-selective channel protein 2 (VDAC-2) (Outer mitochondrial membrane protein porin 2) (B36-VDAC)	3	P81155
ENSRNOP00000004798	2	-14.2	No description available.Protein Family: MICROSOMAL GLUTATHIONE S TRANSFERASE 3 EC_2.5.1.18 MICROSOMAL GST 3 MICROSOMAL GST III	0	
ENSRNOP00000015810	7	-49.5	solute carrier family 37 (glucose-6-phosphate transporter), member 4 Source: RefSeq_peptide NP_113777	1	
ENSRNOP00000058260	5	-39.4	No other features on this peptide	1	
ENSRNOP00000015684	4	-30.5	No description available.Protein Family: AMBIGUOUS	1	
ENSRNOP00000007870	9	-51.6	Corticosteroid 11-beta-dehydrogenase isozyme 1 (EC 1.1.1.146) (11-DH) (11-beta-hydroxysteroid dehydrogenase 1) (11-beta-HSD1)	2	P16232
ENSRNOP00000000749	5	-28.8	No description available.Protein Family: CDGSH IRON SULFUR DOMAIN CONTAINING 1 ZINC FINGER CDGSH DOMAIN CONTAINING 1	0	
ENSRNOP00000034135	5	-40	Ndufa9 protein (Fragment).	1	Q5BK63
ENSRNOP00000021638	6	-40	Vesicular integral-membrane protein VIP36 precursor (Lectin mannose- binding 2).	1	Q9DBH5
ENSRNOP00000039545	3	-15.3	Protein FAM82A.	3	Q498D5
ENSRNOP00000012425	2	-28.9	No description available.Protein Family: NADH DEHYDROGENASE IRON SULFUR 3 MITOCHONDRIAL PRECURSOR EC_1.6.5.3 EC_1.6.99.- 3 NADH UBIQUINONE OXIDOREDUCTASE 30 KDA SUBUNIT COMPLEX I 30KD CI 30KD	0	
ENSRNOP00000054924	9	-47.2	inner membrane protein, mitochondrial Source: RefSeq_peptide NP_001030100	3	

ENSRNOP00000017101	10	-65.5	Membrane-associated progesterone receptor component 1 (Acidic 25 kDa protein) (25-DX) (Ventral midline antigen) (VEMA).	0	P70580
ENSRNOP00000045886	8	-48.5	Fatty aldehyde dehydrogenase (EC 1.2.1.3) (Aldehyde dehydrogenase, microsomal) (Aldehyde dehydrogenase family 3 member A2) (Aldehyde dehydrogenase 10).	0	P30839
ENSRNOP00000010760	6	-25.1	Methyltransferase-like protein 7B precursor (EC 2.1.1.-) (Associated with lipid droplet protein 1) (ALDI).	0	Q562C4
ENSRNOP00000020681	3	-14.9	Vesicle-associated membrane protein-associated protein A (VAMP- associated protein A) (VAMP-A) (VAP-A) (33 kDa Vamp-associated protein) (VAP-33).	5	Q9Z270
ENSRNOP00000003004	2	-16.5	Dehydrogenase/reductase SDR family member 8 precursor (EC 1.1.1.-) (17-beta-hydroxysteroid dehydrogenase 11) (17-beta-HSD 11) (17-beta- HSD XI) (17betaHSDXI) (17bHSD11) (17betaHSD11).	0	Q6AYS8
ENSRNOP00000007223	4	-22.9	SAC1 (supressor of actin mutations 1, homolog)-like Source: RefSeq_peptide NP_446250	2	
ENSRNOP00000026197	5	-35	Voltage-dependent anion-selective channel protein 3 (VDAC-3) (rVDAC3) (Outer mitochondrial membrane protein porin 3).	2	Q9R1Z0
ENSRNOP00000025254	6	-18.5	Asialoglycoprotein receptor 1 (ASGPR 1) (ASGP-R 1) (Hepatic lectin 1) (RHL-1).	3	P02706
ENSRNOP00000020015	6	-43.9	aldehyde dehydrogenase 8 family, member A1	0	
ENSRNOP00000025240	6	-46.4	solute carrier family 25 (mitochondrial carrier, glutamate), member 22 Source: RefSeq_peptide NP_001014049	1	
ENSRNOP00000002705	3	-17.7	No description available.Protein Family: UDP GLUCURONOSYLTRANSFERASE PRECURSOR EC_2.4.1.17	3	
ENSRNOP00000006855	2	-20.5	Surfeit locus protein 1	1	Q9QXU2
ENSRNOP00000040969	5	-31.1	ATP synthase, H+ transporting, mitochondrial F0 complex, subunit G Source: RefSeq_peptide NP_997681	0	
ENSRNOP00000001816	6	-45.6	Aldehyde dehydrogenase, mitochondrial precursor (EC 1.2.1.3) (ALDH class 2) (ALDH1) (ALDH-E2).	2	P11884
ENSRNOP00000040087	7	-52.5	No description available.Protein Family: DOLICHYL DIPHOSPHOOLIGOSACCHARIDE GLYCOSYLTRANSFERASE SUBUNIT EC_2.4.1.119 OLIGOSACCHARYL TRANSFERASE SUBUNIT STT3	2	
ENSRNOP00000018973	1	-6.2	No description available.Protein Family: ERLIN 2 PRECURSOR ENDOPLASMIC RETICULUM LIPID RAFT ASSOCIATED 2 STOMATIN PROHIBITIN FLOTILLIN HFLC/K DOMAIN CONTAINING 2 SPFH DOMAIN CONTAINING 2	1	

ENSRNOP00000017180	4	-17.3	similar to eukaryotic translation elongation factor 1 alpha 2 (LOC364172), mRNA Source: RefSeq_dna XR_006078	1	
ENSRNOP00000004941	4	-14.2	Leucine-rich repeat-containing protein 59 (Protein p34).	1	Q5RJR8
ENSRNOP00000015598	6	-14.8	Ras-related protein Rab-11A (Rab-11) (24KG).	1	P62494
ENSRNOP00000023152	4	-25.4	Cytochrome P450 27, mitochondrial precursor (EC 1.14.13.15) (Cytochrome P-450C27/25) (Sterol 26-hydroxylase) (Sterol 27-hydroxylase) (Vitamin D(3) 25-hydroxylase) (5-beta-cholestane-3-alpha,7-alpha,12-alpha-triol 27-hydroxylase)	0	P17178
ENSRNOP00000017282	6	-15	Brain protein 44-like protein (Apoptosis-regulating basic protein).	0	P63031
ENSRNOP00000055824	2	-14.8	Dipeptidyl peptidase 4 (EC 3.4.14.5) (Dipeptidyl peptidase IV) (DPP IV) (T-cell activation antigen CD26) (GP110 glycoprotein) (Bile canaliculus domain-specific membrane glycoprotein) [Contains: Dipeptidyl peptidase 4 membrane form (Dipeptidyl peptidase IV	10	P14740
ENSRNOP00000051412	4	-25.5	Multidrug resistance-associated protein 6 (ATP-binding cassette sub- family C member 6) (MRP-like protein 1) (MLP-1).	8	O88269
ENSRNOP00000000177	2	-4.9	Lysosome-associated membrane glycoprotein 2 precursor (LAMP-2) (Lysosomal membrane glycoprotein-type B) (LGP-B) (LGP-96) (LGP-110) (CD107b antigen).	16	P17046
ENSRNOP00000051361	4	-19.7	Dimethylaniline monooxygenase 1 (EC 1.14.13.8) (Hepatic flavin-containing monooxygenase 1) (FMO 1) (Dimethylaniline oxidase 1).	2	P36365
ENSRNOP00000022703	3	-13.3	L-gulonolactone oxidase (EC 1.1.3.8) (LGO) (L-gulono-gamma-lactone oxidase) (GLO).	2	P10867
ENSRNOP00000025649	3	-13	Ras-related protein Rab-14.	2	P61107
ENSRNOP00000005153	2	-10.1	LRRGT00013.	1	Q6TXI6
ENSRNOP00000053215	5	-36.1	Translocon-associated protein subunit delta precursor (TRAP-delta) (Signal sequence receptor subunit delta) (SSR-delta).	0	Q07984
ENSRNOP00000015217	3	-15	NADH dehydrogenase iron-sulfur protein 4, mitochondrial precursor (EC 1.6.5.3) (EC 1.6.99.3) (NADH-ubiquinone oxidoreductase 18 kDa subunit) (Complex I-18 kDa) (CI-18 kDa).	2	Q5XIF3
ENSRNOP00000028033	4	-23.5	Glucose-6-phosphatase (EC 3.1.3.9) (G6Pase) (G-6-Pase).	3	P43428
ENSRNOP00000029426	3	-15.9	No description available.Protein Family: AMBIGUOUS	0	
ENSRNOP00000018001	5	-20.5	No description available.Protein Family: COILED COIL HELIX COILED COIL HELIX DOMAIN CONTAINING	2	
ENSRNOP00000036810	2	-4.7	No description available.Protein Family: UNCHARACTERIZED	0	
ENSRNOP00000056976	3	-16.3	Translocon-associated protein subunit alpha precursor (TRAP-alpha) (Signal sequence receptor subunit alpha) (SSR-alpha) (Liver regeneration-related protein LRRG137).	2	Q7TPJ0

ENSRNOP00000001545	4	-11.2	Translocation-associated membrane protein 1.	3	Q5XI41
ENSRNOP00000027760	2	-14.8	CD81 antigen (26 kDa cell surface protein TAPA-1) (Target of the antiproliferative antibody 1).	1	Q62745
ENSRNOP00000014235	49	-351.4	Long-chain-fatty-acid--CoA ligase 1 (EC 6.2.1.3) (Long-chain acyl-CoA synthetase 1) (LACS 1) (Long-chain-fatty-acid--CoA ligase, liver isozyme).	3	P18163
ENSRNOP00000050252	7	-49.4	Basigin precursor (OX-47 antigen) (Glycoprotein CE9) (CD147 antigen).	3	P26453
ENSRNOP00000035966	5	-31.2	ERGIC-53 protein precursor (ER-Golgi intermediate compartment 53 kDa protein) (Lectin, mannose-binding 1) (p58)	1	Q62902
ENSRNOP00000030069	5	-21.9	Cytochrome P450 2B1 (EC 1.14.14.1) (CYPIIB1) (P450-B) (P450b) (P450- PB1 and P450-PB2) (P450-LM2).	1	P00176
ENSRNOP00000051608	3	-21.7	Cytochrome P450 2C70 (EC 1.14.14.1) (CYPIIC70) (P-450Md) (P450 P49).	2	P19225
ENSRNOP00000054078	5	-31.7	Cytochrome P450 2A3 (EC 1.14.14.1) (CYPIIA3) (Coumarin 7-hydroxylase).	1	P20812
ENSRNOP00000002728	5	-36.4	No description available.Protein Family: UDP GLUCURONOSYLTRANSFERASE PRECURSOR EC_2.4.1.17	2	
ENSRNOP00000024609	3	-12.4	Ubiquinol-cytochrome c reductase iron-sulfur subunit, mitochondrial precursor (EC 1.10.2.2) (Rieske iron-sulfur protein) (RISP) (Liver regeneration-related protein LRRGT00195).	0	P20788
ENSRNOP00000003611	3	-10.8	Nucleoside diphosphate kinase B (EC 2.7.4.6) (NDK B) (NDP kinase B) (P18)	0	P19804
ENSRNOP00000052490	2	-25.8	solute carrier organic anion transporter family, member 1a1	6	
ENSRNOP00000019624	8	-40.7	similar to NADH-ubiquinone oxidoreductase PDSW subunit (Complex I-PDSW) (CI-PDSW) (LOC681418), mRNA Source: RefSeq_dna NM_001109443	1	
ENSRNOP00000007015	2	-22.6	3-beta-hydroxysteroid-Delta(8),Delta(7)-isomerase (EC 5.3.3.5) (Cholestenol Delta-isomerase) (Delta(8)-Delta(7) sterol isomerase) (D8-D7 sterol isomerase) (Emopamil-binding protein) (Sterol 8- isomerase).	0	Q9JJ46
ENSRNOP00000009777	3	-13.4	Bile acid CoA:amino acid N-acyltransferase (EC 2.3.1.65) (BAT) (BACAT) (Glycine N-choloyltransferase) (Kan-1) (Long-chain fatty-acyl-CoA hydrolase) (EC 3.1.2.2).	1	Q63276
ENSRNOP00000015866	8	-29.2	Solute carrier family 2, facilitated glucose transporter member 2 (Glucose transporter type 2, liver) (GLUT-2).	1	P12336
ENSRNOP00000015956	4	-23.7	Aspartate aminotransferase, mitochondrial precursor (EC 2.6.1.1) (Transaminase A) (Glutamate oxaloacetate transaminase 2).	1	P00507
ENSRNOP00000036896	13	-64.8	No other features on this peptide	0	

ENSRNOP00000032909	4	-16.5	solute carrier family 25 (mitochondrial carrier, Aralar), member 12	1	
ENSRNOP00000039338	3	-15.1	Protein transport protein Sec61 subunit alpha isoform 1 (Sec61 alpha- 1).	2	P61621
ENSRNOP00000011158	3	-10.3	Nipsnap1 protein (Fragment)	0	Q5EBA4
ENSRNOP00000042159	4	-24.8	No description available.Protein Family: UNKNOWN	6	
ENSRNOP00000049222	2	-9.4	No description available.Protein Family: UNKNOWN	0	
ENSRNOP00000048358	14	-81	No description available.Protein Family: ADP/ATP TRANSLOCASE ADENINE NUCLEOTIDE TRANSLOCATOR ANT ADP ATP CARRIER SOLUTE CARRIER FAMILY 25 MEMBER	2	
ENSRNOP00000015667	7	-63.3	Fatty-acid amide hydrolase 1 (EC 3.1.-.-) (Oleamide hydrolase 1) (Anandamide amidohydrolase 1)	1	P97612
ENSRNOP00000016043	8	-49.8	solute carrier family 25 member 15 Source: RefSeq_peptide NP_001041345	0	
ENSRNOP00000053689	3	-27	No description available.Protein Family: UNKNOWN	0	
ENSRNOP00000016739	4	-26.5	ATP-binding cassette sub-family D member 3 (70 kDa peroxisomal membrane protein) (PMP70).	2	P16970
ENSRNOP00000035416	4	-25.6	No description available.Protein Family: SYNAPTIC GLYCOPROTEIN SC2 EC_1.3.1.- TRANS 2 3 ENOYL COA REDUCTASE TER	3	
ENSRNOP00000008045	5	-23.3	Protein FAM82A.	1	Q498D5
ENSRNOP00000030668	3	-22.2	transmembrane emp24 protein transport domain containing 9 Source: RefSeq_peptide NP_001009703	1	
ENSRNOP00000010512	2	-17.1	No description available.Protein Family: PRECURSOR	1	
ENSRNOP00000003436	4	-12.6	Implantation-associated protein precursor (IAP).	2	O35777
ENSRNOP00000017002	2	-12.5	No description available.Protein Family: AMBIGUOUS	1	
ENSRNOP00000057449	3	-11.1	Ras-related C3 botulinum toxin substrate 1 precursor (p21-Rac1).	1	Q6RUV5
ENSRNOP00000001285	3	-10.9	Cytochrome P450 3A18 (EC 1.14.14.1) (CYPIIIA18) (P450(6)beta-2).	2	Q64581
ENSRNOP00000043148	2	-10.5	Catechol O-methyltransferase (EC 2.1.1.6).	0	P22734
ENSRNOP00000057476	2	-10.4	No description available.Protein Family: UNKNOWN	0	
ENSRNOP00000021215	2	-6.3	similar to prohibitin (LOC364817), mRNA Source: RefSeq_dna XR_005946	1	
ENSRNOP00000002410	3	-21.7	Peroxisomal bifunctional enzyme (PBE) (PBFE)	1	P07896
ENSRNOP00000003020	5	-11.7	succinate dehydrogenase complex, subunit C Source: RefSeq_peptide NP_001005534	0	

ENSRNOP00000003674	3	-14.3	NADH dehydrogenase (ubiquinone) 1 beta subcomplex, 4, 15kDa Source: RefSeq_peptide NP_001032415	0	
ENSRNOP00000005144	2	-10.7	Mitochondrial 2-oxoglutarate/malate carrier protein (OGCP) (Solute carrier family 25 member 11)	0	P97700
ENSRNOP00000006950	3	-18.9	Ras-related protein Rab-1A. Source: Uniprot/SWISSPROT Q6NYB7	1	
ENSRNOP00000007825	2	-4.1	Sodium/bile acid cotransporter (Na(+)/bile acid cotransporter) (Na(+)/taurocholate transport protein) (Sodium/taurocholate cotransporting polypeptide) (Solute carrier family 10 member 1).	6	P26435
ENSRNOP00000007840	2	-11.9	NADH dehydrogenase (ubiquinone) 1 alpha subcomplex, 8 Source: RefSeq_peptide NP_001041327	0	
ENSRNOP00000009511	3	-12.2	Ras-related protein Rap-1b precursor (GTP-binding protein smg p21B).	0	Q62636
ENSRNOP00000011521	3	-18.9	Mannosyl-oligosaccharide glucosidase (EC 3.2.1.106) (Glycoprotein- processing glucosidase I).	1	O88941
ENSRNOP00000014684	3	-11.9	ATPase family AAA domain-containing protein 1.	2	Q505J9
ENSRNOP00000016432	3	-14.9	Ras-related C3 botulinum toxin substrate 1 precursor (p21-Rac1).	0	Q6RUV5
ENSRNOP00000018761	3	-13.1	Arylacetamide deacetylase (EC 3.1.1.-) (AADAC).	3	Q9QZH8
ENSRNOP00000018795	4	-25.6	Estradiol 17-beta-dehydrogenase 2 (EC 1.1.1.62) (17-beta-HSD 2) (17- beta-hydroxysteroid dehydrogenase 2)	2	Q62730
ENSRNOP00000020544	4	-41.3	Electron transfer flavoprotein subunit alpha, mitochondrial precursor (Alpha-ETF). Source: Uniprot/SWISSPROT P13803	1	
ENSRNOP00000022985	2	-12.3	NAD(P) dependent steroid dehydrogenase-like Source: RefSeq_peptide NP_001009399	2	
ENSRNOP00000024772	3	-10.9	No description available.Protein Family: SIGNAL PEPTIDASE COMPLEX SUBUNIT 2 EC_3.4.-.- MICROSOMAL SIGNAL PEPTIDASE 25 KDA SUBUNIT SPASE 25 KDA SUBUNIT	0	
ENSRNOP00000025327	2	-5	Vesicle-trafficking protein SEC22b (SEC22 vesicle-trafficking protein homolog B) (SEC22 vesicle-trafficking protein-like 1) (ERS24) (ERS- 24).	1	Q4KM74
ENSRNOP00000027234	2	-11.2	Translocon-associated protein subunit alpha precursor (TRAP-alpha) (Signal sequence receptor subunit alpha) (SSR-alpha) (Liver regeneration-related protein LRRG137).	1	Q7TPJ0
ENSRNOP00000028196	5	-40.6	Cytochrome P450 2B2 (EC 1.14.14.1) (CYPIIB2) (P450E) (P450 PB4).	1	P04167
ENSRNOP00000040338	3	-17.3	methyltransferase like 7A Source: RefSeq_peptide NP_001032432	0	
ENSRNOP00000044573	1	-5.8	NADH-ubiquinone oxidoreductase chain 5 (EC 1.6.5.3) (NADH dehydrogenase subunit 5)	3	P11661

ENSRNOP00000048723	6	-33.2	No other features on this peptide	1	
ENSRNOP00000053518	2	-20.4	Peroxisomal membrane protein 2 (22 kDa peroxisomal membrane protein)	1	Q07066
ENSRNOP00000057446	2	-11.8	Son protein (Fragment).	0	Q6PDU3
ENSRNOP00000017643	2	-11.1	C-type lectin domain family 4 member F (C-type lectin superfamily member 13) (C-type lectin 13) (Kupffer cell receptor).	6	P10716
ENSRNOP00000021612	2	-12.7	Cadherin-17 precursor (Liver-intestine-cadherin) (LI-cadherin).	7	P55281
ENSRNOP00000027346	3	-25.9	Epithelial-cadherin precursor (E-cadherin) (Uvomorulin) (Cadherin-1) (CD324 antigen) . Source: Uniprot/SWISSPROT	2	Q9R0T4
ENSRNOP00000021170	3	-26	Cadherin-2 precursor (Neural-cadherin) (N-cadherin) (CD325 antigen).	8	Q9Z1Y3
ENSRNOP00000005853	2	-14.3	Polymeric-immunoglobulin receptor precursor (Poly-Ig receptor) (PIGR) . Source: Uniprot/SWISSPROT	4	P15083

Supplementary Table 4
Membrane Proteins identified by ConA fractionation (Chapter 3)

Identifier	# peptides	log (e) score	Description	Glycosylation (N-X-S/T)	Accession No
ENSRNOP00000000306	2	-9.4	Tricarboxylate transport protein, mitochondrial precursor (Citrate transport protein) (CTP) (Tricarboxylate carrier protein) (Solute carrier family 25 member 1).	0	P32089
ENSRNOP00000000749	2	-15.1	No description available.Protein Family: CDGSH IRON SULFUR DOMAIN CONTAINING 1 ZINC FINGER CDGSH DOMAIN CONTAINING 1	0	
ENSRNOP00000001299	8	-72.9	Scavenger receptor class B member 1 (SRB1) (SR-BI).	8	P97943
ENSRNOP00000001315	5	-3.5	Actin-related protein 2/3 complex subunit 1B (ARP2/3 complex 41 kDa subunit) (p41-ARC).	0	O88656
ENSRNOP00000001816	2	-3.7	Aldehyde dehydrogenase, mitochondrial precursor (EC 1.2.1.3) (ALDH class 2) (ALDH1) (ALDH-E2).	2	P11884
ENSRNOP00000001924	3	-14.7	Mitochondrial fission 1 protein (Fis1 homolog) (rFis1) (Tetratricopeptide repeat protein 11) (TPR repeat protein 11).	0	P84817
ENSRNOP00000002712	8	-27.8	UDP-glucuronosyltransferase 2B4 precursor (EC 2.4.1.17) (UDPGT) (UDP- glucuronosyltransferase 2B12).	0	P36511
ENSRNOP00000002738	8	-46.3	CD166 antigen precursor (Activated leukocyte-cell adhesion molecule) (ALCAM) (MEMD protein) (HB2) (SB-10 antigen) (KG-CAM).	5	O35112
ENSRNOP00000003601	3	-15.7	No description available.Protein Family: AMBIGUOUS	1	
ENSRNOP00000003791	2	-3.6	Probable saccharopine dehydrogenase (EC 1.5.1.9).	2	Q6AY30
ENSRNOP00000004311	4	-16.2	RAB37, member of RAS oncogene family	1	
ENSRNOP00000004836	4	-7.7	No description available.Protein Family: ATP SYNTHASE D CHAIN MITOCHONDRIAL EC_3.6.3.14	1	
ENSRNOP00000005755	2	-4	Calmodulin (CaM).	1	P62161
ENSRNOP00000005853	8	-56.6	Polymeric-immunoglobulin receptor precursor (Poly-Ig receptor) (PIGR) .	4	P15083
ENSRNOP00000005875	13	-29.5	Retinol dehydrogenase 7 (EC 1.1.1.105) (Retinol dehydrogenase type III) (RODH III).	1	P55006
ENSRNOP00000006087	2	-12.4	epidermal growth factor receptor Source: RefSeq_peptide NP_113695	6	

ENSRNOP00000006141	2	-10.8	Junctional adhesion molecule A precursor (JAM-A) (Junctional adhesion molecule 1) (JAM-1) (CD321 antigen).	2	Q9JHY1
ENSRNOP00000007233	2	-3.3	Dynein-like protein 11 (Fragment).	1	Q63162
ENSRNOP00000007870	4	-26.8	Corticosteroid 11-beta-dehydrogenase isozyme 1 (EC 1.1.1.146) (11-DH) (11-beta-hydroxysteroid dehydrogenase 1) (11-beta-HSD1).	2	P16232
ENSRNOP00000008045	2	-11.9	Protein FAM82A.	1	Q498D5
ENSRNOP00000008163	2	-8.7	No other features on this peptide	2	
ENSRNOP00000008477	9	-21.5	Voltage-dependent anion-selective channel protein 1 (VDAC-1) (rVDAC1) (Outer mitochondrial membrane protein porin 1)	2	Q9Z2L0
ENSRNOP00000008932	18	-128.7	similar to RIKEN cDNA 2310001A20 (RGD1308874), mRNA Source: RefSeq_dna NM_001034003	1	
ENSRNOP00000008987	2	-6.2	CD302 antigen precursor (C-type lectin domain family 13 member A).	0	Q5FVR3
ENSRNOP00000009989	2	-14.5	Protein LYRIC (Lysine-rich CEACAM1 co-isolated protein) (Metastasis adhesion protein) (Metadherin)	3	Q9Z1W6
ENSRNOP00000010209	6	-40	Dolichyl-diphosphooligosaccharide--protein glycosyltransferase 63 kDa subunit precursor (EC 2.4.1.119) (Ribophorin II) (RPN-II).	2	P25235
ENSRNOP00000010467	2	-9.6	No description available.Protein Family: PLEXIN PRECURSOR	11	
ENSRNOP00000010579	20	-47.2	Microsomal glutathione S-transferase 1 (EC 2.5.1.18) (Microsomal GST- 1) (Microsomal GST-I).	0	P08011
ENSRNOP00000010663	2	-9.1	UDP-glucose pyrophosphorylase 2 Source: RefSeq_peptide NP_001019914	4	
ENSRNOP00000010760	6	-4.6	Methyltransferase-like protein 7B precursor (EC 2.1.1.-) (Associated with lipid droplet protein 1) (ALDI).	0	Q562C4
ENSRNOP00000011158	3	-16.1	Nipsnap1 protein (Fragment).	0	Q5EBA4
ENSRNOP00000011275	8	-54.5	Basigin precursor (OX-47 antigen) (Glycoprotein CE9) (CD147 antigen).	3	P26453
ENSRNOP00000011880	3	-15.2	Cytochrome P450 2D18 (EC 1.14.14.1) (CYPIID18) (P450 2D-29/2D-35).	1	Q64680
ENSRNOP00000012260	2	-9.2	No other features on this peptide	0	
ENSRNOP00000012413	13	-29.6	Cytochrome P450 2D26 (EC 1.14.14.1) (CYPIID26) (P450-DB2) (P450-CMF2) (Debrisoquine 4-hydroxylase).	3	P10634
ENSRNOP00000012661	2	-8.3	No description available.Protein Family: TENSIN	1	

ENSRNOP00000012681	7	-23.4	No other features on this peptide	1	
ENSRNOP00000012878	2	-4	NADH-cytochrome b5 reductase 3 (EC 1.6.2.2) (Cytochrome b5 reductase) (B5R) (Diaphorase-1)	0	P20070
ENSRNOP00000013262	64	-441.8	Electron transfer flavoprotein-ubiquinone oxidoreductase, mitochondrial precursor (EC 1.5.5.1) (ETF-QO) (ETF-ubiquinone oxidoreductase) (ETF dehydrogenase) (Electron-transferring- flavoprotein dehydrogenase).	1	Q6UPE1
ENSRNOP00000013607	2	-10.5	Solute carrier family 27 (Fatty acid transporter), member 2.	2	Q66HN6
ENSRNOP00000013816	18	-65.7	No other features on this peptide	0	
ENSRNOP00000013935	2	-8.6	No other features on this peptide	3	
ENSRNOP00000014058	2	-4.6	Cytochrome c, somatic.	0	P62898
ENSRNOP00000014235	50	-154.1	Long-chain-fatty-acid--CoA ligase 1 (EC 6.2.1.3) (Long-chain acyl-CoA synthetase 1) (LACS 1) (Long-chain-fatty-acid--CoA ligase, liver isozyme).	3	P18163
ENSRNOP00000014630	3	-8.8	No description available.Protein Family: MICROSOMAL TRIGLYCERIDE TRANSFER LARGE SUBUNIT PRECURSOR	1	
ENSRNOP00000014704	4	-17	ADP/ATP translocase 1 (Adenine nucleotide translocator 1) (ANT 1) (ADP,ATP carrier protein 1) (Solute carrier family 25 member 4).	0	Q05962
ENSRNOP00000014819	2	-6.5	Uncharacterized protein C10orf58 homolog precursor.	0	Q6AXX6
ENSRNOP00000015302	3	-15.7	No description available.Protein Family: PDZ AND LIM DOMAIN	2	
ENSRNOP00000015851	3	-16.6	NADH-ubiquinone oxidoreductase 75 kDa subunit, mitochondrial precursor (EC 1.6.5.3) (EC 1.6.99.3).	1	Q66HF1
ENSRNOP00000015866	2	-3.6	Solute carrier family 2, facilitated glucose transporter member 2 (Glucose transporter type 2, liver) (GLUT-2).	1	P12336
ENSRNOP00000015913	11	-49.3	ADP/ATP translocase 2 (Adenine nucleotide translocator 2) (ANT 2) (ADP,ATP carrier protein 2) (Solute carrier family 25 member 5).	1	Q09073
ENSRNOP00000016205	2	-10.2	Cysteine sulfinic acid decarboxylase (EC 4.1.1.29) (Sulfinoalanine decarboxylase) (Cysteine-sulfinate decarboxylase).	2	Q64611
ENSRNOP00000016423	5	-28.8	Collagen alpha-2(I) chain precursor (Alpha-2 type I collagen).	0	P02466
ENSRNOP00000016954	4	-9.8	Carnitine O-palmitoyltransferase 2, mitochondrial precursor (EC 2.3.1.21) (Carnitine palmitoyltransferase II) (CPT II).	6	P18886

ENSRNOP00000016965	2	-3.1	NADH dehydrogenase flavoprotein 2, mitochondrial precursor (EC 1.6.5.3) (EC 1.6.99.3) (NADH-ubiquinone oxidoreductase 24 kDa subunit).	0	P19234
ENSRNOP00000017067	2	-4.8	No description available.Protein Family: CYTOCHROME C1 HEME PROTEIN MITOCHONDRIAL PRECURSOR CYTOCHROME C 1 CYTOCHROME B C1 COMPLEX SUBUNIT 4 UBIQUINOL CYTOCHROME C REDUCTASE COMPLEX CYTOCHROME C1 SUBUNIT COMPLEX III SUBUNIT 4 COMPLEX III SUBUNIT IV	0	
ENSRNOP00000017067	2	-4.8	No description available.Protein Family: CYTOCHROME C1 HEME PROTEIN MITOCHONDRIAL PRECURSOR CYTOCHROME C 1 CYTOCHROME B C1 COMPLEX SUBUNIT 4 UBIQUINOL CYTOCHROME C REDUCTASE COMPLEX CYTOCHROME C1 SUBUNIT COMPLEX III SUBUNIT 4 COMPLEX III SUBUNIT IV	0	
ENSRNOP00000017101	3	-22.4	Membrane-associated progesterone receptor component 1 (Acidic 25 kDa protein) (25-DX) (Ventral midline antigen) (VEMA).	0	P70580
ENSRNOP00000017237	3	-15.3	Cytochrome P450 2C6 (EC 1.14.14.1) (CYPIIC6) (P450 PB1) (PTF2).	2	P05178
ENSRNOP00000017310	10	-50.3	Cytochrome P450 2C11 (EC 1.14.14.1) (CYPIIC11) (P-450(M-1)) (P450H) (P450-UT-A) (UT-2).	1	P08683
ENSRNOP00000018116	4	-23.3	Collagen alpha-1(IX) chain (Fragment).	0	P20850
ENSRNOP00000020184	5	-23.5	procollagen, type IV, alpha 4 Source: RefSeq_peptide NP_001008333	0	
ENSRNOP00000020302	5	-39.7	Dihydroorotate dehydrogenase, mitochondrial precursor (EC 1.3.3.1) (Dihydroorotate oxidase) (DHOdehase).	3	Q63707
ENSRNOP00000020306	13	-105	dolichyl-di-phosphooligosaccharide-protein glycotransferase (predicted) Source: RefSeq_peptide NP_001012104	0	
ENSRNOP00000020364	5	-33	Cation-dependent mannose-6-phosphate receptor precursor (CD Man-6-P receptor) (CD-MPR).	5	Q6AY20
ENSRNOP00000020446	27	-147.1	Cytochrome b5.	0	P00173
ENSRNOP00000020554	9	-29.6	No description available.Protein Family: RRNA 2- O METHYLTRANSFERASE FIBRILLARIN EC_2.1.1.-	1	
ENSRNOP00000021170	2	-6.7	Cadherin-2 precursor (Neural-cadherin) (N-cadherin) (CD325 antigen).	7	Q9Z1Y3
ENSRNOP00000021407	38	-283.4	choline dehydrogenase precursor Source: RefSeq_peptide NP_942026	0	

ENSRNOP00000021512	4	-21.5	Peroxisomal trans-2-enoyl-CoA reductase (EC 1.3.1.38) (RLF98) (Peroxisomal 2,4-dienoyl CoA reductase) (PX-2,4-DCR1).	3	Q9WVK3
ENSRNOP00000021514	2	-9.3	Ubiquinol-cytochrome-c reductase complex core protein 2, mitochondrial precursor (EC 1.10.2.2) (Core protein II) (Complex III subunit II).	3	P32551
ENSRNOP00000021920	5	-17.2	ATP synthase B chain, mitochondrial precursor (EC 3.6.3.14).	0	P19511
ENSRNOP00000022703	6	-34.8	L-gulonolactone oxidase (EC 1.1.3.8) (LGO) (L-gulono-gamma-lactone oxidase) (GLO).	2	P10867
ENSRNOP00000022892	2	-4.5	ATP synthase subunit alpha, mitochondrial precursor (EC 3.6.3.14). \	1	P15999
ENSRNOP00000023601	2	-8.2	Ryanodine receptor type II (Fragment).	1	O08661
ENSRNOP00000024106	6	-46	Alpha-enolase (EC 4.2.1.11) (2-phospho-D-glycerate hydro-lyase) (Non- neural enolase) (NNE) (Enolase 1).	2	P04764
ENSRNOP00000024423	3	-3.8	Dimethylaniline monooxygenase 5 (EC 1.14.13.8) (Hepatic flavin-containing monooxygenase 5) (FMO 5) (Dimethylaniline oxidase 5).	2	Q8K4C0
ENSRNOP00000024824	2	-7.6	tau tubulin kinase 1	1	
ENSRNOP00000025045	4	-11.7	UDP-glucuronosyltransferase 1-1 precursor (EC 2.4.1.17) (UDPGT) (UGT1*1) (UGT1-01) (UGT1.1) (UGT1A1) (B1).	2	Q64550
ENSRNOP00000025254	10	-86.6	Asialoglycoprotein receptor 1 (ASGPR 1) (ASGP-R 1) (Hepatic lectin 1) (RHL-1).	3	P02706
ENSRNOP00000025525	3	-15.1	Cytochrome c oxidase subunit 5A, mitochondrial precursor (EC 1.9.3.1) (Cytochrome c oxidase polypeptide Va).	0	P11240
ENSRNOP00000026122	4	-22	Hydroxymethylglutaryl-CoA synthase, mitochondrial precursor (EC 2.3.3.10) (HMG-CoA synthase) (3-hydroxy-3-methylglutaryl coenzyme A synthase).	0	P22791
ENSRNOP00000026279	2	-6.1	Proteasome activator complex subunit 2 (Proteasome activator 28- subunit beta) (PA28beta) (PA28b) (Activator of multicatalytic protease subunit 2) (11S regulator complex subunit beta) (REG-beta).	0	Q63798
ENSRNOP00000026290	13	-80.6	3 beta-hydroxysteroid dehydrogenase type 5 (3 beta-hydroxysteroid dehydrogenase type V) (3-beta-HSD V) (NADPH-dependent 3-beta-hydroxy- Delta(5)-steroid dehydrogenase) (EC 1.1.1.-) (3-beta-hydroxy-5-ene steroid dehydrogenase) (Progesterone reductase).	2	

ENSRNOP00000003052	2	-11.2	Lysosome membrane protein 2 (Lysosome membrane protein II) (LIMP II) (Scavenger receptor class B member 2)	11	P27615
ENSRNOP00000026347	2	-8.5	Vitamin K epoxide reductase complex subunit 1 (EC 1.1.4.1) (Vitamin K1 2,3-epoxide reductase subunit 1).	1	Q6TEK4
ENSRNOP00000026574	5	-17.6	Bile acyl-CoA synthetase (EC 6.2.1.7) (BACS) (Bile acid CoA ligase) (BA-CoA ligase) (BAL) (Cholate--CoA ligase) (Very long chain acyl-CoA synthetase-related protein) (VLACS-related) (VLACSR) (Fatty acid transport protein 5) (FATP-5) (Solute carrier family	1	Q9ES38
ENSRNOP00000027520	2	-12	Mitochondrial carnitine/acylcarnitine carrier protein (Carnitine/acylcarnitine translocase) (CAC) (Solute carrier family 25 member 20).	0	P97521
ENSRNOP00000027754	2	-17.5	Up-regulated during skeletal muscle growth protein 5 (Diabetes- associated protein in insulin-sensitive tissues).	0	Q9JJW3
ENSRNOP00000027760	6	-53.8	CD81 antigen (26 kDa cell surface protein TAPA-1) (Target of the antiproliferative antibody 1).	0	Q62745
ENSRNOP00000028066	2	-9.8	Intercellular adhesion molecule 1 precursor (ICAM-1) (CD54 antigen).	8	Q00238
ENSRNOP00000028237	2	-5	Cytochrome P450 2A1 (EC 1.14.14.1) (CYPIIA1) (Steroid hormones 7- alpha-hydroxylase) (Testosterone 7-alpha-hydroxylase) (P450-UT-F).	1	P11711
ENSRNOP00000028680	3	-9.4	No description available.Protein Family: NODAL MODULATOR PRECURSOR PM5	5	
ENSRNOP00000028760	2	-9.9	Synaptic vesicle glycoprotein 2A (Synaptic vesicle protein 2A) (Synaptic vesicle protein 2).	3	Q02563
ENSRNOP00000029426	2	-4.6	No description available.Protein Family: ATP SYNTHASE F CHAIN MITOCHONDRIAL EC_3.6.3.14	0	
ENSRNOP00000030046	2	-8	No description available.Protein Family: UNCHARACTERIZED	1	
ENSRNOP00000031599	2	-3.1	hydroxysteroid (17-beta) dehydrogenase 6 Source: RefSeq_peptide NP_775427	3	
ENSRNOP00000031896	5	-39	Collagen alpha-1(I) chain precursor (Alpha-1 type I collagen).	2	P02454
ENSRNOP00000033706	2	-3.8	No description available.Protein Family: CYTOCHROME B C1 COMPLEX SUBUNIT 7 EC_1.10.2.2 UBIQUINOL CYTOCHROME C REDUCTASE COMPLEX 14 KDA COMPLEX III SUBUNIT 7 COMPLEX III SUBUNIT VII	0	
ENSRNOP00000034293	9	-69.9	Epoxide hydrolase 1 (EC 3.3.2.9) (Microsomal epoxide hydrolase) (Epoxide hydratase).	1	P07687

ENSRNOP00000034723	7	-50.8	UDP-glucuronosyltransferase 2B2 precursor (EC 2.4.1.17) (UDPGT) (3- hydroxyandrogen specific) (UDPGTr-4) (RLUG23).	1	P08541
ENSRNOP00000034954	6	-26.6	Perlecan (Fragment).	5	O08591
ENSRNOP00000035031	2	-7.3	No description available.Protein Family: UNKNOWN	5	
ENSRNOP00000035416	2	-4.6	No description available.Protein Family: SYNAPTIC GLYCOPROTEIN SC2 EC_1.3.1.- TRANS 2 3 ENOYL COA REDUCTASE TER	3	
ENSRNOP00000035423	7	-42.4	Retinol dehydrogenase 2 (EC 1.1.1.105) (Retinol dehydrogenase type II) (RODH II) (29 k-protein).	0	P50170
ENSRNOP00000035497	14	-113.1	Uncharacterized protein KIAA0152 homolog precursor.	1	Q5FVQ4
ENSRNOP00000038602	3	-15.7	No other features on this peptide	2	
ENSRNOP00000040139	2	-4.6	Metalloreductase STEAP4 (EC 1.16.1.-) (Six-transmembrane epithelial antigen of prostate 4).	2	Q4V8K1
ENSRNOP00000055824	2	-15.3	Dipeptidyl peptidase 4 (EC 3.4.14.5) (Dipeptidyl peptidase IV) (DPP IV) (T-cell activation antigen CD26) (GP110 glycoprotein)	8	P14740
ENSRNOP00000040266	12	-69.5	Cytochrome P450 2D10 (EC 1.14.14.1) (CYPIID10) (P450-DB5) (P450-CMF1B) (Debrisoquine 4-hydroxylase).	4	P12939
ENSRNOP00000040513	2	-9.9	No description available.Protein Family: CATION DEPENDENT MANNOSE 6 PHOSPHATE RECEPTOR PRECURSOR CD MAN 6 P RECEPTOR CD MPR 46 KDA MANNOSE 6 PHOSPHATE RECEPTOR MPR 46	4	
ENSRNOP00000040859	36	-257.1	Calnexin precursor.	1	P35565
ENSRNOP00000041174	30	-62.7	Cytochrome P450 2D1 (EC 1.14.14.1) (CYPIID1) (P450-DB1) (P450-CMF1A) (P450-UT-7) (Debrisoquine 4-hydroxylase).	4	P10633
ENSRNOP00000041608	10	-10.4	Phosphate carrier protein, mitochondrial precursor (PTP) (Solute carrier family 25 member 3).	0	P16036
ENSRNOP00000043032	6	-20.4	poliovirus receptor related 2 Source: RefSeq_peptide NP_001012064	3	
ENSRNOP00000043239	10	-45	UDP-glucuronosyltransferase 2B3 precursor (EC 2.4.1.17) (UDPGT) (Testosterone, dihydrotestosterone, and beta-estradiol specific) (17- beta-hydroxysteroid specific) (UDPGTr-3) (RLUG38).	0	P08542
ENSRNOP00000043466	2	-12.8	Amine oxidase B (EC 1.4.3.4) (Monoamine oxidase type B) (MAO-B).	1	P19643
ENSRNOP00000043524	14	-75.9	similar to RIKEN cDNA 2310001A20 (RGD1308874), mRNA Source: RefSeq_dna NM_001034003	1	

ENSRNOP00000043567	2	-4.8	actin, gamma, cytoplasmic 1	0	
ENSRNOP00000044296	6	-8.2	Actin, cytoplasmic 1 (Beta-actin).	1	P60711
ENSRNOP00000045002	10	-33.7	UDP-glucuronosyltransferase 2B3 precursor (EC 2.4.1.17) (UDPGT) (Testosterone, dihydrotestosterone, and beta-estradiol specific) (17- beta-hydroxysteroid specific) (UDPGTr-3) (RLUG38).	0	P08542
ENSRNOP00000045029	3	-11.8	Cytochrome P450 2C7 (EC 1.14.14.1) (CYPIIC7) (P450F) (PTF1).	1	P05179
ENSRNOP00000045388	2	-9.4	RT1 class I, CE2 Source: RefSeq_peptide NP_001008840	2	
ENSRNOP00000045650	3	-9	ATPase, Na+/K+ transporting, alpha 1 polypeptide	3	
ENSRNOP00000045886	6	-35	Fatty aldehyde dehydrogenase (EC 1.2.1.3) (Aldehyde dehydrogenase, microsomal) (Aldehyde dehydrogenase family 3 member A2) (Aldehyde dehydrogenase 10).	0	P30839
ENSRNOP00000045952	2	-3.3	solute carrier family 25 member 15 Source: RefSeq_peptide NP_001041345	0	
ENSRNOP00000047647	2	-3.7	Glycerol kinase (EC 2.7.1.30) (ATP:glycerol 3-phosphotransferase) (Glycerokinase) (GK) (ATP-stimulated glucocorticoid-receptor translocation promoter) (ASTP).	1	Q63060
ENSRNOP00000048417	4	-14.3	RT1 class Ia, locus A2 Source: RefSeq_peptide NP_001008829	1	
ENSRNOP00000048711	6	-48.4	Cytochrome P450 2D3 (EC 1.14.14.1) (CYPIID3) (P450-DB3) (Debrisoquine 4-hydroxylase).	1	P12938
ENSRNOP00000048723	9	-44.7	No other features on this peptide	0	
ENSRNOP00000049689	2	-4.6	similar to Tricarboxylate transport protein, mitochondrial precursor (Citrate transport protein) (CTP) (Tricarboxylate carrier protein) (Solute carrier family 25 member 1) (LOC288311), mRNA Source: RefSeq_dna XR_006058	1	
ENSRNOP00000049883	2	-9.6	RT1 class Ib gene, H2-TL-like, grc region (N1) Source: RefSeq_peptide NP_036778	3	
ENSRNOP00000050252	11	-90.3	Basigin precursor (OX-47 antigen) (Glycoprotein CE9) (CD147 antigen).	3	P26453
ENSRNOP00000050322	2	-4	Actin, gamma-enteric smooth muscle (Smooth muscle gamma actin) (Gamma- 2-actin) (Alpha-actin-3).	1	P63269
ENSRNOP00000051614	2	-13.5	No other features on this peptide	2	

ENSRNOP00000051841	8	-47.5	Protein disulfide-isomerase precursor (EC 5.3.4.1) (PDI) (Prolyl 4- hydroxylase subunit beta) (Cellular thyroid hormone-binding protein).	0	P04785
ENSRNOP00000052247	3	-9.2	RAB30, member RAS oncogene family Source: RefSeq_peptide NP_001015012	2	
ENSRNOP00000052513	2	-8.3	No description available.Protein Family: UNKNOWN	0	
ENSRNOP00000053689	2	-8	No description available.Protein Family: UNKNOWN	0	
ENSRNOP00000054537	5	-31	lysosomal-associated membrane protein 1	18	
ENSRNOP00000056312	4	-15.4	tumor rejection antigen gp96 (predicted) Source: RefSeq_peptide NP_001012197	4	
ENSRNOP00000056976	2	-9	Translocon-associated protein subunit alpha precursor (TRAP-alpha) (Signal sequence receptor subunit alpha) (SSR-alpha) (Liver regeneration-related protein LRRG137).	2	Q7TPJ0
ENSRNOP00000057369	2	-9.1	No description available.Protein Family: FRAGMENT	0	
ENSRNOP00000057476	2	-7.5	No description available.Protein Family: UNKNOWN	0	
ENSRNOP00000057564	2	-8.1	No description available.Protein Family: PRECURSOR	0	
ENSRNOP00000057699	3	-10.2	RT1 class I, CE5 isoform 1 Source: RefSeq_peptide NP_001008843	1	

Supplementary Table 4 (continued)
Membrane Proteins identified by Jacalin fractionation (Chapter 3)

Identifier	# peptides	log (e) score	Description	Glycosylation (N-X-S/T)	Accession No
ENSRNOP00000024187	34	-224.2	Liver carboxylesterase 4 precursor (EC 3.1.1.1) (Carboxyesterase ES-4) (Microsomal palmitoyl-CoA hydrolase) (Kidney microsomal carboxylesterase).	0	Q64573
ENSRNOP00000014235	69	-179.3	Long-chain-fatty-acid--CoA ligase 1 (EC 6.2.1.3) (Long-chain acyl-CoA synthetase 1) (LACS 1) (Long-chain-fatty-acid--CoA ligase, liver isozyme).	3	P18163
ENSRNOP00000034210	23	-169.1	Lrp1 protein (Fragment).	3	Q5I0H1
ENSRNOP00000021812	24	-149.3	Carboxylesterase 3 precursor (EC 3.1.1.1) (Liver carboxylesterase 10) (Carboxyesterase ES-10) (pI 6.1 esterase) (ES-HVEL).	2	P16303
ENSRNOP00000041174	32	-94.5	Cytochrome P450 2D1 (EC 1.14.14.1) (CYPIID1) (P450-DB1) (P450-CMF1A) (P450-UT-7) (Debrisoquine 4-hydroxylase).	4	P10633
ENSRNOP00000044296	20	-79	Actin, cytoplasmic 1 (Beta-actin).	1	P60711
ENSRNOP00000040266	26	-78.6	Cytochrome P450 2D10 (EC 1.14.14.1) (CYPIID10) (P450-DB5) (P450-CMF1B) (Debrisoquine 4-hydroxylase).	4	P12939
ENSRNOP00000013816	23	-69.7	No other features on this peptide	0	
ENSRNOP00000020775	7	-57.9	Liver carboxylesterase 3 precursor (EC 3.1.1.1) (Carboxyesterase ES-3) (pI 5.5 esterase) (ES-HTEL).	3	Q63108
ENSRNOP00000051841	12	-56.5	Protein disulfide-isomerase precursor (EC 5.3.4.1) (PDI) (Prolyl 4- hydroxylase subunit beta) (Cellular thyroid hormone-binding protein).	0	P04785
ENSRNOP00000020446	19	-56.4	Cytochrome b5.	1	P00173
ENSRNOP00000010579	23	-51.4	Microsomal glutathione S-transferase 1 (EC 2.5.1.18) (Microsomal GST- 1) (Microsomal GST-I).	0	P08011
ENSRNOP00000005875	20	-49.8	Retinol dehydrogenase 7 (EC 1.1.1.105) (Retinol dehydrogenase type III) (RODH III).	1	P55006
ENSRNOP00000035423	14	-48	Retinol dehydrogenase 2 (EC 1.1.1.105) (Retinol dehydrogenase type II) (RODH II) (29 k-protein).	0	P50170
ENSRNOP00000025254	6	-43.7	Asialoglycoprotein receptor 1 (ASGPR 1) (ASGP-R 1) (Hepatic lectin 1) (RHL-1).	3	P02706
ENSRNOP00000045567	10	-43.2	Cytochrome P450 4A14 precursor (EC 1.14.15.3) (CYPIVA14) (Lauric acid omega-hydroxylase) (P450-LA-omega 3).	3	P20817

ENSRNOP00000015913	21	-40.6	ADP/ATP translocase 2 (Adenine nucleotide translocator 2) (ANT 2) (ADP,ATP carrier protein 2) (Solute carrier family 25 member 5).	1	Q09073
ENSRNOP00000045886	14	-39.8	Fatty aldehyde dehydrogenase (EC 1.2.1.3) (Aldehyde dehydrogenase, microsomal) (Aldehyde dehydrogenase family 3 member A2) (Aldehyde dehydrogenase 10).	0	P30839
ENSRNOP00000020558	6	-38.6	UDP-glucose:glycoprotein glucosyltransferase 1 precursor (EC 2.4.1.-) (UDP-glucose ceramide glucosyltransferase-like 1) (UDP-- Glc:glycoprotein glucosyltransferase) (RUGT).	3	Q9JLA3
ENSRNOP00000019772	8	-37	Fibronectin precursor (FN).	6	P04937
ENSRNOP00000058524	5	-34.6	carboxylesterase 6 Source: RefSeq_peptide NP_653344	1	
ENSRNOP00000042597	6	-34.4	Liver carboxylesterase 4 precursor (EC 3.1.1.1) (Carboxyesterase ES-4) (Microsomal palmitoyl-CoA hydrolase) (Kidney microsomal carboxylesterase).	1	Q64573
ENSRNOP00000024622	5	-34.2	No description available.Protein Family: CARBOXYLESTERASE PRECURSOR EC_3.1.1.1	4	
ENSRNOP00000018649	6	-34.1	Dsp protein (Fragment).	4	Q4QQR7
ENSRNOP00000034723	7	-33.9	UDP-glucuronosyltransferase 2B2 precursor (EC 2.4.1.17) (UDPGT) (3- hydroxyandrogen specific) (UDPGTr-4) (RLUG23).	1	P08541
ENSRNOP00000021514	6	-33.5	Ubiquinol-cytochrome-c reductase complex core protein 2, mitochondrial precursor (EC 1.10.2.2) (Core protein II) (Complex III subunit II).	3	P32551
ENSRNOP00000043239	8	-33.4	UDP-glucuronosyltransferase 2B3 precursor (EC 2.4.1.17) (UDPGT) (Testosterone, dihydrotestosterone, and beta-estradiol specific) (17- beta-hydroxysteroid specific) (UDPGTr-3) (RLUG38).	0	P08542
ENSRNOP00000003334	5	-33	Guanine nucleotide-binding protein subunit beta 2-like 1 (Receptor of activated protein kinase C 1) (RACK1) (Receptor for activated C kinase).	1	P63245
ENSRNOP00000026794	6	-31.1	No description available.Protein Family: NEUTRAL ALPHA GLUCOSIDASE AB PRECURSOR EC_3.2.1.84 GLUCOSIDASE II SUBUNIT ALPHA	1	
ENSRNOP00000045002	7	-30.8	UDP-glucuronosyltransferase 2B3 precursor (EC 2.4.1.17) (UDPGT) (Testosterone, dihydrotestosterone, and beta-estradiol specific) (17- beta-hydroxysteroid specific) (UDPGTr-3) (RLUG38).	0	P08542
ENSRNOP00000017310	5	-30	Cytochrome P450 2C11 (EC 1.14.14.1) (CYPIIC11) (P-450(M-1)) (P450H) (P450-UT-A) (UT-2).	1	P08683
ENSRNOP00000022892	4	-29.4	ATP synthase subunit alpha, mitochondrial precursor (EC 3.6.3.14).	1	P15999
ENSRNOP00000001299	3	-28.8	Scavenger receptor class B member 1 (SRB1) (SR-BI).	8	P97943

ENSRNOP00000012796	5	-27.5	No description available.Protein Family: FILAMIN B FLN B BETA FILAMIN ACTIN BINDING ABP 280	4	
ENSRNOP00000002738	5	-26.6	CD166 antigen precursor (Activated leukocyte-cell adhesion molecule) (ALCAM) (MEMD protein) (HB2) (SB-10 antigen) (KG-CAM).	5	O35112
ENSRNOP00000038602	5	-26.4	No other features on this peptide	2	
ENSRNOP00000042268	6	-26.4	Basigin precursor (OX-47 antigen) (Glycoprotein CE9) (CD147 antigen).	3	P26453
ENSRNOP00000024423	3	-25.7	Dimethylaniline monooxygenase 5 (EC 1.14.13.8) (Hepatic flavin-containing monooxygenase 5) (FMO 5) (Dimethylaniline oxidase 5).	2	Q8K4C0
ENSRNOP00000043950	4	-25.4	Junction plakoglobin.	7	Q6P0K8
ENSRNOP00000053689	4	-24.7	No description available.Protein Family: UNKNOWN	0	
ENSRNOP00000016353	4	-23.5	Integrin alpha-1 precursor (Laminin and collagen receptor) (VLA-1) (CD49a antigen).	21	P18614
ENSRNOP00000004864	5	-22.9	Dimethylaniline monooxygenase 3 (EC 1.14.13.8) (Hepatic flavin-containing monooxygenase 3) (FMO 3) (Dimethylaniline oxidase 3).	3	Q9EQ76
ENSRNOP00000024736	4	-22.7	No description available.Protein Family: PRECURSOR	3	
ENSRNOP00000010209	4	-22	Dolichyl-diphosphooligosaccharide--protein glycosyltransferase 63 kDa subunit precursor (EC 2.4.1.119) (Ribophorin II) (RPN-II).	2	P25235
ENSRNOP00000021170	5	-21.9	Cadherin-2 precursor (Neural-cadherin) (N-cadherin) (CD325 antigen).	7	Q9Z1Y3
ENSRNOP00000013532	4	-21	No description available.Protein Family: PLAKOPHILIN	5	
ENSRNOP00000021920	5	-20.6	ATP synthase B chain, mitochondrial precursor (EC 3.6.3.14).	0	P19511
ENSRNOP00000005755	3	-19.9	Calmodulin (CaM).	1	P62161
ENSRNOP00000026290	6	-19.7	3 beta-hydroxysteroid dehydrogenase type 5 (3 beta-hydroxysteroid dehydrogenase type V) (3-beta-HSD V) (NADPH-dependent 3-beta-hydroxy- Delta(5)-steroid dehydrogenase) (EC 1.1.1.-) (3-beta-hydroxy-5-ene steroid dehydrogenase) (Progesterone reductase).	2	P27364
ENSRNOP00000008477	16	-19.6	Voltage-dependent anion-selective channel protein 1 (VDAC-1) (rVDAC1) (Outer mitochondrial membrane protein porin 1).	2	Q9Z2L0
ENSRNOP00000054924	4	-19.3	inner membrane protein, mitochondrial Source: RefSeq_peptide NP_001030100	3	
ENSRNOP00000008987	2	-17.7	CD302 antigen precursor (C-type lectin domain family 13 member A).	0	Q5FVR3
ENSRNOP00000019285	3	-17.6	Cathepsin H precursor (EC 3.4.22.16) (Cathepsin B3) (Cathepsin BA) .	2	P00786
ENSRNOP00000035497	2	-17.6	Uncharacterized protein KIAA0152 homolog precursor.	1	Q5FVQ4

ENSRNOP00000037093	3	-16.9	No description available.Protein Family: COPINE COPINE	2	
ENSRNOP00000043466	4	-16.9	Amine oxidase B (EC 1.4.3.4) (Monoamine oxidase type B) (MAO-B).	1	P19643
ENSRNOP00000004091	4	-16.3	Calreticulin precursor (CRP55) (Calregulin) (HACBP) (ERp60) (CALBP) (Calcium-binding protein 3) (CABP3).	0	P18418
ENSRNOP00000026574	3	-15.9	Bile acyl-CoA synthetase (EC 6.2.1.7) (BACS) (Bile acid CoA ligase) (BA-CoA ligase) (BAL) (Cholate--CoA ligase) (Very long chain acyl-CoA synthetase-related protein) (VLACS-related) (VLACSR) (Fatty acid transport protein 5) (FATP-5) (Solute carrier family	1	Q9ES38
ENSRNOP00000046111	3	-15.6	LRRGT00082.	3	Q6TUG2
ENSRNOP00000001095	3	-15.3	Tubulin beta-5 chain.	2	P69897
ENSRNOP00000044376	2	-14.3	Asialoglycoprotein receptor 2 (ASGP-R 2) (ASGPR 2) (Hepatic lectin R2/3) (RHL-2).	3	P08290
ENSRNOP00000011880	2	-14.2	Cytochrome P450 2D18 (EC 1.14.14.1) (CYPIID18) (P450 2D-29/2D-35).	3	Q64680
ENSRNOP00000030301	3	-14.2	Elastin precursor (Tropoelastin).	0	Q99372
ENSRNOP00000050167	3	-14.1	Elastin precursor (Tropoelastin).	0	Q99372
ENSRNOP00000004836	5	-13.5	No description available.Protein Family: ATP SYNTHASE D CHAIN MITOCHONDRIAL EC_3.6.3.14	1	
ENSRNOP00000044696	4	-12.9	Ubiquinol-cytochrome-c reductase complex core protein 1, mitochondrial precursor (EC 1.10.2.2) (Core I protein).	2	Q68FY0
ENSRNOP00000005459	4	-12.6	LOC690745 protein (Fragment).	0	Q5I0K9
ENSRNOP00000050581	5	-12.3	Corticosteroid 11-beta-dehydrogenase isozyme 1 (EC 1.1.1.146) (11-DH) (11-beta-hydroxysteroid dehydrogenase 1) (11-beta-HSD1).	2	P16232
ENSRNOP00000013262	3	-12.1	Electron transfer flavoprotein-ubiquinone oxidoreductase, mitochondrial precursor (EC 1.5.5.1) (ETF-QO) (ETF-ubiquinone oxidoreductase) (ETF dehydrogenase) (Electron-transferring- flavoprotein dehydrogenase).	1	Q6UPE1
ENSRNOP00000003965	2	-11.6	ATP synthase subunit beta, mitochondrial precursor (EC 3.6.3.14).	0	P10719
ENSRNOP00000015956	2	-11.2	Aspartate aminotransferase, mitochondrial precursor (EC 2.6.1.1) (Transaminase A) (Glutamate oxaloacetate transaminase 2).	1	P00507
ENSRNOP00000048723	3	-11.1	No other features on this peptide	1	
ENSRNOP00000013607	2	-11	Solute carrier family 27 (Fatty acid transporter), member 2.	2	Q66HN6
ENSRNOP00000003052	2	-10.8	Lysosome membrane protein 2 (Lysosome membrane protein II) (LIMP II) (Scavenger receptor class B member 2)	11	P27615
ENSRNOP00000027520	5	-10.8	Mitochondrial carnitine/acylcarnitine carrier protein (Carnitine/acylcarnitine translocase) (CAC) (Solute carrier family 25 member 20).	0	P97521

ENSRNOP00000049879	6	-10.3	ATP synthase gamma chain, mitochondrial (EC 3.6.3.14).	4	P35435
ENSRNOP00000057476	2	-10	No description available.Protein Family: UNKNOWN	0	
ENSRNOP00000028237	3	-9.6	Cytochrome P450 2A1 (EC 1.14.14.1) (CYPIIA1) (Steroid hormones 7- alpha-hydroxylase) (Testosterone 7-alpha-hydroxylase) (P450-UT-F).	1	P11711
ENSRNOP00000034293	2	-9.6	Epoxide hydrolase 1 (EC 3.3.2.9) (Microsomal epoxide hydrolase) (Epoxide hydratase).	1	P07687
ENSRNOP00000011485	2	-9.2	MAL2 proteolipid protein Source: RefSeq_peptide NP_942081	1	
ENSRNOP00000022487	3	-9.2	Cytochrome c oxidase subunit 5B, mitochondrial precursor (EC 1.9.3.1) (Cytochrome c oxidase polypeptide Vb) (Cytochrome c oxidase subunit VIA*).	1	P12075
ENSRNOP00000014058	3	-8.9	Cytochrome c, somatic.	0	P62898
ENSRNOP00000019624	2	-8.9	No description available.Protein Family: NADH DEHYDROGENASE 1 BETA SUBCOMPLEX SUBUNIT 10 EC_1.6.5.3 EC_1.6.99.- 3 NADH UBIQUINONE OXIDOREDUCTASE PDSW SUBUNIT COMPLEX I PDSW CI PDSW	1	
ENSRNOP00000021407	4	-8.9	choline dehydrogenase precursor Source: RefSeq_peptide NP_942026	0	
ENSRNOP00000018455	3	-8.8	Protein transport protein Sec61 subunit alpha isoform 1 (Sec61 alpha- 1).	0	P61621
ENSRNOP00000028194	3	-8.6	7-dehydrocholesterol reductase (EC 1.3.1.21) (7-DHC reductase) (Sterol Delta(7)-reductase).	3	Q9Z2Z8
ENSRNOP00000004365	2	-8.5	No description available.Protein Family: WD REPEAT CONTAINING	0	
ENSRNOP00000027773	3	-8.5	Alpha-actinin-4 (Non-muscle alpha-actinin 4) (F-actin cross-linking protein).	3	Q9QXQ0
ENSRNOP00000052801	2	-8.4	Perlecan (Fragment).	0	O08591
ENSRNOP00000024106	2	-8.2	Alpha-enolase (EC 4.2.1.11) (2-phospho-D-glycerate hydro-lyase) (Non- neural enolase) (NNE) (Enolase 1).	2	P04764
ENSRNOP00000035416	2	-8.2	No description available.Protein Family: SYNAPTIC GLYCOPROTEIN SC2 EC_1.3.1.- TRANS 2 3 ENOYL COA REDUCTASE TER	3	
ENSRNOP00000049615	2	-8.2	No description available.Protein Family: COLLAGEN ALPHA 1 CHAIN	1	
ENSRNOP00000010043	2	-8.1	Ras-related protein Rab-15.	1	P35289
ENSRNOP00000015338	2	-8	src homology 2 domain-containing transforming protein B	0	
ENSRNOP00000040018	2	-8	Plectin-1 (PLTN) (PCN).	9	P30427
ENSRNOP00000006087	2	-7.9	epidermal growth factor receptor Source: RefSeq_peptide NP_113695	6	

ENSRNOP00000029578	2	-7.9	nicotinamide nucleotide transhydrogenase Source: RefSeq_peptide NP_001013175	5	
ENSRNOP00000009989	2	-7.8	Protein LYRIC (Lysine-rich CEACAM1 co-isolated protein) (Metastasis adhesion protein) (Metadherin).	3	Q9Z1W6
ENSRNOP00000001284	2	-7.7	No description available.Protein Family: GUANINE NUCLEOTIDE EXCHANGE FACTOR LYMPHOID BLAST CRISIS ONCOGENE	2	
ENSRNOP00000010333	2	-7.4	procollagen, type XXVII, alpha 1 Source: RefSeq_peptide NP_942042	3	
ENSRNOP00000013496	3	-7.4	Low-density lipoprotein receptor precursor (LDL receptor).	4	P35952
ENSRNOP00000020554	2	-7.4	No description available.Protein Family: RRNA 2- O METHYLTRANSFERASE FIBRILLARIN EC_2.1.1.-		
ENSRNOP00000033098	2	-7.3	sidekick homolog 2 (chicken)	17	
ENSRNOP00000051703	2	-7.2	predicted gene, ENSMUSG00000072030	0	
ENSRNOP00000015684	2	-6.9	No description available.Protein Family: AMBIGUOUS	1	
ENSRNOP00000017101	2	-7	Membrane-associated progesterone receptor component 1 (Acidic 25 kDa protein) (25-DX) (Ventral midline antigen) (VEMA).	0	P70580
ENSRNOP00000002410	2	-6.3	Peroxisomal bifunctional enzyme (PBE) (PBFE) .	1	P07896
ENSRNOP00000022233	2	-6.3	Prothrombin precursor (EC 3.4.21.5) (Coagulation factor II) .	4	P18292
ENSRNOP00000005853	2	-6.1	Polymeric-immunoglobulin receptor precursor (Poly-Ig receptor) (PIGR) .	4	P15083
ENSRNOP00000029426	4	-5.6	No description available.Protein Family: ATP SYNTHASE F CHAIN MITOCHONDRIAL EC_3.6.3.14	0	
ENSRNOP00000015851	2	-5.5	NADH-ubiquinone oxidoreductase 75 kDa subunit, mitochondrial precursor (EC 1.6.5.3) (EC 1.6.99.3).	1	Q66HF1
ENSRNOP00000016965	2	-5.3	NADH dehydrogenase flavoprotein 2, mitochondrial precursor (EC 1.6.5.3) (EC 1.6.99.3) (NADH-ubiquinone oxidoreductase 24 kDa subunit).	0	P19234
ENSRNOP00000003645	2	-5.1	homogentisate 1, 2-dioxygenase Source: RefSeq_peptide NP_001012145	0	
ENSRNOP00000045650	2	-4.9	ATPase, Na+/K+ transporting, alpha 1 polypeptide	3	
ENSRNOP00000030508	2	-4.7	No description available.Protein Family: F BOX ONLY	0	
ENSRNOP00000040859	2	-4.7	Calnexin precursor.	1	P35565
ENSRNOP00000002712	5	-4.3	UDP-glucuronosyltransferase 2B4 precursor (EC 2.4.1.17) (UDPGT) (UDP- glucuronosyltransferase 2B12).	1	P36511
ENSRNOP00000041608	11	-4.1	Phosphate carrier protein, mitochondrial precursor (PTP) (Solute carrier family 25 member 3)	0	P16036

ENSRNOP00000000177	2	-4	Lysosome-associated membrane glycoprotein 2 precursor (LAMP-2) (Lysosomal membrane glycoprotein-type B) (LGP-B) (LGP-96) (LGP-110) (CD107b antigen).	16	P17046
ENSRNOP00000048004	2	-4	No description available.Protein Family: SKIN SPECIFIC 32	0	
ENSRNOP00000036896	2	-3.9	No other features on this peptide	0	
ENSRNOP00000010760	8	-3.5	Methyltransferase-like protein 7B precursor (EC 2.1.1.-) (Associated with lipid droplet protein 1) (ALDI).	0	Q562C4
ENSRNOP00000012448	3	-3.5	Cytochrome P450 4X1 (EC 1.14.14.1) (CYPIVX1).	3	Q8K4D6
ENSRNOP00000013629	2	-3.5	AP-2 complex subunit beta-1 (Adapter-related protein complex 2 beta-1 subunit) (Beta-adaptin) (Plasma membrane adaptor HA2/AP2 adaptin beta subunit) (Clathrin assembly protein complex 2 beta large chain) (AP105B).	3	P62944
ENSRNOP00000015866	3	-3.5	Solute carrier family 2, facilitated glucose transporter member 2 (Glucose transporter type 2, liver) (GLUT-2).	1	P12336
ENSRNOP00000038428	2	-3.5	Annexin A2 (Annexin-2) (Annexin II) (Lipocortin II) (Calpactin I heavy chain) (Chromobindin-8) (p36) (Protein I) (Placental anticoagulant protein IV) (PAP-IV).	1	Q07936
ENSRNOP00000020306	2	-3.4	dolichyl-di-phosphooligosaccharide-protein glycotransferase (predicted) Source: RefSeq_peptide NP_001012104	2	
ENSRNOP00000037521	2	-3.3	No description available.Protein Family: AMBIGUOUS	0	
ENSRNOP00000042136	2	-3.2	Latrophilin-2 precursor (Calcium-independent alpha-latrotoxin receptor 2) (CIRL-2).	12	O88923
ENSRNOP00000052656	2	-3.2	Clathrin heavy chain.	6	P11442
ENSRNOP00000055369	2	-3.2	cytochrome P450, family 1, subfamily a, polypeptide 2	3	
ENSRNOP00000034511	2	-3.1	No description available.Protein Family: NADH DEHYDROGENASE 1 BETA SUBCOMPLEX SUBUNIT 7 EC_1.6.5.3 EC_1.6.99.- 3 NADH UBIQUINONE OXIDOREDUCTASE B18 SUBUNIT COMPLEX I B18 CI B18	0	

Supplementary Table 4 (continued)
Membrane Proteins identified by WGA fractionation (Chapter 3)

Identifier	# peptides	log (e) score	Description	Glycosylation (N-X-S/T)	Accession No
ENSRNOP00000014235	39	-164.2	Long-chain-fatty-acid--CoA ligase 1 (EC 6.2.1.3) (Long-chain acyl-CoA synthetase 1) (LACS 1) (Long-chain-fatty-acid--CoA ligase, liver isozyme).	3	P18163
ENSRNOP00000041174	31	-109.4	Cytochrome P450 2D1 (EC 1.14.14.1) (CYPIID1) (P450-DB1) (P450-CMF1A) (P450-UT-7) (Debrisoquine 4-hydroxylase).	4	P10633
ENSRNOP00000013816	21	-107.1	No other features on this peptide	0	
ENSRNOP00000003334	13	-85.7	Guanine nucleotide-binding protein subunit beta 2-like 1 (Receptor of activated protein kinase C 1) (RACK1) (Receptor for activated C kinase).	1	P63245
ENSRNOP00000040266	20	-84.3	Cytochrome P450 2D10 (EC 1.14.14.1) (CYPIID10) (P450-DB5) (P450-CMF1B) (Debrisoquine 4-hydroxylase).	4	P12939
ENSRNOP00000034293	12	-77.7	Epoxide hydrolase 1 (EC 3.3.2.9) (Microsomal epoxide hydrolase) (Epoxide hydratase).	1	P07687
ENSRNOP00000005875	18	-62.2	Retinol dehydrogenase 7 (EC 1.1.1.105) (Retinol dehydrogenase type III) (RODH III).	1	P55006
ENSRNOP00000015913	15	-60.8	ADP/ATP translocase 2 (Adenine nucleotide translocator 2) (ANT 2) (ADP,ATP carrier protein 2) (Solute carrier family 25 member 5).	1	Q09073
ENSRNOP00000042597	11	-55.3	Liver carboxylesterase 4 precursor (EC 3.1.1.1) (Carboxyesterase ES-4) (Microsomal palmitoyl-CoA hydrolase) (Kidney microsomal carboxylesterase).	1	Q64573
ENSRNOP00000010579	12	-50.3	Microsomal glutathione S-transferase 1 (EC 2.5.1.18) (Microsomal GST- 1) (Microsomal GST-I).	0	P08011
ENSRNOP00000012413	16	-48.2	Cytochrome P450 2D26 (EC 1.14.14.1) (CYPIID26) (P450-DB2) (P450-CMF2) (Debrisoquine 4-hydroxylase).	3	P10634
ENSRNOP00000044296	13	-47.7	Actin, cytoplasmic 1 (Beta-actin).	1	P60711
ENSRNOP00000043466	8	-44.8	Amine oxidase B (EC 1.4.3.4) (Monoamine oxidase type B) (MAO-B).	1	P19643
ENSRNOP00000026574	9	-44.7	Bile acyl-CoA synthetase (EC 6.2.1.7) (BACS) (Bile acid CoA ligase) (BA-CoA ligase) (BAL) (Cholate--CoA ligase) (Very long chain acyl-CoA synthetase-related protein) (VLACS-related) (VLACSR) (Fatty acid transport protein 5) (FATP-5) (Solute carrier family	1	Q9ES38

ENSRNOP00000043239	7	-44.6	UDP-glucuronosyltransferase 2B3 precursor (EC 2.4.1.17) (UDPGT) (Testosterone, dihydrotestosterone, and beta-estradiol specific) (17-beta-hydroxysteroid specific) (UDPGTr-3) (RLUG38).	0	P08542
ENSRNOP00000035423	7	-42.5	Retinol dehydrogenase 2 (EC 1.1.1.105) (Retinol dehydrogenase type II) (RODH II) (29 k-protein).	0	P50170
ENSRNOP00000021812	7	-42.4	Carboxylesterase 3 precursor (EC 3.1.1.1) (Liver carboxylesterase 10) (Carboxyesterase ES-10) (pI 6.1 esterase) (ES-HVEL).	2	P16303
ENSRNOP00000010209	6	-42.2	Dolichyl-diphosphooligosaccharide--protein glycosyltransferase 63 kDa subunit precursor (EC 2.4.1.119) (Ribophorin II) (RPN-II).	2	P25235
ENSRNOP00000045886	9	-41.5	Fatty aldehyde dehydrogenase (EC 1.2.1.3) (Aldehyde dehydrogenase, microsomal) (Aldehyde dehydrogenase family 3 member A2) (Aldehyde dehydrogenase 10).	0	P30839
ENSRNOP00000003965	7	-40.8	ATP synthase subunit beta, mitochondrial precursor (EC 3.6.3.14).	0	P10719
ENSRNOP00000020446	20	-40.1	Cytochrome b5.	1	P00173
ENSRNOP00000002724	7	-39.3	UDP-glucuronosyltransferase 2B1 precursor (EC 2.4.1.17) (UDPGT) (UDPGTr-2).	2	P09875
ENSRNOP00000024973	6	-38.7	Very-long-chain specific acyl-CoA dehydrogenase, mitochondrial precursor (EC 1.3.99.-) (VLCAD).	3	P45953
ENSRNOP00000027994	6	-37.5	No description available.Protein Family: COLLAGEN ALPHA 1 CHAIN	4	
ENSRNOP00000048358	11	-37.4	No description available.Protein Family: ADP/ATP TRANSLOCASE ADENINE NUCLEOTIDE TRANSLOCATOR ANT ADP ATP CARRIER SOLUTE CARRIER FAMILY 25 MEMBER	2	
ENSRNOP00000021920	6	-37.1	ATP synthase B chain, mitochondrial precursor (EC 3.6.3.14).	0	P19511
ENSRNOP00000045002	13	-35.8	UDP-glucuronosyltransferase 2B3 precursor (EC 2.4.1.17) (UDPGT) (Testosterone, dihydrotestosterone, and beta-estradiol specific) (17-beta-hydroxysteroid specific) (UDPGTr-3) (RLUG38).	0	P08542
ENSRNOP00000054537	7	-34.9	lysosomal-associated membrane protein 1	18	
ENSRNOP00000045567	9	-34.4	Cytochrome P450 4A14 precursor (EC 1.14.15.3) (CYPIVA14) (Lauric acid omega-hydroxylase) (P450-LA-omega 3).	3	P20817
ENSRNOP00000015956	5	-34.2	Aspartate aminotransferase, mitochondrial precursor (EC 2.6.1.1) (Transaminase A) (Glutamate oxaloacetate transaminase 2).	1	P00507

ENSRNOP00000008477	4	-33.6	Voltage-dependent anion-selective channel protein 1 (VDAC-1) (rVDAC1) (Outer mitochondrial membrane protein porin 1).	2	Q9Z2L0
ENSRNOP00000016083	7	-33.4	Ceruloplasmin precursor (EC 1.16.3.1) (Ferroxidase).	4	P13635
ENSRNOP00000005853	5	-32.1	Polymeric-immunoglobulin receptor precursor (Poly-Ig receptor) (PIGR) .	4	P15083
ENSRNOP00000004091	7	-31.7	Calreticulin precursor (CRP55) (Calregulin) (HACBP) (ERp60) (CALBP) (Calcium-binding protein 3) (CABP3).	0	P18418
ENSRNOP00000034723	10	-31.7	UDP-glucuronosyltransferase 2B2 precursor (EC 2.4.1.17) (UDPGT) (3- hydroxyandrogen specific) (UDPGTr-4) (RLUG23).	1	P08541
ENSRNOP00000014630	8	-31.5	No description available.Protein Family: MICROSOMAL TRIGLYCERIDE TRANSFER LARGE SUBUNIT PRECURSOR	1	
ENSRNOP00000018649	5	-31.4	Dsp protein (Fragment).	4	Q4QQR7
ENSRNOP00000021514	7	-30.6	Ubiquinol-cytochrome-c reductase complex core protein 2, mitochondrial precursor (EC 1.10.2.2) (Core protein II) (Complex III subunit II).	3	P32551
ENSRNOP00000019772	4	-29	Fibronectin precursor (FN).	6	P04937
ENSRNOP00000046654	3	-25.3	Carcinoembryonic antigen-related cell adhesion molecule 1 precursor (Cell-CAM 105) (C-CAM 105) (Ecto-ATPase) (ATP-dependent taurocolate- carrier protein) (GP110) (pp120).	15	P16573
ENSRNOP00000025254	5	-24.6	Asialoglycoprotein receptor 1 (ASGPR 1) (ASGP-R 1) (Hepatic lectin 1) (RHL-1).	3	P02706
ENSRNOP00000002738	4	-24.5	CD166 antigen precursor (Activated leukocyte-cell adhesion molecule) (ALCAM) (MEMD protein) (HB2) (SB-10 antigen) (KG-CAM).	5	O35112
ENSRNOP00000027773	3	-24.1	Alpha-actinin-4 (Non-muscle alpha-actinin 4) (F-actin cross-linking protein).	3	Q9QXQ0
ENSRNOP00000005311	5	-23.8	Collagen alpha-1(I) chain precursor (Alpha-1 type I collagen).	2	P02454
ENSRNOP00000005073	4	-23.3	Collagen alpha 2 type V (Fragment).	2	O70598
ENSRNOP00000024106	3	-23.3	Alpha-enolase (EC 4.2.1.11) (2-phospho-D-glycerate hydro-lyase) (Non- neural enolase) (NNE) (Enolase 1).	2	P04764
ENSRNOP00000019547	4	-23.2	No description available.Protein Family: BRAIN SPECIFIC ANGIOGENESIS INHIBITOR PRECURSOR	5	
ENSRNOP00000033956	7	-22.9	No description available.Protein Family: ADP/ATP TRANSLOCASE ADENINE NUCLEOTIDE TRANSLOCATOR ANT ADP ATP CARRIER SOLUTE CARRIER FAMILY 25 MEMBER	2	

ENSRNOP00000021407	5	-22.8	choline dehydrogenase precursor Source: RefSeq_peptide NP_942026	0	
ENSRNOP00000020775	9	-21.6	Liver carboxylesterase 3 precursor (EC 3.1.1.1) (Carboxyesterase ES-3) (pI 5.5 esterase) (ES-HTEL).	3	Q63108
ENSRNOP00000051445	10	-21.3	Long-chain-fatty-acid--CoA ligase 5 (EC 6.2.1.3) (Long-chain acyl-CoA synthetase 5) (LACS 5). O88813	1	O88813
ENSRNOP00000019408	4	-21.1	No description available.Protein Family: ZINC FINGER HOMEOBOX ZINC FINGER HOMEODOMAIN ZFH	14	
ENSRNOP00000022892	6	-20.9	ATP synthase subunit alpha, mitochondrial precursor (EC 3.6.3.14).	1	P15999
ENSRNOP00000004864	3	-20.4	Dimethylaniline monooxygenase 3 (EC 1.14.13.8) (Hepatic flavin-containing monooxygenase 3) (FMO 3) (Dimethylaniline oxidase 3).	3	Q9EQ76
ENSRNOP00000043950	7	-19.8	Junction plakoglobin.	7	Q6P0K8
ENSRNOP00000049879	8	-19.3	ATP synthase gamma chain, mitochondrial (EC 3.6.3.14).	4	P35435
ENSRNOP00000051841	4	-18.6	Protein disulfide-isomerase precursor (EC 5.3.4.1) (PDI) (Prolyl 4- hydroxylase subunit beta) (Cellular thyroid hormone-binding protein).	0	P04785
ENSRNOP00000021512	4	-18.1	Peroxisomal trans-2-enoyl-CoA reductase (EC 1.3.1.38) (RLF98) (Peroxisomal 2,4-dienoyl CoA reductase) (PX-2,4-DCR1).	3	Q9WVK3
ENSRNOP00000026290	3	-17.5	3 beta-hydroxysteroid dehydrogenase type 5 (3 beta-hydroxysteroid dehydrogenase type V) (3-beta-HSD V) (NADPH-dependent 3-beta-hydroxy- Delta(5)-steroid dehydrogenase) (EC 1.1.1.-) (3-beta-hydroxy-5-ene steroid dehydrogenase) (Progesterone reductase).	2	P27364
ENSRNOP00000003965	7	-40.8	ATP synthase subunit beta, mitochondrial precursor (EC 3.6.3.14).	0	P10719
ENSRNOP00000033185	3	-16.2	No description available.Protein Family: AMBIGUOUS	1	
ENSRNOP00000005459	3	-16	LOC690745 protein (Fragment).	0	Q5I0K9
ENSRNOP00000044696	3	-15.5	Ubiquinol-cytochrome-c reductase complex core protein 1, mitochondrial precursor (EC 1.10.2.2) (Core I protein).	2	Q68FY0
ENSRNOP00000027234	4	-15.2	Monocarboxylate transporter 1 (MCT 1) (Solute carrier family 16 member 1).	1	P53987
ENSRNOP00000017310	5	-14.8	Cytochrome P450 2C11 (EC 1.14.14.1) (CYPIIC11) (P-450(M-1)) (P450H) (P450-UT-A) (UT-2).	1	P08683
ENSRNOP00000052856	5	-14.4	similar to solute carrier family 25, member 5 (LOC673916), mRNA Source: RefSeq_dna XR_004388	1	

ENSRNOP00000020184	3	-14	procollagen, type IV, alpha 4 Source: RefSeq_peptide NP_001008333	3	
ENSRNOP00000015851	2	-13.5	NADH-ubiquinone oxidoreductase 75 kDa subunit, mitochondrial precursor (EC 1.6.5.3) (EC 1.6.99.3).	1	Q66HF1
ENSRNOP00000019552	3	-13.5	Annexin A5 (Annexin-5) (Annexin V) (Lipocortin V) (Endonexin II) (Calphobindin I) (CBP-I) (Placental anticoagulant protein I) (PAP-I) (PP4) (Thromboplastin inhibitor) (Vascular anticoagulant-alpha) (VAC- alpha) (Anchorin CII).	0	
ENSRNOP00000028237	3	-13.2	Cytochrome P450 2A1 (EC 1.14.14.1) (CYPIIA1) (Steroid hormones 7- alpha-hydroxylase) (Testosterone 7-alpha-hydroxylase) (P450-UT-F).	1	P11711
ENSRNOP00000050581	4	-13	Corticosteroid 11-beta-dehydrogenase isozyme 1 (EC 1.1.1.146) (11-DH) (11-beta-hydroxysteroid dehydrogenase 1) (11-beta-HSD1).	2	P16232
ENSRNOP00000001816	4	-11.5	Aldehyde dehydrogenase, mitochondrial precursor (EC 1.2.1.3) (ALDH class 2) (ALDH1) (ALDH-E2).	2	P11884
ENSRNOP00000012878	4	-11.5	NADH-cytochrome b5 reductase 3 (EC 1.6.2.2) (Cytochrome b5 reductase) (B5R) (Diaphorase-1) .	0	P20070
ENSRNOP00000022532	2	-11.3	Prenylcysteine oxidase precursor (EC 1.8.3.5) (Chloride ion pump- associated 55 kDa protein).	3	Q99ML5
ENSRNOP00000022233	3	-11.1	Prothrombin precursor (EC 3.4.21.5) (Coagulation factor II) .	4	P18292
ENSRNOP00000014464	3	-10.6	Annexin A6 (Annexin-6) (Annexin VI) (Lipocortin VI) (P68) (P70) (Protein III) (Chromobindin-20) (67 kDa calelectrin) (Calphobindin-II) (CPB-II) (Calcium-binding protein CATA 65/67).	1	P48037
ENSRNOP00000051613	4	-10.4	No description available.Protein Family: CYTOCHROME P450 2	2	
ENSRNOP00000003052	2	-10.2	Lysosome membrane protein 2 (Lysosome membrane protein II) (LIMP II) (Scavenger receptor class B member 2) (85 kDa lysosomal membrane sialoglycoprotein) (LGP85) (CD36 antigen-like 2).	9	P27615
ENSRNOP00000052152	2	-10.2	Fibronectin receptor alpha chain (Fragments).	6	Q7M074
ENSRNOP00000018462	2	-9.9	Voltage-dependent anion-selective channel protein 2 (VDAC-2) (Outer mitochondrial membrane protein porin 2) (B36-VDAC).	3	P81155
ENSRNOP00000025570	2	-9.9	Golgi apparatus protein 1 precursor (Golgi sialoglycoprotein MG-160) (E-selectin ligand 1) (ESL-1).	5	Q62638
ENSRNOP00000046414	2	-9.9	Cytochrome c oxidase subunit 2 (EC 1.9.3.1) (Cytochrome c oxidase polypeptide II).	0	P00406

ENSRNOP00000017101	2	-9.8	Membrane-associated progesterone receptor component 1 (Acidic 25 kDa protein) (25-DX) (Ventral midline antigen) (VEMA).	0	P70580
ENSRNOP00000010663	2	-9.7	UDP-glucose pyrophosphorylase 2 Source: RefSeq_peptide NP_001019914	4	
ENSRNOP00000052490	2	-9.7	No description available.Protein Family: SOLUTE CARRIER ORGANIC ANION TRANSPORTER FAMILY MEMBER SOLUTE CARRIER FAMILY 21 MEMBER ORGANIC ANION TRANSPORTER ORGANIC ANION TRANSPORTING POLYPEPTIDE	6	
ENSRNOP00000055369	2	-9.7	cytochrome P450, family 1, subfamily a, polypeptide 2	3	
ENSRNOP00000008851	2	-9.4	24-dehydrocholesterol reductase Source: RefSeq_peptide NP_001073617	0	
ENSRNOP00000020364	3	-9.3	Cation-dependent mannose-6-phosphate receptor precursor (CD Man-6-P receptor) (CD-MPR).	5	Q6AY20
ENSRNOP00000054267	2	-9.3	No description available.Protein Family: COLLAGEN ALPHA IV CHAIN	1	
ENSRNOP00000048004	3	-9.2	No description available.Protein Family: SKIN SPECIFIC 32	0	
ENSRNOP00000013262	2	-9.1	Electron transfer flavoprotein-ubiquinone oxidoreductase, mitochondrial precursor (EC 1.5.5.1) (ETF-QO) (ETF-ubiquinone oxidoreductase) (ETF dehydrogenase) (Electron-transferring- flavoprotein dehydrogenase).	1	Q6UPE1
ENSRNOP00000020669	2	-9.1	Alpha-3 type IV collagen (Fragment).	1	Q63122
ENSRNOP00000012219	3	-8.8	No other features on this peptide	1	
ENSRNOP00000018796	2	-8.6	Membrane-associated progesterone receptor component 2.	0	Q5XIU9
ENSRNOP00000034954	2	-8.6	Perlecan (Fragment).	5	O08591
ENSRNOP00000009777	2	-8.3	Bile acid CoA:amino acid N-acyltransferase (EC 2.3.1.65) (BAT) (BACAT) (Glycine N-choloyltransferase) (Kan-1) (Long-chain fatty-acyl-CoA hydrolase) (EC 3.1.2.2).	1	Q63276
ENSRNOP00000052513	2	-8.1	No description available.Protein Family: UNKNOWN	0	
ENSRNOP00000004836	4	-8	No description available.Protein Family: ATP SYNTHASE D CHAIN MITOCHONDRIAL EC_3.6.3.14	1	
ENSRNOP00000042268	2	-8	Basigin precursor (OX-47 antigen) (Glycoprotein CE9) (CD147 antigen).	3	P26453
ENSRNOP00000012425	3	-7.9	No description available.Protein Family: NADH DEHYDROGENASE IRON SULFUR 3 MITOCHONDRIAL PRECURSOR EC_1.6.5.3 EC_1.6.99.- 3 NADH UBIQUINONE OXIDOREDUCTASE 30 KDA SUBUNIT COMPLEX I	0	

			30KD CI 30KD		
ENSRNOP00000029204	2	-7.9	No description available.Protein Family: ZINC FINGER	0	
ENSRNOP00000034851	3	-7.8	No description available.Protein Family: E3 UBIQUITIN LIGASE MARCH4 PRECURSOR EC_6.3.2.- MEMBRANE ASSOCIATED RING FINGER 4 MEMBRANE ASSOCIATED RING CH IV MARCH IV	1	
ENSRNOP00000025045	2	-7.7	UDP-glucuronosyltransferase 1-1 precursor (EC 2.4.1.17) (UDPGT) (UGT1*1) (UGT1-01) (UGT1.1) (UGT1A1) (B1).	2	Q64550
ENSRNOP00000016423	2	-7.6	Collagen alpha-2(I) chain precursor (Alpha-2 type I collagen).	0	P02466
ENSRNOP00000011641	2	-7.5	No description available.Protein Family: ZINC FINGER HOMEOBOX ZINC FINGER HOMEODOMAIN ZFH	11	
ENSRNOP00000038770	2	-7.5	No description available.Protein Family: FIBRONECTIN TYPE III DOMAIN CONTAINING 3B FACTOR ADIPOCYTE DIFFERENTIATION 104 HCV NS5A BINDING 37	3	
ENSRNOP00000019624	2	-7.4	No description available.Protein Family: NADH DEHYDROGENASE 1 BETA SUBCOMPLEX SUBUNIT 10 EC_1.6.5.3 EC_1.6.99.- 3 NADH UBIQUINONE OXIDOREDUCTASE PDSW SUBUNIT COMPLEX I PDSW CI PDSW	1	
ENSRNOP00000000095	2	-7.3	No description available.Protein Family: EC_3.6.1.-	5	
ENSRNOP00000015006	2	-7.3	Cytochrome b5 type B precursor (Cytochrome b5 outer mitochondrial membrane isoform).	0	P04166
ENSRNOP00000026333	2	-7.3	No description available.Protein Family: RING FINGER 31	2	
ENSRNOP00000041026	2	-7.3	ectonucleoside triphosphate diphosphohydrolase 5 Source: RefSeq_peptide NP_955426	1	
ENSRNOP00000055547	2	-7.3	No description available.Protein Family: NESPRIN NUCLEAR ENVELOPE SPECTRIN REPEAT SYNAPTIC NUCLEAR ENVELOPE	10	
ENSRNOP00000000177	2	-6.8	Lysosome-associated membrane glycoprotein 2 precursor (LAMP-2) (Lysosomal membrane glycoprotein-type B) (LGP-B) (LGP-96) (LGP-110) (CD107b antigen).	16	P17046
ENSRNOP00000006855	2	-6.6	Surfeit locus protein 1.	1	Q9QXU2
ENSRNOP00000018761	2	-6.5	Arylacetamide deacetylase (EC 3.1.1.-) (AADAC).	3	Q9QZH8

ENSRNOP00000012233	2	-6.4	Dolichyl-diphosphooligosaccharide--protein glycosyltransferase subunit DAD1 (EC 2.4.1.119) (Oligosaccharyl transferase subunit DAD1) (Defender against cell death 1) (DAD-1).	0	P61805
ENSRNOP00000024707	2	-6.4	Sideroflexin-1 (Tricarboxylate carrier protein) (TCC).	3	Q63965
ENSRNOP00000001299	2	-6.3	Scavenger receptor class B member 1 (SRB1) (SR-BI).	8	P97943
ENSRNOP00000014058	2	-6.1	Cytochrome c, somatic.	0	P62898
ENSRNOP00000015684	3	-6.1	No description available.Protein Family: AMBIGUOUS	1	
ENSRNOP00000018711	2	-6.1	Adenylyl cyclase-associated protein 1 (CAP 1).	3	Q08163
ENSRNOP00000013532	2	-5.8	No description available.Protein Family: PLAKOPHILIN	5	
ENSRNOP00000001905	2	-5.7	No description available.Protein Family: TRANSFERRIN RECEPTOR	5	
ENSRNOP00000056312	2	-5.6	tumor rejection antigen gp96 (predicted) Source: RefSeq_peptide NP_001012197	4	
ENSRNOP00000040859	2	-5.5	Calnexin precursor.	1	P35565
ENSRNOP00000007567	2	-5.2	NADH dehydrogenase (ubiquinone) 1 alpha subcomplex, 4	0	
ENSRNOP00000049568	2	-4.9	No description available.Protein Family: PRECURSOR	6	
ENSRNOP00000025045	2	-7.7	UDP-glucuronosyltransferase 1-1 precursor (EC 2.4.1.17) (UDPGT) (UGT1*1) (UGT1-01) (UGT1.1) (UGT1A1) (B1).	2	Q64550
ENSRNOP00000027760	2	-4.6	CD81 antigen (26 kDa cell surface protein TAPA-1) (Target of the antiproliferative antibody 1).	1	Q62745
ENSRNOP00000003910	2	-4.4	Amine oxidase A (EC 1.4.3.4) (Monoamine oxidase type A) (MAO-A).	1	P21396
ENSRNOP00000029426	2	-4.2	No description available.Protein Family: ATP SYNTHASE F CHAIN MITOCHONDRIAL EC_3.6.3.14	0	
ENSRNOP00000041608	6	-4.2	Phosphate carrier protein, mitochondrial precursor (PTP) (Solute carrier family 25 member 3).	0	P16036
ENSRNOP00000051608	2	-4.2	Cytochrome P450 2C70 (EC 1.14.14.1) (CYPIIC70) (P-450Md) (P450 P49).	2	P19225
ENSRNOP00000024736	2	-4.1	No description available.Protein Family: PRECURSOR	3	
ENSRNOP00000026347	2	-4.1	Vitamin K epoxide reductase complex subunit 1 (EC 1.1.4.1) (Vitamin K1 2,3-epoxide reductase subunit 1).	1	Q6TEK4
ENSRNOP00000010760	6	-3.9	Methyltransferase-like protein 7B precursor (EC 2.1.1.-) (Associated with lipid droplet protein 1) (ALDI).	0	Q562C4
ENSRNOP00000012681	2	-3.6	No other features on this peptide	1	

ENSRNOP00000038428	2	-3.6	Annexin A2 (Annexin-2) (Annexin II) (Lipocortin II) (Calpactin I heavy chain) (Chromobindin-8) (p36) (Protein I) (Placental anticoagulant protein IV) (PAP-IV).	1	Q07936
ENSRNOP00000043148	2	-3.6	Catechol O-methyltransferase (EC 2.1.1.6).	0	P22734
ENSRNOP00000015802	2	-3.5	No description available.Protein Family: CYTOCHROME P450 2	1	
ENSRNOP00000050137	10	-3.5	No description available.Protein Family: VOLTAGE DEPENDENT ANION SELECTIVE CHANNEL VDAC OUTER MITOCHONDRIAL MEMBRANE PORIN	1	
ENSRNOP00000001315	2	-3.4	Actin-related protein 2/3 complex subunit 1B (ARP2/3 complex 41 kDa subunit) (p41-ARC).	0	O88656
ENSRNOP00000026197	2	-3.4	Voltage-dependent anion-selective channel protein 3 (VDAC-3) (rVDAC3) (Outer mitochondrial membrane protein porin 3).	2	Q9R1Z0
ENSRNOP00000028066	2	-3.4	Intercellular adhesion molecule 1 precursor (ICAM-1) (CD54 antigen).	8	Q00238
ENSRNOP00000042986	2	-3.4	cytochrome P450, family 2, subfamily b, polypeptide 13 Source: RefSeq_peptide NP_942028	1	
ENSRNOP00000002712	2	-3	UDP-glucuronosyltransferase 2B4 precursor (EC 2.4.1.17) (UDPGT) (UDP- glucuronosyltransferase 2B12).	0	P36511
ENSRNOP00000015866	2	-3	Solute carrier family 2, facilitated glucose transporter member 2 (Glucose transporter type 2, liver) (GLUT-2).	1	P12336
ENSRNOP00000028194	2	-3	7-dehydrocholesterol reductase (EC 1.3.1.21) (7-DHC reductase) (Sterol Delta(7)-reductase).	3	Q9Z2Z8
ENSRNOP00000007398	2	-7.7	Myosin-9 (Myosin heavy chain 9) (Myosin heavy chain, nonmuscle IIa) (Nonmuscle myosin heavy chain IIa) (NMMHC II-a) (NMMHC-IIA) (Cellular myosin heavy chain, type A) (Nonmuscle myosin heavy chain-A) (NMMHC- A).	6	Q62812
ENSRNOP00000028458	2	-4.4	Myosin light polypeptide 3 (Myosin light chain 1, slow-twitch muscle B/ventricular isoform) (MLC1SB) (Ventricular/slow twitch myosin alkali light chain).	1	P16409

Supplementary Table 4 (continued)
Membrane Proteins identified by hydrazine chemistry (Chapter 3)

Identifier	# peptides	log (e) score	Description	Glycosylation (N-X-S/T)	Accession No
ENSRNOP00000000072	13	-39.6	ATP synthase subunit e, mitochondrial.	0	P29419
ENSRNOP00000003022	10	-18.3	Cytochrome c oxidase polypeptide VIIa-liver/heart, mitochondrial precursor (Cytochrome c oxidase subunit VIIa-L).	0	P35171
ENSRNOP00000040969	20	-50.8	ATP synthase, H+ transporting, mitochondrial F0 complex, subunit G	0	NP_997681
ENSRNOP00000001545	6	-19.5	Cytochrome c oxidase polypeptide VIa-liver, mitochondrial precursor.	1	P10818
ENSRNOP00000042135	2	-5.7	NADH dehydrogenase 1 beta 4 (Fragment).	0	Q2XTA8
ENSRNOP00000037647	2	-13.8	Protein Mpv17.	0	Q5BK62
ENSRNOP00000040759	2	-12.5	Myosin light polypeptide 6 (Smooth muscle and nonmuscle myosin light chain alkali 6) (Myosin light chain alkali 3) (Myosin light chain 3) (MLC-3) (LC17).	1	Q64119
ENSRNOP00000020670	2	-9.5	ATP synthase subunit delta, mitochondrial precursor.	0	P35434
ENSRNOP00000038100	1	-4.3	translocase of inner mitochondrial membrane 17 homolog B Source: RefSeq_peptide	0	NP_001101719
ENSRNOP00000053215	5	-18.1	Translocon-associated protein subunit delta precursor (TRAP-delta) (Signal sequence receptor subunit delta) (SSR-delta).	0	Q07984
ENSRNOP00000024033	9	-13.6	Cytochrome c oxidase subunit 4 isoform 1, mitochondrial precursor (Cytochrome c oxidase subunit IV isoform 1) (COX IV-1) (Cytochrome c oxidase polypeptide IV).	0	P10888
ENSRNOP00000021274	2	-4.1	Myosin regulatory light chain 2-B, smooth muscle isoform (Myosin RLC- B).	2	P18666
ENSRNOP00000017692	18	-23.3	ADP-ribosylation factor 4.	1	P61751
ENSRNOP00000054063	7	-10.7	Ras-related protein Rab-4B.	1	P51146
ENSRNOP00000040401	8	-5.4	No description available.Protein Family: MITOCHONDRIAL IMPORT INNER MEMBRANE TRANSLOCASE SUBUNIT TIM23	2	
ENSRNOP00000006950	11	-19.8	Ras-related protein Rab-1A.	1	Q6NYB7
ENSRNOP00000053518	8	-8.5	Peroxisomal membrane protein 2 (22 kDa peroxisomal membrane protein).	1	Q07066

ENSRNOP00000002732	38	-93.6	ATP synthase subunit O, mitochondrial precursor (Oligomycin sensitivity conferral protein) (OSCP).	0	Q06647
ENSRNOP00000053675	6	-11.5	No other features on this peptide	1	
ENSRNOP00000057446	4	-15.3	NADH dehydrogenase (ubiquinone) Fe-S protein 7	0	NP_001008525
ENSRNOP00000025327	3	-12.6	Vesicle-trafficking protein SEC22b (SEC22 vesicle-trafficking protein homolog B) (SEC22 vesicle-trafficking protein-like 1) (ERS24) (ERS- 24).	1	Q4KM74
ENSRNOP00000040879	4	-6.4	similar to CG7582-PA (LOC690610), mRNA Source: RefSeq_	0	dna NM_001109604
ENSRNOP00000030668	9	-5.7	transmembrane emp24 protein transport domain containing 9	1	NP_001009703
ENSRNOP00000034299	16	-53.8	No description available.Protein Family: ARACHIDONATE LIPOXYGENASE	1	
ENSRNOP00000018897	10	-24.4	catechol-O-methyltransferase domain containing 1	1	NP_001100719
ENSRNOP00000023562	6	-5.9	membrane-associated ring finger (C3HC4) 5	1	NP_001099842
ENSRNOP00000051846	26	-89.5	solute carrier family 25 (mitochondrial carrier; dicarboxylate transporter), member 10	1	NP_596909
ENSRNOP00000022519	5	-7	Uncharacterized protein C18orf19 homolog.	0	Q5XIJ4
ENSRNOP00000010593	4	-14.8	Succinate dehydrogenase iron-sulfur subunit (EC 1.3.5.1) (Ip) (Iron-sulfur subunit of complex II) (Fragment).	1	P21913
ENSRNOP00000016043	12	-52.6	solute carrier family 25 member 15	0	NP_001041345
ENSRNOP00000021893	2	-7.7	Iodotyrosine dehalogenase 1 precursor (EC 1.-.-.-) (IYD-1).	0	Q5BK17
ENSRNOP00000003004	11	-32.6	Estradiol 17-beta-dehydrogenase 11 precursor (EC 1.1.1.-) (17-beta- hydroxysteroid dehydrogenase 11) (17-beta-HSD 11) (17-beta-HSD XI) (17betaHSDXI) (17bHSD11) (17betaHSD11) (Dehydrogenase/reductase SDR family member 8).	0	Q6AYS8
ENSRNOP00000002044	6	-4.5	Alpha-soluble NSF attachment protein (SNAP-alpha) (N-ethylmaleimide- sensitive factor attachment protein, alpha).	1	P54921
ENSRNOP00000017472	22	-55.8	Prohibitin-2 (B-cell receptor-associated protein BAP37) (BAP-37).	2	Q5XIH7
ENSRNOP00000042462	51	-69.8	No description available.Protein Family: UNKNOWN	1	
ENSRNOP00000005144	17	-69.3	Mitochondrial 2-oxoglutarate/malate carrier protein (OGCP) (Solute carrier family 25 member 11).	0	P97700
ENSRNOP00000011846	18	-54.9	mitochondrial carrier homolog 2 Source:	1	NP_001099958
ENSRNOP00000025240	5	-32.6	solute carrier family 25 (mitochondrial carrier, glutamate), member 22	1	NP_001014049

ENSRNOP00000004941	10	-18.1	Leucine-rich repeat-containing protein 59 (Protein p34).	1	Q5RJR8
ENSRNOP00000020544	5	-5.9	Electron transfer flavoprotein subunit alpha, mitochondrial precursor (Alpha-ETF).	1	P13803
ENSRNOP00000027615	2	-6.2	Solute carrier family 25 member 42.	0	P0C546
ENSRNOP00000015844	2	-6	retinol dehydrogenase 11	2	NP_001012193
ENSRNOP00000036519	16	-47.8	dehydrogenase/reductase (SDR family) member 7	0	NP_001013116
ENSRNOP00000034963	2	-10.2	MOSC domain-containing protein 2, mitochondrial precursor (EC 1.-.-.-).	0	Q922Q1
ENSRNOP00000025523	2	-5.9	carbonic anhydrase 14	1	NP_001103125
ENSRNOP00000021017	2	-4.5	eukaryotic translation initiation factor 3, subunit 5 (epsilon)	2	NP_001099762
ENSRNOP00000013151	3	-4.7	Stomatin-like protein 2 (SLP-2).	2	Q4FZT0
ENSRNOP00000027815	6	-10.5	Secretory carrier membrane protein 3 (Fragment).	0	Q9ERM8
ENSRNOP00000043885	3	-5.9	NADH-ubiquinone oxidoreductase chain 2 (EC 1.6.5.3) (NADH dehydrogenase subunit 2).	3	P11662
ENSRNOP00000017268	2	-8.6	SPFH domain family, member 1	2	NP_001099823
ENSRNOP00000011494	23	-81.5	Phosphate carrier protein, mitochondrial precursor (PTP) (Solute carrier family 25 member 3).	0	P16036
ENSRNOP00000022985	7	-45	NAD(P) dependent steroid dehydrogenase-like	2	NP_001009399
ENSRNOP00000028033	2	-5.7	Glucose-6-phosphatase (EC 3.1.3.9) (G6Pase) (G-6-Pase).	3	P43428
ENSRNOP00000022550	3	-3.8	Guanine nucleotide-binding protein G(i), alpha-2 subunit (Adenylate cyclase-inhibiting G alpha protein).	1	P04897
ENSRNOP00000018795	8	-15.3	Estradiol 17-beta-dehydrogenase 2 (EC 1.1.1.62) (Testosterone 17-beta- dehydrogenase) (EC 1.1.1.63) (17-beta-HSD 2) (17-beta-hydroxysteroid dehydrogenase 2).	2	Q62730
ENSRNOP00000034135	11	-60.2	NADH dehydrogenase 1 alpha subcomplex subunit 9, mitochondrial precursor (NADH-ubiquinone oxidoreductase 39 kDa subunit) (Complex I-39kD) (CI-39kD) (Fragment).	1	Q5BK63
ENSRNOP00000005912	6	-30.3	lysophosphatidylglycerol acyltransferase 1	1	NP_001102846
ENSRNOP00000028084	3	-16.1	vesicle amine transport protein 1 homolog (T californica)	2	NP_001028855
ENSRNOP00000039584	25	-115.8	Cytochrome P450 4A14 precursor (EC 1.14.15.3) (CYPIVA14) (Lauric acid omega-hydroxylase) (P450-LA-omega 3).	2	P20817

ENSRNOP00000050691	2	-5.3	3-ketoacyl-CoA thiolase B, peroxisomal precursor (EC 2.3.1.16) (Beta- ketothiolase B) (Acetyl-CoA acyltransferase B) (Peroxisomal 3-oxoacyl- CoA thiolase B).	3	P07871
ENSRNOP00000027925	4	-11.3	Organic cation transporter-like protein 2 (Solute carrier family 22 member 18).	0	Q6AY78
ENSRNOP00000001556	19	-34.7	Short-chain specific acyl-CoA dehydrogenase, mitochondrial precursor (EC 1.3.99.2) (SCAD) (Butyryl-CoA dehydrogenase).	3	P15651
ENSRNOP00000023215	4	-8.7	COX15 homolog	1	NP_001028871
ENSRNOP00000049419	4	-11.1	eukaryotic translation initiation factor 4A1	1	NP_955404
ENSRNOP00000015810	9	-24	solute carrier family 37 (glucose-6-phosphate transporter), member 4	1	NP_113777
ENSRNOP00000016561	5	-10.7	No description available.Protein Family: AMBIGUOUS	2	
ENSRNOP00000007552	5	-24.2	Suclg2 protein (Fragment).	0	Q68FT4
ENSRNOP00000027999	3	-4.6	Short/branched chain specific acyl-CoA dehydrogenase, mitochondrial precursor (EC 1.3.99.-) (SBCAD) (2-methyl branched chain acyl-CoA dehydrogenase) (2-MEBCAD) (2-methylbutyryl-coenzyme A dehydrogenase) (2-methylbutyryl-CoA dehydrogenase).	1	P70584
ENSRNOP00000025203	10	-11.4	Tu translation elongation factor, mitochondrial	1	NP_001099765
ENSRNOP00000048850	3	-16.5	No description available.Protein Family: AMBIGUOUS	2	
ENSRNOP00000006322	44	-92	Tubulin alpha-1A chain (Tubulin alpha-1 chain) (Alpha-tubulin 1).	1	P68370
ENSRNOP00000027305	2	-7.9	Elongation factor 1-gamma (EF-1-gamma) (eEF-1B gamma).	1	Q68FR6
ENSRNOP00000042628	51	-109.2	tubulin, alpha 1B (Tuba1b),	1	dna NM_001044270
ENSRNOP00000017180	27	-53.5	No description available.Protein Family: ELONGATION FACTOR 1 ALPHA EF 1 ALPHA	1	
ENSRNOP00000023516	3	-7.9	succinate-Coenzyme A ligase, ADP-forming, beta subunit	0	NP_001101857
ENSRNOP00000032909	35	-30.8	Calcium-binding mitochondrial carrier protein Aralar1 (Mitochondrial aspartate glutamate carrier 1) (Solute carrier family 25 member 12).	1	Q8BH59
ENSRNOP00000028392	13	-40.3	Probable proline dehydrogenase 2 (EC 1.5.99.8) (Proline oxidase-like protein).	2	Q2V057
ENSRNOP00000016520	5	-4.5	Sorting and assembly machinery component 50 homolog.	1	Q6AXV4

ENSRNOP00000055224	17	-27	NADH dehydrogenase iron-sulfur protein 2, mitochondrial precursor (EC 1.6.5.3) (EC 1.6.99.3) (NADH-ubiquinone oxidoreductase 49 kDa subunit) (Complex I-49kD) (CI-49kD).	1	Q91WD5
ENSRNOP00000043141	9	-22.4	NADH-ubiquinone oxidoreductase chain 4 (EC 1.6.5.3) (NADH dehydrogenase subunit 4).	4	P05508
ENSRNOP00000016356	2	-8.4	Protein FAM82C.	1	Q66H15
ENSRNOP00000053174	2	-4.2	No description available.Protein Family: AMBIGUOUS	1	
ENSRNOP00000020015	13	-43.4	Aldehyde dehydrogenase family 8 member A1 (EC 1.2.1.-) (Retinal dehydrogenase 4).	0	Q8BH00
ENSRNOP00000014051	3	-7.7	cytochrome P450, family 39, subfamily a, polypeptide 1	2	NP_001100363
ENSRNOP00000005005	18	-53.5	Kynurenine 3-monooxygenase (EC 1.14.13.9) (Kynurenine 3-hydroxylase). Source:	2	O88867
ENSRNOP00000003691	2	-3.6	UDP-glucose 6-dehydrogenase (EC 1.1.1.22) (UDP-Glc dehydrogenase) (UDP-GlcDH) (UDPGDH).	0	O70199
ENSRNOP00000012533	3	-5.2	Coiled-coil domain-containing protein 47 precursor.	1	Q5U2X6
ENSRNOP00000045196	26	-89.5	Cytochrome P450 2B1 (EC 1.14.14.1) (CYPIIB1) (P450-B) (P450b) (P450- PB1 and P450-PB2) (P450-LM2).	1	P00176
ENSRNOP00000012300	2	-3.6	Alpha-(1,3)-fucosyltransferase 11 (EC 2.4.1.-) (Galactoside 3-L- fucosyltransferase 11) (Fucosyltransferase 11) (FucT-XI) (Fuc-TXI).	4	Q68FV3
ENSRNOP00000028249	42	-125.5	Cytochrome P450 2A2 (EC 1.14.14.1) (CYPIIA2) (Testosterone 15-alpha- hydroxylase) (P450-UT-4).	2	P15149
ENSRNOP00000002054	4	-12.8	Cytochrome P450 2B15 (EC 1.14.14.1) (CYPIIB15).	2	Q64583
ENSRNOP00000017840	62	-102.8	Cytochrome P450 2C23 (EC 1.14.14.1) (CYPIIC23) (Arachidonic acid epoxygenase).	1	P24470
ENSRNOP00000016883	26	-101.4	Cytochrome P450 2E1 (EC 1.14.14.1) (CYPIIE1) (P450-J) (P450RLM6).	2	P05182
ENSRNOP00000054078	13	-39.3	No description available.Protein Family: CYTOCHROME P450 EC_1.14.14.1	1	
ENSRNOP00000028196	28	-99.1	Cytochrome P450 2B2 (EC 1.14.14.1) (CYPIIB2) (P450E) (P450 PB4).	1	P04167
ENSRNOP00000020478	9	-38.6	Protein disulfide-isomerase A3 precursor (EC 5.3.4.1) (Disulfide isomerase ER-60) (ERp60) (58 kDa microsomal protein) (p58) (ERp57) (HIP-70) (Q-2).	0	P11598
ENSRNOP00000001285	9	-50.2	Cytochrome P450 3A18 (EC 1.14.14.1) (CYPIIIA18) (P450(6)beta-2).	2	Q64581

ENSRNOP00000001291	45	-110	No description available.Protein Family: CYTOCHROME P450 EC_1.14.14.1	2	
ENSRNOP00000035966	7	-3.9	Protein ERGIC-53 precursor (ER-Golgi intermediate compartment 53 kDa protein) (Lectin mannose-binding 1) (p58).	0	Q62902
ENSRNOP00000025094	6	-31.2	solute carrier family 22 member 7	3	NP_445989
ENSRNOP00000025652	33	-63.8	UDP-glucuronosyltransferase 1-1 precursor (EC 2.4.1.17) (UDPGT) (UGT1*1) (UGT1-01) (UGT1.1) (UGT1A1) (B1).	2	Q64550
ENSRNOP00000051361	23	-84.2	Dimethylaniline monooxygenase 1 (EC 1.14.13.8) (Hepatic flavin-containing monooxygenase 1) (FMO 1) (Dimethylaniline oxidase 1).	2	P36365
ENSRNOP00000040239	8	-28	UDP-glucuronosyltransferase 2A1 precursor (EC 2.4.1.17) (UDPGT) (UGT- OLF).	4	P36510
ENSRNOP00000006533	4	-23.1	Cytochrome P450 4F1 (EC 1.14.14.1) (CYPIVF1) (P450-A3).	2	P33274
ENSRNOP00000045670	33	-67.3	UDP-glucuronosyltransferase 1-1 precursor (EC 2.4.1.17) (UDPGT) (UGT1*1) (UGT1-01) (UGT1.1) (UGT1A1) (B1).	4	Q64550
ENSRNOP00000039545	5	-25.5	Cytochrome P450 4F4 (EC 1.14.14.1) (CYPIVF4).	3	P51869
ENSRNOP00000030374	32	-63.4	UDP-glucuronosyltransferase 1-1 precursor (EC 2.4.1.17) (UDPGT) (UGT1*1) (UGT1-01) (UGT1.1) (UGT1A1) (B1).	2	Q64550
ENSRNOP00000024452	10	-35.8	lactamase, beta Source:	1	NP_001100303
ENSRNOP00000028787	11	-14.6	Atlastin-3.	4	Q0ZHH6
ENSRNOP00000023152	15	-46.8	Cytochrome P450 27, mitochondrial precursor (EC 1.14.13.15) (Cytochrome P-450C27/25) (Sterol 26-hydroxylase) (Sterol 27- hydroxylase) (Vitamin D(3) 25-hydroxylase) (5-beta-cholestane-3- alpha,7-alpha,12-alpha-triol 27-hydroxylase).	0	P17178
ENSRNOP00000002728	18	-70.8	No description available.Protein Family: UDP GLUCURONOSYLTRANSFERASE PRECURSOR EC_2.4.1.17	2	
ENSRNOP00000013392	2	-5.6	Acetyl-coenzyme A transporter 1 (AT-1) (Acetyl-CoA transporter) (Solute carrier family 33 member 1). Source: Uniprot/SWISSPROT	1	Q6AYY8
ENSRNOP00000002705	11	-48.3	No description available.Protein Family: UDP GLUCURONOSYLTRANSFERASE PRECURSOR EC_2.4.1.17	3	
ENSRNOP00000013789	17	-74.4	Glutamate dehydrogenase 1, mitochondrial precursor (EC 1.4.1.3) (GDH) (Memory-related protein 2) (MRG-2).	1	P10860

ENSRNOP00000021257	4	-6.5	Probable oxidoreductase C10orf33 homolog (EC 1.-.-.-).	0	Q68FT3
ENSRNOP00000028995	4	-19.7	Arl6ip2 protein (Fragment).	3	Q562A0
ENSRNOP00000007223	5	-14.9	SAC1 (supressor of actin mutations 1, homolog)-like	2	NP_446250
ENSRNOP00000019571	12	-49.4	All-trans-retinol 13,14-reductase precursor (EC 1.3.99.23) (All-trans- 13,14-dihydroretinol saturase) (RetSat) (RMT-7).	0	Q8VHE9
ENSRNOP00000002238	5	-11.7	Mitochondrial precursor proteins import receptor (Translocase of outer membrane TOM70).	2	Q75Q39
ENSRNOP00000036958	2	-12.6	ilvB (bacterial acetolactate synthase)-like	1	NP_001102208
ENSRNOP00000034828	4	-4.4	eukaryotic translation elongation factor 1 delta	2	NP_001013122
ENSRNOP00000018336	18	-47.1	Succinate dehydrogenase flavoprotein subunit, mitochondrial precursor (EC 1.3.5.1) (Fp) (Flavoprotein subunit of complex II).	0	Q920L2
ENSRNOP00000029702	5	-28.9	DEAD/H (Asp-Glu-Ala-Asp/His) box polypeptide 3, X-linked	5	NP_001101716
ENSRNOP00000018185	2	-15.1	DEAD (Asp-Glu-Ala-Asp) box polypeptide 17	3	NP_001015018
ENSRNOP00000057949	6	-17.2	ATP-binding cassette, sub-family G (WHITE), member 3	2	NP_001004076
ENSRNOP00000039792	4	-22.2	Solute carrier organic anion transporter family member 1A6 (Solute carrier family 21 member 13) (Kidney-specific organic anion- transporting polypeptide 5) (OATP-5).	5	Q9QYE2
ENSRNOP00000016739	15	-55.8	ATP-binding cassette sub-family D member 3 (70 kDa peroxisomal membrane protein) (PMP70).	2	P16970
ENSRNOP00000010260	5	-11.2	Acyl-coenzyme A oxidase 2, peroxisomal (EC 1.17.99.3) (3-alpha,7- alpha,12-alpha-trihydroxy-5-beta-cholestanoyl-CoA 24-hydroxylase) (3- alpha,7-alpha,12-alpha-trihydroxy-5-beta-cholestanoyl-CoA oxidase) (Trihydroxycoprostanoyl-CoA oxidase) (THCCox) (THCA-	2	P97562
ENSRNOP00000001961	12	-70.3	NADPH--cytochrome P450 reductase (EC 1.6.2.4) (CPR) (P450R).	1	P00388
ENSRNOP00000034745	5	-21.1	Ac1573.	5	Q7TQ74
ENSRNOP00000015667	16	-74.3	Fatty-acid amide hydrolase 1 (EC 3.1.-.-) (Oleamide hydrolase 1) (Anandamide amidohydrolase 1).	1	P97612
ENSRNOP00000055824	7	-15.3	Dipeptidyl peptidase 4 (EC 3.4.14.5) (Dipeptidyl peptidase IV) (DPP IV) (T-cell activation antigen CD26) (GP110 glycoprotein) (Bile canaliculus domain-specific membrane glycoprotein) [Contains: Dipeptidyl peptidase 4 membrane form (Dipeptidyl peptidase IV	9	P14740

ENSRNOP00000003739	8	-4.5	ATP-binding cassette sub-family B member 7, mitochondrial precursor (ATP-binding cassette transporter 7) (ABC transporter 7 protein).	3	Q704E8
ENSRNOP00000040087	5	-18	No description available.Protein Family: DOLICHYL DIPHOSPHOOLIGOSACCHARIDE GLYCOSYLTRANSFERASE SUBUNIT EC_2.4.1.119 OLIGOSACCHARYL TRANSFERASE SUBUNIT STT3	2	
ENSRNOP00000036574	5	-24.5	acyl-Coenzyme A dehydrogenase family, member 11	3	NP_001101651
ENSRNOP00000000345	3	-16.3	Translocation protein SEC63 homolog.	1	Q8VHE0
ENSRNOP00000013985	3	-15.2	Carnitine O-palmitoyltransferase I, muscle isoform (EC 2.3.1.21) (CPT I) (CPTI-M) (Carnitine palmitoyltransferase 1B) (Carnitine palmitoyltransferase I-like protein).	2	Q63704
ENSRNOP00000024632	2	-3.7	Afg3l2 protein.	0	Q5BJM6
ENSRNOP00000040121	3	-7.2	Transitional endoplasmic reticulum ATPase (TER ATPase) (15S Mg(2+)- ATPase p97 subunit) (Valosin-containing protein) (VCP).	1	P46462
ENSRNOP00000011521	18	-47.6	Mannosyl-oligosaccharide glucosidase (EC 3.2.1.106) (Glycoprotein- processing glucosidase I).	1	O88941
ENSRNOP00000025627	2	-7.7	Mitochondrial ATP-binding cassette sub-family B member 6 (Ubiquitously-expressed mammalian ABC half transporter).	4	O70595
ENSRNOP00000050050	2	-13.3	Glycerol-3-phosphate acyltransferase, mitochondrial precursor (EC 2.3.1.15) (GPAT).	3	P97564
ENSRNOP00000006582	2	-18.7	Extended synaptotagmin-2 (E-Syt2) (Protein FAM62B).	5	Q3TZZ7
ENSRNOP00000058268	19	-52.6	No description available.Protein Family: RAS GTPASE ACTIVATING	2	
ENSRNOP00000028445	5	-29.5	Band 3 anion transport protein (Anion exchange protein 1) (AE 1) (Solute carrier family 4 member 1) (CD233 antigen).	2	P23562
ENSRNOP00000047113	3	-11.7	Armadillo repeat protein deleted in velo-cardio-facial syndrome homolog.	5	P98203
ENSRNOP00000001738	25	-58	Sarcoplasmic/endoplasmic reticulum calcium ATPase 2 (EC 3.6.3.8) (Calcium pump 2) (SERCA2) (SR Ca(2+)-ATPase 2) (Calcium-transporting ATPase sarcoplasmic reticulum type, slow twitch skeletal muscle isoform) (Endoplasmic reticulum class 1/2 Ca(2+) ATPase).	3	P11507
ENSRNOP00000027497	10	-13.1	Sodium/potassium-transporting ATPase subunit alpha-3 (EC 3.6.3.9) (Sodium pump subunit alpha-3) (Na(+)/K(+) ATPase alpha-3 subunit) (Na(+)/K(+) ATPase alpha(III) subunit).	5	P06687

ENSRNOP00000006119	3	-9.6	Extended-synaptotagmin-1 (E-Syt1) (Membrane-bound C2 domain-containing protein) (vp115) (Protein FAM62A).	2	Q9Z1X1
ENSRNOP00000039718	7	-11.2	No description available.Protein Family: PROBABLE PHOSPHOLIPID TRANSPORTING ATPASE EC_3.6.3.1 ATPASE CLASS I TYPE	3	
ENSRNOP00000048088	2	-15.8	Myosin-Ib (Myosin I alpha) (MMI-alpha) (MMIa) (Myosin heavy chain myr 1).	2	Q05096
ENSRNOP00000048476	10	-29.5	Vigilin (High density lipoprotein-binding protein) (HDL-binding protein).	2	Q9Z1A6
ENSRNOP00000042749	3	-11.9	Nuclear pore complex protein Nup155 (Nucleoporin Nup155) (155 kDa nucleoporin) (P140).	4	P37199
ENSRNOP00000051412	13	-41.5	Multidrug resistance-associated protein 6 (ATP-binding cassette sub- family C member 6) (MRP-like protein 1) (MLP-1).	8	O88269
ENSRNOP00000014833	2	-4.9	nucleoporin 205kDa	5	NP_001102090
ENSRNOP00000003983	4	-20.4	Myosin-10 (Myosin heavy chain 10) (Myosin heavy chain, non-muscle IIb) (Non-muscle myosin heavy chain IIb) (NMMHC II-b) (NMMHC-IIB) (Cellular myosin heavy chain, type B) (Non-muscle myosin heavy chain-B) (NMMHC- B).	7	Q9JLT0
ENSRNOP00000026573	3	-8.7	Spectrin beta chain, brain 2 (Spectrin, non-erythroid beta chain 2) (Beta-III spectrin) (SPNB-3) (Beta SpIII sigma 1) (Glutamate transporter EAAT4-associated protein 41) (Spectrin-like protein GTRAP41).	2	Q9QWN8
ENSRNOP00000008210	2	-10.2	spectrin beta 2	4	NP_001013148
ENSRNOP00000042382	3	-11.9	Spectrin alpha chain, brain (Spectrin, non-erythroid alpha chain) (Alpha-II spectrin) (Fodrin alpha chain).	5	P16086
ENSRNOP00000001517	7	-16.9	No description available.Protein Family: AMBIGUOUS	3	
ENSRNOP00000032156	3	-11.4	E3 ubiquitin-protein ligase UBR4 (EC 6.3.2.-) (N-recognin-4) (Zinc finger UBR1-type protein 1).	19	Q2TL32
ENSRNOP00000027754	16	-22.5	Up-regulated during skeletal muscle growth protein 5 (Diabetes- associated protein in insulin-sensitive tissues).	0	Q9JJW3
ENSRNOP00000029426	2	-7.1	No description available.Protein Family: ATP SYNTHASE F CHAIN MITOCHONDRIAL EC_3.6.3.14	0	
ENSRNOP00000000749	3	-3.7	No description available.Protein Family: CDGSH IRON SULFUR DOMAIN CONTAINING 1 ZINC FINGER CDGSH DOMAIN CONTAINING 1	0	

ENSRNOP00000012233	10	-15.3	Dolichyl-diphosphooligosaccharide--protein glycosyltransferase subunit DAD1 (EC 2.4.1.119) (Oligosaccharyl transferase subunit DAD1) (Defender against cell death 1) (DAD-1).	0	P61805
ENSRNOP00000022487	5	-3.5	Cytochrome c oxidase subunit 5B, mitochondrial precursor (EC 1.9.3.1) (Cytochrome c oxidase polypeptide Vb) (Cytochrome c oxidase subunit VIA*).	1	P12075
ENSRNOP00000020446	36	-45.4	Cytochrome b5.	0	P00173
ENSRNOP00000025525	8	-24.1	Cytochrome c oxidase subunit 5A, mitochondrial precursor (EC 1.9.3.1) (Cytochrome c oxidase polypeptide Va).	0	P11240
ENSRNOP00000037521	3	-4.2	No description available.Protein Family: AMBIGUOUS	0	
ENSRNOP00000010579	62	-157.8	Microsomal glutathione S-transferase 1 (EC 2.5.1.18) (Microsomal GST- 1) (Microsomal GST-I).	0	P08011
ENSRNOP00000026347	4	-7.3	Vitamin K epoxide reductase complex subunit 1 (EC 1.1.4.1) (Vitamin K1 2,3-epoxide reductase subunit 1).	1	Q6TEK4
ENSRNOP00000019624	4	-22.3	No description available.Protein Family: NADH DEHYDROGENASE 1 BETA SUBCOMPLEX SUBUNIT 10 EC_1.6.5.3 EC_1.6.99.- 3 NADH UBIQUINONE OXIDOREDUCTASE PDSW SUBUNIT COMPLEX I PDSW CI PDSW	1	
ENSRNOP00000015684	6	-18	No description available.Protein Family: AMBIGUOUS	1	
ENSRNOP00000017101	13	-31.4	Membrane-associated progesterone receptor component 1 (Acidic 25 kDa protein) (25-DX) (Ventral midline antigen) (VEMA).	0	P70580
ENSRNOP00000031599	6	-25.3	hydroxysteroid (17-beta) dehydrogenase 6 Source: RefSeq_peptide NP_775427	3	
ENSRNOP00000014819	2	-6.5	Uncharacterized protein C10orf58 homolog precursor.	0	Q6AXX6
ENSRNOP00000027760	2	-6	CD81 antigen (26 kDa cell surface protein TAPA-1) (Target of the antiproliferative antibody 1).	0	Q62745
ENSRNOP00000046414	7	-19.7	Cytochrome c oxidase subunit 2 (EC 1.9.3.1) (Cytochrome c oxidase polypeptide II).	0	P00406
ENSRNOP00000010760	24	-81.7	Methyltransferase-like protein 7B precursor (EC 2.1.1.-) (Associated with lipid droplet protein 1) (ALDI).	0	Q562C4
ENSRNOP00000021920	20	-50.8	ATP synthase B chain, mitochondrial precursor (EC 3.6.3.14).	0	P19511

ENSRNOP00000012425	6	-25.1	No description available.Protein Family: NADH DEHYDROGENASE IRON SULFUR 3 MITOCHONDRIAL PRECURSOR EC_1.6.5.3 EC_1.6.99.- 3 NADH UBIQUINONE OXIDOREDUCTASE 30 KDA SUBUNIT COMPLEX I 30KD CI 30KD	0	
ENSRNOP00000026197	16	-38.8	Voltage-dependent anion-selective channel protein 3 (VDAC-3) (rVDAC3) (Outer mitochondrial membrane protein porin 3).	2	Q9R1Z0
ENSRNOP00000015802	25	-68.2	No description available.Protein Family: CYTOCHROME P450 2	1	
ENSRNOP00000018462	11	-22.6	Voltage-dependent anion-selective channel protein 2 (VDAC-2) (Outer mitochondrial membrane protein porin 2) (B36-VDAC).	3	P81155
ENSRNOP00000007870	26	-80.6	Corticosteroid 11-beta-dehydrogenase isozyme 1 (EC 1.1.1.146) (11-DH) (11-beta-hydroxysteroid dehydrogenase 1) (11-beta-HSD1).	2	P16232
ENSRNOP00000008477	23	-47.3	Voltage-dependent anion-selective channel protein 1 (VDAC-1) (rVDAC1) (Outer mitochondrial membrane protein porin 1)	2	Q9Z2L0
ENSRNOP00000035497	5	-16.9	Uncharacterized protein KIAA0152 homolog precursor.	1	Q5FVQ4
ENSRNOP00000056976	5	-15.2	Translocon-associated protein subunit alpha precursor (TRAP-alpha) (Signal sequence receptor subunit alpha) (SSR-alpha) (Liver regeneration-related protein LRRG137).	2	Q7TPJ0
ENSRNOP00000021512	44	-92.9	Peroxisomal trans-2-enoyl-CoA reductase (EC 1.3.1.38) (RLF98) (Peroxisomal 2,4-dienoyl CoA reductase) (PX-2,4-DCR1).	3	Q9WVK3
ENSRNOP00000014704	22	-56.7	ADP/ATP translocase 1 (Adenine nucleotide translocator 1) (ANT 1) (ADP,ATP carrier protein 1) (Solute carrier family 25 member 4).	0	Q05962
ENSRNOP00000015913	66	-101.3	ADP/ATP translocase 2 (Adenine nucleotide translocator 2) (ANT 2) (ADP,ATP carrier protein 2) (Solute carrier family 25 member 5).	1	Q09073
ENSRNOP00000027520	23	-66.2	Mitochondrial carnitine/acylcarnitine carrier protein (Carnitine/acylcarnitine translocase) (CAC) (Solute carrier family 25 member 20).	0	P97521
ENSRNOP00000011158	7	-26.6	Nipsnap1 protein (Fragment).	0	Q5EBA4
ENSRNOP00000000306	9	-39.5	Tricarboxylate transport protein, mitochondrial precursor (Citrate transport protein) (CTP) (Tricarboxylate carrier protein) (Solute carrier family 25 member 1).	0	P32089

ENSRNOP00000012878	37	-56.6	NADH-cytochrome b5 reductase 3 (EC 1.6.2.2) (Cytochrome b5 reductase) (B5R) (Diaphorase-1)	0	P20070
ENSRNOP00000017067	9	-22.9	No description available.Protein Family: CYTOCHROME C1 HEME PROTEIN MITOCHONDRIAL PRECURSOR CYTOCHROME C 1 CYTOCHROME B C1 COMPLEX SUBUNIT 4 UBIQUINOL CYTOCHROME C REDUCTASE COMPLEX CYTOCHROME C1 SUBUNIT COMPLEX III SUBUNIT 4 COMPLEX III SUBUNIT IV	0	0
ENSRNOP00000003334	4	-14.4	Guanine nucleotide-binding protein subunit beta 2-like 1 (Receptor of activated protein kinase C 1) (RACK1) (Receptor for activated C kinase).	1	P63245
ENSRNOP00000035423	30	-100.2	Retinol dehydrogenase 2 (EC 1.1.1.105) (Retinol dehydrogenase type II) (RODH II) (29 k-protein).	0	P50170
ENSRNOP00000024707	12	-49.2	Sideroflexin-1 (Tricarboxylate carrier protein) (TCC).	3	Q63965
ENSRNOP00000005875	37	-109.8	Retinol dehydrogenase 7 (EC 1.1.1.105) (Retinol dehydrogenase type III) (RODH III).	1	P55006
ENSRNOP00000036896	23	-94.8	No other features on this peptide	0	
ENSRNOP00000041608	19	-71.6	Phosphate carrier protein, mitochondrial precursor (PTP) (Solute carrier family 25 member 3).	0	P16036
ENSRNOP00000044296	60	-194.2	Actin, cytoplasmic 1 (Beta-actin).	1	P60711
ENSRNOP00000035416	4	-18.1	No description available.Protein Family: SYNAPTIC GLYCOPROTEIN SC2 EC_1.3.1.- TRANS 2 3 ENOYL COA REDUCTASE TER	3	0
ENSRNOP00000026290	27	-95.8	3 beta-hydroxysteroid dehydrogenase type 5 (3 beta-hydroxysteroid dehydrogenase type V) (3-beta-HSD V) (NADPH-dependent 3-beta-hydroxy-Delta(5)-steroid dehydrogenase) (EC 1.1.1.-) (3-beta-hydroxy-5-ene steroid dehydrogenase) (Progesterone reductase).	2	
ENSRNOP00000012681	24	-99.6	No other features on this peptide	1	
ENSRNOP00000011275	4	-16.6	Basigin precursor (OX-47 antigen) (Glycoprotein CE9) (CD147 antigen).	3	P26453
ENSRNOP00000018761	9	-35.2	Arylacetamide deacetylase (EC 3.1.1.-) (AADAC).	3	Q9QZH8
ENSRNOP00000008932	3	-16.5	similar to RIKEN cDNA 2310001A20 (RGD1308874), mRNA Source: RefSeq_dna NM_001034003	1	
ENSRNOP00000003791	5	-13.3	Probable saccharopine dehydrogenase (EC 1.5.1.9).	2	Q6AY30
ENSRNOP00000021514	28	-119.7	Ubiquinol-cytochrome-c reductase complex core protein 2, mitochondrial precursor (EC 1.10.2.2) (Core protein II) (Complex III subunit II).	3	P32551

ENSRNOP00000020306	24	-51.1	dolichyl-di-phosphooligosaccharide-protein glycotransferase (predicted) Source: RefSeq_peptide NP_001012104	0	
ENSRNOP00000001095	35	-124.1	Tubulin beta-5 chain.	2	P69897
ENSRNOP00000045029	29	-75	Cytochrome P450 2C7 (EC 1.14.14.1) (CYPIIC7) (P450F) (PTF1).	1	P05179
ENSRNOP00000018455	16	-32.4	Protein transport protein Sec61 subunit alpha isoform 1 (Sec61 alpha- 1).	0	P61621
ENSRNOP00000034293	57	-158	Epoxide hydrolase 1 (EC 3.3.2.9) (Microsomal epoxide hydrolase) (Epoxide hydratase).	2	P07687
ENSRNOP00000044696	13	-34	Ubiquinol-cytochrome-c reductase complex core protein 1, mitochondrial precursor (EC 1.10.2.2) (Core I protein).	2	Q68FY0
ENSRNOP00000026122	25	-98	Hydroxymethylglutaryl-CoA synthase, mitochondrial precursor (EC 2.3.3.10) (HMG-CoA synthase) (3-hydroxy-3-methylglutaryl coenzyme A synthase).	0	P22791
ENSRNOP00000003052	3	-9.9	Lysosome membrane protein 2 (Lysosome membrane protein II) (LIMP II) (Scavenger receptor class B member 2) (85 kDa lysosomal membrane sialoglycoprotein) (LGP85) (CD36 antigen-like 2).	9	P27615
ENSRNOP00000028237	63	-154.9	Cytochrome P450 2A1 (EC 1.14.14.1) (CYPIIA1) (Steroid hormones 7- alpha-hydroxylase) (Testosterone 7-alpha-hydroxylase) (P450-UT-F).	1	P11711
ENSRNOP00000017237	74	-179.4	Cytochrome P450 2C6 (EC 1.14.14.1) (CYPIIC6) (P450 PB1) (PTF2).	2	P05178
ENSRNOP00000001816	3	-10.7	Aldehyde dehydrogenase, mitochondrial precursor (EC 1.2.1.3) (ALDH class 2) (ALDH1) (ALDH-E2).	2	P11884
ENSRNOP00000003965	212	-372	ATP synthase subunit beta, mitochondrial precursor (EC 3.6.3.14).	0	P10719
ENSRNOP00000042986	8	-15.6	cytochrome P450, family 2, subfamily b, polypeptide 13 Source: RefSeq_peptide NP_942028	1	
ENSRNOP00000001299	2	-5.3	Scavenger receptor class B member 1 (SRB1) (SR-BI).	8	P97943
ENSRNOP00000051608	21	-61.5	Cytochrome P450 2C70 (EC 1.14.14.1) (CYPIIC70) (P-450Md) (P450 P49).	2	P19225
ENSRNOP00000045886	42	-125.2	Fatty aldehyde dehydrogenase (EC 1.2.1.3) (Aldehyde dehydrogenase, microsomal) (Aldehyde dehydrogenase family 3 member A2) (Aldehyde dehydrogenase 10).	0	P30839
ENSRNOP00000043466	25	-92.1	Amine oxidase B (EC 1.4.3.4) (Monoamine oxidase type B) (MAO-B).	1	P19643

ENSRNOP00000040266	55	-206.2	Cytochrome P450 2D10 (EC 1.14.14.1) (CYPIID10) (P450-DB5) (P450-CMF1B) (Debrisoquine 4-hydroxylase).	4	P12939
ENSRNOP00000048711	29	-133.7	Cytochrome P450 2D3 (EC 1.14.14.1) (CYPIID3) (P450-DB3) (Debrisoquine 4-hydroxylase).	1	P12938
ENSRNOP00000041174	71	-230.4	Cytochrome P450 2D1 (EC 1.14.14.1) (CYPIID1) (P450-DB1) (P450-CMF1A) (P450-UT-7) (Debrisoquine 4-hydroxylase).	4	P10633
ENSRNOP00000015866	13	-13.5	Solute carrier family 2, facilitated glucose transporter member 2 (Glucose transporter type 2, liver) (GLUT-2).	1	P12336
ENSRNOP00000055369	11	-42.2	cytochrome P450, family 1, subfamily a, polypeptide 2	3	
ENSRNOP00000012413	61	-182.9	Cytochrome P450 2D26 (EC 1.14.14.1) (CYPIID26) (P450-DB2) (P450-CMF2) (Debrisoquine 4-hydroxylase).	3	P10634
ENSRNOP00000045567	35	-146.9	Cytochrome P450 4A14 precursor (EC 1.14.15.3) (CYPIVA14) (Lauric acid omega-hydroxylase) (P450-LA-omega 3).	3	P20817
ENSRNOP00000017310	115	-253.3	Cytochrome P450 2C11 (EC 1.14.14.1) (CYPIIC11) (P-450(M-1)) (P450H) (P450-UT-A) (UT-2).	1	P08683
ENSRNOP00000003910	11	-58.8	Amine oxidase A (EC 1.4.3.4) (Monoamine oxidase type A) (MAO-A).	1	P21396
ENSRNOP00000025045	52	-130.3	UDP-glucuronosyltransferase 1-1 precursor (EC 2.4.1.17) (UDPGT) (UGT1*1) (UGT1-01) (UGT1.1) (UGT1A1) (B1).	2	Q64550
ENSRNOP00000022892	174	-326.7	ATP synthase subunit alpha, mitochondrial precursor (EC 3.6.3.14). \	1	P15999
ENSRNOP00000004864	48	-144.6	Dimethylaniline monooxygenase 3 (EC 1.14.13.8) (Hepatic flavin-containing monooxygenase 3) (FMO 3) (Dimethylaniline oxidase 3).	3	Q9EQ76
ENSRNOP00000024423	32	-128.2	Dimethylaniline monooxygenase 5 (EC 1.14.13.8) (Hepatic flavin-containing monooxygenase 5) (FMO 5) (Dimethylaniline oxidase 5).	2	Q8K4C0
ENSRNOP00000043239	73	-229.8	UDP-glucuronosyltransferase 2B3 precursor (EC 2.4.1.17) (UDPGT) (Testosterone, dihydrotestosterone, and beta-estradiol specific) (17- beta-hydroxysteroid specific) (UDPGTr-3) (RLUG38).	0	P08542
ENSRNOP00000002724	36	-94	UDP-glucuronosyltransferase 2B1 precursor (EC 2.4.1.17) (UDPGT) (UDPGTr-2).	2	P09875

ENSRNOP00000045002	54	-172.5	UDP-glucuronosyltransferase 2B3 precursor (EC 2.4.1.17) (UDPGT) (Testosterone, dihydrotestosterone, and beta-estradiol specific) (17- beta-hydroxysteroid specific) (UDPGTr-3) (RLUG38).	0	P08542
ENSRNOP00000002712	46	-144.1	UDP-glucuronosyltransferase 2B4 precursor (EC 2.4.1.17) (UDPGT) (UDP- glucuronosyltransferase 2B12).	0	P36511
ENSRNOP00000034723	58	-188.1	UDP-glucuronosyltransferase 2B2 precursor (EC 2.4.1.17) (UDPGT) (3- hydroxyandrogen specific) (UDPGTr-4) (RLUG23).	1	P08541
ENSRNOP00000021407	16	-43	choline dehydrogenase precursor Source: RefSeq_peptide NP_942026	0	
ENSRNOP00000040859	8	-24.7	Calnexin precursor.	1	P35565
ENSRNOP00000049879	33	-80.2	ATP synthase gamma chain, mitochondrial (EC 3.6.3.14).	4	P35435
ENSRNOP00000013262	45	-132.3	Electron transfer flavoprotein-ubiquinone oxidoreductase, mitochondrial precursor (EC 1.5.5.1) (ETF-QO) (ETF-ubiquinone oxidoreductase) (ETF dehydrogenase) (Electron-transferring- flavoprotein dehydrogenase).	1	Q6UPE1
ENSRNOP00000010209	61	-183.5	Dolichyl-diphosphooligosaccharide--protein glycosyltransferase 63 kDa subunit precursor (EC 2.4.1.119) (Ribophorin II) (RPN-II).	2	P25235
ENSRNOP00000013607	25	-62.3	Solute carrier family 27 (Fatty acid transporter), member 2.	2	Q66HN6
ENSRNOP00000024973	37	-148.6	Very-long-chain specific acyl-CoA dehydrogenase, mitochondrial precursor (EC 1.3.99.-) (VLCAD).	3	P45953
ENSRNOP00000013816	130	-358.4	No other features on this peptide	0	
ENSRNOP00000016954	3	-16.8	Carnitine O-palmitoyltransferase 2, mitochondrial precursor (EC 2.3.1.21) (Carnitine palmitoyltransferase II) (CPT II).	6	P18886
ENSRNOP00000056312	16	-41.7	tumor rejection antigen gp96 (predicted) Source: RefSeq_peptide NP_001012197	4	
ENSRNOP00000052490	11	-26.8	No description available.Protein Family: SOLUTE CARRIER ORGANIC ANION TRANSPORTER FAMILY MEMBER SOLUTE CARRIER FAMILY 21 MEMBER ORGANIC ANION TRANSPORTER ORGANIC ANION TRANSPORTING POLYPEPTIDE	6	

ENSRNOP00000026574	41	-158.5	Bile acyl-CoA synthetase (EC 6.2.1.7) (BACS) (Bile acid CoA ligase) (BA-CoA ligase) (BAL) (Cholate--CoA ligase) (Very long chain acyl-CoA synthetase-related protein) (VLACS-related) (VLACSR) (Fatty acid transport protein 5) (FATP-5) (Solute carrier family	1	Q9ES38
ENSRNOP00000051445	21	-56	Long-chain-fatty-acid--CoA ligase 5 (EC 6.2.1.3) (Long-chain acyl-CoA synthetase 5) (LACS 5). O88813	1	O88813
ENSRNOP00000014235	111	-262.2	Long-chain-fatty-acid--CoA ligase 1 (EC 6.2.1.3) (Long-chain acyl-CoA synthetase 1) (LACS 1) (Long-chain-fatty-acid--CoA ligase, liver isozyme).	3	P18163
ENSRNOP00000002410	12	-49	Peroxisomal bifunctional enzyme (PBE) (PBFE) .	1	P07896
ENSRNOP00000015851	4	-19.1	NADH-ubiquinone oxidoreductase 75 kDa subunit, mitochondrial precursor (EC 1.6.5.3) (EC 1.6.99.3).	1	Q66HF1
ENSRNOP00000043950	5	-24.7	Junction plakoglobin.	7	Q6P0K8
ENSRNOP00000006855	6	-17.6	Surfeit locus protein 1.	1	Q9QXU2
ENSRNOP00000045650	17	-45.4	ATPase, Na+/K+ transporting, alpha 1 polypeptide	3	
ENSRNOP00000054924	9	-34.6	inner membrane protein, mitochondrial Source: RefSeq_peptide NP_001030100	3	
ENSRNOP00000001905	4	-7.4	No description available.Protein Family: TRANSFERRIN RECEPTOR	5	
ENSRNOP00000014630	5	-28.1	No description available.Protein Family: MICROSOMAL TRIGLYCERIDE TRANSFER LARGE SUBUNIT PRECURSOR	1	
ENSRNOP00000029578	21	-76.7	nicotinamide nucleotide transhydrogenase Source: RefSeq_peptide NP_001013175	5	0
ENSRNOP00000052656	19	-74.3	Clathrin heavy chain.	6	P11442
ENSRNOP00000007398	38	-151.2	Myosin-9 (Myosin heavy chain 9) (Myosin heavy chain, nonmuscle IIa) (Nonmuscle myosin heavy chain IIa) (NMMHC II-a) (NMMHC-IIA) (Cellular myosin heavy chain, type A) (Nonmuscle myosin heavy chain-A) (NMMHC- A).	6	Q62812
ENSRNOP00000019772	3	-11.7	Fibronectin precursor (FN).	6	P04937
ENSRNOP00000034954	3	-17.2	Perlecan (Fragment).	5	O08591
ENSRNOP00000040018	6	-30.7	Plectin-1 (PLTN) (PCN).	9	P30427

Supplementary Table 6
Enzymes involved in the Glycosylation pathway and cell surface lectins
EHS-bearing mice Chapter 4

			Control 1	Control 2	Control 3			
Identifier	**Glycosylation enzymes**	**Abrev**	**#peptides (control 1)**	**#peptides (control 2)**	**# peptides (control 3)**	**Control (AvgNSAF)**	**SD**	**SE**
ENSMUSP00000003843	mannosidase 1, alpha	Man1a1	63	63	67	9.332075654	0.495901871	0.286309079
ENSMUSP00000036996	mannosidase, alpha, class 1B, member 1	Man1b1	3	3	1	0.365104662	0.164235082	0.094821169
ENSMUSP00000083928	mannosidase 2, alpha 1	Man2a1	89	109	149	9.108451016	1.823922886	1.053042369
ENSMUSP00000080484	mannoside acetylglucosaminyltransferase 1	Mgat1	5	10	10	1.465457349	0.276359436	0.159556195
ENSMUSP00000057905	mannoside acetylglucosaminyltransferase 2	Mgat2	6	7	7	1.488337166	0.108293356	0.062523198
ENSMUSP00000038359	mannoside acetylglucosaminyltransferase 5	Mgat5	0	0	0	0.023406591	0.001136845	0.000656358
ENSMUSP00000090307	ST3 beta-galactoside alpha-2,3-sialyltransferase 3	St3Gal1	15	22	8	4.010906483	1.443234817	0.83325201
ENSMUSP00000023601	beta galactoside alpha 2,6 sialyltransferase 1	St6Gal1	1	11	2	0.732574536	0.767178809	0.442930892
ENSMUSP00000092655	Alpha-N-acetylgalactosaminide alpha-2,6-sialyltransferase 6	St6GalNAc6	0	0	0	0.055338266	0.002687748	0.001551772
ENSMUSP00000060247	UDP-GlcNAc:betaGal beta-1,3-N-acetylglucosaminyltransferase 2	B3galt7	0	0	0	0.043629414	0.002119055	0.001223437
ENSMUSP00000066353	Beta-1,4-galactosyltransferase 3	B4galt3	0	0	0	0.043850322	0.002129785	0.001229632
ENSMUSP00000047931	core 1 synthase, glycoprotein-N-acetylgalactosamine 3-beta-galactosyltransferase, 1	C1GalT1	4	4	0	0.495490039	0.573508724	0.331115416
ENSMUSP00000059224	C1GALT1-specific chaperone 1	C1GalT2	0	0	1	0.158868752	0.181438367	0.10475349
ENSMUSP00000034458	Polypeptide N-acetylgalactosaminyltransferase 1	Galnt1	5	7	0	0.085153497	0.092319494	0.053300685
ENSMUSP00000072764	lectin, galactose binding, soluble 9	Lgals9	9	13	8	2.752415865	0.572788682	0.3306997
ENSMUSP00000014686	C-type lectin domain family 4, member f	Clec4f	2	4	4	0.49805957	0.092404488	0.053349756

ENSMUSP00000028794	Sialoadhesin precursor (Sialic acid-binding Ig-like lectin 1) (Siglec- 1)	Siglec1	0	0	0	0.010218807	0.000496322	0.000286551

Supplementary Table 6 (continued)
Enzymes involved in the Glycosylation pathway and cell surface lectins
EHS-bearing mice Chapter 4

	Control 1				Control 2				Control 3			
Identifier	LogE	%	Unique Pep	Total Pep	LogE	%	Unique Pep	Total Pep	LogE	%	Unique Pep	Total Pep
ENSMUSP00000003843	-198.8	33	17	63	-228	42	20	63	-215.2	37	19	67
ENSMUSP00000036996	-14.4	5.8	2	3	-20.4	5.3	2	3	-3.4	2.9	1	1
ENSMUSP00000083928	-390.8	35	33	89	-412.4	37	37	109	-436.6	41	39	149
ENSMUSP00000080484	-33	7.2	3	5	-54.5	18	6	10	-46.3	13	5	10
ENSMUSP00000057905	-18.6	5.2	2	6	-33.5	13	4	7	-16.8	11	3	7
ENSMUSP00000038359	#N/A	#N/A	#N/A	#N/A	#N/A	#N/A	#N/A	#N/A	#N/A	#N/A	#N/A	#N/A
ENSMUSP00000090307	-47.7	26	6	15	-53.8	25	6	22	-16	13	2	8
ENSMUSP00000023601	-12.9	3.5	1	1	-31.9	9.7	3	11	-6.6	3.7	1	2
ENSMUSP00000092655	#N/A	#N/A	#N/A	#N/A	#N/A	#N/A	#N/A	#N/A	#N/A	#N/A	#N/A	#N/A
ENSMUSP00000060247	#N/A	#N/A	#N/A	#N/A	#N/A	#N/A	#N/A	#N/A	#N/A	#N/A	#N/A	#N/A
ENSMUSP00000066353	#N/A	#N/A	#N/A	#N/A	#N/A	#N/A	#N/A	#N/A	#N/A	#N/A	#N/A	#N/A
ENSMUSP00000047931	-18.2	6.3	2	4	-12.5	6.9	2	4	#N/A	#N/A	#N/A	#N/A
ENSMUSP00000059224	#N/A	#N/A	#N/A	#N/A	#N/A	#N/A	#N/A	#N/A	-6.1	6.3	1	1
ENSMUSP00000034458	-24.1	7.5	3	5	-47.4	11	5	7	#N/A	#N/A	#N/A	#N/A
ENSMUSP00000072764	-33.3	13	3	9	-46.5	17	5	13	-38.3	15	4	8
ENSMUSP00000014686	-9.9	5.1	2	2	-16.4	3.8	2	4	-27.9	4.6	2	3

ENSMUSP00000028794	#N/A	#N/A	#N/A	#N/A	#N/A	#N/A	#N/A	#N/A	#N/A	#N/A	#N/A	#N/A

Supplementary Table 7 (Chapter 4)

Assigned glycan structures identified in both control and EHS-bearing mice

N-glycans		
(M-H)2-	**(M-H)1-**	**Glycan assignment**
617.3	1235.6	$(Hex)_2 + (Man)_3(GlcNAc)_2$
658.2	1317.4	$(HexNAc)_2 + (Man)_3(GlcNAc)_2$
698.3	1397.6	$(Hex)_3 + (Man)_3(GlcNAc)_2$
779.3	1559.6	$(Hex)_4 + (Man)_3(GlcNAc)_2$
791.3	1583.6	$(Hex)_1\ (HexNAc)_1\ (NeuGc)_1 + (Man)_3(GlcNAc)_2$
799.8	1600.6	(Hex)3(HexNAc)1 + (Man)3(GlcNAc)2
812.3	1625.6	(Hex)1(HexNAc)2(Deoxyhexose)1 + (Man)3(GlcNAc)2
820.3	1641.6	$(Hex)_2\ (HexNAc)_2 + (Man)_3(GlcNAc)_2$
832.8	1666.6	$(HexNAc)_3\ (Deoxyhexose)_1 + (Man)_3(GlcNAc)_2$
860.3	1721.6	$(Hex)_5 + (Man)_3(GlcNAc)_2$
872.3	1745.6	$(Hex)_2\ (HexNAc)_1\ (NeuGc)_1 + (Man)_3(GlcNAc)_2$
884.8	1770.6	$(Hex)_1\ (HexNAc)_2\ (NeuAc)_1 + (Man)_3(GlcNAc)_2$
893.9	1788.8	$(Hex)_1\ (HexNAc)_2\ (NeuGc)_1 + (Man)_3(GlcNAc)_2$
913.8	1828.6	$(Hex)_1\ (HexNAc)_3\ (Deoxyhexose)_1 + (Man)_3(GlcNAc)_2$
941.3	1883.6	$(Hex)_6 + (Man)_3(GlcNAc)_2$
952.9	1906.8	$(Hex)_3\ (HexNAc)_1\ (NeuGc)_1 + (Man)_3(GlcNAc)_2$
961.8	1924.6	$(Hex)_5\ (HexNAc)_1 + (Man)_3(GlcNAc)_2$
965.9	1932.8	$(Hex)_2\ (HexNAc)_2\ (NeuAc)_1 + (Man)_3(GlcNAc)_2$
973.8	1948.6	$(Hex)_2\ (HexNAc)_2\ (NeuGc)_1 + (Man)_3(GlcNAc)_2$
994.5	1990	$(Hex)_2\ (HexNAc)_3\ (Deoxyhexose)_1 + (Man)_3(GlcNAc)_2$
1022.4	2045.8	$(Hex)_7 + (Man)_3(GlcNAc)_2$
1038.9	2078.8	$(Hex)_2\ (HexNAc)_2\ (Deoxyhexose)_1\ (NeuAc)_1 + (Man)_3(GlcNAc)_2$
1046.4	2093.8	$(Hex)_1\ (HexNAc)_2\ (NeuGc)_2 + (Man)_3(GlcNAc)_2$
1067.5	2136	(Hex)2(HexNAc)3(Deoxyhexose)2 + (Man)3(GlcNAc)2
1103.4	2207.8	$(Hex)_8 + (Man)_3(GlcNAc)_2$
1111.4	2223.8	$(Hex)_2\ (HexNAc)_2\ (NeuAc)_2 + (Man)_3(GlcNAc)_2$
1119.9	2240.8	$(Hex)_3\ (HexNAc)_2\ (Deoxyhexose)_1\ (NeuAc)_1 + (Man)_3(GlcNAc)_2$
1127.5	2256	$(Hex)_2\ (HexNAc)_2\ (NeuGc)_2 + (Man)_3(GlcNAc)_2$
1148.6	2298.2	$(Hex)_2\ (HexNAc)_3\ (Deoxyhexose)_1\ (NeuGc)_1 + (Man)_3(GlcNAc)_2$
1148.6	2298.2	$(Hex)_3\ (HexNAc)_3\ (NeuAc)_1 + (Man)_3(GlcNAc)_2$
1184.4	2369.8	$(Hex)_2\ (HexNAc)_2\ (Deoxyhexose)_1\ (NeuAc)_2 + (Man)_3(GlcNAc)_2$

1200.5	2402	$(Hex)_2$ $(HexNAc)_2$ $(Deoxyhexose)_1$ $(NeuGc)_2$ + $(Man)_3(GlcNAc)_2$
1280.9	2562.8	$(Hex)_2$ $(HexNAc)_2$ $(NeuGc)_3$ + $(Man)_3(GlcNAc)_2$
1309.9	2620.8	$(Hex)_3$ $(HexNAc)_3$ $(NeuGc)_2$ + $(Man)_3(GlcNAc)_2$
1463.5	2928	$(Hex)_3$ $(HexNAc)_3$ $(NeuGc)_3$ + $(Man)_3(GlcNAc)_2$
O-glycans		
	675.5	$(Hex)_1$ $(HexNAc)_1$ $(NeuAc)_1$
	691.3	$(Hex)_1$ $(HexNAc)_1$ $(NeuGc)_1$
	966.5	$(Hex)_1$ $(HexNAc)_1$ $(NeuAc)_2$
	982.3	$(Hex)_1$ $(HexNAc)_1$ $(NeuAc)_1$ $(NeuGc)_1$
	998.3	$(Hex)_1$ $(HexNAc)_1$ $(NeuGc)_2$
681.3	1363.6	$(Hex)_2$ $(HexNAc)_2$ $(NeuGc)_2$

Supplementary Table 8

Chapter 5

Protein identification from control, non-cachectic and cachectic mouse liver membrane preparations

Identifier: ENSEMBL number

Mr: Molecular weight

Description: Protein Description

AA: Amino Acid Length

Identifier	Mr	Description	AA
ENSMUSP00000068282	60.8	UDP-glucuronosyltransferase 2B5 Precursor (UDPGT 2B5)(EC 2.4.1.17)(M-1) Source: 2.4.1.17 IPR002213 UDP glucos trans	533.33333
ENSMUSP00000071573	35.7	retinol dehydrogenase 16 IPR003560 DHB DHaseIPR002198 DHase sc/Rdtase SDRIPR002347 Glc/ribitol DHaseIPR016040 NAD(P)-bd	313.15789
ENSMUSP00000037665	57.8	Cytochrome P450 3A11 (EC 1.14.14.1)(CYPIIIA11)(P-450IIIAM1)(P-450UT) Source: 1.14.14.1 IPR001128 Cyt P450IPR002397 Cyt P450 BIPR017973 Cyt P450 CIPR017972 Cyt P450 CSIPR008072 Cyt P450 E CYP3AIPR002401 Cyt P450 E grp-IIPR002402 Cyt P450 E grp-IIIPR002403 Cyt P450 E grp-IV	507.01754
ENSMUSP00000072598	60.9	UDP glucuronosyltransferase 2 family, polypeptide B38 IPR002213 UDP glucos trans	534.21053
ENSMUSP00000031633	57.8	Cytochrome P450 3A16 (EC 1.14.14.1)(CYPIIIA16) Source: 1.14.14.1 IPR001128 Cyt P450IPR002397 Cyt P450 BIPR017973 Cyt P450 CIPR017972 Cyt P450 CSIPR008072 Cyt P450 E CYP3AIPR002401 Cyt P450 E grp-IIPR002402 Cyt P450 E grp-IIIPR002403 Cyt P450 E grp-IV	507.01754
ENSMUSP00000052945	164.8	hypothetical protein LOC545428 IPR007110 Ig-likeIPR013098 Ig I-setIPR018159 Spectrin/alpha-actininIPR002017 Spectrin repeat	1445.614
ENSMUSP00000033086	46.5	Phosphorylase b kinase gamma catalytic chain, testis/liver isoform (PHK-gamma-T)(EC 2.7.11.19)(Phosphorylase kinase subunit gamma 2) Source: 2.7.11.19 IPR011009 Kinase likeIPR002291 Phosph kin gammaIPR000719 Prot kinase coreIPR017441 Protein kinase ATP BSIPR017442 Se/Thr pkinase-relIPR008271 Ser thr pkin ASIPR002290 Ser thr pkinaseIPR001245 Tyr pkinase	407.89474
ENSMUSP00000034173	61.5	Liver carboxylesterase 22 Precursor (Esterase-22)(Es-22)(EC 3.1.1.1)(Egasyn) Source: 3.1.1.1 IPR002018 CarbesteraseBIPR000997 Cholinesterase	539.47368
ENSMUSP00000020266	32	Phenazine biosynthesis-like domain-containing protein 1 (EC 5.1.-.-) Source: 5.1.-.- IPR003719 PhzC PhzF	280.70175
ENSMUSP00000102636	41.9	3 beta-hydroxysteroid dehydrogenase/Delta 5-->4-isomerase type 2 (3-beta-HSD II) Source: 1.1.1.145 IPR002225 3Beta OHSteriod DHase/EstaseIPR001509 Epimerase deHydtaseIPR013120 Male sterile NAD-bdIPR016040 NAD(P)-bdIPR003869 Polysac CapD	367.54386
ENSMUSP00000023709	61.7	Keratin, type II cytoskeletal 5 (Cytokeratin-5)(CK-5)(Keratin-5)(K5) IPR016044 FIPR018039 Intermediate filament CSIPR002957 Keratin IIPR003054 Keratin IIIPR009053 PrefoldinIPR000533 Tropomyosin	541.22807
ENSMUSP00000004478	88.9	Cullin-3 (CUL-3) IPR016157 Cullin CSIPR001373 Cullin NIPR016158 Cullin homologyIPR016159 Cullin repeat-like	779.82456
ENSMUSP00000017597	43.8	Peroxisomal sarcosine oxidase (PSO)(EC 1.5.3.1)(EC 1.5.3.7)(L-pipecolate oxidase)(L-pipecolic acid oxidase) Source: 1.5.3.1 IPR006076 FAD-dep OxRdtaseIPR006281 SoxA mon	384.21053
ENSMUSP00000004396	13.4	V-type proton ATPase subunit F (V-ATPase subunit F)(Vacuolar proton pump subunit F)(V-ATPase 14 kDa subunit) IPR005772 ATPase V1-cplx fsu eukIPR008218 ATPase V1/A1-cplx fsu	117.54386
ENSMUSP00000094929	82.8	Methylmalonyl-CoA mutase, mitochondrial Precursor (MCM)(EC 5.4.99.2)(Methylmalonyl-CoA isomerase) Source: 5.4.99.2 IPR006159 Acid CoA mut CIPR016176 Cbl-dep enz catIPR006158 Cobalamin-bdIPR006099 MMCoA mutase a/b catIPR006098 MMCoA mutase a cat	726.31579
ENSMUSP00000077972	53	G-rich sequence factor 1 (GRSF-1) IPR000104 Antifreeze 1IPR003072 NOR1 rcptIPR000504 RRM RNP1	464.91228
ENSMUSP00000072558	16.3	no description availableIPR001971 Ribosomal S11IPR018102 Ribosomal S11 CS	142.98246
ENSMUSP00000099436	22.9	Proteasome subunit beta type-3 (EC 3.4.25.1)(Proteasome theta chain)(Proteasome chain 13)(Proteasome component C10-II) Source: 3.4.25.1 IPR001353 Proteasome A B suIPR016050 Proteasome bsu CS	200.87719

ENSMUSP00000066990	10.6	28S ribosomal protein S21, mitochondrial (S21mt)(MRP-S21) IPR001911 Ribosomal S21	92.982456
ENSMUSP00000001497	24.8	Cell death activator CIDE-B (Cell death-inducing DFFA-like effector B) IPR003508 CAD	217.54386
ENSMUSP00000103034	49.5	Keratin, type I cytoskeletal 15 (Cytokeratin-15)(CK-15)(Keratin-15)(K15) IPR016044 FIPR018039 Intermediate filament CSIPR002957 Keratin IIPR009053 PrefoldinIPR000817 PrionIPR003536 Transloc intimin rcpt	434.21053
ENSMUSP00000034046	77.9	Long-chain-fatty-acid--CoA ligase 1 (EC 6.2.1.3)(Long-chain acyl-CoA synthetase 1)(LACS 1) Source: 6.2.1.3 IPR000873 AMP-dep Synth/Lig	683.33333
ENSMUSP00000057069	100.1	Endoplasmic reticulum metallopeptidase 1 (EC 3.4.-.-)(Felix-ina) Source: 3.4.-.- IPR002933 Peptidase M20IPR007484 Peptidase M28	878.07018
ENSMUSP00000044012	174.2	amylo-1,6-glucosidase, 4-alpha-glucanotransferase IPR008928 6-hairpin glycosidase-likeIPR010401 GDE CIPR006421 Glyc debranchIPR017853 Glyco hydro cat	1528.0702
ENSMUSP00000018727	51.8	Ras GTPase-activating protein-binding protein 1 (EC 3.6.1.-)(G3BP-1)(ATP-dependent DNA helicase VIII)(HDH-VIII)(GAP SH3 domain-binding protein 1) Source: 3.6.1.- IPR002075 NTF2IPR018222 Nuclear transport factor 2 eukIPR000694 PRO richIPR000504 RRM RNP1	454.38596
sp|K1C15_SHEEP|	48.7	Keratin, type I cytoskeletal 15; Cytokeratin-15; CK-15; Keratin-15; K15;	427.19298
ENSMUSP00000032074	25.7	Probable N-acetyltransferase CML5 (EC 2.3.1.-)(Camello-like protein 5) Source: 2.3.1.- IPR016181 Acyl CoA acyltransferaseIPR000182 GCN5-rel AcTrfase	225.4386
ENSMUSP00000039784	17.1	39S ribosomal protein L23, mitochondrial (L23mt)(MRP-L23)(L23 mitochondrial-related protein) IPR012678 Ribosomal L23/L15e coreIPR013025 Ribosomal L25/23	150
ENSMUSP00000029387	64.4	Eukaryotic translation initiation factor 2A (eIF-2A) IPR011046 WD40 repeat-likeIPR011387 eIF2AIPR013979 eIF2A central-region	564.91228
ENSMUSP00000040580	37.8	Aldose 1-epimerase (EC 5.1.3.3)(Galactose mutarotase) Source: 5.1.3.3 IPR008183 Ald1 epimeraseIPR018052 Ald1 epimerase CSIPR011013 Glyco hydro-type carb-bd	331.57895
ENSMUSP00000073444	60	UDP-glucuronosyltransferase 1-7C Precursor (UDPGT)(UGT1*7C)(EC 2.4.1.17)(UGT1-07C)(UGT1.7C)(UGT1A7C)(UGT1A10) Source: 2.4.1.17 IPR002213 UDP glucos trans	526.31579
ENSMUSP00000059943	8.5	UPF0608 protein C19orf42 homolog Precursor	74.561404
ENSMUSP00000034860	58.1	Cytochrome P450 1A2 (EC 1.14.14.1)(CYPIA2)(P450-P2/P450-P3) Source: 1.14.14.1 IPR001128 Cyt P450IPR002397 Cyt P450 BIPR017973 Cyt P450 CIPR017972 Cyt P450 CSIPR002401 Cyt P450 E grp-IIPR002403 Cyt P450 E grp-IVIPR008066 Cyt P450 E grp-I CYP1IPR008067 Cyt P450 E grp-I CYP2A-likeIPR008071 Cyt P450 E grp-I CYP2J-like	509.64912
ENSMUSP00000089691	35.9	cis-retinol/3alpha hydroxysterol short-chain dehydrogenase-like IPR003560 DHB DHaseIPR002198 DHase sc/Rdtase SDRIPR002347 Glc/ribitol DHaseIPR002424 Insect AlcDHase famIPR016040 NAD(P)-bd	314.91228
ENSMUSP00000026462	36.1	Hydroxysteroid 17-beta dehydrogenase 6 Precursor (EC 1.1.1.62)(EC 1.1.1.63)(EC 1.1.1.105)(17-beta-HSD6)(17-beta-HSD9)(Oxidative 3-alpha hydroxysteroid dehydrogenase)(3-alpha->beta-hydroxysteroid epimerase)(3-alpha->beta-HSE) Source: 1.1.1.62 IPR003560 DHB DHaseIPR002198 DHase sc/Rdtase SDRIPR002347 Glc/ribitol DHaseIPR016040 NAD(P)-bd	316.66667
ENSMUSP00000074990	56.1	Cytochrome P450 2A12 (EC 1.14.14.1)(CYPIIA12)(Steroid hormones 7-alpha-hydroxylase)(Testosterone 7-alpha-hydroxylase) Source: 1.14.14.1 IPR001128 Cyt P450IPR017973 Cyt P450 CIPR017972 Cyt P450 CSIPR002401 Cyt P450 E grp-IIPR002403 Cyt P450 E grp-IVIPR008067 Cyt P450 E grp-I CYP2A-likeIPR008068 Cyt P450 E grp-I CYP2B-likeIPR008071 Cyt P450 E grp-I CYP2J-like	492.10526
ENSMUSP00000081370	58.3	Cytochrome P450 4A12A (EC 1.14.14.1)(CYPIVA12) Source: 1.14.14.1 IPR001128 Cyt P450IPR002397 Cyt P450 BIPR017973 Cyt P450 CIPR017972 Cyt P450 CSIPR002401 Cyt P450 E grp-IIPR002402 Cyt P450 E grp-IIIPR002403 Cyt P450 E grp-IV	511.40351
ENSMUSP00000003100	55.9	Cytochrome P450 2F2 (EC 1.14.14.-)(CYPIIF2)(Naphthalene dehydrogenase)(Naphthalene hydroxylase)(P450-NAH-2) Source: 1.14.14.- IPR001128 Cyt P450IPR002397 Cyt P450 BIPR017973 Cyt P450 CIPR017972 Cyt P450 CSIPR002401 Cyt P450 E grp-IIPR002403 Cyt P450 E grp-IVIPR008067 Cyt P450 E grp-I CYP2A-likeIPR008068 Cyt P450 E grp-I CYP2B-likeIPR008071 Cyt P450 E grp-I CYP2J-like	490.35088
ENSMUSP00000082352	35.1	Retinol dehydrogenase 11 (EC 1.1.1.-)(Retinal reductase 1)(RalR1)(Prostate short-chain dehydrogenase/reductase 1)(Androgen-regulated short-chain dehydrogenase/reductase 1)(Short-chain aldehyde dehydrogenase)(SCALD)(Cell line	307.89474

		MC/9.IL4-derived protein 1)(M42C60) Source: 1.1.1.- IPR003560 DHB DHaseIPR002198 DHase sc/Rdtase SDRIPR002347 Glc/ribitol DHaseIPR002424 Insect AlcDHase famIPR016040 NAD(P)-bd	
ENSMUSP00000029569	36	UDP-N-acetylglucosamine transporter (Golgi UDP-GlcNAc transporter)(Solute carrier family 35 member A3) IPR007271 Nuc sug transptIPR004689 UDPgal transpt	315.78947
sp|K1C10_HUMAN|	59.5	Keratin, type I cytoskeletal 10; Cytokeratin-10; CK-10; Keratin-10; K10;	521.92982
ENSMUSP00000065796	56.1	cytochrome P450, family 2, subfamily c, polypeptide 67 IPR001128 Cyt P450IPR002397 Cyt P450 BIPR017973 Cyt P450 CIPR017972 Cyt P450 CSIPR002401 Cyt P450 E grp-IIPR002403 Cyt P450 E grp-IVIPR008068 Cyt P450 E grp-I CYP2B-likeIPR008069 Cyt P450 E grp-I CYP2D-likeIPR008070 Cyt P450 E grp-I CYP2E-likeIPR008071 Cyt P450 E grp-I CYP2J-like	492.10526
ENSMUSP00000031195	61.1	UDP-glucuronosyltransferase 2A3 Precursor (UDPGT 2A3)(EC 2.4.1.17) Source: 2.4.1.17 IPR002213 UDP glucos trans	535.96491
ENSMUSP00000057732	35.7	retinol dehydrogenase 9 IPR003560 DHB DHaseIPR002198 DHase sc/Rdtase SDRIPR002347 Glc/ribitol DHaseIPR016040 NAD(P)-bd	313.15789
ENSMUSP00000034567	67.9	Dihydrolipoyllysine-residue acetyltransferase component of pyruvate dehydrogenase complex, mitochondrial Precursor (EC 2.3.1.12)(Dihydrolipoamide acetyltransferase component of pyruvate dehydrogenase complex)(PDC-E2)(E2) Source: 2.3.1.12 IPR003016 2-oxoA DHase lipoyl-BSIPR001078 2-oxoacid DHase actylTfraseIPR006257 AcTrfase Pyrv DHase cplx LIPR000089 Biotin lipoylIPR004167 E3 bdIPR000694 PRO richIPR011053 Single hybrid motifIPR001412 aa-tRNA-synth I CS	595.61404
ENSMUSP00000023832	33.4	Regucalcin (RC)(Senescence marker protein 30)(SMP-30) IPR008367 RegucalcinIPR013658 SGLIPR005511 SMP-30	292.98246
ENSMUSP00000026398	28	Methyltransferase-like protein 7B Precursor (EC 2.1.1.-) Source: 2.1.1.- IPR013216 Methyltransf 11IPR013217 Methyltransf 12	245.61404
ENSMUSP00000028807	46.3	Isovaleryl-CoA dehydrogenase, mitochondrial Precursor (IVD)(EC 1.3.99.10) Source: 1.3.99.10 IPR006091 Acyl-CoA DHase/Oxase MIPR013107 Acyl-CoA DHase 2 CIPR006089 Acyl-CoA DHase CSIPR006092 Acyl-CoA DHase NIPR006090 Acyl-CoA Oxase/DHase 1IPR009100 AcylCoA DH/oxidase M/N	406.14035
ENSMUSP00000045351	49.8	GPI-anchor transamidase Precursor (GPI transamidase)(EC 3.-.-.-)(Phosphatidylinositol-glycan biosynthesis class K protein)(PIG-K) Source: 3.-.-.- IPR001096 Peptidase C13	436.84211
ENSMUSP00000002840	104.5	Peroxisome assembly factor 2 (PAF-2)(Peroxisomal-type ATPase 1)(Peroxisomal biogenesis factor 6)(Peroxin-6) IPR003593 AAA+ ATPase coreIPR003960 AAA ATPase CSIPR003959 AAA ATPase core	916.66667
ENSMUSP00000047551	52.5	Epoxide hydrolase 1 (EC 3.3.2.9)(Microsomal epoxide hydrolase)(Epoxide hydratase) Source: 3.3.2.9 IPR000073 AB hydrolase 1IPR000639 Epox hydrolase-likeIPR010497 Epoxide hydro NIPR016292 Epoxide hydrolaseIPR002410 Peptidase S33	460.52632
ENSMUSP00000066958	67.5	Transmembrane 9 superfamily member 3 Precursor IPR004240 EMP70	592.10526
ENSMUSP00000030299	57.7	Cytochrome P450 2J5 (EC 1.14.14.1)(CYPIIJ5)(Arachidonic acid epoxygenase) Source: 1.14.14.1 IPR001128 Cyt P450IPR002397 Cyt P450 BIPR017973 Cyt P450 CIPR017972 Cyt P450 CSIPR002401 Cyt P450 E grp-IIPR002402 Cyt P450 E grp-IIIPR002403 Cyt P450 E grp-IVIPR008068 Cyt P450 E grp-I CYP2B-likeIPR008069 Cyt P450 E grp-I CYP2D-likeIPR008071 Cyt P450 E grp-I CYP2J-like	506.14035
ENSMUSP00000004381	56.1	Lysophosphatidylcholine acyltransferase 3 (EC 2.3.1.23)(Membrane-bound O-acyltransferase domain-containing protein 5)(O-acyltransferase domain-containing protein 5) Source: 2.3.1.23 IPR004299 MBOAT fam	492.10526
ENSMUSP00000027478	40.6	NADH dehydrogenase IPR002624 Deoxynucleoside kinaseIPR015828 NADH UbQ OxRdtase 42KD su	356.14035
ENSMUSP00000043061	33.1	3-mercaptopyruvate sulfurtransferase (MST)(EC 2.8.1.2) Source: 2.8.1.2 IPR001763 Rhodanese-likeIPR001307 Thiosulphate STrfase CS	290.35088
ENSMUSP00000042095	46.6	Serine protease inhibitor A3K Precursor (Serpin A3K)(Contrapsin)(SPI-2) IPR000295 Prot inh Lserp2IPR000215 Protease inhib I4 serpin	408.77193
ENSMUSP00000065425	36.8	Tartrate-resistant acid phosphatase type 5 Precursor (TR-AP)(EC 3.1.3.2)(Tartrate-resistant acid ATPase)(TrATPase)(Acid phosphatase 5, tartrate resistant) Source: 3.1.3.2 IPR004843 M-pesterase	322.80702
ENSMUSP00000061851	47.7	Adenosylhomocysteinase (AdoHcyase)(EC 3.3.1.1)(S-adenosyl-L-homocysteine hydrolase)(Liver copper-binding protein)(CUBP) Source: 3.3.1.1 IPR000043 Ad hcy hydrolaseIPR015878 Ado hCys hydrolase NAD-bd	418.42105
ENSMUSP00000001834	55.2	UPF0027 protein C22orf28 homolog IPR001233 UPF0027	484.21053

ENSMUSP00000032078	59.6	T-complex protein 1 subunit eta (TCP-1-eta)(CCT-eta) IPR012720 Chap CCT etaIPR017998 Chaperone TCP-1IPR002194 Chaperonin TCP-1 CSIPR001844 Chaprnin Cpn60IPR002423 Cpn60/TCP-1	522.80702
ENSMUSP00000035417	62.2	Pyruvate kinase isozymes R/L (EC 2.7.1.40)(L-PK) Source: 2.7.1.40 IPR001697 Pyr KnaseIPR015813 Pyrv/PenolPyrv Kinase catIPR018209 Pyrv Knase ASIPR015795 Pyrv Knase C-likeIPR015794 Pyrv Knase a/bIPR015793 Pyrv Knase brl	545.61404
ENSMUSP00000025279	142.8	Niemann-Pick C1 protein Precursor IPR004765 NP C typeIPR003392 PatchedIPR000731 SSD 5TM	1252.6316
ENSMUSP00000021370	50.9	L-2-hydroxyglutarate dehydrogenase, mitochondrial Precursor (Duranin)(EC 1.1.99.2) Source: 1.1.99.2 IPR006076 FAD-dep OxRdtaseIPR003042 Rng hydrolase	446.49123
ENSMUSP00000024963	16.2	Multiple coagulation factor deficiency protein 2 homolog Precursor (Neural stem cell-derived neuronal survival protein) IPR018247 EF HAND 1IPR018249 EF HAND 2	142.10526
ENSMUSP00000000394	71.5	Protein TBRG4 (Transforming growth factor beta regulator 4) IPR013579 FAST 2IPR010622 FAST Leu-richIPR013584 RAP	627.19298
ENSMUSP00000001183	58.9	Formimidoyltransferase-cyclodeaminase (Formiminotransferase-cyclodeaminase)(FTCD) Source: 2.1.2.5 IPR007044 Cyclodeamin/CycOHaseIPR004227 FormiminotransferaseIPR013802 Formiminotransferase CIPR012886 Formiminotransferase N	516.66667
ENSMUSP00000034624	46	solute carrier family 37 (glucose-6-phosphate transporter), member 4 IPR000849 GlpT transporterIPR011701 MFS 1IPR016196 MFS gen sb transpt	403.50877
ENSMUSP00000041442	41.9	3 beta-hydroxysteroid dehydrogenase type 5 (3 beta-hydroxysteroid dehydrogenase type V)(3-beta-HSD V)(NADPH-dependent 3-beta-hydroxy-Delta(5)-steroid dehydrogenase)(EC 1.1.1.-)(3-beta-hydroxy-5-ene steroid dehydrogenase)(Progesterone reductase) Source: 1.1.1.- IPR002225 3Beta OHSteriod DHase/EstaseIPR002198 DHase sc/Rdtase SDRIPR001509 Epimerase deHydtaseIPR013120 Male sterile NAD-bdIPR016040 NAD(P)-bdIPR003869 Polysac CapD	367.54386
ENSMUSP00000086530	56.9	Cytochrome P450 2D9 (EC 1.14.14.1)(CYPIID9)(P450-16-alpha)(CA)(Testosterone 16-alpha hydroxylase) Source: 1.14.14.1 IPR001128 Cyt P450IPR002397 Cyt P450 BIPR017973 Cyt P450 CIPR017972 Cyt P450 CSIPR002401 Cyt P450 E grp-IIPR002403 Cyt P450 E grp-IVIPR008069 Cyt P450 E grp-I CYP2D-likeIPR008071 Cyt P450 E grp-I CYP2J-like	499.12281
ENSMUSP00000051293	75.2	Cleft lip and palate transmembrane protein 1 homolog (Thymic epithelial cell surface antigen) IPR008429 CLPTM1	659.64912
ENSMUSP00000086528	56.8	Cytochrome P450 2D11 (EC 1.14.14.1)(CYPIID11)(P450-16-alpha)(CC)(Testosterone 16-alpha hydroxylase) Source: 1.14.14.1 IPR001128 Cyt P450IPR002397 Cyt P450 BIPR017973 Cyt P450 CIPR017972 Cyt P450 CSIPR002401 Cyt P450 E grp-IIPR002403 Cyt P450 E grp-IVIPR008069 Cyt P450 E grp-I CYP2D-likeIPR008071 Cyt P450 E grp-I CYP2J-like	498.24561
ENSMUSP00000022976	134	Strumpellin IPR001756 ATPase P-typ Cu-transptrIPR014756 Ig E-set	1175.4386
ENSMUSP00000051621	14.7	Membrane magnesium transporter 1 Precursor (Transmembrane protein 32)	128.94737
sp|K1C9_HUMAN|	62.1	Keratin, type I cytoskeletal 9; Cytokeratin-9; CK-9; Keratin-9; K9;	544.73684
ENSMUSP00000101999	42.4	Phosphoribosyl pyrophosphate synthetase-associated protein 1 (PRPP synthetase-associated protein 1)(39 kDa phosphoribosypyrophosphate synthetase-associated protein)(PAP39) IPR005946 PRPP kinaseIPR000836 PRibTrfase	371.92982
ENSMUSP00000034414	35	Ester hydrolase C11orf54 homolog (EC 3.1.-.-) Source: 3.1.-.- IPR015021 DUF1907	307.01754
ENSMUSP00000051441	51.7	Transmembrane protein 195	453.50877
ENSMUSP00000029240	56.9	Solute carrier family 2, facilitated glucose transporter member 2 (Glucose transporter type 2, liver)(GLUT-2) IPR002440 Glc transpt 2IPR011701 MFS 1IPR016196 MFS gen sb transptIPR005828 Sub transporterIPR003663 Sugar/inositol transptIPR005829 Sugar transporter CS	499.12281
ENSMUSP00000034623	24.4	Trafficking protein particle complex subunit 4 (Synbindin)(TRS23 homolog) IPR011012 Longin likeIPR007233 Sybindin	214.03509
ENSMUSP00000111510	60.4	Nuclear protein NP60 IPR006183 6-phosphogluconate DHaseIPR006115 6PGDH NAD-bdIPR017956 AT hook DNA-bd CSIPR016040 NAD(P)-bdIPR004455 NADP OxRdtase F420IPR000313 PWWPIPR006151 Shikm DHase/Glu-tRNA Rdtase	529.82456
sp|K2C1_HUMAN|	65.8	Keratin, type II cytoskeletal 1; Cytokeratin-1; CK-1; Keratin-1; K1; 67 kDa cytokeratin; Hair alpha protein;	577.19298

ENSMUSP00000086418	60.4	T-complex protein 1 subunit alpha B (TCP-1-alpha)(CCT-alpha)(Tailless complex polypeptide 1B)(TCP-1-B) IPR012715 Chap CCT alphaIPR017998 Chaperone TCP-1IPR002194 Chaperonin TCP-1 CSIPR001844 Chaprnin Cpn60IPR002423 Cpn60/TCP-1	529.82456
ENSMUSP00000025713	46.5	Delta(14)-sterol reductase (Delta-14-SR)(EC 1.3.1.70)(C-14 sterol reductase)(Sterol C14-reductase)(Transmembrane 7 superfamily member 2) Source: 1.3.1.70 IPR001171 ERG4 ERG24IPR018083 Sterol reductase CS	407.89474
ENSMUSP00000017946	51.6	Protein FAM134C	452.63158
ENSMUSP00000051700	80.7	Fatty-acid amide hydrolase 1 (EC 3.1.-.-)(Oleamide hydrolase 1)(Anandamide amidohydrolase 1) Source: 3.1.-.- IPR000120 Amidase sig enzIPR006206 Mev galkinaseIPR003979 Tropoelastin	707.89474
ENSMUSP00000034848	29.5	Proteasome subunit alpha type-4 (EC 3.4.25.1)(Proteasome component C9)(Macropain subunit C9)(Multicatalytic endopeptidase complex subunit C9)(Proteasome subunit L) Source: 3.4.25.1 IPR001353 Proteasome A B suIPR000426 Proteasome alpha CSIPR016050 Proteasome bsu CS	258.77193
ENSMUSP00000047790	23.6	Glutathione S-transferase P 1 (Gst P1)(EC 2.5.1.18)(GST YF-YF)(GST-piB)(GST class-pi)(Preadipocyte growth factor) Source: 2.5.1.18 IPR004046 GST CIPR003080 GST alphaIPR003082 GST piIPR010987 Glutathione-S-Trfase C-likeIPR004045 Glutathione S-Trfase NIPR012336 Thioredoxin-like fold	207.01754
ENSMUSP00000097860	184.1	ATP-binding cassette sub-family A member 8-A IPR003593 AAA+ ATPase coreIPR003439 ABC transporter-likeIPR017871 ABC transporter CS	1614.9123
ENSMUSP00000034172	61.7	Carboxylesterase 3 Precursor (EC 3.1.1.1)(EC 3.1.1.67)(Triacylglycerol hydrolase)(TGH)(Fatty acid ethyl ester synthase)(FAEE synthase) Source: 3.1.1.1 IPR002018 CarbesteraseBIPR000997 Cholinesterase	541.22807
ENSMUSP00000041244	23.4	28S ribosomal protein S26, mitochondrial Precursor (S26mt)(MRP-S26)	205.26316
ENSMUSP00000040424	74.5	Probable urocanate hydratase (Urocanase)(EC 4.2.1.49)(Imidazolonepropionate hydrolase) Source: 4.2.1.49 IPR000193 Urocanase	653.50877
ENSMUSP00000005923	29.1	Proteasome subunit beta type-4 Precursor (Proteasome beta chain)(EC 3.4.25.1)(Macropain beta chain)(Multicatalytic endopeptidase complex beta chain)(Proteasome chain 3) Source: 3.4.25.1 IPR001353 Proteasome A B suIPR016050 Proteasome bsu CSIPR016295 Proteasome endopept cplx B	255.26316
ENSMUSP00000031181	60.8	UDP glucuronosyltransferase 2 family, polypeptide B34 IPR002213 UDP glucos trans	533.33333
ENSMUSP00000027464	37.5	39S ribosomal protein L44, mitochondrial Precursor (L44mt)(EC 3.1.26.-)(MRP-L44) Source: 3.1.26.- IPR001159 Ds-RNA bdIPR000999 RNase III	328.94737
ENSMUSP00000003843	73.2	Mannosyl-oligosaccharide 1,2-alpha-mannosidase IA (EC 3.2.1.113)(Processing alpha-1,2-mannosidase IA)(Alpha-1,2-mannosidase IA)(Mannosidase alpha class 1A member 1)(Man(9)-alpha-mannosidase)(Man9-mannosidase) Source: 3.2.1.113 IPR001382 Glyco hydro 47	642.10526
ENSMUSP00000104806	116.3	Probable phospholipid-transporting ATPase IIA (EC 3.6.3.1)(ATPase class II type 9A) Source: 3.6.3.1 IPR001757 ATPase PIPR006539 ATPase P-typ Plipid-transIIPR006069 ATPase P-typ cation-exchng asuIPR018303 ATPase P-typ phosphor siteIPR005834 Dehalogen-like hydro	1020.1754
ENSMUSP00000107118	22.4	Proteasome subunit beta type-5 Precursor (EC 3.4.25.1)(Proteasome epsilon chain)(Macropain epsilon chain)(Multicatalytic endopeptidase complex epsilon chain)(Proteasome subunit X)(Proteasome chain 6) Source: 3.4.25.1 IPR000243 Pept T1A subBIPR001353 Proteasome A B suIPR016050 Proteasome bsu CS	196.49123
ENSMUSP00000076578	55.8	cytochrome P450, family 2, subfamily b, polypeptide 23 IPR001128 Cyt P450IPR002397 Cyt P450 BIPR017973 Cyt P450 CIPR017972 Cyt P450 CSIPR002401 Cyt P450 E grp-IIPR002403 Cyt P450 E grp-IVIPR008067 Cyt P450 E grp-I CYP2A-likeIPR008068 Cyt P450 E grp-I CYP2B-likeIPR008071 Cyt P450 E grp-I CYP2J-like	489.47368
ENSMUSP00000023083	56.4	cytochrome P450, family 2, subfamily d, polypeptide 22 IPR001128 Cyt P450IPR002397 Cyt P450 BIPR017973 Cyt P450 CIPR017972 Cyt P450 CSIPR002401 Cyt P450 E grp-IIPR002403 Cyt P450 E grp-IVIPR008066 Cyt P450 E grp-I CYP1IPR008069 Cyt P450 E grp-I CYP2D-likeIPR008071 Cyt P450 E grp-I CYP2J-like	494.73684
ENSMUSP00000026208	173.6	Canalicular multispecific organic anion transporter 1 (ATP-binding cassette sub-family C member 2) IPR003593 AAA+ ATPase coreIPR011527 ABC TM 1IPR001140 ABC TM transptIPR003439 ABC transporter-likeIPR017940 ABC transporter type1IPR005292 Multidrug-R assoc MRP	1522.807
ENSMUSP00000034178	61.6	hypothetical protein LOC234564 IPR002018 CarbesteraseB	540.35088
ENSMUSP00000025356	19.1	Protein MAL2 IPR013295 MALIPR008253 Marvel	167.54386

ENSMUSP00000014913	26.4	Proteasome subunit beta type-1 Precursor (EC 3.4.25.1)(Proteasome component C5)(Macropain subunit C5)(Multicatalytic endopeptidase complex subunit C5)(Proteasome gamma chain) Source: 3.4.25.1 IPR001353 Proteasome A B suIPR016050 Proteasome bsu CS	231.57895
ENSMUSP00000025196	30.2	Proteasome subunit beta type-8 Precursor (EC 3.4.25.1)(Proteasome subunit beta-5i)(Proteasome component C13)(Macropain subunit C13)(Multicatalytic endopeptidase complex subunit C13) Source: 3.4.25.1 IPR000243 Pept T1A subBIPR001353 Proteasome A B suIPR016050 Proteasome bsu CS	264.91228
ENSMUSP00000084445	16.9	OCIA domain-containing protein 2 IPR009764 OCIA	148.24561
ENSMUSP00000080996	25.1	ATP synthase subunit a (F-ATPase protein 6) IPR000568 ATPase F0-cplx asu	220.17544
ENSMUSP00000072555	57.2	Cytochrome P450 2D10 (EC 1.14.14.1)(CYPIID10)(P450-16-alpha)(P450CB)(Testosterone 16-alpha hydroxylase) Source: 1.14.14.1 IPR001128 Cyt P450IPR002397 Cyt P450 BIPR017973 Cyt P450 CIPR017972 Cyt P450 CSIPR002401 Cyt P450 E grp-IIPR002403 Cyt P450 E grp-IVIPR008069 Cyt P450 E grp-I CYP2D-likeIPR008071 Cyt P450 E grp-I CYP2J-like	501.75439
ENSMUSP00000109355	64	RNA-binding protein 47 (RNA-binding motif protein 47) IPR006535 HnRNP R QIPR003954 RRM 1IPR000504 RRM RNP1	561.40351
ENSMUSP00000028657	40.1	Sorbitol dehydrogenase (EC 1.1.1.14)(L-iditol 2-dehydrogenase) Source: 1.1.1.14 IPR013154 AlcDHase GroES-likeIPR013149 AlcDHase Zn-bdIPR002328 AlcDHase Zn CSIPR013027 FAD pyr nucl-diS OxRdtaseIPR011032 GroES likeIPR000103 Pyridine nuc-diS OxRdtase 2	351.75439
ENSMUSP00000031251	32.9	Estradiol 17-beta-dehydrogenase 11 Precursor (EC 1.1.1.62)(17-beta-hydroxysteroid dehydrogenase 11)(17-beta-HSD 11)(17betaHSD11)(17bHSD11)(17-beta-HSD XI)(17betaHSDXI)(Dehydrogenase/reductase SDR family member 8) Source: 1.1.1.62 IPR003560 DHB DHaseIPR002198 DHase sc/Rdtase SDRIPR002347 Glc/ribitol DHaseIPR002424 Insect AlcDHase famIPR016040 NAD(P)-bd	288.59649
ENSMUSP00000022148	61.3	Methylcrotonoyl-CoA carboxylase beta chain, mitochondrial Precursor (MCCase subunit beta)(EC 6.4.1.4)(3-methylcrotonyl-CoA:carbon dioxide ligase subunit beta)(3-methylcrotonyl-CoA carboxylase non-biotin-containing subunit)(3-methylcrotonyl-CoA carboxylase 2) Source: 6.4.1.4 IPR011763 COA CT CIPR011762 COA CT NIPR000022 Carboxyl trans	537.7193
ENSMUSP00000073061	21.7	Membrane-associated progesterone receptor component 1 IPR001199 Cyt B5IPR000417 Hyethyz kinase	190.35088
ENSMUSP00000037022	74.3	Solute carrier organic anion transporter family member 1A1 (Solute carrier family 21 member 1)(Sodium-independent organic anion-transporting polypeptide 1)(OATP1) IPR011701 MFS 1IPR016196 MFS gen sb transptIPR004156 OA transporterIPR011497 Prot Inh Kazal 2	651.75439
ENSMUSP00000075235	65.6	APOBEC1 complementation factor (APOBEC1-stimulating protein) IPR001159 Ds-RNA bdIPR006535 HnRNP R QIPR003954 RRM 1IPR000504 RRM RNP1	575.4386
ENSMUSP00000055206	80.3	Putative uncharacterized protein Fragment Source: UniProtKB/TrEMBL Q8BNL1	704.38596
ENSMUSP00000112236	35.5	2-oxoisovalerate dehydrogenase subunit beta, mitochondrial Precursor (EC 1.2.4.4)(Branched-chain alpha-keto acid dehydrogenase E1 component beta chain)(BCKDH E1-beta) Source: 1.2.4.4 IPR005476 Transketo CIPR005475 Transketo Cen R	311.40351
ENSMUSP00000032422	45.7	Cysteine-rich with EGF-like domain protein 1 Precursor IPR006210 EGFIPR000152 EGF-type Asp/Asn hydroxyl CSIPR000742 EGF 3IPR001881 EGF Ca bdIPR013091 EGF Ca bd 2IPR018097 EGF Ca bd CSIPR002049 EGF lamininIPR013032 EGF like reg CSIPR006212 Furin repeatIPR009030 Growth fac rcpt	400.87719
ENSMUSP00000037259	59.9	Dimethylaniline monooxygenase Source: 1.14.13.8 IPR000759 Adrndx reductaseIPR013027 FAD pyr nucl-diS OxRdtaseIPR000960 Flavin mOaseIPR002253 Flavin mOase 1IPR002254 Flavin mOase 2IPR002255 Flavin mOase 3IPR002257 Flavin mOase 5IPR002345 LipocalinIPR012143 dManiline mOase	525.4386
ENSMUSP00000056152	39.7	Ornithine carbamoyltransferase, mitochondrial Precursor (EC 2.1.3.3)(Ornithine transcarbamylase)(OTCase) Source: 2.1.3.3 IPR006130 Asp/Orn carbamoylTrfaseIPR006132 Asp/Orn carbamoyltranf P bdIPR006131 Asp carbamoyltransf Asp/Orn bdIPR002082 Aspartate carbamoyltransf eukIPR002292 Orn carbamltrans	348.24561
ENSMUSP00000076735	35.9	retinol dehydrogenase similar protein 2 IPR003560 DHB DHaseIPR002198 DHase sc/Rdtase SDRIPR002347 Glc/ribitol DHaseIPR002424 Insect AlcDHase famIPR016040 NAD(P)-bd	314.91228
ENSMUSP00000028083	29.9	Proteasome subunit beta type-7 Precursor (EC 3.4.25.1)(Proteasome subunit Z)(Macropain chain Z)(Multicatalytic endopeptidase complex chain Z) Source: 3.4.25.1 IPR000243 Pept T1A subBIPR001353 Proteasome A B suIPR016050	262.2807

		Proteasome bsu CS	
ENSMUSP00000022341	28.1	UPF0568 protein C14orf166 homolog	246.49123
ENSMUSP00000003137	55.7	Cytochrome P450 2C29 (EC 1.14.14.1)(CYPIIC29)(P-450 MUT-2)(Aldehyde oxygenase) Source: 1.14.14.1 IPR001128 Cyt P450IPR017973 Cyt P450 CIPR017972 Cyt P450 CSIPR002401 Cyt P450 E grp-IIPR002403 Cyt P450 E grp-IVIPR008067 Cyt P450 E grp-I CYP2A-likeIPR008068 Cyt P450 E grp-I CYP2B-likeIPR008069 Cyt P450 E grp-I CYP2D-likeIPR008070 Cyt P450 E grp-I CYP2E-likeIPR008071 Cyt P450 E grp-I CYP2J-like	488.59649
ENSMUSP00000046585	76.2	Long-chain-fatty-acid--CoA ligase 5 (EC 6.2.1.3)(Long-chain acyl-CoA synthetase 5)(LACS 5) Source: 6.2.1.3 IPR000873 AMP-dep Synth/Lig	668.42105
ENSMUSP00000002663	39.5	Serum paraoxonase/arylesterase 1 (PON 1)(EC 3.1.1.2)(EC 3.1.8.1)(Serum aryldialkylphosphatase 1)(A-esterase 1)(Aromatic esterase 1) Source: 3.1.1.2 IPR002640 ArylesteraseIPR008363 Paraoxonase1IPR008364 Paraoxonase2IPR013658 SGL	346.49123
ENSMUSP00000108763	60.5	UDP-glucuronosyltransferase 1-7C Precursor (UDPGT)(UGT1*7C)(EC 2.4.1.17)(UGT1-07C)(UGT1.7C)(UGT1A7C)(UGT1A10) Source: 2.4.1.17 IPR002213 UDP glucos trans	530.70175
ENSMUSP00000084959	35	Putative deoxyribose-phosphate aldolase (EC 4.1.2.4)(Phosphodeoxyriboaldolase)(Deoxyriboaldolase)(DERA) Source: 4.1.2.4 IPR011343 DeoCIPR002915 DeoC/AroFGH archIPR002953 Filo VP35	307.01754
ENSMUSP00000030051	11.7	Thioredoxin (Trx)(ATL-derived factor)(ADF) IPR012336 Thioredoxin-like foldIPR006662 Thioredoxin-like subdomIPR017937 Thioredoxin CSIPR013766 Thioredoxin dom	102.63158
ENSMUSP00000010049	35.9	3-ketodihydrosphingosine reductase Precursor (KDS reductase)(EC 1.1.1.102)(3-dehydrosphinganine reductase)(Follicular variant translocation protein 1 homolog)(FVT-1) Source: 1.1.1.102 IPR003560 DHB DHaseIPR002198 DHase sc/Rdtase SDRIPR002347 Glc/ribitol DHaseIPR016040 NAD(P)-bdIPR013968 Polyketide synth KR	314.91228
ENSMUSP00000008801	61.2	cytochrome P450, family 4, subfamily f, polypeptide 15 IPR001128 Cyt P450IPR002397 Cyt P450 BIPR017973 Cyt P450 CIPR017972 Cyt P450 CSIPR002401 Cyt P450 E grp-IIPR002402 Cyt P450 E grp-IIIPR002403 Cyt P450 E grp-IV	536.84211
ENSMUSP00000036245	41.1	3 beta-hydroxysteroid dehydrogenase type 7 (3 beta-hydroxysteroid dehydrogenase type VII)(3-beta-HSD VII)(3-beta-hydroxy-Delta(5)-C27 steroid oxidoreductase)(EC 1.1.1.-)(C(27) 3-beta-HSD) Source: 1.1.1.- IPR002225 3Beta OHSteriod DHase/EstaseIPR002198 DHase sc/Rdtase SDRIPR001509 Epimerase deHydtaseIPR013120 Male sterile NAD-bdIPR016040 NAD(P)-bdIPR013968 Polyketide synth KRIPR003869 Polysac CapD	360.52632
ENSMUSP00000031183	60.1	UDP glucuronosyltransferase 2 family, polypeptide B1 IPR002213 UDP glucos trans	527.19298
ENSMUSP00000039543	31.1	Syntaxin-16 IPR006012 Syntaxin/epimorphin CSIPR006011 Syntaxin NIPR000727 T SNAREIPR010989 t-SNARE	272.80702
ENSMUSP00000031822	73	ATP-binding cassette sub-family G member 2 (Breast cancer resistance protein 1 homolog)(CD338 antigen) IPR003593 AAA+ ATPase coreIPR013525 ABC 2 transIPR003439 ABC transporter-likeIPR002091 ArAA permease	640.35088
ENSMUSP00000079065	55.7	Cytochrome P450 2C50 (EC 1.14.14.1)(CYPIIC50) Source: 1.14.14.1 IPR001128 Cyt P450IPR002397 Cyt P450 BIPR017973 Cyt P450 CIPR017972 Cyt P450 CSIPR002401 Cyt P450 E grp-IIPR002403 Cyt P450 E grp-IVIPR008067 Cyt P450 E grp-I CYP2A-likeIPR008068 Cyt P450 E grp-I CYP2B-likeIPR008069 Cyt P450 E grp-I CYP2D-likeIPR008070 Cyt P450 E grp-I CYP2E-likeIPR008071 Cyt P450 E grp-I CYP2J-like	488.59649
ENSMUSP00000042188	94.4	Two pore calcium channel protein 1 (Voltage-dependent calcium channel protein TPC1) IPR005821 Ion transIPR001220 Lectin legB	828.07018
ENSMUSP00000053877	127.8	Constitutive coactivator of PPAR-gamma-like protein 1 (Oxidative stress-associated Src activator)(Protein FAM120A) IPR006030 Mollsc rhodpsn CIPR000694 PRO rich	1121.0526
ENSMUSP00000025602	41.5	Guanine nucleotide-binding protein subunit alpha-14 (G-protein subunit alpha-14)(G alpha-14) IPR002975 Fungi GproteinAIPR001019 Gprotein alph bdIPR000469 Gprotein alpha12IPR001408 Gprotein alpha IIPR000654 Gprotein alpha Q	364.03509
ENSMUSP00000032399	21.5	GTPase KRas Precursor (K-Ras 2)(Ki-Ras)(c-K-ras)(c-Ki-ras) IPR006689 ARF/SARIPR003579 GTPase RabIPR003577 GTPase RasIPR003578 GTPase RhoIPR013684 Miro-likeIPR002041 Ran GTPaseIPR013753 RasIPR001806 Ras GTPaseIPR005225 Small GTP bd	188.59649
ENSMUSP00000039663	97.2	Dimethylglycine dehydrogenase, mitochondrial Precursor (EC 1.5.99.2)(ME2GLYDH) Source: 1.5.99.2 IPR006076 FAD-dep OxRdtaseIPR013027 FAD pyr nucl-diS OxRdtaseIPR013977 GCV T CIPR006222 GCV T N	852.63158

ENSMUSP00000000349	53.2	Lipoamide acyltransferase component of branched-chain alpha-keto acid dehydrogenase complex, mitochondrial Precursor (EC 2.3.1.168)(Dihydrolipoyllysine-residue (2-methylpropanoyl)transferase)(Dihydrolipoamide branched chain transacylase)(BCKAD E2 subunit)(E2) Source: 2.3.1.168 IPR003016 2-oxoA DHase lipoyl-BSIPR001078 2-oxoacid DHase actylTfraseIPR000089 Biotin lipoylIPR004167 E3 bdIPR000694 PRO richIPR011053 Single hybrid motif	466.66667
ENSMUSP00000085244	139.8	Tripeptidyl-peptidase 2 (EC 3.4.14.10)(Tripeptidyl-peptidase II)(TPP-II)(Tripeptidyl aminopeptidase) Source: 3.4.14.10 IPR003006 Ig/MHC CSIPR000209 Pept S8 S53	1226.3158
ENSMUSP00000099848:reversed	111.5		978.07018
ENSMUSP00000022317	24.4	Uncharacterized protein C10orf58 homolog Precursor IPR012336 Thioredoxin-like fold	214.03509
ENSMUSP00000073939	25	Probable N-acetyltransferase CML1 (EC 2.3.1.-)(Camello-like protein 1) Source: 2.3.1.- IPR016181 Acyl CoA acyltransferaseIPR000182 GCN5-rel AcTrfase	219.29825
ENSMUSP00000099770	146.7	Bile salt export pump (ATP-binding cassette sub-family B member 11)(Sister of P-glycoprotein) IPR003593 AAA+ ATPase coreIPR011527 ABC TM 1IPR001140 ABC TM transptIPR003439 ABC transporter-likeIPR017871 ABC transporter CSIPR017940 ABC transporter type1IPR017970 Homeobox CS	1286.8421
ENSMUSP00000103436	169.1	Canalicular multispecific organic anion transporter 2 (ATP-binding cassette sub-family C member 3)(Multidrug resistance-associated protein 3) IPR003593 AAA+ ATPase coreIPR011527 ABC TM 1IPR001140 ABC TM transptIPR003439 ABC transporter-likeIPR017871 ABC transporter CSIPR017940 ABC transporter type1IPR005292 Multidrug-R assoc MRP	1483.3333
ENSMUSP00000048832	21.2	Transmembrane protein 205	185.96491
ENSMUSP00000092966	60.9	Cytochrome P450 4V3 (EC 1.14.-.-) Source: 1.14.-.- IPR001128 Cyt P450IPR017973 Cyt P450 CIPR017972 Cyt P450 CSIPR002401 Cyt P450 E grp-IIPR002402 Cyt P450 E grp-IIIPR002403 Cyt P450 E grp-IV	534.21053
ENSMUSP00000105754	35.2	Solute carrier family 25 member 42 IPR002113 Aden trnslctorIPR014762 DNA mismatch repair CSIPR002167 Graves DCIPR002067 Mit carrierIPR001993 Mitoch carrierIPR018108 Mitochondrial sb/sol carrierIPR003842 VacA	308.77193
ENSMUSP00000033074	17.8	Vitamin K epoxide reductase complex subunit 1 (EC 1.1.4.1)(Vitamin K1 2,3-epoxide reductase subunit 1) Source: 1.1.4.1 IPR012932 VKOR	156.14035
ENSMUSP00000109150	98.6	10-formyltetrahydrofolate dehydrogenase (EC 1.5.1.6) (10-FTHFDH) (Aldehyde dehydrogenase family 1 member L1). Source: Uniprot/SWISSPROT Q8R0Y6	864.91228
ENSMUSP00000101096	41.3	Apoptosis-inducing factor 2 (EC 1.-.-.-)(Apoptosis-inducing factor-like mitochondrion-associated inducer of death)(Apoptosis-inducing factor homologous mitochondrion-associated inducer of death) Source: 1.-.-.- IPR000759 Adrndx reductaseIPR013027 FAD pyr nucl-diS OxRdtaseIPR001327 Pyr OxRdtase NAD bdIPR000103 Pyridine nuc-diS OxRdtase 2IPR003042 Rng hydrolase	362.2807
ENSMUSP00000002844	33.3	39S ribosomal protein L2, mitochondrial Precursor (L2mt)(MRP-L2) IPR016027 NA-bd OB-fold-likeIPR002171 Ribosomal L2IPR008991 Translation prot SH3-like	292.10526
ENSMUSP00000017365	60.7	26S proteasome non-ATPase regulatory subunit 3 (26S proteasome regulatory subunit S3)(Proteasome subunit p58)(Transplantation antigen P91A)(Tum-P91A antigen) IPR013586 26S Psome reg CIPR013143 PAMIPR000717 PCI	532.45614
sp|K22E_HUMAN|	65.8	Keratin, type II cytoskeletal 2 epidermal; Cytokeratin-2e; CK 2e; K2e; keratin-2;	577.19298
ENSMUSP00000007977	84.7	Aldehyde dehydrogenase family 16 member A1 IPR011408 ADH duplIPR016161 Ald DHase/Histidinol DHaseIPR015590 Aldehyde DHase	742.98246
ENSMUSP00000088246	42	3 beta-hydroxysteroid dehydrogenase/Delta 5-->4-isomerase type 3 (3-beta-HSD III) Source: 1.1.1.145 IPR002225 3Beta OHSteriod DHase/EstaseIPR001509 Epimerase deHydtaseIPR013120 Male sterile NAD-bdIPR016040 NAD(P)-bdIPR003869 Polysac CapD	368.42105
ENSMUSP00000097395	21.9	Peroxiredoxin-5, mitochondrial Precursor (EC 1.11.1.15)(Prx-V)(Peroxisomal antioxidant enzyme)(PLP)(Thioredoxin reductase)(Thioredoxin peroxidase PMP20)(Antioxidant enzyme B166)(AOEB166)(Liver tissue 2D-page spot 2D-0014IV) Source: 1.11.1.15 IPR000866 Alkyl hydroperoxide RdtaseIPR013740 RedoxinIPR012336 Thioredoxin-like fold	192.10526
ENSMUSP00000023519	49.9	Homogentisate 1,2-dioxygenase (EC 1.13.11.5)(Homogentisic acid oxidase)(Homogentisate oxygenase)(Homogentisicase) Source: 1.13.11.5 IPR011051 Cupin RmlC typeIPR005708 Homogentis dOase	437.7193
ENSMUSP00000102665	60	Dimethylaniline monooxygenase Source: 1.14.13.8 IPR000759 Adrndx reductaseIPR013027 FAD pyr nucl-diS OxRdtaseIPR000960 Flavin mOaseIPR002253 Flavin mOase 1IPR002254 Flavin mOase 2IPR002255 Flavin mOase 3IPR002257 Flavin mOase 5IPR012143 dManiline mOase	526.31579

ENSMUSP00000075089	123.9	Regulator of nonsense transcripts 1 (EC 3.6.1.-)(ATP-dependent helicase RENT1)(Nonsense mRNA reducing factor 1)(NORF1)(Up-frameshift suppressor 1 homolog)(mUpf1) Source: 3.6.1.- IPR003593 AAA+ ATPase coreIPR014001 DEAD-like NIPR006935 Restrct endonuc I R/III Res	1086.8421
ENSMUSP00000025804	22.2	Ras-related protein Rab-1B IPR006688 ARFIPR006689 ARF/SARIPR003579 GTPase RabIPR003577 GTPase RasIPR003578 GTPase RhoIPR013684 Miro-likeIPR002078 RNA pol sigma 54 intIPR002041 Ran GTPaseIPR013753 RasIPR001806 Ras GTPaseIPR005225 Small GTP bd	194.73684
ENSMUSP00000056643	23.3	Membrane-associated progesterone receptor component 2 IPR001199 Cyt B5	204.38596
ENSMUSP00000072803	60	UDP-glucuronosyltransferase 1-7C Precursor (UDPGT)(UGT1*7C)(EC 2.4.1.17)(UGT1-07C)(UGT1.7C)(UGT1A7C)(UGT1A10) Source: 2.4.1.17 IPR002213 UDP glucos trans	526.31579
ENSMUSP00000052872	272.3	Fatty acid synthase (EC 2.3.1.85) Source: 2.3.1.85 IPR009081 ACP likeIPR016035 Acyl Trfase/lysoPlipaseIPR014043 Acyl transferaseIPR013149 AlcDHase Zn-bdIPR002198 DHase sc/Rdtase SDRIPR018201 Ketoacyl synth ASIPR014031 Ketoacyl synth CIPR014030 Ketoacyl synth NIPR013217 Methyltransf 12IPR016040 NAD(P)-bdIPR006163 Phsphopanteth bdIPR013968 Polyketide synth KRIPR006162 Ppantne SIPR001031 ThioesteraseIPR016039 Thiolase-like	2388.5965
ENSMUSP00000093390	34.8	hypothetical protein LOC328099 IPR005946 PRPP kinaseIPR000842 PRib-PP synthetase CSIPR000836 PRibTrfase	305.26316
ENSMUSP00000037487	58.4	Cytochrome P450 7B1 (EC 1.14.13.100)(25-hydroxycholesterol 7-alpha-hydroxylase)(Oxysterol 7-alpha-hydroxylase)(HCT-1) Source: 1.14.13.100 IPR001128 Cyt P450IPR017973 Cyt P450 CIPR002401 Cyt P450 E grp-IIPR002403 Cyt P450 E grp-IV	512.2807
ENSMUSP00000045362	55.6	Cytochrome P450 2C37 (EC 1.14.14.1)(CYPIIC37) Source: 1.14.14.1 IPR001128 Cyt P450IPR002397 Cyt P450 BIPR017973 Cyt P450 CIPR017972 Cyt P450 CSIPR002401 Cyt P450 E grp-IIPR002403 Cyt P450 E grp-IVIPR008067 Cyt P450 E grp-I CYP2A-likeIPR008068 Cyt P450 E grp-I CYP2B-likeIPR008069 Cyt P450 E grp-I CYP2D-likeIPR008070 Cyt P450 E grp-I CYP2E-likeIPR008071 Cyt P450 E grp-I CYP2J-like	487.7193
ENSMUSP00000031492	23	Ras-related protein Rab-35 IPR003593 AAA+ ATPase coreIPR006688 ARFIPR003579 GTPase RabIPR003577 GTPase RasIPR003578 GTPase RhoIPR001019 Gprotein alph bdIPR013684 Miro-likeIPR002078 RNA pol sigma 54 intIPR002041 Ran GTPaseIPR013753 RasIPR001806 Ras GTPaseIPR005225 Small GTP bd	201.75439
ENSMUSP00000046497	61.4	Putative uncharacterized protein Source: UniProtKB/TrEMBL Q8BZP6 IPR006091 Acyl-CoA DHase/Oxase MIPR013107 Acyl-CoA DHase 2 CIPR006090 Acyl-CoA Oxase/DHase 1IPR009100 AcylCoA DH/oxidase M/N	538.59649
ENSMUSP00000048096	144.2	Isoleucyl-tRNA synthetase, cytoplasmic (EC 6.1.1.5)(Isoleucine--tRNA ligase)(IleRS)(IRS) Source: 6.1.1.5 IPR002301 Ile-tRNA-synt IaIPR015905 Ile-tRNA-synt Ia NIPR013155 V/L/I-tRNA-synth anticodon-bdIPR002303 Val-tRNA synth IaIPR015413 aa-tRNA-synt IIPR001412 aa-tRNA-synth I CSIPR002300 aa-tRNA-synth IaIPR009080 tRNAsynth 1a anticodon-bd	1264.9123
ENSMUSP00000004910	38.9	Translation initiation factor eIF-2B subunit beta (eIF-2B GDP-GTP exchange factor subunit beta) IPR000649 IF-2B related	341.22807
ENSMUSP00000045285	191.8	ATP-binding cassette sub-family A member 3 IPR003593 AAA+ ATPase coreIPR003439 ABC transporter-likeIPR017871 ABC transporter CS	1682.4561
ENSMUSP00000021412	27.4	Proteasome subunit alpha type-6 (EC 3.4.25.1)(Proteasome iota chain)(Macropain iota chain)(Multicatalytic endopeptidase complex iota chain) Source: 3.4.25.1 IPR001353 Proteasome A B suIPR000426 Proteasome alpha CS	240.35088
ENSMUSP00000032228	165.2	Murinoglobulin-1 Precursor (MuG1) IPR009048 A-macroglobulin rcpt-bdIPR002890 A2M NIPR011625 A2M N 2IPR011626 A2M compIPR001599 MacroglobInA2IPR008930 Terpenoid cyclase/PrenylTrfaseIPR010916 TonB box CS	1449.1228
ENSMUSP00000104358	33.2	Dehydrogenase/reductase SDR family member 7B (EC 1.1.-.-) Source: 1.1.-.- IPR003560 DHB DHaseIPR002198 DHase sc/Rdtase SDRIPR002347 Glc/ribitol DHaseIPR002424 Insect AlcDHase famIPR016040 NAD(P)-bdIPR013968 Polyketide synth KR	291.22807
ENSMUSP00000038763	79.9	Propionyl-CoA carboxylase alpha chain, mitochondrial Precursor (PCCase subunit alpha)(EC 6.4.1.3)(Propanoyl-CoA:carbon dioxide ligase subunit alpha) Source: 6.4.1.3 IPR011761 ATP-graspIPR013651 ATP-grasp RimK-typeIPR003135 ATP-grasp carboxylate-amineIPR001249 AcCoA biotinCCIPR011764 BCIPR001882 Biotin BSIPR005482 Biotin COase CIPR000089 Biotin lipoylIPR005483 CarbamoylP synth lsuIPR005479 CarbamoylP synth lsu ATP-bdIPR005481 CarbamoylP synth lsu NIPR008992 Enterotoxin bacIPR016185 PreATP-grasp-likeIPR011054 Rudment hybrid motifIPR011053 Single hybrid motif	700.87719

ENSMUSP00000033683	29.6	40S ribosomal protein S4, X isoform IPR005824 KOWIPR000876 Ribosomal S4eIPR013843 Ribosomal S4e NIPR018199 Ribosomal S4e N CSIPR013845 Ribosomal S4e centralIPR002942 S4 RNA bd	259.64912
ENSMUSP00000031186	60.4	UDP glucuronosyltransferase 2 family, polypeptide B35 IPR002213 UDP glucos trans	529.82456
ENSMUSP00000021273	12.7	Vesicle-associated membrane protein 2 (VAMP-2)(Synaptobrevin-2) IPR001388 SynaptobrevinIPR016444 Synaptobrevin met/fun	111.40351
ENSMUSP00000032419	48	N-acylneuraminate cytidylyltransferase (EC 2.7.7.43)(CMP-N-acetylneuraminic acid synthetase)(CMP-NeuNAc synthetase) Source: 2.7.7.43 IPR003329 Cytidylyl trans	421.05263
ENSMUSP00000016031	72.2	Histidine ammonia-lyase (Histidase)(EC 4.3.1.3) Source: 4.3.1.3 IPR005921 HutHIPR008948 L-Aspartase-likeIPR001106 Phe/His NH3-lyase	633.33333
ENSMUSP00000090727	23.6	Ras-related protein Rab-4B IPR006688 ARFIPR003579 GTPase RabIPR003577 GTPase RasIPR003578 GTPase RhoIPR013684 Miro-likeIPR002041 Ran GTPaseIPR013753 RasIPR001806 Ras GTPaseIPR005225 Small GTP bd	207.01754
ENSMUSP00000059404	34.9	Transcriptional activator protein Pur-alpha (Purine-rich single-stranded DNA-binding protein alpha) IPR006628 PUR DNA RNA bd	306.14035
ENSMUSP00000031377	54	Lysosome membrane protein 2 (Lysosome membrane protein II)(LIMP II)(Scavenger receptor class B member 2)(85 kDa lysosomal membrane sialoglycoprotein)(LGP85) IPR002159 CD36IPR005428 CD36 antigenIPR005429 LimpII	473.68421
ENSMUSP00000043424	87.3	Nephrocystin-3 IPR002575 APH transIPR006091 Acyl-CoA DHase/Oxase MIPR013107 Acyl-CoA DHase 2 CIPR006090 Acyl-CoA Oxase/DHase 1IPR009100 AcylCoA DH/oxidase M/NIPR011009 Kinase likeIPR008271 Ser thr pkin AS	765.78947
ENSMUSP00000044877	13.3	BET1 homolog (mBET1)(Golgi vesicular membrane-trafficking protein p18) IPR000727 T SNARE	116.66667
ENSMUSP00000048284	55.8	Cytochrome P450 2C54 (EC 1.14.14.1)(CYPIIC54) Source: 1.14.14.1 IPR001128 Cyt P450IPR002397 Cyt P450 BIPR017973 Cyt P450 CIPR017972 Cyt P450 CSIPR002401 Cyt P450 E grp-IIPR002403 Cyt P450 E grp-IVIPR008067 Cyt P450 E grp-I CYP2A-likeIPR008068 Cyt P450 E grp-I CYP2B-likeIPR008069 Cyt P450 E grp-I CYP2D-likeIPR008070 Cyt P450 E grp-I CYP2E-likeIPR008071 Cyt P450 E grp-I CYP2J-like	489.47368
ENSMUSP00000022268	38.9	Pyruvate dehydrogenase E1 component subunit beta, mitochondrial Precursor (PDHE1-B)(EC 1.2.4.1) Source: 1.2.4.1 IPR005476 Transketo CIPR005475 Transketo Cen R	341.22807
ENSMUSP00000108422	33.4	17-beta hydroxysteroid dehydrogenase 13 Precursor (EC 1.1.-.-)(Short-chain dehydrogenase/reductase 9)(Alcohol dehydrogenase PAN1B-like) Source: 1.1.-.- IPR003560 DHB DHaseIPR002198 DHase sc/Rdtase SDRIPR002347 Glc/ribitol DHaseIPR002424 Insect AlcDHase famIPR016040 NAD(P)-bdIPR013968 Polyketide synth KR	292.98246
ENSMUSP00000029076	29.3	Carbonic anhydrase 3 (EC 4.2.1.1)(Carbonic anhydrase III)(CA-III)(Carbonate dehydratase III) Source: 4.2.1.1 IPR018338 Carbonic anhydrase a-class CSIPR001148 Carbonic anhydrase a-class cat	257.01754
ENSMUSP00000035458	183.2	ATP-binding cassette sub-family A member 6 IPR003593 AAA+ ATPase coreIPR003439 ABC transporter-like	1607.0175
ENSMUSP00000003038	104	AP-2 complex subunit alpha-2 (Adapter-related protein complex 2 alpha-2 subunit)(Adaptor protein complex AP-2 subunit alpha-2)(Alpha2-adaptin)(Plasma membrane adaptor HA2/AP2 adaptin alpha C subunit)(Alpha-adaptin C)(Clathrin assembly protein complex 2 alpha-C large chain)(100 kDa coated vesicle protein C) IPR017104 AP2 complex asuIPR016024 ARM-type foldIPR009028 Calthrin/coatomer app sub CIPR002553 Clathrin/coatomer adapt-like NIPR013041 Clathrin/coatomer app Ig-likeIPR003164 Clathrin a-adaptin app sub CIPR008152 Clathrin a/b/g-adaptin app Ig	912.2807
ENSMUSP00000025549	15.2	Cytochrome b5 IPR001199 Cyt B5IPR018506 Cyt B5 heme-BS	133.33333
ENSMUSP00000022946	14.2	Ribonuclease UK114 (EC 3.1.-.-)(Heat-responsive protein 12) Source: 3.1.-.- IPR013813 Endoribo LPSP/chorism mut-likeIPR006175 Endoribon LPSPIPR006056 YjgF-like	124.5614
ENSMUSP00000023712	70.9	Keratin, type II cytoskeletal 2 epidermal (Cytokeratin-2e)(CK2e)(K2e)(keratin-2)(keratin-2 epidermis) IPR016044 FIPR018039 Intermediate filament CSIPR002957 Keratin IIPR003054 Keratin IIIPR009053 PrefoldinIPR000817 Prion	621.92982
ENSMUSP00000024823	20.8	Lactoylglutathione lyase (EC 4.4.1.5)(Methylglyoxalase)(Aldoketomutase)(Glyoxalase I)(Glx I)(Ketone-aldehyde mutase)(S-D-lactoylglutathione methylglyoxal lyase) Source: 4.4.1.5 IPR004360 Glyas bleo-R dOaseIPR004361 Glyoxalase 1IPR018146 Glyoxalase 1 CS	182.45614
ENSMUSP00000026427	121.5	Extended synaptotagmin-1 (E-Syt1)(Membrane-bound C2 domain-containing protein)(Protein FAM62A) IPR000008 C2 Ca-depIPR008973 C2 Ca/lipid-bd reg CaLBIPR018029 C2 membr targeting	1065.7895
ENSMUSP00000082519	107.6	AP-2 complex subunit alpha-1 (Adapter-related protein complex 2 alpha-1 subunit)(Adaptor protein complex AP-2 subunit	943.85965

		alpha-1)(Alpha1-adaptin)(Plasma membrane adaptor HA2/AP2 adaptin alpha A subunit)(Alpha-adaptin A)(Clathrin assembly protein complex 2 alpha-A large chain)(100 kDa coated vesicle protein A) IPR017104 AP2 complex asuIPR016024 ARM-type foldIPR009028 Calthrin/coatomer app sub CIPR002553 Clathrin/coatomer adapt-like NIPR013041 Clathrin/coatomer app Ig-likeIPR003164 Clathrin a-adaptin app sub CIPR008152 Clathrin a/b/g-adaptin app IgIPR000694 PRO rich	
ENSMUSP00000060346	49	Dihydrolipoyllysine-residue succinyltransferase component of 2-oxoglutarate dehydrogenase complex, mitochondrial Precursor (EC 2.3.1.61)(Dihydrolipoamide succinyltransferase component of 2-oxoglutarate dehydrogenase complex)(E2)(E2K) Source: 2.3.1.61 IPR003016 2-oxoA DHase lipoyl-BSIPR001078 2-oxoacid DHase actylTfraseIPR000089 Biotin lipoylIPR000694 PRO richIPR011053 Single hybrid motifIPR006255 SucB	429.82456
ENSMUSP00000081485	13.3	no description availableIPR008195 Ribosomal L34eIPR018065 Ribosomal L34e CS	116.66667
ENSMUSP00000007272	52.8	Keratin, type I cytoskeletal 14 (Cytokeratin-14)(CK-14)(Keratin-14)(K14) IPR016044 FIPR018039 Intermediate filament CSIPR002957 Keratin IIPR009053 Prefoldin	463.15789
ENSMUSP00000028610	59.8	Catalase (EC 1.11.1.6) Source: 1.11.1.6 IPR002226 CatalaseIPR011614 Catalase NIPR018028 Catalase rel subgroup	524.5614
ENSMUSP00000032998	26.7	40S ribosomal protein S3 IPR004087 KHIPR009019 KH prok-typeIPR004044 KH type 2IPR001351 Ribosomal S3 CIPR018280 Ribosomal S3 CSIPR005703 Ribosomal S3 euk/arc	234.21053
ENSMUSP00000027153	47.9	Long-chain specific acyl-CoA dehydrogenase, mitochondrial Precursor (LCAD)(EC 1.3.99.13) Source: 1.3.99.13 IPR006091 Acyl-CoA DHase/Oxase MIPR013107 Acyl-CoA DHase 2 CIPR006089 Acyl-CoA DHase CSIPR006092 Acyl-CoA DHase NIPR006090 Acyl-CoA Oxase/DHase 1IPR009100 AcylCoA DH/oxidase M/N	420.17544
ENSMUSP00000031729	88.3	Transferrin receptor protein 2 (TfR2) IPR003137 PAIPR007484 Peptidase M28IPR007365 Transferrin rcpt-like dimerise	774.5614
ENSMUSP00000071292	50.7	2-oxoisovalerate dehydrogenase subunit alpha, mitochondrial Precursor (EC 1.2.4.4)(Branched-chain alpha-keto acid dehydrogenase E1 component alpha chain)(BCKDH E1-alpha) Source: 1.2.4.4 IPR001017 DHase E1	444.73684
ENSMUSP00000027381	32.4	Peroxisomal trans-2-enoyl-CoA reductase (EC 1.3.1.38) Source: 1.3.1.38 IPR003560 DHB DHaseIPR002198 DHase sc/Rdtase SDRIPR002347 Glc/ribitol DHaseIPR016040 NAD(P)-bd	284.21053
ENSMUSP00000025778	113.2	Glycine dehydrogenase Source: 1.4.4.2 IPR017871 ABC transporter CSIPR003437 GDC-PIPR015424 PyrdxlP-dep Trfase major	992.98246
ENSMUSP00000039252	35.6	Retinol dehydrogenase 7 (EC 1.1.1.105)(Cis-retinol/androgen dehydrogenase type 2)(CRAD-2)(Cis-retinol/3alpha-hydroxysterol short-chain dehydrogenase isozyme 2) Source: 1.1.1.105 IPR003560 DHB DHaseIPR002198 DHase sc/Rdtase SDRIPR002347 Glc/ribitol DHaseIPR016040 NAD(P)-bd	312.2807
ENSMUSP00000034355	62.3	carboxylesterase 5 IPR002018 CarbesteraseBIPR000997 Cholinesterase	546.49123
ENSMUSP00000031334	33.8	Translation initiation factor eIF-2B subunit alpha (eIF-2B GDP-GTP exchange factor subunit alpha) IPR000649 IF-2B related	296.49123
ENSMUSP00000031411	56.5	Aldehyde dehydrogenase, mitochondrial Precursor (EC 1.2.1.3)(ALDH class 2)(AHD-M1)(ALDHI)(ALDH-E2) Source: 1.2.1.3 IPR016161 Ald DHase/Histidinol DHaseIPR016160 Ald DHase CSIPR015590 Aldehyde DHase	495.61404
ENSMUSP00000104955	206.1	Putative uncharacterized proteinMCG140951Plexin B2Plxnb2 protein ;;; Source: UniProtKB/TrEMBL B2RXS4 IPR002909 IPT TIG rcptIPR014756 Ig E-setIPR003659 Plexin-likeIPR016201 Plexin-like foldIPR013548 Plexin cytopIIPR002165 Plexin repeatIPR008936 Rho GTPase activation protIPR001627 Semaphorin/CD100 Ag	1807.8947
ENSMUSP00000029770	75.4	ATP-binding cassette sub-family D member 3 (70 kDa peroxisomal membrane protein)(PMP70)(PMP68) IPR003593 AAA+ ATPase coreIPR010509 ABC Ald NIPR011527 ABC TM 1IPR003439 ABC transporter-likeIPR017871 ABC transporter CSIPR017940 ABC transporter type1IPR005283 FA transporter	661.40351
ENSMUSP00000029663	35.1	Multisynthetase complex auxiliary component p43 IPR016027 NA-bd OB-fold-likeIPR010989 t-SNAREIPR002547 tRNA bd	307.89474
ENSMUSP00000090593	151.7	hypothetical protein LOC74148 IPR016160 Ald DHase CSIPR010916 TonB box CS	1330.7018
ENSMUSP00000021001	22.5	Ras-related protein Rab-10 IPR006688 ARFIPR006689 ARF/SARIPR003579 GTPase RabIPR003577 GTPase RasIPR003578 GTPase RhoIPR013684 Miro-likeIPR002078 RNA pol sigma 54 intIPR002041 Ran GTPaseIPR013753 RasIPR001806 Ras GTPaseIPR005225 Small GTP bd	197.36842
ENSMUSP00000090909	63	Liver carboxylesterase 31-like Precursor (EC 3.1.1.1) Source: 3.1.1.1 IPR002018 CarbesteraseB	552.63158

ENSMUSP00000029877	36.2	2,4-dienoyl-CoA reductase, mitochondrial Precursor (EC 1.3.1.34)(2,4-dienoyl-CoA reductase Source: 1.3.1.34 IPR003560 DHB DHaseIPR002198 DHase sc/Rdtase SDRIPR002347 Glc/ribitol DHaseIPR016040 NAD(P)-bd	317.54386
ENSMUSP00000020948	182.9	ATP-binding cassette sub-family A member 8-B IPR003593 AAA+ ATPase coreIPR003439 ABC transporter-likeIPR017871 ABC transporter CS	1604.386
ENSMUSP00000090155	63.6	Sphingosine-1-phosphate lyase 1 (SP-lyase)(mSPL)(EC 4.1.2.27)(Sphingosine-1-phosphate aldolase) Source: 4.1.2.27 IPR000192 Aminotrans V/Cys dSaseIPR015424 PyrdxlP-dep Trfase majorIPR002129 PyrdxlP-dep de-COase	557.89474
ENSMUSP00000032073	25.6	Probable N-acetyltransferase CML4 (EC 2.3.1.-)(Camello-like protein 4) Source: 2.3.1.- IPR016181 Acyl CoA acyltransferaseIPR000182 GCN5-rel AcTrfase	224.5614
ENSMUSP00000029987	39.5	Fructose-bisphosphate aldolase B (EC 4.1.2.13)(Liver-type aldolase)(Aldolase 2) Source: 4.1.2.13 IPR000741 Aldolase I	346.49123
ENSMUSP00000054322	36.1	Starch-binding domain-containing protein 1 (Genethonin-1) IPR013784 Carb-bd-like foldIPR002044 Glyco hydro carb-bd	316.66667
ENSMUSP00000032841	32.1	39S ribosomal protein L46, mitochondrial Precursor (L46mt)(MRP-L46) IPR015797 NUDIX	281.57895
sp|ALBU_HUMAN|	69.3	Serum albumin; Flags: Precursor;	607.89474
ENSMUSP00000092283	52	Regulator of microtubule dynamics protein 3 (RMD-3)(mRMD-3)(Protein FAM82A2)(Protein FAM82C)	456.14035
ENSMUSP00000034426	67.8	Lysyl-tRNA synthetase (EC 6.1.1.6)(Lysine--tRNA ligase)(LysRS) Source: 6.1.1.6 IPR002312 Asp-tRNA-synth IIbIPR002313 Lys-tRNA-synth IIIPR018149 Lys-tRNA-synth II CIPR016027 NA-bd OB-fold-likeIPR004365 NA bd OB tRNA-helicaseIPR004364 aa-tRNA-synt IIIPR006195 aa-tRNA-synth II	594.73684
ENSMUSP00000023462	41.2	Mitogen-activated protein kinase 1 (EC 2.7.11.24)(Extracellular signal-regulated kinase 2)(ERK-2)(Mitogen-activated protein kinase 2)(MAP kinase 2)(MAPK 2)(p42-MAPK)(ERT1) Source: 2.7.11.24 IPR008349 Erk 1 2 MAPKIPR008350 Erk 3 4 MAPKIPR008351 JNK MAPKIPR011009 Kinase likeIPR008352 MAPK p38IPR003527 MAP kinase CSIPR000719 Prot kinase coreIPR017441 Protein kinase ATP BSIPR017442 Se/Thr pkinase-relIPR008271 Ser thr pkin ASIPR002290 Ser thr pkinaseIPR001245 Tyr pkinase	361.40351
ENSMUSP00000018186	34.1	NADH-cytochrome b5 reductase 3 (Cytochrome b5 reductase)(B5R)(EC 1.6.2.2)(Diaphorase-1) Source: 1.6.2.2 IPR013113 FAD bd 9 SIPIPR001709 Flavoprot Pyr Nucl cyt RdtaseIPR001834 NADH-Cyt B5 reductaseIPR008333 OxRdtase FAD-bdIPR001433 OxRdtase FAD/NAD bdIPR001221 Phe hydroxylase	299.12281
ENSMUSP00000076472	35.9	Dehydrogenase/reductase SDR family member on chromosome X homolog Precursor (EC 1.1.-.-)(DHRSXY)(SCAD family protein) Source: 1.1.-.- IPR002198 DHase sc/Rdtase SDRIPR002347 Glc/ribitol DHaseIPR016040 NAD(P)-bd	314.91228
ENSMUSP00000003569	29.4	Indolethylamine N-methyltransferase (Indolamine N-methyltransferase)(EC 2.1.1.49)(Aromatic alkylamine N-methyltransferase)(Arylamine N-methyltransferase)(Amine N-methyltransferase) Source: 2.1.1.49 IPR000940 NNMT TEMT trans	257.89474
ENSMUSP00000052989	57.7	Cytochrome P450 8B1 (EC 1.14.13.95)(CYPVIIIB1)(7-alpha-hydroxycholest-4-en-3-one 12-alpha-hydroxylase)(7-alpha-hydroxy-4-cholesten-3-one 12-alpha-hydroxylase)(Sterol 12-alpha-hydroxylase) Source: 1.14.13.95 IPR001128 Cyt P450IPR017973 Cyt P450 CIPR002401 Cyt P450 E grp-IIPR002403 Cyt P450 E grp-IV	506.14035
ENSMUSP00000037555	62.6	Liver carboxylesterase 1 Precursor (EC 3.1.1.1)(Acyl coenzyme A:cholesterol acyltransferase)(ES-x) Source: 3.1.1.1 IPR002018 CarbesteraseB	549.12281
ENSMUSP00000106140	25.9	Proteasome subunit alpha type-2 (EC 3.4.25.1)(Proteasome component C3)(Macropain subunit C3)(Multicatalytic endopeptidase complex subunit C3) Source: 3.4.25.1 IPR001353 Proteasome A B suIPR000426 Proteasome alpha CS	227.19298
ENSMUSP00000023559	78.3	Peroxisomal bifunctional enzyme (PBE)(PBFE) Source: 4.2.1.17 IPR006180 3-OHacyl-CoA DHase CSIPR006176 3-OHacyl-CoA DHase NAD-bdIPR006108 3HC DHase CIPR008927 6-PGluconate DH C likeIPR001753 Crotonase coreIPR018376 Enoyl-CoA hyd/isom CSIPR016040 NAD(P)-bd	686.84211
ENSMUSP00000002549	46.2	Abhydrolase domain-containing protein 3 (EC 3.1.1.-)(Lung alpha/beta hydrolase 3)(MmLABH3) Source: 3.1.1.- IPR012020 AB-Hydro YheTIPR000073 AB hydrolase 1IPR000952 UPF0017 hydro-like CS	405.26316
ENSMUSP00000004774	28.8	Aquaporin-1 (AQP-1)(Aquaporin-CHIP)(Water channel protein for red blood cells and kidney proximal tubule)(Delayed early response protein 2)(DER2) IPR012269 AquaporinIPR000425 MIP	252.63158
ENSMUSP00000070944	38.1	no description availableIPR002735 Transl init fac IF2/IF5IPR016189 Transl init fac IF2/IF5 N	334.21053
ENSMUSP00000035116	58.4	Propionyl-CoA carboxylase beta chain, mitochondrial Precursor (PCCase subunit beta)(EC 6.4.1.3)(Propanoyl-CoA:carbon dioxide ligase subunit beta) Source: 6.4.1.3 IPR000438 Acetyl CoA COase Trfase b suIPR011763 COA CT CIPR011762 COA CT NIPR000022 Carboxyl trans	512.2807

ENSMUSP00000077223	16.5	Eukaryotic translation initiation factor 1A (eIF-1A)(eIF-4C) IPR016027 NA-bd OB-fold-likeIPR006196 S1 IF1IPR001253 TIF eIF-1AIPR018104 TIF eIF-1A CS	144.73684
ENSMUSP00000008684	17.5	Microsomal glutathione S-transferase 1 (Microsomal GST-1)(EC 2.5.1.18)(Microsomal GST-I) Source: 2.5.1.18 IPR001129 MAPEG	153.50877
ENSMUSP00000038305	20.5	28S ribosomal protein S28, mitochondrial (S28mt)(MRP-S28) IPR016027 NA-bd OB-fold-likeIPR003029 S1 RNA-bd	179.82456
ENSMUSP00000103136	17.5	Major urinary proteins 11 and 8 Fragment (MUP11 and MUP8) IPR002968 A1-microglobInIPR011038 Calycin likeIPR002345 LipocalinIPR000566 Lipocln cytFABPIPR002971 Maj urinaryIPR003087 N gelatinaseIPR002448 Odour bdIPR002972 PstgldnD synthIPR002450 vonEbner gland	153.50877
ENSMUSP00000103903	36.5	Galectin-9 IPR008985 ConA like lec glIPR001079 Galectin CRD	320.17544
ENSMUSP00000042967	50.8	NADH dehydrogenase Source: 1.6.5.3 IPR011538 NADH-UbQ OxRdtase 51KDa suIPR011537 NADH-UbQ OxRdtase F suIPR001949 NADH-ubq OxRdtase 51KDa CS	445.61404
ENSMUSP00000006094	56.9	Cytochrome P450 2D26 (EC 1.14.14.1)(CYPIID26) Source: 1.14.14.1 IPR001128 Cyt P450IPR002397 Cyt P450 BIPR017973 Cyt P450 CIPR017972 Cyt P450 CSIPR002401 Cyt P450 E grp-IIPR002403 Cyt P450 E grp-IVIPR008066 Cyt P450 E grp-I CYP1IPR008069 Cyt P450 E grp-I CYP2D-likeIPR008071 Cyt P450 E grp-I CYP2J-like	499.12281
ENSMUSP00000099435	14.9	60S ribosomal protein L23 IPR000218 Ribosomal L14b/L23e	130.70175
ENSMUSP00000010807	52.3	Fatty acid desaturase 1 (EC 1.14.19.-)(Delta(5) fatty acid desaturase)(Delta(5) desaturase)(D5D) Source: 1.14.19.- IPR001199 Cyt B5IPR012171 Fatty acid/sphinglp desaturaseIPR005804 Fatty acid desaturase-1	458.77193
ENSMUSP00000028063	28.6	Phosphotriesterase-related protein (Parathion hydrolase-related protein) IPR017947 AryldialkylPase Zn-BSIPR001559 Aryldialkylphosphatase	250.87719
ENSMUSP00000019622	23.8	Ras-related protein Rab-4A IPR006688 ARFIPR006689 ARF/SARIPR003579 GTPase RabIPR003577 GTPase RasIPR003578 GTPase RhoIPR013684 Miro-likeIPR002041 Ran GTPaseIPR013753 RasIPR001806 Ras GTPaseIPR005225 Small GTP bd	208.77193
ENSMUSP00000002850	164.8	Multidrug resistance-associated protein 6 (ATP-binding cassette sub-family C member 6) IPR003593 AAA+ ATPase coreIPR011527 ABC TM 1IPR001140 ABC TM transptIPR003439 ABC transporter-likeIPR017871 ABC transporter CSIPR017940 ABC transporter type1IPR009147 CysFib conduc TMIPR005292 Multidrug-R assoc MRP	1445.614
ENSMUSP00000026470	55.7	serine hydroxymethyltransferase 2 (mitochondrial) IPR001085 Gly HO-MeTrfaseIPR015424 PyrdxlP-dep Trfase major	488.59649
ENSMUSP00000031093:reversed	48.4		424.5614
ENSMUSP00000041361:reversed	175.5		1539.4737
ENSMUSP00000033662	43.2	Pyruvate dehydrogenase E1 component subunit alpha, somatic form, mitochondrial Precursor (EC 1.2.4.1)(PDHE1-A type I) Source: 1.2.4.1 IPR001017 DHase E1	378.94737
ENSMUSP00000030112	99	Cytoplasmic aconitate hydratase (Aconitase)(EC 4.2.1.3)(Citrate hydro-lyase)(Iron-responsive element-binding protein 1)(IRE-BP 1)(Iron regulatory protein 1)(IRP1) Source: 4.2.1.3 IPR001030 Acoase/IPM deHydtase lsu abaIPR015928 Aconitase/3IPM dehydase swvIIPR006249 Aconitase/Fe reg prot 2IPR000573 AconitaseA/IPMdHydase ssu swvIIPR018136 Aconitase 4Fe-4S BS	868.42105
ENSMUSP00000021443	101.1	C-1-tetrahydrofolate synthase, cytoplasmic (C1-THF synthase) Source: 1.5.1.5 IPR000559 For THF ligaseIPR016040 NAD(P)-bdIPR000672 THF DHase/CycOHase	886.84211
ENSMUSP00000036288	57.4	T-complex protein 1 subunit beta (TCP-1-beta)(CCT-beta) IPR012716 Chap CCT betaIPR017998 Chaperone TCP-1IPR002194 Chaperonin TCP-1 CSIPR001844 Chaprnin Cpn60IPR002423 Cpn60/TCP-1IPR017441 Protein kinase ATP BS	503.50877
ENSMUSP00000007212	100.1	26S proteasome non-ATPase regulatory subunit 2 (26S proteasome regulatory subunit RPN1)(26S proteasome regulatory subunit S2)(26S proteasome subunit p97) IPR016643 26S Psome Rpn1IPR002015 APC proteasomeIPR016024 ARM-type fold	878.07018
ENSMUSP00000086252	37.4	Killer cell lectin-like receptor 2 (T-cell surface glycoprotein Ly-49B)(Lymphocyte antigen 49b)(Ly-49b) IPR001304 C-type lectinIPR016187 C-type lectin foldIPR013600 Ly49	328.07018
ENSMUSP00000086987	8.5	Small nuclear ribonucleoprotein G (snRNP-G)(Sm protein G)(Sm-G)(SmG) IPR006649 Euk arc LSM coreIPR010920 LSM related coreIPR001163 LSM snRNP core	74.561404

ENSMUSP00000000090	16.1	Cytochrome c oxidase subunit 5A, mitochondrial Precursor (Cytochrome c oxidase polypeptide Va) IPR003204 Cyt c oxidase su5A	141.22807
ENSMUSP00000105288	89.5	85 kDa calcium-independent phospholipase A2 (CaI-PLA2)(iPLA2)(EC 3.1.1.4)(Group VI phospholipase A2)(GVI PLA2) Source: 3.1.1.4 IPR002110 ANKIPR016035 Acyl Trfase/lysoPlipaseIPR002641 Patatin	785.08772
ENSMUSP00000015858	45	LAG1 longevity assurance homolog 2 (Translocating chain-associating membrane protein homolog 3)(TRAM homolog 3) IPR001356 HomeoboxIPR009057 Homeodomain likeIPR016439 Longevity assurance LAG1 LAC1IPR006634 TLC	394.73684
ENSMUSP00000033289	77.5	Stromal interaction molecule 1 Precursor IPR001660 SAMIPR011510 SAM 2IPR010993 SAM homology	679.82456
ENSMUSP00000025667	27.3	Reticulon-3 IPR003388 Reticulon	239.47368
ENSMUSP00000112196	36.1	ELAV-like protein 1 (Hu-antigen R)(HuR)(Elav-like generic protein)(MelG) IPR006548 ELAD HUD SFIPR002343 Hud Sxl RNAIPR003954 RRM 1IPR000504 RRM RNP1	316.66667
ENSMUSP00000032882	14.2	NADH dehydrogenase IPR009423 NADH-UbQ OxRdtase b14.5b	124.5614
ENSMUSP00000103940	16.4	40S ribosomal protein S16 IPR000754 Ribosomal S9	143.85965
ENSMUSP00000088057	26.4	Proteasome subunit alpha type-5 (EC 3.4.25.1)(Proteasome zeta chain)(Macropain zeta chain)(Multicatalytic endopeptidase complex zeta chain) Source: 3.4.25.1 IPR001353 Proteasome A B suIPR000426 Proteasome alpha CS	231.57895
ENSMUSP00000034400	16.3	Cytochrome b5 type B Precursor (Cytochrome b5 outer mitochondrial membrane isoform) IPR001199 Cyt B5IPR018506 Cyt B5 heme-BSIPR000425 MIP	142.98246
ENSMUSP00000032371	80.8	Glycogen Source: 2.4.1.11 IPR008631 Glycogen synth	708.77193
ENSMUSP00000026565	14.9	interferon induced transmembrane protein 3 IPR007593 CD225 TM	130.70175
ENSMUSP00000007216	49.6	AP-2 complex subunit mu-1 (Mu2-adaptin)(AP-2 mu-2 chain)(Plasma membrane adaptor AP-2 50 kDa protein)(Clathrin assembly protein complex 2 medium chain)(Clathrin coat assembly protein AP50)(Clathrin coat-associated protein AP50) IPR001392 Clathrin muIPR008968 Clathrin mu CIPR018240 Clathrin mu CSIPR011012 Longin like	435.08772
ENSMUSP00000083281	17	AP-2 complex subunit sigma-1 (Adapter-related protein complex 2 sigma-1 subunit)(Sigma2-adaptin)(Sigma-adaptin 3b)(Plasma membrane adaptor AP-2 17 kDa protein)(Clathrin assembly protein 2 small chain)(Clathrin coat assembly protein AP17)(Clathrin coat-associated protein AP17) IPR016635 AP complex ssuIPR000804 Clathrin sigma/coatomer zetaIPR011012 Longin like	149.12281
ENSMUSP00000025161	49.8	Tapasin Precursor (TPSN)(TPN)(TAP-binding protein)(TAP-associated protein) IPR007110 Ig-likeIPR003006 Ig/MHC CSIPR003597 Ig C1-setIPR003599 Ig subIPR008056 Tapasin	436.84211
ENSMUSP00000003066	35.8	Apolipoprotein E Precursor (Apo-E) IPR000074 ApoA1 A4 E	314.03509
ENSMUSP00000040954	63.5	Selenocysteine-specific elongation factor (Elongation factor sec)(Eukaryotic elongation factor, selenocysteine-tRNA-specific)(mSelB) IPR000795 ProtSyn GTP bdIPR004161 Transl elong EFTu/EF1A 2	557.01754
ENSMUSP00000045127	22.9	Ras-related protein Rab-9A (Rab-9A)(Sid 99) IPR003579 GTPase RabIPR003577 GTPase RasIPR003578 GTPase RhoIPR006036 K uptake TrkAIPR013684 Miro-likeIPR002041 Ran GTPaseIPR013753 RasIPR001806 Ras GTPaseIPR005225 Small GTP bd	200.87719
ENSMUSP00000002846	32.7	Glycine N-methyltransferase (EC 2.1.1.20) Source: 2.1.1.20 IPR014369 Gly N MeTrfaseIPR013216 Methyltransf 11IPR013217 Methyltransf 12	286.84211
ENSMUSP00000047665	40.1	Adenosine kinase (AK)(EC 2.7.1.20)(Adenosine 5--phosphotransferase) Source: 2.7.1.20 IPR001805 AdenokinaseIPR011611 Carb/pur kinaseIPR002173 Carboh/pur kinase PfkB CSIPR002139 Ribokinase	351.75439
ENSMUSP00000034346	61.9	carboxylesterase 6 IPR002018 CarbesteraseBIPR000997 Cholinesterase	542.98246
ENSMUSP00000022861	59.7	UDP-glucuronosyltransferase 3A1 Precursor (UDPGT 3A1)(EC 2.4.1.17) Source: 2.4.1.17 IPR007235 Glyco trans 28 CIPR002213 UDP glucos trans	523.68421
ENSMUSP00000022256	45.5	26S proteasome non-ATPase regulatory subunit 6 (26S proteasome regulatory subunit S10)(p42A) IPR000717 PCI	399.12281
ENSMUSP00000099730	23.4	60S ribosomal protein L13a (Transplantation antigen P198)(Tum-P198 antigen) IPR005822 Ribosomal L13IPR005755 Ribosomal L13 euk/arc	205.26316
ENSMUSP00000070449	15.1	Uncharacterized protein C19orf12 homolog	132.45614
ENSMUSP00000099534	13.8	Beta-2-microglobulin Precursor IPR013151 IgIPR007110 Ig-likeIPR003006 Ig/MHC CSIPR003597 Ig C1-set	121.05263

ENSMUSP00000102289	25.7	Glutathione S-transferase Mu 3 (EC 2.5.1.18)(GST class-mu 3)(Glutathione S-transferase GT9.3) Source: 2.5.1.18 IPR004046 GST CIPR003081 GST muIPR010987 Glutathione-S-Trfase C-likeIPR004045 Glutathione S-Trfase NIPR012336 Thioredoxin-like fold	225.4386
ENSMUSP00000029830	43.5	Cystathionine gamma-lyase (EC 4.4.1.1)(Gamma-cystathionase) Source: 4.4.1.1 IPR000277 Cys/Met-Metab PyrdxlP-dep enzIPR015424 PyrdxlP-dep Trfase major	381.57895
ENSMUSP00000051561	75.7	Sulfate anion transporter 1 (SAT-1)(Solute carrier family 26 member 1) IPR018045 S04 transporter CSIPR002645 SO4 transptr/STASIPR001902 SulP transptIPR011547 Sulph transpt	664.03509
ENSMUSP00000099490	265.1	Acetyl-CoA carboxylase 1 (EC 6.4.1.2)(ACC-alpha)(Acetyl-CoA carboxylase 265) Source: 6.4.1.2 IPR011761 ATP-graspIPR013537 AcCoA COase cenIPR011764 BCIPR001882 Biotin BSIPR005482 Biotin COase CIPR000089 Biotin lipoylIPR011763 COA CT CIPR011762 COA CT NIPR005479 CarbamoylP synth lsu ATP-bdIPR005481 CarbamoylP synth lsu NIPR000022 Carboxyl transIPR016185 PreATP-grasp-likeIPR011054 Rudment hybrid motifIPR011053 Single hybrid motif	2325.4386
ENSMUSP00000025563	21.1	Ferritin heavy chain (Ferritin H subunit)(EC 1.16.3.1) Source: 1.16.3.1 IPR009078 Ferritin/RR likeIPR014034 Ferritin CSIPR008331 Ferritin DpsIPR009040 Ferritin like	185.08772
ENSMUSP00000071624	28.4	Proteasome subunit alpha type-3 (EC 3.4.25.1)(Proteasome component C8)(Macropain subunit C8)(Multicatalytic endopeptidase complex subunit C8)(Proteasome subunit K) Source: 3.4.25.1 IPR001353 Proteasome A B suIPR000426 Proteasome alpha CS	249.12281
ENSMUSP00000002171	50.4	26S protease regulatory subunit 6A (Proteasome 26S subunit ATPase 3)(TAT-binding protein 1)(TBP-1) IPR005937 26S Psome P45IPR003593 AAA+ ATPase coreIPR003960 AAA ATPase CSIPR003959 AAA ATPase core	442.10526
ENSMUSP00000029402	61	Acetyl-coenzyme A transporter 1 (AT-1)(Acetyl-CoA transporter)(Solute carrier family 33 member 1) IPR004752 AmpG permeaseIPR016196 MFS gen sb transpt	535.08772
ENSMUSP00000072858	14	Histone H2A type 2-B (H2a-613A) IPR003958 CBFA NFYB domainIPR009072 Histone-foldIPR002119 Histone H2AIPR007125 Histone core D	122.80702
ENSMUSP00000031402	58.5	T-complex protein 1 subunit zeta (TCP-1-zeta)(CCT-zeta)(CCT-zeta-1) IPR012722 Chap CCT zetaIPR017998 Chaperone TCP-1IPR002194 Chaperonin TCP-1 CSIPR001844 Chaprnin Cpn60IPR002423 Cpn60/TCP-1	513.15789
ENSMUSP00000037348	41.8	3-ketoacyl-CoA thiolase, mitochondrial (EC 2.3.1.16)(Beta-ketothiolase)(Acetyl-CoA acyltransferase)(Mitochondrial 3-oxoacyl-CoA thiolase) Source: 2.3.1.16 IPR000870 Homoser kinIPR002155 ThiolaseIPR016039 Thiolase-like	366.66667
ENSMUSP00000089551	21.3	no description availableIPR001063 Ribosomal L22IPR018260 Ribosomal L22/L17 CSIPR005721 Ribosomal L22/L17 euk/arc	186.84211
ENSMUSP00000088372	20.8	Ferritin light chain 1 (Ferritin L subunit 1) IPR009078 Ferritin/RR likeIPR014034 Ferritin CSIPR008331 Ferritin DpsIPR009040 Ferritin like	182.45614
ENSMUSP00000028121	52.3	Acyl-CoA-binding domain-containing protein 5 IPR000582 Acyl-CoA-binding proteinIPR016347 M-assoc diazepam-bd-inh	458.77193
ENSMUSP00000078123	20.7	39S ribosomal protein L18, mitochondrial Precursor (L18mt)(MRP-L18)	181.57895
ENSMUSP00000025668	60.5	Atlastin-3 IPR015900 Guanylate-bd-like CIPR015894 Guanylate-bd N	530.70175
ENSMUSP00000023312	65.1	CD166 antigen Precursor (Activated leukocyte cell adhesion molecule)(Protein DM-GRASP)(CD166 antigen) IPR013162 CD80 C2-setIPR013151 IgIPR007110 Ig-likeIPR003596 Ig V-set subIPR003599 Ig subIPR003598 Ig sub2	571.05263
ENSMUSP00000090844	91.7	AP-1 complex subunit gamma-1 (Adapter-related protein complex 1 subunit gamma-1)(Adaptor protein complex AP-1 subunit gamma-1)(Golgi adaptor HA1/AP1 adaptin subunit gamma-1)(Gamma1-adaptin)(Gamma-adaptin)(Clathrin assembly protein complex 1 gamma-1 large chain) IPR017107 AP1 complex gsuIPR016024 ARM-type foldIPR002553 Clathrin/coatomer adapt-like NIPR013041 Clathrin/coatomer app Ig-likeIPR008152 Clathrin a/b/g-adaptin app IgIPR008153 Clathrin g-adaptin app	804.38596
ENSMUSP00000013737	52.6	NADH dehydrogenase Source: 1.6.5.3 IPR014029 NADH-UbQ OxRdtase 49kDa CSIPR010219 NADH DH 1 dsuIPR001135 NADH UbQ OxRdtase 49kDa	461.40351
ENSMUSP00000003521	18.4	40S ribosomal protein S11 IPR016027 NA-bd OB-fold-likeIPR000266 Ribosomal S17	161.40351
ENSMUSP00000075953	9.3	NADH dehydrogenase	81.578947
ENSMUSP00000034227	19.8	Plasmolipin (Plasma membrane proteolipid) IPR013295 MALIPR008253 Marvel	173.68421

ENSMUSP00000080058	81.5	Acylamino-acid-releasing enzyme (AARE)(EC 3.4.19.1)(Acyl-peptide hydrolase)(APH)(Acylaminoacyl-peptidase) Source: 3.4.19.1 IPR002471 Pept S9 ASIPR001375 Peptidase S9IPR002470 Peptidase S9A	714.91228
ENSMUSP00000111831	16.7		146.49123
ENSMUSP00000045621	31.3	Peroxisomal 2,4-dienoyl-CoA reductase (EC 1.3.1.34)(2,4-dienoyl-CoA reductase 2) Source: 1.3.1.34 IPR003560 DHB DHaseIPR002198 DHase sc/Rdtase SDRIPR002347 Glc/ribitol DHaseIPR016040 NAD(P)-bdIPR013968 Polyketide synth KR	274.5614
ENSMUSP00000102363	48.3	26S proteasome non-ATPase regulatory subunit 12 (26S proteasome regulatory subunit p55) IPR000717 PCI	423.68421
ENSMUSP00000020504	13.8	Histidine triad nucleotide-binding protein 1 (EC 3.-.-.-)(Adenosine 5--monophosphoramidase)(Protein kinase C inhibitor 1)(Protein kinase C-interacting protein 1)(PKCI-1) Source: 3.-.-.- IPR011146 His triad-like motifIPR001310 Histidine triad HIT	121.05263
ENSMUSP00000096222	64	Heterogeneous nuclear ribonucleoprotein L (hnRNP L) IPR006536 HnRNP-L PTBIPR005404 K chnl volt-dep Kv3.3IPR001399 Orbi VP6IPR000694 PRO richIPR000504 RRM RNP1	561.40351
ENSMUSP00000030940	37.4	Guanine nucleotide-binding protein G(I)/G(S)/G(T) subunit beta-1 (Transducin beta chain 1) IPR001632 Gprotein BIPR016346 Guanine nucleotide-bd bsuIPR001680 WD40 repeatIPR011046 WD40 repeat-likeIPR017986 WD40 repeat region	328.07018
ENSMUSP00000034141	94.5	Peroxisomal Lon protease homolog 2 (EC 3.4.21.-)(Lon protease-like protein 2)(Lon protease 2) Source: 3.4.21.- IPR003593 AAA+ ATPase coreIPR011704 AAA 5IPR003959 AAA ATPase coreIPR001270 Chaprnin clpA/BIPR008269 Pept S16 CIPR003111 Pept S16 NIPR004815 Pept S16 lonIPR001984 Peptidase S16IPR008268 Peptidase S16 AS	828.94737
ENSMUSP00000017065	39	arginine/serine-rich splicing factor 6 IPR000504 RRM RNP1	342.10526
ENSMUSP00000026704	59.5	T-complex protein 1 subunit theta (TCP-1-theta)(CCT-theta) IPR012721 Chap CCT thetaIPR017998 Chaperone TCP-1IPR002194 Chaperonin TCP-1 CSIPR001844 Chaprnin Cpn60IPR002423 Cpn60/TCP-1	521.92982
ENSMUSP00000034881	9.3	Cytochrome c oxidase polypeptide 7A2, mitochondrial Precursor (Cytochrome c oxidase polypeptide VIIa-liver/heart)(Cytochrome c oxidase subunit VIIa-L) IPR003177 Cyt c oxidase su7a	81.578947
ENSMUSP00000028238	23.9	Ras-related protein Rab-14 IPR006688 ARFIPR001270 Chaprnin clpA/BIPR003579 GTPase RabIPR003577 GTPase RasIPR003578 GTPase RhoIPR013684 Miro-likeIPR002041 Ran GTPaseIPR013753 RasIPR001806 Ras GTPaseIPR005225 Small GTP bd	209.64912
ENSMUSP00000028062	53.7	Vimentin IPR016044 FIPR006821 Intermed filament DNA bdIPR018039 Intermediate filament CSIPR002957 Keratin IIPR009053 PrefoldinIPR000533 Tropomyosin	471.05263
ENSMUSP00000029259	79.3	Methylcrotonoyl-CoA carboxylase subunit alpha, mitochondrial Precursor (MCCase subunit alpha)(EC 6.4.1.4)(3-methylcrotonyl-CoA carboxylase 1)(3-methylcrotonyl-CoA:carbon dioxide ligase subunit alpha)(3-methylcrotonyl-CoA carboxylase biotin-containing subunit) Source: 6.4.1.4 IPR011761 ATP-graspIPR013651 ATP-grasp RimK-typeIPR003135 ATP-grasp carboxylate-amineIPR001249 AcCoA biotinCCIPR011764 BCIPR001882 Biotin BSIPR005482 Biotin COase CIPR000089 Biotin lipoylIPR005483 CarbamoylP synth lsuIPR005479 CarbamoylP synth lsu ATP-bdIPR005481 CarbamoylP synth lsu NIPR016185 PreATP-grasp-likeIPR011054 Rudment hybrid motifIPR011053 Single hybrid motif	695.61404
ENSMUSP00000023749	26.5	Bax inhibitor 1 (BI-1)(Transmembrane BAX inhibitor motif-containing protein 6)(Testis-enhanced gene transcript protein) IPR006213 Bax inhbtr1 CSIPR006214 UPF0005	232.45614
ENSMUSP00000064655	14.2	Fatty acid-binding protein, liver (L-FABP)(14 kDa selenium-binding protein) IPR011038 Calycin likeIPR000463 Fatty acid bdIPR000566 Lipocln cytFABP	124.5614
ENSMUSP00000030455	36.6	Alcohol dehydrogenase Source: 1.1.1.2 IPR001395 Aldo/ket redIPR018170 Aldo/ket reductase CS	321.05263
ENSMUSP00000000001	40.5	Guanine nucleotide-binding protein G(k) subunit alpha (G(i) alpha-3) IPR006688 ARFIPR002975 Fungi GproteinAIPR001019 Gprotein alph bdIPR000469 Gprotein alpha12IPR001408 Gprotein alpha IIPR006036 K uptake TrkAIPR001806 Ras GTPase	355.26316
ENSMUSP00000098076	91.3	Eukaryotic translation initiation factor 3 subunit B (eIF3b)(Eukaryotic translation initiation factor 3 subunit 9)(eIF-3-eta)(eIF3 p116) IPR003954 RRM 1IPR000504 RRM RNP1IPR013979 eIF2A central-regionIPR011400 eIF3b	800.87719
ENSMUSP00000005685	56.7	Cytochrome P450 2A5 (EC 1.14.14.1)(CYPIIA5)(Coumarin 7-hydroxylase)(P450-15-COH)(P450-IIA3.2) Source: 1.14.14.1 IPR001128 Cyt P450IPR002397 Cyt P450 BIPR017973 Cyt P450 CIPR017972 Cyt P450 CSIPR002401 Cyt P450 E grp-IIPR002403 Cyt P450 E grp-IVIPR008067 Cyt P450 E grp-I CYP2A-likeIPR008068 Cyt P450 E grp-I CYP2B-likeIPR008069 Cyt P450 E grp-I CYP2D-likeIPR008071 Cyt P450 E grp-I CYP2J-like	497.36842

ENSMUSP00000089374	45	Betaine--homocysteine S-methyltransferase 1 (EC 2.1.1.5) Source: 2.1.1.5 IPR017226 Betaine-hCys S-MeTrfase BHMTIPR003726 S MeTrfase	394.73684
ENSMUSP00000084918	54.4	Retinal dehydrogenase 1 (RALDH 1)(RalDH1)(EC 1.2.1.36)(Aldehyde dehydrogenase family 1 member A1)(Aldehyde dehydrogenase, cytosolic)(ALHDII)(ALDH-E1) Source: 1.2.1.36 IPR016161 Ald DHase/Histidinol DHaseIPR016160 Ald DHase CSIPR015590 Aldehyde DHase	477.19298
ENSMUSP00000033480	127.7	Probable phospholipid-transporting ATPase 11C (EC 3.6.3.1)(ATPase class VI type 11C) Source: 3.6.3.1 IPR001757 ATPase PIPR006539 ATPase P-typ Plipid-transIIPR018303 ATPase P-typ phosphor siteIPR005834 Dehalogen-like hydro	1120.1754
ENSMUSP00000099642	275.6	acetyl-Coenzyme A carboxylase beta IPR011761 ATP-graspIPR013537 AcCoA COase cenIPR011764 BCIPR005482 Biotin COase CIPR000089 Biotin lipoylIPR011763 COA CT CIPR011762 COA CT NIPR005479 CarbamoylP synth lsu ATP-bdIPR005481 CarbamoylP synth lsu NIPR000022 Carboxyl transIPR016185 PreATP-grasp-likeIPR011054 Rudment hybrid motifIPR011053 Single hybrid motif	2417.5439
ENSMUSP00000090184	24.1	no description availableIPR001047 Ribosomal S8eIPR018283 Ribosomal S8e CS	211.40351
ENSMUSP00000018430	25.4	Proteasome subunit beta type-6 Precursor (EC 3.4.25.1)(Proteasome delta chain)(Macropain delta chain)(Multicatalytic endopeptidase complex delta chain)(Proteasome subunit Y) Source: 3.4.25.1 IPR000243 Pept T1A subBIPR001353 Proteasome A B suIPR016050 Proteasome bsu CS	222.80702
ENSMUSP00000027067	25.3	Glutathione S-transferase A3 (EC 2.5.1.18)(Glutathione S-transferase Yc)(Ya3)(GST class-alpha member 3) Source: 2.5.1.18 IPR004046 GST CIPR003080 GST alphaIPR010987 Glutathione-S-Trfase C-likeIPR004045 Glutathione S-Trfase NIPR012336 Thioredoxin-like fold	221.92982
ENSMUSP00000091541	51.1	Abhydrolase domain-containing protein UNQ6510/PRO21435 homolog Precursor (EC 3.1.1.-) Source: 3.1.1.- IPR012020 AB-Hydro YheT	448.24561
ENSMUSP00000099819	30.7	Voltage-dependent anion-selective channel protein 1 (VDAC-1)(mVDAC1)(Voltage-dependent anion-selective channel protein 5)(VDAC-5)(mVDAC5)(Outer mitochondrial membrane protein porin 1)(Plasmalemmal porin) IPR001925 Porin Euk	269.29825
ENSMUSP00000054421	29.5	Eukaryotic translation initiation factor 3 subunit J (eIF3j)(Eukaryotic translation initiation factor 3 subunit 1)(eIF-3-alpha)(eIF3 p35) IPR000104 Antifreeze 1IPR013906 eIF3 subunit	258.77193
ENSMUSP00000077917	14.9	28S ribosomal protein S14, mitochondrial (S14mt)(MRP-S14) IPR001209 Ribosomal S14	130.70175
ENSMUSP00000003461	116.4	2-oxoglutarate dehydrogenase E1 component, mitochondrial Precursor (EC 1.2.4.2)(Alpha-ketoglutarate dehydrogenase) Source: 1.2.4.2 IPR011603 2oxoglutarate DHase E1IPR001017 DHase E1IPR005475 Transketo Cen R	1021.0526
ENSMUSP00000034097	47.4	Aspartate aminotransferase, mitochondrial Precursor (mAspAT)(EC 2.6.1.1)(Transaminase A)(Glutamate oxaloacetate transaminase 2)(Fatty acid-binding protein)(FABP-1)(FABPpm) Source: 2.6.1.1 IPR004839 Aminotrans I/IIIPR000796 Asp transIPR008120 Dense granule Gra7 proteinIPR004838 NHTrfase class1 PyrdxlP-BSIPR015424 PyrdxlP-dep Trfase major	415.78947
ENSMUSP00000004232	39.7	Alcohol dehydrogenase 1 (EC 1.1.1.1)(Alcohol dehydrogenase A subunit)(ADH-A2) Source: 1.1.1.1 IPR013154 AlcDHase GroES-likeIPR013149 AlcDHase Zn-bdIPR002328 AlcDHase Zn CSIPR011032 GroES likeIPR016040 NAD(P)-bd	348.24561
ENSMUSP00000031773	39.3	Serum paraoxonase/lactonase 3 (EC 3.1.1.-) Source: 3.1.1.- IPR002640 ArylesteraseIPR008364 Paraoxonase2	344.73684
ENSMUSP00000069359:reversed	33.7		295.61404
ENSMUSP00000103557	22.3	Selenoprotein T Precursor (SelT) IPR011893 CXXU selWTH	195.61404
ENSMUSP00000099415	52.1	Keratin, type I cytoskeletal 16 (Cytokeratin-16)(CK-16)(Keratin-16)(K16) IPR016044 FIPR018039 Intermediate filament CSIPR002957 Keratin IIPR013253 Kinetochore Spc7IPR009053 Prefoldin	457.01754
ENSMUSP00000001507	56.7	cytochrome P450, family 51 IPR001128 Cyt P450IPR017973 Cyt P450 CIPR017972 Cyt P450 CSIPR002401 Cyt P450 E grp-IIPR002403 Cyt P450 E grp-IVIPR018114 Peptidase S1/S6 AS	497.36842
ENSMUSP00000047960	11.4	ATP synthase subunit g, mitochondrial (ATPase subunit g) IPR016702 ATP-Synthase su G mt metIPR006808 ATPase F0-cplx gsu mt	100
ENSMUSP00000017975	23.6	Ras-related protein Rab-5A IPR006688 ARFIPR003579 GTPase RabIPR003577 GTPase RasIPR003578 GTPase RhoIPR001019 Gprotein alph bdIPR013684 Miro-likeIPR002041 Ran GTPaseIPR013753 RasIPR001806 Ras GTPaseIPR005225 Small GTP bd	207.01754
ENSMUSP00000088252	18	Peptidyl-prolyl cis-trans isomerase A (PPIase A)(Rotamase A)(EC 5.2.1.8)(Cyclophilin A)(Cyclosporin A-binding	157.89474

		protein)(SP18) Source: 5.2.1.8 IPR015891 Cyclophilin-likeIPR002130 PPIase cyclophilin	
ENSMUSP00000080995	7.8	ATP synthase subunit a (F-ATPase protein 6) IPR001421 ATPase F0-cplx su8 mt metazoan	68.421053
ENSMUSP00000099908	17.9	40S ribosomal protein S27a IPR002906 Ribosomal S27aIPR000626 Ubiquitin	157.01754
ENSMUSP00000110223	11.4	UPF0569 transmembrane protein	100
ENSMUSP00000028278	34.6	26S proteasome non-ATPase regulatory subunit 14 (26S proteasome regulatory subunit rpn11)(MAD1) IPR000555 Mov34 MPN PAD1	303.50877
ENSMUSP00000106968	18.4	Succinate dehydrogenase cytochrome b560 subunit, mitochondrial Precursor (Integral membrane protein CII-3)(QPs-1)(QPs1) IPR000701 Succ DHase cyt bsuIPR018495 Succ DHase cyt bsu CSIPR014314 Succ DHase cytb556IPR014361 Succ DHase cytb560	161.40351
ENSMUSP00000034304	41.8	Estradiol 17-beta-dehydrogenase 2 (EC 1.1.1.62)(Testosterone 17-beta-dehydrogenase)(EC 1.1.1.63)(17-beta-hydroxysteroid dehydrogenase 2)(17-beta-HSD 2) Source: 1.1.1.62 IPR003560 DHB DHaseIPR002198 DHase sc/Rdtase SDRIPR002347 Glc/ribitol DHaseIPR002424 Insect AlcDHase famIPR016040 NAD(P)-bd	366.66667
ENSMUSP00000088358	52.6	Selenium-binding protein 2 (56 kDa acetaminophen-binding protein)(AP56) IPR011048 Cyt cd1 nitrite Rdtase haem CIPR008826 Se bd	461.40351
ENSMUSP00000089302	13.6		119.29825
ENSMUSP00000029476	24.7	Vesicle-trafficking protein SEC22b (SEC22 vesicle-trafficking protein homolog B)(SEC22 vesicle-trafficking protein-like 1)(mSec22b)(ERS24)(ERS-24) IPR010908 LonginIPR011012 Longin likeIPR001388 Synaptobrevin	216.66667
ENSMUSP00000000284	70.7	Tripartite motif-containing protein 25 (Zinc finger protein 147)(Estrogen-responsive finger protein)(Efp) IPR001870 B302IPR003879 ButyrophylinIPR006574 PRYIPR003877 SPRY rcptIPR018355 SPla/RYanodine receptor sgIPR000315 Znf B-boxIPR001841 Znf RINGIPR017907 Znf RING CS	620.17544
ENSMUSP00000081567	135.9	Bromodomain and WD repeat-containing protein 2 (WD repeat-containing protein 11) IPR018215 Pept S14 ClpP CSIPR001680 WD40 repeatIPR011046 WD40 repeat-like	1192.1053
ENSMUSP00000002452	14.9	NADH dehydrogenase IPR003397 Tim17 Tim22	130.70175
ENSMUSP00000025095	12.4	Cytochrome c oxidase subunit 7A-related protein, mitochondrial Precursor (Cytochrome c oxidase subunit VIIa-related protein)(Silica-induced gene 81 protein)(SIG-81) IPR003177 Cyt c oxidase su7aIPR017267 Cyt c oxidase su7a-rel mt	108.77193
ENSMUSP00000007251	63	Protein BAT5 (HLA-B-associated transcript 5) IPR000073 AB hydrolase 1	552.63158
ENSMUSP00000108003	15.4	40S ribosomal protein S24 IPR001976 Ribosomal S24eIPR018098 Ribosomal S24e CS	135.08772
ENSMUSP00000029325	45.2	Arylacetamide deacetylase (AADAC)(EC 3.1.1.-) Source: 3.1.1.- IPR013094 AB hydrolase 3IPR017157 Arylacetamide deacetylaseIPR002168 Lipase GDXG AS	396.49123
ENSMUSP00000104816	23.4	Dolichol-phosphate mannosyltransferase (EC 2.4.1.83)(Dolichol-phosphate mannose synthase)(DPM synthase)(Dolichyl-phosphate beta-D-mannosyltransferase)(Mannose-P-dolichol synthase)(MPD synthase) Source: 2.4.1.83 IPR001173 Glyco trans 2	205.26316
ENSMUSP00000037446	101.4	Methionyl-tRNA synthetase, cytoplasmic (EC 6.1.1.10)(Methionine--tRNA ligase)(MetRS) Source: 6.1.1.10 IPR004046 GST CIPR010987 Glutathione-S-Trfase C-likeIPR002304 Met-tRNA-synth IaIPR009068 S15 NS1 RNA bdIPR012336 Thioredoxin-like foldIPR000738 WHEP-TRSIPR015413 aa-tRNA-synt IIPR001412 aa-tRNA-synth I CSIPR014758 tRNA-synt met NIPR009080 tRNAsynth 1a anticodon-bd	889.47368
ENSMUSP00000034326	132.3	Probable cation-transporting ATPase 13A1 (CATP)(EC 3.6.3.-) Source: 3.6.3.- IPR001757 ATPase PIPR008250 ATPase P-typ ATPase-assoc-regIPR018303 ATPase P-typ phosphor siteIPR006544 ATPase P-typ unknown-pump-spIPR005834 Dehalogen-like hydro	1160.5263
ENSMUSP00000032888	23.4	ADP-ribosylation factor-like protein 6-interacting protein 1 (ARL-6-interacting protein 1)(Aip-1)(Protein TBX2)	205.26316
ENSMUSP00000032761	28.1	Peroxisomal membrane protein 11A (Peroxin-11A)(Peroxisomal biogenesis factor 11A)(PEX11alpha) IPR008733 PEX11	246.49123
ENSMUSP00000060892	12	Transmembrane protein 93 IPR008504 DUF786	105.26316
ENSMUSP00000092557	104.5	GPI inositol-deacylase (EC 3.1.-.-)(Post-GPI attachment to proteins factor 1) Source: 3.1.-.- IPR012908 PGAP1	916.66667
ENSMUSP00000046856	83.1	Lanosterol synthase (EC 5.4.99.7)(Oxidosqualene--lanosterol cyclase)(OSC)(2,3-epoxysqualene--lanosterol cyclase)	728.94737

		Source: 5.4.99.7 IPR000923 BlueCu 1IPR001330 PrenyltransIPR018333 Squalene cyclaseIPR002365 Terpene synthIPR008930 Terpenoid cyclase/PrenylTrfase	
ENSMUSP00000100593	16.9	no description availableIPR012678 Ribosomal L23/L15e coreIPR005633 Ribosomal L23/L25 NIPR001014 Ribosomal L23 CSIPR013025 Ribosomal L25/23	148.24561
ENSMUSP00000022070	106.5	Endoplasmic reticulum aminopeptidase 1 (EC 3.4.11.-)(Adipocyte-derived leucine aminopeptidase)(A-LAP)(ARTS-1)(Aminopeptidase PILS)(Puromycin-insensitive leucyl-specific aminopeptidase)(PILS-AP)(VEGF-induced aminopeptidase) Source: 3.4.11.- IPR014782 Peptidase M1 N	934.21053
ENSMUSP00000021676	15.8	Probable ergosterol biosynthetic protein 28 IPR005352 Erg28	138.59649
ENSMUSP00000109310	31.4	Transmembrane protein 33 (Protein DB83) IPR005344 UPF0121	275.4386
ENSMUSP00000047218	35.3	Glyoxylate reductase/hydroxypyruvate reductase (EC 1.1.1.79) Source: 1.1.1.79 IPR006139 D-isomer 2 OHA DHaseIPR006140 D-isomer 2 OHA DHase NAD-bdIPR016040 NAD(P)-bd	309.64912
ENSMUSP00000092233	61	UDP glucuronosyltransferase 2 family, polypeptide B36 IPR002213 UDP glucos trans	535.08772
ENSMUSP00000066238	20.8	Ras-related protein Rap-1b Precursor (GTP-binding protein smg p21B) IPR003579 GTPase RabIPR003577 GTPase RasIPR003578 GTPase RhoIPR013684 Miro-likeIPR002041 Ran GTPaseIPR013753 RasIPR001806 Ras GTPaseIPR005225 Small GTP bd	182.45614
ENSMUSP00000049584	307.3	Inositol 1,4,5-trisphosphate receptor type 2 (Type 2 inositol 1,4,5-trisphosphate receptor)(Type 2 InsP3 receptor)(IP3 receptor isoform 2)(InsP3R2)(Inositol 1,4,5-trisphosphate type V receptor) IPR016024 ARM-type foldIPR000699 Ca-rel channelIPR014821 Ins145 P3 rcptIPR000493 InsP3 rcpt bdIPR005821 Ion transIPR003608 MIRIPR016093 MIR motifIPR013662 RIH assoc	2695.614
ENSMUSP00000007959	21.8	Transforming protein RhoA Precursor IPR006689 ARF/SARIPR003579 GTPase RabIPR003577 GTPase RasIPR003578 GTPase RhoIPR013684 Miro-likeIPR002041 Ran GTPaseIPR013753 RasIPR001806 Ras GTPaseIPR005225 Small GTP bd	191.22807
ENSMUSP00000031423	114.8	Sarcoplasmic/endoplasmic reticulum calcium ATPase 2 (SERCA2)(EC 3.6.3.8)(Calcium pump 2)(Calcium-transporting ATPase sarcoplasmic reticulum type, slow twitch skeletal muscle isoform)(SR Ca(2+)-ATPase 2)(Endoplasmic reticulum class 1/2 Ca(2+) ATPase) Source: 3.6.3.8 IPR001757 ATPase PIPR008250 ATPase P-typ ATPase-assoc-regIPR005782 ATPase P-typ Ca-transpIPR000695 ATPase P-typ H-transpIPR006069 ATPase P-typ cation-exchng asuIPR006068 ATPase P-typ cation-transptr CIPR004014 ATPase P-typ cation-transptr NIPR018303 ATPase P-typ phosphor siteIPR005834 Dehalogen-like hydro	1007.0175
ENSMUSP00000032824	47.4	26S protease regulatory subunit 6B (Proteasome 26S subunit ATPase 4)(MB67-interacting protein)(MIP224)(TAT-binding protein 7)(TBP-7)(CIP21) IPR005937 26S Psome P45IPR003593 AAA+ ATPase coreIPR011704 AAA 5IPR003960 AAA ATPase CSIPR003959 AAA ATPase coreIPR001957 Bac DnaAIPR001270 Chaprnin clpA/B	415.78947
ENSMUSP00000024223	26.7	Triosephosphate isomerase (TIM)(EC 5.3.1.1)(Triose-phosphate isomerase) Source: 5.3.1.1 IPR000652 Triosephosphate isomerase	234.21053
ENSMUSP00000090911	57.8	Liver carboxylesterase 31 Precursor (Esterase-31)(EC 3.1.1.1)(ES-male) Source: 3.1.1.1 IPR002018 CarbesteraseB	507.01754
ENSMUSP00000099769	19.7	Actin-related protein 2/3 complex subunit 4 (Arp2/3 complex 20 kDa subunit)(p20-ARC) IPR008384 ARPC4	172.80702
ENSMUSP00000101011	22.2	Phospholipid hydroperoxide glutathione peroxidase, mitochondrial Precursor (PHGPx)(EC 1.11.1.12)(GPX-4) Source: 1.11.1.12 IPR000889 Glutathione peroxidaseIPR012336 Thioredoxin-like fold	194.73684
ENSMUSP00000059501	11.4	Vesicle-associated membrane protein 8 (VAMP-8)(Endobrevin)(Edb) IPR001388 SynaptobrevinIPR016444 Synaptobrevin met/fun	100
ENSMUSP00000005953	50.2	Sulfide:quinone oxidoreductase, mitochondrial Precursor (EC 1.-.-.-) Source: 1.-.-.- IPR013027 FAD pyr nucl-diS OxRdtaseIPR000103 Pyridine nuc-diS OxRdtase 2	440.35088
ENSMUSP00000018875	105.7	AP-2 complex subunit beta-1 (Adapter-related protein complex 2 beta-1 subunit)(Beta2-adaptin)(Beta-adaptin)(Plasma membrane adaptor HA2/AP2 adaptin beta subunit)(Clathrin assembly protein complex 2 beta large chain)(AP105B) IPR016342 AP complex bsuIPR016024 ARM-type foldIPR000225 ArmadilloIPR009028 Calthrin/coatomer app sub CIPR002553 Clathrin/coatomer adapt-like NIPR013041 Clathrin/coatomer app Ig-likeIPR008152 Clathrin a/b/g-adaptin app IgIPR015151 Clathrin b-adaptin app sub CIPR000357 HEAT	927.19298
ENSMUSP00000045048	45.7	Heterogeneous nuclear ribonucleoprotein F (hnRNP F) IPR000504 RRM RNP1IPR012996 Znf CHHC	400.87719

ENSMUSP00000037341	16.3	NADH dehydrogenase IPR008698 NADH UbQ OxRdtase B18 su	142.98246
ENSMUSP00000011492	68.7	Acyl-CoA dehydrogenase family member 9, mitochondrial Precursor (ACAD-9)(EC 1.3.99.-) Source: 1.3.99.- IPR006091 Acyl-CoA DHase/Oxase MIPR013107 Acyl-CoA DHase 2 CIPR006089 Acyl-CoA DHase CSIPR006092 Acyl-CoA DHase NIPR006090 Acyl-CoA Oxase/DHase 1IPR009100 AcylCoA DH/oxidase M/NIPR009075 AcylCo DHase/oxidase C	602.63158
ENSMUSP00000018992	75.6	Arginyl-tRNA synthetase, cytoplasmic (EC 6.1.1.19)(Arginine--tRNA ligase)(ArgRS) Source: 6.1.1.19 IPR001278 Arg-tRNA-synth IcIPR005148 Arg-tRNA-synth Ic NIPR015945 Arg-tRNA-synth Ic coreIPR008909 DALR anticod bdIPR001412 aa-tRNA-synth I CSIPR009080 tRNAsynth 1a anticodon-bd	663.15789
ENSMUSP00000051921	19.1	Bone marrow stromal antigen 2 Precursor (BST-2)(HM1.24 antigen)(CD317 antigen)	167.54386
ENSMUSP00000023707	15.9	Superoxide dismutase Source: 1.15.1.1 IPR018152 SOD Cu/Zn BSIPR001424 SOD Cu Zn	139.47368
ENSMUSP00000110532	18.9	40S ribosomal protein S10 IPR005326 S10 plectin N	165.78947
ENSMUSP00000027810	54.3	Fumarate hydratase, mitochondrial Precursor (Fumarase)(EC 4.2.1.2)(EF-3) Source: 4.2.1.2 IPR003031 D crystallinIPR005677 Fum hydIIIPR000362 Fumarate lyaseIPR008948 L-Aspartase-like	476.31579
ENSMUSP00000044955	43.1	Protein tyrosine phosphatase-like protein PTPLAD1 (Protein-tyrosine phosphatase-like A domain-containing protein 1)(Butyrate-induced protein 1)(B-ind1) IPR017447 CSIPR007052 CS domainIPR008978 HSP20-like chaperoneIPR007482 Tyr Pase-like PTPLA	378.07018
ENSMUSP00000034277	23.3	Neighbor of COX4 IPR005366 UPF0172	204.38596
ENSMUSP00000021217	17.4	Nucleoside diphosphate kinase B (NDP kinase B)(NDK B)(EC 2.7.4.6)(nm23-M2)(P18) Source: 2.7.4.6 IPR001564 Nuc diP kinase core	152.63158
ENSMUSP00000095263	60	UDP-glucuronosyltransferase 1-7C Precursor (UDPGT)(UGT1*7C)(EC 2.4.1.17)(UGT1-07C)(UGT1.7C)(UGT1A7C)(UGT1A10) Source: 2.4.1.17 IPR002213 UDP glucos trans	526.31579
ENSMUSP00000021512	38.1	Dehydrogenase/reductase SDR family member 7 Precursor (EC 1.1.-.-)(Retinal short-chain dehydrogenase/reductase 4) Source: 1.1.-.- IPR003560 DHB DHaseIPR002198 DHase sc/Rdtase SDRIPR002347 Glc/ribitol DHaseIPR002424 Insect AlcDHase famIPR016040 NAD(P)-bdIPR013968 Polyketide synth KR	334.21053
ENSMUSP00000107237	34.4	Heterogeneous nuclear ribonucleoproteins C1/C2 (hnRNP C1 / hnRNP C2) IPR003954 RRM 1IPR000504 RRM RNP1IPR017347 hnRNP C Raly	301.75439
ENSMUSP00000047571	87.9	heterogeneous nuclear ribonucleoprotein U IPR000850 Adenylate kinIPR001870 B302IPR003034 SAP DNA bdIPR003877 SPRY rcptIPR018355 SPla/RYanodine receptor sg	771.05263
ENSMUSP00000021940	40.4	Vesicular integral-membrane protein VIP36 Precursor (Lectin mannose-binding 2) IPR008985 ConA like lec glIPR005052 Lectin leg	354.38596
ENSMUSP00000077909	46	Alpha-1-antitrypsin 1-4 Precursor (Serine protease inhibitor 1-4)(Serine protease inhibitor A1d)(Alpha-1 protease inhibitor 4) IPR000215 Protease inhib I4 serpin	403.50877
ENSMUSP00000099563	121.9	Myosin-Ic (Myosin I beta)(MMIb) IPR003593 AAA+ ATPase coreIPR000048 IQ CaM bd regionIPR001609 Myosin headIPR010926 Myosin tail 2	1069.2982
ENSMUSP00000006496	22.6	40S ribosomal protein S9 IPR001912 Ribosomal S4IPR005710 Ribosomal S4/S9 euk/arcIPR018079 Ribosomal S4 CSIPR002942 S4 RNA bd	198.24561
ENSMUSP00000004057	17.7	UPF0389 protein FAM162A (E2-induced gene 5 protein homolog) IPR009432 DUF1075	155.26316
ENSMUSP00000020241	51.9	Phenylalanine-4-hydroxylase (PAH)(EC 1.14.16.1)(Phe-4-monooxygenase) Source: 1.14.16.1 IPR002912 ACT bdIPR001273 ArAA hydroxylaseIPR018301 ArAA hydroxylase Fe/CU BSIPR005961 Phe-4-hydroxylase tetra	455.26316
ENSMUSP00000044405	60.9	Dimethylaniline monooxygenase Source: 1.14.13.8 IPR000759 Adrndx reductaseIPR013027 FAD pyr nucl-diS OxRdtaseIPR000960 Flavin mOaseIPR002253 Flavin mOase 1IPR002254 Flavin mOase 2IPR002255 Flavin mOase 3IPR002256 Flavin mOase 4IPR002257 Flavin mOase 5IPR012143 dManiline mOase	534.21053
ENSMUSP00000060912	50.4	L-gulonolactone oxidase (LGO)(EC 1.1.3.8)(L-gulono-gamma-lactone oxidase)(GLO) Source: 1.1.3.8 IPR007173 ALOIPR016166 FAD-bd 2IPR010031 FAD lactone oxidaseIPR006094 Oxid FAD bind NIPR006093 Oxy OxRdtase FAD BS	442.10526
ENSMUSP00000104179	22.9	40S ribosomal protein S5 IPR000235 Ribosomal S7IPR005716 Ribosomal S7 euk/arc	200.87719
ENSMUSP00000043580	47.4	Alpha-1,3-mannosyltransferase ALG2 (EC 2.4.1.-)(GDP-Man:Man(1)GlcNAc(2)-PP-dolichol	415.78947

		mannosyltransferase)(Asparagine-linked glycosylation protein 2) Source: 2.4.1.- IPR001296 Glyco trans 1	
ENSMUSP00000078236	41.7	Minor histocompatibility antigen H13 (EC 3.4.23.-)(Signal peptide peptidase)(Presenilin-like protein 3) Source: 3.4.23.- IPR006639 Peptidase A22IPR007369 Peptidase A22B SPP	365.78947
ENSMUSP00000108760	60.4	UDP-glucuronosyltransferase 1-7C Precursor (UDPGT)(UGT1*7C)(EC 2.4.1.17)(UGT1-07C)(UGT1.7C)(UGT1A7C)(UGT1A10) Source: 2.4.1.17 IPR002213 UDP glucos trans	529.82456
ENSMUSP00000031061	90.9	Putative pre-mRNA-splicing factor ATP-dependent RNA helicase DHX15 (EC 3.6.1.-)(DEAH box protein 15) Source: 3.6.1.- IPR003593 AAA+ ATPase coreIPR014001 DEAD-like NIPR001650 DNA/RNA helicase CIPR002464 DNA/RNA helicase DEAH CSIPR011709 DUF1605IPR007502 Helicase-assoc regIPR014021 Helicase SF1/SF2 ATP-bd	797.36842
ENSMUSP00000031726	37.3	Guanine nucleotide-binding protein G(I)/G(S)/G(T) subunit beta-2 (Transducin beta chain 2)(G protein subunit beta-2) IPR001632 Gprotein BIPR016346 Guanine nucleotide-bd bsuIPR001680 WD40 repeatIPR011046 WD40 repeat-likeIPR017986 WD40 repeat region	327.19298
ENSMUSP00000052258	72.7	Autocrine motility factor receptor (AMF receptor)(EC 6.3.2.19) Source: 6.3.2.19 IPR003892 CUEIPR001841 Znf RINGIPR011016 Znf RING-CH	637.7193
ENSMUSP00000016338	32.3	Corticosteroid 11-beta-dehydrogenase isozyme 1 (EC 1.1.1.146)(11-beta-hydroxysteroid dehydrogenase 1)(11-beta-HSD1)(11beta-HSD1A)(11-DH) Source: 1.1.1.146 IPR002198 DHase sc/Rdtase SDRIPR002347 Glc/ribitol DHaseIPR002424 Insect AlcDHase famIPR016040 NAD(P)-bd	283.33333
ENSMUSP00000043559	12.1	CDGSH iron sulfur domain-containing protein 1 (MitoNEET) IPR006622 FeS-containing CDGSH-typ	106.14035
ENSMUSP00000101105	61	Sulfated glycoprotein 1 Precursor (SGP-1)(Prosaposin) IPR003119 SapAIPR007856 SapB 1IPR008138 SapB 2IPR008373 SaposinIPR008139 SaposinBIPR011001 Saposin like	535.08772
ENSMUSP00000092746	15.5	NADH dehydrogenase	135.96491
ENSMUSP00000074935	43.5	FK506-binding protein 8 (EC 5.2.1.8)(Peptidyl-prolyl cis-trans isomerase)(PPIase)(Rotamase)(38 kDa FK506-binding protein)(mFKBP38)(FKBPR38) Source: 5.2.1.8 IPR001179 PPIase FKBPIPR001440 TPR-1IPR013105 TPR 2IPR013026 TPR region	381.57895
ENSMUSP00000029684	38.4	Secretory carrier-associated membrane protein 3 (Secretory carrier membrane protein 3) IPR000694 PRO richIPR007273 SCAMP	336.84211
ENSMUSP00000048363	52.6	Presenilin-1 (PS-1)(EC 3.4.23.-)(Protein S182) Source: 3.4.23.- IPR003568 Cyt c biogenesis CcmFIPR002031 Pept A22A PS1IPR006639 Peptidase A22IPR001108 Peptidase A22A	461.40351
ENSMUSP00000087192	38.3	D-beta-hydroxybutyrate dehydrogenase, mitochondrial Precursor (BDH)(EC 1.1.1.30)(3-hydroxybutyrate dehydrogenase) Source: 1.1.1.30 IPR003560 DHB DHaseIPR002198 DHase sc/Rdtase SDRIPR002347 Glc/ribitol DHaseIPR016040 NAD(P)-bd	335.96491
ENSMUSP00000029805	99	Microsomal triglyceride transfer protein large subunit Precursor IPR001747 Lipid transpt N	868.42105
ENSMUSP00000041149	12.5	Macrophage migration inhibitory factor (MIF)(EC 5.3.2.1)(Phenylpyruvate tautomerase)(Glycosylation-inhibiting factor)(GIF)(Delayed early response protein 6)(DER6) Source: 5.3.2.1 IPR001398 Macrophage inhib fac	109.64912
ENSMUSP00000029837	35	Uricase (EC 1.7.3.3)(Urate oxidase) Source: 1.7.3.3 IPR002042 Uricase	307.01754
ENSMUSP00000065585	58.1	Cytochrome P450 3A25 (EC 1.14.14.1)(CYPIIIA25) Source: 1.14.14.1 IPR001128 Cyt P450IPR002397 Cyt P450 BIPR017973 Cyt P450 CIPR017972 Cyt P450 CSIPR008072 Cyt P450 E CYP3AIPR002401 Cyt P450 E grp-IIPR002402 Cyt P450 E grp-IIIPR002403 Cyt P450 E grp-IV	509.64912
ENSMUSP00000059395	51	Eukaryotic translation initiation factor 2 subunit 3, X-linked (Eukaryotic translation initiation factor 2 subunit gamma, X-linked)(eIF-2-gamma X) IPR000795 ProtSyn GTP bdIPR001806 Ras GTPaseIPR009001 Transl elong EF1A/Init IF2 CIPR004161 Transl elong EFTu/EF1A 2IPR009000 Transl elong init/rib B-barrelIPR015256 eIF2 C	447.36842
ENSMUSP00000098053	63.9	Eukaryotic translation initiation factor 3 subunit D (eIF3d)(Eukaryotic translation initiation factor 3 subunit 7)(eIF-3-zeta)(eIF3 p66) IPR007783 EIF-3 zeta	560.52632
ENSMUSP00000023790	65.6	Keratin, type II cytoskeletal 1 (Cytokeratin-1)(CK-1)(Keratin-1)(K1)(67 kDa cytokeratin)(Krt1 protein) IPR016044 FIPR018039 Intermediate filament CSIPR002957 Keratin IIPR003054 Keratin IIIPR009053 PrefoldinIPR000817 PrionIPR003536 Transloc intimin rcpt	575.4386
ENSMUSP00000046910	17.8	15 kDa selenoprotein Precursor IPR014912 Sep15 SelM	156.14035

ENSMUSP00000063744	62.6	Heterogeneous nuclear ribonucleoprotein Q (hnRNP Q)(hnRNP-Q)(Synaptotagmin-binding, cytoplasmic RNA-interacting protein)(Glycine- and tyrosine-rich RNA-binding protein)(GRY-RBP)(NS1-associated protein 1)(pp68) IPR006535 HnRNP R QIPR002343 Hud Sxl RNAIPR000504 RRM RNP1	549.12281
ENSMUSP00000000137	44.7	Actin-related protein 2 (Actin-like protein 2) IPR004000 Actin like	392.10526
ENSMUSP00000039844	42.6	Alpha-centractin (Centractin)(Centrosome-associated actin homolog)(Actin-RPV)(ARP1) IPR004001 Actin CSIPR004000 Actin like	373.68421
ENSMUSP00000029217	21.7	NADH dehydrogenase	190.35088
ENSMUSP00000069004	17	40S ribosomal protein S15 (RIG protein) IPR005713 Ribosomal S15 euk/arcIPR002222 Ribosomal S19	149.12281
ENSMUSP00000023486	85.7	Transferrin receptor protein 1 (TfR1)(TfR)(TR)(Trfr)(CD71 antigen) IPR003137 PAIPR007365 Transferrin rcpt-like dimerise	751.75439
ENSMUSP00000030642	22.9	Proteasome subunit beta type-2 (EC 3.4.25.1)(Proteasome component C7-I)(Macropain subunit C7-I)(Multicatalytic endopeptidase complex subunit C7-I) Source: 3.4.25.1 IPR001353 Proteasome A B suIPR016050 Proteasome bsu CS	200.87719
ENSMUSP00000051657	32.7	26S proteasome non-ATPase regulatory subunit 8 (26S proteasome regulatory subunit S14) IPR005062 SAC3/GANP/Nin1/mts3/eIF-3-p25	286.84211
ENSMUSP00000035034	41.2	28S ribosomal protein S22, mitochondrial (S22mt)(MRP-S22)	361.40351
ENSMUSP00000037962	28.7	Peroxisomal membrane protein 11B (Peroxin-11B)(Peroxisomal biogenesis factor 11B)(PEX11beta)(Pex11pbeta) IPR008733 PEX11	251.75439
ENSMUSP00000040222	56.1	Cytosol aminopeptidase (EC 3.4.11.1)(Leucine aminopeptidase)(Leucyl aminopeptidase)(Leucine aminopeptidase 3)(LAP)(Proline aminopeptidase)(EC 3.4.11.5)(Prolyl aminopeptidase) Source: 3.4.11.1 IPR000819 Peptidase M17 CIPR008283 Peptidase M17 N	492.10526
ENSMUSP00000010254	39.7	Syntaxin-5 IPR004090 Chemotax Me-accpt rcptIPR006012 Syntaxin/epimorphin CSIPR006011 Syntaxin NIPR000727 T SNAREIPR010989 t-SNARE	348.24561
ENSMUSP00000029082	27.8	Proteasome subunit alpha type-7 (EC 3.4.25.1)(Proteasome subunit RC6-1) Source: 3.4.25.1 IPR001353 Proteasome A B suIPR000426 Proteasome alpha CS	243.85965
ENSMUSP00000091429	559.2	Ring finger protein 213 Fragment Source: UniProtKB/TrEMBL B1ATE2 IPR003593 AAA+ ATPase coreIPR009003 Pept Trypsin-like Ser/CysIPR001841 Znf RINGIPR017907 Znf RING CS	4905.2632
ENSMUSP00000085523	42.5	NADH dehydrogenase IPR002225 3Beta OHSteriod DHase/EstaseIPR001509 Epimerase deHydtaseIPR013120 Male sterile NAD-bdIPR016040 NAD(P)-bdIPR008030 NmrA	372.80702
ENSMUSP00000021719	6.7	6.8 kDa mitochondrial proteolipid IPR012574 Mit proteolip	58.77193
ENSMUSP00000002090	18.9	Translocon-associated protein subunit delta Precursor (TRAP-delta)(Signal sequence receptor subunit delta)(SSR-delta) IPR008855 TRAP-delta	165.78947
ENSMUSP00000080302	44.5	Phosphoglycerate kinase 1 (EC 2.7.2.3) Source: 2.7.2.3 IPR001576 Phosphoglycerate kinaseIPR015911 Phosphoglycerate kinase CS	390.35088
ENSMUSP00000095197	134.1	Leucyl-tRNA synthetase, cytoplasmic (EC 6.1.1.4)(Leucine--tRNA ligase)(LeuRS) Source: 6.1.1.4 IPR004493 Leu-tRNA-synth Ia arc/eukIPR013155 V/L/I-tRNA-synth anticodon-bdIPR015413 aa-tRNA-synt IIPR001412 aa-tRNA-synth I CSIPR002300 aa-tRNA-synth IaIPR009080 tRNAsynth 1a anticodon-bd	1176.3158
ENSMUSP00000055743	33.4	Thiosulfate sulfurtransferase (EC 2.8.1.1)(Rhodanese) Source: 2.8.1.1 IPR001763 Rhodanese-likeIPR001307 Thiosulphate STrfase CS	292.98246
ENSMUSP00000095655	20.7	Major urinary protein 2 Precursor (MUP 2) IPR002968 A1-microglobInIPR002447 BlactoglobulinIPR011038 Calycin likeIPR002345 LipocalinIPR000566 LipocIn cytFABPIPR002971 Maj urinaryIPR003087 N gelatinaseIPR002448 Odour bdIPR002972 PstgldnD synthIPR002450 vonEbner gland	181.57895
ENSMUSP00000099475	191.4	Clathrin heavy chain 1 IPR016024 ARM-type foldIPR000547 Clathrin H-chain/VPS repeatIPR015348 Clathrin H-chain linker coreIPR001473 Clathrin H-chain propeller NIPR016341 Clathrin heavy chain	1678.9474
ENSMUSP00000022437	63.6	2-hydroxyacyl-CoA lyase 1 (EC 4.1.-.-)(2-hydroxyphytanoyl-CoA lyase)(2-HPCL)(Phytanoyl-CoA 2-hydroxylase 2) Source: 4.1.-.- IPR012001 TPP bd enzyme NIPR012000 TPP enzyme MIPR011766 TPP enzyme bd C	557.89474
ENSMUSP00000014457	8.5	Cytochrome c oxidase polypeptide VIc IPR004204 Cyt c oxidase su6c	74.561404

ENSMUSP00000031910	26.1	protease, serine, 1 IPR009003 Pept Trypsin-like Ser/CysIPR018114 Peptidase S1/S6 ASIPR001314 Peptidase S1AIPR001254 Peptidase S1 S6	228.94737
ENSMUSP00000110027	77.6	Heterogeneous nuclear ribonucleoprotein M (hnRNP M) IPR000504 RRM RNP1	680.70175
ENSMUSP00000023085	15.3	NADH dehydrogenase IPR000104 Antifreeze 1IPR008011 Complex1 LYRIPR016488 NADH Ub cplx-1 asu su-6	134.21053
ENSMUSP00000003906	57.6	Phenylalanyl-tRNA synthetase alpha chain (EC 6.1.1.20)(Phenylalanine--tRNA ligase alpha chain)(PheRS) Source: 6.1.1.20 IPR013196 HTH 11IPR018157 Phe-tRNA-synth IIc CIPR004529 Phe-tRNA-synth IIc asuIPR006195 aa-tRNA-synth II	505.26316
ENSMUSP00000002043	55.8	Coiled-coil domain-containing protein 47 Precursor (Adipocyte-specific protein 4) IPR012879 DUF1682	489.47368
ENSMUSP00000021049	45.6	26S protease regulatory subunit 8 (Proteasome 26S subunit ATPase 5)(Proteasome subunit p45)(p45/SUG)(mSUG1) IPR005937 26S Psome P45IPR003593 AAA+ ATPase coreIPR011704 AAA 5IPR003960 AAA ATPase CSIPR003959 AAA ATPase coreIPR001806 Ras GTPase	400
ENSMUSP00000042285	37.3	UPF0554 protein C2orf43 homolog	327.19298
ENSMUSP00000034276	19.5	Cytochrome c oxidase subunit 4 isoform 1, mitochondrial Precursor (Cytochrome c oxidase subunit IV isoform 1)(COX IV-1)(Cytochrome c oxidase polypeptide IV) IPR004203 Cyt c oxidase su4IPR013288 Cyt c oxidase su4 sub	171.05263
ENSMUSP00000021329	24.7	Golgi SNAP receptor complex member 2 (27 kDa Golgi SNARE protein)(Membrin) IPR007705 V-SNARE	216.66667
ENSMUSP00000001452	60.6	T-complex protein 1 subunit gamma (TCP-1-gamma)(CCT-gamma)(Matricin)(mTRiC-P5) IPR012719 Chap CCT gammaIPR017998 Chaperone TCP-1IPR002194 Chaperonin TCP-1 CSIPR001844 Chaprnin Cpn60IPR002423 Cpn60/TCP-1	531.57895
ENSMUSP00000087948	112.4	Sec24 related gene family, member C IPR007123 GelsolnIPR018120 Glyco hydro 1 ASIPR000694 PRO richIPR012990 Sec23 24 beta SIPR006900 Sec23 helicalIPR006896 Sec23 trunkIPR006895 Znf Sec23 Sec24	985.96491
ENSMUSP00000008036	11.5	60S acidic ribosomal protein P1 IPR001813 Ribosomal 60SIPR001859 Ribosomal P2IPR017859 TCS treacle-like	100.87719
ENSMUSP00000081000	51.8	NADH-ubiquinone oxidoreductase chain 4 (EC 1.6.5.3)(NADH dehydrogenase subunit 4) Source: 1.6.5.3 IPR010227 NADH quinone OxRdtase I MIPR003918 NADHub OxRdtase 4IPR003916 NADHub OxRdtase 5IPR000260 OxRdtase q5 NIPR001750 Oxidored q1	454.38596
ENSMUSP00000085379	37.9	Prolactin regulatory element-binding protein (Mammalian guanine nucleotide exchange factor mSec12) IPR001680 WD40 repeatIPR011046 WD40 repeat-likeIPR017986 WD40 repeat region	332.45614
ENSMUSP00000032919	95.9	Major vault protein (MVP) IPR018247 EF HAND 1IPR002499 Vault N	841.22807
ENSMUSP00000013304	40.3	V-type proton ATPase subunit d 1 (V-ATPase subunit d 1)(Vacuolar proton pump subunit d 1)(V-ATPase AC39 subunit)(V-ATPase 40 kDa accessory protein)(P39)(Physophilin) IPR016727 ATPase V0-cplx dsuIPR002843 ATPase V0/A0-cplx csu/dsu	353.50877
ENSMUSP00000034586	10.9	Apolipoprotein C-III Precursor (Apo-CIII)(ApoC-III) IPR008403 Apo-CIII	95.614035
ENSMUSP00000014221	22.4	Calcium-binding protein p22 (Calcium-binding protein CHP)(Calcineurin homologous protein)(Sid 470) IPR018247 EF HAND 1IPR018249 EF HAND 2IPR018248 EF handIPR002048 EF hand Ca bdIPR008080 ParvalbuminIPR001125 Recoverin	196.49123
ENSMUSP00000021790	11.6	Transmembrane protein 14C IPR005349 UPF0136 TM	101.75439
ENSMUSP00000032065	56.5	Prenylcysteine oxidase Precursor (EC 1.8.3.5) Source: 1.8.3.5 IPR000759 Adrndx reductaseIPR006076 FAD-dep OxRdtaseIPR013027 FAD pyr nucl-diS OxRdtaseIPR010795 Prenylcys lyaseIPR017046 Prenylcysteine Oxase	495.61404
ENSMUSP00000023514	15.1	NADH dehydrogenase IPR009866 NADH UbQ OxRdtase NDUFB4 su	132.45614
ENSMUSP00000026735	45.1	Coiled-coil domain-containing protein 51	395.61404
ENSMUSP00000093955	50	Elongation factor 1-gamma (EF-1-gamma)(eEF-1B gamma) IPR004046 GST CIPR010987 Glutathione-S-Trfase C-likeIPR004045 Glutathione S-Trfase NIPR012336 Thioredoxin-like foldIPR001662 Transl elong EF1 G con	438.59649
ENSMUSP00000029815	15.2	CDGSH iron sulfur domain-containing protein 2 (MitoNEET-related 1 protein)(Miner1)(Nervous system over-expressed protein 70) IPR006622 FeS-containing CDGSH-typ	133.33333
ENSMUSP00000022865	63.8	Protein LYRIC (Lysine-rich CEACAM1 co-isolated protein)(3D3/LYRIC)(Metastasis adhesion protein)(Metadherin)	559.64912

ENSMUSP00000018851	531.7	Cytoplasmic dynein 1 heavy chain 1 (Cytoplasmic dynein heavy chain 1)(Dynein heavy chain, cytosolic) IPR003593 AAA+ ATPase coreIPR011704 AAA 5IPR004273 Dynein heavyIPR013594 Dynein heavy N 1IPR013602 Dynein heavy N 2IPR010987 Glutathione-S-Trfase C-likeIPR000169 Pept cys ASIPR012336 Thioredoxin-like fold	4664.0351
ENSMUSP00000075954	47.6	Glyceraldehyde-3-phosphate dehydrogenase, testis-specific (EC 1.2.1.12)(Spermatogenic glyceraldehyde-3-phosphate dehydrogenase)(Spermatogenic cell-specific glyceraldehyde 3-phosphate dehydrogenase 2)(GAPDH-2) Source: 1.2.1.12 IPR000173 GlycerAld 3-P DHaseIPR006424 Glyceraldehyde-3-P DHase 1IPR000381 Inhibin betaBIPR006030 Mollsc rhodpsn CIPR016040 NAD(P)-bdIPR000694 PRO richIPR003882 Pistil extensinIPR003267 Small Pro richIPR017997 Vinculin	417.54386
ENSMUSP00000024932	15.8	V-type proton ATPase 16 kDa proteolipid subunit (V-ATPase 16 kDa proteolipid subunit)(Vacuolar proton pump 16 kDa proteolipid subunit)(PL16) IPR002379 ATPase F0/V0-cplx csuIPR000245 ATPase V0-cplx csuIPR011555 ATPase V0-cplx csu eukIPR001036 Acrflvin-RIPR013281 Apop reg Mc1	138.59649
ENSMUSP00000080403	36	TraB domain containing (Trabd), mRNA IPR002816 Pheromone shutdown-rel TraB	315.78947
ENSMUSP00000106014	12.8	60S ribosomal protein L30 IPR000948 Ribosomal HS6IPR000231 Ribosomal L30eIPR004038 Ribosomal L7Ae/L30e/S12e/Gad45	112.2807
ENSMUSP00000079340	12.2	60S ribosomal protein L36 IPR000509 Ribosomal L36e	107.01754
ENSMUSP00000031707	102.9	Alpha-aminoadipic semialdehyde synthase, mitochondrial Precursor (LKR/SDH) Source: 1.5.1.8 IPR007698 Ala DHase/PNT CIPR007886 Ala DHase/PNT NIPR016040 NAD(P)-bdIPR005097 Saccharopine DHase	902.63158
ENSMUSP00000083973	14.5	40S ribosomal protein S12 IPR004038 Ribosomal L7Ae/L30e/S12e/Gad45IPR000530 Ribosomal S12e	127.19298
ENSMUSP00000108229	31.2	Cation-dependent mannose-6-phosphate receptor Precursor (CD Man-6-P receptor)(CD-MPR)(46 kDa mannose 6-phosphate receptor)(MPR 46) IPR009011 Man6P isomerase rcpt bdIPR000296 Man 6 P rcpt	273.68421
ENSMUSP00000030698	31.2	Syntaxin-12 IPR006012 Syntaxin/epimorphin CSIPR006011 Syntaxin NIPR000727 T SNAREIPR010989 t-SNARE	273.68421
ENSMUSP00000076589	57.6	Glucosylceramidase Precursor (EC 3.2.1.45)(Beta-glucocerebrosidase)(Acid beta-glucosidase)(D-glucosyl-N-acylsphingosine glucohydrolase) Source: 3.2.1.45 IPR001139 Glyco hydro 30IPR017853 Glyco hydro cat	505.26316
ENSMUSP00000005647	30.1	NADH dehydrogenase Source: 1.6.5.3 IPR010218 NADH DH csuIPR001268 NADH DHase Ub 30kDa su	264.03509
ENSMUSP00000015100	37.2	Serine/threonine-protein phosphatase PP1-beta catalytic subunit (PP-1B)(EC 3.1.3.16) Source: 3.1.3.16 IPR004843 M-pesteraseIPR006186 T phtase apaH	326.31579
ENSMUSP00000080998	13.2	NADH-ubiquinone oxidoreductase chain 3 (EC 1.6.5.3)(NADH dehydrogenase subunit 3) Source: 1.6.5.3 IPR000440 Oxidored q4	115.78947
ENSMUSP00000106104	14.9	Histone H2B type 1-F/J/L (H2B 291A) IPR009072 Histone-foldIPR000558 Histone H2BIPR007125 Histone core D	130.70175
ENSMUSP00000042150	23.7	Ras-related protein R-Ras Precursor (p23) IPR006688 ARFIPR003579 GTPase RabIPR003577 GTPase RasIPR003578 GTPase RhoIPR013684 Miro-likeIPR002041 Ran GTPaseIPR013753 RasIPR001806 Ras GTPaseIPR005225 Small GTP bd	207.89474
ENSMUSP00000041968	36.5	26S proteasome non-ATPase regulatory subunit 7 (26S proteasome regulatory subunit rpn8)(26S proteasome regulatory subunit S12)(Proteasome subunit p40)(Mov34 protein) IPR000555 Mov34 MPN PAD1	320.17544
ENSMUSP00000039264	78.8	Antigen peptide transporter 1 (APT1)(Peptide transporter TAP1)(ATP-binding cassette sub-family B member 2)(Histocompatibility antigen modifier 1) IPR003593 AAA+ ATPase coreIPR013305 ABC B2IPR011527 ABC TM 1IPR001140 ABC TM transptIPR003439 ABC transporter-likeIPR017871 ABC transporter CSIPR017940 ABC transporter type1IPR005293 Ag transporter2	691.22807
ENSMUSP00000033008	29.5	Proteasome subunit alpha type-1 (EC 3.4.25.1)(Proteasome component C2)(Macropain subunit C2)(Multicatalytic endopeptidase complex subunit C2)(Proteasome nu chain) Source: 3.4.25.1 IPR001353 Proteasome A B suIPR000426 Proteasome alpha CS	258.77193
ENSMUSP00000071214	36.1	Eukaryotic translation initiation factor 2 subunit 1 (Eukaryotic translation initiation factor 2 subunit alpha)(eIF-2-alpha)(EIF-2alpha)(EIF-2A) IPR011488 EIF 2 alphaIPR016027 NA-bd OB-fold-likeIPR003029 S1 RNA-bd	316.66667
ENSMUSP00000027853	14.3	Brain protein 44 IPR005336 UPF0041	125.4386
ENSMUSP00000090284	17.8	60S ribosomal protein L12 IPR000911 Ribosomal L11	156.14035
ENSMUSP00000081474	11.6	60S acidic ribosomal protein P2 IPR001813 Ribosomal 60SIPR001859 Ribosomal P2IPR017859 TCS treacle-like	101.75439

ENSMUSP00000021993	13.6	Cytochrome b-c1 complex subunit 7 (Ubiquinol-cytochrome c reductase complex 14 kDa protein)(Complex III subunit 7)(Complex III subunit VII) IPR003197 Cyt bd ubiquinol oxidase 14kDa	119.29825
ENSMUSP00000042988	17.1	Thyroid hormone-inducible hepatic protein (Spot 14 protein)(SPOT14)(S14 protein) IPR009786 Spot 14	150
ENSMUSP00000030914	23	Protein RER1 IPR004932 Rer1	201.75439
ENSMUSP00000107966:reversed	371.7		3260.5263
ENSMUSP00000107749	32.4	Malectin Precursor	284.21053
ENSMUSP00000060523	9.5	40S ribosomal protein S27 IPR000592 Ribosomal S27eIPR011332 Ribosomal zn-bd	83.333333
ENSMUSP00000030340	59.1	Non-specific lipid-transfer protein (EC 2.3.1.176)(Propanoyl-CoA C-acyltransferase)(NSL-TP)(Sterol carrier protein 2)(SCP-2)(Sterol carrier protein X)(SCP-X)(SCP-chi)(SCPX) Source: 2.3.1.176 IPR003033 SCP2 sterol bdIPR016083 Sterol-binding-likeIPR002155 ThiolaseIPR016039 Thiolase-like	518.42105
ENSMUSP00000029610	34.4	Hydroxyacyl-coenzyme A dehydrogenase, mitochondrial Precursor (HCDH)(EC 1.1.1.35)(Short chain 3-hydroxyacyl-CoA dehydrogenase)(Medium and short chain L-3-hydroxyacyl-coenzyme A dehydrogenase) Source: 1.1.1.35 IPR006180 3-OHacyl-CoA DHase CSIPR006176 3-OHacyl-CoA DHase NAD-bdIPR006108 3HC DHase CIPR008927 6-PGluconate DH C likeIPR000447 FAD-dep Gly3P DHaseIPR006036 K uptake TrkAIPR016040 NAD(P)-bd	301.75439
ENSMUSP00000036541	20.8	Trafficking protein particle complex subunit 5 IPR007194 TRAPP Bet3IPR016696 TRAPP I complex Trs31	182.45614
ENSMUSP00000032196	21.5	ADP-ribosylation factor-like protein 8B (ADP-ribosylation factor-like protein 10C)(Novel small G protein indispensable for equal chromosome segregation 1) IPR006688 ARFIPR006689 ARF/SARIPR003579 GTPase RabIPR003577 GTPase RasIPR001019 Gprotein alph bdIPR013684 Miro-likeIPR013753 RasIPR001806 Ras GTPaseIPR006687 SAR1 GTP bdIPR005225 Small GTP bd	188.59649
ENSMUSP00000030169	38.4	Stomatin-like protein 2 (SLP-2) IPR001107 Band 7IPR001972 Stomatin	336.84211
ENSMUSP00000020920	76.9	Regulator of G-protein signaling 9 (RGS9) IPR015898 G-protein gamma-likeIPR000591 Pleckstrin/G-protein interactIPR000342 Regulat G prot signalIPR016137 Regulat G prot signal superfam	674.5614
ENSMUSP00000023851	13.4	NADH dehydrogenase IPR006806 ETC CI 29 9	117.54386
ENSMUSP00000105886	36	Uncharacterized protein C20orf116 homolog precursor. Source: Uniprot/SWISSPROT Q80WW9	315.78947
ENSMUSP00000095433	571.9	E3 ubiquitin-protein ligase UBR4 (EC 6.3.2.-)(N-recognin-4)(Zinc finger UBR1-type protein 1)(p600) Source: 6.3.2.-IPR016024 ARM-type foldIPR018187 Asp/Glu racemase CSIPR000694 PRO richIPR011046 WD40 repeat-likeIPR007087 Znf C2H2IPR003126 Znf N-recogninIPR013993 Znf N-recognin met	5016.6667
ENSMUSP00000032425	30	Transmembrane protein 111 IPR008568 DUF850 TM euk	263.15789
ENSMUSP00000022781	12.5	Dolichyl-diphosphooligosaccharide--protein glycosyltransferase subunit DAD1 (Oligosaccharyl transferase subunit DAD1)(EC 2.4.1.119)(Defender against cell death 1)(DAD-1) Source: 2.4.1.119 IPR003038 DAD	109.64912
ENSMUSP00000015950	25.6	Dihydropteridine reductase (EC 1.5.1.34)(HDHPR)(Quinoid dihydropteridine reductase) Source: 1.5.1.34 IPR002198 DHase sc/Rdtase SDRIPR002347 Glc/ribitol DHaseIPR016040 NAD(P)-bd	224.5614
ENSMUSP00000001547	137.9	Collagen alpha-1(I) chain Precursor (Alpha-1 type I collagen) IPR008160 CollagenIPR000885 Fib collagen CIPR002181 Fibrinogen a/b/g CIPR000694 PRO richIPR003979 TropoelastinIPR006552 VWC outIPR001007 VWF C	1209.6491
ENSMUSP00000066682	65	Lipase maturation factor 1 (Transmembrane protein 112) IPR009613 DUF1222	570.17544
ENSMUSP00000045394	37.2	aldo-keto reductase family 1, member C14 IPR001395 Aldo/ket redIPR018170 Aldo/ket reductase CS	326.31579
ENSMUSP00000039657	112.9	Sodium/potassium-transporting ATPase subunit alpha-1 Precursor (Sodium pump subunit alpha-1)(EC 3.6.3.9)(Na(+)/K(+) ATPase alpha-1 subunit) Source: 3.6.3.9 IPR001757 ATPase PIPR008250 ATPase P-typ ATPase-assoc-regIPR000695 ATPase P-typ H-transpIPR005775 ATPase P-typ cation-ex asu eukIPR006069 ATPase P-typ cation-exchng asuIPR006068 ATPase P-typ cation-transptr CIPR004014 ATPase P-typ cation-transptr NIPR018303 ATPase P-typ phosphor siteIPR005834 Dehalogen-like hydro	990.35088
ENSMUSP00000054634	21.2	Cell division control protein 42 homolog Precursor (G25K GTP-binding protein) IPR006689 ARF/SARIPR003579 GTPase RabIPR003577 GTPase RasIPR003578 GTPase RhoIPR006036 K uptake TrkAIPR013684 Miro-likeIPR002041 Ran GTPaseIPR013753 RasIPR001806 Ras GTPaseIPR005225 Small GTP bd	185.96491

ENSMUSP00000030660	20.3	Trafficking protein particle complex subunit 3 (BET3 homolog) IPR007194 TRAPP Bet3IPR016721 TRAPP I complex Bet3	178.07018
ENSMUSP00000019382	36.1	Synaptic glycoprotein SC2 (EC 1.3.1.-)(Trans-2,3-enoyl-CoA reductase)(TER) Source: 1.3.1.- IPR001104 3-oxo-5 a-steroid 4-DHase C	316.66667
ENSMUSP00000026649	24.8	Synaptogyrin-2 (Cellugyrin) IPR008253 MarvelIPR016579 Synaptogyrin	217.54386
ENSMUSP00000100505	21.9	no description availableIPR000554 Ribosomal S7e	192.10526
ENSMUSP00000045930	517.4	Probable E3 ubiquitin-protein ligase MYCBP2 (EC 6.3.2.-)(Myc-binding protein 2)(Protein associated with Myc)(Pam/highwire/rpm-1 protein) Source: 6.3.2.- IPR001298 FilaminIPR017868 Filamin/ABP280 repeat likeIPR008979 Galactose-bd-likeIPR014756 Ig E-setIPR012983 PHRIPR000408 Reg chr condensIPR009091 Reg csome cond/b-lactamase inhIPR000315 Znf B-boxIPR001841 Znf RING	4538.5965
ENSMUSP00000102211	8.2	60S ribosomal protein L38 IPR002675 Ribosomal L38e	71.929825
ENSMUSP00000025217	73.4	Stress-70 protein, mitochondrial Precursor (75 kDa glucose-regulated protein)(GRP 75)(Heat shock 70 kDa protein 9)(Peptide-binding protein 74)(PBP74)(P66 MOT)(Mortalin) IPR012725 DnaK prokIPR018247 EF HAND 1IPR018181 Heat shock 70 CSIPR001023 Hsp70IPR013126 Hsp 70	643.85965
ENSMUSP00000018905	26.4	Mannose-P-dolichol utilization defect 1 protein (Suppressor of Lec15 and Lec35 glycosylation mutation homolog)(SL15) IPR006603 CTNSIPR005282 LC transporterIPR016817 MannP-dilichol defect-1	231.57895
ENSMUSP00000015725	26.2	Vesicle transport protein SEC20 IPR005606 Sec20	229.82456
ENSMUSP00000106709	18.7	AP-1 complex subunit sigma-1A (Adapter-related protein complex 1 sigma-1A subunit)(Adaptor protein complex AP-1 sigma-1A subunit)(Sigma-adaptin 1A)(Sigma1A-adaptin)(Golgi adaptor HA1/AP1 adaptin sigma-1A subunit)(HA1 19 kDa subunit)(Clathrin assembly protein complex 1 sigma-1A small chain)(Clathrin coat assembly protein AP19)(Sigma 1a subunit of AP-1 clathrin) IPR016635 AP complex ssuIPR000804 Clathrin sigma/coatomer zetaIPR011012 Longin like	164.03509
ENSMUSP00000087974	18.6	ATP synthase, H+ transporting, mitochondrial F0 complex, subunit d Fragment Source: UniProtKB/TrEMBL B1ASE2 IPR008689 ATPase F0-cplx dsu mt	163.15789
ENSMUSP00000056604	14.2	Histone H2B type 1-A (Histone H2B, testis)(Testis-specific histone H2B) IPR009072 Histone-foldIPR000558 Histone H2BIPR007125 Histone core D	124.5614
ENSMUSP00000053900	54.7	CAAX prenyl protease 1 homolog (EC 3.4.24.84)(Prenyl protein-specific endoprotease 1)(Farnesylated proteins-converting enzyme 1)(FACE-1)(Zinc metalloproteinase Ste24 homolog) Source: 3.4.24.84 IPR001915 Peptidase M48	479.82456
ENSMUSP00000088581	44.7	Ferrochelatase, mitochondrial Precursor (EC 4.99.1.1)(Protoheme ferro-lyase)(Heme synthetase) Source: 4.99.1.1 IPR001015 Ferrochelatase	392.10526
ENSMUSP00000096435	54.2	Probable ATP-dependent RNA helicase DDX6 (EC 3.6.1.-)(DEAD box protein 6)(ATP-dependent RNA helicase p54)(Oncogene RCK homolog) Source: 3.6.1.- IPR014001 DEAD-like NIPR001650 DNA/RNA helicase CIPR011545 DNA/RNA helicase DEAD/DEAH NIPR014021 Helicase SF1/SF2 ATP-bdIPR000629 RNA-helicase DEAD-box CSIPR014014 RNA helicase DEAD Q motif	475.4386
ENSMUSP00000006435	56.5	V-type proton ATPase subunit B, brain isoform (V-ATPase subunit B 2)(Vacuolar proton pump subunit B 2)(Endomembrane proton pump 58 kDa subunit) IPR000793 ATPase F1/V1/A1-cplx a/bsu CIPR004100 ATPase F1/V1/A1-cplx a/bsu NIPR000194 ATPase F1/V1/A1 a/bsu nucl-bdIPR005723 ATPase V1-cplx bsu	495.61404
ENSMUSP00000085251	12.5	60S ribosomal protein L35a IPR001780 Ribosomal L35AeIPR018266 Ribosomal L35Ae CS	109.64912
ENSMUSP00000068568	67.3	All-trans-retinol 13,14-reductase Precursor (EC 1.3.99.23)(All-trans-13,14-dihydroretinol saturase)(RetSat) Source: 1.3.99.23 IPR000759 Adrndx reductaseIPR006076 FAD-dep OxRdtaseIPR002005 Rab GDI REP	590.35088
ENSMUSP00000025955	161.8	Eukaryotic translation initiation factor 3 subunit A (eIF3a)(Eukaryotic translation initiation factor 3 subunit 10)(eIF-3-theta)(eIF3 p167)(eIF3 p180)(eIF3 p185)(p162)(Centrosomin) IPR000717 PCI	1419.2982
ENSMUSP00000079232	36.8	aldo-keto reductase family 1, member C20 IPR001395 Aldo/ket redIPR018170 Aldo/ket reductase CS	322.80702
ENSMUSP00000099788	75.2	Annexin A6 (Annexin-6)(Annexin VI)(Lipocortin VI)(p68)(p70)(Protein III)(Chromobindin-20)(67 kDa calelectrin)(Calphobindin-II)(CPB-II) IPR001464 AnnexinIPR002391 AnnexinIVIPR002392 AnnexinVIPR002393 AnnexinVIIPR018502 Annexin repeatIPR018252 Annexin repeat CS	659.64912
ENSMUSP00000109671	265.5	SON protein IPR001159 Ds-RNA bdIPR000467 G patchIPR000694 PRO richIPR011046 WD40 repeat-like	2328.9474

ENSMUSP00000093965	109.3	Neutral alpha-glucosidase AB Precursor (EC 3.2.1.84)(Glucosidase II subunit alpha)(Alpha-glucosidase 2) Source: 3.2.1.84 IPR000322 Glyco hydro 31IPR017853 Glyco hydro cat	958.77193
ENSMUSP00000029722	29.9	40S ribosomal protein S3a IPR001593 Ribosomal S3AeIPR018281 Ribosomal S3Ae CS	262.2807
ENSMUSP00000047356	48.5	interferon gamma induced GTPase IPR007743 Interferon-inducible GTPase	425.4386
ENSMUSP00000039726	10.3	ATP synthase subunit f, mitochondrial	90.350877
ENSMUSP00000072775	32.9	no description availableIPR000504 RRM RNP1	288.59649
ENSMUSP00000075987	39.6	Phosphate carrier protein, mitochondrial Precursor (Phosphate transport protein)(PTP)(Solute carrier family 25 member 3) IPR002113 Aden trnslctorIPR002067 Mit carrierIPR001993 Mitoch carrierIPR018108 Mitochondrial sb/sol carrier	347.36842
ENSMUSP00000044050	87.4	Dipeptidyl peptidase 4 (EC 3.4.14.5)(Dipeptidyl peptidase IV)(DPP IV)(T-cell activation antigen CD26)(Thymocyte-activating molecule)(THAM)(CD26 antigen) Source: 3.4.14.5 IPR002471 Pept S9 ASIPR001375 Peptidase S9IPR002469 Peptidase S9B	766.66667
ENSMUSP00000019198	17	Mitochondrial fission 1 protein (Fis1 homolog)(Tetratricopeptide repeat protein 11)(TPR repeat protein 11) IPR016543 Tetratricopeptide rpt 11 Fis1	149.12281
ENSMUSP00000050446	46.5	Immunity-related GTPase family M protein (EC 3.6.5.-)(Immunity-related GTPase family M protein 1)(Interferon-inducible protein 1)(LPS-stimulated RAW 264.7 macrophage protein 47)(LRG-47) Source: 3.6.5.- IPR007743 Interferon-inducible GTPase	407.89474
ENSMUSP00000028225	55.9	26S proteasome non-ATPase regulatory subunit 5 (26S proteasome subunit S5B)(26S protease subunit S5 basic) IPR016024 ARM-type fold	490.35088
ENSMUSP00000054856	7.4	Cytochrome b-c1 complex subunit 9 (Ubiquinol-cytochrome c reductase complex 7.2 kDa protein)(Cytochrome c1 non-heme 7 kDa protein)(Complex III subunit X)(Complex III subunit 9) IPR008027 Ubiquinol cyt c Rdtase QCR9	64.912281
ENSMUSP00000067681	10	Protein transport protein Sec61 subunit beta IPR005609 Sec61 betaIPR016482 Sec61 beta euk	87.719298
sp|TRY1_BOVIN|	25.4	Cationic trypsin; EC 3.4.21.4; Beta-trypsin; Contains: Alpha-trypsin chain 1; Contains: Alpha-trypsin chain 2; Flags: Precursor;	222.80702
ENSMUSP00000100074	13.4	40S ribosomal protein S20 IPR001848 Ribosomal S10IPR018268 Ribosomal S10 CSIPR005729 Ribosomal S10 euk/arc	117.54386
ENSMUSP00000031931	26.4	trypsinogen 7 IPR009003 Pept Trypsin-like Ser/CysIPR018114 Peptidase S1/S6 ASIPR001314 Peptidase S1AIPR001254 Peptidase S1 S6	231.57895
ENSMUSP00000030164	89.3	Transitional endoplasmic reticulum ATPase (TER ATPase)(15S Mg(2+)-ATPase p97 subunit)(Valosin-containing protein)(VCP) IPR003593 AAA+ ATPase coreIPR011704 AAA 5IPR003960 AAA ATPase CSIPR003959 AAA ATPase coreIPR005938 AAA CDC48IPR003338 ATPaseVAT NIPR009010 Asp de-COase-like foldIPR000641 CbxX CfqX	783.33333
ENSMUSP00000024797	69.8	molybdenum cofactor synthesis 1 isoform 1 IPR006638 Elp3/MiaB/NifBIPR013483 MoaAIPR000385 MoaA NifB PqqE Fe-S bd CSIPR010505 Mob synth CIPR002820 Mopterin CF MoaC regIPR007197 Radical SAM	612.2807
ENSMUSP00000045111	25.8	28S ribosomal protein S34, mitochondrial (S34mt)(MRP-S34)(T-complex expressed gene 2 protein)	226.31579
ENSMUSP00000101139	16.3	Sorting nexin-3 (SDP3 protein) IPR001683 PX	142.98246
ENSMUSP00000035105	32.8	40S ribosomal protein SA (Laminin receptor 1)(p40)(34/67 kDa laminin receptor)(37 kDa oncofetal antigen)(OFA/iLRP) IPR001865 Ribosomal S2IPR018130 Ribosomal S2 CSIPR005707 Ribosomal S2 euk/arc	287.7193
ENSMUSP00000023677	23.3	ATP synthase subunit O, mitochondrial Precursor (Oligomycin sensitivity conferral protein)(OSCP) IPR000711 ATPase F1-cplx OSCP/dsu	204.38596
ENSMUSP00000093959	75	Metastasis-associated protein MTA2 (Metastasis-associated 1-like 1) IPR001025 BAHIPR000949 ELM2IPR009057 Homeodomain likeIPR014778 Myb DNA-bdIPR001005 SANT DNA-bdIPR000679 Znf GATA	657.89474
ENSMUSP00000034000	44.6	Acid ceramidase Precursor (AC)(EC 3.5.1.23)(Acylsphingosine deacylase)(N-acylsphingosine amidohydrolase) Source: 3.5.1.23 IPR016699 Acid ceramidase-likeIPR003199 Chologlycine hydro	391.22807
ENSMUSP00000023238	53.2	Gasdermin-D (Gasdermin domain-containing protein 1) IPR007677 DFNA5	466.66667
ENSMUSP00000059801	85.2	6-phosphofructokinase, muscle type (EC 2.7.1.11)(Phosphofructokinase 1)(Phosphohexokinase)(Phosphofructo-1-kinase isozyme A)(PFK-A)(Phosphofructokinase-M) Source: 2.7.1.11 IPR009161 6-phosphofructokinase eukIPR015912 Phosphofructokinase CSIPR000023 Ppfruckinase	747.36842

ENSMUSP00000025802	23.2	Nucleoside diphosphate-linked moiety X motif 8, mitochondrial Precursor (Nudix motif 8)(EC 3.6.1.-) Source: 3.6.1.- IPR015797 NUDIXIPR000086 NUDIX hydrolase core	203.50877
ENSMUSP00000033483	70.8	Coiled-coil domain-containing protein 22 IPR008530 DUF812IPR000533 Tropomyosin	621.05263
ENSMUSP00000045654	12.4	Brain protein 44-like protein IPR005336 UPF0041	108.77193
ENSMUSP00000029777	31.2	Transmembrane protein 56 IPR006634 TLC	273.68421
ENSMUSP00000060940	43.4	Reticulon-4-interacting protein 1 Precursor (NOGO-interacting mitochondrial protein) IPR013154 AlcDHase GroES-likeIPR013149 AlcDHase Zn-bdIPR011032 GroES likeIPR016040 NAD(P)-bdIPR002364 Quin OxRdtase/zeta-crystal CS	380.70175
ENSMUSP00000020640	35.1	Guanine nucleotide-binding protein subunit beta-2-like 1 (Receptor of activated protein kinase C 1)(RACK1)(Receptor for activated C kinase)(p205)(12-3) IPR001680 WD40 repeatIPR011046 WD40 repeat-likeIPR017986 WD40 repeat region	307.89474
ENSMUSP00000023513	19	cytochrome P450, family 2, subfamily ab, polypeptide 1 IPR001128 Cyt P450IPR017973 Cyt P450 CIPR017972 Cyt P450 CSIPR002401 Cyt P450 E grp-IIPR002403 Cyt P450 E grp-IV	166.66667
ENSMUSP00000040853	38.2	Agmatinase, mitochondrial Precursor (EC 3.5.3.11)(Agmatine ureohydrolase)(AUH) Source: 3.5.3.11 IPR005925 AgmatinaseIPR005924 ArginaseIPR006035 Ureohydrolase	335.08772
ENSMUSP00000099480	14.7	60S ribosomal protein L22 (Heparin-binding protein HBp15) IPR002671 Ribosomal L22e	128.94737
ENSMUSP00000041907	32.4	Junctional adhesion molecule A Precursor (JAM-A)(Junctional adhesion molecule 1)(JAM-1)(CD321 antigen) IPR013151 IgIPR007110 Ig-likeIPR003597 Ig C1-setIPR013098 Ig I-setIPR013106 Ig V-setIPR003596 Ig V-set subIPR003599 Ig subIPR003598 Ig sub2	284.21053
ENSMUSP00000095081	21.2	Transmembrane and coiled-coil domain-containing protein 1 IPR008559 DUF841 euk	185.96491
ENSMUSP00000053145	9.8	Cytochrome b-c1 complex subunit 8 (Ubiquinol-cytochrome c reductase complex ubiquinone-binding protein QP-C)(Ubiquinol-cytochrome c reductase complex 9.5 kDa protein)(Complex III subunit VIII)(Complex III subunit 8) IPR004205 UcrQ	85.964912
ENSMUSP00000088736	51.1	Eukaryotic translation initiation factor 2 subunit 3, Y-linked (Eukaryotic translation initiation factor 2 subunit gamma, Y-linked)(eIF-2-gamma Y) IPR000795 ProtSyn GTP bdIPR001806 Ras GTPaseIPR009001 Transl elong EF1A/Init IF2 CIPR004161 Transl elong EFTu/EF1A 2IPR009000 Transl elong init/rib B-barrelIPR015256 eIF2 C	448.24561
ENSMUSP00000056082	43.3	Solute carrier family 22 member 18 (Organic cation transporter-like protein 2)(ORCTL-2)(Imprinted multi-membrane spanning polyspecific transporter-related protein 1)(Multi-membrane spanning polyspecific transporter) IPR001226 Flavodoxin CSIPR011701 MFS 1IPR016196 MFS gen sb transptIPR001958 Tet-R TetA	379.82456
ENSMUSP00000079628	15.5	40S ribosomal protein S17 IPR001210 Ribosomal S17eIPR018273 Ribosomal S17e CS	135.96491
ENSMUSP00000030903	66.7	ATPase family AAA domain-containing protein 3 (AAA-ATPase TOB3) IPR003593 AAA+ ATPase coreIPR003959 AAA ATPase core	585.08772
ENSMUSP00000032192	313	Inositol 1,4,5-trisphosphate receptor type 1 (Type 1 inositol 1,4,5-trisphosphate receptor)(Type 1 InsP3 receptor)(IP3 receptor isoform 1)(InsP3R1)(Inositol 1,4,5-trisphosphate-binding protein P400)(Purkinje cell protein 1)(Protein PCD-6) IPR016024 ARM-type foldIPR000699 Ca-rel channelIPR014821 Ins145 P3 rcptIPR000493 InsP3 rcpt bdIPR005821 Ion transIPR003608 MIRIPR016093 MIR motifIPR013662 RIH assoc	2745.614
sp|TRYP_PIG|	24.4	Trypsin; EC 3.4.21.4; Flags: Precursor;	214.03509
ENSMUSP00000025178	82	Vacuolar protein sorting-associated protein 52 homolog IPR007258 Vps52	719.29825
ENSMUSP00000089348	15.4	Histone H3.1 IPR009072 Histone-foldIPR000164 Histone H3IPR007125 Histone core D	135.08772
ENSMUSP00000103086	10.1	Dolichol-phosphate mannosyltransferase subunit 3 (Dolichyl-phosphate beta-D-mannosyltransferase subunit 3)(Dolichol-phosphate mannose synthase subunit 3)(DPM synthase complex subunit 3)(Mannose-P-dolichol synthase subunit 3)(MPD synthase subunit 3) IPR013174 DPM3	88.596491
ENSMUSP00000043540	24	Keratinocytes-associated protein 2 (KCP-2)	210.52632
ENSMUSP00000057595	70.4	Very long-chain acyl-CoA synthetase (VLACS)(VLCS)(EC 6.2.1.-)(Very long-chain-fatty-acid-CoA ligase)(THCA-CoA ligase)(Fatty-acid-coenzyme A ligase, very long-chain 1)(Long-chain-fatty-acid--CoA ligase)(EC 6.2.1.3)(Fatty acid transport protein 2)(FATP-2)(Solute carrier family 27 member 2) Source: 6.2.1.- IPR000873 AMP-dep Synth/Lig	617.54386
ENSMUSP00000074448	45.8	Lysosome-associated membrane glycoprotein 2 Precursor (LAMP-2)(Lysosomal membrane glycoprotein type B)(LGP-	401.75439

		B)(CD107 antigen-like family member B)(CD107b antigen) IPR018133 LAMP/LAMP-like membraneIPR018134 LAMP CSIPR002000 LampIPR001412 aa-tRNA-synth I CS	
ENSMUSP00000003620	68	Proline dehydrogenase, mitochondrial Precursor (EC 1.5.99.8)(Proline oxidase) Source: 1.5.99.8 IPR002872 Proline DHase	596.49123
ENSMUSP00000107927	156.5	Leucine-rich PPR motif-containing protein, mitochondrial Precursor (130 kDa leucine-rich protein)(LRP 130)(mLRP130) IPR002885 Pentatricopeptide repeatIPR001420 X opioid rcpt	1372.807
ENSMUSP00000005431	82.9	LETM1 and EF-hand domain-containing protein 1, mitochondrial Precursor (Leucine zipper-EF-hand-containing transmembrane protein 1) IPR018247 EF HAND 1IPR011685 LETM1	727.19298
ENSMUSP00000016771	226.2	Myosin-9 (Myosin heavy chain 9)(Myosin heavy chain, non-muscle IIa)(Non-muscle myosin heavy chain IIa)(NMMHC II-a)(NMMHC-IIA)(Cellular myosin heavy chain, type A)(Non-muscle myosin heavy chain-A)(NMMHC-A) IPR000048 IQ CaM bd regionIPR004009 Myosin NIPR001609 Myosin headIPR002928 Myosin tailIPR009053 PrefoldinIPR016137 Regulat G prot signal superfamIPR002661 Ribosome recyc facIPR000533 TropomyosinIPR006077 Vinculin/cateninIPR004174 gpW	1984.2105
ENSMUSP00000023806	60.6	Sterol O-acyltransferase 2 (EC 2.3.1.26)(Cholesterol acyltransferase 2)(Acyl coenzyme A:cholesterol acyltransferase 2)(ACAT-2) Source: 2.3.1.26 IPR004299 MBOAT fam	531.57895
ENSMUSP00000057664	23.5	Ras-related protein Rab-2A IPR006688 ARFIPR003579 GTPase RabIPR003577 GTPase RasIPR003578 GTPase RhoIPR013684 Miro-likeIPR002078 RNA pol sigma 54 intIPR002041 Ran GTPaseIPR013753 RasIPR001806 Ras GTPaseIPR005225 Small GTP bd	206.14035
ENSMUSP00000002551	13.3	Small nuclear ribonucleoprotein Sm D1 (Sm-D1)(snRNP core protein D1)(Sm-D autoantigen) IPR006649 Euk arc LSM coreIPR010920 LSM related coreIPR001163 LSM snRNP core	116.66667
ENSMUSP00000066038	25.1	Eukaryotic translation initiation factor 3 subunit K (eIF3k)(Eukaryotic translation initiation factor 3 subunit 12)(eIF-3 p25) IPR016024 ARM-type foldIPR005062 SAC3/GANP/Nin1/mts3/eIF-3-p25	220.17544
ENSMUSP00000110434	51.4	Trifunctional enzyme subunit beta, mitochondrial Precursor (TP-beta) Source: 2.3.1.16 IPR002155 ThiolaseIPR016039 Thiolase-like	450.87719
ENSMUSP00000020820	23.8	39S ribosomal protein L22, mitochondrial Precursor (L22mt)(MRP-L22) IPR001063 Ribosomal L22	208.77193
ENSMUSP00000041104	66.7	Apoptosis-inducing factor 1, mitochondrial Precursor (EC 1.-.-.-)(Programmed cell death protein 8) Source: 1.-.-.- IPR016156 FAD/NAD-linked Rdtase dimerIPR013027 FAD pyr nucl-diS OxRdtaseIPR000815 Hg reductaseIPR001327 Pyr OxRdtase NAD bdIPR000103 Pyridine nuc-diS OxRdtase 2	585.08772
ENSMUSP00000020637	67.2	Calnexin Precursor IPR001580 Calret/calnexIPR018124 Calret/calnex CSIPR009033 Calreticulin/calnexin PIPR008985 ConA like lec gl	589.47368
ENSMUSP00000022821	29.9	Dehydrogenase/reductase SDR family member 4 (EC 1.1.1.184)(NADPH-dependent carbonyl reductase/NADP-retinol dehydrogenase)(PHCR)(CR)(Peroxisomal short-chain alcohol dehydrogenase)(NADPH-dependent retinol dehydrogenase/reductase)(NDRD)(mouNRDR) Source: 1.1.1.184 IPR003560 DHB DHaseIPR002198 DHase sc/Rdtase SDRIPR002347 Glc/ribitol DHaseIPR002424 Insect AlcDHase famIPR016040 NAD(P)-bdIPR013968 Polyketide synth KR	262.2807
ENSMUSP00000070149	26.3	Coiled-coil-helix-coiled-coil-helix domain-containing protein 3, mitochondrial Precursor IPR010625 CHCHIPR007964 DUF737	230.70175
ENSMUSP00000103257	9.8		85.964912
ENSMUSP00000065987	82.4	ATP-dependent RNA helicase DDX1 (EC 3.6.1.-)(DEAD box protein 1) Source: 3.6.1.- IPR001870 B302IPR014001 DEAD-like NIPR001650 DNA/RNA helicase CIPR011545 DNA/RNA helicase DEAD/DEAH NIPR014021 Helicase SF1/SF2 ATP-bdIPR014014 RNA helicase DEAD Q motifIPR003877 SPRY rcptIPR018355 SPla/RYanodine receptor sg	722.80702
ENSMUSP00000101665	13.6	5-hydroxyisourate hydrolase (HIU hydrolase)(HIUase)(EC 3.5.2.17)(Transthyretin-related protein) Source: 3.5.2.17 IPR000895 Transthyretin	119.29825
ENSMUSP00000047254	59.5	Xylulose kinase (Xylulokinase)(EC 2.7.1.17) Source: 2.7.1.17 IPR018485 Carb kinase FGGY CIPR018484 Carb kinase FGGY N	521.92982
ENSMUSP00000091608	11.6	UPF0451 protein C17orf61 homolog Precursor IPR006696 DUF423	101.75439
ENSMUSP00000069962	40.7	ATPase family AAA domain-containing protein 1 IPR003593 AAA+ ATPase coreIPR003960 AAA ATPase CSIPR003959 AAA ATPase coreIPR000850 Adenylate kinIPR014001 DEAD-like N	357.01754
ENSMUSP00000107659	39.2	Erlin-1 (Endoplasmic reticulum lipid raft-associated protein 1)(Stomatin-prohibitin-flotillin-HflC/K domain-containing protein 1)(SPFH domain-containing protein 1)(Protein KE04 homolog) IPR001107 Band 7	343.85965

ENSMUSP00000028619	34.7	Estradiol 17-beta-dehydrogenase 12 (EC 1.1.1.62)(17-beta-hydroxysteroid dehydrogenase 12)(17-beta-HSD 12)(3-ketoacyl-CoA reductase)(KAR)(EC 1.3.1.-)(KIK-I) Source: 1.1.1.62 IPR002198 DHase sc/Rdtase SDRIPR002347 Glc/ribitol DHaseIPR016040 NAD(P)-bd	304.38596
ENSMUSP00000103012	120.7	ATP-citrate synthase (EC 2.3.3.8)(ATP-citrate (pro-S-)-lyase)(Citrate cleavage enzyme) Source: 2.3.3.8 IPR014608 ATP-citrate synthaseIPR017440 Cit synth/succinyl-CoA lig ASIPR002020 Citrate synthase-likeIPR016141 Citrate synthase-like coreIPR003781 CoA bdIPR005810 CoA lig alphaIPR005811 CoA ligaseIPR017866 Succ-CoA synthase bsu CSIPR016102 Succinyl-CoA synth-like	1058.7719
ENSMUSP00000026818	20.6	Signal peptidase complex catalytic subunit SEC11A (EC 3.4.-.-)(SEC11 homolog A)(SEC11-like protein 1)(Microsomal signal peptidase 18 kDa subunit)(SPase 18 kDa subunit)(SPC18)(Endopeptidase SP18)(Sid 2895) Source: 3.4.-.-IPR000223 Pept S26A signal pept 1IPR015927 Peptidase S24 S26A/B/CIPR011056 Peptidase S24 S26 CIPR001733 Peptidase S26B	180.70175
ENSMUSP00000020358	22.4	Ras-related protein Rab-1A (YPT1-related protein) IPR006688 ARFIPR006689 ARF/SARIPR003579 GTPase RabIPR003577 GTPase RasIPR003578 GTPase RhoIPR013684 Miro-likeIPR002078 RNA pol sigma 54 intIPR002041 Ran GTPaseIPR013753 RasIPR001806 Ras GTPaseIPR005225 Small GTP bd	196.49123
ENSMUSP00000032539	76.2	Bile acyl-CoA synthetase (BACS)(EC 6.2.1.7)(Bile acid-CoA ligase)(BA-CoA ligase)(BAL)(Cholate--CoA ligase)(Very long-chain acyl-CoA synthetase-related protein)(VLACS-related)(VLACSR)(Fatty acid transport protein 5)(FATP-5)(Solute carrier family 27 member 5) Source: 6.2.1.7 IPR000873 AMP-dep Synth/Lig	668.42105
ENSMUSP00000092502	31.2	40S ribosomal protein S2 (S4)(LLRep3 protein) IPR005324 Ribosomal S5 CIPR013810 Ribosomal S5 NIPR018192 Ribosomal S5 N CSIPR005711 Ribosomal S5 euk/arc	273.68421
ENSMUSP00000026924	102.7	Probable 2-oxoglutarate dehydrogenase E1 component DHKTD1, mitochondrial Precursor (EC 1.2.4.2)(Dehydrogenase E1 and transketolase domain-containing protein 1) Source: 1.2.4.2 IPR011603 2oxoglutarate DHase E1IPR001017 DHase E1IPR005475 Transketo Cen R	900.87719
ENSMUSP00000006181	33.2	Alpha-soluble NSF attachment protein (SNAP-alpha)(N-ethylmaleimide-sensitive factor attachment protein alpha) IPR000744 NSF attach	291.22807
ENSMUSP00000102062	15.3	Histone H3.3 IPR009072 Histone-foldIPR000164 Histone H3IPR007125 Histone core D	134.21053
ENSMUSP00000001592	81.7	Junction plakoglobin (Desmoplakin-3)(Desmoplakin III) IPR016024 ARM-type foldIPR000225 ArmadilloIPR013284 Beta-cateninIPR000357 HEAT	716.66667
ENSMUSP00000072483	46.5	Medium-chain specific acyl-CoA dehydrogenase, mitochondrial Precursor (MCAD)(EC 1.3.99.3) Source: 1.3.99.3 IPR006091 Acyl-CoA DHase/Oxase MIPR013107 Acyl-CoA DHase 2 CIPR006089 Acyl-CoA DHase CSIPR006092 Acyl-CoA DHase NIPR006090 Acyl-CoA Oxase/DHase 1IPR009100 AcylCoA DH/oxidase M/NIPR009075 AcylCo DHase/oxidase C	407.89474
ENSMUSP00000071939	49.8	Ectonucleoside triphosphate diphosphohydrolase 5 Precursor (NTPDase 5)(EC 3.6.1.6)(Nucleoside diphosphatase)(CD39 antigen-like 4)(ER-UDPase) Source: 3.6.1.6 IPR000407 GDA1 CD39 NTPase	436.84211
ENSMUSP00000025197	77.4	Antigen peptide transporter 2 (APT2)(ATP-binding cassette sub-family B member 3)(Histocompatibility antigen modifier 2) IPR003593 AAA+ ATPase coreIPR013305 ABC B2IPR013306 ABC B3IPR011527 ABC TM 1IPR001140 ABC TM transptIPR003439 ABC transporter-likeIPR017871 ABC transporter CSIPR017940 ABC transporter type1IPR005293 Ag transporter2	678.94737
ENSMUSP00000004673	40.8	Protein NDRG2 (Protein Ndr2) IPR004142 Ndr	357.89474
ENSMUSP00000040140	57.8	Protein ERGIC-53 Precursor (ER-Golgi intermediate compartment 53 kDa protein)(Lectin mannose-binding 1)(p58) IPR008985 ConA like lec glIPR005052 Lectin leg	507.01754
ENSMUSP00000027602	57.1	Aspartyl-tRNA synthetase, cytoplasmic (EC 6.1.1.12)(Aspartate--tRNA ligase)(AspRS) Source: 6.1.1.12 IPR002312 Asp-tRNA-synth IIbIPR004523 Asp-tRNA-synth IIb arc/eukIPR004365 NA bd OB tRNA-helicaseIPR004364 aa-tRNA-synt IIIPR006195 aa-tRNA-synth II	500.87719
ENSMUSP00000017572	47.4	26S proteasome non-ATPase regulatory subunit 11 (26S proteasome regulatory subunit S9)(26S proteasome regulatory subunit p44.5) IPR013143 PAMIPR000717 PCI	415.78947
ENSMUSP00000032114	91.8	Mannosyl-oligosaccharide glucosidase (EC 3.2.1.106)(Glycoprotein-processing glucosidase I)(Glucosidase 1) Source: 3.2.1.106 IPR008928 6-hairpin glycosidase-likeIPR004888 Glyco hydro 63	805.26316
ENSMUSP00000018437	14.9	Profilin-1 (Profilin I) IPR002097 ProfilinIPR005454 Profilin mammal	130.70175

ENSMUSP00000024596	61.5	Solute carrier family 22 member 1 (Organic cation transporter 1)(mOCT1) IPR011701 MFS 1IPR016196 MFS gen sb transptIPR004749 Orgcat transpIPR005828 Sub transporterIPR005829 Sugar transporter CS	539.47368
ENSMUSP00000108237	82.8	Glycerol-3-phosphate dehydrogenase, mitochondrial Precursor (GPDH-M)(GPD-M)(EC 1.1.99.5)(Protein TISP38) Source: 1.1.99.5 IPR018247 EF HAND 1IPR018249 EF HAND 2IPR018248 EF handIPR002048 EF hand Ca bdIPR000447 FAD-dep Gly3P DHaseIPR006076 FAD-dep OxRdtase	726.31579
ENSMUSP00000040840	46.4	Adipocyte plasma membrane-associated protein (Protein DD16) IPR013658 SGLIPR018119 Strictosidine synth cons-reg	407.01754
ENSMUSP00000008812	17.7	40S ribosomal protein S18 (Ke-3)(Ke3) IPR001892 Ribosomal S13IPR010979 Ribosomal S13-like H2THIPR018269 Ribosomal S13 CS	155.26316
ENSMUSP00000015256	74.4	Calcium-binding mitochondrial carrier protein Aralar2 (Mitochondrial aspartate glutamate carrier 2)(Solute carrier family 25 member 13)(Citrin) IPR002113 Aden trnslctorIPR018249 EF HAND 2IPR018248 EF handIPR002048 EF hand Ca bdIPR002067 Mit carrierIPR001993 Mitoch carrierIPR018108 Mitochondrial sb/sol carrier	652.63158
ENSMUSP00000051222	8.2	ATP synthase subunit e, mitochondrial IPR008386 ATPase F0-cplx esu mt	71.929825
ENSMUSP00000031524	44.9	Short-chain specific acyl-CoA dehydrogenase, mitochondrial Precursor (SCAD)(EC 1.3.99.2)(Butyryl-CoA dehydrogenase) Source: 1.3.99.2 IPR006091 Acyl-CoA DHase/Oxase MIPR013107 Acyl-CoA DHase 2 CIPR006089 Acyl-CoA DHase CSIPR006092 Acyl-CoA DHase NIPR006090 Acyl-CoA Oxase/DHase 1IPR009100 AcylCoA DH/oxidase M/N	393.85965
ENSMUSP00000019726	47.2	Mannose-6-phosphate receptor-binding protein 1 (Cargo selection protein TIP47) IPR017993 Atrophin-1IPR004279 Perilipin	414.03509
ENSMUSP00000103145	20	major urinary protein (Mup)-like precursor IPR002968 A1-microglobinIPR002447 BlactoglobulinIPR011038 Calycin likeIPR002345 LipocalinIPR000566 Lipocln cytFABPIPR002971 Maj urinaryIPR003087 N gelatinaseIPR002448 Odour bdIPR002972 PstgldnD synthIPR002450 vonEbner gland	175.4386
ENSMUSP00000074994	15.4	Histone H3.2 IPR009072 Histone-foldIPR000164 Histone H3IPR007125 Histone core D	135.08772
ENSMUSP00000072236	59.6	UDP-glucuronosyltransferase 3A2 Precursor (UDPGT 3A2)(EC 2.4.1.17) Source: 2.4.1.17 IPR007235 Glyco trans 28 CIPR002213 UDP glucos trans	522.80702
ENSMUSP00000088837	155.5	Insulin receptor Precursor (IR)(EC 2.7.10.1)(CD220 antigen) Source: 2.7.10.1 IPR000494 EGF rcpt LIPR003961 FN IIIIPR008957 Fibronectin typ-III-like foldIPR003962 FnIII subdIPR006211 Furin-likeIPR006212 Furin repeatIPR000174 IL8 rcptIPR016246 Insulin rcptIPR011009 Kinase likeIPR000719 Prot kinase coreIPR017441 Protein kinase ATP BSIPR002011 Recept tyr kinase-II CSIPR017442 Se/Thr pkinase-relIPR002290 Ser thr pkinaseIPR001245 Tyr pkinaseIPR008266 Tyr pkinase AS	1364.0351
ENSMUSP00000020209	17.6	NADH dehydrogenase IPR007763 NADH UbQ OxRdtase 17.2kD su	154.38596
ENSMUSP00000018561	132	Myosin-Ib (Myosin I alpha)(MMI-alpha)(MMIa)(MIH-L) IPR000048 IQ CaM bd regionIPR001609 Myosin headIPR010926 Myosin tail 2	1157.8947
ENSMUSP00000025598	33.7	Glycine N-acyltransferase-like protein Keg1 (EC 2.3.1.13)(Acyl-CoA:glycine N-acyltransferase protein Keg1)(Kidney-expressed gene 1 protein) Source: 2.3.1.13 IPR016181 Acyl CoA acyltransferaseIPR013652 Glycine N-acyltransferase CIPR015938 Glycine N-acyltransferase N	295.61404
ENSMUSP00000105796	16.8	NADH dehydrogenase IPR009346 GRIM-19	147.36842
ENSMUSP00000087632	30	no description availableIPR001921 Ribosomal L7AIPR018492 Ribosomal L7A/RS6 famIPR004037 Ribosomal L7AeIPR004038 Ribosomal L7Ae/L30e/S12e/Gad45	263.15789
ENSMUSP00000101495	43.5	Platelet-activating factor acetylhydrolase 2, cytoplasmic (EC 3.1.1.47)(Serine-dependent phospholipase A2) Source: 3.1.1.47 IPR016715 Ac Ohase PAFIPR005065 PAF acetylhydro II	381.57895
ENSMUSP00000090564	36.9	Fructose-1,6-bisphosphatase 1 (FBPase 1)(EC 3.1.3.11)(D-fructose-1,6-bisphosphate 1-phosphohydrolase 1) Source: 3.1.3.11 IPR000146 Fructose bisphosphataseIPR017955 IMPase/FBPase	323.68421
ENSMUSP00000109215	33.4	Monoglyceride lipase (MGL)(EC 3.1.1.23) Source: 3.1.1.23 IPR000073 AB hydrolase 1IPR002410 Peptidase S33	292.98246
ENSMUSP00000097561	3904.1	Titin (EC 2.7.11.1)(Connectin) Source: 2.7.11.1 IPR018483 Carb kinase FGGY CSIPR003883 Extensin likeIPR003961 FN IIIIPR008957 Fibronectin typ-III-like foldIPR003962 FnIII subdIPR002016 Haem peroxidase pln/fun/bacIPR013151 IgIPR007110 Ig-likeIPR003006 Ig/MHC CSIPR003597 Ig C1-setIPR013098 Ig I-setIPR013106 Ig V-setIPR003596 Ig V-set subIPR003599 Ig subIPR003598 Ig sub2IPR011009 Kinase likeIPR004168 PPAK motifIPR000694 PRO	34246.491

		richIPR000719 Prot kinase coreIPR017442 Se/Thr pkinase-relIPR002290 Ser thr pkinaseIPR015129 Titin ZIPR001245 Tyr pkinaseIPR008266 Tyr pkinase AS	
ENSMUSP00000031314	68.6	Serum albumin Precursor IPR001703 Alpha-fetoproteinIPR000264 Serum albuminIPR014760 Serum albumin N	601.75439
ENSMUSP00000111272	29.5	Catechol O-methyltransferase (EC 2.1.1.6) Source: 2.1.1.6 IPR017128 Catechol O-MeTrfase eukIPR002935 O-MeTrfase 3	258.77193
ENSMUSP00000031472	22.1	Peroxisomal membrane protein 2 (22 kDa peroxisomal membrane protein) IPR007248 Mpv17 PMP22	193.85965
ENSMUSP00000090897	15.1	Hemoglobin subunit alpha (Hemoglobin alpha chain)(Alpha-globin) IPR013314 Globin lamprey/hagfishIPR009050 Globin likeIPR000971 Globin subsetIPR002338 Haemoglobin aIPR002339 Haemoglobin piIPR002335 Myoglobin	132.45614
ENSMUSP00000083928	131.5	Alpha-mannosidase 2 (EC 3.2.1.114)(Alpha-mannosidase II)(AMAN II)(MAN II)(Mannosyl-oligosaccharide 1,3-1,6-alpha-mannosidase)(Golgi alpha-mannosidase II)(Mannosidase alpha class 2A member 1) Source: 3.2.1.114 IPR011013 Glyco hydro-type carb-bdIPR011330 Glyco hydro/deAcase b/a-brIIPR011682 Glyco hydro 38 CIPR015341 Glyco hydro 38 centralIPR000602 Glyco hydro 38 core	1153.5088
ENSMUSP00000088729	73.4	ATP-dependent RNA helicase DDX3Y (EC 3.6.1.-)(DEAD box protein 3, Y-chromosomal)(DEAD-box RNA helicase DEAD2)(mDEAD2)(D1Pas1-related sequence 1) Source: 3.6.1.- IPR014001 DEAD-like NIPR001650 DNA/RNA helicase CIPR011545 DNA/RNA helicase DEAD/DEAH NIPR014021 Helicase SF1/SF2 ATP-bdIPR000629 RNA-helicase DEAD-box CSIPR014014 RNA helicase DEAD Q motif	643.85965
ENSMUSP00000005477	56.8	Cytochrome P450 2B10 (EC 1.14.14.1)(CYPIIB10)(Testosterone 16-alpha hydroxylase)(P450-16-alpha)(Clone PF3/46)(Cytochrome P450 2B20)(CYPIIB20)(P24) Source: 1.14.14.1 IPR001128 Cyt P450IPR017973 Cyt P450 CIPR002401 Cyt P450 E grp-IIPR002403 Cyt P450 E grp-IVIPR008067 Cyt P450 E grp-I CYP2A-likeIPR008068 Cyt P450 E grp-I CYP2B-likeIPR008069 Cyt P450 E grp-I CYP2D-likeIPR008071 Cyt P450 E grp-I CYP2J-like	498.24561
ENSMUSP00000030078	54.2	Hydroxysteroid dehydrogenase-like protein 2 (EC 1.-.-.-) Source: 1.-.-.- IPR002198 DHase sc/Rdtase SDRIPR002347 Glc/ribitol DHaseIPR000815 Hg reductaseIPR016040 NAD(P)-bdIPR003033 SCP2 sterol bdIPR016083 Sterol-binding-like	475.4386
ENSMUSP00000026144	25.7	L-xylulose reductase (XR)(EC 1.1.1.10)(Dicarbonyl/L-xylulose reductase) Source: 1.1.1.10 IPR003560 DHB DHaseIPR002198 DHase sc/Rdtase SDRIPR002347 Glc/ribitol DHaseIPR016040 NAD(P)-bdIPR013968 Polyketide synth KR	225.4386
ENSMUSP00000075825	62.9	Probable oxidoreductase C10orf33 homolog (EC 1.-.-.-) Source: 1.-.-.- IPR000759 Adrndx reductaseIPR000447 FAD-dep Gly3P DHaseIPR006076 FAD-dep OxRdtase	551.75439
ENSMUSP00000019937	87.8	Translocation protein SEC63 homolog IPR001623 DnaJ NIPR003095 Hsp DnaJIPR004179 Sec63IPR018127 Sec63-dom subgr	770.17544
ENSMUSP00000105420	82	Transmembrane 9 superfamily member 4 Precursor IPR004240 EMP70	719.29825
ENSMUSP00000022380	44.1	26S protease regulatory subunit S10B (Proteasome 26S subunit ATPase 6)(Proteasome subunit p42) IPR005937 26S Psome P45IPR003593 AAA+ ATPase coreIPR003960 AAA ATPase CSIPR003959 AAA ATPase coreIPR000641 CbxX CfqX	386.84211
ENSMUSP00000032992	105.5	Eukaryotic translation initiation factor 3 subunit C (eIF3c)(Eukaryotic translation initiation factor 3 subunit 8)(eIF3 p110) IPR000717 PCIIPR008905 eIF3c N	925.4386
ENSMUSP00000026270	66.9	Phosphatidylinositide phosphatase SAC1 (EC 3.1.3.-)(Suppressor of actin mutations 1-like protein) Source: 3.1.3.- IPR002013 Syja N	586.84211
ENSMUSP00000002091	27.9	B-cell receptor-associated protein 31 (BCR-associated protein Bap31)(p28 Bap31) IPR008417 Bap31IPR000533 Tropomyosin	244.73684
ENSMUSP00000044827	151.9	Myb-binding protein 1A (Myb-binding protein of 160 kDa) IPR016024 ARM-type foldIPR007015 DNA pol V	1332.4561
ENSMUSP00000091035	17.2	40S ribosomal protein S13 IPR012606 Ribosomal S13/S15 NIPR000589 Ribosomal S15IPR009068 S15 NS1 RNA bd	150.87719
ENSMUSP00000038135	149.6	ATP-dependent RNA helicase A (EC 3.6.1.-)(Nuclear DNA helicase II)(NDH II)(DEAH box protein 9)(mHEL-5) Source: 3.6.1.- IPR003593 AAA+ ATPase coreIPR014001 DEAD-like NIPR001650 DNA/RNA helicase CIPR011545 DNA/RNA helicase DEAD/DEAH NIPR002464 DNA/RNA helicase DEAH CSIPR011709 DUF1605IPR001159 Ds-RNA bdIPR007502 Helicase-assoc regIPR014021 Helicase SF1/SF2 ATP-bdIPR000817 Prion	1312.2807
ENSMUSP00000081142	33.6	TAR DNA-binding protein 43 (TDP-43) IPR002343 Hud Sxl RNAIPR000504 RRM RNP1	294.73684

ENSMUSP00000022062	72.5	Succinate dehydrogenase Source: 1.3.5.1 IPR003953 FAD bind2 NIPR013027 FAD pyr nucl-diS OxRdtaseIPR003952 FRD SDH FAD BSIPR015939 Fum Rdtase/Succ DH flav-like CIPR004112 Fum Rdtase/Succ DHase flav CIPR011281 Succ DHase flav su fwdIPR014006 Succ Dhase frdA Gneg	635.96491
ENSMUSP00000034234	35.1	Ubiquinone biosynthesis protein COQ9, mitochondrial Precursor IPR013718 COQ9IPR009057 Homeodomain likeIPR012762 Ubiq biosynth COQ9	307.89474
ENSMUSP00000029645	47.7	Tryptophan 2,3-dioxygenase (TDO)(EC 1.13.11.11)(Tryptophan pyrrolase)(Tryptophanase)(Tryptophan oxygenase)(TRPO)(TO)(Tryptamin 2,3-dioxygenase) Source: 1.13.11.11 IPR004981 Trp 2 3 dOase	418.42105
ENSMUSP00000018449	273.4	Pre-mRNA-processing-splicing factor 8 (Splicing factor Prp8) IPR008972 CupredoxinIPR000555 Mov34 MPN PAD1IPR012591 PRO8NTIPR012592 PROCNIPR012984 PRO C	2398.2456
ENSMUSP00000016072	158.3	ribosome binding protein 1 isoform a IPR003914 RabaptinIPR007794 Rib rcpt KPIPR000533 TropomyosinIPR010989 t-SNARE	1388.5965
ENSMUSP00000075150	10.1	Cytochrome c oxidase subunit VIb isoform 1 (COX VIb-1) IPR003213 Cyt c oxidase su6B	88.596491
ENSMUSP00000108058	30.4	COP9 signalosome complex subunit 7a (Signalosome subunit 7a)(SGN7a)(JAB1-containing signalosome subunit 7a) IPR000717 PCI	266.66667
ENSMUSP00000021630	37	Estradiol 17 beta-dehydrogenase 5 (EC 1.1.1.-)(17-beta-HSD 5) Source: 1.1.1.- IPR001395 Aldo/ket redIPR018170 Aldo/ket reductase CS	324.5614
ENSMUSP00000109228	23.5	Ras-related protein Rab-7a IPR003579 GTPase RabIPR003577 GTPase RasIPR003578 GTPase RhoIPR013684 Miro-likeIPR002078 RNA pol sigma 54 intIPR002041 Ran GTPaseIPR013753 RasIPR001806 Ras GTPaseIPR005225 Small GTP bd	206.14035
ENSMUSP00000025511	16.3	40S ribosomal protein S14 IPR001971 Ribosomal S11IPR018102 Ribosomal S11 CS	142.98246
ENSMUSP00000067767	59.2	Fatty aldehyde dehydrogenase (EC 1.2.1.3)(Aldehyde dehydrogenase family 3 member A2)(Aldehyde dehydrogenase 3) Source: 1.2.1.3 IPR016161 Ald DHase/Histidinol DHaseIPR016160 Ald DHase CSIPR012394 Ald DHase NAD(P)IPR015590 Aldehyde DHase	519.29825
ENSMUSP00000101006	17.6	ATP synthase subunit delta, mitochondrial Precursor (F-ATPase delta subunit) IPR001469 ATPase F1-cplx dsu/esu	154.38596
ENSMUSP00000104884	69.7	Clathrin interactor 1 (Epsin-4)(Epsin-related protein)(EpsinR)(Enthoprotin) IPR008942 ENTH VHSIPR013809 Epsin-like NIPR001026 Epsin N	611.40351
ENSMUSP00000104163	27.8	Derlin-2 (Der1-like protein 2)(Degradation in endoplasmic reticulum protein 2)(F-LANa) IPR007599 DER1	243.85965
ENSMUSP00000099950	101.6	Sarcosine dehydrogenase, mitochondrial Precursor (SarDH)(EC 1.5.99.1) Source: 1.5.99.1 IPR000447 FAD-dep Gly3P DHaseIPR006076 FAD-dep OxRdtaseIPR013977 GCV T CIPR006222 GCV T N	891.22807
ENSMUSP00000089769	22.7	Transmembrane emp24 domain-containing protein 2 Precursor (Membrane protein p24A)(Sid 394) IPR000348 Emp24 gp25L p24IPR009038 GOLD	199.12281
ENSMUSP00000000804	73.1	ATP-dependent RNA helicase DDX3X (EC 3.6.1.-)(DEAD box protein 3, X-chromosomal)(DEAD box RNA helicase DEAD3)(mDEAD3)(Embryonic RNA helicase)(D1Pas1-related sequence 2) Source: 3.6.1.- IPR003593 AAA+ ATPase coreIPR014001 DEAD-like NIPR001650 DNA/RNA helicase CIPR011545 DNA/RNA helicase DEAD/DEAH NIPR014021 Helicase SF1/SF2 ATP-bdIPR000629 RNA-helicase DEAD-box CSIPR014014 RNA helicase DEAD Q motif	641.22807
ENSMUSP00000048469	24.8	60S ribosomal protein L10a (CSA-19)(Neural precursor cell expressed developmentally down-regulated protein 6)(NEDD-6) IPR002143 Ribosomal L1	217.54386
ENSMUSP00000105177	75.8	SAM domain and HD domain-containing protein 1 (Interferon-gamma-inducible protein Mg11) IPR003607 Met-dep phosphohydro HDIPR006674 Met-dep phosphohydro HD subIPR001660 SAMIPR011510 SAM 2	664.91228
ENSMUSP00000053270	45.3	Lysosomal acid lipase/cholesteryl ester hydrolase Precursor (LAL)(Acid cholesteryl ester hydrolase)(EC 3.1.1.13)(Sterol esterase)(Lipase A)(Cholesteryl esterase) Source: 3.1.1.13 IPR006693 AB hydro lipaseIPR000073 AB hydrolase 1	397.36842
ENSMUSP00000011526	36.3	Trans-1,2-dihydrobenzene-1,2-diol dehydrogenase (EC 1.3.1.20)(Dimeric dihydrodiol dehydrogenase)(D-xylose-NADP dehydrogenase)(EC 1.1.1.179)(D-xylose 1-dehydrogenase) Source: 1.3.1.20 IPR016040 NAD(P)-bdIPR004104 OxRdtase CIPR000683 Oxidoreductase N	318.42105
ENSMUSP00000078996	18.8	no description availableIPR001147 Ribosomal L21eIPR008991 Translation prot SH3-like	164.91228
ENSMUSP00000038744	18.7	S-phase kinase-associated protein 1 (S-phase kinase-associated protein 1A)(Cyclin A/CDK2-associated protein p19)(p19skp1)(p19A) IPR011333 BTB/POZ foldIPR016897 E3 ubiquit lig SCF SkpIPR001232 Skp1 compIPR016073	164.03509

		Skp1 comp POZIPR016072 Skp1 comp dimer	
ENSMUSP00000020562	58	T-complex protein 1 subunit delta (TCP-1-delta)(CCT-delta)(A45) IPR012717 Chap CCT deltaIPR017998 Chaperone TCP-1IPR002194 Chaperonin TCP-1 CSIPR001844 Chaprnin Cpn60IPR002423 Cpn60/TCP-1	508.77193
ENSMUSP00000062670	39.6	Serum paraoxonase/arylesterase 2 (PON 2)(EC 3.1.1.2)(EC 3.1.8.1)(Serum aryldialkylphosphatase 2)(A-esterase 2)(Aromatic esterase 2) Source: 3.1.1.2 IPR002640 ArylesteraseIPR008364 Paraoxonase2	347.36842
ENSMUSP00000043543	21	NADH dehydrogenase	184.21053
ENSMUSP00000058368	20.7	60S ribosomal protein L18a IPR002670 Ribosomal L18ae	181.57895
ENSMUSP00000004172	35.7	Heme oxygenase 2 (HO-2)(EC 1.14.99.3) Source: 1.14.99.3 IPR002051 Haem OaseIPR016053 Haem Oase-likeIPR016084 Haem Oase-like multi-hlxIPR018207 Haem oxygenase CS	313.15789
ENSMUSP00000054391	48.6	Protein kinase C and casein kinase II substrate protein 3 IPR001060 Cdc15 Fes CIP4IPR011511 SH3 2IPR001452 SH3 domain	426.31579
ENSMUSP00000041152	25	Signal peptidase complex subunit 2 (EC 3.4.-.-)(Microsomal signal peptidase 25 kDa subunit)(SPase 25 kDa subunit) Source: 3.4.-.- IPR009582 SPC25	219.29825
ENSMUSP00000021595	49.2	26S protease regulatory subunit 4 (P26s4)(Proteasome 26S subunit ATPase 1) IPR005937 26S Psome P45IPR003593 AAA+ ATPase coreIPR003960 AAA ATPase CSIPR003959 AAA ATPase coreIPR001957 Bac DnaA	431.57895
ENSMUSP00000027193	11.7	NADH dehydrogenase IPR012576 NADH UbQ OxRdtase B12 su	102.63158
ENSMUSP00000110314	68.3	V-type proton ATPase catalytic subunit A (V-ATPase subunit A)(EC 3.6.3.14)(Vacuolar proton pump subunit alpha)(V-ATPase 69 kDa subunit) Source: 3.6.3.14 IPR003593 AAA+ ATPase coreIPR018118 ATPase F1/A1-cplx a/bsu NIPR000793 ATPase F1/V1/A1-cplx a/bsu CIPR004100 ATPase F1/V1/A1-cplx a/bsu NIPR000194 ATPase F1/V1/A1 a/bsu nucl-bdIPR005725 ATPase V1-cplx asuIPR008378 Ubiq surface	599.12281
ENSMUSP00000100992	19.4	Receptor expression-enhancing protein 6 (Polyposis locus protein 1-like 1)(TB2 protein-like 1) IPR004345 TB2 DP1 HVA22	170.17544
ENSMUSP00000053540	24.3	Maleylacetoacetate isomerase (MAAI)(EC 5.2.1.2)(Glutathione S-transferase zeta 1)(EC 2.5.1.18)(GSTZ1-1) Source: 5.2.1.2 IPR004046 GST CIPR010987 Glutathione-S-Trfase C-likeIPR004045 Glutathione S-Trfase NIPR005955 Mal ac isomIPR012336 Thioredoxin-like fold	213.15789
ENSMUSP00000035222	33	Mitochondrial carnitine/acylcarnitine carrier protein (Carnitine/acylcarnitine translocase)(mCAC)(CAC)(Solute carrier family 25 member 20) IPR002113 Aden trnslctorIPR002067 Mit carrierIPR001993 Mitoch carrierIPR018108 Mitochondrial sb/sol carrier	289.47368
ENSMUSP00000028852	48.2	28S ribosomal protein S5, mitochondrial (S5mt)(MRP-S5) IPR005324 Ribosomal S5 CIPR013810 Ribosomal S5 NIPR018192 Ribosomal S5 N CS	422.80702
ENSMUSP00000021471	31.4	Thioredoxin domain-containing protein 1 Precursor IPR012336 Thioredoxin-like foldIPR006662 Thioredoxin-like subdomIPR017937 Thioredoxin CSIPR013766 Thioredoxin dom	275.4386
ENSMUSP00000046480	16.8	UPF0527 transmembrane protein	147.36842
ENSMUSP00000035033	102.4	Coatomer subunit beta- (Beta--coat protein)(Beta--COP)(p102) IPR006692 Coatomer WD-assoc regIPR016453 Coatomer beta' subunitIPR001680 WD40 repeatIPR011046 WD40 repeat-likeIPR017986 WD40 repeat region	898.24561
ENSMUSP00000070267	20.2	signal peptidase complex subunit 3 IPR007653 SPC22IPR010916 TonB box CS	177.19298
sp|CASB_BOVIN|	25.1	Beta-casein; Contains: Casoparan; Contains: Antioxidant peptide; Contains: Casohypotensin; Flags: Precursor;	220.17544
ENSMUSP00000021930	35.6	Sideroflexin-1 IPR004686 Mtc	312.2807
ENSMUSP00000030191	117	Atrial natriuretic peptide receptor B Precursor (ANP-B)(ANPRB)(GC-B)(Guanylate cyclase B)(EC 4.6.1.2)(NPR-B)(Atrial natriuretic peptide B-type receptor) Source: 4.6.1.2 IPR001054 A/G cyclaseIPR018297 A/G cyclase CSIPR001828 ANF lig bd rcptIPR011009 Kinase likeIPR001170 Ntpep rcpt NIPR000719 Prot kinase coreIPR017442 Se/Thr pkinase-relIPR002290 Ser thr pkinaseIPR001245 Tyr pkinase	1026.3158
ENSMUSP00000073975	51.7	Programmed cell death protein 4 (Topoisomerase-inhibitor suppressed protein)(Protein MA-3) IPR003891 Initiation fac eIF4g MI	453.50877
ENSMUSP00000032597	15.7	60S ribosomal protein L28 IPR002672 Ribosomal L28e	137.7193

ENSMUSP00000009790	21.7	Group XIIB secretory phospholipase A2-like protein Precursor (Group XIII secretory phospholipase A2-like protein)(GXIII sPLA2-like)(sPLA2-GXIIB)(GXIIB) IPR016090 Phospholipase A2IPR010711 Phospholipase A2 secretory G12	190.35088
ENSMUSP00000101027	43.3	1-acyl-sn-glycerol-3-phosphate acyltransferase gamma (EC 2.3.1.51)(1-AGP acyltransferase 3)(1-AGPAT 3)(Lysophosphatidic acid acyltransferase gamma)(LPAAT-gamma)(1-acylglycerol-3-phosphate O-acyltransferase 3) Source: 2.3.1.51 IPR002123 Acyltransferase	379.82456
ENSMUSP00000025567	52.4	Fatty acid desaturase 2 (EC 1.14.19.-)(Delta(6) fatty acid desaturase)(Delta(6) desaturase)(D6D) Source: 1.14.19.- IPR001199 Cyt B5IPR012171 Fatty acid/sphinglp desaturaseIPR005804 Fatty acid desaturase-1IPR001635 Flag hook	459.64912
ENSMUSP00000033121	133.3	nodal modulator 1 IPR013784 Carb-bd-like foldIPR008969 CarboxyPept-like regulatoryIPR008454 Collagen-bd Cna-like B-reg	1169.2982
ENSMUSP00000000727	23.7	Ras-related protein Rab-5B IPR006688 ARFIPR003579 GTPase RabIPR003577 GTPase RasIPR003578 GTPase RhoIPR001019 Gprotein alph bdIPR013684 Miro-likeIPR002041 Ran GTPaseIPR013753 RasIPR001806 Ras GTPaseIPR005225 Small GTP bd	207.89474
ENSMUSP00000030432	34.2	Hydroxymethylglutaryl-CoA lyase, mitochondrial Precursor (HMG-CoA lyase)(HL)(EC 4.1.3.4)(3-hydroxy-3-methylglutarate-CoA lyase) Source: 4.1.3.4 IPR000138 HMG CoA lyase ASIPR000891 PYR CT	300
ENSMUSP00000095695	37.7	Ubiquinone biosynthesis protein COQ7 homolog (Coenzyme Q biosynthesis protein 7 homolog)(Timing protein clk-1 homolog) IPR004916 COQ7IPR009078 Ferritin/RR like	330.70175
ENSMUSP00000065271	28.1	methyltransferase like 7A1 IPR013216 Methyltransf 11IPR013217 Methyltransf 12	246.49123
ENSMUSP00000099938	36.5	Malate dehydrogenase, cytoplasmic (EC 1.1.1.37)(Cytosolic malate dehydrogenase) Source: 1.1.1.37 IPR001557 L-lactate/malate DHaseIPR001236 Lactate/malate DHaseIPR015955 Lactate DHase/Glyco Ohase 4 CIPR001252 Malate DHase ASIPR011274 Malate DHase NAD-dep eukIPR010945 Malate DHase SF1IPR016040 NAD(P)-bd	320.17544
ENSMUSP00000004140	26	Glutathione S-transferase Mu 1 (EC 2.5.1.18)(GST class-mu 1)(Glutathione S-transferase GT8.7)(pmGT10)(GST 1-1) Source: 2.5.1.18 IPR004046 GST CIPR003081 GST muIPR010987 Glutathione-S-Trfase C-likeIPR004045 Glutathione S-Trfase NIPR012336 Thioredoxin-like fold	228.07018
ENSMUSP00000065542	66.4	Choline dehydrogenase, mitochondrial Precursor (CHD)(CDH)(EC 1.1.99.1) Source: 1.1.99.1 IPR011533 Choline dehydrogenaseIPR012132 GMC OxRdtaseIPR000172 GMC OxRdtase NIPR007867 GMC OxRtase C	582.45614
ENSMUSP00000019896	32.8	Iodotyrosine dehalogenase 1 Precursor (IYD-1)(EC 1.-.-.-) Source: 1.-.-.- IPR000415 Nitroreductase	287.7193
ENSMUSP00000069209	62.5	Epoxide hydrolase 2 (EC 3.3.2.10)(Soluble epoxide hydrolase)(SEH)(Epoxide hydratase)(Cytosolic epoxide hydrolase)(CEH) Source: 3.3.2.10 IPR000073 AB hydrolase 1IPR005834 Dehalogen-like hydroIPR000639 Epox hydrolase-likeIPR006402 HAD-SF hydro IA v3IPR005833 Haloacid DHase/epoxide hydro	548.24561
ENSMUSP00000106471	43.9	Lysosome-associated membrane glycoprotein 1 Precursor (LAMP-1)(Lysosomal membrane glycoprotein A)(LGP-A)(120 kDa lysosomal membrane glycoprotein)(LGP-120)(P2B)(CD107 antigen-like family member A)(CD107a antigen) IPR018133 LAMP/LAMP-like membraneIPR018134 LAMP CSIPR002000 Lamp	385.08772
ENSMUSP00000062005:reversed	27.4		240.35088
ENSMUSP00000108056	46.8	Atlastin-2 (ADP-ribosylation factor-like protein 6-interacting protein 2)(ARL-6-interacting protein 2)(Aip-2) IPR015900 Guanylate-bd-like CIPR015894 Guanylate-bd N	410.52632
ENSMUSP00000091840	14.2	NHP2-like protein 1 (High mobility group-like nuclear protein 2 homolog 1)(U4/U6.U5 tri-snRNP 15.5 kDa protein)(Sperm-specific antigen 1)(Fertilization antigen 1)(FA-1) IPR002415 HMG nuclearIPR000948 Ribosomal HS6IPR018492 Ribosomal L7A/RS6 famIPR004037 Ribosomal L7AeIPR004038 Ribosomal L7Ae/L30e/S12e/Gad45	124.5614
ENSMUSP00000092888	28.5	60S ribosomal protein L7-like 1 IPR000295 Prot inh Lserp2IPR016082 Ribosomal L30 CIPR000517 Ribosomal L30 coreIPR005998 Ribosomal L7 eukIPR018038 Ribosomal protein L30	250
sp|CAS1_BOVIN|	24.5	Alpha-S1-casein; Contains: Antioxidant peptide; Flags: Precursor;	214.91228
ENSMUSP00000034607	57.2	Coatomer subunit delta (Delta-coat protein)(Delta-COP)(Archain) IPR008968 Clathrin mu CIPR011012 Longin like	501.75439
ENSMUSP00000043660	25.3	no description availableIPR000348 Emp24 gp25L p24IPR009038 GOLD	221.92982
ENSMUSP00000071636	24.8	Peroxiredoxin-6 (EC 1.11.1.15)(Antioxidant protein 2)(1-Cys peroxiredoxin)(1-Cys PRX)(Acidic calcium-independent phospholipase A2)(aiPLA2)(EC 3.1.1.-)(Non-selenium glutathione peroxidase)(NSGPx)(EC 1.11.1.7) Source: 1.11.1.15 IPR000866 Alkyl hydroperoxide RdtaseIPR013740 RedoxinIPR012336 Thioredoxin-like fold	217.54386

ENSMUSP00000108956	110.8	26S proteasome non-ATPase regulatory subunit 1 (26S proteasome regulatory subunit RPN2)(26S proteasome regulatory subunit S1) IPR016642 26S Psome Rpn2IPR002015 APC proteasomeIPR016024 ARM-type foldIPR004155 PBS lyase HEAT	971.92982
ENSMUSP00000004729	27.6	Electron transfer flavoprotein subunit beta (Beta-ETF) IPR014730 ETF a/b NIPR012255 ETF bIPR000049 ETF b core	242.10526
ENSMUSP00000079180	13.7	40S ribosomal protein S25 IPR000079 HMG 14 17IPR004977 Ribosomal S25	120.17544
ENSMUSP00000026425	43.7	Proliferation-associated protein 2G4 (Proliferation-associated protein 1)(Protein p38-2G4)(Mpp1)(IRES-specific cellular trans-acting factor 45 kDa)(ITAF45) IPR004545 Pap 1IPR018349 Pept M24A MAP2 BSIPR000994 Pept M24 structural-domain	383.33333
ENSMUSP00000023433	67.5	Mitochondrial import receptor subunit TOM70 (Translocase of outer membrane 70 kDa subunit)(Mitochondrial precursor proteins import receptor) IPR001440 TPR-1IPR013105 TPR 2IPR013026 TPR region	592.10526
ENSMUSP00000005066	43.4	Dual specificity mitogen-activated protein kinase kinase 1 (MAP kinase kinase 1)(MAPKK 1)(EC 2.7.12.2)(ERK activator kinase 1)(MAPK/ERK kinase 1)(MEK1) Source: 2.7.12.2 IPR011009 Kinase likeIPR000719 Prot kinase coreIPR017441 Protein kinase ATP BSIPR017442 Se/Thr pkinase-relIPR008271 Ser thr pkin ASIPR002290 Ser thr pkinaseIPR001245 Tyr pkinase	380.70175
ENSMUSP00000030028	46.8	Thioredoxin domain-containing protein 4 Precursor (Endoplasmic reticulum resident protein ERp44) IPR001393 CalsequestrinIPR012336 Thioredoxin-like foldIPR006662 Thioredoxin-like subdomIPR013766 Thioredoxin dom	410.52632
ENSMUSP00000083375	42.1	Glutamine synthetase (GS)(EC 6.3.1.2)(Glutamate--ammonia ligase) Source: 6.3.1.2 IPR008147 Gln synt betaIPR008146 Gln synth cat	369.29825
ENSMUSP00000060584	56	Cytochrome P450 2C70 (EC 1.14.14.1)(CYPIIC70) Source: 1.14.14.1 IPR001128 Cyt P450IPR002397 Cyt P450 BIPR017973 Cyt P450 CIPR017972 Cyt P450 CSIPR002401 Cyt P450 E grp-IIPR002403 Cyt P450 E grp-IVIPR008067 Cyt P450 E grp-I CYP2A-likeIPR008068 Cyt P450 E grp-I CYP2B-likeIPR008069 Cyt P450 E grp-I CYP2D-like	491.22807
ENSMUSP00000027111	79.7	NADH-ubiquinone oxidoreductase 75 kDa subunit, mitochondrial Precursor (EC 1.6.5.3)(EC 1.6.99.3)(Complex I-75kD)(CI-75kD) Source: 1.6.5.3 IPR001041 FerredoxinIPR006656 Mopterin OxRdtaseIPR000283 NADH DHase 75KDa su CSIPR010228 NADH quinone OxRdtase GIPR015405 NuoG C	699.12281
ENSMUSP00000024946	32.2	3,2-trans-enoyl-CoA isomerase, mitochondrial Precursor (EC 5.3.3.8)(Dodecenoyl-CoA isomerase)(Delta(3),Delta(2)-enoyl-CoA isomerase)(D3,D2-enoyl-CoA isomerase) Source: 5.3.3.8 IPR001753 Crotonase coreIPR018376 Enoyl-CoA hyd/isom CS	282.45614
ENSMUSP00000078369	60.6	60 kDa lysophospholipase (EC 3.1.1.5) Source: 3.1.1.5 IPR002110 ANKIPR006033 AsnASEIIPR006034 Asp/Glutamnse	531.57895
ENSMUSP00000036265	137.4	superkiller viralicidic activity 2-like IPR003593 AAA+ ATPase coreIPR014001 DEAD-like NIPR001650 DNA/RNA helicase CIPR011545 DNA/RNA helicase DEAD/DEAH NIPR012961 DSH CIPR014021 Helicase SF1/SF2 ATP-bdIPR016438 RNA helicase ATP-dep SK12/DOB1IPR013324 RNA pol sigma r3 r4	1205.2632
ENSMUSP00000040550	58.5	Amine oxidase Source: 1.4.3.4 IPR000759 Adrndx reductaseIPR001613 Amineoxid flIPR002937 Amino oxidase	513.15789
ENSMUSP00000087110	72.9	Elongation factor 1-delta (EF-1-delta) IPR001326 Transl elong EF1B B/D CSIPR014038 Transl elong EF1B B/D G exch	639.47368
ENSMUSP00000032927	32.9	PCTP-like protein (PCTP-L)(StAR-related lipid transfer protein 10)(START domain-containing protein 10)(StARD10)(Serologically defined colon cancer antigen 28 homolog) IPR002913 START lipid bd	288.59649
ENSMUSP00000047661	12.5	Cytochrome c oxidase polypeptide 6A1, mitochondrial Precursor (Cytochrome c oxidase polypeptide VIa-liver) IPR001349 Cyt c oxidase su6aIPR018507 Cyt c oxidase su6a CS	109.64912
ENSMUSP00000080614	39.8	Mitochondrial import inner membrane translocase subunit TIM50 Precursor IPR004274 NIF	349.12281
ENSMUSP00000046016	9.5	40S ribosomal protein S27-like protein IPR000592 Ribosomal S27eIPR011332 Ribosomal zn-bd	83.333333
ENSMUSP00000037930	173.8	UDP-glucose:glycoprotein glucosyltransferase 1 Precursor (EC 2.4.1.-)(UDP-glucose ceramide glucosyltransferase-like 1)(UDP--Glc:glycoprotein glucosyltransferase) Source: 2.4.1.- IPR009448 UDP-g GGtrans	1524.5614
ENSMUSP00000089808	36.3	Transmembrane protein 19 IPR002794 DUF92 TM	318.42105
ENSMUSP00000034131	91.7	Vacuolar protein sorting-associated protein 35 (Vesicle protein sorting 35)(Maternal-embryonic 3) IPR005378 Vps35	804.38596
ENSMUSP00000070751	42.4	Basigin Precursor (Basic immunoglobulin superfamily)(Membrane glycoprotein gp42)(HT7 antigen)(CD147 antigen) IPR013151 IgIPR007110 Ig-likeIPR013098 Ig I-setIPR003599 Ig subIPR003598 Ig sub2	371.92982

ENSMUSP00000044004	504.4	Prolow-density lipoprotein receptor-related protein 1 Precursor (LRP)(Alpha-2-macroglobulin receptor)(A2MR)(CD91 antigen) IPR006150 Cys repeat 1IPR006210 EGFIPR000152 EGF-type Asp/Asn hydroxyl CSIPR000742 EGF 3IPR001881 EGF Ca bdIPR013091 EGF Ca bd 2IPR018097 EGF Ca bd CSIPR002049 EGF lamininIPR006209 EGF likeIPR013032 EGF like reg CSIPR006212 Furin repeatIPR000033 LDLRIPR002172 LDL rcpt classA cys-richIPR003566 Tcell CD5	4424.5614
ENSMUSP00000070993	29.2	14-3-3 protein epsilon (14-3-3E) IPR000308 14-3-3	256.14035
ENSMUSP00000022842	59.6	T-complex protein 1 subunit epsilon (TCP-1-epsilon)(CCT-epsilon) IPR012718 Chap CCT epsiIPR017998 Chaperone TCP-1IPR002194 Chaperonin TCP-1 CSIPR001844 Chaprnin Cpn60IPR002423 Cpn60/TCP-1	522.80702
ENSMUSP00000023210	35.3	Cytochrome c1, heme protein, mitochondrial Precursor (Ubiquinol-cytochrome-c reductase complex cytochrome c1 subunit)(Cytochrome c-1)(Cytochrome b-c1 complex subunit 4)(Complex III subunit 4)(Complex III subunit IV) IPR002326 Cyt C1IPR009056 Cyt c monohaem	309.64912
ENSMUSP00000005508	49.6	Transducin beta-like protein 2 IPR001632 Gprotein BIPR001680 WD40 repeatIPR011046 WD40 repeat-likeIPR017986 WD40 repeat region	435.08772
ENSMUSP00000053842	52.4	DnaJ homolog subfamily A member 3, mitochondrial Precursor (Tumorous imaginal discs protein Tid56 homolog)(DnaJ protein Tid-1)(mTid-1) IPR002939 DnaJ CIPR001623 DnaJ NIPR008971 HSP40/DnaJ pept-bdIPR001305 HSP DnaJ cys-richIPR018253 Heat shock DnaJ CSIPR003095 Hsp DnaJ	459.64912
ENSMUSP00000055313	48.1	Squalene synthetase (SQS)(SS)(EC 2.5.1.21)(Farnesyl-diphosphate farnesyltransferase)(FPP:FPP farnesyltransferase) Source: 2.5.1.21 IPR002060 Squ/phyt synthseIPR006449 Squal synthIPR008949 Terpenoid synth	421.92982
ENSMUSP00000025294	65.4	Tetratricopeptide repeat protein 39C (TPR repeat protein 39C)	573.68421
ENSMUSP00000064699	26.9	Vesicle-associated membrane protein-associated protein B (VAMP-associated protein B)(VAMP-B)(VAP-B)(VAMP-associated protein 33b) IPR000535 Major spermIPR008962 PapD-likeIPR016763 Vesicle-associated membrane	235.96491
ENSMUSP00000104831	116.2	nicotinamide nucleotide transhydrogenase (Nnt), transcript variant 2, transcribed RNA IPR007698 Ala DHase/PNT CIPR008142 Ala DHase/PNT CS1IPR008143 Ala DHase/PNT CS2IPR007886 Ala DHase/PNT NIPR004003 NADP transhyd b	1019.2982
ENSMUSP00000010007	31.8	Succinate dehydrogenase Source: 1.3.5.1 IPR006058 2Fe2S fd BSIPR017900 4Fe4S Fe S CSIPR001041 FerredoxinIPR009051 Helical ferredxnIPR004489 Succ DHase/fum Rdtase Fe-S	278.94737
ENSMUSP00000066181	83.8	Mitochondrial inner membrane protein (Mitofilin)	735.08772
ENSMUSP00000026495	59.7	ATP synthase subunit alpha, mitochondrial Precursor IPR005294 ATPase F1-cplx asuIPR018118 ATPase F1/A1-cplx a/bsu NIPR000793 ATPase F1/V1/A1-cplx a/bsu CIPR004100 ATPase F1/V1/A1-cplx a/bsu NIPR000194 ATPase F1/V1/A1 a/bsu nucl-bd	523.68421
ENSMUSP00000021806	27.6	Thiopurine S-methyltransferase (EC 2.1.1.67)(Thiopurine methyltransferase) Source: 2.1.1.67 IPR008854 Thiopurine S-MeTrfaseIPR016822 Thiopurine S-MeTrfase sub	242.10526
ENSMUSP00000099664	25.6	Adenylate kinase 2, mitochondrial (AK 2)(EC 2.7.4.3)(ATP-AMP transphosphorylase 2) Source: 2.7.4.3 IPR006259 Adenyl kin subIPR000850 Adenylate kinIPR007862 Adenylate kinase Znf lid	224.5614
ENSMUSP00000046079	55.6	Probable carboxypeptidase PM20D1 Precursor (EC 3.4.17.-)(Peptidase M20 domain-containing protein 1) Source: 3.4.17.- IPR002933 Peptidase M20IPR011650 Peptidase M20 dimer	487.7193
ENSMUSP00000097738	20.2	Coatomer subunit zeta-1 (Zeta-1-coat protein)(Zeta-1 COP) IPR000804 Clathrin sigma/coatomer zetaIPR011012 Longin like	177.19298
ENSMUSP00000052086	42	Beta-actin-like protein 2 (Kappa-actin) IPR004001 Actin CSIPR004000 Actin like	368.42105
ENSMUSP00000026420	13	40S ribosomal protein S26 IPR000892 Ribosomal S26e	114.03509
ENSMUSP00000101300	20	Protein DJ-1 (Parkinson disease protein 7 homolog) IPR006287 DJ1IPR002818 ThiJ/PfpI	175.4386
ENSMUSP00000101023	68.1	Acetolactate synthase-like protein (EC 2.2.1.-)(IlvB-like protein) Source: 2.2.1.- IPR000399 TPP bd CSIPR012001 TPP bd enzyme NIPR012000 TPP enzyme MIPR011766 TPP enzyme bd C	597.36842
ENSMUSP00000080354	46.1	60S ribosomal protein L3 (J1 protein) IPR000597 Ribosomal L3IPR009000 TranslI elong init/rib B-barrel	404.38596
ENSMUSP00000026843	82.6	Trifunctional enzyme subunit alpha, mitochondrial Precursor (TP-alpha) Source: 4.2.1.17 IPR006180 3-OHacyl-CoA DHase CSIPR006176 3-OHacyl-CoA DHase NAD-bdIPR006108 3HC DHase CIPR008927 6-PGluconate DH C	724.5614

		likeIPR001753 Crotonase coreIPR018376 Enoyl-CoA hyd/isom CSIPR012803 Fa ox alpha mitIPR006036 K uptake TrkAIPR016040 NAD(P)-bd	
ENSMUSP00000033176	48.2	Cytochrome b-c1 complex subunit 2, mitochondrial Precursor (Ubiquinol-cytochrome-c reductase complex core protein 2)(Core protein II)(Complex III subunit 2) IPR011249 Metalloenz metal-bdIPR011765 Pept M16 NIPR001431 Pept M16 Zn BSIPR007863 Peptidase M16 C	422.80702
ENSMUSP00000057543	40.5	Guanine nucleotide-binding protein G(i), alpha-2 subunit (Adenylate cyclase-inhibiting G alpha protein) IPR006688 ARFIPR002975 Fungi GproteinAIPR001019 Gprotein alph bdIPR000469 Gprotein alpha12IPR001408 Gprotein alpha IIPR000367 Gprotein alpha SIPR001806 Ras GTPase	355.26316
ENSMUSP00000020262	32	Phenazine biosynthesis-like domain-containing protein 2 (EC 5.1.-.-) Source: 5.1.-.- IPR003719 PhzC PhzF	280.70175
ENSMUSP00000073322	35.9	retinol dehydrogenase 1 (all trans) IPR003560 DHB DHaseIPR002198 DHase sc/Rdtase SDRIPR002347 Glc/ribitol DHaseIPR002424 Insect AlcDHase famIPR016040 NAD(P)-bd	314.91228
ENSMUSP00000038063	60.1	24-dehydrocholesterol reductase Precursor (EC 1.3.1.-)(3-beta-hydroxysterol delta-24-reductase) Source: 1.3.1.- IPR016166 FAD-bd 2IPR006094 Oxid FAD bind N	527.19298
ENSMUSP00000044587	26.4	Probable N-acetyltransferase CML2 (EC 2.3.1.-)(Camello-like protein 2) Source: 2.3.1.- IPR016181 Acyl CoA acyltransferaseIPR000182 GCN5-rel AcTrfase	231.57895
ENSMUSP00000071976	26.2	trypsin 10 IPR009003 Pept Trypsin-like Ser/CysIPR018114 Peptidase S1/S6 ASIPR001314 Peptidase S1AIPR001254 Peptidase S1 S6	229.82456
ENSMUSP00000061152	33.5	Mitochondrial carrier homolog 2 IPR001993 Mitoch carrierIPR018108 Mitochondrial sb/sol carrier	293.85965
ENSMUSP00000027108	24.7	Elongation factor 1-beta (EF-1-beta) IPR010987 Glutathione-S-Trfase C-likeIPR001326 Transl elong EF1B B/D CSIPR014038 Transl elong EF1B B/D G exch	216.66667
ENSMUSP00000032946	23.6	Ras-related protein Rab-6A (Rab-6) IPR006688 ARFIPR006689 ARF/SARIPR003579 GTPase RabIPR003577 GTPase RasIPR003578 GTPase RhoIPR013684 Miro-likeIPR002041 Ran GTPaseIPR013753 RasIPR001806 Ras GTPaseIPR005225 Small GTP bd	207.01754
ENSMUSP00000077021	56	Cytochrome P450 2B19 (EC 1.14.14.1)(CYPIIB19) Source: 1.14.14.1 IPR001128 Cyt P450IPR017973 Cyt P450 CIPR017972 Cyt P450 CSIPR002401 Cyt P450 E grp-IIPR002403 Cyt P450 E grp-IVIPR008067 Cyt P450 E grp-I CYP2A-likeIPR008068 Cyt P450 E grp-I CYP2B-likeIPR008071 Cyt P450 E grp-I CYP2J-like	491.22807
ENSMUSP00000032143	68.5	Dolichyl-diphosphooligosaccharide--protein glycosyltransferase subunit 1 Precursor (EC 2.4.1.119)(Dolichyl-diphosphooligosaccharide--protein glycosyltransferase 67 kDa subunit)(Ribophorin-1)(Ribophorin I)(RPN-I) Source: 2.4.1.119 IPR007676 Ribophorin I	600.87719
ENSMUSP00000026459	56.3	ATP synthase subunit beta, mitochondrial Precursor (EC 3.6.3.14) Source: 3.6.3.14 IPR003593 AAA+ ATPase coreIPR005722 ATPase F1-cplx bsuIPR018118 ATPase F1/A1-cplx a/bsu NIPR000793 ATPase F1/V1/A1-cplx a/bsu CIPR004100 ATPase F1/V1/A1-cplx a/bsu NIPR000194 ATPase F1/V1/A1 a/bsu nucl-bd	493.85965
ENSMUSP00000019226	34.6	Mitochondrial glutamate carrier 1 (GC-1)(Glutamate/H(+) symporter 1)(Solute carrier family 25 member 22) IPR002113 Aden trnslctorIPR002067 Mit carrierIPR001993 Mitoch carrierIPR018108 Mitochondrial sb/sol carrier	303.50877
ENSMUSP00000002837	26.2	Transmembrane emp24 domain-containing protein 5 Precursor IPR000348 Emp24 gp25L p24IPR009038 GOLD	229.82456
ENSMUSP00000019323	35.6	Malate dehydrogenase, mitochondrial Precursor (EC 1.1.1.37) Source: 1.1.1.37 IPR001557 L-lactate/malate DHaseIPR001236 Lactate/malate DHaseIPR015955 Lactate DHase/Glyco Ohase 4 CIPR001252 Malate DHase ASIPR010097 Malate DHase NAD-dep euk g bacIPR016040 NAD(P)-bd	312.2807
ENSMUSP00000097754	62.8	Keratin, type II cytoskeletal 2 oral (Keratin-76)(K76) IPR016044 FIPR018039 Intermediate filament CSIPR002957 Keratin IIPR003054 Keratin IIIPR009053 Prefoldin	550.87719
ENSMUSP00000021062	69.2	Probable ATP-dependent RNA helicase DDX5 (EC 3.6.1.-)(DEAD box protein 5)(RNA helicase p68)(DEAD box RNA helicase DEAD1)(mDEAD1) Source: 3.6.1.- IPR014001 DEAD-like NIPR001650 DNA/RNA helicase CIPR011545 DNA/RNA helicase DEAD/DEAH NIPR014021 Helicase SF1/SF2 ATP-bdIPR012587 P68HRIPR000629 RNA-helicase DEAD-box CSIPR014014 RNA helicase DEAD Q motif	607.01754
ENSMUSP00000073261	35.6	Metaxin-1 IPR010987 Glutathione-S-Trfase C-likeIPR017410 Metaxin	312.2807
ENSMUSP00000103365	21.6	60S ribosomal protein L18 IPR000039 Ribosomal L18e	189.47368
ENSMUSP00000027966	37.8	Low affinity immunoglobulin gamma Fc region receptor II Precursor (IgG Fc receptor II beta)(Fc gamma receptor IIB)(Fc-	331.57895

		gamma-RIIB)(Fc-gamma RII)(FcRII)(Lymphocyte antigen 17)(Ly-17)(CD32 antigen) IPR013151 IgIPR007110 Ig-likeIPR003599 Ig subIPR003598 Ig sub2	
ENSMUSP00000049394	30.6	Carbonyl reductase Source: 1.1.1.184 IPR003560 DHB DHaseIPR002198 DHase sc/Rdtase SDRIPR002347 Glc/ribitol DHaseIPR016040 NAD(P)-bd	268.42105
ENSMUSP00000069508	65.7	Phenylalanyl-tRNA synthetase beta chain (EC 6.1.1.20)(Phenylalanine--tRNA ligase beta chain)(PheRS) Source: 6.1.1.20 IPR005146 B3/B4 tRNA-bdIPR005147 B5IPR009061 DNA bd putIPR004531 Phe-tRNA-synth IIc bsu arc	576.31579
ENSMUSP00000020329	134.8	Epidermal growth factor receptor Precursor (EC 2.7.10.1) Source: 2.7.10.1 IPR016060 Complement control moduleIPR000494 EGF rcpt LIPR006211 Furin-likeIPR006212 Furin repeatIPR011009 Kinase likeIPR000719 Prot kinase coreIPR017441 Protein kinase ATP BSIPR017442 Se/Thr pkinase-relIPR002290 Ser thr pkinaseIPR016245 Tyr kinase rcpt EGF/ERB/XmrKIPR001245 Tyr pkinaseIPR008266 Tyr pkinase AS	1182.4561
ENSMUSP00000099441	57	CDK5 regulatory subunit-associated protein 3 IPR008491 DUF773	500
ENSMUSP00000068408	59.1	Cleavage and polyadenylation specificity factor subunit 6 IPR013286 AnnexinVIIIPR000694 PRO richIPR003882 Pistil extensinIPR000504 RRM RNP1IPR017997 Vinculin	518.42105
ENSMUSP00000045841	170	Bifunctional aminoacyl-tRNA synthetase Source: 6.1.1.17 IPR004154 Anticodon bdIPR004526 Glu-tRNA-synth Ic arc/eukIPR000924 Glu/Gln-tRNA-synth IcIPR010987 Glutathione-S-Trfase C-likeIPR002316 Pro-tRNA-synth IIaIPR004499 Pro-tRNA-synth IIa pro-typeIPR017449 Pro-tRNA synth IIIPR016061 Pro-tRNA synth II CIPR011035 Ribosomal L25/Gln-tRNA synthIPR009068 S15 NS1 RNA bdIPR000738 WHEP-TRSIPR002314 aa-tRNA-synt IIbIPR006195 aa-tRNA-synth IIIPR001412 aa-tRNA-synth I CS	1491.2281
ENSMUSP00000019469	40.4	Glucose-6-phosphatase (G-6-Pase)(G6Pase)(EC 3.1.3.9) Source: 3.1.3.9 IPR016275 Glucose-6-phosphataseIPR000326 P Acid Pase 2/haloperoxidase	354.38596
ENSMUSP00000020463	62.9	Nicalin Precursor (Nicastrin-like protein) IPR016574 Nicalin	551.75439
ENSMUSP00000042364	19.8	Myosin regulatory light chain MRLC2 (Myosin regulatory light chain 2-B, smooth muscle isoform) IPR018247 EF HAND 1IPR018249 EF HAND 2IPR018248 EF handIPR002048 EF hand Ca bd	173.68421
ENSMUSP00000009003	23.5	Ras-related protein Ral-A Precursor IPR006689 ARF/SARIPR003579 GTPase RabIPR003577 GTPase RasIPR003578 GTPase RhoIPR013684 Miro-likeIPR002041 Ran GTPaseIPR013753 RasIPR001806 Ras GTPaseIPR005225 Small GTP bd	206.14035
ENSMUSP00000027975	38.6	Phytanoyl-CoA dioxygenase, peroxisomal Precursor (EC 1.14.11.18)(Phytanoyl-CoA alpha-hydroxylase)(PhyH)(Phytanic acid oxidase)(Lupus nephritis-associated peptide 1) Source: 1.14.11.18 IPR008775 Phytyl CoA dOase	338.59649
ENSMUSP00000049732	34.4	Glycolipid transfer protein domain-containing protein 2 IPR014830 Glycolipid transfer prot	301.75439
ENSMUSP00000109305	35.9	Annexin A4 (Annexin-4)(Annexin IV) IPR001464 AnnexinIPR002389 AnnexinIIIPR002390 AnnexinIIIIPR002391 AnnexinIVIPR002392 AnnexinVIPR009115 AnnexinVIIIIPR018502 Annexin repeatIPR018252 Annexin repeat CS	314.91228
ENSMUSP00000006838	87.6	glutaminyl-tRNA synthetase IPR004514 Gln-tRNA-synth IcIPR007639 Gln-tRNA-synth Ic RNA-bd 1IPR007638 Gln-tRNA-synth Ic RNA-bd 2IPR000924 Glu/Gln-tRNA-synth IcIPR011035 Ribosomal L25/Gln-tRNA synthIPR001412 aa-tRNA-synth I CS	768.42105
ENSMUSP00000035157	29.6	Signal recognition particle receptor subunit beta (SR-beta) IPR006688 ARFIPR006689 ARF/SARIPR006687 SAR1 GTP bd	259.64912
ENSMUSP00000002403	34	Dehydrogenase/reductase SDR family member 1 (EC 1.1.-.-) Source: 1.1.-.- IPR003560 DHB DHaseIPR002198 DHase sc/Rdtase SDRIPR002347 Glc/ribitol DHaseIPR016040 NAD(P)-bd	298.24561
ENSMUSP00000048460	10.3	Phospholemman Precursor (FXYD domain-containing ion transport regulator 1) IPR000272 Ion-transport regulator FXYD	90.350877
ENSMUSP00000074600	24	NADH dehydrogenase Source: 1.6.5.3 IPR001080 3Fe4S ferredoxinIPR017900 4Fe4S Fe S CSIPR001450 4Fe4S Fe S bd subgrIPR009051 Helical ferredxnIPR010226 NADH quinone OxRdtase I	210.52632
ENSMUSP00000038839	66.6	Eukaryotic translation initiation factor 3 subunit L (eIF3l)(Eukaryotic translation initiation factor 3 subunit E-interacting protein)(Eukaryotic translation initiation factor 3 subunit 6-interacting protein)(67 kDa polymerase-associated factor)(PAF67)(66 kDa tyrosine-rich heat shock protein)(HSP-66Y)	584.21053
ENSMUSP00000075990	28.9	Synaptophysin-like protein 1 (Pantophysin) IPR008253 MarvelIPR001285 Synaptophysin/porin	253.50877
ENSMUSP00000022734	57.4	DnaJ homolog subfamily C member 3 Precursor (Interferon-induced, double-stranded RNA-activated protein kinase inhibitor)(Protein kinase inhibitor of 58 kDa)(Protein kinase inhibitor p58) IPR001623 DnaJ NIPR001440 TPR-1IPR013105	503.50877

		TPR 2IPR013026 TPR region	
ENSMUSP00000004574	40.5	DnaJ homolog subfamily B member 11 Precursor (ER-associated dnaJ protein 3)(ERj3p)(ERdj3)(ER-associated Hsp40 co-chaperone)(ER-associated DNAJ)(APOBEC1-binding protein 2)(ABBP-2) IPR002939 DnaJ CIPR001623 DnaJ NIPR008971 HSP40/DnaJ pept-bdIPR018253 Heat shock DnaJ CSIPR003095 Hsp DnaJ	355.26316
ENSMUSP00000044871	61.7	GPI transamidase component PIG-S (Phosphatidylinositol-glycan biosynthesis class S protein)	541.22807
ENSMUSP00000028396	74.5	Calcium-binding mitochondrial carrier protein Aralar1 (Mitochondrial aspartate glutamate carrier 1)(Solute carrier family 25 member 12) IPR002113 Aden trnslctorIPR018247 EF HAND 1IPR018249 EF HAND 2IPR018248 EF handIPR002048 EF hand Ca bdIPR002167 Graves DCIPR002067 Mit carrierIPR001993 Mitoch carrierIPR018108 Mitochondrial sb/sol carrier	653.50877
ENSMUSP00000099653	36.4	Eukaryotic translation initiation factor 3 subunit I (eIF3i)(Eukaryotic translation initiation factor 3 subunit 2)(eIF-3-beta)(eIF3 p36)(TGF-beta receptor-interacting protein 1)(TRIP-1) IPR001680 WD40 repeatIPR011046 WD40 repeat-likeIPR017986 WD40 repeat region	319.29825
ENSMUSP00000103015	109.6	Aminopeptidase N (mAPN)(EC 3.4.11.2)(Alanyl aminopeptidase)(Microsomal aminopeptidase)(Aminopeptidase M)(Membrane protein p161)(CD13 antigen) Source: 3.4.11.2 IPR014782 Peptidase M1 N	961.40351
ENSMUSP00000099417	73.5	Dolichyl-diphosphooligosaccharide--protein glycosyltransferase subunit 2 Precursor (EC 2.4.1.119)(Dolichyl-diphosphooligosaccharide--protein glycosyltransferase 63 kDa subunit)(Ribophorin-2)(Ribophorin II)(RPN-II) Source: 2.4.1.119 IPR008814 Ribophorin II	644.73684
ENSMUSP00000078670	20.6	no description availableIPR002132 Ribosomal L5	180.70175
ENSMUSP00000047606	65.4	Complement component C8 alpha chain Precursor (Complement component 8 subunit alpha) IPR013032 EGF like reg CSIPR002172 LDL rcpt classA cys-richIPR001862 MAC perforinIPR000884 Thrombospondin 1 rptIPR008085 Thrombospondin 1 rpt sub	573.68421
ENSMUSP00000020741	40.5	Developmentally-regulated GTP-binding protein 1 (DRG-1)(Neural precursor cell expressed developmentally down-regulated protein 3)(NEDD-3) IPR006074 GTP1-OBG CSIPR006073 GTP1 OBGIPR002917 MMR HSR1 GTP bdIPR005225 Small GTP bdIPR004095 TGS	355.26316
ENSMUSP00000022322	61.3	Glutamate dehydrogenase 1, mitochondrial Precursor (GDH)(EC 1.4.1.3) Source: 1.4.1.3 IPR006095 Glu/Leu/Phe/Val DHaseIPR006096 Glu/Leu/Phe/Val DHase CIPR006097 Glu/Leu/Phe/Val DHase dimerIPR016040 NAD(P)-bd	537.7193
ENSMUSP00000006900	15.2	Thioesterase superfamily member 2 IPR003736 PAAIIPR006683 Thioestr supf	133.33333
ENSMUSP00000004375	33.3	Prohibitin-2 (B-cell receptor-associated protein BAP37)(Repressor of estrogen receptor activity) IPR001107 Band 7IPR000163 Prohibitin	292.10526
ENSMUSP00000103657	19.5	Peptidyl-tRNA hydrolase 2, mitochondrial Precursor (PTH 2)(EC 3.1.1.29) Source: 3.1.1.29 IPR002833 Pep tRNA hydro PTH2	171.05263
ENSMUSP00000090910	61.4	Liver carboxylesterase 31 Precursor (Esterase-31)(EC 3.1.1.1)(ES-male) Source: 3.1.1.1 IPR002018 CarbesteraseB	538.59649
ENSMUSP00000022925	39.8	Eukaryotic translation initiation factor 3 subunit H (eIF3h)(Eukaryotic translation initiation factor 3 subunit 3)(eIF-3 gamma)(eIF3 p40 subunit) IPR000555 Mov34 MPN PAD1	349.12281
ENSMUSP00000017488	54.8	Vitronectin Precursor (Serum-spreading factor)(S-protein) IPR000585 HemopexinIPR018486 Hemopexin/matrixin CSIPR018487 Hemopexin/matrixin repeatIPR001212 Somatomedin B	480.70175
ENSMUSP00000026899	31.7	Mitochondrial dicarboxylate carrier (Solute carrier family 25 member 10) IPR002113 Aden trnslctorIPR002067 Mit carrierIPR002030 Mit uncouplingIPR001993 Mitoch carrierIPR018108 Mitochondrial sb/sol carrier	278.07018
ENSMUSP00000022894	27.8	14-3-3 protein zeta/delta (Protein kinase C inhibitor protein 1)(KCIP-1)(SEZ-2) IPR000308 14-3-3	243.85965
ENSMUSP00000096932	17.2	Ubiquitin-conjugating enzyme E2 N (EC 6.3.2.19)(Ubiquitin-protein ligase N)(Ubiquitin carrier protein N)(Ubc13)(Bendless-like ubiquitin-conjugating enzyme) Source: 6.3.2.19 IPR016135 UBQ-conjugat/RWD-likeIPR000608 UBQ-conjugat E2	150.87719
ENSMUSP00000026222	21.9	NADH dehydrogenase IPR008699 NADH UbQ OxRdtase ASHI suIPR016551 NADH Ub cplx-1 bsu su-8	192.10526
ENSMUSP00000095287	15.8	60S ribosomal protein L27 IPR005824 KOWIPR001141 Ribosomal L27eIPR018262 Ribosomal L27e CS	138.59649
ENSMUSP00000036246	59.7	Keratin, type II cytoskeletal 75 (Cytokeratin-75)(CK-75)(Keratin-75)(K75)(Type II keratin-18)(Type II keratin-K6hf)(Keratin-6 hair follicle)(mK6hf) IPR016044 FIPR018039 Intermediate filament CSIPR002957 Keratin IIPR003054 Keratin IIIPR009053 PrefoldinIPR003536 Transloc intimin rcptIPR000533 Tropomyosin	523.68421

ENSMUSP00000055535	72.5	Probable ATP-dependent RNA helicase DDX17 (EC 3.6.1.-)(DEAD box protein 17) Source: 3.6.1.- IPR014001 DEAD-like NIPR001650 DNA/RNA helicase CIPR011545 DNA/RNA helicase DEAD/DEAH NIPR014021 Helicase SF1/SF2 ATP-bdIPR000694 PRO richIPR000629 RNA-helicase DEAD-box CSIPR014014 RNA helicase DEAD Q motif	635.96491
ENSMUSP00000056027	25.2	Sigma 1-type opioid receptor (Sigma1-receptor)(Sigma1R) IPR006716 ERG2 sigma1 rcpt like	221.05263
ENSMUSP00000080854	34.4	60S ribosomal protein L5 IPR005484 Ribosomal L18/L5IPR005485 Ribosomal L5 euk	301.75439
ENSMUSP00000046324	27.6	Glutathione S-transferase theta-2 (EC 2.5.1.18)(GST class-theta-2) Source: 2.5.1.18 IPR004046 GST CIPR010987 Glutathione-S-Trfase C-likeIPR004045 Glutathione S-Trfase NIPR012336 Thioredoxin-like fold	242.10526
ENSMUSP00000041872	37.3	Sideroflexin-5 IPR004686 Mtc	327.19298
ENSMUSP00000033873	37.8	Erlin-2 (Endoplasmic reticulum lipid raft-associated protein 2)(Stomatin-prohibitin-flotillin-HflC/K domain-containing protein 2)(SPFH domain-containing protein 2) IPR001107 Band 7	331.57895
ENSMUSP00000028704	41	Hydroxyacid oxidase 1 (HAOX1)(EC 1.1.3.15)(Glycolate oxidase)(GOX) Source: 1.1.3.15 IPR000262 FMN-dep DHaseIPR008259 FMN hydac DHase ASIPR012133 a-Hydoxy acid DHase FMN	359.64912
ENSMUSP00000066715	38.2	MOSC domain-containing protein 2, mitochondrial Precursor (EC 1.-.-.-) Source: 1.-.-.- IPR005303 MOSC NIPR005302 MoCF Sase CIPR011037 Pyrv Knase b-brl-likeIPR000231 Ribosomal L30e	335.08772
ENSMUSP00000022980	22	NADH dehydrogenase IPR008011 Complex1 LYR	192.98246
ENSMUSP00000016400	34	Cathepsin Z Precursor (EC 3.4.18.1) Source: 3.4.18.1 IPR000169 Pept cys ASIPR000668 Peptidase C1A C	298.24561
ENSMUSP00000010795	44	3-ketoacyl-CoA thiolase B, peroxisomal Precursor (EC 2.3.1.16)(Beta-ketothiolase B)(Acetyl-CoA acyltransferase B)(Peroxisomal 3-oxoacyl-CoA thiolase B) Source: 2.3.1.16 IPR013747 ACP syn III CIPR002155 ThiolaseIPR016039 Thiolase-like	385.96491
ENSMUSP00000043047	141.7	Vigilin (High density lipoprotein-binding protein)(HDL-binding protein) IPR004087 KHIPR004088 KH type 1IPR018111 KH type 1 subgr	1242.9825
ENSMUSP00000033953	44.4	Indoleamine 2,3-dioxygenase-like protein 1 (EC 1.13.11.-)(Indoleamine-pyrrole 2,3-dioxygenase-like protein 1) Source: 1.13.11.- IPR000898 Indolamine dOase	389.47368
ENSMUSP00000037617	33.8	solute carrier family 35 (UDP-glucuronic acid/UDP-N-acetylgalactosamine dual transporter), member D1	296.49123
ENSMUSP00000083271	85.8	Dolichyl-diphosphooligosaccharide--protein glycosyltransferase subunit STT3A (Oligosaccharyl transferase subunit STT3A)(STT3-A)(EC 2.4.1.119)(B5)(Integral membrane protein 1) Source: 2.4.1.119 IPR003674 Oligo trans STT3	752.63158
ENSMUSP00000049025	19.3	Splicing factor, arginine/serine-rich 3 (Pre-mRNA-splicing factor SRP20)(Protein X16) IPR000504 RRM RNP1	169.29825
ENSMUSP00000043111	14.5	60S ribosomal protein L22-like 1 IPR002671 Ribosomal L22e	127.19298
ENSMUSP00000093394	49.3	t-complex protein 10b IPR009852 Tcp10/CenJ C	432.45614
ENSMUSP00000033342	38	Eukaryotic translation initiation factor 3 subunit F (eIF3f)(Eukaryotic translation initiation factor 3 subunit 5)(eIF-3-epsilon)(eIF3 p47) IPR000104 Antifreeze 1IPR000555 Mov34 MPN PAD1IPR001013 NK3 rcptIPR000694 PRO rich	333.33333
ENSMUSP00000105531	27.1	Transmembrane emp24 domain-containing protein 9 Precursor (Glycoprotein 25L2) IPR000348 Emp24 gp25L p24IPR009038 GOLD	237.7193
ENSMUSP00000003912	48	Calreticulin Precursor (CRP55)(Calregulin)(HACBP)(ERp60) IPR001580 Calret/calnexIPR018124 Calret/calnex CSIPR009169 CalreticulinIPR008985 ConA like lec gl	421.05263
ENSMUSP00000099907	126.5	Reticulon-4 (Neurite outgrowth inhibitor)(Nogo protein) IPR000694 PRO richIPR003388 Reticulon	1109.6491
ENSMUSP00000106961	50.4	Rho GTPase-activating protein 1 (Rho-type GTPase-activating protein 1) IPR001251 CRAL bd TRIO CIPR000198 RhoGAPIPR008936 Rho GTPase activation prot	442.10526
ENSMUSP00000021335	72.3	Sec1 family domain-containing protein 1 (Syntaxin-binding protein 1-like 2) IPR001619 Sec1-like	634.21053
ENSMUSP00000089350	13.9	Histone H2B type 1-F/J/L (H2B 291A) IPR009072 Histone-foldIPR000558 Histone H2BIPR007125 Histone core D	121.92982
ENSMUSP00000109399	21.9	60S ribosomal protein L9 IPR000702 Ribosomal L6IPR002359 Ribosomal L6 CS2	192.10526
ENSMUSP00000031697	89.6	Cullin-1 (CUL-1) IPR016157 Cullin CSIPR001373 Cullin NIPR016158 Cullin homologyIPR016159 Cullin repeat-like	785.96491
ENSMUSP00000045284	29.3	Cytochrome b-c1 complex subunit Rieske, mitochondrial Precursor (EC 1.10.2.2)(Ubiquinol-cytochrome c reductase iron-	257.01754

		sulfur subunit)(Rieske iron-sulfur protein)(RISP)(Complex III subunit 5) Source: 1.10.2.2 IPR011070 Globular prot asu/bsuIPR005805 Rieske Fe-S prot CIPR005806 Rieske regIPR015248 Ubiqinol cyt c Rdtase NIPR004192 Ubiquinol cyt Rdtase TMIPR006317 Ubiquinol cyt c Rdtase Fe-S-su	
ENSMUSP00000024897	27.8	Vesicle-associated membrane protein-associated protein A (VAMP-associated protein A)(VAMP-A)(VAP-A)(33 kDa Vamp-associated protein)(VAP-33) IPR000535 Major spermIPR008962 PapD-likeIPR016763 Vesicle-associated membrane	243.85965
ENSMUSP00000006235	37.3	Cathepsin B Precursor (EC 3.4.22.1)(Cathepsin B1) Source: 3.4.22.1 IPR002016 Haem peroxidase pln/fun/bacIPR000169 Pept cys ASIPR000668 Peptidase C1A CIPR012599 Propeptide C1A	327.19298
ENSMUSP00000061059	31.6	Phosphatidylinositol transfer protein beta isoform (PtdIns transfer protein beta)(PtdInsTP)(PI-TP-beta) IPR001666 PI transfer	277.19298
ENSMUSP00000102987	23.4	Ras-related protein Rab-5C IPR006688 ARFIPR003579 GTPase RabIPR003577 GTPase RasIPR003578 GTPase RhoIPR001019 Gprotein alph bdIPR013684 Miro-likeIPR002041 Ran GTPaseIPR013753 RasIPR001806 Ras GTPaseIPR005225 Small GTP bd	205.26316
ENSMUSP00000009256	46.7	Bcl-2-like 13 protein (Protein Mil1)(Bcl-rambo) IPR002475 BCL2 apoptsisIPR000712 Bcl2 BH	409.64912
ENSMUSP00000031038	27.6	OCIA domain-containing protein 1 IPR009764 OCIA	242.10526
ENSMUSP00000015800	70.8	Heat shock cognate 71 kDa protein (Heat shock 70 kDa protein 8) IPR018181 Heat shock 70 CSIPR001023 Hsp70IPR013126 Hsp 70	621.05263
ENSMUSP00000071777:reversed	395.4		3468.4211
ENSMUSP00000049338	33.3	Protein NipSnap homolog 1 (NipSnap1) IPR012577 NIPSNAP	292.10526
ENSMUSP00000108940	35.1	sulfotransferase family 1D, member 1 IPR000863 Sulfotransferase	307.89474
ENSMUSP00000031637	9.3	NADH dehydrogenase	81.578947
ENSMUSP00000073541	53.9	7-dehydrocholesterol reductase (7-DHC reductase)(EC 1.3.1.21)(Sterol Delta(7)-reductase) Source: 1.3.1.21 IPR001171 ERG4 ERG24IPR018083 Sterol reductase CS	472.80702
ENSMUSP00000030118	44.8	DnaJ homolog subfamily A member 1 (Heat shock 40 kDa protein 4)(DnaJ protein homolog 2)(HSJ-2) IPR002939 DnaJ CIPR001623 DnaJ NIPR008971 HSP40/DnaJ pept-bdIPR001305 HSP DnaJ cys-richIPR018253 Heat shock DnaJ CSIPR003095 Hsp DnaJ	392.98246
ENSMUSP00000034547	44.8	Acetyl-CoA acetyltransferase, mitochondrial Precursor (EC 2.3.1.9)(Acetoacetyl-CoA thiolase) Source: 2.3.1.9 IPR002155 ThiolaseIPR016039 Thiolase-like	392.98246
ENSMUSP00000033229	16.1	Hemoglobin subunit epsilon-Y2 (Hemoglobin epsilon-Y2 chain)(Epsilon-Y2-globin) IPR013314 Globin lamprey/hagfishIPR009050 Globin likeIPR000971 Globin subsetIPR002337 Haemoglobin bIPR002339 Haemoglobin piIPR001032 LeghaemoglobinIPR002335 Myoglobin	141.22807
ENSMUSP00000032898	123.5	Importin-5 (Imp5)(Importin subunit beta-3)(Karyopherin beta-3)(Ran-binding protein 5)(RanBP5) IPR016024 ARM-type foldIPR000357 HEATIPR001494 Importin-b N	1083.3333
ENSMUSP00000029266	35.7	Annexin A5 (Annexin-5)(Annexin V)(Lipocortin V)(Endonexin II)(Calphobindin I)(CBP-I)(Placental anticoagulant protein I)(PAP-I)(Placental anticoagulant protein 4)(PP4)(Thromboplastin inhibitor)(Vascular anticoagulant-alpha)(VAC-alpha)(Anchorin CII) IPR001464 AnnexinIPR002390 AnnexinIIIIPR002391 AnnexinIVIPR002392 AnnexinVIPR018502 Annexin repeatIPR018252 Annexin repeat CS	313.15789
ENSMUSP00000071486	41.8	Actin, cytoplasmic 2 (Gamma-actin) IPR004001 Actin CSIPR004000 Actin like	366.66667
ENSMUSP00000110021	24.5	Ras-related protein Rab-11B IPR006688 ARFIPR003579 GTPase RabIPR003577 GTPase RasIPR003578 GTPase RhoIPR013684 Miro-likeIPR002078 RNA pol sigma 54 intIPR002041 Ran GTPaseIPR013753 RasIPR001806 Ras GTPaseIPR005225 Small GTP bd	214.91228
ENSMUSP00000101651	49.8	Ribonuclease inhibitor (Ribonuclease/angiogenin inhibitor 1) IPR001611 Leu-rich rptIPR003590 Leu-rich rpt RNase inh sub-typ	436.84211
ENSMUSP00000066419	37.2	H-2 class I histocompatibility antigen, Q10 alpha chain Precursor IPR002411 Allergen/amylase inhib riceIPR013151 IgIPR007110 Ig-likeIPR003006 Ig/MHC CSIPR003597 Ig C1-setIPR011162 MHC I/II-like Ag-recogIPR001039 MHC I a a1/a2	326.31579

ENSMUSP00000087524	38	GTPase IMAP family member 4 (Immunity-associated protein 4)(Immunity-associated nucleotide 1 protein) IPR006703 AIG1IPR000048 IQ CaM bd regionIPR001806 Ras GTPase	333.33333
ENSMUSP00000023510	52.3	Uridine 5--monophosphate synthase (UMP synthase) Source: 2.4.2.10 IPR014732 OMPdecase 1 coreIPR018089 OMPdecase ASIPR001754 OMPdecase coreIPR004467 Or phspho transIPR000836 PRibTrfaseIPR011060 RibuloseP-bd barrel	458.77193
ENSMUSP00000032844	21.5	Transmembrane protein 126A IPR009801 DUF1370	188.59649
ENSMUSP00000006764	19.7	Adenine phosphoribosyltransferase (APRT)(EC 2.4.2.7) Source: 2.4.2.7 IPR005764 Ade phspho transIPR000836 PRibTrfase	172.80702
ENSMUSP00000079672	14.5	60S ribosomal protein L35 IPR001854 Ribosomal L29IPR018254 Ribosomal L29 CS	127.19298
ENSMUSP00000003445	22.1	FK506-binding protein 11 Precursor (EC 5.2.1.8)(Peptidyl-prolyl cis-trans isomerase)(PPIase)(Rotamase)(19 kDa FK506-binding protein)(FKBP-19) Source: 5.2.1.8 IPR001179 PPIase FKBP	193.85965
ENSMUSP00000058919	10.3	60S ribosomal protein L37a IPR002674 Ribosomal L37aeIPR011332 Ribosomal zn-bd	90.350877
ENSMUSP00000098591	138.3	Inverted formin-2 IPR016024 ARM-type foldIPR018299 Alkaline phosphatase ASIPR010472 Drf FH3IPR010473 Drf GTPase bdIPR015425 FH2 actin bdIPR003104 FH2 actin bd DRFIPR000694 PRO richIPR003882 Pistil extensinIPR003124 WH2 actin bd	1213.1579
ENSMUSP00000105028	102.3	Transportin-1 (Importin beta-2)(Karyopherin beta-2) IPR016024 ARM-type foldIPR000225 ArmadilloIPR000357 HEATIPR001494 Importin-b N	897.36842
ENSMUSP00000110364	71.3	Transmembrane protein 214	625.4386
ENSMUSP00000028286	31	1-acyl-sn-glycerol-3-phosphate acyltransferase beta (EC 2.3.1.51)(1-AGP acyltransferase 2)(1-AGPAT 2)(Lysophosphatidic acid acyltransferase beta)(LPAAT-beta)(1-acylglycerol-3-phosphate O-acyltransferase 2) Source: 2.3.1.51 IPR004552 AGP acyltransIPR002123 Acyltransferase	271.92982
ENSMUSP00000033087	51.1	RuvB-like 2 (EC 3.6.1.-)(p47 protein) Source: 3.6.1.- IPR003593 AAA+ ATPase coreIPR003959 AAA ATPase coreIPR004504 DNA repair RadAIPR010339 TIP49 CIPR000764 Uridine kinase	448.24561
ENSMUSP00000031398	45	4-hydroxyphenylpyruvate dioxygenase (EC 1.13.11.27)(4-hydroxyphenylpyruvic acid oxidase)(HPPDase)(4HPPD)(HPD)(F Alloantigen)(F protein) Source: 1.13.11.27 IPR005956 4OHPhenylPyrv dOaseIPR004360 Glyas bleo-R dOase	394.73684
ENSMUSP00000095794	15.7	Hemoglobin subunit beta-1 (Hemoglobin beta-1 chain)(Beta-1-globin)(Hemoglobin beta-major chain) IPR013314 Globin lamprey/hagfishIPR009050 Globin likeIPR000971 Globin subsetIPR002338 Haemoglobin aIPR002337 Haemoglobin bIPR002339 Haemoglobin piIPR002335 Myoglobin	137.7193
ENSMUSP00000104725	118.7	Protein transport protein Sec24A (SEC24-related protein A) IPR017993 Atrophin-1IPR007123 GelsolnIPR000694 PRO richIPR012990 Sec23 24 beta SIPR006900 Sec23 helicalIPR006896 Sec23 trunkIPR006895 Znf Sec23 Sec24	1041.2281
ENSMUSP00000072717	74.6	Peroxisomal acyl-coenzyme A oxidase 1 (AOX)(EC 1.3.3.6)(Palmitoyl-CoA oxidase) Source: 1.3.3.6 IPR006091 Acyl-CoA DHase/Oxase MIPR012258 Acyl-CoA oxidaseIPR002655 Acyl-CoA oxidase CIPR009100 AcylCoA DH/oxidase M/NIPR009075 AcylCo DHase/oxidase CIPR001412 aa-tRNA-synth I CS	654.38596
ENSMUSP00000061227	61.4	Phosphoglucomutase-1 (PGM 1)(EC 5.4.2.2)(Glucose phosphomutase 1) Source: 5.4.2.2 IPR005843 A-D-PHexomutase CIPR016066 A-D-PHexomutase CSIPR005841 A-D-PHexomutase NIPR005844 A-D-PHexomutase a/b/a-IIPR016055 A-D-PHexomutase a/b/a-I/II/IIIIPR005845 A-D-PHexomutase a/b/a-IIIPR005846 A-D-PHexomutase a/b/a-III	538.59649
ENSMUSP00000027989	37.3	3-keto-steroid reductase (EC 1.1.1.270)(Estradiol 17-beta-dehydrogenase 7)(EC 1.1.1.62)(17-beta-hydroxysteroid dehydrogenase 7)(17-beta-HSD 7) Source: 1.1.1.270 IPR002198 DHase sc/Rdtase SDRIPR002347 Glc/ribitol DHaseIPR016040 NAD(P)-bd	327.19298
ENSMUSP00000066897	33.3	sulfotransferase-like protein 1 IPR000863 Sulfotransferase	292.10526
ENSMUSP00000020653	22.4	GTP-binding protein SAR1b IPR006688 ARFIPR006689 ARF/SARIPR003579 GTPase RabIPR013684 Miro-likeIPR001806 Ras GTPaseIPR006687 SAR1 GTP bdIPR005225 Small GTP bd	196.49123
ENSMUSP00000089978	56.9	Polypyrimidine tract-binding protein 1 (PTB)(Heterogeneous nuclear ribonucleoprotein I)(hnRNP I) IPR000104 Antifreeze 1IPR006536 HnRNP-L PTBIPR000870 Homoser kinIPR003954 RRM 1IPR000504 RRM RNP1	499.12281
ENSMUSP00000003655	41.8	Arsenite methyltransferase (EC 2.1.1.137)(S-adenosyl-L-methionine:arsenic(III) methyltransferase)(Methylarsonite methyltransferase) Source: 2.1.1.137 IPR013216 Methyltransf 11IPR013217 Methyltransf 12IPR004033 UbiE/COQ5	366.66667

		MeTrFase	
ENSMUSP00000023396	27.6	Phosphomannomutase 2 (PMM 2)(EC 5.4.2.8) Source: 5.4.2.8 IPR013200 HAD-SF hydro-like 3IPR006379 HAD-SF hydro IIBIPR005002 PMM	242.10526
ENSMUSP00000109611	61.2	Glycerol kinase (EC 2.7.1.30)(ATP:glycerol 3-phosphotransferase)(Glycerokinase)(GK) Source: 2.7.1.30 IPR018485 Carb kinase FGGY CIPR018483 Carb kinase FGGY CSIPR018484 Carb kinase FGGY NIPR005999 Glycerol kin	536.84211
ENSMUSP00000000175	17	Succinate dehydrogenase IPR007992 Cyt b succ DHase CybS	149.12281
ENSMUSP00000106540	70.1		614.91228
ENSMUSP00000071752	22.6	COMM domain-containing protein 7 IPR009886 HCaRG	198.24561
ENSMUSP00000081009	47.8	Selenide, water dikinase 2 (EC 2.7.9.3)(Selenophosphate synthetase 2)(Selenium donor protein 2) Source: 2.7.9.3 IPR000728 AIR synthIPR010918 AIR synth CIPR016188 PurM N-likeIPR004536 SelD	419.29825
ENSMUSP00000027429	17.9	Uncharacterized protein C2orf72 homolog Precursor	157.01754
ENSMUSP00000025218	49	Eukaryotic peptide chain release factor subunit 1 (Eukaryotic release factor 1)(eRF1) IPR004403 eRF1IPR005140 eRF1 1IPR005141 eRF1 2IPR005142 eRF1 3	429.82456
ENSMUSP00000030076	56.7	Regulator of differentiation 1 (Rod1) IPR006536 HnRNP-L PTBIPR000504 RRM RNP1	497.36842
ENSMUSP00000038772	62.6	MAGUK p55 subfamily member 6 (Protein associated with Lin-7 2)(Dlgh4 protein)(P55T protein) IPR008144 Guanylate kinIPR008145 Guanylt/CaIPR004172 L27IPR014775 L27 CIPR001478 PDZ/DHR/GLGFIPR011511 SH3 2IPR001452 SH3 domain	549.12281
ENSMUSP00000068174	30.4	Inositol monophosphatase (EC 3.1.3.25)(Inositol-1(or 4)-monophosphatase)(IMPase)(IMP)(Lithium-sensitive myo-inositol monophosphatase A1) Source: 3.1.3.25 IPR017955 IMPase/FBPaseIPR000760 Inositol P	266.66667
ENSMUSP00000078914	19.5	Ufm1-conjugating enzyme 1 (Ubiquitin-fold modifier-conjugating enzyme 1) IPR014806 DUF1782IPR016135 UBQ-conjugat/RWD-like	171.05263
ENSMUSP00000003117	48.5	AP-1 complex subunit mu-1 (Adaptor-related protein complex 1 mu-1 subunit)(Adaptor protein complex AP-1 mu-1 subunit)(Golgi adaptor HA1/AP1 adaptin mu-1 subunit)(Mu-adaptin 1)(AP-mu chain family member mu1A)(Mu1A-adaptin)(Clathrin assembly protein complex 1 medium chain 1)(Clathrin coat assembly protein AP47)(Clathrin coat-associated protein AP47) IPR001392 Clathrin muIPR008968 Clathrin mu CIPR018240 Clathrin mu CSIPR011012 Longin like	425.4386
ENSMUSP00000103181	23.2	60S ribosomal protein L19 IPR005819 Histone H5IPR000196 Ribosomal L19/L19e	203.50877
ENSMUSP00000005651	77	NADPH--cytochrome P450 reductase (CPR)(P450R)(EC 1.6.2.4) Source: 1.6.2.4 IPR003097 FAD-binding 1IPR001094 Flavdoxin likeIPR008254 Flavodoxin/NO synthIPR001709 Flavoprot Pyr Nucl cyt RdtaseIPR001834 NADH-Cyt B5 reductaseIPR001433 OxRdtase FAD/NAD bdIPR017938 Riboflavin synthase like b-brl	675.4386
ENSMUSP00000000687	32.8	3-hydroxyanthranilate 3,4-dioxygenase (EC 1.13.11.6)(3-hydroxyanthranilic acid dioxygenase)(HAD)(3-hydroxyanthranilate oxygenase)(3-HAO) Source: 1.13.11.6 IPR010329 3hydroanth dOaseIPR016700 3hydroanth dOase metIPR011051 Cupin RmlC type	287.7193
ENSMUSP00000102857	40.7	26S proteasome non-ATPase regulatory subunit 4 (26S proteasome regulatory subunit S5A)(Rpn10)(Multiubiquitin chain-binding protein) IPR003903 Ubiquitin-int motifIPR002035 VWF A	357.01754
ENSMUSP00000026625	37.5	Citrate lyase subunit beta-like protein, mitochondrial Precursor (Citrate lyase beta-like)(EC 4.1.-.-) Source: 4.1.-.-IPR011206 Citrate lyase betaIPR005000 HpcH HpaIIPR015813 Pyrv/PenolPyrv Kinase cat	328.94737
ENSMUSP00000034834	57.8	Pyruvate kinase isozymes M1/M2 (EC 2.7.1.40)(Pyruvate kinase muscle isozyme) Source: 2.7.1.40 IPR001697 Pyr KnaseIPR015813 Pyrv/PenolPyrv Kinase catIPR018209 Pyrv Knase ASIPR015795 Pyrv Knase C-likeIPR015794 Pyrv Knase a/bIPR015793 Pyrv Knase brl	507.01754
ENSMUSP00000065113	35	Succinyl-CoA ligase Source: 6.2.1.4 IPR017440 Cit synth/succinyl-CoA lig ASIPR003781 CoA bdIPR005810 CoA lig alphaIPR005811 CoA ligaseIPR016040 NAD(P)-bdIPR016102 Succinyl-CoA synth-like	307.01754
ENSMUSP00000022271	76.8	Peroxisomal acyl-coenzyme A oxidase 2 (EC 1.17.99.3)(3-alpha,7-alpha,12-alpha-trihydroxy-5-beta-cholestanoyl-CoA 24-hydroxylase)(3-alpha,7-alpha,12-alpha-trihydroxy-5-beta-cholestanoyl-CoA oxidase)(Trihydroxycoprostanoyl-CoA oxidase)(THCA-CoA oxidase)(THCCox) Source: 1.17.99.3 IPR006091 Acyl-CoA DHase/Oxase MIPR012258 Acyl-CoA oxidaseIPR002655 Acyl-CoA oxidase CIPR009100 AcylCoA DH/oxidase M/NIPR009075 AcylCo DHase/oxidase C	673.68421

ENSMUSP00000025679	31.3	Ubiquitin thioesterase OTUB1 (EC 3.1.2.-)(Otubain-1)(OTU domain-containing ubiquitin aldehyde-binding protein 1)(Ubiquitin-specific-processing protease OTUB1)(Deubiquitinating enzyme OTUB1) Source: 3.1.2.- IPR003323 OTUIPR016615 Ubiquitin thioesterase Otubain	274.5614
ENSMUSP00000021425	38.1	Activator of 90 kDa heat shock protein ATPase homolog 1 (AHA1) IPR013538 AHSA1IPR015310 AHSA1 N	334.21053
ENSMUSP00000027356	60.7	Cytochrome P450 27, mitochondrial Precursor (EC 1.14.13.15)(Cytochrome P-450C27/25)(Sterol 26-hydroxylase)(Sterol 27-hydroxylase)(Vitamin D(3) 25-hydroxylase)(5-beta-cholestane-3-alpha,7-alpha,12-alpha-triol 27-hydroxylase) Source: 1.14.13.15 IPR001128 Cyt P450IPR002397 Cyt P450 BIPR017973 Cyt P450 CIPR017972 Cyt P450 CSIPR002401 Cyt P450 E grp-IIPR002403 Cyt P450 E grp-IVIPR002399 Cyt P450 mit	532.45614
ENSMUSP00000099754	22.6	Phosphatidylethanolamine N-methyltransferase (PEAMT)(PEMT)(EC 2.1.1.17)(PEMT2) Source: 2.1.1.17 IPR007318 PEMT	198.24561
ENSMUSP00000095285	23	Ras-related protein Rab-18 IPR006688 ARFIPR006689 ARF/SARIPR003579 GTPase RabIPR003577 GTPase RasIPR003578 GTPase RhoIPR013684 Miro-likeIPR002078 RNA pol sigma 54 intIPR002041 Ran GTPaseIPR013753 RasIPR001806 Ras GTPaseIPR005225 Small GTP bd	201.75439
ENSMUSP00000028004	55.9	4-trimethylaminobutyraldehyde dehydrogenase (TMABADH)(EC 1.2.1.47)(Aldehyde dehydrogenase family 9 member A1)(EC 1.2.1.3) Source: 1.2.1.47 IPR016161 Ald DHase/Histidinol DHaseIPR016160 Ald DHase CSIPR015590 Aldehyde DHase	490.35088
ENSMUSP00000104825	46.8	interferon gamma inducible protein 47 IPR007743 Interferon-inducible GTPase	410.52632
ENSMUSP00000030769	52.8	26S protease regulatory subunit 7 (Proteasome 26S subunit ATPase 2)(Protein MSS1) IPR005937 26S Psome P45IPR003593 AAA+ ATPase coreIPR003960 AAA ATPase CSIPR003959 AAA ATPase core	463.15789
ENSMUSP00000026743	52.8	Cytochrome b-c1 complex subunit 1, mitochondrial Precursor (Ubiquinol-cytochrome-c reductase complex core protein 1)(Core protein I)(Complex III subunit 1) IPR011249 Metalloenz metal-bdIPR011765 Pept M16 NIPR007863 Peptidase M16 C	463.15789
ENSMUSP00000054490	15.8	40S ribosomal protein S23 IPR016027 NA-bd OB-fold-likeIPR006032 Ribosomal S12/S23IPR005679 Ribosomal S12 bac-typeIPR005680 Ribosomal S23 euk/arc	138.59649
ENSMUSP00000022960	52.2	Eukaryotic translation initiation factor 3 subunit E (eIF3e)(Eukaryotic translation initiation factor 3 subunit 6)(eIF-3 p48)(Mammary tumor-associated protein INT-6)(Viral integration site protein INT-6)(MMTV integration site 6) IPR000717 PCIIPR016650 Transl init fac 3 su6 euk	457.89474
ENSMUSP00000015829	47.8	Short/branched chain specific acyl-CoA dehydrogenase, mitochondrial Precursor (SBCAD)(EC 1.3.99.-)(2-methyl branched chain acyl-CoA dehydrogenase)(2-MEBCAD)(2-methylbutyryl-coenzyme A dehydrogenase)(2-methylbutyryl-CoA dehydrogenase) Source: 1.3.99.- IPR006091 Acyl-CoA DHase/Oxase MIPR013107 Acyl-CoA DHase 2 CIPR006089 Acyl-CoA DHase CSIPR006092 Acyl-CoA DHase NIPR006090 Acyl-CoA Oxase/DHase 1IPR009100 AcylCoA DH/oxidase M/N	419.29825
ENSMUSP00000068594	111.1	Hypoxia up-regulated protein 1 Precursor (170 kDa glucose-regulated protein)(GRP-170)(140 kDa Ca(2+)-binding protein)(CBP-140) IPR018181 Heat shock 70 CSIPR001312 HexokinaseIPR001023 Hsp70IPR013126 Hsp 70	974.5614
ENSMUSP00000109196	41.6	Magnesium transporter protein 1 Precursor (MagT1)(Implantation-associated protein)(IAP) IPR006844 OST3 OST6IPR012336 Thioredoxin-like fold	364.91228
ENSMUSP00000101003	24.7	NADH dehydrogenase Source: 1.6.5.3 IPR006138 NADH DHase 20kDa suIPR006137 OxRdtase q6	216.66667
ENSMUSP00000065352	20	NADH dehydrogenase IPR010625 CHCHIPR016680 NADH Ub cplx-1 asu su-8	175.4386
ENSMUSP00000026560	42.8	26S proteasome non-ATPase regulatory subunit 13 (26S proteasome regulatory subunit S11)(26S proteasome regulatory subunit p40.5) IPR007985 Hemolysn expr modulating HHAIPR000717 PCI	375.4386
ENSMUSP00000021313	26.5	Dephospho-CoA kinase domain-containing protein IPR001977 Depp CoAkinase	232.45614
ENSMUSP00000026827	22.7	UPF0585 protein C16orf13 homolog IPR010342 DUF938	199.12281
ENSMUSP00000023237	58.2	Nicotinate phosphoribosyltransferase (NAPRTase)(EC 2.4.2.11)(Nicotinate phosphoribosyltransferase domain-containing protein 1) Source: 2.4.2.11 IPR015977 Nic PRibTrfase-likeIPR007229 Nic PRibTrfase-relIPR006405 Nic PRibTrfase put	510.52632
ENSMUSP00000031383	24.4	GTP-binding nuclear protein Ran (GTPase Ran)(Ras-related nuclear protein)(Ras-like protein TC4) IPR006688 ARFIPR006689 ARF/SARIPR018210 GTP-bd nuclear protein CSIPR003579 GTPase RabIPR003577 GTPase RasIPR003578 GTPase RhoIPR001019 Gprotein alph bdIPR013684 Miro-likeIPR002041 Ran GTPaseIPR013753	214.03509

		RasIPR001806 Ras GTPaseIPR005225 Small GTP bd	
ENSMUSP00000008991	270.8	spectrin beta 3 IPR001589 Actinin actin-bd CSIPR016146 Calponin-homologyIPR001715 Calponin act bdIPR001849 Pleckstrin homologyIPR018159 Spectrin/alpha-actininIPR001605 Spectrin PHIPR016343 Spectrin bsuIPR002017 Spectrin repeat	2375.4386
ENSMUSP00000084053	32.7	Translocon-associated protein subunit alpha Precursor (TRAP-alpha)(Signal sequence receptor subunit alpha)(SSR-alpha) IPR005595 TRAP alpha	286.84211
ENSMUSP00000018506	57.9	Importin subunit alpha-2 (Karyopherin subunit alpha-2)(SRP1-alpha)(RAG cohort protein 1)(Pendulin)(Pore targeting complex 58 kDa subunit)(PTAC58)(Importin alpha P1) IPR016024 ARM-type foldIPR000225 ArmadilloIPR000357 HEATIPR002652 Importin-a-like IBB-bd	507.89474
ENSMUSP00000025375:reversed	123.7		1085.0877
ENSMUSP00000035220	45.6	cAMP-dependent protein kinase type II-alpha regulatory subunit IPR012198 PK regulatoryIPR010916 TonB box CSIPR003117 cAMP-dep prot kin reg I/II a/bIPR002373 cAMP/cGMP kinIPR000595 cNMP bdIPR018490 cNMP bd-likeIPR018488 cNMP bd CS	400
ENSMUSP00000099763:reversed	21.9		192.10526
ENSMUSP00000014750	34.1	Mitochondrial 2-oxoglutarate/malate carrier protein (OGCP)(Solute carrier family 25 member 11) IPR002113 Aden trnslctorIPR002067 Mit carrierIPR002030 Mit uncouplingIPR001993 Mitoch carrierIPR018108 Mitochondrial sb/sol carrier	299.12281
ENSMUSP00000034866	35	Electron transfer flavoprotein subunit alpha, mitochondrial Precursor (Alpha-ETF) IPR001308 ETF aIPR014730 ETF a/b NIPR014731 ETF a CIPR018206 ETF asu C CS	307.01754
ENSMUSP00000080994	26	Cytochrome c oxidase subunit 2 (Cytochrome c oxidase polypeptide II) IPR001505 Copper CuAIPR008972 CupredoxinIPR011759 Cyt c oxidase II TMIPR014222 Cyt c oxidase su2IPR015964 Cyt c oxidase su2-like TMIPR002429 Cyt c oxidase su2 C	228.07018
ENSMUSP00000051092	80.1	Phosphatidylinositol-binding clathrin assembly protein (Clathrin assembly lymphoid myeloid leukemia)(CALM) IPR011417 ANTHIPR008942 ENTH VHSIPR013809 Epsin-like NIPR001026 Epsin N	702.63158
ENSMUSP00000070109	87.1	Vitamin K-dependent gamma-carboxylase (EC 6.4.-.-)(Gamma-glutamyl carboxylase)(Vitamin K gamma glutamyl carboxylase) Source: 6.4.-.- IPR011051 Cupin RmlC typeIPR011020 HTTMIPR007782 VKG COase	764.03509
ENSMUSP00000005606	40.5	cAMP-dependent protein kinase catalytic subunit alpha (PKA C-alpha)(EC 2.7.11.11) Source: 2.7.11.11 IPR000961 AGC-kinase CIPR011009 Kinase likeIPR017892 Pkinase CIPR000719 Prot kinase coreIPR017441 Protein kinase ATP BSIPR017442 Se/Thr pkinase-relIPR008271 Ser thr pkin ASIPR002290 Ser thr pkinaseIPR001245 Tyr pkinase	355.26316
ENSMUSP00000028691	58.1	ADP-ribosylation factor GTPase-activating protein 2 (ARF GAP 2)(GTPase-activating protein ZNF289)(Zinc finger protein 289) IPR001164 ArfGAP	509.64912
ENSMUSP00000030385	33.8	Phosphopantothenate--cysteine ligase (EC 6.3.2.5)(Phosphopantothenoylcysteine synthetase)(PPC synthetase) Source: 6.3.2.5 IPR007085 DNA/pantothenate-metab flavo C	296.49123
ENSMUSP00000094167	46.1	DEP domain-containing protein 6 IPR001478 PDZ/DHR/GLGFIPR000591 Pleckstrin/G-protein interact	404.38596
ENSMUSP00000036555	119.2	Importin-4 (Imp4)(Importin-4a)(Imp4a)(Ran-binding protein 4)(RanBP4) IPR016024 ARM-type foldIPR000357 HEATIPR001494 Importin-b N	1045.614
ENSMUSP00000036881	94.9	ATP-binding cassette sub-family F member 1 IPR003593 AAA+ ATPase coreIPR003439 ABC transporter-likeIPR017871 ABC transporter CSIPR001984 Peptidase S16IPR009068 S15 NS1 RNA bd	832.45614
sp|CASK_BOVIN|	21.3	Kappa-casein; Contains: Casoxin-C; Contains: Casoxin-6; Contains: Casoxin-A; Contains: Casoxin-B; Contains: Casoplatelin; Flags: Precursor;	186.84211
ENSMUSP00000033673	54.5	Non-POU domain-containing octamer-binding protein (NonO protein) IPR012975 NOPSIPR000504 RRM RNP1	478.07018
ENSMUSP00000032920	23.6	CDP-diacylglycerol--inositol 3-phosphatidyltransferase (EC 2.7.8.11)(Phosphatidylinositol synthase)(PtdIns synthase)(PI synthase) Source: 2.7.8.11 IPR000462 CDP-OH P transIPR014387 CDP diag ino 3 P euk	207.01754
ENSMUSP00000105447	51.9	Glucokinase (EC 2.7.1.2)(Hexokinase type IV)(HK IV)(Hexokinase-4)(HK4)(Hexokinase-D) Source: 2.7.1.2 IPR001312 HexokinaseIPR001023 Hsp70	455.26316
ENSMUSP00000027491	45.9	Serine--pyruvate aminotransferase, mitochondrial Precursor (SPT)(EC 2.6.1.51)(Alanine--glyoxylate aminotransferase)(AGT)(EC 2.6.1.44) Source: 2.6.1.51 IPR000192 Aminotrans V/Cys dSaseIPR015424 PyrdxlP-dep Trfase major	402.63158

ENSMUSP00000110094	19.5	60S ribosomal protein L24 IPR000988 Ribosomal L24eIPR011017 TRASH	171.05263
ENSMUSP00000025476	32.2	Thioredoxin-like protein 1 (32 kDa thioredoxin-related protein) IPR010400 DUF1000IPR012336 Thioredoxin-like foldIPR006662 Thioredoxin-like subdomIPR017937 Thioredoxin CSIPR013766 Thioredoxin dom	282.45614
ENSMUSP00000027863	35.2	Sodium/potassium-transporting ATPase subunit beta-1 (Sodium/potassium-dependent ATPase subunit beta-1) IPR000402 ATPase H Na/K b	308.77193
ENSMUSP00000026289	27.3	3-hydroxyacyl-CoA dehydrogenase type-2 (EC 1.1.1.35)(3-hydroxyacyl-CoA dehydrogenase type II)(Type II HADH)(3-hydroxy-2-methylbutyryl-CoA dehydrogenase)(EC 1.1.1.178)(17-beta-hydroxysteroid dehydrogenase 10)(Mitochondrial ribonuclease P protein 2)(Mitochondrial RNase P protein 2)(Endoplasmic reticulum-associated amyloid beta-peptide-binding protein) Source: 1.1.1.35 IPR003560 DHB DHaseIPR002198 DHase sc/Rdtase SDRIPR001509 Epimerase deHydtaseIPR002347 Glc/ribitol DHaseIPR002424 Insect AlcDHase famIPR016040 NAD(P)-bdIPR013968 Polyketide synth KR	239.47368
ENSMUSP00000015877	32.9	F-actin-capping protein subunit alpha-2 (CapZ alpha-2) IPR002189 F-actin cap asuIPR017865 F-actin cap asu CSIPR018315 F-actin cap asu actin bd	288.59649
ENSMUSP00000018470	28.1	14-3-3 protein beta/alpha (Protein kinase C inhibitor protein 1)(KCIP-1) IPR000308 14-3-3	246.49123
ENSMUSP00000027529	23.6	Ras-related protein Rab-17 IPR006688 ARFIPR003579 GTPase RabIPR003577 GTPase RasIPR003578 GTPase RhoIPR013684 Miro-likeIPR002041 Ran GTPaseIPR013753 RasIPR001806 Ras GTPaseIPR005225 Small GTP bd	207.01754
ENSMUSP00000031741	57.5	Cytochrome P450 3A13 (EC 1.14.14.1)(CYPIIIA13) Source: 1.14.14.1 IPR001128 Cyt P450IPR002397 Cyt P450 BIPR017973 Cyt P450 CIPR017972 Cyt P450 CSIPR008072 Cyt P450 E CYP3AIPR002401 Cyt P450 E grp-IIPR002402 Cyt P450 E grp-IIIPR002403 Cyt P450 E grp-IV	504.38596
ENSMUSP00000035804	38	MOSC domain-containing protein 1, mitochondrial Precursor (EC 1.-.-.-) Source: 1.-.-.- IPR005303 MOSC NIPR005302 MoCF Sase CIPR011037 Pyrv Knase b-brl-like	333.33333
ENSMUSP00000033715	40.7	Sterol-4-alpha-carboxylate 3-dehydrogenase, decarboxylating (EC 1.1.1.170) Source: 1.1.1.170 IPR002225 3Beta OHSteriod DHase/EstaseIPR001509 Epimerase deHydtaseIPR013120 Male sterile NAD-bdIPR016040 NAD(P)-bdIPR003869 Polysac CapD	357.01754
ENSMUSP00000003622	33.9	solute carrier family 25, member 1 IPR002113 Aden trnslctorIPR002067 Mit carrierIPR001993 Mitoch carrierIPR018108 Mitochondrial sb/sol carrier	297.36842
ENSMUSP00000029386	68	Electron transfer flavoprotein-ubiquinone oxidoreductase, mitochondrial Precursor (ETF-ubiquinone oxidoreductase)(ETF-QO)(EC 1.5.5.1)(Electron-transferring-flavoprotein dehydrogenase)(ETF dehydrogenase) Source: 1.5.5.1 IPR007859 ETFD OxRdtaseIPR006076 FAD-dep OxRdtaseIPR000103 Pyridine nuc-diS OxRdtase 2	596.49123
ENSMUSP00000069432	292.8	GCN1 general control of amino-acid synthesis 1-like 1 IPR016024 ARM-type foldIPR000225 ArmadilloIPR000357 HEATIPR004155 PBS lyase HEAT	2568.4211
ENSMUSP00000099482	21.9	Inosine triphosphate pyrophosphatase (ITPase)(Inosine triphosphatase)(EC 3.6.1.19) Source: 3.6.1.19 IPR002637 Ham1p like	192.10526
ENSMUSP00000042232	21.1	Heme-binding protein 1 (p22HBP) IPR006917 SOUL haem bd	185.08772
ENSMUSP00000022962	34.9	Tetratricopeptide repeat protein 35 (TPR repeat protein 35) IPR013105 TPR 2IPR013026 TPR region	306.14035
ENSMUSP00000101478	24.8	Acyl-protein thioesterase 2 (EC 3.1.2.-)(Lysophospholipase II)(Lysophospholipase 2)(mLyso II) Source: 3.1.2.- IPR003140 Phospholipase/Carboxylesterase	217.54386
ENSMUSP00000022293	31.7	Voltage-dependent anion-selective channel protein 2 (VDAC-2)(mVDAC2)(Voltage-dependent anion-selective channel protein 6)(VDAC-6)(mVDAC6)(Outer mitochondrial membrane protein porin 2) IPR001925 Porin Euk	278.07018
ENSMUSP00000080888	111.5	Uncharacterized protein KIAA0090 Precursor IPR011678 DUF1620IPR011047 Quino AlcDHase-like	978.07018
ENSMUSP00000020343	24.1	Ras-related protein Rab-21 (Rab-12) IPR006688 ARFIPR003579 GTPase RabIPR003577 GTPase RasIPR003578 GTPase RhoIPR006036 K uptake TrkAIPR013684 Miro-likeIPR002041 Ran GTPaseIPR013753 RasIPR001806 Ras GTPaseIPR005225 Small GTP bd	211.40351
ENSMUSP00000045864	45.7	Arylacetamide deacetylase-like 1 (EC 3.1.1.-)(Chlorpyrifos oxon-binding protein)(CPO-BP)(Neutral cholesterol ester hydrolase)(NCEH) Source: 3.1.1.- IPR013094 AB hydrolase 3IPR017157 Arylacetamide deacetylaseIPR002168 Lipase GDXG AS	400.87719
ENSMUSP00000034947	23.7	Peptidyl-prolyl cis-trans isomerase B Precursor (PPIase)(Rotamase)(EC 5.2.1.8)(Cyclophilin B)(S-	207.89474

		cyclophilin)(SCYLP)(CYP-S1) Source: 5.2.1.8 IPR015891 Cyclophilin-likeIPR002130 PPIase cyclophilin	
ENSMUSP00000001566	49.6	Tubulin beta-5 chain IPR002452 Alpha tubulinIPR013838 Beta-tubulin BSIPR002453 Beta tubulinIPR000158 Cell division FtsZ NIPR002967 Delta tubulinIPR004057 Epsilon tubulinIPR002454 Gamma tubulinIPR008280 Tub FtsZ CIPR000217 TubulinIPR018316 Tubulin/FtsZ 2-layer-sand-domIPR017975 Tubulin CSIPR003008 Tubulin FtsZ	435.08772
ENSMUSP00000021854	39.5	Peroxisomal 3,2-trans-enoyl-CoA isomerase (EC 5.3.3.8)(Dodecenoyl-CoA isomerase)(Delta(3),delta(2)-enoyl-CoA isomerase)(D3,D2-enoyl-CoA isomerase) Source: 5.3.3.8 IPR000582 Acyl-CoA-binding proteinIPR001753 Crotonase core	346.49123
ENSMUSP00000025968	55.8	Cytochrome P450 2C39 (EC 1.14.14.1)(CYPIIC39) Source: 1.14.14.1 IPR004090 Chemotax Me-accpt rcptIPR001128 Cyt P450IPR017973 Cyt P450 CIPR017972 Cyt P450 CSIPR002401 Cyt P450 E grp-IIPR002403 Cyt P450 E grp-IVIPR008067 Cyt P450 E grp-I CYP2A-likeIPR008068 Cyt P450 E grp-I CYP2B-likeIPR008069 Cyt P450 E grp-I CYP2D-likeIPR008070 Cyt P450 E grp-I CYP2E-likeIPR008071 Cyt P450 E grp-I CYP2J-likeIPR000362 Fumarate lyase	489.47368
ENSMUSP00000081030	16.7	no description availableIPR001196 Ribosomal L15	146.49123
ENSMUSP00000029414	21.1	Translocon-associated protein subunit gamma (TRAP-gamma)(Signal sequence receptor subunit gamma)(SSR-gamma) IPR009779 TRAP-gamma	185.08772
ENSMUSP00000026610	55.7	Argininosuccinate lyase (ASAL)(EC 4.3.2.1)(Arginosuccinase) Source: 4.3.2.1 IPR009049 Argininosuccinate lyaseIPR003031 D crystallinIPR000362 Fumarate lyaseIPR008948 L-Aspartase-like	488.59649
ENSMUSP00000025617	17.4	Riboflavin kinase (EC 2.7.1.26)(ATP:riboflavin 5--phosphotransferase)(Flavokinase)(KOI-4) Source: 2.7.1.26 IPR015865 Riboflavin kinase	152.63158
ENSMUSP00000027036	24.7	Acyl-protein thioesterase 1 (EC 3.1.2.-)(Lysophospholipase 1)(Lysophospholipase I)(LysoPLA I) Source: 3.1.2.- IPR003140 Phospholipase/Carboxylesterase	216.66667
ENSMUSP00000099649	46.1	Eukaryotic initiation factor 4A-I (eIF-4A-I)(eIF4A-I)(EC 3.6.1.-)(ATP-dependent RNA helicase eIF4A-1) Source: 3.6.1.- IPR014001 DEAD-like NIPR001650 DNA/RNA helicase CIPR011545 DNA/RNA helicase DEAD/DEAH NIPR014021 Helicase SF1/SF2 ATP-bdIPR000629 RNA-helicase DEAD-box CSIPR014014 RNA helicase DEAD Q motif	404.38596
ENSMUSP00000077118	23.5	60S ribosomal protein L14 IPR000104 Antifreeze 1IPR005819 Histone H5IPR005824 KOWIPR002784 Ribosomal L14e	206.14035
ENSMUSP00000088168	28.9	ATP synthase subunit b, mitochondrial Precursor IPR008688 ATPase F0-cplx bsu mt	253.50877
ENSMUSP00000109451	34.3	Actin-related protein 2/3 complex subunit 2 (Arp2/3 complex 34 kDa subunit)(p34-ARC) IPR007188 P34-arc	300.87719
ENSMUSP00000105356	21.8	Peroxiredoxin-2 (EC 1.11.1.15)(Thioredoxin peroxidase 1)(Thioredoxin-dependent peroxide reductase 1)(Thiol-specific antioxidant protein)(TSA) Source: 1.11.1.15 IPR000866 Alkyl hydroperoxide RdtaseIPR013740 RedoxinIPR012336 Thioredoxin-like fold	191.22807
ENSMUSP00000027916	33.2	3-(2-),5--bisphosphate nucleotidase 1 (EC 3.1.3.7)(Bisphosphate 3--nucleotidase 1)(PAP-inositol-1,4-phosphatase)(PIP) Source: 3.1.3.7 IPR018062 HTH AraC-typ sub 2IPR000760 Inositol P	291.22807
ENSMUSP00000016463	32.9	ADP/ATP translocase 2 (Adenine nucleotide translocator 2)(ANT 2)(ADP,ATP carrier protein 2)(Solute carrier family 25 member 5) IPR002113 Aden trnslctorIPR002067 Mit carrierIPR002030 Mit uncouplingIPR001993 Mitoch carrierIPR018108 Mitochondrial sb/sol carrier	288.59649
ENSMUSP00000037583	24.9	Transmembrane emp24 domain-containing protein 10 Precursor (21 kDa transmembrane-trafficking protein)(Transmembrane protein Tmp21) IPR009038 GOLD	218.42105
ENSMUSP00000100059	89.5	UPF0555 protein KIAA0776	785.08772
ENSMUSP00000093229	39.4	Sodium/bile acid cotransporter (Na(+)/bile acid cotransporter)(Na(+)/taurocholate transport protein)(Sodium/taurocholate cotransporting polypeptide)(Solute carrier family 10 member 1) IPR002657 BilAc/Na symportIPR004710 Bil ac transpt	345.61404
ENSMUSP00000080523	15.8	60S ribosomal protein L32 IPR001515 Ribosomal L32eIPR018263 Ribosomal L32e CS	138.59649
ENSMUSP00000098648	74.6	signal recognition particle 72 IPR005819 Histone H5IPR013699 Signal recog part SRP72 RNA-bdIPR001440 TPR-1IPR013105 TPR 2IPR013026 TPR region	654.38596
ENSMUSP00000023550	59.2	Protein disulfide-isomerase A5 Precursor (EC 5.3.4.1)(Protein disulfide isomerase-related protein) Source: 5.3.4.1 IPR012336 Thioredoxin-like foldIPR006662 Thioredoxin-like subdomIPR017937 Thioredoxin CSIPR013766 Thioredoxin dom	519.29825
ENSMUSP00000023952	54.5	Keratin, type II cytoskeletal 8 (Cytokeratin-8)(CK-8)(Keratin-8)(K8)(Cytokeratin endo A) IPR016044 FIPR018039 Intermediate filament CSIPR002957 Keratin IIPR003054 Keratin IIIPR009053 PrefoldinIPR017441 Protein kinase ATP	478.07018

		BSIPR003536 Transloc intimin rcpt	
ENSMUSP00000003681	46.3	SEC14-like protein 2 (Alpha-tocopherol-associated protein)(TAP) IPR001251 CRAL bd TRIO CIPR008273 CRAL bd TRIO NIPR001071 CRAL bd toc tranIPR000348 Emp24 gp25L p24IPR009038 GOLDIPR011074 Sec14p like N	406.14035
ENSMUSP00000051223	28.3	14-3-3 protein gamma IPR000308 14-3-3	248.24561
ENSMUSP00000098041	204.4	kinesin family member 13B IPR000938 Cytoskel-assoc-prot CAP-GlyIPR000253 FHAIPR001752 Kinesin motorIPR008984 SMAD FHA dom	1792.9825
ENSMUSP00000010208	55.6	Sodium-coupled neutral amino acid transporter 3 (Na(+)-coupled neutral amino acid transporter 3)(System N amino acid transporter 1)(N-system amino acid transporter 1)(Solute carrier family 38 member 3)(mNAT) IPR013057 AA transpt TMIPR003975 K chnl volt-dep Kv4	487.7193
ENSMUSP00000003907	48.6	Glutaryl-CoA dehydrogenase, mitochondrial Precursor (GCD)(EC 1.3.99.7) Source: 1.3.99.7 IPR006091 Acyl-CoA DHase/Oxase MIPR013107 Acyl-CoA DHase 2 CIPR006089 Acyl-CoA DHase CSIPR006092 Acyl-CoA DHase NIPR006090 Acyl-CoA Oxase/DHase 1IPR009100 AcylCoA DH/oxidase M/NIPR009075 AcylCo DHase/oxidase C	426.31579
ENSMUSP00000076575	39.3	Porphobilinogen deaminase (PBG-D)(EC 2.5.1.61)(Pre-uroporphyrinogen synthase)(Hydroxymethylbilane synthase)(HMBS) Source: 2.5.1.61 IPR000860 4pyrrol synth OHMeBilane synth	344.73684
ENSMUSP00000097561:reversed	3904.1		34246.491
ENSMUSP00000084572	140.1	Valyl-tRNA synthetase (EC 6.1.1.9)(Valine--tRNA ligase)(ValRS)(Protein G7a) Source: 6.1.1.9 IPR004046 GST CIPR010987 Glutathione-S-Trfase C-likeIPR004045 Glutathione S-Trfase NIPR013155 V/L/I-tRNA-synth anticodon-bdIPR002303 Val-tRNA synth IaIPR015413 aa-tRNA-synt IIPR001412 aa-tRNA-synth I CSIPR002300 aa-tRNA-synth IaIPR009080 tRNAsynth 1a anticodon-bd	1228.9474
ENSMUSP00000103904	40	Galectin-9 IPR008985 ConA like lec gIIPR001079 Galectin CRD	350.87719
ENSMUSP00000018699	32.6	Asialoglycoprotein receptor 1 (ASGP-R 1)(ASGPR 1)(Hepatic lectin 1)(MHL-1) IPR002353 AntifreezeIIIPR001304 C-type lectinIPR018378 C-type lectin CSIPR016187 C-type lectin foldIPR005640 Lectin NIPR003990 Pancreatis ac	285.96491
ENSMUSP00000026552	56.8	Cytochrome P450 2E1 (EC 1.14.14.1)(CYPIIE1)(P450-J)(P450-ALC) Source: 1.14.14.1 IPR001128 Cyt P450IPR002397 Cyt P450 BIPR017973 Cyt P450 CIPR017972 Cyt P450 CSIPR002401 Cyt P450 E grp-IIPR002403 Cyt P450 E grp-IVIPR008068 Cyt P450 E grp-I CYP2B-likeIPR008070 Cyt P450 E grp-I CYP2E-likeIPR008071 Cyt P450 E grp-I CYP2J-like	498.24561
ENSMUSP00000081782	119.4	Importin-7 (Imp7)(Ran-binding protein 7)(RanBP7) IPR016024 ARM-type foldIPR003006 Ig/MHC CSIPR001494 Importin-b N	1047.3684
ENSMUSP00000073175	17.2	60S ribosomal protein L26 (Silica-induced gene 20 protein)(SIG-20) IPR005824 KOWIPR005825 Ribosomal L24/26 CSIPR005756 Ribosomal L26 euk/arcIPR008991 Translation prot SH3-like	150.87719
ENSMUSP00000104830	16.3	Ubiquitin-conjugating enzyme E2 variant 1 (UEV-1)(CROC-1) IPR016135 UBQ-conjugat/RWD-likeIPR000608 UBQ-conjugat E2	142.98246
ENSMUSP00000087046	28.7	Proteasome activator complex subunit 1 (Proteasome activator 28 subunit alpha)(PA28alpha)(PA28a)(Activator of multicatalytic protease subunit 1)(11S regulator complex subunit alpha)(REG-alpha) IPR003185 Proteasome activ REG asuIPR009077 Proteasome activ REG asu/bsuIPR003186 Proteasome activ REG bsu	251.75439
ENSMUSP00000029353	57.9	Importin subunit alpha-4 (Karyopherin subunit alpha-4)(Importin alpha Q1)(Qip1) IPR016024 ARM-type foldIPR000225 ArmadilloIPR000357 HEATIPR002652 Importin-a-like IBB-bd	507.89474
ENSMUSP00000031160	47	Multifunctional protein ADE2 Source: 6.3.2.6 IPR000031 AIR COase coreIPR001636 SAICAR syntIPR018236 SAICAR synthetase CS	412.2807
ENSMUSP00000022993	28.8	Derlin-1 (Der1-like protein 1)(Degradation in endoplasmic reticulum protein 1) IPR007599 DER1	252.63158
ENSMUSP00000106250	12.4	60S ribosomal protein L36a (60S ribosomal protein L44) IPR000552 Ribosomal L44eIPR011332 Ribosomal zn-bd	108.77193
ENSMUSP00000100968	44.3	Dual specificity mitogen-activated protein kinase kinase 2 (MAP kinase kinase 2)(MAPKK 2)(EC 2.7.12.2)(ERK activator kinase 2)(MAPK/ERK kinase 2)(MEK2) Source: 2.7.12.2 IPR000960 Flavin mOaseIPR011009 Kinase likeIPR000719 Prot kinase coreIPR017441 Protein kinase ATP BSIPR017442 Se/Thr pkinase-relIPR008271 Ser thr pkin ASIPR002290 Ser thr pkinaseIPR001245 Tyr pkinase	388.59649
ENSMUSP00000049007	100	Catenin alpha-1 (102 kDa cadherin-associated protein)(CAP102)(Alpha E-catenin) IPR001033 Alpha cateninIPR017997	877.19298

		VinculinIPR006077 Vinculin/cateninIPR000633 Vinculin CS	
ENSMUSP00000080974	52.7	Platelet glycoprotein 4 (Platelet glycoprotein IV)(GPIV)(GPIIIB)(PAS IV)(PAS-4)(CD36 antigen) IPR002159 CD36IPR005428 CD36 antigenIPR005429 LimpII	462.2807
ENSMUSP00000020522	85.3	6-phosphofructokinase, liver type (EC 2.7.1.11)(Phosphofructokinase 1)(Phosphohexokinase)(Phosphofructo-1-kinase isozyme B)(PFK-B) Source: 2.7.1.11 IPR009161 6-phosphofructokinase eukIPR015912 Phosphofructokinase CSIPR000023 Ppfruckinase	748.24561
ENSMUSP00000100802	24.1	60S ribosomal protein L15 Fragment Source: UniProtKB/TrEMBL B8JKK2 IPR000439 Ribosomal L15eIPR012678 Ribosomal L23/L15e core	211.40351
ENSMUSP00000029405	76.7	GMP synthase Source: 6.3.5.2 IPR006220 Anth synthIIIPR001317 CarbamoylP synth GATaseIPR011702 GATASEIPR000991 GATase class1 CIPR001674 GMP synth CIPR004739 GMP synth NIPR018317 Queuosine synth-like	672.80702
ENSMUSP00000051935	48	Basic leucine zipper and W2 domain-containing protein 1 IPR016024 ARM-type foldIPR003307 eIF5C	421.05263
ENSMUSP00000025483	64.2	Asparaginyl-tRNA synthetase, cytoplasmic (EC 6.1.1.22)(Asparagine--tRNA ligase)(AsnRS) Source: 6.1.1.22 IPR004522 Asn-tRNA-synth IIbIPR002312 Asp-tRNA-synth IIbIPR004365 NA bd OB tRNA-helicaseIPR004364 aa-tRNA-synt IIIPR006195 aa-tRNA-synth II	563.15789
ENSMUSP00000028241	31.4	Erythrocyte band 7 integral membrane protein (Stomatin)(Protein 7.2b) IPR001107 Band 7IPR018080 Band 7/stomatin-like CSIPR001972 Stomatin	275.4386
ENSMUSP00000047898	53.9	ATP-dependent RNA helicase DDX19A (EC 3.6.1.-)(DEAD box protein 19A)(DEAD box RNA helicase DEAD5)(mDEAD5)(Eukaryotic translation initiation factor 4A-related sequence 1) Source: 3.6.1.- IPR014001 DEAD-like NIPR001650 DNA/RNA helicase CIPR011545 DNA/RNA helicase DEAD/DEAH NIPR014021 Helicase SF1/SF2 ATP-bdIPR014014 RNA helicase DEAD Q motif	472.80702
ENSMUSP00000022060	21.9	Programmed cell death protein 6 (Probable calcium-binding protein ALG-2)(PMP41)(ALG-257) IPR018247 EF HAND 1IPR018249 EF HAND 2IPR018248 EF handIPR002048 EF hand Ca bd	192.10526
ENSMUSP00000001713	27.4	Glutathione S-transferase theta-1 (EC 2.5.1.18)(GST class-theta-1) Source: 2.5.1.18 IPR004046 GST CIPR010987 Glutathione-S-Trfase C-likeIPR004045 Glutathione S-Trfase NIPR012336 Thioredoxin-like fold	240.35088
ENSMUSP00000107760	165.7	Alpha-2-macroglobulin Precursor (Alpha-2-M)(Pregnancy zone protein) IPR009048 A-macroglobulin rcpt-bdIPR002890 A2M NIPR011625 A2M N 2IPR011626 A2M compIPR001599 MacrogloblnA2IPR008930 Terpenoid cyclase/PrenylTrfase	1453.5088
ENSMUSP00000028222	72.4	78 kDa glucose-regulated protein Precursor (GRP 78)(Heat shock 70 kDa protein 5)(Immunoglobulin heavy chain-binding protein)(BiP) IPR018181 Heat shock 70 CSIPR001023 Hsp70IPR013126 Hsp 70	635.08772
ENSMUSP00000038368	97.6	Coatomer subunit gamma-2 (Gamma-2-coat protein)(Gamma-2-COP) IPR016024 ARM-type foldIPR009028 Calthrin/coatomer app sub CIPR002553 Clathrin/coatomer adapt-like NIPR017106 Coatomer gamma subunitIPR014863 Coatomer gsu appIPR000357 HEAT	856.14035
ENSMUSP00000080531	40.6	Farnesyl pyrophosphate synthetase (FPP synthetase)(FPS)(Farnesyl diphosphate synthetase)(Cholesterol-regulated 39 kDa protein)(CR 39) Source: 2.5.1.1 IPR000092 Polyprenyl syntIPR008949 Terpenoid synth	356.14035
ENSMUSP00000029630	61.3	fibrinogen, alpha polypeptide isoform 2 IPR014814 Fibrinogen alpha N	537.7193
ENSMUSP00000100067	27.8	14-3-3 protein theta (14-3-3 protein tau) IPR000308 14-3-3	243.85965
ENSMUSP00000020285	22.4	GTP-binding protein SAR1a IPR006688 ARFIPR006689 ARF/SARIPR013684 Miro-likeIPR001806 Ras GTPaseIPR006687 SAR1 GTP bdIPR005225 Small GTP bd	196.49123
ENSMUSP00000004508	26	Transmembrane emp24 domain-containing protein 4 Precursor (Endoplasmic reticulum stress-response protein 25)(ERS25)(p26) IPR000348 Emp24 gp25L p24IPR009038 GOLD	228.07018
ENSMUSP00000093944	82.6	Dynamin-1-like protein (EC 3.6.5.5)(Dynamin-related protein 1)(Dynamin family member proline-rich carboxyl-terminal domain less)(Dymple) Source: 3.6.5.5 IPR001401 Dynamin GTPaseIPR000375 Dynamin centralIPR003130 GED	724.5614
ENSMUSP00000081010	22.3	Glutathione peroxidase 1 (EC 1.11.1.9)(GSHPx-1)(GPx-1)(Cellular glutathione peroxidase) Source: 1.11.1.9 IPR000889 Glutathione peroxidaseIPR012336 Thioredoxin-like fold	195.61404
ENSMUSP00000045927	31.6	Uncharacterized protein C18orf19 homolog IPR009688 DUF1279	277.19298
ENSMUSP00000096677	202.1	ADP-ribosylation factor guanine nucleotide-exchange factor 2 (brefeldin A-inhibited) IPR016024 ARM-type foldIPR015403 DUF1981 SEC7 assocIPR000904 Sec7	1772.807

ENSMUSP00000100564	27	Proteasome activator complex subunit 2 (Proteasome activator 28 subunit beta)(PA28beta)(PA28b)(Activator of multicatalytic protease subunit 2)(11S regulator complex subunit beta)(REG-beta) IPR003185 Proteasome activ REG asuIPR009077 Proteasome activ REG asu/bsuIPR003186 Proteasome activ REG bsu	236.84211
ENSMUSP00000008826	24.6	60S ribosomal protein L10 (Protein QM homolog) IPR001197 Ribosomal L10eIPR016180 Ribosomal L10e/L16IPR018255 Ribosomal L10e CS	215.78947
ENSMUSP00000073213	26.8	Peroxisomal coenzyme A diphosphatase NUDT7 (EC 3.6.1.-)(Nucleoside diphosphate-linked moiety X motif 7)(Nudix motif 7) Source: 3.6.1.- IPR015797 NUDIXIPR000059 NUDIX hydrolase CSIPR000086 NUDIX hydrolase core	235.08772
ENSMUSP00000041814	105.8	Lon protease homolog, mitochondrial Precursor (EC 3.4.21.-)(Lon protease-like protein)(LONP)(Mitochondrial ATP-dependent protease Lon)(Serine protease 15) Source: 3.4.21.- IPR003593 AAA+ ATPase coreIPR011704 AAA 5IPR003959 AAA ATPase coreIPR001270 Chaprnin clpA/BIPR008269 Pept S16 CIPR003111 Pept S16 NIPR004815 Pept S16 lonIPR001984 Peptidase S16IPR008268 Peptidase S16 AS	928.07018
ENSMUSP00000030345	73.9	Carnitine O-palmitoyltransferase 2, mitochondrial Precursor (EC 2.3.1.21)(Carnitine palmitoyltransferase II)(CPT II) Source: 2.3.1.21 IPR000542 Carn acyl trans	648.24561
ENSMUSP00000102140	21.9	5-(3-)-deoxyribonucleotidase, cytosolic type (EC 3.1.3.-)(Cytosolic 5-,3--pyrimidine nucleotidase)(Deoxy-5--nucleotidase 1)(dNT-1) Source: 3.1.3.- IPR010708 5'(3')-deoxyribonucleotidase	192.10526
ENSMUSP00000083705	34.2	60S acidic ribosomal protein P0 (L10E) IPR000104 Antifreeze 1IPR001813 Ribosomal 60SIPR001790 Ribosomal L10	300
ENSMUSP00000085623	37.5	5--AMP-activated protein kinase subunit gamma-1 (AMPK gamma-1 chain)(AMPKg) IPR000644 Cysta beta synth core	328.94737
ENSMUSP00000105795	24.2	Maleylacetoacetate isomerase (MAAI)(EC 5.2.1.2)(Glutathione S-transferase zeta 1)(EC 2.5.1.18)(GSTZ1-1) Source: 5.2.1.2 IPR004046 GST CIPR010987 Glutathione-S-Trfase C-likeIPR004045 Glutathione S-Trfase NIPR005955 Mal ac isomIPR012336 Thioredoxin-like fold	212.2807
ENSMUSP00000044326	76.7	Solute carrier organic anion transporter family member 1B2 (Solute carrier family 21 member 10)(Liver-specific organic anion transporter 1)(LST-1)(SLC21A6) IPR011701 MFS 1IPR016196 MFS gen sb transptIPR004156 OA transporterIPR011497 Prot Inh Kazal 2IPR002350 Prot inh Kazal	672.80702
ENSMUSP00000087694	102.2	E3 ubiquitin-protein ligase MARCH6 (EC 6.3.2.-)(Membrane-associated RING finger protein 6)(Membrane-associated RING-CH protein VI)(MARCH-VI) Source: 6.3.2.- IPR011016 Znf RING-CH	896.49123
ENSMUSP00000045216	53.2	Monocarboxylate transporter 1 (MCT 1)(Solute carrier family 16 member 1) IPR011701 MFS 1IPR016196 MFS gen sb transptIPR004743 Monocarb transpt	466.66667
ENSMUSP00000071078	34.5	Coatomer subunit epsilon (Epsilon-coat protein)(Epsilon-COP) IPR006822 Coatomer esu	302.63158
ENSMUSP00000034966	47.1	60S ribosomal protein L4 IPR016160 Ald DHase CSIPR002136 Ribosomal L4/L1eIPR013000 Ribosomal L4/L1e euk/arc CS	413.15789
ENSMUSP00000099634	70.8	Very long-chain specific acyl-CoA dehydrogenase, mitochondrial Precursor (EC 1.3.99.-)(MVLCAD)(VLCAD) Source: 1.3.99.- IPR006091 Acyl-CoA DHase/Oxase MIPR013107 Acyl-CoA DHase 2 CIPR006089 Acyl-CoA DHase CSIPR006092 Acyl-CoA DHase NIPR006090 Acyl-CoA Oxase/DHase 1IPR009100 AcylCoA DH/oxidase M/NIPR009075 AcylCo DHase/oxidase C	621.05263
ENSMUSP00000030830	89.9	GDH/6PGL endoplasmic bifunctional protein Precursor Source: 1.1.1.47 IPR005900 6-phosphogluconolactonaseIPR001282 Glc-6-P DHaseIPR006148 Glc/Gal-6P isomerase	788.59649
ENSMUSP00000107433	28.8	Endoplasmic reticulum protein ERp29 Precursor IPR016855 ER p29IPR011679 ER p29 CIPR012883 ERp29 NIPR012336 Thioredoxin-like fold	252.63158
ENSMUSP00000081001	68.4	NADH-ubiquinone oxidoreductase chain 5 (EC 1.6.5.3)(NADH dehydrogenase subunit 5) Source: 1.6.5.3 IPR010934 NADH DHase su5 CIPR003945 NADHpl OxRdtase 5IPR018393 NADHpl OxRdtase 5 sgIPR003918 NADHub OxRdtase 4IPR003916 NADHub OxRdtase 5IPR001516 OxRdtase q1 NIPR001750 Oxidored q1	600
ENSMUSP00000038914	54.5	Kynurenine 3-monooxygenase (EC 1.14.13.9)(Kynurenine 3-hydroxylase) Source: 1.14.13.9 IPR003042 Rng hydrolaseIPR002938 mOase FAD bd	478.07018
ENSMUSP00000055862	20.1	ADP-ribosylation factor 6 IPR006688 ARFIPR006689 ARF/SARIPR003579 GTPase RabIPR013684 Miro-likeIPR013753 RasIPR001806 Ras GTPaseIPR006687 SAR1 GTP bdIPR005225 Small GTP bd	176.31579
ENSMUSP00000108126	55	Protein FAM98A IPR001174 Galkinase	482.45614
ENSMUSP00000020161	36.2	Arginase-1 (EC 3.5.3.1)(Type I arginase)(Liver-type arginase) Source: 3.5.3.1 IPR005924 ArginaseIPR014033 Arginase	317.54386

		subIPR006035 Ureohydrolase	
ENSMUSP00000036093	115.9	Importin-9 (Imp9)(Importin-9a)(Imp9a)(Importin-9b)(Imp9b)(Ran-binding protein 9)(RanBP9) IPR016024 ARM-type foldIPR001494 Importin-b N	1016.6667
ENSMUSP00000025385	79.4	Peroxisomal multifunctional enzyme type 2 (MFE-2)(D-bifunctional protein)(DBP)(17-beta-hydroxysteroid dehydrogenase 4)(17-beta-HSD 4) Source: 1.1.1.35 IPR003560 DHB DHaseIPR002198 DHase sc/Rdtase SDRIPR003965 Fatty acid synthaseIPR002347 Glc/ribitol DHaseIPR002539 MaoC deHydtaseIPR016040 NAD(P)-bdIPR013968 Polyketide synth KRIPR003033 SCP2 sterol bdIPR016083 Sterol-binding-like	696.49123
ENSMUSP00000034541	69.6	Signal recognition particle receptor subunit alpha (SR-alpha)(Docking protein alpha)(DP-alpha) IPR003593 AAA+ ATPase coreIPR007222 Sig recog particle rcpt asu NIPR000897 Signal recog part SRP54 GTPaseIPR013822 Signal recog particl SRP54 hlx	610.52632
ENSMUSP00000047536	29.8	Prohibitin (B-cell receptor-associated protein 32)(BAP 32) IPR001107 Band 7IPR000163 Prohibitin	261.40351
ENSMUSP00000037783	25.8	Growth arrest and DNA-damage-inducible proteins-interacting protein 1	226.31579
ENSMUSP00000021239	34.9	Leucine-rich repeat-containing protein 59 IPR005819 Histone H5IPR001611 Leu-rich rptIPR003591 Leu-rich rpt typical-subtyp	306.14035
ENSMUSP00000028916	86.4	Protein transport protein Sec23B (SEC23-related protein B) IPR007123 GelsolnIPR012990 Sec23 24 beta SIPR006900 Sec23 helicalIPR006896 Sec23 trunkIPR006895 Znf Sec23 Sec24	757.89474
ENSMUSP00000037018	49.4	Fibrinogen gamma chain Precursor IPR002181 Fibrinogen a/b/g C	433.33333
ENSMUSP00000110998	46.5	Eukaryotic initiation factor 4A-II (eIF-4A-II)(eIF4A-II)(EC 3.6.1.-)(ATP-dependent RNA helicase eIF4A-2) Source: 3.6.1.- IPR014001 DEAD-like NIPR001650 DNA/RNA helicase CIPR011545 DNA/RNA helicase DEAD/DEAH NIPR014021 Helicase SF1/SF2 ATP-bdIPR000629 RNA-helicase DEAD-box CSIPR014014 RNA helicase DEAD Q motif	407.89474
ENSMUSP00000060218	20	Probable gluconokinase (EC 2.7.1.12)(Gluconate kinase) Source: 2.7.1.12 IPR000623 Shik kinaseIPR006001 Therm gnt kinIPR000764 Uridine kinase	175.4386
ENSMUSP00000002790	110.4	Exportin-2 (Exp2)(Importin-alpha re-exporter)(Chromosome segregation 1-like protein) IPR016024 ARM-type foldIPR005043 CAS CSE1 CIPR013713 Exportin Cse1-likeIPR001494 Importin-b N	968.42105
ENSMUSP00000030538	49	Dolichyl-diphosphooligosaccharide--protein glycosyltransferase 48 kDa subunit Precursor (Oligosaccharyl transferase 48 kDa subunit)(DDOST 48 kDa subunit)(EC 2.4.1.119) Source: 2.4.1.119 IPR005013 DDOST 48kDa	429.82456
ENSMUSP00000023803	47.5	Keratin, type I cytoskeletal 18 (Cytokeratin-18)(CK-18)(Keratin-18)(K18)(Cytokeratin endo B)(Keratin D) IPR016044 FIPR018039 Intermediate filament CSIPR002957 Keratin IIPR003054 Keratin IIIPR009053 Prefoldin	416.66667
ENSMUSP00000106481	54.2	Dihydrolipoyl dehydrogenase, mitochondrial Precursor (EC 1.8.1.4)(Dihydrolipoamide dehydrogenase) Source: 1.8.1.4 IPR016156 FAD/NAD-linked Rdtase dimerIPR013027 FAD pyr nucl-diS OxRdtaseIPR000815 Hg reductaseIPR006036 K uptake TrkAIPR006258 Lipoamide DHaseIPR012999 Pyr OxRdtase I ASIPR001327 Pyr OxRdtase NAD bdIPR004099 Pyr nucl-diS OxRdtase dimerIPR000103 Pyridine nuc-diS OxRdtase 2	475.4386
ENSMUSP00000034164	39.4	Uncharacterized protein KIAA0174 IPR005061 DUF292 eukIPR000694 PRO rich	345.61404
ENSMUSP00000112334	58.8	Alpha-aminoadipic semialdehyde dehydrogenase (Alpha-AASA dehydrogenase)(EC 1.2.1.31)(Delta1-piperideine-6-carboxylate dehydrogenease)(P6c dehydrogenase)(Aldehyde dehydrogenase family 7 member A1)(Antiquitin-1) Source: 1.2.1.31 IPR016161 Ald DHase/Histidinol DHaseIPR016160 Ald DHase CSIPR015590 Aldehyde DHase	515.78947
ENSMUSP00000067685	180.4	Ras GTPase-activating-like protein IQGAP2 IPR016146 Calponin-homologyIPR001715 Calponin act bdIPR003197 Cyt bd ubiquinol oxidase 14kDaIPR000048 IQ CaM bd regionIPR001936 RasGAPIPR000593 RasGAP CIPR008936 Rho GTPase activation protIPR001202 WW Rsp5 WWP	1582.4561
ENSMUSP00000099364	82.6	Vesicle-fusing ATPase (EC 3.6.4.6)(N-ethylmaleimide-sensitive fusion protein)(NEM-sensitive fusion protein)(Vesicular-fusion protein NSF)(Suppressor of K(+) transport growth defect 2)(Protein SKD2) Source: 3.6.4.6 IPR003593 AAA+ ATPase coreIPR003960 AAA ATPase CSIPR003959 AAA ATPase coreIPR003338 ATPaseVAT NIPR009010 Asp de-COase-like foldIPR004201 Cdc48 2IPR001984 Peptidase S16	724.5614
ENSMUSP00000020717	20.5	ADP-ribosylation factor 5 IPR006688 ARFIPR006689 ARF/SARIPR003579 GTPase RabIPR013684 Miro-likeIPR013753 RasIPR001806 Ras GTPaseIPR006687 SAR1 GTP bdIPR005225 Small GTP bd	179.82456
ENSMUSP00000033509	26.2	3-beta-hydroxysteroid-Delta(8),Delta(7)-isomerase (EC 5.3.3.5)(Cholestenol Delta-isomerase)(Delta(8)-Delta(7) sterol isomerase)(D8-D7 sterol isomerase)(Emopamil-binding protein) Source: 5.3.3.5 IPR007905 EBP	229.82456

ENSMUSP00000091180	49.5	no description availableIPR000795 ProtSyn GTP bdIPR009001 Transl elong EF1A/Init IF2 CIPR004161 Transl elong EFTu/EF1A 2IPR004160 Transl elong EFTu/EF1A CIPR004541 Transl elong EFTu/EF1A bac/org	434.21053
ENSMUSP00000095845	32	Alpha-tocopherol transfer protein (Alpha-TTP) IPR001251 CRAL bd TRIO CIPR008273 CRAL bd TRIO NIPR001071 CRAL bd toc tranIPR011074 Sec14p like N	280.70175
ENSMUSP00000035761	503.7	apolipoprotein B precursor IPR016024 ARM-type foldIPR015819 Lipid transp b-sht shellIPR001747 Lipid transpt NIPR009454 Lipid transpt open b-shtIPR015255 Vitellinogen open b-sht	4418.4211
ENSMUSP00000021375	86.1	Protein transport protein Sec23A (SEC23-related protein A) IPR007123 GelsolnIPR012990 Sec23 24 beta SIPR006900 Sec23 helicalIPR006896 Sec23 trunkIPR006895 Znf Sec23 Sec24	755.26316
ENSMUSP00000000756	24.3	60S ribosomal protein L13 (A52) IPR001380 Ribosomal L13eIPR018256 Ribosomal L13e CS	213.15789
ENSMUSP00000107914	39.9	Mannose-1-phosphate guanyltransferase beta (EC 2.7.7.13)(GTP-mannose-1-phosphate guanylyltransferase beta)(GDP-mannose pyrophosphorylase B) Source: 2.7.7.13 IPR001451 Hexapep transfIPR018357 Hexapep transf CSIPR005835 NTP transferaseIPR011004 Trimer LpxA like	350
ENSMUSP00000023583	37.3	Alpha-2-HS-glycoprotein Precursor (Fetuin-A)(Countertrypin) IPR000010 Prot inh cystatIPR001363 Prot inh fetuin CS	327.19298
ENSMUSP00000007130	85.4	Catenin beta-1 (Beta-catenin) IPR016024 ARM-type foldIPR000225 ArmadilloIPR013284 Beta-cateninIPR000357 HEAT	749.12281
ENSMUSP00000039202	30.3	Putative L-aspartate dehydrogenase (EC 1.4.1.21) Source: 1.4.1.21 IPR005106 Asp/hSer DHase NAD-bdIPR002811 Asp DHaseIPR011182 Asp DHase NAD synIPR001312 HexokinaseIPR016040 NAD(P)-bd	265.78947
ENSMUSP00000001460	102	Staphylococcal nuclease domain-containing protein 1 (p100 co-activator)(100 kDa coactivator) IPR008191 Maternal tudorIPR016685 Silence cplx Nase-comp TudorSNIPR016071 Staphylococal nuclease OB-foldIPR006021 Staphylococcal nucleaseIPR002071 Thermonucl ASIPR002999 TudorIPR018351 Tudor subgroup	894.73684
ENSMUSP00000023087	40.1	Twinfilin-1 (Protein A6) IPR002108 Actin-bd cofilin/tropomyosin	351.75439
ENSMUSP00000021133	70.5	Signal recognition particle 68 kDa protein (SRP68) IPR013026 TPR region	618.42105
ENSMUSP00000031355	106.9	General vesicular transport factor p115 (Protein USO1 homolog)(Transcytosis-associated protein)(TAP)(Vesicle-docking protein) IPR016024 ARM-type foldIPR000225 ArmadilloIPR006955 Uso1 p115 CIPR006953 Uso1 p115 head	937.7193
ENSMUSP00000033093	21.4	Apoptosis regulator BAX IPR013282 Apop reg Bcl2RelIPR002475 BCL2 apoptsisIPR000712 Bcl2 BH	187.7193
ENSMUSP00000107937	20.5	ADP-ribosylation factor 4 IPR006688 ARFIPR006689 ARF/SARIPR003579 GTPase RabIPR003577 GTPase RasIPR013684 Miro-likeIPR013753 RasIPR001806 Ras GTPaseIPR006687 SAR1 GTP bdIPR005225 Small GTP bd	179.82456
ENSMUSP00000072199	98.1	Dynamin-2 (EC 3.6.5.5)(Dynamin UDNM) Source: 3.6.5.5 IPR001401 Dynamin GTPaseIPR000375 Dynamin centralIPR003130 GEDIPR000694 PRO richIPR001849 Pleckstrin homology	860.52632
ENSMUSP00000026538	31.5	Enoyl-CoA hydratase, mitochondrial Precursor (EC 4.2.1.17)(Short chain enoyl-CoA hydratase)(SCEH)(Enoyl-CoA hydratase 1) Source: 4.2.1.17 IPR001753 Crotonase coreIPR018376 Enoyl-CoA hyd/isom CS	276.31579
ENSMUSP00000025835	88.2	Carnitine O-palmitoyltransferase 1, liver isoform (CPT1-L)(EC 2.3.1.21)(Carnitine O-palmitoyltransferase I, liver isoform)(CPTI-L)(CPT I)(Carnitine palmitoyltransferase 1A) Source: 2.3.1.21 IPR000542 Carn acyl trans	773.68421
ENSMUSP00000086021	14.5	60S ribosomal protein L31 IPR000054 Ribosomal L31e	127.19298
ENSMUSP00000001715	27.4	glutathione S-transferase, theta 3 IPR004046 GST CIPR010987 Glutathione-S-Trfase C-likeIPR004045 Glutathione S-Trfase NIPR012336 Thioredoxin-like fold	240.35088
ENSMUSP00000021793	34.2	Elongation of very long chain fatty acids protein 2 IPR006028 GABAA rcptIPR002076 GNS1 SUR4	300
ENSMUSP00000071616	31.4	60S ribosomal protein L7 IPR016082 Ribosomal L30 CIPR012988 Ribosomal L30 NIPR000517 Ribosomal L30 coreIPR005998 Ribosomal L7 eukIPR018038 Ribosomal protein L30	275.4386
ENSMUSP00000015011	30.4	Surfeit locus protein 4 IPR002995 Surf4	266.66667
ENSMUSP00000106359	24.4	ER lumen protein retaining receptor 2 (KDEL endoplasmic reticulum protein retention receptor 2)(KDEL receptor 2) IPR000133 ER ret rcpt	214.03509
ENSMUSP00000036386	36.5	L-lactate dehydrogenase A chain (LDH-A)(EC 1.1.1.27)(LDH muscle subunit)(LDH-M) Source: 1.1.1.27 IPR001557 L-lactate/malate DHaseIPR011304 L-lactate DHaseIPR018177 L-lactate DHase ASIPR001236 Lactate/malate DHaseIPR015955 Lactate DHase/Glyco Ohase 4 CIPR016040 NAD(P)-bdIPR001806 Ras GTPase	320.17544
ENSMUSP00000066035	52.2	Annexin A7 (Annexin-7)(Annexin VII)(Synexin) IPR001464 AnnexinIPR002391 AnnexinIVIPR013286	457.89474

		AnnexinVIIIPR009115 AnnexinVIIIIPR018502 Annexin repeatIPR018252 Annexin repeat CSIPR006030 Mollsc rhodpsn CIPR000694 PRO rich	
ENSMUSP00000025833	70.3	Bifunctional 3--phosphoadenosine 5--phosphosulfate synthetase 2 (PAPS synthetase 2)(PAPSS 2)(Sulfurylase kinase 2)(SK 2)(SK2) Source: 2.7.7.4 IPR002891 APS kinase CIPR002650 ATP-sulfurylaseIPR015947 PUA-like	616.66667
ENSMUSP00000032168	52.2	Protein transport protein Sec61 subunit alpha isoform 1 (Sec61 alpha-1) IPR002208 SecY	457.89474
ENSMUSP00000063825	129.6	Pyruvate carboxylase, mitochondrial Precursor (EC 6.4.1.1)(Pyruvic carboxylase)(PCB) Source: 6.4.1.1 IPR011761 ATP-graspIPR003135 ATP-grasp carboxylate-amineIPR011764 BCIPR001882 Biotin BSIPR005482 Biotin COase CIPR000089 Biotin lipoylIPR005483 CarbamoylP synth lsuIPR005479 CarbamoylP synth lsu ATP-bdIPR005481 CarbamoylP synth lsu NIPR003379 PYC OADAIPR000891 PYR CTIPR016185 PreATP-grasp-likeIPR005930 Pyruv COaseIPR011054 Rudment hybrid motifIPR011053 Single hybrid motif	1136.8421
ENSMUSP00000072084	64.6	Glucokinase regulatory protein (Glucokinase regulator) IPR005486 Glucokinase regulatory CS	566.66667
ENSMUSP00000056433	20.6	Ras-related protein Rap-2a Precursor IPR003579 GTPase RabIPR003577 GTPase RasIPR003578 GTPase RhoIPR013684 Miro-likeIPR002041 Ran GTPaseIPR013753 RasIPR001806 Ras GTPaseIPR005225 Small GTP bd	180.70175
ENSMUSP00000082125	46.7	Serine protease inhibitor A3C Precursor (Serpin A3C)(Kallikrein-binding protein)(KBP) IPR000295 Prot inh Lserp2IPR000215 Protease inhib I4 serpin	409.64912
ENSMUSP00000031617	33.5	60S ribosomal protein L6 (TAX-responsive enhancer element-binding protein 107)(TAXREB107) IPR000915 Ribosomal L6EIPR005568 Ribosomal L6 N	293.85965
ENSMUSP00000038214	116.1	Uncharacterized protein KIAA0564 homolog Precursor IPR003593 AAA+ ATPase coreIPR011704 AAA 5IPR001984 Peptidase S16	1018.4211
ENSMUSP00000035010	93.3	Dolichyl-diphosphooligosaccharide--protein glycosyltransferase subunit STT3B (Oligosaccharyl transferase subunit STT3B)(STT3-B)(EC 2.4.1.119)(Source of immunodominant MHC-associated peptides)(B6dom1 antigen) Source: 2.4.1.119 IPR003674 Oligo trans STT3	818.42105
ENSMUSP00000079379	67.3	ATP-binding cassette sub-family E member 1 (RNase L inhibitor)(Ribonuclease 4 inhibitor)(RNS4I) IPR017900 4Fe4S Fe S CSIPR001450 4Fe4S Fe S bd subgrIPR003593 AAA+ ATPase coreIPR013283 ABC EIPR003439 ABC transporter-likeIPR017871 ABC transporter CSIPR007209 RLI metal bd	590.35088
ENSMUSP00000075321	34.6	Sulfotransferase 1A1 (EC 2.8.2.1)(Aryl sulfotransferase)(Phenol sulfotransferase)(Sulfokinase)(Phenol/aryl sulfotransferase)(mSTp1)(ST1A4) Source: 2.8.2.1 IPR000863 Sulfotransferase	303.50877
ENSMUSP00000006703	104.6	inter alpha-trypsin inhibitor, heavy chain 4 IPR010600 ITI HC CIPR000694 PRO richIPR013694 VITIPR006587 VIT metIPR002035 VWF A	917.54386
ENSMUSP00000052544	40.5	Zinc-binding alcohol dehydrogenase domain-containing protein 2 (EC 1.-.-.-) Source: 1.-.-.- IPR013154 AlcDHase GroES-likeIPR013149 AlcDHase Zn-bdIPR011032 GroES likeIPR016040 NAD(P)-bdIPR002364 Quin OxRdtase/zeta-crystal CS	355.26316
ENSMUSP00000034058	25.4	Carbonyl reductase 4 (EC 1.1.1.-) Source: 1.1.1.- IPR003560 DHB DHaseIPR002198 DHase sc/Rdtase SDRIPR002347 Glc/ribitol DHaseIPR002424 Insect AlcDHase famIPR016040 NAD(P)-bdIPR013968 Polyketide synth KR	222.80702
ENSMUSP00000026667	46.8	Eukaryotic initiation factor 4A-III (EC 3.6.1.-)(Eukaryotic translation initiation factor 4A isoform 3)(ATP-dependent RNA helicase eIF4A-3)(ATP-dependent RNA helicase DDX48)(DEAD box protein 48) Source: 3.6.1.- IPR003593 AAA+ ATPase coreIPR014001 DEAD-like NIPR001650 DNA/RNA helicase CIPR011545 DNA/RNA helicase DEAD/DEAH NIPR014021 Helicase SF1/SF2 ATP-bdIPR000629 RNA-helicase DEAD-box CSIPR014014 RNA helicase DEAD Q motif	410.52632
ENSMUSP00000042860	20.8	Glucosamine 6-phosphate N-acetyltransferase (EC 2.3.1.4)(Phosphoglucosamine transacetylase)(Phosphoglucosamine acetylase)(EMeg32 protein) Source: 2.3.1.4 IPR016181 Acyl CoA acyltransferaseIPR000182 GCN5-rel AcTrfase	182.45614
ENSMUSP00000028683	56.6	Protein disulfide-isomerase A3 Precursor (EC 5.3.4.1)(Disulfide isomerase ER-60)(ERp60)(58 kDa microsomal protein)(p58)(ERp57) Source: 5.3.4.1 IPR005788 Disulphide isomeraseIPR005792 Prot disulphide isomeraseIPR012336 Thioredoxin-like foldIPR006662 Thioredoxin-like subdomIPR017937 Thioredoxin CSIPR013766 Thioredoxin dom	496.49123
ENSMUSP00000028592	42.5	Eukaryotic translation initiation factor 3 subunit M (eIF3m)(PCI domain-containing protein 1) IPR016024 ARM-type foldIPR000717 PCI	372.80702
ENSMUSP00000026122	57	Protein disulfide-isomerase Precursor (PDI)(EC 5.3.4.1)(Prolyl 4-hydroxylase subunit beta)(Cellular thyroid hormone-binding protein)(p55)(Erp59) Source: 5.3.4.1 IPR005788 Disulphide isomeraseIPR005792 Prot disulphide isomeraseIPR012336 Thioredoxin-like foldIPR006662 Thioredoxin-like subdomIPR017937 Thioredoxin CSIPR013766 Thioredoxin dom	500

ENSMUSP00000004072	28	60S ribosomal protein L8 IPR016027 NA-bd OB-fold-likeIPR002171 Ribosomal L2IPR008991 Translation prot SH3-like	245.61404
ENSMUSP00000076521	72.3	Protein disulfide-isomerase A4 Precursor (EC 5.3.4.1)(Protein ERp-72)(ERp72) Source: 5.3.4.1 IPR001393 CalsequestrinIPR017068 DS-Isoase A4IPR005788 Disulphide isomeraseIPR005792 Prot disulphide isomeraseIPR012336 Thioredoxin-like foldIPR006662 Thioredoxin-like subdomIPR017937 Thioredoxin CSIPR013766 Thioredoxin dom	634.21053
ENSMUSP00000001479	97.1	Importin subunit beta-1 (Karyopherin subunit beta-1)(Nuclear factor P97)(Pore targeting complex 97 kDa subunit)(PTAC97)(SCG) IPR016024 ARM-type foldIPR000225 ArmadilloIPR000357 HEATIPR001494 Importin-b N	851.75439
ENSMUSP00000020238	92.4	Endoplasmin Precursor (Heat shock protein 90 kDa beta member 1)(94 kDa glucose-regulated protein)(GRP94)(ERP99)(Polymorphic tumor rejection antigen 1)(Tumor rejection antigen gp96) IPR003594 ATP bd ATPaseIPR001404 Hsp90IPR004358 Sig transdc His kin-like C	810.52632
ENSMUSP00000027123	60.9	60 kDa heat shock protein, mitochondrial Precursor (Heat shock protein 60)(HSP-60)(Hsp60)(60 kDa chaperonin)(Chaperonin 60)(CPN60)(Mitochondrial matrix protein P1)(HSP-65) IPR017998 Chaperone TCP-1IPR018370 Chaperonin Cpn60 CSIPR001844 Chaprnin Cpn60IPR002423 Cpn60/TCP-1	534.21053
ENSMUSP00000075513	47.1	Alpha-enolase (EC 4.2.1.11)(2-phospho-D-glycerate hydro-lyase)(Non-neural enolase)(NNE)(Enolase 1) Source: 4.2.1.11 IPR000941 Enolase	413.15789
ENSMUSP00000019512	46	SEC14-like protein 4 IPR001251 CRAL bd TRIO CIPR008273 CRAL bd TRIO NIPR001071 CRAL bd toc tranIPR000348 Emp24 gp25L p24IPR009038 GOLDIPR011074 Sec14p like N	403.50877
ENSMUSP00000099453	67.9	Acyl-CoA synthetase family member 2, mitochondrial Precursor (EC 6.2.1.-) Source: 6.2.1.- IPR000873 AMP-dep Synth/Lig	595.61404
ENSMUSP00000111081	53	Metalloreductase STEAP4 (EC 1.16.1.-)(Six-transmembrane epithelial antigen of prostate 4)(Tumor necrosis factor-alpha-induced adipose-related protein)(Dudulin-4) Source: 1.16.1.- IPR013130 Fe3 reduct TM NIPR018486 Hemopexin/matrixin CSIPR016040 NAD(P)-bdIPR004455 NADP OxRdtase F420	464.91228
ENSMUSP00000039269	50.9	Heterogeneous nuclear ribonucleoprotein K (hnRNP K) IPR004087 KHIPR004088 KH type 1IPR018111 KH type 1 subgrIPR004044 KH type 2IPR000694 PRO richIPR012987 ROK N	446.49123
ENSMUSP00000101823	43.4	Actin, cytoplasmic 2 (Gamma-actin) IPR004001 Actin CSIPR004000 Actin like	380.70175
ENSMUSP00000099841	25	Adenylate kinase isoenzyme 4, mitochondrial (EC 2.7.4.3)(Adenylate kinase 3-like)(ATP-AMP transphosphorylase) Source: 2.7.4.3 IPR006259 Adenyl kin subIPR000850 Adenylate kinIPR007862 Adenylate kinase Znf lidIPR000623 Shik kinase	219.29825
ENSMUSP00000078774	46.8	Succinyl-CoA ligase Source: 6.2.1.4 IPR013650 ATP-grasp succ-CoA synth-typeIPR005811 CoA ligaseIPR002347 Glc/ribitol DHaseIPR017866 Succ-CoA synthase bsu CSIPR005809 Succ CoA synthase bsuIPR016102 Succinyl-CoA synth-like	410.52632
ENSMUSP00000023760	37.5	Glycerol-3-phosphate dehydrogenase Source: 1.1.1.8 IPR008927 6-PGluconate DH C likeIPR006036 K uptake TrkAIPR016040 NAD(P)-bdIPR006168 NAD-dep Gly3P DHaseIPR011128 NAD-dep Gly3P DHase NIPR006109 NAD Gly3P DHase C	328.94737
ENSMUSP00000052912	48.7	Protein disulfide-isomerase A6 Precursor (EC 5.3.4.1)(Thioredoxin domain-containing protein 7) Source: 5.3.4.1 IPR005788 Disulphide isomeraseIPR012336 Thioredoxin-like foldIPR006662 Thioredoxin-like subdomIPR017937 Thioredoxin CSIPR013766 Thioredoxin dom	427.19298
ENSMUSP00000005122	39.4	Translation initiation factor eIF-2B subunit alpha/beta/delta-like protein IPR000649 IF-2B relatedIPR011559 Initiation fac 2B a/b/d	345.61404
ENSMUSP00000100000	79.1	Bifunctional UDP-N-acetylglucosamine 2-epimerase/N-acetylmannosamine kinase (UDP-GlcNAc-2-epimerase/ManAc kinase) Source: 5.1.3.14 IPR001312 HexokinaseIPR000600 ROKIPR003331 UDP GlcNAc Epimerase 2	693.85965
ENSMUSP00000039472	54.7	Fibrinogen beta chain Precursor IPR002181 Fibrinogen a/b/g C	479.82456
ENSMUSP00000042351	43.9	3-ketoacyl-CoA thiolase A, peroxisomal Precursor (EC 2.3.1.16)(Beta-ketothiolase A)(Acetyl-CoA acyltransferase A)(Peroxisomal 3-oxoacyl-CoA thiolase A) Source: 2.3.1.16 IPR013747 ACP syn III CIPR002155 ThiolaseIPR016039 Thiolase-like	385.08772
ENSMUSP00000024988	186.4	Complement C3 Precursor (HSE-MSF) IPR009048 A-macroglobulin rcpt-bdIPR002890 A2M NIPR011625 A2M N 2IPR011626 A2M compIPR000020 AnaphylatoxinIPR018081 Anaphylatoxin IPR001840 AnaphylatoxnIPR001599 MacroglobInA2IPR001134 Netrin CIPR018933 Netrin module non-TIMPIPR008930 Terpenoid cyclase/PrenylTrfase	1635.0877

ENSMUSP00000033012	107	Coatomer subunit beta (Beta-coat protein)(Beta-COP) IPR016024 ARM-type foldIPR002553 Clathrin/coatomer adapt-like NIPR016460 Coatomer beta subunitIPR011710 Coatomer bsu CIPR000357 HEAT	938.59649
ENSMUSP00000048111	27.9	Sepiapterin reductase (SPR)(EC 1.1.1.153) Source: 1.1.1.153 IPR003560 DHB DHaseIPR002198 DHase sc/Rdtase SDRIPR002347 Glc/ribitol DHaseIPR016040 NAD(P)-bdIPR006393 Sepiapterin red	244.73684
ENSMUSP00000020315	136.2	Cullin-associated NEDD8-dissociated protein 1 (Cullin-associated and neddylation-dissociated protein 1)(p120 CAND1) IPR016024 ARM-type foldIPR000225 ArmadilloIPR000357 HEATIPR013932 TATA bd TIP120	1194.7368
ENSMUSP00000111471	78.5	Pyridoxal-dependent decarboxylase domain-containing protein 1 (EC 4.1.1.-) Source: 4.1.1.- IPR015424 PyrdxlP-dep Trfase majorIPR002129 PyrdxlP-dep de-COase	688.59649
ENSMUSP00000111363	17.9	Ubiquitin-conjugating enzyme E2 L3 (EC 6.3.2.19)(Ubiquitin-protein ligase L3)(Ubiquitin carrier protein L3)(UbcM4) Source: 6.3.2.19 IPR016135 UBQ-conjugat/RWD-likeIPR000608 UBQ-conjugat E2	157.01754
ENSMUSP00000095129:reversed	41.7		365.78947
ENSMUSP00000031897	25.7	Glutathione S-transferase kappa 1 (EC 2.5.1.18)(Glutathione S-transferase subunit 13)(GST 13-13)(GST class-kappa)(GSTK1-1)(mGSTK1) Source: 2.5.1.18 IPR014440 HCCAis GSTkIPR001853 OxRdtase DSBAIPR012336 Thioredoxin-like fold	225.4386
ENSMUSP00000002064	33.5	Biliverdin reductase A Precursor (BVR A)(EC 1.3.1.24)(Biliverdin-IX alpha-reductase) Source: 1.3.1.24 IPR017094 Biliverdin Rdtase AIPR015249 Biliverdin Rdtase catIPR016040 NAD(P)-bdIPR000683 Oxidoreductase N	293.85965
ENSMUSP00000087118	43.7	S-adenosylmethionine synthetase isoform type-2 (AdoMet synthetase 2)(EC 2.5.1.6)(Methionine adenosyltransferase 2)(MAT 2) Source: 2.5.1.6 IPR002133 S-AdoMet synthetase	383.33333
ENSMUSP00000086165	20.3	Sorcin IPR018247 EF HAND 1IPR018249 EF HAND 2IPR018248 EF handIPR002048 EF hand Ca bd	178.07018
ENSMUSP00000078382	50.9	FK506-binding protein 5 (EC 5.2.1.8)(Peptidyl-prolyl cis-trans isomerase)(PPIase)(Rotamase)(51 kDa FK506-binding protein)(FKBP-51) Source: 5.2.1.8 IPR001179 PPIase FKBPIPR001440 TPR-1IPR013105 TPR 2IPR013026 TPR region	446.49123
ENSMUSP00000033871	32.8	Mitochondrial ornithine transporter 1 (Solute carrier family 25 member 15) IPR002113 Aden trnslctorIPR003949 K chnl volt-dep EAGIPR002067 Mit carrierIPR001993 Mitoch carrierIPR018108 Mitochondrial sb/sol carrier	287.7193
ENSMUSP00000038755	22.4	Abhydrolase domain-containing protein 14B (EC 3.-.-.-)(CCG1-interacting factor B) Source: 3.-.-.-	196.49123
ENSMUSP00000079246	20.4	ADP-ribosylation factor-like protein 1 IPR006688 ARFIPR006689 ARF/SARIPR003579 GTPase RabIPR003577 GTPase RasIPR013684 Miro-likeIPR000795 ProtSyn GTP bdIPR013753 RasIPR001806 Ras GTPaseIPR006687 SAR1 GTP bdIPR005225 Small GTP bd	178.94737
ENSMUSP00000023214	56.8	Diacylglycerol O-acyltransferase 1 (EC 2.3.1.20)(Diglyceride acyltransferase) Source: 2.3.1.20 IPR004299 MBOAT fam	498.24561
ENSMUSP00000034453	42	Actin, alpha skeletal muscle (Alpha-actin-1) IPR004001 Actin CSIPR004000 Actin like	368.42105
ENSMUSP00000098963	55.7	Signal recognition particle 54 kDa protein (SRP54) IPR003593 AAA+ ATPase coreIPR001270 Chaprnin clpA/BIPR014001 DEAD-like NIPR000897 Signal recog part SRP54 GTPaseIPR013822 Signal recog particl SRP54 hlxIPR006325 Signal recog particle SRP54IPR004125 Signal recog particle SRP54 M	488.59649
ENSMUSP00000026585	26	Tetraspanin-4 (Tspan-4)(Transmembrane 4 superfamily member 7) IPR018499 TetraspaninIPR008952 TetraspaninIPR018503 Tetraspanin CSIPR000301 Tetraspanin sub	228.07018
ENSMUSP00000098000	20	2-oxo-4-hydroxy-4-carboxy-5-ureidoimidazoline decarboxylase (OHCU decarboxylase)(EC 4.-.-.-)(Parahox neighbor) Source: 4.-.-.-	175.4386
ENSMUSP00000038878	53.6	Aldehyde dehydrogenase family 8 member A1 (EC 1.2.1.-)(Retinal dehydrogenase 4) Source: 1.2.1.- IPR016161 Ald DHase/Histidinol DHaseIPR016160 Ald DHase CSIPR015590 Aldehyde DHase	470.17544
ENSMUSP00000066878	61.5	Cystathionine beta-synthase (EC 4.2.1.22)(Serine sulfhydrase)(Beta-thionase) Source: 4.2.1.22 IPR001216 Cys synth BSIPR005857 Cysta beta synthIPR000644 Cysta beta synth coreIPR001926 PyrdxlP-dep enz bsu	539.47368
ENSMUSP00000109237	97.5	Coatomer subunit gamma (Gamma-coat protein)(Gamma-COP) IPR016024 ARM-type foldIPR009028 Calthrin/coatomer app sub CIPR002553 Clathrin/coatomer adapt-like NIPR013041 Clathrin/coatomer app Ig-likeIPR017106 Coatomer gamma subunitIPR014863 Coatomer gsu appIPR000357 HEAT	855.26316
ENSMUSP00000099461	18.5	Destrin (Actin-depolymerizing factor)(ADF)(Sid 23) IPR017904 ADF/Cofilin/DestrinIPR002108 Actin-bd cofilin/tropomyosin	162.2807
ENSMUSP00000033230	43.5	threonine aldolase 1 IPR001597 ArAA b-elim lyase/Thr aldolaseIPR015424 PyrdxlP-dep Trfase major	381.57895

ENSMUSP00000001806	62	Bifunctional coenzyme A synthase (CoA synthase) Source: 2.7.7.3 IPR004821 Cyt trans relIPR004820 CytidylyltransfIPR001977 Depp CoAkinase	543.85965
ENSMUSP00000069418	192.8	Complement C4-B Precursor IPR009048 A-macroglobulin rcpt-bdIPR002890 A2M NIPR011625 A2M N 2IPR011626 A2M compIPR000020 AnaphylatoxinIPR018081 Anaphylatoxin IPR001840 AnaphylatoxnIPR001599 MacrogloblnA2IPR001134 Netrin CIPR018933 Netrin module non-TIMPIPR008930 Terpenoid cyclase/PrenylTrfase	1691.2281
ENSMUSP00000019109	28.2	14-3-3 protein eta IPR000308 14-3-3	247.36842
ENSMUSP00000046101	95.3	Elongation factor 2 (EF-2) IPR009022 EFG III VIPR000795 ProtSyn GTP bdIPR005225 Small GTP bdIPR000640 Transl elong EFG/EF2 CIPR005517 Transl elong EFG/EF2 IVIPR004161 Transl elong EFTu/EF1A 2IPR009000 Transl elong init/rib B-barrel	835.96491
ENSMUSP00000022706	50.1	Succinyl-CoA ligase Source: 6.2.1.5 IPR013650 ATP-grasp succ-CoA synth-typeIPR005811 CoA ligaseIPR017866 Succ-CoA synthase bsu CSIPR005809 Succ CoA synthase bsuIPR016102 Succinyl-CoA synth-like	439.47368
ENSMUSP00000021639	50	Tubulin alpha chain-like 3 IPR002452 Alpha tubulinIPR002453 Beta tubulinIPR000158 Cell division FtsZ NIPR000183 De-COase2IPR002967 Delta tubulinIPR004057 Epsilon tubulinIPR002454 Gamma tubulinIPR008280 Tub FtsZ CIPR000217 TubulinIPR018316 Tubulin/FtsZ 2-layer-sand-domIPR017975 Tubulin CSIPR003008 Tubulin FtsZ	438.59649
ENSMUSP00000107544	50	Protein odr-4 homolog (mODR-4)	438.59649
ENSMUSP00000044288	43.5	S-adenosylmethionine synthetase isoform type-1 (AdoMet synthetase 1)(EC 2.5.1.6)(Methionine adenosyltransferase 1)(MAT 1) Source: 2.5.1.6 IPR002133 S-AdoMet synthetase	381.57895
ENSMUSP00000078429	49.9	Tubulin alpha-4A chain (Tubulin alpha-4 chain)(Alpha-tubulin 4)(Alpha-tubulin isotype M-alpha-4) IPR002452 Alpha tubulinIPR002453 Beta tubulinIPR000158 Cell division FtsZ NIPR002967 Delta tubulinIPR004057 Epsilon tubulinIPR002454 Gamma tubulinIPR008280 Tub FtsZ CIPR000217 TubulinIPR018316 Tubulin/FtsZ 2-layer-sand-domIPR017975 Tubulin CSIPR003008 Tubulin FtsZ	437.7193
ENSMUSP00000107492	96.7	Programmed cell death 6-interacting protein (ALG-2-interacting protein X)(ALG-2-interacting protein 1)(E2F1-inducible protein)(Eig2) IPR004116 AmelogeninIPR004328 BRO1IPR000694 PRO rich	848.24561
ENSMUSP00000070983	27.4	Splicing factor, arginine/serine-rich 7 IPR000504 RRM RNP1IPR001878 Znf CCHC	240.35088
ENSMUSP00000029769	30.5	Glutamate--cysteine ligase regulatory subunit (Gamma-glutamylcysteine synthetase regulatory subunit)(Gamma-ECS regulatory subunit)(GCS light chain)(Glutamate--cysteine ligase modifier subunit) IPR001395 Aldo/ket red	267.54386
ENSMUSP00000092157	132	Protein transport protein Sec31A (SEC31-related protein A)(SEC31-like 1) IPR000694 PRO richIPR001680 WD40 repeatIPR011046 WD40 repeat-likeIPR017986 WD40 repeat region	1157.8947
ENSMUSP00000022120	61.7	Acyl-coenzyme A thioesterase 12 (Acyl-CoA thioesterase 12)(EC 3.1.2.1)(Acyl-CoA thioester hydrolase 12)(Cytoplasmic acetyl-CoA hydrolase 1)(mCACH-1)(CACH-1) Source: 3.1.2.1 IPR002913 START lipid bdIPR006683 Thioestr supf	541.22807
ENSMUSP00000003572	81.8	Glycyl-tRNA synthetase (EC 6.1.1.14)(Glycine--tRNA ligase)(GlyRS) Source: 6.1.1.14 IPR004154 Anticodon bdIPR002316 Pro-tRNA-synth IIaIPR009068 S15 NS1 RNA bdIPR000738 WHEP-TRSIPR002314 aa-tRNA-synt IIbIPR006195 aa-tRNA-synth IIIPR002315 tRNA-synt gly	717.54386
ENSMUSP00000025846	94.6	Serine/threonine-protein phosphatase 6 regulatory subunit 3 (SAPS domain family member 3) IPR016024 ARM-type foldIPR007587 SAPS	829.82456
ENSMUSP00000032508	51.5	FK506-binding protein 4 (EC 5.2.1.8)(Peptidyl-prolyl cis-trans isomerase)(PPIase)(Rotamase)(HSP-binding immunophilin)(HBI)(FKBP52 protein)(52 kDa FK506-binding protein)(FKBP59)(p59 protein) Source: 5.2.1.8 IPR001179 PPIase FKBPIPR001440 TPR-1IPR013105 TPR 2IPR013026 TPR region	451.75439
ENSMUSP00000033050	34.6	Lymphatic vessel endothelial hyaluronic acid receptor 1 Precursor (LYVE-1)(Cell surface retention sequence-binding protein 1)(CRSBP-1)(Extracellular link domain-containing protein 1) IPR016187 C-type lectin foldIPR000538 Link	303.50877
ENSMUSP00000062215	56.7	Ubiquitin carboxyl-terminal hydrolase 14 (EC 3.1.2.15)(Ubiquitin thioesterase 14)(Ubiquitin-specific-processing protease 14)(Deubiquitinating enzyme 14) Source: 3.1.2.15 IPR018200 Pept C19ubi-hydrolase C CSIPR001394 Peptidase C19IPR000626 Ubiquitin	497.36842
ENSMUSP00000064557	24.5	Cofilin-1 (Cofilin, non-muscle isoform) IPR017904 ADF/Cofilin/DestrinIPR002108 Actin-bd cofilin/tropomyosin	214.91228
ENSMUSP00000066413	67.1	SET domain-containing protein 3 (Endothelial differentiation inhibitory protein D10) IPR015353 Rubisco subst bdIPR001214 SET	588.59649
ENSMUSP00000084114	46.2	Heterogeneous nuclear ribonucleoprotein D-like (hnRPD-like protein)(hnRNP-DL)(JKT41-binding protein) IPR000504	405.26316

		RRM RNP1	
ENSMUSP00000088334	91.7	Mitogen-activated protein kinase kinase kinase MLT (EC 2.7.11.25)(MLK-like mitogen-activated protein triple kinase)(Leucine zipper- and sterile alpha motif kinase ZAK)(Sterile alpha motif- and leucine zipper-containing kinase AZK)(Mixed lineage kinase-related kinase)(MLK-related kinase)(MRK) Source: 2.7.11.25 IPR000194 ATPase F1/V1/A1 a/bsu nucl-bdIPR011009 Kinase likeIPR000719 Prot kinase coreIPR001660 SAMIPR011510 SAM 2IPR010993 SAM homologyIPR017442 Se/Thr pkinase-reIIPR008271 Ser thr pkin ASIPR002290 Ser thr pkinaseIPR001245 Tyr pkinase	804.38596
ENSMUSP00000088663	34.6	Phytanoyl-CoA dioxygenase domain-containing protein 1 (EC 1.-.-.-) Source: 1.-.-.- IPR008775 Phytyl CoA dOase	303.50877
ENSMUSP00000097097:reversed	107.5		942.98246
ENSMUSP00000098112	50.2	Arf-GAP domain and FG repeats-containing protein 2 (HIV-1 Rev-binding protein-like protein)(Rev/Rex activation domain-binding protein related)(RAB-R) IPR001164 ArfGAP	440.35088
ENSMUSP00000107983	47.6	Annexin A11 (Annexin-11)(Annexin XI)(Calcyclin-associated annexin 50)(CAP-50) IPR001464 AnnexinIPR013286 AnnexinVIIIPR008157 AnnexinXI NIPR018502 Annexin repeatIPR018252 Annexin repeat CSIPR006030 Mollsc rhodpsn CIPR000694 PRO rich	417.54386
ENSMUSP00000111892	17.3		151.75439
ENSMUSP00000029564	21.9	Phosphomevalonate kinase (PMKase)(EC 2.7.4.2) Source: 2.7.4.2 IPR005919 Pmev kin anim	192.10526
ENSMUSP00000027766	71.7	Chaperone activity of bc1 complex-like, mitochondrial Precursor (Chaperone-ABC1-like)(aarF domain-containing protein kinase 3) IPR004147 ABC 1IPR011009 Kinase likeIPR002290 Ser thr pkinase	628.94737
ENSMUSP00000034529	90.9	Cullin-5 (CUL-5) IPR016157 Cullin CSIPR001373 Cullin NIPR016158 Cullin homologyIPR016159 Cullin repeat-like	797.36842
ENSMUSP00000035208:reversed	418.6		3671.9298
ENSMUSP00000047376	66.3	Glutaminase liver isoform, mitochondrial Precursor (GLS)(EC 3.5.1.2)(L-glutamine amidohydrolase)(L-glutaminase) Source: 3.5.1.2 IPR002110 ANKIPR012338 B-lactamase-typ transpept foldIPR015868 Glutaminase core	581.57895
ENSMUSP00000014546	44.1	Tumor susceptibility gene 101 protein (ESCRT-I complex subunit TSG101) IPR000694 PRO richIPR008883 Tsg101IPR016135 UBQ-conjugat/RWD-likeIPR000608 UBQ-conjugat E2	386.84211
ENSMUSP00000020886	55.4	Nicotinamide phosphoribosyltransferase (NAmPRTase)(Nampt)(EC 2.4.2.12)(Pre-B-cell colony-enhancing factor 1 homolog)(PBEF)(Visfatin) Source: 2.4.2.12 IPR015977 Nic PRibTrfase-likeIPR016471 Nicotinamide PRibTrfase	485.96491
ENSMUSP00000029125	31.2	Armadillo repeat-containing protein 1 IPR016024 ARM-type foldIPR000225 ArmadilloIPR006121 HeavyMe transptIPR016617 UCP013899 metal bd	273.68421
ENSMUSP00000030935	21.7	Uncharacterized protein C1orf93 homolog	190.35088
ENSMUSP00000035237	108.3	Ubiquitin carboxyl-terminal hydrolase 4 (EC 3.1.2.15)(Ubiquitin thioesterase 4)(Ubiquitin-specific-processing protease 4)(Deubiquitinating enzyme 4)(Ubiquitous nuclear protein) Source: 3.1.2.15 IPR006615 Pept C19 DUSPIPR010460 Pept C19 N 2IPR018200 Pept C19ubi-hydrolase C CSIPR001394 Peptidase C19	950
ENSMUSP00000043703:reversed	117.5		1030.7018
ENSMUSP00000045998	123.9	Ubiquitin-protein ligase E3C (EC 6.3.2.-) Source: 6.3.2.- IPR000569 HECTIPR000048 IQ CaM bd region	1086.8421
ENSMUSP00000051033	49.9	Tubulin alpha-1C chain (Tubulin alpha-6 chain)(Alpha-tubulin 6)(Alpha-tubulin isotype M-alpha-6) IPR002452 Alpha tubulinIPR002453 Beta tubulinIPR000158 Cell division FtsZ NIPR002967 Delta tubulinIPR004057 Epsilon tubulinIPR002454 Gamma tubulinIPR008280 Tub FtsZ CIPR000217 TubulinIPR018316 Tubulin/FtsZ 2-layer-sand-domIPR017975 Tubulin CSIPR003008 Tubulin FtsZ	437.7193
ENSMUSP00000075722	62.7	hypothetical protein LOC71903 IPR002018 CarbesteraseBIPR000997 Cholinesterase	550
ENSMUSP00000079905	20.7	ADP-ribosylation factor 1 IPR006688 ARFIPR006689 ARF/SARIPR003579 GTPase RabIPR013684 Miro-likeIPR013753 RasIPR001806 Ras GTPaseIPR006687 SAR1 GTP bdIPR005225 Small GTP bd	181.57895
ENSMUSP00000097582	28.4	Putative uncharacterized protein Source: UniProtKB/TrEMBL Q3V3K5	249.12281
ENSMUSP00000108098	59.9	poly (ADP-ribose) polymerase family, member 3 IPR012317 PARP catalyticIPR004102 PARP regIPR008893 WGR	525.4386
ENSMUSP00000111551	32.9	Translin-associated protein X (Translin-associated factor X) IPR002848 Translin	288.59649

sp|CAS2_BOVIN|	26	Alpha-S2-casein; Contains: Casocidin-1; Casocidin-I; Flags: Precursor;	228.07018
ENSMUSP00000007708:reversed	65.3		572.80702
ENSMUSP00000034391	71.6	Conserved oligomeric Golgi complex subunit 8 (COG complex subunit 8)(Component of oligomeric Golgi complex 8) IPR000276 7TM GPCR RhodpsnIPR016632 COG8IPR007255 Dor1	628.07018
ENSMUSP00000063548	56.4	4-aminobutyrate aminotransferase, mitochondrial Precursor (EC 2.6.1.19)(Gamma-amino-N-butyrate transaminase)(GABA transaminase)(GABA-T)(GABA aminotransferase)(GABA-AT)(L-AIBAT)((S)-3-amino-2-methylpropionate transaminase)(EC 2.6.1.22) Source: 2.6.1.19 IPR004631 4NH2But aminotransferase eukIPR005814 Aminotrans 3IPR015424 PyrdxlP-dep Trfase major	494.73684
ENSMUSP00000073102	34.2	Probable arylformamidase (EC 3.5.1.9)(Kynurenine formamidase)(KF) Source: 3.5.1.9	300
ENSMUSP00000073861	54.2	Threonine synthase-like 2 (TSH2)(mTSH2)(EC 4.2.3.-) Source: 4.2.3.- IPR001926 PyrdxlP-dep enz bsuIPR004450 Thr synthase	475.4386
ENSMUSP00000076093	392.5	utrophin IPR016024 ARM-type foldIPR001589 Actinin actin-bd CSIPR016146 Calponin-homologyIPR001715 Calponin act bdIPR016344 Dystrophin/utrophinIPR015153 EF-hand regn-1IPR015154 EF-hand regn-2IPR018159 Spectrin/alpha-actininIPR002017 Spectrin repeatIPR001202 WW Rsp5 WWPIPR000433 Znf ZZ	3442.9825
ENSMUSP00000078845:reversed	69.1		606.14035
ENSMUSP00000099420:reversed	57		500
ENSMUSP00000106953	11.3	Apolipoprotein A-II Precursor (Apo-AII)(ApoA-II) IPR006801 ApoA-II	99.122807
ENSMUSP00000043821	61.8	Delta-1-pyrroline-5-carboxylate dehydrogenase, mitochondrial Precursor (P5C dehydrogenase)(EC 1.5.1.12)(Aldehyde dehydrogenase family 4 member A1) Source: 1.5.1.12 IPR016161 Ald DHase/Histidinol DHaseIPR016160 Ald DHase CSIPR015590 Aldehyde DHaseIPR005931 d-1-pyrroline-5-COlate DHase-1	542.10526
ENSMUSP00000073459	40.6	Aflatoxin B1 aldehyde reductase member 2 (EC 1.-.-.-) Source: 1.-.-.- IPR001395 Aldo/ket red	356.14035
ENSMUSP00000028892	42.2	isocitrate dehydrogenase 3, beta subunit IPR004434 IsoCit DHase NAD mitIPR001804 IsoCit IM DHase	370.17544
ENSMUSP00000013773	243.1	carbamoyl-phosphate synthetase 2, aspartate transcarbamylase, and dihydroorotase IPR011761 ATP-graspIPR013651 ATP-grasp RimK-typeIPR003135 ATP-grasp carboxylate-amineIPR006680 Amidohydro 1IPR006220 Anth synthIIIPR006130 Asp/Orn carbamoylTrfaseIPR006132 Asp/Orn carbamoyltranf P bdIPR006131 Asp carbamoyltransf Asp/Orn bdIPR002082 Aspartate carbamoyltransf eukIPR001317 CarbamoylP synth GATaseIPR005483 CarbamoylP synth lsuIPR005479 CarbamoylP synth lsu ATP-bdIPR006275 CarbamoylP synth lsu Gln-depIPR005481 CarbamoylP synth lsu NIPR005480 CarbamoylP synth lsu oligoIPR006274 CarbamoylP synth ssuIPR002474 CarbamoylP synth ssu NIPR004722 DHOmultIPR002195 Dihydroorotase CSIPR011702 GATASEIPR000991 GATase class1 CIPR011607 MGSIPR011059 Metal-dep hydrolase compositeIPR000694 PRO richIPR016185 PreATP-grasp-like	2132.4561
ENSMUSP00000024944	78.1	solute carrier family 3, member 1 IPR006046 Glyco hydro 13IPR006047 Glyco hydro 13 catIPR006589 Glyco hydro 13 sub catIPR017853 Glyco hydro cat	685.08772
ENSMUSP00000076777	50.1	Tubulin alpha-1B chain (Tubulin alpha-2 chain)(Alpha-tubulin 2)(Alpha-tubulin isotype M-alpha-2) IPR002452 Alpha tubulinIPR002453 Beta tubulinIPR000158 Cell division FtsZ NIPR002967 Delta tubulinIPR004057 Epsilon tubulinIPR002454 Gamma tubulinIPR008280 Tub FtsZ CIPR000217 TubulinIPR018316 Tubulin/FtsZ 2-layer-sand-domIPR017975 Tubulin CSIPR003008 Tubulin FtsZ	439.47368
ENSMUSP00000047054	75.8	Dymeclin	664.91228
ENSMUSP00000077040	419.8	Vacuolar protein sorting-associated protein 13C IPR008374 SF assemblinIPR009543 VPSAP	3682.4561
ENSMUSP00000043220:reversed	81.3		713.15789
ENSMUSP00000038339	53.4	Mitochondrial antiviral-signaling protein (Interferon-beta promoter stimulator protein 1)(IPS-1)(Virus-induced-signaling adapter)(CARD adapter inducing interferon-beta)(Cardif)	468.42105
ENSMUSP00000022196	122.7	AP-3 complex subunit beta-1 (Adapter-related protein complex 3 subunit beta-1)(Adaptor protein complex AP-3 beta-1 subunit)(Beta3A-adaptin)(Clathrin assembly protein complex 3 beta-1 large chain) IPR017108 AP3 complex bsuIPR016024 ARM-type foldIPR002553 Clathrin/coatomer adapt-like N	1076.3158
ENSMUSP00000030742	40.3	Trans-2-enoyl-CoA reductase, mitochondrial Precursor (EC 1.3.1.38) Source: 1.3.1.38 IPR013154 AlcDHase GroES-	353.50877

		likeIPR013149 AlcDHase Zn-bdIPR011032 GroES likeIPR016040 NAD(P)-bd	
ENSMUSP00000054370	45.1	Isobutyryl-CoA dehydrogenase, mitochondrial Precursor (EC 1.3.99.-)(Acyl-CoA dehydrogenase family member 8)(ACAD-8) Source: 1.3.99.- IPR006091 Acyl-CoA DHase/Oxase MIPR013107 Acyl-CoA DHase 2 CIPR006089 Acyl-CoA DHase CSIPR006092 Acyl-CoA DHase NIPR006090 Acyl-CoA Oxase/DHase 1IPR009100 AcylCoA DH/oxidase M/NIPR009075 AcylCo DHase/oxidase C	395.61404
ENSMUSP00000007708	65.3	Serine/threonine-protein phosphatase 2A 65 kDa regulatory subunit A alpha isoform (PP2A, subunit A, PR65-alpha isoform)(PP2A, subunit A, R1-alpha isoform) IPR016024 ARM-type foldIPR000357 HEATIPR001160 Peptidase M20C	572.80702
ENSMUSP00000021698	84.7	Heat shock protein HSP 90-alpha (HSP 86)(Tumor-specific transplantation 86 kDa antigen)(TSTA) IPR003594 ATP bd ATPaseIPR001404 Hsp90	742.98246
ENSMUSP00000006137	80.2	Heat shock protein 75 kDa, mitochondrial Precursor (HSP 75)(Tumor necrosis factor type 1 receptor-associated protein)(TRAP-1)(TNFR-associated protein 1) IPR003594 ATP bd ATPaseIPR001404 Hsp90	703.50877
ENSMUSP00000027833	138.3	Coatomer subunit alpha (Alpha-coat protein)(Alpha-COP) IPR009033 Calreticulin/calnexin PIPR006692 Coatomer WD-assoc regIPR016391 Coatomer alpha subunitIPR010714 Coatomer asu CIPR011044 Quino amine DHase bsuIPR001680 WD40 repeatIPR011046 WD40 repeat-likeIPR017986 WD40 repeat region	1213.1579
ENSMUSP00000030454	22.2	Peroxiredoxin-1 (EC 1.11.1.15)(Thioredoxin peroxidase 2)(Thioredoxin-dependent peroxide reductase 2)(Osteoblast-specific factor 3)(OSF-3)(Macrophage 23 kDa stress protein) Source: 1.11.1.15 IPR000866 Alkyl hydroperoxide RdtaseIPR013740 RedoxinIPR012336 Thioredoxin-like fold	194.73684
ENSMUSP00000088249	56.8	Hydroxymethylglutaryl-CoA synthase, mitochondrial Precursor (HMG-CoA synthase)(EC 2.3.3.10)(3-hydroxy-3-methylglutaryl coenzyme A synthase) Source: 2.3.3.10 IPR000590 HMG CoA synt ASIPR013746 HMG CoA synt CIPR013528 HMG CoA synth NIPR010122 HMG CoA synthase eukIPR016039 Thiolase-like	498.24561
ENSMUSP00000076294	38.2	Poly(rC)-binding protein 2 (Alpha-CP2)(Putative heterogeneous nuclear ribonucleoprotein X)(hnRNP X)(CTBP)(CBP) IPR004087 KHIPR004088 KH type 1IPR018111 KH type 1 subgrIPR004044 KH type 2	335.08772
ENSMUSP00000025696	25.4	GTP:AMP phosphotransferase mitochondrial (EC 2.7.4.10)(Adenylate kinase 3)(AK 3)(Adenylate kinase 3 alpha-like 1) Source: 2.7.4.10 IPR006259 Adenyl kin subIPR000850 Adenylate kinIPR007862 Adenylate kinase Znf lidIPR000623 Shik kinase	222.80702
ENSMUSP00000050689	20.6	ADP-ribosylation factor 3 IPR006688 ARFIPR006689 ARF/SARIPR003579 GTPase RabIPR013684 Miro-likeIPR013753 RasIPR001806 Ras GTPaseIPR006687 SAR1 GTP bdIPR005225 Small GTP bd	180.70175
ENSMUSP00000054863	37.5	Poly(rC)-binding protein 1 (Alpha-CP1)(hnRNP-E1) IPR004087 KHIPR004088 KH type 1IPR018111 KH type 1 subgrIPR004044 KH type 2	328.94737
ENSMUSP00000082288	57.9	Methylmalonate-semialdehyde dehydrogenase Source: 1.2.1.27 IPR016161 Ald DHase/Histidinol DHaseIPR016160 Ald DHase CSIPR015590 Aldehyde DHaseIPR010061 MeMal-semiAld DHase	507.89474
ENSMUSP00000032473	47.5	Interferon-inducible GTPase 1 (EC 3.6.5.-) Source: 3.6.5.- IPR007743 Interferon-inducible GTPase	416.66667
ENSMUSP00000033185	51.3	Hemopexin Precursor IPR000585 HemopexinIPR018486 Hemopexin/matrixin CSIPR018487 Hemopexin/matrixin repeatIPR016358 Hemopexin chordata	450
ENSMUSP00000002389	89.7	Protein-glutamine gamma-glutamyltransferase K (EC 2.3.2.13)(Transglutaminase K)(TGase K)(TGK)(TG(K))(Transglutaminase-1)(Epidermal TGase) Source: 2.3.2.13 IPR001951 Histone H4IPR014756 Ig E-setIPR008958 Transglutaminase CIPR013808 Transglutaminase CSIPR001102 Transglutaminase NIPR002931 Trnsglumase like	786.84211
ENSMUSP00000101002	26.3	Guanidinoacetate N-methyltransferase (EC 2.1.1.2) Source: 2.1.1.2 IPR016550 GuanidinoAc N-MeTrfase	230.70175
ENSMUSP00000031105	22.4	Ubiquitin-conjugating enzyme E2 K (EC 6.3.2.19)(Ubiquitin-conjugating enzyme E2-25 kDa)(E2(25K))(Ubiquitin-protein ligase)(Ubiquitin carrier protein)(Huntingtin-interacting protein 2)(HIP-2) Source: 6.3.2.19 IPR000449 UBA/transl elong EF1B NIPR015940 UBA/transl elong EF1B N eukIPR009060 UBA likeIPR016135 UBQ-conjugat/RWD-likeIPR000608 UBQ-conjugat E2	196.49123
ENSMUSP00000024739	83.2	Heat shock protein HSP 90-beta (HSP 84)(Tumor-specific transplantation 84 kDa antigen)(TSTA) IPR003594 ATP bd ATPaseIPR001404 Hsp90	729.82456
ENSMUSP00000099904	46.6	Argininosuccinate synthase (EC 6.3.4.5)(Citrulline--aspartate ligase) Source: 6.3.4.5 IPR001518 Arginosuc synthIPR018223 Arginosuc synth CS	408.77193

ENSMUSP00000101833	43.4	Nucleolysin TIAR (TIA-1-related protein) IPR008111 RNA bd 8IPR003954 RRM 1IPR000504 RRM RNP1	380.70175
ENSMUSP00000039243	58.4	Sorting nexin-2 IPR001683 PXIPR005329 Sorting nexin NIPR015404 Vps5	512.2807
ENSMUSP00000086716	290	Probable ubiquitin carboxyl-terminal hydrolase FAF-X (EC 3.1.2.15)(Ubiquitin thioesterase FAF-X)(Ubiquitin-specific-processing protease FAF-X)(Deubiquitinating enzyme FAF-X)(Fat facets protein-related, X-linked)(Ubiquitin-specific protease 9, X chromosome)(Ubiquitin carboxyl-terminal hydrolase FAM)(Fat facets homolog) Source: 3.1.2.15 IPR017853 Glyco hydro catIPR018200 Pept C19ubi-hydrolase C CSIPR001394 Peptidase C19	2543.8596
ENSMUSP00000086626	117.7	Ubiquitin-like modifier-activating enzyme 1 (Ubiquitin-activating enzyme E1)(Ubiquitin-like modifier-activating enzyme 1 X)(Ubiquitin-activating enzyme E1 X) IPR009036 Molybdenum cofac synth MoeBIPR000594 ThiF NAD FAD bdIPR018075 UBQ-activ enz E1IPR000011 UBQ-activ enz E1IPR018074 UBQ-activ enz E1 ASIPR000127 UBact repeat	1032.4561
ENSMUSP00000099807	70.5	SUMO-activating enzyme subunit 2 (EC 6.3.2.-)(Ubiquitin-like 1-activating enzyme E1B)(Anthracycline-associated resistance ARX) Source: 6.3.2.- IPR009036 Molybdenum cofac synth MoeBIPR000594 ThiF NAD FAD bdIPR018074 UBQ-activ enz E1 ASIPR000127 UBact repeat	618.42105
ENSMUSP00000027144	164.5	Carbamoyl-phosphate synthase Source: 6.3.4.16 IPR011761 ATP-graspIPR003135 ATP-grasp carboxylate-amineIPR001317 CarbamoylP synth GATaseIPR005483 CarbamoylP synth lsuIPR005479 CarbamoylP synth lsu ATP-bdIPR006275 CarbamoylP synth lsu Gln-depIPR005481 CarbamoylP synth lsu NIPR005480 CarbamoylP synth lsu oligoIPR006274 CarbamoylP synth ssuIPR002474 CarbamoylP synth ssu NIPR011702 GATASEIPR000991 GATase class1 CIPR011607 MGSIPR016185 PreATP-grasp-like	1442.9825
ENSMUSP00000071135	49.6	Tubulin beta-4 chain IPR002452 Alpha tubulinIPR013838 Beta-tubulin BSIPR002453 Beta tubulinIPR000158 Cell division FtsZ NIPR002967 Delta tubulinIPR004057 Epsilon tubulinIPR002454 Gamma tubulinIPR008280 Tub FtsZ CIPR000217 TubulinIPR018316 Tubulin/FtsZ 2-layer-sand-domIPR017975 Tubulin CSIPR003008 Tubulin FtsZ	435.08772
ENSMUSP00000110006:reversed	147.8		1296.4912
ENSMUSP00000105647	49.3	Legumain Precursor (EC 3.4.22.34)(Asparaginyl endopeptidase)(Protease, cysteine 1) Source: 3.4.22.34 IPR001096 Peptidase C13	432.45614
ENSMUSP00000095316	46.6	Isocitrate dehydrogenase Source: 1.1.1.42 IPR004790 IsoCit DHase NADP-dep eukIPR001804 IsoCit IM DHase	408.77193
ENSMUSP00000042457	50.1	Elongation factor 1-alpha 1 (EF-1-alpha-1)(Elongation factor 1 A-1)(eEF1A-1)(Elongation factor Tu)(EF-Tu) IPR000795 ProtSyn GTP bdIPR009001 Transl elong EF1A/Init IF2 CIPR004539 Transl elong EF1A euk/arcIPR004161 Transl elong EFTu/EF1A 2IPR004160 Transl elong EFTu/EF1A C	439.47368
ENSMUSP00000042342	49.8	Tubulin beta-2C chain IPR002452 Alpha tubulinIPR013838 Beta-tubulin BSIPR002453 Beta tubulinIPR000158 Cell division FtsZ NIPR002967 Delta tubulinIPR004057 Epsilon tubulinIPR002454 Gamma tubulinIPR008280 Tub FtsZ CIPR000217 TubulinIPR018316 Tubulin/FtsZ 2-layer-sand-domIPR017975 Tubulin CSIPR003008 Tubulin FtsZ	436.84211
ENSMUSP00000034818	39.6	Isocitrate dehydrogenase Source: 1.1.1.41 IPR004434 IsoCit DHase NAD mitIPR001804 IsoCit IM DHase	347.36842
ENSMUSP00000044556	59.7	Dihydroxyacetone kinase (DHA kinase)(EC 2.7.1.29)(Glycerone kinase) Source: 2.7.1.29 IPR004006 Dak1IPR004007 Dak2IPR012734 DhaK ATP	523.68421
ENSMUSP00000097469	56.2	EH domain-containing protein 1 (mPAST1) IPR001401 Dynamin GTPaseIPR002917 MMR HSR1 GTP bd	492.98246
ENSMUSP00000031103	54.8	UDP-glucose 6-dehydrogenase (UDP-Glc dehydrogenase)(UDP-GlcDH)(UDPGDH)(EC 1.1.1.22) Source: 1.1.1.22 IPR016040 NAD(P)-bdIPR014027 UDP-Glc/GDP-Man DHase CIPR001732 UDP-Glc/GDP-Man DHase NIPR014026 UDP-Glc/GDP-Man DHase dimer	480.70175
ENSMUSP00000021114	42.3	Galactokinase (EC 2.7.1.6)(Galactose kinase) Source: 2.7.1.6 IPR006204 GHMP kinaseIPR013750 GHMP kinase CIPR006203 GHMP knse ATP bd CSIPR000705 GalactokinaseIPR001174 GalkinaseIPR006206 Mev galkinase	371.05263
ENSMUSP00000020286	32.6	Inorganic pyrophosphatase (EC 3.6.1.1)(Pyrophosphate phospho-hydrolase)(PPase) Source: 3.6.1.1 IPR008162 Pyrophosphatase	285.96491
ENSMUSP00000060246	49.9	Tubulin beta-2A chain IPR002452 Alpha tubulinIPR013838 Beta-tubulin BSIPR002453 Beta tubulinIPR000158 Cell division FtsZ NIPR002967 Delta tubulinIPR004057 Epsilon tubulinIPR002454 Gamma tubulinIPR008280 Tub FtsZ CIPR000217 TubulinIPR018316 Tubulin/FtsZ 2-layer-sand-domIPR017975 Tubulin CSIPR003008 Tubulin FtsZ	437.7193
ENSMUSP00000050292	18.7	Prostaglandin E synthase 3 (EC 5.3.99.3)(Cytosolic prostaglandin E2 synthase)(cPGES)(Telomerase-binding protein p23)(Hsp90 co-chaperone)(Progesterone receptor complex p23)(Sid 3177) Source: 5.3.99.3 IPR017447 CSIPR007052 CS domainIPR008978 HSP20-like chaperone	164.03509

ENSMUSP00000027824	26.2	Serum amyloid P-component Precursor (SAP) IPR008985 ConA like lec glIPR001759 Pentaxin	229.82456
ENSMUSP00000108734	23.2	5, 10-methenyltetrahydrofolate synthetase-like IPR002698 FTHF cligase	203.50877
ENSMUSP00000068086	51.8	Probable D-lactate dehydrogenase, mitochondrial Precursor (Lactate dehydrogenase D)(DLD)(EC 1.1.2.4) Source: 1.1.2.4 IPR016166 FAD-bd 2IPR016164 FAD-linked Oxase-like CIPR004113 FAD-linked oxidase CIPR006094 Oxid FAD bind N	454.38596
ENSMUSP00000034808	29.6	Nicotinamide N-methyltransferase (EC 2.1.1.1) Source: 2.1.1.1 IPR000940 NNMT TEMT trans	259.64912
ENSMUSP00000030187	269.7	Talin-1 IPR000299 Band 4.1 NIPR009065 FERM 3-hlxIPR002558 ILWEQIPR000159 Ras-assocIPR015224 Talin centIPR015009 VBS bdIPR006077 Vinculin/catenin	2365.7895
ENSMUSP00000026168	113	MMS19 nucleotide excision repair protein homolog (MMS19-like protein)(MET18 homolog) IPR016024 ARM-type foldIPR000357 HEATIPR002016 Haem peroxidase pln/fun/bac	991.22807
ENSMUSP00000102254	42.3	Alpha-parvin (Actopaxin) IPR016146 Calponin-homologyIPR001715 Calponin act bd	371.05263
ENSMUSP00000026012	57.6	Cytochrome P450 17A1 (EC 1.14.99.9)(CYPXVII)(P450-C17)(P450c17)(Steroid 17-alpha-hydroxylase/17,20 lyase) Source: 1.14.99.9 IPR001128 Cyt P450IPR002397 Cyt P450 BIPR017973 Cyt P450 CIPR017972 Cyt P450 CSIPR002401 Cyt P450 E grp-IIPR002403 Cyt P450 E grp-IVIPR008069 Cyt P450 E grp-I CYP2D-like	505.26316
ENSMUSP00000064849	34.6	L-serine dehydratase (EC 4.3.1.17)(L-serine deaminase) Source: 4.3.1.17 IPR001926 PyrdxlP-dep enz bsuIPR000634 Ser/Thr deHydtase PyrdxlP-BS	303.50877
ENSMUSP00000101862	51.5	Adenylyl cyclase-associated protein 1 (CAP 1) IPR013912 Adenylate cyclase-assoc CAP CIPR013992 Adenylate cyclase-assoc CAP NIPR018106 CAP CSIPR006599 CARP motifIPR000694 PRO rich	451.75439
ENSMUSP00000047761	55.3	Glycerate kinase (EC 2.7.1.31) Source: 2.7.1.31 IPR007835 MOFRL	485.08772
ENSMUSP00000020034	35.4	Enoyl-CoA hydratase domain-containing protein 1 IPR001753 Crotonase coreIPR018376 Enoyl-CoA hyd/isom CS	310.52632
ENSMUSP00000070682	49	Spliceosome RNA helicase Bat1 (EC 3.6.1.-)(DEAD box protein UAP56)(56 kDa U2AF65-associated protein)(HLA-B-associated transcript 1) Source: 3.6.1.- IPR014001 DEAD-like NIPR001650 DNA/RNA helicase CIPR011545 DNA/RNA helicase DEAD/DEAH NIPR014021 Helicase SF1/SF2 ATP-bdIPR014014 RNA helicase DEAD Q motif	429.82456
ENSMUSP00000036337	28	Haloacid dehalogenase-like hydrolase domain-containing protein 3 IPR005834 Dehalogen-like hydroIPR011949 HAD-SF hydro IA REG-2-likeIPR006439 HAD-SF hydro IA v1IPR005833 Haloacid DHase/epoxide hydro	245.61404
ENSMUSP00000024860	60.8	EH domain-containing protein 3 IPR001401 Dynamin GTPaseIPR018247 EF HAND 1IPR018249 EF HAND 2IPR002048 EF hand Ca bdIPR000261 EPS15 homology	533.33333
ENSMUSP00000051366	57.6	FAD synthetase (EC 2.7.7.2)(FMN adenylyltransferase)(FAD pyrophosphorylase)(Flavin adenine dinucleotide synthetase) Source: 2.7.7.2 IPR012183 FAD synth Mopterin-bdIPR001453 Mopterin bdIPR002500 PAPS reduct	505.26316
ENSMUSP00000110576	49.5	Zinc finger and BTB domain-containing protein 9 IPR000210 BTB/POZ-likeIPR011333 BTB/POZ foldIPR013069 BTB POZIPR003072 NOR1 rcptIPR007087 Znf C2H2IPR015880 Znf C2H2-like	434.21053
ENSMUSP00000052174:reversed	55.9		490.35088
ENSMUSP00000099403	83.1	Signal transducer and activator of transcription 3 (Acute-phase response factor) IPR013289 ETOIPR000980 SH2IPR013801 STAT TF DNA-bdIPR013800 STAT TF alphaIPR015988 STAT TF coiled-coilIPR013799 STAT TF prot interactionIPR008967 p53 like TF DNA-bd	728.94737
ENSMUSP00000022369	116.6	Vinculin (Metavinculin) IPR000694 PRO richIPR017997 VinculinIPR006077 Vinculin/cateninIPR000633 Vinculin CS	1022.807
ENSMUSP00000044554	77.8	Fermitin family homolog 2 (Pleckstrin homology domain-containing family C member 1)(Kindlin-2) IPR000299 Band 4.1 NIPR009065 FERM 3-hlxIPR001849 Pleckstrin homology	682.45614
ENSMUSP00000021506	46.7	Serine protease inhibitor A3N Precursor (Serpin A3N) IPR000295 Prot inh Lserp2IPR000215 Protease inhib I4 serpin	409.64912
ENSMUSP00000108953	62.2	UDP-glucuronosyltransferase 2B5 Precursor (UDPGT 2B5)(EC 2.4.1.17)(M-1) Source: 2.4.1.17 IPR002213 UDP glucos trans	545.61404
ENSMUSP00000035823	112.6	SEC24 related gene family, member D IPR007123 GelsolnIPR000694 PRO richIPR012990 Sec23 24 beta SIPR006900 Sec23 helicalIPR006896 Sec23 trunkIPR006895 Znf Sec23 Sec24	987.7193

Supplementary Table 8
(continued)
Protein identifications from control, non-cachectic and cachectic mouse liver membrane preparations

Identifier: ENSEMBL number
cachectic/control/nc (1-3): number of nonredundant peptides
LogNSAF: log of the average NSAF
n.b. NSAF=(Spc/L)/Σ(Spc/L)
Spc: spectral counts L: length of the protein

Identifier	cachectic_3.csv	cachectic_2.csv	cachectic_1.csv	control_1.csv	control_2.csv	control_3.csv	nc_1.csv	nc_2.csv	nc_3.csv	Log.NSAF.cachectic	Log.NSAF.control	Log.NSAF.nc
ENSMUSP00000068282	0	0	0	186	185	163	0	0	143	-11.06014	-5.420473	-6.762545
ENSMUSP00000071573	0	0	0	157	126	120	79	101	68	-10.5277	-5.168587	-5.683907
ENSMUSP00000037665	0	0	0	210	220	166	89	83	102	-11.00954	-5.260317	-6.066614
ENSMUSP00000072598	0	0	0	123	128	99	0	79	92	-11.06179	-5.843114	-6.587063
ENSMUSP00000031633	0	0	0	89	91	66	0	0	0	-11.00954	-6.141677	-11.28415
ENSMUSP00000052945	0	0	0	6	5	5	2	2	3	-12.05729	-9.838983	-10.59364
ENSMUSP00000033086	0	0	0	2	2	2	1	0	0	-10.79201	-9.421507	-10.55401
ENSMUSP00000034173	0	0	0	21	16	21	9	7	9	-11.07159	-7.629244	-8.470332
ENSMUSP00000020266	0	0	0	5	5	4	0	0	2	-10.41829	-8.321396	-9.843062
ENSMUSP00000102636	0	0	0	28	25	17	0	0	0	-10.68784	-7.061753	-10.96245
ENSMUSP00000023709	0	0	0	34	57	45	44	0	39	-11.07484	-6.79478	-7.3138
ENSMUSP00000004478	0	0	0	1	1	1	0	0	0	-11.44007	-10.58098	-11.71467
ENSMUSP00000017597	0	0	0	1	1	1	1	0	3	-10.73219	-9.873106	-9.704283
ENSMUSP00000004396	0	0	0	1	1	1	0	0	0	-9.547809	-8.688726	-9.822418
ENSMUSP00000094929	0	0	0	1	1	1	0	0	0	-11.36898	-10.5099	-11.64359

ENSMUSP00000077972	0	0	0	1	1	1	0	0	0	-10.92285	-10.06376	-11.19745
ENSMUSP00000072558	0	0	0	24	44	26	0	0	0	-9.743719	-5.82818	-10.01833
ENSMUSP00000099436	0	0	0	5	5	7	3	4	3	-10.08369	-7.809797	-8.317556
ENSMUSP00000066990	0	0	0	3	4	3	0	0	3	-9.313408	-7.515156	-8.486443
ENSMUSP00000001497	0	0	0	3	4	3	0	0	0	-10.1634	-8.365146	-10.43801
ENSMUSP00000103034	0	0	0	22	39	21	0	20	15	-10.85453	-7.073277	-7.933031
ENSMUSP00000034046	121	120	124	258	264	246	179	183	217	-5.805026	-5.305765	-5.619736
ENSMUSP00000057069	0	0	0	3	3	2	0	2	0	-11.55872	-9.951649	-10.9835
ENSMUSP00000044012	0	0	0	3	3	2	0	0	3	-12.11276	-10.50568	-11.28579
ENSMUSP00000018727	0	0	0	3	2	2	0	0	0	-10.89994	-9.404177	-11.17455
sp|K1C15_SHEEP|	0	0	0	28	74	52	42	0	46	-10.83823	-6.435148	-7.019703
ENSMUSP00000032074	0	0	0	3	2	3	0	0	0	-10.19905	-8.59197	-10.47365
ENSMUSP00000039784	0	0	0	7	4	4	2	0	0	-9.791633	-7.632192	-9.216404
ENSMUSP00000029387	0	0	0	2	3	3	1	0	0	-11.11767	-9.510593	-10.87967
ENSMUSP00000040580	0	0	0	4	3	2	2	0	0	-10.58486	-8.877638	-10.00963
ENSMUSP00000073444	92	89	103	206	204	179	113	161	156	-5.793706	-5.309458	-5.655281
ENSMUSP00000059943	0	0	0	4	2	3	0	0	0	-9.09262	-7.385395	-9.367229
ENSMUSP00000034860	22	29	39	299	257	204	59	89	89	-6.899479	-5.022956	-6.216013
ENSMUSP00000089691	25	24	29	60	54	51	42	63	34	-6.558644	-6.061853	-6.263766
ENSMUSP00000026462	80	71	89	230	209	177	119	138	98	-5.453031	-4.756696	-5.338166
ENSMUSP00000074990	89	81	92	207	207	169	52	49	69	-5.806688	-5.252462	-6.51078
ENSMUSP00000081370	21	20	18	99	86	65	16	24	14	-7.316649	-6.134257	-7.677527
ENSMUSP00000003100	83	87	117	326	286	301	175	170	189	-5.712472	-4.801266	-5.368565
ENSMUSP00000082352	4	4	6	21	25	19	9	17	9	-8.17137	-6.957171	-7.58926
ENSMUSP00000029569	0	0	0	4	2	2	1	0	0	-10.53607	-8.928998	-10.29808

sp|K1C10_HUMAN|	156	137	150	286	311	331	311	324	266	-5.342621	-4.847408	-4.909004
ENSMUSP00000065796	26	25	19	78	73	83	16	0	30	-7.111111	-6.161525	-7.794735
ENSMUSP00000031195	21	21	31	80	87	73	23	24	31	-7.155382	-6.221741	-7.365027
ENSMUSP00000057732	68	70	77	163	134	137	87	102	79	-5.551171	-5.094743	-5.606796
ENSMUSP00000034567	4	4	4	13	11	16	11	12	11	-8.969419	-8.088574	-8.276879
ENSMUSP00000023832	5	6	5	27	19	31	10	14	5	-8.000315	-6.741613	-7.719236
ENSMUSP00000026398	23	24	33	81	72	69	47	67	55	-6.285263	-5.518894	-5.821697
ENSMUSP00000028807	0	0	0	3	2	5	0	2	0	-10.7877	-8.989444	-10.21247
ENSMUSP00000045351	0	0	0	2	2	1	0	0	0	-10.86057	-9.633307	-11.13518
ENSMUSP00000002840	0	0	0	2	2	1	0	0	0	-11.60174	-10.37448	-11.87635
ENSMUSP00000047551	19	20	11	138	155	97	47	0	0	-7.37294	-5.586916	-7.707575
ENSMUSP00000066958	0	0	0	3	5	9	4	4	1	-11.16468	-8.890788	-9.489574
ENSMUSP00000030299	29	30	31	95	91	66	21	24	30	-6.892571	-6.115991	-7.346242
ENSMUSP00000004381	5	4	5	11	9	11	3	7	3	-8.640305	-8.142172	-8.981634
ENSMUSP00000027478	6	6	5	16	16	21	6	5	5	-8.139937	-7.301761	-8.470136
ENSMUSP00000043061	0	0	0	2	1	1	0	0	0	-10.45209	-9.392065	-10.7267
ENSMUSP00000042095	0	0	0	2	1	1	0	0	0	-10.79415	-9.734133	-11.06876
ENSMUSP00000065425	0	0	0	2	1	1	3	0	1	-10.55805	-9.49803	-9.530147
ENSMUSP00000061851	19	23	26	68	85	61	34	30	38	-6.97728	-6.088073	-6.853613
ENSMUSP00000001834	5	6	5	18	14	20	7	3	4	-8.502722	-7.627477	-8.89874
ENSMUSP00000032078	12	7	8	29	30	27	29	26	35	-8.091565	-7.212164	-7.199578
ENSMUSP00000035417	0	0	0	7	4	2	9	0	9	-11.08291	-9.052736	-8.78847
ENSMUSP00000025279	0	0	0	2	4	6	0	0	0	-11.914	-9.955319	-12.18861
ENSMUSP00000021370	0	0	0	1	2	2	2	1	1	-10.88242	-9.655155	-9.854512
ENSMUSP00000024963	0	0	0	1	2	2	0	0	0	-9.737565	-	-10.01217

											8.510303	
ENSMUSP00000000394	0	0	0	1	2	2	1	1	1	-11.22225	-9.994989	-10.39529
ENSMUSP00000001183	23	20	13	73	76	75	53	56	96	-7.377752	-6.253622	-6.373762
ENSMUSP00000034624	3	1	4	24	41	29	4	7	6	-8.931629	-6.865656	-8.539419
ENSMUSP00000041442	0	1	0	16	10	10	2	0	0	-10.17524	-7.707194	-10.11261
ENSMUSP00000086530	112	117	158	374	397	297	206	238	265	-5.432599	-4.662427	-5.103524
ENSMUSP00000051293	3	4	3	10	14	13	0	0	0	-9.231962	-8.265737	-11.54731
ENSMUSP00000086528	143	133	163	332	311	253	196	206	232	-5.305221	-4.836002	-5.213323
ENSMUSP00000022976	0	0	0	1	2	1	0	0	0	-11.85039	-10.79037	-12.125
ENSMUSP00000051621	0	0	0	1	2	1	0	2	0	-9.640402	-8.58038	-9.065173
sp|K1C9_HUMAN|	66	51	64	171	281	179	166	142	171	-6.275612	-5.275148	-5.582121
ENSMUSP00000101999	0	0	1	12	6	7	0	1	0	-10.1871	-8.066326	-10.46171
ENSMUSP00000034414	0	0	0	3	2	1	0	0	0	-10.5079	-9.137403	-10.78251
ENSMUSP00000051441	0	0	0	3	2	1	0	0	0	-10.89801	-9.527513	-11.17262
ENSMUSP00000029240	5	2	3	15	26	23	11	3	12	-8.953106	-7.455418	-8.35554
ENSMUSP00000034623	0	0	0	1	1	2	0	0	0	-10.14714	-9.087115	-10.42175
ENSMUSP00000111510	0	0	0	1	1	2	1	0	1	-11.05354	-9.993521	-10.47831
sp|K2C1_HUMAN|	164	116	142	330	433	318	348	307	364	-5.491662	-4.795669	-4.886767
ENSMUSP00000086418	10	9	10	23	33	38	27	27	27	-8.03706	-7.138004	-7.31646
ENSMUSP00000025713	3	3	3	12	12	7	1	0	0	-8.84229	-7.954488	-10.55401
ENSMUSP00000017946	0	0	0	2	1	3	0	0	0	-10.89608	-9.525576	-11.17068
ENSMUSP00000051700	15	20	21	44	56	52	13	16	0	-7.692649	-6.953153	-8.601418
ENSMUSP00000034848	0	0	0	3	3	1	2	1	0	-10.33694	-8.841178	-9.509979
ENSMUSP00000047790	25	15	34	108	181	104	95	92	96	-6.190782	-4.779716	-5.138725
ENSMUSP00000097860	0	0	2	15	58	53	6	3	5	-11.3182	-7.963486	-10.10326

ENSMUSP00000034172	19	23	17	78	69	47	29	26	35	-7.37333	-6.442829	-7.234206
ENSMUSP00000041244	0	0	0	3	1	3	4	2	1	-10.10529	-8.609523	-8.64164
ENSMUSP00000040424	1	2	3	12	11	9	3	0	8	-9.650362	-8.395524	-9.413791
ENSMUSP00000005923	0	1	1	10	8	8	3	4	4	-9.473455	-7.652865	-8.47373
ENSMUSP00000031181	26	33	24	73	81	63	22	32	36	-7.024497	-6.316906	-7.219512
ENSMUSP00000027464	0	0	0	1	3	2	1	0	0	-10.5769	-9.206396	-10.3389
ENSMUSP00000003843	0	0	0	1	3	2	0	0	1	-11.24575	-9.87525	-11.00775
ENSMUSP00000104806	0	0	0	1	2	3	0	0	0	-11.70873	-10.33823	-11.98334
ENSMUSP00000107118	0	0	1	9	4	8	1	3	1	-9.549011	-7.591912	-8.86647
ENSMUSP00000076578	0	0	0	4	10	2	0	0	0	-10.97433	-8.756024	-11.24894
ENSMUSP00000023083	94	99	107	231	215	167	88	104	92	-5.677301	-5.207743	-6.006439
ENSMUSP00000026208	0	1	0	5	9	8	0	0	0	-11.5967	-9.596108	-12.38392
ENSMUSP00000034178	10	20	15	65	50	76	14	33	22	-7.634932	-6.456672	-7.493332
ENSMUSP00000025356	0	1	0	6	8	5	0	1	1	-9.389639	-7.525659	-9.327014
ENSMUSP00000014913	1	1	0	7	9	10	3	7	6	-9.376081	-7.555491	-8.039732
ENSMUSP00000025196	0	0	0	3	4	1	0	0	1	-10.3604	-8.753321	-10.1224
ENSMUSP00000084445	0	0	0	4	1	3	1	0	0	-9.779868	-8.172793	-9.541873
ENSMUSP00000080996	0	0	0	4	2	1	0	0	0	-10.17542	-8.679655	-10.45003
ENSMUSP00000072555	187	191	235	423	429	339	284	300	356	-4.979336	-4.558824	-4.827275
ENSMUSP00000109355	0	0	0	3	1	4	0	0	0	-11.11144	-9.504362	-11.38605
ENSMUSP00000028657	1	1	4	16	11	15	2	12	8	-9.03094	-7.51484	-8.162847
ENSMUSP00000031251	9	6	12	39	47	24	11	14	9	-7.497382	-6.375579	-7.552316
ENSMUSP00000022148	0	2	1	23	11	17	15	6	10	-9.96676	-7.751165	-8.262933
ENSMUSP00000073061	31	29	52	99	118	93	69	76	102	-5.699148	-4.932006	-5.190085
ENSMUSP00000037022	2	2	10	36	43	39	12	15	9	-8.92128	-7.120922	-8.312136

ENSMUSP00000075235	0	0	2	9	12	21	2	2	2	-10.28629	-8.007039	-9.797748
ENSMUSP00000055206	0	0	0	1	3	4	0	0	0	-11.33832	-9.731249	-11.61293
ENSMUSP00000112236	14	8	13	32	26	37	34	29	28	-7.325983	-6.59613	-6.670585
ENSMUSP00000032422	0	0	1	4	5	3	1	0	0	-10.26205	-8.815972	-10.53666
ENSMUSP00000037259	20	37	44	127	123	103	46	60	79	-6.816459	-5.818058	-6.49247
ENSMUSP00000056152	17	10	11	35	29	28	18	26	18	-7.358799	-6.739532	-7.158605
ENSMUSP00000076735	83	83	94	169	137	134	0	118	81	-5.367908	-5.086646	-5.908145
ENSMUSP00000028083	0	0	0	5	1	4	0	0	0	-10.35041	-8.552161	-10.62502
ENSMUSP00000022341	0	0	0	1	4	4	0	0	0	-10.28832	-8.581099	-10.56293
ENSMUSP00000003137	190	165	202	458	441	303	226	306	265	-5.048317	-4.523068	-4.965442
ENSMUSP00000046585	78	89	91	189	191	140	110	89	112	-6.12821	-5.672736	-6.216967
ENSMUSP00000002663	20	29	15	61	68	64	21	35	30	-6.847932	-6.001974	-6.832926
ENSMUSP00000108763	82	83	101	178	153	138	88	121	121	-5.867129	-5.544933	-5.927224
ENSMUSP00000084959	0	1	1	9	5	16	2	6	0	-9.658065	-7.701643	-8.932945
ENSMUSP00000030051	0	0	0	1	3	5	2	4	1	-9.412143	-7.704918	-7.948493
ENSMUSP00000010049	0	0	0	4	6	1	0	0	0	-10.53329	-8.651612	-10.8079
ENSMUSP00000008801	4	8	5	22	24	15	6	5	2	-8.550316	-7.575158	-9.068646
ENSMUSP00000036245	2	0	0	10	8	7	6	3	7	-9.818725	-8.035186	-8.482376
ENSMUSP00000031183	21	35	47	101	113	102	53	70	66	-6.800466	-5.931624	-6.474581
ENSMUSP00000039543	0	0	0	2	1	5	0	0	0	-10.38976	-8.782687	-10.66437
ENSMUSP00000031822	0	1	0	3	7	9	2	1	0	-10.73041	-8.86643	-10.41605
ENSMUSP00000079065	63	63	93	246	230	138	58	127	85	-5.977693	-5.193628	-6.044231
ENSMUSP00000042188	0	0	0	1	5	2	0	0	0	-11.5001	-9.89302	-11.7747
ENSMUSP00000053877	2	1	1	4	10	9	0	2	2	-10.50051	-9.248136	-10.77512
ENSMUSP00000025602	1	1	1	2	3	3	0	4	2	-9.576674	-9.071173	-9.339865

ENSMUSP00000032399	1	0	1	4	6	4	2	2	1	-9.17077	-7.923713	-8.825462
ENSMUSP00000039663	0	1	0	4	3	6	0	0	5	-11.01672	-9.499152	-10.33418
ENSMUSP00000000349	14	20	14	53	34	62	23	25	14	-7.4258	-6.556211	-7.451312
ENSMUSP00000085244	1	2	6	14	23	22	5	5	2	-9.943051	-8.433751	-9.966204
ENSMUSP00000099848:reversed	0	1	0	4	3	7	4	8	6	-11.15398	-9.569685	-9.37214
ENSMUSP00000022317	6	6	10	16	16	16	4	3	7	-7.391446	-6.888816	-8.082361
ENSMUSP00000073939	3	7	4	18	13	18	5	12	3	-7.832045	-6.893106	-7.779321
ENSMUSP00000099770	16	9	16	29	48	40	15	4	8	-8.592622	-7.809604	-9.266907
ENSMUSP00000103436	0	0	1	3	8	3	0	0	0	-11.57044	-9.98615	-12.35765
ENSMUSP00000048832	10	13	11	24	23	19	5	10	8	-6.838236	-6.438044	-7.483788
ENSMUSP00000092966	0	5	1	29	30	18	4	2	4	-9.448796	-7.342291	-9.295653
ENSMUSP00000105754	1	0	1	8	5	3	0	0	0	-9.663763	-8.295296	-10.78821
ENSMUSP00000033074	4	2	2	8	6	8	6	5	11	-7.982186	-7.318552	-7.350669
ENSMUSP00000109150	48	75	116	249	199	265	70	91	54	-6.461959	-5.615569	-6.8417
ENSMUSP00000101096	1	0	0	4	3	2	1	1	2	-10.16081	-8.966192	-9.645512
ENSMUSP00000002844	1	0	0	3	4	2	0	3	1	-9.945508	-8.750887	-9.430207
ENSMUSP00000017365	0	2	4	18	23	20	21	16	12	-9.445507	-7.566955	-7.812291
sp|K22E_HUMAN|	59	70	87	131	211	177	200	167	172	-6.158032	-5.527914	-5.522326
ENSMUSP00000007977	1	4	4	18	12	13	19	22	14	-9.441953	-8.239847	-8.033181
ENSMUSP00000088246	3	7	12	39	34	24	7	13	9	-7.934532	-6.743752	-7.948349
ENSMUSP00000097395	0	0	1	2	3	4	0	1	0	-9.526437	-8.331816	-9.801046
ENSMUSP00000023519	2	6	6	23	23	14	5	3	3	-8.52319	-7.387163	-9.013013
ENSMUSP00000102665	141	116	185	298	253	261	148	154	132	-5.353242	-4.989078	-5.646054
ENSMUSP00000075089	0	0	0	1	4	1	0	1	0	-11.77203	-10.40153	-11.53403
ENSMUSP00000025804	9	11	13	24	23	18	10	18	12	-6.912906	-	-7.002748

											6.499062	
ENSMUSP00000056643	3	4	8	15	19	13	0	11	0	-7.699076	-6.863098	-8.251445
ENSMUSP00000072803	94	106	117	193	170	159	120	181	162	-5.684323	-5.429892	-5.581586
ENSMUSP00000052872	77	60	91	183	124	197	416	357	468	-7.52461	-6.977441	-6.110218
ENSMUSP00000093390	2	3	3	20	6	13	5	2	3	-8.652605	-7.444551	-8.736037
ENSMUSP00000037487	27	22	65	115	106	146	31	37	27	-6.671683	-5.753965	-7.12603
ENSMUSP00000045362	62	69	88	199	207	119	0	115	80	-5.975896	-5.348016	-6.365743
ENSMUSP00000031492	0	0	4	11	15	11	0	0	8	-8.785535	-7.08108	-8.513091
ENSMUSP00000046497	1	0	0	2	6	3	0	4	0	-10.55736	-9.188284	-10.04206
ENSMUSP00000048096	3	1	6	13	14	28	4	4	1	-9.883012	-8.53315	-10.24865
ENSMUSP00000004910	0	0	1	3	2	2	1	0	0	-10.10094	-9.117782	-10.37555
ENSMUSP00000045285	0	0	0	1	8	2	0	0	1	-12.20901	-10.32733	-11.97101
ENSMUSP00000021412	0	0	2	6	5	4	3	2	2	-9.41326	-8.103657	-8.799447
ENSMUSP00000032228	0	3	1	7	14	15	0	0	0	-10.7572	-9.079065	-12.33432
ENSMUSP00000104358	0	0	1	2	2	3	0	0	0	-9.9425	-8.959337	-10.72971
ENSMUSP00000038763	2	5	4	19	9	12	8	3	4	-9.209159	-8.251314	-9.206007
ENSMUSP00000033683	55	48	77	112	105	104	76	59	49	-5.540135	-5.207763	-5.792944
ENSMUSP00000031186	2	1	13	41	36	24	15	19	20	-8.592748	-7.067263	-7.712914
ENSMUSP00000021273	0	0	1	2	4	2	2	2	2	-8.981552	-7.887081	-8.155774
ENSMUSP00000032419	0	0	0	1	1	5	0	0	0	-10.82376	-9.327988	-11.09836
ENSMUSP00000016031	0	0	3	5	11	9	3	5	1	-10.13042	-8.598618	-9.556886
ENSMUSP00000090727	0	0	3	8	12	5	0	8	0	-9.012227	-7.480424	-8.538843
ENSMUSP00000059404	0	2	0	7	4	5	0	2	0	-9.655204	-8.286737	-9.929813
ENSMUSP00000031377	5	5	2	11	11	15	4	6	6	-8.740367	-7.93457	-8.755352
ENSMUSP00000043424	5	12	7	20	36	22	16	11	10	-8.584513	-7.689749	-8.447053
ENSMUSP00000044877	1	0	0	2	2	2	0	0	0	-9.027715	-	-9.814927

											8.169819	
ENSMUSP00000048284	99	96	125	247	249	155	64	146	105	-5.602377	-5.137044	-5.89266
ENSMUSP00000022268	11	6	6	35	14	36	13	8	8	-7.816172	-6.796998	-7.871674
ENSMUSP00000108422	39	36	38	81	54	62	40	34	25	-6.121619	-5.813872	-6.526653
ENSMUSP00000029076	6	0	5	38	40	22	23	20	17	-8.205971	-6.353666	-6.886847
ENSMUSP00000035458	5	9	20	30	46	48	13	10	12	-8.994813	-7.974397	-9.241637
ENSMUSP00000003038	24	29	32	50	51	74	19	38	34	-7.537903	-7.067179	-7.745443
ENSMUSP00000025549	35	7	23	130	105	56	108	92	103	-5.877773	-4.638925	-4.630835
ENSMUSP00000022946	1	0	1	5	2	5	2	5	5	-8.755959	-7.647116	-7.679233
ENSMUSP00000023712	19	0	0	60	82	44	0	58	62	-8.59475	-6.623599	-7.0896
ENSMUSP00000024823	1	0	0	2	2	6	2	1	5	-9.474903	-8.189255	-8.412549
ENSMUSP00000026427	5	2	3	7	9	8	0	1	2	-9.711725	-9.157568	-10.9255
ENSMUSP00000082519	5	13	12	25	28	39	15	21	17	-8.582224	-7.736602	-8.308531
ENSMUSP00000060346	1	1	0	8	3	3	6	5	2	-9.994537	-8.747481	-8.846319
ENSMUSP00000081485	4	1	6	13	22	11	13	13	10	-7.416147	-6.323246	-6.591789
ENSMUSP00000007272	12	9	17	27	53	26	17	23	18	-7.643959	-6.885154	-7.508835
ENSMUSP00000028610	31	65	46	137	92	122	48	69	57	-6.478297	-5.822045	-6.551593
ENSMUSP00000032998	64	67	67	141	93	145	106	115	70	-5.342463	-4.939266	-5.23441
ENSMUSP00000027153	0	1	0	2	5	2	3	1	1	-10.30907	-9.114445	-9.626525
ENSMUSP00000031729	3	10	13	27	36	31	10	5	13	-8.520376	-7.517755	-8.724764
ENSMUSP00000071292	14	24	14	51	38	33	56	29	30	-7.299948	-6.70581	-6.79628
ENSMUSP00000027381	3	0	0	14	7	4	17	20	14	-9.329139	-7.797336	-7.14566
ENSMUSP00000025778	1	1	2	3	3	5	2	1	2	-10.3792	-9.800031	-10.48657
ENSMUSP00000039252	117	118	147	269	213	182	152	183	132	-4.976603	-4.667888	-5.051012
ENSMUSP00000034355	0	2	0	4	5	4	12	13	19	-10.23468	-9.054343	-7.942584

ENSMUSP00000031334	2	1	3	4	7	7	6	2	3	-8.860024	-8.146459	-8.623453
ENSMUSP00000031411	11	13	11	43	18	44	30	31	14	-7.79069	-6.96223	-7.325225
ENSMUSP00000104955	0	0	0	1	1	7	0	0	0	-12.28092	-10.57369	-12.55552
ENSMUSP00000029770	20	34	32	55	86	58	37	26	28	-7.204824	-6.618098	-7.423859
ENSMUSP00000029663	1	1	0	7	2	5	0	2	0	-9.660918	-8.413861	-9.935527
ENSMUSP00000090593	0	1	1	2	7	10	2	4	1	-11.12462	-9.597876	-10.51081
ENSMUSP00000021001	6	8	8	17	26	12	8	9	9	-7.310378	-6.675464	-7.42776
ENSMUSP00000090909	15	26	37	74	64	50	47	0	57	-7.121041	-6.494852	-7.112675
ENSMUSP00000029877	8	10	6	34	13	25	12	10	8	-7.704221	-6.887936	-7.767471
ENSMUSP00000020948	0	0	2	2	6	8	0	1	0	-11.31166	-9.94319	-11.9235
ENSMUSP00000090155	0	4	0	5	13	10	2	1	0	-9.802654	-8.36452	-10.2782
ENSMUSP00000032073	0	0	1	3	3	1	0	0	0	-9.682543	-8.69938	-10.46976
ENSMUSP00000029987	32	47	40	78	97	62	42	36	52	-6.238286	-5.798031	-6.425533
ENSMUSP00000054322	6	0	2	14	16	12	7	19	10	-8.689281	-7.409756	-7.590318
ENSMUSP00000032841	1	0	0	4	1	3	0	0	0	-9.908807	-8.814335	-10.69602
sp|ALBU_HUMAN|	10	7	12	15	38	41	25	7	6	-8.174516	-7.27546	-8.190501
ENSMUSP00000092283	6	1	1	9	8	11	3	5	0	-9.054232	-8.16315	-9.32884
ENSMUSP00000034426	2	6	3	8	11	18	3	5	2	-9.044945	-8.162148	-9.402982
ENSMUSP00000023462	0	0	1	3	1	5	6	6	7	-10.15839	-8.963767	-8.326526
ENSMUSP00000018186	62	54	41	156	102	82	65	99	75	-5.817165	-5.292041	-5.674794
ENSMUSP00000076472	0	1	1	6	3	2	0	0	0	-9.683454	-8.651612	-10.8079
ENSMUSP00000003569	5	0	0	7	7	15	4	9	5	-8.863795	-7.559557	-8.03911
ENSMUSP00000052989	1	10	0	19	21	21	10	11	13	-8.88364	-7.516268	-8.1141
ENSMUSP00000037555	18	24	23	60	31	49	13	20	13	-7.293243	-6.780584	-7.904364
ENSMUSP00000106140	0	0	4	5	6	10	2	2	2	-8.904284	-7.737095	-8.868415
ENSMUSP00000023559	23	19	14	44	28	42	49	45	60	-7.662458	-7.207406	-6.942133

ENSMUSP00000002549	1	2	3	6	4	5	0	0	2	-9.172543	-8.626094	-10.21031
ENSMUSP00000004774	1	10	4	16	25	19	18	11	11	-7.910998	-6.837518	-7.263031
ENSMUSP00000070944	2	3	3	8	4	7	1	4	2	-8.743202	-8.216185	-9.129119
ENSMUSP00000035116	5	10	6	26	11	25	13	6	2	-8.307676	-7.512452	-8.582285
ENSMUSP00000077223	1	0	0	3	1	2	0	0	0	-9.243311	-8.385415	-10.03052
ENSMUSP00000008684	251	146	329	552	534	392	207	270	264	-3.626176	-3.158817	-3.880376
ENSMUSP00000038305	1	0	0	4	1	2	2	2	3	-9.460375	-8.477212	-8.509329
ENSMUSP00000103136	7	7	0	40	24	26	0	22	16	-7.47537	-5.942006	-6.814257
ENSMUSP00000103903	0	20	0	34	37	33	0	0	0	-7.883148	-6.534736	-10.82448
ENSMUSP00000042967	3	3	1	7	5	14	7	4	6	-9.142192	-8.210023	-8.638673
ENSMUSP00000006094	200	185	210	345	364	254	216	217	233	-5.003807	-4.765764	-5.165955
ENSMUSP00000099435	20	17	14	30	27	26	24	19	11	-6.094255	-5.86076	-6.313287
ENSMUSP00000010807	0	1	0	3	7	1	0	4	0	-10.39695	-9.027871	-9.881646
ENSMUSP00000028063	0	0	1	2	1	2	0	0	0	-9.793357	-9.078699	-10.58057
ENSMUSP00000019622	3	5	2	9	13	6	0	9	9	-8.081496	-7.381592	-7.827801
ENSMUSP00000002850	1	1	0	2	3	8	0	0	2	-11.20745	-10.02711	-11.48206
ENSMUSP00000026470	1	6	3	14	7	18	3	0	2	-8.931791	-7.914914	-9.777389
ENSMUSP00000031093:reversed	1	0	0	2	2	1	0	0	1	-10.31945	-9.604792	-10.59406
ENSMUSP00000041361:reversed	0	0	1	2	5	1	0	1	1	-11.60759	-10.51312	-11.54496
ENSMUSP00000033662	4	10	3	20	11	18	4	3	4	-8.202009	-7.44007	-8.868832
ENSMUSP00000030112	0	1	2	3	4	6	1	3	4	-10.4461	-9.517501	-9.972716
ENSMUSP00000021443	57	52	103	121	133	146	87	93	81	-6.606084	-6.216991	-6.674073
ENSMUSP00000036288	4	14	13	33	22	32	55	49	48	-7.922589	-7.163188	-6.644576
ENSMUSP00000007212	5	6	12	25	12	20	11	15	11	-8.761348	-8.133328	-8.583873
ENSMUSP00000086252	1	0	0	1	2	2	0	0	0	-10.06162	-9.346963	-10.84883

ENSMUSP00000086987	1	0	0	1	2	2	0	2	2	-8.580017	-7.865358	-8.064715
ENSMUSP00000000090	2	0	6	12	9	12	10	13	4	-7.881807	-6.834124	-7.057337
ENSMUSP00000105288	0	1	0	3	1	2	0	0	2	-10.93419	-10.07629	-10.87156
ENSMUSP00000015858	2	4	4	6	9	7	0	1	1	-8.718473	-8.246016	-10.18399
ENSMUSP00000033289	0	1	0	2	3	1	0	1	2	-10.79023	-9.932333	-10.47587
ENSMUSP00000025667	4	4	0	11	14	12	5	11	5	-8.409875	-7.252473	-7.821855
ENSMUSP00000112196	1	2	0	10	2	8	4	7	3	-9.437273	-8.114621	-8.47407
ENSMUSP00000032882	0	0	1	2	1	7	0	4	1	-9.093192	-7.807544	-8.410651
ENSMUSP00000103940	42	8	29	70	74	67	65	63	50	-5.762687	-5.034442	-5.235332
ENSMUSP00000088057	0	3	4	11	9	10	0	7	0	-8.48766	-7.419659	-8.762268
ENSMUSP00000034400	14	4	3	19	15	22	27	38	29	-7.031525	-6.335567	-5.860297
ENSMUSP00000032371	0	0	4	8	3	7	17	12	19	-10.04202	-9.017975	-8.118327
ENSMUSP00000026565	4	0	1	7	6	5	9	9	6	-8.184162	-7.327359	-7.091132
ENSMUSP00000007216	7	16	6	25	17	42	11	14	16	-7.840062	-7.051624	-7.782832
ENSMUSP00000083281	2	0	0	2	3	3	0	7	0	-8.935931	-8.178693	-8.322118
ENSMUSP00000025161	0	1	0	2	2	1	2	2	2	-10.34797	-9.633307	-9.522187
ENSMUSP00000003066	12	10	8	27	14	19	14	30	14	-7.481751	-7.05509	-7.120272
ENSMUSP00000040954	1	5	10	23	10	35	10	4	10	-8.642799	-7.50588	-8.540811
ENSMUSP00000045127	1	1	0	3	2	2	0	0	0	-9.233854	-8.587924	-10.3583
ENSMUSP00000002846	3	3	5	6	6	8	6	7	8	-8.315758	-8.015703	-8.002344
ENSMUSP00000047665	2	2	4	6	6	4	1	4	11	-8.794364	-8.425627	-8.457744
ENSMUSP00000034346	1	6	0	12	8	7	2	7	13	-9.339816	-8.371921	-8.596991
ENSMUSP00000022861	4	4	0	16	9	9	2	7	1	-9.19232	-8.116058	-9.275752
ENSMUSP00000022256	11	7	6	14	13	23	10	7	13	-7.932874	-7.472331	-7.996124
ENSMUSP00000099730	14	17	26	29	43	34	28	31	31	-6.437403	-6.071378	-6.264658

ENSMUSP00000070449	5	0	1	8	5	7	0	6	6	-8.054258	-7.243022	-7.740686
ENSMUSP00000099534	2	0	0	2	2	4	1	4	0	-8.727386	-7.970148	-8.382078
ENSMUSP00000102289	11	0	0	9	13	13	8	0	8	-8.074874	-7.245432	-8.012859
ENSMUSP00000029830	0	3	2	4	8	8	4	0	3	-9.255561	-8.301089	-9.261665
ENSMUSP00000051561	0	0	2	6	5	1	1	2	0	-10.4295	-9.320652	-10.45237
ENSMUSP00000099490	0	7	0	6	9	10	23	20	48	-10.7944	-9.899285	-8.681159
ENSMUSP00000025563	4	4	5	11	7	6	10	8	6	-7.729163	-7.406927	-7.439044
ENSMUSP00000071624	0	0	2	5	6	1	2	2	2	-9.449106	-8.340263	-8.960561
ENSMUSP00000002171	1	3	4	14	4	9	11	12	4	-9.022979	-8.166392	-8.198509
ENSMUSP00000029402	8	3	5	10	9	13	0	2	1	-8.602633	-8.195598	-10.23646
ENSMUSP00000072858	0	0	0	9	0	11	18	21	39	-9.591612	-7.167385	-5.891573
ENSMUSP00000031402	4	10	7	13	13	20	16	26	17	-8.309387	-7.804508	-7.594682
ENSMUSP00000037348	87	62	69	125	107	98	106	127	89	-5.695154	-5.52536	-5.581906
ENSMUSP00000089551	26	24	24	41	31	43	28	39	22	-6.088242	-5.896944	-6.181619
ENSMUSP00000088372	9	15	19	27	30	23	40	33	30	-6.593193	-6.230503	-6.014018
ENSMUSP00000028121	2	0	4	6	7	6	4	6	4	-9.29656	-8.532967	-8.844774
ENSMUSP00000078123	0	0	4	5	3	5	0	1	1	-8.680174	-7.952515	-9.40746
ENSMUSP00000025668	3	11	18	33	31	21	10	4	8	-7.944876	-7.238647	-8.574114
ENSMUSP00000023312	0	1	2	4	2	5	1	1	0	-10.0269	-9.246799	-10.55325
ENSMUSP00000090844	0	1	3	3	4	11	12	0	13	-10.16856	-9.14452	-8.869817
ENSMUSP00000013737	9	0	0	12	5	12	0	0	0	-8.965554	-8.141279	-11.18988
ENSMUSP00000003521	30	14	31	43	45	46	25	32	30	-5.928727	-5.5995	-6.057612
ENSMUSP00000075953	0	0	1	1	2	1	0	0	1	-8.669965	-8.122547	-8.944574
ENSMUSP00000034227	0	0	1	1	2	1	0	1	0	-9.425632	-8.878214	-9.700241
ENSMUSP00000080058	0	0	1	1	2	1	0	0	0	-10.84055	-10.29314	-11.62777

ENSMUSP00000111831	5	0	6	12	12	13	2	4	2	-7.643792	-6.760995	-8.193005
ENSMUSP00000045621	8	9	4	13	12	20	10	13	10	-7.683978	-7.20038	-7.53104
ENSMUSP00000102363	0	2	4	6	10	5	0	6	5	-9.216995	-8.360283	-8.980423
ENSMUSP00000020504	0	0	1	1	1	2	1	3	4	-9.064619	-8.517201	-8.002265
ENSMUSP00000096222	1	0	0	1	1	3	1	3	2	-10.59883	-9.884175	-9.773055
ENSMUSP00000030940	0	0	3	2	4	4	0	7	2	-9.472651	-8.775973	-8.899117
ENSMUSP00000034141	1	0	1	4	3	1	3	1	1	-10.65132	-9.894079	-10.30601
ENSMUSP00000017065	0	0	0	0	5	12	2	3	1	-10.61612	-8.342222	-9.277734
ENSMUSP00000026704	12	9	13	19	15	26	40	22	30	-7.870211	-7.563119	-7.176275
ENSMUSP00000034881	3	0	0	2	6	3	18	15	11	-8.080995	-7.300889	-6.040637
ENSMUSP00000028238	0	11	5	18	25	16	16	0	12	-7.665637	-6.667416	-7.417902
ENSMUSP00000028062	0	1	1	1	5	4	2	1	1	-10.08613	-9.137715	-9.908062
ENSMUSP00000029259	4	8	3	21	6	23	28	27	13	-8.923861	-8.027857	-7.760196
ENSMUSP00000023749	2	0	3	6	8	3	1	1	1	-8.759945	-7.955805	-9.402734
ENSMUSP00000064655	4	0	6	10	9	13	10	15	19	-7.565053	-6.737966	-6.463864
ENSMUSP00000030455	0	3	3	4	9	9	2	6	5	-8.939612	-8.039402	-8.554547
ENSMUSP00000000001	0	0	5	7	3	5	0	0	0	-9.184103	-8.494416	-10.92846
ENSMUSP00000098076	5	2	2	4	9	10	3	6	6	-9.516989	-8.91182	-9.339382
ENSMUSP00000005685	0	36	51	223	159	86	18	32	0	-6.908427	-5.482192	-7.72451
ENSMUSP00000089374	0	0	36	37	16	29	19	32	23	-7.536079	-6.977967	-7.110807
ENSMUSP00000084918	8	21	18	32	29	31	6	6	15	-7.468517	-7.054545	-8.274882
ENSMUSP00000033480	16	32	20	36	40	53	19	9	17	-7.962033	-7.574433	-8.638563
ENSMUSP00000099642	1	0	4	6	3	6	10	3	9	-11.10175	-10.41206	-10.09042
ENSMUSP00000090184	22	38	27	52	47	47	43	41	45	-6.052864	-5.7845	-5.939078
ENSMUSP00000018430	1	0	4	4	4	6	2	0	4	-8.71755	-8.090409	-8.848921

ENSMUSP00000027067	2	7	4	13	14	6	7	9	11	-7.910694	-7.286109	-7.509322
ENSMUSP00000091541	0	1	0	7	1	1	0	0	0	-10.37373	-9.179114	-11.16095
ENSMUSP00000099819	12	11	13	45	17	19	0	17	13	-7.153679	-6.607616	-7.602675
ENSMUSP00000054421	0	0	0	2	0	2	2	1	2	-10.33694	-9.276922	-9.141799
ENSMUSP00000077917	0	0	0	2	0	2	3	6	1	-9.653915	-8.593893	-7.887781
ENSMUSP00000003461	2	4	9	15	7	15	3	0	4	-9.307655	-8.702618	-10.24594
ENSMUSP00000034097	1	2	0	5	3	2	2	9	1	-9.709602	-9.012925	-8.884613
ENSMUSP00000004232	9	3	2	11	7	17	16	18	17	-8.29452	-7.680292	-7.348853
ENSMUSP00000031773	6	19	12	32	18	32	4	8	5	-7.374319	-6.842529	-8.382002
ENSMUSP00000069359:reversed	0	1	0	1	2	1	2	0	0	-9.957448	-9.41003	-9.894824
ENSMUSP00000103557	0	0	5	3	7	4	0	2	0	-8.587387	-7.960247	-9.481913
ENSMUSP00000099415	15	0	15	26	43	36	20	25	18	-7.856968	-6.881154	-7.414791
ENSMUSP00000001507	6	7	26	33	26	22	3	2	2	-7.690216	-7.221128	-9.526679
ENSMUSP00000047960	11	0	4	17	11	16	5	13	4	-6.984236	-6.212119	-6.905084
ENSMUSP00000017975	6	0	2	7	6	9	0	0	0	-8.264235	-7.600601	-10.38841
ENSMUSP00000088252	0	2	8	9	7	12	0	4	5	-7.802183	-7.102278	-8.167818
ENSMUSP00000080995	2	0	1	2	3	3	1	2	3	-7.905104	-7.399603	-7.668296
ENSMUSP00000099908	9	11	16	17	23	20	9	11	9	-6.614217	-6.361943	-7.095481
ENSMUSP00000110223	2	0	0	1	3	3	0	0	0	-8.536331	-7.890401	-9.660776
ENSMUSP00000028278	5	5	2	8	7	8	4	1	2	-8.295236	-7.941523	-9.032758
ENSMUSP00000106968	1	0	1	4	1	2	1	3	1	-9.015068	-8.369138	-8.66976
ENSMUSP00000034304	24	34	30	51	71	37	17	21	23	-6.592312	-6.250715	-7.226025
ENSMUSP00000088358	19	28	39	45	43	81	27	22	19	-6.844733	-6.420091	-7.349674
ENSMUSP00000089302	12	2	0	12	8	18	22	30	44	-7.223239	-6.530009	-5.658474
ENSMUSP00000029476	12	12	10	16	16	19	2	12	4	-6.991038	-	-7.864918

											6.842188	
ENSMUSP00000000284	0	0	0	2	0	1	1	2	2	-11.211	-10.35192	-10.01585
ENSMUSP00000081567	0	0	0	2	0	1	3	2	1	-11.86447	-11.00539	-10.52609
ENSMUSP00000002452	0	0	0	2	0	1	4	3	2	-9.653915	-8.794833	-7.978808
ENSMUSP00000025095	1	0	1	1	4	2	2	1	2	-8.620414	-7.974484	-8.275106
ENSMUSP00000007251	0	0	1	1	1	1	0	0	0	-10.58309	-10.23661	-11.3703
ENSMUSP00000108003	22	5	14	25	21	46	21	23	11	-6.3386	-5.792549	-6.328433
ENSMUSP00000029325	17	41	34	57	60	49	35	53	36	-6.626787	-6.286225	-6.607033
ENSMUSP00000104816	0	0	6	3	8	4	1	2	0	-8.492299	-7.94585	-9.278325
ENSMUSP00000037446	8	0	10	13	19	19	10	11	14	-9.002579	-8.254458	-8.650132
ENSMUSP00000034326	2	8	6	8	12	17	2	5	1	-9.376831	-8.830658	-10.26267
ENSMUSP00000032888	0	0	0	1	0	2	1	1	1	-10.10529	-9.246208	-9.278325
ENSMUSP00000032761	0	2	0	1	3	3	0	0	0	-9.438487	-8.792557	-10.56293
ENSMUSP00000060892	2	0	2	3	3	4	1	1	0	-8.134947	-7.639209	-8.862232
ENSMUSP00000092557	1	0	0	1	1	1	0	0	0	-11.08914	-10.74266	-11.87635
ENSMUSP00000046856	0	0	9	6	5	7	3	2	2	-9.422882	-9.046043	-9.908949
ENSMUSP00000100593	12	4	9	12	15	23	7	17	7	-6.904	-6.481932	-6.974467
ENSMUSP00000022070	3	3	2	7	3	14	1	5	0	-9.771133	-9.025799	-10.28232
ENSMUSP00000021676	1	0	5	4	5	5	1	3	3	-8.099573	-7.61567	-8.248914
ENSMUSP00000109310	4	6	4	14	13	5	5	9	2	-8.059977	-7.531532	-8.213175
ENSMUSP00000047218	0	2	0	2	5	1	1	0	0	-9.6666	-8.909362	-10.27844
ENSMUSP00000092233	79	70	82	142	145	87	93	104	107	-6.015592	-5.778705	-6.017135
ENSMUSP00000066238	4	0	14	13	20	12	9	11	15	-7.418459	-6.791715	-7.066011
ENSMUSP00000049584	0	1	2	2	2	6	0	0	0	-11.5788	-10.88213	-12.95499
ENSMUSP00000007959	5	7	6	7	17	13	7	11	10	-7.465416	-7.027496	-7.325934

ENSMUSP00000031423	49	60	77	90	103	89	28	20	19	-6.863028	-6.692074	-8.144643
ENSMUSP00000032824	7	10	6	12	11	20	12	14	8	-8.0138	-7.659354	-7.917465
ENSMUSP00000024223	4	2	2	7	4	4	1	4	0	-8.387651	-8.077777	-9.042073
ENSMUSP00000090911	32	0	67	125	109	65	0	0	0	-6.800477	-5.947635	-11.28415
ENSMUSP00000099769	0	1	1	1	4	2	0	1	0	-9.083336	-8.437406	-9.695178
ENSMUSP00000101011	2	1	4	5	4	4	2	7	3	-8.314388	-8.022473	-8.126084
ENSMUSP00000059501	3	0	4	10	5	4	4	5	4	-7.647909	-7.009584	-7.388112
ENSMUSP00000005953	9	10	14	23	13	20	23	12	16	-7.728828	-7.460417	-7.583517
ENSMUSP00000018875	0	27	40	58	62	79	49	52	52	-7.787448	-6.955895	-7.248642
ENSMUSP00000045048	4	4	0	5	7	10	0	0	0	-8.925086	-8.261452	-11.04926
ENSMUSP00000037341	5	0	2	7	3	9	9	3	3	-8.005461	-7.367136	-7.616396
ENSMUSP00000011492	1	2	0	1	4	10	2	0	3	-10.08073	-9.022863	-9.987158
ENSMUSP00000018992	5	7	19	18	15	27	16	21	9	-8.198001	-7.802599	-8.093055
ENSMUSP00000051921	0	2	0	3	1	2	2	2	0	-9.052406	-8.531743	-8.874338
ENSMUSP00000023707	0	0	5	4	5	2	2	5	4	-8.24912	-7.837194	-7.869311
ENSMUSP00000110532	17	11	16	26	21	19	22	31	25	-6.475176	-6.323204	-6.191677
ENSMUSP00000027810	3	2	0	3	6	4	2	1	2	-9.477325	-8.916905	-9.751933
ENSMUSP00000044955	10	13	15	17	19	25	13	10	8	-7.440971	-7.224534	-7.910676
ENSMUSP00000034277	0	2	1	2	4	2	2	0	3	-8.999434	-8.493933	-8.905863
ENSMUSP00000021217	3	0	3	10	3	4	0	6	0	-8.196033	-7.53513	-8.470642
ENSMUSP00000095263	0	65	83	155	136	127	0	0	0	-6.440673	-5.651368	-11.32151
ENSMUSP00000021512	2	1	1	4	2	2	0	1	1	-9.290255	-8.985694	-10.01754
ENSMUSP00000107237	2	1	4	8	2	14	5	8	0	-8.752352	-7.89571	-8.492555
ENSMUSP00000047571	8	5	5	11	7	24	7	5	1	-8.859706	-8.299663	-9.430698
ENSMUSP00000021940	14	20	18	25	25	28	20	19	15	-7.072852	-6.919228	-7.310755

ENSMUSP00000077909	0	0	2	2	1	2	0	0	0	-9.931359	-9.553933	-11.0558
ENSMUSP00000099563	0	1	9	5	9	6	3	3	5	-9.715012	-9.331529	-9.906193
ENSMUSP00000006496	23	34	45	45	69	56	25	33	34	-5.832023	-5.569477	-6.208248
ENSMUSP00000004057	4	0	1	3	3	5	2	5	0	-8.356365	-7.944439	-8.362469
ENSMUSP00000020241	4	0	2	5	4	4	57	30	55	-9.288882	-8.8717	-6.611219
ENSMUSP00000044405	4	1	2	3	5	6	1	2	0	-9.323529	-8.964893	-10.23482
ENSMUSP00000060912	32	44	50	67	106	51	35	34	36	-6.425507	-6.097772	-6.880097
ENSMUSP00000104179	25	21	30	33	38	37	34	49	36	-6.134525	-6.031345	-5.967731
ENSMUSP00000043580	1	1	2	2	4	2	0	2	0	-9.508663	-9.204102	-10.23595
ENSMUSP00000078236	1	3	7	14	16	3	0	0	1	-8.558884	-7.785806	-10.44506
ENSMUSP00000108760	0	87	101	182	161	138	0	122	121	-6.210215	-5.518093	-6.22999
ENSMUSP00000031061	0	0	3	2	1	7	1	0	0	-10.36074	-9.664062	-11.22432
ENSMUSP00000031726	0	5	4	8	4	11	6	8	3	-8.621831	-8.016663	-8.32977
ENSMUSP00000052258	0	0	4	1	9	3	0	0	1	-9.936382	-9.208723	-11.0009
ENSMUSP00000016338	85	81	73	140	110	98	43	46	49	-5.345955	-5.214654	-6.165239
ENSMUSP00000043559	25	3	8	28	15	25	14	24	5	-6.222622	-5.848046	-6.326054
ENSMUSP00000101105	2	0	3	3	3	5	7	10	6	-9.593674	-9.181748	-8.540661
ENSMUSP00000092746	3	0	2	3	3	5	0	4	0	-8.223641	-7.811715	-8.665489
ENSMUSP00000074935	0	2	0	2	1	2	0	0	0	-9.875478	-9.498053	-10.99992
ENSMUSP00000029684	0	3	6	6	9	5	1	2	1	-8.650895	-8.176385	-9.572707
ENSMUSP00000048363	1	1	0	2	1	2	1	0	0	-10.06543	-9.688008	-10.67728
ENSMUSP00000087192	38	25	18	46	53	34	38	39	37	-6.586312	-6.340007	-6.524426
ENSMUSP00000029805	29	66	45	70	74	84	14	20	14	-6.996447	-6.755317	-8.32147
ENSMUSP00000041149	2	0	5	7	3	5	7	0	7	-7.740024	-7.318843	-7.413506
ENSMUSP00000029837	7	1	5	20	3	20	2	9	5	-8.235238	-7.35608	-8.321716

ENSMUSP00000065585	0	1	9	4	7	7	0	3	0	-8.973977	-8.688163	-10.18775
ENSMUSP00000059395	0	7	9	14	6	21	0	0	0	-8.423585	-7.778549	-11.15899
ENSMUSP00000098053	0	3	5	4	5	10	6	5	5	-9.260307	-8.73329	-8.923687
ENSMUSP00000023790	28	19	0	25	56	29	44	34	45	-7.655729	-7.065682	-6.987512
ENSMUSP00000046910	0	0	2	1	4	1	2	1	0	-8.981916	-8.461253	-9.004787
ENSMUSP00000063744	0	2	3	2	7	4	3	1	2	-9.619566	-9.059146	-9.750937
ENSMUSP00000000137	1	3	0	1	5	8	0	0	0	-9.450014	-8.655634	-11.02714
ENSMUSP00000039844	3	1	0	2	2	7	1	1	1	-9.401895	-8.822729	-9.877443
ENSMUSP00000029217	1	0	3	2	3	3	1	4	1	-8.727353	-8.422792	-8.691484
ENSMUSP00000069004	9	9	13	15	18	13	27	28	25	-6.705758	-6.568695	-6.060881
ENSMUSP00000023486	0	0	3	1	2	4	0	1	0	-10.30183	-9.90764	-11.16541
ENSMUSP00000030642	0	4	2	3	10	3	2	6	2	-8.4707	-7.865387	-8.317556
ENSMUSP00000051657	5	0	3	7	5	4	5	8	2	-8.590363	-8.221625	-8.312606
ENSMUSP00000035034	0	0	2	3	1	1	0	1	0	-9.821155	-9.44373	-10.433
ENSMUSP00000037962	0	0	4	2	2	3	0	1	0	-9.006938	-8.813684	-10.07146
ENSMUSP00000040222	1	4	0	5	1	15	0	0	0	-9.509936	-8.509987	-11.2543
ENSMUSP00000010254	4	0	1	2	4	4	3	3	1	-9.164152	-8.835654	-9.170256
ENSMUSP00000029082	2	0	2	2	6	2	1	3	0	-8.975077	-8.479338	-9.249685
ENSMUSP00000091429	0	4	1	1	5	15	6	1	1	-11.80931	-10.80936	-11.7041
ENSMUSP00000085523	15	12	8	24	14	19	9	15	8	-7.505954	-7.276662	-7.866346
ENSMUSP00000021719	2	0	0	1	3	1	9	0	3	-8.004825	-7.6274	-6.928099
ENSMUSP00000002090	14	0	16	22	26	12	7	9	6	-6.842965	-6.416304	-7.410633
ENSMUSP00000080302	0	3	0	2	4	1	1	0	0	-9.646469	-9.252277	-10.51005
ENSMUSP00000095197	1	1	4	2	4	8	3	2	2	-10.23815	-9.754246	-10.38749
ENSMUSP00000055743	4	0	1	5	2	3	0	0	0	-8.991356	-8.662858	-10.73572
ENSMUSP00000095655	0	6	0	37	21	0	9	20	13	-8.369697	-	-6.885714

											6.540341	
ENSMUSP00000099475	197	0	341	301	301	350	304	277	250	-6.317315	-5.990305	-6.158129
ENSMUSP00000022437	3	4	2	3	6	13	3	3	0	-9.155451	-8.591967	-9.766785
ENSMUSP00000014457	9	0	5	5	10	13	6	9	4	-6.753235	-6.351973	-6.748154
ENSMUSP00000031910	7	10	3	12	8	17	13	10	15	-7.547771	-7.207521	-7.213992
ENSMUSP00000110027	4	0	3	4	4	5	1	7	0	-9.565863	-9.273949	-9.729164
ENSMUSP00000023085	6	0	4	8	3	11	6	8	3	-7.639664	-7.167207	-7.43863
ENSMUSP00000003906	9	10	8	17	9	23	10	9	11	-8.057432	-7.727752	-8.231935
ENSMUSP00000002043	0	3	0	3	1	2	0	0	0	-9.872754	-9.603829	-11.24894
ENSMUSP00000021049	9	6	9	10	11	16	11	14	6	-7.93507	-7.765494	-7.967061
ENSMUSP00000042285	1	2	0	3	3	1	0	0	0	-9.469974	-9.075781	-10.84616
ENSMUSP00000034276	15	1	7	18	8	15	24	22	13	-7.125593	-6.817138	-6.49607
ENSMUSP00000021329	4	2	5	5	8	5	2	3	6	-8.035186	-7.832801	-8.309795
ENSMUSP00000001452	8	21	21	39	17	35	51	39	41	-7.516422	-7.17323	-6.845951
ENSMUSP00000087948	2	2	6	4	9	5	18	15	18	-9.633875	-9.348062	-8.389566
ENSMUSP00000008036	12	0	11	12	8	25	17	22	9	-6.597525	-6.199109	-6.168697
ENSMUSP00000081000	0	3	1	4	2	2	6	0	5	-9.597431	-9.292869	-9.050382
ENSMUSP00000085379	0	0	4	1	5	2	3	2	2	-9.284992	-8.98043	-9.123856
ENSMUSP00000032919	43	54	92	83	106	94	50	34	31	-6.667269	-6.508668	-7.43366
ENSMUSP00000013304	2	4	8	7	6	11	3	4	7	-8.30952	-8.054005	-8.584129
ENSMUSP00000034586	2	0	0	0	5	6	4	4	3	-8.49148	-7.459637	-7.491754
ENSMUSP00000014221	1	3	0	2	2	4	0	0	0	-8.759102	-8.45454	-10.33622
ENSMUSP00000021790	5	1	7	6	6	10	4	5	1	-7.130895	-6.890359	-7.637425
ENSMUSP00000032065	2	3	3	6	2	14	3	4	3	-9.137228	-8.473594	-9.22066
ENSMUSP00000023514	5	0	0	4	1	3	10	6	8	-8.197495	-8.060174	-7.104466
ENSMUSP00000026735	0	2	0	1	1	2	2	0	0	-9.911599	-	-10.18621

											9.701414	
ENSMUSP00000093955	2	9	6	11	13	6	35	35	21	-8.348192	-8.058318	-7.013075
ENSMUSP00000029815	1	0	4	3	2	3	2	2	1	-8.204096	-8.066775	-8.478705
ENSMUSP00000022865	1	0	2	2	1	3	2	4	3	-10.00673	-9.737808	-9.4332
ENSMUSP00000018851	36	56	35	44	65	117	77	65	49	-8.773782	-8.44503	-8.644206
ENSMUSP00000075954	0	0	0	11	0	0	15	17	15	-10.81539	-8.933707	-7.609595
ENSMUSP00000024932	7	2	1	5	4	7	0	0	0	-7.671821	-7.49426	-9.987173
ENSMUSP00000080403	3	0	0	1	1	4	0	0	1	-9.434499	-9.165574	-10.29808
ENSMUSP00000106014	14	0	21	15	15	19	18	31	15	-6.305895	-6.223675	-5.995685
ENSMUSP00000079340	31	13	0	20	14	28	13	25	0	-6.03745	-5.946572	-6.453492
ENSMUSP00000031707	13	6	11	23	14	11	5	6	7	-8.537561	-8.327991	-9.291873
ENSMUSP00000083973	4	0	5	3	4	10	7	14	3	-7.676986	-7.352809	-7.063919
ENSMUSP00000108229	5	14	8	10	15	19	9	6	4	-7.444327	-7.218923	-8.048506
ENSMUSP00000030698	0	3	3	3	3	4	0	1	0	-8.779981	-8.59472	-10.15498
ENSMUSP00000076589	0	2	1	2	1	3	0	0	0	-9.904503	-9.635577	-11.28069
ENSMUSP00000005647	5	8	7	16	6	13	9	7	4	-7.690361	-7.403466	-7.96497
ENSMUSP00000015100	1	0	0	2	2	0	3	5	1	-10.05626	-9.508841	-8.893755
ENSMUSP00000080998	1	0	0	2	0	2	2	2	1	-9.020167	-8.472749	-8.337626
ENSMUSP00000106104	0	1	8	5	1	16	0	0	0	-7.704199	-7.140715	-9.928524
ENSMUSP00000042150	0	1	3	2	6	1	2	5	0	-8.815516	-8.410804	-8.65438
ENSMUSP00000041968	4	9	0	8	5	6	4	4	4	-8.277202	-8.173283	-8.623304
ENSMUSP00000039264	0	1	1	1	1	2	1	0	0	-10.46963	-10.25945	-11.08147
ENSMUSP00000033008	2	0	2	1	7	2	2	0	4	-9.034431	-8.538693	-8.998562
ENSMUSP00000071214	14	12	20	24	15	35	7	16	7	-7.079283	-6.85832	-7.764705
ENSMUSP00000027853	3	0	1	5	1	2	3	3	4	-8.3103	-8.005739	-7.846679
ENSMUSP00000090284	0	25	41	25	19	39	25	38	28	-6.020749	-6.038597	-5.98025

ENSMUSP00000081474	13	0	13	10	13	11	9	20	12	-6.490641	-6.477731	-6.329846
ENSMUSP00000021993	6	0	5	5	4	7	15	16	5	-7.438453	-7.34432	-6.614095
ENSMUSP00000042988	0	0	0	0	0	4	7	11	11	-9.791633	-8.731611	-7.049758
ENSMUSP00000030914	0	14	8	9	31	4	0	0	2	-7.332357	-6.913999	-9.51282
ENSMUSP00000107966:reversed	0	0	0	3	0	0	2	1	1	-12.87064	-12.01156	-11.84274
ENSMUSP00000107749	4	0	0	0	9	4	1	2	1	-9.128199	-8.40054	-9.402808
ENSMUSP00000060523	11	0	13	9	7	17	4	13	5	-6.366454	-6.306597	-6.722763
ENSMUSP00000030340	92	48	17	73	76	73	114	132	127	-6.367098	-6.265921	-5.781846
ENSMUSP00000029610	4	4	1	5	3	7	2	5	3	-8.540894	-8.33117	-8.724476
ENSMUSP00000036541	0	0	1	1	3	0	2	2	1	-9.474903	-8.927485	-8.792362
ENSMUSP00000032196	4	7	7	8	10	8	7	5	5	-7.451559	-7.35018	-7.77883
ENSMUSP00000030169	0	7	0	3	1	4	2	4	2	-8.862353	-8.993537	-9.025654
ENSMUSP00000020920	2	0	0	1	1	1	8	8	10	-10.44522	-10.43598	-8.65675
ENSMUSP00000023851	4	0	2	5	1	5	4	1	3	-7.934818	-7.666129	-7.972851
ENSMUSP00000105886	3	2	1	3	3	3	6	3	0	-8.923082	-8.828848	-8.860965
ENSMUSP00000095433	2	4	3	3	4	10	5	4	3	-11.3518	-11.02762	-11.37496
ENSMUSP00000032425	0	5	1	3	2	3	0	0	0	-8.740761	-8.746677	-10.62836
ENSMUSP00000022781	21	5	6	18	9	20	8	16	14	-6.367962	-6.240373	-6.477785
ENSMUSP00000015950	0	4	3	3	3	4	0	0	1	-8.456888	-8.396895	-9.957151
ENSMUSP00000001547	0	2	0	1	1	1	0	0	0	-11.02925	-11.02	-12.15369
ENSMUSP00000066682	0	5	5	3	8	4	2	0	0	-9.086198	-8.967501	-10.55171
ENSMUSP00000045394	14	4	0	5	6	10	27	21	18	-7.999815	-8.09916	-7.032468
ENSMUSP00000039657	94	96	100	110	143	143	67	46	39	-6.405065	-6.337396	-7.321034
ENSMUSP00000054634	10	14	14	18	16	18	9	10	17	-6.731449	-6.670515	-7.058026
ENSMUSP00000030660	1	0	2	1	1	4	1	5	1	-8.861601	-8.592676	-8.499525
ENSMUSP00000019382	12	9	19	23	15	18	3	8	6	-7.21434	-7.130695	-8.29707

ENSMUSP00000026649	2	2	3	1	9	8	3	3	3	-8.425139	-7.836841	-8.48829
ENSMUSP00000100505	29	21	42	39	36	54	32	35	33	-5.902176	-5.811236	-6.094682
ENSMUSP00000045930	6	0	0	3	2	1	4	0	1	-11.58838	-11.83087	-12.00623
ENSMUSP00000102211	8	0	4	2	6	10	6	7	7	-6.855517	-6.730132	-6.664579
ENSMUSP00000025217	1	1	1	1	2	2	9	2	7	-10.1469	-10.02122	-8.954039
ENSMUSP00000018905	0	6	8	5	6	6	0	1	0	-7.886533	-7.952024	-9.987923
ENSMUSP00000015725	0	4	0	3	1	1	0	0	0	-8.9158	-8.991051	-10.49292
ENSMUSP00000106709	0	0	1	1	0	2	1	1	1	-9.368474	-9.021995	-9.054112
ENSMUSP00000087974	29	13	14	27	26	23	42	38	25	-6.225072	-6.169041	-5.883268
ENSMUSP00000056604	3	0	4	6	1	5	0	4	2	-7.867538	-7.647116	-8.267414
ENSMUSP00000053900	1	2	1	2	2	2	0	0	0	-9.651904	-9.583918	-11.22903
ENSMUSP00000088581	0	0	1	0	1	2	3	4	1	-10.23992	-9.893445	-9.17757
ENSMUSP00000096435	1	0	0	0	1	2	2	2	1	-10.43263	-10.08615	-9.75009
ENSMUSP00000006435	0	1	0	2	1	0	3	1	3	-10.47419	-10.12771	-9.523145
ENSMUSP00000085251	2	0	5	3	1	9	4	6	2	-7.740024	-7.44811	-7.55172
ENSMUSP00000068568	21	24	5	22	30	18	0	5	3	-7.621287	-7.535627	-9.586757
ENSMUSP00000025955	22	30	21	27	30	52	40	24	34	-8.129231	-7.977477	-8.114459
ENSMUSP00000079232	18	0	0	10	0	18	11	17	19	-7.989004	-7.817404	-7.35226
ENSMUSP00000099788	0	3	1	1	1	7	0	1	0	-9.970192	-9.56548	-11.03471
ENSMUSP00000109671	1	3	0	3	2	1	3	3	0	-11.23166	-11.16367	-11.19579
ENSMUSP00000093965	9	19	30	23	28	28	4	4	6	-7.961812	-7.901993	-9.581874
ENSMUSP00000029722	61	45	37	88	42	84	54	51	36	-5.778205	-5.621	-6.066752
ENSMUSP00000047356	2	3	0	4	3	1	0	2	1	-9.364364	-9.227043	-10.00715
ENSMUSP00000039726	4	3	2	7	2	7	12	7	8	-7.334982	-7.066394	-6.610662
ENSMUSP00000072775	0	15	13	11	3	30	3	9	2	-7.462888	-7.271978	-8.38125

ENSMUSP00000075987	76	48	34	89	56	74	39	44	34	-5.960407	-5.879033	-6.532161
ENSMUSP00000044050	4	4	11	15	12	4	2	5	11	-8.803975	-8.585531	-9.12861
ENSMUSP00000019198	0	0	9	5	8	0	4	6	5	-7.836051	-7.755595	-7.658444
ENSMUSP00000050446	6	8	5	8	9	9	2	2	5	-8.172932	-8.121579	-9.116899
ENSMUSP00000028225	0	0	2	2	0	2	3	8	6	-10.12628	-9.916097	-8.734342
ENSMUSP00000054856	1	0	1	0	2	4	1	2	2	-8.104197	-7.583535	-7.758889
ENSMUSP00000067681	4	0	5	3	2	7	11	8	7	-7.305423	-7.296459	-6.616829
sp|TRY1_BOVIN|	12	0	0	2	2	3	10	5	11	-7.986132	-8.691536	-7.548993
ENSMUSP00000100074	35	8	13	25	16	33	20	29	12	-5.897165	-5.867282	-6.088383
ENSMUSP00000031931	20	6	3	10	14	11	14	12	19	-7.209435	-7.272305	-7.062243
ENSMUSP00000030164	21	16	24	20	26	43	22	25	30	-7.710521	-7.582797	-7.757176
ENSMUSP00000024797	0	0	0	1	0	0	2	1	2	-11.19819	-10.92808	-10.00304
ENSMUSP00000045111	0	0	0	1	0	0	1	1	1	-10.20293	-9.932816	-9.375963
ENSMUSP00000101139	0	0	0	1	0	0	5	9	1	-9.743719	-9.473607	-7.616396
ENSMUSP00000035105	38	33	43	64	36	59	108	97	65	-6.094796	-6.008247	-5.51468
ENSMUSP00000023677	48	35	26	48	49	47	54	55	37	-5.797078	-5.764394	-5.782859
ENSMUSP00000093959	0	0	0	0	1	0	2	1	1	-11.27004	-10.99993	-10.24214
ENSMUSP00000034000	0	0	3	1	1	1	0	0	0	-9.648714	-9.891206	-11.0249
ENSMUSP00000023238	0	0	0	0	0	1	5	15	3	-10.92661	-10.6565	-8.403845
ENSMUSP00000059801	0	0	0	0	0	1	4	4	3	-11.39756	-11.12744	-9.547993
ENSMUSP00000025802	0	0	0	0	0	1	5	1	6	-10.09671	-9.826594	-8.170144
ENSMUSP00000033483	0	0	0	0	0	1	4	3	5	-11.21241	-10.9423	-9.28585
ENSMUSP00000045654	0	0	0	0	0	1	4	2	3	-9.470251	-9.200138	-7.795143
ENSMUSP00000029777	1	1	0	1	1	1	0	0	0	-9.543135	-9.53389	-10.66758
ENSMUSP00000060940	0	3	0	1	1	1	0	0	0	-9.62144	-9.863931	-10.99762

ENSMUSP00000020640	4	8	1	10	2	8	8	11	7	-8.238091	-8.086529	-7.872445
ENSMUSP00000023513	0	2	0	3	1	0	1	2	1	-9.047156	-8.836971	-8.869088
ENSMUSP00000040853	11	4	4	10	6	9	15	28	11	-7.976315	-7.962013	-7.254761
ENSMUSP00000099480	8	3	11	8	8	13	6	11	6	-6.88471	-6.86641	-7.117634
ENSMUSP00000041907	0	3	0	0	5	1	3	2	3	-9.329139	-9.060213	-8.855755
ENSMUSP00000095081	3	2	3	3	10	2	0	2	1	-8.156989	-7.847115	-9.17959
ENSMUSP00000053145	3	0	1	3	0	6	1	3	4	-7.932423	-7.527712	-7.659979
ENSMUSP00000088736	1	0	7	10	5	0	5	3	4	-9.036772	-8.726898	-8.959776
ENSMUSP00000056082	1	5	6	4	6	5	2	0	0	-8.519535	-8.561267	-10.14548
ENSMUSP00000079628	16	11	16	24	12	25	17	29	8	-6.29908	-6.201851	-6.352765
ENSMUSP00000030903	4	5	4	4	9	6	2	2	4	-8.880095	-8.776176	-9.577801
ENSMUSP00000032192	0	3	7	8	2	2	1	0	0	-10.65801	-10.74008	-12.46076
sp|TRYP_PIG|	393	300	326	433	403	489	539	447	553	-3.620122	-3.60036	-3.482914
ENSMUSP00000025178	1	0	0	0	1	1	1	4	1	-10.84667	-10.75193	-10.02089
ENSMUSP00000089348	4	0	0	0	1	6	5	12	7	-8.384408	-8.191155	-7.124138
ENSMUSP00000103086	2	0	2	2	1	2	1	2	2	-7.962576	-8.037827	-8.069945
ENSMUSP00000043540	2	0	6	4	2	2	0	2	1	-8.281042	-8.523533	-9.303643
ENSMUSP00000057595	162	185	215	227	292	220	139	152	202	-5.273618	-5.242948	-5.678848
ENSMUSP00000074448	0	2	1	0	5	2	1	2	2	-9.675264	-9.281071	-9.581693
ENSMUSP00000003620	1	5	12	6	7	6	6	2	4	-8.603014	-8.795478	-9.245499
ENSMUSP00000107927	5	2	5	7	4	5	13	1	5	-9.804439	-9.787306	-9.661144
ENSMUSP00000005431	3	3	1	3	5	2	1	0	1	-9.631931	-9.571937	-10.79496
ENSMUSP00000016771	14	39	58	23	33	133	32	16	6	-8.052105	-7.767874	-9.033345
ENSMUSP00000023806	2	2	3	3	12	1	2	0	0	-9.318591	-8.838545	-10.48162
ENSMUSP00000057664	4	9	4	8	8	6	4	15	5	-7.593169	-7.596354	-7.546771

ENSMUSP00000002551	4	0	3	0	3	18	6	11	3	-7.80206	-7.070616	-7.148209
ENSMUSP00000066038	1	0	4	4	1	1	6	10	7	-8.705668	-8.804923	-7.652655
ENSMUSP00000110434	87	81	40	91	84	88	108	82	76	-5.948526	-5.957894	-5.978732
ENSMUSP00000020820	0	4	1	4	1	1	0	0	0	-8.652486	-8.75174	-10.39685
ENSMUSP00000041104	8	19	15	17	14	24	16	10	11	-7.781177	-7.762153	-8.177908
ENSMUSP00000020637	16	38	44	33	44	46	27	28	18	-6.961162	-6.979492	-7.525152
ENSMUSP00000022821	2	2	0	4	4	0	1	1	2	-9.047899	-8.743338	-9.322508
ENSMUSP00000070149	1	4	0	1	4	1	4	3	2	-8.752369	-8.851624	-8.547015
ENSMUSP00000103257	1	4	0	1	1	4	0	0	0	-7.765183	-7.864437	-9.509545
ENSMUSP00000065987	7	5	12	13	5	17	5	12	3	-8.526748	-8.410527	-8.97203
ENSMUSP00000101665	3	0	5	4	2	2	2	9	8	-7.713058	-7.955549	-7.218158
ENSMUSP00000047254	1	0	1	2	2	0	7	11	7	-10.18869	-9.978508	-8.437271
ENSMUSP00000091608	1	2	3	3	2	3	2	2	1	-7.790568	-7.796484	-8.208414
ENSMUSP00000069962	1	5	2	8	2	2	2	1	0	-8.809216	-8.700102	-9.831817
ENSMUSP00000107659	0	7	6	4	3	4	0	0	0	-8.348566	-8.739551	-10.89584
ENSMUSP00000028619	15	15	18	26	18	19	11	21	8	-6.998481	-6.976249	-7.449395
ENSMUSP00000103012	9	1	3	20	15	0	10	7	23	-9.473198	-8.792249	-8.695963
ENSMUSP00000026818	6	6	6	4	10	13	2	4	1	-7.408797	-7.271692	-8.514196
ENSMUSP00000020358	11	0	12	0	23	21	10	16	13	-7.264239	-6.887566	-7.036112
ENSMUSP00000032539	126	149	162	224	187	156	112	152	168	-5.603597	-5.586443	-5.889674
ENSMUSP00000092502	0	42	50	107	77	0	66	66	42	-6.256108	-5.813471	-5.901006
ENSMUSP00000026924	6	6	9	9	9	9	49	27	67	-8.872172	-8.878213	-7.286767
ENSMUSP00000006181	2	8	6	7	4	9	5	4	2	-7.994309	-8.030878	-8.605542
ENSMUSP00000102062	0	0	3	9	0	0	6	14	23	-8.578833	-7.973182	-6.560702
ENSMUSP00000001592	0	6	1	1	1	5	4	3	3	-9.61735	-	-9.589474

											9.859841	
ENSMUSP00000072483	7	6	1	6	7	3	6	8	10	-8.452621	-8.573703	-8.229223
ENSMUSP00000071939	8	6	2	7	7	5	1	2	3	-8.399774	-8.483986	-9.522187
ENSMUSP00000025197	6	14	15	17	11	15	1	4	5	-8.105437	-8.149718	-9.535406
ENSMUSP00000004673	3	7	8	7	5	11	6	7	9	-8.092188	-8.106352	-8.180153
ENSMUSP00000040140	14	15	6	14	9	22	6	7	6	-7.813439	-7.813751	-8.665077
ENSMUSP00000027602	12	19	12	16	12	30	32	19	20	-7.603044	-7.555011	-7.389498
ENSMUSP00000017572	11	8	6	8	7	20	14	10	6	-7.935308	-7.857564	-8.037034
ENSMUSP00000032114	5	6	6	4	8	12	0	3	1	-8.955781	-8.877266	-10.44426
ENSMUSP00000018437	5	0	5	6	8	0	2	7	5	-7.613172	-7.557021	-7.589139
ENSMUSP00000024596	3	2	3	5	4	2	0	0	4	-9.222025	-9.189912	-10.04369
ENSMUSP00000108237	1	9	0	1	2	3	1	0	0	-9.328239	-9.998483	-11.13099
ENSMUSP00000040840	5	7	3	5	5	9	0	4	0	-8.387922	-8.41327	-9.761949
ENSMUSP00000008812	59	0	111	0	120	74	115	146	108	-5.0826	-5.19411	-4.586918
ENSMUSP00000015256	63	79	45	86	62	84	59	47	46	-6.423973	-6.452374	-6.903987
ENSMUSP00000051222	6	0	5	4	1	4	3	4	4	-6.932517	-7.349463	-7.207126
ENSMUSP00000031524	14	15	10	18	8	28	14	19	13	-7.45688	-7.384246	-7.572037
ENSMUSP00000019726	0	6	0	3	0	1	3	8	4	-9.193957	-9.746926	-8.679625
ENSMUSP00000103145	0	2	2	2	1	1	0	3	0	-8.645773	-8.888264	-9.121321
ENSMUSP00000074994	7	0	5	9	0	6	8	14	20	-7.48575	-7.527481	-6.589948
ENSMUSP00000072236	29	29	32	43	39	33	19	28	20	-6.924969	-6.925893	-7.489107
ENSMUSP00000088837	1	2	0	1	1	1	0	0	0	-10.89763	-11.14012	-12.27381
ENSMUSP00000020209	2	1	1	7	2	0	3	7	5	-8.51794	-8.113228	-7.69313
ENSMUSP00000018561	3	12	13	4	14	15	14	10	11	-8.852217	-8.938107	-8.91386
ENSMUSP00000025598	2	0	1	2	0	2	24	30	23	-9.368478	-9.41003	-6.782673
ENSMUSP00000105796	6	0	5	2	4	2	2	9	6	-7.649762	-	-7.532156

											8.166858	
ENSMUSP00000087632	59	0	0	0	58	0	30	46	32	-6.652244	-6.911404	-6.333522
ENSMUSP00000101495	1	1	1	4	0	2	0	0	1	-9.623741	-9.354816	-10.48732
ENSMUSP00000090564	10	18	12	15	10	27	2	15	4	-7.236258	-7.224726	-8.12318
ENSMUSP00000109215	3	4	3	3	5	5	6	4	4	-8.420367	-8.430937	-8.396333
ENSMUSP00000097561	3	1	7	6	1	6	2	10	0	-13.09817	-13.19216	-13.29577
ENSMUSP00000031314	4	12	2	4	9	5	6	7	9	-8.611799	-8.85429	-8.699764
ENSMUSP00000111272	63	67	102	90	101	93	80	104	75	-5.284817	-5.326243	-5.450002
ENSMUSP00000031472	11	8	12	14	14	11	11	11	10	-6.968122	-6.990511	-7.212419
ENSMUSP00000090897	74	3	2	12	3	18	11	25	23	-5.6801	-6.77	-6.24035
ENSMUSP00000083928	6	3	15	4	13	9	1	1	4	-8.994169	-9.161134	-10.49318
ENSMUSP00000088729	0	14	0	0	14	0	16	14	12	-8.909093	-9.151584	-8.151504
ENSMUSP00000005477	2	8	10	39	0	12	1	4	4	-8.325372	-7.674921	-9.316983
ENSMUSP00000030078	5	9	0	2	2	5	12	6	8	-8.60585	-9.23801	-8.306925
ENSMUSP00000026144	0	0	2	0	3	0	51	21	25	-9.349208	-9.339963	-6.284691
ENSMUSP00000075825	0	3	0	4	0	0	2	4	4	-9.992526	-10.03408	-9.327966
ENSMUSP00000019937	3	14	15	7	21	7	1	0	1	-8.317294	-8.474003	-10.85239
ENSMUSP00000105420	2	5	2	1	5	6	0	0	3	-9.409557	-9.400593	-10.53231
ENSMUSP00000022380	9	5	5	7	8	8	9	8	12	-8.119939	-8.184129	-7.99714
ENSMUSP00000032992	4	11	8	8	3	21	6	10	7	-8.813889	-8.743435	-9.088498
ENSMUSP00000026270	12	22	20	24	28	14	0	9	13	-7.540516	-7.587241	-8.67467
ENSMUSP00000002091	8	12	15	22	20	5	8	8	5	-7.085076	-7.043271	-7.843595
ENSMUSP00000044827	1	2	5	1	1	11	1	4	0	-10.12621	-9.945604	-10.78063
ENSMUSP00000091035	22	19	19	26	38	14	45	36	39	-6.07956	-6.065307	-5.673238
ENSMUSP00000038135	7	9	14	10	4	30	7	7	6	-8.911768	-8.78647	-9.56841
ENSMUSP00000081142	2	1	2	6	0	3	1	2	1	-8.997327	-8.759855	-9.439175

ENSMUSP00000022062	40	54	34	55	24	87	39	23	27	-6.773537	-6.758714	-7.406499
ENSMUSP00000034234	2	6	1	5	2	2	8	4	3	-8.561039	-8.80353	-8.383432
ENSMUSP00000029645	1	10	11	9	3	6	4	11	11	-8.061794	-8.490929	-8.179176
ENSMUSP00000018449	1	1	1	2	0	3	0	0	1	-11.46192	-11.33623	-12.3255
ENSMUSP00000016072	5	19	8	12	10	10	5	14	3	-8.906725	-9.149216	-9.535963
ENSMUSP00000075150	2	0	3	1	1	2	1	2	3	-7.795336	-8.205068	-7.926707
ENSMUSP00000108058	1	2	1	1	2	2	5	9	3	-9.064483	-9.139735	-8.12522
ENSMUSP00000021630	34	8	16	13	17	29	20	36	35	-6.878633	-7.104456	-6.71197
ENSMUSP00000109228	8	15	18	15	19	13	6	12	10	-6.761233	-6.871645	-7.401024
ENSMUSP00000025511	33	25	43	39	50	33	26	53	37	-5.514947	-5.571049	-5.652972
ENSMUSP00000067767	22	20	7	67	0	55	3	20	14	-7.51266	-6.860806	-8.058625
ENSMUSP00000101006	6	0	6	3	2	2	8	5	5	-7.619282	-8.324686	-7.526014
ENSMUSP00000104884	3	1	0	1	1	1	0	0	0	-9.894241	-10.33767	-11.47136
ENSMUSP00000104163	0	1	3	1	1	1	0	0	0	-8.975077	-9.418508	-10.5522
ENSMUSP00000099950	1	3	3	0	6	5	2	2	0	-9.835339	-9.691918	-10.54569
ENSMUSP00000089769	4	5	15	6	11	7	4	11	2	-7.237527	-7.480019	-7.833142
ENSMUSP00000000804	16	15	20	15	23	25	16	17	14	-7.684722	-7.721338	-8.03859
ENSMUSP00000048469	24	21	27	30	27	33	22	39	22	-6.267229	-6.290649	-6.402359
ENSMUSP00000105177	0	0	4	1	1	0	1	1	3	-9.978139	-10.67331	-10.08551
ENSMUSP00000053270	3	0	1	1	0	3	16	19	13	-9.463348	-9.705839	-7.539657
ENSMUSP00000011526	3	0	1	3	1	0	1	6	4	-9.241858	-9.48435	-8.694809
ENSMUSP00000078996	10	0	14	12	6	0	15	18	10	-7.049019	-7.559855	-6.766706
ENSMUSP00000038744	2	0	0	2	0	0	2	6	1	-9.031241	-9.273732	-8.20597
ENSMUSP00000020562	8	19	6	12	5	19	28	30	26	-7.873256	-8.032351	-7.240193
ENSMUSP00000062670	6	7	8	7	7	12	1	2	0	-7.919189	-7.960956	-9.804418

ENSMUSP00000043543	6	9	1	4	2	8	2	7	3	-7.536281	-7.900183	-8.070514
ENSMUSP00000058368	7	11	14	13	11	13	11	14	10	-6.872367	-6.97572	-7.061192
ENSMUSP00000004172	2	4	4	6	4	2	0	0	0	-8.486962	-8.569025	-10.80231
ENSMUSP00000054391	0	1	2	1	0	2	1	2	2	-9.734604	-9.977095	-9.641033
ENSMUSP00000041152	1	4	6	3	3	4	1	6	3	-8.047259	-8.373178	-8.405295
ENSMUSP00000021595	9	6	7	16	8	4	19	16	17	-8.092756	-8.1078	-7.544525
ENSMUSP00000027193	2	0	4	3	0	2	1	4	2	-7.799152	-8.184881	-7.948493
ENSMUSP00000110314	0	6	7	1	2	4	0	2	2	-8.903799	-9.680697	-10.14856
ENSMUSP00000100992	12	9	37	18	22	13	11	28	23	-6.232988	-6.563266	-6.442526
ENSMUSP00000053540	0	0	100	0	0	15	206	231	187	-5.924063	-7.98359	-4.380124
ENSMUSP00000035222	38	25	6	22	12	22	7	3	1	-6.594569	-7.04091	-8.599499
ENSMUSP00000028852	1	1	2	3	1	1	0	0	0	-9.5254	-9.600651	-11.10252
ENSMUSP00000021471	3	6	5	5	6	5	0	0	0	-8.059977	-8.181058	-10.67397
ENSMUSP00000046480	12	9	14	12	17	13	4	6	4	-6.577829	-6.644842	-7.709156
ENSMUSP00000035033	16	12	3	10	5	12	11	12	12	-8.501431	-8.875287	-8.659945
ENSMUSP00000070267	0	4	9	3	5	0	2	2	1	-7.685572	-8.351162	-8.763092
sp|CASB_BOVIN|	0	0	7	0	0	3	59	39	39	-8.437164	-9.31634	-5.920234
ENSMUSP00000021930	26	14	11	23	11	21	11	5	7	-6.965239	-7.134294	-8.002132
ENSMUSP00000030191	1	0	0	0	0	1	3	2	2	-11.20212	-11.44462	-10.25108
ENSMUSP00000073975	0	4	0	0	2	0	4	5	4	-9.595498	-10.29067	-8.899956
ENSMUSP00000032597	8	22	12	11	11	21	4	13	6	-6.334633	-6.554392	-7.183447
ENSMUSP00000009790	2	3	7	4	6	2	2	6	5	-7.828695	-8.071186	-8.031811
ENSMUSP00000101027	0	8	6	1	5	1	1	0	0	-8.381321	-9.22494	-10.48271
ENSMUSP00000025567	8	9	5	4	13	8	5	1	0	-8.155769	-8.278084	-9.573079
ENSMUSP00000033121	2	1	1	0	2	3	0	0	0	-10.54264	-10.61789	-12.11977
ENSMUSP00000000727	4	8	2	5	5	3	0	0	0	-7.778644	-8.087856	-10.39264

ENSMUSP00000030432	13	3	1	4	1	6	11	15	10	-7.968394	-8.6031	-7.536251
ENSMUSP00000095695	4	2	1	4	4	0	6	7	6	-8.843956	-8.975139	-8.237748
ENSMUSP00000065271	15	36	33	81	68	0	21	35	32	-6.240911	-5.917922	-6.469794
ENSMUSP00000099938	7	4	0	1	0	7	8	8	14	-8.425695	-8.942792	-7.775724
ENSMUSP00000004140	27	22	25	64	76	0	0	0	47	-6.287632	-5.901915	-7.004858
ENSMUSP00000065542	7	16	0	3	8	0	6	8	5	-8.350875	-9.266572	-8.803785
ENSMUSP00000019896	8	5	14	12	7	9	2	2	1	-7.494338	-7.702335	-9.247838
ENSMUSP00000069209	55	35	12	31	31	24	99	87	129	-6.849239	-7.259675	-6.006053
ENSMUSP00000106471	6	13	9	10	8	12	2	6	2	-7.751329	-7.928209	-8.968334
ENSMUSP00000062005:reversed	1	2	4	4	2	1	1	2	4	-8.524839	-8.76733	-8.799447
ENSMUSP00000108056	1	6	9	9	0	6	0	2	3	-8.337642	-8.638997	-9.603292
ENSMUSP00000091840	1	0	4	1	0	2	5	5	4	-8.136043	-8.746714	-7.541019
ENSMUSP00000092888	3	0	3	2	2	0	1	1	1	-8.689467	-9.242436	-9.475493
sp|CAS1_BOVIN|	0	0	32	0	0	4	98	67	77	-7.040906	-9.091205	-5.331772
ENSMUSP00000034607	1	3	3	2	3	2	17	13	15	-9.26085	-9.503341	-7.835433
ENSMUSP00000043660	7	4	4	1	7	9	1	5	2	-7.781427	-7.909464	-8.608401
ENSMUSP00000071636	0	6	3	1	1	2	5	9	6	-8.213681	-9.103376	-7.771288
ENSMUSP00000108956	0	4	9	14	0	0	10	12	9	-9.387616	-9.563387	-8.85488
ENSMUSP00000004729	1	3	1	3	1	1	1	5	6	-8.800616	-9.043108	-8.343807
ENSMUSP00000079180	16	12	16	14	17	21	17	26	10	-6.15341	-6.23391	-6.247506
ENSMUSP00000026425	13	28	22	19	9	40	9	12	1	-6.964366	-7.132188	-8.248819
ENSMUSP00000023433	2	2	1	2	0	4	1	2	0	-9.694928	-9.794182	-10.33772
ENSMUSP00000005066	2	1	0	0	3	0	7	4	3	-9.62144	-9.863931	-8.658237
ENSMUSP00000030028	2	1	1	0	4	1	2	0	0	-9.495924	-9.571175	-10.22321
ENSMUSP00000083375	12	29	14	13	17	24	18	9	9	-7.059505	-7.319856	-7.744073

ENSMUSP00000060584	41	50	110	68	71	56	15	14	17	-6.068225	-6.340795	-7.792951
ENSMUSP00000027111	21	26	13	25	19	20	22	14	6	-7.61292	-7.792392	-8.23385
ENSMUSP00000024946	6	4	0	3	0	2	2	4	2	-8.383777	-9.197258	-8.849563
ENSMUSP00000078369	2	0	0	0	1	0	8	7	9	-10.20701	-10.78674	-8.494066
ENSMUSP00000036265	0	0	2	0	0	1	1	3	2	-11.02561	-11.60534	-10.53707
ENSMUSP00000040550	8	19	10	17	6	14	14	11	28	-7.772121	-8.014613	-7.699137
ENSMUSP00000087110	0	0	2	0	1	0	2	6	6	-10.39181	-10.97153	-9.176866
ENSMUSP00000032927	2	0	0	1	0	0	3	4	4	-9.59619	-10.17591	-8.596464
ENSMUSP00000047661	8	0	5	0	2	4	9	6	12	-7.205618	-8.107783	-6.804246
ENSMUSP00000080614	5	2	2	4	2	3	0	1	0	-8.686705	-8.929196	-10.39843
ENSMUSP00000046016	7	2	12	0	7	13	0	14	0	-6.491652	-6.779619	-7.139069
ENSMUSP00000037930	11	15	14	10	8	27	1	11	1	-8.785952	-8.914667	-10.1124
ENSMUSP00000089808	14	11	7	16	7	11	4	8	2	-7.434051	-7.618544	-8.479595
ENSMUSP00000034131	0	1	2	0	1	1	1	2	5	-10.3695	-10.86373	-9.896119
ENSMUSP00000070751	6	0	11	2	5	0	4	1	1	-8.183317	-9.203936	-9.36132
ENSMUSP00000044004	11	29	22	9	14	38	15	9	1	-9.426014	-9.684381	-10.57466
ENSMUSP00000070993	10	6	4	9	4	7	11	13	7	-7.660005	-7.902496	-7.521322
ENSMUSP00000022842	6	11	13	11	12	8	19	18	27	-7.991459	-8.202691	-7.533896
ENSMUSP00000023210	19	24	11	23	15	17	7	5	5	-6.9012	-7.125831	-8.27466
ENSMUSP00000005508	2	8	3	5	7	0	0	3	2	-8.583881	-8.897865	-9.6614
ENSMUSP00000053842	3	4	1	1	2	4	4	5	4	-9.061894	-9.415694	-8.913405
ENSMUSP00000055313	1	3	4	2	2	3	0	0	0	-8.97627	-9.330069	-11.10045
ENSMUSP00000025294	1	1	5	1	5	0	20	18	38	-9.394818	-9.762577	-7.458519
ENSMUSP00000064699	8	6	5	8	10	2	2	0	1	-7.625606	-7.820454	-9.417715

ENSMUSP00000104831	25	32	10	21	14	23	8	6	5	-7.882156	-8.26552	-9.363401
ENSMUSP00000010007	27	18	8	19	10	17	7	9	7	-6.814968	-7.194948	-7.889253
ENSMUSP00000066181	3	19	7	7	5	7	2	5	2	-8.364504	-9.004404	-9.705879
ENSMUSP00000026495	244	220	151	227	165	271	215	168	133	-5.018864	-5.186379	-5.468524
ENSMUSP00000021806	5	0	0	0	1	0	3	3	2	-8.800616	-10.00026	-8.695412
ENSMUSP00000099664	4	6	9	5	11	3	11	9	5	-7.576072	-7.818563	-7.593887
ENSMUSP00000046079	28	44	37	31	54	32	30	31	23	-6.666808	-6.839398	-7.197933
ENSMUSP00000097738	1	2	4	0	1	6	6	15	5	-8.219978	-8.46247	-7.319927
ENSMUSP00000052086	55	58	0	0	0	54	81	75	65	-6.350733	-7.317478	-5.960961
ENSMUSP00000026420	15	17	19	15	20	23	13	14	12	-5.957843	-6.075156	-6.492
ENSMUSP00000101300	2	1	0	0	2	0	2	4	1	-8.846712	-9.340941	-8.484637
ENSMUSP00000101023	5	3	6	5	6	4	0	2	0	-8.834146	-9.014091	-10.5983
ENSMUSP00000080354	43	73	55	41	68	67	31	41	25	-6.034034	-6.247951	-6.869013
ENSMUSP00000026843	222	252	158	190	256	229	234	162	199	-5.31634	-5.493159	-5.65113
ENSMUSP00000033176	72	75	46	77	44	78	24	30	26	-5.958541	-6.170649	-7.103026
ENSMUSP00000057543	2	7	5	8	0	4	2	4	2	-8.314471	-8.695176	-9.078898
ENSMUSP00000020262	1	2	1	5	0	0	1	0	0	-9.115777	-9.191028	-10.1803
ENSMUSP00000073322	85	90	94	0	142	138	0	0	0	-5.33407	-5.5367	-10.8079
ENSMUSP00000038063	4	5	9	2	14	2	0	1	0	-8.479516	-8.722008	-10.81057
ENSMUSP00000044587	20	23	22	17	28	27	9	17	9	-6.429842	-6.572241	-7.304422
ENSMUSP00000071976	25	10	12	12	6	24	19	9	30	-6.737913	-7.089223	-6.808083
ENSMUSP00000061152	55	36	25	46	32	36	22	19	15	-6.098744	-6.358404	-7.088065
ENSMUSP00000027108	1	3	3	1	3	2	2	4	1	-8.421099	-8.788858	-8.695708
ENSMUSP00000032946	7	8	13	11	15	0	10	0	10	-7.130662	-7.443374	-7.721692
ENSMUSP00000077021	5	5	6	11	0	5	0	0	0	-8.517111	-8.759602	-11.25251

ENSMUSP00000032143	46	90	87	63	89	66	30	34	33	-6.166568	-6.431583	-7.265033
ENSMUSP00000026459	240	252	171	261	177	272	218	210	178	-4.88525	-5.0594	-5.249542
ENSMUSP00000019226	17	14	9	15	5	18	0	5	1	-7.1719	-7.463793	-9.158026
ENSMUSP00000002837	5	9	8	5	7	10	0	6	0	-7.462622	-7.705113	-8.879931
ENSMUSP00000019323	5	6	1	3	0	5	3	0	0	-8.323728	-8.917825	-9.697934
ENSMUSP00000097754	20	23	28	23	34	21	24	16	17	-7.21004	-7.360353	-7.699231
ENSMUSP00000021062	15	18	15	14	12	25	10	6	10	-7.688742	-7.872386	-8.551245
ENSMUSP00000073261	6	6	4	8	0	6	0	0	1	-8.064105	-8.428006	-10.2869
ENSMUSP00000103365	59	42	37	46	40	60	15	34	28	-5.488256	-5.674982	-6.337868
ENSMUSP00000027966	1	0	4	0	0	2	1	2	1	-9.11511	-9.977518	-9.556958
ENSMUSP00000049394	6	4	0	1	2	0	4	4	7	-8.332811	-9.514472	-8.246231
ENSMUSP00000069508	4	10	14	5	2	15	7	15	2	-8.154514	-8.624453	-8.57487
ENSMUSP00000020329	27	18	16	11	19	29	12	16	5	-8.122312	-8.39733	-8.991214
ENSMUSP00000099441	1	3	2	0	1	4	3	1	6	-9.382615	-9.768343	-9.229471
ENSMUSP00000068408	4	1	3	4	2	0	2	1	0	-9.182219	-9.661286	-10.20482
ENSMUSP00000045841	8	10	20	11	9	14	12	5	12	-8.813246	-9.162524	-9.346478
ENSMUSP00000019469	11	10	13	12	17	3	0	1	0	-7.483064	-7.783554	-10.41339
ENSMUSP00000020463	2	3	3	3	3	3	0	0	0	-9.244534	-9.386875	-11.36871
ENSMUSP00000042364	0	1	7	0	0	2	1	1	2	-8.08867	-9.330891	-8.910331
ENSMUSP00000009003	2	4	2	1	3	3	0	1	0	-8.259988	-8.613788	-9.87156
ENSMUSP00000027975	0	2	2	2	0	0	3	4	6	-9.303293	-9.998461	-8.607751
ENSMUSP00000049732	10	5	5	5	6	8	1	3	3	-7.823893	-8.114027	-9.026961
ENSMUSP00000109305	5	7	0	0	1	2	2	1	2	-8.33212	-9.674209	-9.338146
ENSMUSP00000006838	15	19	25	11	19	27	17	16	19	-7.723827	-7.999939	-8.121412
ENSMUSP00000035157	16	12	17	15	17	19	6	14	4	-6.902045	-7.023159	-7.777545

ENSMUSP00000002403	34	52	32	50	27	40	22	26	18	-6.09668	-6.347575	-6.94252
ENSMUSP00000048460	3	4	9	3	4	6	3	5	4	-6.823903	-7.254525	-7.358135
ENSMUSP00000074600	3	5	1	2	1	3	5	13	1	-8.180892	-8.760109	-7.786142
ENSMUSP00000038839	11	15	19	9	23	11	20	16	22	-7.712975	-7.999436	-7.741029
ENSMUSP00000075990	2	6	5	9	1	1	0	1	0	-8.043731	-8.434716	-10.0784
ENSMUSP00000022734	1	5	3	2	1	3	1	1	0	-9.052882	-9.632099	-10.42737
ENSMUSP00000004574	3	8	1	1	0	6	0	0	0	-8.452685	-9.158089	-10.92846
ENSMUSP00000044871	2	3	5	2	6	0	2	1	1	-9.034095	-9.467763	-10.04693
ENSMUSP00000028396	9	18	13	18	0	12	0	0	0	-7.938846	-8.457094	-11.53796
ENSMUSP00000099653	4	12	10	10	3	7	1	3	0	-7.634204	-8.122896	-9.519218
ENSMUSP00000103015	2	15	11	6	2	6	3	1	1	-8.666252	-9.552498	-10.45425
ENSMUSP00000099417	46	115	113	57	93	74	22	28	26	-6.032302	-6.475066	-7.575282
ENSMUSP00000078670	12	22	24	17	20	18	13	27	12	-6.293006	-6.58724	-6.673922
ENSMUSP00000047606	2	3	3	2	2	4	0	0	0	-9.28351	-9.526002	-11.40769
ENSMUSP00000020741	2	5	7	4	1	5	2	3	2	-8.314471	-8.855604	-9.190206
ENSMUSP00000022322	147	150	124	166	71	175	61	86	38	-5.423186	-5.68721	-6.515573
ENSMUSP00000006900	2	0	3	0	0	2	3	4	4	-8.204096	-9.066504	-7.824287
ENSMUSP00000004375	28	30	17	30	13	26	15	22	9	-6.521934	-6.84611	-7.273156
ENSMUSP00000103657	3	1	4	2	3	1	0	2	0	-8.073402	-8.552469	-9.34774
ENSMUSP00000090910	0	56	0	0	0	0	64	107	80	-7.41932	-11.31246	-6.214214
ENSMUSP00000022925	2	7	7	7	3	1	1	5	6	-8.175626	-8.754741	-8.709858
ENSMUSP00000017488	0	1	1	0	0	1	2	1	2	-10.10641	-10.68613	-9.761099
ENSMUSP00000026899	19	15	16	16	18	22	7	15	6	-6.868444	-7.000719	-7.70034
ENSMUSP00000022894	6	4	0	3	0	0	6	7	5	-8.236847	-9.418508	-7.983151
ENSMUSP00000096932	5	0	10	4	0	0	5	11	5	-7.395532	-8.737442	-7.359878

ENSMUSP00000026222	3	1	5	1	3	2	4	4	4	-8.089324	-8.668541	-8.112478
ENSMUSP00000095287	14	15	11	12	18	12	15	24	14	-6.388057	-6.583473	-6.39012
ENSMUSP00000036246	43	49	41	38	53	0	46	27	33	-6.541397	-7.158267	-7.040092
ENSMUSP00000055535	16	16	13	14	0	18	0	5	0	-7.797857	-8.368311	-10.041
ENSMUSP00000056027	0	3	5	1	0	1	1	4	3	-8.329832	-9.572053	-8.60444
ENSMUSP00000080854	32	65	52	47	20	59	11	21	6	-5.877718	-6.286064	-7.490113
ENSMUSP00000046324	6	3	0	1	0	1	3	2	6	-8.320654	-9.663024	-8.420807
ENSMUSP00000041872	6	2	1	1	0	4	0	1	0	-8.621831	-9.344285	-10.33355
ENSMUSP00000033873	10	8	15	15	10	6	3	5	2	-7.445122	-7.747345	-8.818729
ENSMUSP00000028704	4	8	15	7	1	9	17	10	10	-7.717481	-8.392232	-7.691275
ENSMUSP00000066715	52	46	23	44	34	26	16	15	14	-6.188359	-6.580259	-7.431715
ENSMUSP00000022980	5	8	3	5	5	3	4	9	2	-7.582801	-8.013424	-7.916273
ENSMUSP00000016400	1	2	3	2	0	2	0	0	0	-8.865924	-9.418893	-10.75352
ENSMUSP00000010795	44	36	28	50	32	23	127	181	162	-6.441906	-6.712179	-5.256473
ENSMUSP00000043047	81	48	16	25	34	24	55	65	46	-7.320312	-8.113111	-7.460957
ENSMUSP00000033953	0	2	14	2	0	0	12	10	15	-8.284998	-10.13845	-7.770942
ENSMUSP00000037617	15	14	19	16	22	11	0	11	0	-6.972202	-7.194691	-8.623453
ENSMUSP00000083271	4	25	28	5	12	8	5	6	1	-7.736686	-8.771197	-9.47801
ENSMUSP00000049025	5	5	16	2	2	13	2	9	4	-6.999741	-7.638765	-7.785336
ENSMUSP00000043111	1	0	1	1	0	0	2	3	1	-8.776866	-9.356591	-8.288321
ENSMUSP00000093394	2	1	3	2	0	2	1	4	2	-9.237487	-9.790456	-9.386829
ENSMUSP00000033342	6	9	6	8	1	7	19	14	10	-7.877946	-8.371837	-7.470435
ENSMUSP00000105531	12	21	12	13	16	13	9	14	5	-6.813804	-7.122997	-7.543557
ENSMUSP00000003912	4	19	4	5	3	5	2	4	0	-7.87511	-8.793582	-9.485373

ENSMUSP00000099907	2	3	1	3	1	0	1	3	0	-10.17981	-10.73277	-10.76489
ENSMUSP00000106961	0	4	0	0	0	0	3	1	2	-9.570032	-11.11504	-9.534163
ENSMUSP00000021335	1	3	1	1	2	0	4	6	3	-9.763625	-10.3743	-9.235322
ENSMUSP00000089350	7	0	0	0	0	0	12	29	16	-7.846185	-9.826935	-6.191164
ENSMUSP00000109399	42	31	37	36	27	0	23	35	22	-5.726102	-6.515996	-6.314154
ENSMUSP00000031697	4	1	4	2	0	3	5	1	2	-9.498193	-10.22065	-9.872952
ENSMUSP00000045284	6	1	3	3	0	2	4	3	1	-8.289398	-9.10288	-8.755184
ENSMUSP00000024897	9	3	6	8	0	3	4	6	0	-7.708542	-8.395911	-8.511456
ENSMUSP00000006235	2	1	4	2	1	2	2	2	0	-8.833289	-9.344285	-9.543643
ENSMUSP00000061059	0	3	0	0	0	0	9	4	2	-9.304137	-10.6482	-8.278388
ENSMUSP00000102987	9	11	5	7	5	9	2	12	5	-7.229422	-7.635588	-7.760824
ENSMUSP00000009256	1	6	1	1	0	2	0	1	1	-8.946732	-9.937216	-10.22107
ENSMUSP00000031038	3	4	3	5	0	2	1	0	0	-8.229627	-8.774603	-10.03237
ENSMUSP00000015800	35	80	74	45	48	61	42	52	37	-6.363822	-6.809328	-7.001515
ENSMUSP00000071777:reversed	4	1	1	0	2	1	4	3	2	-11.31946	-12.07337	-11.25734
ENSMUSP00000049338	8	7	4	6	3	7	15	17	23	-7.839037	-8.239808	-7.099623
ENSMUSP00000108940	0	0	5	0	0	0	6	6	7	-9.041002	-10.75325	-8.166289
ENSMUSP00000031637	7	0	5	1	1	0	6	10	7	-6.981397	-8.575223	-6.659801
ENSMUSP00000073541	12	13	21	17	16	12	6	17	7	-7.480121	-7.743893	-8.165543
ENSMUSP00000030118	6	6	2	5	1	3	2	2	0	-8.415377	-9.047537	-9.726857
ENSMUSP00000034547	5	14	12	6	3	12	1	2	10	-7.674753	-8.28506	-8.756706
ENSMUSP00000033229	4	0	0	0	0	0	7	10	14	-8.42886	-9.973865	-6.925972
ENSMUSP00000032898	0	0	4	0	0	0	5	1	5	-10.46628	-12.01129	-9.919233
ENSMUSP00000029266	6	4	1	3	2	0	0	0	0	-8.403534	-9.300443	-10.80231
ENSMUSP00000071486	231	230	242	167	137	0	0	252	0	-4.528997	-5.60704	-5.825747
ENSMUSP00000110021	10	15	11	10	15	10	14	18	11	-6.928089	-7.197614	-7.031522

ENSMUSP00000101651	0	2	0	0	0	0	28	33	27	-10.01073	-11.10306	-7.042039
ENSMUSP00000066419	0	2	0	0	0	0	5	2	1	-9.719026	-10.81135	-8.993905
ENSMUSP00000087524	0	2	0	0	0	0	1	2	2	-9.740303	-10.83263	-9.394995
ENSMUSP00000023510	0	2	0	0	0	0	6	3	4	-10.05971	-11.15204	-8.911495
ENSMUSP00000032844	1	3	3	2	1	2	1	1	0	-8.282349	-8.793345	-9.445379
ENSMUSP00000006764	7	0	4	0	0	2	7	7	4	-7.809002	-9.325827	-7.638734
ENSMUSP00000079672	29	22	24	22	27	31	11	32	6	-5.690525	-5.869699	-6.380496
ENSMUSP00000003445	2	4	3	2	1	4	1	4	0	-8.098415	-8.552365	-8.852987
ENSMUSP00000058919	0	0	3	0	0	0	2	11	3	-8.183124	-9.52719	-7.098511
ENSMUSP00000098591	0	0	3	0	0	0	4	1	2	-10.78041	-12.12447	-10.41833
ENSMUSP00000105028	0	0	3	0	0	0	3	2	2	-10.47889	-11.82296	-10.11681
ENSMUSP00000110364	4	6	7	0	7	3	1	1	0	-8.703065	-9.421199	-10.64422
ENSMUSP00000028286	10	19	16	16	10	14	0	0	0	-6.948258	-7.304525	-10.66115
ENSMUSP00000033087	0	2	2	0	0	1	5	5	2	-9.583825	-10.61623	-8.959776
ENSMUSP00000031398	5	8	12	2	9	6	2	13	13	-7.883349	-8.485322	-8.050686
ENSMUSP00000095794	158	7	12	7	0	17	34	49	85	-4.922689	-7.111314	-5.249036
ENSMUSP00000104725	14	9	21	7	5	20	28	23	29	-8.312613	-8.861324	-8.004266
ENSMUSP00000072717	29	55	37	40	16	39	29	18	25	-6.857664	-7.338738	-7.643134
ENSMUSP00000061227	27	9	7	5	7	12	30	23	47	-7.67565	-8.475063	-7.125605
ENSMUSP00000027989	8	7	8	7	6	0	0	0	0	-7.774171	-8.541375	-10.84616
ENSMUSP00000066897	11	4	9	6	7	6	76	59	92	-7.62072	-8.081528	-5.702239
ENSMUSP00000020653	7	17	13	10	12	6	14	24	34	-6.812155	-7.320967	-6.440055
ENSMUSP00000089978	30	41	25	22	0	21	24	46	30	-6.815091	-7.842027	-7.049491
ENSMUSP00000003655	2	0	0	0	0	0	5	3	3	-9.835614	-10.92794	-8.835888
ENSMUSP00000023396	2	0	0	0	0	0	8	10	6	-9.420533	-	-7.707587

											10.51286	
ENSMUSP00000109611	2	0	0	0	0	0	3	3	1	-10.21686	-11.30919	-9.603052
ENSMUSP00000000175	2	0	0	0	0	0	3	3	1	-8.935931	-10.02826	-8.322118
ENSMUSP00000106540	2	0	0	0	0	0	2	2	1	-10.35264	-11.44497	-10.00733
ENSMUSP00000071752	2	0	0	0	0	0	1	2	2	-9.220667	-10.313	-8.875359
ENSMUSP00000081009	2	0	0	0	0	0	3	10	7	-9.969743	-11.06207	-8.42747
ENSMUSP00000027429	1	2	2	0	1	2	2	0	0	-8.367601	-8.978272	-9.262127
ENSMUSP00000025218	3	4	1	3	0	1	5	7	4	-8.994808	-9.784352	-8.658188
ENSMUSP00000030076	3	6	2	3	1	3	2	3	3	-8.866157	-9.494562	-9.415371
ENSMUSP00000038772	0	0	2	0	0	0	3	1	3	-10.23948	-11.33181	-9.62567
ENSMUSP00000068174	0	0	2	0	0	0	3	4	4	-9.51716	-10.60949	-8.517434
ENSMUSP00000078914	0	0	2	0	0	0	5	7	5	-9.073132	-10.16546	-7.681192
ENSMUSP00000003117	1	2	2	0	0	3	9	5	3	-9.364364	-9.975035	-8.592341
ENSMUSP00000103181	7	5	5	7	5	6	3	5	3	-7.580321	-7.77015	-8.247144
ENSMUSP00000005651	97	129	191	127	137	116	50	76	58	-5.660724	-5.995783	-6.748975
ENSMUSP00000000687	0	1	0	0	0	0	3	3	2	-9.930379	-10.68547	-8.868025
ENSMUSP00000102857	0	1	0	0	0	0	3	2	3	-10.14618	-10.90127	-9.083825
ENSMUSP00000026625	0	1	0	0	0	0	9	9	6	-10.06429	-10.81939	-8.014112
ENSMUSP00000034834	0	1	0	0	0	0	3	4	2	-10.49694	-11.25203	-9.334435
ENSMUSP00000065113	1	4	1	1	1	1	16	4	6	-8.894911	-9.64882	-7.869592
ENSMUSP00000022271	8	15	24	12	2	12	35	19	19	-7.813358	-8.623332	-7.658683
ENSMUSP00000025679	3	0	2	0	0	1	8	7	4	-8.926419	-10.12606	-8.051706
ENSMUSP00000021425	4	2	5	0	5	1	6	8	9	-8.468597	-9.222269	-8.070001
ENSMUSP00000027356	25	30	30	37	28	26	7	4	7	-6.999456	-7.174878	-8.764059
ENSMUSP00000099754	1	4	4	1	3	0	0	2	0	-8.120788	-9.010482	-9.495276
ENSMUSP00000095285	7	6	6	7	3	7	10	14	14	-7.468974	-	-7.08755

											7.814154	
ENSMUSP00000028004	2	3	1	0	2	1	7	10	7	-9.363128	-10.11704	-8.413335
ENSMUSP00000104825	6	3	0	1	0	0	6	7	7	-8.848721	-10.52833	-8.406328
ENSMUSP00000030769	4	9	5	7	3	3	9	7	11	-8.350018	-8.888892	-8.245029
ENSMUSP00000026743	26	40	16	21	12	24	11	22	11	-6.895324	-7.49367	-7.777134
ENSMUSP00000054490	19	11	21	17	11	17	11	14	11	-6.152903	-6.516772	-6.764035
ENSMUSP00000022960	8	19	6	6	6	8	12	3	11	-7.767896	-8.48341	-8.269327
ENSMUSP00000015829	8	1	5	0	0	5	28	32	30	-8.480194	-9.592318	-6.978948
ENSMUSP00000068594	21	15	25	7	13	25	25	27	24	-7.92895	-8.467193	-7.988427
ENSMUSP00000109196	11	4	10	5	7	6	0	3	0	-7.804786	-8.354098	-9.853689
ENSMUSP00000101003	8	5	9	5	3	9	2	1	4	-7.403666	-7.885463	-8.695708
ENSMUSP00000065352	2	2	3	2	2	0	5	8	1	-8.210028	-8.888264	-7.88351
ENSMUSP00000026560	10	14	12	13	9	13	13	7	8	-7.485954	-7.755479	-8.000562
ENSMUSP00000021313	4	3	2	1	4	1	1	2	1	-8.279982	-8.8592	-9.201794
ENSMUSP00000026827	5	2	8	4	3	1	10	15	10	-7.672987	-8.467844	-7.153423
ENSMUSP00000023237	3	5	4	3	0	3	19	15	16	-8.815268	-9.64594	-7.750621
ENSMUSP00000031383	4	1	2	0	0	3	5	10	2	-8.408879	-9.288055	-7.90536
ENSMUSP00000008991	1	7	5	1	0	3	21	12	12	-10.28127	-11.49391	-9.39026
ENSMUSP00000084053	4	4	6	3	2	6	4	1	2	-8.100544	-8.55825	-8.97628
ENSMUSP00000018506	1	0	0	0	0	0	1	3	2	-10.49867	-11.25376	-9.672889
ENSMUSP00000025375:reversed	1	0	0	0	0	0	1	2	1	-11.25781	-12.0129	-10.74251
ENSMUSP00000035220	1	0	0	0	0	0	4	3	1	-10.25986	-11.01495	-9.197504
ENSMUSP00000099763:reversed	1	1	2	0	0	2	0	0	0	-8.736527	-9.431695	-10.31365
ENSMUSP00000014750	11	15	8	10	11	8	2	0	1	-7.313532	-7.70786	-9.654886
ENSMUSP00000034866	14	16	5	10	5	5	9	9	13	-7.311798	-8.083676	-7.702501
ENSMUSP00000080994	25	27	14	22	16	16	21	24	18	-6.399647	-6.837905	-6.719723
ENSMUSP00000051092	11	14	7	8	1	8	4	4	5	-8.225509	-9.061936	-9.337774

ENSMUSP00000070109	2	3	9	0	4	1	0	1	0	-9.080226	-10.19235	-11.18162
ENSMUSP00000005606	0	0	1	0	0	0	2	3	1	-10.14125	-10.89635	-9.315474
ENSMUSP00000028691	0	0	1	0	0	0	1	1	4	-10.50212	-11.25721	-9.676338
ENSMUSP00000030385	0	0	1	0	0	0	7	4	2	-9.960411	-10.71551	-8.474959
ENSMUSP00000094167	0	0	1	0	0	0	1	2	1	-10.27076	-11.02586	-9.755462
ENSMUSP00000036555	0	0	1	0	0	0	2	1	1	-11.22075	-11.97585	-10.70545
ENSMUSP00000036881	0	0	1	0	0	0	2	3	2	-10.99277	-11.74787	-10.04173
sp|CASK_BOVIN|	0	0	1	0	0	0	19	24	13	-9.498658	-10.25375	-6.635226
ENSMUSP00000033673	10	3	8	3	0	5	3	6	3	-8.238561	-9.34368	-9.024192
ENSMUSP00000032920	3	4	8	4	2	4	1	2	0	-7.711869	-8.315549	-9.286836
ENSMUSP00000105447	1	1	9	2	0	0	17	13	24	-8.777702	-10.29453	-7.561244
ENSMUSP00000027491	1	2	3	2	1	1	1	0	3	-9.166028	-9.718997	-9.751114
ENSMUSP00000110094	22	13	14	9	9	0	5	15	2	-6.402153	-7.596412	-7.441885
ENSMUSP00000025476	1	3	1	0	1	1	0	2	1	-8.954767	-9.817175	-9.597555
ENSMUSP00000027863	5	14	6	0	2	7	1	1	0	-7.637732	-8.806375	-9.938372
ENSMUSP00000026289	8	14	14	17	0	0	5	8	7	-7.036303	-7.985547	-7.867332
ENSMUSP00000015877	1	2	1	1	1	0	0	0	0	-9.143513	-9.838681	-10.72064
ENSMUSP00000018470	6	3	3	0	4	1	13	13	12	-8.087152	-9.061062	-7.287826
ENSMUSP00000027529	4	3	2	1	2	3	2	1	1	-8.164084	-8.743301	-9.085896
ENSMUSP00000031741	7	27	30	9	12	5	0	4	0	-7.223416	-8.333912	-9.976434
ENSMUSP00000035804	27	26	19	25	17	24	24	21	21	-6.693971	-7.021629	-7.053746
ENSMUSP00000033715	17	20	34	20	19	20	4	8	4	-6.776313	-7.199766	-8.472596
ENSMUSP00000003622	11	9	7	7	7	10	4	3	0	-7.527324	-7.881069	-9.012319
ENSMUSP00000029386	27	39	25	14	17	34	22	16	8	-7.045951	-7.618477	-7.987107
ENSMUSP00000069432	33	61	64	26	48	38	42	43	49	-7.961068	-	-8.398756

											8.543817	
ENSMUSP00000099482	0	5	1	0	0	0	4	9	3	-8.42605	-10.28153	-7.852854
ENSMUSP00000042232	7	7	1	1	1	2	3	8	7	-7.599895	-8.941805	-7.707388
ENSMUSP00000022962	2	9	3	1	0	3	1	0	0	-8.165656	-9.445019	-10.26705
ENSMUSP00000101478	0	1	6	0	0	0	6	6	10	-8.425139	-10.40589	-7.682315
ENSMUSP00000022293	12	13	8	12	8	8	2	7	2	-7.26913	-7.668223	-8.559308
ENSMUSP00000080888	8	6	12	8	7	3	1	0	2	-8.75366	-9.340022	-10.83961
ENSMUSP00000020343	1	5	8	0	1	2	1	4	2	-7.795381	-9.275684	-8.671116
ENSMUSP00000045864	4	3	2	2	2	3	0	0	1	-8.824936	-9.278886	-10.53666
ENSMUSP00000034947	14	11	26	9	16	5	12	19	7	-6.558368	-7.31177	-7.117531
ENSMUSP00000001566	169	208	182	0	45	48	237	243	227	-4.928753	-6.951533	-4.969039
ENSMUSP00000021854	7	6	9	7	7	3	18	18	15	-7.873163	-8.354961	-7.343803
ENSMUSP00000025968	63	57	48	0	0	64	0	56	0	-6.24254	-7.435897	-7.598293
ENSMUSP00000081030	5	4	5	6	0	0	0	13	0	-7.428577	-8.397463	-7.769907
ENSMUSP00000029414	5	6	11	3	4	7	2	0	3	-7.246135	-7.904933	-8.806682
ENSMUSP00000026610	24	19	21	21	10	21	51	45	57	-7.191611	-7.636494	-6.608018
ENSMUSP00000025617	11	0	2	0	0	0	4	2	3	-7.53636	-10.05152	-8.133917
ENSMUSP00000027036	4	2	10	1	2	3	22	25	21	-7.698562	-8.788858	-6.593761
ENSMUSP00000099649	93	93	93	27	27	0	149	123	148	-5.547843	-7.410621	-5.415198
ENSMUSP00000077118	62	46	43	49	34	52	20	30	14	-5.483459	-5.836796	-6.60324
ENSMUSP00000088168	53	44	47	57	55	56	58	56	51	-5.737291	-5.827099	-5.877075
ENSMUSP00000109451	1	2	5	0	0	2	2	0	0	-8.638133	-9.880354	-9.912471
ENSMUSP00000105356	3	1	2	0	0	2	14	14	9	-8.421473	-9.427119	-7.059613
ENSMUSP00000027916	3	3	6	4	2	1	27	32	19	-8.253932	-8.959337	-6.755065
ENSMUSP00000016463	147	114	70	99	64	75	61	61	50	-5.040433	-5.611018	-5.965522

ENSMUSP00000037583	12	12	19	11	8	15	5	16	7	-6.773108	-7.241594	-7.458891
ENSMUSP00000100059	5	6	2	1	2	3	0	0	1	-9.174128	-10.07629	-11.2088
ENSMUSP00000093229	12	37	15	12	11	9	4	0	0	-6.845397	-7.75849	-9.598415
ENSMUSP00000080523	8	8	12	9	4	8	4	17	5	-6.729425	-7.242861	-7.074254
ENSMUSP00000098648	9	9	4	1	0	6	9	8	10	-8.509003	-9.768928	-8.590658
ENSMUSP00000023550	1	9	3	0	0	2	0	4	1	-8.760811	-10.42613	-9.838331
ENSMUSP00000023952	91	122	65	50	90	35	100	88	69	-5.718802	-6.420989	-6.071519
ENSMUSP00000003681	6	15	2	0	2	2	1	6	15	-7.99032	-9.727674	-8.306613
ENSMUSP00000051223	7	5	2	0	3	1	11	9	8	-7.956031	-9.235394	-7.586885
ENSMUSP00000098041	0	11	7	0	0	0	2	1	2	-9.703585	-12.51512	-11.07749
ENSMUSP00000010208	6	37	37	7	7	6	5	3	4	-6.971242	-8.546511	-9.044174
ENSMUSP00000003907	6	7	3	4	3	1	14	11	14	-8.375382	-9.229103	-7.810674
ENSMUSP00000076575	1	0	4	0	0	0	8	4	5	-9.154025	-10.86627	-8.382002
ENSMUSP00000097561:reversed	2	4	1	0	1	1	3	1	3	-13.48408	-14.61499	-13.75869
ENSMUSP00000084572	30	24	36	28	20	32	50	62	50	-7.77967	-8.137906	-7.473773
ENSMUSP00000103904	20	0	24	0	0	0	7	28	13	-7.224893	-10.88393	-7.41523
ENSMUSP00000018699	39	47	36	40	43	36	21	20	19	-6.021705	-6.288789	-6.993572
ENSMUSP00000026552	267	269	277	292	290	184	122	187	136	-4.69055	-4.992478	-5.5663
ENSMUSP00000081782	6	0	2	0	0	0	3	2	6	-9.885467	-11.97752	-9.885471
ENSMUSP00000073175	10	15	14	12	6	11	0	12	10	-6.497351	-7.023472	-7.31638
ENSMUSP00000104830	7	0	13	0	0	0	13	14	18	-7.077001	-9.986211	-6.580044
ENSMUSP00000087046	3	3	0	0	0	0	6	8	3	-8.69646	-10.55194	-8.067674
ENSMUSP00000029353	0	2	1	0	0	0	1	4	3	-9.909698	-11.25376	-9.436314
ENSMUSP00000031160	0	2	1	0	0	0	4	4	2	-9.701128	-11.04519	-9.036567
ENSMUSP00000022993	2	6	2	1	2	1	0	2	1	-8.272186	-	-9.485964

											9.252908	
ENSMUSP00000106250	2	0	5	0	0	0	1	1	2	-7.731992	-9.712742	-8.442346
ENSMUSP00000100968	3	0	1	0	0	0	3	7	2	-9.441025	-10.98603	-8.816976
ENSMUSP00000049007	1	2	2	1	0	1	3	7	3	-10.08797	-10.95038	-9.559669
ENSMUSP00000080974	1	3	4	2	0	0	1	3	3	-9.067603	-10.30982	-9.45352
ENSMUSP00000020522	0	2	3	0	0	0	10	13	8	-9.928975	-11.64122	-8.593327
ENSMUSP00000100802	27	23	24	16	11	27	17	24	14	-6.211747	-6.76202	-6.776277
ENSMUSP00000029405	1	0	3	0	0	0	10	1	4	-9.989942	-11.53495	-9.165133
ENSMUSP00000051935	2	1	0	0	0	0	1	1	2	-9.722181	-11.06625	-9.79585
ENSMUSP00000025483	1	5	5	0	0	2	5	22	6	-8.990386	-10.50721	-8.249425
ENSMUSP00000028241	4	7	1	2	0	0	1	1	0	-8.198191	-9.792017	-9.824134
ENSMUSP00000047898	0	1	2	0	0	0	3	1	3	-9.838111	-11.18218	-9.476035
ENSMUSP00000022060	4	0	2	0	0	0	2	4	2	-8.42605	-10.28153	-8.464083
ENSMUSP00000001713	7	5	7	3	3	0	40	56	58	-7.644022	-8.892598	-5.892129
ENSMUSP00000107760	5	10	1	1	0	1	0	0	0	-9.601938	-11.45539	-12.33734
ENSMUSP00000028222	61	160	131	61	58	72	34	73	32	-5.767922	-6.618216	-6.965235
ENSMUSP00000038368	10	11	13	5	0	4	20	15	22	-8.365112	-9.826207	-8.140153
ENSMUSP00000080531	3	0	4	0	0	0	2	6	6	-8.918064	-10.89881	-8.591545
ENSMUSP00000029630	28	22	6	0	0	9	0	0	0	-7.41769	-9.361109	-11.34294
ENSMUSP00000100067	5	2	4	3	0	0	9	13	7	-8.153419	-9.418508	-7.535716
ENSMUSP00000020285	6	9	9	0	0	6	3	9	7	-7.224223	-8.691116	-7.717149
ENSMUSP00000004508	9	11	7	8	7	4	8	11	5	-7.262006	-7.834067	-7.647867
ENSMUSP00000093944	3	5	9	4	0	0	15	16	16	-8.850178	-10.30654	-8.160772
ENSMUSP00000081010	18	18	21	11	18	18	48	68	38	-6.389254	-6.819231	-5.686172
ENSMUSP00000045927	2	2	2	2	0	0	0	1	1	-8.79272	-9.798366	-9.830483

ENSMUSP00000096677	1	1	0	0	0	0	3	5	4	-11.41148	-12.50381	-10.33475
ENSMUSP00000100564	5	5	8	1	0	4	22	13	7	-7.679343	-9.021129	-7.151417
ENSMUSP00000008826	31	30	25	25	16	28	12	22	12	-6.084764	-6.543299	-6.970345
ENSMUSP00000073213	26	17	11	13	4	8	52	35	41	-6.625719	-7.607579	-6.052961
ENSMUSP00000041814	4	4	8	1	4	2	26	18	35	-9.153309	-10.11834	-7.901565
ENSMUSP00000030345	25	50	26	24	19	18	20	15	24	-7.026495	-7.763724	-7.828368
ENSMUSP00000102140	1	2	1	0	0	1	6	2	6	-8.736527	-9.768929	-7.974264
ENSMUSP00000083705	59	66	77	58	47	71	47	47	34	-5.570172	-5.949364	-6.296785
ENSMUSP00000085623	4	1	1	1	0	0	5	8	7	-8.963904	-10.30678	-8.184786
ENSMUSP00000105795	57	66	100	15	12	0	210	232	191	-5.126087	-7.432753	-4.361714
ENSMUSP00000044326	17	18	20	22	17	18	13	2	12	-7.659359	-7.86706	-8.618419
ENSMUSP00000087694	1	1	1	1	0	0	0	0	1	-10.47791	-11.30937	-11.34149
ENSMUSP00000045216	7	25	13	7	3	1	1	0	0	-7.488329	-9.044933	-10.68862
ENSMUSP00000071078	5	5	8	1	3	4	7	2	0	-7.924466	-8.886439	-8.818406
ENSMUSP00000034966	51	83	61	41	34	56	21	50	26	-5.925224	-6.561812	-6.890473
ENSMUSP00000099634	42	59	37	37	36	34	42	28	53	-6.675422	-7.169242	-7.063795
ENSMUSP00000030830	6	12	15	5	4	7	4	3	3	-8.311511	-9.232948	-9.685117
ENSMUSP00000107433	2	3	7	0	2	0	2	0	0	-8.111758	-9.705584	-9.737701
ENSMUSP00000081001	3	5	3	2	3	2	0	1	1	-9.053756	-9.68216	-10.6027
ENSMUSP00000038914	54	53	23	24	14	22	14	9	7	-6.472824	-7.475343	-8.176613
ENSMUSP00000055862	7	6	10	4	7	3	10	12	9	-7.155898	-7.85638	-7.147873
ENSMUSP00000108126	1	0	1	0	0	0	1	1	1	-10.11005	-11.20238	-10.13292
ENSMUSP00000020161	47	48	22	5	2	20	0	5	1	-6.167782	-7.83546	-9.203231
ENSMUSP00000036093	6	1	2	0	1	0	3	2	10	-9.755565	-11.43517	-9.577959
ENSMUSP00000025385	69	67	38	39	28	40	95	69	72	-6.560477	-7.283881	-6.532547
ENSMUSP00000034541	20	14	11	2	10	4	5	6	5	-7.757035	-	-9.009132

											8.977015	
ENSMUSP00000047536	21	18	14	9	14	14	20	13	13	-6.75001	-7.340094	-7.162107
ENSMUSP00000037783	2	1	1	1	0	0	0	0	0	-8.900415	-9.932816	-10.47754
ENSMUSP00000021239	15	20	16	16	12	15	6	9	4	-6.94538	-7.353218	-8.160575
ENSMUSP00000028916	8	9	13	0	0	5	17	16	15	-8.362791	-10.18428	-8.185338
ENSMUSP00000037018	20	11	7	0	0	5	0	1	0	-7.577398	-9.625242	-10.61451
ENSMUSP00000110998	67	70	70	23	0	0	114	109	0	-5.853125	-8.237122	-6.053795
ENSMUSP00000060218	1	2	4	0	1	0	6	3	10	-8.210028	-9.678174	-7.60382
ENSMUSP00000002790	11	9	22	3	7	1	19	16	31	-8.285082	-9.774985	-8.12027
ENSMUSP00000030538	18	25	26	9	12	19	2	5	6	-6.989882	-7.762358	-8.846319
ENSMUSP00000023803	62	108	44	35	34	27	87	86	67	-5.84138	-6.877017	-6.002076
ENSMUSP00000106481	11	7	3	2	0	1	0	6	2	-8.233041	-10.08615	-9.370277
ENSMUSP00000034164	2	2	1	1	0	0	0	0	0	-9.156566	-10.35621	-10.90093
ENSMUSP00000112334	8	10	6	3	3	6	81	76	81	-8.189304	-9.068016	-6.223805
ENSMUSP00000067685	52	68	77	34	18	46	72	99	68	-7.258001	-8.191157	-7.340673
ENSMUSP00000099364	5	5	5	4	2	1	9	5	2	-8.964632	-9.870797	-9.180377
ENSMUSP00000020717	20	16	22	7	15	12	23	32	26	-6.28814	-7.047151	-6.235896
ENSMUSP00000033509	41	62	49	44	34	35	27	38	23	-5.585682	-6.121314	-6.399784
ENSMUSP00000091180	6	9	7	1	0	3	6	11	5	-8.098835	-9.794505	-8.373444
ENSMUSP00000095845	18	18	25	4	0	4	19	17	24	-6.684256	-8.811215	-6.974995
ENSMUSP00000035761	12	15	18	7	11	11	20	6	5	-9.736251	-10.40054	-10.36913
ENSMUSP00000021375	30	29	31	18	17	29	45	32	55	-7.292823	-7.869632	-7.189646
ENSMUSP00000000756	33	46	39	36	30	26	16	22	16	-5.760796	-6.248657	-6.802402
ENSMUSP00000107914	2	1	3	1	0	0	2	0	3	-9.02594	-10.36882	-9.443786
ENSMUSP00000023583	15	6	11	3	4	6	4	6	3	-7.461226	-	-8.573492

											8.541375	
ENSMUSP00000007130	2	3	3	1	0	1	5	3	0	-9.550334	-10.79255	-9.824943
ENSMUSP00000039202	11	10	9	3	0	2	11	21	5	-7.314951	-9.13644	-7.388851
ENSMUSP00000001460	74	77	75	43	46	71	100	89	84	-6.551432	-7.13658	-6.638234
ENSMUSP00000023087	1	6	1	0	0	0	0	3	0	-8.794364	-10.88642	-9.816965
ENSMUSP00000021133	8	13	12	1	5	3	27	33	20	-8.068426	-9.500942	-7.48328
ENSMUSP00000031355	12	6	11	0	3	1	25	17	22	-8.607965	-10.56443	-8.118134
ENSMUSP00000033093	3	6	6	2	0	0	2	3	2	-7.614013	-9.4086	-8.552295
ENSMUSP00000107937	35	19	31	11	17	18	28	38	32	-5.913937	-6.755907	-6.048523
ENSMUSP00000072199	1	17	12	0	0	0	9	4	10	-8.489791	-11.78103	-9.015774
ENSMUSP00000026538	31	26	9	6	6	4	68	72	84	-6.591538	-8.184238	-5.659886
ENSMUSP00000025835	67	80	39	26	34	18	8	16	5	-6.599444	-7.700005	-8.690287
ENSMUSP00000086021	25	12	21	11	5	9	9	19	7	-5.941864	-6.993326	-6.705207
ENSMUSP00000001715	4	5	4	2	0	0	8	11	14	-7.990433	-9.655752	-7.397965
ENSMUSP00000021793	5	6	5	4	4	5	2	0	0	-8.023985	-8.454607	-9.909551
ENSMUSP00000071616	72	50	43	42	38	33	47	65	45	-5.685433	-6.302363	-6.009284
ENSMUSP00000015011	57	49	58	52	52	60	24	22	11	-5.659092	-5.901583	-6.973718
ENSMUSP00000106359	13	20	16	13	10	9	2	9	4	-6.626321	-7.279308	-8.019814
ENSMUSP00000036386	15	16	14	11	14	9	12	11	12	-7.111583	-7.624038	-7.628371
ENSMUSP00000066035	1	5	1	0	0	0	5	8	5	-9.169378	-11.15013	-8.613197
ENSMUSP00000025833	5	5	7	1	2	0	18	30	32	-8.68894	-10.34624	-7.480439
ENSMUSP00000032168	71	119	99	49	65	55	15	32	13	-5.637082	-6.412458	-7.464342
ENSMUSP00000063825	184	103	63	42	23	38	211	184	215	-6.355842	-7.811401	-6.076737
ENSMUSP00000072084	4	2	3	1	2	1	2	5	2	-9.171052	-10.06075	-9.445661
ENSMUSP00000056433	2	2	2	0	0	1	0	2	2	-8.364854	-9.707733	-8.94994
ENSMUSP00000082125	7	12	13	2	0	2	0	2	0	-7.685977	-	-10.22107

											9.736276	
ENSMUSP00000031617	110	112	133	80	87	111	46	64	47	-4.98881	-5.474638	-6.074021
ENSMUSP00000038214	6	13	7	1	2	0	24	13	28	-8.794088	-10.84792	-8.185539
ENSMUSP00000035010	6	10	11	5	3	2	1	2	0	-8.539729	-9.690123	-10.66141
ENSMUSP00000079379	5	9	9	3	2	4	35	23	31	-8.364338	-9.454489	-7.332072
ENSMUSP00000075321	19	15	52	0	4	0	37	53	0	-6.425871	-9.436386	-6.655776
ENSMUSP00000006703	9	6	1	0	0	0	2	0	1	-9.141902	-11.84519	-10.77573
ENSMUSP00000052544	7	6	8	1	0	2	8	8	7	-7.941662	-9.794774	-8.131089
ENSMUSP00000034058	5	6	11	2	0	0	5	4	1	-7.431612	-9.579958	-8.421169
ENSMUSP00000026667	8	5	9	0	0	2	11	13	10	-8.042746	-10.19109	-7.904726
ENSMUSP00000042860	1	4	9	0	0	0	4	14	5	-7.648122	-10.23	-7.46474
ENSMUSP00000028683	138	196	156	62	66	108	35	37	26	-5.192141	-6.161941	-7.064107
ENSMUSP00000028592	15	7	9	2	4	4	1	3	2	-7.622048	-8.903806	-9.363676
ENSMUSP00000026122	50	82	38	24	18	22	25	48	30	-6.252087	-7.457174	-7.022116
ENSMUSP00000004072	38	55	45	35	26	27	31	34	21	-5.747768	-6.434112	-6.48883
ENSMUSP00000076521	18	58	38	6	7	9	0	6	1	-6.885191	-8.720178	-9.769729
ENSMUSP00000001479	11	12	18	2	5	1	29	28	35	-8.179974	-9.921221	-7.66604
ENSMUSP00000020238	115	179	149	40	44	79	108	107	71	-5.782772	-7.019328	-6.493116
ENSMUSP00000027123	79	95	63	40	20	35	162	119	115	-5.988472	-7.135831	-5.752244
ENSMUSP00000075513	78	67	23	4	2	0	94	98	119	-6.073039	-9.434328	-5.735878
ENSMUSP00000019512	4	6	1	0	0	0	3	6	7	-8.657024	-11.02369	-8.595009
ENSMUSP00000099453	36	43	44	5	0	2	131	117	99	-6.747364	-9.674823	-5.992606
ENSMUSP00000111081	38	38	34	2	1	9	7	9	0	-6.609907	-8.964166	-8.736659
ENSMUSP00000039269	27	33	27	24	22	19	39	36	28	-6.800515	-7.328832	-6.908928
ENSMUSP00000101823	189	174	187	134	100	152	0	0	0	-4.81141	-5.406832	-10.99762

ENSMUSP00000099841	3	6	4	0	0	1	14	12	3	-7.898766	-9.901318	-7.429556
ENSMUSP00000078774	20	15	9	0	2	1	15	16	17	-7.381897	-9.939355	-7.572233
ENSMUSP00000023760	9	15	11	6	4	3	12	19	16	-7.380791	-8.546722	-7.371103
ENSMUSP00000052912	69	107	80	32	45	43	63	74	50	-5.688265	-6.681891	-6.274805
ENSMUSP00000005122	4	5	1	0	0	0	6	12	13	-8.585577	-10.86881	-7.820919
ENSMUSP00000100000	17	19	30	3	0	0	42	36	19	-7.512264	-10.46418	-7.408912
ENSMUSP00000039472	8	14	2	0	0	0	0	0	0	-8.117026	-11.19691	-11.22903
ENSMUSP00000042351	76	77	58	42	23	22	148	192	155	-5.776584	-6.895058	-5.202533
ENSMUSP00000024988	11	27	22	0	2	1	0	0	0	-8.462546	-11.32137	-12.45506
ENSMUSP00000033012	38	32	38	8	3	11	32	23	33	-7.330545	-9.112183	-7.806853
ENSMUSP00000048111	6	6	16	1	1	2	19	29	14	-7.298042	-9.221159	-6.80588
ENSMUSP00000020315	34	41	37	5	13	11	53	48	64	-7.53596	-9.092687	-7.427358
ENSMUSP00000111471	6	10	4	0	1	0	3	3	3	-8.648935	-11.04554	-9.640545
ENSMUSP00000111363	4	4	1	0	0	0	1	2	1	-7.887638	-10.07985	-8.80945
ENSMUSP00000095129:reversed	4	4	1	0	0	0	0	0	0	-8.733339	-10.92555	-10.95766
ENSMUSP00000031897	24	24	23	6	1	3	16	23	23	-6.316576	-8.400793	-6.723744
ENSMUSP00000002064	2	4	1	0	0	0	3	5	3	-8.725841	-10.70659	-8.614537
ENSMUSP00000087118	2	4	1	0	0	0	0	6	4	-8.991644	-10.97239	-8.963768
ENSMUSP00000086165	1	4	2	0	0	0	0	3	1	-8.224917	-10.20567	-8.93527
ENSMUSP00000078382	1	4	2	0	0	0	1	1	0	-9.144159	-11.12491	-10.30719
ENSMUSP00000033871	20	32	26	14	12	13	10	8	5	-6.468335	-7.385362	-7.920215
ENSMUSP00000038755	17	12	10	6	3	4	63	77	51	-6.761503	-8.031442	-5.477188
ENSMUSP00000079246	4	5	4	3	2	2	6	10	6	-7.695425	-8.472322	-7.487006
ENSMUSP00000023214	4	7	7	0	1	0	0	0	0	-8.423043	-10.72198	-11.2667

ENSMUSP00000034453	85	83	84	63	55	73	143	139	122	-5.555912	-6.073679	-5.360754
ENSMUSP00000098963	8	5	3	1	1	1	4	6	5	-8.511739	-10.11345	-8.845211
ENSMUSP00000026585	1	3	4	0	0	0	1	0	0	-8.361084	-10.45314	-9.972656
ENSMUSP00000098000	1	3	4	0	0	0	5	7	2	-8.09872	-10.19078	-7.88351
ENSMUSP00000038878	14	20	12	7	6	5	66	64	68	-7.474539	-8.607547	-6.313957
ENSMUSP00000066878	9	4	7	1	1	2	20	12	19	-8.404873	-10.01157	-7.786539
ENSMUSP00000109237	35	46	51	9	16	16	106	93	109	-7.039381	-8.426576	-6.473104
ENSMUSP00000099461	1	1	3	0	0	0	5	8	2	-8.400571	-10.11282	-7.743002
ENSMUSP00000033230	4	1	4	0	0	0	3	3	2	-8.775599	-10.96781	-9.150357
ENSMUSP00000001806	8	18	12	1	0	1	34	30	34	-7.804582	-10.47234	-7.155232
ENSMUSP00000069418	3	16	7	0	0	0	1	2	0	-9.301289	-12.4567	-11.38724
ENSMUSP00000019109	3	3	1	0	0	0	0	0	0	-8.553618	-10.53437	-10.56648
ENSMUSP00000046101	163	106	80	9	21	19	171	137	166	-6.051268	-8.23126	-6.020866
ENSMUSP00000022706	23	18	17	3	4	7	59	45	37	-7.181736	-8.769681	-6.582914
ENSMUSP00000021639	7	8	2	0	0	0	16	0	21	-8.348192	-11.10707	-7.889726
ENSMUSP00000107544	1	3	3	0	0	0	0	0	0	-9.126319	-11.10707	-11.13919
ENSMUSP00000044288	69	67	58	3	2	0	57	45	59	-5.850815	-9.498053	-6.310312
ENSMUSP00000078429	93	83	57	29	18	26	177	150	186	-5.806174	-7.195383	-5.295027
ENSMUSP00000107492	6	7	9	0	0	1	17	13	16	-8.768476	-11.25406	-8.339212
ENSMUSP00000070983	3	3	11	0	0	0	0	4	0	-7.746712	-10.50559	-9.235192
ENSMUSP00000029769	3	2	1	0	0	0	5	6	8	-8.75729	-10.61277	-8.025815
ENSMUSP00000092157	18	7	19	1	0	0	27	24	25	-8.418816	-11.56524	-8.160798
ENSMUSP00000022120	0	0	0	0	0	0	7	9	13	-11.07484	-11.31733	-8.332964
ENSMUSP00000003572	0	0	0	0	0	0	3	1	4	-11.35683	-11.59932	-9.781874
ENSMUSP00000025846	0	0	0	0	0	0	2	1	1	-11.50221	-11.7447	-10.47431

ENSMUSP00000032508	0	0	0	0	0	0	1	2	2	-10.89414	-11.13663	-9.698991
ENSMUSP00000033050	0	0	0	0	0	0	3	6	2	-10.49641	-10.7389	-8.646845
ENSMUSP00000062215	0	0	0	0	0	0	1	5	1	-10.99033	-11.23282	-9.526679
ENSMUSP00000064557	0	0	0	0	0	0	5	6	1	-10.15123	-10.39372	-8.224664
ENSMUSP00000066413	0	0	0	0	0	0	1	2	1	-11.15874	-11.40123	-10.13083
ENSMUSP00000084114	0	0	0	0	0	0	1	1	1	-10.78553	-11.02803	-9.958569
ENSMUSP00000088334	0	0	0	0	0	0	2	1	1	-11.47108	-11.71357	-10.44317
ENSMUSP00000088663	0	0	0	0	0	0	1	2	2	-10.49641	-10.7389	-9.301263
ENSMUSP00000097097:reversed	0	0	0	0	0	0	1	1	2	-11.63005	-11.87254	-10.60214
ENSMUSP00000098112	0	0	0	0	0	0	1	1	1	-10.86857	-11.11106	-10.0416
ENSMUSP00000107983	0	0	0	0	0	0	2	1	3	-10.81539	-11.05788	-9.477005
ENSMUSP00000111892	0	0	0	0	0	0	60	85	53	-9.803261	-10.04575	-5.183114
ENSMUSP00000029564	0	0	0	0	0	0	1	4	2	-10.03904	-10.28153	-8.575391
ENSMUSP00000027766	0	0	0	0	0	0	3	4	4	-11.22504	-11.46754	-9.375482
ENSMUSP00000034529	0	0	0	0	0	0	2	2	2	-11.46231	-11.70481	-10.12393
ENSMUSP00000035208:reversed	0	0	0	0	0	0	1	1	1	-12.98947	-13.23196	-12.1625
ENSMUSP00000047376	0	0	0	0	0	0	5	7	4	-11.14674	-11.38924	-8.960557
ENSMUSP00000014546	0	0	0	0	0	0	1	2	1	-10.73901	-10.98151	-9.711109
ENSMUSP00000020886	0	0	0	0	0	0	3	2	3	-10.96713	-11.20963	-9.392176
ENSMUSP00000029125	0	0	0	0	0	0	1	2	1	-10.39297	-10.63546	-9.365067
ENSMUSP00000030935	0	0	0	0	0	0	5	9	4	-10.02987	-10.27236	-7.735427
ENSMUSP00000035237	0	0	0	0	0	0	1	1	1	-11.63746	-11.87995	-10.81049
ENSMUSP00000043703:reversed	0	0	0	0	0	0	2	3	1	-11.71899	-11.96148	-10.38061
ENSMUSP00000045998	0	0	0	0	0	0	1	2	4	-11.77203	-12.01452	-10.30838
ENSMUSP00000051033	0	0	0	0	0	0	184	175	213	-10.86258	-11.10507	-5.186463

ENSMUSP00000075722	0	0	0	0	0	0	1	3	8	-11.09092	-11.33341	-9.164353
ENSMUSP00000079905	0	0	0	0	0	0	31	48	40	-9.982688	-10.22518	-5.866728
ENSMUSP00000097582	0	0	0	0	0	0	2	2	1	-10.29894	-10.54143	-9.103798
ENSMUSP00000108098	0	0	0	0	0	0	2	1	3	-11.04523	-11.28772	-9.706848
ENSMUSP00000111551	0	0	0	0	0	0	3	1	2	-10.44603	-10.68852	-9.107645
sp|CAS2_BOVIN|	0	0	0	0	0	0	25	10	18	-10.21065	-10.45314	-6.888206
ENSMUSP00000007708:reversed	0	0	0	0	0	0	1	1	1	-11.13155	-11.37404	-10.30458
ENSMUSP00000034391	0	0	0	0	0	0	1	1	1	-11.22365	-11.46614	-10.39668
ENSMUSP00000063548	0	0	0	0	0	0	1	2	1	-10.98502	-11.22751	-9.957118
ENSMUSP00000073102	0	0	0	0	0	0	7	6	9	-10.48478	-10.72727	-8.003697
ENSMUSP00000073861	0	0	0	0	0	0	4	2	3	-10.94524	-11.18773	-9.270127
ENSMUSP00000076093	0	0	0	0	0	0	1	1	1	-12.92509	-13.16758	-12.09813
ENSMUSP00000078845:reversed	0	0	0	0	0	0	2	2	2	-11.18811	-11.4306	-9.849727
ENSMUSP00000099420:reversed	0	0	0	0	0	0	1	1	1	-10.99561	-11.2381	-10.16864
ENSMUSP00000106953	0	0	0	0	0	0	3	11	10	-9.377357	-9.619848	-6.814574
ENSMUSP00000043821	51	32	27	10	6	9	90	91	114	-6.763518	-8.443081	-6.060067
ENSMUSP00000073459	4	18	8	0	0	0	12	11	12	-7.607571	-10.89881	-7.734827
ENSMUSP00000028892	1	2	3	0	0	0	4	1	2	-9.081984	-10.93747	-9.231325
ENSMUSP00000013773	5	19	6	0	0	0	20	23	17	-9.397276	-12.68852	-9.002732
ENSMUSP00000024944	2	3	7	0	0	0	0	0	0	-9.109373	-11.55304	-11.58515
ENSMUSP00000076777	132	114	85	37	22	33	192	186	0	-5.460981	-6.972202	-5.603373
ENSMUSP00000047054	3	1	3	0	0	0	1	0	0	-9.542394	-11.52314	-11.04266
ENSMUSP00000077040	1	2	1	0	0	0	4	1	0	-11.68982	-13.23482	-11.79719
ENSMUSP00000043220:reversed	1	2	1	0	0	0	1	0	1	-10.04819	-11.59319	-10.77547
ENSMUSP00000038339	1	2	1	0	0	0	3	4	5	-9.627851	-11.17286	-9.003802

ENSMUSP00000022196	1	2	1	0	0	0	0	1	0	-10.45978	-12.00479	-11.5243
ENSMUSP00000030742	1	2	1	0	0	0	1	1	0	-9.346392	-10.8914	-10.07368
ENSMUSP00000054370	8	13	11	1	0	0	32	29	17	-7.651115	-10.49132	-7.061397
ENSMUSP00000007708	10	11	14	0	0	1	38	33	29	-7.935442	-10.86143	-7.187187
ENSMUSP00000021698	101	137	125	17	15	31	218	176	212	-5.894187	-7.868625	-5.657963
ENSMUSP00000006137	16	27	31	4	3	5	56	29	46	-7.414059	-9.378398	-7.12618
ENSMUSP00000027833	48	38	47	16	11	19	61	65	69	-7.38149	-8.664907	-7.276985
ENSMUSP00000030454	32	24	37	8	12	11	40	68	46	-5.905143	-7.215128	-5.681678
ENSMUSP00000088249	301	297	139	35	31	29	393	315	411	-4.788504	-7.066134	-4.646201
ENSMUSP00000076294	24	23	22	13	11	15	15	26	14	-6.740897	-7.537769	-7.236901
ENSMUSP00000025696	21	16	15	1	1	0	25	41	35	-6.608772	-9.579958	-6.23314
ENSMUSP00000050689	29	26	31	11	16	13	0	0	0	-5.907308	-6.895829	-10.25245
ENSMUSP00000054863	30	29	23	12	10	13	13	19	17	-6.553154	-7.623282	-7.330688
ENSMUSP00000082288	91	53	43	6	3	2	220	150	154	-6.173235	-9.129592	-5.422569
ENSMUSP00000032473	25	34	21	4	2	4	22	36	39	-6.813788	-9.015032	-6.898929
ENSMUSP00000033185	3	8	4	0	0	0	1	1	0	-8.488313	-11.13274	-10.31502
ENSMUSP00000002389	2	4	2	0	0	0	0	0	0	-9.599459	-11.69152	-11.72363
ENSMUSP00000101002	1	2	2	0	0	0	14	19	20	-8.752369	-10.46461	-6.899679
ENSMUSP00000031105	1	2	2	0	0	0	5	10	12	-8.591862	-10.30411	-7.387579
ENSMUSP00000024739	177	212	191	29	49	44	350	299	337	-5.409228	-7.201132	-5.154266
ENSMUSP00000099904	143	122	116	63	67	74	343	286	335	-5.248469	-6.112258	-4.59715
ENSMUSP00000101833	1	1	2	0	0	0	0	0	0	-9.4205	-10.96551	-10.99762
ENSMUSP00000039243	1	1	2	0	0	0	2	9	5	-9.717357	-11.26236	-8.833683
ENSMUSP00000086716	3	3	7	0	0	0	18	0	8	-10.34977	-12.86493	-9.984125
ENSMUSP00000086626	8	3	8	0	0	0	7	11	18	-9.101618	-	-8.772164

											11.96318	
ENSMUSP00000099807	4	4	2	0	0	0	0	0	0	-9.167424	-11.45066	-11.48278
ENSMUSP00000027144	1313	1212	963	472	417	418	2583	2329	2332	-4.298979	-5.52235	-3.842964
ENSMUSP00000071135	143	180	149	36	42	48	220	224	216	-5.097433	-6.651998	-5.03768
ENSMUSP00000110006:reversed	2	4	3	0	0	0	5	4	2	-9.998698	-12.19091	-10.09885
ENSMUSP00000105647	2	2	4	0	0	0	0	1	0	-9.000912	-11.09297	-10.61248
ENSMUSP00000095316	19	23	22	9	9	10	29	36	36	-7.013232	-8.053507	-6.839991
ENSMUSP00000042457	283	284	203	63	64	68	389	377	398	-4.619273	-6.229464	-4.48131
ENSMUSP00000042342	181	229	181	55	57	64	287	288	297	-4.877255	-6.325153	-4.763703
ENSMUSP00000034818	9	5	4	0	0	0	8	10	8	-8.062335	-10.87387	-7.993073
ENSMUSP00000044556	47	36	33	12	10	9	153	122	172	-6.67653	-8.204368	-5.611627
ENSMUSP00000097469	7	17	11	0	0	0	0	15	15	-7.785367	-11.22396	-8.207329
ENSMUSP00000031103	83	50	45	4	5	3	161	152	153	-6.167132	-8.997564	-5.484494
ENSMUSP00000021114	8	12	6	0	0	0	18	15	20	-7.784423	-10.93983	-7.374897
ENSMUSP00000020286	8	6	4	0	0	0	13	19	14	-7.867819	-10.67936	-7.251911
ENSMUSP00000060246	176	207	172	46	49	54	238	246	238	-4.941946	-6.492174	-4.954118
ENSMUSP00000050292	5	5	3	0	0	0	4	7	2	-7.608413	-10.12357	-7.883022
ENSMUSP00000027824	6	9	5	0	0	0	0	2	0	-7.551596	-10.46081	-9.643085
ENSMUSP00000108734	3	3	2	0	0	0	3	6	6	-8.24714	-10.3392	-7.969383
ENSMUSP00000068086	2	3	3	0	0	0	26	8	9	-9.050378	-11.14244	-7.780239
ENSMUSP00000034808	5	8	9	0	0	0	0	0	0	-7.584637	-10.58282	-10.61494
ENSMUSP00000030187	15	25	13	0	0	0	25	32	36	-8.952811	-12.79236	-8.676969
ENSMUSP00000026168	3	2	2	0	0	0	1	0	1	-9.941684	-11.92243	-11.10471
ENSMUSP00000102254	2	2	3	0	0	0	1	3	4	-8.959083	-10.93983	-9.122384
ENSMUSP00000026012	20	22	41	0	0	0	0	0	0	-6.97043	-11.24857	-11.28069

ENSMUSP00000064849	30	22	49	0	0	0	80	76	61	-6.267636	-10.7389	-5.785287
ENSMUSP00000101862	17	14	18	5	4	4	20	23	21	-7.37332	-8.863963	-7.387822
ENSMUSP00000047761	12	18	12	0	0	0	44	28	38	-7.593745	-11.20782	-6.926997
ENSMUSP00000020034	5	3	4	0	0	0	12	15	8	-8.318094	-10.76176	-7.59777
ENSMUSP00000070682	14	13	10	0	0	0	29	33	36	-7.594915	-11.08687	-6.919918
ENSMUSP00000036337	3	3	4	0	0	0	22	11	8	-8.244015	-10.52725	-7.211045
ENSMUSP00000024860	11	14	15	0	0	0	32	30	33	-7.735636	-11.30264	-7.166304
ENSMUSP00000051366	1	1	1	0	0	0	3	5	1	-9.904503	-11.24857	-9.330969
ENSMUSP00000110576	1	1	1	0	0	0	0	0	0	-9.752953	-11.09702	-11.12914
ENSMUSP00000052174:reversed	1	1	1	0	0	0	0	0	0	-9.874545	-11.21861	-11.25073
ENSMUSP00000099403	9	9	12	0	0	0	14	14	6	-8.323848	-11.61509	-8.478888
ENSMUSP00000022369	21	14	19	0	0	0	16	27	19	-8.096066	-11.95379	-8.236003
ENSMUSP00000044554	5	5	6	0	0	0	5	5	7	-8.8459	-11.54919	-9.064919
ENSMUSP00000021506	3	3	3	0	0	0	0	0	0	-8.846582	-11.03879	-11.07091
ENSMUSP00000108953	57	50	70	0	0	0	130	130	0	-6.299384	-11.3254	-6.192135
ENSMUSP00000035823	11	9	10	0	0	0	6	8	16	-8.627645	-11.91889	-8.902254

Supplementary Table 8
(continued)

Protein identification from control, non-cachectic and cachectic mouse liver membrane preparations

Identifier: ENSEMBL number
LogNSAF(cachectic/control/non-cachectic): log of the individual NSAF
Log p.value: p value
ratio: fold change difference compared to the control
invratio: inverse of the ratio

Identifier	Log.NSAF.cachectic_3.csv	Log.NSAF.cachectic_2.csv	Log.NSAF.cachectic_1.csv	Log.NSAF.control_1.csv	Log.NSAF.control_2.csv	Log.NSAF.control_3.csv	Log.NSAF.nc_1.csv	Log.NSAF.nc_2.csv	Log.NSAF.nc_3.csv	Log.p.value	ratio	invratio
ENSMUSP00000068282	-11.08277	-11.00059	-11.09447	-5.40878	-5.37183	-5.48544	-11.28942	-11.42272	-5.62204	0.00000	0.00355	281.37018
ENSMUSP00000071573	-10.55033	-10.46816	-10.56203	-5.04535	-5.22221	-5.25817	-5.68367	-5.57266	-5.82912	0.00000	0.00471	212.53740
ENSMUSP00000037665	-11.03217	-10.94999	-11.04387	-5.23712	-5.14839	-5.41666	-6.04702	-6.24971	-5.90792	0.00000	0.00319	313.94752
ENSMUSP00000072598	-11.08442	-11.00224	-11.09612	-5.82262	-5.74061	-5.98375	-11.29106	-6.35105	-6.06282	0.00000	0.00541	184.68903
ENSMUSP00000031633	-11.03217	-10.94999	-11.04387	-6.09238	-6.02796	-6.33447	-11.23882	-11.37212	-11.23535	0.00000	0.00769	130.04316
ENSMUSP00000052945	-12.07991	-11.99774	-12.09162	-9.76288	-9.88767	-9.87504	-10.67357	-10.80687	-10.33337	0.00000	0.10879	9.19173
ENSMUSP00000033086	-10.81463	-10.73246	-10.82634	-9.45365	-9.41134	-9.39870	-9.91971	-11.15458	-11.01781	0.00000	0.25398	3.93732
ENSMUSP00000034173	-11.09422	-11.01204	-11.10592	-7.58069	-7.80310	-7.52574	-8.35222	-8.72197	-8.34875	0.00000	0.03199	31.26025
ENSMUSP00000020266	-10.44092	-10.35874	-10.45262	-8.29100	-8.24868	-8.43680	-10.64757	-10.78087	-9.03110	0.00001	0.12284	8.14084
ENSMUSP00000102636	-10.71047	-10.62829	-10.72217	-6.91507	-6.98398	-7.34786	-10.91712	-11.05042	-10.91364	0.00001	0.02662	37.56554
ENSMUSP00000023709	-11.09747	-11.01529	-11.10917	-7.11100	-6.55783	-6.77927	-6.81109	-11.43741	-6.92681	0.00001	0.01384	72.24465
ENSMUSP00000004478	-11.46269	-11.38052	-11.47440	-10.61313	-10.57081	-10.55818	-11.66934	-11.80264	-11.66587	0.00001	0.42355	2.36099
ENSMUSP00000017597	-10.75482	-10.67264	-10.76652	-9.90525	-9.86293	-9.85030	-9.85989	-11.09476	-9.00828	0.00001	0.42355	2.36099
ENSMUSP00000004396	-9.57044	-9.48826	-9.58214	-8.72087	-8.67855	-8.66592	-9.77709	-9.91038	-9.77361	0.00001	0.42355	2.36099
ENSMUSP00000094929	-11.39161	-11.30943	-11.40331	-10.54205	-10.49973	-10.48709	-11.59826	-11.73156	-11.59479	0.00001	0.42355	2.36099
ENSMUSP00000077972	-10.94547	-10.86330	-10.95718	-10.09591	-10.05359	-10.04096	-11.15212	-11.28542	-11.14865	0.00001	0.42355	2.36099
ENSMUSP00000072558	-9.76635	-9.68417	-9.77805	-6.12219	-5.48301	-5.98876	-9.97300	-10.10630	-9.96952	0.00004	0.01993	50.17613
ENSMUSP00000099436	-10.10632	-10.02414	-10.11802	-7.95640	-7.91408	-7.59118	-8.36325	-8.24510	-8.35978	0.00005	0.10291	9.71717
ENSMUSP00000066990	-9.33604	-9.25386	-9.34774	-7.63833	-7.34456	-7.58338	-9.54268	-9.67598	-7.58950	0.00005	0.16559	6.03908

ENSMUSP00000001497	-10.18603	-10.10385	-10.19773	-8.48832	-8.19455	-8.43337	-10.39267	-10.52597	-10.38920	0.00005	0.16559	6.03908
ENSMUSP00000103034	-10.87715	-10.79498	-10.88886	-7.31816	-6.71302	-7.30867	-11.08380	-7.49920	-7.64205	0.00005	0.02279	43.87083
ENSMUSP00000034046	-5.83313	-5.75921	-5.82044	-5.33015	-5.26488	-5.32272	-5.64951	-5.76077	-5.45401	0.00008	0.60698	1.64750
ENSMUSP00000057069	-11.58135	-11.49917	-11.59305	-9.88365	-9.84133	-10.16542	-11.78800	-10.30831	-11.78453	0.00011	0.20047	4.98820
ENSMUSP00000044012	-12.13539	-12.05321	-12.14709	-10.43768	-10.39536	-10.71945	-12.34203	-12.47533	-10.38885	0.00011	0.20047	4.98820
ENSMUSP00000018727	-10.92257	-10.84039	-10.93427	-9.22487	-9.51927	-9.50664	-11.12922	-11.26252	-11.12575	0.00012	0.22408	4.46276
sp|K1C15_SHEEP|	-10.86086	-10.77868	-10.87256	-7.06546	-6.06220	-6.39956	-6.62047	-11.20081	-6.52705	0.00013	0.01224	81.70259
ENSMUSP00000032074	-10.22167	-10.13950	-10.23337	-8.52397	-8.81837	-8.46901	-10.42832	-10.56162	-10.42485	0.00014	0.20047	4.98820
ENSMUSP00000039784	-9.81426	-9.73208	-9.82596	-7.35408	-7.82278	-7.81015	-8.40792	-10.15421	-10.01744	0.00017	0.11539	8.66629
ENSMUSP00000029387	-11.14030	-11.05812	-11.15200	-9.77932	-9.40027	-9.38764	-10.24537	-11.48024	-11.34347	0.00027	0.20047	4.98820
ENSMUSP00000040580	-10.60749	-10.52531	-10.61919	-8.65833	-8.86747	-9.19156	-9.20115	-10.94744	-10.81067	0.00044	0.18137	5.51364
ENSMUSP00000073444	-5.84476	-5.79555	-5.74409	-5.29366	-5.26108	-5.37883	-5.84681	-5.62740	-5.52207	0.00045	0.61616	1.62295
ENSMUSP00000059943	-9.11525	-9.03307	-9.12695	-7.16609	-7.71195	-7.36259	-9.32190	-9.45520	-9.31842	0.00049	0.18137	5.51364
ENSMUSP00000034860	-7.22634	-6.87327	-6.67522	-4.88966	-4.99844	-5.21626	-6.46047	-6.18550	-6.04872	0.00055	0.15312	6.53076
ENSMUSP00000089691	-6.61974	-6.57757	-6.48572	-6.00774	-6.06986	-6.11385	-6.31553	-6.04728	-6.52061	0.00058	0.60848	1.64344
ENSMUSP00000026462	-5.47566	-5.51204	-5.38138	-4.67566	-4.72887	-4.88199	-5.28724	-5.27298	-5.47703	0.00069	0.49841	2.00639
ENSMUSP00000074990	-5.81052	-5.82198	-5.78925	-5.22162	-5.17930	-5.36895	-6.55061	-6.74275	-6.26661	0.00070	0.57452	1.74059
ENSMUSP00000081370	-7.27525	-7.24070	-7.43725	-5.99507	-6.09277	-6.35824	-7.74662	-7.48456	-7.87238	0.00071	0.30654	3.26217
ENSMUSP00000003100	-5.87634	-5.74737	-5.54644	-4.76475	-4.85312	-4.78945	-5.34018	-5.50239	-5.25996	0.00076	0.40204	2.48732
ENSMUSP00000082352	-8.33221	-8.25003	-7.97604	-7.01986	-6.80690	-7.06255	-7.79139	-7.31367	-7.78791	0.00079	0.29695	3.36760
ENSMUSP00000029569	-10.55870	-10.47652	-10.57040	-8.60954	-9.15540	-9.14277	-9.66378	-10.89865	-10.76188	0.00101	0.20047	4.98820
sp|K1C10_HUMAN|	-5.31053	-5.35779	-5.36133	-4.95785	-4.83187	-4.75701	-4.82883	-4.92124	-4.98138	0.00125	0.60944	1.64085
ENSMUSP00000065796	-7.02767	-6.98396	-7.34613	-6.19367	-6.21717	-6.07697	-7.70815	-11.34227	-7.09025	0.00143	0.38690	2.58464
ENSMUSP00000031195	-7.32216	-7.23998	-6.95189	-6.25389	-6.12819	-6.28991	-7.43985	-7.53147	-7.14337	0.00151	0.39312	2.54375
ENSMUSP00000057732	-5.62594	-5.51499	-5.51420	-5.00796	-5.16089	-5.12619	-5.58778	-5.56285	-5.68019	0.00158	0.63354	1.57843
ENSMUSP00000034567	-8.99205	-8.90987	-9.00375	-8.14512	-8.26317	-7.88946	-8.26013	-8.31003	-8.25665	0.00160	0.41443	2.41294
ENSMUSP00000023832	-8.08181	-7.83251	-8.09351	-6.72406	-7.02554	-6.53329	-7.64164	-7.45210	-8.28498	0.00173	0.28402	3.52085
ENSMUSP00000026398	-6.45289	-6.32904	-6.11002	-5.46123	-5.53594	-5.56556	-5.95577	-5.73765	-5.79663	0.00178	0.46470	2.15194
ENSMUSP00000028807	-10.81032	-10.72815	-10.82203	-9.11262	-9.40703	-8.60545	-11.01697	-9.53728	-11.01350	0.00178	0.16559	6.03908
ENSMUSP00000045351	-10.88320	-10.80102	-10.89490	-9.52222	-9.47990	-9.97868	-11.08985	-11.22315	-11.08637	0.00179	0.29309	3.41188
ENSMUSP00000002840	-11.62437	-11.54219	-11.63607	-10.26339	-10.22107	-10.71985	-11.83102	-11.96432	-11.82755	0.00179	0.29309	3.41188
ENSMUSP00000047551	-7.26811	-7.13591	-7.80796	-5.55957	-5.40147	-5.85564	-6.58437	-11.27594	-11.13917	0.00183	0.16763	5.96569
ENSMUSP00000066958	-11.18731	-11.10513	-11.19901	-9.48960	-8.99507	-8.43572	-9.19279	-9.32609	-10.28891	0.00201	0.10291	9.71717
ENSMUSP00000030299	-6.94854	-6.83302	-6.89464	-6.02576	-6.02623	-6.33274	-7.47155	-7.47422	-7.11838	0.00208	0.45998	2.17402
ENSMUSP00000004381	-8.60039	-8.71897	-8.61209	-8.11459	-8.26336	-8.05963	-9.25925	-8.63007	-9.25578	0.00225	0.60766	1.64565

ENSMUSP00000027478	-8.10990	-8.02772	-8.28872	-7.43015	-7.38783	-7.11047	-8.31655	-8.61697	-8.48019	0.00275	0.43250	2.31215
ENSMUSP00000043061	-10.47472	-10.39254	-10.48642	-9.11374	-9.58283	-9.57020	-10.68136	-10.81466	-10.67789	0.00281	0.34645	2.88643
ENSMUSP00000042095	-10.81678	-10.73461	-10.82848	-9.45580	-9.92490	-9.91226	-11.02343	-11.15673	-11.01996	0.00281	0.34645	2.88643
ENSMUSP00000065425	-10.58068	-10.49850	-10.59238	-9.21970	-9.68880	-9.67616	-8.83761	-10.92063	-9.68228	0.00281	0.34645	2.88643
ENSMUSP00000061851	-7.17223	-6.90344	-6.87717	-6.16774	-5.90373	-6.22058	-6.80828	-7.06482	-6.69510	0.00285	0.41098	2.43320
ENSMUSP00000001834	-8.58421	-8.33492	-8.59591	-7.62292	-7.82425	-7.46530	-8.48060	-9.37638	-8.98815	0.00296	0.41676	2.39946
ENSMUSP00000032078	-7.83970	-8.26847	-8.23715	-7.23295	-7.15729	-7.24820	-7.18758	-7.42814	-6.99896	0.00305	0.41503	2.40945
ENSMUSP00000035417	-11.10554	-11.02336	-11.11724	-8.64535	-9.11406	-9.68960	-8.36354	-11.44549	-8.36007	0.00312	0.13131	7.61540
ENSMUSP00000025279	-11.93663	-11.85445	-11.94833	-10.57565	-9.94515	-9.56464	-12.14328	-12.27658	-12.13980	0.00313	0.14104	7.08996
ENSMUSP00000021370	-10.90504	-10.82287	-10.91675	-10.05548	-9.50175	-9.48911	-9.49870	-10.14342	-10.00665	0.00316	0.29309	3.41188
ENSMUSP00000024963	-9.76019	-9.67802	-9.77189	-8.91063	-8.35689	-8.34426	-9.96684	-10.10014	-9.96337	0.00316	0.29309	3.41188
ENSMUSP00000000394	-11.24488	-11.16270	-11.25658	-10.39532	-9.84158	-9.82894	-10.34995	-10.48325	-10.34648	0.00316	0.29309	3.41188
ENSMUSP00000001183	-7.19653	-7.25094	-7.76261	-6.30819	-6.22587	-6.22639	-6.58045	-6.65918	-5.98709	0.00323	0.32494	3.07754
ENSMUSP00000034624	-8.85411	-9.62007	-8.61435	-7.15966	-6.59029	-6.91898	-8.80930	-8.43158	-8.43795	0.00345	0.12669	7.89297
ENSMUSP00000041442	-10.71047	-9.52672	-10.72217	-7.46167	-7.87141	-7.85877	-9.30413	-11.05042	-10.91364	0.00348	0.08475	11.79933
ENSMUSP00000086530	-5.59596	-5.47029	-5.26485	-4.64532	-4.54339	-4.82054	-5.19525	-5.18448	-4.94046	0.00356	0.46293	2.16014
ENSMUSP00000051293	-9.34562	-9.01198	-9.35732	-8.49859	-8.13344	-8.19228	-11.50198	-11.63528	-11.49851	0.00384	0.38052	2.62801
ENSMUSP00000086528	-5.35081	-5.34087	-5.23203	-4.76251	-4.78543	-4.97883	-5.24313	-5.32679	-5.07143	0.00404	0.62549	1.59874
ENSMUSP00000022976	-11.87302	-11.79084	-11.88472	-11.02346	-10.46972	-10.96850	-12.07967	-12.21297	-12.07620	0.00450	0.34645	2.88643
ENSMUSP00000051621	-9.66303	-9.58085	-9.67473	-8.81347	-8.25973	-8.75851	-9.86968	-8.38999	-9.86621	0.00450	0.34645	2.88643
sp|K1C9_HUMAN|	-6.20917	-6.38263	-6.25141	-5.51378	-4.97591	-5.41323	-5.49801	-5.78696	-5.46495	0.00480	0.36771	2.71954
ENSMUSP00000101999	-10.72233	-10.64015	-9.63246	-7.75120	-8.36297	-8.20719	-10.92898	-9.96070	-10.92551	0.00492	0.11994	8.33758
ENSMUSP00000034414	-10.53053	-10.44835	-10.54223	-8.83282	-9.12723	-9.62601	-10.73718	-10.87048	-10.73371	0.00493	0.25398	3.93732
ENSMUSP00000051441	-10.92064	-10.83846	-10.93234	-9.22293	-9.51734	-10.01612	-11.12729	-11.26059	-11.12382	0.00493	0.25398	3.93732
ENSMUSP00000029240	-8.61455	-9.32131	-9.07846	-7.83020	-7.25152	-7.35904	-8.08339	-9.40671	-7.99652	0.00505	0.22365	4.47134
ENSMUSP00000034623	-10.16977	-10.08759	-10.18147	-9.32020	-9.27788	-8.75383	-10.37641	-10.50971	-10.37294	0.00507	0.34645	2.88643
ENSMUSP00000111510	-11.07617	-10.99399	-11.08787	-10.22661	-10.18429	-9.66024	-10.18125	-11.41612	-10.17777	0.00507	0.34645	2.88643
sp|K2C1_HUMAN|	-5.36132	-5.62417	-5.51659	-4.91563	-4.60202	-4.89766	-4.81723	-5.07570	-4.76887	0.00543	0.49858	2.00570
ENSMUSP00000086418	-8.02742	-8.04535	-8.03912	-7.47369	-7.07680	-6.92504	-7.27113	-7.40443	-7.26766	0.00581	0.40695	2.45728
ENSMUSP00000025713	-8.86492	-8.78274	-8.87662	-7.84351	-7.80119	-8.29950	-9.91971	-11.15458	-11.01781	0.00608	0.41156	2.42978
ENSMUSP00000017946	-10.91870	-10.83653	-10.93041	-9.55772	-10.02682	-9.16604	-11.12535	-11.25865	-11.12188	0.00636	0.25398	3.93732
ENSMUSP00000051700	-7.92764	-7.56584	-7.61209	-7.12491	-6.84382	-6.90462	-8.27246	-8.20506	-11.56910	0.00637	0.47735	2.09488
ENSMUSP00000034848	-10.35957	-10.27739	-10.37127	-8.66187	-8.61955	-9.45505	-8.95323	-9.59795	-10.56275	0.00647	0.22408	4.46276
ENSMUSP00000047790	-6.20025	-6.61597	-5.90965	-5.00412	-4.44729	-4.98673	-5.08639	-5.25161	-5.07250	0.00650	0.24388	4.10032
ENSMUSP00000097860	-12.19066	-12.10848	-10.58937	-9.00439	-7.63378	-7.71049	-9.82826	-10.58089	-9.99191	0.00683	0.03492	28.63730

ENSMUSP00000034172	-7.42958	-7.16080	-7.54951	-6.28882	-6.36828	-6.73625	-7.22221	-7.46277	-7.03359	0.00697	0.39436	2.53578
ENSMUSP00000041244	-10.12792	-10.04574	-10.13962	-8.43021	-9.23604	-8.37526	-8.13340	-8.85488	-9.22952	0.00703	0.22408	4.46276
ENSMUSP00000040424	-10.18441	-9.59081	-9.34797	-8.31485	-8.35593	-8.53439	-9.54291	-11.62593	-8.65177	0.00711	0.28512	3.50727
ENSMUSP00000005923	-10.34592	-9.16217	-9.25605	-7.54918	-7.71822	-7.70558	-8.60285	-8.48470	-8.34793	0.00733	0.16193	6.17550
ENSMUSP00000031181	-7.10812	-6.79153	-7.19830	-6.33994	-6.19430	-6.43124	-7.47842	-7.24396	-6.99111	0.00734	0.49283	2.02910
ENSMUSP00000027464	-10.59952	-10.51735	-10.61122	-9.74996	-8.85950	-9.18359	-9.70460	-10.93947	-10.80270	0.00744	0.25398	3.93732
ENSMUSP00000003843	-11.26838	-11.18620	-11.28008	-10.41881	-9.52835	-9.85244	-11.47503	-11.60833	-10.36998	0.00744	0.25398	3.93732
ENSMUSP00000104806	-11.73135	-11.64918	-11.74306	-10.88179	-10.32806	-9.97869	-11.93800	-12.07130	-11.93453	0.00772	0.25398	3.93732
ENSMUSP00000107118	-10.08424	-10.00207	-8.99437	-7.38761	-8.09276	-7.44391	-9.18932	-8.47447	-9.18585	0.00793	0.14127	7.07876
ENSMUSP00000076578	-10.99696	-10.91478	-11.00866	-9.04780	-8.15790	-9.58102	-11.20360	-11.33690	-11.20013	0.00797	0.10879	9.19173
ENSMUSP00000023083	-5.76149	-5.62775	-5.64430	-5.11751	-5.14681	-5.38615	-6.03374	-6.00085	-5.98606	0.00830	0.62528	1.59929
ENSMUSP00000026208	-12.13194	-10.94818	-12.14364	-9.98201	-9.39298	-9.49160	-12.33858	-12.47188	-12.33511	0.00830	0.13525	7.39347
ENSMUSP00000034178	-8.04709	-7.29576	-7.66926	-6.46825	-6.68602	-6.25805	-7.93091	-7.22673	-7.48802	0.00860	0.30781	3.24872
ENSMUSP00000025356	-9.92487	-8.74112	-9.93657	-7.60783	-7.29717	-7.71999	-10.13152	-9.16324	-9.02647	0.00873	0.15505	6.44935
ENSMUSP00000014913	-9.14697	-9.06479	-10.26025	-7.78836	-7.50959	-7.39685	-8.50548	-7.87630	-7.88267	0.00876	0.16193	6.17550
ENSMUSP00000025196	-10.38302	-10.30085	-10.39473	-8.68532	-8.39154	-9.47851	-10.58967	-10.72297	-9.48463	0.00984	0.20047	4.98820
ENSMUSP00000084445	-9.80250	-9.72032	-9.81420	-7.85333	-8.91061	-8.04984	-8.90757	-10.14244	-10.00567	0.00985	0.20047	4.98820
ENSMUSP00000080996	-10.19805	-10.11587	-10.20975	-8.24889	-8.79475	-9.29353	-10.40470	-10.53800	-10.40123	0.01000	0.22408	4.46276
ENSMUSP00000072555	-5.09038	-4.98710	-4.87415	-4.52761	-4.47123	-4.69374	-4.88007	-4.95866	-4.65100	0.01011	0.65671	1.52274
ENSMUSP00000109355	-11.13406	-11.05189	-11.14577	-9.43636	-10.24218	-9.12995	-11.34071	-11.47401	-11.33724	0.01060	0.20047	4.98820
ENSMUSP00000028657	-9.56498	-9.48281	-8.47709	-7.41776	-7.73651	-7.42533	-9.26022	-7.78337	-8.03234	0.01071	0.21957	4.55443
ENSMUSP00000031251	-7.52001	-7.81743	-7.25722	-6.34683	-6.12008	-6.76954	-7.53556	-7.43702	-7.72319	0.01098	0.32569	3.07038
ENSMUSP00000022148	-11.09096	-9.39579	-10.00109	-7.48848	-8.16091	-7.72836	-7.85933	-8.86186	-8.24539	0.01132	0.10909	9.16686
ENSMUSP00000073061	-5.90499	-5.88842	-5.40584	-5.00678	-4.78971	-5.01403	-5.32026	-5.35759	-4.92824	0.01136	0.46434	2.15360
ENSMUSP00000037022	-9.67030	-9.58812	-8.24624	-7.24047	-7.02269	-7.10652	-8.26680	-8.18496	-8.53782	0.01179	0.16524	6.05181
ENSMUSP00000075235	-11.15876	-11.07658	-9.55747	-8.46212	-8.14531	-7.59028	-9.75242	-9.88571	-9.74894	0.01199	0.10236	9.76939
ENSMUSP00000055206	-11.36095	-11.27877	-11.37265	-10.51139	-9.62093	-9.35684	-11.56760	-11.70090	-11.56413	0.01263	0.20047	4.98820
ENSMUSP00000112236	-7.17313	-7.62515	-7.25630	-6.61797	-6.77976	-6.41990	-6.51288	-6.80276	-6.70048	0.01268	0.48198	2.07477
ENSMUSP00000032422	-10.79728	-10.71510	-9.70741	-8.84812	-8.60504	-9.04462	-9.90236	-11.13723	-11.00046	0.01345	0.23549	4.24642
ENSMUSP00000037259	-7.34996	-6.66381	-6.58653	-5.77418	-5.76374	-5.92778	-6.73752	-6.60761	-6.19772	0.01362	0.36847	2.71394
ENSMUSP00000056152	-7.09687	-7.52561	-7.52849	-6.64149	-6.78432	-6.80618	-7.24794	-7.02183	-7.24447	0.01373	0.53834	1.85756
ENSMUSP00000076735	-5.43351	-5.35134	-5.32146	-4.97750	-5.14442	-5.15384	-10.76257	-5.42339	-5.66093	0.01400	0.75483	1.32480
ENSMUSP00000028083	-10.37304	-10.29086	-10.38474	-8.22312	-9.48116	-8.36893	-10.57969	-10.71299	-10.57622	0.01411	0.16559	6.03908
ENSMUSP00000022341	-10.31095	-10.22877	-10.32265	-9.46139	-8.31947	-8.30684	-10.51760	-10.65090	-10.51413	0.01431	0.18137	5.51364
ENSMUSP00000003137	-5.04793	-5.10644	-4.99855	-4.42163	-4.41709	-4.77926	-5.08149	-4.91231	-4.91915	0.01452	0.59141	1.69088

ENSMUSP00000046585	-6.24789	-6.03457	-6.10634	-5.61859	-5.56577	-5.86282	-6.11261	-6.45669	-6.09120	0.01570	0.63415	1.57692
ENSMUSP00000002663	-6.93358	-6.48740	-7.22490	-6.08691	-5.93679	-5.98432	-7.09260	-6.72437	-6.73942	0.01593	0.42915	2.33021
ENSMUSP00000108763	-5.96747	-5.87324	-5.77190	-5.44767	-5.55624	-5.64644	-6.10391	-5.92029	-5.78352	0.01638	0.72456	1.38015
ENSMUSP00000084959	-10.53053	-9.34678	-9.44066	-7.83390	-8.33829	-7.22677	-9.12419	-8.30143	-10.73371	0.01660	0.14136	7.07397
ENSMUSP00000030051	-9.43477	-9.35259	-9.44647	-8.58521	-7.69475	-7.22990	-8.02843	-7.57355	-8.53637	0.01683	0.18137	5.51364
ENSMUSP00000010049	-10.55592	-10.47374	-10.56762	-8.60676	-8.19656	-9.65140	-10.76257	-10.89587	-10.75910	0.01683	0.15233	6.56452
ENSMUSP00000008801	-8.88816	-8.16976	-8.69910	-7.53034	-7.40285	-7.84810	-8.72693	-9.02735	-9.67951	0.01712	0.37713	2.65158
ENSMUSP00000036245	-9.07820	-10.60901	-10.70289	-7.89445	-8.06349	-8.17605	-8.32879	-9.08142	-8.18217	0.01735	0.16804	5.95088
ENSMUSP00000031183	-7.30566	-6.72196	-6.52462	-6.00558	-5.85151	-5.94082	-6.60061	-6.45797	-6.37961	0.01836	0.41944	2.38415
ENSMUSP00000039543	-10.41239	-10.33021	-10.42409	-9.05141	-9.52051	-8.20751	-10.61904	-10.75234	-10.61557	0.01917	0.20047	4.98820
ENSMUSP00000031822	-11.26564	-10.08189	-11.27734	-9.56794	-8.76314	-8.51405	-9.85930	-10.50402	-11.46882	0.01927	0.15505	6.44935
ENSMUSP00000079065	-6.14657	-6.06439	-5.77134	-5.04223	-5.06703	-5.56378	-6.43524	-5.78942	-6.05226	0.01971	0.45655	2.19036
ENSMUSP00000042188	-11.52272	-11.44055	-11.53442	-10.67316	-9.33048	-10.10679	-11.72937	-11.86267	-11.72590	0.02000	0.20047	4.98820
ENSMUSP00000053877	-10.21266	-10.64190	-10.73578	-9.87649	-8.98659	-9.07406	-12.03230	-10.55261	-10.41583	0.02015	0.28583	3.49863
ENSMUSP00000025602	-9.59930	-9.51712	-9.61100	-9.33990	-8.96085	-8.94822	-10.90752	-8.83965	-9.29106	0.02016	0.60320	1.65782
ENSMUSP00000032399	-8.94166	-9.96106	-8.95336	-8.09407	-7.68388	-8.03912	-8.63689	-8.77019	-9.14484	0.02040	0.28735	3.48009
ENSMUSP00000039663	-11.55195	-10.36820	-11.56365	-9.60279	-9.81193	-9.17996	-11.75860	-11.89190	-9.35320	0.02045	0.21924	4.56113
ENSMUSP00000000349	-7.57766	-7.14916	-7.58936	-6.52402	-6.92045	-6.31358	-7.30140	-7.35301	-7.78083	0.02053	0.41912	2.38593
ENSMUSP00000085244	-10.81382	-10.22023	-9.35805	-8.79582	-8.27059	-8.30145	-9.72011	-9.85341	-10.50558	0.02128	0.22106	4.52356
ENSMUSP00000099848:reversed	-11.68921	-10.50546	-11.70091	-9.74005	-9.94918	-9.17407	-9.69468	-9.19176	-9.32334	0.02171	0.20509	4.87583
ENSMUSP00000022317	-7.60072	-7.51854	-7.13272	-6.92096	-6.87864	-6.86601	-8.17524	-8.56000	-7.66075	0.02194	0.60494	1.65306
ENSMUSP00000073939	-8.24434	-7.39969	-8.00459	-6.83083	-7.10364	-6.77588	-7.99877	-7.31087	-8.44752	0.02247	0.39104	2.55727
ENSMUSP00000099770	-8.46276	-8.93275	-8.47446	-8.13368	-7.59416	-7.76179	-8.73194	-10.10235	-9.32936	0.02335	0.45702	2.18807
ENSMUSP00000103436	-12.10567	-12.02349	-11.01580	-10.40797	-9.47797	-10.35301	-12.31232	-12.44562	-12.30885	0.02404	0.20509	4.87583
ENSMUSP00000048832	-6.98043	-6.64689	-6.90114	-6.38502	-6.38438	-6.55835	-7.83390	-7.32038	-7.39497	0.02609	0.67019	1.49211
ENSMUSP00000092966	-11.08442	-8.60031	-9.99454	-7.25452	-7.17887	-7.66623	-9.08989	-9.81137	-9.08642	0.02632	0.12166	8.21947
ENSMUSP00000105754	-9.43465	-10.45405	-9.44636	-7.95085	-8.34399	-8.78357	-10.74288	-10.87618	-10.73940	0.02675	0.25450	3.92932
ENSMUSP00000033074	-7.65321	-8.15921	-8.25309	-7.26900	-7.49502	-7.21404	-7.49198	-7.79240	-6.91782	0.02750	0.51498	1.94184
ENSMUSP00000109150	-6.98715	-6.46239	-6.12250	-5.60123	-5.78256	-5.48412	-6.81973	-6.69230	-7.07368	0.02758	0.42896	2.33122
ENSMUSP00000101096	-9.59447	-10.61387	-10.70775	-8.74688	-8.95602	-9.28011	-9.80112	-9.93442	-9.28623	0.02798	0.30282	3.30231
ENSMUSP00000002844	-9.37917	-10.39856	-10.49244	-8.78303	-8.48926	-9.06480	-10.68739	-8.87097	-9.58234	0.02901	0.30282	3.30231
ENSMUSP00000017365	-11.08113	-9.38596	-8.89166	-7.71790	-7.43633	-7.56028	-7.52224	-7.92026	-8.06116	0.02950	0.15281	6.54402
sp|K22E_HUMAN|	-6.37828	-6.12646	-6.00430	-5.83724	-5.31969	-5.48231	-5.37006	-5.68319	-5.51701	0.02967	0.53253	1.87783
ENSMUSP00000007977	-10.31272	-9.13095	-9.22483	-8.05107	-8.40085	-8.31124	-7.95306	-7.94324	-8.24589	0.02970	0.30056	3.32712
ENSMUSP00000088246	-8.76314	-7.91848	-7.50142	-6.59103	-6.68406	-7.01374	-8.20731	-7.75269	-7.96738	0.02977	0.30398	3.28965

ENSMUSP00000097395	-10.06167	-9.97949	-8.97180	-8.70069	-8.32164	-8.05755	-10.26832	-9.30004	-10.26485	0.02987	0.30282	3.30231
ENSMUSP00000023519	-9.27221	-8.23398	-8.32786	-7.28272	-7.24040	-7.71068	-8.68992	-9.27543	-9.13866	0.03001	0.32109	3.11437
ENSMUSP00000102665	-5.41966	-5.53189	-5.16060	-4.92519	-5.04628	-5.00257	-5.57802	-5.67171	-5.68855	0.03037	0.69478	1.43931
ENSMUSP00000075089	-11.79466	-11.71248	-11.80636	-10.94509	-9.80318	-10.89014	-12.00131	-11.03303	-11.99783	0.03038	0.25398	3.93732
ENSMUSP00000025804	-7.12663	-6.85336	-6.78686	-6.43112	-6.43047	-6.65709	-7.23317	-6.79998	-7.05531	0.03170	0.66110	1.51262
ENSMUSP00000056643	-8.17392	-7.84029	-7.29794	-6.93736	-6.66544	-7.02058	-10.33028	-7.32384	-10.32681	0.03176	0.43345	2.30707
ENSMUSP00000072803	-5.82336	-5.62164	-5.61722	-5.35868	-5.44291	-5.49697	-5.78696	-5.51064	-5.48445	0.03222	0.77536	1.28973
ENSMUSP00000052872	-7.53425	-7.69972	-7.37989	-6.92431	-7.26990	-6.79583	-6.05927	-6.34532	-5.93815	0.03282	0.57859	1.72835
ENSMUSP00000093390	-8.91181	-8.49291	-8.58678	-7.05891	-8.16544	-7.42174	-8.32952	-9.25176	-8.77826	0.03320	0.29878	3.34697
ENSMUSP00000037487	-7.03081	-7.14932	-6.17460	-5.84767	-5.88648	-5.55496	-7.10164	-7.06058	-7.23398	0.03452	0.39943	2.50357
ENSMUSP00000045362	-6.16065	-5.97231	-5.82450	-5.25199	-5.17035	-5.70954	-11.20001	-5.88648	-6.11073	0.03493	0.53372	1.87363
ENSMUSP00000031492	-10.11068	-10.02850	-7.92121	-7.22295	-6.88208	-7.16799	-10.31733	-10.45062	-7.47646	0.03540	0.18187	5.49839
ENSMUSP00000046497	-9.99102	-11.01041	-11.10429	-9.73161	-8.73324	-9.33993	-11.29924	-9.23137	-11.29577	0.03560	0.25434	3.93172
ENSMUSP00000048096	-9.99667	-10.76263	-9.38904	-8.89828	-8.78449	-8.09603	-9.95186	-10.08516	-11.04799	0.03622	0.25928	3.85689
ENSMUSP00000004910	-10.63618	-10.55400	-9.54630	-8.93847	-9.23288	-9.22024	-9.74125	-10.97612	-10.83935	0.03734	0.37413	2.67290
ENSMUSP00000045285	-12.23164	-12.14946	-12.24334	-11.38207	-9.60394	-10.81570	-12.43828	-12.57158	-11.33324	0.03764	0.15233	6.56452
ENSMUSP00000021412	-10.28572	-10.20355	-8.68444	-7.96869	-8.09349	-8.28161	-8.54266	-9.01268	-8.87591	0.03816	0.26993	3.70470
ENSMUSP00000032228	-12.08234	-10.05045	-10.99247	-9.62216	-8.92045	-8.84111	-12.28899	-12.42229	-12.28552	0.03984	0.18672	5.35555
ENSMUSP00000104358	-10.47773	-10.39555	-9.38786	-9.11675	-9.07443	-8.72507	-10.68438	-10.81768	-10.68091	0.03997	0.37413	2.67290
ENSMUSP00000038763	-9.74297	-8.87185	-9.16649	-7.94008	-8.61700	-8.32988	-8.72521	-9.74619	-9.35796	0.04023	0.38372	2.60607
ENSMUSP00000033683	-5.64903	-5.70167	-5.32682	-5.19445	-5.21637	-5.21326	-5.53476	-5.91938	-5.96662	0.04026	0.71722	1.39427
ENSMUSP00000031186	-9.46318	-9.89242	-7.78776	-6.90496	-6.99103	-7.37706	-7.84454	-7.74823	-7.56144	0.04104	0.21752	4.59737
ENSMUSP00000021273	-9.51678	-9.43461	-8.42691	-8.15580	-7.52530	-8.10085	-8.11044	-8.24374	-8.10697	0.04134	0.33472	2.98760
ENSMUSP00000032419	-10.84638	-10.76421	-10.85808	-9.99682	-9.95450	-8.64151	-11.05303	-11.18633	-11.04956	0.04422	0.22408	4.46276
ENSMUSP00000016031	-11.25462	-11.17244	-9.31661	-9.10470	-8.32457	-8.50303	-9.51155	-9.19264	-10.35622	0.04554	0.21615	4.62651
ENSMUSP00000090727	-10.13643	-10.05425	-8.19841	-7.55105	-7.12298	-7.93155	-10.34308	-7.63898	-10.33961	0.04601	0.21615	4.62651
ENSMUSP00000059404	-10.52767	-8.83250	-10.53937	-8.06749	-8.53619	-8.32279	-10.73432	-9.25463	-10.73085	0.04670	0.25450	3.92932
ENSMUSP00000031377	-8.56223	-8.48006	-9.36288	-8.07644	-8.03412	-7.72294	-8.96964	-8.73507	-8.59829	0.04731	0.44673	2.23848
ENSMUSP00000043424	-9.04260	-8.13922	-8.74404	-7.97864	-7.35939	-7.83059	-8.15037	-8.64474	-8.59896	0.04734	0.40870	2.44676
ENSMUSP00000044877	-8.46137	-9.48077	-9.57465	-8.20197	-8.15965	-8.14701	-9.76959	-9.90289	-9.76612	0.04833	0.42405	2.35819
ENSMUSP00000048284	-5.69923	-5.64767	-5.47878	-5.03998	-4.98961	-5.44979	-6.33939	-5.65231	-5.84386	0.04876	0.62793	1.59254
ENSMUSP00000022268	-7.49644	-7.98495	-8.07883	-6.62113	-7.47429	-6.53839	-7.54271	-8.13873	-8.00196	0.04921	0.36089	2.77091
ENSMUSP00000108422	-6.10991	-6.10672	-6.14725	-5.63759	-5.99768	-5.84808	-6.29155	-6.58520	-6.75074	0.04938	0.73510	1.36036
ENSMUSP00000029076	-7.78372	-10.27059	-7.96254	-6.25659	-6.16363	-6.73882	-6.70493	-6.97481	-6.99629	0.04950	0.15688	6.37450
ENSMUSP00000035458	-9.78383	-9.15494	-8.47956	-8.32253	-7.85846	-7.80371	-9.09230	-9.47696	-9.16580	0.04957	0.36045	2.77435

ENSMUSP00000003038	-7.72340	-7.45549	-7.45252	-7.25207	-7.19014	-6.80827	-8.15833	-7.61133	-7.58427	0.04957	0.62455	1.60115
ENSMUSP00000025549	-5.42942	-6.90211	-5.85369	-4.37955	-4.54989	-5.16175	-4.51881	-4.81165	-4.56252	0.05187	0.28972	3.45164
ENSMUSP00000022946	-8.52685	-9.54625	-8.53855	-7.47850	-8.22513	-7.42355	-8.22208	-7.56644	-7.42967	0.05243	0.32994	3.03085
ENSMUSP00000023712	-7.56856	-11.15428	-11.24815	-6.68827	-6.33579	-6.94048	-11.44310	-6.80983	-6.60691	0.05269	0.13930	7.17894
ENSMUSP00000024823	-8.90856	-9.92796	-10.02184	-8.64915	-8.60684	-7.63814	-8.60379	-9.24851	-7.81138	0.05301	0.27647	3.61701
ENSMUSP00000026427	-9.37316	-10.07993	-9.83708	-9.31491	-9.03614	-9.13476	-11.98175	-11.01347	-10.36528	0.05413	0.57456	1.74047
ENSMUSP00000082519	-9.25167	-8.27131	-8.44217	-7.96944	-7.81588	-7.47683	-8.42197	-8.22801	-8.29712	0.05494	0.42929	2.32943
ENSMUSP00000060346	-9.76543	-9.68325	-10.87870	-8.28162	-9.12698	-9.11434	-8.50460	-8.80502	-9.45719	0.05624	0.28735	3.48009
ENSMUSP00000081485	-7.36177	-8.37919	-7.00560	-6.51484	-5.96163	-6.62026	-6.46948	-6.60278	-6.71737	0.05710	0.33524	2.98292
ENSMUSP00000007272	-7.71856	-7.91087	-7.39373	-7.18201	-6.47416	-7.16410	-7.58868	-7.42715	-7.52963	0.05728	0.46823	2.13572
ENSMUSP00000028610	-6.91868	-6.10441	-6.54090	-5.69700	-6.05111	-5.75756	-6.69373	-6.46725	-6.52003	0.05730	0.51879	1.92755
ENSMUSP00000032998	-5.39563	-5.26799	-5.36187	-4.86199	-5.23401	-4.77915	-5.10078	-5.15296	-5.50985	0.05731	0.66818	1.49660
ENSMUSP00000027153	-10.84430	-9.66055	-10.85600	-9.48332	-8.65206	-9.42836	-9.10123	-10.08267	-9.94590	0.05738	0.30282	3.30231
ENSMUSP00000031729	-9.50621	-8.32499	-8.16751	-7.69624	-7.37078	-7.50547	-8.61382	-9.39394	-8.35899	0.05767	0.36692	2.72542
ENSMUSP00000071292	-7.52953	-6.92276	-7.54123	-6.51399	-6.76261	-6.88910	-6.37597	-7.15915	-6.98904	0.05846	0.55204	1.81147
ENSMUSP00000027381	-8.50362	-10.37116	-10.46504	-7.33377	-7.95084	-8.44923	-7.10033	-7.07539	-7.28493	0.05933	0.21615	4.62651
ENSMUSP00000025778	-10.60276	-10.52059	-10.10305	-10.00663	-9.96431	-9.49946	-10.29800	-10.94271	-10.29452	0.05947	0.56037	1.78455
ENSMUSP00000039252	-5.08352	-4.99287	-4.86783	-4.50539	-4.69601	-4.84026	-5.02944	-4.97769	-5.16655	0.05959	0.73439	1.36167
ENSMUSP00000034355	-11.10714	-9.41198	-11.11885	-9.15798	-8.91490	-9.10303	-8.09065	-8.14698	-7.64243	0.05997	0.30718	3.25547
ENSMUSP00000031334	-8.88265	-9.31189	-8.55763	-8.54648	-7.99314	-7.98050	-8.13324	-9.22260	-8.74910	0.06069	0.48989	2.04126
ENSMUSP00000031411	-7.86968	-7.62713	-7.88138	-6.79114	-7.60388	-6.71345	-7.10083	-7.20187	-7.84102	0.06323	0.43672	2.28979
ENSMUSP00000104955	-12.30354	-12.22137	-12.31525	-11.45398	-11.41166	-9.78841	-12.51019	-12.64349	-12.50672	0.06389	0.18137	5.51364
ENSMUSP00000029770	-7.58009	-6.97733	-7.13093	-6.83607	-6.34998	-6.72847	-7.18277	-7.66329	-7.45375	0.06437	0.55614	1.79809
ENSMUSP00000029663	-9.43181	-9.34963	-10.54508	-8.07320	-9.13008	-8.32851	-10.74003	-9.26034	-10.73656	0.06468	0.28735	3.48009
ENSMUSP00000090593	-11.99709	-10.81334	-10.90721	-10.63611	-9.49458	-9.14539	-10.59074	-10.13586	-11.09869	0.06581	0.21724	4.60318
ENSMUSP00000021001	-7.51965	-7.16913	-7.26301	-6.78105	-6.32374	-7.06262	-7.45795	-7.48000	-7.34323	0.06791	0.52998	1.88686
ENSMUSP00000090909	-7.68003	-7.06149	-6.80815	-6.36197	-6.46379	-6.69586	-6.76670	-11.45826	-6.57216	0.07127	0.53463	1.87047
ENSMUSP00000029877	-7.72685	-7.43331	-8.00689	-6.57777	-7.47382	-6.82512	-7.54775	-7.85544	-7.93003	0.07207	0.44207	2.26208
ENSMUSP00000020948	-12.18412	-12.10194	-10.58283	-10.82314	-9.82477	-9.54379	-12.39077	-11.42250	-12.38730	0.07429	0.25450	3.92932
ENSMUSP00000090155	-11.12780	-8.84445	-11.13950	-8.97787	-8.03738	-8.27610	-9.72145	-10.36617	-11.33097	0.07561	0.23737	4.21283
ENSMUSP00000032073	-10.21777	-10.13560	-9.12790	-8.52007	-8.47775	-9.31326	-10.42442	-10.55772	-10.42095	0.07573	0.37413	2.67290
ENSMUSP00000029987	-6.47272	-6.01104	-6.26435	-5.84284	-5.58376	-6.01582	-6.41109	-6.69659	-6.19630	0.07640	0.64387	1.55310
ENSMUSP00000054322	-7.99243	-10.47930	-8.96019	-7.44190	-7.27035	-7.53539	-8.05593	-7.23354	-7.71590	0.07648	0.27817	3.59493
ENSMUSP00000032841	-9.34246	-10.36186	-10.45574	-8.49488	-9.55216	-8.69138	-10.65069	-10.78399	-10.64721	0.07720	0.33472	2.98760
sp|ALBU_HUMAN|	-8.16488	-8.41926	-8.00219	-8.02735	-7.07513	-6.98746	-7.48410	-8.84138	-8.84776	0.07869	0.40695	2.45728

ENSMUSP00000092283	-8.35738	-9.74267	-9.83655	-8.22979	-8.29873	-7.98374	-9.18336	-8.86444	-11.12960	0.07931	0.41021	2.43776
ENSMUSP00000034426	-9.57875	-8.54052	-9.25373	-8.60636	-8.26170	-7.77356	-9.44868	-9.12976	-9.78193	0.08005	0.41362	2.41765
ENSMUSP00000023462	-10.69362	-10.61144	-9.60375	-8.99591	-9.80174	-8.48874	-8.33122	-8.46452	-8.18460	0.08039	0.30282	3.30231
ENSMUSP00000018186	-5.67176	-5.72656	-6.09295	-5.00586	-5.38674	-5.59118	-5.83153	-5.54671	-5.68597	0.08110	0.59148	1.69067
ENSMUSP00000076472	-10.55592	-9.37217	-9.46605	-8.23888	-8.81590	-9.13998	-10.76257	-10.89587	-10.75910	0.08234	0.35635	2.80623
ENSMUSP00000003569	-7.95424	-10.27400	-10.36788	-7.89599	-7.85367	-7.11495	-8.36165	-7.74748	-8.15742	0.08255	0.27138	3.68488
ENSMUSP00000052989	-9.92887	-7.89951	-11.04214	-7.61456	-7.47459	-7.46196	-8.18834	-8.23065	-7.93350	0.08418	0.25478	3.92502
ENSMUSP00000037555	-7.49671	-7.13360	-7.26916	-6.56376	-7.17414	-6.70949	-8.01848	-7.73399	-8.01501	0.08485	0.59890	1.66973
ENSMUSP00000106140	-10.22942	-10.14725	-8.03995	-8.07950	-7.87007	-7.37773	-8.82308	-8.95638	-8.81961	0.08537	0.31124	3.21295
ENSMUSP00000023559	-7.48124	-7.58566	-7.97585	-7.09471	-7.49801	-7.08575	-6.94286	-7.16043	-6.73871	0.08841	0.63441	1.57626
ENSMUSP00000002549	-9.70659	-9.11299	-8.87015	-8.49112	-8.81668	-8.60329	-11.01481	-11.14811	-9.39835	0.08985	0.57900	1.72711
ENSMUSP00000004774	-9.23398	-7.20463	-8.14609	-7.08676	-6.60907	-6.86473	-6.92697	-7.53576	-7.39899	0.08992	0.34182	2.92554
ENSMUSP00000070944	-9.00241	-8.58350	-8.67738	-8.03001	-8.62392	-8.10026	-9.72047	-8.75417	-9.20558	0.09032	0.59036	1.69387
ENSMUSP00000035116	-8.64057	-7.91157	-8.48515	-7.31986	-8.11245	-7.30338	-7.94903	-8.81340	-9.63268	0.09154	0.45148	2.21494
ENSMUSP00000077223	-8.67697	-9.69637	-9.79024	-8.08084	-8.88666	-8.36261	-9.98519	-10.11849	-9.98172	0.09173	0.42405	2.35819
ENSMUSP00000008684	-3.61236	-4.07061	-3.35393	-3.07736	-3.06816	-3.36432	-4.01132	-3.87948	-3.76514	0.09229	0.62666	1.59577
ENSMUSP00000038305	-8.89403	-9.91343	-10.00731	-8.04645	-9.10373	-8.57967	-8.58926	-8.72256	-8.24907	0.09357	0.37413	2.67290
ENSMUSP00000103136	-7.12519	-7.04301	-9.84908	-5.69056	-6.15091	-6.05979	-10.04403	-6.36633	-6.53975	0.09412	0.21581	4.63374
ENSMUSP00000103903	-10.57249	-6.77241	-10.58420	-6.58602	-6.46032	-6.56048	-10.77914	-10.91244	-10.77567	0.09415	0.25965	3.85131
ENSMUSP00000042967	-8.95336	-8.87118	-9.81321	-8.44289	-8.71084	-7.72855	-8.39753	-9.04185	-8.53721	0.09421	0.39370	2.54001
ENSMUSP00000006094	-5.01809	-5.01367	-4.98112	-4.72592	-4.63006	-4.97665	-5.14796	-5.27665	-5.06889	0.09468	0.78817	1.26876
ENSMUSP00000099435	-5.95864	-6.03471	-6.31666	-5.81331	-5.87454	-5.89895	-5.98702	-6.34860	-6.73998	0.09738	0.79176	1.26301
ENSMUSP00000010807	-10.93218	-9.74843	-10.94388	-9.23447	-8.42968	-10.02766	-11.13883	-9.07095	-11.13535	0.09744	0.25434	3.93172
ENSMUSP00000028063	-10.32859	-10.24641	-9.23872	-8.96761	-9.43671	-8.91265	-10.53524	-10.66854	-10.53177	0.09845	0.48936	2.04349
ENSMUSP00000019622	-8.19515	-7.66076	-8.54358	-7.44823	-7.05445	-7.77288	-10.35152	-7.53617	-7.39940	0.09866	0.49663	2.01356
ENSMUSP00000002850	-10.97834	-10.89616	-12.09162	-10.71893	-10.33989	-9.43958	-12.28656	-12.41986	-10.67010	0.09942	0.30718	3.25547
ENSMUSP00000026470	-9.89359	-8.34394	-9.05715	-7.87559	-8.49266	-7.57698	-9.25209	-11.33511	-9.58535	0.09954	0.36172	2.76455
ENSMUSP00000031093:reversed	-9.75311	-10.77250	-10.86638	-9.49370	-9.45138	-9.95016	-11.06133	-11.19463	-9.95628	0.10013	0.48936	2.04349
ENSMUSP00000041361:reversed	-12.14282	-12.06064	-11.05295	-10.78184	-9.95058	-11.23830	-12.34947	-11.38120	-11.24442	0.10042	0.33472	2.98760
ENSMUSP00000033662	-8.53985	-7.61009	-8.80301	-7.27513	-7.81097	-7.32284	-8.74650	-9.13125	-8.74303	0.10153	0.46676	2.14243
ENSMUSP00000030112	-11.57030	-10.38655	-9.96901	-9.87260	-9.57882	-9.19831	-10.67538	-9.96053	-9.57231	0.10259	0.39511	2.53096
ENSMUSP00000021443	-6.84196	-6.85076	-6.26586	-6.34582	-6.20931	-6.10375	-6.62874	-6.69572	-6.69631	0.10307	0.67767	1.47564
ENSMUSP00000036288	-8.82405	-7.57147	-7.73682	-7.06817	-7.42392	-7.04352	-6.51795	-6.76566	-6.64930	0.10334	0.46795	2.13699
ENSMUSP00000007212	-9.17942	-8.93013	-8.36992	-7.89718	-8.56791	-8.06050	-8.64826	-8.48302	-8.64479	0.10606	0.53365	1.87390
ENSMUSP00000086252	-9.49528	-10.51468	-10.60855	-9.74729	-9.19355	-9.18092	-10.80350	-10.93680	-10.80003	0.10746	0.48936	2.04349

ENSMUSP00000086987	-8.01367	-9.03307	-9.12695	-8.26568	-7.71195	-7.69931	-9.32190	-7.84221	-7.70543	0.10746	0.48936	2.04349
ENSMUSP00000000090	-8.14101	-9.67182	-7.19666	-6.78287	-7.01505	-6.72792	-6.91190	-6.79384	-7.75601	0.10881	0.35075	2.85104
ENSMUSP00000105288	-11.46942	-10.28567	-11.48112	-9.77171	-10.57754	-10.05349	-11.67607	-11.80937	-10.05961	0.11013	0.42405	2.35819
ENSMUSP00000015858	-9.16885	-8.49850	-8.59237	-8.46481	-8.04289	-8.26671	-10.98849	-10.02022	-9.88345	0.11065	0.62347	1.60393
ENSMUSP00000033289	-11.32546	-10.14171	-11.33716	-9.96448	-9.58544	-10.42094	-11.53211	-10.56383	-9.91565	0.11168	0.42405	2.35819
ENSMUSP00000025667	-8.08090	-7.99872	-10.29377	-7.39434	-7.12018	-7.25599	-8.08679	-7.48228	-8.08331	0.11223	0.31430	3.18166
ENSMUSP00000112196	-9.45990	-8.86631	-10.57318	-7.76473	-9.15818	-7.92114	-8.56695	-8.18923	-8.81493	0.11254	0.26643	3.75336
ENSMUSP00000032882	-9.62842	-9.54625	-8.53855	-8.26744	-8.73654	-7.11329	-9.83507	-7.76720	-8.73003	0.11471	0.27647	3.61701
ENSMUSP00000103940	-5.32542	-6.85289	-5.70226	-5.07131	-4.97380	-5.05984	-5.09951	-5.26382	-5.35612	0.11488	0.48276	2.07144
ENSMUSP00000088057	-10.24855	-8.21665	-8.05908	-7.36082	-7.50959	-7.39685	-10.45519	-7.87630	-10.45172	0.11498	0.34369	2.90956
ENSMUSP00000034400	-6.39476	-7.48300	-7.82833	-6.35047	-6.53776	-6.15240	-5.96130	-5.75811	-5.88762	0.11720	0.49860	2.00563
ENSMUSP00000032371	-11.36716	-11.28498	-9.17769	-8.78178	-9.62713	-8.85202	-8.01415	-8.48397	-7.90245	0.11769	0.35914	2.78443
ENSMUSP00000026565	-7.47537	-9.59437	-8.58667	-7.21636	-7.31719	-7.47167	-6.93455	-7.06785	-7.31067	0.11957	0.42452	2.35562
ENSMUSP00000007216	-8.16698	-7.29618	-8.32183	-7.19501	-7.52920	-6.62919	-7.94608	-7.84754	-7.58154	0.12146	0.45455	2.19996
ENSMUSP00000083281	-8.19540	-9.72622	-9.82010	-8.44742	-8.06837	-8.05574	-10.01504	-7.43615	-10.01157	0.12304	0.46896	2.13238
ENSMUSP00000025161	-10.88320	-9.69945	-10.89490	-9.52222	-9.47990	-9.97868	-9.47685	-9.61015	-9.47338	0.12341	0.48936	2.04349
ENSMUSP00000003066	-7.32999	-7.42220	-7.72744	-6.79345	-7.39124	-7.08230	-7.38820	-6.77784	-7.38472	0.12693	0.65268	1.53213
ENSMUSP00000040954	-10.02465	-8.64211	-8.08917	-7.52374	-8.28716	-7.05622	-8.28412	-9.26500	-8.28065	0.12856	0.32081	3.11715
ENSMUSP00000045127	-9.00474	-8.92257	-10.11802	-8.40861	-8.70302	-8.69038	-10.31297	-10.44627	-10.30950	0.13296	0.52417	1.90776
ENSMUSP00000002846	-8.51284	-8.43066	-8.07233	-8.14552	-8.10320	-7.82222	-8.10016	-8.09031	-7.82834	0.13593	0.74078	1.34993
ENSMUSP00000047665	-9.05357	-8.97139	-8.47709	-8.34952	-8.30720	-8.66244	-9.77163	-8.80533	-7.72999	0.13648	0.69161	1.44591
ENSMUSP00000034346	-9.99913	-8.44948	-11.11240	-8.12958	-8.47300	-8.58556	-9.69436	-8.72846	-8.00377	0.13661	0.37988	2.63240
ENSMUSP00000022861	-8.86334	-8.78117	-11.07622	-7.81571	-8.32556	-8.31293	-9.65817	-8.69227	-10.16612	0.13856	0.34087	2.93369
ENSMUSP00000022256	-7.65315	-7.99852	-8.23555	-7.67332	-7.70247	-7.13546	-7.95079	-8.42065	-7.69596	0.14064	0.63094	1.58494
ENSMUSP00000099730	-6.75634	-6.48608	-6.16497	-6.29803	-5.86731	-6.08649	-6.28715	-6.32036	-6.18359	0.14249	0.69349	1.44199
ENSMUSP00000070449	-7.28794	-9.60770	-8.60000	-7.10450	-7.49764	-7.17474	-9.89653	-7.46078	-7.32401	0.14345	0.44431	2.25069
ENSMUSP00000099534	-7.98686	-9.51767	-9.61155	-8.23887	-8.19655	-7.59574	-8.70493	-7.73863	-9.80303	0.14346	0.46896	2.13238
ENSMUSP00000102289	-7.08193	-10.13950	-10.23337	-7.52504	-7.13125	-7.11862	-7.59093	-10.56162	-7.58746	0.14389	0.43629	2.29204
ENSMUSP00000029830	-10.74794	-8.71605	-9.14665	-8.79878	-8.12024	-8.10761	-8.75342	-11.08789	-9.00140	0.14406	0.38502	2.59730
ENSMUSP00000051561	-11.30196	-11.21978	-9.70067	-8.98492	-9.10972	-10.39744	-10.40704	-10.02892	-11.50514	0.14549	0.32994	3.03085
ENSMUSP00000099490	-12.55529	-9.76092	-12.56699	-10.23825	-9.81634	-9.70359	-8.90745	-9.17733	-8.17936	0.14573	0.40856	2.44763
ENSMUSP00000025563	-7.82328	-7.74111	-7.63422	-7.13672	-7.52195	-7.65246	-7.18235	-7.52701	-7.65858	0.14597	0.72453	1.38021
ENSMUSP00000071624	-10.32157	-10.23939	-8.72028	-8.17165	-7.96222	-9.41705	-8.91523	-9.04853	-8.91176	0.14624	0.32994	3.03085
ENSMUSP00000002171	-9.79360	-8.86328	-8.70570	-7.77560	-8.90369	-8.14358	-7.96208	-8.01198	-8.89718	0.14923	0.42461	2.35511
ENSMUSP00000029402	-8.24866	-9.05416	-8.69583	-8.28932	-8.34710	-7.98300	-11.29270	-9.81301	-10.18766	0.15048	0.66562	1.50236

ENSMUSP00000072858	-9.61424	-9.53206	-9.62594	-6.91760	-9.82393	-6.67155	-6.20565	-6.18865	-5.44358	0.15251	0.08855	11.29349
ENSMUSP00000031402	-8.84304	-7.91328	-8.34372	-7.99611	-7.95379	-7.52336	-7.75005	-7.40951	-7.68772	0.15330	0.60358	1.65678
ENSMUSP00000037348	-5.53888	-5.79318	-5.78090	-5.43021	-5.54271	-5.61751	-5.54902	-5.50234	-5.71945	0.15362	0.84384	1.18506
ENSMUSP00000089551	-6.05924	-6.05554	-6.14942	-5.86267	-6.09608	-5.76065	-6.19313	-6.00001	-6.42606	0.15544	0.82589	1.21082
ENSMUSP00000088372	-7.06149	-6.48967	-6.35395	-6.25045	-6.10459	-6.35270	-5.81795	-6.14102	-6.09807	0.15552	0.69580	1.43719
ENSMUSP00000028121	-9.31919	-10.85000	-8.74271	-8.61514	-8.42968	-8.56019	-8.93766	-8.70308	-8.93418	0.15567	0.46599	2.14597
ENSMUSP00000078123	-10.00532	-9.92314	-7.81585	-7.85539	-8.26529	-7.80044	-10.21196	-9.24369	-9.10692	0.15639	0.48304	2.07023
ENSMUSP00000025668	-9.12811	-7.85591	-7.47429	-7.12077	-7.14001	-7.50935	-8.23572	-9.21660	-8.44361	0.15729	0.49350	2.02634
ENSMUSP00000023312	-11.15111	-9.96736	-9.54982	-9.20195	-9.74781	-8.94623	-10.25618	-10.38948	-11.35428	0.15899	0.45836	2.18170
ENSMUSP00000090844	-11.49370	-10.30995	-9.55569	-9.79600	-9.50222	-8.55102	-8.47722	-11.83365	-8.39677	0.15934	0.35914	2.78443
ENSMUSP00000013737	-7.98925	-10.85572	-10.94960	-7.96677	-8.74566	-7.91182	-11.14455	-11.27785	-11.14107	0.16253	0.43855	2.28023
ENSMUSP00000003521	-5.77229	-6.43377	-5.75173	-5.66925	-5.58197	-5.54760	-6.15800	-6.04872	-5.97547	0.16386	0.71948	1.38989
ENSMUSP00000075953	-9.20520	-9.12302	-8.11532	-8.35563	-7.80190	-8.30068	-9.41185	-9.54514	-8.30680	0.16679	0.57844	1.72878
ENSMUSP00000034227	-9.96086	-9.87869	-8.87099	-9.11130	-8.55757	-9.05635	-10.16751	-9.19924	-10.16404	0.16679	0.57844	1.72878
ENSMUSP00000080058	-11.37578	-11.29361	-10.28591	-10.52622	-9.97249	-10.47127	-11.58243	-11.71573	-11.57896	0.16679	0.57844	1.72878
ENSMUSP00000111831	-7.38866	-9.70841	-7.23324	-6.81946	-6.77714	-6.68753	-8.38425	-7.92937	-8.38078	0.16765	0.41362	2.41765
ENSMUSP00000045621	-7.58141	-7.38798	-8.22933	-7.37070	-7.40535	-6.89795	-7.57670	-7.45864	-7.57323	0.16824	0.61656	1.62190
ENSMUSP00000102363	-10.85261	-9.15745	-8.66314	-8.53558	-8.01355	-8.64774	-11.05926	-8.62351	-8.65386	0.16894	0.42456	2.35540
ENSMUSP00000020504	-9.59985	-9.51767	-8.50998	-8.75029	-8.70797	-8.18392	-8.70493	-7.99008	-7.60186	0.16910	0.57844	1.72878
ENSMUSP00000096222	-10.03249	-11.05189	-11.14577	-10.28450	-10.24218	-9.38140	-10.23914	-9.52430	-9.72425	0.16933	0.48936	2.04349
ENSMUSP00000030940	-10.59685	-10.51468	-8.65884	-9.23587	-8.60537	-8.59274	-10.80350	-8.22461	-9.18704	0.17098	0.49824	2.00707
ENSMUSP00000034141	-10.42221	-11.44160	-10.43391	-9.57462	-9.78376	-10.61926	-9.78071	-10.76216	-10.62538	0.17144	0.46896	2.13238
ENSMUSP00000017065	-10.63874	-10.55657	-10.65045	-10.89075	-8.44650	-7.61266	-9.23240	-9.02898	-9.74035	0.17259	0.10291	9.71717
ENSMUSP00000026704	-7.83802	-8.03034	-7.77275	-7.64528	-7.83257	-7.28357	-6.86897	-7.59010	-7.14909	0.17619	0.73558	1.35947
ENSMUSP00000034881	-7.25548	-9.12302	-9.21690	-7.84422	-6.84584	-7.45254	-5.79661	-6.10686	-6.26863	0.17629	0.45836	2.18170
ENSMUSP00000028238	-10.14906	-6.92714	-7.75883	-6.78583	-6.42257	-6.84530	-6.85490	-10.48901	-7.12910	0.17735	0.36853	2.71345
ENSMUSP00000028062	-10.95859	-9.77484	-9.86872	-10.10903	-8.76636	-8.95448	-9.55225	-10.19697	-10.06020	0.17795	0.38735	2.58161
ENSMUSP00000029259	-9.14725	-8.42885	-9.41041	-7.83489	-8.98906	-7.69098	-7.50766	-7.67668	-8.25148	0.17800	0.40820	2.44979
ENSMUSP00000023749	-8.63934	-10.17015	-8.31431	-7.93529	-7.62463	-8.49967	-9.35740	-9.49070	-9.35393	0.17858	0.44747	2.23478
ENSMUSP00000064655	-7.42725	-9.54625	-7.07108	-6.83168	-6.88947	-6.52537	-6.78632	-6.53009	-6.16371	0.18023	0.43732	2.28665
ENSMUSP00000030455	-10.57523	-8.54334	-8.63722	-8.62607	-7.83628	-7.82364	-9.16889	-8.34613	-8.37648	0.18029	0.40648	2.46012
ENSMUSP00000000001	-10.67648	-10.59431	-8.28625	-8.21630	-8.93646	-8.47161	-10.88313	-11.01643	-10.87966	0.18143	0.50173	1.99309
ENSMUSP00000098076	-9.08740	-9.79416	-9.88804	-9.54017	-8.75038	-8.63764	-9.74627	-9.26023	-9.12346	0.18163	0.54598	1.83156
ENSMUSP00000005685	-11.01296	-6.63594	-6.38553	-5.15798	-5.45303	-6.05231	-7.60437	-7.17415	-11.21613	0.18251	0.24021	4.16300
ENSMUSP00000089374	-10.78184	-10.69967	-6.49871	-6.71199	-7.49072	-6.89700	-7.32061	-6.94303	-7.13053	0.18489	0.57229	1.74737

ENSMUSP00000084918	-8.13415	-7.12383	-7.36801	-7.04480	-7.09934	-7.02110	-8.60915	-8.74245	-7.73644	0.18589	0.66102	1.51281
ENSMUSP00000033480	-8.32405	-7.56393	-8.11866	-7.78204	-7.63572	-7.34470	-8.36363	-9.21617	-8.46838	0.18710	0.67868	1.47344
ENSMUSP00000099642	-11.49256	-12.51196	-10.40466	-10.27710	-10.85411	-10.22214	-9.75203	-10.98436	-9.84866	0.18731	0.50173	1.99309
ENSMUSP00000090184	-6.34639	-5.72703	-6.15740	-5.75105	-5.80882	-5.79618	-5.89375	-6.07412	-5.84532	0.18840	0.76463	1.30782
ENSMUSP00000018430	-9.10836	-10.12775	-8.02046	-8.26077	-8.21845	-7.83794	-8.80359	-10.54988	-8.21194	0.19095	0.53412	1.87225
ENSMUSP00000027067	-8.59300	-7.41161	-8.01652	-7.15789	-7.04410	-7.83399	-7.70044	-7.59729	-7.26942	0.19097	0.53548	1.86747
ENSMUSP00000091541	-10.90897	-9.72522	-10.92067	-8.44878	-10.01708	-10.00445	-11.11562	-11.24891	-11.11214	0.19128	0.30282	3.30231
ENSMUSP00000099819	-7.17631	-7.17753	-7.11103	-6.13621	-7.04948	-6.92861	-10.60609	-7.17973	-7.30251	0.19213	0.57923	1.72644
ENSMUSP00000054421	-10.35957	-10.27739	-10.37127	-8.99859	-10.56926	-8.94364	-8.95323	-9.59795	-8.94976	0.19396	0.34645	2.88643
ENSMUSP00000077917	-9.67654	-9.59437	-9.68824	-8.31556	-9.88624	-8.26061	-7.93348	-7.44744	-8.77815	0.19396	0.34645	2.88643
ENSMUSP00000003461	-10.11922	-9.44887	-8.79527	-8.54594	-9.22971	-8.49099	-9.98915	-12.07216	-9.73422	0.19539	0.54605	1.83132
ENSMUSP00000034097	-9.73223	-9.13864	-10.84551	-8.68388	-9.09378	-9.41787	-9.42746	-8.22511	-9.93541	0.19699	0.49824	2.00707
ENSMUSP00000004232	-7.70789	-8.62464	-9.05524	-7.76880	-8.15403	-7.29393	-7.36237	-7.38124	-7.30005	0.19750	0.54106	1.84823
ENSMUSP00000031773	-8.07736	-6.89634	-7.43497	-6.71966	-7.24086	-6.66470	-8.65188	-8.14896	-8.44765	0.19987	0.58755	1.70198
ENSMUSP00000069359:reversed	-10.49268	-9.30893	-10.50438	-9.64312	-9.08938	-9.58816	-9.08634	-10.83263	-10.69586	0.20191	0.57844	1.72878
ENSMUSP00000103557	-10.07977	-9.99759	-7.68954	-8.38206	-7.57727	-8.07565	-10.28642	-8.80673	-10.28295	0.20286	0.53412	1.87225
ENSMUSP00000099415	-7.49006	-10.84617	-7.50176	-7.20571	-6.66774	-6.83057	-7.41709	-7.33212	-7.51629	0.20385	0.37689	2.65333
ENSMUSP00000001507	-8.44391	-8.21858	-7.05001	-7.05590	-7.24800	-7.39901	-9.26989	-9.73991	-9.60314	0.20527	0.62557	1.59854
ENSMUSP00000047960	-6.26905	-9.32662	-7.21933	-6.10115	-6.47875	-6.10504	-7.21351	-6.44863	-7.41080	0.20571	0.46203	2.16434
ENSMUSP00000017975	-7.56738	-10.05425	-8.53514	-7.67625	-7.77707	-7.38484	-10.34308	-10.47638	-10.33961	0.20589	0.51498	1.94184
ENSMUSP00000088252	-9.86555	-8.17039	-7.03986	-7.16892	-7.36305	-6.83947	-10.07220	-8.00433	-7.66680	0.21338	0.49663	2.01356
ENSMUSP00000080995	-7.41631	-8.94713	-7.93943	-7.66833	-7.28928	-7.27665	-8.13438	-7.75626	-7.28277	0.21405	0.60320	1.65782
ENSMUSP00000099908	-6.91134	-6.63806	-6.37087	-6.55233	-6.21518	-6.33914	-7.11799	-7.06019	-7.11451	0.21550	0.77703	1.28695
ENSMUSP00000110223	-7.79580	-9.32662	-9.42050	-8.55923	-7.66877	-7.65614	-9.61544	-9.74874	-9.61197	0.21715	0.52417	1.90776
ENSMUSP00000028278	-8.11710	-8.03493	-8.91775	-7.93365	-8.01653	-7.87870	-8.52451	-9.75741	-9.10922	0.21954	0.70208	1.42435
ENSMUSP00000106968	-8.78596	-9.80536	-8.79766	-7.93837	-8.99565	-8.47160	-8.99261	-8.27776	-8.98914	0.22014	0.52417	1.90776
ENSMUSP00000034304	-6.81191	-6.38742	-6.60454	-6.32096	-5.95052	-6.58327	-7.35507	-7.28249	-7.05676	0.22501	0.71063	1.40719
ENSMUSP00000088358	-7.27001	-6.80831	-6.57577	-6.67466	-6.67729	-6.03679	-7.13286	-7.46684	-7.47319	0.22599	0.65400	1.52904
ENSMUSP00000089302	-6.36211	-7.89008	-9.59695	-6.61412	-6.95755	-6.16707	-5.98090	-5.80996	-5.29540	0.22745	0.49996	2.00017
ENSMUSP00000029476	-6.95885	-6.87667	-7.14494	-6.93318	-6.89086	-6.71115	-8.77564	-7.29880	-8.18399	0.22872	0.86170	1.16050
ENSMUSP00000000284	-11.23363	-11.15145	-11.24533	-9.87265	-11.44332	-10.32911	-10.33870	-9.96058	-9.82381	0.22976	0.42355	2.36099
ENSMUSP00000081567	-11.88710	-11.80492	-11.89880	-10.52612	-12.09679	-10.98258	-10.14403	-10.61406	-10.98870	0.22976	0.42355	2.36099
ENSMUSP00000002452	-9.67654	-9.59437	-9.68824	-8.31556	-9.88624	-8.77203	-7.68202	-8.06677	-8.26673	0.22976	0.42355	2.36099
ENSMUSP00000025095	-8.39130	-9.41070	-8.40301	-8.64332	-7.50140	-8.07694	-8.08654	-8.73125	-8.08306	0.23395	0.52417	1.90776
ENSMUSP00000007251	-11.11832	-11.03614	-10.02844	-10.26875	-10.22643	-10.21380	-11.32497	-11.45826	-11.32149	0.23395	0.70717	1.41408

ENSMUSP00000108003	-5.89855	-7.22544	-6.34967	-6.02538	-6.15371	-5.36961	-6.15066	-6.19500	-6.77299	0.23468	0.57923	1.72642
ENSMUSP00000029325	-7.22662	-6.28088	-6.55950	-6.28896	-6.19578	-6.38382	-6.72587	-6.44900	-6.69462	0.23471	0.71137	1.40574
ENSMUSP00000104816	-10.12792	-10.04574	-7.57057	-8.43021	-7.50022	-8.12380	-9.23299	-8.85488	-10.33109	0.23586	0.57900	1.72711
ENSMUSP00000037446	-8.75686	-11.51208	-8.55721	-8.54615	-8.13606	-8.12342	-8.75215	-8.79446	-8.42585	0.23661	0.47325	2.11303
ENSMUSP00000034326	-10.24726	-8.94068	-9.30291	-9.27487	-8.84681	-8.49765	-10.45391	-9.79827	-10.96186	0.23762	0.57916	1.72663
ENSMUSP00000032888	-10.12792	-10.04574	-10.13962	-9.27835	-10.33761	-8.71198	-9.23299	-9.36629	-9.22952	0.23789	0.42355	2.36099
ENSMUSP00000032761	-10.31095	-8.61578	-10.32265	-9.46139	-8.57093	-8.55829	-10.51760	-10.65090	-10.51413	0.23896	0.52417	1.90776
ENSMUSP00000060892	-7.84710	-9.37791	-7.85880	-7.76238	-7.72006	-7.45597	-8.56516	-8.69846	-9.66327	0.23901	0.60912	1.64171
ENSMUSP00000092557	-10.52279	-11.54219	-11.63607	-10.77481	-10.73249	-10.71985	-11.83102	-11.96432	-11.82755	0.24063	0.70717	1.41408
ENSMUSP00000046856	-11.39523	-11.31305	-8.45828	-9.07819	-9.20299	-8.88009	-9.65216	-10.12218	-9.98541	0.24078	0.68603	1.45767
ENSMUSP00000100593	-6.57936	-7.51915	-6.86555	-6.83137	-6.57390	-6.14506	-7.29695	-6.58278	-7.29348	0.24105	0.65569	1.52511
ENSMUSP00000022070	-9.69361	-9.61143	-10.04204	-9.18314	-9.90330	-8.46880	-10.74840	-9.58134	-11.84650	0.24135	0.47458	2.10715
ENSMUSP00000021676	-8.63362	-9.65301	-7.34496	-7.78603	-7.54295	-7.53032	-8.84027	-8.12542	-7.98865	0.24163	0.61637	1.62239
ENSMUSP00000109310	-8.22082	-7.77076	-8.23252	-7.30242	-7.33157	-8.21711	-8.22671	-7.81329	-9.01218	0.24536	0.58952	1.69629
ENSMUSP00000047218	-10.53906	-8.84390	-10.55077	-9.17808	-8.34683	-9.63455	-9.64414	-10.87901	-10.74224	0.24596	0.46896	2.13238
ENSMUSP00000092233	-6.01274	-6.05071	-5.98740	-5.68115	-5.61800	-6.11391	-6.05718	-6.07925	-5.91418	0.24697	0.78908	1.26730
ENSMUSP00000066238	-7.80896	-9.92796	-6.65025	-6.96203	-6.50192	-6.98405	-7.26814	-7.21034	-6.77503	0.24826	0.53433	1.87151
ENSMUSP00000049584	-12.70301	-11.51926	-11.10172	-11.34203	-11.29971	-10.33101	-12.90966	-13.04295	-12.90618	0.24950	0.49824	2.00707
ENSMUSP00000007959	-7.65516	-7.26272	-7.49975	-7.59691	-6.70712	-6.95404	-7.55155	-7.25730	-7.21152	0.25166	0.64538	1.54948
ENSMUSP00000031423	-7.11886	-6.83600	-6.68224	-6.76747	-6.59093	-6.72363	-7.87761	-8.34042	-8.25366	0.25235	0.84286	1.18644
ENSMUSP00000032824	-8.12161	-7.70288	-8.27646	-7.86268	-7.90376	-7.31296	-7.81732	-7.80217	-8.19959	0.25451	0.70156	1.42539
ENSMUSP00000024223	-8.05867	-8.56468	-8.65856	-7.79966	-8.26837	-8.25573	-9.36492	-8.39862	-10.46302	0.25707	0.73354	1.36325
ENSMUSP00000090911	-6.85341	-10.94999	-6.13419	-5.75431	-5.84837	-6.34962	-11.23882	-11.37212	-11.23535	0.25724	0.42620	2.34631
ENSMUSP00000099769	-9.95580	-8.77205	-8.86593	-9.10624	-7.96432	-8.53987	-10.16245	-9.19417	-10.15898	0.25902	0.52417	1.90776
ENSMUSP00000101011	-8.46228	-8.89152	-7.88580	-7.92535	-8.08379	-8.07116	-8.66893	-7.70303	-8.32873	0.26142	0.74683	1.33899
ENSMUSP00000059501	-7.45908	-9.32662	-7.21933	-6.61206	-7.21656	-7.40468	-7.41427	-7.34681	-7.41080	0.26174	0.52818	1.89331
ENSMUSP00000005953	-7.94255	-7.76027	-7.53132	-7.28872	-7.80078	-7.37035	-7.24335	-8.00801	-7.59356	0.26328	0.76459	1.30788
ENSMUSP00000018875	-11.63579	-7.54192	-7.24865	-7.12122	-7.01276	-6.75953	-7.24292	-7.31738	-7.18061	0.26385	0.43537	2.29688
ENSMUSP00000045048	-8.59611	-8.51393	-10.80898	-8.64736	-8.29478	-7.94559	-11.00393	-11.13723	-11.00046	0.26411	0.51498	1.94184
ENSMUSP00000037341	-7.36442	-9.68417	-8.16506	-7.30616	-8.02632	-7.01476	-7.02435	-8.15658	-8.01981	0.26826	0.52818	1.89331
ENSMUSP00000011492	-10.10336	-9.50976	-11.21663	-10.35537	-9.21345	-8.35324	-9.79859	-11.54488	-9.45839	0.27437	0.34720	2.88022
ENSMUSP00000018992	-8.89871	-8.50627	-7.64445	-7.93741	-8.07205	-7.48600	-8.00647	-7.87505	-8.55517	0.27571	0.67341	1.48498
ENSMUSP00000051921	-9.92487	-8.22970	-9.93657	-8.22716	-9.03299	-8.50894	-8.51853	-8.65183	-10.12805	0.27611	0.59413	1.68314
ENSMUSP00000023707	-9.74150	-9.65932	-7.35127	-7.79234	-7.54926	-8.32557	-8.33516	-7.67952	-7.74351	0.27624	0.66237	1.50972
ENSMUSP00000110532	-6.35468	-6.69243	-6.42523	-6.19171	-6.35850	-6.44351	-6.30999	-6.10679	-6.18134	0.27639	0.85901	1.16413

ENSMUSP00000027810	-9.01999	-9.27454	-10.98141	-9.27200	-8.61035	-8.96559	-9.56336	-10.20808	-9.55989	0.27773	0.57097	1.75141
ENSMUSP00000044955	-7.68995	-7.35642	-7.31212	-7.43105	-7.28051	-6.99958	-7.64524	-8.02990	-8.10449	0.28223	0.80538	1.24164
ENSMUSP00000034277	-10.12364	-8.42847	-9.03376	-8.76266	-8.13216	-8.70770	-8.71729	-10.46358	-8.37710	0.28447	0.60320	1.65782
ENSMUSP00000021217	-7.88194	-9.74947	-7.89364	-7.03491	-8.09163	-7.82754	-10.03830	-7.60255	-10.03483	0.28629	0.51638	1.93654
ENSMUSP00000095263	-11.06953	-6.10775	-5.95882	-5.57732	-5.66532	-5.72090	-11.27618	-11.40947	-11.27270	0.28783	0.45416	2.20186
ENSMUSP00000021512	-9.00241	-9.43165	-9.52552	-8.66624	-9.21210	-9.19946	-10.82205	-9.85377	-9.71700	0.29034	0.73745	1.35603
ENSMUSP00000107237	-8.90025	-9.32949	-8.32377	-7.92786	-9.10994	-7.33871	-8.31796	-8.01579	-10.71642	0.29082	0.42459	2.35524
ENSMUSP00000047571	-8.61399	-8.96727	-9.06115	-8.56365	-8.94888	-7.75227	-8.94584	-9.38940	-10.55298	0.29126	0.57118	1.75075
ENSMUSP00000021940	-7.30243	-6.87393	-7.07048	-6.98984	-6.94753	-6.82366	-7.16276	-7.34607	-7.43890	0.29186	0.85759	1.16605
ENSMUSP00000077909	-10.80382	-10.72165	-9.20253	-9.44284	-9.91194	-9.38789	-11.01047	-11.14377	-11.00700	0.29259	0.68562	1.45852
ENSMUSP00000099563	-11.77838	-10.59463	-8.84144	-9.62846	-9.03943	-9.40639	-10.03532	-10.16861	-9.57963	0.29538	0.68148	1.46739
ENSMUSP00000006496	-6.23864	-5.77247	-5.58958	-5.82989	-5.36394	-5.55840	-6.36360	-6.22401	-6.05783	0.29652	0.76909	1.30024
ENSMUSP00000004057	-7.64757	-9.76657	-8.75887	-8.15104	-8.10872	-7.64387	-8.44240	-7.78676	-10.05192	0.29817	0.66237	1.50972
ENSMUSP00000020241	-8.72333	-10.84232	-9.32321	-8.77458	-8.93302	-8.92039	-6.38182	-7.14921	-6.41375	0.29941	0.65890	1.51768
ENSMUSP00000044405	-8.88324	-9.90066	-9.48313	-9.38671	-8.89218	-8.71242	-10.18949	-9.81137	-11.28759	0.30006	0.69863	1.43138
ENSMUSP00000060912	-6.71641	-6.31997	-6.28736	-6.23750	-5.73915	-6.45310	-6.83477	-6.99664	-6.80351	0.30319	0.72055	1.38782
ENSMUSP00000104179	-6.17014	-6.25861	-6.00278	-6.14926	-5.96782	-5.98151	-6.07449	-5.84675	-6.01466	0.30772	0.90196	1.10869
ENSMUSP00000043580	-9.73223	-9.65005	-9.23251	-9.47282	-8.84232	-9.41787	-11.04045	-9.56076	-11.03698	0.31183	0.73745	1.35603
ENSMUSP00000078236	-9.60411	-8.67379	-8.00519	-7.58611	-7.41456	-8.95302	-10.91233	-11.04563	-9.80729	0.31236	0.46159	2.16642
ENSMUSP00000108760	-11.07617	-5.82479	-5.77025	-5.42386	-5.50379	-5.64479	-11.28282	-5.91044	-5.78187	0.31256	0.50051	1.99795
ENSMUSP00000031061	-11.48494	-11.40276	-9.54693	-10.12396	-10.59306	-8.96980	-10.59002	-11.82489	-11.68812	0.31377	0.49824	2.00707
ENSMUSP00000031726	-10.59418	-8.11007	-8.40471	-8.00879	-8.60270	-7.65149	-8.23178	-8.09673	-8.84764	0.31744	0.54598	1.83156
ENSMUSP00000052258	-11.26152	-11.17935	-9.07205	-10.41196	-8.52257	-9.50886	-11.46817	-11.60147	-10.36313	0.31936	0.48304	2.07023
ENSMUSP00000016338	-5.30417	-5.26991	-5.46711	-5.05948	-5.25736	-5.35968	-6.18660	-6.25321	-6.05391	0.31967	0.87695	1.14031
ENSMUSP00000043559	-5.53221	-7.43649	-6.64270	-5.67299	-6.23980	-5.72927	-6.30345	-5.91217	-7.26963	0.32165	0.68758	1.45437
ENSMUSP00000101105	-9.47306	-11.00388	-9.14804	-9.38835	-9.34603	-8.88118	-8.58051	-8.37725	-8.72018	0.32311	0.66237	1.50972
ENSMUSP00000092746	-7.76631	-9.63384	-8.11473	-8.01832	-7.97600	-7.51115	-9.92267	-7.85480	-9.91920	0.32390	0.66237	1.50972
ENSMUSP00000074935	-10.74794	-9.05277	-10.75964	-9.38696	-9.85606	-9.33201	-10.95459	-11.08789	-10.95112	0.32543	0.68562	1.45852
ENSMUSP00000029684	-10.62324	-8.59135	-8.06589	-8.30620	-7.88429	-8.41836	-9.72831	-9.35020	-9.72484	0.32617	0.62219	1.60723
ENSMUSP00000048363	-9.83632	-9.75415	-10.94960	-9.57692	-10.04602	-9.52196	-10.04297	-11.27785	-11.14107	0.33012	0.68562	1.45852
ENSMUSP00000087192	-6.27244	-6.60228	-7.01710	-6.33565	-6.15310	-6.57921	-6.47909	-6.58675	-6.50194	0.33073	0.78168	1.27929
ENSMUSP00000029805	-7.48840	-6.59337	-7.06675	-6.86914	-6.77164	-6.63305	-8.40537	-8.19235	-8.40190	0.33689	0.78574	1.27269
ENSMUSP00000041149	-7.88792	-9.41873	-7.11068	-7.04073	-7.76089	-7.29604	-6.99537	-9.84086	-6.99189	0.33736	0.65627	1.52376
ENSMUSP00000029837	-7.81834	-9.34678	-8.14030	-7.06464	-8.79051	-7.00968	-9.12419	-7.92183	-8.33177	0.33743	0.41513	2.40887
ENSMUSP00000065585	-11.03735	-9.85360	-8.10040	-9.08819	-8.53485	-8.52221	-11.24400	-9.42758	-11.24052	0.33841	0.75140	1.33084

ENSMUSP00000059395	-10.90701	-8.11264	-7.97006	-7.78744	-8.54765	-7.33853	-11.11366	-11.24696	-11.11018	0.33910	0.52464	1.90605
ENSMUSP00000098053	-11.13250	-9.10061	-8.74227	-9.18334	-8.94026	-8.28081	-8.77010	-9.07052	-8.93375	0.33987	0.59036	1.69387
ENSMUSP00000023790	-7.11134	-7.40869	-11.17046	-7.47459	-6.63666	-7.27391	-6.87238	-7.26022	-6.84668	0.34146	0.55430	1.80407
ENSMUSP00000046910	-9.85438	-9.77220	-8.25309	-9.00482	-7.86290	-8.94986	-8.44804	-9.09275	-10.05756	0.34312	0.59413	1.68314
ENSMUSP00000063744	-11.11195	-9.41678	-9.17393	-9.75097	-8.60945	-9.10783	-9.36888	-10.35032	-9.70213	0.34322	0.57097	1.75141
ENSMUSP00000000137	-9.67358	-8.74326	-10.78686	-9.92559	-8.58292	-8.13482	-10.98180	-11.11510	-10.97833	0.34563	0.45186	2.21307
ENSMUSP00000039844	-8.77732	-9.54328	-10.73874	-9.36606	-9.32374	-8.21190	-9.83211	-9.96541	-9.82864	0.35266	0.56037	1.78455
ENSMUSP00000029217	-8.95092	-9.97032	-8.11448	-8.69151	-8.31247	-8.29983	-9.15757	-8.19127	-9.15410	0.35450	0.73745	1.35603
ENSMUSP00000069004	-6.85975	-6.77757	-6.51998	-6.62212	-6.40285	-6.70534	-6.00335	-6.10093	-6.07539	0.35574	0.87192	1.14690
ENSMUSP00000023486	-11.42603	-11.34386	-9.48802	-10.57647	-10.02274	-9.42192	-11.63268	-10.66441	-11.62921	0.35604	0.67422	1.48319
ENSMUSP00000030642	-10.10632	-7.82297	-8.50503	-8.40861	-7.26726	-8.35366	-8.69998	-7.87722	-8.69650	0.35778	0.54590	1.83183
ENSMUSP00000051657	-8.06063	-10.38038	-8.52454	-8.00237	-8.27032	-8.45844	-8.26727	-7.96511	-9.05274	0.35993	0.69161	1.44591
ENSMUSP00000035034	-10.69362	-10.61144	-9.09233	-8.99591	-9.80174	-9.78910	-10.90027	-9.93199	-10.89680	0.36041	0.68562	1.45852
ENSMUSP00000037962	-10.33208	-10.24990	-8.14261	-8.97110	-8.92878	-8.57942	-10.53873	-9.57045	-10.53526	0.36154	0.82427	1.21319
ENSMUSP00000040222	-9.90074	-8.71897	-11.01402	-8.85240	-10.11044	-7.76109	-11.20897	-11.34227	-11.20549	0.36434	0.36790	2.71814
ENSMUSP00000010254	-8.45536	-10.57436	-9.56666	-9.29555	-8.66505	-8.65242	-8.91347	-9.04676	-9.75814	0.36512	0.72000	1.38888
ENSMUSP00000029082	-8.68723	-10.21804	-8.69893	-8.93924	-7.94086	-8.88428	-9.40529	-8.69045	-10.50339	0.36652	0.60912	1.64171
ENSMUSP00000091429	-13.30169	-11.01834	-12.21182	-12.45213	-11.10945	-10.06046	-10.93929	-12.54006	-12.40329	0.36767	0.36790	2.71814
ENSMUSP00000085523	-7.28640	-7.41937	-7.89900	-7.08053	-7.56280	-7.25385	-7.98269	-7.62635	-8.09047	0.36950	0.79510	1.25771
ENSMUSP00000021719	-7.26430	-8.79511	-8.88899	-8.02773	-7.13727	-7.97277	-6.13529	-9.21724	-7.13075	0.37156	0.68562	1.45852
ENSMUSP00000002090	-6.54276	-9.83217	-6.42523	-6.35535	-6.14939	-6.88826	-7.40880	-7.30565	-7.54847	0.37479	0.65268	1.53213
ENSMUSP00000080302	-10.77067	-8.73878	-10.78237	-9.40969	-8.77919	-9.86615	-9.87575	-11.11062	-10.97385	0.37574	0.67422	1.48319
ENSMUSP00000095197	-10.77219	-10.69002	-9.68430	-10.51279	-9.88229	-9.23343	-10.13070	-10.60072	-10.46395	0.37614	0.61637	1.62239
ENSMUSP00000055743	-8.28257	-10.40156	-9.39387	-8.33382	-9.08044	-8.73108	-10.69039	-10.82369	-10.68691	0.37697	0.72000	1.38888
ENSMUSP00000095655	-10.00532	-7.35409	-10.01702	-5.93546	-6.44947	-10.20237	-7.26332	-6.62736	-6.90838	0.37763	0.16052	6.22988
ENSMUSP00000099475	-6.24623	-12.14737	-5.71032	-6.07521	-6.03289	-5.86966	-6.01995	-6.24610	-6.21169	0.37831	0.72108	1.38682
ENSMUSP00000022437	-9.17808	-8.84445	-9.52651	-9.43009	-8.76844	-8.02474	-9.38473	-9.51803	-11.33097	0.38278	0.56922	1.75678
ENSMUSP00000014457	-6.16660	-9.03307	-6.72502	-6.96533	-6.27619	-6.01219	-6.75285	-6.50655	-7.11725	0.38900	0.66947	1.49371
ENSMUSP00000031910	-7.52492	-7.10619	-8.29910	-7.26599	-7.60942	-6.87451	-7.14365	-7.52831	-7.00201	0.39041	0.71159	1.40530
ENSMUSP00000110027	-9.12558	-11.24457	-9.38873	-9.37759	-9.33527	-9.12187	-10.43182	-8.95450	-11.52993	0.39359	0.74683	1.33899
ENSMUSP00000023085	-7.13399	-9.62086	-7.51356	-7.11765	-7.96301	-6.76035	-7.34064	-7.20559	-7.95649	0.39591	0.62347	1.60393
ENSMUSP00000003906	-8.08006	-7.89778	-8.20301	-7.72105	-8.28975	-7.37127	-8.18660	-8.42001	-8.09214	0.39846	0.71915	1.39052
ENSMUSP00000002043	-10.99696	-8.96506	-11.00866	-9.29925	-10.10507	-9.58102	-11.20360	-11.33690	-11.20013	0.40951	0.76420	1.30856
ENSMUSP00000021049	-7.84644	-8.14386	-7.85815	-7.99835	-7.86504	-7.49133	-7.86200	-7.76346	-8.42922	0.41284	0.84402	1.18480
ENSMUSP00000042285	-9.49260	-8.89901	-10.60588	-8.89647	-8.85415	-9.68966	-10.80082	-10.93412	-10.79735	0.41348	0.67422	1.48319

ENSMUSP00000034276	-6.50731	-8.76185	-7.24510	-6.58237	-7.31790	-6.70437	-6.25608	-6.47454	-6.84866	0.41557	0.73458	1.36132
ENSMUSP00000021329	-7.98081	-8.48682	-7.79176	-8.03206	-7.55429	-7.97711	-8.77564	-8.57222	-7.81611	0.41706	0.81678	1.22432
ENSMUSP00000001452	-8.24208	-7.23176	-7.32564	-6.95766	-7.72951	-7.00948	-6.64700	-7.04559	-6.85943	0.41781	0.70950	1.40944
ENSMUSP00000087948	-10.08425	-10.00208	-9.13990	-9.74809	-8.95829	-9.49237	-8.28866	-8.59891	-8.28519	0.41979	0.75140	1.33084
ENSMUSP00000008036	-6.19439	-9.33535	-6.28949	-6.44640	-6.78983	-5.67841	-6.06452	-5.94647	-6.67206	0.42168	0.67138	1.48946
ENSMUSP00000081000	-10.92257	-8.89068	-9.83270	-8.97341	-9.51927	-9.50664	-8.56017	-11.26252	-8.72382	0.42189	0.73745	1.35603
ENSMUSP00000085379	-10.61013	-10.52796	-8.42066	-9.76057	-8.41789	-9.19420	-8.86707	-9.33709	-9.20032	0.42200	0.73745	1.35603
ENSMUSP00000032919	-7.06819	-6.76056	-6.32542	-6.66809	-6.38247	-6.48938	-7.12562	-7.63995	-7.59416	0.42554	0.85334	1.17187
ENSMUSP00000013304	-9.05854	-8.38818	-7.84584	-8.21135	-8.31218	-7.72885	-8.92847	-8.81031	-8.16252	0.42878	0.77452	1.29113
ENSMUSP00000034586	-7.75095	-9.28177	-9.37565	-9.61596	-7.17171	-6.99195	-7.36942	-7.50272	-7.61740	0.42899	0.35635	2.80623
ENSMUSP00000014221	-8.98267	-8.05235	-10.09594	-8.72326	-8.68094	-8.08013	-10.29089	-10.42419	-10.28742	0.43021	0.73745	1.35603
ENSMUSP00000021790	-7.02426	-8.24244	-6.72569	-7.10915	-7.06683	-6.57449	-7.43166	-7.36420	-8.52779	0.44971	0.78621	1.27193
ENSMUSP00000032065	-9.39643	-8.97753	-9.07141	-8.69239	-9.60612	-7.83490	-9.26636	-9.14820	-9.26288	0.45322	0.51498	1.94184
ENSMUSP00000023514	-7.28794	-9.60770	-9.70158	-7.74072	-8.79799	-7.93722	-6.84777	-7.46078	-7.05566	0.45399	0.87169	1.14720
ENSMUSP00000026735	-10.78406	-9.08890	-10.79577	-9.93450	-9.89218	-9.36813	-9.37772	-11.12401	-10.98724	0.45575	0.81043	1.23391
ENSMUSP00000093955	-9.27421	-7.85638	-8.32986	-7.99947	-7.79679	-8.51521	-6.82680	-6.96010	-7.32485	0.45947	0.74836	1.33626
ENSMUSP00000029815	-8.59490	-9.61430	-7.50701	-7.99877	-8.29318	-7.94382	-8.29014	-8.42343	-8.79808	0.46931	0.87169	1.14720
ENSMUSP00000022865	-10.02936	-11.04876	-9.52965	-9.76996	-10.23905	-9.37827	-9.72459	-9.26971	-9.38440	0.47100	0.76420	1.30856
ENSMUSP00000018851	-8.95642	-8.43730	-8.99591	-9.01025	-8.58135	-7.98431	-8.41007	-8.71161	-8.85492	0.47891	0.71982	1.38923
ENSMUSP00000075954	-10.83801	-10.75584	-10.84972	-7.95028	-11.04771	-11.03507	-7.60638	-7.61830	-7.60291	0.47923	0.15233	6.56452
ENSMUSP00000024932	-7.02300	-8.04002	-8.64532	-7.58527	-7.74371	-7.22005	-9.94184	-10.07514	-9.93837	0.48115	0.83731	1.19430
ENSMUSP00000080403	-8.60898	-10.47652	-10.57040	-9.70914	-9.66682	-8.55459	-10.76535	-10.89865	-9.66030	0.48166	0.76420	1.30856
ENSMUSP00000106014	-6.15304	-9.44245	-5.77079	-6.33835	-6.29604	-6.05380	-6.11604	-5.71707	-6.28952	0.48756	0.92107	1.08569
ENSMUSP00000079340	-5.32911	-6.09433	-9.48832	-6.01073	-6.31473	-5.62626	-6.38315	-5.88039	-9.67979	0.48810	0.91313	1.09513
ENSMUSP00000031707	-8.30883	-8.95771	-8.48090	-8.00646	-8.44705	-8.66625	-9.41366	-9.37984	-9.09992	0.48828	0.81093	1.23315
ENSMUSP00000083973	-7.44816	-9.56715	-7.25910	-7.95162	-7.65785	-6.79764	-7.14379	-6.61770	-7.90279	0.48853	0.72312	1.38289
ENSMUSP00000108229	-8.01367	-6.96184	-7.58991	-7.61886	-7.18701	-6.94477	-7.67360	-8.18650	-8.41761	0.49663	0.79819	1.25283
ENSMUSP00000030698	-10.41560	-8.38371	-8.47759	-8.71789	-8.67558	-8.41148	-10.62225	-9.65397	-10.61878	0.50405	0.83089	1.20353
ENSMUSP00000076589	-11.02870	-9.33354	-9.93883	-9.66772	-10.13682	-9.27604	-11.23535	-11.36865	-11.23188	0.50411	0.76420	1.30856
ENSMUSP00000005647	-7.97778	-7.46014	-7.67921	-7.13091	-8.02035	-7.27665	-7.63771	-8.00746	-8.38171	0.50446	0.75059	1.33228
ENSMUSP00000015100	-9.48992	-10.50931	-10.60319	-9.23051	-9.18819	-10.78855	-8.84842	-8.52951	-9.69309	0.50509	0.57844	1.72878
ENSMUSP00000080998	-8.45382	-9.47322	-9.56710	-8.19442	-9.76509	-8.13946	-8.14906	-8.28236	-8.65700	0.50842	0.57844	1.72878
ENSMUSP00000106104	-9.67654	-8.49279	-6.85085	-7.52662	-8.78466	-6.37279	-9.88319	-10.01649	-9.87972	0.50905	0.56922	1.75678
ENSMUSP00000042150	-10.14066	-8.95691	-8.20264	-8.77968	-7.78130	-9.23614	-8.73432	-8.07867	-10.34383	0.51875	0.66717	1.49887
ENSMUSP00000041968	-8.37132	-7.54167	-10.58420	-7.98711	-8.38025	-8.20050	-8.57797	-8.71127	-8.57450	0.52096	0.90130	1.10951

ENSMUSP00000039264	-11.34209	-10.15834	-10.25222	-10.49253	-10.45021	-9.92616	-10.44717	-11.68204	-11.54527	0.52295	0.81043	1.23391
ENSMUSP00000033008	-8.74658	-10.27739	-8.75828	-9.51001	-7.85707	-8.94364	-8.95323	-10.69952	-8.36158	0.52353	0.60912	1.64171
ENSMUSP00000071214	-7.18989	-7.25616	-6.85527	-6.91732	-7.33288	-6.49147	-8.05593	-7.40061	-8.05246	0.53157	0.80175	1.24728
ENSMUSP00000027853	-7.68572	-9.55326	-8.54557	-7.48552	-8.74356	-8.21951	-7.89237	-8.02567	-7.63745	0.53177	0.73745	1.35603
ENSMUSP00000090284	-9.85438	-5.83603	-5.44286	-6.17021	-6.39619	-5.67761	-6.12485	-5.84614	-6.01014	0.53631	1.01801	0.98231
ENSMUSP00000081474	-6.12607	-9.34401	-6.13778	-6.62945	-6.33577	-6.48350	-6.68419	-6.04823	-6.40623	0.53950	0.98717	1.01299
ENSMUSP00000021993	-7.01620	-9.50307	-7.19502	-7.43533	-7.59377	-7.07011	-6.35362	-6.42439	-7.38650	0.54532	0.91016	1.09871
ENSMUSP00000042988	-9.81426	-9.73208	-9.82596	-10.06627	-10.02395	-7.81015	-7.30872	-7.01447	-6.87770	0.54649	0.34645	2.88643
ENSMUSP00000030914	-10.11068	-6.65692	-7.28499	-7.41404	-6.17286	-8.10656	-10.31733	-10.45062	-8.70086	0.54912	0.65813	1.51946
ENSMUSP00000107966:reversed	-12.89327	-12.81109	-12.90497	-11.19556	-13.10296	-13.09033	-11.48693	-12.13164	-11.99487	0.55624	0.42355	2.36099
ENSMUSP00000107749	-8.25217	-10.37116	-10.46504	-10.70535	-7.71439	-8.44923	-9.55842	-9.18030	-9.55494	0.55636	0.48304	2.07023
ENSMUSP00000060523	-6.08673	-9.14430	-5.93806	-6.52984	-6.72397	-5.86387	-7.23195	-6.26631	-7.02772	0.55992	0.94190	1.06169
ENSMUSP00000030340	-5.82964	-6.39313	-7.50645	-6.31158	-6.22926	-6.25663	-5.82292	-5.81021	-5.71190	0.56308	0.90377	1.10647
ENSMUSP00000029610	-8.31207	-8.22989	-9.42337	-8.36332	-8.77321	-7.99810	-9.10690	-8.45125	-8.76670	0.56770	0.81081	1.23334
ENSMUSP00000036541	-10.01013	-9.92796	-8.92026	-9.16057	-8.27011	-10.20719	-8.60379	-8.73709	-9.11174	0.57121	0.57844	1.72878
ENSMUSP00000032196	-7.84206	-7.24886	-7.34274	-7.45785	-7.20418	-7.40290	-7.53769	-7.98125	-7.84448	0.57128	0.90359	1.10670
ENSMUSP00000030169	-10.62324	-7.82887	-10.63494	-8.92553	-9.73136	-8.61912	-9.21690	-8.76202	-9.21343	0.57517	1.14018	0.87706
ENSMUSP00000020920	-9.70470	-11.23551	-11.32939	-10.46812	-10.42581	-10.41317	-8.68694	-8.82024	-8.47211	0.57546	0.99080	1.00929
ENSMUSP00000023851	-7.36927	-9.48826	-7.96915	-7.42052	-8.67855	-7.36556	-7.57591	-8.80881	-7.82390	0.58365	0.76438	1.30825
ENSMUSP00000105886	-8.60898	-8.86353	-9.46883	-8.86100	-8.81868	-8.80604	-8.19630	-8.94893	-10.76188	0.58428	0.91007	1.09882
ENSMUSP00000095433	-11.71116	-11.04080	-11.38613	-11.62644	-11.33267	-10.47245	-11.12886	-11.46292	-11.57761	0.58465	0.72312	1.38289
ENSMUSP00000032425	-10.37638	-7.89227	-9.28651	-8.67867	-8.97308	-8.62372	-10.58303	-10.71633	-10.57956	0.58891	1.00593	0.99410
ENSMUSP00000022781	-5.73537	-7.01680	-6.94356	-6.13768	-6.76196	-5.98006	-6.87017	-6.34005	-6.33250	0.60061	0.88022	1.13609
ENSMUSP00000015950	-10.21777	-7.93443	-8.27976	-8.52007	-8.47775	-8.21366	-10.42442	-10.55772	-9.31938	0.60078	0.94177	1.06183
ENSMUSP00000001547	-11.90171	-10.20654	-11.91341	-11.05215	-11.00983	-10.99719	-12.10836	-12.24166	-12.10489	0.60190	0.99080	1.00929
ENSMUSP00000066682	-11.14957	-8.66546	-8.75934	-9.45186	-8.52187	-9.14545	-9.74323	-11.48952	-11.35275	0.60191	0.88808	1.12603
ENSMUSP00000045394	-7.21991	-8.30814	-10.60319	-8.44157	-8.23214	-7.73980	-6.78645	-7.16590	-7.17943	0.60405	1.10445	0.90543
ENSMUSP00000039657	-6.45552	-6.35240	-6.40566	-6.55111	-6.24747	-6.23483	-6.99865	-7.50464	-7.53103	0.60647	0.93457	1.07001
ENSMUSP00000054634	-6.98043	-6.57542	-6.66930	-6.66596	-6.73806	-6.61100	-7.28719	-7.32038	-6.67270	0.61279	0.94089	1.06283
ENSMUSP00000030660	-8.88423	-9.90363	-8.38451	-9.13624	-9.09392	-7.98169	-9.09088	-7.92382	-9.08741	0.61351	0.76420	1.30856
ENSMUSP00000019382	-7.33834	-7.53065	-6.90529	-6.95899	-7.33288	-7.14329	-8.81841	-8.06403	-8.19560	0.62550	0.91976	1.08724
ENSMUSP00000026649	-8.57303	-8.49086	-8.24801	-9.33646	-7.44707	-7.54569	-8.44296	-8.57626	-8.43949	0.62616	0.55527	1.80092
ENSMUSP00000100505	-5.97977	-6.21395	-5.62633	-5.93985	-5.97652	-5.56298	-6.08956	-6.13456	-6.05578	0.62677	0.91307	1.09520
ENSMUSP00000045930	-10.65495	-13.14182	-13.23570	-11.52629	-11.82070	-12.31948	-11.22948	-13.56395	-12.32560	0.63072	1.27442	0.78467
ENSMUSP00000102211	-6.24192	-8.99714	-6.88985	-7.71834	-6.71996	-6.22762	-6.71692	-6.70707	-6.57030	0.63137	0.88216	1.13358

ENSMUSP00000025217	-10.16953	-10.08735	-10.18123	-10.42154	-9.86781	-9.85517	-8.52911	-9.99806	-8.76209	0.63198	0.88189	1.13393
ENSMUSP00000018905	-10.24855	-7.59732	-7.42286	-8.09862	-7.88919	-7.87655	-10.45519	-9.48692	-10.45172	0.63661	1.06768	0.93661
ENSMUSP00000015725	-10.24094	-7.95759	-10.25264	-8.54324	-9.34906	-9.33642	-10.44759	-10.58089	-10.44412	0.64067	1.07816	0.92751
ENSMUSP00000106709	-9.90371	-9.82153	-8.81383	-9.05414	-10.11340	-8.48777	-9.00878	-9.14208	-9.00531	0.64454	0.70717	1.41408
ENSMUSP00000087974	-5.81644	-6.51605	-6.53846	-6.13866	-6.13339	-6.24091	-5.65795	-5.89010	-6.16534	0.64458	0.94551	1.05763
ENSMUSP00000056604	-7.67871	-9.54625	-7.43895	-7.31139	-8.73654	-7.42355	-9.83507	-7.76720	-8.21861	0.64857	0.80218	1.24660
ENSMUSP00000053900	-9.87547	-9.28188	-9.88717	-9.61607	-9.57375	-9.56111	-11.18369	-11.31699	-11.18022	0.65107	0.93427	1.07035
ENSMUSP00000088581	-10.77516	-10.69298	-9.68528	-11.02717	-9.88327	-9.35922	-9.03209	-8.91393	-9.87676	0.65148	0.70717	1.41408
ENSMUSP00000096435	-9.86629	-10.88569	-10.97956	-11.21987	-10.07598	-9.55193	-9.56152	-9.69482	-10.06947	0.65332	0.70717	1.41408
ENSMUSP00000006435	-11.00942	-9.82567	-11.02112	-9.64844	-10.11754	-11.20648	-9.26636	-10.24780	-9.26288	0.65359	0.70717	1.41408
ENSMUSP00000085251	-7.88792	-9.41873	-7.11068	-7.80320	-8.60903	-6.74932	-7.50639	-7.27181	-8.09110	0.65403	0.74683	1.33899
ENSMUSP00000068568	-7.41881	-7.20600	-8.79411	-7.62535	-7.27879	-7.76616	-11.39099	-9.12236	-9.43780	0.65538	0.91791	1.08944
ENSMUSP00000025955	-8.25054	-7.86413	-8.30771	-8.30186	-8.15599	-7.60024	-7.86936	-8.50532	-8.02624	0.65897	0.85920	1.16387
ENSMUSP00000079232	-6.96544	-10.49850	-10.59238	-7.78394	-10.79037	-7.16250	-7.64759	-7.36097	-7.11597	0.66131	0.84232	1.18720
ENSMUSP00000099788	-11.29533	-9.26344	-10.20546	-10.44577	-10.40345	-8.78020	-11.50198	-10.53371	-11.49851	0.66224	0.66717	1.49887
ENSMUSP00000109671	-11.45522	-10.52490	-12.56850	-10.85909	-11.15350	-11.65228	-10.81373	-10.94703	-12.75997	0.66657	0.93427	1.07035
ENSMUSP00000093965	-8.72063	-7.91921	-7.56574	-8.06680	-7.83156	-7.81892	-9.67476	-9.80805	-9.30341	0.66697	0.94194	1.06164
ENSMUSP00000029722	-5.55645	-5.77561	-6.06287	-5.44449	-6.13569	-5.43578	-5.88394	-6.07386	-6.28138	0.66910	0.85453	1.17024
ENSMUSP00000047356	-9.24375	-8.82485	-10.86845	-8.90758	-9.11672	-9.95223	-11.06339	-9.58370	-9.95835	0.67121	0.87169	1.14720
ENSMUSP00000039726	-7.10615	-7.27543	-7.70604	-6.84714	-7.90403	-6.79219	-6.29084	-6.93508	-6.67311	0.67625	0.76446	1.30812
ENSMUSP00000072775	-10.46865	-6.94819	-7.18024	-7.58092	-8.72863	-6.55047	-8.72559	-7.85996	-9.05884	0.67890	0.82621	1.21035
ENSMUSP00000075987	-5.61916	-5.99273	-6.42723	-5.71422	-6.13192	-5.84271	-6.48683	-6.50093	-6.61871	0.68132	0.92185	1.08478
ENSMUSP00000044050	-9.24451	-9.16233	-8.31764	-8.25940	-8.43223	-9.44156	-10.03934	-9.38369	-8.50911	0.69824	0.80377	1.24414
ENSMUSP00000019198	-9.80840	-9.72622	-6.87145	-7.65847	-7.18070	-10.00545	-7.81387	-7.57930	-7.60964	0.70969	0.92269	1.08378
ENSMUSP00000050446	-8.24559	-7.89507	-8.42440	-8.22925	-8.07568	-8.06305	-9.40829	-9.54159	-8.61588	0.70986	0.94994	1.05269
ENSMUSP00000028225	-10.99875	-10.91657	-9.39746	-9.63777	-11.20844	-9.58281	-9.25568	-8.50130	-8.63288	0.71273	0.81043	1.23391
ENSMUSP00000054856	-7.87509	-8.89448	-7.88679	-9.22867	-7.57336	-6.97255	-8.08174	-7.70362	-7.56685	0.71670	0.59413	1.68314
ENSMUSP00000067681	-7.07660	-9.19559	-6.88754	-7.58006	-7.87447	-6.76263	-6.34468	-6.78032	-6.76875	0.71824	0.99108	1.00900
sp|TRY1_BOVIN|	-6.98679	-10.12775	-10.22163	-8.84895	-8.80663	-8.45727	-7.36783	-8.14795	-7.27337	0.72256	2.02467	0.49391
ENSMUSP00000100074	-5.30338	-6.65087	-6.28203	-5.88627	-6.27932	-5.55843	-6.05918	-5.82848	-6.55048	0.72527	0.97056	1.03033
ENSMUSP00000031931	-6.53064	-7.59732	-8.31053	-7.45181	-7.08666	-7.30586	-7.08361	-7.36536	-6.78384	0.72660	1.06489	0.93907
ENSMUSP00000030164	-7.70165	-7.88419	-7.58272	-8.00129	-7.70223	-7.19394	-7.86283	-7.87095	-7.55512	0.73747	0.88010	1.13624
ENSMUSP00000024797	-11.22082	-11.13864	-11.23252	-10.37125	-11.43051	-11.41787	-9.81447	-10.45919	-9.81100	0.74235	0.76329	1.31011
ENSMUSP00000045111	-10.22556	-10.14338	-10.23726	-9.37599	-10.43525	-10.42261	-9.33063	-9.46393	-9.32716	0.74235	0.76329	1.31011
ENSMUSP00000101139	-9.76635	-9.68417	-9.77805	-8.91678	-9.97604	-9.96340	-7.57106	-7.15765	-8.86795	0.74235	0.76329	1.31011

ENSMUSP00000035105	-6.11742	-6.17437	-6.00702	-5.85340	-6.38046	-5.87914	-5.28794	-5.52814	-5.78918	0.74604	0.91709	1.09040
ENSMUSP00000023677	-5.54453	-5.77440	-6.16069	-5.79654	-5.73381	-5.76242	-5.63454	-5.74965	-6.00494	0.74768	0.96784	1.03322
ENSMUSP00000093959	-11.29267	-11.21049	-11.30437	-11.54468	-10.40079	-11.48973	-9.88633	-10.53104	-10.39427	0.75644	0.76329	1.31011
ENSMUSP00000034000	-10.77292	-10.69074	-8.83490	-9.92335	-9.88103	-9.86840	-10.97956	-11.11286	-10.97609	0.75828	1.27442	0.78467
ENSMUSP00000023238	-10.94924	-10.86706	-10.96094	-11.20125	-11.15893	-10.04472	-8.75396	-7.85090	-9.20270	0.76022	0.76329	1.31011
ENSMUSP00000059801	-11.42018	-11.33801	-11.43189	-11.67219	-11.62988	-10.51567	-9.42566	-9.55896	-9.67364	0.76022	0.76329	1.31011
ENSMUSP00000025802	-10.11933	-10.03716	-10.13104	-10.37135	-10.32903	-9.21482	-7.92405	-9.35771	-7.75346	0.76022	0.76329	1.31011
ENSMUSP00000033483	-11.23504	-11.15286	-11.24674	-11.48705	-11.44473	-10.33052	-9.24052	-9.62527	-9.03629	0.76022	0.76329	1.31011
ENSMUSP00000045654	-9.49288	-9.41070	-9.50458	-9.74489	-9.70257	-8.58836	-7.49836	-8.21984	-7.74634	0.76022	0.76329	1.31011
ENSMUSP00000029777	-9.31403	-9.23185	-10.42730	-9.56604	-9.52372	-9.51108	-10.62225	-10.75555	-10.61878	0.76383	0.99080	1.00929
ENSMUSP00000060940	-10.74564	-8.71375	-10.75734	-9.89608	-9.85376	-9.84112	-10.95229	-11.08559	-10.94882	0.77417	1.27442	0.78467
ENSMUSP00000020640	-8.33221	-7.61381	-9.44351	-7.73664	-9.13008	-7.89305	-7.90264	-7.73359	-8.02437	0.77644	0.85936	1.16365
ENSMUSP00000023513	-9.91962	-8.22445	-9.93132	-8.22192	-9.02774	-10.11668	-9.02470	-8.64658	-9.02122	0.77950	0.81043	1.23391
ENSMUSP00000040853	-7.47828	-8.33467	-8.42855	-7.82128	-8.25866	-7.86643	-7.38638	-6.91055	-7.68145	0.78218	0.98580	1.01440
ENSMUSP00000099480	-6.82564	-7.63114	-6.53499	-7.07765	-7.03533	-6.55997	-7.30063	-6.86324	-7.29716	0.78680	0.98187	1.01847
ENSMUSP00000041907	-10.45334	-8.42145	-10.46504	-10.70535	-8.26110	-9.54882	-8.71027	-9.18030	-8.70680	0.79296	0.76420	1.30856
ENSMUSP00000095081	-8.07947	-8.33401	-8.09117	-8.33148	-7.19012	-8.61325	-10.23583	-8.75614	-9.13079	0.79457	0.73354	1.36325
ENSMUSP00000053145	-7.30785	-9.17539	-8.16769	-7.55986	-9.46726	-6.88557	-8.36264	-7.64780	-7.25957	0.80698	0.66717	1.49887
ENSMUSP00000088736	-9.80739	-10.82679	-8.20847	-8.11223	-8.71673	-11.10602	-8.71368	-9.29920	-8.91097	0.81183	0.73354	1.36325
ENSMUSP00000056082	-9.64176	-8.25923	-8.18599	-8.79417	-8.38398	-8.53846	-9.33699	-11.08328	-10.94651	0.81290	1.04261	0.95913
ENSMUSP00000079628	-6.21521	-6.49410	-6.22691	-6.07186	-6.70258	-5.97690	-6.36301	-5.97407	-7.08181	0.81398	0.90735	1.10211
ENSMUSP00000030903	-8.97422	-8.69128	-8.98592	-9.22623	-8.43643	-8.80340	-9.76904	-9.90234	-9.17739	0.81530	0.90130	1.10951
ENSMUSP00000032192	-12.72139	-10.68949	-10.02089	-10.13600	-11.31809	-11.30545	-11.82646	-13.06133	-12.92456	0.81597	1.08552	0.92121
sp|TRYP_PIG|	-3.49710	-3.68456	-3.69546	-3.65230	-3.68170	-3.47585	-3.38819	-3.70846	-3.35910	0.81746	0.98043	1.01996
ENSMUSP00000025178	-10.28033	-11.29972	-11.39360	-11.63391	-10.49002	-10.47738	-10.48698	-9.52068	-10.48350	0.82425	0.90961	1.09937
ENSMUSP00000089348	-7.50838	-9.62737	-9.72125	-9.96156	-8.81767	-7.33756	-7.51427	-6.82636	-7.20053	0.82548	0.82427	1.21319
ENSMUSP00000103086	-7.67473	-9.20554	-7.68643	-7.92674	-8.39584	-7.87178	-8.39279	-8.01467	-7.87790	0.82788	1.07816	0.92751
ENSMUSP00000043540	-8.54024	-10.07106	-7.59589	-8.20407	-8.74994	-8.73730	-10.35988	-8.88019	-9.25484	0.82839	1.27442	0.78467
ENSMUSP00000057595	-5.44112	-5.22657	-5.17054	-5.35666	-5.06302	-5.33296	-5.80039	-5.84459	-5.42424	0.83088	0.96980	1.03114
ENSMUSP00000074448	-10.79947	-9.10430	-9.70959	-11.05148	-8.60723	-9.38353	-9.90454	-9.52642	-9.38965	0.83844	0.67422	1.48319
ENSMUSP00000003620	-10.09312	-8.71058	-7.98325	-8.87765	-8.69219	-8.82270	-8.83229	-9.92165	-9.19669	0.84274	1.21223	0.82492
ENSMUSP00000107927	-9.62631	-10.33307	-9.63801	-9.56805	-10.03676	-9.82336	-8.93477	-11.26661	-9.82948	0.84479	0.98301	1.01728
ENSMUSP00000005431	-9.44310	-9.36092	-10.30294	-9.69511	-9.20058	-9.97688	-10.49789	-11.73277	-10.49442	0.84599	0.94177	1.06183
ENSMUSP00000016771	-9.02502	-7.94059	-7.64173	-8.79412	-8.39723	-7.00199	-8.42449	-9.23574	-10.03073	0.85059	0.75259	1.32874
ENSMUSP00000023806	-9.46649	-9.38431	-9.14146	-9.38177	-8.06603	-10.17496	-9.67313	-11.41942	-11.28265	0.85285	0.61876	1.61615

ENSMUSP00000057664	-7.93101	-7.10136	-7.94271	-7.54680	-7.50448	-7.76019	-8.13766	-7.03385	-7.93343	0.85977	1.00319	0.99682
ENSMUSP00000002551	-7.36177	-9.48077	-7.62493	-9.81496	-7.82292	-6.14476	-7.20055	-6.76315	-7.81641	0.86429	0.48121	2.07808
ENSMUSP00000066038	-9.09648	-10.11587	-8.00858	-8.24889	-9.30617	-9.29353	-7.83565	-7.48925	-7.68903	0.86827	1.10435	0.90551
ENSMUSP00000110434	-5.74562	-5.73448	-6.52769	-5.95293	-5.99020	-5.93131	-5.73715	-6.14441	-6.08315	0.87405	1.00941	0.99068
ENSMUSP00000020820	-10.14487	-7.86152	-9.05500	-8.19571	-9.25299	-9.24035	-10.35152	-10.48482	-10.34804	0.87605	1.10435	0.90551
ENSMUSP00000041104	-8.33799	-7.42532	-7.74880	-7.86774	-8.01350	-7.47627	-7.88122	-8.46658	-8.23882	0.87666	0.98116	1.01921
ENSMUSP00000020637	-7.68204	-6.75249	-6.70153	-7.22580	-6.89952	-6.84292	-7.37781	-7.47539	-7.77079	0.87739	1.01850	0.98184
ENSMUSP00000022821	-8.76005	-8.67787	-10.38474	-8.42388	-8.38156	-10.57010	-9.47812	-9.61141	-8.96323	0.87805	0.73745	1.35603
ENSMUSP00000070149	-9.14318	-7.96140	-10.25645	-9.39519	-8.25327	-9.34023	-8.25023	-8.63498	-8.83494	0.87817	1.10435	0.90551
ENSMUSP00000103257	-8.15599	-6.97422	-9.26927	-8.40800	-8.36568	-7.25345	-9.46421	-9.59751	-9.46074	0.87865	1.10435	0.90551
ENSMUSP00000065987	-8.67457	-8.90266	-8.17533	-8.33867	-9.19453	-8.02416	-9.19148	-8.50358	-9.64023	0.88170	0.89028	1.12324
ENSMUSP00000101665	-7.63554	-9.50307	-7.19502	-7.63609	-8.18195	-8.16932	-8.17891	-6.97655	-6.95104	0.88202	1.27442	0.78467
ENSMUSP00000047254	-9.95958	-10.97898	-9.97129	-9.70018	-9.65786	-11.25821	-8.55561	-8.26137	-8.55214	0.88327	0.81043	1.23391
ENSMUSP00000091608	-8.32461	-7.73102	-7.48817	-7.72848	-8.02289	-7.67353	-8.01985	-8.15314	-8.52779	0.89082	1.00593	0.99410
ENSMUSP00000069962	-9.57984	-8.19730	-9.08012	-8.09603	-9.27811	-9.26548	-9.27507	-9.91978	-10.88459	0.90369	0.89663	1.11529
ENSMUSP00000107659	-10.64386	-7.84949	-8.08651	-8.69470	-8.90383	-8.63974	-10.85051	-10.98381	-10.84704	0.90524	1.47844	0.67639
ENSMUSP00000028619	-7.08364	-7.00146	-6.91839	-6.79928	-7.11638	-7.05109	-7.58883	-7.09633	-7.88771	0.91504	0.97801	1.02248
ENSMUSP00000103012	-8.81984	-10.58474	-9.83048	-8.30260	-8.53990	-11.96555	-8.92639	-9.39624	-8.11717	0.91740	0.50614	1.97575
ENSMUSP00000026818	-7.43143	-7.34925	-7.44313	-8.05131	-7.16141	-6.89742	-8.59413	-8.13925	-9.10208	0.91908	0.87188	1.14695
ENSMUSP00000020358	-6.94450	-10.00207	-6.87281	-10.33625	-6.43944	-6.51576	-7.24214	-6.92338	-6.98731	0.92014	0.68614	1.45743
ENSMUSP00000032539	-5.77073	-5.52150	-5.53199	-5.44910	-5.58688	-5.75497	-6.09467	-5.92375	-5.68721	0.93092	0.98299	1.01730
ENSMUSP00000092502	-10.41560	-5.88638	-5.80779	-5.29255	-5.57746	-10.61266	-5.72749	-5.86079	-6.17174	0.93205	0.64234	1.55681
ENSMUSP00000026924	-9.03795	-8.95577	-8.67005	-8.91036	-8.86804	-8.85541	-7.21413	-7.93525	-6.90049	0.93366	1.00606	0.99398
ENSMUSP00000006181	-8.86474	-7.55816	-7.92039	-8.01755	-8.48625	-7.72614	-8.28245	-8.61651	-9.06792	0.93684	1.03725	0.96409
ENSMUSP00000102062	-9.70303	-9.62086	-7.76502	-7.00640	-9.91273	-9.90009	-7.34064	-6.67140	-6.05172	0.94172	0.54572	1.83244
ENSMUSP00000001592	-11.37824	-8.72701	-10.28836	-10.52867	-10.48635	-9.17336	-9.38371	-9.76847	-9.63170	0.94234	1.27442	0.78467
ENSMUSP00000072483	-8.10244	-8.16341	-9.72476	-8.49760	-8.31213	-9.06197	-8.45224	-8.31719	-7.96906	0.94851	1.12872	0.88596
ENSMUSP00000071939	-8.04580	-8.23197	-9.28191	-8.42301	-8.38070	-8.67832	-9.98827	-9.61015	-9.13666	0.95100	1.08786	0.91924
ENSMUSP00000025197	-8.75512	-7.87041	-7.89759	-8.01652	-8.39412	-8.08294	-10.42924	-9.46295	-9.12541	0.97641	1.04528	0.95668
ENSMUSP00000004673	-8.73415	-7.88949	-7.85817	-8.22368	-8.49162	-7.74118	-8.32147	-8.31162	-7.93840	0.98247	1.01426	0.98594
ENSMUSP00000040140	-7.66059	-7.51171	-8.47482	-7.91260	-8.29322	-7.41822	-8.66977	-8.65992	-8.66630	0.98528	1.00031	0.99969
ENSMUSP00000027602	-7.79685	-7.26992	-7.80855	-7.77118	-8.00654	-7.10180	-7.04788	-7.69205	-7.50526	0.99675	0.95310	1.04921
ENSMUSP00000017572	-7.69406	-7.91423	-8.27646	-8.24842	-8.33130	-7.31296	-7.66887	-8.12500	-8.46793	0.99462	0.92520	1.08085
ENSMUSP00000032114	-9.09286	-8.84357	-8.93745	-9.54563	-8.86709	-8.46871	-11.70144	-9.88503	-10.59640	0.99414	0.92449	1.08168
ENSMUSP00000018437	-7.27461	-9.59437	-7.28631	-7.35951	-7.04884	-9.87360	-8.27020	-7.30430	-7.47779	0.97320	0.94540	1.05776

ENSMUSP00000024596	-9.14450	-9.39905	-9.15620	-8.94430	-9.10274	-9.67828	-11.30087	-11.43417	-9.09622	0.97315	0.96840	1.03263
ENSMUSP00000108237	-10.29004	-8.36079	-11.40331	-10.54205	-9.98831	-9.63895	-10.49668	-11.73156	-11.59479	0.96895	1.95471	0.51158
ENSMUSP00000040840	-8.41055	-8.01811	-8.87447	-8.66256	-8.62024	-8.06089	-11.01913	-8.95126	-11.01566	0.96775	1.02567	0.97497
ENSMUSP00000008812	-5.06522	-9.76657	-4.44886	-10.10076	-4.56922	-5.03745	-4.60856	-4.50410	-4.66761	0.95631	1.11796	0.89448
ENSMUSP00000015256	-6.43605	-6.12915	-6.78109	-6.37894	-6.66161	-6.34738	-6.70776	-7.06632	-6.95082	0.95119	1.02881	0.97200
ENSMUSP00000051222	-6.51027	-8.99714	-6.68909	-7.13016	-8.18743	-7.07520	-7.33625	-7.21809	-7.08132	0.94422	1.51732	0.65906
ENSMUSP00000031524	-7.40804	-7.25916	-7.74257	-7.41639	-8.15192	-6.92926	-7.61469	-7.45168	-7.68268	0.94276	0.92994	1.07534
ENSMUSP00000019726	-10.82958	-8.17835	-10.84128	-9.13187	-11.03927	-9.92506	-9.08651	-8.33213	-8.83158	0.94095	1.73841	0.57524
ENSMUSP00000103145	-9.97091	-8.27575	-8.36962	-8.60993	-9.07903	-9.06640	-10.17756	-8.36115	-10.17409	0.93922	1.27442	0.78467
ENSMUSP00000074994	-6.99736	-9.62737	-7.31932	-7.01292	-9.91924	-7.33756	-7.07881	-6.67792	-6.19482	0.93431	1.04261	0.95913
ENSMUSP00000072236	-6.98094	-6.89876	-6.89578	-6.84455	-6.89870	-7.05083	-7.60160	-7.35537	-7.54811	0.93148	1.00092	0.99908
ENSMUSP00000088837	-10.92025	-10.32666	-12.03353	-11.17226	-11.12995	-11.11731	-12.22848	-12.36178	-12.22500	0.93066	1.27442	0.78467
ENSMUSP00000020209	-8.23009	-8.65933	-8.75321	-7.38290	-8.43978	-10.04014	-8.10001	-7.47083	-7.64433	0.93036	0.66717	1.49887
ENSMUSP00000018561	-9.90827	-8.55267	-8.56957	-9.90882	-8.69609	-8.61676	-8.69305	-9.14918	-8.92142	0.92228	1.08969	0.91770
ENSMUSP00000025598	-8.87969	-10.41050	-9.40281	-9.13170	-10.70237	-9.07675	-6.80316	-6.71739	-6.84136	0.92205	1.04243	0.95930
ENSMUSP00000105796	-7.22751	-9.71438	-7.40633	-8.43558	-7.80508	-8.38063	-8.39022	-7.18786	-7.43069	0.91754	1.67715	0.59625
ENSMUSP00000087632	-5.59285	-10.29420	-10.38808	-10.62839	-5.81950	-10.57344	-6.46779	-6.17934	-6.40080	0.91717	1.29584	0.77170
ENSMUSP00000101495	-9.64637	-9.56419	-9.65807	-8.79878	-10.95764	-9.33201	-10.95459	-11.08789	-9.84955	0.91568	0.76420	1.30856
ENSMUSP00000090564	-7.53464	-6.88598	-7.37196	-7.39712	-7.74433	-6.76876	-9.17705	-7.48506	-8.58540	0.91515	0.98853	1.01160
ENSMUSP00000109215	-8.53402	-8.20039	-8.54572	-8.78603	-8.29150	-8.27886	-8.12134	-8.62251	-8.48574	0.90581	1.01063	0.98949
ENSMUSP00000097561	-13.29525	-14.06121	-12.54447	-12.92793	-14.35308	-12.87297	-13.83862	-12.53616	-15.44814	0.90346	1.09856	0.91028
ENSMUSP00000031314	-9.00230	-7.89816	-9.60219	-9.25431	-8.46452	-8.99860	-8.84108	-8.83123	-8.45801	0.90282	1.27442	0.78467
ENSMUSP00000111272	-5.51098	-5.36771	-5.04385	-5.40867	-5.25164	-5.32110	-5.48041	-5.35277	-5.54106	0.89918	1.04230	0.95942
ENSMUSP00000031472	-6.93102	-7.15119	-6.85932	-6.95119	-6.90887	-7.12807	-7.13767	-7.27097	-7.22519	0.89504	1.02264	0.97786
ENSMUSP00000090897	-4.68152	-7.65798	-8.08859	-6.71875	-7.94985	-6.27170	-6.75678	-6.09365	-6.03856	0.89221	2.97397	0.33625
ENSMUSP00000083928	-9.28514	-9.82230	-8.42761	-9.90503	-8.76377	-9.10260	-10.95926	-11.09256	-9.85619	0.88874	1.18171	0.84623
ENSMUSP00000088729	-11.27111	-7.81735	-11.28281	-11.52312	-8.10922	-11.46816	-7.97694	-8.23947	-8.25114	0.88756	1.27442	0.78467
ENSMUSP00000005477	-9.40173	-8.09515	-7.97767	-6.89290	-11.22441	-7.98864	-10.11979	-9.15349	-9.01672	0.88601	0.52181	1.91641
ENSMUSP00000030078	-8.56593	-7.93704	-10.97956	-9.60688	-9.56456	-8.76299	-7.95137	-8.73876	-8.33365	0.88377	1.88167	0.53144
ENSMUSP00000026144	-10.22167	-10.13950	-8.62038	-10.47368	-8.48165	-10.41873	-5.78920	-6.79608	-6.48867	0.88332	0.99080	1.00929
ENSMUSP00000075825	-11.11673	-9.08483	-11.12843	-9.16757	-11.32642	-11.31378	-9.71039	-9.25550	-9.11873	0.87976	1.04243	0.95930
ENSMUSP00000019937	-9.50053	-7.99648	-8.02366	-8.99006	-7.89440	-8.93511	-10.55532	-11.79019	-10.55185	0.87847	1.16965	0.85495
ENSMUSP00000105420	-9.76891	-8.89779	-9.78061	-10.53234	-9.18966	-9.00991	-11.58855	-11.72185	-9.63536	0.87421	0.99108	1.00900
ENSMUSP00000022380	-7.81300	-8.27753	-8.37141	-8.30146	-8.13394	-8.12131	-8.01965	-8.26420	-7.74168	0.87073	1.06630	0.93783
ENSMUSP00000032992	-9.43272	-8.41197	-8.80820	-9.04851	-9.89387	-8.06541	-9.27149	-8.92509	-9.12488	0.85478	0.93197	1.07299

ENSMUSP00000026270	-7.95524	-7.28520	-7.47218	-7.53422	-7.34066	-8.00385	-11.38503	-8.56968	-8.08145	0.85308	1.04783	0.95435
ENSMUSP00000002091	-7.46642	-6.99849	-6.87723	-6.74482	-6.79560	-8.09893	-7.67307	-7.80636	-8.10505	0.84599	0.95906	1.04269
ENSMUSP00000044827	-10.89683	-10.30324	-9.60817	-11.14884	-11.10652	-9.05572	-11.10348	-10.13718	-12.20158	0.84131	0.83476	1.19794
ENSMUSP00000091035	-6.00909	-6.07003	-6.16391	-6.09745	-5.68160	-6.64557	-5.51149	-5.86520	-5.64944	0.84095	0.98585	1.01435
ENSMUSP00000038135	-9.27095	-8.95232	-8.62327	-9.18641	-9.99167	-8.06496	-9.47760	-9.61090	-9.61728	0.83349	0.88223	1.13349
ENSMUSP00000081142	-8.87672	-9.30596	-8.88842	-8.17267	-10.69940	-8.73705	-9.59478	-9.21667	-9.59131	0.82913	0.78862	1.26804
ENSMUSP00000022062	-6.85993	-6.48084	-7.03199	-6.79685	-7.57229	-6.28662	-7.09159	-7.74422	-7.45025	0.82837	0.98529	1.01493
ENSMUSP00000034234	-8.92039	-7.88216	-9.44351	-8.38346	-9.13008	-9.11745	-7.90264	-8.67216	-8.78684	0.81758	1.27442	0.78467
ENSMUSP00000029645	-9.73854	-7.70919	-7.71207	-8.14348	-9.10009	-8.46812	-8.84559	-8.04032	-7.90355	0.81395	1.53593	0.65107
ENSMUSP00000018449	-11.48454	-11.40237	-11.49625	-11.22514	-12.79581	-10.83346	-12.79277	-12.92607	-11.68772	0.80650	0.88189	1.13393
ENSMUSP00000016072	-9.63774	-8.28961	-9.21398	-9.06855	-9.20062	-9.18798	-9.84439	-9.00804	-10.29313	0.80553	1.27442	0.78467
ENSMUSP00000075150	-7.67473	-9.20554	-7.34970	-8.43815	-8.39584	-7.87178	-8.39279	-8.01467	-7.54118	0.80473	1.50641	0.66383
ENSMUSP00000108058	-9.28805	-8.69446	-9.29975	-9.54006	-8.98633	-8.97369	-8.19434	-7.78093	-8.64308	0.80377	1.07816	0.92751
ENSMUSP00000021630	-6.34762	-7.66653	-7.09699	-7.53800	-7.23613	-6.70125	-7.07485	-6.63121	-6.52222	0.80217	1.25335	0.79786
ENSMUSP00000109228	-7.29479	-6.61172	-6.52865	-6.94591	-6.67399	-7.02913	-7.76978	-7.24899	-7.28661	0.80148	1.11674	0.89546
ENSMUSP00000025511	-5.55728	-5.74799	-5.30775	-5.64453	-5.35652	-5.75434	-5.99835	-5.42907	-5.64766	0.79870	1.05771	0.94544
ENSMUSP00000067767	-7.24510	-7.25602	-8.35561	-6.39843	-11.26580	-6.53923	-9.31304	-7.67815	-7.88770	0.79801	0.52108	1.91910
ENSMUSP00000101006	-7.27403	-9.76090	-7.28573	-8.14538	-8.43978	-8.42715	-7.21234	-7.78110	-7.64433	0.79557	2.02467	0.49391
ENSMUSP00000104884	-9.26967	-10.03563	-11.23108	-10.36982	-10.32750	-10.31486	-11.42603	-11.55933	-11.42256	0.79495	1.55804	0.64183
ENSMUSP00000104163	-10.30022	-9.11647	-8.36220	-9.45065	-9.40834	-9.39570	-10.50687	-10.64017	-10.50339	0.79259	1.55804	0.64183
ENSMUSP00000099950	-10.49465	-9.56433	-9.65821	-11.84824	-9.23687	-9.39135	-10.18988	-10.32318	-11.79940	0.79162	0.86639	1.15422
ENSMUSP00000089769	-7.89638	-7.61344	-6.67096	-7.78051	-7.16750	-7.58241	-8.10302	-7.29775	-8.68773	0.79136	1.27442	0.78467
ENSMUSP00000000804	-7.76620	-7.74655	-7.56081	-8.08074	-7.62221	-7.52789	-7.97285	-8.04730	-8.09860	0.78857	1.03729	0.96405
ENSMUSP00000048469	-6.28986	-6.33831	-6.18604	-6.32280	-6.38403	-6.17402	-6.58167	-6.15214	-6.57820	0.78692	1.02370	0.97685
ENSMUSP00000105177	-11.30328	-11.22110	-9.11381	-10.45372	-10.41140	-11.50034	-10.40836	-10.54165	-9.55674	0.77702	2.00405	0.49899
ENSMUSP00000053270	-8.83877	-10.70631	-9.69862	-9.93893	-10.99818	-9.03583	-7.49433	-7.46055	-7.69155	0.77168	1.27442	0.78467
ENSMUSP00000011526	-8.61728	-10.48482	-9.47713	-8.86929	-9.67512	-10.76406	-9.67207	-8.33790	-8.56900	0.76798	1.27442	0.78467
ENSMUSP00000078996	-6.86029	-9.82686	-6.54916	-6.93791	-7.54968	-10.10610	-6.67740	-6.63375	-7.06346	0.76685	1.66668	0.59999
ENSMUSP00000038744	-8.29071	-9.82153	-9.91541	-8.54273	-10.11340	-10.10076	-8.49736	-7.67461	-9.00531	0.75937	1.27442	0.78467
ENSMUSP00000020562	-8.19823	-7.28556	-8.47828	-8.06450	-8.84339	-7.56479	-7.19486	-7.26033	-7.26415	0.75885	1.17245	0.85292
ENSMUSP00000062670	-8.08496	-7.85964	-7.82832	-8.19383	-8.15151	-7.62793	-9.75909	-9.38097	-10.85719	0.75421	1.04265	0.95909
ENSMUSP00000043543	-7.45066	-6.98888	-8.92983	-8.07054	-8.61641	-7.37937	-8.61336	-7.64746	-8.27316	0.75195	1.43893	0.69496
ENSMUSP00000058368	-7.29312	-6.78340	-6.64543	-6.95721	-7.07527	-6.90226	-7.07222	-6.97368	-7.15974	0.74497	1.10888	0.90181
ENSMUSP00000004172	-8.93734	-8.26698	-8.36086	-8.23330	-8.55885	-9.13440	-10.75698	-10.89028	-10.75351	0.73856	1.08552	0.92121
ENSMUSP00000054391	-10.85881	-9.67505	-9.25752	-10.00924	-11.06850	-9.44287	-9.96388	-9.58576	-9.44899	0.73733	1.27442	0.78467

ENSMUSP00000041152	-9.09248	-7.91071	-7.63671	-8.49635	-8.45403	-8.18994	-9.29913	-7.96496	-8.44752	0.73349	1.38530	0.72186
ENSMUSP00000021595	-7.92243	-8.21985	-8.17058	-7.62227	-8.24338	-8.86696	-7.40984	-7.71021	-7.51459	0.72517	1.01516	0.98507
ENSMUSP00000027193	-7.82178	-9.35259	-7.24530	-7.73707	-9.64446	-8.01884	-8.53985	-7.57355	-8.02496	0.72478	1.47069	0.67995
ENSMUSP00000110314	-11.19909	-8.54787	-8.49860	-10.34953	-9.79579	-9.19498	-11.40574	-9.92605	-9.78928	0.72108	2.17472	0.45983
ENSMUSP00000100992	-6.71732	-6.90963	-5.63029	-6.57723	-6.33914	-6.83740	-7.00736	-6.23299	-6.28914	0.71584	1.39135	0.71872
ENSMUSP00000053540	-10.16566	-10.08348	-4.86964	-10.41767	-10.37535	-6.92443	-4.34443	-4.36345	-4.43748	0.70108	7.84226	0.12751
ENSMUSP00000035222	-6.12350	-6.45333	-7.91434	-6.91270	-7.45824	-6.85774	-7.96614	-8.86192	-9.57329	0.69479	1.56258	0.63997
ENSMUSP00000028852	-9.74897	-9.66679	-9.24925	-9.15284	-9.95866	-9.94602	-11.05719	-11.19049	-11.05372	0.69300	1.07816	0.92751
ENSMUSP00000021471	-8.47227	-7.77076	-8.03176	-8.27207	-8.06263	-8.21711	-10.62864	-10.76194	-10.62517	0.68847	1.12872	0.88596
ENSMUSP00000046480	-6.57342	-6.76574	-6.43668	-6.82543	-6.44659	-6.69350	-7.80204	-7.56746	-7.79857	0.68810	1.06931	0.93518
ENSMUSP00000035033	-8.10326	-8.29875	-9.66605	-8.80733	-9.41183	-8.57799	-8.67098	-8.72088	-8.58411	0.68192	1.45333	0.68808
ENSMUSP00000070267	-9.98086	-7.69752	-7.04392	-8.28316	-7.78862	-10.17792	-8.57452	-8.70782	-9.08247	0.68088	1.94564	0.51397
sp|CASB_BOVIN|	-10.19805	-10.11587	-7.49756	-10.45006	-10.40774	-8.44539	-5.62117	-6.16417	-6.02740	0.67635	2.40891	0.41512
ENSMUSP00000021930	-6.57288	-7.09377	-7.41949	-6.94505	-7.61748	-6.97905	-7.61444	-8.48554	-8.03851	0.66899	1.18419	0.84446
ENSMUSP00000030191	-10.63578	-11.65518	-11.74906	-11.98937	-11.94705	-10.83284	-9.99429	-10.46431	-10.32754	0.66453	1.27442	0.78467
ENSMUSP00000073975	-10.92064	-8.63729	-10.93234	-11.17265	-9.51734	-11.11770	-8.92612	-8.85866	-8.92264	0.66353	2.00405	0.49899
ENSMUSP00000032597	-6.89145	-5.83566	-6.51741	-6.84111	-6.79879	-6.16036	-7.73432	-6.76868	-7.36297	0.65099	1.24578	0.80271
ENSMUSP00000009790	-8.43950	-8.02060	-7.35200	-8.10333	-7.69314	-8.63656	-8.64615	-7.82339	-7.85374	0.64660	1.27442	0.78467
ENSMUSP00000101027	-10.74333	-7.82377	-8.18599	-9.89377	-8.55110	-9.83882	-9.84841	-11.08328	-10.94651	0.64262	2.32476	0.43015
ENSMUSP00000025567	-8.09670	-7.90327	-8.54386	-8.98493	-7.84367	-8.29375	-8.73881	-10.17246	-11.13727	0.64046	1.13011	0.88487
ENSMUSP00000033121	-10.25479	-10.68403	-10.77791	-12.11979	-10.46449	-10.11512	-12.07443	-12.20773	-12.07096	0.63518	1.07816	0.92751
ENSMUSP00000000727	-7.93949	-7.22109	-8.53937	-7.99074	-7.94842	-8.38800	-10.34731	-10.48061	-10.34383	0.63371	1.36235	0.73402
ENSMUSP00000030432	-7.20730	-8.47551	-9.41754	-8.55825	-9.61553	-8.13542	-7.57432	-7.40907	-7.66183	0.63143	1.88647	0.53009
ENSMUSP00000095695	-8.40367	-8.90967	-9.51497	-8.65568	-8.61336	-10.80190	-8.24244	-8.23260	-8.23897	0.62809	1.14018	0.87706
ENSMUSP00000065271	-6.87267	-5.93394	-6.11359	-5.46480	-5.59626	-10.50801	-6.75206	-6.38384	-6.33537	0.62784	0.72398	1.38125
ENSMUSP00000099938	-7.86030	-8.28915	-10.58420	-9.72293	-10.78219	-8.05736	-7.94175	-8.07505	-7.40409	0.62680	1.67715	0.59625
ENSMUSP00000004140	-6.22159	-6.34010	-6.30880	-5.62107	-5.40812	-10.43033	-10.43993	-10.57323	-5.87819	0.62658	0.67996	1.47067
ENSMUSP00000065542	-8.45868	-7.58789	-11.18258	-9.47317	-8.54318	-11.36794	-8.80848	-8.67344	-8.97212	0.62650	2.49851	0.40024
ENSMUSP00000019896	-7.62822	-7.98150	-7.10573	-7.49448	-7.96311	-7.71402	-9.05927	-9.19257	-9.56721	0.62564	1.23121	0.81221
ENSMUSP00000069209	-6.39642	-6.76111	-7.89891	-7.21486	-7.17254	-7.41124	-6.01928	-6.28110	-5.75227	0.61805	1.50747	0.66336
ENSMUSP00000106471	-8.18805	-7.37481	-7.82015	-7.96036	-8.12940	-7.73101	-9.35075	-8.52800	-9.34728	0.60716	1.19349	0.83788
ENSMUSP00000062005:reversed	-9.18415	-8.59056	-8.09626	-8.33656	-8.88243	-9.38121	-9.39080	-9.01268	-8.28773	0.60672	1.27442	0.78467
ENSMUSP00000108056	-9.71949	-8.16984	-7.88412	-8.12443	-11.03076	-8.44907	-11.02771	-9.54802	-9.07453	0.60283	1.35169	0.73982
ENSMUSP00000091840	-8.52685	-9.54625	-7.43895	-8.77886	-9.83812	-8.21249	-7.43314	-7.56644	-7.63043	0.60023	1.84167	0.54299
ENSMUSP00000092888	-8.37537	-10.24291	-8.38707	-8.96411	-8.92179	-10.52214	-9.43016	-9.56346	-9.42669	0.59639	1.73841	0.57524

sp|CAS1_BOVIN|	-10.17385	-10.09168	-6.00680	-10.42587	-10.38355	-8.16974	-5.09288	-5.60412	-5.32920	0.59500	7.77023	0.12870
ENSMUSP00000034607	-9.92016	-8.98984	-9.08372	-9.66076	-9.28171	-9.60580	-7.66872	-8.06157	-7.78663	0.59276	1.27442	0.78467
ENSMUSP00000043660	-7.49379	-7.92264	-8.01652	-9.35642	-7.70348	-7.45440	-9.31106	-8.14400	-8.79617	0.59111	1.13660	0.87982
ENSMUSP00000071636	-10.18603	-7.53480	-8.24801	-9.33646	-9.29414	-8.77009	-7.99074	-7.57733	-7.82015	0.58859	2.43439	0.41078
ENSMUSP00000108956	-11.68291	-9.39956	-8.74597	-8.56334	-11.89260	-11.87996	-8.84081	-8.79972	-8.93744	0.58803	1.19216	0.83881
ENSMUSP00000004729	-9.19142	-8.26110	-9.20313	-8.59529	-9.40112	-9.38848	-9.39807	-8.23101	-7.92713	0.58551	1.27442	0.78467
ENSMUSP00000079180	-6.09177	-6.28726	-6.10347	-6.47301	-6.24261	-6.02410	-6.23957	-5.95788	-6.74700	0.58422	1.08383	0.92265
ENSMUSP00000026425	-7.45242	-6.62294	-6.95323	-7.33665	-8.01358	-6.55075	-8.01053	-7.86934	-9.85413	0.58229	1.18273	0.84550
ENSMUSP00000023433	-9.57432	-9.49214	-10.09744	-9.82633	-11.39700	-9.18319	-10.29238	-9.91427	-11.39049	0.57763	1.10435	0.90551
ENSMUSP00000005066	-9.13265	-9.56189	-10.75734	-10.99765	-9.00562	-10.94270	-8.24010	-8.88442	-8.99910	0.57448	1.27442	0.78467
ENSMUSP00000030028	-9.20807	-9.63731	-9.73119	-11.07308	-8.82959	-9.91655	-9.41472	-11.16101	-11.02424	0.56849	1.07816	0.92751
ENSMUSP00000083375	-7.49209	-6.55115	-7.35535	-7.66713	-7.36526	-7.01612	-7.30664	-8.10653	-7.96976	0.56799	1.29739	0.77078
ENSMUSP00000060584	-6.57731	-6.29884	-5.60965	-6.32816	-6.24297	-6.46580	-7.76890	-7.96890	-7.64405	0.56699	1.31334	0.76142
ENSMUSP00000027111	-7.58792	-7.29663	-8.06504	-7.66928	-7.89526	-7.83260	-7.74910	-8.32182	-8.98758	0.55824	1.19659	0.83571
ENSMUSP00000024946	-7.87810	-8.16380	-10.45885	-8.74944	-10.65684	-9.03121	-9.04081	-8.58592	-9.03733	0.55754	2.25575	0.44331
ENSMUSP00000078369	-9.46649	-10.99730	-11.09118	-11.33149	-10.18760	-11.27653	-8.44873	-8.70723	-8.33401	0.55632	1.78555	0.56005
ENSMUSP00000036265	-11.89808	-11.81590	-10.29679	-12.15009	-12.10777	-10.99356	-11.00315	-10.28831	-10.48826	0.55558	1.78555	0.56005
ENSMUSP00000040550	-8.20682	-7.29414	-8.00716	-7.73656	-8.68485	-7.86968	-7.87928	-8.24442	-7.19997	0.55505	1.27442	0.78467
ENSMUSP00000087110	-11.26427	-11.18209	-9.66298	-11.51628	-10.37239	-11.46133	-9.85793	-9.03517	-8.89840	0.55345	1.78555	0.56005
ENSMUSP00000032927	-8.85566	-10.38648	-10.48036	-9.61909	-10.67835	-10.66571	-8.72559	-8.60743	-8.47066	0.54912	1.78555	0.56005
ENSMUSP00000047661	-6.66352	-9.41873	-7.11068	-9.75292	-8.09761	-7.49680	-6.75891	-7.27181	-6.48095	0.54531	2.46493	0.40569
ENSMUSP00000080614	-8.25712	-8.96388	-9.05776	-8.70989	-9.25575	-8.90639	-10.86570	-9.89742	-10.86223	0.54437	1.27442	0.78467
ENSMUSP00000046016	-6.51428	-7.53131	-6.01504	-9.47848	-6.72397	-6.12342	-9.43312	-6.19484	-9.42965	0.53892	1.33371	0.74979
ENSMUSP00000037930	-8.99335	-8.61263	-8.77321	-9.33635	-9.50539	-8.31845	-11.23816	-9.33329	-11.23469	0.53777	1.13737	0.87922
ENSMUSP00000089808	-7.19542	-7.34508	-7.86651	-7.31820	-8.06450	-7.62432	-8.57248	-8.06956	-9.15719	0.53776	1.20261	0.83153
ENSMUSP00000034131	-11.49370	-10.30995	-9.89242	-11.74572	-10.60182	-10.58919	-10.59878	-10.22066	-9.29495	0.53752	1.63923	0.61004
ENSMUSP00000070751	-8.15328	-10.64015	-7.59429	-9.36135	-8.53009	-10.91939	-8.72781	-9.96070	-9.82393	0.52764	2.77491	0.36037
ENSMUSP00000044004	-10.05881	-9.03447	-9.39925	-10.50192	-10.03666	-9.04742	-9.96692	-10.58985	-12.30015	0.52441	1.29481	0.77231
ENSMUSP00000070993	-7.30060	-7.69813	-8.15988	-7.65272	-8.35787	-7.83421	-7.41626	-7.38919	-7.84033	0.52169	1.27442	0.78467
ENSMUSP00000022842	-8.49379	-7.84092	-7.77443	-8.17511	-8.04939	-8.42250	-7.60160	-7.78755	-7.25432	0.51974	1.23520	0.80959
ENSMUSP00000023210	-6.87118	-6.56072	-7.41103	-6.93658	-7.31047	-7.17646	-8.03352	-8.47708	-8.34031	0.51523	1.25186	0.79881
ENSMUSP00000005508	-9.26618	-7.95960	-8.94116	-8.72925	-8.37667	-11.07623	-11.08582	-9.26940	-9.46936	0.51172	1.36887	0.73053
ENSMUSP00000053842	-8.98437	-8.65074	-9.84422	-10.08453	-9.53079	-8.92997	-8.93957	-8.87210	-8.93609	0.50637	1.42447	0.70202
ENSMUSP00000055313	-9.74689	-8.81657	-8.65899	-9.48748	-9.44517	-9.09580	-11.05511	-11.18841	-11.05164	0.49854	1.42447	0.70202
ENSMUSP00000025294	-10.05413	-9.97195	-8.76547	-10.30614	-8.96346	-11.35276	-7.64445	-7.88041	-7.01069	0.49174	1.44449	0.69228

ENSMUSP00000064699	-7.42992	-7.61608	-7.87708	-7.68193	-7.42825	-8.85137	-8.86097	-10.60726	-9.36891	0.49098	1.21513	0.82296
ENSMUSP00000104831	-7.79432	-7.46956	-8.69345	-8.21697	-8.56860	-8.07306	-9.09975	-9.50140	-9.53174	0.48877	1.46721	0.68157
ENSMUSP00000010007	-6.42296	-6.73723	-7.60896	-7.01877	-7.59559	-7.07204	-7.92910	-7.82595	-7.92563	0.48688	1.46226	0.68387
ENSMUSP00000066181	-9.45390	-7.65355	-8.70312	-8.94343	-9.21138	-8.88848	-9.99727	-9.34163	-9.99380	0.48264	1.89629	0.52735
ENSMUSP00000026495	-4.86772	-4.88886	-5.35806	-5.19180	-5.46766	-4.96003	-5.20063	-5.57995	-5.67602	0.48157	1.18236	0.84576
ENSMUSP00000021806	-7.89107	-10.21082	-10.30470	-10.54501	-9.40112	-10.49005	-8.54993	-8.68323	-8.88318	0.48155	3.31893	0.30130
ENSMUSP00000099664	-8.01660	-7.56655	-7.28083	-8.06785	-7.28773	-8.46511	-7.28468	-7.60908	-8.01902	0.47686	1.27442	0.78467
ENSMUSP00000046079	-6.94595	-6.41816	-6.68320	-7.09787	-6.50731	-7.01166	-7.08477	-7.18581	-7.34205	0.47152	1.18838	0.84148
ENSMUSP00000097738	-8.87929	-8.28570	-7.79139	-10.23288	-9.08898	-7.60887	-7.61847	-6.88253	-7.78211	0.46824	1.27442	0.78467
ENSMUSP00000052086	-5.99892	-5.86410	-10.72455	-10.96486	-10.92254	-6.21416	-5.82134	-6.03111	-6.03643	0.45891	2.62937	0.38032
ENSMUSP00000026420	-6.10185	-5.89829	-5.88395	-6.35386	-6.03192	-5.88269	-6.44667	-6.50850	-6.52017	0.45710	1.12447	0.88931
ENSMUSP00000101300	-8.35792	-8.78716	-9.98262	-10.22293	-8.56762	-10.16797	-8.56457	-8.10969	-9.07252	0.44943	1.63923	0.61004
ENSMUSP00000101023	-8.79423	-9.16427	-8.63881	-9.04624	-8.83680	-9.19204	-11.40281	-9.92312	-11.39934	0.44207	1.19715	0.83532
ENSMUSP00000080354	-6.33570	-5.72898	-6.10377	-6.63478	-6.09130	-6.09337	-6.86514	-6.72272	-7.07299	0.43917	1.23852	0.80742
ENSMUSP00000026843	-5.28669	-5.07803	-5.63757	-5.69398	-5.35418	-5.45277	-5.44081	-5.94089	-5.59898	0.43535	1.19341	0.83793
ENSMUSP00000033176	-5.86940	-5.74667	-6.32525	-6.05472	-6.56721	-5.98694	-7.16102	-7.07525	-7.07907	0.43052	1.23628	0.80888
ENSMUSP00000057543	-9.06349	-7.88211	-8.28625	-8.09110	-10.88618	-8.67237	-9.27014	-8.81526	-9.26667	0.43019	1.46332	0.68338
ENSMUSP00000020262	-9.33934	-8.74575	-9.35105	-8.29100	-10.65061	-10.63797	-9.54599	-10.78087	-10.64409	0.42729	1.07816	0.92751
ENSMUSP00000073322	-5.40984	-5.27083	-5.32146	-10.80793	-5.10870	-5.12453	-10.76257	-10.89587	-10.75910	0.42606	1.22462	0.81658
ENSMUSP00000038063	-8.87002	-8.58708	-8.13425	-9.71021	-7.90930	-9.65526	-11.27784	-10.30957	-11.27437	0.42274	1.27442	0.78467
ENSMUSP00000044587	-6.53064	-6.31188	-6.44924	-6.94090	-6.41083	-6.43391	-7.50655	-7.02883	-7.50308	0.42239	1.15304	0.86728
ENSMUSP00000071976	-6.30476	-7.11001	-7.02951	-7.26981	-7.88159	-6.54183	-6.77970	-7.63224	-6.32888	0.42054	1.42093	0.70377
ENSMUSP00000061152	-5.77280	-6.10971	-6.56225	-6.20175	-6.51766	-6.38895	-6.88237	-7.15879	-7.25162	0.42011	1.29649	0.77131
ENSMUSP00000027108	-9.08041	-8.15009	-8.24397	-9.33242	-8.44196	-8.76605	-8.77564	-8.32076	-9.28359	0.41802	1.44449	0.69228
ENSMUSP00000032946	-7.42423	-7.21686	-6.84802	-7.24870	-6.90784	-10.33348	-7.29433	-10.47638	-7.29085	0.41555	1.36713	0.73146
ENSMUSP00000077021	-8.59860	-8.51642	-8.44319	-8.11280	-11.21023	-8.79566	-11.20718	-11.34048	-11.20371	0.41554	1.27442	0.78467
ENSMUSP00000032143	-6.66502	-5.91693	-6.04452	-6.60543	-6.21991	-6.50432	-7.29342	-7.30348	-7.19613	0.41545	1.30345	0.76719
ENSMUSP00000026459	-4.82558	-4.69471	-5.17542	-4.99387	-5.33902	-4.89772	-5.12816	-5.29876	-5.32689	0.41513	1.19023	0.84017
ENSMUSP00000019226	-6.95937	-7.06528	-7.58209	-7.33276	-8.32680	-7.10085	-10.72568	-8.45705	-9.62064	0.41406	1.33896	0.74685
ENSMUSP00000002837	-7.83901	-7.21012	-7.41525	-8.09102	-7.73844	-7.38925	-10.44759	-8.01184	-10.44412	0.41143	1.27442	0.78467
ENSMUSP00000019323	-8.14560	-7.89630	-9.45766	-8.84982	-10.75722	-8.34265	-8.80446	-10.88748	-10.75070	0.40602	1.81139	0.55206
ENSMUSP00000097754	-7.39723	-7.17847	-7.07943	-7.51266	-7.08635	-7.54666	-7.42562	-7.95427	-7.75865	0.40387	1.16220	0.86044
ENSMUSP00000021062	-7.77390	-7.51477	-7.78560	-8.09261	-8.19874	-7.47306	-8.37008	-8.98308	-8.36661	0.39729	1.20159	0.83223
ENSMUSP00000073261	-7.97848	-7.89630	-8.35806	-7.96215	-10.75722	-8.17554	-10.75418	-10.88748	-9.64913	0.38445	1.43893	0.69496
ENSMUSP00000103365	-5.26435	-5.51866	-5.73771	-5.76289	-5.85873	-5.44474	-6.81624	-6.14934	-6.20364	0.38206	1.20530	0.82967

ENSMUSP00000027966	-9.50592	-10.52531	-8.41802	-10.85950	-10.81718	-9.19156	-9.71257	-9.33445	-9.70909	0.38088	2.36886	0.42214
ENSMUSP00000049394	-7.82713	-8.11283	-10.40788	-9.54662	-8.99288	-10.59324	-8.40166	-8.53496	-7.88716	0.38019	3.25978	0.30677
ENSMUSP00000069508	-8.95911	-8.02935	-7.80040	-9.01036	-9.75698	-7.91905	-8.65474	-8.06195	-9.75047	0.37933	1.59990	0.62504
ENSMUSP00000020329	-7.86728	-8.18156	-8.38986	-8.99124	-8.42078	-7.99413	-8.86249	-8.71811	-9.68022	0.37901	1.31655	0.75956
ENSMUSP00000099441	-9.91666	-8.98634	-9.41694	-11.27024	-10.12635	-9.01412	-9.27517	-10.25661	-8.65236	0.37860	1.47069	0.67995
ENSMUSP00000068408	-8.85324	-9.87066	-9.11640	-9.10525	-9.65111	-11.25147	-9.64807	-10.29279	-11.25759	0.36793	1.61457	0.61936
ENSMUSP00000045841	-9.27359	-8.98005	-8.40478	-9.22325	-9.37203	-8.93645	-9.09449	-10.04900	-9.09102	0.36539	1.41804	0.70520
ENSMUSP00000019469	-7.53427	-7.54308	-7.38560	-7.70288	-7.32404	-8.92135	-10.88066	-9.91239	-10.87719	0.36467	1.35052	0.74046
ENSMUSP00000020463	-9.50374	-9.08483	-9.17871	-9.41902	-9.37670	-9.36407	-11.32338	-11.45668	-11.31990	0.36449	1.15297	0.86733
ENSMUSP00000042364	-9.96086	-8.77711	-7.26037	-10.21287	-10.17056	-8.54493	-9.06594	-9.19924	-8.55105	0.36433	3.46330	0.28874
ENSMUSP00000009003	-8.51919	-7.84883	-8.53089	-9.28262	-8.39216	-8.37952	-10.33883	-9.37056	-10.33536	0.36180	1.42447	0.70202
ENSMUSP00000027975	-10.62843	-8.93327	-9.02714	-9.26745	-10.83813	-10.82549	-8.88537	-8.76721	-8.26256	0.36119	2.00405	0.49899
ENSMUSP00000049732	-7.46449	-8.02913	-8.12301	-8.36332	-8.15388	-7.87290	-9.61831	-8.90347	-8.76670	0.36060	1.33661	0.74816
ENSMUSP00000109305	-8.15399	-7.76155	-10.56762	-10.80793	-9.66404	-9.13998	-9.14958	-9.79429	-9.14610	0.35845	3.82703	0.26130
ENSMUSP00000006838	-8.00968	-7.69790	-7.52349	-8.56023	-7.98977	-7.63333	-8.09495	-8.28710	-7.98325	0.35692	1.31800	0.75873
ENSMUSP00000035157	-6.86214	-7.05764	-6.81500	-7.17668	-7.01299	-6.89213	-8.00056	-7.33132	-8.36496	0.35613	1.12875	0.88593
ENSMUSP00000002403	-6.26306	-5.76101	-6.33449	-6.13404	-6.69954	-6.29976	-6.89719	-6.86684	-7.08948	0.35378	1.28518	0.77810
ENSMUSP00000048460	-7.35761	-7.02398	-6.37038	-7.60962	-7.31585	-6.93533	-7.56426	-7.24534	-7.30933	0.34992	1.53821	0.65010
ENSMUSP00000074600	-8.20352	-7.66913	-9.06336	-8.79226	-9.26135	-8.40058	-7.95795	-7.19307	-9.25484	0.34789	1.78464	0.56034
ENSMUSP00000038839	-8.03415	-7.65343	-7.51770	-8.47725	-7.52909	-8.23120	-7.66263	-8.01302	-7.56606	0.34731	1.33171	0.75092
ENSMUSP00000075990	-8.72603	-7.68780	-7.94879	-7.64239	-9.44714	-9.43451	-10.54567	-9.57740	-10.54220	0.34641	1.47844	0.67639
ENSMUSP00000022734	-9.92365	-8.54112	-9.08721	-9.66425	-10.13334	-9.27257	-10.13030	-10.26360	-11.22840	0.34475	1.78464	0.56034
ENSMUSP00000004574	-8.72677	-7.75691	-9.58661	-9.82692	-10.88618	-8.30449	-10.88313	-11.01643	-10.87966	0.34430	2.02467	0.49391
ENSMUSP00000044871	-9.48447	-9.06557	-8.70724	-9.73649	-8.73811	-11.29452	-9.69112	-10.33584	-10.19907	0.34188	1.54291	0.64813
ENSMUSP00000028396	-8.33734	-7.58857	-7.99757	-7.92275	-11.49567	-8.25990	-11.49263	-11.62593	-11.48916	0.34107	1.67908	0.59556
ENSMUSP00000099653	-8.36858	-7.26444	-7.53270	-7.77301	-8.82973	-8.05461	-9.67483	-8.95998	-10.77293	0.33931	1.63018	0.61343
ENSMUSP00000103015	-10.05903	-8.15156	-8.54398	-9.35498	-10.26872	-9.30003	-9.92895	-10.91039	-10.77362	0.33545	2.42600	0.41220
ENSMUSP00000099417	-6.73548	-5.74345	-5.85480	-6.77515	-6.24664	-6.46117	-7.66811	-7.56500	-7.50100	0.33435	1.55701	0.64226
ENSMUSP00000078670	-6.77734	-6.10729	-6.11601	-6.69282	-6.49226	-6.58229	-6.90701	-6.32873	-6.98051	0.32758	1.34210	0.74510
ENSMUSP00000047606	-9.54271	-9.12381	-9.21769	-9.79472	-9.75241	-9.15159	-11.36235	-11.49565	-11.35888	0.32713	1.27442	0.78467
ENSMUSP00000020741	-9.06349	-8.19237	-7.97599	-8.72732	-9.78460	-8.47161	-9.27014	-9.06672	-9.26667	0.32556	1.71795	0.58209
ENSMUSP00000022322	-5.39956	-5.29725	-5.58079	-5.53040	-6.33340	-5.42281	-6.48102	-6.27320	-6.94595	0.32358	1.30216	0.76796
ENSMUSP00000006900	-8.08349	-9.61430	-7.75846	-9.94849	-9.90617	-8.28054	-7.95341	-7.83525	-7.69848	0.32313	2.36886	0.42214
ENSMUSP00000004375	-6.43333	-6.28332	-6.93278	-6.61751	-7.39032	-6.70315	-7.24910	-7.00968	-7.73527	0.32230	1.38289	0.72312
ENSMUSP00000103657	-7.99588	-8.76185	-7.75613	-8.58462	-8.20557	-9.04108	-10.15225	-8.67255	-10.14877	0.32066	1.61457	0.61936

ENSMUSP00000090910	-11.09259	-6.27863	-11.10429	-11.34460	-11.30228	-11.28965	-6.43502	-6.05748	-6.20995	0.32053	49.06447	0.02038
ENSMUSP00000022925	-9.04606	-7.86468	-7.95856	-8.19887	-8.91902	-9.75453	-9.76412	-8.59707	-8.29318	0.31958	1.78446	0.56039
ENSMUSP00000017488	-10.97887	-9.79512	-9.88900	-11.23088	-11.18856	-10.07435	-9.57253	-10.21725	-9.56906	0.31875	1.78555	0.56005
ENSMUSP00000026899	-6.76361	-6.91104	-6.94239	-7.18270	-7.02595	-6.81755	-7.92595	-7.33316	-8.06563	0.31657	1.14142	0.87610
ENSMUSP00000022894	-7.73117	-8.01687	-10.31192	-8.60251	-10.50991	-10.49727	-7.93782	-7.92797	-8.10146	0.31623	3.25978	0.30677
ENSMUSP00000096932	-7.41816	-9.73791	-6.78304	-7.87093	-10.02978	-10.01715	-7.62481	-7.02030	-7.62134	0.31283	3.82634	0.26135
ENSMUSP00000026222	-8.11195	-8.87792	-7.67144	-9.21211	-8.32164	-8.64573	-8.06715	-8.20045	-8.06367	0.31237	1.78464	0.56034
ENSMUSP00000095287	-6.36361	-6.21473	-6.60715	-6.76406	-6.32965	-6.70911	-6.50356	-6.17897	-6.56679	0.31234	1.21582	0.82249
ENSMUSP00000036246	-6.59422	-6.38282	-6.65299	-6.96834	-6.59698	-11.26157	-6.73417	-7.39277	-7.05862	0.31218	1.85312	0.53963
ENSMUSP00000055535	-7.75796	-7.67578	-7.97036	-8.13920	-11.46846	-7.84059	-11.46542	-9.19678	-11.46195	0.31199	1.76907	0.56527
ENSMUSP00000056027	-10.20203	-8.17013	-7.81180	-9.35246	-10.41172	-9.29751	-9.30710	-8.34080	-8.45549	0.31105	3.46330	0.28874
ENSMUSP00000080854	-6.33448	-5.55146	-5.86658	-6.20698	-7.00503	-5.92677	-7.58015	-7.08765	-8.14737	0.30709	1.50433	0.66475
ENSMUSP00000046324	-7.72395	-8.26110	-10.30470	-9.44343	-10.50269	-9.38848	-8.54993	-9.01995	-7.92713	0.30612	3.82811	0.26123
ENSMUSP00000041872	-8.02513	-8.89901	-9.50430	-9.74461	-10.80387	-8.59006	-10.80082	-9.83255	-10.79735	0.30584	2.05948	0.48556
ENSMUSP00000033873	-7.55874	-7.68792	-7.18091	-7.42122	-7.76843	-8.23550	-8.86442	-8.54551	-9.19768	0.30174	1.35286	0.73917
ENSMUSP00000028704	-8.48758	-7.76918	-7.26217	-8.22857	-9.79687	-7.93717	-7.33574	-7.97995	-7.84318	0.29595	1.96354	0.50928
ENSMUSP00000066715	-5.95966	-5.99885	-6.77523	-6.37700	-6.58923	-6.84043	-7.32385	-7.51968	-7.44961	0.29550	1.47979	0.67577
ENSMUSP00000022980	-7.66429	-7.14666	-8.12821	-7.91630	-7.87398	-8.31356	-8.07170	-7.45753	-8.65641	0.28680	1.53821	0.65010
ENSMUSP00000016400	-9.39997	-8.80637	-8.56353	-9.14056	-10.71123	-9.08561	-10.70819	-10.84149	-10.70472	0.28652	1.73841	0.57524
ENSMUSP00000010795	-6.26635	-6.38236	-6.72366	-6.39187	-6.79031	-7.10194	-5.42034	-5.20049	-5.17430	0.28613	1.31032	0.76317
ENSMUSP00000043047	-6.83073	-7.26761	-8.43978	-8.24473	-7.90010	-8.22978	-7.42161	-7.38924	-7.59508	0.28249	2.20957	0.45258
ENSMUSP00000033953	-10.76842	-9.07325	-7.40854	-9.40744	-10.97811	-10.96548	-7.75193	-8.05962	-7.53331	0.28232	6.38180	0.15670
ENSMUSP00000037617	-7.05736	-7.04188	-6.83946	-7.24684	-6.89433	-7.55296	-10.70229	-7.69585	-10.69882	0.28224	1.24918	0.80052
ENSMUSP00000083271	-9.22603	-7.40885	-7.39149	-9.27728	-8.41376	-8.78687	-9.23192	-9.19810	-10.52880	0.28211	2.81373	0.35540
ENSMUSP00000049025	-7.53336	-7.45118	-6.44618	-8.57431	-8.53199	-6.83223	-8.52895	-7.32659	-7.93729	0.28133	1.89463	0.52781
ENSMUSP00000043111	-8.54776	-9.56715	-8.55946	-8.79977	-9.85902	-9.84639	-8.24299	-8.03956	-8.75093	0.27857	1.78555	0.56005
ENSMUSP00000093394	-9.26012	-9.68935	-8.93509	-9.51213	-11.08280	-9.45717	-9.97818	-9.01188	-9.46329	0.27799	1.73841	0.57524
ENSMUSP00000033342	-8.04372	-7.58195	-8.05542	-8.02739	-9.72089	-8.09763	-7.15153	-7.58113	-7.76719	0.27761	1.63868	0.61025
ENSMUSP00000105531	-7.05158	-6.42700	-7.06328	-7.22661	-6.98360	-7.17166	-7.53272	-7.24308	-8.07596	0.27700	1.36232	0.73404
ENSMUSP00000003912	-8.64521	-7.09632	-8.65691	-8.69646	-9.10636	-8.64151	-9.44004	-8.98516	-11.04956	0.27417	2.50546	0.39913
ENSMUSP00000099907	-10.20243	-9.78353	-10.72555	-10.11772	-10.92354	-12.01248	-10.92050	-10.20566	-12.01860	0.27171	1.73841	0.57524
ENSMUSP00000106961	-10.89517	-8.61182	-10.90687	-11.14718	-11.10487	-11.09223	-9.15211	-10.13355	-9.48536	0.26981	4.68800	0.21331
ENSMUSP00000021335	-10.15443	-9.22411	-10.16613	-10.40644	-9.85271	-11.45306	-9.26148	-9.02691	-9.50947	0.26907	1.84167	0.54299
ENSMUSP00000089350	-6.89488	-9.52489	-9.61877	-9.85908	-9.81676	-9.80413	-6.59058	-5.86512	-6.30943	0.26823	7.24818	0.13797
ENSMUSP00000109399	-5.61463	-5.83199	-5.75150	-6.01884	-6.25967	-10.25872	-6.41382	-6.13456	-6.45384	0.26562	2.20316	0.45389

ENSMUSP00000031697	-9.26937	-10.28679	-9.28107	-10.10956	-11.68023	-9.71788	-9.27525	-10.70891	-10.06072	0.26533	2.05948	0.48556
ENSMUSP00000045284	-7.78372	-9.16902	-8.41475	-8.65506	-10.56246	-8.93683	-8.35825	-8.74300	-9.45437	0.26466	2.25575	0.44331
ENSMUSP00000024897	-7.35157	-8.26832	-7.74287	-7.71484	-10.50991	-8.54756	-8.30570	-8.07112	-10.50339	0.26152	1.98848	0.50290
ENSMUSP00000006235	-8.98118	-9.41042	-8.40471	-9.23320	-9.70229	-9.17824	-9.18783	-9.32113	-10.79735	0.26066	1.66695	0.59990
ENSMUSP00000061059	-10.42834	-8.39645	-10.44004	-10.68035	-10.63803	-10.62540	-7.68634	-8.56712	-9.01852	0.25906	3.83460	0.26078
ENSMUSP00000102987	-7.17927	-6.90600	-7.73769	-7.66773	-7.93568	-7.37633	-8.72158	-7.24473	-7.92916	0.25884	1.50105	0.66620
ENSMUSP00000009256	-9.71735	-8.16770	-9.72905	-9.96936	-11.02862	-9.40299	-11.02558	-10.05730	-9.92053	0.25753	2.69254	0.37140
ENSMUSP00000031038	-8.34328	-8.00965	-8.35498	-8.14308	-10.50269	-8.87706	-9.39807	-10.63295	-10.49617	0.25475	1.72457	0.57986
ENSMUSP00000015800	-6.96798	-6.06705	-6.23839	-6.97180	-6.86563	-6.61551	-6.99465	-6.91663	-7.11635	0.25443	1.56128	0.64050
ENSMUSP00000071777:reversed	-10.75391	-11.77133	-11.86521	-13.20709	-11.55178	-12.05056	-10.96056	-11.34531	-11.54527	0.25397	2.12529	0.47052
ENSMUSP00000049338	-7.64335	-7.68637	-8.29127	-8.16370	-8.74072	-7.96560	-7.24910	-7.26103	-6.82942	0.25391	1.49298	0.66980
ENSMUSP00000108940	-10.53338	-10.45121	-8.14315	-10.78539	-10.74308	-10.73044	-8.17098	-8.30428	-8.02437	0.25369	5.54139	0.18046
ENSMUSP00000031637	-6.49300	-9.12302	-6.81497	-8.35563	-8.31331	-9.40225	-6.84280	-6.49639	-6.69618	0.24956	4.92255	0.20315
ENSMUSP00000073541	-7.73917	-7.58002	-7.20848	-7.65466	-7.67119	-7.93623	-8.59991	-7.74260	-8.45329	0.24933	1.30183	0.76815
ENSMUSP00000030118	-8.20834	-8.12617	-9.17610	-8.62747	-9.88551	-9.02473	-9.37105	-9.50435	-10.98057	0.24913	1.88167	0.53144
ENSMUSP00000034547	-8.37546	-7.32363	-7.56595	-8.46035	-9.03737	-7.75131	-9.88247	-9.50435	-7.93182	0.24791	1.84100	0.54318
ENSMUSP00000033229	-7.55283	-9.67182	-9.76570	-10.00601	-9.96369	-9.95106	-7.24846	-7.04520	-6.58560	0.24787	4.68800	0.21331
ENSMUSP00000032898	-11.79142	-11.70925	-9.60195	-12.04343	-12.00112	-11.98848	-9.59614	-11.02980	-9.59267	0.24460	4.68800	0.21331
ENSMUSP00000029266	-7.98128	-8.26698	-9.46046	-8.85263	-9.14703	-10.74739	-10.75698	-10.89028	-10.75351	0.24444	2.45201	0.40783
ENSMUSP00000071486	-4.56592	-4.48807	-4.53120	-5.14153	-5.29658	-10.90513	-10.91473	-4.81904	-10.91125	0.24430	2.93892	0.34026
ENSMUSP00000110021	-7.12510	-6.65339	-7.04582	-7.37712	-6.94526	-7.32216	-7.00892	-6.89857	-7.23729	0.24186	1.30934	0.76374
ENSMUSP00000101651	-10.88320	-9.18803	-10.89490	-11.13521	-11.09289	-11.08025	-7.04243	-7.01408	-7.07468	0.24074	2.98121	0.33543
ENSMUSP00000066419	-10.59149	-8.89632	-10.60319	-10.84350	-10.80118	-10.78855	-8.39621	-9.31845	-9.69309	0.24074	2.98121	0.33543
ENSMUSP00000087524	-10.61277	-8.91760	-10.62447	-10.86478	-10.82246	-10.80982	-9.71784	-9.33973	-9.20295	0.24074	2.98121	0.33543
ENSMUSP00000023510	-10.93218	-9.23701	-10.94388	-11.18419	-11.14187	-11.12923	-8.56978	-9.32241	-8.93418	0.24074	2.98121	0.33543
ENSMUSP00000032844	-8.94166	-8.01134	-8.10522	-8.68225	-9.15135	-8.62730	-9.14831	-9.28161	-10.24641	0.24021	1.66695	0.59990
ENSMUSP00000006764	-7.24361	-9.87362	-7.76633	-10.20781	-10.16549	-8.53987	-7.45026	-7.58355	-7.95781	0.23975	4.55773	0.21941
ENSMUSP00000079672	-5.56743	-5.75615	-5.76486	-6.09034	-5.84733	-5.69888	-6.71624	-5.81052	-7.28346	0.23564	1.19623	0.83596
ENSMUSP00000003445	-8.45777	-7.78741	-8.13274	-8.70978	-9.17888	-8.06664	-9.17583	-8.20954	-10.27394	0.23457	1.57452	0.63511
ENSMUSP00000058919	-9.30733	-9.22515	-7.36931	-9.55934	-9.51702	-9.50438	-7.90098	-6.50753	-7.56079	0.23114	3.83460	0.26078
ENSMUSP00000098591	-11.90461	-11.82243	-9.96659	-12.15662	-12.11430	-12.10166	-9.91008	-11.14298	-10.49479	0.23114	3.83460	0.26078
ENSMUSP00000105028	-11.60309	-11.52091	-9.66508	-11.85510	-11.81278	-11.80015	-9.86002	-10.33005	-10.19328	0.23114	3.83460	0.26078
ENSMUSP00000110364	-9.04091	-8.59085	-8.54159	-11.49409	-8.73958	-9.48942	-10.34715	-10.48045	-11.44525	0.23053	2.05060	0.48766
ENSMUSP00000028286	-7.36042	-6.65910	-6.92006	-7.16037	-7.57011	-7.23464	-10.61582	-10.74912	-10.61235	0.22801	1.42799	0.70029
ENSMUSP00000033087	-10.90897	-9.21380	-9.30768	-11.16098	-11.11866	-10.00445	-8.71368	-8.84698	-9.49915	0.22745	2.80780	0.35615

ENSMUSP00000031398	-8.37991	-7.86228	-7.57041	-9.42086	-8.04289	-8.40985	-9.37550	-7.82168	-7.68491	0.22175	1.82572	0.54773
ENSMUSP00000095794	-3.96552	-6.93447	-6.51741	-7.26866	-9.93853	-6.36624	-5.69701	-5.46928	-4.78594	0.22148	8.92294	0.11207
ENSMUSP00000104725	-8.38020	-8.72096	-7.99795	-9.29160	-9.55954	-8.23093	-7.91102	-8.23724	-7.87306	0.22099	1.73102	0.57769
ENSMUSP00000072717	-7.20542	-6.49122	-6.97716	-7.14050	-7.99620	-7.11055	-7.41207	-8.01203	-7.55432	0.21750	1.61781	0.61812
ENSMUSP00000061227	-7.08090	-8.06177	-8.39210	-8.94267	-8.59009	-8.06651	-7.18400	-7.57805	-6.73750	0.21606	2.22424	0.44959
ENSMUSP00000027989	-7.75678	-7.79980	-7.76848	-8.13399	-8.23482	-10.79123	-10.80082	-10.93412	-10.79735	0.21547	2.15373	0.46431
ENSMUSP00000066897	-7.34100	-8.19739	-7.54380	-8.16370	-7.97824	-8.10875	-5.65254	-6.03716	-5.45914	0.21438	1.58536	0.63077
ENSMUSP00000020653	-7.37205	-6.44240	-6.79583	-7.28750	-7.07080	-7.71225	-6.91931	-6.52802	-6.04894	0.21421	1.66331	0.60121
ENSMUSP00000089978	-6.90124	-6.51107	-7.09200	-7.45748	-11.22617	-7.44800	-7.32696	-6.81943	-7.10441	0.21355	2.79250	0.35810
ENSMUSP00000003655	-9.09509	-10.62590	-10.71978	-10.96009	-10.91777	-10.90513	-8.51280	-9.09831	-8.96154	0.21251	2.98121	0.33543
ENSMUSP00000023396	-8.68001	-10.21082	-10.30470	-10.54501	-10.50269	-10.49005	-7.66225	-7.58420	-7.92713	0.21251	2.98121	0.33543
ENSMUSP00000109611	-9.47634	-11.00715	-11.10103	-11.34134	-11.29902	-11.28639	-9.34626	-9.47956	-10.19093	0.21251	2.98121	0.33543
ENSMUSP00000000175	-8.19540	-9.72622	-9.82010	-10.06041	-10.01809	-10.00545	-8.06533	-8.19863	-8.91000	0.21251	2.98121	0.33543
ENSMUSP00000106540	-9.61211	-11.14293	-11.23681	-11.47712	-11.43480	-11.42216	-9.81876	-9.95206	-10.32671	0.21251	2.98121	0.33543
ENSMUSP00000071752	-8.48014	-10.01095	-10.10483	-10.34514	-10.30282	-10.29019	-9.19821	-8.82009	-8.68332	0.21251	2.98121	0.33543
ENSMUSP00000081009	-9.22922	-10.76003	-10.85391	-11.09422	-11.05190	-11.03926	-9.09914	-8.13340	-8.33319	0.21251	2.98121	0.33543
ENSMUSP00000027429	-8.75841	-8.16481	-8.25869	-10.11199	-8.96810	-8.44405	-8.45364	-10.19993	-10.06316	0.21174	1.84167	0.54299
ENSMUSP00000025218	-8.91729	-8.58365	-9.77713	-9.16930	-11.07669	-9.96248	-8.67172	-8.49476	-8.86901	0.21162	2.20239	0.45405
ENSMUSP00000030076	-9.06324	-8.36173	-9.41167	-9.31525	-10.12107	-9.26030	-9.60661	-9.40319	-9.26642	0.21003	1.87462	0.53344
ENSMUSP00000038772	-11.11195	-11.02977	-9.51066	-11.36396	-11.32164	-11.30900	-9.36888	-10.35032	-9.36541	0.20827	2.98121	0.33543
ENSMUSP00000068174	-10.38962	-10.30745	-8.78834	-10.64164	-10.59932	-10.58668	-8.64656	-8.52840	-8.39163	0.20827	2.98121	0.33543
ENSMUSP00000078914	-9.94560	-9.86342	-8.34431	-10.19761	-10.15529	-10.14265	-7.75031	-7.57335	-7.74684	0.20827	2.98121	0.33543
ENSMUSP00000003117	-9.75517	-9.16158	-9.25546	-11.10876	-11.06644	-9.10409	-8.11475	-8.79476	-9.11021	0.20587	1.84167	0.54299
ENSMUSP00000103181	-7.40714	-7.63523	-7.72910	-7.65915	-7.92709	-7.74734	-8.37627	-8.05735	-8.37279	0.20504	1.20904	0.82710
ENSMUSP00000005651	-6.04157	-5.67556	-5.37823	-6.02531	-5.90749	-6.06058	-6.90612	-6.62409	-6.75559	0.20389	1.39802	0.71530
ENSMUSP00000000687	-10.46561	-9.28186	-10.47731	-10.71762	-10.67530	-10.66267	-8.72254	-8.85584	-9.05580	0.19896	2.12781	0.46997
ENSMUSP00000102857	-10.68141	-9.49766	-10.69311	-10.93342	-10.89110	-10.87847	-8.93834	-9.40837	-8.93487	0.19896	2.12781	0.46997
ENSMUSP00000026625	-10.59952	-9.41577	-10.61122	-10.85153	-10.80922	-10.79658	-7.85753	-7.99083	-8.23365	0.19896	2.12781	0.46997
ENSMUSP00000034834	-11.03217	-9.84842	-11.04387	-11.28418	-11.24186	-11.22923	-9.28910	-9.17095	-9.62236	0.19896	2.12781	0.46997
ENSMUSP00000065113	-9.42896	-8.24718	-9.44066	-9.68097	-9.63865	-9.62601	-7.23637	-8.66931	-8.16466	0.19875	2.12529	0.47052
ENSMUSP00000022271	-8.47899	-7.79593	-7.43192	-8.34526	-9.91309	-8.29030	-7.25598	-7.98845	-7.85168	0.19786	2.24785	0.44487
ENSMUSP00000025679	-8.46908	-10.33662	-8.81751	-10.67081	-10.62849	-9.51428	-7.78806	-8.04655	-8.42081	0.19659	3.31893	0.30130
ENSMUSP00000021425	-8.41422	-8.92023	-8.22517	-10.86741	-8.42316	-9.71088	-8.25300	-8.11795	-7.86993	0.19395	2.12479	0.47064
ENSMUSP00000027356	-7.14495	-6.88371	-6.97759	-7.01127	-7.24341	-7.30353	-8.57558	-9.21990	-8.57211	0.19207	1.19175	0.83910
ENSMUSP00000099754	-8.99156	-7.80978	-7.90366	-9.24357	-8.35311	-10.29019	-10.29978	-8.82009	-10.29631	0.19182	2.43439	0.41078

ENSMUSP00000095285	-7.39848	-7.45945	-7.55333	-7.65049	-8.37065	-7.59554	-7.26857	-7.07904	-6.94227	0.18848	1.41225	0.70809
ENSMUSP00000028004	-9.38576	-8.96685	-9.90887	-11.25076	-9.59545	-10.09423	-8.49320	-8.28994	-8.48973	0.18659	2.12529	0.47052
ENSMUSP00000104825	-8.25202	-8.78917	-10.83277	-9.97150	-11.03076	-11.01812	-8.45867	-8.44882	-8.31205	0.18369	5.36343	0.18645
ENSMUSP00000030769	-8.74052	-7.91087	-8.55146	-8.48151	-9.20167	-9.18903	-8.19970	-8.56945	-8.00513	0.18298	1.71408	0.58340
ENSMUSP00000026743	-6.96705	-6.46068	-7.45258	-7.42817	-7.92825	-7.24258	-8.00860	-7.47064	-8.00513	0.17898	1.81911	0.54972
ENSMUSP00000054490	-6.06730	-6.51327	-5.98136	-6.42754	-6.80514	-6.37259	-6.80210	-6.70356	-6.79863	0.17896	1.43889	0.69498
ENSMUSP00000022960	-8.09287	-7.18020	-8.37292	-8.61323	-8.57091	-8.28993	-7.91378	-9.32050	-7.99370	0.17868	2.04524	0.48894
ENSMUSP00000015829	-8.00482	-9.65846	-8.45198	-11.09422	-11.05190	-8.63733	-7.00144	-7.00340	-6.93014	0.17691	3.04081	0.32886
ENSMUSP00000068594	-7.92008	-8.16515	-7.76114	-9.22543	-8.59519	-7.94649	-7.95608	-8.01387	-7.99262	0.17379	1.71299	0.58377
ENSMUSP00000109196	-7.56354	-8.41993	-7.66623	-8.55336	-8.20078	-8.33129	-10.90993	-9.09351	-10.90646	0.17299	1.73206	0.57735
ENSMUSP00000101003	-7.34459	-7.69788	-7.24504	-8.03206	-8.44196	-7.43040	-8.77564	-9.42036	-8.18399	0.17186	1.61898	0.61767
ENSMUSP00000065352	-8.35792	-8.27575	-8.03290	-8.60993	-8.56762	-10.16797	-7.77563	-7.47347	-9.07252	0.17073	1.97040	0.50751
ENSMUSP00000026560	-7.68297	-7.27796	-7.52028	-7.68362	-7.99277	-7.62866	-7.63826	-8.35947	-8.09750	0.16806	1.30934	0.76374
ENSMUSP00000021313	-8.05116	-8.22043	-8.65104	-9.40276	-8.26085	-9.34781	-9.35740	-8.97928	-9.35393	0.16668	1.78464	0.56034
ENSMUSP00000026827	-7.69562	-8.40238	-7.27186	-8.14839	-8.35752	-9.19303	-7.25545	-6.99921	-7.25197	0.16593	2.21412	0.45165
ENSMUSP00000023237	-9.08935	-8.55496	-8.84960	-9.34136	-11.24876	-9.28641	-7.57783	-7.94073	-7.74143	0.16443	2.29486	0.43576
ENSMUSP00000031383	-7.96859	-8.98601	-8.56848	-10.42178	-10.37946	-8.41710	-7.97448	-7.46096	-8.75995	0.16420	2.40891	0.41512
ENSMUSP00000008991	-11.47499	-9.78219	-10.18633	-11.72700	-12.78625	-10.82390	-9.01768	-9.69337	-9.55660	0.16414	3.36236	0.29741
ENSMUSP00000084053	-8.26139	-8.17921	-7.90521	-8.76485	-9.05926	-8.09057	-8.46803	-9.70093	-9.05274	0.16291	1.58044	0.63273
ENSMUSP00000018506	-9.93233	-10.95172	-11.04560	-11.28591	-11.24359	-11.23096	-10.13897	-9.42413	-9.62409	0.16242	2.12781	0.46997
ENSMUSP00000025375:reversed	-10.69147	-11.71086	-11.80474	-12.04505	-12.00273	-11.99010	-10.89812	-10.52000	-10.89464	0.16242	2.12781	0.46997
ENSMUSP00000035220	-9.69352	-10.71291	-10.80679	-11.04710	-11.00478	-10.99215	-8.80057	-9.18532	-9.89669	0.16242	2.12781	0.46997
ENSMUSP00000099763:reversed	-8.96009	-8.87792	-8.46038	-10.31368	-10.27136	-8.64573	-10.26832	-10.40162	-10.26485	0.16177	2.00405	0.49899
ENSMUSP00000014750	-7.36474	-6.98402	-7.67879	-7.70774	-7.57443	-7.86414	-9.09814	-10.84443	-9.60608	0.16175	1.48339	0.67413
ENSMUSP00000034866	-7.15895	-6.94754	-8.14030	-7.73379	-8.33829	-8.32565	-7.78853	-7.92183	-7.43359	0.16151	2.16383	0.46214
ENSMUSP00000080994	-6.29710	-6.13941	-6.87340	-6.67429	-6.94216	-6.92952	-6.67439	-6.67706	-6.82122	0.16053	1.55000	0.64516
ENSMUSP00000051092	-8.21872	-7.90470	-8.65797	-8.77308	-10.46658	-8.71812	-9.36394	-9.49723	-9.15970	0.15975	2.30811	0.43326
ENSMUSP00000070109	-9.82925	-9.41035	-8.50530	-11.69425	-9.45076	-10.53772	-11.64889	-10.68061	-11.64542	0.15771	3.04081	0.32886
ENSMUSP00000005606	-10.67648	-10.59431	-9.58661	-10.92849	-10.88618	-10.87354	-9.27014	-9.06672	-9.77809	0.15690	2.12781	0.46997
ENSMUSP00000028691	-11.03735	-10.95517	-9.94748	-11.28936	-11.24704	-11.23440	-10.14242	-10.27572	-9.03935	0.15690	2.12781	0.46997
ENSMUSP00000030385	-10.49564	-10.41347	-9.40577	-10.74765	-10.70533	-10.69270	-7.99010	-8.63442	-9.08583	0.15690	2.12781	0.46997
ENSMUSP00000094167	-10.80599	-10.72382	-9.71612	-11.05801	-11.01569	-11.00305	-9.91107	-9.53295	-9.90760	0.15690	2.12781	0.46997
ENSMUSP00000036555	-11.75598	-11.67381	-10.66611	-12.00800	-11.96568	-11.95304	-10.34964	-10.99436	-10.85759	0.15690	2.12781	0.46997
ENSMUSP00000036881	-11.52801	-11.44583	-10.43813	-11.78002	-11.73770	-11.72506	-10.12166	-9.91824	-10.11819	0.15690	2.12781	0.46997
sp|CASK_BOVIN|	-10.03389	-9.95171	-8.94402	-10.28590	-10.24358	-10.23095	-6.57265	-6.47767	-6.93695	0.15690	2.12781	0.46997

ENSMUSP00000033673	-7.92463	-8.94149	-8.14769	-9.27568	-11.18307	-8.76851	-9.23032	-8.74428	-9.22684	0.15290	3.01958	0.33117
ENSMUSP00000032920	-8.18671	-7.85308	-7.31074	-8.18727	-8.73313	-8.13231	-9.24150	-8.86339	-10.33961	0.15018	1.82884	0.54680
ENSMUSP00000105447	-9.82293	-9.74075	-7.98756	-9.56352	-11.13419	-11.12156	-7.57149	-7.96434	-7.23151	0.14759	4.55773	0.21941
ENSMUSP00000027491	-9.70007	-9.10648	-8.86363	-9.44067	-9.90977	-9.89713	-9.90672	-11.14160	-9.05511	0.14660	1.73841	0.57524
ENSMUSP00000110094	-6.13459	-6.56331	-6.58572	-7.24896	-7.20664	-10.14265	-7.75031	-6.84726	-8.53578	0.14578	3.30111	0.30293
ENSMUSP00000025476	-9.34557	-8.41525	-9.35728	-10.69916	-9.55527	-9.54263	-10.65380	-9.17411	-9.54875	0.14517	2.36886	0.42214
ENSMUSP00000027863	-8.13430	-7.08247	-7.97888	-10.78824	-9.13293	-8.02109	-9.64130	-9.77460	-10.73940	0.14247	3.21762	0.31079
ENSMUSP00000026289	-7.44468	-6.82831	-6.92219	-6.97442	-10.49176	-10.47912	-8.08679	-7.78462	-7.77305	0.13065	2.58375	0.38703
ENSMUSP00000015877	-9.36708	-8.77349	-9.37878	-9.61909	-9.57677	-10.66571	-10.67530	-10.80860	-10.67183	0.12848	2.00405	0.49899
ENSMUSP00000018470	-7.74190	-8.27906	-8.37294	-10.56296	-8.31947	-9.40643	-7.21749	-7.35079	-7.29099	0.12756	2.64828	0.37760
ENSMUSP00000027529	-7.93526	-8.10453	-8.53514	-9.28687	-8.73313	-8.38377	-8.73009	-9.37480	-9.23803	0.12755	1.78464	0.56034
ENSMUSP00000031741	-8.31477	-6.93310	-6.92343	-8.33033	-8.01352	-8.82209	-11.23362	-9.16574	-11.23014	0.12656	3.03586	0.32940
ENSMUSP00000035804	-6.60108	-6.55594	-6.95658	-6.92860	-7.26280	-6.91366	-6.92325	-7.18718	-7.05041	0.12448	1.38771	0.72061
ENSMUSP00000033715	-7.12175	-6.88133	-6.45463	-7.21552	-7.22321	-7.16056	-8.68689	-8.18397	-8.68342	0.12425	1.52723	0.65478
ENSMUSP00000003622	-7.35886	-7.46777	-7.79810	-8.03841	-7.99610	-7.64690	-8.50407	-8.88883	-10.70177	0.12381	1.42439	0.70205
ENSMUSP00000029386	-7.18300	-6.73868	-7.27021	-8.07512	-7.84472	-7.15326	-7.59034	-8.03383	-8.56047	0.12349	1.77274	0.56410
ENSMUSP00000069432	-8.44561	-7.75591	-7.80216	-8.93203	-8.28526	-8.50354	-8.41428	-8.52432	-8.25833	0.12212	1.79096	0.55836
ENSMUSP00000099482	-10.06167	-7.57756	-8.97180	-10.31368	-10.27136	-10.25872	-8.06715	-7.45297	-8.31513	0.12126	6.39478	0.15638
ENSMUSP00000042232	-7.31226	-7.23008	-8.93458	-9.17489	-9.13257	-8.60852	-8.28139	-7.52701	-7.51544	0.12120	3.82634	0.26135
ENSMUSP00000022962	-8.91468	-7.49685	-8.58965	-9.67811	-10.73736	-8.77501	-9.63274	-10.86762	-10.73085	0.12098	3.59435	0.27821
ENSMUSP00000101478	-10.18603	-9.00227	-7.62868	-10.43804	-10.39572	-10.38308	-7.82363	-7.95693	-7.34045	0.11822	7.24818	0.13797
ENSMUSP00000022293	-7.20836	-7.04921	-7.60581	-7.46037	-7.80380	-7.79116	-9.02516	-8.05925	-9.02168	0.11802	1.49047	0.67093
ENSMUSP00000080888	-8.85181	-9.03798	-8.47777	-9.10383	-9.18670	-9.93655	-10.79428	-12.02915	-10.27939	0.11781	1.79744	0.55635
ENSMUSP00000020343	-9.05582	-7.67328	-7.33170	-10.40940	-9.26551	-8.74146	-9.26247	-8.29617	-8.74758	0.11444	4.39428	0.22757
ENSMUSP00000045864	-8.59611	-8.76539	-9.19599	-9.43630	-9.39398	-9.04462	-11.00393	-11.13723	-9.89888	0.11357	1.57452	0.63511
ENSMUSP00000034947	-6.76907	-6.91874	-6.17771	-7.44402	-6.84954	-7.93578	-7.12417	-6.81272	-7.63164	0.11147	2.12421	0.47076
ENSMUSP00000001566	-5.04875	-4.75948	-4.98655	-11.13118	-6.57361	-6.49712	-4.91808	-5.02643	-4.95762	0.11053	7.55931	0.13229
ENSMUSP00000021854	-7.93929	-8.00026	-7.71454	-8.19130	-8.14898	-8.89882	-7.24289	-7.37619	-7.41638	0.11021	1.61898	0.61767
ENSMUSP00000025968	-6.14836	-6.16545	-6.42955	-11.24897	-11.20665	-6.32979	-11.20360	-6.60512	-11.20013	0.11007	3.29813	0.30320
ENSMUSP00000081030	-7.38866	-7.50724	-7.40036	-7.47355	-10.00028	-9.98765	-9.99724	-6.83043	-9.99377	0.11003	2.63501	0.37951
ENSMUSP00000029414	-7.62252	-7.37323	-6.89642	-8.32675	-8.03298	-7.50932	-8.61811	-10.36440	-8.27792	0.10870	1.93247	0.51747
ENSMUSP00000026610	-7.09899	-7.24510	-7.24133	-7.48164	-8.15610	-7.42668	-6.56269	-6.81986	-6.44901	0.10853	1.56031	0.64090
ENSMUSP00000025617	-6.69191	-9.74947	-8.23036	-10.08366	-10.04134	-10.02871	-7.83713	-8.55861	-8.08511	0.10724	12.36854	0.08085
ENSMUSP00000027036	-7.98081	-8.48682	-7.14494	-9.33242	-8.77869	-8.42932	-6.57763	-6.58576	-6.61963	0.10718	2.97515	0.33612
ENSMUSP00000099649	-5.57047	-5.48829	-5.58217	-7.04631	-7.00400	-11.00305	-5.30778	-5.63213	-5.31102	0.10201	6.44161	0.15524

ENSMUSP00000077118	-5.29946	-5.51301	-5.67359	-5.78468	-6.10339	-5.67088	-6.62093	-6.35689	-6.96378	0.10151	1.42381	0.70234
ENSMUSP00000088168	-5.66180	-5.76382	-5.79246	-5.84170	-5.83479	-5.80429	-5.77910	-5.94718	-5.90307	0.10121	1.09396	0.91411
ENSMUSP00000109451	-9.40875	-8.81516	-8.12010	-10.76234	-10.72002	-9.09439	-9.10399	-10.85028	-10.71350	0.10058	3.46330	0.28874
ENSMUSP00000105356	-8.10738	-8.87334	-8.45580	-10.30910	-10.26678	-8.64116	-6.89216	-7.02546	-7.31162	0.10037	2.73367	0.36581
ENSMUSP00000027916	-8.52802	-8.44584	-7.92039	-8.52857	-9.07443	-9.57321	-6.67269	-6.63892	-7.01302	0.09992	2.02467	0.49391
ENSMUSP00000016463	-4.77725	-4.94834	-5.52719	-5.42294	-5.81413	-5.64402	-5.85872	-5.99202	-6.05232	0.09905	1.76930	0.56519
ENSMUSP00000037583	-6.96691	-6.88473	-6.53386	-7.30232	-7.56235	-6.94882	-7.99477	-7.02919	-7.68103	0.09853	1.59757	0.62595
ENSMUSP00000100059	-9.06749	-8.81820	-9.86813	-10.61986	-10.06612	-9.71676	-11.67607	-11.80937	-10.57102	0.09852	2.46493	0.40569
ENSMUSP00000093229	-7.42581	-6.24490	-7.22237	-7.67782	-7.71890	-7.89736	-8.65443	-10.98890	-10.85212	0.09698	2.49202	0.40128
ENSMUSP00000080523	-6.89780	-6.81562	-6.52376	-7.03856	-7.74371	-7.09486	-7.74067	-6.51548	-7.53644	0.09693	1.67102	0.59844
ENSMUSP00000098648	-8.33868	-8.25650	-9.09785	-10.43776	-11.49701	-8.91533	-8.54533	-8.78988	-8.44175	0.09684	3.52516	0.28368
ENSMUSP00000023550	-9.95453	-8.02528	-9.11809	-11.30811	-11.26580	-9.64017	-11.26275	-9.19488	-10.15771	0.09502	5.28736	0.18913
ENSMUSP00000023952	-5.75948	-5.38553	-6.10548	-6.60588	-5.98016	-6.90338	-5.87231	-6.13277	-6.23768	0.09478	2.01816	0.49550
ENSMUSP00000003681	-8.24128	-7.28986	-9.20903	-11.06233	-9.40703	-9.39439	-9.91540	-8.58122	-7.57522	0.09474	5.68229	0.17599
ENSMUSP00000051223	-7.60585	-7.83393	-8.71675	-10.57005	-8.57802	-9.41353	-7.38495	-7.70935	-7.68383	0.09337	3.59435	0.27821
ENSMUSP00000098041	-12.29526	-9.07334	-9.59477	-12.54727	-12.50495	-12.49232	-10.88892	-11.53363	-10.88545	0.09299	16.63551	0.06011
ENSMUSP00000010208	-8.42432	-6.58932	-6.68320	-8.53318	-8.49086	-8.62137	-8.79808	-9.38360	-8.99537	0.09250	4.83204	0.20695
ENSMUSP00000003907	-8.28976	-8.06443	-8.92079	-8.90964	-9.11878	-9.95429	-7.69387	-8.05901	-7.69040	0.09212	2.34837	0.42583
ENSMUSP00000076575	-9.54483	-10.56423	-8.45694	-10.89842	-10.85610	-10.84346	-8.01566	-8.78518	-8.44765	0.09182	5.54139	0.18046
ENSMUSP00000097561:reversed	-13.63197	-12.96162	-14.15509	-15.49698	-14.35308	-14.34045	-13.50190	-14.48334	-13.49842	0.09029	3.09848	0.32274
ENSMUSP00000084572	-7.80230	-7.93919	-7.63440	-8.12214	-8.40933	-7.93584	-7.50467	-7.42477	-7.50120	0.09011	1.43080	0.69891
ENSMUSP00000103904	-6.94616	-10.58188	-6.77959	-10.91607	-10.87375	-10.86112	-8.15852	-6.95660	-7.56713	0.08847	38.82374	0.02576
ENSMUSP00000018699	-6.08566	-5.81905	-6.17636	-6.31267	-6.19889	-6.36171	-6.90061	-7.08154	-6.99478	0.08804	1.30615	0.76561
ENSMUSP00000026552	-4.72802	-4.63839	-4.70302	-4.89069	-4.85523	-5.29655	-5.71569	-5.42331	-5.60400	0.08751	1.35246	0.73939
ENSMUSP00000081782	-9.18861	-11.67548	-10.15637	-12.00967	-11.96735	-11.95472	-10.01459	-10.48462	-9.39179	0.08655	8.10157	0.12343
ENSMUSP00000073175	-6.77134	-6.29963	-6.46021	-6.84896	-7.46074	-6.87741	-10.02674	-6.93690	-6.97452	0.08534	1.69235	0.59089
ENSMUSP00000104830	-7.05415	-9.68417	-6.47794	-10.01836	-9.97604	-9.96340	-6.67288	-6.73471	-6.35429	0.08508	18.34229	0.05452
ENSMUSP00000087046	-8.38236	-8.30019	-10.34378	-10.58409	-10.54177	-10.52914	-7.96968	-7.83464	-8.58554	0.08210	6.39478	0.15638
ENSMUSP00000029353	-11.03390	-9.33873	-9.94403	-11.28591	-11.24359	-11.23096	-10.13897	-9.17268	-9.28736	0.08174	3.83460	0.26078
ENSMUSP00000031160	-10.82533	-9.13016	-9.73546	-11.07734	-11.03502	-11.02239	-8.83081	-8.96411	-9.41552	0.08174	3.83460	0.26078
ENSMUSP00000022993	-8.72257	-7.68433	-8.73427	-9.48599	-8.93226	-9.43104	-10.54221	-9.06251	-9.43716	0.08166	2.66638	0.37504
ENSMUSP00000106250	-7.87989	-9.41070	-7.10265	-9.74489	-9.70257	-9.68993	-8.59795	-8.73125	-8.08306	0.08010	7.24818	0.13797
ENSMUSP00000100968	-8.81645	-10.68399	-9.67629	-11.01818	-10.97586	-10.96322	-9.02310	-8.39392	-9.35635	0.07991	4.68800	0.21331
ENSMUSP00000049007	-10.47878	-9.88518	-9.97906	-10.73079	-11.79004	-10.67583	-9.83728	-9.20811	-9.83381	0.07948	2.36886	0.42214
ENSMUSP00000080974	-9.83822	-8.90790	-8.75033	-9.57882	-11.14949	-11.13685	-10.04487	-9.33003	-9.19326	0.07934	3.46330	0.28874

ENSMUSP00000020522	-11.42136	-9.72619	-9.48334	-11.67337	-11.63105	-11.61841	-8.57925	-8.46119	-8.78714	0.07885	5.54139	0.18046
ENSMUSP00000100802	-6.14570	-6.22072	-6.27293	-6.90859	-7.22735	-6.34276	-6.80438	-6.60117	-6.98899	0.07881	1.73373	0.57679
ENSMUSP00000029405	-10.21351	-11.23291	-9.37707	-11.56709	-11.52478	-11.51214	-8.47298	-10.55346	-9.31709	0.07875	4.68800	0.21331
ENSMUSP00000051935	-9.23339	-9.66263	-10.85808	-11.09839	-11.05608	-11.04344	-9.95146	-10.08476	-9.43657	0.07764	3.83460	0.26078
ENSMUSP00000025483	-10.03561	-8.65308	-8.74696	-11.38920	-11.34688	-9.72125	-8.94190	-7.66613	-8.77131	0.07713	4.55773	0.21941
ENSMUSP00000028241	-8.22082	-7.62762	-9.33212	-9.06101	-10.63168	-10.61905	-9.52706	-9.66036	-10.62517	0.07695	4.92255	0.20315
ENSMUSP00000047898	-10.96231	-9.77856	-9.36102	-11.21432	-11.17200	-11.15937	-9.21924	-10.20069	-9.21577	0.07498	3.83460	0.26078
ENSMUSP00000022060	-7.86050	-9.97949	-8.46038	-10.31368	-10.27136	-10.25872	-8.65533	-8.20045	-8.65185	0.07429	6.39478	0.15638
ENSMUSP00000001713	-7.57353	-7.80162	-7.58523	-8.58802	-8.54570	-10.48278	-6.09354	-5.89389	-5.72233	0.07327	3.48537	0.28691
ENSMUSP00000107760	-9.68343	-8.95443	-10.99549	-11.23580	-12.29505	-11.18084	-12.29201	-12.42531	-12.28854	0.07253	6.38180	0.15670
ENSMUSP00000028222	-6.44080	-5.39934	-5.69251	-6.69281	-6.70051	-6.47330	-7.22556	-6.60249	-7.28181	0.07123	2.34034	0.42729
ENSMUSP00000038368	-8.50731	-8.33414	-8.26765	-9.40614	-11.76575	-9.55194	-8.04481	-8.45772	-7.94823	0.07113	4.31068	0.23198
ENSMUSP00000080531	-8.72923	-10.59677	-8.48948	-10.93096	-10.88864	-10.87601	-9.27261	-8.44985	-8.31308	0.07110	7.24818	0.13797
ENSMUSP00000029630	-7.04355	-7.19778	-8.53362	-11.34297	-11.30065	-8.33937	-11.29761	-11.43091	-11.29414	0.06785	6.98258	0.14321
ENSMUSP00000100067	-7.89829	-8.60505	-8.11075	-8.60251	-10.50991	-10.49727	-7.55822	-7.34005	-7.79120	0.06712	3.54341	0.28221
ENSMUSP00000020285	-7.51519	-7.05342	-7.14730	-10.33625	-10.29394	-7.71225	-8.34118	-7.47555	-7.57523	0.06587	4.33574	0.23064
ENSMUSP00000004508	-7.28463	-7.01136	-7.53279	-7.64790	-7.73078	-8.22916	-7.60254	-7.43349	-8.03452	0.06575	1.77192	0.56436
ENSMUSP00000093944	-9.43948	-8.90508	-8.45225	-9.44003	-11.59888	-11.58625	-8.15756	-8.22833	-8.09156	0.06563	4.29033	0.23308
ENSMUSP00000081010	-6.46453	-6.38235	-6.32593	-7.19204	-6.67422	-6.66159	-5.70731	-5.49533	-5.93476	0.06544	1.53722	0.65052
ENSMUSP00000045927	-8.81535	-8.73317	-8.82705	-9.06736	-10.63803	-10.62540	-10.63499	-9.66671	-9.52994	0.06506	2.73367	0.36581
ENSMUSP00000096677	-11.18237	-11.10019	-12.29565	-12.53596	-12.49364	-12.48100	-10.54088	-10.22196	-10.28595	0.06445	2.98121	0.33543
ENSMUSP00000100564	-7.86909	-7.78691	-7.44533	-9.42146	-10.48071	-8.26690	-6.66666	-7.31085	-7.76200	0.06070	3.82587	0.26138
ENSMUSP00000008826	-6.03042	-5.98051	-6.25345	-6.49376	-6.88681	-6.32757	-7.16144	-6.70687	-7.15797	0.06070	1.58176	0.63221
ENSMUSP00000073213	-6.28894	-6.62175	-7.13554	-7.21548	-8.27210	-7.62325	-5.81188	-6.33648	-6.04353	0.06054	2.66942	0.37461
ENSMUSP00000041814	-9.43556	-9.35338	-8.81104	-10.78717	-9.64525	-10.22080	-7.86873	-8.36144	-7.57285	0.05674	2.62486	0.38097
ENSMUSP00000030345	-7.34172	-6.57620	-7.31495	-7.63374	-7.81970	-7.85971	-7.76664	-8.17956	-7.58490	0.05617	2.09014	0.47844
ENSMUSP00000102140	-8.96009	-8.36650	-8.97180	-10.31368	-10.27136	-9.15715	-7.69927	-8.78863	-7.69580	0.05516	2.80780	0.35615
ENSMUSP00000083705	-5.72388	-5.53048	-5.47127	-5.99284	-6.15883	-5.73721	-6.15579	-6.28909	-6.47210	0.05494	1.46110	0.68441
ENSMUSP00000085623	-8.39835	-9.41577	-9.50965	-9.74996	-10.80922	-10.79658	-8.40424	-8.10208	-8.09051	0.05471	3.83005	0.26109
ENSMUSP00000105795	-5.41220	-5.18460	-4.86551	-6.97526	-7.14809	-10.35859	-4.32112	-4.35502	-4.41225	0.05381	10.04090	0.09959
ENSMUSP00000044326	-7.75542	-7.61767	-7.60888	-7.75609	-7.96512	-7.89690	-8.22162	-10.04204	-8.29512	0.05252	1.23085	0.81245
ENSMUSP00000087694	-10.50054	-10.41836	-10.51224	-10.75255	-11.81181	-11.79917	-11.80876	-11.94206	-10.70372	0.05007	2.29667	0.43541
ENSMUSP00000045216	-8.23705	-6.93089	-7.66083	-8.48906	-9.20922	-10.04472	-10.05432	-11.28919	-11.15242	0.04934	4.74269	0.21085
ENSMUSP00000071078	-8.11421	-8.03203	-7.69045	-9.66658	-8.77612	-8.51203	-8.01060	-9.24310	-10.71932	0.04933	2.61685	0.38214
ENSMUSP00000034966	-6.18833	-5.62287	-6.02257	-6.65624	-6.79867	-6.29272	-7.26857	-6.54789	-7.05598	0.04740	1.89002	0.52909

ENSMUSP00000099634	-6.78800	-6.36934	-6.92487	-7.16518	-7.14990	-7.19362	-6.99465	-7.52758	-6.76099	0.04700	1.63856	0.61029
ENSMUSP00000030830	-8.90483	-8.16856	-8.04730	-9.32396	-9.48240	-8.95874	-9.47936	-9.86411	-9.72734	0.04651	2.51290	0.39795
ENSMUSP00000107433	-8.72257	-8.30366	-7.63506	-10.58757	-8.93226	-10.53261	-8.92922	-10.67551	-10.53873	0.04596	4.92255	0.20315
ENSMUSP00000081001	-9.25084	-8.71645	-9.26254	-9.83957	-9.46053	-9.78462	-11.40720	-10.43893	-10.30216	0.04549	1.87462	0.53344
ENSMUSP00000038914	-6.27764	-6.21398	-7.13059	-7.32922	-7.81149	-7.35944	-7.80845	-8.36469	-8.46437	0.04542	2.72514	0.36695
ENSMUSP00000055862	-7.26371	-7.32468	-6.93885	-8.02674	-7.47340	-8.22324	-7.13380	-7.09271	-7.23043	0.04514	2.01472	0.49635
ENSMUSP00000108126	-9.88094	-10.90034	-9.89264	-11.23453	-11.19221	-11.17957	-10.08759	-10.22089	-10.08412	0.04458	2.98121	0.33543
ENSMUSP00000020161	-6.00597	-5.90296	-6.76494	-8.41432	-9.16094	-7.04339	-10.77089	-8.50226	-9.66584	0.04295	5.29984	0.18868
ENSMUSP00000036093	-9.15886	-10.54416	-10.12662	-11.97992	-10.83603	-11.92497	-9.98484	-10.45487	-8.88234	0.04179	5.36343	0.18645
ENSMUSP00000025385	-6.41080	-6.35782	-7.01319	-7.22786	-7.51196	-7.14790	-6.29964	-6.75075	-6.57171	0.04171	2.06144	0.48510
ENSMUSP00000034541	-7.50004	-7.76419	-8.08991	-9.85697	-8.37889	-9.21383	-9.02266	-8.98885	-9.01919	0.04140	3.38712	0.29524
ENSMUSP00000047536	-6.60415	-6.67228	-7.00981	-7.67306	-7.20780	-7.19516	-6.85844	-7.40953	-7.27275	0.04130	1.80414	0.55428
ENSMUSP00000037783	-8.61257	-9.04181	-9.13568	-9.37599	-10.43525	-10.42261	-10.43221	-10.56550	-10.42873	0.04104	2.80780	0.35615
ENSMUSP00000021239	-7.08939	-6.72759	-7.03856	-7.27887	-7.51422	-7.28644	-8.16527	-7.91897	-8.52967	0.04076	1.50356	0.66509
ENSMUSP00000028916	-8.59678	-8.40335	-8.14576	-11.68618	-11.64386	-9.22929	-8.08116	-8.27331	-8.19906	0.03976	6.18105	0.16178
ENSMUSP00000037018	-7.15723	-7.65321	-8.17464	-11.12714	-11.08482	-8.67026	-11.08178	-10.11351	-11.07831	0.03808	7.75118	0.12901
ENSMUSP00000110998	-5.90495	-5.77929	-5.87317	-7.21215	-11.02433	-11.01169	-5.58314	-5.76109	-11.01781	0.03728	10.84817	0.09218
ENSMUSP00000060218	-8.86934	-8.27575	-7.78144	-10.22293	-9.07903	-10.16797	-7.60852	-8.36115	-7.12534	0.03599	4.34118	0.23035
ENSMUSP00000002790	-8.53955	-8.64847	-7.87999	-9.98159	-9.17679	-10.77477	-8.21805	-8.51843	-7.73497	0.03558	4.43666	0.22539
ENSMUSP00000030538	-7.25176	-6.84865	-6.90406	-8.17037	-7.85356	-7.39617	-9.46066	-8.80502	-8.50113	0.03537	2.16512	0.46187
ENSMUSP00000023803	-6.00319	-5.36942	-6.35459	-6.82087	-6.80712	-7.02128	-5.87336	-6.01815	-6.12941	0.03034	2.81690	0.35500
ENSMUSP00000106481	-7.82812	-8.17349	-9.02985	-9.60688	-11.17756	-10.06335	-11.17451	-8.73876	-9.55805	0.02994	6.37964	0.15675
ENSMUSP00000034164	-9.03596	-8.95378	-9.55908	-9.79938	-10.85864	-10.84600	-10.85560	-10.98890	-10.85212	0.02979	3.31893	0.30130
ENSMUSP00000112334	-8.21193	-7.91840	-8.49198	-9.35162	-9.30930	-8.67733	-6.15781	-6.35442	-6.15434	0.02975	2.40780	0.41532
ENSMUSP00000067685	-7.51200	-7.16379	-7.13422	-8.18389	-8.76481	-7.83042	-7.39587	-7.21258	-7.44915	0.02940	2.54252	0.39331
ENSMUSP00000099364	-8.98726	-8.90508	-8.99896	-9.44003	-9.98589	-10.48467	-8.64720	-9.32721	-9.97938	0.02937	2.47481	0.40407
ENSMUSP00000020717	-6.27770	-6.41262	-6.19631	-7.53542	-6.76702	-6.96953	-6.34776	-6.15680	-6.22414	0.02898	2.13616	0.46813
ENSMUSP00000033509	-5.81771	-5.32605	-5.65313	-5.99993	-6.21215	-6.17094	-6.43590	-6.23270	-6.58963	0.02891	1.70853	0.58530
ENSMUSP00000091180	-8.30811	-7.84633	-8.17666	-10.02759	-11.08685	-9.12449	-8.51476	-8.07736	-8.67840	0.02791	5.45030	0.18348
ENSMUSP00000095845	-6.82568	-6.74350	-6.51644	-8.49176	-10.65061	-8.43680	-6.97968	-7.22121	-6.74793	0.02729	8.38932	0.11920
ENSMUSP00000035761	-9.97402	-9.67670	-9.59363	-10.73698	-10.26711	-10.25448	-9.68591	-10.96806	-10.99841	0.02678	1.94311	0.51464
ENSMUSP00000021375	-7.31545	-7.26661	-7.29489	-8.06746	-8.08072	-7.54585	-7.12209	-7.59188	-6.91994	0.02659	1.78035	0.56169
ENSMUSP00000000756	-5.95659	-5.54649	-5.80353	-6.12283	-6.26011	-6.38807	-6.87149	-6.69460	-6.86802	0.02639	1.62883	0.61394
ENSMUSP00000107914	-9.04857	-9.47781	-8.72354	-9.81200	-10.87125	-10.85861	-9.25522	-11.00151	-8.91502	0.02580	3.83005	0.26109
ENSMUSP00000023583	-7.15589	-7.94295	-7.46614	-8.89647	-8.60270	-8.22218	-8.59965	-8.36508	-8.84764	0.02495	2.94512	0.33955

ENSMUSP00000007130	-9.80954	-9.39063	-9.48451	-10.57296	-11.63222	-10.51801	-9.22725	-9.81276	-11.62570	0.02480	3.46330	0.28874
ENSMUSP00000039202	-7.24659	-7.25540	-7.44939	-8.68862	-10.59602	-8.97039	-7.45324	-6.96074	-8.18757	0.02460	6.18105	0.16178
ENSMUSP00000001460	-6.59180	-6.47014	-6.59017	-7.38187	-7.27286	-6.82996	-6.49908	-6.74830	-6.66902	0.02443	1.79526	0.55702
ENSMUSP00000023087	-9.56498	-8.01533	-9.57669	-10.91857	-10.87625	-10.86361	-10.87321	-9.05679	-10.86973	0.02412	8.10157	0.12343
ENSMUSP00000021133	-8.39340	-7.84851	-8.01936	-10.38123	-9.03856	-9.47813	-7.42575	-7.36168	-7.71607	0.02232	4.18923	0.23871
ENSMUSP00000031355	-8.42394	-8.99585	-8.51904	-11.89909	-9.90705	-10.74256	-7.91755	-8.42736	-8.03925	0.02182	7.07425	0.14136
ENSMUSP00000033093	-8.08886	-7.38735	-7.48123	-8.67759	-10.24827	-10.23563	-8.63223	-8.42880	-8.62876	0.02169	6.01698	0.16620
ENSMUSP00000107937	-5.72855	-6.24554	-5.85980	-7.10788	-6.64564	-6.57743	-6.15484	-5.98737	-6.02003	0.02166	2.32093	0.43086
ENSMUSP00000072199	-10.45960	-7.91933	-8.34973	-11.81318	-11.77086	-11.75823	-8.81917	-9.69995	-8.71560	0.02163	26.87623	0.03721
ENSMUSP00000026538	-6.27767	-6.36834	-7.48823	-8.10813	-8.06581	-8.42105	-5.70743	-5.78398	-5.49403	0.02138	4.91700	0.20338
ENSMUSP00000025835	-6.54511	-6.28680	-7.09266	-7.73215	-7.42600	-8.03661	-8.82405	-8.29392	-9.25603	0.02111	3.00585	0.33268
ENSMUSP00000086021	-5.71315	-6.34402	-5.89550	-6.76160	-7.45709	-6.89774	-6.90733	-6.32139	-7.14031	0.02050	2.86183	0.34943
ENSMUSP00000001715	-8.08455	-7.80162	-8.09626	-8.92474	-10.49542	-10.48278	-7.65498	-7.48593	-7.11732	0.02045	5.28736	0.18913
ENSMUSP00000021793	-8.10548	-7.85618	-8.11718	-8.55825	-8.51593	-8.30253	-9.10107	-10.84736	-10.71058	0.02043	1.53821	0.65010
ENSMUSP00000071616	-5.44085	-5.72030	-5.96339	-6.22696	-6.28349	-6.40998	-6.07037	-5.88234	-6.10992	0.02025	1.85323	0.53960
ENSMUSP00000015011	-5.64029	-5.70793	-5.63475	-5.98328	-5.94096	-5.78649	-6.70010	-6.91857	-7.45306	0.01952	1.27442	0.78467
ENSMUSP00000106359	-6.86965	-6.36968	-6.68065	-7.12166	-7.33071	-7.41818	-8.76342	-7.56107	-8.17177	0.01879	1.92127	0.52049
ENSMUSP00000036386	-7.13421	-6.98950	-7.21261	-7.68476	-7.41060	-7.82091	-7.55601	-7.77270	-7.55253	0.01849	1.66939	0.59902
ENSMUSP00000066035	-9.82869	-8.44616	-9.84039	-11.18228	-11.13996	-11.12732	-8.73498	-8.43282	-8.73151	0.01847	7.24818	0.13797
ENSMUSP00000025833	-8.82602	-8.74384	-8.52746	-10.37839	-9.82466	-11.42501	-7.81937	-7.45266	-7.25237	0.01815	5.24515	0.19065
ENSMUSP00000032168	-5.96301	-5.36720	-5.64424	-6.58276	-6.26035	-6.41339	-7.69863	-7.09145	-7.83333	0.01774	2.17141	0.46053
ENSMUSP00000063825	-5.92441	-6.42032	-7.00274	-7.64461	-8.19483	-7.68850	-5.99448	-6.26436	-5.97227	0.01768	4.28688	0.23327
ENSMUSP00000072084	-8.94222	-9.44823	-9.20538	-10.29383	-9.74010	-10.23888	-9.73705	-9.08141	-9.73358	0.01755	2.43439	0.41078
ENSMUSP00000056433	-8.38748	-8.30530	-8.39918	-10.25248	-10.21017	-9.09596	-10.20712	-8.72743	-8.59066	0.01725	3.83005	0.26109
ENSMUSP00000082125	-8.10673	-7.51361	-7.53052	-9.45795	-11.02862	-9.40299	-11.02558	-9.54588	-11.02210	0.01670	7.77023	0.12870
ENSMUSP00000031617	-5.08415	-4.98403	-4.90676	-5.65292	-5.52722	-5.27219	-6.15639	-5.96246	-6.13163	0.01617	1.62552	0.61519
ENSMUSP00000038214	-9.16059	-8.34734	-9.02914	-10.88007	-10.32634	-11.92669	-8.04011	-8.76947	-7.88540	0.01452	7.79776	0.12824
ENSMUSP00000035010	-8.94195	-8.38007	-8.38296	-9.36108	-9.77098	-10.09507	-10.61608	-10.23796	-11.71418	0.01425	3.15944	0.31651
ENSMUSP00000079379	-8.78241	-8.15352	-8.24740	-9.48664	-9.78104	-9.18023	-7.12393	-7.66980	-7.24002	0.01415	2.97472	0.33617
ENSMUSP00000075321	-6.85115	-6.99857	-5.87238	-10.77105	-8.52756	-10.71609	-6.40382	-6.18176	-10.72221	0.01382	20.29785	0.04927
ENSMUSP00000006703	-8.67668	-8.97410	-10.53545	-11.87734	-11.83502	-11.82238	-10.21898	-11.96527	-10.72693	0.01318	14.92872	0.06698
ENSMUSP00000052544	-7.96429	-8.02526	-7.85079	-9.82692	-10.88618	-9.26055	-8.04574	-8.17904	-8.16747	0.01298	6.37964	0.15675
ENSMUSP00000034058	-7.80800	-7.55871	-7.08189	-8.84895	-10.41962	-10.40699	-8.01465	-8.34871	-9.31153	0.01288	8.57067	0.11668
ENSMUSP00000026667	-7.98367	-8.33696	-7.88412	-11.07308	-11.03076	-9.40513	-7.88797	-7.86090	-7.97549	0.01263	8.57067	0.11668
ENSMUSP00000042860	-8.90856	-7.72679	-7.07319	-10.26215	-10.21983	-10.20719	-8.01561	-6.97850	-7.81138	0.01235	13.22193	0.07563

ENSMUSP00000028683	-5.38275	-4.95078	-5.27226	-6.43048	-6.32613	-5.82393	-6.95078	-7.02927	-7.23972	0.01211	2.63742	0.37916
ENSMUSP00000028592	-7.28640	-7.93031	-7.78774	-9.36371	-8.73321	-8.72057	-9.82976	-9.11492	-9.31487	0.01163	3.60297	0.27755
ENSMUSP00000026122	-6.39872	-5.82570	-6.68175	-7.37407	-7.61269	-7.40429	-7.28870	-6.77908	-7.10617	0.01150	3.33705	0.29967
ENSMUSP00000004072	-5.95920	-5.51128	-5.80384	-6.29234	-6.54243	-6.49275	-6.36653	-6.40885	-6.74503	0.01079	1.98644	0.50341
ENSMUSP00000076521	-7.64077	-6.40725	-6.91952	-8.93897	-8.75350	-8.50442	-11.46265	-9.02691	-10.35761	0.01006	6.26505	0.15962
ENSMUSP00000001479	-8.41118	-8.24561	-7.94739	-10.18994	-9.35868	-10.64641	-7.67567	-7.84346	-7.48704	0.00965	5.70445	0.17530
ENSMUSP00000020238	-6.05447	-5.53138	-5.80814	-7.35449	-7.21798	-6.62505	-6.32364	-6.46620	-6.73723	0.00935	3.44373	0.29038
ENSMUSP00000027123	-6.01110	-5.74555	-6.24753	-6.93759	-7.57620	-7.01441	-5.50281	-5.94348	-5.84075	0.00907	3.14986	0.31747
ENSMUSP00000075513	-5.76680	-5.83560	-6.98466	-8.87829	-9.42416	-11.02451	-5.78794	-5.87978	-5.54975	0.00905	28.82631	0.03469
ENSMUSP00000019512	-8.60265	-8.15260	-9.71395	-11.05583	-11.01352	-11.00088	-9.06076	-8.57472	-8.29481	0.00904	10.66175	0.09379
ENSMUSP00000099453	-6.89838	-6.64074	-6.71189	-9.04330	-11.40291	-9.77728	-5.82329	-6.06916	-6.09867	0.00904	18.68012	0.05353
ENSMUSP00000111081	-6.59729	-6.51511	-6.71869	-9.58449	-10.05359	-8.19388	-8.43993	-8.33678	-11.14865	0.00897	10.53032	0.09496
ENSMUSP00000039269	-6.89335	-6.61380	-6.90505	-7.26089	-7.30373	-7.43421	-6.73786	-6.95015	-7.06081	0.00820	1.69608	0.58960
ENSMUSP00000101823	-4.80368	-4.80397	-4.82599	-5.39852	-5.64761	-5.21796	-10.95229	-11.08559	-10.94882	0.00810	1.81380	0.55133
ENSMUSP00000099841	-8.24434	-7.54283	-8.00459	-10.44607	-10.40375	-9.28954	-7.02912	-7.31087	-8.44752	0.00799	7.40794	0.13499
ENSMUSP00000078774	-7.10316	-7.30060	-7.88412	-11.07308	-9.41777	-9.91655	-7.58943	-7.66020	-7.46458	0.00760	12.90298	0.07750
ENSMUSP00000023760	-7.65088	-7.07906	-7.47148	-8.28249	-8.60804	-8.84686	-7.58303	-7.27158	-7.30189	0.00742	3.20891	0.31163
ENSMUSP00000052912	-5.92198	-5.40363	-5.78675	-6.93411	-6.55530	-6.58762	-6.21892	-6.19245	-6.44452	0.00740	2.70101	0.37023
ENSMUSP00000005122	-8.44778	-8.16484	-9.55908	-10.90096	-10.85864	-10.84600	-8.28655	-7.76576	-7.55201	0.00730	9.80836	0.10195
ENSMUSP00000100000	-7.78623	-7.59583	-7.24236	-9.64819	-11.55559	-11.54295	-7.10551	-7.39100	-7.88118	0.00668	19.14269	0.05224
ENSMUSP00000039472	-8.13965	-7.52329	-9.37576	-11.22906	-11.18674	-11.17410	-11.18369	-11.31699	-11.18022	0.00638	21.75587	0.04596
ENSMUSP00000042351	-5.72225	-5.62708	-6.00222	-6.56207	-7.11230	-7.14315	-5.26559	-5.13937	-5.21605	0.00627	3.06018	0.32678
ENSMUSP00000024988	-9.06334	-8.10921	-8.40378	-12.45509	-10.79978	-11.29856	-12.40973	-12.54302	-12.40625	0.00613	17.44095	0.05734
ENSMUSP00000033012	-7.29982	-7.38708	-7.31153	-9.06263	-9.90799	-8.70533	-7.67590	-8.13347	-7.64212	0.00612	5.93958	0.16836
ENSMUSP00000048111	-7.73476	-7.65258	-6.81470	-9.45425	-9.41193	-8.88787	-6.84257	-6.56186	-7.13540	0.00588	6.84225	0.14615
ENSMUSP00000020315	-7.65082	-7.38390	-7.57914	-9.73939	-8.79889	-8.94662	-7.41873	-7.65015	-7.22827	0.00583	4.74327	0.21082
ENSMUSP00000111471	-8.76923	-8.20735	-9.14881	-11.59029	-10.44640	-11.53534	-9.59521	-9.72851	-9.59174	0.00580	10.98583	0.09103
ENSMUSP00000111363	-7.65881	-7.57663	-8.77011	-10.11199	-10.06967	-10.05704	-8.96506	-8.58694	-8.96159	0.00572	8.95496	0.11167
ENSMUSP00000095129:reversed	-8.50451	-8.42233	-9.61581	-10.95769	-10.91538	-10.90274	-10.91233	-11.04563	-10.90886	0.00572	8.95496	0.11167
ENSMUSP00000031897	-6.32550	-6.24333	-6.37888	-7.90464	-9.32979	-8.46901	-6.92751	-6.70713	-6.57036	0.00565	8.03830	0.12440
ENSMUSP00000002064	-8.87374	-8.20338	-9.39686	-10.73874	-10.69642	-10.68378	-8.74366	-8.42474	-8.74019	0.00554	7.24818	0.13797
ENSMUSP00000087118	-9.13954	-8.46918	-9.66266	-11.00454	-10.96222	-10.94959	-10.95918	-8.52343	-8.75454	0.00554	7.24818	0.13797
ENSMUSP00000086165	-8.88423	-7.70245	-8.38451	-10.23781	-10.19550	-10.18286	-10.19245	-8.37603	-9.08741	0.00537	7.24818	0.13797
ENSMUSP00000078382	-9.80347	-8.62170	-9.30376	-11.15706	-11.11474	-11.10210	-10.01012	-10.14342	-11.10822	0.00537	7.24818	0.13797
ENSMUSP00000033871	-6.74771	-6.20467	-6.50266	-7.34604	-7.45216	-7.36255	-7.62351	-7.96817	-8.26686	0.00492	2.50184	0.39971

ENSMUSP00000038755	-6.52458	-6.77893	-7.04719	-7.76721	-8.34422	-8.08013	-5.44230	-5.37636	-5.64829	0.00470	3.56064	0.28085
ENSMUSP00000079246	-7.78955	-7.50661	-7.80125	-8.29301	-8.58742	-8.57478	-7.62832	-7.28191	-7.62485	0.00446	2.17472	0.45983
ENSMUSP00000023214	-8.81355	-8.22035	-8.31423	-11.26673	-10.12284	-11.21177	-11.22137	-11.35467	-11.21789	0.00434	9.96357	0.10037
ENSMUSP00000034453	-5.56677	-5.50827	-5.59024	-6.11627	-6.20861	-5.91507	-5.25559	-5.41716	-5.41035	0.00431	1.67828	0.59585
ENSMUSP00000098963	-8.15777	-8.51105	-9.05715	-10.14560	-10.10328	-10.09064	-9.00064	-8.76606	-8.79641	0.00422	4.96152	0.20155
ENSMUSP00000026585	-9.13170	-8.20138	-8.04381	-10.48529	-10.44297	-10.43033	-9.33835	-10.57323	-10.43646	0.00421	8.10157	0.12343
ENSMUSP00000098000	-8.86934	-7.93902	-7.78144	-10.22293	-10.18061	-10.16797	-7.77563	-7.59867	-8.56110	0.00421	8.10157	0.12343
ENSMUSP00000038878	-7.58515	-7.15665	-7.74529	-8.49655	-8.59738	-8.75186	-6.26862	-6.43246	-6.23552	0.00421	3.10498	0.32206
ENSMUSP00000066878	-8.14557	-8.81087	-8.39373	-10.24466	-10.20234	-9.67828	-7.58296	-8.21103	-7.62951	0.00393	4.98631	0.20055
ENSMUSP00000109237	-7.28798	-6.93587	-6.92761	-8.85840	-8.26391	-8.25128	-6.39597	-6.65946	-6.36472	0.00378	4.00361	0.24977
ENSMUSP00000099461	-8.79138	-8.70920	-7.95494	-10.14496	-10.10264	-10.09001	-7.69767	-7.39551	-8.48314	0.00365	5.54139	0.18046
ENSMUSP00000033230	-8.54677	-9.56419	-8.55847	-10.99995	-10.95764	-10.94500	-9.00488	-9.13817	-9.33813	0.00354	8.95496	0.11167
ENSMUSP00000001806	-8.26492	-7.40490	-7.89088	-10.25275	-11.31201	-10.19780	-7.07048	-7.32702	-7.06701	0.00341	14.40768	0.06941
ENSMUSP00000069418	-10.28712	-8.65385	-9.53634	-12.48885	-12.44653	-12.43389	-11.34191	-10.96379	-12.44001	0.00329	23.46266	0.04262
ENSMUSP00000019109	-8.36479	-8.28261	-9.22463	-10.56651	-10.52420	-10.51156	-10.52115	-10.65445	-10.51768	0.00319	7.24818	0.13797
ENSMUSP00000046101	-5.73783	-6.08432	-6.45810	-8.83558	-7.97637	-8.06138	-5.89670	-6.25097	-5.92282	0.00306	8.84623	0.11304
ENSMUSP00000022706	-7.03471	-7.19179	-7.34124	-9.19150	-8.89772	-8.37407	-6.31233	-6.71390	-6.77051	0.00306	4.89368	0.20435
ENSMUSP00000021639	-8.17501	-7.96764	-9.28592	-11.13922	-11.09690	-11.08426	-7.59304	-11.22715	-7.32485	0.00302	15.78211	0.06336
ENSMUSP00000107544	-9.78563	-8.85531	-8.94919	-11.13922	-11.09690	-11.08426	-11.09385	-11.22715	-11.09038	0.00298	7.24818	0.13797
ENSMUSP00000044288	-5.80906	-5.75608	-5.99307	-9.05024	-9.34464	-10.94500	-6.20526	-6.57264	-6.16759	0.00270	38.36856	0.02606
ENSMUSP00000078429	-5.64968	-5.68062	-6.14757	-7.05531	-7.47966	-7.10761	-5.21531	-5.51362	-5.16237	0.00268	4.01167	0.24927
ENSMUSP00000107492	-8.97775	-8.75242	-8.60985	-11.79881	-11.75649	-10.64228	-8.19378	-8.58663	-8.24916	0.00265	12.00808	0.08328
ENSMUSP00000070983	-8.33601	-8.25383	-7.15769	-10.53774	-10.49542	-10.48278	-10.49237	-8.42450	-10.48890	0.00243	15.78211	0.06336
ENSMUSP00000029769	-8.44319	-8.69774	-9.30304	-10.64492	-10.60260	-10.58996	-8.19763	-8.16381	-7.75869	0.00215	6.39478	0.15638
ENSMUSP00000092157	-8.24275	-9.06361	-8.20180	-11.00842	-12.06768	-12.05504	-8.05294	-8.30176	-8.12498	0.00204	23.25286	0.04301
ENSMUSP00000022120	-11.09747	-11.01529	-11.10917	-11.34948	-11.30716	-11.29452	-8.59192	-8.48877	-8.00053	0.00200	1.27442	0.78467
ENSMUSP00000003572	-11.37946	-11.29728	-11.39116	-11.63147	-11.58915	-11.57652	-9.63639	-10.61783	-9.38146	0.00200	1.27442	0.78467
ENSMUSP00000025846	-11.52484	-11.44266	-11.53654	-11.77685	-11.73453	-11.72190	-10.11850	-10.76321	-10.62644	0.00200	1.27442	0.78467
ENSMUSP00000032508	-10.91676	-10.83459	-10.92847	-11.16877	-11.12646	-11.11382	-10.02184	-9.64372	-9.50695	0.00200	1.27442	0.78467
ENSMUSP00000033050	-10.51904	-10.43686	-10.53074	-10.77105	-10.72873	-10.71609	-8.77597	-8.28994	-9.10922	0.00200	1.27442	0.78467
ENSMUSP00000062215	-11.01296	-10.93078	-11.02466	-11.26497	-11.22265	-11.21001	-10.11803	-8.95097	-10.11456	0.00200	1.27442	0.78467
ENSMUSP00000064557	-10.17385	-10.09168	-10.18556	-10.42587	-10.38355	-10.37091	-7.97857	-7.94476	-9.27546	0.00200	1.27442	0.78467
ENSMUSP00000066413	-11.18137	-11.09919	-11.19307	-11.43338	-11.39106	-11.37842	-10.28644	-9.90832	-10.28297	0.00200	1.27442	0.78467
ENSMUSP00000084114	-10.80816	-10.72598	-10.81986	-11.06017	-11.01785	-11.00522	-9.91324	-10.04654	-9.90976	0.00200	1.27442	0.78467
ENSMUSP00000088334	-11.49370	-11.41153	-11.50541	-11.74572	-11.70340	-11.69076	-10.08736	-10.73208	-10.59531	0.00200	1.27442	0.78467

ENSMUSP00000088663	-10.51904	-10.43686	-10.53074	-10.77105	-10.72873	-10.71609	-9.62411	-9.24599	-9.10922	0.00200	1.27442	0.78467
ENSMUSP00000097097:reversed	-11.65267	-11.57050	-11.66437	-11.90468	-11.86237	-11.84973	-10.75775	-10.89105	-10.24286	0.00200	1.27442	0.78467
ENSMUSP00000098112	-10.89120	-10.80902	-10.90290	-11.14321	-11.10089	-11.08825	-9.99627	-10.12957	-9.99280	0.00200	1.27442	0.78467
ENSMUSP00000107983	-10.83801	-10.75584	-10.84972	-11.09003	-11.04771	-11.03507	-9.43167	-10.07639	-9.09147	0.00200	1.27442	0.78467
ENSMUSP00000111892	-9.82589	-9.74371	-9.83759	-10.07790	-10.03558	-10.02294	-5.23234	-5.01976	-5.35184	0.00200	1.27442	0.78467
ENSMUSP00000029564	-10.06167	-9.97949	-10.07337	-10.31368	-10.27136	-10.25872	-9.16674	-8.20045	-8.65185	0.00200	1.27442	0.78467
ENSMUSP00000027766	-11.24767	-11.16550	-11.25937	-11.49968	-11.45736	-11.44473	-9.50461	-9.38645	-9.24968	0.00200	1.27442	0.78467
ENSMUSP00000034529	-11.48494	-11.40276	-11.49664	-11.73695	-11.69463	-11.68200	-10.07860	-10.21190	-10.07513	0.00200	1.27442	0.78467
ENSMUSP00000035208:reversed	-13.01210	-12.92992	-13.02380	-13.26411	-13.22179	-13.20915	-12.11717	-12.25047	-12.11370	0.00200	1.27442	0.78467
ENSMUSP00000047376	-11.16937	-11.08719	-11.18107	-11.42138	-11.37906	-11.36643	-8.97409	-8.79713	-9.17138	0.00200	1.27442	0.78467
ENSMUSP00000014546	-10.76164	-10.67946	-10.77334	-11.01365	-10.97133	-10.95870	-9.86672	-9.48860	-9.86324	0.00200	1.27442	0.78467
ENSMUSP00000020886	-10.98976	-10.90758	-11.00146	-11.24177	-11.19945	-11.18682	-9.24669	-9.71672	-9.24322	0.00200	1.27442	0.78467
ENSMUSP00000029125	-10.41560	-10.33342	-10.42730	-10.66761	-10.62529	-10.61266	-9.52067	-9.14256	-9.51720	0.00200	1.27442	0.78467
ENSMUSP00000030935	-10.05249	-9.97032	-10.06420	-10.30450	-10.26219	-10.24955	-7.85721	-7.44380	-8.05450	0.00200	1.27442	0.78467
ENSMUSP00000035237	-11.66009	-11.57791	-11.67179	-11.91210	-11.86978	-11.85714	-10.76516	-10.89846	-10.76169	0.00200	1.27442	0.78467
ENSMUSP00000043703:reversed	-11.74162	-11.65944	-11.75332	-11.99363	-11.95131	-11.93868	-10.33528	-10.13185	-10.84322	0.00200	1.27442	0.78467
ENSMUSP00000045998	-11.79466	-11.71248	-11.80636	-12.04667	-12.00435	-11.99171	-10.89973	-10.52161	-9.79666	0.00200	1.27442	0.78467
ENSMUSP00000051033	-10.88520	-10.80303	-10.89690	-11.13721	-11.09490	-11.08226	-5.17663	-5.35994	-5.02717	0.00200	1.27442	0.78467
ENSMUSP00000075722	-11.11354	-11.03137	-11.12525	-11.36555	-11.32324	-11.31060	-10.21862	-9.50378	-8.47933	0.00200	1.27442	0.78467
ENSMUSP00000079905	-10.00532	-9.92314	-10.01702	-10.25733	-10.21501	-10.20237	-6.06446	-5.76616	-5.80966	0.00200	1.27442	0.78467
ENSMUSP00000097582	-10.32157	-10.23939	-10.33327	-10.57358	-10.53126	-10.51863	-8.91523	-9.04853	-9.42317	0.00200	1.27442	0.78467
ENSMUSP00000108098	-11.06786	-10.98568	-11.07956	-11.31987	-11.27755	-11.26491	-9.66152	-10.30623	-9.32132	0.00200	1.27442	0.78467
ENSMUSP00000111551	-10.46865	-10.38648	-10.48036	-10.72067	-10.67835	-10.66571	-8.72559	-9.70703	-9.05884	0.00200	1.27442	0.78467
sp|CAS2_BOVIN|	-10.23328	-10.15110	-10.24498	-10.48529	-10.44297	-10.43033	-6.50375	-7.52448	-6.82122	0.00200	1.27442	0.78467
ENSMUSP00000007708:reversed	-11.15417	-11.07200	-11.16588	-11.40618	-11.36387	-11.35123	-10.25925	-10.39255	-10.25578	0.00200	1.27442	0.78467
ENSMUSP00000034391	-11.24628	-11.16410	-11.25798	-11.49829	-11.45597	-11.44333	-10.35135	-10.48465	-10.34788	0.00200	1.27442	0.78467
ENSMUSP00000063548	-11.00765	-10.92547	-11.01935	-11.25966	-11.21734	-11.20471	-10.11273	-9.73461	-10.10925	0.00200	1.27442	0.78467
ENSMUSP00000073102	-10.50741	-10.42523	-10.51911	-10.75942	-10.71710	-10.70446	-8.00186	-8.27831	-7.76194	0.00200	1.27442	0.78467
ENSMUSP00000073861	-10.96786	-10.88569	-10.97956	-11.21987	-11.17756	-11.16492	-8.97334	-9.69482	-9.22132	0.00200	1.27442	0.78467
ENSMUSP00000076093	-12.94772	-12.86554	-12.95942	-13.19973	-13.15741	-13.14477	-12.05279	-12.18609	-12.04932	0.00200	1.27442	0.78467
ENSMUSP00000078845:reversed	-11.21074	-11.12856	-11.22244	-11.46275	-11.42043	-11.40779	-9.80439	-9.93769	-9.80092	0.00200	1.27442	0.78467
ENSMUSP00000099420:reversed	-11.01823	-10.93606	-11.02993	-11.27024	-11.22793	-11.21529	-10.12331	-10.25661	-10.11984	0.00200	1.27442	0.78467
ENSMUSP00000106953	-9.39998	-9.31781	-9.41169	-9.65200	-9.60968	-9.59704	-7.65692	-6.60019	-6.55441	0.00200	1.27442	0.78467

ENSMUSP00000043821	-6.45996	-6.83815	-7.09910	-8.30235	-8.73973	-8.34750	-6.10282	-6.22513	-5.86412	0.00199	5.36321	0.18646
ENSMUSP00000073459	-8.47778	-6.98154	-7.85326	-10.93096	-10.88864	-10.87601	-7.66246	-7.87916	-7.65899	0.00197	26.87623	0.03721
ENSMUSP00000028892	-9.61603	-9.02243	-8.77959	-10.96961	-10.92729	-10.91466	-8.72308	-9.95598	-9.30779	0.00195	6.39478	0.15638
ENSMUSP00000013773	-10.06672	-8.71859	-9.91131	-12.72067	-12.67835	-12.66571	-8.95740	-8.95411	-9.11217	0.00185	26.87623	0.03721
ENSMUSP00000024944	-9.72018	-9.30128	-8.63268	-11.58518	-11.54286	-11.53023	-11.53982	-11.67312	-11.53635	0.00181	11.51514	0.08684
ENSMUSP00000076777	-5.30505	-5.36888	-5.75483	-6.81935	-7.28789	-6.87719	-5.13818	-5.30315	-11.09238	0.00173	4.53226	0.22064
ENSMUSP00000047054	-9.35356	-10.11953	-9.36527	-11.55529	-11.51297	-11.50034	-10.40836	-11.64323	-11.50646	0.00167	7.24818	0.13797
ENSMUSP00000077040	-11.91339	-11.31979	-11.92509	-13.26697	-13.22465	-13.21202	-11.02044	-12.25333	-13.21814	0.00164	4.68800	0.21331
ENSMUSP00000043220:reversed	-10.27175	-9.67816	-10.28346	-11.62534	-11.58302	-11.57038	-10.47840	-11.71328	-10.47493	0.00164	4.68800	0.21331
ENSMUSP00000038339	-9.85142	-9.25782	-9.86312	-11.20500	-11.16268	-11.15005	-9.20993	-9.09177	-8.75424	0.00164	4.68800	0.21331
ENSMUSP00000022196	-10.68335	-10.08976	-10.69505	-12.03694	-11.99462	-11.98198	-11.99157	-11.02330	-11.98810	0.00164	4.68800	0.21331
ENSMUSP00000030742	-9.56996	-8.97637	-9.58166	-10.92354	-10.88123	-10.86859	-9.77661	-9.90991	-10.87471	0.00164	4.68800	0.21331
ENSMUSP00000054370	-7.94667	-7.40177	-7.65602	-9.93450	-10.99376	-10.98112	-6.81195	-7.04211	-7.42758	0.00152	17.11934	0.05841
ENSMUSP00000007708	-8.10542	-7.93226	-7.79429	-11.40618	-11.36387	-10.24966	-7.01264	-7.28506	-7.27545	0.00141	18.65272	0.05361
ENSMUSP00000021698	-6.09667	-5.71093	-5.89612	-8.10665	-8.18571	-7.46385	-5.53658	-5.88335	-5.56096	0.00137	7.20257	0.13884
ENSMUSP00000006137	-7.85889	-7.26584	-7.22390	-9.41054	-9.61968	-9.15483	-6.83457	-7.61775	-7.02589	0.00137	7.13020	0.14025
ENSMUSP00000027833	-7.32550	-7.47424	-7.35804	-8.65581	-8.97456	-8.43378	-7.29467	-7.36495	-7.16890	0.00134	3.60895	0.27709
ENSMUSP00000030454	-5.89652	-6.09693	-5.76511	-7.48989	-7.06183	-7.13259	-5.88309	-5.49083	-5.74146	0.00133	3.70612	0.26982
ENSMUSP00000088249	-4.60837	-4.53955	-5.39078	-6.99967	-7.07691	-7.12987	-4.54871	-4.90293	-4.50050	0.00128	9.75353	0.10253
ENSMUSP00000076294	-6.72185	-6.68135	-6.81872	-7.56992	-7.68797	-7.37679	-7.38638	-6.98332	-7.44961	0.00127	2.21859	0.45074
ENSMUSP00000025696	-6.44439	-6.62694	-6.78335	-9.36037	-9.31805	-10.40699	-6.48040	-6.12665	-6.14605	0.00113	19.51505	0.05124
ENSMUSP00000050689	-5.91857	-5.94365	-5.86467	-7.11274	-6.70935	-6.89742	-10.20712	-10.34042	-10.20365	0.00110	2.68726	0.37213
ENSMUSP00000054863	-6.48428	-6.43544	-6.75673	-7.62840	-7.76046	-7.49647	-7.50606	-7.27158	-7.24304	0.00105	2.91575	0.34296
ENSMUSP00000082288	-5.82000	-6.27450	-6.57530	-8.71686	-9.29388	-9.61796	-5.14707	-5.66231	-5.49931	0.00096	19.22780	0.05201
ENSMUSP00000032473	-6.89973	-6.51525	-7.08208	-8.88675	-9.43261	-8.83180	-7.23156	-6.88102	-6.66526	0.00095	9.03625	0.11067
ENSMUSP00000033185	-8.96316	-7.99330	-8.72340	-11.16488	-11.12256	-11.10993	-10.01795	-10.15125	-11.11605	0.00092	14.07533	0.07105
ENSMUSP00000002389	-9.85866	-9.18830	-9.87036	-11.72366	-11.68134	-11.66871	-11.67830	-11.81160	-11.67483	0.00082	8.10157	0.12343
ENSMUSP00000101002	-9.14318	-8.54958	-8.64346	-10.49676	-10.45444	-10.44181	-7.07982	-6.91681	-6.73002	0.00080	5.54139	0.18046
ENSMUSP00000031105	-8.98267	-8.38907	-8.48295	-10.33625	-10.29394	-10.28130	-7.88896	-7.37544	-7.06428	0.00080	5.54139	0.18046
ENSMUSP00000024739	-5.51988	-5.25773	-5.45567	-7.56654	-7.00661	-7.10046	-5.04614	-5.33668	-5.08046	0.00068	6.00087	0.16664
ENSMUSP00000099904	-5.15288	-5.22893	-5.37303	-6.22020	-6.11679	-6.00548	-4.48666	-4.80141	-4.50676	0.00065	2.37213	0.42156
ENSMUSP00000101833	-9.64407	-9.56189	-9.14435	-10.99765	-10.95533	-10.94270	-10.95229	-11.08559	-10.94882	0.00062	4.68800	0.21331
ENSMUSP00000039243	-9.94092	-9.85875	-9.44121	-11.29451	-11.25219	-11.23955	-9.63616	-8.43380	-8.84374	0.00062	4.68800	0.21331
ENSMUSP00000086716	-10.69535	-10.61317	-9.94457	-12.89707	-12.85476	-12.84212	-9.23647	-12.98501	-10.01085	0.00051	12.36854	0.08085
ENSMUSP00000086626	-8.90593	-9.71143	-8.91763	-11.99533	-11.95301	-11.94038	-9.23778	-8.94353	-8.33126	0.00048	17.48890	0.05718

ENSMUSP00000099807	-9.02962	-8.94745	-9.62951	-11.48281	-11.44049	-11.42785	-11.43744	-11.57074	-11.43397	0.00048	9.80836	0.10195
ENSMUSP00000027144	-4.20006	-4.19789	-4.52164	-5.47448	-5.55592	-5.54089	-3.73026	-3.96705	-3.82899	0.00039	3.39863	0.29424
ENSMUSP00000071135	-5.21527	-4.90369	-5.18601	-6.83635	-6.64183	-6.49712	-4.99235	-5.10767	-5.00718	0.00037	4.73303	0.21128
ENSMUSP00000110006:reversed	-10.35805	-9.68769	-10.03303	-12.22305	-12.18073	-12.16810	-9.77576	-10.10982	-10.56123	0.00037	8.95496	0.11167
ENSMUSP00000105647	-9.26012	-9.17794	-8.68364	-11.12512	-11.08280	-11.07016	-11.07975	-10.11148	-11.07628	0.00034	8.10157	0.12343
ENSMUSP00000095316	-7.14890	-6.88011	-7.01748	-8.12015	-8.07783	-7.96509	-6.94153	-6.86189	-6.72512	0.00033	2.83000	0.35336
ENSMUSP00000042457	-4.54441	-4.45871	-4.88766	-6.29262	-6.23468	-6.16187	-4.43341	-4.59800	-4.40709	0.00030	5.00377	0.19985
ENSMUSP00000042342	-4.98437	-4.66754	-4.99607	-6.42128	-6.34356	-6.21604	-4.73104	-4.86087	-4.69338	0.00030	4.25416	0.23506
ENSMUSP00000034818	-7.70537	-8.16990	-8.46454	-10.90602	-10.86370	-10.85107	-8.02327	-7.94521	-8.01980	0.00024	16.63551	0.06011
ENSMUSP00000044556	-6.50624	-6.68750	-6.86715	-8.09339	-8.22546	-8.31293	-5.53989	-5.89878	-5.41972	0.00024	4.60820	0.21700
ENSMUSP00000097469	-8.29190	-7.36226	-7.87606	-11.25611	-11.21379	-11.20115	-11.21075	-7.90576	-7.76899	0.00023	31.14320	0.03211
ENSMUSP00000031103	-5.85647	-6.27718	-6.47532	-9.02971	-8.78663	-9.22621	-5.40344	-5.59408	-5.45078	0.00023	16.95279	0.05899
ENSMUSP00000021114	-7.88258	-7.41465	-8.16262	-10.97198	-10.92966	-10.91703	-7.31138	-7.62163	-7.20524	0.00014	23.46266	0.04262
ENSMUSP00000020286	-7.62210	-7.80827	-8.27002	-10.71151	-10.66919	-10.65655	-7.36603	-7.13155	-7.29109	0.00014	16.63551	0.06011
ENSMUSP00000060246	-5.01431	-4.77032	-5.04893	-6.60022	-6.49538	-6.38651	-4.91991	-5.02021	-4.91643	0.00013	4.71254	0.21220
ENSMUSP00000050292	-7.50177	-7.41960	-7.96569	-10.15572	-10.11340	-10.10076	-7.90918	-7.53146	-8.49389	0.00013	12.36854	0.08085
ENSMUSP00000027824	-7.67189	-7.21012	-7.85071	-10.49295	-10.45063	-10.43800	-10.44759	-8.96790	-10.44412	0.00011	18.34229	0.05452
ENSMUSP00000108734	-8.16962	-8.08744	-8.51804	-10.37135	-10.32903	-10.31639	-8.37627	-7.89023	-7.75346	0.00010	8.10157	0.12343
ENSMUSP00000068086	-9.30958	-8.89068	-8.98456	-11.17458	-11.13226	-11.11963	-7.15457	-8.42513	-8.17710	0.00008	8.10157	0.12343
ENSMUSP00000034808	-7.96102	-7.44339	-7.42601	-10.61497	-10.57265	-10.56001	-10.56961	-10.70290	-10.56613	0.00007	20.04908	0.04988
ENSMUSP00000030187	-9.13421	-8.55414	-9.28408	-12.82450	-12.78218	-12.76955	-8.84296	-8.73368	-8.48083	0.00007	46.50428	0.02150
ENSMUSP00000026168	-9.75285	-10.00740	-10.10128	-11.95458	-11.91226	-11.89963	-10.80764	-12.04252	-10.80417	0.00005	7.24818	0.13797
ENSMUSP00000102254	-9.10698	-9.02480	-8.78195	-10.97198	-10.92966	-10.91703	-9.82504	-9.11020	-8.72197	0.00004	7.24818	0.13797
ENSMUSP00000026012	-7.31080	-7.13552	-6.61718	-11.28072	-11.23840	-11.22576	-11.23535	-11.36865	-11.23188	0.00004	72.10609	0.01387
ENSMUSP00000064849	-6.40380	-6.62586	-5.93122	-10.77105	-10.72873	-10.71609	-5.63987	-5.82414	-5.90562	0.00003	87.46718	0.01143
ENSMUSP00000101862	-7.35710	-7.46300	-7.31323	-8.76684	-8.92528	-8.91265	-7.40551	-7.40222	-7.35440	0.00002	4.43995	0.22523
ENSMUSP00000047761	-7.76482	-7.29054	-7.77652	-11.23997	-11.19765	-11.18501	-6.70158	-7.28049	-6.84294	0.00002	37.11695	0.02694
ENSMUSP00000020034	-8.13996	-8.51000	-8.35242	-10.79390	-10.75159	-10.73895	-7.52540	-7.44356	-7.90768	0.00002	11.51514	0.08684
ENSMUSP00000070682	-7.49542	-7.48471	-7.82995	-11.11901	-11.07669	-11.06406	-6.99175	-6.99788	-6.77534	0.00001	32.84999	0.03044
ENSMUSP00000036337	-8.35767	-8.27549	-8.11792	-10.55940	-10.51708	-10.50444	-6.70303	-7.50759	-7.67317	0.00001	9.80836	0.10195
ENSMUSP00000024860	-7.94303	-7.62901	-7.65619	-11.33478	-11.29246	-11.27983	-7.11066	-7.30748	-7.07688	0.00000	35.41017	0.02824
ENSMUSP00000051366	-9.92713	-9.84495	-9.93883	-11.28072	-11.23840	-11.22576	-9.28564	-8.96672	-10.13031	0.00000	3.83460	0.26078
ENSMUSP00000110576	-9.77558	-9.69340	-9.78728	-11.12917	-11.08685	-11.07421	-11.08380	-11.21710	-11.08033	0.00000	3.83460	0.26078
ENSMUSP00000052174:reversed	-9.89717	-9.81500	-9.90887	-11.25076	-11.20844	-11.19580	-11.20540	-11.33869	-11.20192	0.00000	3.83460	0.26078
ENSMUSP00000099403	-8.44658	-8.36440	-8.18379	-11.64724	-11.60492	-11.59228	-8.23029	-8.36359	-9.02936	0.00000	26.87623	0.03721

ENSMUSP00000022369	-7.96839	-8.28017	-8.07775	-11.98594	-11.94362	-11.93099	-8.43977	-8.06219	-8.26922	0.00000	47.35768	0.02112
ENSMUSP00000044554	-8.92739	-8.84521	-8.77198	-11.58133	-11.53902	-11.52638	-9.13404	-9.26734	-8.82031	0.00000	14.92872	0.06698
ENSMUSP00000021506	-8.86921	-8.78703	-8.88091	-11.07094	-11.02862	-11.01598	-11.02558	-11.15887	-11.02210	0.00000	8.95496	0.11167
ENSMUSP00000108953	-6.35620	-6.40384	-6.16407	-11.35755	-11.31523	-11.30259	-5.74324	-5.87654	-11.30871	0.00000	152.32510	0.00656
ENSMUSP00000035823	-8.55928	-8.66820	-8.66197	-11.95103	-11.90872	-11.89608	-9.33662	-9.20158	-8.40139	0.00000	26.87623	0.03721